Polarons: Part I

Yury Holubeu *

February 17, 2026

This draft is not aimed for distribution.

Contents

Preface **8**

I Polarons in a Nutshell **9**

1 Main Formulas and Ideas from My Notes (?) **9**

2 Main Formulas and Ideas from Alexandrov and Mott (?) **9**

2.1 Main Formalism of Alexandrov and Mott . . . 9

2.2 1 Large and small polaron . . . 10

2.2.1 1.1, 1.2 Strong-coupling large polaron . . . 10

2.2.2 1.3 Fröhlich large polaron . . . 11

2.2.3 1.4 Intermediate-coupling large polaron $1 < \alpha < 10$ . . . 12

2.2.4 1.5,1.6,1.7 Small polaron: two-site Holstein model, adiabatic, fast solutions . . . 13

2.2.5 1.8 From large to small polaron: numerical calculations . . . 14

2.3 3 Electrons and phonons . . . 14

2.3.1 3.1 Electrons, phonons and the Fröhlich interaction . . . 14

2.3.2 3.2 Bare phonons and sound in a metal . . . 16

2.3.3 3.3 Effect of the Fröhlich interaction on electrons in a metal . . . 16

2.3.4 3.4 Broken gauge symmetry and the BCS ground state . . . 16

2.3.5 3.5 Bloch states in semiconductors: Effective mass approximation . . . 16

2.3.6 3.6 Tight-binding approximation . . . 16

2.4 4 The multi-polaron problem . . . 17

2.4.1 4.1 Small-polaron instability within the Migdal approach . . . 17

2.4.2 4.2 Exact solution of the multi-polaron problem for $\lambda \to \infty$ . . . 17

2.4.3 4.3 Polaron band and self-energy . . . 18

2.4.4 4.4 Temperature collapse of the polaron band . . . 19

2.4.5 4.5 Phonons in a strong-coupling system . . . 19

2.4.6 4.6 Screening and polaronic plasmon . . . 19

2.4.7 4.7 Many-body polaronic effect in the phonon spectrum . . . 20

2.4.8 4.8 Polaron thermodynamics . . . 20

2.4.9 4.9 Polaron kinetics: hopping transport . . . 21

2.4.10 4.10 MIR conductivity of polarons . . . 21

2.4.11 4.11 Polaron kinetics: band tunneling transport . . . 21

2.4.12 4.12 Electron Green's function and ARPES of polaronic systems . . . 21

2.5 Articles That Are Used in Alexandrov and Mott's Book . . . 21

2.5.1 The Motion of Slow Electrons in a Polar Crystal by Lee, Low, Pines 1953 . . . 21

II My Theory of Polarons **22**

*https://yuriholubeu.github.io/, yuri.holubev@gmail.com

3 Main Models of Polarons **22**
3.1 Physics Behind Polarons . . . 22
3.1.1 Concept of Polarization for Polarons . . . 22
3.1.2 When Electron-Phonon Coupling is Large . . . 22
3.1.3 Requirements for Semiconductor to Have Polarons . . . 22
3.1.4 Why in TaS_2 there are polarons (form experiments)? . . . 22
3.2 General Conceptual Questions about Single Polarons . . . 22
3.2.1 How to know, which type of polaron is present? . . . 22
3.3 Bipolarons . . . 22
3.3.1 What Is Going On With Theories of Bipolarons? . . . 22

4 Numerical Simulation of Polarons **22**

5 Experimental Consequences of Polarons **22**

III Examples and Solved Problems **23**

IV Well-known and Important Theories **24**

6 Polarons and Bipolarons by Alexandrov, Mott **24**
6.1 Introduction . . . 24
6.1.1 Introduction . . . 24
6.1.2 Electron Motion in Crystall Lattices by Landau 1933 . . . 28
6.2 1 Large and small polaron . . . 29
6.2.1 1.1 Strong-coupling large polaron . . . 29
6.2.2 1.2 Effective mass of large strong-coupling polaron . . . 32
6.2.3 1.3 Fröhlich large polaron . . . 34
6.2.4 1.4 Intermediate-coupling large polaron . . . 38
6.2.5 The Motion of Slow Electrons in a Polar Crystal by Lee, Low, Pines 1953 . . . 41
6.2.6 Self Energy of Slow Electrons in Polar Materials by Gurari 1953 . . . 51
6.2.7 1.5 Small polaron: two-site Holstein model . . . 58
6.2.8 1.6 Nonadiabatic small polaron . . . 61
6.2.9 1.7 Adiabatic small polaron . . . 63
6.2.10 Holstein's Studies of Polaron Motion. Part I. The Molecular-Crystal Model . . . 65
6.2.11 Holstein's Studies of Polaron Motion. Part II. The "Small" Polaron 1 . . . 80
6.2.12 Holstein's Studies of Polaron Motion. Part II. The "Small" Polaron 2 . . . 91
6.2.13 Holstein's Studies of Polaron Motion. Part II. The "Small" Polaron 3 . . . 101
6.2.14 Holstein's Studies of Polaron Motion. Part II. The "Small" Polaron 4 . . . 109
6.2.15 1.8 From large to small polaron: numerical calculations . . . 119
6.3 1-1 Articles about large and small polarons and methods for them . . . 122
6.3.1 Bogoliubov N N 1947 J.Phys.USSR 11, 23-32 . . . 122
6.4 3 Electrons and phonons . . . 123
6.4.1 3.1 Electrons, phonons and the Fröhlich interaction . . . 123
6.4.2 3.2 Bare phonons and sound in a metal . . . 127
6.4.3 3.3 Effect of the Fröhlich interaction on electrons in a metal . . . 131
6.4.4 3.4 Broken gauge symmetry and the BCS ground state . . . 135
6.4.5 3.5 Bloch states in semiconductors: Effective mass approximation . . . 140
6.4.6 3.6 Tight-binding approximation . . . 143
6.5 4 The multi-polaron problem . . . 146
6.5.1 4.1 Small-polaron instability within the Migdal approach . . . 146
6.5.2 Electron-phonons with strong coupling, violation of Migdal-Éliashberg theory . . . 149
6.5.3 4.2 Exact solution of the multi-polaron problem for $\lambda \to \infty$ . . . 159

6.5.4 Many-body effects in the normal-state polaron system by Alexandrov 161
6.5.5 Kinetic Theory of Semiconductors with Low Mobility by Lang, Firsov 1 172
6.5.6 Kinetic Theory of Semiconductors with Low Mobility by Lang, Firsov 2 185
6.5.7 4.3 Polaron band and self-energy 192
6.5.8 4.4 Temperature collapse of the polaron band 196
6.5.9 4.5 Phonons in a strong-coupling system 198
6.5.10 4.6 Screening and polaronic plasmon 199
6.5.11 4.7 Many-body polaronic effect in the phonon spectrum 200
6.5.12 4.8 Polaron thermodynamics 202
6.5.13 4.9 Polaron kinetics: hopping transport 204
6.5.14 4.10 MIR conductivity of polarons 206
6.5.15 4.11 Polaron kinetics: band tunneling transport 208
6.5.16 4.12 Electron Green's function and ARPES of polaronic systems 211
6.6 2 Large and small bipolaron 213
6.6.1 2.1 Strong-coupling large bipolaron 213
6.6.2 2.2 Intermediate-coupling large bipolaron 216
6.6.3 2.3 Path integral approach to large bipolaron 218
6.6.4 2.4 Small bipolaron 222
6.6.5 2.5 Small bipolaron in perovskite structures 223
6.6.6 2.6 Effect of the kinetic energy on small-bipolaron formation 228
6.7 5 Phase transformations of the polaronic Fermi-liquid 231
6.7.1 5.1 Bipolaronic instability 231
6.7.2 5.2 Cooper pairing of nonadiabatic carriers 232
6.7.3 5.3 High T_c polaronic superconductivity 233
6.7.4 5.4 Polaronic CDW 237
6.7.5 5.5 Small polarons in doped Mott insulators 241
6.8 6 Bipolaronic liquid 243
6.8.1 6.1 Coherent tunneling and repulsion of bipolarons 243
6.8.2 6.2 Bipolaron anisotropic flat bands in high- T_c copper oxides 246
6.8.3 6.3 Bipolaron kinetics 250
6.8.4 6.4 MIR conductivity of small bipolarons 252
6.8.5 6.5 Effect of superconducting phase transition on MIR conductivity 253
6.8.6 6.6 Pseudospin representation of the bipolaronic Hamiltonian 258
6.8.7 6.7 Superfluid versus charged ordered ground state 259
6.8.8 6.8 Excitation spectrum of the bipolaronic liquid 260
6.8.9 6.9 $T - n$ phase diagram of the bipolaronic liquid 262
6.8.10 6.10 Mapping on a charged Bose gas 263
6.8.11 6.11 Bipolaron electrodynamics 265
6.9 7 Charged Bose gas 266
6.9.1 7.1 Bogoliubov-de Gennes equations for CBG 267
6.9.2 7.2 Excitation spectrum and ground state energy of CBG 269
6.9.3 7.3 Linear-response function 271
6.9.4 7.4 Collective excitations and screening 273
6.9.5 7.5 Superconducting kinetics of CBG: $2D$ heat superconductor 274
6.9.6 7.6 BEC of charged bosons in a random potential 275
6.9.7 7.7 BEC of charged bosons in a magnetic field 278
6.9.8 7.8 Normal state kinetics of CBG 282
6.10 8 Evidence for mobile small polarons and bipolarons 284
6.10.1 8.1 Small versus large polarons 284
6.10.2 8.2 Small-polaron transport in TiO_2 and NiO 286
6.10.3 8.3 Mobile polarons and bipolarons in WO_{3-x} 288
6.10.4 8.4 Small polarons in high- T_c oxides 289
6.10.5 8.4.1 High- T_c oxides are doped semiconductors 290

6.10.6 8.4.2 Low mobility . . . 290
6.10.7 8.4.3 MIR conductivity of high- T_c oxides . . . 292
6.10.8 8.5 Small bipolarons in high- T_c oxides . . . 294
6.10.9 8.5.1 λ-point in high- T_c oxides . . . 295
6.10.10 8.5.2 Doping dependence of R_H, T_c and λ_H . . . 296
6.10.11 8.5.3 NIR absorption in $YBCO$ . . . 298
6.10.12 8.5.4 Upper critical field of high- T_c oxides . . . 299
6.10.13 8.6 Polaronic ARPES in high- T_c oxides and fullerene . . . 301
6.11 Conclusion . . . 303

7 Fröhlich Polarons by Devreese: Single polaron 305
7.1 Introduction. The "standard" theories . . . 306
7.1.1 The polaron concept . . . 306
7.1.2 Intuitive concepts . . . 307
7.1.3 The Fröhlich Hamiltonian . . . 310
7.1.4 Infinite mass model [“shift”–operators] . . . 311
7.1.5 The "standard" theories . . . 312
7.1.6 Polaron mobility . . . 327
7.2 Optical Absorption. Weak coupling . . . 329
7.2.1 Optical absorption at weak coupling [within the perturbation theory] . . . 329
7.2.2 Optical absorption at weak coupling [within the canonical-transformation method [73] (DHL)] . . . 330
7.3 Optical absorption. Strong coupling . . . 335
7.4 Arbitrary coupling . . . 336
7.4.1 Impedance function of large polarons: An alternative derivation of FHIP [76] . . . 336
7.4.2 Calculation of the memory function (Devreese *et. al.* [50]) . . . 356
7.4.3 Discussion of optical absorption of polarons at arbitrary coupling . . . 358
7.4.4 Scaling relations . . . 364

8 Fröhlich Polarons by Devreese: Many polarons 384
8.1 Optical conductivity of an interacting many-polaron gas . . . 384
8.1.1 Kubo formula for the optical conductivity of the many-polaron gas . . . 384
8.1.2 Force-force correlation function . . . 386
8.1.3 Canonical transformation . . . 388
8.1.4 Dynamic structure factor . . . 391
8.1.5 Comparison to the infrared spectrum of $Nd_{2-x}Ce_xCuO_{2-y}$ . . . 398
8.1.6 Experimental data on the optical absorption in manganites: interpretation in terms of a many-polaron response . . . 399
8.2 Interacting polarons in a quantum dot . . . 401
8.2.1 The partition function and the free energy of a many-polaron system . . . 401
8.2.2 Model system . . . 406
8.2.3 Variational functional . . . 411
8.2.4 Two-point correlation functions . . . 413
8.2.5 Many-polaron ground state in a quantum dot: extrapolation to the homogeneous limit and comparison to the results for a polaron gas in bulk [90] . . . 422
8.2.6 Optical conductivity . . . 425
8.3 Variational path-integral treatment of a translation invariant N-polaron system . . . 432
8.3.1 The many-polaron system . . . 432
8.3.2 Variational principle . . . 433
8.3.3 Results . . . 434
8.4 Ripplonic polarons in multielectron bubbles . . . 437
8.4.1 Ripplon-phonon modes of a MEB . . . 437
8.4.2 Electron-ripplon interaction in the MEB . . . 438
8.4.3 Locally flat approximation . . . 439

8.4.4 Ripplopolaron in a Wigner lattice: the mean-field approach . . . 440
8.4.5 Ripplopolaron Wigner lattice at finite temperature . . . 441
8.4.6 Melting of the ripplopolaron Wigner lattice . . . 442

9 Fröhlich Polarons by Devreese: Appendix 444
9.1 Optical conductivity of a strong-coupling Fröhlich polaron . . . 444
9.1.1 Introduction . . . 445
9.1.2 Optical conductivity . . . 445
9.1.3 Results and discussion . . . 451
9.1.4 Conclusions . . . 453
9.1.5 Appendix 1. Correlation function . . . 453
9.1.6 Appendix 2. Effective phonon modes . . . 455
9.2 Feynman's path-integral polaron treatment approached using time-ordered operator calculus . . . 462
9.3 Many-body large polaron optical conductivity in $SrTi_{1-x}Nb_xO_3$ . . . 469
9.3.1 Introduction . . . 469
9.3.2 Optical conductivity of a gas of large polarons . . . 472
9.3.3 Optical conductivity spectra . . . 477
9.3.4 Conclusions . . . 481
9.4 Notes on the polaron mobility . . . 484

10 Pekar's Research in Electron Theory of Crystals, 1951 490
10.1 I Introduction . . . 491
10.1.1 1 Preliminary remarks . . . 491
10.1.2 § 2. Consequences arising from translational symmetry of crystals . . . 496
10.1.3 § 3. Qualitative study of the states of electrons in a semiconductor with fixed ions 499
10.1.4 § 4. Effective mass method . . . 503
10.2 II Theory of Polarons with Classical Approach to Crystal Motion . . . 511
10.2.1 § 5. Basic Equations . . . 511
10.2.2 § 6. The Resting Polaron [12, 13] . . . 515
10.2.3 § 7. Criteria for the applicability of the theory [12] . . . 520
10.2.4 § 9. Photodissociation and photo-excitation of the polaron [12], [16] . . . 526
10.2.5 § 10. Progressive motion of the polaron [17], [18] . . . 529
10.2.6 § 11. A new look at the electronic conductivity of ionic crystals [15], [17] . . . 536
10.3 III. Polaron Theory with Quantum Mechanical Approach to Ion Motion . . . 540
10.3.1 § 12. Basic Equations . . . 540
10.3.2 § 13. Properties of the wave function arising from the theory of groups . . . 544
10.3.3 § 14. Approximate determination of system energy . . . 545
10.3.4 § 15. System energy operator in adiabatic approximation [22] . . . 549
10.3.5 § 16. Energy spectrum and ψ-functions of the system in adiabatic approximation 555
10.3.6 § 17. Scattering of polaron waves by optical oscillations of ions . . . 562
10.3.7 § 18. Scattering of polaron waves by acoustic oscillations of the crystal . . . 568
10.3.8 § 19. Application of statistics in case of thermal equilibrium . . . 575
10.3.9 § 20. Mobility of Polarons . . . 578
10.4 IV Theory of F-centers and F'-centers with Classical Approach to Motion of Ions . . . 589
10.4.1 § 21. Crystal Staining . . . 589
10.4.2 § 22. Critical review of existing hypotheses about the nature of F-centers . . . 591
10.4.3 § 23. Basic equations for crystal with F-центром . . . 594
10.4.4 § 24. Energy spectrum and ψ-functions of the electron in the F-center . . . 597
10.4.5 § 25. Absorption of light by F-centers [15] . . . 600
10.4.6 § 26. Theory of F'-центров . . . 602
10.5 IV Theory of F-centers and F'-centers with Quantum Approach to Motion of Ions [38] 606
10.5.1 § 27. Energy spectrum and ψ-function of the crystal with F-center . . . 606
10.5.2 § 28. Absorption of light by F-centers . . . 609

10.5.3 § 29. Application of statistics in case of thermal equilibrium 616
10.6 VI Comparison of Theory with Experiments. Application of theory to Specific Crystals 621
10.6.1 § 30. Defining Theory Parameters 621
10.6.2 § 31. Comparison with the experience of thermal dissociation energies of F-centers 624
10.6.3 § 32. Width, shape and temperature dependence of F absorption bands 627
10.6.4 § 33. On the theory of electron recombination in semiconductors [57] 629
10.6.5 § 34. Recombination of conduction electrons at F-centers. Comparison of theory with experience [59] 634
10.6.6 § 35. Quantum Output of Photodissociation F - and F'-центров 636
10.6.7 § 36. Metal-type electronic semiconductorsSulfurous lead 640
10.6.8 § 37. Conclusion 647
10.6.9 Appendix. Attempt to Consider Polarons Under the Assumption of Weak Interaction of Electron with Polarization Oscillations 649

V Old, Fundamental Theories 654

11 Old Articles that Derive Important Properties 654
11.1 Electrons in Lattice Fields by Frolich 1954 654
11.1.1 § 2. Introduction 654
11.1.2 § 2. Lattice Fields 655
11.1.3 §3. General Properties 660
11.1.4 §4. Stationary Solutions I 665
11.1.5 §5. Stationary Solutions II 673
11.1.6 §6. Discussion of Solutions and of Methods 678
11.1.7 § 7. Mobility 683
11.1.8 References 687
11.2 Effective Mass of a Polaron by Landau, Pekar 688
11.3 Mobility of Slow Electrons in a Polar Crystal by Feynman, Hellwarth, et al. 693
11.3.1 I. Introduction 693
11.3.2 II. Formulation of the Mobility Problem in Terms of Electron Coordinate Alone 695
11.3.3 III. A Method of Approximation 697
11.3.4 IV. First Corrected Term 700
11.3.5 V. Behavior of the Impedance 702
11.3.6 VI. Weak-Coupling Limit, Boltzmann Equation 708
11.3.7 VII. Suggestions for Improving Accuracy 710
11.3.8 Appendix A 712
11.3.9 Appendix B 714

12 Old Articles that Are Used in Experiments 715
12.1 Optical Properties of Small Polarons in the Infrared by Reik, 1963 715

VI Special Effects: Useful, Selected Articles 720

VII High Tc Polarons: Useful, Selected Articles 721

VIII Experiments: Main Articles 722

13 Crystallization of polarons through charge, spin ordering transitions in 1T-TaS_2 722

14 Observation of 2D liquid of Fröhlich polarons at the $SrTiO_3$ surface by Chen **737**
14.1 Results . . . 738
14.2 Discussion . . . 744
14.3 Methods . . . 745
14.4 References . . . 746

15 Application of polaron-transport theory to $Tl_2Ba_2Ca_{1-x}Gd_xCu_2O_8$, by Mihailovic **748**
15.0.1 I. Introduction . . . 749
15.0.2 II. Calculation of $\sigma(\omega)$ and Comparison with Experimental Results . . . 750
15.0.3 III. Discussion . . . 752
15.0.4 IV. Conclusion . . . 754

16 Holstein polaron in a valley-degenerate 2D semiconductor by Kang et al. **754**
16.0.1 References . . . 758
16.0.2 Additional Information . . . 760
16.0.3 Methods . . . 761

Bibliography **765**
16.1 Bibliography from Most Useful Articles . . . 765
16.2 Bibliography from Old, Fundamental Articles . . . 787
16.3 Bibliography from Articles about Special Models and Effects . . . 787
16.4 Bibliography from articles about main experiments . . . 787

Preface to Part I

Examples and Solved Problems

Famous Reviews and Important Articles

Old, Fundamental Theories

Special Effects: Useful, Selected Articles

Main experiments

Amazing facts

(I'll reveal it later)

Puzzles for motivation

(I'll reveal it later)

Part I
Polarons in a Nutshell

1 Main Formulas and Ideas from My Notes (?)

(??? I'll write all this later)

2 Main Formulas and Ideas from Alexandrov and Mott (?)

2.1 Main Formalism of Alexandrov and Mott

Definitions

$$\alpha = \frac{e^2}{\kappa}\sqrt{\frac{m}{2\omega}}. \tag{1.40}$$

$$\lambda = E_p / \frac{\hbar^2}{2ma^2}$$

$$\lambda \equiv \frac{E_p}{D} \geq 1 \tag{1.97}$$

$$\lambda = \frac{E_p}{D} \tag{8.1}$$

$$\lambda = 2E_p N(0) \tag{3.61}$$

$$\lambda \simeq r_s \ll 1 \tag{3.62}$$

$$N(0) = \frac{1}{N}\sum_{\mathbf{k}} \delta\left(\xi_{\mathbf{k}} - \mu\right) \tag{3.63}$$

$$E_p = \frac{1}{2N}\sum_{\mathbf{q}} |\gamma(\mathbf{q})|^2 \omega_{\mathbf{q}} \tag{1.98}$$

This originates from ideas in scope of large strong coupling polaron (???)

$$\gamma_{n,n'}(\mathbf{q},\mathbf{k},\nu) = -\frac{N}{\sqrt{M\omega^3_{\mathbf{q},\nu}}}\int d\mathbf{r}\left(\mathbf{e}_{\mathbf{q},\nu}\cdot\nabla v(\mathbf{r})\right)\phi^*_{\mathbf{k},n,s}(\mathbf{r})\phi_{\mathbf{k}-\mathbf{q},n',s}(\mathbf{r}) \tag{3.22}$$

$$\gamma_{n,n'}(\mathbf{q},\mathbf{k},\nu) = \gamma(\mathbf{q}) \tag{3.23}$$

$$u_i(\mathbf{q}) = \frac{1}{\sqrt{2N}}\gamma(\mathbf{q})e^{i\mathbf{q}\cdot\mathbf{m}} \qquad i := (\mathbf{m}, n, s) \tag{3.136}$$

$$V_c(\mathbf{m}) = \frac{1}{N}\sum_{\mathbf{q}} V_c(\mathbf{q})e^{i\mathbf{q}\cdot\mathbf{m}} \tag{3.137}$$

2.2 1 Large and small polaron

2.2.1 1.1, 1.2 Strong-coupling large polaron

There is a very abstract model that takes into account an influence of electron on itself by polarization of its material.

$$E(\psi) = \int d\mathbf{r} \left[\psi^*(\mathbf{r}) \left(-\frac{\nabla^2}{2m} \right) \psi(\mathbf{r}) - \mathbf{P}(\mathbf{r}) \cdot \mathbf{D}(\mathbf{r}) \right]; \qquad \mathbf{D}(\mathbf{r}) = e\nabla \int d\mathbf{r}' \frac{|\psi(\mathbf{r}')|^2}{|\mathbf{r} - \mathbf{r}'|} \tag{1.1,1.2}$$

$$\left(-\frac{\nabla^2}{2m} - e \int d\mathbf{r}' \mathbf{P}(\mathbf{r}') \cdot \nabla' \frac{1}{|\mathbf{r}' - \mathbf{r}|} \right) \psi(\mathbf{r}) = E_0 \psi(\mathbf{r}) \tag{1.3}$$

$$\mathbf{P} = (\chi_0 - \chi)\, \mathbf{D}. \tag{1.4}$$

$$\mathbf{P} = \frac{\mathbf{D}}{4\pi\kappa} \qquad \kappa^{-1} = \epsilon^{-1} - \epsilon_0^{-1} \tag{1.5}$$

Radius and ground state energy of a large strong coupling polaron

$$\left(-\frac{\nabla^2}{2m} - \frac{e^2}{\kappa} \int d\mathbf{r}' \frac{|\psi(\mathbf{r}')|^2}{|\mathbf{r}' - \mathbf{r}|} \right) \psi(\mathbf{r}) = E_0 \psi(\mathbf{r}) \tag{1.8}$$

One can solve it using a clever variational method. Approximately,

$$\psi(\mathbf{r}) = A e^{-r/r_p}, \tag{1.10}$$

$a_B = \kappa / m e^2$

$$r_p = \frac{16 a_B}{5} \tag{1.18}$$

$$E_0 = -0.146 \frac{1}{m a_B^2} \qquad \text{ground state energy} \tag{1.19}$$

1.2 Effective mass of large strong-coupling polaron

$$\omega^{-2} \frac{\partial^2 \mathbf{P}(\mathbf{r}, t)}{\partial t^2} + \mathbf{P}(\mathbf{r}, t) = \frac{\mathbf{D}(\mathbf{r}, t)}{4\pi\kappa}, \tag{1.30}$$

$$v \ll \omega a_B \tag{1.31}$$

$$\mathbf{P}(\mathbf{r}, t) \simeq \frac{1}{4\pi\kappa} \left(\mathbf{D}(\mathbf{r}, t) - \omega^{-2} \frac{\partial^2 \mathbf{D}(\mathbf{r}, t)}{\partial t^2} \right) \tag{1.32}$$

$$E = E(\psi) + 2\pi\kappa \int d\mathbf{r} \left[\mathbf{P}^2(\mathbf{r}, t) + \omega^{-2} \left(\frac{\partial \mathbf{P}(\mathbf{r}, t)}{\partial t} \right)^2 \right] \tag{1.33}$$

$$E = E_0 + U_d + \frac{m^* v^2}{2}, \tag{1.34}$$

where

$$m^* = -\frac{1}{12\pi\omega^2\kappa}\int d\mathbf{r}\mathbf{D}(\mathbf{r})\cdot\nabla^2\mathbf{D}(\mathbf{r}) = \frac{4\pi e^2}{3\omega^2\kappa}\int d\mathbf{r}|\psi(\mathbf{r})|^4 \tag{1.35,1.38}$$

$$\nabla^2\mathbf{D} = -4\pi e\nabla|\psi(\mathbf{r})|^2 \qquad \nabla\cdot\mathbf{D} = -4\pi e|\psi(\mathbf{r})|^2 \tag{1.36,1.37}$$

$$m^* \simeq 0.02\alpha^4 m \tag{1.39}$$

$$\alpha = \frac{e^2}{\kappa}\sqrt{\frac{m}{2\omega}}. \tag{1.40}$$

$$\alpha \ll \sqrt{\frac{D}{z\omega}}, \tag{1.41}$$

$D \simeq z/2ma^2$

$$E = -0.109\alpha^2\omega \tag{1.42}$$

Then somehow we are told that such model can't be in nature.

2.2.2 1.3 Fröhlich large polaron

One can construct a model in a very clever way by using a second quantization.

$$V(\mathbf{r}) = \sum_{\mathbf{l}} v\left(\mathbf{r}-\mathbf{R}_{\mathbf{l}}\right), \tag{1.44}$$

$$v\left(\mathbf{r}-\mathbf{R}_{\mathbf{l}}\right) \simeq v(\mathbf{r}-\mathbf{l}) - \mathbf{u}_{\mathbf{l}}\cdot\nabla v(\mathbf{r}-\mathbf{l}).$$

$$\mathbf{u}_{\mathbf{l}} = \sum_{\mathbf{q}} \frac{\mathbf{e}_{\mathbf{q}}}{\sqrt{2NM\omega_{\mathbf{q}}}} d_{\mathbf{q}} e^{i\mathbf{q}\cdot\mathbf{l}} + \text{ h.c.} \tag{1.46}$$

$$H_{e-ph} = \frac{1}{\sqrt{2N}}\sum_{\mathbf{q}}\gamma(\mathbf{q})\omega_{\mathbf{q}} d_{\mathbf{q}} e^{i\mathbf{q}\cdot\mathbf{r}} + h.c. \qquad \gamma(\mathbf{q}) = -i\frac{N\mathbf{e}_{\mathbf{q}}\cdot\mathbf{q}}{\sqrt{M\omega_{\mathbf{q}}^3}} v_{\mathbf{q}} \qquad v(\mathbf{r}) = \sum_{\mathbf{k}} v_{\mathbf{k}} e^{i\mathbf{k}\cdot\mathbf{r}} \tag{1.48, 1.49}$$

For
$v_{\mathrm{q}} \simeq 4\pi/\Omega\kappa q^2$
$(\mathbf{e}_{\mathbf{q}} \| \mathbf{q})$

$$\frac{\gamma(\mathbf{q})\omega}{2N} \equiv V_{\mathbf{q}} = -\frac{i\omega}{q}\left(\frac{4\pi\alpha}{\Omega\sqrt{2m\omega}}\right)^{1/2} \tag{1.50}$$

$\omega = \sqrt{4\pi Ne^2/M\Omega\kappa}$

$$H = -\frac{\nabla^2}{2m} + \sum_{\mathbf{q}}\left(V_{\mathbf{q}} d_{\mathbf{q}} e^{i\mathbf{q}\cdot\mathbf{r}} + h.c.\right) + \sum_{\mathbf{q}}\omega_{\mathbf{q}}\left(d_{\mathbf{q}}^{\dagger} d_{\mathbf{q}} + 1/2\right) \tag{1.51}$$

This is the model of an electron, that is coupled also to phonon, so totally we have "combined dynamics of electron and phonon". Let's find an energy of quantum of this dynamics.

$$|\mathbf{k}-\mathbf{q}, 1_{\mathbf{q}}\rangle = \frac{1}{\sqrt{\Omega}} e^{i(\mathbf{k}-\mathbf{q})\cdot\mathbf{r}} |1_{\mathbf{q}}\rangle \tag{1.53}$$

$$\langle \mathbf{k}-\mathbf{q}, 1_{\mathbf{q}}| \, H_{e-ph} |\mathbf{k}, 0\rangle = V_{\mathbf{q}}^* \tag{1.54}$$

$$\tilde{E}_{\mathbf{k}} = \frac{k^2}{2m} - \sum_{\mathbf{q}} \frac{|V_{\mathbf{q}}|^2}{(\mathbf{k}-\mathbf{q})^2/2m + \omega - k^2/2m} \tag{1.55}$$

for slow electron,

$$\tilde{E}_{\mathrm{k}} = \frac{k^2}{2m} - \frac{\alpha\omega q_p}{k} \arcsin\left(\frac{k}{q_p}\right) \tag{1.59}$$

and for very slow,

$$\tilde{E}_{\mathbf{k}} \simeq -\alpha\omega + \frac{k^2}{2m^*} \tag{1.60}$$

$$m^* = \frac{m}{1-\alpha/6} \simeq m\left(1+\frac{\alpha}{6}\right) \tag{1.61}$$

2.2.3 1.4 Intermediate-coupling large polaron $1 < \alpha < 10$

$$\tilde{E}_{\mathbf{K}} = -\alpha\omega + \frac{K^2}{2m^*} \tag{1.95}$$

$$m^* = m(1+\alpha/6) \tag{1.96}$$

To get this, we do two transformations. The first one:

$$|\tilde{N}\rangle = \exp(S)|N\rangle \tag{1.72}$$

$$\tilde{H} = \exp(S) H \exp(-S); \qquad S_{LLP} = i\sum_{\mathbf{q}} (\mathbf{q}\cdot\mathbf{r}) d_{\mathbf{q}}^\dagger d_{\mathbf{q}} \tag{1.74,1.75}$$

$$\tilde{H} = \frac{1}{2m}\left(-i\nabla - \sum_{\mathbf{q}} \mathbf{q} d_{\mathbf{q}}^\dagger d_{\mathbf{q}}\right)^2 + \sum_{\mathbf{q}} \left(V_{\mathbf{q}} d_{\mathbf{q}} + h.c.\right) + \omega \sum_{\mathbf{q}} \left(d_{\mathbf{q}}^\dagger d_{\mathbf{q}} + 1/2\right) \tag{1.78}$$

$$|\tilde{N}\rangle = \frac{1}{\sqrt{\Omega}} e^{i\mathbf{K}\cdot\mathbf{r}} \left|\tilde{N}_{ph}\right\rangle \tag{1.79}$$

$$\tilde{H} = \frac{1}{2m}\left(\mathbf{K} - \sum_{\mathbf{q}} \mathbf{q} d_{\mathbf{q}}^\dagger d_{\mathbf{q}}\right)^2 + \sum_{\mathbf{q}} \left(V_{\mathbf{q}} d_{\mathbf{q}} + h.c.\right) + \omega \sum_{\mathbf{q}} \left(d_{\mathbf{q}}^\dagger d_{\mathbf{q}} + 1/2\right) \tag{1.80}$$

And now, we don't like something, so we do the second transformation:

$$S = \sum_{\mathbf{q}} f(\mathbf{q}) d_{\mathbf{q}} - h.c. \qquad f(\mathbf{q}) = \frac{V_{\mathbf{q}}}{\omega + q^2/2m - (1-\eta)\mathbf{q}\cdot\mathbf{K}/m} \tag{1.81, 1.89}$$

$$\tilde{E}_{\mathbf{K}} = \frac{K^2}{2m} - \sum_{\mathbf{q}} \left(V_{\mathbf{q}} f^*(\mathbf{q}) + h.c.\right) + \sum_{\mathbf{q}} |f(\mathbf{q})|^2 \left(\omega - \frac{\mathbf{K}\cdot\mathbf{q}}{m} + \frac{q^2}{2m}\right) + \frac{1}{2m}\sum_{\mathbf{q},\mathbf{q}'} \left|f(\mathbf{q}) f(\mathbf{q}')\right|^2 \mathbf{q}\cdot\mathbf{q}' \tag{1.86}$$

$$\tilde{E}_{\mathbf{K}} = \frac{(1-\eta^2)\,K^2}{2m} - \sum_{\mathbf{q}} \frac{|V_{\mathbf{q}}|^2}{\omega + q^2/2m - (1-\eta)\mathbf{q}\cdot\mathbf{K}/m} \tag{1.90}$$

$$\tilde{E}_{\mathbf{K}} = \frac{(1-\eta^2)\,K^2}{2m} - \frac{\alpha\omega q_p}{K(1-\eta)} \arcsin\left(\frac{K(1-\eta)}{q_p}\right) \tag{1.92}$$

$$\eta(1-\eta)^2 = \frac{\alpha q_p^3}{2K^3}\left(\frac{(1-\eta)K}{\sqrt{q_p^2-(1-\eta)^2K^2}} - \arcsin\frac{(1-\eta)K}{q_p}\right) \quad \overset{K\ll q_p}{\rightarrow} \quad \eta = \frac{\alpha/6}{1+\alpha/6} \tag{1.93, 1.94}$$

$$\lambda \equiv \frac{E_p}{D} \geq 1 \tag{1.97}$$

$$E_p = \frac{1}{2N}\sum_{\mathbf{q}} |\gamma(\mathbf{q})|^2 \omega_{\mathbf{q}} \tag{1.98}$$

$$E_p \simeq \frac{q_D e^2}{\pi\kappa} \tag{1.99}$$

$q_d = (6\pi^2/\Omega)^{1/3}$

2.2.4 1.5,1.6,1.7 Small polaron: two-site Holstein model, adiabatic, fast solutions

two-site Holstein model

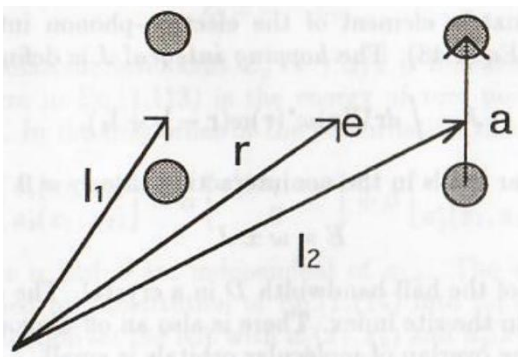

$$H_{ph} = -\frac{1}{2M}\sum_{i=1,2}\left(\frac{\partial^2}{\partial x_i^2} + \frac{M\omega^2 x_i^2}{2}\right) \tag{1.100}$$

$$H_e = -\frac{\nabla^2}{2m} + V(\mathbf{r}-\mathbf{l}_1) + V(\mathbf{r}-\mathbf{l}_2)\,, \qquad V(\mathbf{r}-\mathbf{l}) = v(\mathbf{r}-\mathbf{l}-\mathbf{a}/2) - v(\mathbf{r}-\mathbf{l}+\mathbf{a}/2) \tag{1.101,1.102}$$

$$H_{e-ph} = -\sum_{i=1,2}\frac{x_i}{2}\frac{\partial}{\partial x}\left[v(\mathbf{r}-\mathbf{l}_i-\mathbf{a}/2) + v(\mathbf{r}-\mathbf{l}_i+\mathbf{a}/2)\right]. \tag{1.103}$$

$$|\mathbf{r}, x_1, x_2\rangle = \sum_{i=1,2} a_i\left(x_1, x_2\right) w\left(\mathbf{r}-\mathbf{l}_i\right); \qquad \left(-\frac{\nabla^2}{2m}+V(\mathbf{r})\right) w(\mathbf{r})=0 \tag{1.104,1.105}$$

$$\left[E+\frac{1}{2M}\left(\frac{\partial^2}{\partial x_1^2}+\frac{\partial^2}{\partial x_2^2}\right)-\frac{M\omega^2\left(x_1^2+x_2^2\right)}{2}-\gamma\omega\sqrt{M\omega}x_1\right] a_1\left(x_1, x_2\right)=-Ja_2\left(x_1, x_2\right), \tag{1.106}$$

$$\left[E+\frac{1}{2M}\left(\frac{\partial^2}{\partial x_1^2}+\frac{\partial^2}{\partial x_2^2}\right)-\frac{M\omega^2\left(x_1^2+x_2^2\right)}{2}-\gamma\omega\sqrt{M\omega}x_2\right] a_2\left(x_1, x_2\right)=-Ja_1\left(x_1, x_2\right), \tag{1.107}$$

where

$$\gamma=-\frac{1}{2\omega\sqrt{M\omega}}\int d\mathbf{r}|w(\mathbf{r})|^2\frac{\partial}{\partial x}[v(\mathbf{r}-\mathbf{a}/2)+v(\mathbf{r}+\mathbf{a}/2)] \tag{1.108}$$

$$J=\int d\mathbf{r}V(\mathbf{r})w^*(\mathbf{r})w\left(\mathbf{r}-\mathrm{l}_2+\mathrm{l}_1\right) \tag{1.109}$$

adiabatic parameter: ω/J

$2J=D$, bandwidth

This models describes only small polarons.

1.6 Nonadiabatic small polaron

We somehow solve this model.

1.7 Adiabatic small polaron

$$\Delta E \simeq \sqrt{\frac{4E_p\omega}{\pi}}e^{-\tilde{g}^2} \tag{1.135}$$

$$\tilde{g}^2=g^2\left[1-\frac{1}{4\lambda^2}\ln(4\lambda)-\frac{1}{8\lambda^2}\right] \tag{1.136}$$

This is because some special ansatz gives us an equation for the wave function in a form of 1D potential and quasiclassicak.

2.2.5 1.8 From large to small polaron: numerical calculations

2.3 3 Electrons and phonons

2.3.1 3.1 Electrons, phonons and the Fröhlich interaction

$$H=-\sum_i\frac{\nabla_i^2}{2m_e}+\frac{e^2}{2}\sum_{i\neq i'}\frac{1}{|\mathbf{r}_i-\mathbf{r}_{i'}|}-Ze^2\sum_{ij}\frac{1}{|\mathbf{r}_i-\mathbf{R}_j|}+\frac{Z^2e^2}{2}\sum_{j\neq j'}\frac{1}{|\mathbf{R}_j-\mathbf{R}_{j'}|}-\sum_j\frac{\nabla_j^2}{2M} \tag{3.1}$$

$$\frac{\langle|\mathrm{u}|\rangle}{a}\simeq\left(m_e/Mr_s\right)^{1/4}\ll 1. \tag{3.2}$$

is equivalent to

$$H = H_0 + H_{e-ph} + H_{e-e}, \tag{3.19}$$

$$H_0 = \sum_{\mathbf{k},n,s} \xi_{\mathbf{k},n,s} c^\dagger_{\mathbf{k},n,s} c_{\mathbf{k},n,s} + \sum_{\mathbf{q},\nu} \omega_{\mathbf{q},\nu} \left(d^\dagger_{\mathbf{q},\nu} d_{\mathbf{q},\nu} + 1/2 \right) \tag{3.20}$$

$$H_{e-ph} = \frac{1}{\sqrt{2N}} \sum_{\mathbf{k},\mathbf{q},n,n',\nu,s} \gamma_{n,n'}(\mathbf{q},\mathbf{k},\nu) \omega_{\mathbf{q},\nu} c^\dagger_{\mathbf{k},n,s} c_{\mathbf{k}-\mathbf{q},n',s} d_{\mathbf{q},\nu} + h.c. \tag{3.21}$$

$$H_{e-e} = \frac{1}{2} \sum_{\mathbf{q}} V_c(\mathbf{q}) \rho^\dagger_{\mathbf{q}} \rho_{\mathbf{q}} \qquad \rho^\dagger_{\mathbf{q}} = \sum_{\mathbf{k},s} c^\dagger_{\mathbf{k},s} c_{\mathbf{k}+\mathbf{q},s} \tag{3.24, 3.25}$$

$$\gamma_{n,n'}(\mathbf{q},\mathbf{k},\nu) = -\frac{N}{\sqrt{M\omega^3_{\mathbf{q},\nu}}} \int d\mathbf{r} \left(\mathbf{e}_{\mathbf{q},\nu} \cdot \nabla v(\mathbf{r}) \right) \phi^*_{\mathbf{k},n,s}(\mathbf{r}) \phi_{\mathbf{k}-\mathbf{q},n',s}(\mathbf{r}) \tag{3.22}$$

$$\gamma_{n,n'}(\mathbf{q},\mathbf{k},\nu) = \gamma(\mathbf{q}) \tag{3.23}$$

This can maybe be derived by a very unclear transformations appear:

$$\mathcal{V}(\mathbf{r}) = -Ze^2 \sum_j \frac{1}{|\mathbf{r} - \mathbf{R}_j|} + e^2 \int d\mathbf{r}' \frac{n(\mathbf{r}')}{|\mathbf{r} - \mathbf{r}'|} + \mu_{xc}(\mathbf{r}) \tag{3.3}$$

$$\mu_{xc}(\mathbf{r}) = -\beta [n(\mathbf{r})]^{1/3} \tag{3.4}$$

$$H = H_e + H_{ph} + H_{e-ph} + H_{e-e}, \tag{3.5}$$

we get very messy expressions:

$$H_e = \int d\mathbf{r} \psi^\dagger(\mathbf{r}) \left(\frac{\nabla^2}{2m_e} + V(\mathbf{r}) \right) \psi(\mathbf{r}) \tag{3.6}$$

$$H_{ph} = \sum_{\mathbf{l}} \left(-\frac{\nabla^2_{\mathbf{u}}}{2M} + \mathbf{u}_{\mathbf{l}} \cdot \frac{\partial}{\partial \mathbf{l}} \int d\mathbf{r} n^0(\mathbf{r}) V(\mathbf{r}) \right) + \frac{1}{2} \sum_{\mathbf{l},\mathbf{l}',\alpha,\beta} u^\alpha_{\mathbf{l}} u^\beta_{\mathbf{l}'} D_{\alpha,\beta}(\mathbf{l} - \mathbf{l}') \tag{3.7}$$

and this one has a very messy function

$$D_{\alpha,\beta}(\mathbf{l} - \mathbf{l}') = \frac{\partial^2}{\partial l^\alpha \partial l'^\beta} \left(\frac{Z^2 e^2}{2} \sum_{\mathbf{l}'' \neq \mathbf{l}'''} \frac{1}{|\mathbf{l}'' - \mathbf{l}'''|} + \int d\mathbf{r} n^0(\mathbf{r}) V(\mathbf{r}) \right) \tag{3.8}$$

but don't worry, it will be simplified and forgotten soon.

$$\begin{aligned} H_{e-ph} = & \sum_{\mathbf{1}} \mathbf{u}_{\mathbf{l}} \cdot \frac{\partial}{\partial \mathbf{l}} \int d\mathbf{r} \left(\psi^\dagger(\mathbf{r}) \psi^\dagger(\mathbf{r}) - n^0(\mathbf{r}) \right) V(\mathbf{r}) \\ & + \frac{1}{2} \sum_{\mathbf{1},\mathbf{l}',\alpha,\beta} u^\alpha_{\mathbf{1}} u^\beta_{\mathbf{1}'} \frac{\partial^2}{\partial l^\alpha \partial l'^\beta} \int d\mathbf{r} \left(\psi^\dagger(\mathbf{r}) \psi(\mathbf{r}) - n^0(\mathbf{r}) \right) V(\mathbf{r}) \end{aligned} \tag{3.9}$$

$$\begin{aligned} H_{e-e} = & \int d\mathbf{r} d\mathbf{r}' \left(\frac{e^2}{2|\mathbf{r} - \mathbf{r}'|} \left[\psi^\dagger(\mathbf{r}') \psi(\mathbf{r}') - n^0(\mathbf{r}') \right] - \mu_{xc}(\mathbf{r}) \delta(\mathbf{r} - \mathbf{r}') \right) \psi^\dagger(\mathbf{r}) \psi(\mathbf{r}) \\ & + \frac{Z^2 e^2}{2} \sum_{\mathbf{l} \neq \mathbf{l}'} \frac{1}{|\mathbf{l} - \mathbf{l}'|} - \frac{e^2}{2} \int d\mathbf{r} d\mathbf{r}' \frac{n^0(\mathbf{r}')}{|\mathbf{r} - \mathbf{r}'|} \psi^\dagger(\mathbf{r}) \psi(\mathbf{r}) \end{aligned} \tag{3.10}$$

But somehow quantization of phonons help us to make them better. We quantize:

$$\mathbf{u}_{\mathbf{l}} = \sum_{\mathbf{q}} \frac{\mathbf{e}_{\mathbf{q},\nu}}{\sqrt{2NM\omega_{\mathbf{q},\nu}}} d_{\mathbf{q},\nu} \exp(i\mathbf{q}\cdot\mathbf{l}) + h.c., \tag{3.11}$$

$$\frac{\partial}{\partial \mathbf{u}_{\mathbf{l}}} = \sum_{\mathbf{q}} \mathbf{e}_{\mathbf{q},\nu} \sqrt{\frac{M\omega_{\mathbf{q},\nu}}{2N}} d_{\mathbf{q},\nu} \exp(i\mathbf{q}\cdot\mathbf{l}) - h.c., \tag{3.12}$$

$$H_{ph} = \sum_{\mathbf{q},\nu} \omega_{\mathbf{q},\nu} \left(d^{\dagger}_{\mathbf{q},\nu} d_{\mathbf{q},\nu} + 1/2\right) \tag{3.13}$$

$$M\omega^2_{\mathbf{q},\nu} e^{\alpha}_{\mathbf{q},\nu} = \sum_{\beta} D^{\alpha,\beta}_{\mathbf{q}} e^{\beta}_{\mathbf{q},\nu} \tag{3.14}$$

$$\sum_{\mathbf{q}} e^{*\alpha}_{\mathbf{q},\nu} e^{\beta}_{\mathbf{q},\nu} = N\delta_{\alpha,\beta} \tag{3.15}$$

$$D^{\alpha,\beta}_{\mathbf{q}} = \sum_{\mathbf{m}} \exp(i\mathbf{q}\cdot\mathbf{m}) D_{\alpha,\beta}(\mathbf{m}) \tag{3.16}$$

$$\psi(\mathbf{r}) = \sum_{\mathbf{k},n,s} \phi_{\mathbf{k},n,s}(\mathbf{r}) c_{\mathbf{k},n,s} \tag{3.17}$$

$$\left(-\frac{\nabla^2}{2m_e} + V(\mathbf{r})\right) \phi_{\mathbf{k},n,s}(\mathbf{r}) = E_{\mathbf{k},n,s} \phi_{\mathbf{k},n,s}(\mathbf{r}) \tag{3.18}$$

And from this somehow we can get the second-quantized electron-phonon model.

2.3.2 3.2 Bare phonons and sound in a metal

2.3.3 3.3 Effect of the Fröhlich interaction on electrons in a metal

2.3.4 3.4 Broken gauge symmetry and the BCS ground state

2.3.5 3.5 Bloch states in semiconductors: Effective mass approximation

2.3.6 3.6 Tight-binding approximation

If we somehow transform and simplify the typical electron-phonon model, we can obtain the tight-binding model:

$$H = \sum_{i,j} (T(\mathbf{m}-\mathbf{n})\delta_{s,s'} - \mu\delta_{i,j}) c^{\dagger}_i c_j + \sum_{\mathbf{q},i} \omega_{\mathbf{q}} \hat{n}_i \left(u_i(\mathbf{q}) d_{\mathbf{q}} + h.c.\right) \qquad i := (\mathbf{m}, n, s)$$
$$+ \frac{1}{2} \sum_{i,j} V_c(\mathbf{m}-\mathbf{n}) \hat{n}_i \hat{n}_j + \sum_{\mathbf{q}} \omega_{\mathbf{q}} \left(d^{\dagger}_{\mathbf{q}} d_{\mathbf{q}} + 1/2\right) \tag{3.138}$$

$$u_i(\mathbf{q}) = \frac{1}{\sqrt{2N}} \gamma(\mathbf{q}) e^{i\mathbf{q}\cdot\mathbf{m}} \tag{3.136}$$

$$V_c(\mathbf{m}) = \frac{1}{N} \sum_{\mathbf{q}} V_c(\mathbf{q}) e^{i\mathbf{q}\cdot\mathbf{m}} \tag{3.137}$$

$\hat{n}_i = c_i^\dagger c_i$

$$c_i = \frac{1}{\sqrt{N}} \sum_{\mathbf{k}} e^{i\mathbf{k}\cdot\mathbf{m}} c_{\mathbf{k},s}, \tag{3.128}$$

$$w_i(\mathbf{r}) = \frac{1}{\sqrt{N}} \sum_{\mathbf{k}} e^{-i\mathbf{k}\cdot\mathbf{m}} \phi_{\mathbf{k},n,s}(\mathbf{r}). \tag{3.129}$$

$$T(\mathbf{m}) = \frac{1}{N} \sum_{\mathbf{k}} E_{\mathbf{k},n} e^{i\mathbf{k}\cdot\mathbf{m}} \tag{3.131}$$

$$E_{\mathbf{k}} = \sum_{|\mathbf{m}|=a} T(\mathbf{m}) e^{-i\mathbf{k}\cdot\mathbf{m}} = 2T(a)\left[\cos(k_x a) + \cos(k_y a) + \cos(k_z a)\right] \qquad m = \frac{1}{2a^2|T(a)|} \tag{3.132, 3.133}$$

2.4 4 The multi-polaron problem

2.4.1 4.1 Small-polaron instability within the Migdal approach

In Migdal's approach, there are problems, if $\lambda > 1$, since one contribution to self-energy blows up. This is because we can include change of self-energy to change of chemical potential and test stability by it. So, this theory predicts that system will fill istelf with a lot of particles.

In the Holstein model, there are also the same problems.

So, I don't know what to conclude, maybe another approach is needed for this special region, but we just start to analyze the extreme case $\lambda \to \infty$. Somehow what is below is the correct approach.

2.4.2 4.2 Exact solution of the multi-polaron problem for $\lambda \to \infty$

$$H = \sum_{\mathbf{q},i} \omega_{\mathbf{q}} \hat{n}_i \left(u_i(\mathbf{q}) d_{\mathbf{q}} + h.c.\right) + \frac{1}{2} \sum_{i,j} V_c(\mathbf{m}-\mathbf{n}) \hat{n}_i \hat{n}_j + \sum_{\mathbf{q}} \omega_{\mathbf{q}} \left(d_{\mathbf{q}}^\dagger d_{\mathbf{q}} + 1/2\right) \tag{3.138}$$

$i := (\mathbf{m}, n, s); \qquad j := (\mathbf{n}, n', s')$

Somehow if we transform as

$$\tilde{H} = e^S H e^{-S}; \qquad S = \sum_{\mathbf{q},i} \hat{n}_i \left(u_i(\mathbf{q}) d_{\mathbf{q}} - \text{ h.c. }\right) \tag{4.9}$$

$$\tilde{c}_i = c_i \exp\left(\sum_{\mathbf{q}} u_i(\mathbf{q}) d_{\mathbf{q}} - h.c.\right) \tag{4.10}$$

$$\tilde{d}_{\mathbf{q}} = d_{\mathbf{q}} - \sum_i \hat{n}_i u_i^*(\mathbf{q}) \tag{4.11}$$

we get

$$\tilde{H} = \sum_{i,j} \left(\hat{\sigma}_{ij} - \mu\delta_{i,j}\right) c_i^\dagger c_j - E_p \sum_i \hat{n}_i + \frac{1}{2} \sum_{i,j} v_{ij} c_i^\dagger c_j^\dagger c_j c_i + \sum_{\mathbf{q}} \omega_{\mathbf{q}} \left(d_{\mathbf{q}}^\dagger d_{\mathbf{q}} + 1/2\right) \tag{4.12}$$

$i := (\mathbf{m}, n, s); \qquad j := (\mathbf{n}, n', s')$

$$\hat{\sigma}_{ij} = T(\mathbf{m}-\mathbf{n})\delta_{s.s'} \exp\left(\sum_{\mathbf{q}} \left[u_i(\mathbf{q}) - u_j(\mathbf{q})\right] d_{\mathbf{q}} - h.c.\right) \tag{4.13}$$

$$v_{ij} = V_c(\mathbf{m}-\mathbf{n}) - 2\sum_{\mathbf{q}} \omega_{\mathbf{q}} \left(u_i(\mathbf{q})u_j^*(\mathbf{q})\right) \tag{4.14}$$

and this encodes the energy levels for the multi-polaron problem in this exotic case $\lambda \to \infty$

$$E = (T(0) - E_p - \mu)\sum_i n_i + \frac{1}{2}\sum_{i,j} v_{ij} n_i n_j + \sum_{\mathbf{q}} \omega_{\mathbf{q}} \left(n_{\mathbf{q}} + 1/2\right) \tag{4.15}$$

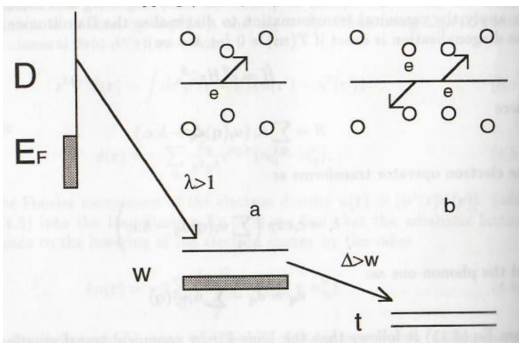

Fig.4.1. Polaron collapse of the electron band (a); bipolaron band (b).

2.4.3 4.3 Polaron band and self-energy

Some parameters tell us that the band width is suppressed like

$$w = De^{-g^2} \tag{4.27}$$

$$g^2_{T=0}(\mathbf{m}-\mathbf{n}) = \frac{1}{2}\sum_{\mathbf{q}} \left(|u_i(\mathbf{q})|^2 + |u_j(\mathbf{q})|^2 - 2u_i^*(\mathbf{q})u_j(\mathbf{q})\right) \tag{4.20}$$

$$g^2_{T\neq 0}(\mathbf{m}) = \frac{1}{2N}\sum_{\mathbf{q}} |\gamma(\mathbf{q})|^2 \coth\left(\frac{\omega_{\mathbf{q}}}{2T}\right)\left[1 - \cos(\mathbf{q}\cdot\mathbf{m})\right] \tag{4.21}$$

This is because of some argument that was also valid for Holstein model.

Also

$$\Sigma \simeq -(1-n)\sum_{\mathbf{a}} \frac{T^2(\mathbf{a})}{2\omega_0 g^2(\mathbf{a})} \tag{4.48}$$

$$\Sigma \simeq -\frac{(1-n)E_p}{2z\lambda^2} \tag{4.49}$$

It is obtaind by some magic struggles with GF method. From the def. of polaron GF, we get formula

$$\Sigma_{ij}(\omega_n) = \sum_{i',j'} \Gamma^{i'j'}_{ii'}(\omega_n)\, \hat{\tilde{g}}^{-1}_{j'j}(\omega_n) \tag{4.32}$$

$$\Gamma^{jj'}_{ii'}(\tau) = -\langle\langle T_\tau \left[\hat{\sigma}_{ii'}(\tau) - \sigma(\mathrm{m}-\mathrm{m}')\right] c_j(\tau) c^\dagger_{j'}\rangle\rangle. \tag{4.33}$$

We will evaluate self energy using special $\tilde{\Phi}$ tensor, which is evaluated by Φ tensor:

$$\Sigma_{ij}\left(\omega_n\right) = T\sum_{\omega_{n'}}\sum_{i',i'',j'}\tilde{\Phi}_{ii'}^{i''j'}\left(\omega_n-\omega_{n'}\right)\tilde{g}_{i'i''}^{(0)}\left(\omega_{n'}\right)\frac{\left(i\omega_n+\mu\right)\delta_{j',j}-\sigma\left(\mathbf{n}-\mathbf{n}'\right)}{i\omega_n+\mu} \tag{4.36}$$

$$\tilde{\Phi}_{ii'}^{jj'}\left(\Omega_n\right) = \Phi_{ii'}^{jj'}\left(\Omega_n\right)-\frac{1}{T}\sigma\left(\mathbf{m}-\mathbf{m}'\right)\sigma\left(\mathbf{n}-\mathbf{n}'\right)\delta_{\Omega_n,0} \qquad \Phi_{ii'}^{jj'}(\tau) = \langle\langle T_\tau\hat{\sigma}_{ii'}(\tau)\hat{\sigma}_{jj'}\rangle\rangle \tag{4.37, 4.38}$$

Somehow we can obatain:

$$\Phi_{ii'}^{jj'}(\tau) = \sigma(\mathbf{a})\sigma(\mathbf{b})\exp\left(\frac{1}{N}\sum_{\mathbf{q}}\gamma^2(\mathbf{q})f_{\mathbf{q}}\frac{\cosh\left[\omega_{\mathbf{q}}\left(\frac{1}{2T}-|\tau|\right)\right]}{\sinh\frac{\omega_{\mathbf{q}}}{2T}}\right) \tag{4.39}$$

$2f_{\mathbf{q}} = \cos(\mathbf{q}\cdot[\mathbf{c}-\mathbf{a}])+\cos(\mathbf{q}\cdot[\mathbf{c}+\mathbf{b}])-\cos(\mathbf{q}\cdot\mathbf{c})-\cos(\mathbf{q}\cdot[\mathbf{c}-\mathbf{a}+\mathbf{b}])$ with $\mathbf{a}=\mathbf{m}-\mathbf{m}'$, $\mathbf{b}=\mathbf{n}-\mathbf{n}'$ and $\mathbf{c}=\mathbf{n}'-\mathbf{m}'$.

And some genius simplifications and substitutions give us the result.

2.4.4 4.4 Temperature collapse of the polaron band

2.4.5 4.5 Phonons in a strong-coupling system

If coupling is strong, there are much more contributions to self-energy, and they give us the initial formula:

$$\Sigma_{ph}\left(\mathbf{q},\Omega_n\right) = -\frac{n(2-n)|\gamma(\mathbf{q})|^2}{2}\sum_{\mathbf{a}}\left(\Phi_{\mathbf{a}}\left(\Omega_n\right)-\Phi_{\mathbf{a}}(0)\right)\left[1-\cos(\mathbf{q}\cdot\mathbf{a})\right] \tag{4.61}$$

after some very complicated transformations, we get

$$i\Omega_n \to \tilde{\omega}+i0^+ \tag{4.63}$$

$$\tilde{\omega}_{\mathbf{q}} \simeq \omega-\Delta(\mathbf{q}) \qquad \Delta(\mathbf{q}) = \frac{n(2-n)|\gamma(\mathbf{q})|^2}{2\omega}\sum_{\mathbf{a}}\frac{T^2(\mathbf{a})[1-\cos(\mathbf{q}\cdot\mathbf{a})]}{g^6(\mathbf{a})} \tag{4.64, 4.65}$$

It is unclear, which exactly this contribution is, but maybe it is very small.

2.4.6 4.6 Screening and polaronic plasmon

Now, suppose light shines on the material. Somehow in the whole formalism, there is an influence of the material to the dielectric constant through v:

$$\epsilon(\mathbf{q},\Omega) = 1-2v(\mathbf{q})\sum_{\mathbf{k}}\frac{n_{\mathbf{k}+\mathbf{q}}-n_{\mathbf{k}}}{\Omega-\epsilon_{\mathbf{k}}+\epsilon_{\mathbf{k}+\mathbf{q}}} \tag{4.66}$$

and somewhere from the polaron theory, we know formulas for v. Thus

$$\epsilon(\mathbf{q},\omega) = 1-\frac{\omega_p^2(\mathbf{q})}{\omega^2} \qquad \omega_p^2(\mathbf{q}) = 2v(\mathbf{q})\sum_{\mathbf{k}}n_{\mathbf{k}}\left(\epsilon_{\mathbf{k}+\mathbf{q}}-\epsilon_{\mathbf{k}}\right) \tag{4.74,4.73}$$

Examples of evaluation of this formula are not known.

2.4.7 4.7 Many-body polaronic effect in the phonon spectrum

All phonon effects can be obtained from phonon GF, so we will just evaluate it and pretand that it is obvious how to get all consequences from it. The resuls is:

$$D(\mathbf{q},\Omega) = \sum_{i=1}^{3} \frac{P_i(\mathbf{q})}{\Omega - \Omega_i(\mathbf{q})} \tag{4.92}$$

$$\frac{P_2}{P_1} = \frac{\left(\Omega_2^2 - \omega_p^2\right)\left(\Omega_3 - \Omega_1\right)}{\left(\Omega_1^2 - \omega_p^2\right)\left(\Omega_3 - \Omega_2\right)} \tag{4.93}$$

$$\Omega_1 = \frac{\tilde{\omega}}{3} + \frac{2}{3}\cos\left(\frac{\alpha}{3}\right)\left[\tilde{\omega}^2 + \omega_p^2\right]^{1/2} \tag{4.89}$$

$$\Omega_{2,3} = \frac{\tilde{\omega}}{3} - \frac{2}{3}\cos\left(\frac{\alpha \pm \pi}{3}\right)\left[\tilde{\omega}^2 + \omega_p^2\right]^{1/2} \tag{4.90}$$

$\tilde{\omega} = \omega - \Delta, \qquad \cos\alpha = \left[\tilde{\omega}^3 - 9\tilde{\omega}\omega_p^2 + 27\beta\omega_p^4/2\omega\right] / \left[\tilde{\omega}^2 + 3\omega_p^2\right]^{3/2}.$

It was deriven by looking at self-energy as a function of polarisation tensor and using the obtained complicated expression for the self-energy. The new step here is to simplify the complicated polarisation tensor, and then from analytical continuation, the dispersion relation pops out. Then we pretand that it is ok to just write the final formula, because maybe it is obvious how would it look like, if we know the characteristic frequences of phonons.

2.4.8 4.8 Polaron thermodynamics

Heat capacity

It is unclear, which model is used, but if $N_p = 1/2w$, then from it with help of maybe usulal statistical physics, we get

$$C_{p|T<0.4w} = \frac{\pi^2 T}{3w} \tag{4.95}$$

$$C_{p|T>w} = \frac{w^2 n(2-n)}{6T^2}. \tag{4.96}$$

Magnetic susceptibility

After using some ideas of chemical potential, we get

$$\chi_{s|T\gg w} \simeq \frac{\mu_B^2 n(2-n)}{2T}, \tag{4.100}$$

$$\chi_{s|T<w} = \frac{\mu_B^2}{w} \tag{4.101}$$

2.4.9 4.9 Polaron kinetics: hopping transport

2.4.10 4.10 MIR conductivity of polarons

2.4.11 4.11 Polaron kinetics: band tunneling transport

2.4.12 4.12 Electron Green's function and ARPES of polaronic systems

2.5 Articles That Are Used in Alexandrov and Mott's Book

2.5.1 The Motion of Slow Electrons in a Polar Crystal by Lee, Low, Pines 1953

Part II
My Theory of Polarons

3 Main Models of Polarons

3.1 Physics Behind Polarons

3.1.1 Concept of Polarization for Polarons

(??? see note on ED, I'll write what is it??? how exactly it is introduced???)

3.1.2 When Electron-Phonon Coupling is Large

(??? this determines the model that can be used. but how to know, what is it from other experiments or from other theory?)

3.1.3 Requirements for Semiconductor to Have Polarons

(??? why exactly semiconductors are assumed???)

3.1.4 Why in TaS_2 there are polarons (form experiments)?

Yes, we see densities of electrons, but why they are polarons????

3.2 General Conceptual Questions about Single Polarons

3.2.1 How to know, which type of polaron is present?

(????????????? I have no idea, I haven't seen a discussion of it here)

3.3 Bipolarons

3.3.1 What Is Going On With Theories of Bipolarons?

(??? Virtor said that they are dead. So I'll write something about them)

4 Numerical Simulation of Polarons

(there are references in Alexandrov, Mott, but it is a complicated topic...)

5 Experimental Consequences of Polarons

(see Alexandrov, Mott for now)

Part III
Examples and Solved Problems

Part IV
Well-known and Important Theories

6 Polarons and Bipolarons by Alexandrov, Mott

(In whole this book, one needs to read original works to figure out what is meant.)

6.1 Introduction

6.1.1 Introduction

The concept of polarons was first introduced by Landau (1933) (I haven't read yet his article about it, I'll look later).

If an electron is placed into the conduction band (meaning that it propagates with some not little energy) of an ionic crystal (meaning that there is one absent electron in each atom) the force on another electron at a distance r from it would be $e^2/\epsilon_0 r^2$. But if the ions did not move the force would be $e^2/\epsilon r^2$, where ϵ_0 and ϵ are the static and high-frequency ("high-frequency" - irrelevant word, it is meant that media is deformed because of filed of electron, thus there is an ε) dielectric constants, respectively.

Thus an electron is acted upon by a potential energy

$$-\frac{e^2\left(\epsilon^{-1}-\epsilon_0^{-1}\right)}{r} \tag{0.1}$$

(this is a genius idea which could get to any head if one thinks deeper about what the dielectric constant is? We consider here some "abstract atom" somewhere near, which effectively takes into account many atoms which contribute to ε. This is a very effective model, because in reality there is no one point, to which we need to place r, all variables here are poorly defined.)

Since this is a Coulomb potential, localised states must exist (this is unclear. Is it because in 1D QM we always have a bound state? I can't imagine another reason.). The electron is 'trapped by digging its own hole'.

Mott and Gurney (1940) argued that the trapped electron must be mobile but heavy, and find it remarkable that no such entity had been observed (read their paper to understand it!).

The concept was treated in much greater detail by Fröhlich (1954), Yamashita and Kurosawa (1958), Sewel (1958), Holstein (1959), Toyozawa (1961), Eagles (1963), Reik (1963), Friedman (1964), Holstein and Friedman (1968), Austin and Mott (1969), Emin and Holstein (1969), Emin (1970), the Russian school: Pekar (1951), Tjablikov (1952), Rashba (1957), Klinger (1961), Lang and Firsov (1962) and later by many others. (I'll add their articles later, if needed. I don't know, what each of them did?)

In Holstein's treatment an electron is trapped by the self induced deformation of two-atomic molecules. (do we really have in that model a molecule? I thought that we have two atoms close to each other in a lattice....)

A Franck-Condon model (in scope of Holstain model) is used to calculate their quasistatic displacement and the frequency with which the polaron can move to a neighboring molecule. (add comments about which exactly results it is referring to? what is exactly the Franck-Condon model???)

This (in the so-called adiabatic approximation) involves the excitation of both the occupied and empty molecules to the same energy, so that the electron can tunnel backwards and forwards

between them. (read more about the Holsten model, then think about this statement again, how is exactly it?)

This excitation involves an activation energy $E_p/2$, and the excitation can occur through the action of temperature or zeropoint motion. (read more about the Holsten model, then think about this statement again, how is exactly it? and why exactly 1/2 is here?)

In the former case (temperature motion) the polaron moves by thermally activated hopping, with a diffusion coefficient

$$\omega a^2 \exp\left(-\frac{E_p}{2k_B T}\right) \tag{0.2}$$

where a is the distance between molecules. (does it mean that the wave function of polaron ψ obeys $\frac{d\psi}{dt} = \omega a^2 \exp\left(-\frac{E_p}{2k_B}\right)\frac{d^2\psi}{dx^2}$?) (is there a derivation of it somewhere??)

In the latter case (zeropoint motion), for $k_B T < \hbar\omega/2$ the motion is coherent (like a wave packet), the polaron behaves like a heavy particle with the mass

$$m^* \sim \exp\left(\frac{E_p}{\hbar\omega}\right) \tag{0.3}$$

and with a mean free path determined by the phonon and impurity scattering. (is it derived somewhere?) Here ω is the characteristic phonon frequency (what is it?).

For ionic crystals we may write

$$E_p = \frac{e^2\left(\epsilon^{-1} - \epsilon_0^{-1}\right)}{r_p} \tag{0.4}$$

where r_p is the radius of the volume within the wave function trapped by the lattice deformation (polaron radius). (I guess r_p is a mean radius, it is very unclear here, what it means exactly, but the idea is that we have some effective atom which is near the electron... Maybe the zero-point and thermal motion of electron is the key thing for it? Now, the fluctuation of electron changes the lattice and thus this "effective atom appears". So we forget at all what is the "conductive band". E_p means that if there is less energy in the system than E_p, then there are no polarons. Also, we can't determine r_p because we even don't know that there should be a charge e of the atom. It is just an abstract vague model) This can be greater than or comparable with the lattice constant a (because only this way some effective model can appear). (but now I don't understand, why the motion is coherent with such low energies?)

It is of course possible that the process described (which? thermal, zero point fluctuations, diffusive motion or coherent motion?) only leads to a small phase shift in the wave function at each hop (which hop?) if $E_p \ll \hbar^2/ma^2$, where m is a rigid band mass (how to find it?). (why there could be only phase shifts???)

The polaron is than called 'large' (why??), and can be described as a free particle moving in an elastic continuum (it was stated before, there is even a formula for effective mass).

The most sophisticated treatment of the large or 'continuum' (it is just another strange word) polaron is due to Feynman and co-workers (1962) (they calculated some impedance, read that strange paper! (???)) following that given by Pekar (1951) and Fröhlich (1954) (what is in that papers???).

This treatment leads to a mass enhancement, but not to a hopping conduction (?? why not to it?? read that articles??) or to a narrow polaron band (there is a subsection about it in the multipolaron problem, maybe it is explained there, what is meant here?).

It is in this sense that we use the term 'large polaron' (an unclear statement, there is no way that it makes sense. Nothing is written about Feynman's polaron. I propose to forget this sentence).

Some authors used the term 'large' to describe only situations where $(\epsilon^{-1} - \epsilon_0^{-1})$ is considerably less than unity (why does it lead to large polaron? maybe it is written in that subsection?).

But even this is by no means the case of large polarons if the bare electron band is sufficiently narrow (nothing is clear, why???).

For non-ionic materials (elements) (which?), large polarons in our sense do not exist (because there will be no that effective atom) (is there an experimental article that confirms that they are not there?) (this is why we will consider some elements of a model of small polaron).

If we take the Holstein model (at this moment a reader has no idea, what the Holsten model is, but okay, I know, because there is a section later about it) with the phonon coordinate x (molecular deformation) which lowers the electron energy by $x\omega\sqrt{2ME_p}$ (why???), then the deformation region of the size r_p with one localised electron in it costs the energy

$$E\left(u, r_p\right) \simeq \frac{\hbar^2}{2mr_p^2} - x\omega\sqrt{2ME_p} + \frac{M\omega^2 x^2}{2}\left(\frac{r_p}{a}\right)^3. \tag{0.5}$$

(why it is so????)

Minimising it with respect to the displacement (despite it is not clear what is going on, there is some x that occurs because of some vibrations. It can be arbitrary, but the model makes sense only if there is some minimal energy, and for it there should be some displacements) one obtains

$$x_0 = \sqrt{\frac{2E_p}{M\omega^2}}\left(\frac{a}{r_p}\right)^3 \tag{0.6}$$

and the minimum

$$E\left(x_0, r_p\right) = \frac{\hbar^2}{2mr_p^2} - E_p\left(\frac{a}{r_p}\right)^3 \tag{0.7}$$

(I just believe mathematics here)

The energy has a minimum for $r_p = 0$; therefore the electron collapses into a point at any value of the polaron binding energy E_p. In fact r_p is restricted from below by the lattice constant a. Therefore there is a critical value of the coupling constant $\lambda = E_p/\frac{\hbar^2}{2ma^2}$ (λ is a very important constant for Holstein model. It is also written as $\lambda = E/2J$)(is it the same constant as in Holstein model)

$$\lambda_c = 1 \tag{0.8}$$

No polarons are formed in the weak coupling region $\lambda < \lambda_c\left(r_p = \infty\right)$ (because energy will not have minimum, so all fluctuations will destroy this model), and only small polarons $(r_p = a)$ exist in the strong-coupling regime $\lambda > \lambda_c$ (is there way to write better this model, and not change 0 to a as it is done here?).

The concept of a small polaron was first applied to an electron or hole in a nonmetal (e.g. in alkali halides) (why??).

For the new superconductors our model is of course that of a degenerate gas of small polarons or bipolarons which are also degenerate below T_c and nondegenerate above (what is this degeneracy??).

(for now, I skipped the text below, I'll return later to it)

The bound state of two large polarons on an elastic polarisable continuum (large bipolaron) was introduced by Vinetskii and Giterman (1957) using a variational approach. Vinetskii and Pashitskii (1983) also discussed low-dimensional large bipolarons with disklike morphology and

the possibility of their Bose-Einstein condensation. In ionic crystals the polarization wells and wave functions of macroscopic (large) bipolarons with the radius $r_B \gg a$, where a is the lattice constant, overlap strongly and this should result in their dissociation if the carrier density is sufficiently high $n > 10^{20}$ cm^{-3}. However at low density (less than 10^{18} cm^{-3}) a gas of large bipolarons can be condensed below some critical temperature T_c without any overlapping of the polarization wells. Eagles (1969) examined a possibility of explaining the superconductivity of $SrTiO_3$ through such particles.

The concept of a small on-site localised bipolaron was introduced by Anderson (1975) and by Street and Mott (1975). It was applied to glassy semiconductors (chalcogenide glasses) to explain their magnetic and electric properties. Small bipolarons different from those were identified by Lakkis et al (1976) in Ti_4O_7 and $Ti_{4-x}V_xO_7$. These are inter-site small bipolarons, which are bound states of two Ti^{+3} ions stabilised by a large lattice distortion. At low temperatures they form a charged ordered state and are immobile. Chakraverty (1981) discussed bipolarons in connection with superconductivity, but considered that bipolarons would be immobile and therefore inactive as superconducting carriers.

The introduction of small mobile bipolarons and small polarons into the theory of superconductivity dated from the work of Alexandrov and Ranninger (1981a,b) and Alexandrov (1983), respectively. Many authors applied the BCS approach to describe the behavior of materials with strong interaction, so that the electron-phonon coupling constant λ increases (for review see Scalapino (1969)). The new point is that $\lambda \simeq 1$ is the condition for polaron formation, and it is shown that for a value of λ in the neighborhood of unity there is a fairly sharp transition to a situation in which all the carriers form small polarons. The electron band collapses into a narrow smallpolaron band (half bandwidth $w < \omega$) so that the gap extends across the whole Fermi distribution. The discovery of the new superconductors by Bednorz and Müller in 1986 lead to renewed interest in the bipolaronic superconductivity. We consider bipolarons as a key element for the understanding of the high- T_c phenomenon. Most of the experimental work has been in copper oxides, for which there is convincing evidence that the carriers are small polarons and bipolarons (Alexandrov and Mott (1994)).

In this book single-particle and cooperative properties of selflocalised carriers on a lattice are discussed at a fairly basic level with an emphasis on developments of the strong-coupling theory of superconductivity. Polaron and bipolaron formation provides a number of new physical phenomena both in the normal and superconducting ntates. Highly non-adiabatic motion of selftrapped carriers results in fundamental difference of low mobility conductors compared with simple metals and BCS superconductors.

(below, there is just repetition of what we see in the table of contents) The book starts with a single polaron problem. Both large and small polarons are discussed in Chapter 1. In the second Chapter the bipolaron formation is considered in ionic and atomic solids (still, I don't understand, why we think that all these models of bipolarons are much more useless than on one polaron?). The canonical theory of the electron-phonon interaction in metals is discussed in Chapter 3. In Chapter 4 we introduce the multi-polaron problem. Polar doped Mott insulators are described in Chapter 5. In chapter are We pay perconductivity and CDW in the strong coupling regime. We pay special attention to a charged Bose gas (CBG) in Chapter 7 as a simple but far-reaching model explaining many thermodynamic and kinetic properties of high-T_c superconductors (a good motivation for this model) (how really useful is it?). A discriminating selection of clear-cut experiments confirming the existence of mobile small polarons and bipolarons is presented in Chapter 8 (how really useful is it?). In conclusion

we suggest an overview of the high- T_c problem.

6.1.2 Electron Motion in Crystall Lattices by Landau 1933

Phys.Z.Sowjetunion 3, 664

(think about his article, what did he derive useful???)

It is well known that in a periodic field an electron can move without resistance. When the lattice is slightly distorted at a point, this only leads to scattering of the electrons at this point. This, however, does not mean the electron is trapped at this point. According to a familiar theorem in wave mechanics this will only be possible if, in addition possible if, in addition to continuous eigenvalues, the distorted lattice would also have discrete eigenvalues. But this is not the case for slight distortions.

Let us consider a free electron, subjected in a certain region to a weak field. we can then demonstrate in accordance with Peierls [1] that the solution of the Schrödinger equation at $E = 0$ has no nodes at weak fields, that is it corresponds to the lowest possible eigenvalue. For, when determining the solution of the Schrödinger equation

$$\nabla^2\psi = \frac{2mU}{\hbar^2}\psi \tag{1}$$

for small U in the form

$$\psi = 1 + \chi \tag{2}$$

where χ is also small, one obtains:

$$\nabla^2\gamma = \frac{2mU}{\hbar^2}. \tag{3}$$

If U decreases at infinity more rapidly than $1/r^2$, then this equation has a solution finite throughout, and whose values are proportional to those of U. For a sufficiently small U one therefore has $|\chi| < 1$ hence $1 + \chi$ vanishes. nowhere. (When denoting the dimension of the region where U is different from zero by a, we find that a discrete eigenvalue can only exist when $mUa^2/\hbar^2$ is of the order of unity.)

An analogous proof is possible for a periodic lattice by taking as starting point the solution corresponding to the lowest eigenvalue which is consequently nodeless for a strictly periodic field, and by writing the "distorted" φ in the form $\psi = \psi_0 + \chi$.

Hence a small distortion does not yet lead to the possible trapping of the electron. This possibility only exists for large distortions. We can now differentiate between two essentially different cases. For, the energetically most favourable state of the total system may correspond, firstly, to the undistorted lattice and the electron moving about "freely" and, secondly, the electron

trapped at a strongly distorted region. In the first case, the electron cannot be trapped at all by the lattice. This situation seems to be realised in the case of diamond. In the second case, the electron can only be trapped when passing over an energy barrier. For, as already stated, in the case of a small distortion, the eigenvalues of the electron are not changed. Hence the energy variation of the total system consists solely in the distortion energy and thus is essentially positive. We must therefore expect that the trapping of the electron is associated with activation effects. This corresponds to the situation in the case of NaCl which cannot be discoloured by X-rays at low temperatures. It would be interesting to verify in this effect the $\exp(-A/kT)$ law and to determine the value of the activation energy A.

[0] L. Landau, Über die Bewegung der Elektronen im Kristallgitter, Phys. Z. Sowjet. 3, 664 (1933).

Reference

1. R. Ptrerls, Z. Phys. 58, 59 (1929).

6.2 1 Large and small polaron

This book is about cooperative properties of self-trapped carriers in solids with strong electron-lattice interaction. To approach the many polaron problem we first discuss a single electron interacting with the lattice deformation.

6.2.1 1.1 Strong-coupling large polaron

(!!!! why does this model describe a large strong coupling polaron??? where are these inputs to the model????)

(the main message here is that there is a simple intuitive model that was proposed to take into account influence of electron on itself through lattice) (right??? is there something else important in it?)

Theory

The simplest case studied by Pekar (1946)(so, people considered all work by Landau as useless and only after Pekar, they continued to thing about this idea more?) (there is no way to find this article!!! I have no idea, what is in it, but there is a book by Pekar, so it should have all theory that is in that article) is a free electron interacting with the dielectric polarisable continuum, described by the static ϵ_0 and the optical (high frequency) dielectric constant ϵ.

This is the case for carriers interacting with optical phonons in ionic crystals under the condition that the size of the self-trapped state is large compared with the lattice constant so the lattice discreteness is irrelevant.

Describing the ionic crystal as a polarisable dielectric continuum one should keep in mind that only the ionic part of the total polarisation contribute to the polaron state. (how it could be otherwise??)

The interaction of a carrier with valence electrons responsible for the optical properties is taken into account with the Hartree-Fock periodic potential and included in the band mass m, Chapter 3 (? I'll think later, how it is done?).

Therefore only ion displacements contribute to the self-trapping.

Following Pekar we minimise the sum $E(\psi)$ of the electron kinetic energy and the potential energy due to the self-induced polarisation field

$$E(\psi) = \int d\mathbf{r} \left[\psi^*(\mathbf{r}) \left(-\frac{\nabla^2}{2m} \right) \psi(\mathbf{r}) - \mathbf{P}(\mathbf{r}) \cdot \mathbf{D}(\mathbf{r}) \right] \tag{1.1}$$

where

$$\mathbf{D}(\mathbf{r}) = e\nabla \int d\mathbf{r}' \frac{|\psi(\mathbf{r}')|^2}{|\mathbf{r} - \mathbf{r}'|} \tag{1.2}$$

in the electric field of an electron in the state with the wave function $\psi(\mathbf{r})$ and $\mathbf{P}$ is the ionic part of the lattice polarisation.

(???? !!! write better, which idea is assumed here???)

(write that discussion with Jaka about why do we have exactly $P \cdot D$??? it is a conceptually important question)

Here and further we set $\hbar = c = k_B = 1$ unless specified otherwise.

Minimising $E(\psi)$ with respect to $\psi^*(\mathbf{r})$ at fixed $\mathbf{P}$ and $\int d\mathbf{r}|\psi(\mathbf{r})|^2 = 1$ one arrives at the equation of motion

$$\left(-\frac{\nabla^2}{2m} - e\int d\mathbf{r}'\mathbf{P}\left(\mathbf{r}'\right)\cdot\nabla'\frac{1}{|\mathbf{r}'-\mathbf{r}|}\right)\psi(\mathbf{r}) = E_0\psi(\mathbf{r}) \tag{1.3}$$

where E_0 is the electron part of the ground state energy.

(I'll check the transformation later, maybe it is not that hard)

The ionic part of the total polarisation is given by the definition of the susceptibilities χ_0 and χ

$$\mathbf{P} = \left(\chi_0 - \chi\right)\mathbf{D}. \tag{1.4}$$

(why???)

The dielectric susceptibilities χ_0 and χ are expressed through the static and high frequency dielectric constants, respectively $(\chi_0 = (\epsilon_0 - 1)/4\pi\epsilon_0, \chi = (\epsilon - 1)/4\pi\epsilon)$ to obtain

$$\mathbf{P} = \frac{\mathbf{D}}{4\pi\kappa} \tag{1.5}$$

with $\kappa^{-1} = \epsilon^{-1} - \epsilon_0^{-1}$ (this is a very used parameter).

(I still need to revise electrodynamics to understand all this better)

Then the equation of motion is

$$\left(-\frac{\nabla^2}{2m} - \frac{e^2}{4\pi\kappa}\int d\mathbf{r}'\int d\mathbf{r}''\left|\psi\left(\mathbf{r}'\right)\right|^2\nabla'\frac{1}{|\mathbf{r}'-\mathbf{r}''|}\cdot\nabla'\frac{1}{|\mathbf{r}'-\mathbf{r}|}\right)\psi(\mathbf{r}) = E_0\psi(\mathbf{r}) \tag{1.6}$$

Differentiating by parts with the use of the equation $\nabla^2\frac{1}{r} = -4\pi\delta(\mathrm{r})$, we obtain

$$\left(-\frac{\nabla^2}{2m} - \frac{e^2}{\kappa}\int d\mathbf{r}'\frac{\left|\psi\left(\mathbf{r}'\right)\right|^2}{|\mathbf{r}'-\mathbf{r}|}\right)\psi(\mathbf{r}) = E_0\psi(\mathbf{r}) \tag{1.8}$$

(I'll check the transformation later, maybe it is not that hard)

(write here the idea better!!! why do we introduce a functional???? what this method is???)

The solution of this nonlinear integral-differential equation can be obtained with the help of a variational minimisation of the functional

$$J(\psi) = \frac{1}{2m}\int d\mathbf{r}|\nabla\psi(\mathbf{r})|^2 - \frac{1}{2ma_B}\int d\mathbf{r}d\mathbf{r}'\frac{|\psi(\mathbf{r})|^2\left|\psi\left(\mathbf{r}'\right)\right|^2}{|\mathbf{r}'-\mathbf{r}|} \tag{1.9}$$

where $a_B = \kappa/me^2$ is the effective Bohr radius (this is the important method, that we don't solve the equation, we guess the functional that solves it and then vary with some anzatz) (which other equations can be solved with this method?).

(note that we started with functional $E(\psi)$, then we got another functional $J(\psi)$, which is another version of the energy of electron)

The simplest choice of the normalised trial function is

$$\psi(\mathbf{r}) = Ae^{-r/r_p}, \qquad A = \frac{1}{\sqrt{\pi r_p^3}} \tag{1.10, 1.11}$$

Here we take the volume of the crystal $\Omega = 1$. Substitution of Eq.(1.10) into Eq.(1.9) yields

$$J(\psi) = T + \frac{1}{2}U \tag{1.12}$$

where the kinetic energy is

$$T = \frac{1}{2mr_p^2} \tag{1.13}$$

(I'll check all what is below later, it is a technical part)

To calculate the potential energy U we first integrate in Eq.(1.9) over the angle θ between $\mathbf{r}$ and $\mathbf{r}'$

$$\int_{-\pi}^{\pi} \frac{\sin\theta d\theta}{|\mathbf{r}-\mathbf{r}'|} = \frac{2\Theta\left(r-r'\right)}{r} + \frac{2\Theta\left(r'-r\right)}{r'} \tag{1.14}$$

to obtain

$$U = -\frac{32\pi^2}{ma_B}\int_0^\infty drr^2\psi^2(r)\int_r^\infty dr'r'\psi^2\left(r'\right) \tag{1.15}$$

Here $\Theta(x) = 1$ for $x > 0$ and zero otherwise. With Eq.(1.10) ($\psi(\mathbf{r}) = Ae^{-r/r_p}$) we find

$$U = -\frac{5}{8ma_Br_p}$$

and the function to be minimised with respect to r_p is

$$J(\psi) = \frac{1}{2mr_p^2} - \frac{5}{16ma_Br_p} \tag{1.17}$$

As a result, for the polaron radius we obtain

$$r_p = \frac{16a_B}{5} \tag{1.18}$$

and the ground state energy $E_0 = T + U$ is

$$E_0 = -0.146\frac{1}{ma_B^2} \tag{1.19}$$

(this is the first important result of this model. it tells us that if we just put electron in a crystal, it will be localized) (which exactly assumptions give us such conclusion??? how does it fit to classification of metals and dielectrics?)

This can be compared with the ground state energy of the hydrogen atom $-0.5m_ee^4$, where m_e is the free electron mass. Their ratio is $0.3m/m_e\kappa^2$. In polar solids $4 < \kappa \simeq 20$. Then the large polaron binding energy is below 0.25 eV if $m \simeq m_e$. The potential energy in the ground state is

$$U = -4T = \frac{4}{3}E_0 \tag{1.20}$$

The lowest photon energy $\nu_{\min}$ to excite a polaron into the electron band is

$$\nu_{\min} = |E_0|\,. \tag{1.21}$$

The ion configuration is not changed during the photoexcitation of a polaron. A lower activation energy W_T is necessary, however, if the self-trapped state disappears together with the polarisation well due to a thermal fluctuation

$$W_T = |E_0| - U_d, \tag{1.22}$$

where U_d is the deformation energy. In ionic crystals

$$U_d = \frac{1}{2}\int d\mathbf{r}\mathbf{P}(\mathbf{r})\cdot\mathbf{D}(\mathbf{r}) \tag{1.23}$$

which for the ground state is

$$U_d = \frac{2}{3}\left|E_0\right|. \tag{1.24}$$

Therefore the thermal activation energy is

$$W_T = \frac{1}{3}\left|E_0\right|. \tag{1.25}$$

The ratio of four characteristic energies for the large strong-coupling polaron is given by

$$W_T : U_d : \nu_{\min} : |U| = 1 : 2 : 3 : 4. \tag{1.26}$$

Different trial functions yield practically the same ground state energy with numerically different polaron radius. In particular, with Pekar's choice

$$\psi(r) = A\left(1 + r/r_p + \beta r^2\right)e^{-r/r_p} \tag{1.27}$$

one obtains $A = 0.12/r_p^{3/2}, \beta = 0.45/r_p^2$ and the polaron radius

$$r_p = 1.51 a_B \tag{1.28}$$

The ground state energy is

$$E_0 = -0.164\frac{1}{ma_B^2} \tag{1.29}$$

(check this) (conceptually all is clear here, just more complicated mathematics.)

(How exactly the strong-coupling large polaron is related to other models??? I'll answer this question in my theory of polarons)

6.2.2 1.2 Effective mass of large strong-coupling polaron

Theory

(somehow another model appears... why???)

Any polaron in a perfect crystal can move because of the translational symmetry. (why???)

However, the dynamical lattice deformation does not follow perfectly well the polaron motion (if it was following, this ground state would travel with any constant velocity?).

The retardation is responsible for the polaron mass enhancement (why exactly retardation?).

Within the continuum harmonic approximation the evolution of the lattice polarisation $\mathbf{P}(\mathbf{r},t)$ is described by the harmonic oscillator subjected to an external force $\sim \mathbf{D}/\kappa$:

$$\omega^{-2}\frac{\partial^2\mathbf{P}(\mathbf{r},t)}{\partial t^2} + \mathbf{P}(\mathbf{r},t) = \frac{\mathbf{D}(\mathbf{r},t)}{4\pi\kappa}, \tag{1.30}$$

where ω is the optical phonon frequency (which is just a constant, so there are infinite waves with different ω-s). (l.h.s. is a wave equation for polarization, and r.h.s. is a field that is also in all coordinates)

(explain where does this equation originate??)

If during the characteristic time of the lattice relaxation $\simeq \omega^{-1}$ the polaron (which is manifested in the D vector) moves a distance much less than the polaron radius, the polarisation practically follows the polaron motion. (is it possible to see it in the formula? suppose D was changed slightly and $\omega^{-1} \ll D$, then changes of P are somehow attached to the changes of D?)

(reminder that $\mathbf{D}(\mathbf{r}) = e\nabla \int d\mathbf{r}' \frac{|\psi(\mathbf{r}')|^2}{|\mathbf{r}-\mathbf{r}'|}$ and ψ is a function that exponentially decreasing with characteristic radius r_p. So I D should be also some rapidly decreasing function of r, but also now we set it linearly changing with speed v.)

Therefore for a slow motion with the velocity

$$v \ll \omega a_B \tag{1.31}$$

(because $r_p \sim a_B$)

the first term in Eq.(1.30), responsible for the retardation is a small perturbation. Then

$$\mathbf{P}(\mathbf{r},t) \simeq \frac{1}{4\pi\kappa}\left(\mathbf{D}(\mathbf{r},t) - \omega^{-2}\frac{\partial^2 \mathbf{D}(\mathbf{r},t)}{\partial t^2}\right) \tag{1.32}$$

(this is a not trivial step that requires physical intuition. Indeed, the zero's order look like $\frac{\partial^2 \mathbf{P}(\mathbf{r},t)}{\partial t^2} \approx \frac{\partial^2 \mathbf{D}(\mathbf{r},t)}{\partial t^2}/(4\pi\kappa)$) (why are we interested only in such waves with low ω?)

The total energy of the crystal with an extra electron

$$E = E(\psi) + 2\pi\kappa \int d\mathbf{r}\left[\mathbf{P}^2(\mathbf{r},t) + \omega^{-2}\left(\frac{\partial \mathbf{P}(\mathbf{r},t)}{\partial t}\right)^2\right] \tag{1.33}$$

is determined in such a way that it gives Eq.(1.30) if minimised with respect to $\mathbf{P}$. (one should or know this formula, or derive this using this minimization argument.) (check that it is true! is this formula written somewhere else?)

(reminder: $E(\psi) = \int d\mathbf{r}\left[\psi^*(\mathbf{r})\left(-\frac{\nabla^2}{2m}\right)\psi(\mathbf{r}) - \mathbf{P}(\mathbf{r})\cdot\mathbf{D}(\mathbf{r})\right]$, but it is also that $J(\psi)$, which is another form of $E(\psi)$)

We note that the first term of the lattice contribution is the deformation energy U_d, discussed in the previous section. As follows from Eq.(1.32) the lattice part of the total energy depends on the polaron velocity and contributes to the effective mass. Replacing the static wave function $\psi(\mathbf{r})$ in all expressions for $\psi(\mathbf{r}-\mathbf{v}t)$ and neglecting a contribution to the total energy of higher order than v^2 one obtains

$$E = E_0 + U_d + \frac{m^* v^2}{2}, \qquad m^* = -\frac{1}{12\pi\omega^2\kappa}\int d\mathbf{r}\mathbf{D}(\mathbf{r})\cdot\nabla^2\mathbf{D}(\mathbf{r}) \tag{1.34, 1.35}$$

is the polaron mass. (how this was obtained??? the ∇ appears somehow here.)

The use of the equations

$$\nabla^2\mathbf{D} = -4\pi e\nabla|\psi(\mathbf{r})|^2 \tag{1.36}$$

$$\nabla\cdot\mathbf{D} = -4\pi e|\psi(\mathbf{r})|^2 \tag{1.37}$$

(the first equation was obtained from the second one. The second one is the Maxwell equation in media, where density of electrons is $e|\psi(\mathbf{r})|^2$. Minus here is because we assume that constant e is positive)

yields

$$m^* = \frac{4\pi e^2}{3\omega^2\kappa}\int d\mathbf{r}|\psi(\mathbf{r})|^4 \tag{1.38}$$

(and what do we plug here as D???)

Calculating the integral in Eq.(1.38) with the trial function Eq.(1.10) ($\psi(\mathbf{r}) = Ae^{-r/r_p}$) one obtains

$$m^* \simeq 0.02\alpha^4 m \tag{1.39}$$

(derive it. it should be not that hard)

where α is the dimensionless constant, defined by Fröhlich as

$$\alpha = \frac{e^2}{\kappa}\sqrt{\frac{m}{2\omega}}. \tag{1.40}$$

(where did Fröhlich define it??? here, we see definition of it from papers definitely not by Fröhlich)

To conclude our discussion of the strong-coupling large polaron let us determine the condition of its existence. The polaron radius should be large compared with the lattice constant, $r_p \gg a$ to justify the continuum effective mass approximation for the electron. Then the value of α should not be very large,

$$\alpha \ll \sqrt{\frac{D}{z\omega}}, \tag{1.41}$$

where $D \simeq z/2ma^2$ is half of the bare electron bandwidth, z is the lattice nearest neighbor number. (why is it such?)

On the other hand the continuum (classical) approximation for the lattice polarisation is justified if the number of phonons taking part in the polaron formation is large. This number is of order U_d/ω. The total energy of the immobile polaron and deformed lattice, Eq.(1.34) is expressed as

$$E = -0.109\alpha^2\omega \tag{1.42}$$

and $U_d = 0.218\alpha^2\omega$. Then α is bounded below by the condition $U_d/\omega \gg 1$, which yields

$$\alpha^2 \gg 5. \tag{1.43}$$

The adiabatic ratio D/ω is of order 10 to 100. In fact in many transition metal oxides with narrow bands and a high optical phonon frequency this ratio is below 10, which makes Eq.(1.41) and Eq.(1.43) incompatible. Therefore the large strong coupling polaron is difficult to realise in practice, and we do not know of any solid in which it has been observed.

6.2.3 1.3 Fröhlich large polaron

(to understand it, read the original article, noting is clear here)

Theory

Fröhlich (1950) (see this article in the prt.2 (but maybe I'll move it to prt 1 later)), Fröhlich et al (1950) (it is impossible to find this article) and other workers applied the second quantisation form of the electron-lattice interaction to describe a week-coupling large polaron when $\alpha \leq 1$ (is their definition of α the same as before??), so the quantum nature of the lattice polarisation becomes important (which effects are not described if we neglect the quantum nature of polarization?).

The electron potential energy in a crystal field distorted by phonons is

$$V(\mathbf{r}) = \sum_{1} v\left(\mathbf{r} - \mathbf{R_l}\right), \tag{1.44}$$

(what is this v??!!!)

where the interaction of an electron with a single ion is described by the potential $v(\mathbf{r})$. The distance of ions $\mathbf{u_l} = \mathbf{R_l} - \mathbf{l}$ from the equilibrium positions 1 is small compared with a lattice constant a, which allows us to expand $v\left(\mathbf{r} - \mathbf{R_l}\right)$ near equilibrium:

$$v\left(\mathbf{r} - \mathbf{R_l}\right) \simeq v(\mathbf{r} - \mathbf{l}) - \mathbf{u_l} \cdot \nabla v(\mathbf{r} - \mathbf{l}).$$

The lattice part of the Hamiltonian can be diagonalised with harmonic phonons (see Chapter 3) such, that the ion displacement is a linear combination of their annihilation $d_{\mathbf{q}}$ and creation $d^{\dagger}_{\mathbf{q}}$ bosonic operators:

$$\mathbf{u_l} = \sum_{\mathbf{q}} \frac{\mathbf{e_q}}{\sqrt{2NM\omega_{\mathbf{q}}}} d_{\mathbf{q}} e^{i\mathbf{q}\cdot\mathbf{l}} + \text{ h.c.} \tag{1.46}$$

where q is the phonon momenta in the first Brillouin zone, ω_q the phonon frequency, M ionic mass, $\mathrm{e_q}$ is a unit polarisation vector, and N is the number of ions (sites) in a crystal. With the help of the Fourier expansion

$$v(\mathbf{r}) = \sum_{\mathbf{k}} v_{\mathbf{k}} e^{i\mathbf{k}\cdot\mathbf{r}} \tag{1.47}$$

the electron-phonon interaction in the second quantization is written as:

$$H_{e-ph} = \frac{1}{\sqrt{2N}} \sum_{\mathbf{q}} \gamma(\mathbf{q}) \omega_{\mathbf{q}} d_{\mathbf{q}} e^{i\mathbf{q}\cdot\mathbf{r}} + h.c. \tag{1.48}$$

where the dimensionless matrix element is

$$\gamma(\mathbf{q}) = -i \frac{N \mathbf{e_q} \cdot \mathbf{q}}{\sqrt{M\omega^3_{\mathbf{q}}}} v_{\mathbf{q}} \tag{1.49}$$

(why we put one ω in denominator in the def. of γ and one in the Hamiltonian? Looks useless) (for all reasonings - see the original article, here nothing is explained)

In ionic crystals (where there is one free electron for each atom)(right?) the interaction $v(\mathbf{r})$ is the Coulomb one with the Fourier component $v_{\mathrm{q}} \simeq 4\pi/\Omega\kappa q^2$ (Ω is the crystal volume).

Then the coupling with longitudinal ($\mathbf{e_q} \| \mathbf{q}$) ionic plasmons is

$$\frac{\gamma(\mathbf{q})\omega}{2N} \equiv V_{\mathbf{q}} = -\frac{i\omega}{q} \left(\frac{4\pi\alpha}{\Omega\sqrt{2m\omega}} \right)^{1/2} \tag{1.50}$$

where α is the Fröhlich constant and $\omega = \sqrt{4\pi N e^2/M\Omega\kappa}$ is the ionic plasma frequency. (so, in this definition, we see that only longitudinal phonons play crucial role.) (why? it is not explained at all here, so read the original paper)

The complete Hamiltonian including the quantised deformation energy has the form

$$H = -\frac{\nabla^2}{2m} + \sum_{\mathbf{q}} \left(V_{\mathbf{q}} d_{\mathbf{q}} e^{i\mathbf{q}\cdot\mathbf{r}} + h.c. \right) + \sum_{\mathbf{q}} \omega_{\mathbf{q}} \left(d^{\dagger}_{\mathbf{q}} d_{\mathbf{q}} + 1/2 \right) \tag{1.51}$$

The quantum states of the noninteracting electron and phonons are classified with the electron momentum $\mathbf{k}$ and with the phonon occupation numbers $\left\langle d^{\dagger}_{\mathbf{q}} d_{\mathbf{q}} \right\rangle \equiv n_{\mathbf{q}} = 0, 1, 2, \ldots \infty$. For zero temperature the unperturbed state is the vacuum $|0\rangle$ of phonons and the electron plane wave

$$|\mathbf{k},0\rangle = \frac{1}{\sqrt{\Omega}} e^{i\mathbf{k}\cdot\mathbf{r}} |0\rangle \tag{1.52}$$

While the coupling is weak one can apply perturbation theory. The interaction couples the state Eq.(1.52) with the energy $k^2/2m$ and states of a single phonon of momentum q and the electron of momentum $\mathbf{k}-\mathrm{q}$ with the energy $(\mathbf{k}-\mathrm{q})^2/2m+\omega$

$$|\mathbf{k}-\mathbf{q},1_{\mathbf{q}}\rangle = \frac{1}{\sqrt{\Omega}} e^{i(\mathbf{k}-\mathbf{q})\cdot\mathbf{r}} |1_{\mathbf{q}}\rangle \tag{1.53}$$

The corresponding matrix element is

$$\langle \mathbf{k}-\mathbf{q},1_{\mathbf{q}}| H_{e-ph} |\mathbf{k},0\rangle = V^*_{\mathbf{q}} \tag{1.54}$$

There are no diagonal matrix elements of H_{e-ph}. Then the renormalised energy $\tilde{E}_{\mathbf{k}}$ in the lowest second order is

$$\tilde{E}_{\mathbf{k}} = \frac{k^2}{2m} - \sum_{\mathbf{q}} \frac{|V_{\mathbf{q}}|^2}{(\mathbf{k}-\mathbf{q})^2/2m+\omega-k^2/2m} \tag{1.55}$$

As in section 1.2 we consider a slow electron, such as

$$k < q_p \tag{1.56}$$

where

$$q_p = \min(m\omega/q + q/2) = \sqrt{2m\omega} \tag{1.57}$$

In this case there is no imaginary part of $\tilde{E}_{\mathbf{k}}$, which means that the momentum is conserved. On substituting the expression for $V_{\mathbf{q}}$, Eq.(1.50), changing the sum over q to integrals, and taking the upper limit infinity for q one obtains

$$\tilde{E}_{\mathbf{k}} = \frac{k^2}{2m} - \frac{\alpha\omega}{\pi} \int_{-1}^{1} dx \int_0^{\infty} \frac{dy}{y^2 - 2yxk/q_p + 1} \tag{1.58}$$

The integral over q converges because the coupling constant ($\sim 1/q$) decreases with q. Therefore long wave optical phonons contribute mainly to the polaron self-energy. That is not the case for molecular or acoustical phonons when all states of the Brillouin zone contribute. Evaluating the integrals one arrives at

$$\tilde{E}_{\mathbf{k}} = \frac{k^2}{2m} - \frac{\alpha\omega q_p}{k} \arcsin\left(\frac{k}{q_p}\right) \tag{1.59}$$

which for a very slow motion $k \ll q_p$ yields

$$\tilde{E}_{\mathbf{k}} \simeq -\alpha\omega + \frac{k^2}{2m^*} \tag{1.60}$$

Here the first term is the polaron binding energy. The effective mass of the polaron is enhanced

$$m^* = \frac{m}{1-\alpha/6} \simeq m\left(1+\frac{\alpha}{6}\right) \tag{1.61}$$

This is due to a phonon cloud accompanying a slow polaron.

Number of virtual phonons

The number of virtual (virtual means that they don't travel anywhere, just affect electron) phonons N_{ph} in the cloud is given by taking the expectation value of the phonon number operator

$$N_{ph} = \left\langle \sum_{\mathbf{q}} d^{\dagger}_{\mathbf{q}} d_{\mathbf{q}} \right\rangle \tag{1.62}$$

where bra and ket refer to the perturbed state

$$|\rangle = |0\rangle + \sum_{\mathbf{q}'} \frac{V^*_{\mathbf{q}'}}{k^2/2m - (\mathbf{k}-\mathbf{q}')^2/2m - \omega} |1_{\mathbf{q}'}\rangle \tag{1.63}$$

For a polaron at rest ($\mathbf{k} = 0$) one obtains

$$N_{ph} = \sum_{\mathbf{q}} \frac{|V_{\mathbf{q}}|^2}{(\omega + q^2/2m)^2} \tag{1.64}$$

The value of the integral in Eq.(1.64) is

$$N_{ph} = \frac{\alpha}{2} \tag{1.65}$$

Therefore the Fröhlich coupling constant measures directly the cloud 'thickness'.

Induced lattice-charge

One can also calculate the lattice-charge density induced by the electron. The electrostatic potential $e\phi(\mathbf{r})$ is given by the average of the interaction term of the Hamiltonian

$$e\phi(\mathbf{r}) = \left\langle \sum_{\mathbf{q}} V_{\mathbf{q}} e^{i\mathbf{q}\cdot\mathbf{r}} d_{\mathbf{q}} + h.c. \right\rangle \tag{1.66}$$

and the charge density $\rho(\mathbf{r})$ is related to the electrostatic potential by Poisson's equation

$$\nabla\phi = -4\pi\rho \tag{1.67}$$

As a result

$$\rho(\mathbf{r}) = -\frac{1}{2\pi e} \sum_{\mathbf{q}} \frac{q^2 |V_{\mathbf{q}}|^2 \cos[\mathbf{q}\cdot\mathbf{r}]}{\omega + q^2/2m} \tag{1.68}$$

By integration over q one obtains

$$\rho(\mathbf{r}) = -\frac{e q_p^3}{4\pi\kappa} \frac{e^{-q_p r}}{q_p r} \tag{1.69}$$

The mean extension of the phonon cloud which can be taken as the radius of a weak coupling polaron is

$$r_p = q_p^{-1} \tag{1.70}$$

The total induced charge is

$$Q = \int d\mathbf{r} \rho(\mathbf{r}) = -\frac{e}{\kappa} \tag{1.71}$$

6.2.4 1.4 Intermediate-coupling large polaron

Theory

Many polar materials are in the intermediate regime $1 < \alpha < 10$. (why??)
(why do we at all need some special method here??)

One can approach this regime applying the Lee-Low-Pines (LLP, 1953) canonical transformation, removing the electron coordinate followed by the displacement transformation (Tjablikov (1952) (this aritcle is forgotten by scientific community, it is impossible to find it. what is there?), Lee and Pines (1952), Gurari (1953)). (why do we need to remove the electron coordinate???)

The latter serves to account for that part of the lattice polarisation which follows the electron instantaneously (why is it so and why instantaneously?).

The remaining part of the polarisation field turns out to be small if the coupling constant is not extremely large. (it is not explained, why?)

In the opposite extreme limit, which is Pekar's strong-coupling regime already discussed one can construct the perturbation theory by an expansion in descending powers of α (Bogoliubov (1950)). (what is in that article?)

Alternatively one can apply Feynman's path-integral formulation (1955) of quantum mechanics to remove the phonon field at the expense of a non-instantaneous interaction of electron with itself. (do it!! a good exercise)

Here we consider the canonical transformation approach referring the reader to the papers by Allcock (1962) and Bogoliubov Jr.(1994) for the strong-coupling large polaron theory and by Schultz (1962) for Feynman's path integral method, which is also discussed in section 2.3. (I am not sure how useful is path integral here, so I'll read it later)

A canonical transformation can be written as

$$|\tilde{N}\rangle = \exp(S)|N\rangle \tag{1.72}$$

where in our case $|N\rangle$ is a single-electron multi-phonon wave function, $|\tilde{N}\rangle$ is a transformed one, satisfying the Schrödinger equation:

$$\tilde{H}|\tilde{N}\rangle = E|\tilde{N}\rangle \tag{1.73}$$

with the transformed Hamiltonian

$$\tilde{H} = \exp(S)H\exp(-S) \tag{1.74}$$

If all operators are transformed according to Eq.(1.74) the physical averages, in particular the energy remain unchanged. LLP transformation eliminating the electron coordinate from the Hamiltonian is defined as

$$S_{LLP} = i\sum_{\mathbf{q}}(\mathbf{q}\cdot\mathbf{r})d^{\dagger}_{\mathbf{q}}d_{\mathbf{q}} \tag{1.75}$$

In the new representation the phonon operator is

$$\tilde{d}_{\mathbf{q}} = e^{S_{LLP}}d_{\mathbf{q}}e^{-S_{LLP}} = d_{\mathbf{q}}e^{-i\mathbf{q}\cdot\mathbf{r}} \tag{1.76}$$

and the electron momentum operator is

$$-i\tilde{\nabla} = -ie^{S_{LLP}}\nabla e^{-S_{LLP}} = -i\nabla - \sum_{\mathbf{q}}\mathbf{q}d^{\dagger}_{\mathbf{q}}d_{\mathbf{q}} \tag{1.77}$$

To derive Eq.(1.76) and Eq.(1.77) one can apply transformed operators to the eigenstates of the phonon-number operator and to the plane waves, respectively. The transformed Hamiltonian is therefore

$$\tilde{H} = \frac{1}{2m}\left(-i\nabla - \sum_{\mathbf{q}} \mathbf{q} d_{\mathbf{q}}^{\dagger} d_{\mathbf{q}}\right)^2 + \sum_{\mathbf{q}} \left(V_{\mathbf{q}} d_{\mathbf{q}} + h.c.\right) + \omega \sum_{\mathbf{q}} \left(d_{\mathbf{q}}^{\dagger} d_{\mathbf{q}} + 1/2\right) \tag{1.78}$$

The electron coordinate is absent from $\tilde{H}$. Hence the eigenstates $|\tilde{N}\rangle$ are classified with the momentum $\mathbf{K}$, which is the conserving total momentum of the system

$$|\tilde{N}\rangle = \frac{1}{\sqrt{\Omega}} e^{i\mathbf{K}\cdot\mathbf{r}} \left|\tilde{N}_{ph}\right\rangle \tag{1.79}$$

where the phonon part of the wave function $\left|\tilde{N}_{ph}\right\rangle$ satisfies to the Schrödinger equation with the phonon Hamiltonian

$$\tilde{H} = \frac{1}{2m}\left(\mathbf{K} - \sum_{\mathbf{q}} \mathbf{q} d_{\mathbf{q}}^{\dagger} d_{\mathbf{q}}\right)^2 + \sum_{\mathbf{q}} \left(V_{\mathbf{q}} d_{\mathbf{q}} + h.c.\right) + \omega \sum_{\mathbf{q}} \left(d_{\mathbf{q}}^{\dagger} d_{\mathbf{q}} + 1/2\right) \tag{1.80}$$

As follows from the Fröhlich perturbation analysis the number of virtual phonons is not small in the intermediate coupling regime. Therefore one cannot apply the perturbation theory to $\tilde{H}$. However, one can remove the essential part of the interaction term from the Hamiltonian by the displacement canonical transformation

$$S = \sum_{\mathbf{q}} f(\mathbf{q}) d_{\mathbf{q}} - h.c. \tag{1.81}$$

where the c-number $f(\mathbf{q})$ is to be determined by minimisation of the ground state energy

$$- \quad \frac{\partial E_0}{\partial f^*(\mathbf{q})} = 0 \tag{1.82}$$

The transformed phonon operator is

$$\tilde{d}_{\mathbf{q}} = e^S d_{\mathbf{q}} e^{-S} = d_{\mathbf{q}} - f^*(\mathbf{q}) \tag{1.83}$$

which is obtained with the help of the expansion

$$e^S d_{\mathbf{q}} e^{-S} = d_{\mathbf{q}} + [d_{\mathbf{q}}, S] + \frac{1}{2}\left[[d_{\mathbf{q}} S], S\right] + \ldots \tag{1.84}$$

Because $[d_{\mathbf{q}}, S] = -f^*(\mathbf{q})$ is a c-number all terms after the second vanish. From Eq.(1.83) it follows that $\exp S$ displaces ions to new equilibrium positions. Assuming that the transformed ground state is a phonon vacuum

$$\left|\tilde{\tilde{N}}_{ph}\right\rangle = e^S \left|\tilde{N}_{ph}\right\rangle = |0\rangle \tag{1.85}$$

one finds for the energy $\tilde{E}_{\mathbf{k}} \equiv \langle 0|\tilde{\tilde{H}}|0\rangle$

$$\tilde{E}_{\mathbf{K}} = \frac{K^2}{2m} - \sum_{\mathbf{q}} \left(V_{\mathbf{q}} f^*(\mathbf{q}) + h.c.\right) + \sum_{\mathbf{q}} |f(\mathbf{q})|^2 \left(\omega - \frac{\mathbf{K}\cdot\mathbf{q}}{m} + \frac{q^2}{2m}\right) + \frac{1}{2m} \sum_{\mathbf{q},\mathbf{q}'} \left|f(\mathbf{q}) f(\mathbf{q}')\right|^2 \mathbf{q}\cdot\mathbf{q}' \tag{1.86}$$

Taking the functional derivative of Eq.(1.86) to be zero one arrives at

$$f(\mathbf{q})\left[\left(\omega-\frac{\mathbf{K}\cdot\mathbf{q}}{m}+\frac{q^2}{2m}\right)+\frac{1}{m}\sum_{\mathbf{q}'}\left|f\left(\mathbf{q}'\right)\right|^2\mathbf{q}\cdot\mathbf{q}'\right]=V_{\mathbf{q}} \tag{1.87}$$

It is essential in eliminating a large part of the Fröhlich interaction that the linear term with respect to the phonon operators vanishes from $\tilde{\tilde{H}}$ if $f(\mathbf{q})$ satisfies to Eq.(1.87). Introducing a constant η determined as

$$\sum_{\mathbf{q}'}\left|f\left(\mathbf{q}'\right)\right|^2\mathbf{q}'=\eta\mathbf{K} \tag{1.88}$$

one finds a formal solution to Eq.(1.87)

$$f(\mathbf{q})=\frac{V_{\mathbf{q}}}{\omega+q^2/2m-(1-\eta)\mathbf{q}\cdot\mathbf{K}/m} \tag{1.89}$$

and with Eq.(1.86)

$$\tilde{E}_{\mathbf{K}}=\frac{\left(1-\eta^2\right)K^2}{2m}-\sum_{\mathbf{q}}\frac{\left|V_{\mathbf{q}}\right|^2}{\omega+q^2/2m-(1-\eta)\mathbf{q}\cdot\mathbf{K}/m} \tag{1.90}$$

The last equation is the same as Eq.(1.55) ($\tilde{E}_{\mathbf{k}}=\frac{k^2}{2m}-\sum_{\mathbf{q}}\frac{|V_{\mathbf{q}}|^2}{(\mathbf{k}-\mathbf{q})^2/2m+\omega-k^2/2m}$, which worked for large polaron) if $\eta=0$.

However, $\eta=0$ is not a solution of the self-consistent equation for η which is obtained by substituting Eq.(1.89) into Eq.(1.88)

$$\eta\mathbf{K}=\sum_{\mathbf{q}}\frac{\left|V_{\mathbf{q}}\right|^2\mathbf{q}}{\left(\omega+q^2/2m-(1-\eta)\mathbf{q}\cdot\mathbf{K}/m\right)^2} \tag{1.91}$$

Integrating gives

$$\tilde{E}_{\mathbf{K}}=\frac{\left(1-\eta^2\right)K^2}{2m}-\frac{\alpha\omega q_p}{K(1-\eta)}\arcsin\left(\frac{K(1-\eta)}{q_p}\right) \tag{1.92}$$

with

$$\eta(1-\eta)^2=\frac{\alpha q_p^3}{2K^3}\left(\frac{(1-\eta)K}{\sqrt{q_p^2-(1-\eta)^2K^2}}-\arcsin\frac{(1-\eta)K}{q_p}\right) \tag{1.93}$$

For a slow polaron with $K\ll q_p$ only the term independent of K needs to be retained in η

$$\eta=\frac{\alpha/6}{1+\alpha/6} \tag{1.94}$$

Then the energy up to order K^2 is

$$\tilde{E}_{\mathbf{K}}=-\alpha\omega+\frac{K^2}{2m^*} \tag{1.95}$$

where the polaron mass is now

$$m^*=m(1+\alpha/6) \tag{1.96}$$

This result shows that the perturbation theory, Eq.(1.61) ($m^*=\frac{m}{1-\alpha/6}\simeq m\left(1+\frac{\alpha}{6}\right)$, which is the case for just large polaron, which was obtained just by perturbation theory) can be extended even to $\alpha>1$.

Lee, Low and Pines evaluated also the corrections due to the off-diagonal part of the transformed Hamiltonian $\tilde{\tilde{H}}$ and found that they are below 0.02α for the polaron shift in Eq.(1.95) and below $-0.02\alpha^2/(1+\alpha/6)$ for the effective mass. A lower value of the ground state energy (approximately by 10%) and heavier effective mass was obtained by Feynman using the path integral. The difficulty with the path integral is that the effective action is not quadratic with respect to the electron coordinate. Therefore to determine an upper bound to the ground state energy the action was approximated by an effective quadratic action with two variational parameters. The general conclusion is that for a wide range of α the Feynman estimate of the ground state energy is lower than that obtained by the canonical transformation. Both the Feynman variational path integral approach and the LLP transformation are inaccurate for the strong coupling large polaron, $\alpha > 10$.

6.2.5 The Motion of Slow Electrons in a Polar Crystal by Lee, Low, Pines 1953

Phys.Rev. 90297

Abstract

A variational technique (is it connected to that S_{LLP} rotation???) is developed to investigate the low-lying energy levels of a conduction electron in a polar crystal.

Because of the strong interaction between the electron and the longitudinal optical mode of the lattice vibrations, perturbation-theoretic methods are inapplicable. (so, coupling is bigger than kinetic terms?)

Our variational technique, which is closely related to the "intermediate coupling" method introduced by Tomonaga (which one?), is equivalent to a simple canonical transformation.

The use of this transformation enables us to obtain the wave functions and energy levels quite simply.

Because the recoil of the electron introduces a correlation between the emission of successive virtual phonons by the electron (which correlation??), our approximation, in which this correlation is neglected, breaks down for very strong electron-phonon coupling.

The validity of our approximation is investigated and corrections are found to be small for coupling strengths occurring in typical polar crystals.

I. INTRODUCTION

When an electron in a polar crystal is excited to a low-lying energy level in the conduction band, it interacts strongly with the longitudinal optical mode of the lattice vibrations. More precisely, as the electron moves through the crystal, its Coulomb field displaces the positive and negative ions with respect to one another; the resultant ionic polarization will, in turn, considerably modify the motion of the electron. We may picture the electron as moving through the crystal accompanied by a cloud of phonons (i.e., the associated waves of ionic polarization); the electron plus its associated phonon cloud is known as a polaron.

The theory of the polaron is of more than usual interest because of the mathematical difficulties inherent in any "strong coupling" problem. The dimensionless parameter α, which describes the strength of the electron-phonon coupling, is of the order of magnitude of 3-6 for typical polar crystals. This may be contrasted to the electron-photon coupling constant which is $e^2/\hbar c = 1/137$.

The reduction in the electron energy as a consequence of its interaction with the lattice was first computed by Pekar, [1] and by Markham and Seitz, [2] using the adiabatic approximation.

Frohlich, Pelzer, and Zienau [3] calculated this energy and the effective mass of the polaron using a one-phonon approximation, which is appropriate provided the electron-lattice coupling is sufficiently weak. However, in most cases of interest, the interaction is so strong that the method of FPZ breaks down; on the other hand, the significant electronic frequencies are comparable to the vibrational frequency of the ionic waves, so that the adiabatic approximation is not applicable.

Our approach to this problem is based on a variational technique which does not suffer from either of the above defects. [4] Our essential assumption, following a method first introduced by Tomonaga [5] in treating meson-theoretic problems, is that there is no correlation in the emission of successive virtual phonons by the electron. This assumption appears to have considerable validity for intermediate values of the coupling constant ($\alpha \sim 4$) and for low-lying energy states of the system ($P^2/2m \ll \hbar\omega$, where P is the total momentum of the system, m is the mass of the electron, and ω is the frequency of lattice oscillations). However, it seems that our method breaks down in the limit of intermediate momenta ($P^2/2m \sim \hbar\omega$) and very strong coupling. The domain of physical applicability of our method is therefore somewhat restricted.

II. METHOD OF CALCULATION

We adopt the Hamiltonian and notation of Frohlich, Pelzer, and Zienau, in which (derive it somewhere)

$$H = \sum_k \frac{1}{2}\left(M\omega^2 X_k^2 + \frac{Y_k^2}{M}\right) + \frac{4\pi e}{\sqrt{V}} \sum_k \frac{1}{k}\left(X_k \sin \mathbf{k}\cdot\mathbf{r} + \frac{Y_k}{M}\cos \mathbf{k}\cdot\mathbf{r}\right) + \frac{p^2}{2m} \tag{1}$$

where ω is the frequency of the longitudinal optical vibrational mode of the lattice oscillation, X_k and Y_k are canonical variables, i.e., $[X_k, Y_{k'}] = \hbar i \delta_{kk'}$, m is the effective mass of the electron (as determined by its interaction with the periodic lattice field), $\mathbf{r}$ and $\mathbf{p}$ are the position and momentum operators of the electron, V is the volume of the crystal, and M is given by

$$M\omega^2 = \left[\frac{1}{4\pi}\left(\frac{1}{n^2} - \frac{1}{\epsilon}\right)\right]^{-1} \tag{2}$$

Here, n and ϵ are the optical index of refraction and the static dielectric constant, respectively. The three terms in this Hamiltonian correspond to the kinetic energy of the electron, the field energy of the phonons, and a term describing the electron-phonon interaction. In using this Hamiltonian we make the following assumptions:
(1) The dielectric may be treated as a continuum. This is a legitimate approximation since the phonons which interact strongly with the electron have a wavelength long compared to the lattice distance, and, as we shall see, the polaron extends over many lattice distances.
(2) The choice of M in Eq. (2) reflects the fact that we consider here only the interaction between the electron and the polarization due to the ionic motion.

As pointed out by FPZ, the interaction between the electron and the polarization owing to the bound electrons of the lattice is independent of the electron velocity, and hence would lead only to a constant term in the Hamiltonian, which we may neglect here.
(3) Finally, it is clear that the polarization associated with the acoustic mode of the lattice

[01] S. Pekar, J. Phys. (U.S.S.R.) 10, 341 (1946).
[2] J. Markham and F. Seitz, Phys. Rev. 74, 1014 (1948).
[3] Frohlich, Pelzer, and Zienau, Phil. Mag. 41, 221 (1950), hereinafter referred to as FPZ.
[04] We have been informed by Professor Frohlich that M. Gurari has developed a method of approach to this problem which is substantially equivalent to ours.
[5] S. Tomonaga, Prog. Theoret. Phys. 2, 6 (1947).

oscillations, in which neighboring ions vibrate in phase, will be small, so that we need only consider the long wavelength longitudinal optical mode, [6] in which alternate ions vibrate out of phase. The frequency of this mode is essentially independent of wavelength in the range of interest, and is given by $\omega = \omega_t \left(\epsilon/n^2\right)^{\frac{1}{2}}$, where ω_t is the experimentally known "reststrahl" frequency for long transverse waves. [7]

We find it convenient to express the Hamiltonian in terms of a new set of variables, a_k and $a_k{}^*$, such that

$$a_k = \frac{1}{\sqrt{2}}\left[\left(\frac{M\omega}{\hbar}\right)^{\frac{1}{2}} X_k + i\left(\frac{1}{\hbar M\omega}\right)^{\frac{1}{2}} Y_k\right], \tag{3a}$$

$$a_k{}^* = \frac{1}{\sqrt{2}}\left[\left(\frac{M\omega}{\hbar}\right)^{\frac{1}{2}} X_k - i\left(\frac{1}{\hbar M\omega}\right)^{\frac{1}{2}} Y_k\right]. \tag{3b}$$

Then

$$H = \sum_k a_k{}^* a_k \hbar\omega + \sum_k \left\{V_k a_k e^{i\mathbf{k}\cdot\mathbf{r}} + V_k{}^* a_k{}^* e^{-i\mathbf{k}\cdot\mathbf{r}}\right\} + p^2/2m \tag{4}$$

where we have neglected a zero-point energy $\sum_k \frac{1}{2}\hbar\omega$, and where

$$V_k = -\frac{\hbar\omega i}{k}\left(\frac{\hbar}{2m\omega}\right)^{\frac{1}{4}}\left(\frac{4\pi\alpha}{V}\right)^{\frac{1}{2}}, \tag{5}$$

and

$$\alpha = \frac{e^2}{2\hbar c}\left(\frac{2mc^2}{\hbar\omega}\right)^{\frac{1}{2}}\left(\frac{1}{n^2} - \frac{1}{\epsilon}\right). \tag{6}$$

The dimensionless number α plays the role of a coupling constant for the lattice-electron interaction. a_k and $a_k{}^*$ may be interpreted as phonon destruction and creation operators, since $[a_k, a_{k'}{}^*] = \delta_{kk'}$. The wave equation corresponding to (4) is then $H\Phi = E\Phi$.

We shall furthermore find it convenient to take advantage of the fact that the total momentum of our system is a constant of the motion. The total momentum operator is

$$\mathbf{P}_{\text{op}} = \sum_k \hbar\mathbf{k} a_k{}^* a_k + \mathbf{p},$$

and, of course, commutes with the Hamiltonian, (4). It is, therefore, possible to transform to a representation in which $\mathbf{P}_{\text{op}}$ becomes, a " c " number, and in which the Hamiltonian no longer contains the electron coordinates. The unitary transformation required is $\Phi = S\psi$,

where

$$S = \exp\left[i/h\left(\mathbf{P} - \sum_k a_k{}^* a_k \mathbf{k}\right)\cdot\mathbf{r}\right]. \tag{7}$$

We find

[6] As is well known, any transverse polarization wave has zero divergence and therefore gives rise to no "bound charge."

[7] For the derivation of this relation, see H. Frohlich, Theory of Dielectrics (Clarendon Press, Oxford, 1949).

$$\begin{aligned}\mathbf{P}_{\text{op}} &\to S^{-1}\mathbf{P}_{\text{op}}S = \mathbf{P} + \mathbf{p},\\ \mathbf{p} &\to S^{-1}\mathbf{p}S = \mathbf{P} - \sum_k \hbar\mathbf{k}a_k^* a_k + \mathbf{p},\\ a_k &\to S^{-1}a_k S = a_k e^{-i\mathbf{k}\cdot\mathbf{r}},\end{aligned} \tag{8}$$

so that

$$H \to \mathcal{H} = S^{-1}HS = \sum_k \hbar\omega a_k^* a_k + \sum_k (V_k a_k + V_k^* a_k^*) + \left(\mathbf{P} - \sum_k a_k^* a_k \mathbf{k}\hbar\right)^2 /2m, \tag{9}$$

provided we set $\mathbf{p} = 0$. The wave equation is now $\mathscr{H}\psi = E\psi$.

Our problem is to calculate for a given momentum P the lowest eigenvalue $E(P)$ of this Hamiltonian. We shall here confine our attention to the low-lying energy levels of the electron, for which $E(P)$ may be well represented by the first two terms of a power series expansion in P^2. Thus $E(P) = E_0 + \beta P^2/2 + \cdots O\left(P^4\right) + \cdots$. The effective mass of the polaron is then β^{-1}.

We use a variational method of calculation, which we will show is equivalent to a simple canonical transformation. We choose for our trial wave function

$$\psi = U\psi_0 \tag{10}$$

where ψ_0 is the eigenstate of the unperturbed Hamiltonian with no phonons present, i.e., the "free" vacuum state. Specifically, ψ_0 is defined by

$$a_k\psi_{\text{e}} = 0, \quad (\psi_0, \psi_0) = 1 \tag{11a}$$

and

$$U = \exp\left\{\sum_k \left(a_k^* f(\mathbf{k}) - a_k f^*(\mathbf{k})\right)\right\}, \tag{11b}$$

where $f(\mathbf{k})$ will subsequently be chosen to minimize the energy. It is clear that U is a unitary operator, so that ψ is normalized. Furthermore, viewed as a unitary transformation, U is a displacement operator on a_k and ${a_k}^*$, since

$$U^{-1}a_k^* U = a_k^* + f^*(\mathbf{k}), \quad U^{-1}a_k U = a_k + f(\mathbf{k}). \tag{12}$$

Our variational calculation, which is based on the use of the state vector ψ [Eq. (10)] is closely related to the approximation introduced by Tomonaga in his treatment of the coupling between mesons and nucleons, which was subsequently named the "intermediate coupling" approximation.

The Tomonaga approximation consists in a variational technique based on the physical assumption that successive virtual phonons (mesons) in the field around the electron (nucleon) are emitted independently, and hence that there is no correlation (i.e., interaction) between different phonons.

The mathematical expression of this assumption is that all phonons associated with the ground state of the electron are emitted into the same single phonon state $f(\mathbf{k})$, so that the Fock wave function for that part of the state containing n phonons is a simple product wave function; furthermore, the form of this wave function $f(k)$ is independent of n.

Let us consider a representation in which the Schrödinger function ψ of our system is described by a set of Schrödinger functions corresponding respectively to states of no phonons, one phonon, two phonons, etc. Let $\langle \mathbf{k}_1 \mathbf{k}_2 \cdots \mathbf{k}_n / \psi \rangle$ be the probability amplitude of finding n phonons of momenta $\mathbf{k}_1, \mathbf{k}_2 \cdots \mathbf{k}_n$ respectively in the phonon field, under the assumption that these phonons are distinguishable. [8] The total probability for finding n phonons in the field around the electron is then given by

$$P(n) = \sum_{k_1} \sum_{k_2} \cdots \sum_{k_n} \langle \mathbf{k}_1 \cdots \mathbf{k}_n / \psi \rangle^2 \tag{13}$$

The Tomonaga approximation consists in assuming that $\langle \mathbf{k}_1 \cdots \mathbf{k}_n / \psi \rangle$ has the following form:

$$\langle \mathbf{k}_1 \cdots \mathbf{k}_n / \psi \rangle = f(\mathbf{k}_1) \cdots f(\mathbf{k}_n) \, c_n \tag{14}$$

If the $f(\mathbf{k}_i)$ are normalized, then $P(n) = |c_n|^2$. The form of $f(\mathbf{k})$ and the constants c_n are determined by means of a variational calculation in which the total energy of the system is minimized.

It is easily verified that the use of the state vector (10) is equivalent to setting

$$\langle \mathbf{k}_1 \cdots \mathbf{k}_n / \psi \rangle = \frac{\exp\left[-\frac{1}{2} \sum_k |f(k)|^2\right]}{(n!)^{\frac{1}{2}}} f(\mathbf{k}_1) \, f(\mathbf{k}_2) \cdots f(\mathbf{k}_n) \, , \tag{15}$$

whence

$$P(n) = \frac{1}{n!} \exp\left[-\sum_k |f(\mathbf{k})|^2\right] \left\{\sum_k |f(\mathbf{k})|^2\right\}^n . \tag{16}$$

Thus we see that our form (15) for $\langle \mathbf{k}_1 \cdots \mathbf{k}_n / \psi \rangle$ is not the most general Tomonaga form, since it represents a particular choice of the c_n in Eq. (14). However, it may be shown that up to and including terms of order P^2 in our power series expansion of the energy, no error over and above that of the Tomonaga approximation itself is introduced by our more special assumption, (15). For this reason our calculation of the effective mass of the polaron will be equivalent to that of Lee and Pines who used the Tomonaga approximation. [9]

We seek to minimize the expression for the energy,

$$E = (\psi, H\psi) = \left(\psi_0, U^{-1} H U \psi_0\right) . \tag{17}$$

In virtue of (12),

$$U^{-1} H U = H_0 + H_1, \tag{18}$$

with

[08] The correct probability for finding n phonons of momenta $k_1, k_2 \cdots k_n$ is $\Sigma_p \langle k_1 \cdots k_n / \psi \rangle^2$ where Σ_p denotes a sum over all permutations of different k 's.

[9] T. D. Lee and D. Pines, Phys. Rev. 88, 960 (1952).

$$
\begin{aligned}
H_0 =& \frac{\left(\mathbf{P} - \sum_k a_k{}^* a_k \mathbf{k}\hbar\right)^2}{2m} + \sum_k \left(V_k f(\mathbf{k}) + V_k{}^* f\left(\mathbf{k}^*\right)\right) \\
&+ \frac{\hbar^2}{2m}\left[\sum_k |f(\mathbf{k})|^2 \mathbf{k}\right]^2 \\
&+ \sum_k |f(\mathbf{k})|^2 \left\{\hbar\omega - \frac{\mathbf{k}\cdot\mathbf{P}\hbar}{m} + \frac{k^2}{2m}\hbar^2\right\} \\
&+ \frac{\hbar^2}{m}\sum_k a_k{}^* a_k \mathbf{k}\cdot\left[\sum_{k'} \left|f\left(\mathbf{k}'\right)\right|^2 \mathbf{k}'\right] \\
&+ \sum_k a_k{}^* \left\{V_k{}^* + f(\mathbf{k})\left[\hbar\omega - \frac{\hbar\mathbf{k}\cdot\mathbf{P}}{m} + \hbar^2\frac{k^2}{2m}\right.\right. \\
&\left.\left.\frac{\hbar^2\mathbf{k}}{m}\cdot\left(\sum_{k'}\left|f\left(\mathbf{k}'\right)\right|^2 \mathbf{k}'\right)\right]\right\} \\
&+ \sum_k a_k \left\{V_k + f^*(\mathbf{k})\left[\hbar\omega - \hbar\frac{\mathbf{k}\cdot\mathbf{P}}{m} + \hbar^2\frac{k^2}{2m}\right.\right. \\
&\left.\left.+\frac{\hbar^2\mathbf{k}}{m}\cdot\left(\sum_{k'}\left|f\left(\mathbf{k}'\right)\right|^2 \mathbf{k}'\right)\right]\right\} + \sum_k a_k{}^* a_k \hbar\omega
\end{aligned}
\tag{19}
$$

and

$$
\begin{aligned}
H_1 =& \sum_{kk'} \frac{\mathbf{k}\cdot\mathbf{k}'}{2m}\left\{a_k a_{k'} f^*(\mathbf{k}) f^*\left(\mathbf{k}'\right) + 2a_k{}^* a_{k'} f(\mathbf{k}) f^*\left(\mathbf{k}'\right) + a_k{}^* a_{k'}{}^* f(\mathbf{k}) f\left(\mathbf{k}'\right)\right\} \\
&+ \sum_{kk'} \hbar^2 \frac{\mathbf{k}\cdot\mathbf{k}'}{m}\left\{a_k{}^* a_k a_{k'} f\left(\mathbf{k}'\right)^* + a_{k'}{}^* a_k{}^* a_k f\left(\mathbf{k}'\right)\right\}
\end{aligned}
\tag{20}
$$

Using Eq. (11), we see that

$$
\begin{aligned}
E =& \frac{P^2}{2m} + \sum_k \left\{V_k f(\mathbf{k}) + V_k^* f^*(\mathbf{k})\right\} + \frac{\hbar^2}{2m}\left\{\sum_k |f(\mathbf{k})|^2 \mathbf{k}\right\}^2 \\
&+ \sum_k |f(\mathbf{k})|^2 \left\{\hbar\omega - \frac{\mathbf{k}\cdot\mathbf{P}}{m}\hbar + \frac{k^2}{2m}\hbar^2\right\}.
\end{aligned}
\tag{21}
$$

We minimize (21) by setting

$$
\delta E/\delta f(\mathbf{k}) = \delta E/\delta f^*(\mathbf{k}) = 0 \tag{22}
$$

We find

$$
V_k + f^*(\mathbf{k})\left\{\hbar\omega - \frac{\mathbf{k}\cdot\mathbf{P}}{m}\hbar + \frac{k^2}{2m}\hbar^2 + \frac{\hbar^2}{m}\left[\sum_{k'}\left|f\left(\mathbf{k}'\right)\right|^2 \mathbf{k}'\right]\cdot\mathbf{k}\right\} = 0, \tag{23}
$$

and the appropriate complex conjugate equation for $f(\mathbf{k})$. On comparing (23) and (19) we see that the linear terms (in a_k and $a_k{}^*$) of (19) are

identically zero provided (23) is satisfied, and hence that H_0 is diagonal in a representation in which ${a_k}^* a_k$ is diagonal. Thus, our variational calculation is completely equivalent to the use of (19) as our total Hamiltonian, provided $f(k)$ satisfies (23). Since $H_0 + H_1$ differs from H by a unitary transformation, we can obtain an estimate of the accuracy of our variational procedure by a simple perturbation-theoretic estimate of the effect of H_1.

We now seek to evaluate the energy of the lowest state of our system, which is given by Eq. (21), with $f(\mathbf{k})$ satisfying Eq. (23). If we note that the only preferred direction in this problem is that of $\mathbf{P}$, we may conveniently introduce the parameter η defined by

$$\eta \mathbf{P} = \sum_k |f(\mathbf{k})|^2 \hbar \mathbf{k}. \tag{24}$$

Equation (23) then becomes

$$f(\mathbf{k}) = -V_k^* / \left[\hbar\omega - \frac{\mathbf{k}\cdot\mathbf{P}}{m}(1-\eta) + \frac{\hbar^2 k^2}{2m} \right], \tag{25}$$

and we obtain the following implicit equation for η:

$$\begin{aligned} \eta \mathbf{P} &= \sum_k |f(k)|^2 \hbar \mathbf{k} \\ &= \sum_k |V_k|^2 \hbar \mathbf{k} / \left[\hbar\omega - \hbar \frac{\mathbf{k}\cdot\mathbf{P}}{m}(1-\eta) + \frac{k^2\hbar^2}{2m} \right]^2 . \end{aligned} \tag{26}$$

Using Eq. (5), and transforming the summation in (26) to an integration, [10] we find

$$(\eta - 1)^2 \eta = \frac{\alpha}{2} \left(\frac{2m\omega\hbar}{P^2} \right)^{\frac{3}{2}} \left\{ \sin^{-1} q - \frac{q}{(1-q^2)^{\frac{1}{2}}} \right\} \tag{27}$$

where

$$q = (\eta - 1) \left(P^2 / 2m\omega\hbar \right)^{\frac{1}{2}} . \tag{28}$$

We can also obtain the energy in closed form. It turns out to be

$$E = \left(P^2/2m \right) \left(1 - \eta^2 \right) - (\alpha\omega\hbar/q) \sin^{-1} q \tag{29}$$

As long as $P^2/2m$ is sufficiently small so that no spontaneous emission of phonons can occur (roughly $P^2/2m < \hbar\omega$), Eq. (27) can be solved numerically for a given value of $P^2/2m$, and hence we may obtain $E\left(P^2\right)$. As mentioned earlier, we shall here be content to calculate $E\left(P^2\right)$ to first order in an expansion in powers of $P^2/2m\hbar\omega$. On doing this, one readily obtains:

$$\eta = \frac{\alpha/6}{1+\alpha/6} + O\left(P^2/2m\omega\hbar \right) + \cdots , \tag{30}$$

and

$$E = -\alpha\omega\hbar + \left(P^2/2m \right) \left[1 / \left(1 + \frac{1}{6}\alpha \right) \right] + O\left(P^2/2m\omega\hbar \right)^2 \hbar\omega + \cdots . \tag{31}$$

[010] In carrying out the k integrations we can extend our limits to $\pm\infty$, since the contribution to these integrals falls off quite sharply with increasing k.

III. DISCUSSION OF RESULTS

For the slow electrons we have considered, the interaction therefore introduces two effects: (1) All electronic energy levels are reduced by $\alpha\hbar\omega$. (2) The motion of the polaron is that of a free particle with an effective mass $m_{\text{eff}} = m(1+\alpha/6)$. For higher momenta it is clear that the effective mass becomes P-dependent; we have here given only the $P=0$ contribution.

It is of some interest to calculate the mean number of phonons in the cloud around the electron. This is given by

$$N = \left(\psi, \sum_k a_k^* a_k \psi\right) = \sum_k |f(k)|^2 \tag{32}$$

where we have used Eqs. (10)-(12). Hence, by Eq. (25),

$$N = \frac{1}{2}\alpha\left\{\left(1+\left[1/\left(1+\frac{1}{6}\alpha\right)^2\right]P^2/4m\hbar\omega\right)+O\left(P^4/m^2\hbar^2\omega^2\right)\right\} \tag{33}$$

Another physical quantity of interest is the ionic polarization charge density induced by the electron. In order to calculate this, we note that the interaction term in our Hamiltonian [Eq. (1)] is just the potential energy of the electron in the ionic polarization field. [3] The coefficient of $-e$ in this term is therefore the operator which represents the electrostatic potential at a point $\mathbf{r}$. The mean value of this potential when the electron is at some point $\mathbf{r}_e$ is given by

$$\varphi(\mathbf{r},\mathbf{r}_e) = -(1/e)\left(\psi_{r_e}, \left[\sum_k V_k a_k e^{i\mathbf{k}\cdot\mathbf{r}} + V_k{}^* a_k{}^* e^{-i\mathbf{k}\cdot\mathbf{r}}\right]\psi_{r_e}\right) \tag{34}$$

where

$$\psi_{r_e} = \exp\left\{(i/\hbar)\mathbf{r}_e\cdot\left(\mathbf{P}-\sum_k a_k{}^* a_k \hbar\mathbf{k}\right)\right\}\exp\left\{\sum_k a_k{}^* f(\mathbf{k}) - a_k f^*(\mathbf{k})\right\}\psi_0 \tag{35}$$

(there was a typo in brackets in the original article)

[See Eq. (8) and Eq. (10).] The ionic polarization charge density at $\mathbf{r}$ induced by an electron at $\mathbf{r}_e$ is thus

$$\rho(\mathbf{r},\mathbf{r}_e) = -(1/4\pi)\nabla^2\varphi(\mathbf{r},\mathbf{r}_e) = -(1/4\pi_e)\left(\psi_{r_e}, \sum_k k^2\left(V_k a_k e^{i\mathbf{k}\cdot\mathbf{r}} + V_k^* a_k^* e^{-i\mathbf{k}\cdot\mathbf{r}}\right)\psi_{re}\right) \tag{36}$$

Using (35) we find

$$\begin{aligned}\rho(\mathbf{r},\mathbf{r}_e) &= -(1/4\pi_e)\sum_k k^2\left\{V_k f(k) e^{i\mathbf{k}\cdot(\mathbf{r}-\mathbf{r}_e)} + V_k^* f^*(k) e^{-i\mathbf{k}\cdot(\mathbf{r}-\mathbf{r}_e)}\right\} \\ &= -\frac{e\hbar\omega}{2V}\left(1/n^2 - 1/\epsilon\right)\sum_k\left\{1/\left[\hbar\omega - \hbar(\mathbf{k}\cdot\mathbf{P}/m)(1-\eta) + \left(k^2/2m\right)\hbar^2\right]\right. \\ &\quad \times\left\{e^{i\mathbf{k}\cdot\mathbf{r}-\mathbf{r}_e} + e^{-i\mathbf{k}\cdot(\mathbf{r}-\mathbf{r}_e)}\right\}.\end{aligned} \tag{37}$$

We may immediately calculate the total induced charge,

$$q = \int dr \rho\left(\mathbf{r}, \mathbf{r}_e\right) = -e\left(1/n^2 - 1/\epsilon\right) \tag{38}$$

which is the classically expected result for the induced ionic charge on the inner surface of a dielectric medium surrounding a point charge e.

The charge density is, on changing the summation in
(37) to an integral,

$$\rho\left(\mathbf{r}, \mathbf{r}_e\right) = -e(\hbar\omega/2V)\left(1/n^2 - 1/\epsilon\right) 2m/\hbar^2 \int dk/(2\pi)^3 \left\{ \frac{e^{i\mathbf{k}\cdot(\mathbf{r}-\mathbf{r}_e)} + e^{-i\mathbf{k}\cdot(\mathbf{r}-\mathbf{r}_e)}}{k^2 + (2m\omega/\hbar) - 2(\mathbf{k}\cdot\mathbf{P}/\hbar)(1-\eta)} \right\} \tag{39}$$

The integration in (39) is straightforward, and yields

$$\rho\left(\mathbf{r}, \mathbf{r}_e\right) = -e\frac{\hbar\omega}{2}\left(\frac{1}{n^2} - \frac{1}{\epsilon}\right)\left(\frac{2m}{\hbar^2}\right)\left\{\left(\frac{1}{2\pi}\right)\cos\left(\frac{(1-\eta)\mathbf{P}\cdot\mathbf{r} - \mathbf{r}_e}{\hbar}\right)\right.$$
$$\times \frac{\exp\left[-\left\{2m\omega/\hbar - (1-\eta)^2 P^2/\hbar^2\right\}^{\frac{1}{2}} \left|\mathbf{r} - \mathbf{r}_e\right|\right]}{\left|\mathbf{r} - \mathbf{r}_e\right|} \tag{40}$$

This induced charge distribution is flattened in the forward and backward directions (with respect to the motion of the polaron). Its mean extension is just $(\hbar/2m\omega)^{\frac{1}{2}}$. This may be considered a good measure of the extension of the polaron. As pointed out by FPZ, since $(\hbar/2m\omega)^{\frac{1}{2}}$ is large with respect to the lattice distance, we are justified in using the continuum approximation in our Hamiltonian. [1]

Comparing our energy, Eq. (31) with that obtained by FPZ, we see that in the limit of weak coupling $\alpha \ll 1$, our results reduce to those of FPZ, and that for larger values of α, our result always gives a lower energy. For a typical polar crystal, NaCl, $\alpha = 5.2$, [11] $\omega = 4.8 \times 10^{13}\text{sec}^{-1}$, so that we find $E_0 = -\alpha\hbar\omega = -0.16\text{ev}$, and $m_{\text{eff}} = 1.9m$. In this case FPZ, and also Pekar, obtain $E_0 = -0.09\text{ev}$.

Pekar, [12] and Landau and Pekar, [13] using the adiabatic approximation, have found an effective mass for the polaron (in NaCl) of ~ 17 m.[11] However, as might be suspected from Pekar's much higher value of E_0, this high effective mass is due to the lack of applicability of the adiabatic approximation. The condition of validity of the adiabatic approximation is essentially that the frequencies of interest in the problem shall be large compared to the ionic frequency ω. This is, however, not the case for the polarons we have been considering. A convenient measure of the electronic frequencies of interest is provided by the mean kinetic energy of the electron. For $P = 0$, one finds

$$\langle T\rangle_{\text{Av}} = \left(\psi, \sum_k \frac{\left(a_k{}^* a_k \hbar\mathbf{k}\right)^2}{2m}\psi\right) = \sum_k |f(\mathbf{k})|^2 \frac{\hbar^2 k^2}{2m} = \frac{\alpha\hbar\omega}{2}.$$

Clearly, there is no external mechanism, such as exists in a molecule, which can provide the electron with an appreciably higher frequency than ω. The validity of the adiabatic approach is therefore roughly determined

by $(\alpha/2)^{\frac{1}{2}}$, which is never as large as 2 for polar crystals. Whether the adiabatic approximation applies in principle to the case of extremely large coupling is not clear.

[011] Here we have taken m to be the mass of a free electron.
[12] S. Pekar, J. Exptl. Theor. Phys. 19, 796 (1949).
[13] L. Landau and S. Pekar, J. Exptl. Theor. Phys. 18, 419 (1948).

IV. VALIDITY OF OUR METHOD

As is well known, in the limit of infinite electron mass, an exact solution is possible, and follows, in fact, from our canonical transformation. In the case of finite electron mass, the electron's recoil kinetic energy plays an essential role, since it introduces a correlation between the emission of successive virtual phonons. This correlation will tend to limit the validity of our method.

Furthermore, since the Hamiltonian [Eq. (4)] is a function of only four parameters $\alpha, P, \hbar\omega$, and m, of which α is dimensionless, and P^2/m and $\hbar\omega$ are energies, the energy of the system when expanded in powers of P^2 can only be of the form

$$\hbar\omega f_0(\alpha) + P^2/2m f_1(\alpha) + \left(P^2/2m\right)^2 (1/\hbar\omega) f_2(\alpha) + \cdots$$

Therefore, in estimating corrections to our results for $f_0(\alpha)$ and $f_1(\alpha)$, we have no dimensional arguments to fall back upon. Our hope is that our variational method has taken into account, to a higher extent than might be obvious, the effect of the correlations introduced by electron recoil, although our wave function is chosen under the assumption of no correlation. This situation is quite analogous to that obtaining in the use of the Hartree-Fock wave functions in the treatment of atomic problems; i.e., although the wave function appears to contain no correlation between different particles (phonons), an "average" effect of the correlation energy is taken into account in the choice of that wave function which minimizes the energy.

The validity of our calculation may best be estimated by calculating the lowest order correction to the energy resulting from that part of the Hamiltonian which we have neglected, viz. H_1 [Eq. (20)]. The lowest nonvanishing order in which H_{i} affects the energy is the second. The energy shift, which we calculate using conventional perturbation theory, is given by:

$$\Delta E_1 = -\sum_n{}' \frac{\left|(H_1)_{0n}\right|^2}{E_n - E_0}, \tag{41}$$

where $\sum_n{}'$ is a sum over all the excited states of H_0 to which H_1 has nonvanishing matrix elements. These correspond to two-phonon states. One readily finds:

$$\Delta E_1 = -\frac{1}{4m^2} \sum_{k_1 k_2} \frac{(\mathbf{k}_1 \cdot \mathbf{k}_2)^2 \left|f(\mathbf{k}_1)\right|^2 \left|f(\mathbf{k}_2)\right|^2}{\left\{2\hbar\omega - (\hbar/m)\left[(\mathbf{k}_1 \cdot \mathbf{P}) + \hbar(\mathbf{k}_2 \cdot \mathbf{P})\right](1-\eta) + \hbar^2 (\mathbf{k}_1 + \mathbf{k}_2)^2/2m\right\}}, \tag{42}$$

with $f(\mathbf{k})$ given by Eq. (23). The indicated summations in (42) have been carried out numerically up to order $P^2/2m\hbar\omega$. The result is: (how to do it???)

$$\Delta E_1 = -0.007\alpha^2\hbar\omega - 0.01\frac{\alpha^2}{(1+\alpha/6)^2}\frac{P^2}{2m} \tag{43}$$

This is to be compared with our result [Eq. (31)], $E = -\alpha\hbar\omega + (P^2/2m)\left[1/\left(1+\frac{1}{6}\alpha\right)\right]$. If we set $\alpha = 6$, we find a relative correction to the P-independent term of approximately 4 percent; the correction to the $P^2/2m$ term is larger, and is approximately 18 percent. It is perhaps not surprising that the P-dependent correction is larger than the P-independent one, since we might expect that correlation between the emission of successive quanta will play a more important role when a preferred direction exists.

On the whole, therefore, our method provides a reasonable approximation for intermediate values of the coupling constant α, i.e., $\alpha \lesssim 6$. This point of view is confirmed by a detailed one-dimensional calculation of Gross. [14] Gross uses a variational method, with a state vector which may contain zero, one, two, and three phonon parts, to consider the case in which V_k [Eq. (5)] is now independent of k. He finds, for an equivalent coupling constant of $3-4$, that the

energy of the lowest state, when calculated with a maximum of one, two, and three phonons, respectively, appears to approach a limit which is in substantial agreement with the result we obtain for the same one-dimensional problem using our variational method.

We should like to thank Professor John Bardeen and Dr. C. N. Yang for stimulating discussions. We are grateful to Mrs. Jean Kellom for her assistance in carrying out the numerical work. One of us (D.P.) would like to acknowledge the support of the Office of Ordnance Research, U. S. Army.

6.2.6 Self Energy of Slow Electrons in Polar Materials by Gurari 1953

(???)
Phil.Mag. 44329

Summary

A new variational method is developed to treat the properties of slow electrons in ionic crystals, and similar problems.

It is shown that the true energy of the ground state is always lower than the energy obtained from second order perturbation theory, however strong the interaction.

The corresponding wave functions differ, however, from those of perturbation theory unless the interaction is sufficiently weak.

For NaCl the energy of the ground state is found lower than by any previous method, and hence closer to the true energy.

The effective mass is of the order of twice the electronic mass; no trapping takes place, therefore.

§1. Introduction and Discussion

It is well known that slow electrons in strictly periodic crystal lattices behave in many respects like free electrons. A slow electron, however, polarizes an ionic lattice so that the field in which the electron moves is no longer periodic. Frobhlich, Pelzer and Zienau (1950, quoted as I) have pointed out that this energy corresponds to the self energy of the electron in a field theory if the polarization of the crystal is considered as a field. They found that although the energy of the ground state is depressed by this interaction, the electron together with the polarization attached to it can still move nearly freely through the lattice. This result differs from an earlier suggestion by Landau (1933) who neglected the dynamic properties of the lattice. He thus treated the electron as moving in a static field due to the polarization produced by the electron. This would lead to the trapping of an electron near a given point in space. Although such a trapped electron could still move through the lattice, its effective mass might be very large, in contrast to the result of I.

The calculations in I hold only for relatively weak interaction. The purpose of the present paper is to develop a new variational method which applies also to stronger interaction. The result shows that for a very general type of interaction the energy of the ground state is the same as found from second order perturbation theory. Since a variational method has been used now, however, it follows that this energy is always

[014] E. P. Gross, private communication. We are indebted to Dr. Gross for informing us of his results.
0

- Based on E. R. A. Report L/T 284.
  † Mark Gurari died on May 8, 1952. The present paper was prepared from notes left by him.-H. Fröhlich.
  ‡ Communicated by Professor H. Fröhlich.

higher than the true energy, however strong the interaction. The wave functions used in the variational method tend towards those of perturbation theory only in the case of weak interaction. They may differ from them very considerably for strong interaction.

In the case of ionic crystals assumed to have a single vibrational frequency $\omega/2\pi$ for long longitudinal waves, a static dielectric constant ϵ and an optical refractive index $\epsilon_\infty^{\frac{1}{2}}$ the energy $E(0)$ of the ground state is then (cf. 2.29) found to be $-W$ where (cf. I, 1.5)

$$W = \frac{1}{2}\left(\frac{1}{\epsilon_\infty} - \frac{1}{\epsilon}\right) e^2 u. \quad \ldots . \tag{1.1}$$

Here u is an inverse length satisfying

$$\hbar\omega = \hbar^2 u^2/2m \tag{1.2}$$

It should be noted (cf. I, 4.1) that ω is connected with the frequency $\omega_t/2\pi$ of residual waves by

$$\omega = \omega_t \left(\epsilon/\epsilon_\infty\right)^{\frac{1}{2}} \tag{1.3}$$

It will also be shown below that the ratio of effective mass m^* to the electron mass is †

$$\frac{m^*}{m} = 1 + \frac{W}{6\hbar\omega} \tag{1.4}$$

In the case of NaCl (for numerical values of parameters cf. I) (1.1) leads to $-W = -0.17$ev. This value is lower than both Markham and Seitz's (1948) value of -0.13 ev obtained by Landau's method, and Pekar's (1949) value of $-0 \cdot 10$ev (obtained with an approximation which is good for large $W/\hbar\omega$) and it thus represents a better approximation. Since $\hbar\omega \simeq 0.03$ev it follows from (1.4) that the effective mass is only about twice the electronic mass. It is thus confirmed that as was suggested in I no trapping takes place.

§ 2. Derivation of the Results

Consider the Hamiltonian used in I, eqn. (2.6),

$$H = H_{\text{osc}} + H_{\text{int}} + {p_{\text{op}}}^2/2m \tag{2.1}$$

where $\mathbf{p}_{\text{op}}$ is the momentum operator of the electron,

$$H_{\text{osc}} = \sum_{\mathbf{w}} H_{\mathbf{w}} \quad \cdot \quad \cdot \quad \cdot \quad \cdot \quad \cdot \tag{2.2}$$

refers to the oscillators representing the lattice vibrations and H_{int} is their interaction with the electron. The lattice vibrations can be expressed in terms of plane waves with wave number $\mathbf{w}$, and $H_{\mathbf{w}}$ refers to a single one of them. Clearly if $|\mathbf{K}\rangle$ is the electronic wave function,

$$\frac{p_{\text{op}}^2}{2m}|\mathbf{K}\rangle = \frac{\hbar^2 K^2}{2m}|\mathbf{K}\rangle \tag{2.3}$$

† From a preprint received recently **I** found that Tsung-Dao Lee and David Pines have independently derived the same results. They have not yet published details.-H. Fröhlich.

where $\hbar\mathbf{K}$ is the electronic momentum. Also if $|n_{\mathbf{w}}\rangle$ is an oscillator wave function

$$H_{\mathbf{w}}\,|n_{\mathbf{w}'}\rangle = \delta_{\mathbf{w}\mathbf{w}'} n_{\mathbf{w}} \hbar\omega\,|n_{\mathbf{w}}\rangle \tag{2.4}$$

where the quantum number $n_{\mathbf{w}}$ is a positive integer or zero. Here we have omitted the zero point energy of the oscillator which can be done by an appropriate choice of the zero of energy. Clearly

$$(H - H_{\text{int}}) \left\{ |\mathbf{K}\rangle \prod_{\mathbf{w}} |n_{\mathbf{w}}\rangle \right\} = \left(\frac{\hbar^2 K^2}{2m} + \sum_{\mathbf{w}} n_{\mathbf{w}} \hbar\omega \right) \left\{ |\mathbf{K}\rangle \prod_{\mathbf{w}} |n_{\mathbf{w}}\rangle \right\} \tag{2.5}$$

which means that the product of the electronic and all oscillator wave functions are eigenfunctions of the operator $H - H_{\text{int}}$. They form a complete set, obtained by using all combinations of all possible values for the quantum numbers $n_{\mathbf{w}}$ and for $\mathbf{K}$.

It has been shown in I that the interaction term H_{int} leads to transitions between these eigenfunctions provided the total wave number

$$\mathbf{k} = \mathbf{K} + \sum_{\mathbf{w}} n_{\mathbf{w}} \mathbf{w} \tag{2.6}$$

is not altered. It is useful, therefore, to denote these eigenfunctions by $|\mathbf{k}; \ldots n_{\mathbf{w}} \ldots\rangle$. Clearly in ordinary space ($\mathbf{r}$) representation the normalized electronic wave function is

$$|\mathbf{K}\rangle = V^{-\frac{1}{2}} \exp(-i\mathbf{K}, \mathbf{r}) \tag{2.7}$$

where V is the volume. Thus using (2.6),

$$|\mathbf{k}; \ldots n_{\mathbf{w}} \ldots\rangle = |\mathbf{K}\rangle \prod_{\mathbf{w}} |n_{\mathbf{w}}\rangle = V^{-\frac{1}{2}} \exp(i\mathbf{k} \cdot \mathbf{r}) \Pi_{\mathbf{w}} \exp\left(-i n_{\mathbf{w}} \mathbf{w} \cdot \mathbf{r}\right) |n_{\mathbf{w}}\rangle \tag{2.8}$$

are the eigenfunctions of $H - H_{\text{int}}$. Hence with (2.5),

$$\begin{aligned} \langle \ldots n'_{\mathbf{w}} \ldots; \mathbf{k}'| \left(H - H_{\text{int}}\right) | \mathbf{k}; \ldots n_{\mathbf{w}} \ldots\rangle = \delta_{\mathbf{k}\mathbf{k}'} \ldots \delta_{n_{\mathbf{w}} n_{\mathbf{w}'}} \cdots \frac{\hbar^2}{2m} \\ \times \left\{ \left(\mathbf{k} - \sum_{\mathbf{w}} n_{\mathbf{w}} \mathbf{w} \right)^2 + \sum_{\mathbf{w}} n_{\mathbf{w}} u^2 \right\} \end{aligned} \tag{2.9}$$

where use has been made of eqn. (1.2). Thus in the matrix representation based on the eigenfunctions (2.8) the operator $H - H_{\text{int}}$ has diagonal elements only. For the interaction operator H_{int} on the other hand all diagonal elements vanish. The non-diagonal elements are different from zero only for transitions which leave $\mathbf{k}$ as well as all $n_{\mathbf{w}}$ but one unaltered, the excepted one differing by unity. Thus from I , eqns. (2.15) and (2.16)

$$\begin{aligned} \langle \ldots, n_{\mathbf{w}''}, \ldots, n_{\mathbf{w}}, \ldots n_{\mathbf{w}'}, \ldots; \mathbf{k}| \, H_{\text{int}} \; | \, \mathbf{k}; \ldots, n_{\mathbf{w}'}, \ldots, n_{\mathbf{w}} + 1 \\ \ldots, n_{\mathbf{w}'}, \ldots, \rangle = \langle n_{\mathbf{w}}| \, H_{\text{int}} \; |n_{\mathbf{w}} + 1\rangle = \tfrac{C}{w} \left(\tfrac{n_{\mathbf{w}}+1}{V}\right)^{\frac{1}{2}} \end{aligned} \tag{2.10}$$

where using (1.2)

$$C = \left(4\pi W \hbar^2 u/2m\right)^{\frac{1}{2}} . \tag{2.11}$$

To find an approximate solution of our problem with the help of the variational method it is required that

$$\delta\langle\psi(\mathbf{k})|H|\psi(\mathbf{k})\rangle = 0 \tag{2.12}$$

where δ represents a variation of the normalized trial wave function $|\psi(\mathbf{k})\rangle$. The latter will be assumed of the form

$$|\psi(\mathbf{k})\rangle = V^{-\frac{1}{2}} \exp(i\mathbf{k}.\mathbf{r}) \prod_{\mathbf{w}} |\psi(\mathbf{k},\mathbf{w})\rangle \tag{2.13}$$

where

$$|\psi(\mathbf{k},\mathbf{w})\rangle = \frac{|0_{\mathbf{w}}\rangle + V^{-\frac{1}{2}} c(k,w,x) \exp(-i\mathbf{w},\mathbf{r}) \, |\mathbf{l}_{\mathbf{w}}\rangle}{(1+V^{-1}c^2(k,w,x))^{\frac{1}{2}}} \tag{2.14}$$

Here the coefficients $c(k,w,x)$ are assumed to depend on the magnitudes k and w and on the angle between $\mathbf{k}$ and $\mathbf{w}$ whose cosine is denoted by x; they will be determined from (2.12). As required the wave functions (2.13) using (2.14) can be written as a linear superposition of eigenfunctions (2.8). They all have the same value of $\mathbf{k}$ and contain all combinations of the values $n_{\mathbf{w}} = 0$, and $n_{\mathbf{w}} = 1$ of all w's. We thus admit states which may contain a very great number of vibrational quanta provided they all belong to different wave vectors $\mathbf{w}$. In contrast more restrictive wave functions were used in I where, as in perturbation theory, no states were used with more than a single quantum.

Using orthogonality and normalization of the wave functions, eqns. (2.1), (2.13), (2.14), together with (2.3), (2.4), (1.2), (2.6), (2.7) and (2.10) yield

$$\begin{aligned}\langle\psi(\mathbf{k})|H|\psi(\mathbf{k})\rangle =& \frac{\hbar^2}{2m}\left\{k^2 + \sum_{\mathbf{w}} \frac{V^{-1}c^2(k,w,x)\,(u^2+w^2-2kwx)}{1+V^{-1}c^2(k,w,x)}\right. \\ &\left. + \sum_{\mathbf{w}_2,\mathbf{w_x}} \frac{V^{-2}c^2\,(k,w_1,x_1)\,c^2\,(k,w_2,x_2)\,(\mathbf{w}_1,\mathbf{w}_2)}{(1+V^{-1}c^2\,(k,w_1,x_1))\,(1+V^{-1}c^2\,(k,w_2,x_2))}\right\} \\ &+ 2C\sum_{\mathbf{w}} \frac{V^{-1}c(k,w,x)}{w\,(1+V^{-1}c^2(k,w,x))}\end{aligned} \tag{2.15}$$

Here the dash at the summation sign means that $\mathbf{w}_1 \neq \mathbf{w}_2$. The last term arises from H_{int} ; the rest are due to the electronic terms apart from u^2 which is due to H_{osc} . Clearly as $V \to \infty, V^{-1}c^2$ can be neglected against unity (anticipating c to be independent of V). Furthermore, if polar coordinates in $\mathbf{w}$-space are introduced with $\mathbf{k}$ as axis and ϕ as azimuth then only $\mathbf{w}_1 \cdot \mathbf{w}_2$ depends on ϕ,

$$\mathbf{w}_1 \cdot \mathbf{w}_2 == w_1 w_2 \left(\cos\theta_1 \cos\theta_2 + \sin\theta_1 \sin\theta_2 \cos\left(\phi_1 - \phi_2\right)\right) \tag{2.16}$$

Clearly ϕ integration removes the $\cos\left(\phi_1 - \phi_2\right)$ term so that in (2.15), $\mathbf{w}_1.\mathbf{w}_2$ can be replaced by

$$w_1 w_2 \cos\theta_1 \cos\theta_2 = w_1 x_1 w_2 x_2 \ldots\ldots\ldots \tag{2.17}$$

For $V \to \infty$, eqn. (2.15) can thus be written as

$$\begin{aligned}\langle\psi(\mathbf{k})|H|\psi(\mathbf{k})\rangle =& \frac{\hbar^2\left(k^2+\gamma^2\right)}{2m} \\ &+ V^{-1}\sum_{\mathbf{w}}\left\{\frac{\hbar^2}{2m}\left(u^2+w^2-2kwx\right)c^2(k,w,x) + \frac{2Cc(k,w,x)}{w}\right\}.\end{aligned} \tag{2.18}$$

where

$$\gamma = V^{-1}\sum_{w} wxc^2(k,w,x) \tag{2.19}$$

According to (2.12) the variation of (2.18) with respect to all coefficients $c(k,w,x)$ must vanish. Hence

$$\left(u^2+w^2-2kwx+2\gamma wx\right)c(k,w,x)=-\frac{2m}{\hbar^2}\frac{C}{w},\ldots \tag{2.20}$$

which requires that

$$u^2+w^2-2(k-\gamma)wx\neq 0 \tag{2.21}$$

Denoting by $E(k)$ the expectation value of H when these values of $c(k,w,x)$ have been inserted one finds from eqns. (2.18), (2.19) and (2.20)

$$\begin{aligned}E(k)=&\frac{\hbar^2\left(k^2+\gamma^2\right)}{2m}+\frac{2m}{\hbar^2}V^{-1}C^2\sum_w\frac{1}{w^2}\left\{\frac{u^2+w^2-2kwx}{\left(u^2+w^2-2(k-\gamma)wx\right)^2}\right.\\&\left.-\frac{2}{u^2+w^2-2(k-\gamma)wx}\right\}=\frac{\hbar^2\left(k^2-\gamma^2\right)}{2m}\\&-\frac{2m}{\hbar^2}V^{-1}C^2\sum_w\frac{1}{w^2\left(u^2+w^2-2(k-\gamma)wx\right)}.\end{aligned} \tag{2.22}$$

Introducing now for γ the dimensionless variable

$$v=(k-\gamma)/u,\ldots\ldots\ldots\ldots\ldots \tag{2.23}$$

we find from (2.22) and (2.21) the following parametric representation of $E(k)$,

$$E(k)=\frac{\hbar^2}{2m}\left[k^2-(k-uv)^2\right]-\frac{2m}{\hbar^2}V^{-1}C^2\sum_w\frac{1}{w^2\left(u^2+w^2-2uvwx\right)},\ldots \tag{2.24}$$

$$k-uv=\left(\frac{2m}{\hbar}\right)^2V^{-1}C^2\sum_w\frac{wx}{w^2\left(u^2+w^2-2uvwx\right)^2}. \tag{2.25}$$

To evaluate the sums they will be replaced by integrals,

$$V^{-1}\Sigma_w\ldots\rightarrow\frac{2\pi}{(2\pi)^3}\int\ldots w^2dwdx\ldots\ldots. \tag{2.26}$$

The w-integration can be extended to infinity as has been discussed in I . All integrations are elementary. With the use of (2.11) and (1.2) eqns. (2.24) and (2.25) then become

$$E(k)=\hbar\omega\left[\frac{k^2}{u^2}-\left(\frac{k}{u}-v\right)^2\right]-W\frac{\sin^{-1}v}{v},\ldots \tag{2.27}$$

and

$$\frac{k}{u}-v=\frac{W}{\hbar\omega}\frac{1}{2v^2}\left(\frac{v}{(1-v^2)^{\frac{1}{3}}}-\sin^{-1}v\right) \tag{2.28}$$

Clearly if $v=0$ then from (2.28) also $k=0$. Hence

$$E(0)=-W \tag{2.29}$$

If $v\rightarrow 1$ then from (2.28) $k\rightarrow\infty$ and with (2.27) $E(k)\simeq 2\hbar\omega k/u\rightarrow\infty$. The case $v>1$ has to be excluded to satisfy condition (2.21). It cannot be expected that the choice of the

wave function (2.13) and (2.14) permits
a successful treatment of energies $E(k)$ which are above the ground state by more than $\hbar\omega$. For states below this energy $v \ll 1$. In this case (2.27). and (2.28) can be developed into a power series in v, i.e.

$$E(k) = -W + \hbar\omega \left(2\frac{k}{u}v - v^2 \left(1 + \frac{W}{6\hbar\omega} \right) + \dots \right) \tag{2.30}$$

and

$$\frac{k}{u} = v \left(1 + \frac{W}{6\hbar\omega} \right) + \dots\dots \tag{2.31}$$

Eliminating v leads to

$$E(k) = -W + \frac{\hbar^2 k^2}{2m^*} + \dots \quad \cdot \dots \cdot \tag{2.32}$$

with a value of m^* given by (1.4). Its validity requires

$$E(k) - E(0) \ll \hbar\omega. \quad . \quad . \quad . \quad . \quad . \quad . \tag{2.33}$$

§3. Generalization for $k = 0$

Equation (2.29) shows that for $k = 0$ the energy $E(0)$ is the energy obtained from second order perturbation theory (although the wave functions in the two cases are equal only if $W/\hbar\omega \ll 1$). This result holds not only for the model used in § 2 but also in a much more general case obtained by the replacements

$$C/w \to g(w), \quad u \to u(w), \quad \cdots\cdots \tag{3.1}$$

where $g(w)$ and $u(w)$ are arbitrary functions of w, provided no divergent integrals occur. This can best be seen by making the replacements (3.1) in eqns. (2.24) and (2.25). Then $v = 0$ requires $k = 0$ because the integrand in (2.25) becomes antisymmetric in x. Equation (2.24) is then equal to the second order perturbation formula. This result can also be derived by a more elegant method which will be presented here because it will probably be of use in the discussion of excited states.

Consider the matrix representation of the Hamiltonian H given in §2, and write H as the sum of two terms

$$H = H' + H'', \quad . \quad . \quad . \quad . \quad . \quad . \tag{3.2}$$

such that H'' is a diagonal matrix with elements

$$\langle \dots n_{\mathrm{w}} \dots | \, H'' \, | \dots n_{\mathrm{w}} \dots \rangle = \frac{\hbar^2}{2m} \left\{ \left(\sum_{\mathrm{w}} n_{\mathrm{w}} \mathrm{w} \right)^2 - \sum_{\mathrm{w}} n_{\mathrm{w}} w^2 \right\} \tag{3.3}$$

Then since the diagonal elements of H_{int} vanish the diagonal elements of H are obtained from (2.9) by putting $k = k' = 0$ and $n_{\mathbf{w}} = n_{\mathbf{w}}'$. Use of (3.1), (3.2) and (3.3) then gives

$$\langle \dots n_{\mathrm{w}} \dots | \, H' \, | \dots n_{\mathrm{w}} \dots \rangle = \frac{\hbar^2}{2m} \sum_{\mathrm{w}} n_{\mathrm{w}} \left(w^2 + u^2(w) \right), \tag{3.4}$$

as diagonal elements of H'. The non-diagonal elements are the same as those of H_{int} , given by (2.10). Clearly then, the operator H' can be written as

$$H' = \sum_{\mathbf{w}} H'(\mathbf{w}), \quad . \quad \cdot \quad \cdot \quad \cdot \quad \cdot \quad \cdot \tag{3.5}$$

where

$$\langle n_{\mathbf{w}} | H'(\mathbf{w}) | n_{\mathbf{w}} \rangle = n_{\mathbf{w}} \frac{\hbar^2}{2m} \left(w^2 + u^2(w) \right) \tag{3.6}$$

are the diagonal elements of $H'(\mathbf{w})$. All non-diagonal elements vanish except those next to the diagonal ; they are given by

$$\langle n_{\mathbf{w}} | H'(\mathbf{w}) | (n_{\mathbf{w}} + 1) \rangle = g(w) \left(\frac{n_{\mathbf{w}} + 1}{V} \right)^{\frac{1}{2}} \tag{3.7}$$

Thus $H'(\mathbf{w})$ is identical with the Hamiltonian of an harmonic oscillator (apart from its zero point energy) with frequency $\hbar \left(w^2 + u^2(w) \right) / 2m$ whose origin, through a linear term, has been displaced by

$$\Delta = \left\{ 16 m^3 g^2(w) / V \hbar^4 \left(w^2 + u^2(w) \right)^3 \right\}^{\frac{1}{2}}, \quad \cdot . \quad \cdot \tag{3.8}$$

assuming its mass to be unity. If $|\psi_0{}'(\mathbf{w})\rangle$ is its eigenfunction in the ground level, clearly

$$H'(\mathbf{w}) | \psi_0'(\mathbf{w}) \rangle = - \frac{g^2(w) 2m}{V \hbar^2 \left(w^2 + u^2(w) \right)} | \psi_0'(\mathbf{w}) \rangle \tag{3.9}$$

Using (3.5), therefore,

$$H' | \psi_0' \rangle = E_0 | \psi_0' \rangle , \tag{3.10}$$

where

$$| \psi_0' \rangle = \prod_{\mathbf{w}} | \psi_0'(\mathbf{w}) \rangle , \quad \cdot \quad \cdot \quad \cdot \tag{3.11}$$

and

$$E_0 = - \frac{1}{V} \sum_{\mathrm{w}} \frac{g^2(w) 2m}{\hbar^2 \left(w^2 + u^2(w) \right)} \tag{3.12}$$

Thus the lowest eigenvalue of H' is exactly equal to the expression for the lowest state of H calculated with the help of perturbation theory.

To compare the eigenfunctions it will be noticed that the function $|\psi_0{}'(\mathbf{w})\rangle$ of the displaced oscillator can be developed in a series of eigenfunctions $|n_{\mathbf{w}}\rangle$ of the undisplaced oscillator. It is found that

$$| \psi_0'(\mathbf{w}) \rangle = \exp \left(-s_w^2 \right) \sum_{n_{\mathbf{w}}} \frac{\left(-2^{\frac{1}{2}} s_w \right)^{n_{\mathbf{w}}}}{(n_{\mathbf{w}}!)^{\frac{1}{2}}} | n_{\mathbf{w}} \rangle \tag{3.13}$$

where

$$s_w = \frac{g(w) 2m}{(2V)^{\frac{1}{2}} \hbar^2 (w^2 + u^2(w))}, \quad \cdot \cdot \cdot \cdot \cdot \tag{3.14}$$

It follows that terms with $n_w \geqslant 2$ can be neglected if $V \to \infty$. The eigenfunction $|\psi_0{}'\rangle$ is then seen to be identical with $|\psi(\mathbf{k})\rangle$, eqns. (2.13) and (2.14) if $\mathbf{k} = 0$ and if the coefficients c are introduced from (2.20) considering

the replacements (3.1). Also, since for $\mathbf{k} = 0$ the c 's are independent of the direction of $\mathbf{w}$, the diagonal elements (3.3) of H'' vanish for $n_{\mathbf{w}} = 0$ and $n_{\mathbf{w}} = 1$. Clearly then

$$\langle \psi_0' | H'' | \psi_0' \rangle = 0, \quad \cdot \quad \cdot \quad \cdot \tag{3.15}$$

and hence

$$\langle \psi_0{}' | H | \psi_0{}' \rangle = E_0. \quad \cdot \quad \cdot \quad \cdot \quad . \tag{3.16}$$

It now follows from the variational principle (2.12) that E_0 is larger than the lowest eigenvalue of H.

It is hoped that the present method will permit treatment of excited states by using solutions of H' different from the ground state. Also use of H'' as a perturbation should lead to an estimate of the accuracy of the above solutions.

References

Fröflich, Pelzer and Zienau, 1950, Phil. Mag., 41, 221.

Landad, 1933, Z. Phys. Sowjet., 3, 664.

Markham and Seitz, 1948, Phys. Rev., 74, 1014.

Pekar, 1949, J. Exp. Theor. Phys., U.S.S.R., 19, 796.

6.2.7 1.5 Small polaron: two-site Holstein model

Theory

When the coupling with phonons increases the polaron radius decreases and becomes of the order of the lattice constant.

Then all momenta of the Brillouin zone contribute to the polaron wave function and the effective mass approximation cannot be applied.

This regime occurs if the characteristic potential energy E_p (see below discussion of it) due to the local lattice deformation is comparable or larger than the half bandwidth D (what is it in the original Hamiltonian?).

The strong coupling regime with the dimensionless coupling constant

$$\lambda \equiv \frac{E_p}{D} \geq 1 \tag{1.97}$$

is called a small polaron. (it is not clear, why it is so? or it will be shown further?)

In general, E_p is estimated using the perturbation theory, Eq.(1.55) ($\tilde{E}_{\mathbf{k}} = \frac{k^2}{2m} - \sum_{\mathbf{q}} \frac{|V_{\mathbf{q}}|^2}{(\mathbf{k}-\mathbf{q})^2/2m+\omega-k^2/2m}$):

$$E_p = \frac{1}{2N} \sum_{\mathbf{q}} |\gamma(\mathbf{q})|^2 \omega_{\mathbf{q}} \tag{1.98}$$

(derive it!!! I don't see it right now. add formula for γ) for any type of phonons involved in the polaron cloud.

For the Fröhlich interaction with optical phonons one estimates

$$E_p \simeq \frac{q_D e^2}{\pi \kappa} \tag{1.99}$$

where $q_d = (6\pi^2/\Omega)^{1/3}$ is the Debye momentum. (derive!!! what is Ω?)

With parameters appropriate for high T_c copper oxides $\epsilon_0 \gg \epsilon_\infty \simeq 5$ and $q_D \simeq 0.7\text{Å}^{-1}$, one obtains $E_p \simeq 0.6\text{eV}$.

The exact value of λ_c when the large polaron collapses into a small one depends on the lattice structure and phonon frequency dispersion (and how does it depend?).

The transition occurs around $\lambda_c \simeq 0.5$ in the Holstein model (see Section 1.8) (and why is it so?).

Small polarons are expected to be the carriers in high- T_c oxides, which are strongly polarisible doped semiconductors with rather narrow electron bands (Chapter 8) (what is there??l why they are expected there?).

The band structure (can we sketch two band structures for different regimes?) and kinetic properties (how they are different?) are drastically different in the small polaron regime compared with the large polaron as was discussed by Tjablikov (1952) (it is impossible to find this article), Yamashita and Kurosava (1958) (read it below!), Sewell (1958), Holstein (1959) (who developed a special model for it), and by the Russian school: Rashba (1957)(it is impossible to find this article), Klinger (1962), Firsov and co-workers(1962) (it is meant a book at 1975, which is available only in Russian, there is a lot of theory) and others.

(it is not written here, but as far as I understand, there are some problems with Frolich polarons at this regime, so we need a new model)(why we can't work only with models above???)

The main features of the small polaron are revealed in the simplest Holstein model consisting of only two vibrating molecular sites and one electron between them (by "molecular cites" we mean that there are electron that glue atoms, otherwise they would fly away shortly).

Neglecting the intermolecular coupling the vibration (molecular) part of the Hamiltonian is written as

$$H_{ph} = -\frac{1}{2M}\sum_{i=1,2}\left(\frac{\partial^2}{\partial x_i^2} + \frac{M\omega^2 x_i^2}{2}\right) \tag{1.100}$$

(there is a typo, $-\frac{1}{2M}$ should be inside the bracket)(right?)

where $x_{1,2}$ is the intramolecular coordinate, which is the change of the distance between two ions of a diatomic molecule on site 1 and 2 , respectively, and M is the relative mass. (also, here we introduce the parameter ω which is a constant for this model)(right? it is not changed?? or motion of electron can somehow change ω?)

The interaction of an electron with two rigid molecules is described by the 'electronic' part of the Hamiltonian

$$H_e = -\frac{\nabla^2}{2m} + V(\mathbf{r}-\mathbf{l}_1) + V(\mathbf{r}-\mathbf{l}_2), \tag{1.101}$$

where $\mathbf{l}_{1,2}$ are site coordinates, and the interaction term is

$$V(\mathbf{r}-\mathbf{l}) = v(\mathbf{r}-\mathbf{l}-\mathbf{a}/2) - v(\mathbf{r}-\mathbf{l}+\mathbf{a}/2) \tag{1.102}$$

(write the formula for v!)

in case of the molecules consisting of two ions with the opposite charge (this is why there is a minus in front of the second term) (why do we need different sign? how realistic is it? why would they just not collapse, if they are of different sign?) and the equilibrium distance a between them, Fig.1.1.

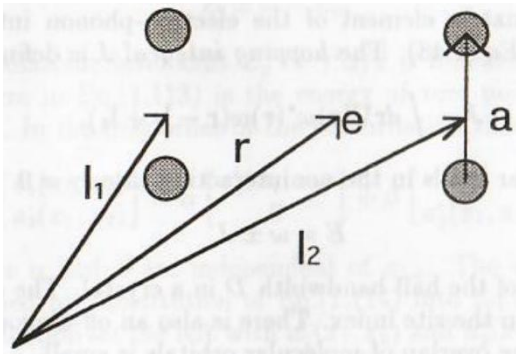

Fig.1.1. Two-site one-electron Holstein model.

And finally, the electron-phonon interaction with a stretching molecular mode is a linear function of the displacements

$$H_{e-ph} = -\sum_{i=1,2} \frac{x_i}{2} \frac{\partial}{\partial x} \left[v\left(\mathbf{r} - \mathbf{l}_i - \mathbf{a}/2\right) + v\left(\mathbf{r} - \mathbf{l}_i + \mathbf{a}/2\right) \right]. \tag{1.103}$$

(this is a term like $x \cdot F$, so we find force from the energy by a derivative.) (discuss with Viktor it ones again!! I forgot why 1/2 is really here, because of change of some parameter of differentiation...)

The state of the system is expressed as a linear superposition

$$|\mathbf{r}, x_1, x_2\rangle = \sum_{i=1,2} a_i\left(x_1, x_2\right) w\left(\mathbf{r} - \mathbf{l}_i\right) \tag{1.104}$$

of electron wave functions, $w(\mathrm{r} - \mathbf{l})$ each localised about particular molecular site $\mathbf{l}$ and assumed to be normalised and orthogonal.

If the molecules are separated by a large distance these Wannier (site) wave functions are molecular orbitals satisfying the Schrödinger equation for an isolated molecule

$$\left(-\frac{\nabla^2}{2m} + V(\mathbf{r})\right) w(\mathbf{r}) = 0 \tag{1.105}$$

where the electron energy of a rigid molecule is taken to be zero (so it means that the conducting electron can take the form of the one that connects these molecules.)(right?). (why can we just take like this energy of conducting electron equal to zero???)

Equations for the $a_i\left(x_1, x_2\right)$ are obtained by substitution of Eq.(1.104) into the Schrödinger equation of the system with the complete Hamiltonian

$$H_e + H_{e-ph} + H_{ph}$$

followed by multiplication on the left with $w^*\left(\mathrm{r} - \mathrm{l}_i\right)$ and integration over the electron coordinate, r. (do this transformation, maybe it is easy?)

This procedure gives

$$\left[E + \frac{1}{2M}\left(\frac{\partial^2}{\partial x_1^2} + \frac{\partial^2}{\partial x_2^2}\right) - \frac{M\omega^2\left(x_1^2 + x_2^2\right)}{2} - \gamma\omega\sqrt{M\omega}x_1\right] a_1\left(x_1, x_2\right) = -J a_2\left(x_1, x_2\right), \tag{1.106}$$

$$\left[E + \frac{1}{2M}\left(\frac{\partial^2}{\partial x_1^2} + \frac{\partial^2}{\partial x_2^2}\right) - \frac{M\omega^2\left(x_1^2 + x_2^2\right)}{2} - \gamma\omega\sqrt{M\omega}x_2\right] a_2\left(x_1, x_2\right) = -J a_1\left(x_1, x_2\right), \tag{1.107}$$

where

$$\gamma = -\frac{1}{2\omega\sqrt{M\omega}} \int d\mathbf{r} |w(\mathbf{r})|^2 \frac{\partial}{\partial x} [v(\mathbf{r} - \mathbf{a}/2) + v(\mathbf{r} + \mathbf{a}/2)] \tag{1.108}$$

is the dimensionless matrix element of the electron-phonon interaction as in the Fröhlich Hamiltonian, Eq.(1.48) (where there was $\gamma(\mathbf{q}) = -i\frac{N\mathbf{e_q}\cdot\mathbf{q}}{\sqrt{M\omega_\mathbf{q}^3}} v_\mathbf{q}$).

(how solutions for $w(r)$ can look for example? then one can plug them here and get the value of γ)

The hopping integral J is defined as

$$J = \int d\mathbf{r} V(\mathbf{r}) w^*(\mathbf{r}) w(\mathbf{r} - \mathbf{l}_2 + \mathbf{l}_1) \tag{1.109}$$

(I think, there shouldn't be many problems in evaluation of this equation, if we know the w...)

There are two molecular levels (options for total levels of the system) in the noninteracting case, $\gamma = 0$

$$E = \omega \pm J$$

with $2J$ playing a role of the half bandwidth D in a crystal.

The matrix element γ is diagonal with respect to the site index. (why? it is just a number, no? or is it at all correct formula for γ, because there are no sites in it?)

There is also an off-diagonal matrix element, which is negligible if the overlap of molecular orbitals is small (and where does it come from?).

The strong coupling condition $\lambda > 1$ corresponds to $\gamma^2 > 4J/\omega$. (why???) (it means that there is an input of two constants: ω and some positions of molecules, which through w give the constant of model J. We compare it with some λ from the very different model.)

Two limiting methods are available for the treatment of the system of two coupled differential equations (1.106, 107) in this strong-coupling regime; the perturbation and the adiabatic approaches, valid in the case of large or small adiabatic parameter ω/J, respectively.

(why does this models describe only small polarons????)

6.2.8 1.6 Nonadiabatic small polaron

(how physically we understand the word "nonadiabatic" for this model???)

Theory

(we try to solve equations

$$\left[E + \frac{1}{2M}\left(\frac{\partial^2}{\partial x_1^2} + \frac{\partial^2}{\partial x_2^2}\right) - \frac{M\omega^2(x_1^2 + x_2^2)}{2} - \gamma\omega\sqrt{M\omega}x_1\right] a_1(x_1, x_2) = -Ja_2(x_1, x_2), \tag{1.106}$$

$$\left[E + \frac{1}{2M}\left(\frac{\partial^2}{\partial x_1^2} + \frac{\partial^2}{\partial x_2^2}\right) - \frac{M\omega^2(x_1^2 + x_2^2)}{2} - \gamma\omega\sqrt{M\omega}x_2\right] a_2(x_1, x_2) = -Ja_1(x_1, x_2), \tag{1.107}$$

)

In the perturbation (meaning "perturbative"?) nonadiabatic approach the lattice moves fast and the electron slow. (why is it connected to the J at all????) Then one can take $J = 0$ in zero approximation with two degenerate eigenstates $a^{l,r}$, corresponding to the polaron 'sitting' on the 'left' a^l and on the 'right' a^r molecule, Fig.1.2 (no, I don't understand intuition behind these formulas. These are gaussian functions, no dynamics... but why do we have 4 functions??)

$$a_1^l\left(x_1,x_2\right)=\exp\left[-\frac{M\omega}{2}\left(\left(x_1+\frac{\gamma}{\sqrt{M\omega}}\right)^2+x_2^2\right)\right];\qquad a_2^l\left(x_1,x_2\right)=0 \tag{1.111}$$

and

$$a_1^r\left(x_1,x_2\right)=0;\qquad a_2^r\left(x_1,x_2\right)=\exp\left[-\frac{M\omega}{2}\left(\left(x_2+\frac{\gamma}{\sqrt{M\omega}}\right)^2+x_1^2\right)\right] \tag{1.112}$$

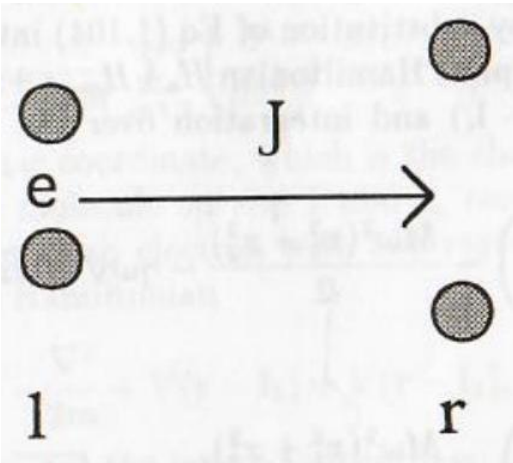

Fig.1.2. Zero-order deformation of the molecules.

The electron-phonon interaction leads to the shrinking of the molecular size (why??)by the value $\gamma/\sqrt{M\omega}$ and to the lowering of the molecular level by the polaronic level shift

$$E\simeq\omega-E_p. \tag{1.113}$$

We note that the polaronic level shift $E_p=\gamma^2\omega/2$ (where was it obtained?) is independent of the molecular mass.

The first term in Eq.(1.113) is the energy of zero point fluctuations of two vibrating molecules.

In the first order of the perturbation theory

$$\left[\begin{array}{c}a_1\left(x_1,x_2\right)\\a_2\left(x_1,x_2\right)\end{array}\right]=\alpha\left[\begin{array}{c}a_1^l\left(x_1,x_2\right)\\0\end{array}\right]+\beta\left[\begin{array}{c}0\\a_2^r\left(x_1,x_2\right)\end{array}\right]. \tag{1.114}$$

Here the coefficients α and β are independent of $x_{1,2}$. The standard secular equation for E is obtained by substitution of Eq.(1.114) into Eq.(1.106) and Eq.(1.107) followed by multiplication on the left with $a_1^l\left(x_1,x_2\right)$ and $a_2^r\left(x_1,x_2\right)$, respectively and integration over the vibration coordinates, $x_{1,2}$. The result is

$$\det\left|\begin{array}{cc}E-\omega+E_p & \tilde{J}\\ \tilde{J} & E-\omega+E_p\end{array}\right|=0 \tag{1.115}$$

with the renormalised hopping integral

$$\tilde{J}=J\frac{\int dx_1\int dx_2 a_1^l\left(x_1,x_2\right)a_2^r\left(x_1,x_2\right)}{\int dx_1\int dx_2\left|a_1^l\left(x_1,x_2\right)\right|^2}. \tag{1.116}$$

The corresponding eigenvalues, $E_{\pm}$are

$$E_{\pm} = \omega - E_p \pm \tilde{J} \tag{1.117}$$

The hopping integral splits the molecular level. The effective 'bandwidth' is significantly reduced compared with the bare one

$$\tilde{J} = Je^{-g^2} \tag{1.118}$$

where $g = \gamma/\sqrt{2}$. The origin of the polaron band narrowing e^{-g^2} lies in a small overlap integral, Eq.(1.116) of two displaced oscillator wave functions a_1^l and a_2^r. This effect is beyond the large-polaron approximation.

6.2.9 1.7 Adiabatic small polaron

(how physically we understand the word "adiabatic" for this model???)

Theory

In the adiabatic approach when $J \gg \omega$, one assumes a wave function of the form

$$\begin{pmatrix} a_1(x_1, x_2) \\ a_2(x_1, x_2) \end{pmatrix} = \chi(x_1, x_2) \begin{pmatrix} \psi(x_1, x_2) \\ \phi(x_1, x_2) \end{pmatrix} \tag{1.119}$$

where ψ and ϕ are solutions of the 'electronic' hopping Hamiltonian with a frozen molecular deformation $x_{1,2}$

$$\begin{pmatrix} E(x_1, x_2) - \gamma\omega\sqrt{M\omega}x_1 & J \\ J & E(x_1, x_2) - \gamma\omega\sqrt{M\omega}x_2 \end{pmatrix} \begin{pmatrix} \psi(x_1, x_2) \\ \phi(x_1, x_2) \end{pmatrix} = 0. \tag{1.120}$$

The lowest eigenvalue of Eq.(1.120) is of interest in the adiabatic approximation

$$E(x_1, x_2) = \frac{\gamma\omega\sqrt{M\omega}(x_1 + x_2)}{2} - \left[\frac{\gamma^2 M\omega^3 (x_1 - x_2)^2}{4} + J^2\right]^{1/2} \tag{1.121}$$

As is known, $E(x_1, x_2)$ plays the role of a potential energy term in the equation for the 'vibration' wave function, $\chi(x_1, x_2)$, which reads

$$\left[E + \frac{1}{2M}\left(\frac{\partial^2}{\partial x_1^2} + \frac{\partial^2}{\partial x_2^2}\right) - \frac{M\omega^2(x_1^2 + x_2^2)}{2} - E(x_1, x_2)\right]\chi(x_1, x_2) = 0. \tag{1.122}$$

Terms with the first and second derivatives of the 'electronic' functions ψ and ϕ are small compared with the corresponding terms with the derivatives of χ for the case in hand. The transformation

$$X = \frac{x_1 + x_2}{2}, x = x_2 - x_1 \tag{1.123}$$

leads to a product solution of the form $\chi(x_1, x_2) = F(X)\chi(x)$, where $F(X)$ is the ground state of a harmonic oscillator in the presence of a constant force $\gamma\omega\sqrt{M\omega}$ with the ground state energy $(\omega - E_p)/2$. The equation for $\chi(x)$ is

$$\left[E + \frac{E_p}{2} - \frac{\omega}{2} + \frac{1}{2\mu}\frac{\partial^2}{\partial x^2} - U(x)\right]\chi(x) = 0 \tag{1.124}$$

where $\mu = M/2$ and

$$U(x) = \frac{\mu\omega^2 x^2}{2} - \left[E_p \mu\omega^2 x^2 + J^2\right]^{1/2} \tag{1.125}$$

The potential energy of the problem $U(x)$ consists of two symmetrical potential wells, separated by a barrier, Fig.1.3.

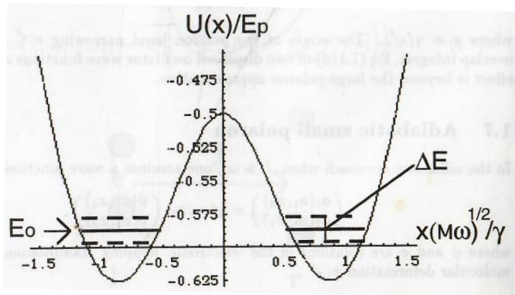

Fig.1.3. Double well potential of the adiabatic Holstein model for $\lambda = 1$.

Minima are located at

$$x_{\min} = \pm\sqrt{\frac{E_p}{\mu\omega^2}\left(1 - \frac{1}{4\lambda^2}\right)} \tag{1.126}$$

and have the common value

$$U_{\min} = -\frac{E_p}{2}\left(1 + \frac{1}{4\lambda^2}\right). \tag{1.127}$$

The barrier height is $-(J + U_{\min})$. If the barrier were impenetrable, there would be the ground state energy level E_0, the same for both wells. To determine its position one can expand the potential near the minimum as

$$U(x) \simeq U_{\min} + \frac{\mu\tilde{\omega}^2 (x - x_{\min})^2}{2} \tag{1.128}$$

where

$$\tilde{\omega} = \omega\sqrt{1 - \frac{1}{4\lambda^2}}. \tag{1.129}$$

Then the system is a harmonic oscillator with the renormalised frequency $\tilde{\omega}$ and the ground state energy

$$E_0 - U_{\min} = \frac{\tilde{\omega}}{2} \tag{1.130}$$

The tunneling through the barrier results in the splitting of this level into two, corresponding to states in which electron moves simultaneously in both wells. This is a well known double well potential problem, which can be solved by the quasi-classical technique, if the condition

$$\left|\frac{d}{dx}\frac{1}{p(x)}\right| \ll 1 \tag{1.131}$$

is satisfied. Here $p(x) = \sqrt{2\mu\left[E_0 - U(x)\right]}$ is the classical momentum. Because $\omega \ll J < E_p$ the quasiclassical condition is satisfied practically for all x. The splitting is given by the textbook expression (Landau and Lifshitz (1977))

$$\Delta E = \frac{\tilde{\omega}}{\pi} \exp\left[-2\int_0^a |p(x)|dx\right] \tag{1.132}$$

where $a \simeq x_{\min} - 1/\sqrt{\mu\tilde{\omega}}$ is the classical turning point corresponding to the energy E_0. Fig.1.3. In the extreme strong coupling limit $\lambda \gg 1$ the integral in Eq.(1.132) is

$$\int_0^a |p(x)|dx \simeq \frac{E_p}{2\omega} + \frac{1}{4}\ln\frac{E_p}{\omega} + O(1) \tag{1.133}$$

Omitting a multiplier of the order of unity, one finds

$$\Delta E \sim \sqrt{E_p\omega}e^{-g^2}. \tag{1.134}$$

Holstein found corrections to this expression up to terms of the order of $1/\lambda^2$

$$\Delta E \simeq \sqrt{\frac{4E_p\omega}{\pi}}e^{-\tilde{g}^2} \tag{1.135}$$

where

$$\tilde{g}^2 = g^2\left[1 - \frac{1}{4\lambda^2}\ln(4\lambda) - \frac{1}{8\lambda^2}\right] \tag{1.136}$$

In the strong-coupling limit $\lambda \gg 1$ the exponent in the renormalised bandwidth Eq.(1.135) $(\Delta E \simeq \sqrt{\frac{4E_p\omega}{\pi}}e^{-\tilde{g}^2})$ is the same, as for the nonadiabatic regime, Eq.(1.118) $(\tilde{J} = Je^{-g^2})$ $\tilde{g} = g$.

However, the term in front of the exponent differs from $2J$ for any value of λ. There is also an essential exponential difference between Eq.(1.135) $(\Delta E \simeq \sqrt{\frac{4E_p\omega}{\pi}}e^{-\tilde{g}^2})$ and twice of Eq.(1.118) $(\tilde{J} = Je^{-g^2})$ in the intermediate coupling region, where $\tilde{g}$ differs from g.

As a result the adiabatic small polaron has much lower effective mass for the intermediate coupling compared with that estimated with the nonadiabatic expression (1.118) $(\tilde{J} = Je^{-g^2})$.

It is thus apparent that the perturbation nonadiabatic approach covers only part of the total small polaron region $\lambda \geq 1$. The upper limit of applicability of perturbation theory is given by $J < \sqrt{E_p\omega}$.

For the remainder of this region, the adiabatic Eq.(1.135), rather than the perturbation approach is to be employed.

Finally, using the expression for the minima position $x_{\min}$ of the double well potential, Eq.(1.126) one can determine the critical value of λ at which the transition to small adiabatic polaron is expected.

The double well disappears when $x_{\min} = 0$ and $\lambda = \lambda_c = 0.5$. At this coupling the renormalised phonon frequency $\tilde{\omega}$ is zero as one can see from Eq.(1.129).

6.2.10 Holstein's Studies of Polaron Motion. Part I. The Molecular-Crystal Model

Holstein T 1959 Ann.Phys. 8, 325-42; ibid p. 343-89

Abstract

In this paper is described a model for polaron motion which incorporates, in simplified form, the principal physical features of the problem. The (crystalline) medium, within which a single excess electron (or hole) is contained, is taken to be a one-dimensional molecular crystal, consisting of diatomic molecular sites; each site possesses a single vibrational degree of freedom, represented by the deviation, x_n, of its

internuclear separation from equilibrium. The motion of the electron in this medium is treated by a tight-binding approach, in which the wave function is represented as a superposition of local "molecular" functions, $\phi(\mathbf{r} - n\mathbf{a}, x_n)$. In line with the x_n dependence of the ϕ 's, it is also assumed that the "local" electronic energy, E_n, (which, in the conventional tight-binding theory, has one and the same value for all sites) depends (linearly) on x_n. This dependence gives rise to electron-lattice interaction; alternatively, it may be regarded as removing the electronic translational degeneracy, characteristic of the undistorted crystal, and thereby providing the possibility for electron trapping.

On the basis of the above-described model, the zeroth order adiabatic treatment of the polaron problem is developed. For values of the parameters such that the linear dimension of the polaron is large compared to a lattice spacing ("large" polaron), an exact solution is obtained; the correspondence between it and Pekar's zeroth-order solution is established. The conditions under which the size of the polaron becomes comparable to a lattice spacing ("small" polaron) are discussed. Finally, by way of exhibiting the relationship of the molecular-crystal concept to the real situation, a description is given of an alternate molecular-crystal model which, in the case of the large polaron, is completely equivalent to the continuum-polarization model of conventional polaron theory.

Theory

This note presents a description of a one-dimensional molecular-crystal model which will form the basis for a number of studies of the polaron problem, to be reported subsequently. [1] It is felt that the model, although physically different

from the cases encountered in practice, corresponds conceptually to them in sufficient degree, so as to merit investigation.

Let us first recall the principal features of the real polaron problem. The physical situation is that of a slow electron (or hole) in an insulating crystal. The Hamiltonian of the system may be regarded as a sum of three terms, H_e, H_L, and H_{int} .H_e, the electronic component, consists of the kinetic energy of the electron and the effective one-electron periodic potential. H_L, the lattice component, is the sum of the kinetic energy of the lattice particles and the lattice potential energy; the latter is taken as a known (invariably quadratic) function of the particle displacements from their equilibrium positions. Finally, H_{int} , the electron-lattice interaction, is a function of the electron coordinate and the lattice displacements; the latter dependence is usually assumed to be linear.

In the standard theory of the motion of slow electrons in insulating crystals, H_{int} is treated as a small perturbation, giving rise to electronic transitions (scattering) in which lattice-vibration quanta are simultaneously absorbed or emitted. The basic problem of polaron theory is that H_{int} is often too large to be treated as a perturbation, but must be considered in zeroth order. Probably the most important physical concept of the theory is that of "self-trapping" of the electron. Qualitatively, this may be understood as follows.

Let us imagine that an electron is momentarily fixed at some point of the crystal. As a result of electron-lattice interaction, the surrounding lattice particles will be displaced to new equilibrium positions; according to general mechanical principles, the "induced" displacements will be such as to provide a potential "well" for the electron. If the well is sufficiently deep, the electon will occupy a bound state, unable to move unless accompanied by the well, that is to say, by the induced lattice-deformation. The unit consisting of the electron, together with its induced lattice deformation, is called the "polaron." [2]

With these preliminaries out of the way, the molecular-crystal model may now be described.

[01] As exemplified by the following paper (to be referred to hereafter as II), these studies will be focussed primarily on the case of the "small" polaron, whose linear dimensions are of the order of a lattice-spacing.

In the absence of the electron, the system is taken to be a linear chain of N identical diatomic molecules, whose orientations and centers of gravity are fixed, but whose internuclear separations are allowed to vary. The "latticevibrations" thus consist of the vibrations of the individual internuclear separations. For the time being, the latter will be assumed, in the absence of the electron, to be uncoupled. If, in addition, the potential energy curve of an individual molecule be assumed parabolic, the lattice Hamiltonian reads

$$H_L = \frac{1}{2M}\sum_{n=1}^{N} {p_n}^2 + \frac{1}{2}\sum_{n=1}^{N} M{\omega_0}^2{x_n}^2, \tag{1}$$

where x_n is the deviation of a typical internuclear separation from its equilibrium value, $p_n \equiv (\hbar/i)\partial/\partial x_n$ is the associated canonical momentum, M the relative mass, and ω_0 the harmonic vibration frequency. [3]

The motion of a single electron (or hole) in the above-described onedimensional molecular-crystal medium will here be formulated in terms of the tight-binding approximation. The details of this formulation are presented in Appendix I; the principal features are as follows. The state of the system is expressed as a linear superposition

$$\psi\left(\mathbf{r}, x_1, \cdots, x_n\right) = \sum a_n\left(x_1, \cdots, x_n\right)\phi\left(\mathbf{r} - n\mathbf{a}, x_n\right), \tag{2}$$

of "molecular" electron wave functions, $\phi\left(\mathbf{r} - n\mathbf{a}, x_n\right)$, each localized about a particular (n th) molecular site ($\mathbf{a}$ is a unit lattice vector) and depending upon the internuclear coordinate, x_n, of that site. The coefficients of the superposition, $a_n\left(x_1, x_2, \cdots, x_N\right)$, are each functions of all the internuclear coordinates, x_1, $x_2, \cdots, x_N$. The equations which they obey are obtained from the time-dependent Schrödinger equation of the system by a standard "projection" procedure. With approximations appropriate to the tight-binding case (smallness of overlap and nonorthogonality integrals) and to the large mass ratio of electrons and nuclei, they take the form (see I-16)

$$\begin{aligned}&\left[i\hbar\frac{\partial}{\partial t} - \sum_m\left(-\frac{\hbar^2}{2M}\frac{\partial^2}{\partial x_m^2} + \frac{1}{2}M\omega_0^2 x_m^2\right) - E\left(x_n\right) - W\left(x_1, \cdots, x_n\right)\right] \\ &\times a_n\left(x_1, \cdots, x_n\right) = \sum_{(\pm)} J\left(x_n, x_{n\pm1}\right) a_{n\pm1}\left(x_1, \cdots, x_n\right)\end{aligned} \tag{3}$$

where the sum on the right-hand side goes over the two neighbors of a given nth site. The quantities $E\left(x_n\right), W_n\left(x_1, \cdots, x_N\right)$, and $J\left(x_n, x_{n\pm1}\right)$ are defined by appendix equations (I-3), (I-14), and (I-15), respectively. Physically, $E\left(x_n\right)$ is the electron energy of an isolated "molecular-ion," i.e., of the system of the electron and an isolated molecule; in conformance with standard concepts of molecular theory, it is to be regarded as a function of the internuclear displacement coordinate of the molecule. $W_n\left(x_1, \cdots, x_N\right)$ represents the perturbation on $E\left(x_n\right)$ due to the presence of the other molecules. Finally, the $J\left(x_n, x_{n\pm1}\right)$ are overlap integrals, depending on the ϕ 's of typical neighbor sites $n, n\pm1$, and are hence functions of the internuclear coordinates x_n and $x_{n\pm1}$ of these sites.

Let us at this point note that, if the internuclear coordinates are all "frozen"

[3] In some studies (e.g., II), coupling terms of the form

[02] The term owes its origin to the circumstance that the problem was first considered for the case of polar crystals, in which the interaction of the electron with the optical polarization modes is especially strong. However, in principle, the self-trapping phenomenon is not limited to polar crystals, but may apply to any medium in which H_{int} is sufficiently strong, relative to H_e and H_{L}.

$$H_c \equiv 1/2M\omega_1^2\Sigma_{n=1}^N x_n x_{n+1},$$

will be introduced into (1). It may be remarked here that the neglect of coupling is a simplification of a type comparable to that often employed in treatments of polaron theory, in which the actual optical frequency spectrum of a polar crystal is replaced by a single frequency (Einstein model).
at one and the same value, say x, the system becomes equivalent to the conventional atomic tight-binding case, in which the localized states, $\phi(\mathbf{r} - n\mathbf{a}, x)$ form a degenerate set. Then, by virtue of the translational symmetry of the system, the stationary solutions of (3) take the standard form

$$a_n^{(k)} = e^{ikn} \tag{4}$$

with eigenvalues

$$E_k' = E(x) + W + (N/2)M\omega_0^2 x^2 - 2J\cos k \tag{5}$$

[where $W = W(x, x, \cdots)$ and where $J(x_n, x_{n\pm1})$ is set equal to a negative constant, $-J$, in recognition of the fact that the potential, $U(\mathbf{r} - n\mathbf{a}, x_n)$, which enters into the overlap integral, (I-15), is intrinsically negative], and group velocities

$$V_K = \frac{a}{\hbar}\frac{\partial E_k}{\partial k} = -\frac{2Ja}{\hbar}\sin k \tag{6}$$

The system thus exhibits typical band character; in particular, at the band extrema ($k = 0, \pi$), the motion may be described in terms of an effective mass

$$m^* \equiv \left(\frac{a}{\hbar}\frac{\partial v_k}{\partial k}\right)^{-1} = \pm\hbar^2/2Ja^2 \tag{7}$$

In proceeding further, it is desirable to introduce a number of simplifications into (3). These are:
(a) The neglect of the energies, $W_n(x_1, \cdots, x_N)$.
(b) The neglect of the x-dependence of the $J(x_n, x_{n\pm1})$; this simplification means that the $J(x_n, x_{n\pm1})$ are all to be taken equal to a single constant, $-J$.
(c) The x-dependence of $E(x_n)$ is taken to be linear, i.e.,

$$E(x_n) = -Ax_n \tag{8}$$

(the sign being chosen negative, and the additive energy constant being set equal to zero, both in the interests of notational convenience).

The physical significance of (a) is that, when the electron is localized on a given molecular site, the perturbation of its expectation-energy due to the potentials of other molecules is assumed small-an assumption which is appropriate to the tight-binding case. Its employment has the effect of restricting the x-dependence of the expectation-energy of a localized electron to a single coordinate, x_n-that of the occupied site. This restriction appears to be a special feature of the molecular-crystal model; in particular, it does not apply to the real situation, in which the energy of a localized electron depends upon lattice displacements at a number of more or less neighboring sites. However, at the present time, it is not at all established whether this difference is significant, as far as physical results are concerned. In fact, the point of view of the present studies is
that such questions will best be answered by a systematic consideration of various hypothetical cases, starting with the simplest. In the spirit of this approach, $W_n(x_1, \cdots, x_N)$ will be neglected, as a suitable first step.

Similarly, the procedure of taking the J 's equal to a constant may be inapplicable in some cases. In principle, the J 's do depend on the x 's mainly via the local wave functions, $\phi\left(\mathrm{r}-n\mathrm{a}, x_n\right)$; however, as will be seen, e.g., in II, the primary physical property of the J 's is their order of magnitude relative to other energies. Hence, at least in the initial phases of the program, their x-dependence will be neglected. Finally, with regard to assumption (c), it may be pointed out that the term $E\left(x_n\right)$ plays the role of electron-lattice interaction; its approximation by (8) leads to a linear dependence of this interaction of the lattice-vibration coordinates, a feature which is characteristic of all treatments of the problem (known to the present author).

With the simplifications discussed above-namely, the neglect of the W 's, the equating of the J 's to a constant $(-J)$, and the use of (1.13), the equations of "motion," (1.3) reduce to

$$\left[i\hbar\frac{\partial}{\partial t}-\sum_m\left(-\frac{\hbar^2}{2M}\frac{\partial^2}{\partial {x_m}^2}+\frac{1}{2}M{\omega_0}^2{x_m}^2\right)+Ax_n\right]a_n\left(x_1,\cdots,x_n\right)+J\left(a_{n+1}+a_{n-1}\right)=0 \quad (9)$$

Equation (9) will form the basis for a number of studies of the polaron problem (the first of which is presented in II). These studies will be focussed primarily on the case of the "small" polaron, the linear dimensions of which are of the order of a lattice spacing. For introductory purposes, it will be convenient at this time to discuss the alternate case of the "large" polaron. In this case, the linear dimensions of the polaron are sufficiently large compared to a lattice spacing so that the "wave function," $a_n\left(x_1,\cdots,x_n\right)$ may be taken to a be a continuous, differentiable function of a continuous position variable, with, e.g.,

$$a_{n+1}=a_n+\frac{\partial a_n}{\partial n}+\frac{1}{2}\frac{\partial^2 a_n}{\partial n^2} \quad (10)$$

The present discussion will be concerned with the adiabatic theory of the large polaron as developed by Pekar (1). Specifically, it will be found that the "molec-ular-crystal" analog of the Pekar-type adiabatic solution (see Ref. 1, Chapter II)-i.e., that solution which, with neglect of the vibrational kinetic energy, minimizes the sum of electronic and vibrational potential energies-may be obtained exactly in closed form.

The starting-point is the system of equations

$$E\left(x_1,\cdots,x_N\right)a_n\left(x_1,\cdots,x_N\right)=\left(1/2\sum_m M\omega_0^2x_m^2-Ax_n\right)a_n\left(x_1,\cdots,x_N\right)-J\left(a_{n-1}+a_{n-1}\right) \quad (11)$$

which, subject to the neglect of the vibrational kinetic energy operator,

$$-\frac{\hbar^2}{2\bar{M}}\sum_m\frac{\partial^2}{\partial x_m^2}$$

is the stationary equivalent of (9). Here, the energy eigenvalue, $E\left(x_1,\cdots,x_N\right)$, is a parametric function of the vibration coordinates, $x_1,\cdots,x_N$; one seeks those values, $x_N^{(0)},\cdots,x_1^{(0)}$, for which $E\left(x_1,\cdots,x_N\right)$ is a minimum.

Upon multiplying (11) by ${a_n}^*$ and summing over n, one obtains

$$E\left(x_1,\cdots,x_N\right)=1/2\sum_m M\omega_0^2x_m^2-\sum_n Ax_n\mid a_n\mid^2 + \sum_n J\left(a_{n-1}+a_{n+1}\right)a_n^* \quad (12)$$

where use has been made of the normalizing condition

$$\sum_n |a_n|^2 = 1 \tag{13}$$

Upon differentiating (12) with respect to a given vibrational coordinate, x_p [account being taken of (13) by the introduction of a Lagrange multiplier, λ] and rearranging the summations in the J-proportional terms, one obtains

$$\begin{aligned}\frac{\partial E(x_1,\cdots,x_N)}{\partial x_p} =& M\omega_0^2 x_p - A|a_p|^2 \\ &+ \sum_n \frac{\partial a_n^*}{\partial x_p}\left[-Ax_n a_n - J(a_{n-1}+a_{n+1}) + \lambda a_n\right] \\ &+ \sum_n \frac{\partial a_n}{\partial x_p}\left[-Ax_n a_n^* - J\left(a_{n-1}^*+a_{n+1}^*\right) + \lambda a_n^*\right]\end{aligned} \tag{14}$$

(plus "boundary" terms, proportional to products of the a_n 's at $n=0$ and $n=N$, which, as verified below, may be assumed to vanish). One now substitutes (11) and its complex conjugates into the first and second square brackets of (14), respectively, obtaining for the last two terms of (14) the expression.

$$\left[E(x_1,\cdots,x_N) - \frac{1}{2}\sum_m M\omega^2 x_m^2 + \lambda\right]\sum_n\left(a_n\frac{\partial a_n^*}{\partial x_p} + a_n^*\frac{\partial a_n}{\partial x_p}\right)$$

which is obviously zero because of (13). Equation (14) then reduces to

$$\frac{\partial E(x_1,\cdots,x_N)}{\partial x_p} = M\omega_0^2 x_p - A|a_p|^2 . \tag{15}$$

Upon setting the right-hand side of (15) equal to zero for all p, one obtains for the $x_p^{(0)}$ the relations

$$x_p^{(0)} = \frac{A\left|a_p^{(0)}\right|^2}{M\omega_0^2} \tag{16}$$

where $a_p^{(0)}$ is that solution of (11) which corresponds to $x_n = x_n^{(0)}$. Upon substituting (16) into (11), and introducing the quantity

$$-\epsilon \equiv E(x_1,\cdots,x_N) - 1/2\sum_m M\omega_0^2 x_m^{(0)^2} + 2J \tag{17}$$

one obtains

$$\left(\frac{A^2}{M\omega_0^2}|a_n|^2 - \epsilon\right)a_n + J(a_{n+1}+a_{n-1}-2a_n) = 0 \tag{18}$$

where the superscript, "(0)," has been dropped with the understanding that a_n will henceforth denote that solution of (11) for which $E(x_1,\cdots,x_N)$ is a minimum.

At this point it is desirable to make use of the "continuum" approximation, (10) (the applicability of which, as discussed above, characterizes the case of the large polaron). The introduction of (10) into (18) yields

$$\left(\frac{A^2}{M\omega_0^2}\left|a_n\right|^2-\epsilon\right)a_n+J\frac{\partial^2 a_n}{\partial n^2}=0 \tag{19}$$

Upon multiplying (19) and its complex conjugate with $\partial {a_n}^*/\partial n$ and $\partial a_n/\partial n$, respectively, and adding, one obtains

$$\frac{A^2}{2M\omega^2}\left|a_n\right|^4-\epsilon\left|a_n\right|^2+J\frac{\partial a_n}{\partial n}\frac{\partial a_n^*}{\partial n}=C_1 \tag{20}$$

where C_1 is a constant to be determined presently.
In proceeding further, it is expedient to write a_n in the form

$$a_n=b_n e^{i\beta_n} \tag{21}$$

where b_n and β_n are real (and b_n positive, as well). Introducing (21) into (19), and equating real and imaginary parts to zero, one finds for the imaginary part

$$2\frac{d\beta_n}{dn}\frac{db_n}{dn}+b_n\frac{d^2\beta_n}{dn^2}=0 \tag{22}$$

a first integration of which yields

$$\frac{d\beta_n}{dn}b_n^2=C_2 \tag{23}$$

where C_2 is another constant, which will now be shown to vanish.
Introducing (21) and (22) into (20), one has

$$\frac{A^2}{2M\omega_0^2}b_n^4-\epsilon {b_n}^2+J\left[\left(\frac{db_n}{dn}\right)^2+\frac{C_2^2}{b_n^2}\right]=C_1$$

At this point, let us impose the condition that b_n differs from zero only in a limited region of the specimen, so that as $|n|\to\infty, b_n\to 0$ and $db_n/dn\to 0$. It is then immediately seen that, in order for this condition to be obeyed, it is necessary that both C_2 and C_1 vanish. One thus arrives at the result that β_n is equal to a constant (which may for convenience be set equal to zero, so that $b_n=a_n$) and (23) reduces to

$$\frac{A^2}{2M\omega_0^2}{a_n}^4-\epsilon a_n^2+J\left(\frac{da_n}{dn}\right)^2=0. \tag{24}$$

Introducing the notations

$$\alpha^2=\frac{A^2}{2M\omega_0^2 J}, \tag{25}$$

$$\gamma^2\equiv\epsilon/J, \tag{26}$$

one may write (24) in the form

$$\frac{da_n}{dn}=\pm a_n\left(\gamma^2-\alpha^2 a_n^2\right)^{1/2} \tag{27}$$

The integration of (27) is straightforward, the result being

$$a_n=\frac{\gamma}{\alpha}\operatorname{sech}\left[\gamma\left(n-n_0\right)\right] \tag{28}$$

where n_0 is a constant of integration, indicative of the fact that the centroid of the polaron may be located at an arbitrary point in the specimen.

The application to (28) of the normalizing condition, which in the continuum approximation, reads

$$\int a_n^2 dn = 1$$

yields the relation

$$\gamma = \alpha^2/2 = \frac{A^2}{4M\omega_0^2 J} \tag{29}$$

so that

$$a_n = \left(\frac{A^2}{8M\omega_0^2 J}\right)^{1/2} \operatorname{sech}\left[\left(\frac{A^2}{4M\omega_0^2 J}\right)(n-n_0)\right] \tag{30}$$

and

$$\epsilon = \frac{1}{16J}\left(A^2/M\omega_0^2\right)^2. \tag{31}$$

Inserting (31) and (16) into (17), one has for the total energy (exclusive, of course, of the vibrational kinetic energy)

$$\begin{aligned} E\left(x_1^{(0)},\cdots,x_N^{(0)}\right) \equiv & E^{(0)} = -2J - \frac{1}{16J}\left(A^2/M\omega_0^2\right)^2 \\ & + \frac{1}{2}M\omega_0^2\left(\frac{A^2}{M\omega_0^2}\right)^2 \int a_n^4 dn \\ = & -2J - \frac{1}{16J}\left(\frac{A^2}{M\omega_0^2}\right)^2 + \frac{1}{24J}\left(\frac{A^2}{M\omega_0^2}\right)^2 \\ = & -2J - \frac{1}{48J}\left(\frac{A^2}{M\omega_0^2}\right)^2 \end{aligned} \tag{32}$$

It should at this point be noted that (20) has an alternate solution, namely, the one which was excluded by the requirement [stated in the paragraph subsequent to (23)] that $a_n \to 0$ as $|n| \to \infty$. If this condition be withdrawn, (20) is also solved by

$$a_n = N^{-1/2} e^{ikn} \tag{33}$$

with

$$\epsilon = -Jk^2 \tag{34}$$

(plus the term $(1/N)\left(A^2/M{\omega_0}^2\right)$ which is to be discarded, since it is of order N^{-1}). Inserting (34) into (17), and continuing to discard terms of order N^{-1}, one has

$$E\left(x_1^{(B)},\cdots,x_N^{(B)}\right) \equiv E^{(B)} = -2J + Jk^2 \tag{35}$$

where the superscript, (B), is used in recognition of the fact that (33) is an unbounded, "band-type," solution of the form discussed earlier [see Eq. (4) and subsequent].

The minimum energy for the band-type solution is attained when $k = 0$, and is

$$E_{\min}^{(B)} = -2J \tag{36}$$

Comparing (36) with (32), we observe that the energy of the bound state is lower than that of the free state by an amount

$$E_p = \frac{1}{48J}\left(A^2/M\omega_0^2\right)^2 \tag{37}$$

E_p may be considered to be the zeroth order binding energy of the large polaron, i.e., the binding energy obtained in the approximation in which the vibrational kinetic energies are neglected. [4]

With the aid of (30), explicit formulas may be obtained for a number of physical properties of the large polaron state.

(a) The equilibrium vibrational displacement, $x_n^{(0)}$, given by (17) and (30), is

$$x_n^{(n)} = \frac{A}{M\omega_0^2}\frac{A^2}{8M\omega_0^2 J}\operatorname{sech}^2\left[\frac{A^2}{4M\omega_0^2 J}(n-n_0)\right]. \tag{38}$$

(b) The potential-well, within which the electron is trapped, is described by the expression

$$V(n) \equiv \frac{A^2}{M\omega_0^2}|a_n|^2 = \frac{\left(A^2/M\omega_0^2\right)^2}{8J}\operatorname{sech}^2\left[\frac{A^2}{4M\omega_0^2 J}(n-n_0)\right]. \tag{39}$$

Its maximum value, achieved at the polaron centroid, n_0, is

$$V_{\max} = \frac{\left(A^2/M\omega_0^2\right)^2}{8J} \tag{40}$$

which is twice the "electronic binding-energy," ϵ, as given by (31), and six times the net binding energy of the polaron, as given by (37). [5]

(c) The linear dimension, L_p, of the large polaron, as may be seen from (30), (38), or (39), is of the order

$$L_p \approx a\left(\frac{4J}{A^2/M\omega_0^2}\right) \tag{41}$$

where a is the lattice spacing. It is in particular to be observed that the condition for the existence of the large polaron, for which $L_p \gg a$, is

$$2J \gg A^2/2M\omega_0^2, \tag{42}$$

i.e., the electronic "bandwidth," $2J$, is to be large compared to $A^2/2M{\omega_0}^2$.

The physical significance of the quantity, $A^2/2M{\omega_0}^2$, may be understood by considering briefly the case of the small polaron, for which the opposite condition

$$2J \ll A^2/2M\omega_0^2 \tag{43}$$

parameter. If, in this "thought-variability," the "restoring-force constant," $M{\omega_0}^2$, be kept fixed, so that the $\omega_0 \propto M^{-1/2}$, E_p gives the polaron binding energy in the limit of $M \to \infty$. It is then apparent that in the further development of the adiabatic theory, higher-order corrections to E_p occur in increasing powers of $1/M$.

[5] It may be remarked in passing that the difference between ϵ and E_p is the energy required to "polarize" the lattice, i.e., it is the work done against the restoring forces, $M{\omega_0}^2 x_n$, in displacing each x_n from zero to $x_n^{(0)}$. Comparison of (31) and (37) demonstrates that two thirds of the gain in electron-lattice interaction energy (as given by ϵ) has to be returned to the lattice in the form of vibrational potential energy, leaving a net binding energy, $\mathrm{E}_p = (1/3)\epsilon$. This

[04] For formal purposes, it is convenient to consider the vibrational mass, M, as a variable

numerological feature is also characteristic of Pekar's solution (see Ref. 1, Chapter II).
holds. In this case (18) is to be solved by a perturbation expansion in powers of J. To the first order in J, the self-consistent solutions are found to be

$$a_n = \delta_{n,n_0} + \frac{J}{A^2/M\omega_0^2}\left[\delta_{n-1,n_0} + \delta_{n+1,n_0}\right] \tag{44}$$

with

$$\begin{aligned} \epsilon &= A^2/M\omega_0^2 - 2J \\ E^{(0)}\left(x_1, \cdots, x_N\right) &= -A^2/2M\omega_0^2 \end{aligned} \tag{45}$$

and n_0 an arbitrary site. Since the minimum energy of the band-type solution is still given by (36), the polaron binding energy is

$$E_p = A^2/2M\omega_0^2 - 2J. \tag{46}$$

From (46) it is seen that the quantity $A^2/2M{\omega_0}^2$ is the maximum binding energy of the polaron, attained in the limit of an infinitely narrow electronic band width ($J = 0$). Both from (41) and (44), it is clear that the ratio of this maximum binding energy to the electronic bandwidth determines the size of the polaron.

MOLECULAR-CRYSTAL POLARIZATION (MCP) MODEL

It is finally of interest to discuss an alternate molecular-crystal model-to be designated as the "Molecular-Crystal Polarization (MCP) Model"-which is closely related to the standard continuum-polarization model, but in addition takes explicit account of the discreteness of crystal structure.

The host crystal of the MCP model is the three-dimensional analog of the onedimensional molecular-crystal described at the beginning of this paper. The lattice vibrations consist, as before, of the internuclear vibrations, x_g, of the individual diatomic molecules; the only difference is that the site-index, $\mathbf{g}$, is now a three-dimensional lattice-site vector. [6]

The interaction term of the MCP model is taken to have the form

$$H_{\text{int}} = -A\sum_{g'} x_{g'}/\left|\mathbf{g} - \mathbf{g}'\right|^2 \tag{47}$$

where the sum goes over $\mathbf{g}' \neq \mathbf{g}$. This basically long-range interaction, which replaces the short-range interaction

$$H_{\text{int}} = -Ax_n = -A\sum_{n'} \delta_{nn'} x_{n'} \tag{48}$$

of the previously discussed one-dimensional model, in effect, invests the displacements, x_g, with a dipolar character; in line with this property, the interaction

is seen to depend on the inverse square of the distance between the electron site, $\mathbf{g}$, and the "dipole" site,$^{\mathbf{g}}$.

The principal difference between (47) and a real electron-dipole interaction is that (47) is a scalar interaction involving a scalar dipole moment, x_g, in place of the vector-dipole moment of the real interaction. However, as will be seen below, this feature does not invalidate the correspondence of the MCP model with the standard continuum-polarization model.

[06] When appearing as subscripts, lattice-site vectors, g, g', etc., will be denoted by lightface roman letters.

Finally, it is necessary to generalize the overlap term of (9) so as to apply to the three-dimensional case. The most obvious such generalization is the replacement of $J\left(a_{n+1}+a_{n-1}\right)$ by

$$J\sum_{h} a_{g+h}$$

where the relative site-vector, h, goes over nearest neighbors.
Introducing these modifications into Eq. (9), one has

$$\left[i\hbar\frac{\partial}{\partial t}-\sum_{g}\left(-\frac{\hbar^2}{2M}\frac{\partial^2}{\partial {x_g}^2}\ +\frac{1}{2}M{\omega_0}^2{x_g}^2\right)+\Lambda\sum_{g}x_{g'}/\left|\mathbf{g}-\mathbf{g}'\right|^2\right] \tag{49}$$
$$\cdot a_g\left(x_p,\cdots,x_N\right)+J\sum_{h}a_{g+h}\left(x_1,\cdots,x_N\right)=0.$$

In order to exhibit the relationship of (49) to the continuum-polarization model, it is desirable to express the vibration coordinates in terms of normal modes. [7]

$$q_k=\left(\frac{2}{N}\right)^{1/2}\sum_{g=1}^{N}x_g\sin(\mathbf{k}\cdot\mathbf{g}+\pi/4) \tag{50}$$

Introducing (50) into (49), one obtains, after some algebra

$$\begin{gathered}\left[i\hbar\tfrac{\partial}{\partial t}-\textstyle\sum_k\left(-\tfrac{\hbar^2}{2M}\tfrac{\partial^2}{\partial {g_k}^2}+\tfrac{1}{2}M\omega_0^2q_k^2\right)+\left(\tfrac{2}{N}\right)^{1/2}A_k\sin(\mathbf{k}\cdot\mathbf{g}+\pi/4)\right]\\ \cdot a_g\left[\cdots q_k\cdots\right]+J\textstyle\sum_g a_{g+h}\left(\cdots q_k\cdots\right)=0\end{gathered} \tag{51}$$

where, with $\mathbf{f}$ a relative site-vector,

$$A_k\equiv A\sum_{f}\cos(\mathbf{k}\cdot\mathbf{f})/f^2 \tag{52}$$

use having been made of the fact that, for the simple monomolecular cubic crystal under consideration, lattice sums involving odd functions of $\mathbf{f}$ vanish.

It will now be noted that, in the continuum approximation (in which $\mathbf{k}$ is to be restricted to magnitudes small compared to those of reciprocal lattice vectors), the sum in (52) may be approximated by an integral, i.e.,

$$A_k\cong A\int\frac{\cos\mathbf{k}\cdot\mathbf{f}}{f^2}d^3\mathbf{f}=2\pi^2A/k \tag{53}$$

Furthermore, in the spirit of the continuum approximation, one may introduce the three-dimensional analog of the expansion (10), i.e.,

$$a_{g+h}=a_g+\sum_{i}h_i\frac{\partial a}{\partial g_i}+\frac{1}{2}\sum_{ij}h_ih_j\frac{\partial^2 a}{\partial g_i^2} \tag{54}$$

which, when substituted into the last term of (51), yields $J{\nabla_g}^2a_g$. The continuum approximation to (51) is thus

[07] For the sake of straightforwardness of enumeration, the sample will be assumed to have the shape of a cube, each side of which has a length equal to $(2G+1)$ lattice spacings (with G integral), so that $N=(2G+1)^3$. The permissible values of the cartesian components of $\mathbf{k}$ are, then, $k_i=2\pi\kappa_i/(2G+1)$, where $-G\leqq\kappa\leqq G$. With these specifications, the transformation given by (50) is orthogonal and hence immediately applicable to (49). It may be remarked here that the particular choice of transformation coefficients, $\sin(\mathbf{k}\cdot\mathbf{g}+\pi/4)$, is the same as that employed by Pekar and Buimistrov (2).

$$ih\frac{\partial}{\partial t} - \sum_k \left(-\frac{\hbar^2}{2M}\frac{\partial^2}{\partial {q_k}^2} + \frac{1}{2}M{\omega_0}^2{q_k}^2 \right)$$
$$+\sum_k \left(\frac{2\pi^2 A}{k}\right) q_k \left(\frac{2}{N}\right)^{1/2} \sin(\mathbf{k}\cdot\mathbf{g}+\pi/4)\Bigg] \tag{55}$$
$$\times\, a_0\left(\cdots q_k \cdots\right) + J{\nabla_0}^2 a_0 = 0$$

In order to bring (55) into a more standard form, it is desirable to introduce dimensionless oscillator coordinates

$$Q_k = \left(\frac{M\omega_0}{\hbar}\right)^{1/2} q_k \tag{56}$$

in terms of which (55) becomes

$$i\hbar\frac{\partial a_a}{\partial t} = H a_g \tag{57}$$

where

$$H = -\frac{\hbar^2}{2m^*}{\nabla_g}^2 + \sum_k \frac{\hbar\omega_0}{2}\left(-\frac{\partial^2}{\partial {Q_k}^2} + {Q_k}^2\right)$$
$$+\sum C_k Q_k \left(\frac{2}{N}\right)^{1/2} \sin(\mathbf{k}\cdot\mathbf{g}+\pi/4) \tag{58}$$

with

$$m^* = \hbar^2/2J \tag{59}$$

and

$$C_k = -\frac{2\pi^2 A}{k}\left(\frac{\hbar}{M\omega_0}\right)^{1/2} \tag{60}$$

Comparison with the continuum-polarization Hamiltonian (given, e.g., in Ref. 6) demonstrates a complete equivalence, provided that the interaction constant, A, hitherto unspecified, be set equal to [8]

$$A = \left(\frac{M\omega_0^2\beta e^2}{\pi^3 a}\right)^{1/2} \tag{61}$$

where $\beta \equiv 1/\epsilon_\infty - 1/\epsilon$ (ϵ_∞ and ϵ representing the high-frequency and static dielectric constants, respectively).

The above-established identity of the MCP and continuum-polarization models demonstrates that, in the degree of approximation commonly employed in polaron theory-i.e., in the continuum approximation-systems of different crystallographic constitution may nevertheless be equivalent. This equivalence, of course, gets lost when the theory is applied to problems in which distances comparable to lattice spacings are important, as is the situation for the small polaron. In the case of a real ionic crystal, it then becomes necessary to consider the coupling of the electron, not only to the longitudinal optical modes, as is done in the continuum-polarization model, but also to the two transverse optical and three acoustical branches. Hence, any small-polaron treatment in which the electron is assumed to interact with but a single branch of

vibration modes, will necessarily be based on a model, which, like the MCP-model, differs physically from the real case. However, as stated earlier, the basic point of view of this and the following paper is that the general features of the small-polaron problem are sufficiently independent of the details of the physical system, so that the methods developed for treating the simplified models should eventually be applicable to the real situation.

APPENDIX I

The motion of the electron (or hole) in the one-dimensional molecular-crystal medium, described in the text, will here be formulated in terms of the tight-binding approximation. In analogy with the corresponding treatment for atomic sites, one assumes that the one-electron potential may be written as a sum of "molecular" potentials, viz.,

$$V\left(\mathbf{r}, x_1, \cdots, x_n\right) = \sum_{n=1} U\left(\mathbf{r} - n\mathbf{a}, x_n\right) \tag{I-1}$$

where $\mathbf{a}$ is the (one-dimensional) unit lattice vector and where the molecular potential, $U\left(\mathbf{r}, x_n\right)$ is assumed to be sufficiently short-range so that, e.g.,

$$U\left(\mathbf{a}, x_n\right) \ll U\left(0, x_n\right) \tag{I-2}$$

The basic electron wave functions, $\varphi\left(\mathbf{r} - n\mathbf{a}, x_n\right)$, appropriate to the tight-binding approximation, are obtained as solutions of the equation

$$\left[-\frac{\hbar^2}{2m}\nabla^2 + U\left(\mathbf{r} - n\mathbf{a}, x_n\right)\right] \phi\left(\mathbf{r} - n\mathbf{a}, x_n\right) = E\left(x_n\right) \phi\left(\mathbf{r} - n\mathbf{a}, x_n\right) \tag{I-3}$$

with eigenvalues $E\left(x_n\right)$, which all depend upon the local internuclear displacement coordinate in the same way. The total wave function of the system is then represented as a superposition

$$\psi\left(\mathbf{r}, x_1, \cdots, x_n\right) = \sum_{\mathbf{n}} a_n\left(x_1, \cdots, x_n\right) \phi_n\left(\mathbf{r}, x_n\right) \tag{I-4}$$

Equations for the $a_n\left(x_1, \cdots, x_n\right)$ are obtained by substitution of (I-4) into the Schrödinger equation of the system [9]

$$i\hbar\frac{\partial\psi}{\partial t} = \left[-\frac{\hbar^2}{2m}\nabla^2 + \sum_{n=1}^{n} U\left(\mathbf{r} - n\mathbf{a}, x_n\right) + \sum_{n=1}^{n}\left(-\frac{\hbar^2}{2M}\frac{\partial^2}{\partial x_n^2} + \frac{1}{2}M\omega_0^2 x_n^2\right)\right]\psi \tag{I-5}$$

followed by multiplication on the left with ${\phi_n}^*\left(\mathrm{r}, x_n\right)$ and integration over the electron coordinate, r. This procedure gives

[08] The occurrence in (61) of the lattice spacing, a, arises from the circumstance that, in the present work, k is expressed in units of $1/a$, whereas the wave-vector, κ, of Footnote 7 is given in cgs.

$$\sum_m T_{nm}\left[i\hbar\frac{\partial}{\partial t}-\sum_p\left(-\frac{\hbar^2}{2M}\frac{\partial^2}{\partial x_p^2}+\frac{1}{2}M\omega_0^2x_p^2\right)-E\left(x_m\right)\right]a_m\left(x_1,\cdots,x_p\right)$$
$$=\sum_m\left[\int\phi^*\left(\mathbf{r}-n\mathbf{a},x_n\right)U\left(\mathbf{r}-p\mathbf{a},x_p\right)\phi\left(\mathbf{r}-m\mathbf{a},x_m\right)dV\right] \tag{I-6}$$
$$\cdot\, a_m\left(x_1,\cdots,x_p\right)-\frac{\hbar^2}{2M}\sum_m\int\phi^*\left(\mathbf{r}-n\mathbf{a},x_n\right)$$
$$\cdot\left[2\frac{\partial\phi\left(\mathbf{r}-m\mathbf{a},x_m\right)}{\partial x_m}\frac{\partial a_m}{\partial x_m}+a_m\frac{\partial^2\phi\left(\mathbf{r}-m\mathbf{a},x_m\right)}{\partial x_m^2}\right]dV$$

where

$$T_{nm}\equiv\int\phi^*\left(\mathrm{r}-n\mathrm{a},x_n\right)\phi\left(\mathrm{r}-m\mathrm{a},x_m\right)dV \tag{I-7}$$
$$=\delta_{nm}+S_{nm}$$

The S_{nm} are the well-known nonorthogonality integrals which will here be assumed to differ from zero only for nearest neighbors and to be small compared to unity; also, with normalized φ 's, one has $S_{nn}=0$.

It is now expedient to multiply (I-6) by the matrix $\breve{T}_{nm}$, which is the inverse of T_{nm}, as defined by the relation

$$\sum_p\breve{T}_{np}T_{pm}=\delta_{nm} \tag{I-8}$$

and as given to first order in the S_{nm} by the expression

$$\breve{T}_{nm}=\delta_{nm}-S_{nm}+\cdots. \tag{I-9}$$

One then obtains in place of (I-6)

$$\left[i\hbar\frac{\partial}{\partial t}-\sum_p\left(-\frac{\hbar^2}{2M}\frac{\partial^2}{\partial x_p^2}+\frac{1}{2}M\omega_0^2x_p^2\right)-E\left(x_n\right)\right]a_n\left(x_1,\cdots,x_p\right)$$
$$=\sum_{\substack{l,m\\p\neq m}}\breve{T}_{nl}\left[\int\phi^*\left(\mathbf{r}-l\mathbf{a},x_l\right)U\left(\mathbf{r}-p\mathbf{a},x_p\right)\phi\left(\mathbf{r}-m\mathbf{a},x_m\right)dV\right] \tag{I-10}$$
$$\cdot\, a_m\left(x_1,\cdots,x_p\right)-\frac{\hbar^2}{2M}\sum_{l,m}\breve{T}_{nl}\int\phi^*\left(\mathbf{r}-l\mathbf{a},x_l\right)$$
$$\cdot\left[2\frac{\partial\phi\left(\mathbf{r}-m\mathbf{a},x_m\right)}{\partial x_m}\frac{\partial a_m}{\partial x_m}+\frac{\partial^2\phi\left(\mathbf{r}-m\mathbf{a},x_m\right)}{\partial x_m^2}a_m\right]dV$$

The rather complicated expressions on the right-hand side of (I-10) may be simplified by the introduction of assumptions appropriate to the case of tightbinding. The principal assumption is that of the smallness of overlap integrals i.e., integrals involving electron wave functions localized at different sites. These integrals are of two types: nonorthogonality integrals, as

[09] H_{int} is implicitly contained in (I-5) by virtue of the x_n dependence of the U 's.

given by the S_{nm}, and those terms on the right-hand side of (I-10) for which $l \neq m$. In line with the above assumption, all terms containing products of more than one such overlap integral will henceforth be discarded.

When the terms of (I-10) involving the U 's are subjected to this procedure, they reduce to the expression

$$\begin{aligned}
&\sum_{\substack{m \\ p\neq m}} \left[\int \phi^* (\mathbf{r} - n\mathbf{a}, x_n)\, U (\mathbf{r} - p\mathbf{a}, x_p)\, \phi (\mathbf{r} - m\mathbf{a}, x_m)\, dV \right] a_m (x_1, \cdots, x_p) \\
&\quad - \sum_{\substack{m \\ p\neq m}} S_{nm} \left[\int \phi^* (\mathbf{r} - m\mathbf{a}, x_m)\, U (\mathbf{r} - p\mathbf{a}, x_p)\, \phi (\mathbf{r} - m\mathbf{a}, x_m)\, dV \right] \\
&\quad \cdot a_m (x_1, \cdots, x_p)
\end{aligned} \tag{I-11}$$

At this stage we may employ a second assumption, also appropriate to the case of tight-binding, which involves the local character of the molecular potential $U (\mathbf{r} - p\mathbf{a}, x_p)$. Specifically, it will be assumed that those terms in (I-11) which
contain products of wave functions and potentials localized at different sites are an order of magnitude smaller than terms for which two (or more) such factors refer to the same site. It then follows that the first member of (I-11) may be approximated by

$$\begin{aligned}
&\sum_{m\neq n} \left[\int \phi^* (\mathbf{r} - n\mathbf{a}, x_n)\, U (\mathbf{r} - n\mathbf{a}, x_n)\, \phi (\mathbf{r} - m\mathbf{a}, x_n)\, dV \right] a_m (x_1, \cdots, x_p) \\
&\quad \cdot \left[+ \int |\phi (\mathbf{r} - n\mathbf{a}, x_n)|^2 \left(\sum_{p\neq n} U (\mathbf{r} - p\mathbf{a}, x_p) \right) dV \right] a_n (x_1, \cdots, x_p)
\end{aligned} \tag{I-12}$$

(i.e., one of the two summation indices gets suppressed), and that the second member of (I-11) may be dropped. [10]

Applying a comparable simplification to the terms of (I-10) which contain derivatives of the φ 's with respect to the internuclear coordinates, one obtains

$$\begin{aligned}
&- \frac{\hbar^2}{2M} \left[\int \phi^* (\mathbf{r} - n\mathbf{a}, x_n) \frac{\partial^2 \phi (\mathbf{r} - n\mathbf{a}, x_n)}{\partial {x_n}^2} \right] a_n (x_1, \cdots, x_n) \\
&- \frac{\hbar^2}{2M} \sum_{m\neq n} \int \phi^* (\mathbf{r} - n\mathbf{a}, x_n) \\
&\quad \cdot \left[2 \frac{\partial \phi (\mathbf{r} - m\mathbf{a}, x_m)}{\partial x_m} \frac{\partial a_m}{\partial x_m} + \frac{\partial^2 \phi (\mathbf{r} - m\mathbf{a}, x_m)}{\partial {x_m}^2} a_m \right] dV \\
&- \frac{\hbar^2}{2M} \sum_{m} S_{nm} \left[\int \phi^* (\mathbf{r} - m\mathbf{a}, x_m) \frac{\partial^2 \phi (\mathbf{r} - m\mathbf{a}, x_m)}{\partial {x_m}^2} dV \right] a_m
\end{aligned} \tag{I-13}$$

in which use has been made of the fact that, since $\phi (\mathbf{r} - n\mathbf{a}, x_n)$ is nondegenerate, and hence, real, the integral $\int \phi^*(\mathbf{r} - n\mathbf{a}) (\partial/\partial x_n) \phi(\mathbf{r} - n\mathbf{a}) dV$ vanishes.

Equation (I-13) is listed here primarily for reference purposes. In line with the standard procedure in which terms involving derivatives of electronic functions with respect to nuclear coordinates are considered to be small (they represent, in essence, the effect of the nuclear kinetic energy on the localized electron wave functions), and also in view of the fact that the

molecular-crystal model, itself, constitutes a simplified abstraction of the real problem, (I-13) will herewith be discarded.

With these approximations, the right-hand side of (I-10) reduces to (I-12). Introducing the notations

$$W_n\left(x_1, \cdots, x_n\right) \equiv \int\left|\phi\left(\mathbf{r}-n \mathbf{a}, x_n\right)\right|^2\left[\sum_{p \neq n} U\left(\mathbf{r}-p \mathbf{a}, x_p\right)\right] d V \tag{I-14}$$

$$J\left(x_n, x_m\right) \equiv \int \phi^*\left(\mathbf{r}-n \mathbf{a}, x_n\right) U\left(\mathbf{r}-n \mathbf{a}, x_n\right) \phi\left(\mathbf{r}-m \mathbf{a}, x_m\right) d V \tag{I-15}$$

and assuming $J\left(x_n, x_m\right)$ appreciable only for nearest neighbors, one may write (I-10) in the form

$$\left[i \hbar \frac{\partial}{\partial t}-\sum_p\left(-\frac{\hbar}{2 M} \frac{\partial^2}{\partial x_p^2}+\frac{1}{2} M \omega_0^2 x_p^2\right)-E\left(x_n\right)-W_n\left(x_1, \cdots, x_n\right)\right] \tag{I-16}$$
$$\times a_n\left(x_1, \cdots, x_n\right)=\sum_{(\pm)} J\left(x_n, x_n \pm 1\right) a_n \pm 1\left(x_1, \cdots, x_n\right)$$

Received: May 11, 1959

REFERENCES

1. See, for example, S. I. Pekar, "Untersuchungen Über die Electronentheorie der Kristalle." Akademie-Verlag, Berlin, 1954.

2. S. I. Pekar and V. M. Buimistrov, J. Tech. Phys. U.S.S.R. 2, 2478 (1957) (Soviet Physics translation).

6.2.11 Holstein's Studies of Polaron Motion. Part II. The "Small" Polaron 1

Received: May 11, 1959

The one-dimensional molecular-crystal model of polaron motion, described in the preceding paper, is here analyzed for the case in which the electronicoverlap term of the total Hamiltonian is a small perturbation. In zeroth order -i.e., in the absence of this term-the electron is localized at a given site, p. The vibrational state of the system is specified by a set of quantum-numbers, N_k, giving the degree of excitation of each vibration-mode; the latter differ from the conventional modes in that in each of them, the equilibrium displacement, about which the system oscillates, depends upon the location of the electron.

The presence of a nonvanishing electronic-overlap term gives rise to transitions in which the electron jumps to a neighboring site ($p \rightarrow p \pm 1$), and in which either all of the N_k remain unaltered ("diagonal" transitions) or in which some of them change by ± 1 ("nondiagonal" transitions). The two types of transitions play fundamentally different roles. At sufficiently low temperatures, the diagonal transitions are dominant. They give rise to the formation of Bloch-type bands whose widths (see Eq. 37) are each given by the product of the electronic-overlap integral, and a vibrational overlap-integral, the latter being an exponentially falling

[010] In particular, it is smaller than the second sum of (I-12) by a factor of the order of a nonorthogonality integral, S_{nm}.

function of the N_k (and, hence, of temperature). In this low-temperature domain, the role of the nondiagonal transitions is essentially one of scattering. In the absence of other scattering mechanisms, such as impurity scattering, they determine the lifetimes of the polaron-band states and, hence, the mean free path for typical transport quantities, such as electron diffusivity.

With rising temperature, the probability of the off-diagonal transitions goes up exponentially. This feature, together with the above-mentioned drop in bandwidth, results, e.g., in an exponentially diminishing diffusivity. Eventually, a temperature, $T_\iota \sim 1/2$ the Debye θ, is reached at which the energy uncertainty, $\hbar/\tau$, associated with the finite lifetime of the states, is equal to the bandwidth. At this point, the Bloch states lose their individual characteristics (in particular, those which depend upon electronic wave number); the bands may then be considered as "washed out." For temperatures $> T_t$, electron motion is predominantly a diffusion process. The elementary steps of this process consist of the random-jumps between neighboring sites associated with the nondiagonal transitions. In conformance with this picture, the electron diffusivity is, apart from a numerical factor, the product of the square of the lattice

distance and the total non-diagonal transition probability, and is therefore an exponentially rising function of temperature.

The limit, $J_{\max}$, of the magnitude of the electronic overlap term, beyond which the perturbation treatment of the present paper becomes inapplicable, is investigated. For representative values of the parameters entering into the theory, $J_{\max} \sim 0.12$ev and 0.035 ev for the extreme cases of (a) width of the ground-state polaron-band and (b) high-temperature site-jump probabilities (these numbers correspond to electronic bandwidths of 0.24 ev and 0.07 ev , respectively). For electronic bandwidths in excess of these limits, a treatment based on the adiabatic approach is required; preliminary results of such a treatment are given for the above two cases.

I. INTRODUCTION

In this paper, the one-dimensional molecular-crystal model, developed in the preceding paper (1), [1] will be applied to the study of the small polaron. The basic features of the molecular-crystal model are contained in Eq. (9) of I, which may be written as

$$i\hbar\frac{\partial a_n\left(x_1,\cdots,x_N\right)}{\partial t} = \left[\sum_{m=1}^{N}\left(-\frac{\hbar^2}{2M}\frac{\partial^2}{\partial {x_m}^2}+\frac{1}{2}M{\omega_0}^{2{x_m}^2}\right)-Ax_n\right]a_n - J\left[a_{n+1}+a_{n-1}\right] \tag{1}$$

IIere, the "wave function," $a_n\left(x_1,\cdots,x_N\right)$, is a function of the "lattice-vibration" coordinates, $x_1,\cdots,x_N$ (each of which describes the internuclear vibration of a single (diatomic) molecular site of the linear chain), and of a discrete "electronic" coordinate, n. The latter is to be understood in terms of the tightbinding approximation, according to which the actual wave function of the system has the form

$$\psi\left(\mathbf{r},x_1,\cdots,x_N\right)=\sum_n a_n\left(x_1,\cdots,x_N\right)\phi\left(\mathbf{r}-n\mathbf{a},x_n\right) \tag{2}$$

(where $\phi\left(\mathbf{r}-n\mathbf{a},x_n\right)$ is a one-electron wave-function, localized about the nth molecular site, its precise definition being given by Eq. (I 3) in the appendix of I).

The sum over m in the square-bracket of (1) represents the "lattice" Hamiltonian, consisting of the vibratory kinetic and potential energies of the molecules in the absence of the electron;

it is expressed in terms of the reduced mass, M, and vibration frequency, ω_0, of the individual molecules. The remaining term in the square bracket, $-Ax_n$, gives the "electron-lattice" interaction as a linear function of the vibration coordinate of the occupied site. Finally, the term pro-

portional to the electronic "overlap" integral, [2] $-J$, describes the motion of the electron through the lattice. As discussed in I, this feature of the model is strictly analogous to the conventional atomic tight-binding approach; in particular, if all the x_n 's are fixed at one and the same value (thereby suppressing vibrational motion), Eq. (1) reduces to the standard tight-binding approximation of the Bloch one-electron equation, as illustrated by Eqs. (4)-(7) of I.

As pointed out in I (Eqs. 43-46, and accompanying text), the case of the small-polaron is realized when the electronic bandwidth, $2J$, is small compared to a characteristic energy, $A^2/2M\omega_0^2$, which (see I, Eq. 46) is, in essence, the binding energy of the small polaron. This circumstance suggests that Eq. (1) be solved by a perturbation approach in which the zeroth order Hamiltonian consists of the square-bracket of (1), whereas the J-proportional term is the perturbation. Such a procedure has, in fact, been applied by Tjablikov (2) and by Yamashita and Kurosawa (3)[3] to the continuum-polarization model, and will form the basis of the present work. In anticipation of results to be obtained below, it may be remarked that the domain of validity of the treatment will not be sufficient to cover the whole range of interest for the small polaron. Namely, as will be shown in Section 6, the small-polaron condition (see Eq. 43 of I)

$$2J < A^2/2M\omega_0^2 \tag{3}$$

is not sufficient for the applicability of the perturbation approach; in particular, the more restrictive conditions

$$\begin{aligned} 2J &< \left(A^2/2M\omega_0^2\right)^{1/2} (\hbar\omega_0)^{1/2} \\ J &< \left(A^2/4M\omega_0^2\right)^{1/4} (2\kappa T/\pi)^{1/4} (\hbar\omega_0/\pi)^{1/2} \end{aligned} \tag{4}$$

will be shown to be necessary.

[2] Strictly speaking, (see I, Eq. 3), this term has the form, $J(x_n, x_{n+1})\, a_{n+1} + J(x_n,\ x_{n-1})\, a_{n-1}$ where the overlap integrals, $J(x_n, x_{n\pm1})$ are defined by Eq. (I-15) in the appendix of I. As discussed in I, the x_n dependence of the J 's is to be ignored for the time being, so that all the J 's are assumed equal to a single constant, $-J$.

[3] Referred to hereafter as Y and K. It should be stated at the outset that the treatment of the present paper overlaps, in considerable measure, the earlier work of Y and K . However, there are a number of features of the problem, which constitute important elements of the present paper, and which are absent from Y and K 's treatment. Examples are (a) the roles of the diagonal and off-diagonal transitions at temperatures above and below the "transition" temperature, T_t [as given by Eq. (88) and subsequent text], (b) the classical activation approach in the high-temperature region ($\kappa T \gg \hbar\omega_k$), and (c) the estimation of the limits of validity of the perturbation treatment (together with the question of the alternate applicability of the adiabatic approach). Moreover, in the opinion of the present author, the specific results obtained by **Y** and **K** are not correct in detail. A discussion of these results is presented at the end of the paper.

Before entering upon detailed calculation, let us generalize Eq. (1) by adding to the lattice Hamiltonian coupling terms of the form mentioned in footnote 3 of I. The augmented equation

[01] To be referred to hereafter as I. Here, as in I, the term "small polaron" designates the case in which the linear dimension of the polaron is of the order of a lattice spacing.

reads
$i\hbar\frac{\partial a_n(x_1,\cdots,x_n)}{\partial t}$

$$= \sum_{m=1}^{N}\left(-\frac{h^2}{2M}\frac{\partial^2}{\partial x_m^2}+\frac{1}{2}M{\omega_0}^2{x_m}^2+\frac{1}{2}M{\omega_1}^2x_mx_{m+1}\right)+Ax_n]\,a_n \tag{5}$$
$$-\,J\left[a_{n+1}+a_{n-1}\right]$$

As is known, the presence of coupling terms gives rise to dispersion of the lattice vibration frequencies. It will later be seen that this dispersion has to be taken into account in the calculation of probabilities of transitions in which a change of electron-site variable is accompanied by the simultaneous absorption and emission of vibrational quanta. In particular, it will turn out that the standard approximation of replacing the vibration frequencies by a single frequency (Einstein model) yields meaningless results for these probabilities.

For the treatment of (5) it is desirable to express the vibrational coordinates, x_n, in terms of the normal-mode coordinates of the host crystal. This is done by means of the one-dimensional analog of Eq. (50) of I [the transformation is also given by Eq. (II-2) of Appendix II]; one then has

$$\begin{aligned} i\hbar\frac{\partial a_n\left(\cdots q_k\cdots\right)}{\partial t} \\ = \sum_k\left[\left(-\frac{\hbar^2}{2M}\frac{\partial^2}{\partial q_k}+\frac{1}{2}M\omega_k^2q_k^2\right)-\left(\frac{2}{N}\right)^{1/2}Aq_k\sin(kn+\pi/4)\right] \\ \times\, a_n\left(\cdots q_k\cdots\right)-J\left(a_{n+1}+a_{n-1}\right) \end{aligned} \tag{6}$$

where ω_k is given by the dispersion relation

$$\omega_k^2=\omega_0^2+\omega_1^2\cos k \tag{7}$$

and where $k=2\pi\kappa/N$, the integer κ lying in the range $-1/2(N-1)\leqq\kappa\leqq 1/2(N-1)$ (N being assumed odd for the sake of convenience).

The zeroth-order wave equation is obtained by setting J equal to zero in (6). The zeroth-order eigenstates are then seen to have the form

$${a_n}^{(p)}\left(\cdots q_k\cdots\right)=\delta_{np}\chi^{(p)}\left(\cdots q_k\cdots\right) \tag{8}$$

where δ_{n_p} is the Krönecker delta-unity for $n=p$ and zero otherwise-and where $\chi^{(p)}$ satisfies the equation

$$E_\chi^{(p)}=\sum_k\left[\begin{array}{c}\hbar^2\quad\partial^2\\ -2M\frac{\partial}{\partial q_k}\end{array}+\frac{1}{2}M\omega_k^2q_k^2-\left(\frac{2}{N}\right)^{1/2}Aq_k\sin(kp+\pi/4)\right]\chi^{(p)}. \tag{9}$$

Noting that the square-bracket of (9) represents a system of independent harmonic oscillators, with equilibrium points

$$q_k^{(p)}=\frac{A}{M\omega_k^2}\left(\frac{2}{N}\right)^{1/2}\sin(kp+\pi/4) \tag{10}$$

one readily obtains for the eigenfunctions and eigenvalues of (8)

$$\chi^{(p)}_{\cdots N_k \cdots}(\cdots q_k \cdots) = \pi_k \Phi_{N_k}\left[(M\omega_k/\hbar)^{1/2}\left(q_k - q_k^{(p)}\right)\right] \tag{11}$$

$$E \cdots N_k \cdots = \sum_k \hbar\omega_k (N_k + 1/2) + E_b \tag{12}$$

where

$$\Phi_N(z) \equiv \left(2^N N! \pi^{1/2}\right)^{-1/2} e^{-z^2/2} H_N(z)$$

are normalized harmonic oscillator eigenfunctions [the $H_N(z)$ being Hermite polynomials] and where

$$Eb = -\sum_k \frac{A^2}{2M\omega_k^2}\left(\frac{2}{N}\right)\sin^2(kp + \pi/4) \tag{13}$$

Finally, from (8) and (11), one has for the zeroth order eigenstates of the total system

$$a_{p,\cdots N_k} \cdots (n, \cdots q_k \cdots) = \delta_{np}\pi_k \Phi_{N_k}\left[(M\omega_k/\hbar)^{1/2}\left(q_k - q_k^{(p)}\right)\right]. \tag{14}$$

In the representation of these zeroth order eigenstates, the wave function of the system takes the form

$$\begin{aligned} a_n(\cdots q_k \cdots) &= \textstyle\sum_{p',\cdots N_k}, \cdots \\ &\times \exp\left[-(it/\hbar)E \ldots N_k{}' \cdots\right] \end{aligned} \tag{15}$$

Inserting this expression into (6), multiplying on the left by $a_p \ldots N_k \ldots (n, \cdots q_k \cdots)$, and integrating with respect to the vibration coordinates, q_k, one obtains, with the aid of (8)-(13)

$$\begin{aligned} i\hbar\frac{\partial C(p, \cdots N_k \cdots)}{\partial t} &= \sum_{p', N_k}(p, \cdots N_k \cdots |V| p', \cdots N_k' \cdots) \\ &\times C(p', \cdots N_k' \cdots)\exp\left[(it/\hbar)(E \ldots N_k \cdots - E \ldots N_k' \cdots)\right] \end{aligned} \tag{16}$$

where

$$\begin{aligned} &(p, \cdots N_k \cdots |V| p', \cdots N_k' \cdots) = -J\sum_{\epsilon=\pm 1}\delta_{p,p'+\epsilon} \\ &\times \pi_k\left[\int_{-\infty}^{+\infty}\Phi_{N_k}\left[(M\omega_k/\hbar)^{1/2}\left(q_k - q_k^{(p)}\right)\right]\phi_{N_k}\left[(M\omega_k/\hbar)^{1/2}\left(q_k - q_k^{(p')}\right]\right] \\ &\cdot (M\omega_k/\hbar)\, dq_k \end{aligned} \tag{17}$$

the product, π_k, going over all vibration modes. Taking advantage of the circumstance that the $q_k^{(p)}$ are actually infinitesimal (i.e., $\sim 1/N$), one may evaluate the multiplicands of π_k simply by developing, say, $\phi_{N_k}\left[(M_{\omega_k}/\hbar)^{1/2}\left(q_k - q_k^{(p)}\right)\right]$ as a Taylor series in $q_k^{(p)} - q_k^{(p')}$, and by making use of the standard formula

$$\frac{\partial\phi_N(z)}{\partial z} = \left(\frac{N}{2}\right)^{1/2}\Phi_{N-1}(z) - \left(\frac{N+1}{2}\right)^{1/2}\Phi_{N+1}(z).$$

The result is, to the second order in $q_k^{(p)} - q_k^{(p')}$,

$$
\begin{aligned}
&(p', \cdots N_k' \cdots |V| p \cdots N_k \cdots) = -J \sum_{\epsilon=\pm 1} \delta_{p', p+\epsilon} \\
&\times \pi_k \left\{ \left[1 - \frac{4}{N} (N_k + 1/2) \gamma_k \cos^2(k(p+\epsilon/2) + \pi/4) \right] \delta_{N_{k'} N_k} \right. \\
&- \left[\left(\frac{8}{N} \right)^{1/2} \epsilon \mu_k \gamma_k^{1/2} \left(\frac{N_k + 1/2 \pm 1/2}{2} \right) \cos(k(p+\epsilon/2) + \pi/4) \right] \\
&\left. \cdot \delta_{N_{k'}, Nk \pm 1} + \frac{\alpha_k^{(\pm)}}{N} \gamma_k \delta_{N_{k'}, N_k \pm 2} \right\}
\end{aligned} \tag{18}
$$

where

$$
\gamma_k \equiv \frac{A^2}{2M\omega_k^2 \hbar \omega_k} (1 - \cos k), \tag{19}
$$

μ_k being equal to ± 1, depending on whether k is positive or negative, and where the ${\alpha_k}^{(\pm)}$are dimensionless quantities of the order of unity or $\langle N_k \rangle_{\mathrm{Av}}$, whichever is larger. They are not given explicitly since, as will be seen later, the two-quantum jumps to which they pertain turn out to be unimportant. In obtaining (18), the expansion parameter, $q_k^{(p)} - q_k^{(p')}$, was eliminated by use of (8). It may be remarked here that the γ_k are important parameters of the theory. Apart from the trigonometric factor, $1 - \cos k$, they represent, in essence, the ratio of the poleron binding energy, ($\sim A^2/2M{\omega_0}^2$), to the quantum of vibrational energy. In order of magnitude, this ratio is to be assumed large compared to unity, e.g., ~ 10 (see footnote 17).

II. DIAGONAL AND NONDIAGONAL TRANSITIONS: COMPLEMENTARITY OF BAND AND LOCAL SITE-JUMP APPROACHES

The transitions arising from the matrix elements (18) may be grouped into two different categories: one in which the vibration quantum numbers remain unaltered ($N_k = N_{k'}$), the other in which some of these numbers change by one (or two) units. These two types will be designated as "diagonal" and "nondiagonal," respectively.

In order to exhibit the role played by the diagonal transitions, let us consider the simplest case-prevalent at the absolute zero of temperature-in which the vibration quantum numbers, N_k, are all zero. In this case, by virtue of energy conservation, transitions of substantial amplitude are all of the diagonal type. It is now to be noted that such transitions connect states, $a_{p,m_0 \cdots} \ldots (n, \cdots q_k \cdots)$, whose unperturbed energies all coincide at one and the same value, $E \ldots 0_k \ldots = E_b + \sum_k \hbar\omega_k/2$. Hence, to the first order in the perturbation parameter, J, the stationary states of the system are of the form [4]

$$
\begin{aligned}
&a_n(x_1, \cdots, x_N) \\
&= \sum_p C_p a_p, \cdots 0_k \cdots (n, \cdots q_k \cdots) \exp \left\{ -i \left[E_b + \sum_k \hbar\omega_k/2 \right] t/\hbar \right\}
\end{aligned} \tag{20}
$$

where the C_p constitute the stationary solution of the equations

$$
ih \frac{\partial C_p}{\partial t} = \sum_p (p, \cdots 0_k \cdots |V| p', \cdots 0_k \cdots) C_{p'} \tag{21}
$$

[obtained from (16) by dropping all terms for which $N_k \neq 0$]. From (18) one has

$$(p, \cdots 0_k \cdots |V| p', \cdots 0_k \cdots) = -J \sum_{\epsilon=\pm 1} \delta_{p,p'+\epsilon} \pi_k \cdot \left\{ 1 - \frac{2}{N} \gamma_k \cos^2 \left[k \left(p' + \frac{\epsilon}{2} \right) + \frac{\pi}{4} \right] \right\}$$

which may be written as [5]

$$(p, \cdots 0_k \cdots |V| p', \cdots 0_k \cdots) = -J \sum_{\epsilon=\pm 1} \delta_{p,p'+\epsilon} \cdot \exp \left\{ -\frac{2}{N} \sum_k \gamma_k \cos^2 \left[k \left(p' + \frac{\epsilon}{2} \right) + \frac{\pi}{4} \right] \right\} = -J \sum_{\epsilon=\pm 1} \delta_{p,p'+\epsilon} \exp \left\{ \sum_k \gamma_k / N \right\} \tag{22}$$

Inserting (22) into (21), and assuming the time dependence of the C_p to be of the form $e^{-iEt/\hbar}$, one has

$$EC_p = -J \exp \left\{ -\sum_k \gamma_k / N \right\} (C_{p+1} + C_{p-1})$$

the solution of which is

$$C_p^{(\sigma)} = e^{ip\sigma} \tag{23}$$

[4] The notation C_p is used as an abbreviation of $C_p, \cdots_0 \cdots$.
[5] The second equality results from the circumstance that $\gamma_k = \gamma_{-k}$, so that, when terms of plus and minus k are combined, one has

$$\sum_{(\pm)} \cos^2 \left[\pm k \left(p' + \frac{\epsilon}{2} \right) + \frac{\pi}{4} \right] = \frac{1}{2} \sum_{(\perp)} \left(1 - \cos \left[\pm k \left(2p' + \epsilon \right) + \frac{\pi}{2} \right] \right) = \frac{1}{2}$$

with

$$E = E_\sigma = -2J \cos \sigma \exp \left\{ -\sum_k \gamma_k / N \right\} \tag{24}$$

where σ ranges over the same values as k.
Referring back to (20) and (14), one observes that the $N_k = 0$ eigenstates of the system are

$$a_{\sigma,\cdots 0}, \ldots (n, \cdots q_k \cdots) = e^{in\sigma} \pi_k \Phi_0 \left[(M\omega_k/\hbar)^{1/2} \left(q_k - q_k^{(p)} \right) \right] \tag{25}$$

with eigenvalues

$$E_{\sigma,\ldots 0\ldots} = E_b + \sum_k \hbar\omega_k/2 - 2J \cos \sigma e^{-s} \tag{26}$$

where

$$S \equiv \sum_k \gamma_k / N = \frac{1}{\pi} \int_0^\pi \gamma_k dk = \frac{1}{\pi} \int_0^\pi \left(A^2 / 2M\omega_k^2 \hbar\omega_k \right) (1 - \cos k) dk \tag{27}$$

The eigenstates (25) may be considered as constituting the groundstate polaron-band. This band is characterized by a half-width

$$\Delta E_{\sigma,\cdots 0_k \cdots} = 2Je^{-s} \tag{28}$$

In practical cases, S may be expected to be of the order of $5-10$, so that the factor e^{-S}, which gives the ratio of the polaron-bandwidth to the original electronic bandwidth, $2J$, will be quite small ($\sim 10^{-2}-10^{-4}$).

Turning now to the excited states, in which some of the N_k differ from zero, and continuing for the moment to neglect the nondiagonal matrix elements, one may approximate (16) by [6]

$$i\hbar\frac{\partial C\left(p,\cdots N_k\cdots\right)}{\partial t}=\sum_{p'}\left(p,\cdots N_k\cdots|V|p',\cdots\ N_k\cdots\right)\qquad(29)$$
$$C\left(p',\cdots N_k\cdots\right)$$

where, in analogy with (21) and (22), one has

$$\left(p,\cdots N_k\cdots|V|\ p,\cdots N_k'\cdots\right)=-J\sum_{\epsilon=\pm1}\delta_{p,p'+\epsilon}$$
$$\cdot\exp\left\{-\sum_k\frac{2\left(1+2N_k\right)}{N}\gamma_k\cos^2\left[k\left(p+\frac{\epsilon}{2}\right)+\frac{\pi}{4}\right]\right\}\qquad(30)$$

For the further simplification of (30) it will be assumed [7] that

$$N_k=N_{-k}.\qquad(31)$$

The step analogous to the last equality of (22) may then be carried out, and one has

$$\left(p,\cdots N_k\cdots|V|p,\cdots N_k'\cdots\right)=-J\sum_{\epsilon=\pm1}\delta_{p,p'+\epsilon}e^{-S(\cdots N_k\cdots)}\qquad(32)$$

where

$$S\left(\cdots N_k\cdots\right)=\sum_k\left(1+2N_k\right)\gamma_k/N=\frac{1}{\pi}\int_0^\pi\left(A^2/2M\omega_k^2\hbar\omega_k\right)\qquad(33)$$
$$\cdot\left(1-\cos k\right)\left(1+2N_k\right)dk$$

Proceeding as before, one then obtains for the stationary solution of (29)

$$C\left(p,\cdots N_k\cdots\right)=e^{ip\sigma}\exp\left[+(it/\hbar)\left(2J\cos\sigma e^{-s(\cdots N_k\cdots)}\right)\right].\qquad(34)$$

The wave functions corresponding to (34) are

$$a_{\sigma,\cdots N_k}\cdots\left(n,\cdots q_k\cdots\right)=e^{in\sigma}\pi_k\Phi_{N_k}\left[\left(M\omega_k/\hbar\right)^{1/2}\left(q_k-q_k^{(p)}\right)\right]\qquad(35)$$

with eigenvalues

$$E_{\sigma,\cdots N_k\cdots}=E_b+\sum_k\left(N_k+1/2\right)\hbar\omega_k-2J\cos\sigma e^{-S(\cdots N_k\cdots)}.\qquad(36)$$

Attention is called to the rather novel feature that the bandwidth

[06] Of special significance is the fact that, due to the coincidence of initial and final unperturbed energies, the time dependent exponential factor in (16) is here unity.

[7] Actually, this assumption would not have been necessary had "running-wave" vibration coordinates been used instead of the "standing-wave" coordinates, q_k. This deficiency,

$$\Delta E_{\sigma,\cdots N_k}\cdots = 2Je^{-S(\cdots N_k\cdots)} \tag{37}$$

is [by virtue of (33)] a function of the vibrational quantum numbers, and, in fact, an exponentially decreasing function of these variables. [8] The bandwidth is thus maximal at absolute zero and diminishes rapidly with rising temperature.

The above discussion has been predicated on the assumption that the nondiagonal transitions play a subordinate, higher-order role. This assumption will now be investigated. One may begin by expressing the equations of motion (16) in the representation of the polaron-band states $a_{\sigma,\cdots N_k}\cdots(n_1\cdots q_k\cdots)$. In this representation, the total wave function takes the form

$$\begin{aligned} a_n&(\cdots q_k\cdots) \\ &= \sum_{\sigma_1\cdots N_k\cdots} C(\sigma,\cdots N_k\cdots)\, a_{\sigma,\cdots N_k\cdots}(n,\cdots q_k\cdots) \\ &\quad\times\exp\left[-(it/\hbar)E_{\sigma,\cdots N_k\cdots}\right] \end{aligned} \tag{38}$$

however, is not serious (since, in practice, N_{-k} and N_k are always, in effect, equal (see footnote 9); the formal advantages of running-wave coordinates are to some extent offset by an increased conceptual complexity of the zeroth order wave functions.

[8] This feature appears to have first been noted by Yamashita and Kurosawa (3).

where $E_{\sigma,\ldots N_k\ldots}$ is given by (36); i.e., it is the original unperturbed energy (taken with reference to localized wave-functions) augmented by the polaronband energy. The $C(\sigma,\cdots N_k\cdots)$ satisfy the equations

$$\begin{aligned} i\hbar\frac{\partial C(\sigma,\cdots N_k\cdots)}{\partial t} &= \sum_{\sigma',\cdots N_k,\ldots}(\sigma,\cdots N_k\cdots|V|\sigma',\cdots N_k{}'\cdots) \\ &\quad\times\exp\left[(it/\hbar)\left(E_{\sigma,\cdots N_k\cdots}-E_{\sigma',\cdots N_k'}\cdots\right)\right] \end{aligned} \tag{39}$$

where

$$\begin{aligned} (\sigma,\cdots N_k\ &\cdots|V|\sigma',\cdots N_k'\cdots) \\ &= \sum_{pp'} e^{-i[\sigma p-\sigma' p']}(p,\cdots N_k\cdots|V|p',\cdots N_k'\cdots) \end{aligned} \tag{40}$$

and where the sum in (39) cxcludes the term for which $\sigma=\sigma'$ and $N_k=N_k{}'$ [this term being automatically subtracted out by the inclusion of the polaronband energy in the time-dependent exponential of (39)].

It is readily verified that the σ dependence of the diagonal matrix elements is of the form [9]$\delta_{\sigma,\sigma'}$, so that, in effect, (39) represents only nondiagonal transitions.

The actual computation of the nondiagonal transitions (in the polaron-band representation) is carried out below (see Section 5). Some of the principal features of these transitions may however be noted here. First of all, the initial and final unperturbed energies no longer coincide exactly. However, primarily because of the dispersion of vibrational frequencies, as represented by (7), the unperturbed energy spectrum is continuous, so that energy conservation (in the sense of time-dependent perturbation theory) is possible for a wide variety of multiphonon processes. It then follows that transitions of the type $\sigma,\cdots N_k\cdots\to\sigma',\cdots N_k'\cdots$ develop uniformly in time, and are therefore describable in terms of the conventional (time-independent) transition probabilities

$$W\left(\sigma,\cdots N_k\cdots\rightarrow\sigma',\ \cdots N_k'\cdots\right)=\frac{2\pi}{\hbar}\Big|\left(\sigma,\cdots N_k\cdots\right.$$
$$\cdot|V|\sigma',\cdots N_k\cdots\left)\right|^2\delta\left(E_{\sigma,\cdots N_k\cdots}-E_{\sigma',\cdots N_k}\cdots\right) \tag{41}$$

where $\delta(E)$ is the Dirac delta function, and where, from (40) and (18),

$$\begin{aligned}&\left(\sigma',\cdots N_k\cdots|V|\sigma,\cdots N_k\cdots\right)=-J\sum_{pp'}\delta_{p',p+\varepsilon}e^{i[\sigma p-\sigma p']}\\&\times\pi_k\left\{\left[1-\frac{4}{N}\left(N_k+1/2\right)\gamma_k\cos^2\left[k\left(p+\frac{\epsilon}{2}\right)+\frac{\pi}{4}\right]\right]\delta_{N_{k'},N_k}\right.\\&-\left(\frac{8}{N}\right)^{1/2}\left(\frac{N_k+\frac{1}{2}\pm\frac{1}{2}}{2}\right)^{1/2}\mu_{k\in\gamma k}^{1/2}\cos\left[k\left(p+\frac{\epsilon}{2}\right)+\frac{\pi}{4}\right]\\&\left.\cdot\delta_{N_{k'},N_{k\pm1}}+\frac{\alpha_k^{(\pm)}}{N}\gamma_k\delta_{N_{k'},N_{k\pm2}}\right\}.\end{aligned} \tag{42}$$

Due to the requirements of energy conservation, the number of phonon absorptions will be comparable to that of phonon emissions. It is to be noticed (from Eq. 42) that each absorption process gives rise to a factor, $N_k^{1/2}$, in the matrix, and hence a factor, N_k, in the transition probability. Thus, for example, the probability of the process $\sigma,\cdots N_{k_1},N_{k_2},N_{k_3},N_{k_4}\rightarrow\sigma'\cdots N_{k_1}-1$, $N_{k_2}-1,N_{k_3}+1,N_{k_4}+1,\cdots$ is proportional to the factor $N_{k_1},N_{k_2}\left(1+N_{k_3}\right)\left(1+N_{k_4}\right)$. It is therefore to be concluded that, at sufficiently low temperatures (such that $\langle\gamma_kN_k\rangle_{\mathrm{Av}}\ll 1$), those transitions which are of lowest order in the number of photon absorptions will dominate.

In discussing these lowest-order transitions, let us assume that all vibrational frequencies, ω_k, differ from zero, [10] i.e., $\omega_1<\omega_0$ in (7). It then follows, by virtue of energy conservation, that a one-phonon (emissive) transition is forbidden; the lowest-order transition is a two-phonon process of the type $\sigma,\cdots N_{k_1},N_{k_2}\rightarrow\sigma',\cdots N_{k_1}-1,N_{k_2}+1,\cdots$; in conformity with the above remarks, its probability is proportional to N_{k_1}. Hence, although this type of transition is the dominant one at low temperatures, its probability also vanishes as the temperature approaches absolute zero.

From this discussion, it is apparent that, in the limit of very low temperatures, the nondiagonal transitions play a role subordinate to that of the diagonal transitions. In particular, in the domain of temperatures such that the mean life of a polaron-band state

$$\tau_{\sigma,\cdots N_k\cdots}=1/\sum_{\sigma',\cdots N_k'\cdots}W\left(\sigma,\cdots N_k\cdots\rightarrow\sigma',\cdots N_k'\cdots\right) \tag{43}$$

is large enough for the fulfillment of the inequality

$$\hbar/\tau_{\sigma_1\cdots N_k}\cdots\ll\Delta E_{\sigma,\cdots N_k}\cdots=2Je^{-s(\cdots N_k\cdots)}, \tag{44}$$

[09] As in the case of footnote 7, this statement is strictly true only when $N_k=N_{-k}$. Here, also, the need for this qualification arises from the use of standing-wave vibration coordinates, and could have been avoided by the use of running-wave coordinates. Actually, however, it is only required that the average quantum number (the average being taken over a range Δk small compared to unity but large compared to the spacings of the individual modes) be the same for plus and minus k. Since this condition is always obeyed in practice, the equality $N_k=N_{-k}$ may be applied to (30). It then follows that

$$\left(p,\cdots N_k\cdots|V|p',\cdots N_k'\cdots\right)$$

depends only of the difference, $p-p'$, in site variable; this feature, in turn, leads straightforwardly to the above-mentioned factor, $\delta_{\sigma,\sigma'}$.

[10] This assumption means simply that the vibrational spectrum is of optical, rather than acoustical, character, this being the relevant case for polaron theory.
a sufficiently accurate description of the physical situation is indeed provided by the polaron-band approach, according to which the principal characteristics of the states depend on the diagonal matrix elements, the role of the off-diagonal elements being limited to determining their lifetimes.

However, as the temperature increases from some low value, at which (44) is valid, the situation changes. First of all, $\tau_\sigma, \ldots N_k \ldots$ decreases by virtue of the fact that, the probability for a given transition, $\sigma, \cdots N_k \cdots \to \sigma', \cdots N_k{}' \cdots$ is proportional to the product of those N_k which are involved in absorption, and these all increase rapidly with temperature. Secondarily, as shown by Eqs. (33) and (37), the bandwidth, $\Delta E_{\sigma,\cdots N_k} \ldots$ diminishes with increasing temperature. Thus a temperature is eventually reached [11] at which (44) breaks down, i.e., at which the polaron-bandwidth becomes smaller than the energy uncertainty of the individual band states. Regarded from another point of view, the lifetime is less than the time ($\sim h/\Delta E_\sigma, \ldots N_k \ldots$) required for the polaron to move a distance equal to a lattice spacing. Under such circumstances, the band approach is clearly inapplicable. The fact is that, at this point, the relative importance of the diagonal and nondiagonal transitions has been reversed. The appropriate zeroth-order states, to be used in a perturbation treatment, are the original localized polaron states, $a_{p,\cdots N_k} \cdots (n, \cdots q_k \cdots)$, given by (14), rather than their plane wave combinations, $a_{\sigma,\cdots N_k} \cdots (n, \cdots q_k \cdots)$. The nondiagonal matrix elements, $(p, \cdots N_k \cdots |V| p', \cdots N_k{}' \cdots)$, between these localized states (which have now to be taken into account before the diagonal elements) give rise to transitions of the type $p, \cdots N_k \cdots \to p \pm 1, \cdots N_k{}' \cdots$ in which a jump to a neighboring site is accompanied by the emission and absorption of a number of phonons. The computation of the probabilities of these transitions, $W\,(p, \cdots N_k \to p', \cdots N_k{}' \cdots)$, by conventional time-dependent perturbation theory is presented below.

The subsequent inclusion of the diagonal matrix elements in the perturbation treatment leads to a state of affairs which, although somewhat novel, is actually not unexpected. Namely, it is found that, by virtue of the exact conservation of energy which characterized the diagonal transitions, the resultant transition probabilitics are not time-independent-as is the case for the nondiagonal vari-ety-but increase linearly with time. From this it follows that, if the time interval, over which perturbation theory is valid, were arbitrarily large, the diagonal transitions would ultimately dominate. Actually, however, perturbation theory breaks down when the time intervals (over which it is applied) get to be of the order of the mean lives of the individual (localized) states

$$\tau_p, \cdots N_k \cdots = 1/\sum_{N'_k p'} W\,(p, \cdots N_k \cdots \to p', \cdots N'_k \cdots)\,. \tag{45}$$

A proper treatment of the diagonal transitions would then require the introduction of collision-damping into the theory. A criterion for the diagonal transitions to be of subsidiary importance may, however, be stated on simple physical grounds, without recourse to a formal damping theory. It is namely that the probability for a diagonal transition to occur in a time $\sim_{\tau_p,\ldots N_k} \ldots$. (as computed by perturbation theory) must be small compared to unity. Using (29) and (32), the reader may readily establish [12] that this criterion is equivalent to

$$\hbar/\tau_{p,\cdots N_k \cdots \gg 2J} e^{-S(\cdots N_k \cdots)}. \tag{46}$$

If, now, it be assumed (as will be verified in Section 5) that $\tau_p, \ldots N_k \ldots$ has a magnitude comparable to that of the mean life, $\tau_\sigma, \ldots N_k \ldots$, of the polaron-band states, (46) is seen to be

[011] An estimate given below (see Eq. 88 and subsequent text) shows that, for representative values of the parameters of the theory, this temperature is of the order of ($0.5 - 1$) times the Debye θ.

simply the converse of (44) and may thus be considered as defining a regime complementary to that in which (44) obtains.

6.2.12 Holstein's Studies of Polaron Motion. Part II. The "Small" Polaron 2

III. NONDIAGONAL TRANSITIONS BETWEEN LOCALIZED STATES: SITE-JUMP PROBABILITIES

After these general orienting remarks, let us proceed to the perturbation calculation of the probabilities of nondiagonal transition between localized states. Two quantities will be of specific interest. The first of these is the probability

$$W_{\ldots N_k \ldots}(p \to p') = \sum_{N_{N_k \ldots}} W(p, \cdots N_k \cdots \to p', \cdots N'_k \cdots) \tag{47}$$

for a site-jump with arbitrary final vibrational quantum numbers. The second is the thermal average of (47), namely,

$$W_T(p \to p') = Z^{-1} \sum_{\ldots N_k \ldots} W_{\ldots N_k} \ldots (p \to p') \exp\left[-\sum_k \beta\hbar\omega_k (N_k + 1/2)\right] \tag{48}$$

where $\beta \equiv 1/\kappa T$ (κ and T are Boltzmann's constant and absolute temperature, respectively) and

$$Z \equiv \sum_{\ldots N_k \cdots} \exp\left[-\sum_k \beta\hbar\omega_k (N_k + 1/2)\right]$$

is the vibrational partition function.
Standard perturbation theory (4) [13] yields for the elementary transition probabilities the expression

$$\begin{aligned} W(p, \cdots N_k \cdots \to p', \cdots N'_k \cdots) = 2\hbar^{-2} \left|(p', \cdots N'_k \cdots |V| p, \cdots N_k)\right|^2 \\ \cdot \tfrac{\partial}{\partial t}\Omega\left[\textstyle\sum_k \hbar\omega_k (N'_k - N_k)\right] \end{aligned} \tag{49}$$

where

$$\Omega(x) \equiv \frac{1 - \cos(xt/\hbar)}{x^2/\hbar^2} = \frac{2\sin^2(xt/2\hbar)}{x^2/\hbar^2} \tag{50}$$

is the characteristic energy-resonance function of perturbation theory; it has the property

$$\lim_{t\to\infty} \Omega(x) = \pi\hbar t\delta(x)$$

and may be expressed in the integral form

$$\Omega(x) = \frac{1}{2}\int_0^t dt' \int_{-t'}^{+t'} e\frac{ixt''}{\hbar} dt''$$

so that

$$\frac{\partial}{\partial t}\Omega(x) = \frac{1}{2}\int_{-t}^{+t} e\frac{ixt'}{\hbar} dt' \tag{51}$$

[012] An explicit expression for the diagonal transition probability, given by Eq. (63), may be used here.
[13] As will be seen later, some care is required in going to the limit of infinite "interaction" time, t.

Upon substituting (51) and (18) into (49), one observes that the sum over the final occupation numbers, $N_k{}'$, required by (47), splits into a product of sums over the individual multiplicands of π_k. These are easily evaluated; the result is

$$\begin{aligned} W\ldots N_k\ldots(p\to p') =& \frac{J^2}{\hbar^2}\sum_{\epsilon=\pm1}\delta_{p',p+\epsilon}\int_{-t}^{+t}\pi_k\left\{\left[1-\frac{4}{N}\left(N_k+1/2\right)\right.\right. \\ & \times\gamma_k\cos^2\left[k\left(p+\frac{\epsilon}{2}\right)+\frac{\pi}{4}\right]\Big]^2 \\ & \left.+\frac{4\gamma_k}{N}\left(N_k e^{-\omega_k t'}+\left(N_k+1\right)e^{i\omega_k t'}\right)\cos^2\left[k\left(p+\frac{\epsilon}{2}\right)+\frac{\pi}{4}\right]\right\}dt' \\ =& \frac{J^2}{\hbar^2}\sum_{\epsilon=\pm1}\delta_{p,p+\epsilon}\int_{-t}^{+t}\exp\left\{\sum_k\frac{8\gamma_k}{N}\cos^2\left[k\left(p+\frac{\epsilon}{2}\right)+\frac{\pi}{4}\right]\right. \\ & \left.\times\left[-\left(N_k+1/2\right)+\left(N_k+1/2\right)\cos\omega_k t'+\frac{i}{2}\sin\omega_k t'\right]\right\}dt' \end{aligned} \tag{52}$$

wherein the contributions of the transitions $N_k\to N_k\pm2$ have been neglected; this neglect is clearly justified in view of the fact that the terms in question are $\sim 1/N^2$ (in contrast to the retained terms, which are $\sim 1/N$). [14]

As before (see footnotes 7 and 9), one takes $N_k = N_{-k}$, and is thereby free to replace $\cos^2[k(p+1/2\epsilon)+1/4\pi]$ by $1/2$. Thus,

$$\begin{aligned} W_{\ldots N_k}\ldots(p\to p') = \frac{J^2}{\hbar^2}\sum_{\epsilon=\pm1}\delta_{p',p+\epsilon}\int_{-t}^{+t}\exp\left\{\sum_k\frac{4\gamma_k}{N}\left[-\left(N_k+1/2\right)\right.\right. \\ \left.\left.+\left(N_k+1/2\right)\cos\omega_k t'+\frac{i}{2}\sin\omega_k t'\right]\right\}dt' \end{aligned} \tag{53}$$

Further progress in the evaluation of (53) is possible for an arbitrary variation of N_k with k, as long as this variation is well-behaved. However, in practice, the distribution in N_k is always thermal, so that we may as well proceed immediately to the thermal average defined by (48). In the evaluation of this average, it is expedient to employ the product form of the exponential integrand in (53), which reads

$$\pi_k\left\{1+\frac{4\gamma_k}{N}\left[-\left(N_k+1/2\right)+\left(N_k+1/2\right)\cos\omega_k t'+\frac{i}{2}\sin\omega_k t'\right]\right\},$$

It is then apparent that the thermal average over the N_k results in the replacement of each N_k by its equilibrium value, $\left(e^{\beta\hbar\omega_k}-1\right)^{-1}$; this replacement (together with the summation over ϵ) yields

$$\begin{aligned} W_T(p\to p\pm1) = \tfrac{J^2}{\hbar^2}\textstyle\int_{-t}^{+t}\exp\left\{-\sum_k\frac{2\gamma_k}{N}\left[\coth\frac{\beta\hbar\omega_k}{2}\left(1-\cos\omega_k t'\right)\right.\right. \\ \left.\left.-i\sin\omega_k t'\right]\right\}dt' \end{aligned} \tag{54}$$

For the further simplification of (54), it is desirable to introduce the transformation

$$t' = \frac{i\beta\hbar}{2}+\tau \tag{55}$$

which transforms the integrand to

[014] For the same reason, the terms in ${\gamma_k}^2$ coming from the first square-bracket in the first equality of (52) have also been discarded.

$$\exp\left\{-\sum_k \frac{2\gamma_k}{N}\left[\coth\frac{\beta\hbar\omega_k}{2}-\operatorname{csch}\frac{\beta\hbar\omega_k}{2}\cos\omega_k\tau\right]\right\}.$$

The τ-integration, which goes from $-t-i\beta\hbar/2$ to $+t-i\beta\hbar/2$ is now deformed into a component along the real axis (from $-t$ to $+t$) and two components perpendicular to this axis (from $-t-i\beta\hbar/2$ to $-t$, and from t to $t-i\beta\hbar/2$). Combining the latter two into a single integral, one obtains

$$W_T(p\to p\pm 1)=\frac{J^2}{\hbar^2}\left[\mathfrak{g}_1(t)+\mathfrak{g}_2(t)\right] \tag{56}$$

where

$$\mathfrak{I}_1(t)=\int_{-t}^{+t}\exp\left\{-\sum_k \frac{2\gamma_k}{N}\left[\coth\frac{\beta\hbar\omega_k}{2}-\operatorname{csch}\frac{\beta\hbar\omega_k}{2}\cos\omega_k\tau\right]\right\}d\tau \tag{57}$$

and

$$_2(t)\equiv\sum_{(\pm)}\mp\int_0^{\beta\hbar/2}\exp\left\{-\frac{2\gamma_k}{N}\left[\coth\frac{\beta\hbar\omega_k}{2}-\operatorname{csch}\frac{\beta\hbar\omega_k}{2}\right.\right. \tag{58}$$
$$\left.\left.\times\cos\left[\omega_k(t\pm i\sigma)\right]\right]\right\}d\sigma$$

In proceeding further, let us focus attention on the case for which the "interaction" time, t, is large compared to the vibrational periods, i.e.,

$$t\gg 1/\omega_k. \tag{59}$$

It is of specific interest to determine whether $W_T(p\to p\pm 1)$ becomes independent of t in this limit (as would be required in order that $W_T(p\to p\pm 1)$ be interpretable as a conventional transition probability).

One may begin by considering the behavior of the integrands of $_1(t)$ and $_2(t)$ for large τ. Inspection of (57) and (58) indicates that this behavior is conditioned by that of

$$G(\tau)\equiv\sum_k\frac{2\gamma_k}{N}\operatorname{csch}\frac{\beta\hbar\omega_k}{2}\cos\omega_k\tau \tag{60}$$

Asymptotic (large τ) expressions for $G(\tau)$ may be obtained by the method of steepest descents. The details of the computation will not be given; the result is

$$G(\tau)\cong 4\gamma_{k=\pi}\frac{\left(\omega_0^2-\omega_1^2\right)^{1/4}}{\omega_1\tau^{1/2}}\operatorname{csch}\frac{\beta h\left(\omega_0^2-\omega_1^2\right)}{2}\cos\left[\left(\omega_0^2-\omega_1^2\right)^{1/2}\tau+\frac{\pi}{4}\right] \tag{61}$$

i.e., $G(\tau)$ is an oscillatory function whose amplitude diminishes with increasing τ. It will be noticed that the parameter, ω_1, which is a measure of the vibrational dispersion (see Eq. 7), occurs in the denominator of (61). This feature testifies to the fact that, in order for (61) to be valid, dispersion of vibrational frequencies is necessary. In the absence of this dispersion ($\omega_k=\omega_0$, Einstein spectrum), the expressions on the right-hand side of (60) obviously reduce to simple trigonometric functions of τ, and do not go to zero with increasing τ, as indicated by (61). The presence of vibrational frequency dispersion is thus a vital ingredient of the theory.

From (61) it is clear that, in the limit specified by (59), $g_2(t)$ approaches zero as $t^{-1/2}$, and may hence be discarded. On the other hand

$$\lim_{t\to\infty} \mathscr{S}_1(t) = \int_{-t}^{+t} \exp\left\{-\sum_k \frac{2\gamma_k}{N}\left[\coth\frac{\beta\hbar\omega_k}{2} - \mathcal{O}\left(\tau^{-1/2}\right)\right]\right\} d\tau \tag{62}$$

(the notation $\mathcal{O}\left(\tau^{-1/2}\right)$, denoting a term $\sim \tau^{-1/2}$ for large τ), which does not approach a finite limit at all, but simply becomes proportional to t. Thus (56) is itself linear in t, and hence cannot represent a transition-probability in the conventional sense.

Actually, (56) is not the correct expression for the thermal average of the total nondiagonal transition probability. Referring back to (52), one may observe that this expression represents the sum of (49) over all final vibrational quantum numbers, $N_k{}'$, and thus includes the diagonal transitions, $N_k = N_k{}'$, as well. These have now to be subtracted from (56).

A simple way of evaluating the diagonal contribution to (56) is to note that the nondiagonal contributions [see the first equality of (52)] always involve the time-dependent exponentials, $e^{\pm i\omega_k t'}$; the climination of quantitics containing these factors is then equivalent to restricting the $N_{k'}$ sum to $N_{k'} = N_k$. Applying this recipe to (56) and (57), one immediately finds for the diagonal contribution, [15]

$$W_T^{(d)}(p \to p \pm 1) = \frac{J^2}{\hbar^2}\int_{-t}^{+t} \exp\left\{-\sum_k \frac{2\gamma_k}{N}\coth\frac{\beta\hbar\omega_k}{2}\right\} d\tau = \frac{2tJ^2}{\hbar^2}e^{-2S_T} \tag{63}$$

where

$$S_T = \sum_k \frac{\gamma_k}{N}\coth\frac{\beta\hbar\omega_k}{2} \tag{64}$$

is clearly the thermal average of $S\left(\cdots N_k \cdots\right)$, as defined by (33).
Subtracting the first equality of (63) from (56), one obtains the correct expression for $W_T(p \to p \pm 1)$, namely,

$$W_T(p \to p \pm 1) = \frac{J^2}{\hbar^2}e^{-2S_T}\int_{-\infty}^{+\infty}\left\{\exp\left[\sum_k \frac{2\gamma_k}{N}\operatorname{csch}\frac{\beta\hbar\omega_k}{2}\cos\omega_k\tau\right] - 1\right\} d\tau \tag{65}$$

wherein the interaction time, t, has finally been permitted to go to infinity; the fact that no convergence difficulties are thereby occasioned may be seen from the form of the integrand at large τ, which, by (61), is

$$\sim \left(1/\omega_1\tau^{1/2}\right)\cos\left[\left(\omega_0^2 - \omega_1^2\right)^{1/2}\tau + \pi/4\right]$$

and hence clearly integrable over the infinite domain.
It is of interest to evaluate (65) in the two limits in which the argument of the exponential term in the integrand is small or large compared to unity. For fixed values of the parameters, A, M, ω_0, and ω_1, which determine the γ_k, these cases occur at low and high temperatures, respectively.

Considering first the low-temperature case, one expands the second exponent as a power-series in the argument, obtaining

[015] The proportionality of (63) to t was discussed earlier (in the text surrounding Eq. 45) and needs no further comment.

$$
\begin{aligned}
W_T(p \to p \pm 1) = & \frac{J^2}{\hbar^2} e^{-2S_T} \left[\int_{-\infty}^{+\infty} 1 \int_0^{\pi} F(k) \cos \omega_k \tau dk + \frac{1}{2\pi^2} \right. \\
& \times \int_0^{\pi} \int_0^{\pi} F(k) F(k') \cos \omega_k \tau \cos w_{k'} dk dk' \\
& + \frac{1}{6\pi^3} \int_0^{\pi} F(k) F(k') F(k'') \\
& \left. \cos \omega_k \tau \cos \omega_{k'} \tau \cos \omega_{k''\tau} dk dk' dk'' + \cdots \right]
\end{aligned}
$$

where

$$
F(k) = 2\gamma_k \operatorname{csch} \frac{\beta \hbar \omega_k}{2}
$$

The integrations over τ are readily carried out, leading to the replacement of the cosines by delta functions; thus

$$
\begin{aligned}
& W_T(p \to p \pm 1) = \frac{J^2}{\hbar^2} e^{-2S} T \left\{ \int_0^{\pi} F(k) \delta(\omega_k) dk + \frac{1}{2\pi} \int_0^{\pi} \int_0^{\pi} F(k) F(k') \right. \\
& \cdot \left[\frac{1}{2} \delta(\omega_k + \omega_{k'}) + \frac{1}{2} \delta(\omega_k - \omega_{k'}) \right] dk dk' \\
& + \frac{1}{6\pi^3} \int_0^{\pi} \int_0^{\pi} \int_0^{\pi} F(k) F(k') F(k'') \left(\frac{1}{4} \right) [\delta(\omega_k + \omega_{k'} + \omega_{k''}) + \delta(\omega_k + \omega_{k'} - \omega_{k''}) \\
& \left. + \delta(\omega_k - \omega_{k'} + \omega_{k''}) + \delta(\omega_k - \omega_{k'} - \omega_{k''})] dk dk' dk'' \right\} + \cdots
\end{aligned}
\tag{66}
$$

From the form of (66) (as exhibited in particular by the curly bracket of the right-hand side), it is seen that $W_T(p \to p \pm 1)$ may be broken down into a series of processes in which one, two, three, etc. phonons are either emitted or absorbed; for each such process, the delta functions of the individual terms incorporate the requirement of conservation of energy. For example, the first term of the second curly bracket, representing a one-phonon process, is actually zero (since $\omega_k \neq 0$, in accordance with footnote [12]); i.e., a single-phonon process cannot conserve energy. Similarly, the second term represents twophonon processes; the delta function, $\delta(\omega_k + \omega_{k'})$ and $\delta(\omega_k - \omega_{k'})$ occurring in the integrand correspond, respectively, to processes in which both phonons are emitted (or absorbed) and to those in which one phonon is emitted and the other absorbed. Since the condition $\omega_k + \omega_{k'} = 0$ cannot be realized, only the
latter process actually occurs. Finally, the third term represents three-phonon processes in which one has

$$
\omega_k \pm \omega_{k'} \pm \omega_{k''} = 0
$$

i.e., one phonon is emitted (absorbed) and two absorbed (emitted).
The above interpretation also accounts for the temperature dependence of the curly-bracket of (66). For example, in the case of two-phonon processes, which are subject to the restriction, $\omega_k = \omega_{k'}$, it is readily verified that the tem-perature-dependent factor, $\operatorname{csch}(\beta \hbar \omega_k / 2) \operatorname{csch}(\beta \hbar \omega_{k'} / 2)$, may be replaced by $1/8 \left[N_k (N_{k'} + 1) + N_{k'} (N_k + 1) \right]$ (where N_k here represents the equilibrium Planck distribution). The first term of the square bracket is clearly the appropriate Bose-Einstein population factor for the transition $N_k \to N_k - 1, N_{k'} \to N_{k'} + 1$; the second term plays an analogous role for the reverse transition. Similarly, for three-phonon processes obeying, e.g., the condition, $\omega_k = \omega_{k'} + \omega_{k''}$, the temperature-dependent factor

$$\operatorname{csch}\frac{\beta\hbar\omega_k}{2}\operatorname{csch}\frac{\beta\hbar\omega_{k'}}{2}\operatorname{csch}\frac{\beta\hbar\omega_{k^*}}{2}$$

may be shown to be equivalent to

$$1/16\left[N_k\left(N_{k'}+1\right)\left(N_{k''}+1\right)+\left(N_k+1\right)N_{k'}N_{k''}\right].$$

The individual terms of the square bracket are clearly the correct Bose-Einstein population factors for the transitions $N_k \to N_k \pm 1, N_{k'} \to N_{k'} \mp 1, N_{k''} \to N_{k''} \mp 1$.

Let us now consider the behavior of (65) in the high-temperature limit, in which

$$\frac{1}{\pi}\int_0^\pi F(k)dk = \frac{1}{\pi}\int_0^\pi 2\gamma_k \operatorname{csch}\frac{\beta\hbar\omega_k}{2}dk \gg 1 \tag{67}$$

In this case the integral in (65) may be evaluated by the method of steepest descents.

We may begin by considering the contributions to the integral from the neighborhood of the point $\tau = 0$, for which the exponential factor attains an absolute maximum. One then has for the argument of the exponential

$$\frac{1}{\pi}\int_0^\pi F(k)\cos\omega_k\tau dk = \frac{1}{\pi}\int_0^\pi F(k)dk - \frac{\tau^2}{2\pi}\int_0^\pi F(k)\omega_k^2 dk \tag{68}$$

It is now to be observed that the second term of (68) will cause the exponential to drop off sharply from its maximum value. In particular, it is seen that the principal contribution to the integral will come from the region in which

$$\tilde{\tau}\left(\frac{1}{2\pi}\int_0^\pi F(k)\omega_k^2 dk\right)^{-1/2} \tag{69}$$

Noting that, according to (7),

$$\omega_0^2+\omega_1^2 > \omega_k^2 > \omega_0^2-\omega_1^2$$

so that

$$\frac{1}{2\pi}\int_0^\pi F(k)\omega_k^2 dk > \frac{\omega_0^2-\omega_1^2}{2\pi}\int_0^\pi F(k)dk$$

one may conclude that, in the domain specified by (69),

$$\omega_k\tau \succeq \left(\frac{\omega_0^2+\omega_1^2}{\omega_0^2-\omega_1^2}\right)^{1/2} / \left(\frac{1}{2\pi}\right)\int_0^\pi F(k)dk \ll 1 \tag{70}$$

the last inequality holding by virtue of (67). It then follows that the higher order terms of (68), resulting from the expansion of $\cos\omega_k\tau$, may be ignored, so that the substitution of (68) into (65) yields

$$W_T^{(0)}(p\to p\pm 1) = \frac{J^2}{\hbar^2}e^{-2S_T}\left[\frac{1}{\pi}\frac{2\pi}{\int_0^\pi 2\gamma_k\omega_k^2\operatorname{csch}\frac{\beta\hbar\omega_k}{2}dk}\right]^{1/2} \tag{71}$$
$$\cdot\exp\left[\frac{1}{\pi}\int_0^\pi 2\gamma_k\operatorname{csch}\frac{\beta\hbar\omega_k}{2}dk\right]$$

where the superscript "(0)" on the left-hand side indicates that (71) represents only the contribution in the neighborhood of $\tau = 0$.

Let us now consider the contributions to $W_T(p \to p \pm 1)$ from the other points, $\tau_i \neq 0$, which minimize the integrand of (65). It is expedient to write the argument of the exponential term of that integrand in the form

$$2\gamma \operatorname{csch} \frac{\beta\hbar\omega_0}{2} \frac{1}{\pi} \int_0^\pi H(k) \cos \omega_k \tau dk$$

where

$$\gamma \equiv \frac{A^2}{2M\omega_0^3\hbar} \tag{72}$$

and where

$$H(k) \equiv \frac{\omega_0^3}{\omega_k^3} \frac{\operatorname{csch} \frac{\beta\hbar\omega_k}{2}}{\operatorname{csch} \frac{\beta\hbar\omega_0}{2}} (1 - \cos k) \tag{73}$$

is a function of the order of unity (as long as ω_k is not too small compared to ω_0 and $\beta\hbar\omega_0/2 = \hbar\omega_0/2\kappa T$ not too large). The condition (67) is then essentially equivalent to

$$2\gamma \operatorname{csch} \frac{\beta\hbar\omega_0}{2} \gg 1 \tag{74}$$

It is now physically reasonable that, if the vibration spectrum (as given by Eq. 7) exhibits sufficient dispersion (e.g., if $\omega_1 \sim \omega_0$), the numerical values of the quantity

$$\frac{1}{\pi} \int_0^\pi H(k) \cos \omega_k \tau_i dk$$

at the maximal points, τ_i, will be smaller than the absolute maximum

$$\frac{1}{\pi} \int_0^\pi H(k) dk$$

attained at $\tau = 0$, by amounts of the order of unity. If this be granted, it then follows, by virtue of (74), that the values of the maxima of the integrand of (65) at the points τ_i are negligibly small compared to the principal one at $\tau = 0$. The contributions from the neighborhoods of $\tau_i \neq 0$ may thus forthwith be neglected, with the result that the right-hand side of (71) is a sufficiently good approximation to the total $W_T(p \to p \pm 1)$.

As a check of the above qualitative argument, a calculation has been carried out in Appendix I for the case of a narrow frequency band ($\omega_1 \ll \omega_0$). It is found that the contributions associated with the subsidiary maxima at $\tau_i \neq 0$ are negligible provided that (see Eq. I-15)

$$2\gamma \frac{\pi^2 \omega_1^4}{8\omega_0^4} \operatorname{csch} \frac{\beta\hbar\omega_0}{2} \gg 1 \tag{75}$$

If, now, for the purpose of order-of-magnitude comparison (75) be extrapolated to the region of $\omega_1 \sim \omega_0$, it clearly becomes equivalent to (74). This equivalence, in the opinion of the present author, constitutes adequate confirmation of the above qualitative argument for the neglect of the contributions of the subsidiary maxima, and for the consequent applicability of (71) to the total $W_T(p \to p \pm 1)$.

Of course, in the case that the frequency spectrum is actually of narrow-band character, the more stringent condition (75) should be used in place of (74). A significant consequence is that in the limiting case of an Einstein spectrum ($\omega_1 = 0, \omega_k = \omega_0$), in which (75) cannot be fulfilled, the approximation represented by (71) breaks down altogether. This breakdown can be seen more directly by setting $\omega_k = \omega_0$ in (65), whence one obtains upon integrating over k,

$$W_T(p \to p \pm 1) = \frac{J^2}{\hbar^2} \exp\left[-2S_T\right] \int_{-\infty}^{+\infty} \left\{ \exp\left[2\gamma \operatorname{csch} \frac{\beta\hbar\omega_0}{2} \cos\omega_0\tau\right] - 1 \right\} dt \tag{76}$$

which clearly diverges, since the integrand is now a positive periodic function of τ [with a period of $(2\pi/\omega_0)$].

In proceeding further, it is convenient to write (71) in the alternate form

$$W_T(p \to p \pm 1) = \frac{J^2}{\hbar^2} \left[\frac{2\pi}{\pi^{-1} \int_0^\pi 2\gamma_k \omega_k^2 \operatorname{csch} \frac{\beta\hbar\omega_k}{2} dk} \right]^{1/2} \times \exp\left\{ \pi^{-1} \int_0^\pi 2\gamma_k \tanh\left(\beta\hbar\omega_k/4\right) dk \right\} \tag{77}$$

where the superscript (0) has now been dropped, in accordance with the above discussion.

Considerable insight into the physical significance of the various factors in (77) is gained by considering the "classical" limit, for which

$$\beta\hbar\omega_k \equiv \hbar\omega_k/\kappa T \ll 1 \tag{78}$$

In this limit the hyperbolic tangent gets replaced by its argument; then, upon eliminating γ_k by use of its definition (19), one has

$$W_T^{(\mathrm{cl})}(p \to p \pm 1) = \frac{J^2}{\hbar^2} \left[\frac{\pi}{4\kappa T E_a} \right]^{1/2} e^{-E_a/\kappa T} \tag{79}$$

where

$$E_a \equiv \pi^{-1} \int_0^\pi \left(\gamma_k \hbar\omega_k/2\right) dk = \pi^{-1} \int_0^\pi \left(A^2/4M\omega_k^2\right) (1 - \cos k) dk \tag{80}$$

It will be observed that the temperature dependence of (79) is of the type characteristic of an activation process, with E_a playing the role of an activation energy. It turns out, in fact, that, in the approximation in which the vibrational motion is treated classically, (79) may be obtained by a simple "occurrenceprobability" approach. This approach is presented in Appendix II. It is shown therein that site jumps between neighboring sites (say, p and $p \pm 1$) occur principally when the values of the unperturbed "electronic" energies, $-Ax_p$ and $-Ax_{p+1}$, coincide. Specifically, it is found that (79) may be written in the form

$$W_T^{(\mathrm{cl})}(p \to p \pm 1) = \int_{-\infty}^{+\infty} P_T^{(c)}\left(v_r\right) W_c(p \to p+1) dv_r \tag{81}$$

where (see II 18)

$$P_T^{(c)}\left(v_r\right) dv_r = \left(\frac{M}{4\pi\kappa T}\right)^{1/2} e^{-Mv_r^2/4\kappa T} \left|v_r\right| \frac{A}{2\pi} \left(\frac{\pi}{4\kappa T E_a}\right)^{1/2} e^{-E_a/\kappa T} \tag{82}$$

is the probability per unit time for the occurrence of a coincidence event, $x_p = x_{p+1}$, in which the "relative" velocity, $v_r = v_p - v_{p+1} = (d/dt)\left(x_p - x_{p+1}\right)$ lies in a specified differential range, and where (see II 9),

$$W_c(p \to p+1) = \frac{2\pi J^2}{\hbar} \frac{1}{A\left|v_r\right|} \tag{83}$$

is the probability that, in such an event, a site-jump takes place. [16]
One may, in addition, show that the activation energy, E_a, is the minimum potential energy (in excess of the absolute minimum, $-E_b$) of a configuration for which $x_p = x_{p+1}$. It should, in particular, be emphasized that E_a is substantially smaller than the binding energy of the polaron,

$$E_b = \frac{1}{\pi}\int_0^\pi \frac{A^2}{2M\omega_k^2}dk \tag{84}$$

(see Eq. 13). This inequality means simply that the energy necessary to establish a "neighbor" coincidence must always be less than that required for the thermal dissociation of the polaron.

Having discussed the behavior of $W_T(p \to p \pm 1)$ in the classical limit, let us utilize the general quantal expression (77) to estimate the "transition" temperature, T_t, at which the mean life of the localized state,

$$\frac{1}{\tau_{p,T}} \equiv W_T(p \to p+1) + W_T(p \to p-1) = 2W_T(p \to p+1) \tag{85}$$

is equal to $1/\hbar$ times the mean polaron bandwidth

$$\Delta E_T = 2Je^{-S_T} \tag{86}$$

From the discussion of Eqs. (44)-(46), T_t is to be considered as defining the boundary between the two regions of high and low temperature, in which the random site-jump and band descriptions of polaron motion are respectively valid. Equating (85) to $1/\hbar$ times (86), and employing (71) and (64), one obtains

$$\begin{aligned}&\frac{\hbar}{J}\left[\frac{1}{2\pi^2}\int_0^\pi 2\gamma_k\omega_k^2 \operatorname{csch}\frac{\beta\hbar\omega_k}{2}dk\right]^{1/2}\\ &\quad = \exp\left\{\frac{1}{\pi}\int_0^\pi \gamma_k\left[2\operatorname{csch}\frac{\beta\hbar\omega_k}{2} - \coth\frac{\beta\hbar\omega_k}{2}\right]dk\right\}\end{aligned} \tag{87}$$

For an order of magnitude estimate of T_t, it will be sufficient to consider the case of a narrow-band vibrational spectrum (in which $\omega_k \cong \omega_0$). Then, upon taking logarithms on both sides, one has

$$2\operatorname{csch}\frac{\beta_t\hbar\omega_0}{2} - \coth\frac{\beta_t\hbar\omega_0}{2} = \frac{1}{\gamma}\log\left[\frac{\hbar\omega_0}{J}\left(\frac{\gamma\operatorname{csch}\beta_t\hbar\omega_0/2}{\pi}\right)^{1/2}\right] \tag{88}$$

[16] The fact that, when (82) and (83) are inserted into (81), the resultant expression reduces to (79) may readily be verified.
which constitutes a transcendental equation for $\beta_t \equiv 1/\kappa T_t$. Choosing for γ a representative value [17] of 10 , one finds that, for $\hbar\omega_0/J$ contained between the extremes of units and 100, T_t lies in the range 0.4-0.55 times the Debye Θ.

It may be remarked that, in view of the exponential temperature dependence of both ΔE_T and $\hbar/\tau_{p,T}$, the transition region, within which neither the sitejump or band approaches are valid, is quite small, and may in practice be ignored.

It may also be pointed out here, that, in the neighborhood of the transition temperature, and with γ large compared to unity, as is the case at hand, inequality (67) (or (74)) holds; it then follows that (77), rather than (66), is the appropriate formula to use for $W_T(p \to p \pm 1)$ in the high-temperature domain in which the site-jump approach applies.

IV. NONDIAGONAL TRANSITIONS BETWEEN POLARON-BAND STATES: MEAN LIFETIMES

In order to round out the theory, it is desirable to obtain an expression for the mean probability per unit time, $W_T(\sigma \to \sigma')$, that a nondiagonal transition between polaron-band states σ and σ' takes place. Due to limitations of space, the derivation of this expression will not be given in detail; a brief outline follows.

One starts with (41), which, with the aid of (36), (40) and the Fourier integral expression for the delta function, may be written as

$$\begin{aligned} &W(\sigma, \cdots N_k \cdots \to \sigma', \cdots N_k' \cdots) \\ &= \frac{1}{N^2} \sum_{\substack{pp' \\ qq'}} e^{i[\sigma(p-q)-\sigma'(p'-q')]} \times W(p, q, \cdots N_k \cdots \to p', q', \cdots N_k' \cdots) \end{aligned} \tag{89}$$

where

$$\begin{aligned} &W(p, q, \cdots N_k \cdots \to p', q', \cdots N_k' \cdots) \\ &= \frac{1}{\hbar^2} \int_{-t}^{+t} e^{i(\Delta\epsilon\sigma\sigma')t'/\hbar} \exp\left\{\sum_k i\omega t' (N_k' - N_k)\right\} \\ &\quad \times (p', \cdots N_k' \cdots |V| p, \cdots N_k \cdots) \\ &\quad \cdot (q', \cdots N_k' \cdots |V| q, \cdots N_k \cdots)\, dt' \end{aligned} \tag{90}$$

and

$$\Delta\epsilon_{\sigma\sigma'} = -2J\left[\cos\sigma' e^{-s\left(\cdots N_k' \cdots\right)} - \cos\sigma e^{-s(\cdots N_k \cdots)}\right]. \tag{91}$$

Substituting (18) into (90), one carries out the sum over $N_k{}'$ and the thermal average over N_k in essentially [18] the same way as was done for the computation

[17] With this value, the activation energy $E_u \sim \gamma(\hbar\omega_0/2)$ is five times the Debye energy, $\hbar\omega_0$; taking the latter to be, e.g., 0.04 ev , one has $E_a = 0.2$ev. The corresponding value of the polaron binding energy, E_b, is $= 0.4$ev. These estimates are suggested by experiments on hole conduction in transition metal oxides [see Heikes and Johnston (5)] to which the present theory may find application.

[18] Some difficulties arise in principal because of the dependence of the $N_{k'}$ (via the fac- of $W_T(p \to p')$. The result is

$W_T(\sigma \to \sigma')$

$$\begin{aligned} &= \sum_{M=-\frac{N}{2}}^{+M_2} \sum_{\epsilon=\pm 1} \frac{2J^2}{N\hbar^2} \cos[(\sigma - \sigma')M] \cos\left[\frac{(1-\epsilon)(\sigma+\sigma')}{2}\right] e^{-2S_T} \\ &\times \int_{-\infty}^{+\infty} e^{i(\Delta\epsilon\sigma\sigma')t'/\hbar} \exp\left\{\sum_k 2\epsilon\gamma_k \operatorname{csch}\frac{\beta\hbar\omega_k}{2} \cos\omega_k t' \cos kM\right\} dt' \end{aligned} \tag{92}$$

where, in accordance with footnote 18 , the $N_k{}'$ in (91) are to be replaced [19] by the N_k.

One may now treat (92) in a manner analogous to (65) to obtain formulae for the two cases in which $\sum_k (2\gamma_k/N) \operatorname{csch}(\beta\hbar\omega_k/2)$ is small or large compared to unity. In the first case, one obtains an expression analogous to (66), which incorporates the added feature of wave-vector

conservation, via the occurrence of Krönecker-delta factors of the form $\delta_{\sigma-\sigma'\pm k\pm k'\pm k''}\ldots$. This case will not be discussed further, since it is most likely that, in the domain in which it is valid, other scattering mechanisms, such as impurity scattering, would be dominant.

In the alternate case, defined by inequality (67), the method of steepest descents is applicable. One finds here that the term in (92) for which $M = 0$ and $\epsilon = 1$ gives by far the largest contribution. Ignoring the other terms, and replacing $\exp\left[i\left(\Delta\epsilon_{\sigma\sigma'}\right)t'/\hbar\right]$ by unity, in accordance with footnote 19, one then sees that, apart from the factor, $2/N$, the expression for $W_T\left(\sigma\to\sigma'\right)$ is identical with that for $W_T\left(p\to p'\right)$, i.e., [20]

$$W_T\left(\sigma\to\sigma'\right) = \frac{2J^2}{N\hbar^2}e^{-2S_T}\left[\frac{2\pi}{\pi^{-1}\int_0^\pi 2\gamma\omega_k^2\,\mathrm{esch}\,\frac{\beta\hbar\omega_k}{2}dk}\right]^{1/2} \times\exp\left\{\pi^{-1}\int_0^\pi 2\gamma_k\,\mathrm{csch}\,\frac{\beta\hbar\omega_k}{2}dk\right\} \tag{93}$$

tor $\exp\left[-S\left(\cdots N_k,\cdots\right)\right]$). However, as can be inferred by examination of the higher order terms in (66), or in fact verified by a computation of

$$\left\langle\sum_k\left(\Delta N_k\right)^2\right\rangle_{\mathrm{Av}} \equiv \sum_k\left\langle\sum_{N_{k'}}\left(N_k-N_k\right)^2 W\left(\sigma,\cdots N_k\cdots\to\sigma',\cdots N_{k'}\cdots\right)\right\rangle_T \Big/ \left\langle\sum_{N_{k'}} W\left(\sigma,\cdots N_k\cdots\to\sigma',\cdots N_{k'}\cdots\right)\right\rangle_T$$

the average number of phonon emissions and absorptions accompanying a transition is finite [in fact, of the order of $\gamma\,\mathrm{csch}\left(\beta\hbar\omega_0/2\right)$] rather than, say, $\sim N$. For such transitions, the difference between $S\left(\cdots N_k,\cdots\right)$ and $S\left(\cdots N_k\cdots\right)$ is $\sim 1/N$, and hence to be ignored.

[19] Actually, in view of the smallness ($\sim 10^{-2}$) of $\Delta\epsilon_{\sigma\sigma}$, in comparison with $\hbar\omega_k$, one may, for all practical purposes, ignore the factor $\exp\left\{i\Delta\epsilon_{\sigma\sigma'}t/\hbar\right\}$ in (92) altogether.

[20] It is of interest to note, in passing, that (93) does not depend on either the initial or final electron wave vectors, σ and σ'. This feature is analogous to the lack of occurrence in (93) (or 77) of energy delta functions, both features being characteristic of multi-phonon processes.

The mean lifetime of a polaron-band state, $\tau_{\sigma,T}$, is given by summing (93) over all σ', i.e.,

$$\frac{1}{\tau_{\sigma,T}} = \sum_{\sigma'} W_T\left(\sigma\to\sigma'\right) = 2W_T\left(p\to p'\right) = 1/\tau_{p,T} \tag{94}$$

where $1/\tau_{p,T}$ is the total site-jump probability, given by (85). Equation (94) exhibits the fact that the lifetimes of the localized states and the polaron-band states are equal.

6.2.13 Holstein's Studies of Polaron Motion. Part II. The "Small" Polaron 3

V. TRANSPORT PHENOMENA: POLARON DIFFUSIVITY

The stage has now been reached where applications to transport properties may be considered. In what follows, attention will be focussed on the diffusivity, D, which, for the case of a nondegenerate polaron gas, is related to the mobility, b, through the Einstein relation

$$b = \frac{eD}{\kappa T} \tag{95}$$

Two cases have to be considered:

Case $I.T > T_t$: Here, as discussed above, polaron motion takes place via a succession of random

site-jumps, in each of which the electron hops to a neighbor site with probability, $W_T(p \to p \pm 1)$. For the one-dimensional model under consideration, the diffusivity is easily seen to be

$$D = a^2 W_T(p \to p \pm 1) \tag{96}$$

where a is the lattice spacing. For illustrative purposes, let us consider the nar-row-band approximation of $\omega_k = \omega_0$. One then has, from (77) and (96)

$$D = \omega_0 a^2 \frac{J^2}{\hbar^2 \omega_0^2} \left[\frac{2\pi}{2\gamma \operatorname{csch} \frac{\beta\hbar\omega_0}{2}} \right]^{1/2} \exp\left\{ -2\gamma \tanh \frac{\beta\hbar\omega_0}{4} \right\} \tag{97}$$

The "relative" diffusivity

$$\mathfrak{D} \equiv D/\omega_0 a^2 \tag{98}$$

is plotted in Fig. 1 as a function of $\beta\hbar\omega_0 \equiv \kappa T$ for representative values of the model parameters $[J = \hbar\omega_0, \gamma = 10$ (see footnote 17)]. Also, shown (as the dotted curve) is the classical approximation, obtained by using (79) in place of (77).

Case II. $T < T_t$: Here, the band approach applies, and one has the conventional formula [21] (adapted to a one-dimensional model)

$$D = \left\langle v_{\sigma,T}^2 \tau_{\sigma,T} \right\rangle_{\mathrm{Av}}$$

[21] In the case at hand, the independence of $W_T\,(\sigma \to \sigma')$ with respect to σ', permits identification of the momentum-transfer rate with the total collision probability.

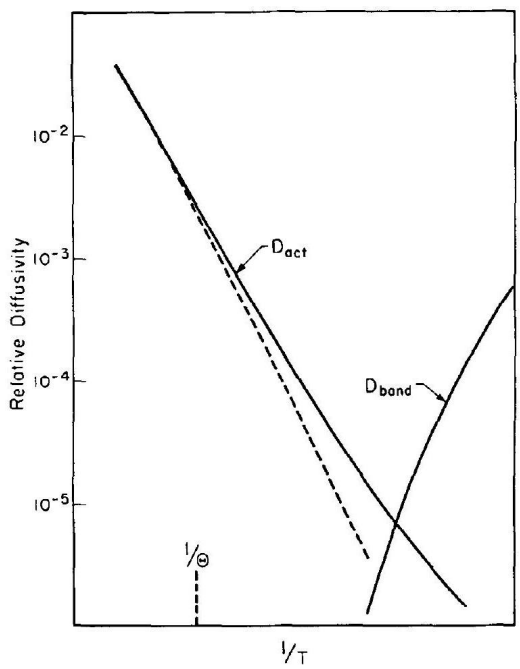

Fig. 1. Polaron diffusivity versus temperature. The solid curves labelled " D_{act} " and " D_{band} " represent the contribution arising from random site jumps and polaron-band motion, respectively. The dashed curve gives the classical approximation to D_{act} .

where, from (36),

$$v_{\sigma,T} \equiv \frac{a}{\hbar} \frac{\partial}{\partial k} E_{\sigma,T} = \frac{2J}{\hbar} \sin \sigma e^{-S_T} \tag{99}$$

is the expectation velocity in a state of wave-number σ, and where the average in (98) is to be taken over the distribution in σ. In view of the extreme smallness of the bandwidth ($\sim 10^{-3}\hbar\omega_0 \ll \kappa T$), one may assume the σ 's to be equally populated, so that

$$D = \pi^{-1} \int_0^{\pi} v_{\sigma,T}^2 \tau_{\sigma,T} d\sigma$$

which, with (99) and (94), becomes

$$D = \frac{2J^2}{\hbar} a^2 \tau_{p,T} e^{-2S_T} \tag{100}$$

Using (85), (71), and (64) (in the narrow-band approximation), one then has for the relative diffusivity

$$\begin{aligned} \mathbb{D} = \frac{D}{\omega_0 a^2} &= \frac{2J^2}{\hbar^2\omega_0^2} \omega_0 \tau_{p,T} e^{-2S} T \\ &= 2\left[\frac{\gamma \operatorname{csch} \frac{\beta\hbar\omega_0}{2}}{\pi}\right]^{1/2} \exp\left\{-2\gamma \operatorname{csch} \frac{\beta\hbar\omega_0}{2}\right\} \end{aligned} \tag{101}$$

This expression is also plotted in Fig. 1 for the same numerical values of the model-parameters as (97) (i.e., $J = \hbar\omega_0, \gamma = 10$). As is to be expected, (101) and (97) attain comparable numerical values in the neighborhood of the transition temperature, T_t.

VI. LIMITS OF APPLICABILITY OF THE PERTURBATION TREATMENT

It is now of interest to discuss the limitations of the perturbation approach, upon which the treatment of the present paper is based. Specifically, one wants an estimate of the upper limit of the electronic bandwidth parameter, $J_{\max}$, for which perturbation theory is valid. Two extreme cases will here be considered: (a) random site-jumps in the classical limit, $\kappa T \gg \hbar_{\omega_0}$, and (b) the polaronband at the absolute zero of temperature.

Case (a): For this case, the limitations of the perturbation approach are treated in Appendix III. It is found [see (III 7) and subsequent discussion], that

$$J_{\max} \sim \left(A\hbar \left|v_{p+1} - v_p\right| / 2\pi\right)^{1/2} \tag{102}$$

where $v_{p+1} - v_p = (d/dt)(x_{p+1} - x_p)$ is the velocity with which a crossing point $x_{p+1} = x_p$ is approached; in line with the discussion of Eqs. (81)-(83) (as well as with Appendix II), such crossing (or coincidence) events are crucially significant for the occurrence of site-jumps. Taking $|v_{p+1} - v_p| \sim (2\kappa T/\pi M)^{1/2}$, one finds

$$J_{\max} \sim \left(\frac{A\hbar}{2\pi}\right)^{1/2} \left(\frac{2\kappa T}{\pi M}\right)^{1/4}$$

which, in the narrow-band case of $\omega_k \cong \omega_0$, may be transformed via (80) to read

$$J_{\max} \sim E_a^{1/4} \left(\frac{2\kappa T}{\pi}\right)^{1/4} \left(\frac{\hbar\omega_0}{\pi}\right)^{1/2} \tag{103}$$

When J is larger than (103), the adiabatic approach (also discussed in Appendix III) becomes valid. In particular, $W_T(p \to p+1)$ is obtained by integrating the coincidence probability (82), over all positive values of $v_r = v_{p+1} -$
v_p. The result of such an integration is

$$W_T(p \to p+1) = \left(\frac{\kappa T}{\pi M}\right)^{1/2} \frac{A}{2\pi} \left(\frac{\pi}{4\kappa T E_a}\right)^{1/2} e^{-E_a/\kappa T}$$

which, again in the narrow-band limit, becomes

$$W_T(p \to p+1) = \frac{\omega_0}{2\pi} e^{-E_a/\kappa T} \tag{104}$$

Case (b): For the polaron-band at absolute zero, the discussion will be based upon preliminary computations which have been carried out for the simplest possible case, namely, a linear chain consisting of only two molecular sites. While this case represents a considerable oversimplification of the multi-site chain, it is, in the opinion of the present author, still relevant. [22] The basic equations are (with neglect of intermolecular coupling, i.e., $\omega_1 = 0$)

$$\begin{aligned}
&\left[E + \frac{\hbar^2}{2M}\left(\frac{\partial^2}{\partial x_1^2} + \frac{\partial^2}{\partial x_2^2}\right) - \frac{1}{2}M\omega_0^2\left(x_1^2 + x_2^2\right) + Ax_1\right] a_1(x_1, x_2) \\
&\qquad\qquad = -Ja_2(x_1, x_2) \\
&\left[E + \frac{\hbar^2}{2M}\left(\frac{\partial^2}{\partial x_1^2} + \frac{\partial^2}{\partial x_2^2}\right) - \frac{1}{2}M\omega_0^2\left(x_1^2 + x_2^2\right) + Ax_2\right] a_2(x_1, x_2) \\
&\qquad\qquad = -Ja_2(x_1, x_2)
\end{aligned} \tag{105}$$

Two limiting methods are available for the treatment of (105); the perturbation and the adiabatic approaches, valid in the extremes of small and large J, respectively. These will now be developed; comparison of the results will then provide an estimate for $J_{\max}$.

In the perturbation approach, one takes odd and even combinations of the zeroth order "wave functions"

$$\begin{aligned}
a_1^{(1)} &= \exp\left\{-\frac{1}{2}\frac{M\omega_0}{\hbar}\left[\left(x_1 - A/M\omega_0^2\right)^2 + x_2^2\right]\right\}; \quad a_2^{(1)} = 0 \\
a_1^{(2)} &= 0; \quad a_2^{(2)} = \exp\left\{-\frac{1}{2}\frac{M\omega_0}{\hbar}\left[x_1^2 + \left(x_2 - A/M\omega_0^2\right)^2\right]\right\}
\end{aligned}$$

These combinations are

$$\begin{aligned}
a_1^{(\pm)} &= \exp\left\{-\frac{1}{2}\frac{M\omega_0}{\hbar}\left[\left(x_1 - A/M\omega_0^2\right)^2 + x_2^2\right]\right\} \\
a_2^{(\pm)} &= \pm\exp\left\{-\frac{1}{2}\frac{M\omega_0}{\hbar}\left[\left(x_2 - A/M\omega_0^2\right)^2 + x_1^2\right]\right\}
\end{aligned} \tag{106}$$

where the superscript ($\pm$) designates the even and odd combinations, respectively. The corresponding eigenvalues, $E^{(\pm)}$, of (105) are obtained by the standard secular calculations, and are

$$E^{(\pm)} = -\frac{A^2}{M\omega_0^2} + \hbar\omega_0 \mp \Delta E \tag{107}$$

where [23]

[022] In particular, preliminary calculations indicate the existence of a rather good possibility that the adiabatic treatment of the two-site case, given below, will be capable of generalization to the multi-site case of physical interest.

$$\Delta E = J \exp\left\{-A^2/2M\omega_0^2\hbar\omega_0\right\}. \tag{108}$$

In the adiabatic approach, one assumes a wave function of the form

$$\begin{aligned} a_1(x_1, x_2) &= \chi(x_1, x_2)\, c_1(x_1, x_2), \\ a_2(x_1, x_2) &= \chi(x_1, x_2)\, c_2(x_1, x_2), \end{aligned} \tag{109}$$

where the c 's are solutions of the "electronic" equations

$$\begin{aligned} (\mathcal{E} + Ax_1)\, c_1 &= -Jc_2, \\ (\mathcal{E} + Ax_2)\, c_2 &= -Jc_1, \end{aligned} \tag{110}$$

the eigenvalue $\mathcal{E}(x_1, x_2)$ constituting the "electronic" energy. As is known, $\varepsilon(x_1, x_2)$ also plays the role of a potential energy term in the equation for the "vibrational" wave function, $\chi(x_1, x_2)$, which reads

$$\left[E + \frac{\hbar^2}{2M}\frac{\partial^2}{\partial {x_1}^2} + \frac{\partial^2}{\partial {x_2}^2} - \frac{1}{2}M{\omega_0}^2\left({x_1}^2 + {x_2}^2\right) - \mathcal{E}(x_1, x_2)\right]\chi(x_1, x_2) = 0. \tag{111}$$

The eigenvalues of (110) have already been obtained in the latter part of Appendix II; of these, only the lowest

$$\varepsilon_{(-)}(x_1, x_2) = -\frac{A(x_1 + x_2)}{2} - \left[\frac{A^2(x_1 - x_2)^2}{4} + J^2\right]^{1/2} \tag{112}$$

is of interest in the adiabatic approximation.
Upon substituting (112) into (111), one observes that the transformation

$$\begin{aligned} X &= \frac{x_1 + x_2}{2}, \\ x &= x_2 - x_1 \end{aligned} \tag{113}$$

leads to a product solution of the form $\chi(x_1, x_2) = \phi(X)\psi(x)$. The equation for $\phi(X)$ is that of a simple harmonic oscillator in the presence of a constant force,

A; apart from the fact that its lowest eigenvalue is $-(A^2/4M{\omega_0}^2) + (\hbar\omega_0/2)$, it is of no further interest.

The equation for $\psi(x)$ is

$$\left[E + \frac{A^2}{8\mu\omega_0^2} - \frac{\hbar\omega_0}{2} + \frac{\hbar^2}{2\mu}\frac{\partial^2}{\partial x^2} - \frac{\mu}{2}\omega_0^2 x^2 + \left\{\left(\frac{Ax}{2}\right)^2 + J^2\right\}^{1/2}\right]\psi(x) = 0 \tag{114}$$

where

$$\mu \equiv M/2 \tag{115}$$

The potential energy for this problem, namely

[023] Apart from a numerical factor of 2, (108) is just what would be obtained from (28) and (27) in the narrow-band limit of $\omega_k = \omega_0$. The absence of the factor of 2 in (108) is due to the special feature of a two-site system, in which the number of nearest neighbors is one, rather than two.

$$V(x) = {}_2^{\mu}\omega_0^2 x^2 - \left\{ \left(\frac{Ax}{2} \right)^2 + J^2 \right\}^{1/2}$$

possesses two minima, which, for J small compared to $A^2/2M{\omega_0}^2$ (small-polaron condition), are approximately located at $x = \pm A/2\mu{\omega_0}^2$, and have the common value

$$V_{\min} \cong -\frac{A^2}{8\mu\omega_0^2}$$

These two minima are separated by a barrier whose height (relative to the minima) is $A^2/8\mu{\omega_0}^2 - J \cong A^2/8\mu{\omega_0}^2$. The potential is thus quite similar to that encountered in the theory of the inversion spectrum of the ammonia molecule. As in that case, the condition, $\hbar\omega_0 \ll$ barrier height, ($\gamma \gg 1$) permits solving for the energy splitting of the two lowest states by WKB tunnelling techniques. Omitting the detailed computations, one finds

$$\Delta E = J \left[\frac{1}{\pi} \frac{A^2}{2M\omega_0^2} \frac{\hbar\omega_0}{J^2} \right]^{1/2} \exp\left\{ -\frac{A^2}{2M\omega_0^2\hbar\omega_0} \right\} \cdot \exp\left\{ \frac{J^2}{2\hbar\omega_0\left(A^2/2M\omega_0^2\right)} + \frac{J^2}{\hbar\omega_0\left(A^2/2M\omega_0^2\right)} \log \frac{A^2}{M\omega_0^2 J} \right\} \tag{116}$$

It will now be noticed that, apart from the logarithmic term, (116) and (108) are of comparable magnitude when

$$J \sim J_{\max} \equiv \left(A^2/2M\omega_0^2\right)^{1/2} (\hbar\omega_0)^{1/2} \tag{117}$$

From this comparison it may be inferred that $J_{\max}$, as defined by (117), gives the upper limit of applicability of perturbation theory.

Considering, now, the logarithmic term, one sees that, since, for $J \sim J_{\max}$,

$$\frac{A^2}{M\omega_0^2 J} \sim \left(\frac{A^2}{M\omega_0^2\hbar\omega_0} \right)^{1/2} \gg 1$$

deviations between (112) and (108) occur at J values somewhat smaller than the right-hand side of (117). Strictly speaking, then, $J_{\max}$ should be redefined as

$$J_{\max} = \left(A^2/2M\omega_0^2\right)^{1/2} (\hbar\omega_0)^{1/2} / \log\left(A^2/M\omega_0^2\hbar\omega_0\right)^{1/2}$$

However, in view of the circumstance that the logarithm is numerically comparable to unity, this last expression is essentially equivalent to (117).

Let us note, in passing, that (117) may be written in a form analogous to the high-temperature limit, namely,

$$J_{\max} = \left(Ahv_r^{(\text{eff})}/2\pi\right)^{1/2} \tag{118}$$

where

$$v_r^{(\text{eff})} = (\pi A/M\omega_0) = (\pi A/2\mu\omega_0)\,. \tag{119}$$

It may now be noted, from (114) and subsequent text, that (119) is of the same order as the "imaginary" velocity

$$\left(\frac{2}{\mu} \frac{A^2}{8\mu\omega_0^2} \right)^{1/2} = \frac{A}{2\mu\omega_0}$$

which the system possesses in the neighborhood of the barrier maximum at $x = 0$, i.e., in the neighborhood of the crossing point of the unperturbed ($J = 0$) potential energy curves. In the high-temperature case, this point is classically accessible, so that, in the general formula, $v_r = (2E_{\text{kin}}/\mu)$, the actual kinetic energy $\sim_\kappa T$ is to be used. In the case of the ground state, the crossing point is classically inaccessible; from the analogy to conventional barrier problems, one takes $E_{\text{kin}} \sim A^2/8\mu\omega_0{}^2$.

It is now of interest to obtain numerical estimates for $J_{\max}$. In terms of the numbers given in footnote 9 , these estimates are

$$J_{\max}^{(T)} \cong 0.67\hbar\omega_0(T/\theta)^{1/4} = 0.027(T/\theta)^{1/4}\text{ev}$$

and

$$J_{\max}^{(0)} \cong 3\hbar\omega_0 = 0.12\text{ev}$$

for the cases of high-temperature site-jumps and ground-state bandwidths, respectively. Selecting for T/θ a representative value of 3 (while this choice pushes (108) to the limit of its domain of applicability, the formula should still be serviceable for order-of-magnitude considerations), one has $J_{\max}^{(T)} \sim 0.035$ev; both this value and that of 0.12 ev , cited for the ground-state limit, $J_{\max}^{(0)}$, represent rather small electronic bandwidths, indeed. It is thus apparent that the perturbation approach covers only part of the total region ($J < A^2/2M\omega_0{}^2 \sim 0.4$ev) of significance for the small polaron; for the remainder of this region, the adiabatic, rather than the perturbation, approach is to be employed.

Some orienting calculations, based on the adiabatic approach, have been performed for the energy levels of the ground-state polaron band. On the basis of these calculations, it appears likely that the levels in question are given by an expression of the form of (26), in which the coefficient, $2Je^{-S}$, gets replaced by twice the right-hand side of (116).

In the other extreme of high-temperature site-jumps, it appears that the adiabatic expression (104) will hold, subject to the stipulation that formula (80) for the activation energy will have to be modified to take account of the progressive lowering of the potential barrier [24] with increasing J.

VII. COMPARISON WITH OTHER SMALL POLARON TREATMENTS

The discussion given here will deal exclusively [25] with the paper of Y and K (3). These authors were primarily concerned with computing the probabilities of thermally activated site-jumps. Using a method originally developed for the treatment of optical transitions in F-centers (which is substantially equivalent to that of the present paper), but also restricting themselves to the Einstein approximation ($\omega_k = \omega_0$), they obtain an expression for the site-jump probability, which reads (see their Eq. 43)

$$W = \tfrac{2\pi}{\hbar}|M|^2 \exp\{-S(2n+1)\}\tfrac{1}{2\pi\hbar}\int_{-\infty}^{+\infty} \exp\left\{2S[n(n+1)]^{1/2} \cdot \cos\omega t\right\}dt \tag{120}$$

where $n \equiv \left[e^{\beta\hbar\omega_0/2} - 1\right]^{-1}$, M is the electronic-overlap parameter ($\equiv J$), and where S apparently [26] corresponds to twice the vibrational overlap parameter, $\gamma = A^2/2M\omega_0{}^2$, employed in the present paper. Noting that $2n+1 = \coth(\beta\hbar\omega_0/2)$, and $[n(n+1)]^{1/2} = 1/2\,\text{csch}\,(\beta\hbar\omega_0/2)$, one sees that, apart from the term, -1 , in the integrand of (76) (this term being absent from Y and K 's formula, because of their neglect to subtract the diagonal transitions from the total transition probability expression), (120) is completely equivalent [27] to (76), and is hence also infinite. The finite result given by Y and K , namely

$$W = \frac{2\pi}{\hbar}|M|^2 \exp\{-S(2n+1)\}\frac{1}{\hbar\omega}I_0\left\{2S[n(n+1)]^{1/2}\right\} \tag{121}$$

[where $I_0(x)$ is the modified Bessel function of the first kind] was apparently obtained by replacing the infinite integral of (120) by one going from zero to 2π.

It should here be remarked that, despite the above-discussed error in its derivation, Y and K's formula (121) is still applicable to the case of a narrowband vibrational spectrum in the region defined by inequality (75). As discussed above, in connection with the derivation of (77), a consequence of this inequality is that the maximum of the integrand of (65) at $t = 0$ is so large, relative to the other maxima, that in effect the integration may be restricted to the interval $-\pi \leqq t \leqq +\pi$, thereby coinciding with Y and K 's procedure. [The actual equivalence of (121) to (77) is readily demonstrated by inserting for $I_0(x)$ the standard asymptotic expression, $e^x/(2\pi x)^{1/2}$.]

On the other hand, in the domain in which the converse of (75) holds (either at low temperatures or for small values of γ), (121) is clearly incorrect. In this region, as shown by equation (66) and subsequent discussion, the site-jump probability is expressed as a sum of terms each representing site-jumps in which two, three, etc., phonons are emitted or absorbed, and hence possessing both the temperature variation and dependence on vibrational frequency spectrum [28] characteristic of such processes. These features are not exhibited by (121).

Y and K have also obtained an expression analogous to (36) for the energy bands of the polaron-bands (see their Eq. 26 and its generalization, stated in the subsequent paragraph)

$$E = E_0 + 2M\left\{\cos(k_x a) + \cos(k_y a) + \cos(k_z a)\right\} e^{-(2n+1)s} \tag{122}$$

where M and S have the same significance as in (120). (Also, the band energy is here a function of three wave numbers, since Y and K 's treatment is threedimensional.) If, now, one introduces Y and K 's symbols into Eq. (36) of the present paper and goes over to the narrow-band approximation in which $\omega_k \to \omega_0$ and $N_k \to n$, one has

$$E_{\sigma,\cdots N_k}\cdots = E_b + \sum_k (n+1/2)\hbar\omega_0 - 2J\cos\sigma e^{-(n+1/2)S} \tag{123}$$

which differs from (122) by a factor of 1/2 in the exponent of the last term.
This numerical difference is far from trivial; in particular, from (122) Y and K apparently concluded that band-type motion of the polaron could never be of any practical significance (irrespective of temperature), and that thermallyinduced, site-jump transport would always be dominant.

Due to the circumstance that Y and K gave only a brief outline of their cal-

[28] The dependence of (66) in the vibrational frequency spectrum is contained implicitly in the frequency delta functions. Integration over any one of the k 's contained in a given delta function results in its replacement by a typical "frequency-density" factor, of the form, $\partial k/\partial\omega_k$.

culation, the present author has not succeeded in tracking down the discrepancy. However, the fact that the exponent of (122) is too large by a factor of two may be established by the following considerations.

[024] It may be remarked that barrier lowering also results in an enhancement of quantal barrier penetration; this feature is responsible for the appearance of the positive terms, proportional to J^2, in the exponent of (116).

[25] The treatment of Tjablikov, cited in Ref. 2 (as well as that of a recent paper by Sewell) is limited to the consideration of the polaron-band states (Tjablikov, in particular, to the ground state band at absolute zero). In neither of these papers, is any attempt made to include the non-diagonal transitions within the framework of the theory.

[26] The reason for this uncertainty will become evident shortly.

[27] Note that, in (76), S_T is to be equated to $\gamma\coth(\beta h\omega_0/2)$.

If one takes the special case of absolute zero, at which the vibrational quantum numbers are all zero, one may establish a simple correspondence between the exponents occurring in (122) and the site-jump-probability expression, (120). Disregarding the question of the actual divergence of (120), which was discussed earlier, one sees that, for $n = 0$, the exponents are apparently identical. It is now to be realized that, in both cases, the exponential factor enters in as part of the matrix element for the transition $p \to p + 1$. This matrix element, given by the product of the right-hand-side of Y and K 's Eq. (27) and the vibrational overlap integral immediately following [or, in the present paper by (17), enters linearly into the band-energy (123)], but quadratically into the random-jump probability (120) (as is evidenced by the M dependence of these two expressions). It therefore follows that the exponent occurring in (122) should actually be half that contained in (120).

6.2.14 Holstein's Studies of Polaron Motion. Part II. The "Small" Polaron 4

APPENDIX I

In this appendix, the maxima of the integrand of the text Eq. (65) will be computed for the "narrow-band" case, in which

$$\omega_1 \ll \omega_0. \tag{I-1}$$

In this case, (7) may be approximated by

$$\omega_k = \omega_0 + \omega_b \cos k \tag{I-2}$$

where

$$\omega_b = \omega_1^2/2\omega_0 \tag{I-3}$$

is the half-width of the band.
Subject to (I-1), one may also introduce the approximations

$$\omega_0^3/\omega_k^3 \cong 1 - 3\,(\omega_b/\omega_0)\cos k \tag{I-4a}$$

$$\operatorname{csch}\frac{\hbar\omega_k}{2\kappa T} = \frac{\hbar\omega_0}{2\kappa T}\left(1 - (\beta\hbar\omega_0)\left(\frac{\omega_b}{\omega_0}\right)(\cos k)\coth\frac{\beta\hbar\omega_0}{2}\right) \tag{I-4b}$$

so that the quantity $H(k)$, defined by the text equation (73), becomes
$H(k) \cong \left(1 - \frac{3\omega_b}{\omega_0}\cos k\right)(1 - \cos k)\left(1 - (\beta\hbar\omega_0)\left(\frac{\omega_b}{\omega_0}\right)\cos k \coth\frac{\beta\hbar\omega_0}{2}\right)$.

Neglecting terms of quadratic or higher order in ω_b/ω_0, one may further approximate $H(k)$ by

$$H(k) \cong 1 - (1 + a)\cos k + a\cos^2 k \tag{I-6}$$

where

$$a_a = \left(3 + \frac{\beta h\omega_0}{2}\coth\frac{\beta h\omega_0}{2}\right)_{\omega_0}^{\omega_b} \tag{I-7}$$

Using (I-6), one then has for the argument of the exponential term in the integrand of (65)

$$\begin{aligned}
\mathscr{K}(\tau) &\equiv 2\gamma \operatorname{csch} \frac{\beta\hbar\omega_0}{2} \frac{1}{\pi} \int_0^\pi H(k) \cos\omega_k \tau dk \\
&= 2\gamma \operatorname{csch} \frac{\beta\hbar\omega_0}{2} \frac{1}{\pi} \int_0^\pi \left[1 - (1+a)\cos k + a\cos^2 k\right] \\
&\cdot \left[\cos\omega_0\tau \cos\left(\omega_0\tau\cos k\right) - \sin\omega_0\tau \sin\left(\omega_0\tau\cos k\right)\right] dk \qquad \text{(I-8)} \\
&= 2\gamma \operatorname{csch} \frac{\beta\hbar\omega_0}{2} \left\{\cos\omega_0\tau \left[\left(1+\frac{a}{2}\right) J_0\left(\omega_b\tau\right) - \frac{a}{2} J_2\left(\omega_b\tau\right)\right] + \sin\omega_0\tau \left[(1+a) J_1\left(\omega_b\tau\right)\right]\right\}
\end{aligned}$$

where the J 's are Bessel functions.
The absolute maximum of $\mathfrak{K}(\tau)$ is attained at $\tau = 0$, and is

$$\mathfrak{K}(0) = 2\gamma \operatorname{csch} \frac{\beta\hbar\omega_0}{2} \left(1 + \frac{a}{2}\right).$$

For the computation of the other maxima, it is expedient to rewrite (I-8) in the form

$$\begin{aligned}
\mathscr{K}(\tau) = \mathscr{K}(0) \Bigg\{ &\left[J_0\left(\frac{\omega_b}{\omega_0}x\right) - \frac{a}{2+a} J_2\left(\frac{\omega_0}{\omega_0}x\right)\right]^2 \\
&+ \left(\frac{(1+a)}{1+a/2}\right)^2 J_1^2\left(\frac{\omega_b}{\omega_0}x\right)\Bigg\}^{1/2} \cos[x - \varphi(\tau)] \qquad \text{(I-9)}
\end{aligned}$$

where

$$\varphi(\tau) \equiv \arctan \frac{(1+a) J_1\left(\omega_b\tau\right)}{\left(1+\frac{a}{2}\right) J_0\left(\omega_b\tau\right) - \frac{a}{2} J_2\left(\omega_b\tau\right)} \qquad \text{(I-10)}$$

and

$$x = \omega_0\tau \qquad \text{(I-11)}$$

In the case of those maximal points for which $(\omega_b/\omega_0)\, x_i < 1$, the Bessel functions may be expanded, yielding, to the lowest order in ω_b/ω_0,

$$\operatorname{Re}(\tau) \cong \operatorname{Re}(0) \left(1 - \frac{\omega_b^2 x^2}{8\omega_0^2}\right) \cos[x - \varphi(\tau)] \qquad \text{(I-12)}$$

$$\varphi(\tau) \cong \omega_b x / 2\omega_0 \qquad \text{(I-13)}$$

It is now to be noted, that, since $\varphi(\tau)$ is small, the maximal points, x_i, may to a sufficiently good approximation, be set equal to $2\pi n_i$. One then has

$$\mathfrak{K}_i(\tau) = \mathfrak{K}(0) \left[1 - \left(\frac{\pi^2\omega_b^2}{2\omega_0^2}\right) n_i\right]. \qquad \text{(I-14)}$$

From (I-14), it is then seen that, in order for the contributions of these maxima to (65) to be negligible, it is required that

$$\mathfrak{K}(0) \frac{\pi^2\omega_b^2}{2\omega_0^2} \gg 1$$

or, in view of (I-3), and of the definition of $\mathfrak{K}(0)$ [given between (I-8) and (I-9)]

$$2\gamma \operatorname{csch} \frac{\beta h \omega_0}{2} \frac{\pi^2 \omega_1^4}{8\omega_0^4} \gg 1 \tag{I-15}$$

Turning now briefly to the other maxima, for which $(\omega_b/\omega_0)\, x_i > 1$, one sees that their magnitudes are essentially given by the curly bracket of (I-9). In particular, if this bracket does not approach unity in the domain $(\omega_b/\omega_0)\, x_i > 1$, the contributions to (65) will be negligible. The fact that this is actually the case may be established by numerical analysis of the curly bracket. However, in view of the above results, and of the arguments already presented in the text subsequent to Eq. (74), this analysis will not be carried out here.

APPENDIX II

In this appendix, the classical occurrence-probability derivation of the text Eq. (79) for $W_T(p \to p \pm 1)$ will be presented. The basis of the treatment is the set of equations

$$i\hbar \frac{\partial a_n}{\partial t} = -A x_n(t) a_n - J\left(a_{n+1} + a_{n-1}\right) \tag{II-1}$$

which is obtained from the text set (5) by omitting the vibrational Hamiltonian. The $x_n(t)$ are to be considered as given functions of time, determined by classical trajectorics. [29] It is assumed that, at some initial time, t_i, the electron

is in a definite (p th) site, so that

$$a_n\left(t_i\right) = \delta_{np}. \tag{II-2}$$

The application of first-order perturbation theory then gives, say, for $a_{p+1}(t)$, at a time $t > t_i$

$$a_{p+1}(t) = -\frac{J}{i\hbar} \exp\left\{\left(\frac{iA}{\hbar}\right) \int^t x_{p+1}\left(t'\right) dt'\right\} \tag{II-3}$$
$$\int_{t_i}^t \exp\left\{\frac{iA}{\hbar} \int^{t'} \left[x_p\left(t''\right) - x_{p+1}\left(t''\right)\right] dt''\right\} dt'$$

where the lower limit of the "phase integrals," occurring in the exponents of (II-3), is to be specified later.

The procedure to be used in the evaluation of the integral on the right-hand side of (II-3) is based on the fact that, over the region of interest for the present classical treatment, in which the inequalities

$$A^2/M\omega_0^2 \gg \hbar\omega \tag{II-4}$$
$$\kappa T \gg \hbar\omega \tag{II-5}$$

obtain, the relative variation of $x_p - x_{p+1}$ in a time of the order of an instantaneous "period," $\hbar/A\left(x_p - x_{p+1}\right)$, [i.e., the quantity $(\hbar/A\left|x_p - x_{p+1}\right|)\left(\partial/\partial t\right) \log\left(x_p - x_{p+1}\right)$], is small, except at a "coincidence" point, t_c [at which $x_{p+1}\left(t_c\right) = x_p\left(t_c\right)$] .[30] It then follows that the oscillations in the exponential integrand will interfere destructively, except at the coincidence points, t_c, at which the phase of the exponential is momentarily stationary.

[029] In the zeroth approximation, in which the electron remains localized on a given p th side, the time dependence of $x_n(t)$ is determined by the Hamiltonian, $H^{(p)} = H_L - A x_p$ (H_L representing the purely vibrational Hamiltonian of the host crystal). When, in the

Let us assume that such a point of stationary phase, t_c, occurs in the interval between t_i and t. Let us further introduce the assumption [31] that, in the neighborhood of t_c, the time variation of $x_p(t) - x_{p+1}(t)$ may be considered linear, so that

$$x_p(t) - x_{p+1}(t) = (v_p - v_{p+1})(t - t_c) \tag{II-6}$$

where the velocities v_{p+1} and v_p are evaluated at t_c.
next approximation, site jumps of the type $p \to p+1$ are computed, the question arises as to whether $H^{(p)}$ or $H^{(p+1)}$ (or some mixture thereof) should be used in determining the $x_n(t)$. It turns out, however, that, as will be seen below, within the domain of validity of the classical calculation, this ambiguity does not cause any trouble.
[30] That such a situation prevails when (II-4) and (II-5) are satisfied, can be seen by noting that $|x_p - x_{p+1}| \gtrsim (\kappa T/M\omega_0^2)^{1/2}$ and $|(d/dt)\log(x_p - x_{p+1})| \sim \omega_0$ so that

$$[\hbar/(A|x_p - x_{p+1}|)]\,|(\partial/\partial t)\log(x_p - x_{p+1})| \ll 1.$$

[31] The domain of validity of this assumption will be discussed later.

Inserting (II-6) into (II-3), and choosing the lower limit of the phase integrals to be t_c, one has

$$\begin{aligned} a_{p+1}(t) = &-\frac{J}{i\hbar}\exp\left\{iA\int_{t_c}^{t} x_{p+1}(t')\,dt'\right\} \\ &\int_{t_i}^{t}\exp\left\{\frac{i}{2}\left[A(v_p - v_{p+1})/\hbar\right](t' - t_c)^2\right\}dt \end{aligned} \tag{II-7}$$

It will now be noticed that important contributions to the integral occur over a time interval,

$$\Delta t \sim [\hbar/A(v_p - v_{p+1})]^{1/2} \sim \left[\hbar/A(\kappa T/M)^{1/2}\right]^{1/2} = \frac{1}{\omega_0}\left[\frac{\hbar\omega_0}{(A/M\omega_0^2)^{1/2}(\kappa T)^{1/2}}\right]^{1/2}$$

If the spacing in time between successive coincidence points be assumed large compared to Δt (this assumption also will be examined later), the contributions of different coincidence points will not overlap. One may then replace the integration limits, t and t_i, by plus and minus infinity, respectively, so that

$$\begin{aligned} a_{p+1}(t) = &-\frac{J}{i\hbar}\exp\left\{iA\int_{t_c}^{t} x_{p+1}(t')\,dt'\right\} \\ &\int_{-\infty}^{+\infty}\exp\left\{\frac{i}{2}\left[A(v_p - v_{p+1})/\hbar\right](t' - t_c)^2\right\}dt' \\ = &-\frac{J}{i\hbar}\exp\left\{iA\int_{t_e}^{t} x_{p+1}(t')\,dt'\right\}e^{-i\pi/4}\left(\frac{2\pi\hbar}{A|v_p - v_{p+1}|}\right)^{1/2} \end{aligned} \tag{II-8}$$

In going from occupation amplitudes to occupation probabilities, it will be assumed that there is no phase correlation between successive coincidence points (or, alternatively, that any such correlation for a given classical trajectory averages to zero when all possible trajectories are taken into account). [32] Then, upon taking the absolute square of both sides of (II-8), one has

$$W_c(p \to p+1) = \frac{2\pi J^2}{\hbar}\frac{1}{A|v_p - v_{p+1}|} \tag{II-9}$$

where $W_c(p \to p+1) = |a_{p+1}(\infty)|^2$ represents the probability of a site jump, $p \to p+1$, occurring in a single coincidence event.

In order to obtain the transition probability, $W_T(p \to p+1)$, giving the average site-jump probability per second, one multiplies (II-9) by the proba-

bility per second, $P_{\mathbf{T}}^{(c)}(v_r)\,dv_r$, for a coincidence in which the relative velocity, $v_r = v_p - v_{p+1}$, lies within a given differential range, and integrates over all values of v_r.

To compute $P_T^{(c)}(v_r)\,dv_r$, one notes that, in a time dt, all configurations for which $x_p - x_{p+1} \leqq v_r dt$ will give rise to the coincidence, $x_p = x_{p+1}$, in time dt. The classical occurrence-probability of such a configuration, in which v_r is also specified to lie within a given differential range, is

$$\begin{aligned} Z^{-1} \int \cdots \int e^{-(H_L - Ax_p)/\kappa T} \left[S\left(x_p - x_{p+1}\right) - S\left(x_p - x_{p+1} - v_r dt\right)\right] \\ \times \left[S\left(v_p - v_{p+1} - v_r\right) - S\left(v_p - V_{p+1} - v_r - dv_r\right)\right] \\ \cdot dx_1 \cdots dx_N dv_1 \cdots dv_N \end{aligned}$$

where

$$Z \equiv \int \cdots \int e^{-(H_L - Ax_p)/\kappa T} dx_1 \cdots dx_N dv_1 \cdots dv_N$$

and where

$$S(x) \equiv \int_{-\infty}^{x} \delta\left(x'\right) dx'$$

is the conventional step function. It will be noticed that both of the square brackets are equal to zero, except for the differential intervals, $x_{p+1} \leqq x_p \leqq x_{p+1} + v_r dt$ and $v_{p+1} + v_r \ll v_p \leqq v_{p+1} + v_r + dv_r$, respectively, within which they are unity. These differential impulse functions may more conveniently be represented by the expressions $\delta\left(x_p - x_{p+1}\right) v_r dt$ and $\delta\left(v_p - v_{p+1} - v_r\right) dv_r$. Then, upon carrying out the velocity integrations, and dividing by dt to obtain the occurrence-probability per unit time, one has

$$P_T^{(c)} = \left(\frac{M}{4\pi\kappa T}\right)^{1/2} dv_r e^{-Mv_r^2/4\kappa T} \left|v_r\right| \mathcal{F} \tag{II-10}$$

where

$$\mathcal{F} \equiv \frac{\int \cdots \int e^{-(V_L - Ax_p)/\kappa T} \delta\left(x_p - x_{p+1}\right) dx_1 \cdots dx_N}{\int \cdots \int e^{-(V_L Ax_p)/\kappa T} dx_1 \cdots dx_N} \tag{II-11}$$

V_L representing the vibrational potential energy of the host crystal.
At this point it is expedient to introduce the Fourier-integral formula for the delta function:

$$\delta(x) = \frac{1}{2\pi} \int_{-\infty}^{+\infty} e^{ix\alpha} d\alpha$$

and to transform to the normal coordinates, q_k, via the relations

$$x_n = \sum_n \left(\frac{2}{N}\right)^{1/2} q_k \sin(kn + \pi/4) \tag{II-12}$$

[032] In view of the generally large number of oscillations between successive coincidence points (this number can be estimated from the material given in footnote 30), such correlations would occur only if the motion were perfectly periodic. This possibility, however, is specifically ruled out by the frequency dispersion of the vibrational frequencies.

The numerator and denominator of the resulting expression for $\mathcal{F}$ are each reduced, therewith, to a product of integrals over the q_k. The individual integrations are readily carried out, the result being

$$\mathcal{F} = \frac{1}{2\pi}\int_{-\infty}^{+\infty} \exp\left\{\sum_k \frac{\beta_k^{2^2}(\alpha) - \beta_k^2(0)}{NM\omega_k^2\kappa T}\right\} d\alpha \tag{II-13}$$

where

$$\beta_k(\alpha) = (-A + i\alpha\kappa T)\sin[kp + \pi/4] - i\alpha\kappa T \sin[k(p+1) + \pi/4]. \tag{II-14}$$

One now introduces a new integration variable

$$\gamma \equiv \alpha + \frac{iA}{2\kappa T} \tag{II-15}$$

Then, upon pairing terms of plus and minus k, one may write the exponent of the integrand of (II-13) as

$$\sum_k -\frac{A^2}{4NM\omega_k^2\kappa T}(1-\cos k) - \sum \frac{\kappa T}{NM\omega_k^2}(1-\cos k)\gamma^2 \tag{II-16}$$

From the form of this exponent, it is clear that the γ-integration limits ($-\infty + iA/2\kappa T, +\infty + iA/2\kappa T$) may be replaced by ($-\infty, +\infty$), so that, upon introducing the "activation energy"

$$\begin{aligned} E_a &= \frac{1}{N}\sum_k A^2(1-\cos k)/4M\omega_k^2 \\ &= \frac{1}{\pi}\int_0^\infty \frac{A^2(1-\cos k)dk}{4M\omega_k^2} \end{aligned} \tag{II-17}$$

one obtains

$$\mathcal{F} = \frac{A}{2\pi}\left(\frac{\pi}{4\kappa T E_a}\right)^{1/2} e^{-E_a/\kappa T}$$

which, when inserted into (10), yields

$$P_T^{(c)}(v_r)\, dv_r = \left(\frac{M}{4\pi\kappa T}\right)^{1/2} dv_r e^{-Mv_r^2/4\kappa T}\, |v_r| \frac{A}{2\pi}\left(\frac{\pi}{4\kappa T E_a}\right)^{1/2} e^{-E_a/\kappa T} \tag{II-18}$$

Multiplying (II-18) by (II-9), and integrating over all $v_r \equiv v_p - v_{p+1}$ one obtains the text relation (79), q.e.d.

The assumptions introduced in the derivation of (II-9) will now be examined.

Of these, the most delicate is embodied in (II-6). The significance of the approximation implied by this expression is that the relative velocity, $v_p - v_{p+1}$, does not change appreciably in a time

$$\Delta t \sim [\hbar/A\,(v_p - v_{p+1})]^{1/2} \sim \omega_0^{-1}\left[\hbar\omega_0/\left(A^2/M\omega_0^2\right)^{1/2}(\kappa T)^{1/2}\right]^{1/2};$$

as pointed out in the discussion subsequent to (II-7), Δt defines the neighborhood of a coincidence-point within which the principal contribution to the righthand side of (II-7) is contained.

In order to assess the validity of this assumption, an estimate of the relative acceleration, $(d/dt)\,(v_p - v_{p+1})$, is required. In obtaining this estimate, the vibrational coupling between

the individual molecules will be neglected ($\omega_1 = 0$); this procedure should be quantitatively accurate for a narrow-band vibrational spectrum ($\omega_1 \ll \omega_0$), and should be suitable for at least order-of-magnitude considerations in the more general case of $\omega_1 \sim \omega_0$.

Neglecting, then, the intermolecular vibrational coupling term in the lattice Hamiltonian, one has for the relative acceleration at a coincidence point ($x_p = x_{p+1}$)

$$\frac{d}{dt}\left(v_p - v_{p+1}\right) = -\omega_0^2\left(x_p - x_{p+1}\right) + \frac{A}{M} \tag{II-19}$$

wherein it has been assumed that the effective Hamiltonian is [33] $H^{(p)} \equiv H_L - Ax_p$. On the other hand, the order of magnitude of the relative velocity is

$$|v_p - v_{p+1}| \sim \left(\frac{2\kappa T}{M}\right)^{1/2} \tag{II-20}$$

From (II-19), (II-20), and the estimate for Δt, it follows that, in order for (II-6) to be applicable, it is necessary that

$$\frac{A}{M\omega_0}\left[\frac{\hbar\omega_0}{\left(A^2/M\omega_0^2\right)^{1/2}(\kappa T)^{1/2}}\right]^{1/2} \ll \left(\frac{2\kappa T}{M}\right)^{1/2}$$

or

$$\left(\frac{A^2}{M\omega_0^2}\right)^{1/2}\frac{\hbar\omega_0}{(\kappa T)^{3/2}} \ll 1$$

i.e.,

$$\kappa T \gg \left[\left(\frac{A^2}{M\omega_0^2}\right)(\hbar\omega_0)^2\right]^{1/3}. \tag{II-21}$$

[33] If, instead, one assumed the effective Hamiltonian to be $H^{(p+1)}$, the sign of the righthand side of (II-9) would be changed but the magnitude would remain unaltered; if one took some average of $H^{(p)}$ and $H^{(p+1)}$, the relative acceleration would still be $\sim A$, times a numerical factor $\leqq 1$.

It is of interest to point out that (II-21), rather than $\kappa T \gg \hbar\omega$, is the appropriate condition for the approximation of the quantal relation (77) by (79). Namely, if in the Taylor expansion of the hyperbolic tangent occurring in the exponential factor of (77), one retains two terms, i.e.,

$$\tanh\frac{\beta\hbar\omega_k}{4} \to \frac{\hbar\omega_k}{4\kappa T} - \frac{1}{3}\left(\frac{\hbar\omega_k}{4\kappa T}\right)^3$$

one obtains (79) multiplied by the factor

$$\exp\left[-\frac{1}{\pi}\int_0^\pi \frac{A^2}{M\omega_k^2}\frac{(1-\cos k)\left(\hbar\omega_k\right)^2}{3(4\kappa T)^3}dk\right]$$

which, for order of magnitude considerations, may be approximated by

$$\exp\left[-\left(\frac{A^2}{M\omega_0^3}\right)\frac{\left(\hbar\omega_0\right)^2}{3(4\kappa T)^3}\right]$$

In order for this quantity to be replaceable by unity, it is necessary that

$$\kappa T \gg \frac{1}{4}\left[3\frac{A^2}{M_{\omega_0^2}}\left(\hbar\omega_0\right)^2\right]^{1/3}$$

which, apart from numerical factors, is identical with (II-21).
It remains to discuss the assumption, introduced in the paragraph preceding (II-8), that the time between successive coincidence points is large compared to $\Delta t \sim \omega_0^{-1}\left[\hbar\omega_0/\left(A^2/M{\omega_0}^2\right)^{1/2}(\kappa T)^{1/2}\right]^{1/2}$. Apart from one special feature, said time is of the order of $1/\omega_0$, and hence larger than Δt by a factor

$$\left(A^2/M\omega_0^2/\hbar\omega_0\right)^{1/2}\left(\kappa T/\hbar\omega_0\right)^{1/4} \gg 1.$$

The special feature in question arises from the fact that, when $A^2/M{\omega_0}^2$ is large compared to κT, the coincidences tend to occur in closely-spaced pairs. For example, using the same narrow-band limit of $\omega_1 = 0$, as in the previous discussion, one sees that every coincidence in which $v_p - v_{p+1}$ is positive is preceded by one in which it is numerically equal, but negative, and that the time interval between them is of the order of twice the mean relative velocity divided by the mean relative acceleration [given by (II-20) and (II-19), respectively], i.e., $\Delta t_c \sim \left(2\kappa T/A^2/M{\omega_0}^2\right)^{1/2}(1/\omega_0)$. It is then immediately clear that the requirement that Δt_c be large compared to Δt is equivalent to (II-21).

It may finally be remarked that the uncertainty, discussed in footnote 29, as to the proper choice of vibrational Hamiltonian to be used in computing classical orbits, would affect only the relative acceleration; hence, in the approximation represented by (II-6), in which acceleration effects are neglected altogether, this uncertainty is of no consequence.

APPENDIX III

In this appendix, the classical treatment of site-jump probabilities, given in Appendix II, is further developed to cover the case in which the electronic bandwidth parameter, J, is too large for perturbation theory to be applicable. The problem has actually been discussed rather extensively in the literature, principally from standpoint of the theory of nonadiabatic transitions between molecular potential energy curves. In the case at hand, these potential energy curves are the eigenvalues $E\left(x_1, \cdots, x_N\right)$ of the equations

$$\begin{aligned} &E\left(x_1, \cdots, x_N\right) a_n\left(x_1, \cdots, x_N\right) \\ &\quad = \left[V_L\left(x_1, \cdots, x_N\right) - Ax_n\right] a_n - J\left(a_{n+1} + a_{n-1}\right) \end{aligned} \tag{III-1}$$

obtained from the text Eq. (5) by discarding the vibrational kinetic energies; as in Appendix II, $V_L\left(x_1, \cdots, x_N\right)$ is the vibrational potential energy

$$V_L\left(x_1, \cdots, x_N\right) = \sum_n \left(\frac{M\omega_0^2}{2}x_m^2 + \frac{M\omega_1^2}{2}x_m x_{m+1}\right). \tag{III-2}$$

If one attempts a development of the solution of (III-1) as a power series in J, via perturbation theory, one obtains

$$\begin{aligned} E^{(p)}\left(x_1, \cdots, x_N\right) =& V_L\left(x_1, \cdots, x_N\right) - Ax_p \\ &- \frac{J^2}{A}\left[\frac{1}{x_p - x_{p+1}} + \frac{1}{x_p - x_{p-1}}\right] + \cdots, a_n^{(p)} \\ =& \delta_{n_p} - \frac{J}{A\left(x_n - x_p\right)}\left[\delta_{n+1,p} + \delta_{n-1,p}\right] + \cdots \end{aligned} \tag{III-3}$$

Generally, [34] $x_p - x_{p+1} \sim A/M\omega_0{}^2$, so that in the case of the small polaron for which $J \ll A^2/M\omega_0{}^2$ (see I, Eq. 43), (III-2) and (III-3) are accurate. Within the domain of applicability of these relationships, the electronic state corresponding to a given potential-energy curve, $E^{(p)}(x_1, \cdots, x_N)$, is strongly localized about a single site, p.

However, in the neighborhood of the "crossing-points" of two potential energy curves, say, $E^{(p)}$ and $E^{(p+1)}$, (in particular, when $|x_p - x_{p+1}| < J/A$), the perturbation expansion must be modified to take account of the fact that a_p and a_{p+1} are both appreciable. One is thus led to the consideration of the two equations

$$\begin{aligned} E(x_1, \cdots, x_N)\, a_p &= (V_L - Ax_p)\, a_p - Ja_{p+1} \\ E(x_1, \cdots, x_N)\, a_{p+1} &= (V_L - Ax_{p+1})\, a_{p+1} - Ja_p \end{aligned} \tag{III-4}$$

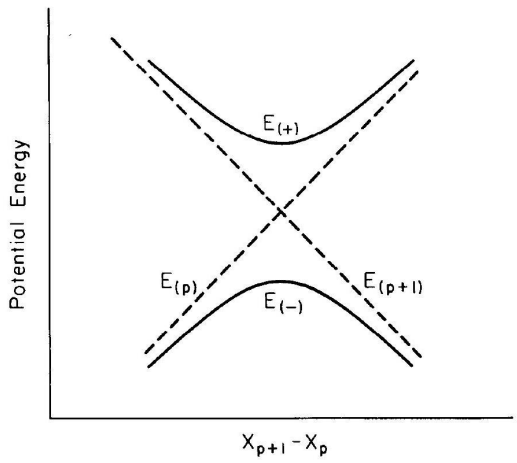

Fig. 2. Potential energy curves for the two-site system

the eigenvalues of which are

$$\begin{aligned} &E_{\oplus)}(x_1, \cdots, x_N) \\ &\quad = V_L(x_1, \cdots, x_N) - A\left(\frac{x_p + x_{p+1}}{2}\right) \pm \left\{\left[\frac{A^2(x_p - x_{p+1})^2}{4} + J^2\right]\right\}^{1/2}. \end{aligned} \tag{III-5}$$

These two solutions are shown in Fig. 2 as the solid curves. The dashed lines, denoted by $E^{(p)}$ and $E^{(p+1)}$, give the unperturbed ($J = 0$) potential curves; they are also the asymptotic limits of the actual curves for sufficiently large $|x_{p+1} - x_p|$.

In a site jump of the type $p \to p+1$, the system is initially in a configuration in which $x_p \gg x_{p+1}$; since the associated electronic state is localized about the p 'th site, its limiting potential energy curve is $E^{(p)}$. It may thus be represented in Fig. 2 by a point which moves along the lower solid curve, $E_{(-)}$, approaching the crossing point from the left. In the neighborhood of the crossing point a variety of possibilities is available.

Firstly, the system may remain on the lower potential curve, $E_{(-)}$, continuing its motion to the right, [35] and thereby eventually attaining the region of

[35] In this discussion, as in the perturbation treatment of Appendix II, the relative velocity,

[034] In the limiting case of $\omega_1 = 0$, for example, the equilibrium x_n 's are (for the small polaron), $x_p = A/M\omega_0{}^2, x_{n\neq p} = 0$.

$v_{p+1} - v_p$, in the vicinity of the crossing point is assumed sufficiently large so as to be considered essentially constant in this vicinity.
$x_{p+1} \gg x_p$ on the curve $E^{(p+1)}$. The net result of this process is the realization of a site-jump event.

The alternate possibility, in which the system jumps from the $E_{(-)}$to the $E_{(+)}$curve, on going to the right, results in a situation in which the system is moving "uphill"; it must then eventually "turn around" and reapproach the crossing point from the right. If in the latter trajectory, it jumps to the lower curve, it moves "downhill" towards the initial configuration, with the net result that no site jump takes place. On the other hand, if the system remains on the $E_{(+)}$curve, it gets another chance to traverse the crossing region from left to right; if, in this traversal, it jumps to the $E_{(-)}$curve, the site-jump event is realized.

By summing over all possibilities of this type, one may compute the site-jump probability, $W_c(p \to p+1)$, in terms of the probability, P_t, of (nonadiabatic) transitions between the potential energy curves. [36] Specifically, one obtains for $W_c(p \to p+1)$ the series

$$W_c(p \to p+1) = 1 - P_t + P_t\,(1 - P_t)\,P_t + P_t\,(1 - P_t)\,P_t + \cdots\,,$$

which is readily summed, the result being

$$W_c(p \to p+1) = 2\frac{1 - P_t}{2 - P_t} \tag{III-6}$$

As stated above, the problem of computing P_t has been treated in the literature. In particular, an explicit solution has been given by Zener (7), which, in the notation of the present paper, reads

$$P_t = \exp\left\{-\frac{2\pi J^2}{\hbar A\,|v_p - v_{p+1}|}\right\} \tag{III-7}$$

From (III-6) and (III-7) it is seen that, when $J^2 \ll hA\,|v_{p+1} - v_p|\,/2\pi$, $W_c(p \to p+1)$ reduces to

$$W_c = 2\frac{2\pi J^2}{\hbar A\,|v_{p+1} - v_p|} \tag{III-8}$$

which is twice the right-hand side of the perturbation result (II-9). In this limit, the system may be considered as moving up and down the zeroth order energy curve, $E^{(p)}$ (represented in Fig. 2 by the appropriately-labelled dashed line). At each of two transits through the crossing point (in which the relative velocity is first positive and then negative) a transfer to the $E^{(p+1)}$ curve may take place with a probability given by (II-9). The total probability (for the two transits) is then equal to the right-hand side of (III-8), as it should be.

In the alternate limit of $J^2 \gg \hbar A\,|v_{p+1} - v_p|\,/2\pi$, the site-jump probability, $W_c(p \to p{+}1)$, is unity. In this limit the system simply stays on the lower potential curve, $E_{(-)}$, in its left-to-right motion, and thus effects an adiabatic site-jump transition, without further ado. [37]

REFERENCES

1. T. Holstein, preceding paper [Annals of Physics 8, 325 (1959)].

2. S. V. Tjablikov, Zhur. Ekspil. i Teort. Fiz. 23, 381 (1952).

3. J. Yamashita and T. Kurosawa, J. Phys. Chem. Solids 5, 34 (1958).

[036] As will be seen immediately below, this probability is symmetrical in the direction of the transition ($E_{\pm} \to E_{\mp}$), and independent of the sign of the relative velocity.

4. A. H. Wilson, "The Theory of Metals," 2nd ed., p. 258, Cambridge Univ. Press, London and New York (1953).

5. R. R. Heikes and W. D. Johnston, J. Chem. Phys. 26, 582 (1957).

6. G. L. Sewell, Phil. Mag. [8], 3, 1361 (1958).

7. C. Zener, Proc. Roy. Soc. A137, 696 (1932).

6.2.15 1.8 From large to small polaron: numerical calculations

Theory

Two analytical approaches discussed above are based on the $1/\lambda$ or ω/J expansions.

(first of all, there are different model before Holstein's model, why are they grouped as one model?? second, I want to write here these models!!! it is not clear, which exactly formulas are meant???)

(what are we doing to compare them numerically??? what is the goal???)

A priori it is difficult to say to what extent they are reliable in the intermediate coupling region, $\lambda \simeq 1$, when the size of a polaron shrinks and for the intermediate value of the adiabatic parameter $\omega/J \simeq 1$.

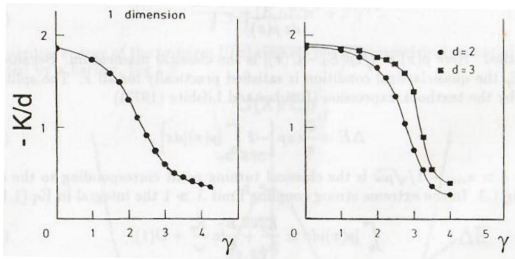

Fig.1.4. The 'Monte-Carlo' polaron collapse of the kinetic energy (K/J) (what is the formula for K?) of one-dimensional, two, $d = 2$, and three-dimensional, $d = 3$ (it would be better if there was one plot with three lines, but okay, without any reason there two plots) fermions interacting with molecular phonons with the interaction constant γ (what is the γ???) for $\omega/J = 1$ (de Raedt and Lagendijk (1983) (read this paper later!! (???))).

The ground state energy is not so sensitive to the parameters (which parameters) being about (above?) $-E_p$ for the small nonadiabatic and small adiabatic polarons.

However, the effective mass and the bandwidth depends strongly on the polaron size and the adiabatic ratio. (why?? I don't remember it)

Several attempts to describe the intermediate region of the coupling $\lambda \simeq 1$ with and without electron-electron correlations are known in the literature (they are written also in the ch. 4).

These are based on the variational approach, the Monte-Carlo calculations (of what?) and on the exact (numerical) solution of a several-site Holstein model (before, we considered only variational approach.).

[037] In all of the above discussion, it has been tacitly assumed that once the system moves downhill from the crossing point (in the $E_{(-)}$curve), in either direction, its energy gets sufficiently dissipated so that the likelihood of an immediate return (say within a time of the order of $1/\omega_0$) is negligible. Without going into this question in detail, it seems safe to say that a necessary and sufficient condition for its validity is the existence of adequate frequency dispersion. For the case in which the perturbation treatment, given in the text of this paper, applies, an estimate of the required amount of dispersion is in fact contained in the inequality (75).

The transition from a wide band electron (or large polaron) to a narrow band small polaron is extremely sharp as seen in the Monte-Carlo simulations, Fig.1.4.

The general conclusion is that there is a continuous but rather sharp evolution from a wide band electron to a narrow band small polaron in the intermediate region of the coupling $\lambda \simeq 1$.

The most reliable results for the intermediate region are obtained with the exact numerical diagonalisation of vibrating clusters (what are they doing???) (Kongeter and Wagner (1990), Ranninger and Thibblin (1992), Alexandrov et al. (1994a), Marsiglio (1995)).

Numerical solution (to what problem??) for several vibrating molecules coupled with one electron in the adiabatic $\omega/J < 1$ as well as in the nonadiabatic $\omega/J > 1$ regimes using numerical diagonalisation with 50 phonons (how to decode N phonons (for example, $N = 50$?)) shows that the adiabatic and the perturbation approximations are in excellent agreement with the exact solution in adiabatic and nonadiabatic regimes respectively for all values of the coupling constant.

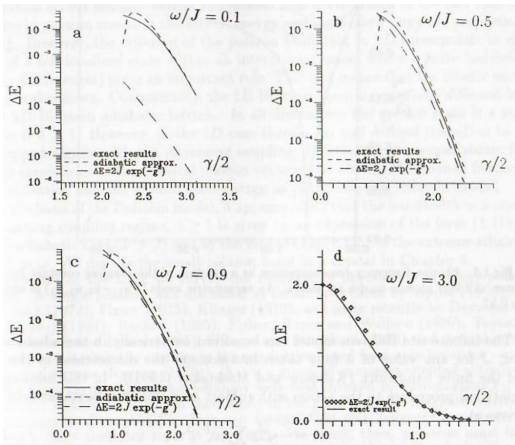

Fig.1.5. Band width (in units of J) of the two-molecular model (Alexandrov et al (1994a)).

To illustrate this we compare in Fig.1.5 the exact splitting of levels (which levels?) for two site cluster with the expression (1.118) ($\tilde{J} = Je^{-g^2}$) for nonadiabatic case and with the Holstein quaniclassical formula Eq.(1.135) in the adiabatic case, generalised for the finite value of λ as

$$\Delta E = \sqrt{\frac{4E_p\omega}{\pi}}\beta^{5/2}\lambda^{1-\beta}[2(1+\beta)]^{-\beta}e^{-\tilde{g}^2} \tag{1.137}$$

where now $\tilde{g}^2 = g^2\{\beta - [\ln(2\lambda(1+\beta))]/4\lambda^2\}$.

This generalisation takes into account the frequency renormalisation $\beta \equiv \tilde{\omega}/\omega = \sqrt{1 - 1/4\lambda^2}$ and the anharmonic corrections of the order of $1/\lambda^2$ to the turning point a in Eq.(1.132).

A much lower effective mass of the adiabatic small polaron in the intermediate coupling region compared with that estimated from the perturbation theory expression (1.118) is revealed in Fig.1.5a.

In the intermediate coupling region, the effective bandwidth of a smal adiabatic polaron ($\omega \ll J$) can be only one order of magnitude smaller than the bare band width. However, perturbation theory is reliable already for $\omega > 0.5J$ as one can see in Fig.1.5c,d for all values of the coupling. The renormalised phonon frequency has a minimum at the transition from large to small polaron. At large λ the frequencies remain unchanged, Fig.1.6 as predicted with the adiabatic formula Eq.(1.129).

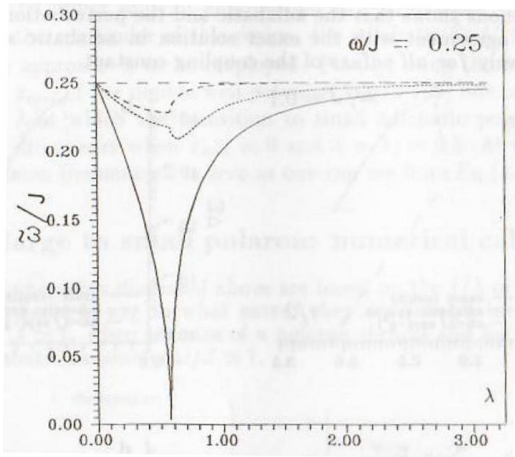

Fig.1.6. Phonon frequency renormalisation as a function of the coupling constant for a 4 -site cluster. All four phonon modes are shown. An asymmetric mode ($-u_{1},-u_{2}, u_{2}, u_{1}$) is unstable at $\lambda \simeq 0.57$.

The infinite-site Holstein model can be solved numerically in the adiabatic limit $\omega \ll J$ for any value of λ fully taken into account the discreteness of the lattice and the finite bandwidth (Kabanov and Mashtakov (1993)). In this limit applying variational procedure to the action with respect to a local displacement field ϕ_i one arrives at

$$\phi_i = -\sqrt{2}g \sum_r \left|\psi_i^{(r)}\right|^2 n_r, \tag{1.138}$$

and

$$J \sum_{j\neq 0} \psi_{i+j}^{(r)} + \sqrt{2}g\omega\psi_i^{(r)}\phi_i = \epsilon_r \psi_i^{(r)} \tag{1.139}$$

These equations are written by the use of the extreme adiabatic approximation $\frac{\partial\phi}{\partial\tau} = 0$ with ψ_i describing an electron localised on a site i. They do not contain spatial derivatives because "bare" phonons are supposed to be dispersionless. n_r means the occupation number in the eigenstate r.

In the weak-coupling regime $\lambda \ll 1$ one can replace the discrete set for a continuous equation with the following exact solution in $1D$ (Rashba (1957)):

$$\psi(x) \sim 1/\cosh\left(\frac{\lambda x}{a}\right) \tag{1.140}$$

The numerical analysis of the discrete set of the adiabatic equations leads to the conclusion that there is a smooth transition at $\lambda \simeq 1$ from large to small polaron, and the self-localization occurs without barrier formation in the $1D$ case.

In $2D$ case the situation changes qualitatively. The formation of a self-localized state in $2D$ case is accompanied by the formation of an energy barrier that separates the self-localized and delocalised state. The formation of the barrier is associated with a finite width $\sim J$ of the bare electronic band, while the numerical study of Eqs. (1.138, 139) in the continuous (effective mass) approximation shows that the selflocalization occurs without barrier formation. This is attributed to the fact that on a decrease in polaron size both the kinetic energy and the strain energy are proportional to $1/r_p^2$. However, the criterion of the polaron formation in $2D$ corresponds to existence of a self-localized state within an interatomic space, where a finite bandwidth (lattice discreteness) plays an important role. This fact means that the kinetic

energy scaling brakes down. Consequently, the $1D$ Holstein chain is essentially different from $2D$ or $3D$ Holstein adiabatic lattices. In all dimensions the ground state is a small polaron if $\lambda \geq 1$. However, in the $1D$ case there is no well defined transition to the self-trapped regime with the increasing coupling. Calculating the nonadiabatic flucfuation corrections to the classical phonon vacuum one obtains the phonon frequency renormalisation and the ground state energy as in the two-site Holstein model.

On the basis of the Holstein model, it appears likely that the bandwidth in a crystal in the strong coupling regime, $\lambda \geq 1$ is given by an expression of the form (1.118) in the nonadiabatic case ($\omega > J$) and by the formula Eq.(1.135) ($\Delta E \simeq \sqrt{\frac{4E_p\omega}{\pi}} e^{-\tilde{g}^2}$) in the extreme adiabatic case, $J \gg \omega$. We discuss the small-polaron band in a crystal in Chapter 4.

In the rest of the book we survey the cooperative phenomena in many-polaron nystems. A single polaron was discussed in detail in reviews by Appel (1968), Devresse(ed.) (1972), Firsov (1975), Klinger (1979), and more recently by Devreese and Peeters (eds) (1984), Rashba (1985), Fisher, Hayes and Wallace (1989), Toyozawa 1990), Gerlach and Lowen (1991), Shluger and Stoneham (1993) and several others. in magnetic materials the carriers in the conduction band form spin polarons - somemos called ferrons (Nagaev (1979)); that is a group of moments oriented antiparallel to that of the carrier. Magnetic polarons were first invoked in ferromagnets by von Molnar and Methfessel (1967) in their study of the giant negative magneto-resistance in ferromagnetic $Eu_{1-x}Gd_xSe$. One can assume that spin polarons are carriers in Clie simple Mott insulator such as La_2CuO_4. We think, then, polarons must be of complex hybrid type. In the highly dielectric materials they will dies. Both spin and lattice will contribute to the mass enhant diin polarons are equivalent to the lattice ass enhancement. To some extent liy the hole is similar to the lattice one. and this fact makes some properties one. However, magnons are not perfect bosons, firent from those of lattice polaries of spin polarons (e.g. effective mass) quite dimily the linearised collective excitat. Nevertheless even in this case the idea that mil the constructive and the proble (magnons) of the spin system matter turns. Then be treated with them can be carrier strongly coupled with the spin powerful polaron formalism. We believe that (lie cooperative properties of spin and lattice bipolarons are those of charged bosons and can be described within the same formalism. Under certain conditions strongly correlated electrons can be described by a single-band $t - J$ model, in which the hole, constrained to a projected Hilbert space without double occupancy of sites, interacts with the spin density. The formation of small polarons in the Holstein $t - J$ model is examined in Chapter 5. It turns out that the correlations between electrons significantly reduce the critical value of the coupling constant λ helping to form small polarons.

6.3 1-1 Articles about large and small polarons and methods for them

6.3.1 Bogoliubov N N 1947 J.Phys.USSR 11, 23-32

1950 Ukr.Mat.Zh. 23;
1958 Zh.Eksp.Teor.Fiz. 34, 58, 73.
(???)
(it is used in "1.4 Intermediate-coupling large polaron")

6.4 3 Electrons and phonons

6.4.1 3.1 Electrons, phonons and the Fröhlich interaction

Theory

In this Chapter, we discuss electrons, phonons and their interaction starting from first principles. Physics and chemistry of solids, liquids and gases are described with the Hamiltonian

$$H = -\sum_i \frac{\nabla_i^2}{2m_e} + \frac{e^2}{2}\sum_{i\neq i'} \frac{1}{|\mathbf{r}_i - \mathbf{r}_{i'}|} - Ze^2 \sum_{ij} \frac{1}{|\mathbf{r}_i - \mathbf{R}_j|} + \frac{Z^2e^2}{2}\sum_{j\neq j'} \frac{1}{|\mathbf{R}_j - \mathbf{R}_{j'}|} - \sum_j \frac{\nabla_j^2}{2M} \quad (3.1)$$

where $\mathbf{r}_i, \mathbf{R}_j$ are coordinates of electrons and nuclei, $i = 1, \dots N_e; j = 1, \dots N; N_e = ZN$, $\nabla_i = \frac{\partial}{\partial \mathbf{r}_i}, \nabla_j = \frac{\partial}{\partial \mathbf{R}_j}$, Z is the number of protons in a nucleus, m_e, M are the electron and nuclear mass, respectively, and e is the elementary charge.

There is no possibility at present to solve the corresponding Schrödinger equation perturbatively because the Coulomb interaction is strong, the ratio of the characteristic interaction energy to the kinetic energy $r_s = m_e e^2/(4\pi n/3)^{1/3} \simeq 1$, or numerically for a condensed matter with the density $n = ZN/\Omega \sim 10^{23}$ cm^{-3}.

Here the normalised volume is taken $\Omega = 1$ unless specified otherwise. (can it play an important role??)

However, one can take advantage of the small value of the adiabatic ratio $m_e/M < 10^{-3}$. Because nuclei are heavy the amplitude $\langle|\mathrm{u}|\rangle \simeq \sqrt{1/M\omega_D}$ (derive this formula btw) of their vibrations near the equilibrium $\mathbf{R}_0 \equiv \mathbf{l}$ in a crystal is much smaller than the lattice constant $a = N^{-1/3}$

$$\frac{\langle|\mathrm{u}|\rangle}{a} \simeq (m_e/Mr_s)^{1/4} \ll 1. \quad (3.2)$$

To obtain this estimate we take into account that the characteristic vibration frequency ω_D is of the order of the ionic plasma frequency $\sqrt{4\pi NZ^2e^2/M}$. (check that it is so)

Using the smallness of the vibration amplitude we can expand the Hamiltonian in powers of $|\mathbf{u}|$ up to quadratic terms, responsible for the quasi-elastic forces returning ions to their equilibrium positions. (it is very not clear, how to do it, because there is no $|\mathbf{u}|$ in the Hamiltonian...)

Further progress requires a simplifying physical idea which is to approach the ground state of the many-electron system via a one-electron picture.

This is called a local density approximation (LDA) introducing an effective one-body potential $\mathcal{V}(\mathbf{r})$

$$\mathcal{V}(\mathbf{r}) = -Ze^2 \sum_j \frac{1}{|\mathbf{r} - \mathbf{R}_j|} + e^2 \int d\mathbf{r}' \frac{n(\mathbf{r}')}{|\mathbf{r} - \mathbf{r}'|} + \mu_{xc}(\mathbf{r}) \quad (3.3)$$

where $\mu_{xc}(\mathbf{r})$ is the exchange interaction, usually expressed by

$$\mu_{xc}(\mathbf{r}) = -\beta[n(\mathbf{r})]^{1/3} \quad (3.4)$$

with constant β. (write more, why is it so??)

Hohenberg and Kohn (1964) proved that $\mathcal{V}(\mathbf{r})$ is a unique functional of the electron density $n(\mathbf{r}) = \langle\psi^\dagger(\mathbf{r})\psi(\mathbf{r})\rangle$. (check their paper???)

As a result the Hamiltonian in the second quantisation for electrons takes the form

$$H = H_e + H_{ph} + H_{e-ph} + H_{e-e}, \quad (3.5)$$

where

$$H_e = \int d\mathbf{r}\psi^\dagger(\mathbf{r})\left(\frac{\nabla^2}{2m_e} + V(\mathbf{r})\right)\psi(\mathbf{r}) \tag{3.6}$$

is the electron energy in a periodic crystal field $V(\mathbf{r}) = \sum_1 v(\mathbf{r}-1)$, which is $\mathcal{V}(\mathbf{r})$ calculated with $\mathbf{R}_j = 1$ and with the periodic density $n^0(\mathbf{r}+1) = n^0(\mathbf{r})$,

$$H_{ph} = \sum_{\mathbf{l}}\left(-\frac{\nabla^2_{\mathbf{u}}}{2M} + \mathbf{u}_{\mathbf{l}}\cdot\frac{\partial}{\partial\mathbf{l}}\int d\mathbf{r}n^0(\mathbf{r})V(\mathbf{r})\right) + \frac{1}{2}\sum_{\mathbf{l},\mathbf{l}',\alpha,\beta} u^\alpha_{\mathbf{l}}u^\beta_{\mathbf{l}'}D_{\alpha,\beta}\left(\mathbf{l}-\mathbf{l}'\right) \tag{3.7}$$

is the vibration energy with $\alpha,\beta = x,y,z$ and

$$D_{\alpha,\beta}\left(\mathbf{l}-\mathbf{l}'\right) = \frac{\partial^2}{\partial l^\alpha \partial l'^\beta}\left(\frac{Z^2e^2}{2}\sum_{\mathbf{l}''\neq\mathbf{l}'''}\frac{1}{|\mathbf{l}''-\mathbf{l}'''|} + \int d\mathbf{r}n^0(\mathbf{r})V(\mathbf{r})\right) \tag{3.8}$$

(derive it!!!)

$$\begin{aligned} H_{e-ph} = &\sum_{1}\mathbf{u}_{\mathbf{l}}\cdot\frac{\partial}{\partial\mathbf{l}}\int d\mathbf{r}\left(\psi^\dagger(\mathbf{r})\psi^\dagger(\mathbf{r}) - n^0(\mathbf{r})\right)V(\mathbf{r}) \\ &+ \frac{1}{2}\sum_{1,\mathbf{l}',\alpha,\beta} u^\alpha_1 u^\beta_{1'}\frac{\partial^2}{\partial l^\alpha\partial l'^\beta}\int d\mathbf{r}\left(\psi^\dagger(\mathbf{r})\psi(\mathbf{r}) - n^0(\mathbf{r})\right)V(\mathbf{r}) \end{aligned} \tag{3.9}$$

is the electron-lattice vibration interaction, and

$$\begin{aligned} H_{e-e} = &\int d\mathbf{r}d\mathbf{r}'\left(\frac{e^2}{2\left|\mathbf{r}-\mathbf{r}'\right|}\left[\psi^\dagger\left(\mathbf{r}'\right)\psi\left(\mathbf{r}'\right) - n^0\left(\mathbf{r}'\right)\right] - \mu_{xc}(\mathbf{r})\delta\left(\mathbf{r}-\mathbf{r}'\right)\right)\psi^\dagger(\mathbf{r})\psi(\mathbf{r}) \\ &+ \frac{Z^2e^2}{2}\sum_{\mathbf{l}\neq\mathbf{l}'}\frac{1}{|\mathbf{l}-\mathbf{l}'|} - \frac{e^2}{2}\int d\mathbf{r}d\mathbf{r}'\frac{n^0\left(\mathbf{r}'\right)}{|\mathbf{r}-\mathbf{r}'|}\psi^\dagger(\mathbf{r})\psi(\mathbf{r}) \end{aligned} \tag{3.10}$$

describes electron-electron correlations.

(derive it!!!)

We include the electrostatic repulsive energy of nuclei in H_{e-e}, so the average of H_{e-e} is zero in a Hartree-Fock approximation. (what is meant by Hartree-Fock a.????)

All integrals above include also summation of spin coordinates. If the magnetic interaction is important the spin-polarised LDA can be applied (for a review see Staunton (1994)). (???)

The vibration Hamiltonian H_{ph} is a quadratic form and therefore can be diagonalised with a linear canonical transformation for the displacement operators

$$\mathbf{u}_{\mathbf{l}} = \sum_{\mathbf{q}}\frac{\mathbf{e}_{\mathbf{q},\nu}}{\sqrt{2NM\omega_{\mathbf{q},\nu}}}d_{\mathbf{q},\nu}\exp(i\mathbf{q}\cdot\mathbf{l}) + h.c., \tag{3.11}$$

$$\frac{\partial}{\partial\mathbf{u}_{\mathbf{l}}} = \sum_{\mathbf{q}}\mathbf{e}_{\mathbf{q},\nu}\sqrt{\frac{M\omega_{\mathbf{q},\nu}}{2N}}d_{\mathbf{q},\nu}\exp(i\mathbf{q}\cdot\mathbf{l}) - h.c., \tag{3.12}$$

(at which point creation, annihilation operators appear? we had just a wave function)

where $\mathbf{q}$ is a phonon momentum, $d_{\mathbf{q},\nu}$ is a phonon (Bose) annihilation operator, $\mathbf{e}_{\mathbf{q},\nu}$ being a unit vector, and ω_{q} a phonon frequency.

Substitution of the last two equations into H_{ph} yields

(check it!!! and the coefficients)

$$H_{ph} = \sum_{\mathbf{q},\nu} \omega_{\mathbf{q},\nu} \left(d^\dagger_{\mathbf{q},\nu} d_{\mathbf{q},\nu} + 1/2 \right) \tag{3.13}$$

if eigenfrequencies $\omega_{\mathbf{q},\nu}$ and eigenstates $\mathbf{e}_{\mathbf{q},\nu}$ satisfy

$$M\omega^2_{\mathbf{q},\nu} e^\alpha_{\mathbf{q},\nu} = \sum_\beta D^{\alpha,\beta}_{\mathbf{q}} e^\beta_{\mathbf{q},\nu} \tag{3.14}$$

and

$$\sum_{\mathbf{q}} e^{*\alpha}_{\mathbf{q},\nu} e^\beta_{\mathbf{q},\nu} = N\delta_{\alpha,\beta} \tag{3.15}$$

The last equation and the bosonic commutation rules $d_{\mathbf{q},\nu} d^\dagger_{\mathbf{q}',\nu'} - d^\dagger_{\mathbf{q}',\nu'} d_{\mathbf{q},\nu} = \delta_{\mathbf{q},\mathbf{q}'}\delta_{\nu,\nu'}$ follow from $\frac{\partial}{\partial u^\alpha_1} u^\beta_1 - u^\beta_1 \frac{\partial}{\partial u^\alpha_1} = \delta_{\alpha,\beta}$. Here

$$D^{\alpha,\beta}_{\mathbf{q}} = \sum_{\mathbf{m}} \exp(i\mathbf{q}\cdot\mathbf{m}) D_{\alpha,\beta}(\mathbf{m}) \tag{3.16}$$

is the Fourier component of the second derivative of the ion potential energy, Eq.(3.8).

The first derivative in Eq.(3.7) is zero in the presence of a symmetry center. The different solutions of Eq.(3.14) are classified with the mode index ν, which is $1, 2, 3$ for a simple lattice, and $1, \ldots 3k$ for a lattice with k ions per unit cell.

The electron (periodic) part of the Hamiltonian is diagonal in the Bloch representation (revise Bloch's theory)

$$\psi(\mathbf{r}) = \sum_{\mathbf{k},n,s} \phi_{\mathbf{k},n,s}(\mathbf{r}) c_{\mathbf{k},n,s} \tag{3.17}$$

where $c_{\mathbf{k},n,s}$ is a fermionic annihilation operator. (the energy bands n and c operators appear at this step.) The Bloch function obeys the Schrödinger equation

$$\left(-\frac{\nabla^2}{2m_e} + V(\mathbf{r}) \right) \phi_{\mathbf{k},n,s}(\mathbf{r}) = E_{\mathbf{k},n,s} \phi_{\mathbf{k},n,s}(\mathbf{r}) \tag{3.18}$$

One-particle states are classified with the momentum $\mathbf{k}$ in the Brillouin zone, band index n (how does it appear??)and spin s.

The solution of this equation is used to obtain the density $n^0(\mathbf{r})$, which determines the crystal field potential $V(\mathbf{r})$. (this is odd... how would we plug V in the equation then, if we need to get if from solution of the eq.?)

The LDA can explain the shape of the Fermi surface of wide band metals and gaps in narrow gap semiconductors. (why??)

The spin polarised version of LDA can explain a variety of properties of many magnetic materials. (why??)This is in contrast to narrow d and f band metals as well as to oxides and other ionic lattices with strong electron-phonon interaction and Coulomb correlations which display much less dispersion and wider gaps than the first-principles band structure methodology can predict.

Substituting Eq.(3.17) into the Hamiltonian one finally obtains

$$H = H_0 + H_{e-ph} + H_{e-e}, \tag{3.19}$$

where

$$H_0 = \sum_{\mathbf{k},n,s} \xi_{\mathbf{k},n,s} c^\dagger_{\mathbf{k},n,s} c_{\mathbf{k},n,s} + \sum_{\mathbf{q},\nu} \omega_{\mathbf{q},\nu} \left(d^\dagger_{\mathbf{q},\nu} d_{\mathbf{q},\nu} + 1/2 \right) \tag{3.20}$$

describes independent electron Bloch bands and phonons, $\xi_{\mathbf{k},n,s} = E_{\mathbf{k},n,s} - \mu$ is the band energy spectrum.

Because the electron-phonon interaction leads to the pairing of electrons it is convenient to consider an open system with a fixed chemical potential μ rather than to fix N_e to avoid some artificial difference between odd and even N_e. (don't understand how will it help to avoid and what is the problem?)

The ground state of an open system has the minimum expectation value of $H - \mu N_e$. That is why the electron energy is related to μ.

The part of the electron-phonon interaction, which is linear in phonon operators can be written as

(derive!!! where the bands at all come into the game??)

$$H_{e-ph} = \frac{1}{\sqrt{2N}} \sum_{\mathbf{k},\mathbf{q},n,n',\nu,s} \gamma_{n,n'}(\mathbf{q},\mathbf{k},\nu) \omega_{\mathbf{q},\nu} c^\dagger_{\mathbf{k},n,s} c_{\mathbf{k}-\mathbf{q},n',s} d_{\mathbf{q},\nu} + h.c. \tag{3.21}$$

with a dimensionless matrix element

$$\gamma_{n,n'}(\mathbf{q},\mathbf{k},\nu) = -\frac{N}{\sqrt{M\omega^3_{\mathbf{q},\nu}}} \int d\mathbf{r} \left(\mathbf{e}_{\mathbf{q},\nu} \cdot \nabla v(\mathbf{r}) \right) \phi^*_{\mathbf{k},n,s}(\mathbf{r}) \phi_{\mathbf{k}-\mathbf{q},n',s}(\mathbf{r}) \tag{3.22}$$

(are there some examples of calculation of this constant???)

Low energy physics is often described within a single band approximation with the matrix element γ depending only on the momentum transfer q. If

$$\gamma_{n,n'}(\mathbf{q},\mathbf{k},\nu) = \gamma(\mathbf{q}) \tag{3.23}$$

we call the interaction the Fröhlich one. Terms of H_{e-ph} quadratic and higher order in phonon operators are small. They play a role only for those phonons which are not coupled with electrons by the linear interaction, Eq.(3.21) ($\gamma = 0$). The correlation energy of a homogeneous electron system is written as

$$H_{e-e} = \frac{1}{2} \sum_{\mathbf{q}} V_c(\mathbf{q}) \rho^\dagger_{\mathbf{q}} \rho_{\mathbf{q}} \tag{3.24}$$

where $V_c(\mathbf{q})$ is a matrix element of the Coulomb interaction, which is zero for $\mathbf{q} = 0$ because of electroneutrality (why??)and

$$\rho^\dagger_{\mathbf{q}} = \sum_{\mathbf{k},s} c^\dagger_{\mathbf{k},s} c_{\mathbf{k}+\mathbf{q},s} \tag{3.25}$$

is the density fluctuation operator. For doped semiconductors and amorphous metals a random potential should be included in H_0. (there are some exotic models about it, maybe I'll learn them later)

The harmonic approximation is sufficient for low temperature kinetics and thermodynamics of solids. Further corrections in $|u|$, especially those of third and fourth order, are known as anharmonic terms, and are of importance for the thermal expansion and lattice thermal conductivity. (I'll maybe meet them in another theory, here they are just not used)

6.4.2 3.2 Bare phonons and sound in a metal

Frequencies of phonons

(in this section, it is not clear, what problem is solved by this formalism, it is just a revision of well-known electron-phonon formalism with some unusual features. Basically, the main conclusion is that phonons are renormalized.)

In wide-band metals such as Na or K the correlation energy is relatively small ($r_s \leq 1$) and carriers are almost free. (what is the input that leads to these properties???)

Core electrons together with nuclei form compact ions with an effective Z. The carrier wave function outside the core can be represented by a plane wave

$$\phi_{\mathbf{k},n,s} \simeq e^{i\mathbf{k}\cdot\mathbf{r}} \tag{3.26}$$

(reminder: we rewrote the initial electron wave function in a quantum-field form, where the ϕ appeared: $\psi(\mathbf{r}) = \sum_{\mathbf{k},n,s} \phi_{\mathbf{k},n,s}(\mathbf{r}) c_{\mathbf{k},n,s}$)

and the carrier density $n^0(\mathbf{r})$ is constant. Therefore the only relevant interaction in the dynamical matrix is the Coulomb repulsion between ions, which yields

(check that it is the same formula as before, but simplified)

$$D_{\alpha,\beta}(\mathbf{l}-\mathbf{l}') = \frac{Z^2e^2}{2}\frac{\partial^2}{\partial l^\alpha \partial l'^\beta}\sum_{\mathbf{l}''\neq\mathbf{l}'''}\frac{1}{|\mathbf{l}''-\mathbf{l}'''|} \tag{3.27}$$

The electron-phonon coupling constant is determined with the Coulomb electron-ion attraction $v(\mathbf{r}) = -Ze^2/r$ and with the plane waves in Eq.(3.22).

(hard task to do: find this coupling constant for some different types of material. maybe I'll do it in another note)

(why do we do such transformations as below???)

The potential $1/r$ may be expanded in a Fourier series as

$$\frac{1}{r} = 4\pi \lim_{\kappa\to 0}\sum_{\mathbf{q}}\frac{1}{q^2+\kappa^2}e^{i\mathbf{q}\cdot\mathbf{r}} \tag{3.28}$$

Substituting this expansion into Eq.(3.27) and Eq.(3.22) we find

$$D_{\alpha,\beta}(\mathbf{m}) = 4\pi \lim_{\kappa\to 0}\sum_{\mathbf{q}}\frac{q_\alpha q_\beta}{q^2+\kappa^2}\cos(\mathbf{q}\cdot\mathbf{m}) \tag{3.29}$$

and

$$\gamma(\mathbf{q}) = i\frac{4\pi NZe^2}{\sqrt{M\omega_{\mathbf{q}}^3}}\lim_{\kappa\to 0}\frac{\mathrm{e}_{\mathbf{q},\nu}\cdot\mathbf{q}}{q^2+\kappa^2} \tag{3.30}$$

Calculating the Fourier component of Eq.(3.29) one obtains for eigenfrequences and three eigenvectors

(how to do it????)

$$\omega_{\mathbf{q},\nu}^2\mathbf{e}_{\mathbf{q},\nu} = \omega_i^2\mathbf{q}\frac{\mathbf{e}_{\mathbf{q},\nu}\cdot\mathbf{q}}{q^2} \tag{3.31}$$

where $\omega_i = \sqrt{4\pi NZ^2e^2/M}$ is the ionic plasma frequency. A longitudinal mode with e $\|$q is an ionic plasmon

$$\omega_{\mathrm{q}} = \omega_i \tag{3.32}$$

and two shear (transverse) modes with $\mathbf{e} \perp \mathbf{q}$ have zero frequency, which is due to a hard core approximation. (why??)

In fact, the core electrons undergo a polarisation when ions are displaced from their equilibrium positions which yields a finite shear mode frequency.

GF method and self-energy

According to Eq.(3.30) carriers interact with the longitudinal phonons. The interaction is strong, giving rise to a significant renormalisation of the bare phonon frequency, Eq.(3.32).

To calculate the renormalised phonon frequency one can apply following Migdal (1958) the Green's function (GF) formalism. The one-particle Green's function (GF) is determined as:

(never saw that GF has both Shr. and Heis. operators. is it ok?)

$$G(\mathbf{k}, t) = -i \left\langle T_t c_{\mathbf{k}}(t) c_{\mathbf{k}}^{\dagger} \right\rangle \tag{3.33}$$

with $c_{\mathbf{k}}(t) = \exp(iHt) c_{\mathbf{k}} \exp(-iHt)$ and $T_t A(t) B = \Theta(t) A(t) B - \Theta(-t) B A(t)$ for any fermionic operators A, B and with the opposite sign of the second term for any bosonic operators, $\Theta(x) = 1$ for $x > 0$ and zero otherwise. The Fourier component of the free-electron GF ($H = H_0$) is given by

$$G^{(0)}(\mathbf{k}, \omega) = \frac{\Theta(\xi_{\mathbf{k}})}{\omega - \xi_{\mathbf{k}} + i0^+} + \frac{\Theta(-\xi_{\mathbf{k}})}{\omega - \xi_{\mathbf{k}} - i0^+}, \tag{3.34}$$

with $\xi_{\mathbf{k}} = k^2/2m_e - \mu$ which is obtained by the direct integration of Eq.(3.33):

$$G^{(0)}(\mathbf{k}, \omega) = \frac{1}{2\pi} \int_{-\infty}^{\infty} dt G^0(\mathbf{k}, t) e^{i\omega t} \tag{3.35}$$

(check this. it should be straightforward)

For interacting electrons the electron self-energy is introduced asы

$$\Sigma(\mathbf{k}, \omega) = \left(G^{(0)}(\mathbf{k}, \omega)\right)^{-1} - (G(\mathbf{k}, \omega))^{-1} \tag{3.36}$$

so

$$G(\mathbf{k}, \omega) = \frac{1}{\omega - \xi_{\mathbf{k}} - \Sigma(\mathbf{k}, \omega)} \tag{3.37}$$

(It is a well-known formalism.)

The phonon GF can be determined as

$$D(\mathbf{q}, t) = -i \frac{\omega_{\mathbf{q}}}{2} \left\langle T_t \left(d_{\mathbf{q}}(t) d_{\mathbf{q}}^{\dagger} + d_{\mathbf{q}}^{\dagger}(t) d_{\mathbf{q}} \right) \right\rangle. \tag{3.38}$$

(check that such defs are in other books...)

Thus the Fourier component of the free phonon GF ($H = H_0$) is the dimensionless even function of frequency

$$D^{(0)}(\mathbf{q}, \omega) = \frac{\omega_{\mathbf{q}}^2}{\omega^2 - \omega_{\mathbf{q}}^2 + i0^+} \tag{3.39}$$

and the phonon self-energy

$$\Pi(\mathbf{q}, \omega) = \left(D^{(0)}(\mathbf{q}, \omega)\right)^{-1} - (D(\mathbf{q}, \omega))^{-1}. \tag{3.40}$$

(nothing is explained below, so one needs to know all this formalism in order to understand it)

The Feynman diagram technique is convenient, Fig.3.1.

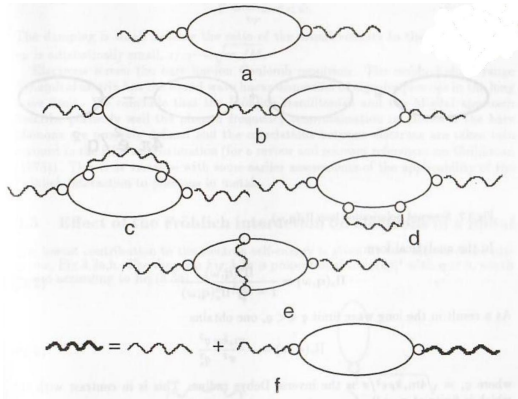

Fig.3.1. Second (a) and fourth order (b,c,d,e) corrections to the phonon GF. The phonon GF in the Migdal approximation, (f).

Thin straight and wavy lines correspond to $G^{(0)}$ and $D^{(0)}$ respectively, a vertex (circle) corresponds to the interaction matrix element $\gamma(\mathbf{q})\sqrt{\omega_{\mathbf{q}}/N}$ and bold lines represent G and D.

The Fröhlich interaction is a sum of two operators describing the emission and absorption of a phonon. Both events are taken into account by the definition of D. Therefore wavy lines have no direction. There are no first or higher odd-order corrections to D because the Fröhlich interaction is off-diagonal with respect to phonon occupation numbers. The second order term of D, Fig.3a includes a so-called polarisation loop Π_e^0, which is a convolution of two $G^{(0)}$. Among different fourth order diagrams the diagram Fig.3.1b with two polarisation loops is the most 'dangerous'. Different from others it is proportional to $1/q^2$, which is large for small q. On the other hand the singularity of internal vertices is integrated out in the diagrams Fig.3.1c,d,e. The sum of all 'dangerous' diagrams is given in Fig.3f, or in the analytical form

$$\Pi(\mathbf{q},\omega) = \frac{|\gamma(\mathbf{q})|^2\omega_{\mathbf{q}}}{N}\Pi_e(\mathbf{q},\omega) \tag{3.41}$$

where

$$\Pi_e(\mathbf{q},\omega) = \Pi_e^0(\mathbf{q},\omega) \tag{3.42}$$

with

$$\Pi_e^0(\mathbf{q},\omega) = -\frac{2i}{(2\pi)^4}\int d\mathbf{k}d\epsilon G^{(0)}(\mathbf{k}+\mathbf{q},\epsilon+\omega)G^{(0)}(\mathbf{k},\epsilon) \tag{3.43}$$

The additional 2 in the phonon self-energy is due to the contribution to the polarisation loop from two electron spins. It is convenient first to integrate over frequency in Eq.(3.43) with the following result:

$$\Pi_e^0(\mathbf{q},\omega) = \frac{1}{4\pi^3}\int d\mathbf{k}\frac{\Theta\left(\xi_{\mathbf{k}}\right)-\Theta\left(\xi_{\mathbf{k}+\mathbf{q}}\right)}{\omega+\xi_{\mathbf{k}}-\xi_{\mathbf{k}+\mathbf{q}}+i0^+\,\mathrm{sgn}\left(\xi_{\mathbf{k}+\mathbf{q}}\right)} \tag{3.44}$$

Because of adiabaticity ω is small, $\omega \ll \mu$. Thus one can take $\omega = 0$ in Re Π_e^0 and the first order term in ω in Im Π_e^0 to obtain

$$\mathrm{Re}\ \Pi_e^0(\mathbf{q},\omega) = -\frac{m_e k_F}{2\pi^2}h\left(\frac{q}{2k_F}\right) \tag{3.45}$$

$$\mathrm{Im}\ \Pi_e^0(\mathbf{q},\omega) = -\frac{m_e^2}{2\pi q}|\omega|\Theta\left(2k_F-q\right) \tag{3.46}$$

with $h(x) = 1+\frac{1-x^2}{2x}\ln\left|\frac{1+x}{1-x}\right|$ and the Fermi momentum $k_F = \sqrt{2m_e\mu} = \left(3\pi^2 n\right)^{1/3}$.

One should also take into account the Coulomb correlations because the corresponding vertex is singular in the long wave limit, $V_c(q) = 4\pi e^2/q^2$.

This leads to a drastic renormalisation of the long wave behavior of Π_e. In the 'loop' or random phase (RPA) approximation we obtain Fig.3.2 as in the case of the electron-plasmon interaction, Fig.3.1f, but with the Coulomb (dashed) line instead of the wavy phonon line.

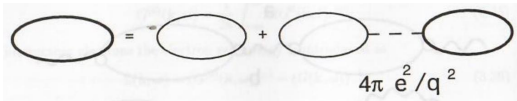

Fig.3.2. Screened polarisation loop $\Pi_{e}(\mathbf{q}, \omega)$.

In the analytical form

$$\Pi_e(\mathbf{q}, \omega) = \frac{\Pi_e^0(\mathbf{q}, \omega)}{1 - \frac{4\pi e^2}{q^2}\Pi_e^0(\mathbf{q}, \omega)} \tag{3.47}$$

As a result in the long wave limit $q \ll q_s$ one obtains

$$\Pi_e(\mathbf{q}, \omega) = -\frac{m_e k_F}{\pi^2}\frac{q^2}{q_s^2} \tag{3.48}$$

where $q_s = \sqrt{4m_e k_F e^2/\pi}$ is the inverse Debye radius. This is in contrast with Π_e^0, which is finite at $q \to 0$.

(this is a bad theory, because before it was written that $\Pi_e(\mathbf{q}, \omega) = \Pi_e^0(\mathbf{q}, \omega)$. Maybe it is meant $\Pi(\mathbf{q}, \omega)$)

With the RPA expression, Eq.(3.41) and $\gamma(\mathbf{q})$ determined in Eq.(3.30) with $\omega_{\mathbf{q},\nu}\omega_i$ the phonon Green's function is

$$D(\mathbf{q}, \omega) = \frac{\omega_i^2}{\omega^2 - \tilde{\omega}_{\mathbf{q}}^2} \tag{3.49}$$

A pole of D determines a new phonon dispersion and a damping Γ due to the interaction with electrons

$$\tilde{\omega}_{\mathbf{q}} = \frac{\omega_i}{\sqrt{\epsilon\left(\mathbf{q}, \tilde{\omega}_{\mathbf{q}}\right)}} \tag{3.50}$$

where

$$\epsilon(\mathbf{q}, \omega) = 1 - \frac{4\pi e^2}{q^2}\Pi_e^0(\mathbf{q}, \omega) \tag{3.51}$$

is the electron dielectric function.

(some formalism is assumed here. write it better! why polarization operator is connected to the dielectric function?)

In the long wave limit

$$\epsilon(\mathbf{q}, 0) = 1 + \frac{q_s^2}{q^2} \tag{3.52}$$

so one obtains a sound wave as the real part of $\tilde{\omega}$

$$\tilde{\omega}_{\mathbf{q}} = sq \tag{3.53}$$

with the sound velocity $s = Zk_F/\sqrt{3Mm_e}$, and a small damping as the imaginary part

$$\Gamma \sim \frac{s}{v_F}\tilde{\omega} \ll \tilde{\omega} \tag{3.54}$$

The damping is small because the ratio of the sound velocity to the Fermi velocity v_F is adiabatically small, $s/v_F \sim \sqrt{m_e/M}$.

Electrons screen the bare ion-ion Coulomb repulsion. The residual short range dynamical matrix has the sound wave linear dispersion of eigenfrequencies in the long wave limit. We conclude that the Fröhlich Hamiltonian and the Migdal approach describe perfectly well the phonon frequency renormalisation in metals if the bare phonons are properly defined and the correlations between electrons are taken into account in the RPA approximation (for a review and relevant references see Geilikman (1975)). This is at variance with some earlier assessments of the applicability of the Fröhlich interaction to phonons in metals.

6.4.3 3.3 Effect of the Fröhlich interaction on electrons in a metal

Theory

(We still consider the model

$$H_0 = \sum_{\mathbf{k},n,s} \xi_{\mathbf{k},n,s} c^\dagger_{\mathbf{k},n,s} c_{\mathbf{k},n,s} + \sum_{\mathbf{q},\nu} \omega_{\mathbf{q},\nu} \left(d^\dagger_{\mathbf{q},\nu} d_{\mathbf{q},\nu} + 1/2 \right) \tag{3.20}$$

$$H_{e-ph} = \frac{1}{\sqrt{2N}} \sum_{\mathbf{k},\mathbf{q},n,n',\nu,s} \gamma_{n,n'}(\mathbf{q},\mathbf{k},\nu) \omega_{\mathbf{q},\nu} c^\dagger_{\mathbf{k},n,s} c_{\mathbf{k}-\mathbf{q},n',s} d_{\mathbf{q},\nu} + h.c. \tag{3.21}$$

$$H_{e-e} = \frac{1}{2} \sum_{\mathbf{q}} V_c(\mathbf{q}) \rho^\dagger_{\mathbf{q}} \rho_{\mathbf{q}} \qquad \rho^\dagger_{\mathbf{q}} = \sum_{\mathbf{k},s} c^\dagger_{\mathbf{k},s} c_{\mathbf{k}+\mathbf{q},s} \tag{3.24, 3.25}$$

)

The lowest contribution to the electron self-energy is given by two second order diagrams, Fig.3.3a,b. The diagram Fig.3.3b is proportional to $|\gamma(\mathbf{q})|^2$ with $\mathbf{q} \equiv 0$, which is zero according to Eq.(3.30).

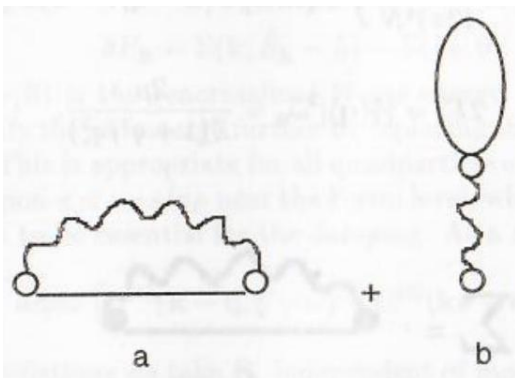

Fig.3.3. Second-order electron self-energy.

Higher order RPA diagrams are taken into account through the replacement of the bare ionic plasmon GF for the renormalised one, Eq.(3.49) and the bare electron-phonon interaction constant γ for a screened one, γ_{sc} as shown in Fig.3.4. In the analytical form the diagram Fig. 3.4 corresponds to

$$\gamma_{sc}(\mathbf{q},\omega) = \gamma(\mathbf{q}) + \frac{4\pi e^2}{q^2}\Pi_e^0(\mathbf{q},\omega)\gamma_{sc}(\mathbf{q},\omega) \tag{3.55}$$

or

$$\gamma_{sc}(\mathbf{q},\omega) = \frac{\gamma(\mathbf{q})}{\epsilon(\mathbf{q},\omega)} \tag{3.56}$$

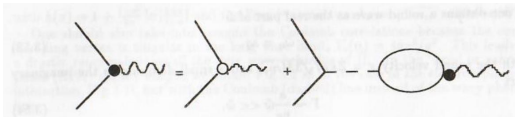

Fig.3.4.Screened electron-phonon interaction (dark circle).

For low-energy excitations $\omega \ll \mu$ the static approximation of the dielectric function, Eq.(3.52) is appropriate. Instead of D and γ_{sc} given in Eq.(3.49) and Eq.(3.56) one can introduce the acoustic phonon GF

$$\tilde{D}(\mathbf{q},\omega) = \frac{\tilde{\omega}_{\mathbf{q}}^2}{\omega^2 - \tilde{\omega}_{\mathbf{q}}^2} \tag{3.57}$$

and the electron-acoustic phonon vertex $\tilde{\gamma}(\mathbf{q})\sqrt{\frac{\bar{\omega}\mathbf{q}}{N}}$ with

$$\tilde{\gamma}(\mathbf{q}) = \frac{\gamma(\mathbf{q})}{\epsilon(\mathbf{q},0)}\left(\frac{\omega_i}{\tilde{\omega}_{\mathbf{q}}}\right)^{3/2} \tag{3.58}$$

Finally one obtains the diagram, Fig.3.5 for the electron self-energy as a result of the summation of the 'most divergent' RPA diagrams (????)

$$\Sigma(\mathbf{k},\epsilon) = \frac{2i}{(2\pi)^4 N}\int d\mathbf{q}d\omega E_p G(\mathbf{k}-\mathbf{q},\epsilon-\omega)\tilde{D}(\mathbf{q},\omega) \tag{3.59}$$

with

$$2E_p = |\tilde{\gamma}(\mathbf{q})|^2\tilde{\omega}_{\mathbf{q}} = \frac{2\mu}{Z\,(1+q^2/q_s^2)} \tag{3.60}$$

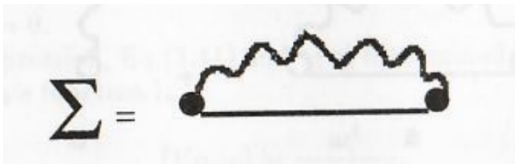

Fig.3.5. Electron self-energy in the Migdal approximation.

Because Z is of order of unity the electron-acoustic phonon interaction E_p is generally not small being of the order of the Fermi-energy in a metal. (??)

Therefore one has to consider fourth and higher order diagrams with the crossing phonon lines as in Fig.3.6, which are absent from Fig.3.5. (??)

Fortunately, as shown by Migdal their contribution is adiabatically small ($\sim s/v_F$) compared with Eq.(3.59). Moreover, the main contribution to the integral in Eq.(3.59) for Σ comes from the region $q \sim k_F \gg q_s$. In this region the dimensionless coupling constant

$$\lambda = 2E_p N(0) \tag{3.61}$$

is small

$$\lambda \simeq r_s \ll 1 \tag{3.62}$$

so the second order is sufficient for Σ. Here

$$N(0) = \frac{1}{N}\sum_{\mathbf{k}} \delta\left(\xi_{\mathbf{k}} - \mu\right) \tag{3.63}$$

is the density of states (DOS) per cell at the Fermi level.

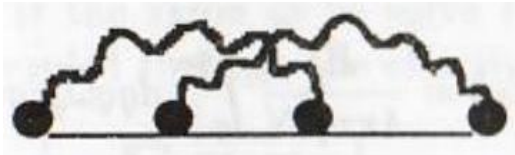

Fig.3.6. Adiabatically small corrections to the electron self-energy.

A new quasiparticle spectrum renormalised by the interaction is determined as a pole of the electron GF:

$$\tilde{E}_{\mathbf{k}} = \tilde{\mu} + v_F\left(k - k_F\right) + \delta E_{\mathbf{k}} \tag{3.64}$$

where

$$\delta E_{\mathbf{k}} = \Sigma\left(\mathbf{k}, \tilde{E}_{\mathbf{k}} - \tilde{\mu}\right) - \Sigma\left(k_F, 0\right) \tag{3.65}$$

and $\tilde{\mu} = \mu + \Sigma\left(k_F, 0\right)$ is the renormalised Fermi energy. The adiabatic condition allows one to simplify the self-energy further by replacing the exact GF in the integral Eq. (3.59) by $G^{(0)}$. This is appropriate for all quasiparticle energies with the exception of a very narrow region $\ll \omega_D s/v_F$ near the Fermi level, where the difference between G and $G^{(0)}$ appears to be essential for the damping. As a result one obtains

$$\delta E_{\mathbf{k}} = \frac{2iE_p}{(2\pi)^4}\int d\mathbf{q}d\omega\left(G^{(0)}(\mathbf{k}-\mathbf{q}, \tilde{\xi} - \omega) - G^{(0)}\left(\mathbf{k}_F - \mathbf{q}, -\omega\right)\right)\tilde{D}(\mathbf{q}, \omega) \tag{3.66}$$

To simplify the calculations we take E_p independent of momentum, apply the Debye approximation for acoustic phonons $\tilde{\omega}_{\mathrm{q}} = sq$ for $q < q_D$ where $q_D \simeq \pi/a$ is the Debye momentum, and consider a half-filled band, $k_F \simeq \pi/2a$ with the energy independent DOS near the Fermi level $N(0) = m_e a^2/4\pi$.

The main contribution to the integral Eq.(3.66) comes from the momentum region close to the Fermi-surface:

$$|\mathbf{k} - \mathrm{q}| \simeq k_F \tag{3.67}$$

This makes it convenient to introduce a new variable $k' = |\mathbf{k} - \mathbf{q}|$ instead of the angle Θ lietween k and q and extend the integration to $\pm\infty$ with the variable $\xi = v_F\left(k' - k_F\right)$. Thus the angular integration in Eq.(3.66) becomes:

$$\int d\Theta \sin\Theta(\ldots) \sim \int_{\infty}^{\infty} d\xi \frac{\tilde{\xi}}{\left[\tilde{\xi} - \omega - \xi + i0^+\,\mathrm{sgn}(\xi)\right]\left[\omega + \xi - i0^+\,\mathrm{sgn}(\xi)\right]} \tag{3.68}$$

This integral is non-zero only if $\tilde{\xi} > \omega > 0$ or $\tilde{\xi} < \omega < 0$. It is $-2\pi i$ in the first region and $2\pi i$ in the second one. Taking into account that $\tilde{D}$ is an even function of ω one obtains

$$\delta E_{\mathbf{k}} = \frac{2E_p}{(2\pi)^2 v_F N} \int_0^{q_D} dqq \int_0^{|\tilde{\xi}|} d\omega \, \mathrm{sgn}(\tilde{\xi}) \frac{\tilde{\omega}_q^2}{\omega^2 - \tilde{\omega}_q^2 + i0^+} \tag{3.69}$$

The real and imaginary parts of Eq.(3.69) determine respectively the renormalised spectrum and the life time of quasiparticles

$$\mathrm{Re}\ (\delta E_{\mathbf{k}}) = \frac{E_p}{4\pi^2 v_F N} \int_0^{q_D} dqq\tilde{\omega}_q \ln \left| \frac{\tilde{\omega}_q - \tilde{\xi}}{\tilde{\omega}_q + \tilde{\xi}} \right| \tag{3.70}$$

$$\mathrm{Im}\ (\delta E_{\mathbf{k}}) = \frac{E_p}{4\pi v_F N} \int_0^{q_m} dqq\tilde{\omega}_q \, \mathrm{sgn}(\tilde{\xi}) \tag{3.71}$$

with $q_m = |\tilde{\xi}|/s$ if $|\tilde{\xi}| < \omega_D$ and $q_m = q_D$ if $|\tilde{\xi}| > \omega_D$. For the excitations far away from the Fermi surface with $|\tilde{\xi}| \gg \omega_D$ we find

$$\mathrm{Re}\ (\delta E_{\mathbf{k}}) = -\lambda \frac{\omega_D^2}{2\tilde{\xi}} \tag{3.72}$$

Here $\omega_D = sq_D$ is the Debye frequency. For low-energy excitations with $|\tilde{\xi}| \ll \omega_D$

$$\mathrm{Re}\ (\delta E_{\mathbf{k}}) = -\lambda \tilde{\xi} \tag{3.73}$$

which means an increase of the effective mass of the excitation due to the electron-phonon interaction

$$\tilde{\xi} = \frac{k_F}{m^*} (k - k_F) \tag{3.74}$$

The renormalised effective mass is

$$m^* = (1 + \lambda) m_e. \tag{3.75}$$

Thus the excitation spectrum of a metal has two different regions with two different values of the effective mass. The thermodynamic properties of a metal at low temperature $T \ll \omega_D$ involve m^*, but the optical properties in a frequency range $\nu \gg \omega_D$ are determined by the high-energy excitations, where according to Eq.(3.72) corrections are small and the mass is equal to the band mass m_e.

The damping has just the opposite behavior. The integral Eq.(3.71) yields

$$\mathrm{Im}\ (\delta E_{\mathbf{k}}) = \begin{cases} \frac{\mathrm{sgn}(\tilde{\xi})\pi\lambda\omega_D}{3}, & |\tilde{\xi}| > \omega_D; \\ \frac{\mathrm{sgn}(\tilde{\xi})\pi\lambda|\tilde{\xi}|^3}{3\omega_D^2}, & |\tilde{\xi}| \ll \omega_D. \end{cases} \tag{3.76,3.77}$$

These expressions describe the rate of decay of the quasiparticles due to emission of phonons. In the immediate neighborhood of the Fermi surface $|\tilde{\xi}| \ll \omega_D$ the decay is small compared with the quasiparticle energy $|\tilde{\xi}|$ even for a relatively strong coupling $\lambda \sim 1$, so that the concept of well-defined quasiparticles has a definite meaning. Hence, within the Migdal approximation the electron-phonon interaction does not destroy the Fermi-liquid behavior of electrons. The Pauli exclusion principle is responsible for the stability of the Fermi liquid. In the intermediate-energy region $|\tilde{\xi}| \sim \omega_D$, however, the decay is comparable with the energy and the quasiparticle spectrum looses its meaning. In the high-energy region $|\tilde{\xi}| \gg \omega_D$ the decay remains the same

in absolute value but again becomes small in comparison with $|\xi|$ and the quasiparticle concept recovers its meaning.

To go beyond Migdal's approximation one has to consider adiabatically small higher order diagrams (is there an example of how it is done somewhere???) which is the same as to solve the Hamiltonian of free electrons and acoustic phonons coupled through the effective Fröhlich interaction

$$H_{e-ph} = \frac{1}{\sqrt{2N}} \sum_{\mathbf{k},\mathbf{q},s} \tilde{\gamma}(\mathbf{q}) \tilde{\omega}_{\mathbf{q}} c^{\dagger}_{\mathbf{k},s} c_{\mathbf{k}-\mathbf{q},s} \tilde{d}_{\mathbf{q}} + h.c. \tag{3.78}$$

(note that now, there are tildes) with $\tilde{d}_{\mathrm{q}}$ the acoustic phonon operator.

From our consideration it follows that applying this Hamiltonian to electrons one should not consider the acoustic phonon self-energy.

Acoustic phonons in a metal appear as the result of the electron-plasmon coupling and the Coulomb screening, so their frequency includes already the self-energy effect as discussed in section 3.2.

6.4.4 3.4 Broken gauge symmetry and the BCS ground state

(All superconductivity is encoded in all the formulas above. This is very not trivial, so here, we are supposed to show how is it?)

(where is Broken gauge symmetry?)

Theory

(We still consider the model

$$H_0 = \sum_{\mathbf{k},n,s} \xi_{\mathbf{k},n,s} c^{\dagger}_{\mathbf{k},n,s} c_{\mathbf{k},n,s} + \sum_{\mathbf{q},\nu} \omega_{\mathbf{q},\nu} \left(d^{\dagger}_{\mathbf{q},\nu} d_{\mathbf{q},\nu} + 1/2 \right) \tag{3.20}$$

$$H_{e-ph} = \frac{1}{\sqrt{2N}} \sum_{\mathbf{k},\mathbf{q},n,n',\nu,s} \gamma_{n,n'}(\mathbf{q},\mathbf{k},\nu) \omega_{\mathbf{q},\nu} c^{\dagger}_{\mathbf{k},n,s} c_{\mathbf{k}-\mathbf{q},n',s} d_{\mathbf{q},\nu} + h.c. \tag{3.21}$$

$$H_{e-e} = \frac{1}{2} \sum_{\mathbf{q}} V_c(\mathbf{q}) \rho^{\dagger}_{\mathbf{q}} \rho_{\mathbf{q}} \qquad \rho^{\dagger}_{\mathbf{q}} = \sum_{\mathbf{k},s} c^{\dagger}_{\mathbf{k},s} c_{\mathbf{k}+\mathbf{q},s} \tag{3.24, 3.25}$$

)

The Migdal approach is justified if the ground state is stable versus a phase transition. Frohlich (1950) realised that the electron-phonon interaction, Eq.(1.48) leads to an attraction between two electrons and Cooper (1957) discovered that any attraction between degenerate electrons leads to their pairing; it does not matter how weak it in. Pairs are bosons, which undergo a Bose-Einstein condensation at some critical temperature T_c. The condensed state is described by the classical field, which is an average of the product of two annihilation field operators $F \sim \langle \psi\psi \rangle$ or two creation operators $F^{+} \sim \langle \psi^{\dagger}\psi^{\dagger} \rangle$. This average is macroscopically large below T_c in an open system. The appearance of the 'anomalous' averages brakes the gauge symmetry of the bare Hamiltonian, Eq.(3.19) and cannot be described perturbatively. Following Hardeen, Cooper and Schrieffer (1957) one has to go beyond the Migdal approximaNon, Fig. 3.5 including the anomalous averages in the ground state. This can be done milfonsistenly using the same self-energy diagram Fig. 3.5 as for the normal state but with the matrix electron GF (Eliashberg (1960)). At finite temperature the diagram in himique can be formulated for the 'temperature' GF defined by Matsubara(1955)

$$g(\mathbf{k},\tau) = -\langle\langle T_\tau c_{\mathbf{k}}(\tau) c^\dagger_{\mathbf{k}} \rangle\rangle, \tag{3.79}$$

will $c_k(\tau) = \exp(H\tau) c_{\mathbf{k}} \exp(-H\tau)$ and $0 < \tau < 1/T$ a 'thermodynamic' time. The imidie angular brackets correspond to the quantum as well as a statistical average willi the Cibbs distribution:

$$\langle\langle \ldots \rangle\rangle = \sum_\nu e^{\frac{\Omega - E_\nu}{T}} \langle\nu| \ldots |\nu\rangle \tag{3.80}$$

where Ω is the thermodynamic potential and $|\nu\rangle$ the eigenstates of $H - \mu N$ with the eigenvalues E_ν. Because the thermodynamic time is restricted by $1/T$ the temperature GF is expanded in the Fourier series:

$$g(\mathbf{k},\tau) = T \sum_{\omega_n} e^{-i\omega_n \tau} g\left(\mathbf{k}, \omega_n\right) \tag{3.81}$$

with the discrete Matsubara frequencies $\omega_n = \pi T(2n+1), n = 0, \pm 1, \pm 2, \ldots$. For free electrons one obtains

$$g^{(0)}\left(\mathbf{k}, \omega_n\right) = \frac{1}{i\omega_n - \xi_{\mathbf{k}}} \tag{3.82}$$

and for phonons

$$\tilde{d}^{(0)}\left(\mathbf{q}, \omega_n - \omega_{n'}\right) = -\frac{\tilde{\omega}^2_{\mathbf{q}}}{\left[\omega_n - \omega_{n'}\right]^2 + \tilde{\omega}^2_{\mathbf{q}}}. \tag{3.83}$$

To take into account the Cooper pairing of two electrons with the opposite momentum and spin one can introduce, following Gor'kov (1958) and Nambu (1960) the matrix GF:

$$\hat{g}(\mathbf{k},\tau) = -\begin{pmatrix} \langle\langle T_\tau c_{\mathbf{k},\uparrow}(\tau) c^\dagger_{\mathbf{k},\uparrow} \rangle\rangle & \langle\langle T_\tau c_{\mathbf{k},\uparrow}(\tau) c_{-\mathbf{k},\downarrow} \rangle\rangle \\ \langle\langle T_\tau c^\dagger_{-\mathbf{k},\downarrow}(\tau) c^\dagger_{\mathbf{k},\uparrow} \rangle\rangle & \langle\langle T_\tau c^\dagger_{-\mathbf{k},\downarrow}(\tau) c_{-\mathbf{k},\downarrow} \rangle\rangle \end{pmatrix}. \tag{3.84}$$

The matrix self-energy

$$\hat{\Sigma}\left(\mathbf{k}, \omega_n\right) = \left(\hat{g}^{(0)}\left(\mathbf{k}, \omega_n\right)\right)^{-1} - \hat{g}^{-1}\left(\mathbf{k}, \omega_n\right) \tag{3.85}$$

with $\hat{g}^{(0)}\left(\mathbf{k}, \omega_n\right) = \left(i\omega_n \tau_0 - \xi_{\mathbf{k}} \tau_3\right)^{-1}$. Here $\tau_{0,1,2,3}$ is a set of the Pauli matrices:

$$\tau_0 = \begin{pmatrix} 1 & 0 \\ 0 & 1 \end{pmatrix}; \qquad \tau_1 = \begin{pmatrix} 0 & 1 \\ 1 & 0 \end{pmatrix}; \qquad \tau_2 = \begin{pmatrix} 0 & -i \\ i & 0 \end{pmatrix}; \qquad \tau_3 = \begin{pmatrix} 1 & 0 \\ 0 & -1 \end{pmatrix}$$

The generalized equation for the matrix $\hat{\Sigma}$ is given by the same diagram as in the normal state, Fig.3.5, with only substitution $\tilde{\gamma}(\mathbf{q})\tau_3$ instead of $\tilde{\gamma}(\mathbf{q})$ and summation over Matsubara frequencies instead of integration:

$$\hat{\Sigma}\left(\mathbf{k}, \omega_n\right) = -T \sum_{\omega_{n'}} \int \frac{d\mathbf{q}}{(2\pi)^3} |\tilde{\gamma}(\mathbf{q})|^2 \tilde{\omega}_{\mathbf{q}} \tau_3 \hat{g}\left(\mathbf{k} - \mathbf{q}, \omega_{n'}\right) \tau_3 \tilde{d}\left(\mathbf{q}, \omega_n - \omega_{n'}\right) \tag{3.86}$$

The most important difference of Eq.(3.86) compared with the normal state Eq.(3.59) is the possibility of obtaining a finite value of the off-diagonal matrix elements $\sim < cc >$ within the self-consistent solution, Fig.3.7. In the second $\left(\hat{g} \to \hat{g}^{(0)}\right)$ or in any finite order of the perturbation theory there are no anomalous averages from Eq.(3.86). That means that within the perturbation theory there is no superconducting phase transition. However if one sums

all diagrams of Fig.3.7 which means solving Eq.(3.86) self-consistently, one obtains the finite anomalous averages. To illustrate this we adopt a particular momentum dependence of the interaction constant as in the previous section and an approximate form of the phonon Green's function:

$$\tilde{d}\left(\mathbf{q}, \omega_n - \omega_{n'}\right) \simeq -1 \tag{3.87}$$

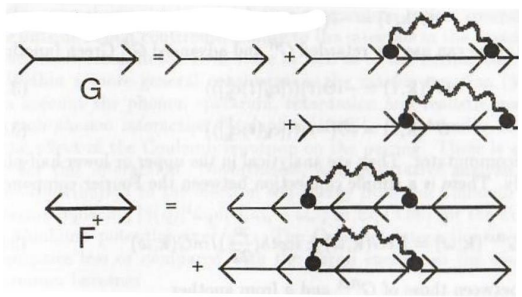

Fig.3.7. Normal G and anomalous F GFs of the BCS superconductor.

If there is no current in the system the phase of the order parameter can be chosen to be zero. In this case $\hat{\Sigma}$ is a sum of three Pauli matrices $\tau_{0,1,3}$ with the coefficients $(1-Z)i\omega_n, \Delta$ and χ respectively, which are the functions of frequency and momentum:

$$\hat{\Sigma}\left(\mathbf{k}, \omega_n\right) = (1-Z)i\omega_n\tau_0 + \Delta\tau_1 + \chi\tau_3. \tag{3.88}$$

Thus

$$\hat{g}^{-1}\left(\mathbf{k}, \omega_n\right) = Zi\omega_n\tau_0 - \Delta\tau_1 - \tilde{\xi}\tau_3 \tag{3.89}$$

and

$$\hat{g}\left(\mathbf{k}, \omega_n\right) = -\frac{Zi\omega_n + \Delta\tau_1 + \tilde{\xi}\tau_3}{Z^2\omega_n^2 + \tilde{\xi}^2 + \Delta^2} \tag{3.90}$$

with $\tilde{\xi} = \xi + \chi$. Substitution of Eq.(3.87,90) into the master equation (3.86) yields

$$(1-Z)i\omega_n = -\lambda T \int d\tilde{\xi} \sum_{\omega_{n'}} \frac{i\omega_{n'}Z}{Z^2\omega_{n'}^2 + \tilde{\xi}^2 + \Delta^2} = 0 \tag{3.91}$$

$$\chi = -\lambda T \int d\tilde{\xi} \sum_{\omega_{n'}} \frac{\tilde{\xi}}{Z^2\omega_{n'}^2 + \tilde{\xi}^2 + \Delta^2} = 0 \tag{3.92}$$

$$\Delta = \lambda T \int d\tilde{\xi} \sum_{\omega_{n'}} \frac{\Delta}{Z^2\omega_{n'}^2 + \tilde{\xi}^2 + \Delta^2} \tag{3.93}$$

It follows from Eq. (3.91, 92) that $Z = 1$ and $\chi = 0$. Applying the formula for tanh to the sum in Eq.(3.93) we obtain the familiar BCS equation for the order parameter

$$1 = \frac{\lambda}{2} \int \frac{d\xi}{\sqrt{\xi^2 + \Delta^2}} \tanh \frac{\sqrt{\xi^2 + \Delta^2}}{2T} \tag{3.94}$$

where the integration is restricted by the region $|\xi| < \omega_D$ because of the approximation, Eq.(3.87) for $\tilde{d}\left(\mathbf{q}, \omega_n - \omega_{n'}\right)$.

There is no direct physical meaning of poles of the temperature GF. To derive the one-particle excitation spectrum one has to calculate the real-time GF determined at finite temperature as

$$G(\mathbf{k},t) = -i\langle\langle T_t c_{\mathbf{k}}(t) c_{\mathbf{k}}^{\dagger}\rangle\rangle, \tag{3.95}$$

with the real time t. One can use the retarded G^R and advanced G^A Green functions:

$$G^R(\mathbf{k},t) = -i\Theta(t)\langle\langle\left[c_{\mathbf{k}}(t)c_{\mathbf{k}}^{\dagger}\right]\rangle\rangle \tag{3.96}$$

$$G^A(\mathbf{k},t) = i\Theta(-t)\langle\langle\left[c_{\mathbf{k}}(t)c_{\mathbf{k}}^{\dagger}\right]\rangle\rangle \tag{3.97}$$

where $[\ldots]$ is an anticommutator. They are analytical in the upper or lower half-plane of ω correspondingly. There is a simple connection between the Fourier components of G and $G^{R,A}$

$$G^{R,A}(\mathbf{k},\omega) = \operatorname{Re} G(\mathbf{k},\omega) \pm i \coth\left(\frac{\omega}{2T}\right) \operatorname{Im} G(\mathbf{k},\omega) \tag{3.98}$$

from one side and between those of $G^{R,A}$ and g from another

$$G^R(\mathbf{k}, i\omega_n) = g(\mathbf{k}, \omega_n) \tag{3.99}$$

for $\omega_n > 0$ and

$$g(\mathbf{k}, -\omega_n) = g^*(\mathbf{k}, \omega_n) \tag{3.100}$$

In our case the temperature GF is

$$g(\mathbf{k},\omega) = \frac{u_{\mathbf{k}}^2}{i\omega_n - \epsilon_{\mathbf{k}}} + \frac{v_{\mathbf{k}}^2}{i\omega_n + \epsilon_{\mathbf{k}}} \tag{3.101}$$

where $u_{\mathbf{k}}^2, v_{\mathbf{k}}^2 = (\epsilon_{\mathbf{k}} \pm \xi_{\mathbf{k}})/2\epsilon_{\mathbf{k}}$ and $\epsilon_{\mathbf{k}} = \sqrt{\xi_{\mathbf{k}}^2 + \Delta^2}$. The analytical continuation of this expression to the upper half-plane yields

$$G^R(\mathbf{k},\omega) = \frac{u_{\mathbf{k}}^2}{\omega - \epsilon_{\mathbf{k}} + i0^+} + \frac{v_{\mathbf{k}}^2}{\omega + \epsilon_{\mathbf{k}} + i0^+} \tag{3.102}$$

and with Eq.(3.98) one obtains

$$G(\mathbf{k},\omega) = \operatorname{Re}\left(\frac{u_{\mathbf{k}}^2}{\omega - \epsilon_{\mathbf{k}}} + \frac{v_{\mathbf{k}}^2}{\omega + \epsilon_{\mathbf{k}}}\right) - i\pi \tanh\left(\frac{\omega}{2T}\right)\left(u_{\mathbf{k}}^2 \delta(\omega - \epsilon_{\mathbf{k}}) + v_{\mathbf{k}}^2 \delta(\omega + \epsilon_{\mathbf{k}})\right) \tag{3.103}$$

At $T = 0, \tanh\left(\frac{\omega}{2T}\right) = \operatorname{sgn}(\omega)$ and

$$G(\mathbf{k},\omega) = \frac{u_{\mathbf{k}}^2}{\omega - \epsilon_{\mathbf{k}} + i0^+} + \frac{v_{\mathbf{k}}^2}{\omega + \epsilon_{\mathbf{k}} - i0^+} \tag{3.104}$$

The poles of GF yield the BCS-quasiparticle energy

$$\epsilon_{\mathbf{k}} = \sqrt{\xi_{\mathbf{k}}^2 + \Delta^2(0)} \tag{3.105}$$

Thus the Migdal-Eliashberg theory reproduces the BCS results if a similar approximation for the attraction between electrons is made. The critical temperature and the BCS gap are adiabatically small ($\sim \omega_D$) compared with the Fermi energy. Therefore, one can worry about the 'crossing' diagrams as in Fig. 3.6, which are neglected with the master equation, Eq.(3.86).

However, the BCS state is essentially the same as the normal one outside the narrow momentum region around the Fermi surface. The outside region contribute mainly to the integrals in the crossing diagrams, which makes them small in the BCS state as well as in the normal one.

Within a more general consideration the master equation (3.86) takes properly into account the phonon spectrum, retardation and realistic matrix element of the electron-phonon interaction (Scalapino (1969)). In particular, it is useful in a study of the effect of the Coulomb repulsion on the pairing. There is no adiabatic parameter for this interaction. Nevertheless, in a qualitative analysis one can adopt the same contribution to the electron self-energy from the Coulomb interaction as from phonons replacing $|\tilde{\gamma}(\mathbf{q})|^2\tilde{\omega}_{\mathbf{q}}\tilde{d}\left(\mathbf{q},\omega_n-\omega_{n'}\right)$ in Eq.(3.86) for the Fourier component of the Coulomb potential $4\pi e^2/q^2\epsilon$. The Coulomb interaction is non-retarded for the frequencies less or compared with the Fermi energy, so the equation for the order parameter becomes

$$\Delta\left(\omega_n\right)=T\int d\xi\sum_{\omega_{n'}}K\left(\omega_n-\omega_{n'}\right)\frac{\Delta\left(\omega_{n'}\right)}{\omega_{n'}^2+\xi^2+\Delta^2\left(\omega_{n'}\right)} \tag{3.106}$$

where the kernel K is given by

$$K\left(\omega_n-\omega_{n'}\right)=\lambda\Theta\left(\omega_D-|\omega_n-\omega_{n'}|\right)-\mu_c\Theta\left(\mu-|\omega_n-\omega_{n'}|\right) \tag{3.107}$$

with μ_c the product of the Fourier component of the Coulomb potential and the normal density of states at the Fermi level. At $T=T_c$ one can neglect the second power of the order parameter in Eq.(3.106) and integrating over ξ obtain

$$\Delta\left(\omega_n\right)=\pi T_c\sum_{\omega_{n'}}K\left(\omega_n-\omega_{n'}\right)\frac{\Delta\left(\omega_{n'}\right)}{|\omega_{n'}|} \tag{3.108}$$

To solve this equation we adopt the BCS-like parametrization of the kernel

$$\begin{aligned}K\left(\omega_n-\omega_{n'}\right)\simeq\lambda\Theta\left(2\omega_D-|\omega_n|\right)\Theta\left(2\omega_D-|\omega_{n'}|\right)\\ -\mu_c\Theta\left(2\mu-|\omega_n|\right)\Theta\left(2\mu-|\omega_{n'}|\right)\end{aligned} \tag{3.109}$$

and replace the summation by the integration

$$\pi T_c\sum\rightarrow\int_{\pi T_c}^{\infty}d\omega \tag{3.110}$$

lecause $T_c\ll\omega_D,\mu$. The solution can be found in the form

$$\Delta(\omega)=\Delta_1\Theta\left(2\omega_D-|\omega|\right)+\Delta_2\Theta(2\mu-|\omega|)\Theta\left(|\omega|-2\omega_D\right) \tag{3.111}$$

with constant but different values of the order parameter below (Δ_1) and above (Δ_2) the cul-off energy $2\omega_D$. Substitution of Eq.(3.109,111) into Eq.(3.108) yields for $\Delta_{1,2}$.

$$\Delta_1\left[1-(\lambda-\mu_c)\ln\frac{2\omega_D}{\pi T_c}\right]+\Delta_2\mu_c\ln\frac{\mu}{\omega_D}=0 \tag{3.112}$$

$$\Delta_1\mu_c\ln\frac{2\omega_D}{\pi T_c}+\Delta_2\left[1+\mu_c\ln\frac{\mu}{\omega_D}\right]=0 \tag{3.113}$$

The condition of the existence of a nontrivial solution of these coupled equations gives for T_c

$$T_c = \frac{2\omega_D}{\pi} \exp\left(-\frac{1}{\lambda - \mu_c^*}\right) \tag{3.114}$$

where

$$\mu_c^* = \frac{\mu_c}{1 + \mu_c \ln(\mu/\omega_D)} \tag{3.115}$$

is the Coulomb pseudopotential (Tolmachev (1958), Morel and Anderson (1962)). This is a remarkable result. It shows that even a large Coulomb repulsion $\mu_c > \lambda$ does not destroy Cooper pairs because its contribution is suppressed down to the value $\sim 1/\ln\frac{\mu}{\omega_D} \ll 1$. The retarded attraction mediated by phonons acts well after two electrons meet each other. This time delay is sufficient for two electrons to be separated by the relative distance, at which the Coulomb repulsion is small.

In the normal state the Coulomb correlations lead to a damping of excitations of order ξ^2/μ, which is relevant only in a narrow region around the Fermi surface of order $\omega_D\sqrt{m_e/M}$. Outside this region the damping due to the Fröhlich interaction dominates.

For metals and their alloys the empirical McMillan (1968) formula for T_c is adopted:

$$T_c = \frac{\omega_D}{1.45} \exp\left(-\frac{1.04(1+\lambda)}{\lambda - \mu_c^*(1+0.62\lambda)}\right) \tag{3.116}$$

which works well for low- T_c materials even if the estimated λ is large (> 1) as in Pb. However, already in materials with a moderate $T_c \sim 20K$ as in $A{-}15$ compounds (Nb_3Sn, V_3Si) the discrepancy between the values of λ estimated with Eq.(3.116) and the direct band-structure calculations exceeds by several times the limit allowed by the experimental and computation accuracy (Klein et al. (1978)) and therefore the credibility of the canonical BCS approach to these materials is low.

The Migdal-Eliashberg theory is based on the assumption that the Fermi liquid is stable and the adiabatic condition $\mu \gg \omega_D$ is satisfied. In original papers Migdal (1958) and Eliashberg (1960) restricted the region of the applicability of their approach by the value of the coupling $\lambda < 1$. We show in this book that the proper extension of the BCS theory to the strong coupling region $\lambda > 1$ inevitably involves small polaron formation.

6.4.5 3.5 Bloch states in semiconductors: Effective mass approximation

(this may be important since we always consider semiconductors)

Theory

(We still consider the model

$$H_0 = \sum_{\mathbf{k},n,s} \xi_{\mathbf{k},n,s} c^\dagger_{\mathbf{k},n,s} c_{\mathbf{k},n,s} + \sum_{\mathbf{q},\nu} \omega_{\mathbf{q},\nu} \left(d^\dagger_{\mathbf{q},\nu} d_{\mathbf{q},\nu} + 1/2\right) \tag{3.20}$$

$$H_{e-ph} = \frac{1}{\sqrt{2N}} \sum_{\mathbf{k},\mathbf{q},n,n',\nu,s} \gamma_{n,n'}(\mathbf{q},\mathbf{k},\nu)\omega_{\mathbf{q},\nu} c^\dagger_{\mathbf{k},n,s} c_{\mathbf{k}-\mathbf{q},n',s} d_{\mathbf{q},\nu} + h.c. \tag{3.21}$$

$$H_{e-e} = \frac{1}{2}\sum_{\mathbf{q}} V_c(\mathbf{q}) \rho^\dagger_{\mathbf{q}} \rho_{\mathbf{q}} \qquad \rho^\dagger_{\mathbf{q}} = \sum_{\mathbf{k},s} c^\dagger_{\mathbf{k},s} c_{\mathbf{k}+\mathbf{q},s} \tag{3.24, 3.25}$$

)

Electron wave functions in semiconductors and narrow band metals differ significantly from plane waves, Eq.(3.26) ($\phi_{\mathbf{k},n,s} \simeq e^{i\mathbf{k}\cdot\mathbf{r}}$). (why??? in terms of formulas, I don't see that they should be different)

Therefore, in general the band structure has to be calculated numerically (because all theory below is not applicable)(why exactly?).

However, in doped semiconductors states in the vicinity of special points of the Brillouin zone matter only at low temperatures and doping. These are points where the energy dispersion $E_{\mathbf{k},n,s}$ of the conduction band has its minimum and the valence band energy has its maximum.

While their positions and band edges are determined experimentally or with the numerical LDA calculations (what is it??), the energy dispersion nearby can be determined analytically with '$\mathbf{k}\cdot\mathbf{p}$' perturbation theory. (what is it??)

To show this we consider a simple cubic lattice having a nondegenerate band of s or d-like symmetry at $\mathbf{k} = 0(\Gamma)$ point lying above by an energy E_g three p-like bands degenerate at $\mathbf{k} = 0$ and transforming at this point like x, y and z under the rotation of the crystal space group. There is no spin-orbit interaction in this example, so spin is irrelevant. The Bloch theorem states that

$$\phi_{\mathbf{k},n}(\mathbf{r}) = e^{i\mathbf{k}\cdot\mathbf{r}} u_{\mathbf{k},n}(\mathbf{r}) \tag{3.117}$$

where $u_{\mathbf{k},n}(\mathbf{r})$ is periodic in $\mathbf{r}$ (do not confuse it with the one that is introduced further $u_i(\mathbf{q})$) and satisfies to

$$\left(-\frac{1}{2m_e}\left(\nabla^2 + 2i\mathbf{k}\cdot\nabla\right) + V(\mathbf{r})\right) u_{\mathbf{k},n}(\mathbf{r}) = \left(E_{\mathbf{k},n} - \frac{k^2}{2m_e}\right) u_{\mathbf{k},n}(\mathbf{r}) \tag{3.118}$$

(how to get this equation??)

At the point $\mathbf{k} = 0$ this equation for $u_{0,n}(\mathbf{r})$ is

$$\left(-\frac{1}{2m_e}\nabla^2 + V(\mathbf{r})\right) u_{0,n}(\mathbf{r}) = E_{0,n} u_{0,n}(\mathbf{r}) \tag{3.119}$$

Thus $u_{0,n}$ has the symmetry of the crystal space group. For small $\mathbf{k}$ one can expand $u_{\mathbf{k},n}$ in series

$$u_{\mathbf{k},n}(\mathbf{r}) = \sum_{n'=s,x,y,z} a_{\mathbf{k},n'} u_{0,n'}(\mathbf{r}) \tag{3.120}$$

to obtain the secular equation

$$\det \begin{vmatrix} E_g + \frac{k^2}{2m_e} - E_{\mathbf{k}} & \frac{k_x p}{m_e} & \frac{k_y p}{m_e} & \frac{k_z p}{m_e} \\ \frac{k_x p}{m_e} & \frac{k^2}{2m_e} - E_{\mathbf{k}} & 0 & 0 \\ \frac{k_y p}{m_e} & 0 & \frac{k^2}{2m_e} - E_{\mathbf{k}} & 0 \\ \frac{k_z p}{m_e} & 0 & 0 & \frac{k^2}{2m_e} - E_{\mathbf{k}} \end{vmatrix} = 0 \tag{3.121}$$

with by symmetry $p \equiv \langle s| - i\nabla_x|x\rangle = \langle s| - i\nabla_y|y\rangle = \langle s| - i\nabla_z|z\rangle$. Different bra and ket correspond to the four different Γ-point Bloch functions $u_{0,n}(\mathbf{r})$. There are four solutions. Two of them correspond to conduction (c) and light hole (lh) valence bands

$$E_{\mathbf{k},c,lh} = \frac{k^2}{2m_e} + \frac{E_g}{2} \pm \sqrt{\frac{E_g^2}{4} + \frac{k^2 p^2}{m_e^2}} \tag{3.122}$$

and the other two, which are degenerate, correspond to heavy holes (hh)

$$E_{\mathbf{k},hh} = \frac{k^2}{2m_e} \tag{3.123}$$

One can split two degenerate heavy hole bands and change the sign of their effective mass if one includes states at Γ point split off from those under consideration by an mergy large in comparison with E_g, as shown with a thin line in Fig.3.8. The effective approximation follows from Eq.(3.122) for small $k \ll m_e E_g/p$

$$E_{\mathbf{k},c} - E_g \simeq \frac{k^2}{2m_c} \tag{3.124}$$

and

$$E_{\mathbf{k},lh} \simeq -\frac{k^2}{2m_{lh}} \tag{3.125}$$

with the effective mass

$$\frac{m_{c,lh}}{m_e} = \frac{1}{\frac{p^2}{m_e E_g} \pm 1} \tag{3.126}$$

In many semiconductors the interband dipole moment is large and the band gap is small so $p^2 \gg m_e E_g$. Therefore the band electron and hole masses can be significantly smaller than the bare mass,

$$\frac{m_c}{m_e} \simeq \frac{m_{lh}}{m_e} \ll 1. \tag{3.127}$$

As a result when experiment does not show very heavy carriers it does not necessary follow that the electron-lattice coupling is small, and the polaronic renormalisation of the band mass is absent.

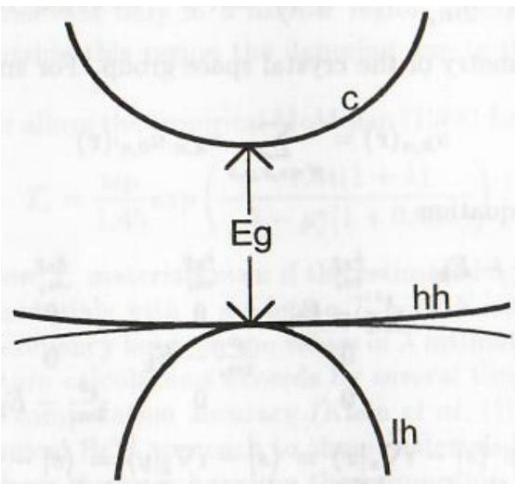

Fig.3.8. $\mathbf{k} \cdot \mathbf{p}$ energy band dispersion near the Γ point in a cubic lattice.

The effective mass approximation, Eq.(3.124,125) as well as $\mathbf{k} \cdot \mathbf{p}$ perturbation theory discussed above can be applied if the external field varies slowly in time and smoothly in space and the electron-phonon and electron-electron interactions are relatively weak, as in the case of large polarons, Chapter 1. If the external or internal fields are strong and contain high frequency and (or) short wave Fourier components they involve large momenta of order of the reciprocical

lattice constant making all states of the electron band to be relevant to the problem. In this case a tight-binding approach is more appropriate.

6.4.6 3.6 Tight-binding approximation

(at which point we approximate and at which we fit???)

Theory

(We continue to working out our obtained model of electron-phonon interactions:

$$H_0 = \sum_{\mathbf{k},n,s} \xi_{\mathbf{k},n,s} c^\dagger_{\mathbf{k},n,s} c_{\mathbf{k},n,s} + \sum_{\mathbf{q},\nu} \omega_{\mathbf{q},\nu} \left(d^\dagger_{\mathbf{q},\nu} d_{\mathbf{q},\nu} + 1/2 \right) \tag{3.20}$$

$$H_{e-ph} = \frac{1}{\sqrt{2N}} \sum_{\mathbf{k},\mathbf{q},n,n',\nu,s} \gamma_{n,n'}(\mathbf{q},\mathbf{k},\nu) \omega_{\mathbf{q},\nu} c^\dagger_{\mathbf{k},n,s} c_{\mathbf{k}-\mathbf{q},n',s} d_{\mathbf{q},\nu} + h.c. \tag{3.21}$$

$$H_{e-e} = \frac{1}{2} \sum_{\mathbf{q}} V_c(\mathbf{q}) \rho^\dagger_{\mathbf{q}} \rho_{\mathbf{q}} \qquad \rho^\dagger_{\mathbf{q}} = \sum_{\mathbf{k},s} c^\dagger_{\mathbf{k},s} c_{\mathbf{k}+\mathbf{q},s} \tag{3.24, 3.25}$$

) (what exactly TB method can give that is impossible to obtain without it????)

For narrow band semiconductors and metals (what are they??) it is convenient to replace the Bloch states for the Wannier states with the canonical linear transformation of electron operators

$$c_i = \frac{1}{\sqrt{N}} \sum_{\mathbf{k}} e^{i\mathbf{k}\cdot\mathbf{m}} c_{\mathbf{k},s}, \tag{3.128}$$

where $i = (\mathbf{m}, n, s)$ includes both site $\mathbf{m}$ (what is this origin of this transformation? it is the answer on the question "why are Wannier functions really useful") ($\mathbf{m}$ connects the origin of the coordinate system with one molecule in the primitive cell in a lattice), band n (it is not that n which is the number of electrons, it is an index. It is very important to note that always by i it will be further meant this multiindex) (where do bands originate from in the derivation before???) and spin s quantum numbers. (Of course, i in the exponent is the imaginary i and not an index.) (where is the index i at the r.h.s.) The Wannier wave function, corresponding to the one-particle state $\{i\}$ is given by the linear combination of the Bloch states

$$w_i(\mathbf{r}) = \frac{1}{\sqrt{N}} \sum_{\mathbf{k}} e^{-i\mathbf{k}\cdot\mathbf{m}} \phi_{\mathbf{k},n,s}(\mathbf{r}). \tag{3.129}$$

(write, how ϕ was connected to c operators???) (why do we have here minus in the exp? should it be obvious?)

In the new representation the periodic Hamiltonian H_e is written as

$$H_e = \sum_{i,j} \left(T(\mathbf{m}-\mathbf{n}) \delta_{s,s'} \delta_{n,n'} - \mu \delta_{i,j} \right) c^\dagger_i c_j \tag{3.130}$$

(where the $\delta_{s,s'}$ come from?)

(how to understand it??? which $\mathbf{m}-\mathbf{n}$ we need to plug in $T(\mathbf{m}-\mathbf{n})$?)

with the bare hopping integral

$$T(\mathbf{m}) = \frac{1}{N} \sum_{\mathbf{k}} E_{\mathbf{k},n} e^{i\mathbf{k}\cdot\mathbf{m}} \tag{3.131}$$

$i = (\mathbf{m}, n, s)$ and $j = (\mathbf{n}, n', s')$ (this is a very used further definition. In general, one can think that this T is just some number and anyway obtain this number from fitting some experiments). (check!!!) (big E appears at the stage of approximation, but where exactly??)

(In general, we see that we have many similar models, since we have a degeneracy in spin and bands. But they are very similar. So, basically, we sum over all cites on a primitive cell and this is our simple Hamiltonian, but it is hard to evaluate coefficients there)

(give an example of calculation of this T element!!)

The idea behind the tight-binding approximation is to fit calculated numerically bands by using a finite number of the hopping integrals (why? I thought, we are simplifying the model?) (of course, if we now forget about many micro parameters and look only on some effective parameters, we can fit them from experiment.)(which exactly we need to fit???).

Many electronic structures, in particular perovskite ones can be fitted with only nearest-neighbor matrix elements between s, p and d-like orbitals (Harrison (1989)). (check that it is true in that paper. do we here use only s orbital? if so, why?)

The second-neighbor matrix elements are somewhat problematic. Their estimate from the nearest-neighbor formulae by scaling with the inter-site distance turns out to be inappropriate. (why??? some people use such models... anyway, nothing is explained here)

Therefore one will not have occasion to use again the second-neighbor hopping integrals fitting well one particular band structure. (not explained, why?)

The hopping integrals could not be calculated by using tabulated atomic wave functions and potentials (which potentials and how exactly? aren't we told that they CAN be calculated?) estimated for the various solids. True atomic orbitals are not orthogonal (why? it is strange) for different sites and they do not provide a quantitative description of bands in solids.

On the other hand atomiclike Wannier orbitals, Eq.(3.129) can provide a very good description already in the tight-binding (nearest-neighbor) approximation. (what is exactly the advantage of Wannier functions?)

For a nondegenerate band in a cubic lattice this approximation yields (derive??? but it is very not clear, T is defined)

$$E_{\mathbf{k}} = \sum_{|\mathbf{m}|=a} T(\mathbf{m}) e^{-i\mathbf{k}\cdot\mathbf{m}} = 2T(a)\left[\cos(k_x a) + \cos(k_y a) + \cos(k_z a)\right] \tag{3.132}$$

if the middle of the band is taken to be zero, $T(0) = 0$. (derive this formula!! maybe it is easy)

If the nearest-neighbor matrix element is negative, the bottom of the band lies at $\mathbf{k} = 0$, where the dispersion is parabolic with the band mass (why??)

$$m = \frac{1}{2a^2|T(a)|} \tag{3.133}$$

The half bandwidth is $D = z|T(a)|$ (because this is the range of all possible E_k), where the nearest-neighbor number $z = 6$ in this example. (where z appears in the game?)

The electron-phonon interaction as well as the Coulomb correlation energy have a simple form in the Wannier representation if the corresponding matrix elements depend on the momentum transfer only, Eq.(3.23)

$$H_{e-ph} = \sum_{\mathbf{q},i} \omega_{\mathbf{q}} \hat{n}_i \left(u_i(\mathbf{q}) d_{\mathbf{q}} + h.c.\right) \tag{3.134}$$

$$H_{e-e} = \frac{1}{2} \sum_{i,j} V_c(\mathbf{m} - \mathbf{n}) \hat{n}_i \hat{n}_j \tag{3.135}$$

with the matrix element of the electron-phonon interaction

$$u_i(\mathbf{q}) = \frac{1}{\sqrt{2N}}\gamma(\mathbf{q})e^{i\mathbf{q}\cdot\mathbf{m}} \qquad i := (\mathbf{m}, n, s) \tag{3.136}$$

and the Coulomb interaction

$$V_c(\mathbf{m}) = \frac{1}{N}\sum_{\mathbf{q}} V_c(\mathbf{q})e^{i\mathbf{q}\cdot\mathbf{m}} \tag{3.137}$$

Here $\hat{n}_i = c_i^\dagger c_i$ is the density operator (reminder: we had $H_{e-e} = \frac{1}{2}\sum_{\mathbf{q}} V_c(\mathbf{q})\rho_{\mathbf{q}}^\dagger\rho_{\mathbf{q}}$ and $V_c(q) = 4\pi e^2/q^2$, for some models.).

It follows from Eq.(3.134,135) that taking the interaction matrix elements depending only on the momentum transfer one neglects (why????) the terms of the electron-phonon and Coulomb interactions, containing the overlap of different site orbitals, which is a good approximation for narrow bands (why????), whose bandwidth $2D$ is less than the characteristic value of the crystal field.

As a result the Hamiltonian appropriate for semiconductors and narrow band metals is given by

$$\begin{aligned} H = \sum_{i,j}\left(T(\mathbf{m}-\mathbf{n})\delta_{s,s'} - \mu\delta_{i,j}\right)c_i^\dagger c_j + \sum_{\mathbf{q},i}\omega_{\mathbf{q}}\hat{n}_i\left(u_i(\mathbf{q})d_{\mathbf{q}} + h.c.\right) \\ + \frac{1}{2}\sum_{i,j}V_c(\mathbf{m}-\mathbf{n})\hat{n}_i\hat{n}_j + \sum_{\mathbf{q}}\omega_{\mathbf{q}}\left(d_{\mathbf{q}}^\dagger d_{\mathbf{q}} + 1/2\right) \end{aligned} \tag{3.138}$$

(We have just collected the terms above.)

For narrow band metals this Hamiltonian can be treated at best as the bare one, in which all matrix elements and phonon frequencies have no direct physical meaning.

Phonons and the interaction matrix elements should be determined using a self-consistent LDA approach as described above. Fortunately, in doped semiconductors one can separate 'carriers' from 'inner' electrons. In this case parent dielectric compounds exist with well defined bare phonons $\omega_{\mathbf{q}}$ and the electronic band structure $E_{\mathbf{k}}$.

The effect of carriers on the crystal field and on the dynamical matrix is negligible while the carrier density is much below the atomic one.

Therefore one can use the band structure and the crystal field of a parent insulator to calculate the parameters of the Hamiltonian, Eq.(3.138). (how???)

Depending on the particular phonon mode the interaction constant $\gamma(\mathbf{q})$ has different $q-$ dependence. For example, as discussed above

$$\begin{aligned} \gamma(\mathbf{q}) &\sim \frac{1}{q}, \\ &\sim \text{ constant }, \\ &\sim \frac{1}{\sqrt{q}} \end{aligned} \tag{3.139}$$

for optical, molecular ($\omega_{\mathbf{q}} \sim$ constant) and acoustic ($\omega_{\mathbf{q}} \sim q$) phonons, respectively in the long wave limit.

Example: values of coefficients of tight-binding model from other parameters of a model

(?????????? how to obtain them???)

6.5 4 The multi-polaron problem

6.5.1 4.1 Small-polaron instability within the Migdal approach

(In Migdal's approach, there are problems, if $\lambda > 1$, since one contribution to self-energy blows up. This is because we can include change of self-energy to change of chemical potential and test stability by it. So, this theory predicts that system will fill istelf with a lot of particles, right?)

(it is a good idea to derive it fully, a very nontrivial statement)

(by the way, here, nothing is said about "Small-polaron", it is just about instability. Maybe we mean that we assume that only small polarons can be at all. But weak-coupled (large) polarons were also observed, so what about them??? read these articles with observations)

Theory

In doped semiconductors the carriers become small polarons or bipolarons at the intermediate value of the coupling constant $\lambda \geq 0.5$, Chapter 2. (why??? and also, where exactly λ originates from and where is located in formulas?)

However, within the adiabatic (why is it adiabatic?) Migdal description of electrons and phonons coupled by the linear electron-phonon interaction there is no instability at any value of λ if the bare ionic plasmon mode is replaced by the acoustic phonon mode as described in Chapter 3. (how is it in terms of formulas?)

The corrections to the normal state spectrum (of conducting electrons, which is determined by their free propagation, without phonons) due to the coupling are adiabatically small ($\sim \omega_D/E_F$) (and how exactly do they look?). In particular, the critical temperature of the BCS superconductor is adiabatically small, $T_c/E_F < \omega_D/E_F \ll 1$ for all relevant values of λ. (So, one can view superconductivity as a correction to the normal spectrum.) (by the way, is something known about SC with not $\cos^2$ spectrum?)

The self-consistent Migdal-Eliashberg (do we mean some Eliashberg equations by it? If so, then what are they?) approach does not allow for the possibility to study the small-(bi)polaron formation in the intermediate and strong-coupling regime because of the following reason. The basic assumption of the canonical theory (of Migdal-Eliashberg theory, right?) that GF is translationally invariant, thus $G(\mathbf{r}, \mathbf{r}', t) = G(\mathbf{r} - \mathbf{r}', t)$. This assumption excludes the possibility of the local violation of the translational symmetry due to the lattice deformation followed by the self-trapping (this is very unclear. I thought, GF for phonons is just added and we don't need that GF of electrons was translationally invariant. Why to we need a violation of translational symmetry of GF to have a polaron? Maybe see Levitov Shitov to answer it...). To enable the electron to relax into the lowest polaron state, one can introduce an infinitesimal translationally noninvariant potenlial, which should be set equal zero only in the final solution for GF (Alexandrov and Mazur (1989)). (at which point such setting to zero produces something that is not producible without it?) (see next section where Alexandrov and Mazur (1989) is written to understand something here)

As in the case of the off-diagonal superconducting order parameter a small potential, violating a translational symmetry (why order parameter violates tr. symmetry?) drives the system into a new ground state at sufficiently large λ (why not at low λ).

Setting it equal to zero in the solution to the equation of motion restore the translational symmetry but in a new polaronic band rather than in the electron one, which turns out to be an excited state. (this is a repetition of a sentence above)

In the Holstein model (which materials does it describe?), in which electrons interact with the local (molecular) phonons (how to distinguish a local (molecular) phonons and typical

phonons?) one can notice the polaronic instability of the Fermi liquid at $\lambda \sim 1$ already within Migdal's diagrams for the electron self-energy (and how to see it?).

The electron self-energy Σ in the Migdal approximation contains two contributions, Σ_M, Fig.3.3a and Σ_μ, Fig.3.3b.

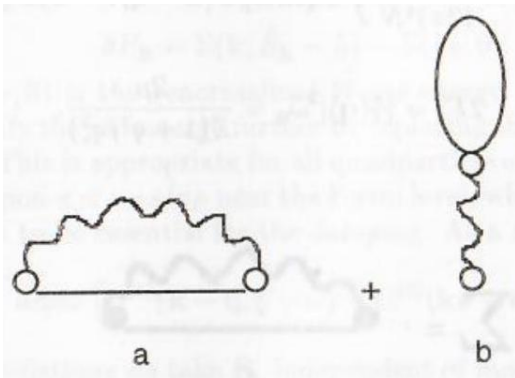

Fig.3.3. Second-order electron self-energy.

$\Sigma_M \simeq \lambda\omega$ (how to see it?) (ω is a frequency of electron, right?), therefore it remains adiabatically small compared with the bandwidth $2D \simeq N(0)^{-1}$ (why the bandwidth is such?) in the relevant region of the coupling ($\lambda < D/\omega$), which guarantees the self-consistency of the approach. (how smallness of self-energy is connected to self-consistency approach?)

On the other hand for the optical or molecular phonons $\Sigma_\mu \simeq D\lambda n$ (how to see it?) is not small and it turns out to be comparable or larger than the Fermi energy already at $\lambda \sim 1$ for any filling of the band (n is the electron density per cell). (why? maybe it is easy to check it, if I understood wha is going on...)

As a rule this diagram, which is momentum and frequency independent, is included in the definition of the chemical potential μ. (why?? how to include a diagram into chem pot?)

While this is justified for a weak-coupling regime, Σ_μ leads to an instability for a strong coupling (which is explained below). To show this let us consider a one-dimensional chain in the tight-binding approximation with the nearest-neighbor hopping integral $D/2$. The renormalised chemical potential is given by (why??)

$$\mu = D \sin\left(\frac{\pi(n-1)}{2}\right) - 2D\lambda n \tag{4.1}$$

(maybe in the article of Alexandrov it is derived somehow? how to derive the first part of this equation?) (note, that the shift is $-2D\lambda n$.)

(important question: why at all we are renormalizing chemical potential? never saw that it was done)

The system is stable if $d\mu/dn$ is positive (this should follow from the sense of chemical potential, but still, I can't derive it immediately, so for me it is not clear, why it is so? was this criterion used somewhere else?), which yields the following region for the stability of the Migdal solution:

$$\lambda < \frac{\pi}{2} \cos\left(\frac{\pi(n-1)}{2}\right) \tag{4.2}$$

(how to determine n, which is the density of conducting electrons? are we still thinking about 3D typical electron-phonon model?) (It means that if we teke away electrons from the system, at some point polarons will start to form, right? Instability means the polaron formation, right?)

For two and three-dimensional lattices the numerical coefficient is different, but the critical value of λ remains of the order of unity. (how to verify this statement?)

In doped semiconductors and metals (reminder that all above was for Holstein model) optical phonons are screened and the diagram Σ_μ with the phonon momentum $\mathbf{q} \equiv 0$ vanishes as for the acoustical phonons. (how to verify this statement?)

In that case one has to violate the translational symmetry to observe the instability of the bare band (and how would this observation look like?).

Because the polaron level shift E_p is independent of the ion mass, the polaronic instability is essentially an adiabatic effect (which increase of the parameter λ, right?).

Therefore, to see how the same self-energy diagram Σ_μ leads to the polaronic collapse independent of the type of phonons we consider the extreme adiabatic limit (limit of which parameter goes to what?) of the classical deformation field $\phi(\mathbf{r})$ coupled with electrons,

$$H = H_e + \int d\mathbf{r}d\mathbf{r}' \left[g\left(\mathbf{r}-\mathbf{r}'\right)\phi\left(\mathbf{r}'\right)\left\{\psi^\dagger(\mathbf{r})\psi(\mathbf{r}) - n^0(\mathbf{r})\right\} + \text{ h.c. }\right] + s^2|\nabla\phi(\mathbf{r})|^2 \tag{4.3}$$

(how to derive it?)

Here s is the sound velocity (how to find it from original model from ch. 3?), $g(\mathbf{r})$ is the coupling constant with the Fourier component $g_\mathbf{q} = \omega_\mathbf{q}^{3/2}\gamma(\mathbf{q})/\sqrt{2N}$,(what is N?,) $n^0(\mathbf{r})$ is the periodic density of carriers respecting the translational symmetry, as defined by Eq.(3.9), and $\omega_\mathrm{q} = sq$. Minimising Eq.(4.3) with respect to the classical field $\phi^*(\mathbf{r})$ we obtain

$$s^2\nabla^2\phi(\mathbf{r}) = \int d\mathbf{r}' g^*\left(\mathbf{r}-\mathbf{r}'\right)\left\{n\left(\mathbf{r}'\right) - n^0\left(\mathbf{r}'\right)\right\} \tag{4.4}$$

(to check it later, it is just mathematical transformation) (here, g^* is because γ can be complex???)

The solution is

$$\phi(\mathbf{r}) = -\sum_\mathbf{q} \frac{g_\mathbf{q}^*}{s^2q^2} e^{i\mathbf{q}\cdot\mathbf{r}}\left\{n_\mathbf{q} - n_\mathbf{q}^0\right\} \tag{4.5}$$

(to check it later, it is just mathematical transformation)

where $n_\mathbf{q}$ is the Fourier component of the electron density $n(\mathbf{r}) \equiv \left\langle\psi^\dagger(\mathbf{r})\psi(\mathbf{r})\right\rangle$. Substituting Eq.(4.5) into the Hamiltonian Eq.(4.3) we find that the adiabatic lattice deformation leads to the lowering of the electron energy by the value

$$\delta\mu(\mathbf{r}) = -2\sum_\mathbf{q} \frac{|g_\mathbf{q}|^2}{\omega_\mathbf{q}^2} e^{i\mathbf{q}\cdot\mathbf{r}}\left\{n_\mathbf{q} - n_\mathbf{q}^0\right\} \tag{4.6}$$

(why is it $\delta\mu$, like a chem. pot?) (to check it later, it is just mathematical transformation)

If the electron density is periodic, $n_\mathbf{q} = n_\mathbf{q}^0$ the shift of the energy is zero. Otherwise, it is not.

For example, one can consider a random statistically uncorrelated distribution with the ansamble average $\langle n_\mathbf{q} n_{\mathbf{q}'}\rangle = Nn^2\delta_{\mathbf{q},-\mathbf{q}'}$.

In that example the chemical potential is shifted by the value

$$\langle|\delta\mu|\rangle = n\left[\frac{1}{N}\sum_\mathbf{q}|\gamma(\mathbf{q})|^4\omega_\mathbf{q}^2\right]^{1/2} \simeq 2n\lambda D, \tag{4.7}$$

(derive it! why γ^4? how the last approx. is done???)

which is the same as in Eq.(4.1). However, now $\lambda D \equiv E_p = (1/2N)\sum_{\mathbf{q}} |\gamma(\mathbf{q})|^2 \omega_{\mathbf{q}}$ (I have no idea how this transformation is done?) depends on the phonon spectrum, integrated over all Brillouin zone rather than on zero momentum phonons.

Breaking of the translational symmetry lowers the energy by the value $2E_p$ (I thought that it is E_p, no?) per particle.

The corresponding increase of the deformation energy is E_p. Therefore, the system prefers to relax into the selftrapped state if $E_p > D$.

The vertex corrections neglected within the Migdal approach are not so crucial if the adiabatic parameter ω/D is small and $\lambda < D/\omega$ (as usual in electrons and phonons).

This consideration shows that the extension of the Migdal approximation to the strong-coupling region $\lambda > 1$ is unacceptable.

In the following we show that depending on the value of the Coulomb repulsion a many electron system strongly coupled with any bosonic field is a polaronic Fermi liquid or a bipolaronic Bose liquid (and to understand their properties, one needs to read other chapters of Alexandrov's and Mott's book.) (They say that it is impossible that there are no polarons, but for which cases?? is it so for all materials?)

6.5.2 Electron-phonon system with strong coupling and violation of the Migdal-Éliashberg theory by Aleksandrov, Mazur, 1988

Zh. Eksp. Teor. Fiz. 96, 1773-1782 (November 1989)

Abstract

It is shown that the traditional theory of electron-phonon interaction is not correct in the case of strong electron-phonon coupling ($\lambda \gtrsim 1$). The ground state described by that theory is unstable to infinitesimal perturbations that violate the translational invariance of the crystal.

INTRODUCTION

Modern theory of strong-coupling superconductors is based in the Éliashberg equations, [1] which are obtained by a natural generalization of the theory of electron-phonon interaction in a normal [2] metal (see, e.g., Ref. 3, pp. 390 and 236 of the Russian original). It is customarily assumed that these equations are valid in the presence of a small adiabatic parameter

$$\omega/D \ll 1, \tag{1}$$

where ω and D are respectively the characteristic phonon frequency and the characteristic kinetic energy of the electrons. (In metals as well as in intermetallic compounds, including high-temperature metal-oxide superconductors, the electron bands have a half-width $D \sim 1$eV and this ensures smallness of the adiabatic parameter (1).)

On the other hand, as noted in Refs. 4-7, the traditional theory of electron-phonon interaction in metals takes no account of the lattice local instability that leads to known polaron effect, viz., electron self-trapping and polaron narrowing of the electron band. A consistent analysis of the multipolaron problem, based on the known methods of the small-radius-polaron (SRP) theory, [8] leads to a picture that differs qualitatively from the classical (BCS) picture of either the normal or the superconducting state of electrons that interact strongly with phonons. [7] This last circumstance is particularly vital for the interpretation of the properties of the new metal-oxide high-temperature superconductors. [9,10] The polaron effect comes into play in the

case of strong elec-tron-phonon interaction, when the depth E_p of the polaron well (the polaron shift of the atomic level) [8] exceeds the halfwidth D of the electron band:

$$E_p/D \geqslant 1. \tag{2}$$

For the usual Fröhlich electron-phonon interaction, the ratio E_p/D coincides with the known electron-phonon coupling constant Λ.[7] The traditional superconductivity theory turns out therefore to be incorrect already for

$$\lambda \gtrsim 1, \tag{3}$$

notwithstanding the adiabaticity of the initial renormalized electron band (1).

Polaron effects in a many-electron system have been heretofore [4−7] considered by using the formalism of singleparticle SRP theory, [8] which takes correct account of both local violation of translational invariance (discreteness of the lattice) and the phonon corrections to the vertex part.

Of undisputed interest is a formulation, for metals and superconductors, of a consistent electron-phonon strong interaction theory that takes the polaron effect into account, using the Green's function (GF) formalism that is universally accepted in traditional superconductivity theory. [1−3]

We formulate in the present paper, for the electron and phonon GF of a normal metal with a Fröhlich electronphonon interaction, equations that make it possible to take the polaron effect into account. We show that from among the three basic assumptions of the classical theory, [1−3], viz.: 1) initial translational invariance of the Green's function

$$G\left(\mathbf{x}, \mathbf{x}', \tau\right) \equiv G\left(\mathbf{x} - \mathbf{x}', \tau\right); \tag{4}$$

2. neglect of phonon corrections to the vertex part, and 3) neglect of the finite width of the electron band, as manifested by the assumption that the single-particle density of the electron states is constant:

$$N(\varepsilon) \approx N(0) \tag{5}$$

the first assumption is incorrect if $\lambda \gtrsim 1$. The last approximation, as shown in Ref. 11, is incorrect for very large λ:

$$\lambda \geqslant D/\omega \gg 1. \tag{6}$$

It appears that allowance for the phonon corrections to the vertex part can lead, even in the presence of polaron narrowing of the band, only to quantitative corrections which do not alter the qualitative picture of the energy spectrum.

1. EQUATIONS FOR GF, WITH ACCOUNT TAKEN OF LOCAL INSTABILITY OF THE LATTICE

The reason for the absence of a polaron effect in the usual theory of electron-phonon interaction in metals is that the electron GF (4) is assumed beforehand (prior to solving the equation) to depend, in view of the translational invariance of the crystal, only on the coordinate difference, so that it is possible to change over the equations for the Fourier transform $\boldsymbol{G}(\mathbf{p}, \omega)$. This excludes automatically the possibility of local violation of the translational invariance due to lattice deformation near the electron site. To enable the electrons to become attuned to one another in a minimum-energy state we introduce in the Hamiltonian, following Refs. 12-15,

an infinitesimal translationally invariant potential of the "sources"; this potential can be set equal to zero only after the calculation of the GF. It is well known here [12–14] that a premature vanishing of this potential can lead to finite differences in the result, i.e., in the GF, the energy spectrum, or thermodynamic and other properties. In our case this is the result of instability of the initial electron band to polaron collapse. [11]

It is important that even for infinitesimal but nonzero sources the average ion deviations $\langle \hat{\mathbf{u}}_n(\tau)\rangle$ from the equilibrium positions R_n^0 differ from zero and are not infinitesimally small. This circumstance was disregarded in the traditional theory of electron-phonon interaction. Furthermore, even in Refs. 15 and 16, in which the general form of the GF contained $\langle \hat{\mathbf{u}}_n(\tau)\rangle$ explicitly, it was assumed that $\langle \hat{\mathbf{u}}_n(\tau)\rangle \neq 0$ corresponds only to an imperfect crystal and does not hold for a perfect one.

We write the Hamiltonian of the electron-phonon system, omitting for simplicity the Coulomb interaction, in the form

$$\begin{aligned}\hat{H} = \hat{H}_e + \hat{H}_i + \hat{H}_{ei} + \int U(\mathbf{r},t)\psi^+(\mathbf{r},t)\psi(\mathbf{r},t)d\mathbf{r} \\ + \textstyle\sum_{n\alpha} J_n^\alpha(t)\hat{u}_n^\alpha(t)\end{aligned} \tag{7}$$

The contributions $\widehat{H}_e$ and $\widehat{H}_i$ to the Hamiltonian, corresponding to the electron and ion subsystems, and that to the electron-ion interaction, are given by

$$\begin{aligned}\hat{H}_e =& \int d\mathbf{r}\psi^+(\mathbf{r},t)\left[-\frac{\nabla^2}{2m} - \mu\right]\psi(\mathbf{r},t) \\ &- \sum_{n\kappa}\int \psi^+(\mathbf{r},t)\psi(\mathbf{r},t)\Phi\left(\mathbf{r} - \mathbf{R}^0_{nx^0}\right)d\mathbf{r}\end{aligned} \tag{8}$$

$$\begin{aligned}\hat{H}_i =& \frac{1}{2}\sum_{n\kappa a} M_\varkappa\left[\dot{\hat{\mathbf{u}}}_n^\alpha\right]^2 + \frac{1}{2}\sum_{\substack{nn'\\ x\kappa}} V\left(\mathbf{R}^0_{nx} - \mathbf{R}^0_{n'x'}\right) \\ &+ \frac{1}{2}\sum_{\substack{nn'\\ xx'}}\left(\hat{u}^\alpha_{nx^\alpha} - \hat{u}^\alpha_{n'x'}\right)\nabla_\alpha V\left(R_{nx^0-} - R^0_{n'x'}\right)\end{aligned} \tag{9}$$

$$\hat{H}_{ei} = \sum_{nx}\int \psi^+(\mathbf{r},t)\psi(\mathbf{r},t)\hat{u}^\alpha_{nx}\nabla_\alpha\Phi\left(\mathbf{r} - \mathbf{R}_{nx}\right)d\mathbf{r} \tag{10}$$

Here $\hat{u}^\alpha_{nx}$ is the ion-displacement operator, and $V\left(R^0_{n\varkappa} - R^0_{n'x'}\right)$ and $\Phi\left(\mathbf{r} - R^0_{n\varkappa}\right)$ are the potentials of the ion-ion and electron-ion interactions. The last two terms of (7) are the aforementioned potentials of the external sources. Terms quadratic in $\hat{u}^\alpha_{nx}$ are assumed to be present in (9) and (10), but are not written out explicitly.

Using (7), we obtain in standard fashion the equations for the electron and phonon temperature GF[12,13,15]:

$$\begin{aligned}\delta\left(\mathbf{r},\mathbf{r}'\right)\delta\left(\tau.\tau'\right) = \int\Bigg[\Bigg(i\frac{\partial}{\partial\tau} + \left(\frac{\nabla^2_{\mathbf{r}}}{2m} + \mu\right) - U + \sum_{n\times}\Phi\left(\mathbf{r} - \mathbf{R}_{n\times}{}^0\right) \\ - \sum_{n\times}\Gamma_x\Phi\left(\mathbf{r} - \mathbf{R}_{n\times}{}^0\right)\langle\hat{u}^\alpha_n(\tau)\rangle\Bigg)\delta_{\mathbf{r}}\mathbf{r}''\delta_{\tau\tau''} \\ -\Sigma\left(\mathbf{r},\mathbf{r}'',\tau-\tau''\right)\Big]G\left(\mathbf{r}'',\mathbf{r}',\tau''-\tau'\right)d\mathbf{r}''\end{aligned} \tag{11}$$

The self-energy part Σ in (11) is given by

$$\begin{aligned}
&\Sigma\left(\mathbf{r}'',\ \mathbf{r}', \tau''-\tau'\right) \\
&\quad = i \sum_{\substack{nn \\ x\kappa}} \nabla_\alpha \Phi\left(\mathbf{r}''-\mathbf{R}_{n\times}^0\right) \nabla_\beta \Phi\left(\mathbf{r}'-\mathbf{R}_{n'x'}^0\right) \\
&\qquad \times D_{nn'xx'}^{\alpha\beta}\left(\tau''-\tau'\right) G\left(\mathbf{r}'', \mathbf{r}', \tau''-\tau'\right)
\end{aligned}$$

where $D_{nn'xx'}^{\alpha\beta}(\tau)$ is the temperature GF for the ion displacements:

$$D_{nn'\times x'}^{\alpha\beta}(\tau) = -i\left\langle T_\tau\left(\hat{u}_{\mathbf{nx}}^\alpha - \langle \hat{u}_{\mathbf{nx}}^\alpha\rangle\right), \left(\hat{u}_{\mathbf{n}'x'}^\beta(\tau) - \left\langle \hat{u}_{\mathbf{n}'x'}^\beta\right\rangle\right)\right\rangle. \tag{12}$$

The expansion of the ion-displacement operator in terms of the phonon operators is

$$\hat{u}_{\mathbf{nx}}^\alpha = \langle \hat{u}_{\mathbf{nx}}^\alpha\rangle + \sum_{\mathbf{qj}} \frac{e^\alpha(\mathbf{q}j \mid x)}{\left[2NM_x\omega_j(\mathbf{q})\right]^{1/2}} \exp\left(i\mathbf{q}R_{\mathbf{nx}}{}^0\right)\left(\hat{b}_{\mathbf{qj}} + \hat{b}_{-\mathbf{q}j}{}^+\right) \tag{13}$$

Here $e^\alpha(\mathbf{q}j \mid x)$ is the polarization vector for an ion x with a radius vector $\rho_\varkappa$ in a unit cell, $M_\varkappa$ is the ion mass, and $\omega_j(\mathbf{q}), \hat{b}_{\mathbf{q}^j}^+, \hat{b}_{\mathbf{q}_j}$ are respectively the frequency and the creation and annihilation operators of a phonon with polarization j. Substitution of (13) in (12) yields

$$\begin{aligned}
D_{nn'xx'}^{\alpha\beta}(\tau) &= \sum_{\mathbf{q}j} \frac{e^{\alpha*}\left(\mathbf{q}j \mid x'\right) e^\beta\left(\mathbf{q}j \mid x'\right)}{N\left(M_x M_{x'}\right)^{1/2}\omega_j(\mathbf{q})} \exp\left[i\mathbf{q}\left(\mathbf{R}_n^0 - \mathbf{R}_{m'}^0\right)\right] \\
&\times \exp\left[i\mathbf{q}\left(\boldsymbol{\rho}_x - \boldsymbol{\rho}_{x'}\right)\right] T \sum_{\mathbf{p}} D_j\left(\mathbf{q}, \omega_p\right) \exp\left(-i\omega_p\tau\right) \\
&\omega_p = \pi n T, n = 0, \pm 1, \pm 2 \ldots
\end{aligned} \tag{14}$$

where $D_j\left(\mathbf{q}, \omega_p\right)$ is the temperature **GF** of the phonons of branch j in the momentum representation.

To calculate $\langle \hat{u}_n^\alpha(\tau)\rangle$ we average the equation for $\hat{u}_n^\alpha(\tau)$:

$$-M_x \frac{\partial^2 \hat{u}_{nx}^\alpha(\tau)}{\partial \tau^2} = \frac{\delta \hat{H}}{\delta \hat{u}_{nx}^\alpha}. \tag{15}$$

As a result we have

$$\langle \hat{u}_{n'}, \beta\rangle = \sum_n \int d\mathbf{r} \rho_e(\mathbf{r}, \tau) \nabla_\alpha \Phi\left(\mathbf{r} - \mathbf{R}_n{}^0\right) D_{nn'}^{\alpha\beta}\left(\omega_p = 0\right) \tag{16}$$

Here $\rho_e(\mathbf{r}, \tau)$ is the coordinate-dependent electron density in the crystal. Substituting (16) in (11), we add the increment to the mean field:

$$\begin{aligned}
&-\sum_{n'} \nabla_\beta \Phi\left(\mathbf{r} - \mathbf{R}_{n'}{}^0\right)\left\langle \hat{u}_{n'}{}^\beta(\tau)\right\rangle \\
&= -\sum_{nn} \int d\mathbf{r}' \rho_e\left(\mathbf{r}', \tau\right) \nabla_\alpha \Phi\left(\mathbf{r} - \mathbf{R}_n{}^0\right) \nabla_k \Phi\left(\mathbf{r} - \mathbf{R}_{n'}{}^0\right) D_{nn'}^{\alpha\beta}\left(\omega_p = 0\right),
\end{aligned} \tag{17}$$

applied to the electron by the polarization (by the shift of the equilibrium positions) of the ions surrounding the given electron.

Since the sources violate translational invariance, we expand the electron field operators $\psi(\mathbf{r}, \tau)$ in terms of functions $\varphi_m(\mathbf{r}) \equiv \varphi\left(\mathbf{r} - \mathbf{R}_m\right)$, that are centered on the lattice sites-in analogy with Wannier functions. The exact form of the functions $\varphi_m(\mathbf{r})$ will be determined later by a variational procedure. We have

$$\psi(\mathbf{r},\tau)=\sum_{\boldsymbol{m}}\hat{a}_m(\tau)\varphi_m(\mathbf{r}). \tag{18}$$

The fact that only one wave function corresponds to the site $\mathbf{R}_m^0$, rather than a complete and orthonormalized set of functions $\varphi_{m,n}(\mathbf{r})$, is equivalent to the single-band approximation.

Substituting (18) in (7)-(10), we separate from the interaction Hamiltonian $\widehat{H}_{ei}(10)$ the term $\widetilde{H}_{ei}$ that leaves the electron on one site:

$$\hat{\tilde{H}}_{ci}=\sum_m \tilde{H}_m\hat{a}_m{}^+\hat{a}_m \tag{19}$$

where

$$\widetilde{H}_m=\int d^3\mathbf{r}\varphi_m^*(\mathbf{r})\varphi_m(\mathbf{r})\sum_n \hat{u}_n^\alpha\nabla_\alpha\Phi\left(\mathbf{r}-\mathbf{R}_n^0\right). \tag{20}$$

We neglect hereafter the difference between $\widehat{\widetilde{H}}_{ei}$ and $\widehat{H}_{ei}$, assuming $\widehat{H}=\widehat{H}_0+\widehat{H}_{ei}$ with $\widehat{H}_0\equiv\widehat{H}_e+\widehat{H}_i$.

It is easy to show, by changing to the momentum representation, that allowance for the terms ($\widehat{H}_{ei}-\widehat{H}_{ei}$) means departure from the framework of a Fröhlich interaction Hamiltonian with a constant that depends only on the phonon momentum. [1]

We rewrite the electron GF in the form

$$\mathscr{G}\left(\mathbf{x},\mathbf{x}',\tau\right)=\sum_{mm'}\varphi_m(\mathbf{x})\varphi_{m'}\left(\mathbf{x}'\right)\mathscr{G}_{mm'}(\tau)$$

$$\mathscr{G}_{mm'}(\tau)=-\sum_{mm'}e^{a/T}\,\mathrm{Sp}\left\{\exp\left(-\frac{\hat{H}_0-\mu\widehat{N}}{T}\right)\right.$$

$$\left.\times T_\tau\left(\hat{a}_m\left(\tau_1\right)\hat{a}_{m'}\left(\tau_2\right)\mathscr{S}\left(\frac{1}{T}\right)\right)\right\} \tag{21}$$

$$e^{-\Omega/T}=\mathrm{Sp}\left\{T\exp\left(-\frac{\hat{H}_0-\mu N}{T}\right)\hat{\mathscr{S}}\left(\frac{1}{T}\right)\right\} \tag{22}$$

$$\mathscr{S}\left(\frac{1}{T}\right)=\exp\left\{-\int_0^{1/T}\hat{H}_{ei}\left(\tau'\right)d\tau'\right\} \tag{23}$$

$$\hat{H}_{ei}(\tau)=\exp\left[\tau\left(\hat{H}_0-\mu\hat{N}\right)\right]\hat{H}_{ei}\exp\left[-\tau\left(\hat{H}_0-\mu\hat{N}\right)\right] \tag{24}$$

Substituting in (17) the explicit expression for $\hat{u}_n^\alpha$ and integrating, we obtain $\mathfrak{S}(1/T)=\exp(-\widetilde{S})$, where

$$\hat{\tilde{S}}=\sum_{\boldsymbol{m}}\int d^3\mathbf{r}\varphi_m\cdot(\mathbf{r})\left[\sum_n\hat{\tilde{u}}_n^\alpha\nabla_a\Phi\left(\mathbf{r}-\mathbf{R}_n{}^0\right)\right]\varphi_m(\mathbf{r})\hat{a}_m{}^+\hat{a}_m. \tag{25}$$

Here

$$\hat{\tilde{u}}_n^\alpha=\sum_{\mathbf{q}jx}\frac{\exp\left(i\mathbf{q}\mathbf{R}_n{}^0\right)}{\left[2NM_x\omega_j(\mathbf{q})\right]^{1/2}\omega_j(\mathbf{q})}e^\alpha(\mathbf{q}j\mid x)\left(\hat{b}_{\mathbf{q}j}-\hat{b}_{-\mathbf{q}j}{}^+\right). \tag{26}$$

i.e., $\hat{\tilde{u}}_n^\alpha$ differs from $\hat{u}_n^\alpha$ by the presence of an extra factor $\omega_j(\mathbf{q})$ in the denominator in the summation over $\mathbf{q}$ and j, and by the sign of $\hat{b}_{-qj}$. The operator $\widetilde{\widetilde{S}}$ is dimensionless. Note now

that by using an identity transformation of the GF $\mathscr{G}_{mm'}(\tau > 0)$ we can rewrite (21) in the form

$$\mathscr{G}_{mm'}(\tau > 0) \equiv -e^{-\Omega/T}\mathrm{Sp}\left\{\mathbb{S}^{+1}(1/T)e^{-\hat{H}_T T}\mathbb{S}^{-1}(1/T)\mathbb{S}(1/T)\right.$$
$$\left.\times\hat{a}_m(\tau_1)\,\mathbb{S}^{-1}(1/T)\mathbb{S}(1/T)\hat{a}_m{}^+(\tau_2)\,\mathbb{S}^{+1}(1/T)\right\} \tag{27}$$

and arrive at the expression

$$\mathscr{G}(\tau > 0)$$
$$= -\,e^{-a/T}\,\mathrm{Sp}\left\{\exp\left(-\frac{\hat{H}-\mu\hat{N}}{T}\right)\hat{\tilde{a}}_m(\tau_1)\right.$$
$$\left.\times\exp\left(\hat{S}_m\right)\hat{\tilde{a}}_m\cdot+(\tau_2)\exp\left(-\hat{S}_{m'}\right)\right\} \tag{28}$$

where

$$\hat{\Pi} = \mathbb{S}^1(1/T)\hat{H}\mathbb{S}^{-1}(1/T)$$
$$\hat{\tilde{\pi}}_m(\tau) = \exp\left[\tau(\hat{H}-\mu\hat{N})\hat{a}_m\exp[-\tau(\hat{\Pi}-u\hat{V})]\right.$$

We have then in (28)

$$\exp\left(-\frac{\hat{H}-\mu\hat{N}}{T}\right) = \mathscr{S}^{+1}\left(\frac{1}{T}\right)\exp\left(-\frac{\hat{H}_0-\mu\hat{N}}{T}\right)$$
$$\equiv \exp\left(-\frac{\hat{H}_e-\mu\hat{N}}{T}\right)\mathscr{S}^{+1}\left(\frac{1}{T}\right)\exp\left(-\frac{\hat{H}_i}{T}\right) \tag{29}$$

Here

$$\hat{H}_e = \mathfrak{S}(1/T)\hat{H}_e\mathfrak{S}^{-1}(1/T). \tag{30}$$

2. ELECTRON GREEN'S FUNCTION AND ENERGY SPECTRUM

Finding the electron energy spectrum calls for an analytic continuation of the temperature GF into the region of real t. To this end, we find the explicit form of the correlator $\left\langle\hat{\tilde{a}}_m(\tau_1)\,\hat{\tilde{a}}^+_{m'}(\tau_2)\right\rangle$ in expression (28) for the GF.

Direct calculations using Eq. (29) lead to the basic property of the transformed part H_i+H_{ei} of the Hamiltonian H: this part of the Hamiltonian was diagonalized with respect to the electron and phonon variables, namely

$$\mathbb{S}^{+1}\left(\frac{1}{T}\right)\exp\left(-\frac{\hat{H}}{T}\right) = \exp\left[-\frac{1}{T}\left(\hat{H}_i+\sum_m\hat{a}_m{}^+\hat{a}_m E_p\right)\right], \tag{31}$$

where

$$
\begin{aligned}
E_p = \langle m| \left| \frac{\nabla_{\mathbf{r}}^2}{2m} + \mu + \sum_n \Phi\left(\mathbf{r} - \mathbf{R}_n^0\right) \right| m \Big\rangle \\
- \langle m|\nabla_\alpha \Phi\left(\mathbf{r} - \mathbf{R}_n^0\right)|m\rangle \langle \hat{u}_n^\alpha \rangle \\
- \sum_{j\mathbf{q}} \hbar\omega_j(\mathbf{q}) \left|\pi_{\mathbf{q}}\right|^2 ; \\
\pi_{\mathbf{q}} = \sum_n \exp\left(i\mathbf{q}\mathbf{R}_n{}'\right) \langle u_n{}^\alpha \rangle \, i\mathbf{q}_\alpha .
\end{aligned} \tag{32}
$$

We now uncouple (28) and assume that

$$
\begin{aligned}
\mathscr{S}_{mm'}(\tau > 0) = \left\langle \hat{\tilde{a}}_m \hat{a}_{m'}^\dagger \right\rangle \left\langle \exp\left(\hat{\tilde{S}}_m\right) \exp\left(-\tilde{\tilde{S}}_{m'}\right) \right\rangle \\
\equiv \left\langle \hat{\tilde{a}}_m(\tau_1) \, \hat{\tilde{a}}_{m'}(\tau_2) \right\rangle \exp\left[- \left\langle \left(\hat{S}_m - \hat{\tilde{S}}_{m'}\right)^2 \right\rangle /2 \right]
\end{aligned} \tag{33}
$$

Averaging over the ion operators in the second factor of (33) leads to the expression

$$
\exp\left(-g_{mm'}^2\right) \equiv \exp\left[- \left\langle \left(\widehat{S}_m - \widehat{S}_{m'}\right)^2 \right\rangle /2 \right], \tag{34}
$$

where

$$
\begin{aligned}
\mathbf{g}_{mm'}^2 = \sum_{\mathbf{q}j} \sum_{nn'} \sum_{\alpha\beta m''} \int \frac{d\omega \, \mathrm{Im}\, D_{\mathbf{q}j}^{\alpha\beta}(\omega)}{\omega^2} \langle m|\nabla_\alpha \Phi\left(\mathbf{r} - \mathbf{R}_n^0\right)|m\rangle \\
\times \langle m''| \nabla_\beta \Phi\left(\mathbf{r}' - \mathbf{R}_{n'}\right)|m''\rangle \cos\left[\mathbf{q}\left(\mathbf{R}_n^0 - \mathbf{R}_{n'}\right)\right] \left(\delta_{mm''} - \delta_{m''m'}\right).
\end{aligned}
$$

We see that $g_{mm'}^2$, vanishes if $m' = m$. For $m' \neq m$ Eq. (34) is a rigorous generalized expression for the polaron factor (see, e.g., Refs. 4 and 8).

Multiplying (11) from the left by $\varphi_m^*(\mathbf{r})$ and from the right by $\varphi_{m'}(\mathbf{r}')$ and integrating with respect to $\mathbf{r}$ and $\mathbf{r}'$, we obtain after changing to the ω representation in imaginary time ($m' \neq m$)

$$
\begin{aligned}
S_{mm'}^0 = \left(i\omega_p + H_{emm}\right) G_{mm'}(\omega_p) + H_{emm'} G_{m'm'}(\omega_p) \\
- \sum_n \langle m|\nabla_\alpha \Phi\left(\mathbf{r} - \mathbf{R}_n^0\right)|m\rangle \\
\times \langle u_n^\alpha(\tau)\rangle \, G_{mm'}(\omega_p) - \sum_n \langle m|\nabla_\alpha \Phi\left(\mathbf{r} - \mathbf{R}_n^0\right)|m'\rangle \\
\times \langle \hat{u}_n^\alpha \rangle \, G_{m'm'}(\omega_p) \\
-2i \sum_{nn'} \sum_{\substack{dd' \\ rr'}} \langle d|\nabla_\alpha \Phi\left(\mathbf{r} - \mathbf{R}_n^0\right)|m\rangle \langle r|\nabla_\beta \Phi\left(\mathbf{r}'' - \mathbf{R}_{n'}\right)|d'\rangle \\
\sum_s D_{nn'}^{\alpha\beta}(\omega_p - \omega_s) \, G_{dd'}(\omega_s) \, G_{rr'}(\omega_p) \, S_{m'r'}^0
\end{aligned} \tag{35}
$$

Here

$$
H_{cmm'} = \langle m| \frac{\nabla_{\mathbf{r}}^2}{2m} + \mu + \sum_n \Phi\left(\mathbf{r} - \mathbf{R}_n{}^0\right)|m'\rangle , \tag{36}
$$

$$
S_{mm'}^{\mathbf{q}} = \langle m| \exp(i\mathbf{q}\mathbf{r})|m'\rangle . \tag{37}
$$

For $m' = m$, the analogous equation is

$$1 = \left[i\omega_p + H_{emm} - \sum_n \langle m|\nabla_\alpha \Phi\left(\mathbf{r} - \mathbf{R}_n^0\right)|m\rangle \langle u_n^\alpha \rangle \right] G_{mm}(\omega_p)$$
$$-i \sum \sum \langle m|\nabla_\alpha \Phi\left(\mathbf{r}' - \mathbf{R}_n^0\right)|m\rangle \langle m|\nabla_\beta \Phi\left(\mathbf{r}'' - \mathbf{R}_{n'}|m\right\rangle$$
$$\times /)_{nn'}^{\alpha\beta}(\omega_s)\, G_{mm}(\omega_p - \omega_s)\, G_{mm}(\omega_p) \tag{38}$$

We substitute in (38) the spectral representation for the GF of the electrons and phonons in the form

$$G_{mm'}(\omega_n) = \frac{1}{2\pi} \int_{-\infty}^{+\infty} dz' \frac{a_{mm'}(z')}{i\omega_n - z'} \tag{39}$$
$$D_j(\mathbf{q}, \omega_n) = \frac{1}{2\pi} \int_{-\infty}^{+\infty} dz' \frac{b_j(\mathbf{q}, z')}{i\omega_n - z'} \tag{40}$$

and recognize that in the case of undamped phonons

$$\mathrm{b}\ \ (\mathbf{q}\cdot \therefore') = 2\pi \left[\delta\left(z' - \omega_j(\mathbf{q})\right) - \delta\left(z' + \omega, (\mathbf{q})\right)\right] \tag{41}$$

In (39) we have

$$a_{mm}(z') = -2\,\mathrm{In}\, G_{\mathrm{R}mm'}(z'), \tag{42}$$

where $G_{Rmm'}(z')$ is the retarded GF of the electrons. The
poles of the electron GF , neglecting the damping of the electronic states, allow us to express $a_{mm'}(z')$ in the form

$$a_{mn'}(z') = -2A_{mm}\delta\left(z - h_{m\cdot n}\right) \tag{43}$$

Substituting (39) and (40) in (38), we sum over n and n' and obtain as a result in the zeroth approximation with respect to the overlap integral $S_{mm'}^{\mathbf{q}}$, recognizing that $h_{mm'} \sim S_{mm'}^{\mathbf{q}}$, the expression

$$G_{mm^{-1}}^{-1}(\omega_p) = \Bigg\{ i\omega_p + HI_{cmm} - \sum_{nn'} \langle m|\nabla_\alpha \Phi\left(\mathbf{r} - \mathbf{R}_n{}^0\right)|m\rangle$$
$$\times \int d\mathbf{r}\rho_e(\mathbf{r}, \tau) \nabla_s \Phi\left(\mathbf{r} - \mathbf{R}_n{}^0\right) D_{nn'}^{\alpha\beta}(\omega_p = 0)$$
$$+ \frac{i}{2} \frac{1}{2\pi} \sum_{q;x'} \int_{-\infty}^{+\infty} d\omega \frac{\mathrm{th}(\omega/2T) + \mathrm{cth}(\Delta/2T)}{i\omega_p - \omega - \Delta} b_j(\mathbf{q}\cdot\omega) \tag{44}$$
$$\times A_{mm} \sum_{nn'} \langle m|\nabla_\alpha \Phi\left(\mathbf{r}' - \mathbf{R}_n{}^0\right)|m\rangle \langle m|\nabla_\beta \Phi\left(\mathbf{r}'' - \mathbf{R}_{n'}{}^n\right)|m\rangle$$
$$\times \frac{e^{\alpha *}(qj \mid x) e^\beta (qj \mid x')}{N\left(M_x M_{x'}\right)^{1/2} \omega_j(q)} \exp\left[iq\left(\rho_x - \rho_{x'}\right)\right].$$

Following an obvious analytic continuation in ω and putting $\omega = h_{mn} \equiv E_p$ we obtain an explicit expression for E_p in the form

$$E_p \approx +H_{emm} - \sum_{\mathbf{q}j\kappa} \frac{|g_{j\mathbf{x}}(\mathbf{q})|^2}{\omega_{\mathbf{q}j}} |S_{mm}{}^{\mathbf{q}}|^2 \tag{45}$$

Here

$$\mathbf{g}_{jx}(\mathbf{q}) = -\frac{\exp(iq\rho_x)}{[2NM_x\omega_j(\mathbf{q})]^{1/2}} \langle p|e(\mathbf{q}j \mid \varkappa)\nabla\Phi_x(\mathbf{r})|p'\rangle \tag{46}$$

is the matrix element of the electron-phonon interaction. Equation (45) was obtained under the assumption that $E_p \gg T$. In the calculation of (45) we took also into account the symmetry change of a crystal by an infinitesimal source, which lowers the total symmetry of the crystal. Expression (45) was obtained with account taken of the lowering of the crystal symmetry by the sources to the site symmetry. In this case $A_{mm} \neq N_{el}/N$, i.e., the filling of the sites of the perturbed crystal is not uniform. Recognizing the smallness of the overlap integral, so that $A_{m_0m'} \sim A_{m_0m_0} \left|S^0_{m_0m'}\right|^2$, and normalizing the GF to an electron number equal to unity, we obtain $A_{m_0m_0} \sim 1$, accurate to the small quantity $\left|S^0_{m_0m'}\right|^2$. The exact form of the function $\varphi_m(\mathbf{r})$ can now be obtained by minimizing E_p with respect to φ.

Substituting the explicit form of $G_{mm}(\omega_p)$ in (35), we have for $\boldsymbol{G}^{(0)}_{mm'}(\omega_p)$:

$$G^{(0)}_{mm'}(\omega_p) = \frac{S^0_{mm'}}{i\omega_p - h_{mm}} - \frac{H_{mm'}}{(i\omega_p - h_{mm})^2} \tag{47}$$

Here

$$H_{m'} = \sum_{\mathbf{q}j} \frac{(2\,\mathrm{Re}\,S^q_{m'm})\,S^0_{mm'} + S^0_{m'm}\left|S^{\mathbf{q}}_{mm}\right|^2}{\omega_j(\mathbf{q})} |g_j(\mathbf{q})|^2 + H_{emm'} \tag{48}$$

Solving (35), which reduces to an integral equation, by an iteration using G^0_{mm}, and G_{mm} to first order in the overlap integral S^q_{mm}, and to arbitrary order in G_{mm}, we arrive, as can be easily checked by direct calculations, at a representa-
tion of the factor $\exp(-g^2_{mm'})$ in expression (33) for $G_{mm'}$, so that

$$G_{mm'}(\omega_p) = \frac{S^0_{mm'}\exp(-\theta_{mm'})}{i\omega_p - h_{mm}} - \frac{H_{mm'}\exp(-\theta_{mm'})}{(i\omega_p - h_{mm})^2} \tag{49}$$

in full agreement with (33).

Carrying out the obvious analytic continuation of $G_{mm}(\omega_p)$ (44) and $G_{mm'}(\omega_p)$ (44) into the regions of real frequencies ω, we calculate the electron dispersion law in the band $\varepsilon(\mathbf{k})$, assuming the potentials of the sources to be zero, and restoring by the same token the total symmetry of the crystal. We have

$$\varepsilon(\mathbf{p}) = -\left[-2i\lim_{t\to 0}\int_{-\infty}^{+\infty} d\omega \sum_{m'} G_{mm'}(\omega)\exp(i\mathbf{p}\mathbf{R}_{mm'})\,\omega\right] \times \left[-2i\lim_{t\to 0}\int_{-\infty}^{+\infty} d\omega \sum_{m'} G_{mm'}(\omega)\exp(i\mathbf{p}\mathbf{R}_{mm'})\right]^{-1} \tag{50}$$

Calculating the intervals with respect to ω in (50), we obtain

$$\varepsilon(\mathbf{p}) = \frac{\sum_{m'} H_{mm'}\exp(-g^2_{mm'})\exp(i\mathbf{p}\mathbf{R}_{mm'})}{\sum_{m'} S^0_{mm'}\exp(-g^2_{mm'})\exp(i\mathbf{p}\mathbf{R}_{mm'})}. \tag{51}$$

The dispersion law obtained for the electrons in the band is polaron-like, and the structure $H_{mm'}$ [Eq. (48)] coincides with the structure of an analogous expression obtained long ago by Tyablikov. [17]

CONCLUSION

A consistent analysis, with allowance for the local lattice deformation ($\langle u_n \rangle \neq 0$), leads to a polaron effect in the electron GF . The spectrum (51) corresponds to an exponentially narrow polaron band of width

$$W = D \exp\left(-g^2\right), \tag{52}$$

where g^2 is the value of g^2_{mm}, for the nearest neighbors. Obviously, narrowing of the band (52) changes qualitatively the cooperative properties (superconducting and others) of the system if the adiabatic regime is disturbed, i.e., if inequality (6) is satisfied:

$$W \leqslant \omega. \tag{53}$$

Recognizing that $\lambda \simeq g^2\omega/D$ (Refs. 4 and 7), we obtain from (53) the following condition for the electron-phonon coupling constant at which polaron effects become significant:

$$\lambda \geqslant (\omega/D)\ln(D/\omega). \tag{54}$$

If the adiabatic condition (1) is met, the left-hand side of inequality (54) turns out to be less than unity! It must be noted here, however, that the inequality (54) that determines the limits of applicability of traditional electronphonon interaction theory is not rigorously exact, in view of the approximate character of the uncoupling (33). A more rigorous analysis, which is possible in the small-radius-polaron theory, shows (see Refs. 8 and 18) that polaron collapse of the band sets in at

$$\lambda \geqslant (2z)^{-1/2}, \tag{55}$$

where z is the coordination number of the lattice; this agrees with the physical condition (2). The transition from a Bloch wide-band electron to a small-radius polaron localized in a narrow band can be jumplike.

The analysis in the present paper, as in the initial ones, [1,2] does not include in explicit form effects of Coulomb interaction of the carriers. Allowance for this interaction influence very little the polaron-formation effects considered here. Indeed, in the case of a small-radius polaron the wave function $\mid m >$ of a polaron localized on site m decreases rapidly outside the limits of the given unit cell. In the polaron factor $g^2_{mm'}$, the only quantity that depends substantially on the electron density is the electron-ion interaction potential $\Phi\left(\mathbf{r} - \mathbf{R}^0_n\right)$, which is screened by free carriers.

The Coulomb interaction of the carriers will influence also the effective electron-electron attraction potential, causing it to decrease by a quantity $\langle m|v_{\text{coul}}\ |m'\rangle$, where m and m' denote neighboring sites or one and the same site.

This effect was investigated for interacting polarons in Refs. 4-6, and will be treated by us in the GF formalism in a separate paper.

We are deeply grateful to A. A. Abrikosov, Yu. M. Kagan, A. I. Larkin, G. M. Éliashberg, D. E. Khmel'nitskii, and E. G. Maksimov for interest in the work and for helpful stimulating discussion of the problem touched upon here.

1) In simple metals the interaction $\widehat{\widetilde{H}}_{ci}$ (crystal field) may turn out to be screened by free electrons, and at the same time $\widetilde{H} - \widehat{H}_{ci}$ is small to the extent that the overlap integrals of the atomic wave functions are small. It seems that $\widehat{H}_{ci}$ will be decisive in metal oxides with relatively low carrier density.

1 G. M. Eliashberg, Zh. Eksp. Theor. Fiz. 38, 966 (1960) [Sov. Phys. JETP 11, 696 (1960)].

[2] A. B. Migdal, ibid. 34, 1438 (1958) [7, 996 (1958)].
[3] A. A. Abrikosov, L. P. Gor'kov, and I. E. Dzyaloshinskii, Quantum Field-Theoretical Methods in Statistical Physics, Pergamon, 1965 (p. 444 of Russian original).
[4] A. S. Alexandrov and V. Ranninger, Phys. Rev. B 23, 1796 (1981).
[5] A. S. Alexandrov, V. Ranninger, and V. Robashkevich, ibid. B 33, 4526 (1986).
[6] A. S. Aleksnadrov, Zh. Fiz. Khim. 57, 273 (1983).
[7] A. S. Aleksandrov, Dokl. Akad. Nauk SSSR 293, 835 (1987) [Sov. Phys. Doklady 32, 286 (1987)].
[8] Polarons [in Russian], Yu. A. Firsov, ed., Nauka, 1975.
[9] A. S. Aleksandrov, Pis'ma Zh. Eksp. Teor. Fiz. 46, Supplement, p. 128 [JETP Lett. 46, Supplement, p. S107].
[10] A. S. Alexandrov, Phys. Rev. B 38, 925 (1988)].
[11] A. S. Aleksandrov, V. N. Grebenev, and E. A. Mazur, Pis'ma Zh. Eksp. Teor. Fiz. 45, 357 (1987) [JETP Lett. 45, 455 (1987)].
[12] G. Baym, Ann. Phys. (N. Y.) 14, 1 (1961).
[13] E. S. Fradkin, Trudy FIAN 29, 7 (1965).
[14] N. N. Bogolyubov, ed., Statistical Physics and Quantum Field Theory [in Russian], Nauka, 1973, pp. 7-80.
[15] E. G. Maksimov, Zh. Eksp. Teor. Fiz. 69, 2236 (1975) [Sov. Phys. JETP 42, 1138 (1975)].
[16] A. K. Rajagopal and M. H. Cohen, Sol. St. Phys. 1, 9 (1972).
[17] S. V. Tyablikov, Zh. Eksp. Teor. Fiz. 23, 381 (1952).
[18] A. S. Aleksandrov and A. B. Krebs, Moscow Engineering-Physics Preprint, 1988.

Translated by J. G. Adashko

6.5.3 4.2 Exact solution of the multi-polaron problem for $\lambda \to \infty$

(so all section 4.1 was for strong coupling? and conclusion is that there is just instability and it means that non of theory is developed at all about it?)

Theory

In the case of large polarons the multi-polaron problem can be solved within the Migdal-Eliashberg approach discussed in Chapter 3. This is the weak coupling regime $\lambda < 1$, where large bipolarons, if they exist, transform into Cooper pairs at finite density.

In the small polaron regime, $\lambda \geq 1$ the kinetic energy remains smaller than the interaction energy and a self-consistent treatment of a many polaron system is possible with the ' $1/\lambda'$ expansion technique (Alexandrov (1992b)). (learn, what is it?)

(why do we consider large polarons at all if we set coupling constant to maximum (which should give small polarons)?)

This possibility results from the fact, known for a long time, that there is an exact solution for a single electron in the strong-coupling limit $\lambda \to \infty$. (where is it written??)

(in which materials there is such a strong coupling???)

We use the tight-binding Hamiltonian of electrons and phonons if hopping coefficient between electrons $T(\mathbf{m}) = 0$ (or $\lambda = \infty$) (for three dimensions)

$$H = \sum_{\mathbf{q},i} \omega_{\mathbf{q}} \hat{n}_i \left(u_i(\mathbf{q}) d_{\mathbf{q}} + h.c.\right) + \frac{1}{2} \sum_{i,j} V_c(\mathbf{m} - \mathbf{n}) \hat{n}_i \hat{n}_j + \sum_{\mathbf{q}} \omega_{\mathbf{q}} \left(d^\dagger_{\mathbf{q}} d_{\mathbf{q}} + 1/2\right) \tag{3.138}$$

(reminder:

$$u_i(\mathbf{q}) = \frac{1}{\sqrt{2N}} \gamma(\mathbf{q}) e^{i\mathbf{q}\cdot\mathbf{m}} \tag{3.136}$$

$$V_c(\mathbf{m}) = \frac{1}{N} \sum_{\mathbf{q}} V_c(\mathbf{q}) e^{i\mathbf{q}\cdot\mathbf{m}} \tag{3.137}$$

$$T(\mathbf{m}) = \frac{1}{N} \sum_{\mathbf{k}} E_{\mathbf{k},n} e^{i\mathbf{k}\cdot\mathbf{m}} \tag{3.131}$$

so they are constants and were obtained at the staged of TB approximation)(I still don't understand what are they???)

Following Lang and Firsov (1962) one can apply the following canonical transformation to diagonalise it:

$$\tilde{H} = e^S H e^{-S}; \qquad S = \sum_{\mathbf{q},i} \hat{n}_i \left(u_i(\mathbf{q}) d_{\mathbf{q}} - \text{ h.c. } \right) \tag{4.9}$$

The electron operator transforms as

$$\tilde{c}_i = c_i \exp\left(\sum_{\mathbf{q}} u_i(\mathbf{q}) d_{\mathbf{q}} - h.c. \right) \tag{4.10}$$

and the phonon one as:

$$\tilde{d}_{\mathbf{q}} = d_{\mathbf{q}} - \sum_i \hat{n}_i u_i^*(\mathbf{q}) \tag{4.11}$$

(okay, I can check it, but it is pure math transformation, it is not that crucial)

From Eq.(4.11) it follows that the Lang-Firsov canonical transformation is the displacement transformation, Eq.(1.81) for the multi-polaron system shifting ions to the new equilibrium positions. (read ch. 1, understand it!)

In a more general sense it changes the boson vacuum. (????)

As a result:

$$\tilde{H} = \sum_{i,j} \left(\hat{\sigma}_{ij} - \mu \delta_{i,j} \right) c_i^\dagger c_j - E_p \sum_i \hat{n}_i + \frac{1}{2} \sum_{i,j} v_{ij} c_i^\dagger c_j^\dagger c_j c_i + \sum_{\mathbf{q}} \omega_{\mathbf{q}} \left(d_{\mathbf{q}}^\dagger d_{\mathbf{q}} + 1/2 \right) \tag{4.12}$$

where

$$\hat{\sigma}_{ij} = T(\mathbf{m} - \mathbf{n}) \delta_{s.s'} \exp\left(\sum_{\mathbf{q}} \left[u_i(\mathbf{q}) - u_j(\mathbf{q}) \right] d_{\mathbf{q}} - h.c. \right) \tag{4.13}$$

is the new hopping integral depending on the phonon variables,

$$v_{ij} = V_c(\mathbf{m} - \mathbf{n}) - 2 \sum_{\mathbf{q}} \omega_{\mathbf{q}} \left(u_i(\mathbf{q}) u_j^*(\mathbf{q}) \right) \tag{4.14}$$

is the polaron-polaron interaction comprising the direct Coulomb repulsion and the attraction via a nonretarded lattice deformation (second term of Eq.(4.14)).

(now, the phonon and electron parts are decoupled and phonons are taken into account effectively.) (u comes from phonons, right?)

(what is the physical meaning of the new parameters here???!!!)

Proof. (???????)

□

In the extreme strong-coupling limit $\lambda \to \infty$ (is this limit physical? I guess definetely no, so why do we need it?) one can neglect the hopping term of the transformed Hamiltonian. The rest has analytically determined eigenstates and eigenvalues.

(!! how the parameters depend on λ???)

The eigenstates $|\tilde{N}\rangle = |n_i, n_{\mathbf{q}}\rangle$ are classified with the polaron $n_{\mathbf{m},s}$ and phonon n_{q} occupation numbers and the energy levels are:

$$E = (T(0) - E_p - \mu) \sum_i n_i + \frac{1}{2} \sum_{i,j} v_{ij} n_i n_j + \sum_{\mathbf{q}} \omega_{\mathbf{q}} \left(n_{\mathbf{q}} + 1/2 \right) \tag{4.15}$$

where $n_i = 0, 1$ and $n_{\mathrm{q}} = 0, 1, 2, 3, \ldots \infty$. The interaction term does not include the on-site interaction $i = j$ for parallel spins because of the Pauli principle.

Thus we conclude that the Hamiltonian Eq.(3.138) in zero order of the hopping describes localised polarons and independent phonons which are vibrations of ions relative to new equilibrium positions depending (how are they dependent quantitatively?) on the polaron occupation numbers (so, a polaron is a shifted electron with different properties. Obviously, if we set hopping term of electron to zero, it means that the polaron will be stable).

The phonon frequencies remain unchanged in this limit. The middle of the electronic band $T(0)$ falls down by E_p as a result of a potential well produced by the lattice deformation due to the self-trapping (see Fig.4.1).

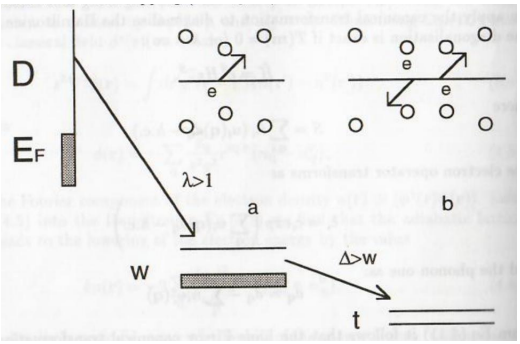

Fig.4.1. Polaron collapse of the electron band (a); bipolaron band (b). (what is D, Δ here???? but it is a part of theory about bipolatons, so I don't know it)

6.5.4 Many-body effects in the normal-state polaron system by Alexandrov 1992

Phys.Rev. B46, 2838-44

Abstract

Dielectric response function of small polarons (SP's) is studied. The Debye radius is small, which reduces a short-range Coulomb repulsion to the magnitude of the order of the small-polaron (SP) bandwidth. Polaron-polaron attraction is enhanced by screening. A critical temperature of the bipolaron formation is found. The dielectric response becomes dynamic in a very low-frequency region. A multiphonon diagram technique is developed to obtain vibration excitations, that are a mixture of phonons with polaronic plasmons. A microscopic model of the anomalous extra modes, observed in neutronscattering experiments in La_2CuO_4, is proposed.

Holstein, [1] and some other workers (for review, see the books in Ref. 1) showed in the framework of the oneelectron problem that at some critical value of the coupling with phonons

$$\lambda > \lambda_c, \tag{1}$$

the electron prefers tunneling in a very narrow polaronic band, having a half bandwidth

$$W = D \exp\left(-g^2\right), \tag{2}$$

which lies well below the bare one, with the half bandwidth D. Here

$$g^2 = \lambda \frac{D}{\omega_0}, \tag{3}$$

with ω_0 being the characteristic phonon frequency. It has now become clear, [2] that the traditional theory of a many-electron system [3] rules out the possibility of the local deformation of the lattice, thus preventing the system from relaxing into the lowest-energy state.

From a more general viewpoint, the instability of a boson vacuum develops in a system of interacting bosons and electrons under the critical value of λ, resulting in a polaron collapse of the electron band. A simple estimation with the perturbation theory in $1/\lambda$ shows [4] a jumplike transition from wide-band electrons with the powerlaw enhanced effective mass [3] to narrow-band small polarons with an exponentially large effective mass, Eq. (2), at

$$\lambda_c = \frac{1}{(2z)^{1/2}} < 1, \tag{4}$$

which agrees well with some variational [5,6] and Monte Carlo [7] calculations, z being the coordination lattice number.

This condition demonstrates the necessity of the development of a theory for a many-electron system, strongly coupled to phonons, taking into account the nonadiabatic character of the carrier motion with the renormalized Fermi energy:

$$\varepsilon_F = E_F \exp\left(-g^2\right) < W < \omega_0. \tag{5}$$

Low-temperature properties of a many-polaron system were first studied in Ref. 8. The ground state of electrons strongly coupled to phonons occurs as a charged Bose liquid, consisting of singlet or triplet pairs [small bipolarons (SB's)] with the charge $2e$ and moving in their narrow band with a heavy effective mass $m^{**} > m^*$.

However, not so much was done for the understanding of many-body effects in the normal state of SP's at temperatures well above the temperature of SB formation. In our recent paper [9] we developed a multiphonon diagram technique to obtain renormalized phonons, using the inverse coupling constant λ^{-1} as a small parameter.

In this paper, the dielectric response of a many-polaron system and the influence of the polaron-polaron interaction on the phonon frequencies are studied. In the first section, using the familiar Holstein-Lang-Firsov transformation [1] I determine a zero-order SP Green function (GF), which contains the main part of the electronphonon interaction in a diagonal form leaving aside the rest in the form of the polaron-polaron interaction and of the residual SP-phonon interaction. For those interactions I adopt the ordinary random-phase approximation (RPA) and the perturbation theory in the inverse coupling λ^{-1}, correspondingly. With RPA the static and the dynamic response of SP's are calculated. Because of the exponentially large mass renormalization, Eq. (2), the Debye radius and the plasma frequency are much smaller than those for a weakly coupled electron-phonon system, and temperature dependent at $T > W$. SP's screen effectively the on-site Coulomb repulsion, reducing it to the value of the order of W. On the contrary the on-site attraction, if it exists, is enhanced by the many-body effects. In Sec. II I generalize our expression for the phonon self-energy, [9] taking into account the polaron-polaron interaction. The SP polarization loop is obtained in a site representation. The spectrum of vibrational excitations is found. One of the most interesting results is that phonons are coupled with polaronic plasmons forming a type of vibration excitations, which are a mixture of the ordinary phonon and the low-frequency plasmon. These vibrations are used to explain the extra modes, observed in neutron-scattering experiments [10] in high- T_c metal oxides.

I. GREEN FUNCTION AND DIELECTRIC RESPONSE OF SP's

After the familiar Holstein-Lang-Firsov transformation [1] and averaging with the phonon density matrix one obtains the free-polaron GF in the form (see for details Ref. 9)

$$G_{\mathbf{k}}(\omega_n) = (i\omega_n - \varepsilon_{\mathbf{k}} + \varepsilon_F)^{-1} \tag{6}$$

with $\omega_n = \pi T(2n+1)$, which corresponds in the site representation to

$$G_{ij}(\omega_n) = \frac{1}{N}\sum_{\mathbf{k}} \exp[-i\mathbf{k}\cdot(\mathbf{m}-\mathbf{n})]\,(i\omega_n - \varepsilon_{\mathbf{k}} + \varepsilon_F)^{-1} \tag{7}$$

Here

$$\epsilon(\mathbf{k}) = \sum_{\mathbf{m}} \sigma(\mathbf{m}) \exp(i\mathbf{k}\cdot\mathbf{m}) \tag{8}$$

is the SP energy dispersion in a narrow polaronic band,

$$\sigma(\mathbf{m}-\mathbf{n}) = t(\mathbf{m}-\mathbf{n}) \exp\left[-g^2(\mathbf{m}-\mathbf{n})\right] \tag{9}$$

is the SP hopping integral, averaged with the density matrix, $\sigma = \langle\hat{\sigma}_{ij}\rangle$,
$g^2(\mathbf{m}) = \frac{1}{2N}\sum_{\mathbf{q}} \gamma^2(\mathbf{q}) \coth\left[\frac{\omega(\mathbf{q})}{2T}\right][1-\cos(\mathbf{q}\cdot\mathbf{m})]$,
with T being the lattice temperature, $t(\mathbf{m})$ is a bare hopping integral in a rigid lattice, and N is the number of lattice sites. The normalization of electron energies is chosen in such a way that the atomic level with the polaronic shift,

$$E_p = \frac{1}{2N}\sum_{\mathbf{q}} \gamma^2(\mathbf{q})\omega(\mathbf{q}) \tag{11}$$

corresponds to zero energy with $\gamma(\mathbf{q})$ and $\omega(\mathbf{q})$ being the matrix element of the electron-phonon Fröhlich interaction and phonon frequencies respectively.

The residual interaction, which remains after this procedure, is a polaron-phonon one: [9]

$$H_{p-\mathrm{ph}} = \sum_{i,j} \left[\hat{\sigma}_{ij} - \sigma(\mathbf{m}-\mathbf{n})\right] c_i^\dagger c_j \tag{12}$$

with

$$\hat{\sigma}_{ij} = t(\mathbf{m}-\mathbf{n}) \exp\left[\sum_{\mathbf{q}} d_{\mathbf{q}}\left[u_i(\mathbf{q}) - u_j(\mathbf{q})\right] - \text{ h.c. }\right]$$
$$u_i(\mathbf{q}) = (1/\sqrt{2N})\gamma(\mathbf{q}) \exp(i\mathbf{q}\cdot\mathbf{m})$$

and the direct (density-density) polaron-polaron interaction (see, for example, Ref. 8),

$$H_{p-p} = \frac{1}{2}\sum_{i,j} v(\mathbf{m}-\mathbf{n}) c_i^\dagger c_j^\dagger c_j c_i \tag{13}$$

where $i = (\mathbf{m}, s), j = (\mathbf{n}, s), c_i^\dagger\,(c_i)$ and $d_{\mathbf{q}}^\dagger\,(d_{\mathbf{q}})$ are electron and phonon operators, and $\mathbf{m}$ and s are a lattice vector and spin, respectively.

As opposed to the usual Fröhlich interaction the polaron-phonon one, Eq. (12), contains multiphonon ver-
tices which are dominant. We further show, that this interaction may be treated as perturbation at $\lambda > 1$ both for phonon and polaron GF's (see, also Ref. 11). At large distances the polaron-polaron interaction, Eq. (13), is an effective Coulomb repulsion, $e^2/|\mathbf{m}-\mathbf{n}|\epsilon$, with ϵ being a

dielectric constant. This fact makes it possible to treat H_{p-p} with the usual RPA at least for long-wave excitations. At short distances the polaron-polaron interaction may be attractive, which leads to instability versus SB formation at a low enough temperature. [8]

We consider the polaron-polaron and the polaronphonon correlations only in the normal state, assuming that the temperature is above the critical temperature of SB's formation (see below), which, in turn, is higher than the critical temperature of the superconducting (superfluid) transition.

Taking into account the exponential smallness of the polaron bandwidth one can obtain the "total localization approximation" (TLA) for the polaron GF:

$$G_{ij}\left(\omega_n\right) = \delta_{ij}\left(i\omega_n + \varepsilon_F\right)^{-1} \tag{14}$$

which is useful in calculations in the temperature range $T \gg W$. In TLA:

$$\varepsilon_F = T \ln\left(\frac{v}{2-v}\right) \tag{15}$$

where v is the atomic concentration of carriers, and the SP distribution function: $n_{\mathbf{k}} = \left[\exp\left(\frac{\varepsilon_{\mathbf{k}}-\varepsilon_F}{T}\right)+1\right]^{-1} \simeq \frac{v}{2}\left[1-\frac{\varepsilon_{\mathbf{k}}(2-v)}{2T}\right]$.

If one takes into account the finite polaronic bandwidth $\varepsilon_k \sim W$ one obtains corrections of the order of $\lambda^{-1}\exp\left(-g^2\right)$. They are exponentially small compared to the main power-law contribution from $H_{p-\mathrm{ph}}$ proportional to λ^{-2}.

This contribution of the second and highest orders k in $H_{p-\mathrm{ph}}$ to the polaron self-energy Σ_p^k comes from multiphonon virtual processes (for details see Refs. 4 and 11):

$$\left|\Sigma_p^k\right| \simeq \frac{D^k}{zE_p^{k-1}} \tag{17}$$

The second-order contribution lowers the energy and increases the SP effective mass, while the third-order one diminishes it.

Comparing this contribution with the polaronic shift E_p, Eq. (11), one obtains the criterion of the SP's existence, Eq. (4), with $\lambda = E_p/D$. For a smoothly varying electron density of states (DOS) this definition of the electron-phonon coupling constant is identical to the usual one. [12] Thus I conclude once more (see Ref. 2) that, at least for the Fröhlich interaction the usual strongcoupling theory, [12] which does not take into account the polaron collapse of the electron band, is unacceptable.

In RPA the effect of the polaron-polaron interaction may be described by the dielectric "constant" $\epsilon(\omega, \mathbf{q})$, which gives the response of SP's to longitudinal electric fields of the arbitrary wave vector $\mathbf{q}$ and the frequency ω.

From this the screening behavior of the system and the plasmon frequency can be calculated:

$$\epsilon(\omega, \mathbf{q}) = 1 - 2v(\mathbf{q})\sum_{\mathbf{k}}\left(n_{\mathbf{k}+\mathbf{q}} - n_{\mathbf{k}}\right)\left(\omega - \varepsilon_{\mathbf{k}} + \varepsilon_{\mathbf{k}+\mathbf{q}}\right)^{-1} \tag{18}$$

where $v(\mathbf{q}) = N^{-1}\sum_{\mathbf{m}} v(\mathbf{m})\exp(-i\mathbf{q}\cdot\mathbf{m})$ is the Fourier component of the polaron-polaron interaction. First I consider the static dielectric constant. For $T = 0$ in the long-wave limit, $q \to 0$, we obtain the usual Debye screening:

$$\epsilon(0, q) = 1 + \left(qr_d\right)^{-2} \tag{19}$$

with the Debye radius

$$r_d = \left(\frac{\epsilon}{4\pi e^2 N_p(0)}\right)^{1/2}, \tag{20}$$

where $N_p(0) = N(0)\exp(g^2)$ is the DOS in the polaronic band on the Fermi level, which is exponentially enhanced compared to the bare DOS $N(0)$. One can see from Eq. (20) that the Debye radius of SP's is much smaller than that of bare electrons due to the strong enhancement of their effective mass.

Now I obtain the temperature behavior of the SP response and show that the correlation effect enhances the short-range attraction opposite to the short-range repulsion.

At temperatures $T \gg W$ one can use TLA, Eq. (16), with the following result:

$$\epsilon(0, \mathbf{q}) = 1 + \frac{v(2-v)v(\mathbf{q})N}{2T}. \tag{21}$$

The screened short-range interaction is given by

$$\widetilde{U} = \frac{UT}{T \pm T^*}, \tag{22}$$

where

$$T^* = \frac{|U|v(2-v)}{2} \tag{23}$$

is the characteristic temperature, the upper sign (+) corresponds to the repulsion and the lower one (-) to the attraction. One can see from Eq. (22) that in the temperature region $T < T^*$ the short-range Coulomb repulsion U is sufficiently suppressed by the screening. The twobody collisions reduce the intraatomic Coulomb selfenergy to a magnitude of the order of the polaronic bandwidth for $T \lesssim W$ (see, also, Ref. 13). In the case of attraction the singularity in the two-particle correlator, Eq. (22), occurs at $T = T^*$. Thus T^* is the critical temperature of the SB's formation. The short-range attraction is enhanced near T^*.

One can estimate T^* at which SB's may be formed in metal oxides using the assumption that a large temperature-independent gap observed in $YBa_2Cu_3O_7$, $\Delta_{\text{gap}} = 8k_BT_c$, is of the order of the attraction of two polarons $|U|$.[14] Thus one can estimate,

$$|U| \simeq 720 \text{ K},$$

and using Eq. (23) obtain for $v = 1$

$$T^* \simeq 360 \text{ K}$$

The SP response becomes dynamic for a rather low frequency $\omega > W$:

$$\epsilon(\omega, \mathbf{q}) = 1 - \frac{\omega_p^2}{\omega^2} \tag{24}$$

with the temperature-dependent plasma frequency

$$\omega_p^2(\mathbf{q}) = 2v(\mathbf{q}) \sum_{\mathbf{k}} n_{\mathbf{k}} \left(\varepsilon_{\mathbf{k}+\mathbf{q}} - \varepsilon_{\mathbf{k}}\right) \tag{25}$$

which is proportional to $1/T$ in the temperature range $T \gg W$. For low temperatures $T < W$ the long-wave plasmon has the frequency

$$\omega_p^2 = \frac{4\pi N e^2 v}{m^* \epsilon} \tag{26}$$

which is much lower than the usual one due to the mass enhancement:

$$m^*/m = \exp\left(g^2\right) \tag{27}$$

The small concentration is assumed in Eq. (26), $v \ll 1$.
Thus compared with the bare electrons response the simple RPA shows a rather unusual response of SP's with a small temperature-dependent Debye radius and plasma frequency. In the case of repulsion the polaronic plasmon has a well-defined dispersion for the whole region of wave vectors with a zero damping, Eq. (25). If $v(q) < 0$ for some q, the plasmon disappears in this region of q space.

II. PHONON SELF-ENERGY

Polaron-phonon and polaron-polaron interactions change the phonon propagation. The second order in $H_{p-\mathrm{ph}}$ phonon self-energy Σ_{ph} is given by the sum of diagrams, Fig. 1, which can be expressed in terms of the multiphonon correlator: [9]

$$\Phi_{ij}^{i'j'}(\tau) = \langle T_\tau \hat{\sigma}_{ij}(\tau) \widehat{\sigma}_{i'j'}(0) \rangle \tag{28}$$

where

$$\widehat{\sigma}_{ij}(\tau) = \exp\left(H_0 \tau\right) \widehat{\sigma}_{ij} \exp\left(-H_0 \tau\right) \tag{29}$$

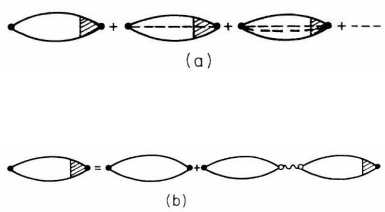

FIG. 1. Phonon self-energy (a) and SP polarization loop (b).

and $-1/T < \tau < 1/T$. The first order in $H_{p-\mathrm{ph}}$ diagrams as well as the second-order terms, containing two polarization loops, are exponentially small, proportional to $\exp\left(-g^2\right)$.[9]

For the real time t the correlator, Eq. (28), was calculated by Lang and Firsov. [15] To obtain $\Phi(\tau)$ one has to make the substitution $t \to -i|\tau|$ with the following result:

$$\Phi_{ij}^{i'j'}(\tau) = \sigma(\mathbf{a})\sigma(\mathbf{b}) \exp\left\{ \frac{1}{N} \sum_{\mathbf{q}} \frac{\gamma^2(\mathbf{q})}{\sinh[\omega(\mathbf{q})/2T]} f_{\mathbf{q}} \cosh\left[\omega(\mathbf{q})\left[\frac{1}{2T} - |\tau|\right]\right]\right\}, \tag{30}$$

where

$$\begin{aligned} f_{\mathbf{q}} = \tfrac{1}{2}\{&\cos(\mathbf{q}\cdot[\mathbf{c}-\mathbf{a}]) + \cos(\mathbf{q}\cdot[\mathbf{c}+\mathbf{b}]) \\ &- \cos(\mathbf{q}\cdot\mathbf{c}) - \cos(\mathbf{q}\cdot[\mathbf{c}-\mathbf{a}+\mathbf{b}])\} \end{aligned} \tag{31}$$

with $\mathbf{a} = \mathbf{m} - \mathbf{n}, \mathbf{b} = \mathbf{m}' - \mathbf{n}', \mathbf{c} = \mathbf{n}' - \mathbf{n}$. The sum of diagrams, Fig. 1(a) gives

$$\Sigma_{\mathrm{ph}}\left(q, \omega_n\right) = -T \sum_{\omega_n} \sum_{iji'j'} \left(u_i^* - u_j^*\right)\left(u_{i'} - u_{j'}\right) \Phi_{ij}^{i'j'}\left(\omega_{n'}\right) \Pi_{iji'j'}\left(\omega_{n'} - \omega_n\right) \tag{32}$$

where

$$\mathbf{\Phi}_{ij}^{i'j'}\left(\omega_n\right) = \frac{1}{2} \int d\tau \left\{ \mathbf{\Phi}_{ij}^{i'j'}(\tau) \exp\left(i\omega_n \tau\right)\right\} \tag{33}$$

and $\omega_n = 2\pi n T$, $\omega_{n'} = 2\pi n' T$.
If one takes for the SP polarization Π a simple loop $\Pi^{(0)}$ (the product of two polaron GF's), one

obtains our previous result. [9] Now I take into account polaronpolaron correlations to obtain in RPA, Fig. 1(b),

$$\Pi_{iji'j'} = \Pi^{(0)}_{iji'j'} + \sum_{l,p} \Pi^{(0)}_{ijll} v(1-\mathbf{p}) \Pi_{ppi'j'}, \tag{34}$$

where the Matsubara frequency ω_n, which is the same in all terms, is omitted. To solve Eq. (34) one can take the Fourier transformation of Π:

$$\Pi_{iji'j'} = \frac{1}{N^3} \sum_{\mathbf{k},\mathbf{k}',\mathbf{g}} \Pi\left(\mathbf{k},\mathbf{k}',\mathbf{g}\right) \exp\left[-i\mathbf{k}\cdot\left(\mathbf{m}'-\mathbf{n}\right) + i\mathbf{k}'\cdot\left(\mathbf{n}'-\mathbf{m}\right) + i\mathbf{g}\cdot\left(\mathbf{m}'-\mathbf{n}'\right)\right] \tag{35}$$

with the Fourier component, which can be derived from the following equation:

$$\Pi\left(\mathbf{k},\mathbf{k}',\mathbf{g}\right) = \Pi^{(0)}\left(\mathbf{k},\mathbf{k}'\right) \left[N\delta_{\mathbf{g},0} + v\left(\mathbf{k}-\mathbf{k}'\right) \sum_{\mathbf{g}'} \Pi\left(\mathbf{k}+\mathbf{g}'-\mathbf{g},\mathbf{k}'+\mathbf{g}'-\mathbf{g},\mathbf{g}'\right) \right] \tag{36}$$

where

$$\Pi^{(0)}\left(\mathbf{k},\mathbf{k}'\right) = 2\frac{n_{\mathbf{k}} - n_{\mathbf{k}'}}{i\omega_n + \varepsilon_{\mathbf{k}} - \varepsilon_{\mathbf{k}'}} \tag{37}$$

One can change in Eq. (36) $\mathbf{k},\mathbf{k}'$ in $\mathbf{k}+\mathbf{g},\mathbf{k}'+\mathbf{g}$, respectively, to obtain

$$\begin{aligned}\Pi\left(\mathbf{k}+\mathbf{g},\mathbf{k}'+\mathbf{g},\mathbf{g}\right) =& \Pi^{(0)}\left(\mathbf{k}+\mathbf{g},\mathbf{k}'+\mathbf{g}\right) \\ & \times \left[N\delta_{\mathbf{g},0} + v\left(\mathbf{k}-\mathbf{k}'\right) A\left(\mathbf{k},\mathbf{k}'\right)\right]\end{aligned} \tag{38}$$

with $A\left(\mathbf{k},\mathbf{k}'\right) = \sum_{\mathbf{g}'} \mathbf{\Pi}\left(\mathbf{k}+\mathbf{g},\mathbf{k}'+\mathbf{g}',\mathbf{g}'\right)$. Taking the sum in Eq. (38) over $\mathbf{g}$ one finds

$$A\left(\mathbf{k},\mathbf{k}'\right) = N\Pi^{(0)}\left(\mathbf{k},\mathbf{k}'\right) \epsilon^{-1}\left(i\omega_n, \mathbf{k}-\mathbf{k}'\right) \tag{39}$$

Substituting Eq. (39) in Eq. (38), one obtains

$$\Pi\left(\mathbf{k},\mathbf{k}',\mathbf{g}\right) = N\Pi^{(0)}\left(\mathbf{k},\mathbf{k}'\right) \left[\delta_{\mathbf{g},0} + v\left(\mathbf{k}-\mathbf{k}'\right) \Pi^{(0)}\left(\mathbf{k}-\mathbf{g},\mathbf{k}'-\mathbf{g}\right) \epsilon^{-1}\left(i\omega_n, \mathbf{k}-\mathbf{k}'\right)\right] \tag{40}$$

To calculate the sum in Eq. (32) one can express $\mathbf{\Phi}(\boldsymbol{\tau})$ in the form

$$\Phi(\tau) = \sigma(\mathbf{a})\sigma(\mathbf{b}) + \widetilde{\Phi}(\tau) \tag{41}$$

The function $\widetilde{\Phi}(\tau)$, defined by Eq. (41), behaves like

$$\widetilde{\Phi}(\tau) \sim \exp\left(2g^2 e^{-\omega|\tau|}\right) - 1 \tag{42}$$

changing very quickly with the characteristic time $\tau < E_p^{-1}$. Thus its Fourier component $\widetilde{\Phi}\left(\omega_n\right)$ weakly depends on the frequency for the entire range of ω_n under consideration. Substituting Eq. (42) in Eqs. (33, 32) one obtains

$$\Sigma_{\mathrm{ph}}\left(\mathbf{q},\omega_n\right) = \Sigma^{\mathrm{res}}_{\mathrm{ph}}\left(\mathbf{q},\omega_n\right) - \widetilde{\Delta}(\mathbf{q}) \tag{43}$$

where

$$\Sigma_{\rm ph}^{\rm res}\left(\mathbf{q},\omega_n\right) = -\sum_{i,j,i',j'}\left(u_i^* - u_j^*\right)\left(u_{i'} - u_{j'}\right)\sigma(\mathbf{m}-\mathbf{n})\sigma\left(\mathbf{m}'-\mathbf{n}'\right)\Pi_{iji'j'}\left(-\omega_n\right) \tag{44}$$

is a frequency-dependent resonance contribution and

$$\widetilde{\Delta}(\mathbf{q}) = T\sum_{i,j,i',j'}\left(u_i^* - u_j^*\right)\left(u_{i'} - u_{j'}\right)\sum_{\omega_{n'}}\widetilde{\Phi}_{ij}^{i'j'}\left(\omega_n+\omega_{n'}\right)\Pi_{iji'j'}\left(\omega_{n'}\right) \tag{45}$$

is a softening. The Fourier transformation in Eqs. (44) and (45) gives

$$\Sigma_{\mathbf{ph}}^{\rm res}\left(\mathbf{q},\omega_n\right) = \frac{\gamma^2(\mathbf{q})}{2N^2}\sum_{\mathbf{k},\mathbf{g}}\left(\varepsilon_{\mathbf{k}}\varepsilon_{\mathbf{k}-\mathbf{q}-\mathbf{g}} + \varepsilon_{\mathbf{k}-\mathbf{q}}\varepsilon_{\mathbf{k}-\mathbf{g}} - \varepsilon_{\mathbf{k}-\mathbf{g}}\varepsilon_{\mathbf{k}-\mathbf{q}-\mathbf{g}} - \varepsilon_{\mathbf{k}}\varepsilon_{\mathbf{k}-\mathbf{g}}\right)\Pi\left(\mathbf{k},\mathbf{k}-\mathbf{q},\mathbf{g};\omega_n\right), \tag{46}$$

$$\begin{aligned}\widetilde{\Delta}(\mathbf{q}) = \frac{\gamma^2(\mathbf{q})}{2N^2}\sum_{\mathbf{k},\mathbf{g},\mathbf{k}'}\sum_{\omega'}\widetilde{\Phi}\left(\mathbf{k},\mathbf{k}'+\mathbf{q},-\mathbf{g}\right)\left[\Pi\left(\mathbf{k},\mathbf{k}',-\mathbf{g}-\mathbf{q};\omega_{n'}\right) - \Pi\left(\mathbf{k}\mathbf{k}',-\mathbf{g};\omega_{n'}\right)\right]\\ + \widetilde{\Phi}\left(\mathbf{k}-\mathbf{q},\mathbf{k}',-g\right)\left[\Pi\left(\mathbf{k},\mathbf{k}',-\mathbf{g}+\mathbf{q};\omega_{n'}\right) - \Pi\left(\mathbf{k},\mathbf{k}',-\mathbf{g};\omega_{n'}\right)\right],\end{aligned} \tag{47}$$

with

$$\widetilde{\Phi}_{ij}^{i'j'} = \frac{1}{N^3}\sum_{\mathbf{k},\mathbf{k}',\mathbf{g}}\widetilde{\Phi}\left(\mathbf{k},\mathbf{k}',\mathbf{g}\right)\exp\left[-i\mathbf{k}\cdot\left(\mathbf{m}'-\mathbf{n}\right) + i\mathbf{k}'\cdot\left(\mathbf{n}'-\mathbf{m}\right) + i\mathbf{g}\cdot\left(\mathbf{m}'-\mathbf{n}'\right)\right] \tag{48}$$

To calculate the frequency-dependent contribution $\Sigma_{\rm ph}^{\rm res}$ one can expand the simple polarization loop, using W/ω as a small parameter:

$$\Pi^{(0)}\left(\mathbf{k},\mathbf{k}'\right) = 2\left\{\frac{n_{\mathbf{k}} - n_{\mathbf{k}'}}{i\omega_n} - \frac{\left(n_{\mathbf{k}'} - n_{\mathbf{k}}\right)\left(\varepsilon_{\mathbf{k}} - \varepsilon_{\mathbf{k}'}\right)}{\omega_n^2} + \cdots\right\}. \tag{49}$$

Substitution of Eq. (49) in Eq. (40) and in Eq. (46) gives

$$\Sigma_{\rm ph}^{\rm res}\left(\mathbf{q},\omega_n\right) = -\frac{\beta(\mathbf{q})\omega_p^4(\mathbf{q})}{\omega(\mathbf{q})\left[\omega_n^2 + \omega_p^2(\mathbf{q})\right]}, \tag{50}$$

where

$$\beta(\mathbf{q}) = \frac{\omega(\mathbf{q})\gamma^2(\mathbf{q})}{v(\mathbf{q})} \tag{51}$$

is a dimensionless plasmon-phonon coupling constant.
To obtain the full expression for $\Delta(\mathbf{q})$ one should use TLA, which gives for the polarization

$$\Pi\left(\mathbf{k},\mathbf{k}',\mathbf{g};\omega_n\right) \simeq -N\delta_{\omega_n,0}\frac{v(2-v)}{2T}\left\{\delta_{\mathbf{g},0} - \frac{v\left(\mathbf{k}-\mathbf{k}'\right)v(2-v)}{2T\epsilon\left(0,\mathbf{k}-\mathbf{k}'\right)}\right\}, \tag{52}$$

and also takes into account the diagrams with two external phonon lines attached to the same vertex of Σ_{ph}. The second term in Eq. (52) does not depend on $\mathbf{g}$. Thus one can see that a direct polaron-polaron interaction does not contribute to the softening of phonons:

$$\Delta(\mathbf{q}) = \frac{v(2-v)\gamma^2(\mathbf{q})}{2}\sum_a\left[\widetilde{\Phi}_{\mathbf{a}}\left(\omega_n\right) - \widetilde{\Phi}_{\mathbf{a}}(0)\right]\left[1-\cos(\mathbf{q}\cdot\mathbf{a})\right] \tag{53}$$

where

$$\widetilde{\Phi}_{\mathrm{a}} = \widetilde{\Phi}_{ij}^{ji}. \tag{54}$$

Expanding the exponent in Eq. (30) we find according to the definitions, Eqs. (33), (41), and (54) for dispersionless phonons, $\omega(\mathbf{q}) = \omega_0$:

$$\widetilde{\Phi}_{\mathbf{a}}(\omega_n) = \frac{2\sigma^2(\mathbf{a})}{\omega_0} \sum_{k=1}^{\infty} \sum_{p=0}^{k} \binom{k}{p} \frac{\sinh\left[(k-2p)\omega_0/2T\right]}{2^k k! \sinh^k(\omega_0/2T)} \left(N^{-1} \sum_{\mathbf{q}'} \gamma^2(\mathbf{q}') \left[1 - \cos(\mathbf{q}' \cdot \mathbf{a})\right] \right)^k \frac{(k-2p)\omega_0^2}{(k-2p)^2\omega_0^2 + \omega_n^2}. \tag{55}$$

For the temperature range $T \ll \omega_0$ the terms with $p = 0$ and $p = k$ dominate. As a result one finds

$$\widetilde{\Phi}_{\mathbf{a}}(\omega_n) - \widetilde{\Phi}_{\mathbf{a}}(0) \simeq \frac{t^2(\mathbf{a})}{\omega_0 g^6(\mathbf{a})} \tag{56}$$

and (in Ref. 9Δ contained g^2 instead of the correct g^6)

$$\Delta(\mathbf{q}) = \frac{v(2-v)\gamma^2(\mathbf{q})}{2\omega_0} \sum_{\mathrm{a}} \frac{t^2(\mathbf{a})[1 - \cos(\mathbf{q} \cdot \mathbf{a})]}{g^6(\mathbf{a})} \tag{57}$$

The estimation of the softening, Eq. (57), shows that it is
small compared with the bare frequency ω_0 as $1/\lambda^2$. At high concentrations of carriers the screening due to the exchange polaron-polaron interaction $\widetilde{v}(\mathbf{m})$ diminishes the value of $\Delta(\mathbf{q})$ (for details see the Appendix):

$$\Delta(\mathbf{q}) = \frac{v(2-v)\gamma^2(\mathbf{q})}{2\omega_0} \sum_{\mathbf{a}} \frac{t^2(\mathbf{a})[1 - \cos(\mathbf{q} \cdot \mathbf{a})]}{g^6(\mathbf{a})[1 + \widetilde{v}(\mathbf{a})v(2-v)/2T]}. \tag{58}$$

Thus the strong electron-phonon interaction, $\lambda > \lambda_c$,
results in a rather small plasma frequency, comparable with the phonon one, Eq. (25), and also in the coupling of bare phonons with polaronic plasmons, Eq. (51). The real vibration excitations are a mixture of phonons and plasmons. To obtain the dispersion relation for the phonon-plasmon mixture one has to carry out the analytic continuation of $\Sigma_{\mathrm{ph}}(\mathbf{q}, \omega_n)$ to real frequencies Ω. Taking into account that $\Sigma_{\mathrm{ph}}^{\mathrm{res}}$ has only simple poles $\omega_n = \pm i\omega_p$, Eq. (50), one can obtain this continuation by a simple substitution in Eq. (50):

$$i\omega_n \to \Omega \tag{59}$$

which gives the following equation for the frequency Ω of the plasmon-phonon mixture:

$$\Omega = \omega(\mathbf{q}) + \Sigma_{\mathrm{ph}}(\mathbf{q}, \Omega) \tag{60}$$

or

$$\Omega - \omega(\mathbf{q}) + \Delta(\mathbf{q}) - \frac{\beta(\mathbf{q})\omega_p^4(\mathbf{q})}{\omega(\mathbf{q})\left[\Omega^2 - \omega_p^2(\mathbf{q})\right]} = 0 \tag{61}$$

There are three solutions of Eq. (61):

$$\Omega_1 = \frac{\widetilde{\omega}}{3} + \frac{2}{3}\cos\left(\frac{\alpha}{3}\right)\sqrt{\widetilde{\omega}^2 + \omega_p^2}, \tag{62}$$

$$\Omega_2 = \frac{\widetilde{\omega}}{3} - \frac{2}{3}\cos\left(\frac{\alpha+\pi}{3}\right)\sqrt{\widetilde{\omega}^2 + \omega_p^2}, \tag{63}$$

$$\Omega_3 = \frac{\widetilde{\omega}}{3} - \frac{2}{3}\cos\left(\frac{\alpha-\pi}{3}\right)\sqrt{\widetilde{\omega}^2 + \omega_p^2}, \tag{64}$$

$$\cos(\alpha) = \frac{\widetilde{\omega}^3 - 9\widetilde{\omega}\omega_p^2 + 27\beta\omega_p^4/2\omega}{\sqrt{\left(\widetilde{\omega}^2 + 3\omega_p^2\right)^3}}, \tag{65}$$

and $\widetilde{\omega} = \omega - \Delta$. The dependence on $\mathbf{q}$ of all parameters is assumed in Eqs. (62)-(65).

Only two solutions, Ω_1 and Ω_2, are real and positive. The last one, Ω_3 (or Ω_2, depending on the choice of α) is negative and has no physical meaning.

Thus I conclude that instead of the bare phonon the vibration spectrum of the lattice, strongly coupled to carriers, consists of two branches of excitations, which describe the propagation of the coupled phonon and plasmon. In the case of weak plasmon-phonon coupling $\beta \ll 1$ the dispersions have the form

$$\Omega_{1,2} = \frac{1}{2}\left\{\widetilde{\omega} + \omega_p \pm \left[\left(\widetilde{\omega} - \omega_p\right)^2 + 2\beta\omega_p^3/\omega\right]^{1/2}\right\} \tag{66}$$

In the limit $\beta \to 0\Omega_1(+)$ and $\Omega_2(-)$ describe the phonon with the renormalized frequency $\widetilde{\omega}$ and the plasmon, respectively. The ratio of weights of two contributions of the phonon-plasmon mixture to the phonon GF,

$$D(\mathbf{q}, \Omega) = \sum_{i=1}^{3} \frac{P_i(\mathbf{q})}{\Omega - \Omega_i(\mathbf{q})}, \tag{67}$$

is given by

$$\frac{P_2}{P_1} = \frac{\left(\Omega_2^2 - \omega_p^2\right)\left(\Omega_3 - \Omega_1\right)}{\left(\Omega_1^2 - \omega_p^2\right)\left(\Omega_3 - \Omega_2\right)} \tag{68}$$

Even for a weak coupling this ratio may be of the order of unity:

$$\frac{P_2}{P_1} \simeq \frac{\Delta - \Delta_0}{\Delta + \Delta_0} \tag{69}$$

if the plasmon and phonon frequencies are close enough to each other. Here $\Delta_0 = \widetilde{\omega} - \omega_p$ and $\Delta = \left[\left(\widetilde{\omega} - \omega_p\right)^2 + 2\beta\omega_p^3/\omega\right]^{1/2}$ are the bare and the renormalized gaps between two branches of excitations.

The anomalous extra branch of high-frequency vibrations, observed in neutron-scattering experiments in La_2CuO_4 and probably in $YBa_2Cu_3O_7$, [10] was connected with the strong electron-phonon interaction.

Capellmann [16] proposed a phenomenological model of this phenomenon, in which phonons are coupled to a collective carrier mode with the frequency well below the one-particle continuous spectrum (see also Ref. 17). I explain the two high-frequency modes as bound states of polaronic plasmons with phonons. This assumption allows an estimation of the parameters $\omega_p, \widetilde{\omega}, \beta$ using the experimental values [10] of frequencies Ω_1 and Ω_2 and also their weight ratio, which is about unity in a certain region of q space:

$$\frac{\Omega_1}{2\pi} = 22(\mathrm{THz}), \frac{\Omega_2}{2\pi} = 14(\mathrm{THz}), \frac{P_2}{P_1} \simeq 1 \tag{70}$$

Substituting these figures in Eqs. (66) and (69) one obtains

$$\frac{\omega_p}{2\pi} \simeq \frac{\widetilde{\omega}}{2\pi} = 18(\mathrm{THz}), \frac{\beta\omega_p^3}{4\pi^2\omega} = 34(\mathrm{THz})^2 \tag{71}$$

If one takes the bare phonon frequency of the order of the renormalized one, $\omega \simeq \widetilde{\omega}$, one finds for the coupling

$$\beta \simeq 0.1, \tag{72}$$

which is a lower estimation because in general $\omega > \widetilde{\omega}$.
The extra mode disappears in the long-wave limit, $\mathbf{q} \to 0$.[10] This is the case for intramolecular and acoustic phonons with $\beta(\mathbf{q} \to 0) = 0$, Eq. (51), but is not the case for long-wave optical phonons, for which $\beta \neq 0$ in this limit. The mode also disappears in the short-wave limit. This fact may be connected with the short-range polaron-polaron attraction, $v(\mathbf{q}) < 0$, resulting in the disappearance of the short-wave polaronic plasmon according to Eq. (25). The estimation of the plasmon frequency, Eq. (26), with experimental values of $\epsilon \simeq 50$,[18] $v = 1$ (half-filled band), and $m^* = 25m_e$ (Ref. 19) gives for $La_2CuO_4\omega_p \simeq 110$ (THz), which is surprisingly close to the value, extracted from the neutron scattering, and supporting the phonon-polaronic-plasmon nature of the extra mode. The existence of the extra mode strongly depends on the parameters Δ_0 and β, small changes of which can lead to its disappearance.

To conclude I have shown that the Debye radius and the plasma frequency of SP's are small and temperature dependent, SP's screen effectively the short-range Coulomb repulsion, and enhance the short-range polaron-polaron attraction, the critical temperature of the SB's formation exists, Eq. (23), vibration excitations
of a strongly coupled many-electron-phonon system exist, which are a mixture of polaronic plasmons and phonons. The anomalous extra mode, observed in the neutronscattering experiments in La_2CuO_4 is explained. Two high-frequency branches of the vibrational spectrum are two of these mixtures.

I would also like to remark that the many-body polaronic effects, discussed above, are a result of the polaron collapse of the bare band, Eq. (2), which is a characteristic feature of the small-polaron theory of metal oxides. [2] The renormalized band structure, including the mass renormalization, can be detected with low-energy experiments. High-energy experiments with the characteristic energy of excitations $\delta\epsilon > \Delta_{\mathrm{gap}} \sim 0.1$eV can only detect the bare band structure with the bare mass $m \simeq m_e$, and with the bare plasma frequency $\omega_p^{(0)} > 1$eV.

APPENDIX

The exchange interaction in the form

$$H_{p-p}^{\mathrm{ex}} = \frac{1}{2} \sum_{m \neq n,s,s'} \widetilde{v}(\mathbf{m}-\mathbf{n}) c_{\mathbf{n},s}^{\dagger} c_{\mathbf{m},s'}^{\dagger} c_{\mathbf{n},s'} c_{\mathbf{m},s} \tag{A1}$$

diminishes $\Delta(\mathbf{q})$. The equation for the polarization is now

$$\Pi(\mathbf{k},\mathbf{k}',\mathbf{g}) = \Pi^{(0)}(\mathbf{k},\mathbf{k}') \left[N\delta_{g,0} + \sum_{\mathbf{g}'} \left[v(\mathbf{k}-\mathbf{k}') + \widetilde{v}(\mathbf{g}-\mathbf{g}') \right] \Pi(\mathbf{k}+\mathbf{g}'-\mathbf{g}, \mathbf{k}'+\mathbf{g}'-\mathbf{g}, \mathbf{g}') \right], \tag{A2}$$

with $\tilde{v}(\mathbf{g})$ being the Fourier component of $\tilde{v}(\mathbf{m})$. In TLA $\Pi^{(0)}(\mathbf{k},\mathbf{k}') = \pi_0$ is momentum independent, and $\Pi(\mathbf{k},\mathbf{k}',\mathbf{g}) = \Pi(\mathbf{k}-\mathbf{k}',\mathbf{g})$. For the Fourier component $\Pi(\mathbf{k}-\mathbf{k}',\mathbf{m})$ defined by

$$\Pi\left(\mathbf{k}-\mathbf{k}',\mathbf{g}\right)=\sum_{\mathbf{m}}\Pi\left(\mathbf{k}-\mathbf{k}',\mathbf{m}\right)\exp(i\mathbf{g}\cdot\mathbf{m}) \tag{A3}$$

one obtains from Eq. (A2),

$$\Pi\left(\mathbf{k}-\mathbf{k}',\mathbf{m}\right)=\frac{\pi_0}{1-\pi_0\left[v\left(\mathbf{k}-k'\right)\delta_{\mathbf{m},0}+\widetilde{v}(\mathbf{m})\right]} \tag{A4}$$

Thus
$\Pi\left(\mathbf{k},\mathbf{k}',\mathbf{g}\right)=\frac{\pi_0}{1-\pi_0 v(\mathbf{k}-\mathbf{k}')}+\sum_{\mathbf{m}\neq 0}\frac{\pi_0\exp(i\mathbf{g}\cdot\mathbf{m})}{1-\widetilde{v}(\mathbf{m})\pi_0}$.
Substituting the last equation in Eq. (47) one obtains Eq. (58).

[1] T. Holstein, Ann. Phys. (N.Y.) 8, 343 (1959); in Polarons, edited by Yu. Firsov (Nauka, Moscow, 1975); in Polarons and Excitons, edited by G. B. Kuper and G. D. Whitfield (Oliver and Boyd, Edinburgh, 1963).
[2] A. S. Alexandrov, Physica C 158, 337 (1989); A. S. Alexandrov and E. A. Mazur, Zh. Eksp. Teor. Fiz. 96, 1773 (1989).
[3] A. B. Migdal, Zh. Eksp. Teor. Fiz. 34, 1438 (1958) [Sov. Phys. JETP 34, 996 (1958)]; G. M. Eliashberg, ibid. 38, 966 (1960) [11, 696 (1960)].
[4] A. S. Alexandrov and A. B. Krebs, Pis'ma, Zh. Eksp. Teor. Fiz. 50, 280 (1989) [JETP Lett. 50, 311 (1989)].
[5] E. Emin, Adv. Phys. 22, 57 (1973).
[6] D. M. Eagles, Phys. Rev. 145, 645 (1966).
[7] H. deRaedt and A. Lagendijk, Phys. Rev. B 27, 6097 (1983); Phys. Rev. 30, 1671 (1984); Z. Phys. B Condens. Matter 65, 43 (1986).
[8] A. S. Alexandrov and J. Ranninger, Phys. Rev. B 23, 1796 (1981).
[9] A. S. Alexandrov and H. Capellmann, Phys. Rev. B 43, 2042 (1991).
[10] H. Rietshel, L. Pintschovious, and W. Reichardt, Physica C 162-164, 1705 (1989).
[11] A. A. Gogolin, Phys. Status Solidi B 109, 95 (1982).
[12] D. J. Scalapino, in Superconductivity (Academic, New York, 1969), Vol. 1, p. 449.
[13] J. Kanamori, Prog. Theor. Phys. 30, 275 (1963).
[14] A. S. Alexandrov and D. K. Ray, Philos. Mag. Lett. 63, 295 (1991).
[15] I. G. Lang and Y. A. Firsov, Zh. Eksp. Teor. Fiz. 43, 1843 (1962) [Sov. Phys. JETP 16, 1301 (1963)].
[16] H. Capellmann (private communication).
[17] P. B. Allen, Phys. Rev. B 43, 2766 (1991).
[18] C. Y. Chen, R. J. Birgeneau, D. R. Gabbe, H. P. Jenssen, M. A. Castner, P. J. Picone, N. W. Preyer, and Tineke Thio, Physica C 162-164, 1031 (1989).
[19] C. M. Foster, A. J. Heeger, G. Stacky, and N. Herron, Solid State Commun. 71, 945 (1989).

6.5.5 Kinetic Theory of Semiconductors with Low Mobility by Lang, Firsov 1

1962 Zh.Eksp.Teor.Fiz. 43, 1843-60
(1963 Sov.Phys.JETP 16, 1301-12 (is it an updated version of this article???)).

Abstract

A low mobility theory for semiconductors with a narrow conductivity band (or valence band) is developed for strong coupling between the current carriers and lattice oscillations. At temperatures below the Debye temperature nonlocalized small-radius polarons are the current carriers. The scattering operator for these polarons is singled out and a transport

equation is set up by which various kinetic coefficients can be calculated. It is demonstrated that at temperatures exceeding the Debye temperature the main mechanism of motion is classical superbarrier current-carrier jumps from site to site, in which the lattice actively participates. The temperature dependence of the mobility in this case is of an activation nature. The problem of the smallness parameters of the theory is considered. The results obtained are compared with the data of other authors.

1. INTRODUCTION

It is known that in many semiconductors [1–3] the mobility u increases with the temperature as $\exp[-\mathrm{E_a/kT}]$, starting near the Debye temperature and above ($\mathrm{E_a}$ is the activation energy). It is important to note that in such substances the mobility is very low ($u \ll 1\ \mathrm{cm^2/V-sec}$), and the Hall effect cannot be measured. It can be shown that these facts are closely related. Several papers [4–6] are devoted to an explanation of this temperature dependence of the mobility, and particular notice should be taken of the interesting paper by Holstein. Inasmuch as a dependence of the type $\exp[-\mathrm{E_a/kT}]$ cannot be due to single-phonon or two-phonon carrier scattering processes, it is clear from the very outset that many phonons must participate simultaneously in the processes. But for this purpose the coupling between the carriers and the lattice vibrations should be strong. The criterion for the applicability of the kinetic equation is not satisfied in this case. Indeed, assuming the usual connection between the mobility and the relaxation time τ, we obtain

$$\frac{\hbar}{\tau kT} \approx 20\frac{m}{m^*}\frac{500^\circ\mathbf{k}}{T}\frac{1\ \mathrm{cm^2/V\cdot sec}}{u}. \tag{1}$$

Here m is the mass of the free electron and m^* is the effective mass. Putting $\mathrm{T} \approx 500^\circ\mathbf{k}, \mathrm{m}^* \approx$ m, and $u \leq 1\ \mathrm{cm^2/V\text{-}sec}$, we find that $\hbar/\tau\mathrm{kT} \gg 1$.

One could hope that the strong electron-phonon interaction would so renormalize the carrier mass (polaron) that the ratio $\mathrm{m/m^*}$ would become much smaller than unity. It may turn out then that the observed temperature dependence of the mobility
is due only to the strong dependence of m^* on the temperature. It will become clear from what follows that such an assumption is untrue. Therefore the activation character of the temperature dependence of the mobility indicates that even after the polarons are separated the transitions should remain multiphonon, and the interaction with the lattice remains strong. But this can lead to a situation wherein the uncertainty in the polaron energy $\hbar W_{\mathbf{k}}$ ($W_{\mathbf{k}}$ is the total probability of scattering of a polaron with momentum $\hbar k$) exceeds the width of the polaron band $\Delta\mathrm{E_p}$, although it does remain much smaller than the dip in the polaron level. In this case one can speak of a localized polaron of small radius, but the concept of "polaron band" would seem to lose its meaning.

Following Yamashita and Kurosawa [4], Holstein proposed that in this case the principal role in the mobility mechanism is played by classical polaron jumps above the barrier from one lattice site to another [1)]. The energy $\mathrm{E_a}$ sufficient to overcome the interatomic barrier is acquired by the polaron

from the lattice vibrations, with the ions vibrating about equilibrium positions that are shifted as a result of the polarization of the lattice by the electron. Such a jump over the

[01)] The concept of jumps from site to site is sometimes identified with the "motion mechanism after Fervey." It must be noted that the use of these ideas without any stipulations contradicts quantum mechanics. Indeed, by virtue of the translational invariance in the stationary state, the electron cannot be connected with some definite site, and no matter how narrow the band, an electron packet localized initially near some site will manage after a time on the order of $\hbar/\Delta E$ (where ΔE is the width of the band) to "smear out" over the entire lattice. Therefore the concepts of jumps from site to site can be used only when the electrons interact sufficiently strongly with the lattice vibrations. In other words, for the latter there is no motion mechanism after Fervey in the customary form.

barrier should occur more rapidly than the ordinary quantum-mechanical penetration through the barrier. The time of this penetration $\hbar/\Delta E_p$ (ΔE_p is the width of the polaron zone), and consequently the polaron effect (narrowing down of the zone and increase in the effective mass) decreases the probability of the tunnel penetration and thereby favors the occurrence of the jumps. According to Holstein, the condition under which the jumps predominate over the ordinary mobility mechanism, that is, $\hbar \mathrm{W(g)} > \Delta \mathrm{E_p}$ (where W(g) is the probability of the polaron jumping from site to site and g is the lattice vector drawn from the given site to the neighboring one) coincides exactly with the condition $\hbar \mathrm{W_{\mathbf{k}}} > \Delta \mathrm{E_p}$, and therefore the jumps actually come into play precisely when the concept of the polaron band loses its meaning. However, such a deduction is a consequence of the erroneous equation $\mathrm{W_{\mathbf{k}}} = \mathrm{W}(\mathbf{g})$. We shall show that in fact the inequality $\mathrm{W_{\mathbf{k}}} \gg \mathrm{W}(\mathbf{g})$ takes place, that is, there exists an intermediate region of temperatures in which the uncertainty in the polaron energy is already large ($\hbar \mathrm{W_{\mathbf{k}}} \gtrsim \Delta \mathrm{E_p}$), and jumps over the barrier still make a small contribution to the electric conductivity. It would be interesting to construct a theory for this temperature range, too.

In addition, the transition to the representation of an electron ascribed to a site, which was made by Yamashita and Kurosawa [4] and by Holstein [5] for temperatures on the order of the Debye temperature and above, needs a more rigorous substantiation. In the papers of Yamashita and Kurosawa [4] there is no proof whatever that the zeroth approximation employed (electron at the site) is the best. Holstein's estimates [5] are not complete and have a somewhat artificial character. By virtue of the considerations advanced above, it is desirable to develop a theory which makes it possible to separate judiciously the zeroth approximation and to estimate the discarded term [2)]. It is desirable to start to learn how to calculate such kinetic coefficients as the thermal emf, the Hall coefficient, etc., for which the measures employed in [5] are generally not applicable. We must therefore develop a special technique for interpreting the Kubo

formula [7] for electric conductivity in the case of strong electron-phonon interaction. The present article is devoted to these questions.

2. INITIAL HAMILTONIAN. CANONICAL TRANSFORMATION

Let us expand the quantized electronic $\hat{\psi}$ function in the orthonormalized system of functions φ_{m}, corresponding to the electron density concentrated near the m-th site, that is,

$$\hat{\psi}(\mathbf{r}) = \sum_m a_m \varphi_m(\mathbf{r}) \tag{2}$$

where a_m $(a_m^+)$are the operators of annihilation (production) of electrons on the m-th site. No detailed information concerning these functions, except for the property

$$\varphi_m(\mathbf{r}) = \varphi\left(\mathbf{r} - \mathbf{R}_m\right) \tag{2a}$$

(where $\mathrm{R_m}$ is the radius vector characterizing the position of the site) will be necessary in what follows. For example, these may be Wannier functions [8]. The functions $\varphi_{\mathrm{m}}(\mathrm{r})$ can be sought in the form of an expansion in the atomic functions $\psi^0\left(r - R_m\right)$ of the electron level corresponding to the investigated band, that is,

$$\varphi_m(\mathbf{r}) = \sum_n c_{nm} \psi^0\left(\mathbf{r} - \mathbf{R}_n\right) \tag{3}$$

(for simplicity we assume that the electron level is not degenerate). The coefficients $\mathrm{c_{nm}}$ must be obtained from the condition that the functions $\varphi_{\mathrm{m}}(\mathrm{r})$ are orthonormal. For example,

[02)] We note that the question of the smallness parameters is far from trivial here. Thus, the equation $W_k = W(g)$ used in [s] is the consequence of an insufficiently rigorous analysis of the series for W_k and $W(g)$ (see Sec. 4).

in the nearest-neighbor approximation ($\sum_{\mathrm{g}}$ is the sum over the nearest neighbors) we have $\varphi_m^{(1)}(\mathbf{r}) = \psi^0(\mathbf{r}-\mathbf{R}_m) - \frac{1}{2}\sum_g L(\mathbf{g})\psi^0(\mathbf{r}-\mathbf{R}_m+\mathbf{g})$,
where L(g) is the overlap of the integral wave functions between the nearest neighbors. Apparently the set of functions $\psi^0(\mathbf{r}-\mathbf{R}_{\mathrm{m}})$ is not complete, since (2) and (3) do not include the states corresponding to excited levels [3)].

As a rule, in substances with small mobility there are several atoms in each elementary cell, and their degree of ionicity is high. Then the

jumps occur over ions of the kind for which the affinity to a charge of a given sign is the largest, and therefore the vector $\mathrm{R_m}$ characterizes uniquely the required ion in the m-th elementary cell. In the self-consistent field approximation we write the electronic Hamiltonian in the form

$$H_e = -\frac{\hbar^2}{2m}\Delta + \sum_{n=1}^{N} U(\mathbf{r}-\mathbf{R}_m) \tag{4}$$

Here $U(r-R_m)$ is the potential energy of the electron in the field of the m -th cell.

In the second-quantization representation, the total Hamiltonian of the system is written in the form

$$\begin{aligned}\hat{H} = &\sum_m \varepsilon a_m^+ a_m + \sum_{m,g} J(\mathbf{g}) a_{m+g}^+ a_m + \sum_{\mathbf{q},j} \hbar\omega_{\mathbf{q},j}\left(b_{\mathbf{q}j}^+ b_{\mathbf{q}j} + \frac{1}{2}\right)\\ &- \sum_m a_m^+ a_m \sum_{\mathbf{q},j} \hbar\omega_{\mathbf{q},j}\left[u_{mj}^*(\mathbf{q}) b_{\mathbf{q}} + u_{mj}(\mathbf{q}) b_{\mathbf{q}}^+\right]\\ &- \sum_{m,g} a_{m+g}^+ a_m \sum_{\mathbf{q},j} \hbar\omega_{\mathbf{q}j}\left[I_j^*(\mathbf{g},\mathbf{q}) u_{mj}^*(\mathbf{q}) b_{\mathbf{q}j}\right.\\ &\left.+ I_i(\mathbf{g},\mathbf{q}) u_{mj}(\mathbf{q}) b_{\mathbf{q}j}^+\right]\end{aligned} \tag{5}$$

where $\mathrm{b_q^+}$ $(\mathrm{b_q})$ are the phonon creation (annihilation) operators, j is the number of the oscillation branch, and $\mathrm{u_{mj}(q)} = -\gamma_{\mathrm{qj}}^*(2\ \mathrm{N})^{-1/2}\exp[-\mathrm{iq}\cdot\mathrm{R_m}]$ are dimensionless quantities that characterize the displacements that result from the polarization of the medium by the electron in the m -th site (here N is the number of cells in the crystal and γ_{qj} are coefficients which determine the interaction between the electrons and the phonons of the j -th branch). For the case of interaction with longitudinal optical oscillations of frequency ω_0 when $\mathbf{q}\cdot\mathbf{g} \ll 1$ we have in accordance with [9]

$$|\gamma_{\mathbf{q}}|^2 = \frac{4\pi e^2}{q^2\Omega\hbar\omega_0}\left(\frac{1}{\varepsilon_\infty} - \frac{1}{\varepsilon_0}\right)$$

where Ω is the volume of the elementary cell, while ϵ_0 and ϵ_∞ are the dielectric constants of the crystal with and without account of its ionic parts, respectively. $\mathrm{I_j(q\cdot g)}$ is the dimensionless quantity that characterizes the ratio of the elec-tron-phonon interaction matrix element which is not diagonal in the functions $\varphi_{\mathrm{m}}(\mathrm{r})$ to the diagonal element

03) This approach corresponds to the known strong-coupling approximation in the calculation of bandwidths. It does not enable us to calculate the dielectric constant and determine the character of the electron-phonon interaction at large momentum transfers. However, this does not prevent us from finding all the temperature dependences, and the main parameters of the theory γ [see(10)] and J [see(6)], which are not calculated very accurately in this approximation, can be determined from experiment.

$$\varepsilon = \int \varphi_m^*(\mathbf{r}) H_e \varphi_m(\mathbf{r}) d^3r$$

$$J(\mathbf{g}) = \int \varphi_{m+g}^*(\mathbf{r}) H_e \varphi_m(\mathbf{r}) d^3r \tag{6}$$

The fact that ϵ and J(g) do not depend on the index m follows from property (2a) and reflects the translational invariance of the problem.

Let us leave in (5) the strongest interaction with the longitudinal polarization vibrations [4)] and let us assume that for these vibrations

$$\sum_{\mathbf{q}} |u_m(\mathbf{q})|^2 = \frac{1}{2N} \sum_{\mathbf{q}} |\gamma_{\mathbf{q}}|^2 = \gamma > 1$$

(that is, strong coupling). To be able to retain in (5) only the linear terms in the displacements (that is, in b_q and b_q^+) it is necessary that the fourth term be smaller than the first and the fifth smaller than the second. This means that the constant displacements that arise upon polarization of the surrounding medium by the electron should be small compared with the interatomic distances. But this requirement does not contradict the condition $\gamma \gg 1$, that is, the situation here is the same as in the case of large-radius polarons.

We assume further that $I(g \cdot q) \ll 1$. In any case, in the case of weak overlap of the functions φ_m and φ_{m+g} [that is, at small values of J(g)] this quantity is as small as the ratio $J(g)/\epsilon$. We leave out for the time being the last term of (5), which by virtue of the foregoing will be the smallest. We shall formulate later exact criteria which show when this can be done. Inasmuch as everything depends on the energy difference between the initial and final states, the constant $\in$ drops out everywhere, that is, the first term of (5) can be left out, and since the ratio of the second to the fourth terms in (5) can be arbitrary, the fourth term in (5) cannot be regarded as perturbed.

Let us carry out the canonical transformation

$$\widetilde{H} = e^{-S} H e^{S} \tag{7}$$

where

$$S = \sum_{\mathbf{q},m} a_m^+ a_m \left(b_{\mathbf{q}}^+ u_m(\mathbf{q}) - b_{\mathbf{q}} u_m^*(\mathbf{q}) \right) \tag{7a}$$

With such a choice of S, the following exact relations hold true:

$$\tilde{a}_m = a_m \exp\left[\sum_{\mathbf{q}} \left(b_{\mathbf{q}}^+ u_m(\mathbf{q}) - b_{\mathbf{q}} u_m^*(\mathbf{q}) \right) \right],$$

$$\tilde{a}_{in}^+ = a_m^+ \exp\left[-\sum_{\mathbf{q}} \left(b_{\mathbf{q}}^+ u_m(\mathbf{q}) - b_{\mathbf{q}} u_m^*(\mathbf{q}) \right) \right]; \tag{8}$$

$$\widetilde{b}_{\mathbf{q}} = b_{\mathbf{q}} + \sum_{\mathbf{q}} u_m(\mathbf{q}) a_m^+ a_m$$

$$\widetilde{b}_{\mathbf{q}}^+ = b_{\mathbf{q}}^+ + \sum_{\mathbf{q}} u_m^*(\mathbf{q}) a_m^+ a_m; \tag{9}$$

[04)] The problem can be solved also without this simplification, but the account of the additional interaction with the acoustical phonons would make the final expressions more cumbersome.

$$\widetilde{H} = \sum_m a_m^+ a_m \left(\varepsilon - E_p\right) + \sum_1 \hbar\omega_{\mathbf{q}} \left(b_{\mathbf{q}}^+ b_{\mathbf{q}} + \frac{1}{2}\right)$$
$$+ \sum_{m,g} J(\mathbf{g}) a_{m+g}^+ a_m \hat{\Phi}_{mg}$$
$$- \sum_{m_1 \neq m_2} a_{m_1}^+ a_{m_1} a_{m_2}^+ a_{m_2} \sum_{\mathbf{q}} \hbar\omega_{\mathbf{q}} \operatorname{Re}\left(u_{m_1}^*(\mathbf{q}) u_{m_2}(\mathbf{q})\right), \tag{10}$$

where

$$E_p = \frac{1}{2N} \sum_{\mathbf{q}} \hbar\omega_{\mathbf{q}} \left|\gamma_{\mathbf{q}}\right|^2 = \hbar\bar{\omega}\chi_\gamma$$
$$\Delta_{\mathbf{q}}(m, m+g) = u_m(\mathbf{q}) - u_{m+g}(\mathbf{q})$$
$$\hat{\Phi}_{mg} = \exp\left[\sum_{\mathbf{q}} \left(b_{\mathbf{q}}^+ \Delta_{\mathbf{q}}(m, m+\mathbf{g}) - b_{\mathbf{q}} \Delta_{\mathbf{q}}^*(m, m+\mathbf{g})\right)\right] \tag{tabular}$$

In the derivation of (10) and (10a) we used the identity $\left|\gamma_q\right|^2 = |\gamma - q|^2$, the consequence of which is

$$\frac{1}{N} \sum_{\mathbf{q}} \left|\gamma_{\mathbf{q}}\right|^2 \sin\left[\mathbf{q}\left(\mathbf{R}_m - \mathbf{R}_{m_1}\right)\right] = 0 \tag{11}$$

The fourth term in (10) characterizes the interaction between two electrons at the different sites by exchange of virtual phonons, but it is inconsistent to retain it, since it is smaller than the electron correlations that have been left out from (4). The pair interaction leads to screening at small momentum transfers [10,11], which overdetermines the constant γ of the theory, in view of the corrections that depend on the electron concentration n . These corrections are observable, since the carrier concentration can be varied in semiconductors. For example, the activation energy $\mathrm{E_a}$, which will be shown later on to be proportional to γ, starts to depend with increasing n on the carrier concentration. It is possible that this explains the dependence of the slope of $\ln u$ (as a function of 1/T) on the concentration of Li observed in NiO [1] when $n > 10^{18} - 10^{19}$. Bearing in mind the low carrier concentrations, we leave out the last term in (10).

The value of $\mathrm{E_p}$ (the polaron atomic level shift) in the first term on (10) is the result of eliminating the term with $\mathrm{m_1 = m_2}$ from the last sum in (10). In fact $\left(a_{m_1}^+ a_{m_1}\right)^2$ has the same matrix elements as the operator $a_{m_1}^+ a_{m_1}$. We analogously obtain

$$I_x = e \sum_{mg} a_{m+g}^+ a_m \langle g|\hat{v}_x|0\rangle \hat{\Phi}_{mg} \tag{12}$$

The diagonal elements of the velocity $\mathrm{v_X}$ are identically equal to zero by virtue of the symmetry with respect to time reversal.

Let us make the following transformation:

$$a_m = N^{-1/2} \sum_{\mathbf{k}} a_{\mathbf{k}} e^{i\mathbf{k}\mathbf{R}_m} \tag{13}$$

We add and subtract in (10) the term

$$\sum_{mg} J(\ \mathrm{g}) a_{m+g}^+ a_m \left\langle \Phi_{\mathrm{g}} \right\rangle,$$

where (see Appendix I)

$$\langle\Phi_g\rangle = e^{-S_T(g)}, S_T(g) = \frac{1}{2N}\sum_q |\gamma_q|^2 (1-\cos qg)\,\mathrm{cth}\,\frac{\hbar\omega_q\beta}{2} \tag{14}$$

We then finally obtain $\tilde{\mathrm{H}} = \tilde{\mathrm{H}}_0 + \tilde{\mathrm{H}}'$, where [5)]

$$\widetilde{H}_0 = \sum_{\mathbf{k}} a^+_{\mathbf{k}} a_{\mathbf{k}} \varepsilon(\mathbf{k}) + \sum_{\mathbf{q}} \hbar\omega_{\mathbf{q}} \left(b^+_{\mathbf{q}} b_{\mathbf{q}} + \frac{1}{2}\right)$$

$$\varepsilon(\mathbf{k}) = \varepsilon - E_p + \sum_{\mathbf{g}} J(\mathbf{g}) e^{-i\mathbf{kg}} e^{-S_T(\mathbf{g})} \tag{15a}$$

$$\widetilde{H}' = \sum_{\mathbf{kk}'} a^+_{\mathbf{k}'} a_{\mathbf{k}} \frac{1}{N} \sum_{m\mathbf{g}} J(\mathbf{g}) \left[\hat{\Phi}_{mg} - \langle\Phi_g\rangle\right]$$

$$\times \exp\left\{i\left(\mathbf{k}-\mathbf{k}'\right)\mathbf{R}_m - i\mathbf{k}'\mathbf{g}\right\} \tag{15b}$$

Carrying out an analogous procedure in (12), we obtain $\tilde{I}_{\mathrm{X}} = I^0_{\mathrm{X}} + I'_{\mathrm{X}}$ where

$$I^{(0)}_x = \frac{e}{\hbar}\sum_k a^+_{\mathbf{k}} a_{\mathbf{k}} \frac{\partial}{\partial k_x}\varepsilon(\mathbf{k}), \tag{16a}$$

$$I'_x = e\sum_{\mathbf{kk}'} a^+_{\mathbf{k}'} a_{\mathbf{k}} \frac{1}{N}\sum_{mg} \langle g|v_x|0\rangle \left\{\hat{\Phi}_{mg} - \langle\Phi_g\rangle\right\} \tag{16b}$$

$$\times \exp\left\{i\left(\mathbf{k}-\mathbf{k}'\right)\mathbf{R}_m - i\mathbf{k}'\mathbf{g}\right\}.$$

We note that the operator $\hat{\Phi}_{\mathrm{mg}}$ has translational invariance, that is, it is not changed by the substitution

$$\mathbf{R}_m \to \mathbf{R}_m + \Delta, b_{\mathbf{q}} \to b_{\mathbf{q}} e^{-i\mathbf{q}\Delta}$$

where Δ is some lattice vector. This operator describes processes which lead to a realignment of the lattice vibration relative to new equilibrium positions as the electron moves. If the phonon occupation numbers do not change (and such transitions are described by terms proportional to $\langle\Phi_g\rangle$), then the realignment is completed within the time of motion of the particle, and the particle drags as it were the entire "load of atomic displacements." This is indeed the polaron effect, which leads to mass renormalization, and $\epsilon(\mathbf{k})$ is the polaron energy (compare with [5]). The terms

proportional to $\Delta\hat{\Phi}_{\mathrm{mg}} = \hat{\Phi}_{\mathrm{mg}} - \langle\Phi_{\mathrm{mg}}\rangle$ describe transitions with change in the occupation number, that is, phonon emission and absorption processes resulting from the fact that the realignment of the lattice vibration relative to new equilibrium positions does not have time to run through its complete course. This is precisely why the second term I'_{x} in the current [see (16b)] plays the principal role in the kinetics of the jumps. In the high temperature region and in the absence of a magnetic field, the k - and m -representations [see (13)] lead in the

[0]*cth = coth

[5)] Inclusion of terms proportional to $I(q,g)$ in (5) would cause J to be replaced by

$$\widetilde{J} = J - \frac{1}{N}\sum_{\mathbf{q}} \hbar\omega_{\mathbf{q}} |\gamma_{\mathbf{q}}|^2 \,\mathrm{Re}\, I(\mathbf{q},\mathbf{g})$$

As noted earlier, $\mathrm{I} \approx \mathrm{J}/\epsilon$, and consequently the ratio of the correction to the main term is equal in order of magnitude to the ratio $\mathrm{E_p}/\epsilon$, which for substances of the type considered is usually much less than unity.

lowest approximation to identical results, but in order to find the contribution to the electric conductivity resulting from the tunnel penetration, it is necessary to ascertain the role played by the continuity of the electronic spectrum. This is particularly important in the case of intermediate and low temperatures.

3. GENERAL TRANSPORT EQUATION AND JUMP PROCESSES

Let us use the Kubo formula for the electric conductivity in the form (compare with [12]):

$$\sigma_{xx} = \frac{\beta}{VZ} \operatorname{Re} \int_0^\infty \exp(-s\tau) \operatorname{Sp} \{\exp(-\beta H_0) \times T_C \left[\exp\left(-\frac{i}{\hbar}\int_C H'(z)dz\right) I_x(\tau) I_x(0)\right]\} d\tau \tag{17}$$

Here $\beta = 1/\mathrm{kT}, \mathrm{V}$ is the crystal volume, and Z is the partition function. The symbol $\mathrm{T_C}$ denotes ordering along the contour (Fig. 1). On the left of the trace symbol are the operators $\mathrm{H'(z)}$ in which z is closer to the point $-\mathrm{i}\hbar\beta.\mathrm{H'(z)}$ and $\mathrm{I_X}(\tau)$ are respectively the perturbation (15b) and the current operator in the interaction representation.

If we consider in the current operators corresponding to the zero and τ terminals only the terms $I'_{\mathbf{X}}$ which are nondiagonal in the phonons, then even in the zeroth approximation in $\mathrm{H'}$ we obtain the following final result:

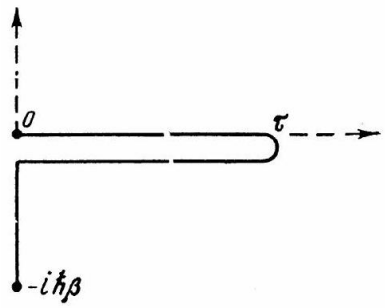

FIG. 1

$$\sigma_{xx}^{(0)} = \frac{ne^2\beta}{V} \operatorname{Re} \frac{1}{N^2} \sum_{\mathbf{k},\mathbf{p}} \sum_{m_1,m_2} \sum_{g_1,g_2} \langle g_1 | v_x | 0\rangle \langle g_2 | v_x | 0\rangle \times \exp\{i[(\mathbf{k}-\mathbf{p})\mathbf{G} - \mathbf{k}\mathbf{g}_1 - \mathbf{p}\mathbf{g}_2]\} Z_0^{-1} e^{-\beta\varepsilon_{\mathbf{k}}} \int_0^\infty \exp\left\{-s\tau + \frac{i}{\hbar}(\varepsilon_{\mathbf{k}} - \varepsilon_p)\tau\right\} \times \{\langle \Phi_{m_1 g_1}(\tau)\Phi_{m_2 g_2}(0)\rangle - \langle \Phi_{g_1}\rangle \langle \Phi_{g_2}\rangle\} d\tau \tag{18}$$

Here n is the electron concentration. It is the result of one "irregular" line (see, for example [12]) from the τ terminal to the zero terminal [6)].

In the derivation of (18), account was taken of the fact that in Boltzmann statistics $\exp[\mu/\mathrm{kT}] = \mathrm{n}/\mathrm{Z_0}$, where μ is the chemical potential and $\mathrm{Z_0} = \mathrm{V}^{-1}\sum_{\mathbf{k}} \exp[-\beta\epsilon(\mathbf{k})]$. Using formula (AI.7) of the Appendix we find that the expression in the curly brackets of (18) is equal to

$$\exp\left[-S_T\left(\mathbf{g}_1\right)-S_T\left(\mathbf{g}_2\right)\right] \times\left\{\exp\left(\frac{1}{N}\sum_{\mathbf{q}}\left|\gamma_{\mathbf{q}}\right|^2\frac{\cos\left[\omega_{\mathbf{q}}(\tau+i\hbar\beta/2)\right]}{\operatorname{sh}\left(\hbar\omega_{\mathbf{q}}\beta/2\right)}a_{1,2}\left(\mathbf{G},\mathbf{g}_1,\mathbf{g}_2\right)\right)-1\right\} \tag{19}$$

where

$$\mathbf{G}=\mathbf{R}_{m_2}-\mathbf{R}_{m_1},$$
$$a_{1,2}=\frac{1}{2}\left[\cos\mathbf{q}\left(\mathbf{G}-\mathbf{g}_1\right)+\cos\mathbf{q}\left(\mathbf{G}+\mathbf{g}_2\right)\right.$$
$$\left.-\cos\mathbf{q}\mathbf{G}-\cos\mathbf{q}\left(\mathbf{G}-\mathbf{g}_1+\mathbf{g}_2\right)\right].$$

It can be shown that if the dispersion of the frequency of the longitudinal optical phonons is taken into account in the form $\omega(\mathrm{q})=\omega_0+\omega_1\cos q\cdot g$ or $\omega^2(q)=\omega_0+\omega_1\cos q\cdot g$ (see [5]), then the sum in the exponent of (19) oscillates and decreases as a function of τ. Consequently, only the contribution near the first saddle point is significant in the integral; at not too small a value of the dispersion the contribution from the next saddle point is exponentially small compared with the contribution from the first point (see, for example [5]).

The subtraction of unity in (19) denotes the elimination of the self-closing of the phonon lines in each of the terminals 0 and τ, that is, they are connected by at least one phonon line, and no divergences of the type 1/s, for which the "free" intersections are responsible, arise (the terminology is taken from [12]).

The saddle-point method is applicable so long as $\gamma/\sinh(\hbar\beta\omega/2)>1$; this is indeed the criterion

that indicates when multiphonon processes are significant. The greatest contribution to (18) is made by the term in which $\mathbf{G}=\mathbf{g}_1=-\mathbf{g}_2$. The remaining terms are small like $\exp\left[-\mathrm{S_T}\right]$. Putting $\epsilon(\mathbf{k})=\epsilon(p)=0$ and summing in (18) with respect to p and k , we again obtain the condition $\mathrm{G}=\mathrm{g}_1=-\mathrm{g}_2$. Here $\mathrm{Z}_0\rightarrow\ \mathrm{N/V}$. Changing over in (18) to a new variable $\mathrm{t}=\tau+\mathrm{i}\hbar\beta/2$, taking the real part of the integral with respect to t (that is, integrating within the limits from 0 to ∞), and expanding $\cos\omega_q t$ in a series near $t=0$ (that is, near the first saddle point), we see that the time within which the integrand decreases sharply (we call this the jump-over time t_0) is

$$t_0^{-1}=\left[\frac{1}{2N}\sum_{\mathbf{q}}\left|\gamma_{\mathbf{q}}\right|^2\frac{\omega_{\mathbf{q}}^2}{\operatorname{sh}\left(\hbar\omega_{\mathbf{q}}\beta/2\right)}(1-\cos\mathbf{qg})\right]^{1/2} \approx\omega_0\left(\frac{\gamma}{\operatorname{sh}\left(\hbar\omega_0\beta/2\right)}\right)^{1/2}>\omega_0 \tag{20}$$

The difference $\epsilon(\mathbf{k})-\epsilon(\mathrm{p})$ in (18) can be neglected if the following conditions are satisfied [7]:

$$\frac{\varepsilon(\mathbf{k})-\varepsilon(\mathbf{p})}{\hbar}t_0\ll 1,\ \text{i.e.},\ \frac{Je^{-S}T}{\hbar\omega_0}\left(\frac{\operatorname{sh}\left(\hbar\omega_0\beta/2\right)}{Y}\right)^{1/2}\ll 1 \tag{21a}$$

$$[\varepsilon(\mathbf{k})-\varepsilon(\mathbf{p})]\beta\ll 1,\ \text{i.e.},\ Je^{-ST}/kT\ll 1 \tag{21b}$$

[06] In asmuch as we confine ourselves in terms linear to the concentration, we shall henceforth consider only graphs with a single irregular electron line.

*sh = sinh.

For the process to be irreversible, that is, for the appearance of a finite resistance, it is necessary that the energy spectrum of the system be continuous. If conditions (21a) and (21b) are satisfied, the continuous spectrum of the polarizationoscillation frequencies plays a more important role than the polaron band. Thus, neglecting the dispersion in the polaron band we obtain [8)]

$$\sigma_{xx}^{(0)} = ne^2\beta\frac{\pi^{1/2}}{2}\sum_g |\langle g|v_x|\,0\Big\rangle|^2\, e^{-E_a/kT}$$
$$\times\left\{\frac{1}{N}\sum_{\mathbf{q}}|\tau_{\mathbf{q}}|^2\,\frac{\omega_{\mathbf{q}}^2}{2}(1-\cos\mathbf{q}g)\,\mathrm{cosec}\,\frac{\hbar\omega_{\mathbf{q}}\beta}{2}\right\}^{-1/2} \tag{22}$$

where

$$E_a = \frac{1}{N\beta}\sum_{\mathbf{q}}|\Upsilon_{\mathbf{q}}|^2\,(1-\cos\mathbf{gq})\ \mathrm{th}\ \frac{\hbar\omega_{\mathbf{q}}\beta}{4}.$$

At high temperatures ($\hbar\omega\beta/4 \ll 1$) we have $\mathrm{E_a} \le \mathrm{E_p}/2$, that is, when $\mathrm{E_p}/2 - \mathrm{E_a} \gg \mathrm{aT}$, the increase in electric conductivity with temperature

like $\exp[-\mathrm{E_a}/\mathrm{kT}]$ is not connected at all with the increase in the number of carriers in the electronic conductivity band due to the dissociation of the localized polarons.

In the nearest-neighbor approximation, when $\langle g|v_X|0\rangle - iJ(g)g_X/\hbar$, we obtain for $\sigma_{XX}^{(0)}$ an expression which coincides, apart from numerical factors (the number of nearest neighbors), with the result of Holstein:

$$\sigma_{xx}^{(0)} \approx \frac{1}{2}ne^{2\beta}\sum_g W_H(g)g_x^2, \tag{23}$$
$$W_H(g) = J^2\sqrt{\pi}e^{-E_{a/k}T}/\hbar^2$$
$$\times\left[\frac{1}{N}\sum_{\mathbf{q}}|\gamma_{\mathbf{q}}|^2\,\frac{\omega_{\mathbf{q}}^2}{2}(1-\cos\mathbf{gq})\,\mathrm{cosec}\,\frac{\hbar\omega_{\mathbf{q}}\beta}{2}\right]^{1/2} \tag{23a}$$

Actually, Holstein's computational procedure was to calculate the jump-over probability $\mathrm{W_H(g)}$ in the first Born approximation, assuming H' to be the perturbation. He then determined the diffusion coefficient as $\mathrm{g}^2\ \mathrm{W_H(g)}$ and calculated the electric conductivity from the Einstein relation. The results coincide, since the operators H' and I' have an identical structure.

It is known that when the integrand of (17) is expanded in powers of H', diverging terms arise, proportional to arbitrary powers of 1/s, starting with the first. In our case, however, because of the terms I'_X in the current, an additional set of finite terms independent of s arises. We call these terms of the Holstein type and replace their subscripts xx by the subscript H. The superscript m is the number of points on the contour (with the exception of the two terminals). The first term of this set, $\sigma_\mathrm{H}^{(0)}$, was just calculated [see (22)]. The term $\sigma_\mathrm{H}^{(1)}$ corresponds to a set of three diagrams, for each of which the operator I'_X is at the terminal 0 and τ, while the third point can be on the upper or lower part of the time contour or on the imaginary axis

077 It follows from the sequel that there are more stringent criteria for the applicability of the theory than (21a) and (21b), that is, the latter are automatically satisfied.

8) If terms proportional to $\mathrm{I(g,q)}$ are taken into account in (5), a correction appears in (22); the ratio of this correction to the principal term is $\left(E_a\hbar\omega_0/\epsilon^2\right)\left(\sinh\left[\hbar\omega_0\beta/2\right]\right)^{-1} \ll 1$.

*th = tanh.

(from 0 to $-i\hbar\beta$) [9]. Using formula (AI.11) with $kT > \hbar\omega_0/2$ we obtain in the nearest-neighbor approximation [10]
a) $\sigma_H^{(1)}/\sigma_H^{(0)} = \eta_1 = J/E_a \ll 1, \quad$ if $g_1 + g_2 + g_3 = 0$,
b) $\sigma_H^{(1)}/\sigma_H^{(0)}$ proportional to e^{-S_T}, if $g_1 + g_2 + g_3 \neq 0$.

For hexagonal and trigonal crystals cases a) and b) are possible, while for cubic crystals only b) is possible. The smallness of the parameter η_1 corresponds to a polaron of small radius (see [5]). The dip in the polaron level E_p exceeds here the width of the electronic band J. Then, owing to the narrowness of the polaron band ($\Delta E_p \approx J \exp[-S_T] \ll J$) it does not overlap the initial band, and all its states are energetically more favored. In the opposite case ($\eta_1 > 1$) the problem becomes more complicated and corresponds to the case of polarons with medium and large radii.

The term $\sigma_H^{(2)}$ (two terminals with operators I'_X and two points on the contour) corresponds to seven diagrams. If at least one of the points lies on the horizontal portions of the contour and each of the terminals is connected by phonon lines only with the point nearest to it, a free intersection arises. This case of closure of the phonon lines will be singled out and included among the diagrams that diverge as 1/s. For example, if the point 1 lies on the lower part of the time contour and point 2 on the upper part, and if 1 is closer to the terminal τ than 2, then the expression under the sign of triple integration with respect to τ, z_1, and z_2 is

$$\begin{gathered}\langle \Delta\Phi_{m_1 g_1}(z_1)\, \Delta\Phi_{mg}(\tau) \Delta\Phi_{m_2 g_2}(z_2)\, \Delta\Phi_{m'g'}(0)\rangle \\ - \langle \Delta\Phi_{m_1 g_1}(z_1)\, \Delta\Phi_{mg}(\tau)\rangle \langle \Delta\Phi_{m_2 g_2}(z_2)\, \Delta\Phi_{m'g'}(0)\rangle \\ \Delta\Phi_{mg}(z) = \hat{\Phi}_{mg}(z) - \langle \Phi_g \rangle \end{gathered} \tag{25}$$

The subtraction procedure must be carried out also for diagrams with a large number of points, and this gives rise to terms proportional to arbitrary powers of 1/s. These must be combined with diagrams with the same order in 1/s, arising when the current $I_X^{(0)}$ is inserted in one or both terminals. The procedure for summing diagrams of the type $(1/s)^n$ will be described below.

For $kT > \hbar\omega_0/2$ we obtain

$$\sigma_H^{(2)}/\sigma_H^{(0)} \approx \eta_2 = J^2/\left(E_a kT\right)^{1/2} \hbar\omega_0,$$

a) $\sigma_H^{(2)}/\sigma_H^{(1)} = (J/\hbar\omega_0)\,(E_a/kT)^{1/2} \geqslant 1$, if $\mathbf{g}_1 + \mathbf{g}_2 + \mathbf{g}_3 = 0$,
b) $\sigma_H^{(2)}/\sigma_H^{(1)}$ proportional to $e^{S_T} \gg 1$, if $\mathbf{g}_1 + \mathbf{g}_2 + \mathbf{g}_3 \neq 0$.

However, the inequality $\sigma_H^{(2)} > \sigma_H^{(1)}$ still does not mean that the series diverges. From an analysis of the next terms of the expansion it follows that

$$\begin{gathered}\sigma_H^{(3)}/\sigma_H^{(1)} \sim \cdots \sim \sigma_H^{(2n+1)}/\sigma_H^{(2n-1)} \sim \cdots \sim \eta_2, \\ \sigma_H^{(2)}/\sigma_H^{(0)} \sim \cdots \sim \sigma_H^{(2n+2)}/\sigma_H^{(2n)} \sim \cdots \sim \eta_2, \end{gathered} \tag{27}$$

and the ratio $\sigma_H^{(2n+1)}/\sigma_H^{(2n)}$ is determined by relations of the type (24).

Thus, the series for the even and odd terms of the Holstein type contain a single parameter η_2, but the first term of the odd series is smaller than the first term of the even series at least in a ratio $\eta_1 : 1$.

---

[09] The diagrams with the current I_x^0 in the left terminal and without free intersections also make a contribution to σ_H, but this contribution is small since it is proportional to $\exp[-S_T]$.

[10] The summation of the diagrams and the integration by the saddle-point method is straightforward but cumbersome. We therefore present only the final results. By way of an example we give in Appendix III a scheme for calculating the second-order probability (block with four points).

Let us proceed to the summation of diagrams containing free intersections. The simplest diagram containing one free intersection is obtained if there are no points on the contour except the terminals 0 and τ, and the latter contain $\mathrm{I}_{\mathrm{x}}^{(0)}$. The next diagram of the type 1/s is obtained if there is at least one point z_1 on the contour. In one of the terminals, say in 0 , we insert I'_X and we close it with point z_1, while in terminal τ we insert $\mathrm{I}_{\mathrm{X}}^{(0)}$. Then a free gap arises between z_1 and τ, and on the left between the points 0 and z_1 lies a multiphonon two-point block. We have already explained how a diagram of the type 1/s arises for four points (two terminals and two points on the contour), etc.

In the general case the factor of the first power of 1/s is a product of two "vertices": the left vertex $r_{1,k}^x$ and the right vertex $r_{2,k}^x$, each of which is a sum of multi-point blocks which contain no free intersections (see Appendix III). The left "vertex" is not equal to the right vertex, since it contains blocks with points on the vertical portion of the contour. Diagrams containing more than one free intersection other than verticles include "horizontal irreducible parts" (see [12]). The sum of all the horizontal irreducible parts (containing no free intersections) will be called the probability W_{pk}. In the aggregate of all the diagrams containing at least one intersection, we separate the right-hand vertex, and the free intersection ahead of it will be included in the left part. For the left part $\mathrm{F}_{\mathbf{k}}^{\mathrm{x}}$ we obtain the equation

$$F_{\mathbf{k}}^x = r_{1,\mathbf{k}}^x \frac{1}{s} + \frac{1}{s} \sum_{\mathbf{p}} F_{\mathbf{p}}^x W_{\mathbf{pk}} \tag{28}$$

Multiplying (28) by s and letting s approach zero, we obtain ultimately

$$r_{1,k}^x + \sum_{\mathbf{p}} F_{\mathbf{p}}^x W_{\mathbf{pk}} = 0 \tag{29}$$

Equation (29) is analogous to the Boltzmann kinetic equation. Therefore we denote the contribution to the electric conductivity associated with it by σ_{B}. In (29) it is possible to segregate the "departure" and "arrival" terms [12]; the former correspond to the probability $\mathrm{W}_{\mathrm{pk}}^{(\mathrm{d})} = -\mathrm{W}_{\mathbf{k}}\delta_{\mathrm{kp}}/\mathrm{N}$. On the diagrams corresponding to these "departure probabilities," in contradiction to those corresponding to "arrival probabilities" $\mathrm{w}_{\mathrm{kp}}^{(\mathrm{ar})}$, there are no phonon lines joining the upper and lower portions of the contour. In the region of low and intermediate temperatures ($\mathrm{kT} < \hbar\omega_0\xi/2$, where
$\xi \leq 1$), this equation determines the entire kinetics for arbitrary coupling between the electrons and the phonons. When $\mathrm{kT} > \hbar\omega_0/2$, it enables us to estimate the contribution made to the electric conductivity by the tunnel penetration, but we shall show that for such temperatures the principal role is played by the jump-over processes.

When $\mathrm{kT} > \hbar\omega_0/2$, Eq. (29) can be readily solved, for by virtue of inequalities of the type (21a) and (21b) the probabilities are practically independent of k and $\mathrm{p}\left(\mathrm{W}_{\mathrm{pk}} \approx \mathrm{W} + \mathrm{W}'_{\mathrm{pk}} \exp\left[-\mathrm{S}_{\mathrm{T}}\right]\right)$. Therefore the arrival terms in (29) vanish (accurate to terms of order $\exp\left[-\mathrm{S}_{\mathrm{T}}\right]$)

$$\sum_{\mathbf{p}} F_{\mathbf{p}}^x W_{\mathbf{pk}}^{(\mathbf{ar})} \approx W \sum_{\mathbf{p}} F_{\mathbf{p}}^x = 0 \tag{30}$$

Equation (30) is satisfied by virtue of the condition $\sum_{\mathrm{p}} \mathrm{F}_{\mathrm{p}}^{\mathrm{x}} = 0$. Consequently

$$F_{\mathbf{k}}^x = r_{1\mathbf{k}}^x / W_{\mathbf{k}} \approx r_{1\mathbf{k}}^x / W \tag{31}$$

It can be shown that the probability $\mathrm{W}_{\mathbf{k}}$ is real, inasmuch as one can set any block, in which l_1 points lie on the upper part of the contour and l_2 points on the lower, in correspondence with a complex-conjugate block with l_2 points on top and l_1 points on the bottom. We ultimately obtain

$$\varsigma_{\mathrm{B}} \approx ne^2\beta W^{-1}\frac{1}{N}\sum_{\mathbf{k}}\mathrm{Re}\,(r^x_{1\mathbf{k}}r^x_{2\mathbf{k}}) \tag{32}$$

We present the results of an analysis of the terms of the series for the departure probability $\mathrm{W}_{\mathbf{k}}$. The first term $\mathrm{W}^{(0)}$ coincides with $\mathrm{W_H(g)}$ [see (23)]. For $\mathrm{W}^{(1)}$ we obtain

$$W^{(1)}/W^{(0)} \approx J/E_a < 1, \quad \text{if} \quad \mathrm{g}_1+\mathrm{g}_2+\mathrm{g}_3 = 0$$

$W^{(1)}/W^{(0)}$ proportional to $\exp\left(-S_{T\gamma_1} - E_a\delta_1/kT\right) \ll 1$,
where $\gamma_1 < 1$ and $\delta_1 \geq 1$ if $\mathbf{g}_1+\mathbf{g}_2+\mathbf{g}_3 \neq 0$.
However, for the term $\mathrm{W}^{(2)}$ (the sum of two blocks P_4 and P_4^* with four points lying either only on the upper part of the contour or only on the lower one) we find (see Appendix III) that when $\hbar\omega_0\beta/2 \ll 1$
$W^{(2)} \approx \left(\frac{J}{E_a}\right)^4 \frac{(kT)^2}{\hbar^2\omega_0}, \quad \frac{W^{(2)}}{W^{(0)}} \approx \frac{J^2}{\hbar\omega_0}\frac{(kT)^{3/2}}{E_a^{7/2}}e^{E_a/kT} \not> 1,$
that is, $\mathrm{W}^{(2)}$, in contradistinction to the Holsteintype term $\sigma_{\mathrm{H}}^{(2)}$, does not contain the factor $\exp\left[-\mathrm{E_a/kT}\right]$. This difference is connected with the fact that in the calculation of $\sigma_{\mathrm{H}}^{(2)}$ we summed seven diagrams (depending on the location of the two additional points on the contour) and in the sum the large terms of the type (34) cancelled out.

We note that the imaginary part of the two-point block lying on the upper part of the contour, which is equal to $\mathrm{J}^2/4\hbar\mathrm{E_a}$, likewise contains no exponential smallness, but it makes no contribution to the probability $\mathrm{W}^{(0)} = \mathrm{W_H(g)} = \mathrm{P}_2 + \mathrm{P}_2^*$.

The calculations show that starting with $\mathrm{W}^{(2)}$ all the even terms of the series $\mathrm{W}^{(2n)}$ contain no exponential smallness of the type $\exp\left[-\mathrm{E_a/kT}\right]$ and $\mathrm{W}^{(2n+2)}/\mathrm{W}^{(2n)} \approx \eta_2$. For the odd terms of the series, starting with $\mathrm{W}^{(3)}$, we obtain $\mathrm{W}^{(2n+1)}/\mathrm{W}^{(2n-1)} \sim \eta_2$, and the ratio $\mathrm{W}^{(3)}/\mathrm{W}^{(2)}$ is small at least as η_1. Thus, we must substitute $\mathrm{W}^{(2)}$ for W in (32). [11)]

In the region of high temperatures ($\mathrm{kT} > \hbar\omega_0/2$), the properties of the series for the vertices are as follows. In the lowest order

$$\begin{aligned} r^{x(0)}_{1\mathbf{k}} = r^{x(0)}_{2\mathbf{k}} &= v_x(\mathbf{k}) = \frac{1}{\hbar}\frac{\partial}{\partial k_x}\varepsilon(\mathbf{k}) \\ &= -\frac{i}{\hbar}\sum_g J(g)g_x e^{-i\mathbf{kg}}e^{-S}T^{(\mathbf{g})} \end{aligned} \tag{35}$$

In the next order (two-point blocks, one of the points is a terminal) we have
$r^{x(1)}_{2\mathbf{k}}/r^{x(0)}_{2\mathbf{k}} \sim e^{-S_T\Upsilon} \ll 1,$
$r^{x(1)}_{1k}/r^{x(0)}_{1k} \approx J/E_a$ for $\mathrm{g}_1+\mathrm{g}_2+\mathrm{g}_3 = 0,$
$r^{x(1)}_{1k}/r^{x(0)}_{1k} \sim e^{-S_T\gamma}$ for $\mathrm{g}_1+\mathrm{g}_2+\mathrm{g}_3 \neq 0,$
where $0 < \gamma < 1$. The series of the odd terms $\mathrm{r}^{\mathrm{x}(2n+1)}_{1\mathbf{k}}$ and $\mathrm{r}^{\mathrm{x}(2n+1)}_{2\mathbf{k}}$ contain as before the parameter η_2, but the saddle points $\mathrm{t}^0_1, \mathrm{t}^0_2, \ldots, \mathrm{t}^0_{2n}$ for all the variables do not lie at zero ($\bar{\omega}\mathrm{t}^0_1, \bar{\omega}\mathrm{t}^0_2, \ldots, \bar{\omega}\mathrm{t}^0_{2n} \approx 1$) in the series of the even terms (starting with two points apart from the terminal). Consequently there is no total cancellation of the factors outside the integrals signs, of the type $\exp\left[-\mathrm{S_T}\left(\mathrm{g}_1\right)\ldots -\mathrm{S_T}\left(\mathrm{g}_{2n+1}\right)\right]$, that is, the even terms are proportional to $\exp\left(-\mathrm{S_T}\gamma_{2n}\right)$, where $0 < \gamma_{2n} < 1$. In addition, near the new saddle points, by virtue of the condition $t_0\omega_0 \ll 1$ [see (20)], we can integrate over all the variables from $-\infty$ to ∞, which yields $\left(\mathrm{Jt_0}/\hbar\right)^{2n}\exp\left(-\mathrm{E_a}\delta_{2n}/\mathrm{kT}\right)$, where $\delta_{2n} > 1$.

We thus have for a vertex with 2 n points

$$r^{x(2n)}_{1\mathbf{k}} \approx r^{x(2n)}_{2\mathbf{k}} \sim v_x(\mathbf{k})\eta_3^n e^{-E_a\delta_{2n}/kT}e^{S_T(1-\gamma_{2n})} \tag{37}$$

where

$$\eta_3 = \left(\frac{Jt_0}{h}\right)^3 = \frac{J^2}{E_a^{kT}} = \eta_2 \frac{\hbar\omega}{(E_a kT)^{1/2}} \ll \eta_2 \tag{37a}$$

It is difficult to obtain the exact values of the

numbers $\delta_{2\mathrm{n}}$ and $\gamma_{2\mathrm{n}}$, for they depend on the form and magnitude of the phonon frequency dispersion and on the form of the dependence of γ_{q} on q . It can be stated, however, that owing to the increase in the number of integration variables ($t_1, \ldots, t_{2n}$), the following relation holds true

$$1 < \delta_2 \lesssim \delta_4 \cdots \leqslant \delta_{2n} \cdots \tag{38}$$

Taking the largest (say the 2 n -th) terms in the series for the vertices, we obtain

$$\frac{\sigma_{\mathrm{B}}^{(2n)}}{\sigma_H^{(0)}} \approx \eta_3^{2n} \eta_2^{-1} \eta_1^{-2} \left(\frac{E_a}{kT}\right)^2 e^{-E_a(2\delta_{2n}-1)/kT} e^{-2S_T\gamma_{2n}} \ll 1, \tag{39}$$

that is, when $\mathrm{E_a} > \mathrm{kT} > \hbar\omega_0/2$ this ratio is exponentially small for any term in the series.

Thus, if $\eta_2 \ll 1$, then the main contribution to the electric conductivity is determined by the equivalent formulas (22) or (23).

6.5.6 Kinetic Theory of Semiconductors with Low Mobility by Lang, Firsov 2

4. DISCUSSION OF RESULTS

Let us present an illustrative physical picture of the phenomena considered above. At sufficiently high temperatures $\sinh(\hbar\omega_0/2\mathrm{kT}) < \gamma(\gamma \gg 1)$, all the processes are essentially multiphonon. When $\mathrm{kT} > \hbar\omega_0/4$ the principal mechanism of motion is by jumps from site to site, and the time Δt between jumps is smaller than the time t_p of tunnel penetration, but much larger than the jump time $\mathrm{t_0}$. Since the jump (collision) time $\mathrm{t_0}$ [see (20)] is much shorter than ω_0^{-1}, the jump occurs so rapidly that the electron jumps out of the polarization well produced by it, shakes off the 'heavy load of atomic displacements' (that is, the process is essentially multiphonon), and ceases to exist as a polaron. But inasmuch as the time between jumps Δt is much longer than ω_0^{-1}, then, on landing on a new site, the electron again has time to produce a polarization well and sink in it (that is, it goes into the polaron state) before it jumps over to a second site, and this jump will occur before the electron can tunnel through the barrier.

Thus, the following inequalities hold true:

$$t_p \geqslant \Delta t \gg t_0, \quad t_0 < \omega_0^{-1}, \quad \Delta t \gg \omega_0^{-1}$$

where

$$t_p = \frac{\hbar}{\Delta E_p} \sim \frac{\hbar}{J} e^S T, \quad t_0 \sim \frac{\hbar}{(E_a kT)^{1/2}},$$
$$\Delta t \approx \frac{1}{W_H} = \frac{\hbar^2}{J^2 t_0} e^{E_a kT}. \tag{40}$$

011) In [4] we actually used for W the zeroth term of the expansion $W^{(0)}$. However, inasmuch as the inequality $W^{(2)} \gg W^{(0)}$ holds true for all temperatures, the results of [4] are incorrect in the region $\mathrm{kT} \leq \hbar\omega_0/2$.

At first glance it is necessary to add to these inequalities still another one, $t_e \approx \hbar/J > \omega_0^{-1}$, which
requires that the electron wave packet spread out more slowly than the time of transition of the electron to the polaron state. It follows from our work, however, that in order for (22) to be valid a weaker condition is necessary:

$$\eta_2 = J^2/\left(E_a kT\right)^{1/2} \hbar\omega_0 \ll 1, \text{ i.e., } t_e > \left(t_0/\omega_0\right)^{1/2}. \tag{41}$$

Condition (41) requires that the initial electron band (of width J) be sufficiently narrow. Incidently, for substances such as NiO , in which it is formed as a result of levels belonging to the unfilled d-shell, the interatomic distances are large; apparently this is precisely the case that is realized.

We note that for arbitrary values of η_2 it is necessary to sum all terms of the series for σ_H, for the probability and for the vertices. From the structure of the terms of the series for σ_H it follows that they are all proportional to $\exp\left(-E_a/kT\right)$, so that we can hope that even in the case of wider bands the contribution to the electric conductivity due to jumps (σ_H) will increase with temperature like $\exp\left(-E_a/kT\right)$, provided the factor preceding the exponential $F\left(\eta_2\right)$ will be a weaker function of the temperature $\left(\eta_2 \sim T^{-1/2}\right)$. If in addition it turns out that the contribution to the electric conductivity due to the jumps is the largest, that is, $\sigma_B < \sigma_H$, then the temperature dependence of the mobility will carry as before an activation character [12)]. The analysis of electric conductivity at low and intermediate temperatures and the calculation of the high frequency conductivity and the hole effect will be the subject of a separate communication.

The authors are grateful to A. I. Ansel'm, L. E. Gurevich, V. L. Gurevich, O. V. Konstantinov, V. I. Perel', G. E. Pikus, and G. M. Éliashberg for useful discussions.

APPENDIX I AVERAGING OF PRODUCTS OF THE TYPE $\hat{\Phi}_{m_1 g_1}\left(z_1\right) \ldots \hat{\Phi}_{m_n g_n}\left(z_n\right)$ OVER THE PHONONS

We consider a block with two points. Representing $\Phi_{ml\ gl}\left(z_l\right)$ in the form $\Pi_q \exp\left[H_l(q)\right]$, where

$$\begin{aligned} H_l(\mathbf{q}) = & \Delta_{\mathbf{q}}\left(m_l, m_l+g_l\right) b_{\mathbf{q}}^{+} e^{i\omega_{\mathbf{q}} z_l} \\ & - \Delta_{\mathbf{q}}^{*}\left(m_l, m_l+\mathbf{g}_l\right) b_{\mathbf{q}} e^{-i\omega_{\mathbf{q}} z_l} \end{aligned} \tag{AI.1}$$

we obtain

$$\begin{aligned} Q_2 = \left\langle \Phi_{m_1 g_1}\left(z_1\right) \Phi_{m_2 g_2}\left(z_2\right)\right\rangle & = \prod_{\mathbf{q}} F_{\mathbf{q}} \\ & = \prod_{\mathbf{q}} 2 \operatorname{sh} \frac{\hbar\omega_{\mathbf{q}}\beta}{2} \left\langle e^{-\hbar\omega_{\mathbf{q}}\beta\left(b_{\mathbf{q}}^{+} b_{\mathbf{q}}+1/2\right)} e^{H_1(\mathbf{q})} e^{H_2(\mathbf{q})} \right\rangle \end{aligned} \tag{AI.2}$$

012) In a recently published article [6] Klinger also investigated the question of low mobility, using the van Hove procedure. [13] However, we strongly disagree with him in many respects, including the question of the limits of validity of the theory (smallness parameters). Klinger states that the main criteria for the applicability of the theory are the conditions (6) in [6], that is, $\Delta t \gg \omega_0^{-1}$ and $t_p \gg \Delta t$. It follows from our work, however, that in order for (22)-(23a) to be valid [compare with (9) and (10) in [6]) it is necessary to satisfy the more stringent requirements $\eta_1 \ll 1$ and $\eta_2 \ll 1$, that is, the initial electron band should be narrow, and the carriers must be polarons of small radius. In [6] no separation is made in the contributions to the mobility made by the transport processes of the ordinary type and made by the jumps, which may lead to an incorrect estimate of the next approximations. Apparently, these are precisely the reasons for the discrepancies.

Inasmuch as the commutator [H_2, H_1] is a number, the following formula holds

$$e^{H_1+H_2} = e^{H_1} e^{H_2} e^{1/2\,[H_2, H_1]}\,. \tag{AI.3}$$

Using twice the formula (AI.3), we reduce F_q to the form

$$\begin{aligned} F_{\mathbf{q}} = &\left(1 - e^{-\hbar\omega_{\mathbf{q}}^{\beta}}\right) e^{-1/2[H_2,H_1]-1/2|\delta_{\mathbf{q}}|^2} \\ &\times \mathrm{Sp}\left\{e^{-\hbar\omega_{\mathbf{q}}\beta_{\mathbf{q}}^{b+b}q^{\delta}e_{\mathbf{q}}^{\delta}b_{\mathbf{q}}^{+}}e^{-\delta_{\mathbf{q}}^{*}b_{\mathbf{q}}}\right\} \end{aligned} \tag{AI.4}$$

where

$$\delta_{\mathbf{q}} = \Delta_{\mathbf{q}}\left(m_1, m_1 + g_1\right) e^{i\omega_{\mathbf{q}} z_1} + \Delta_{\mathbf{q}}\left(m_2, m_2 + g_2\right) e^{i\omega_{\mathbf{q}} z_2} \tag{AI.5}$$

Putting $\exp\left[-\hbar\omega_q\beta\right] = \alpha_q$, we write the trace of the curly bracket in (AI.4) in the form

$$\begin{aligned} &\sum_{N,n<N} \alpha_{\mathbf{q}}^{N}(-1)^n \frac{|\delta_{\mathbf{q}}|^{2n}}{(n!)^2} N(N-1)\ldots(N-n+1) \\ &= \sum_{n=0}^{\infty}(-1)^n \frac{|\delta_{\mathbf{q}}|^{2n}}{(n!)^2}\alpha_{\mathbf{q}}^{n}\frac{d^n}{d\alpha_{\mathbf{q}}^{n}}\sum_{N=0}^{\infty}\alpha_{\mathbf{q}}^{N}. \end{aligned} \tag{AI.6}$$

Taking the sum over N and differentiating it n times, we obtain n in the numerator, after which the series over n adds up to an exponential, that is, (AI.6) turns out equal to $\exp\left[-\left|\delta_q\right|^2 N_q\right] / \left(1 - \alpha_q\right)$, where N_q is the Planck function. We ultimately get

$$\begin{aligned} Q_2 = &\left\langle \hat{\Phi}_{m_1 g_1}\left(z_1\right)\hat{\Phi}_{m_2 g_2}\left(z_2\right)\right\rangle = e^{-S_T(\mathbf{g}_1)-S_T(\mathbf{g}_2)} \\ &\times \exp\left[\frac{1}{N}\sum_{\mathbf{q}}\frac{|r_{\mathbf{q}}|^2}{\mathrm{sh}\left(\hbar\omega_{\mathbf{q}}\beta/2\right)} a_{1,2}\left(\mathbf{G}, \mathbf{g}_1, \mathbf{g}_2\right)\cos\omega_{\mathbf{q}}\left(z_1 - z_2 + \frac{i\hbar\beta}{2}\right)\right] \end{aligned} \tag{AI.7}$$

where

$$\begin{aligned} a_{1,2}\left(\mathbf{G}, \mathbf{g}_1, \mathbf{g}_2\right) = &\frac{1}{2}\left[\cos\mathbf{q}\left(\mathbf{G} - \mathbf{g}_1\right) + \cos\mathbf{q}\left(\mathbf{G} + \mathbf{g}_2\right)\right. \\ &\left. - \cos\mathbf{q}\mathbf{G} - \cos\mathbf{q}\left(\mathbf{G} - \mathbf{g}_1 + \mathbf{g}_2\right)\right], \\ S_T(\mathbf{g}) = &\frac{1}{2N}\sum_{\mathbf{q}}\left|\gamma_{\mathbf{q}}\right|^2 \mathrm{cth}\,\frac{\hbar\omega_{\mathbf{q}}\beta}{2}(1 - \cos\mathbf{q}), \mathbf{G} = \mathbf{R}_{m_2} - \mathbf{R}_{m_1}. \end{aligned} \tag{AI.8}$$

In order to calculate $\left\langle \hat{\Phi}_{m_1 q_1}\left(z_1\right)\right\rangle$, we use (AI.3) and (AI.6). Putting

$$\begin{aligned} H_1(\mathbf{q}) = b_{\mathbf{q}}^{+} e^{i\omega_{\mathbf{q}} z_1}\delta_{\mathbf{q}}, H_2(\mathbf{q}) = b_{\mathbf{q}} e^{-i\omega_{\mathbf{q}} z_1}\delta_{\mathbf{q}}^{*}, \delta_{\mathbf{q}} \\ = \Delta_{\mathbf{q}}\left(m_1, m_1 + g_1\right) \end{aligned} \tag{AI.9}$$

we obtain

$$Q_1 = \left\langle \Phi_{m_1 g_1}\left(z_1\right)\right\rangle = e^{-S_T(g_1)} \tag{AI.10}$$

[0]*cth = coth.

The expression for the case of three points has the form

$$Q_3 = e^{-S_T(\mathbf{g}_1)-S_T(\mathbf{g}_2)-S_T(\mathbf{g}_3)} \times \exp\left\{\frac{1}{N}\sum_{\mathbf{q}} \frac{|\gamma_{\mathbf{q}}|^2}{\operatorname{sh}(\hbar\omega_{\mathbf{q}}\beta/2)}\left(a_{12}f_{12}+a_{13}f_{13}+a_{23}f_{23}\right)\right\} \tag{AI.11}$$

where $f_{ik} = \cos\omega_q\left(z_i - z_k + i\hbar\beta/2\right)$, a_{ik} coincides in form with $a_{1,2}$ in (AI.8), but in this case $G = R_{m_k} - R_{m_i}$. The generalization to include the case of an arbitrary number of points $\mathrm{z}_1, \mathrm{z}_2, \ldots, \mathrm{z}_\mathrm{n}$ is obvious.

APPENDIX II THE 1/s RULE FOR FREE INTERSECTIONS

This rule was proved earlier [12] for weak electron-phonon interaction. Let us prove it for our case. If a free intersection exists between z_n and z_{n+1} (see Fig. 2), then in expressions of the type (AI.11) the time arguments with $\mathrm{m}_1 \geq \mathrm{n}+1$ and $\mathrm{m}_2 \leq \mathrm{n}$ are not coupled. We assume that

$$l_{nm}(z) = \exp\left[\frac{1}{N}\sum_{\mathbf{q}} \frac{|\Upsilon_{\mathbf{q}}|^2}{\operatorname{sh}(\hbar\omega_{\mathbf{q}}\beta/2)} a_{nm} f_{nm}(z)\right]$$

and then the expression corresponding to Fig. 2 is written in the form

$$\begin{aligned}
&\lim_{\substack{T\to\infty\\ s\to 0}}^{T} dz_n \int_{z_n}^{T} d\tau \int_{z_n}^{\tau} dz_1 \ldots \int_{z_n}^{z_{n-2}} dz_{n-1} e^{-s\tau} l_{0,1}\left(\tau - z_1\right) l_{0,2} \\
&\quad \times \left(\tau - z_2\right) \ldots l_{0,n}\left(\tau - z_n\right) \\
&\quad \times l_{1,2}\left(z_1 - z_2\right) \ldots l_{1,n}\left(z_1 - z_n\right) \ldots l_{n-1,n} \\
&\quad \times \left(z_{n-1} - z_n\right) \varphi\left(z_n\right)
\end{aligned} \tag{AII.1}$$

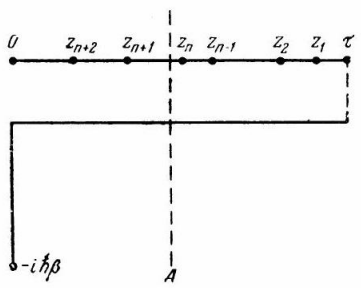

FIG. 2

where $\varphi\left(z_n\right)$ is an expression corresponding to the part to the left of the intersection A:

$$\begin{aligned}
\varphi\left(z_n\right) &= \int_0^{z_n} dz_{n+1} \int_0^{z_{n+1}} dz_{n+2} l_{n+1,n+2}\left(z_{n+1} - z_{n+2}\right) \ldots \\
&= \int_0^{z_n} dz_{n+1} F\left(z_{n+1}\right)
\end{aligned} \tag{AII.2}$$

The expression $F(z_{n+1})$ contains in principle arbitrarily many free intersections, but is independent of z_n. In the Kubo formula it is necessary first to let $T \to \infty$, and then $s \to 0$. Let us make the change of variables

$$\tau = \tau' + z_n, \quad z_1 = z_1' + z_n, \quad z_{n-1} = z_{n-1}' + z_n.$$

(AII.3)
Then expression (AII.1) assumes the form

$$\lim_{\substack{T\to\infty \\ s\to 0}} \int_0^T e^{izn}\varphi(z_n)\,dz_n \int_0^{T-z_n} e^{-s\tau}d\tau \int_0^{\tau} dz_1$$
$$\ldots \int_0^{z_{n-2}} dz_{n-1} l_{0,1}(\tau - z_1)\, l_{0,2}(\tau - z_2)$$
$$\ldots l_{0,n}(\tau) l_{1,2}(z_1 - z_2) \ldots l_{1,n}(z_1) \ldots l_{n-1,n}(z_{n-1}) \qquad \text{(AII.4)}$$

Making the transitions to the limit in the proper sequence, we replace the limit $\mathrm{T} - \mathrm{z_n}$ in the second integral by T and the entire remaining multiple integral, which does not depend on $\mathrm{z_n}$, we denote by $\mathrm{r}_{2,\mathbf{k}}^{\mathrm{x(n)}}$-this is the right vertex of n -th order. Using expression (AII.2) for $\varphi(\mathrm{z_n})$, we integrate with respect to $\mathrm{z_n}$ by parts. We ultimately obtain

$$\frac{1}{s}\int_0^{\infty} e^{-sz_{n+1}} F_{\mathbf{pk}}(z_{n+1})\, dz_{n+1} r_{2,\mathbf{k}}^{x(n)} \qquad \text{(AII.5)}$$

If free intersections are still contained in $F(z_{n+1})$, then, using analogous procedure and denoting again the block separated on the right by $\mathrm{W_{p'}}\mathbf{k}$, we obtain

$$\int_0^{\infty} e^{-sz} F_{\mathrm{pp'}}(z) \frac{1}{s} W_{\mathrm{p'}\mathbf{k}} \frac{1}{s} r_{2,\mathbf{k}}^{x(n)} dz \qquad \text{(AII.6)}$$

etc. This property enables us to write down equations (28) and (29).

APPENDIX III CALCULATIONS OF THE "DEPARTURE PROBABILITY" $\mathrm{W}_{\mathbf{k}}^{(2)}$

The quantity $\mathrm{W}_{\mathbf{k}}^{(2)}$ taken with the opposite sign is equal to twice the real part of P_4, corresponding to the diagram on Fig. 3. The contribution

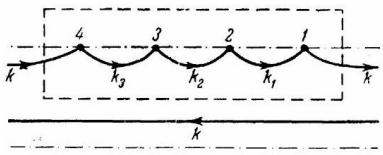

FIG. 3

from diagrams with two overlapping blocks (one in the upper part of the contour, the other under it on the lower part) is omitted, since it is proportional to $\exp[-\mathrm{E_a/kT}]$. We put

$$\Phi_i = \Phi_{m_i g_i}(z_i), \omega_{kp} = (\varepsilon_k - \varepsilon_p)/\hbar, z_4 = 0$$

then

$$
\begin{aligned}
W_{\mathbf{k}}^{(2)} = & -2\,\mathrm{Re}\left(\frac{iJ}{\hbar}\right)^4 \frac{1}{N^4} \sum_{\mathbf{k}_1\mathbf{k}_2\mathbf{k}_3} \sum_{m_1 m_2 m_3 m_4} \exp\{i\,[\mathbf{k}\,(\mathbf{m}_4 - \mathbf{m}_1 - \mathbf{g}_1) \\
& + \mathbf{k}_1\,(\mathbf{m}_1 - \mathbf{m}_2 - \mathbf{g}_2) + \mathbf{k}_2\,(\mathbf{m}_2 - \mathbf{m}_3 - \mathbf{g}_3) \\
& + \mathbf{k}_3\,(\mathbf{m}_3 - \mathbf{m}_4 - \mathbf{g}_4)]\} \int_0^\infty dz_1 \int_0^{z_1} dz_2 \int_0^{z_2} dz_3 \exp\{i\,(\omega_{\mathbf{k}_1} z_1 \\
& + \omega_{\mathbf{k}_1\mathbf{k}_2} z_2 + \omega_{\mathbf{k}_2\mathbf{k}_3} z_3)\} \langle\langle \Phi_1\Phi_2\Phi_3\Phi_4 \rangle\rangle \\
& - \langle \Phi_1\Phi_2 \rangle \langle \Phi_3\Phi_4 \rangle - \langle \Phi_1 \rangle \langle \Phi_2\Phi_3\Phi_4 \rangle - \ldots \\
& + \langle \Phi_2 \rangle \langle \Phi_3 \rangle \langle \Phi_1\Phi_4 \rangle + \ldots - 2\,\langle \Phi_1 \rangle \langle \Phi_2 \rangle \langle \Phi_3 \rangle \langle \Phi_4 \rangle\}
\end{aligned}
\tag{AIII.1}
$$

The third and following terms in the curly bracket in (AIII.1) are small compared with the first two in a ratio $\exp(-\mathrm{S_T}\gamma)$, where $\gamma \gtrsim 1$. We replace quantities of the type $\exp(i\omega_{\mathrm{kk_1}}\mathrm{z_1})$ by unity by virtue of (21a) and (21b). Summing over k_1, k_2, and k_3 we obtain

$$\mathrm{m_1 - m_2 = g_2,\ m_2 - m_3 = g_3,\ m_3 - m_4 = g_4.}$$

The largest result that does not depend on $\mathbf{k}$ is obtained under the condition $\mathbf{g}_1 + \mathbf{g}_2 + \mathbf{g}_3 + \mathbf{g}_4 = 0$. The sum over $\mathrm{m_1}$ is equal to N . Let us put $\mathrm{g_1 = -g_2 = g_3 = -g_4 = g}$. Then

$$a_{1,2} = a_{2,3} = a_{3,4} = a_{\mathbf{q}}, \quad a_{1,3} = a_{2,4} = -a_{\mathbf{q}},$$

where $\mathrm{a_q = 1 - \cos q \cdot g}$ (see AI.8). Making the change of variables $z_1 = t_1 + t_2 + t_3$, $z_2 = t_2 + t_3$, and $\mathrm{z_3 = t_3}$ and putting

$$\cos\omega_{\mathbf{q}}(u + i\hbar\beta/2) = f_{\mathbf{q}}(u)$$

we get

$$
\begin{aligned}
W_{\mathbf{k}}^{(2)} = & -2\,\mathrm{Re}\left(\frac{J}{\hbar}\right)^4 \int_0^\infty dt_1 \int_0^\infty dt_2 \int_0^\infty dt_3 \left\{ \exp\left[\frac{1}{N}\sum_{\mathbf{q}} \Gamma_{\mathbf{q}}\,(f_{\mathbf{q}}\,(t_1)\right.\right. \\
& + f_{\mathbf{q}}\,(t_2) + f_{\mathbf{q}}\,(t_3) + f_{\mathbf{q}}\,(t_1 + t_2 + t_3) - f_{\mathbf{q}}\,(t_1 + t_2) \\
& \left. - f_{\mathbf{q}}\,(t_2 + t_3)) - 4S_T] \right. \\
& \left. - \exp\left[\frac{1}{N}\sum_{\mathbf{q}} \Gamma_{\mathbf{q}}\,(f_{\mathbf{q}}\,(t_1) + f_{\mathbf{q}}\,(t_3)) - 4S_T\right]\right\}, \\
& \Gamma_{\mathbf{q}} = |\gamma_{\mathbf{q}}|^2\, a_{\mathbf{q}} / \operatorname{sh}\frac{\hbar\omega_{\mathbf{q}}\beta}{2}.
\end{aligned}
\tag{AIII.2}
$$

Let us put $\mathrm{t_1' = t_1 + i\hbar\beta/2}$, and let us break up the integral with respect to t_1' into two parts, with limits from $i\hbar\beta/2$ to 0 and from 0 to ∞. The second part is exponentially small, since both exponents in (AIII.2) have for $t_1' = t_2 = t_3 = 0$ a value

$$\frac{1}{N}\sum_{\mathbf{q}} |\Upsilon_{\mathbf{q}}|^2\, a_{\mathbf{q}} \left(\operatorname{cosec}\frac{\hbar\omega_{\mathbf{q}}\beta}{2} + \operatorname{cth}\frac{\hbar\omega_{\mathbf{q}}\beta}{2}\right) - 4S_T \approx -E_a/kT$$

that is, the second part can be discarded. In the first part the essential contribution is near $t_1' = \mathrm{i}\hbar\beta/2$, where the exponents vanish. Let us put $\mathrm{t_2' = t_2 + i\hbar\beta/2}$ and break up the integral with respect to $\mathrm{t_2'}$ into two, with limits from it $\beta/2$ to 0 and from 0 to ∞. We introduce $\mathrm{t_1' = i\hbar\beta/2 - iv_1}$ and $t_2' = iv_2$, and transform the first exponent in the first integral to the form

$$\frac{1}{N}\sum_{\mathbf{q}}\Gamma_{\mathbf{q}}\left[\operatorname{ch}\left(\frac{\hbar\omega_{\mathbf{q}}\beta}{2}-\omega_{\mathbf{q}}v_1\right)-\operatorname{ch}\omega_{\mathbf{q}}\left(v_2-v_1\right)+\operatorname{ch}\omega_{\mathbf{q}}v_2\right.$$
$$\left.+\sqrt{F_1^2(\mathbf{q})-F_2^2(\mathbf{q})}\cos\omega_{\mathbf{q}}\left(t_2+iz\right)-4S_T\right.$$

$F_1(\mathbf{q})=\operatorname{ch}\omega_{\mathbf{q}}\left(v_2-v_1\right)+\operatorname{ch}\frac{\hbar\omega_{\mathbf{q}}\beta}{2}-\operatorname{ch}\omega_{\mathbf{q}}v_2,$
$F_2(\mathbf{q})=\operatorname{sh}\omega_{\mathbf{q}}\left(v_2-v_1\right)+\operatorname{sh}\frac{\hbar\omega_{\mathbf{q}}\beta}{2}-\operatorname{sh}\omega_{\mathbf{q}}v_3,$ (AIII.3)* where $\tanh\omega_{\mathrm{q}}\mathrm{z}=\mathrm{F}_2/\mathrm{F}_1$.

Putting $u_3=t_3+iz$ and leaving the limits of integration with respect to v_3 from 0 to ∞ (since we are taking the real part), we obtain that near $\mathrm{v}_3=0$ (the first saddle point) the exponent does not exceed

$$-\frac{1}{N}\sum_{\mathbf{q}}\left|\gamma_{\mathbf{q}}\right|^2 a_{\mathbf{q}}\ \mathrm{th}\ \frac{\hbar\omega_{\mathbf{q}}\beta}{4}\approx-\frac{E_a}{kT}$$

no matter what the value of v_1 or v_2, that is, the contribution is exponentially small.

Thus, the first integral can be discarded. In the second integral (from 0 to ∞ with respect to t_2') we put $t_1'=i\hbar\beta/2-iv_1$ and expand both exponents (see AIII.2) in powers of v_1, retaining the first term on the expansion. Integrating with respect to v_1 we obtain

$$W^{(2)}=-2\left(\frac{J}{\hbar}\right)^4 e^{-2S_T}\operatorname{Im}\int_0^\infty dt_2'\int_0^\infty dt_3\exp\left[\frac{1}{N}\sum_{\mathbf{q}}\frac{\left|\gamma_{\mathbf{q}}\right|^2 a_{\mathbf{q}}}{\operatorname{sh}\left(\hbar\omega_{\mathbf{q}}\beta/2\right)}\right.$$
$$\left.\times\cos\omega_{\mathbf{q}}\left(t_3\div\frac{i\hbar\beta}{2}\right)\right]R\left(t_2',t_3\right),\qquad\text{(AIII.4)}$$

where

$$R\left(t_2',t_3\right)=\left\{\frac{1}{N}\sum_{\mathbf{q}}\Gamma_{\mathbf{q}}\omega_{\mathbf{q}}\left[\operatorname{sh}\frac{\hbar\omega_{\mathbf{q}}\beta}{2}-i\left(\sin\omega_{\mathbf{q}}\left(t_2'+t_3\right)\right.\right.\right.$$
$$\left.\left.\left.-\sin\omega_{\mathbf{q}}t_2'\right)\right]\right\}^{-1'}-\left\{\frac{1}{N}\sum_{\mathbf{q}}\left|\gamma_{\mathbf{q}}\right|^2 a_{\mathbf{q}}\omega_{\mathbf{q}}\right\}^{-1}$$

Having made the substitution $\mathrm{t}_3'=\mathrm{t}_3+\mathrm{i}\hbar\beta/2$, we discard the integral with respect to t_3' from 0 to ∞, which contains the small factor $\exp\left[-\mathrm{E_a/kT}\right]$. In the remaining integral we put $\mathrm{t}_3'=\mathrm{i}\hbar\beta/2-\mathrm{iv}_3$, in which the essential region is near $\mathrm{v}_3=0$. We expand the exponent and the factor $R\left(t_2',t_3\right)$ in (AIII.3) in powers of v_3, retaining the first term in the exponent, and the first and second terms in $R\left(t_2',t_3\right)$. Integrating with respect to v_3, we obtain

$$W^{(2)}=2\left(\frac{J}{\hbar}\right)^4\int_0^\infty dt_2\left\{\frac{1}{N}\sum_{\mathbf{q}}\Gamma_{\mathbf{q}}\cos\omega_{\mathbf{q}}t_2/\left(\frac{1}{N}\sum_{\mathbf{q}}\left|\gamma_{\mathbf{q}}\right|^2 a_{\mathbf{q}}\omega_{\mathbf{q}}\right)^4\right.$$
$$\left.+2\left(\frac{1}{N}\sum_{\mathbf{q}}\Gamma_{\mathbf{q}}\omega_{\mathbf{q}}^2\cos\omega_{\mathbf{q}}t_2\right)^2/\left(\frac{1}{N}\sum_{\mathbf{q}}\left|\gamma_{\mathbf{q}}\right|^2 a_{\mathbf{q}}\omega_{\mathbf{q}}\right)^6\right\}\cdot\ \text{(AIII.5)}\qquad\text{(AIII.5)}$$

Integrating with respect to t_2, we find that the first term contains a delta function of ω_{q} and is equal to zero ($\omega_{\mathrm{q}}\neq 0$). The second term contains the sum $\delta\left(\omega_{\mathrm{q}_1}+\omega_{\mathrm{q}_2}\right)+\delta\left(\omega_{\mathrm{q}_1}-\omega_{\mathrm{q}_2}\right)$. In the isotropic case we obtain finally

[0]*ch = cosh.

$$W^{(2)} = \frac{J^4}{2\pi^3\hbar^4}\int_0^{q_{\max}} dq\cdot q^4 \frac{|\gamma_{\mathbf{q}}|^4 a_{\mathbf{q}}^2\omega_{\mathbf{q}}^4}{\mathrm{sh}^2\left(\hbar\omega_{\mathbf{q}}\beta/2\right)}\frac{1}{d\omega_{\mathbf{q}}/dq}$$
$$\times\,\Omega^2/\left(\frac{1}{N}\sum_{\mathbf{q}}|\gamma_{\mathbf{q}}|^2 a_{\mathbf{q}}\omega_{\mathbf{q}}\right)^6 \approx \left(\frac{J}{E_a}\right)^4 \frac{\bar{\omega}}{\mathrm{sh}^2(\hbar\bar{\omega}\beta/2)}, \quad \text{(AIII.6)}$$

where Ω is the volume of the elementary cell, $q_{\max}\approx 1/a$, and a is the lattice constant.

[1] F. I. Morin, Phys. Rev. 93, 1199 (1954).
[2] E. Yamaka and K. Sawamoto, Phys. Rev. 112, 1861 (1958).
[3] R. Heikes and W. Johnston, J. Chem. Phys. 26, 582 (1957).
[4] I. Yamashita and T. Kurosawa, J. Chem. Phys. Solids, 5, 34 (1958); J. Phys. Soc. Japan 15, 802 (1960).
[5] T. Holstein, Ann. of Physics 8, 325, 343 (1959).
[6] M. I. Klinger, DAN SSSR 142, 1065 (1962), Soviet Phys. Doklady 7, 123 (1962).
[7] R. Kubo, J. Phys. Soc. Japan 12, 570 (1957).
[8] G. H. Wannier, Phys. Rev. 52, 191 (1937).
[9] M. A. Krivoglaz and S. I. Pekar, Izv. AN SSSR ser. fiz. 21, 3 (1957), Columbia Tech. Transl. p. 1.
[10] Yu. A. Firsov and V. L. Gurevich, JETP 41, 512 (1961), Soviet Phys. JETP 14, 367 (1962).
[11] Gurevich, Larkin, and Firsov, FTT 4, 185 (1962), Soviet Phys. Solid State 4, 131 (1962).
[12] O. V. Konstantinov and V. I. Perel', JETP 39, 197 (1960), Soviet Phys. JETP 12, 142 (1961).
[13] L. van Hove, Physica 21, 901 (1955); 23, 421 (1957).

Translated by J. G. Adashko

314

6.5.7 4.3 Polaron band and self-energy

(this is the celebrated Alexandrov's $1/\lambda$ approach)

The model and energy band

With the finite hopping term polarons tunnel in a narrow band (which narrow band?) because of the degeneracy of the zero order Hamiltonian relative the site position of a single polaron in a regular lattice (which degeneracy?).

To show this self-consistently one can apply perturbation theory using $1/\lambda$ as a small parameter. Because of the degeneracy terms of the first order in $T(\mathbf{m})$ should be included in a zero order Hamiltonian H_0:

$$H_0 = \sum_{i,j}\left(\sigma(\mathbf{m}-\mathbf{n}) - \mu\delta_{i,j}\right)c_i^\dagger c_j + \sum_{\mathbf{q}}\omega_{\mathbf{q}}\left(d_{\mathbf{q}}^\dagger d_{\mathbf{q}} + 1/2\right) \tag{4.16}$$

where

$$\sigma(\mathbf{m}-\mathbf{n}) = \langle\langle\hat{\sigma}_{ij}\rangle\rangle = T(\mathbf{m}-\mathbf{n})\delta_{s,s'}\exp\left[-g^2(\mathbf{m}-\mathbf{n})\right] \tag{4.17}$$

(there is no s-s at the l.h.s., where are they??) (how to calculate these $\langle\langle\ldots\rangle\rangle = \sum_\nu e^{\frac{\Omega-E_\nu}{T}}\langle\nu|\ldots|\nu\rangle$???)

is the hopping integral averaged with the phonon equilibrium distribution. It is calculated by the use of the relation

$$e^{A+B} = e^A e^B e^{-[AB]/2} \tag{4.18}$$

which is valid for any operators A, B with a c-number commutator. For zero temperature one obtains

$$\sigma(\mathbf{m}-\mathbf{n}) = T(\mathbf{m}-\mathbf{n})e^{-g^2(\mathbf{m}-\mathbf{n})}\langle 0|\exp\left[-\sum_{\mathbf{q}}\left[u_i^*(\mathbf{q}) - u_j^*(\mathbf{q})\right]d_{\mathbf{q}}^\dagger\right]\exp\left[\sum_{\mathbf{q}}\left[u_i(\mathbf{q}) - u_j(\mathbf{q})\right]d_{\mathbf{q}}\right]|0\rangle \tag{4.19}$$

where

$$g^2(\mathbf{m}-\mathbf{n}) = \frac{1}{2}\sum_{\mathbf{q}} \left(|u_i(\mathbf{q})|^2 + |u_j(\mathbf{q})|^2 - 2u_i^*(\mathbf{q})u_j(\mathbf{q})\right) \tag{4.20}$$

The bracket in Eq.(4.19) is equal unity for $T = 0$. (it is very not clear, how to obtain these equations, and whyh u-s appear???)

The straightforward generalisation for finite temperatures yields

$$g^2(\mathbf{m}) = \frac{1}{2N}\sum_{\mathbf{q}} |\gamma(\mathbf{q})|^2 \coth\left(\frac{\omega_{\mathbf{q}}}{2T}\right)[1-\cos(\mathbf{q}\cdot\mathbf{m})] \tag{4.21}$$

The renormalised position of the middle of the electron band is taken to be zero, so that $T(0) - E_p = 0$.

The interaction term in the transformed hamiltonian $\tilde{H} = H_0 + H_{\text{int}}$ includes the residual interaction H_{p-ph} of polarons with phonons and the polaron-polaron interaction H_{p-p}:

$$H_{int} = H_{p-ph} + H_{p-p} \tag{4.22}$$

$$H_{p-ph} = \sum_{i,j} \left[\hat{\sigma}_{ij} - \sigma(\mathbf{m}-\mathbf{n})\right] c_i^\dagger c_j \tag{4.23}$$

$$H_{p-p} = \frac{1}{2}\sum_{i,j} v_{ij} c_i^\dagger c_j^\dagger c_j c_i \tag{4.24}$$

(why 4.23 is about p-ph interaction????)

The polaron-phonon interaction leads to the polaron bandwidth and phonon frequency renormalisations and to the scattering of polarons. The polaron-polaron correlations are responsible for the scattering and in case of the attraction for the bipolaron formation. If the temperature is well above the temperature for the formation of bipolarons (see below) one can treat H_{p-ph} with the $1/\lambda$ perturbation expansion and H_{p-p} with the canonical random phase approximation (RPA). We consider first the effect of H_{p-ph} on the polaron self-energy Σ_p.

Because of the translation symmetry H_0 is diagonal in the Bloch-representation Eq.(3.128):

$$H_0 = \sum_{\mathbf{k},s} (\epsilon_{\mathbf{k}} - \mu)\, c_{\mathbf{k},s}^\dagger c_{\mathbf{k},s} + \sum_{\mathbf{q}} \omega_{\mathbf{q}} d_{\mathbf{q}}^\dagger d_{\mathbf{q}} \tag{4.25}$$

with a polaronic band

$$\epsilon_{\mathbf{k}} = \sum_{\mathbf{m}} \sigma(\mathbf{m}) e^{i\mathbf{k}\cdot\mathbf{m}} \tag{4.26}$$

From Eq.(4.26) we conclude that the polaronic band has the bandwidth $2w$ exponentially reduced compared with the bare electronic bandwidth as in the Holstein model(was there the suppression of the bandwidth??? I don't remember it), Chapter 1

$$w = De^{-g^2} \tag{4.27}$$

where g is determined in Eq.(4.21) for the nearest neighbor hopping $|\mathbf{m}| = a$. An increase of the effective mass $m^* = 1/wa^2$ is due to the phonon cloud surrounding a small polaron. The renormalisation factor $\exp(-g^2)$ is closely related to the wellknown Debye-Waller factor, determined by the mean-square displacement of atoms from their equilibrium positions.

Polaron self-energy and solution in terms of GF

To derive the polaron self-energy one can solve perturbatively the equation of motion for the polaronic temperature Green's function defined in the Wannier representation as

$$\tilde{g}_{ij}(\tau) = -\langle\langle T_\tau c_i(\tau) c_j^\dagger \rangle\rangle \tag{4.28}$$

with $c_i(\tau) = e^{\tilde{H}\tau} c_i e^{-\tilde{H}\tau}$. The double angular brackets correspond now to the quantum as well as statistical average over the eigenstates of the transformed Hamiltonian. Differentiating Eq.(4.28) we obtain

$$\frac{d\tilde{g}_{ij}(\tau)}{d\tau} - \mu \tilde{g}_{ij}(\tau) = -\delta(\tau)\delta_{i,j} + \sum_{i'} \langle\langle T_\tau \hat{\sigma}_{ii'}(\tau) c_{i'}(\tau) c_j^\dagger \rangle\rangle \tag{4.29}$$

where $\hat{\sigma}_{ii'}(\tau) = e^{\tilde{H}\tau} \hat{\sigma}_{ii'} e^{-\tilde{H}\tau}$.
For the Fourier component we have:

$$\hat{\tilde{g}}^{-1}(\omega_n) = \left(\hat{\tilde{g}}^{(0)}(\omega_n)\right)^{-1} - \hat{\Sigma}(\omega_n) \tag{4.30}$$

where $\hat{\tilde{g}}$ and $\hat{\Sigma}$ are matrices with respect to site indices i, j. The free polaron GF in determined by

$$\left(\tilde{g}^{(0)}(\omega_n)\right)_{ij}^{-1} = (i\omega_n + \mu)\,\delta_{i,j} - \sigma(\mathbf{m} - \mathbf{n}) \tag{4.31}$$

and the polaron self-energy by

$$\Sigma_{ij}(\omega_n) = \sum_{i',j'} \Gamma_{ii'}^{i'j'}(\omega_n)\, \hat{\tilde{g}}_{j'j}^{-1}(\omega_n) \tag{4.32}$$

where $\hat{\Gamma}(\omega_n)$ is the Fourier component of the polaron-phonon correlation function

$$\Gamma_{ii'}^{jj'}(\tau) = -\langle\langle T_\tau \left[\hat{\sigma}_{ii'}(\tau) - \sigma(\mathrm{m} - \mathrm{m}')\right] c_j(\tau) c_{j'}^\dagger \rangle\rangle. \tag{4.33}$$

This correlation function comprises the second and higher order terms with respect to the hopping integral, as follows from the corresponding equation of motion:

$$\frac{d\Gamma_{ii'}^{jj'}(\tau)}{d\tau} - \mu \Gamma_{ii'}^{jj'}(\tau) = \sum_{i''} \langle\langle T_\tau \left[\hat{\sigma}_{ii'}(\tau) - \sigma(\mathbf{m} - \mathbf{m}')\right] c_j(\tau) c_{i''}^\dagger \hat{\sigma}_{i''j'} \rangle\rangle. \tag{4.34}$$

To obtain Eq.(4.34) one can differentiate the function

$$\Gamma_{ii'}^{jj'}(-\tau) = -\langle\langle T_\tau \left[\hat{\sigma}_{ii'} - \sigma(\mathbf{m} - \mathbf{m}')\right] c_j c_{j'}^\dagger(\tau) \rangle\rangle. \tag{4.35}$$

In the second order of the perturbation theory one can replace $\tilde{H}$ in Eq.(4.34) for H_0 to obtain

$$\Sigma_{ij}(\omega_n) = T \sum_{\omega_{n'}} \sum_{i',i'',j'} \tilde{\Phi}_{ii'}^{i''j'}(\omega_n - \omega_{n'})\, \tilde{g}_{i'i''}^{(0)}(\omega_{n'})\, \frac{(i\omega_n + \mu)\,\delta_{j',j} - \sigma(\mathbf{n} - \mathbf{n}')}{i\omega_n + \mu} \tag{4.36}$$

where

$$\tilde{\Phi}_{ii'}^{jj'}(\Omega_n) = \Phi_{ii'}^{jj'}(\Omega_n) - \frac{1}{T}\sigma(\mathbf{m} - \mathbf{m}')\,\sigma(\mathbf{n} - \mathbf{n}')\,\delta_{\Omega_n,0} \tag{4.37}$$

and $\Phi_{ii'}^{jj'}(\Omega_n)$ is a Fourier component of the multiphonon correlator

$$\Phi_{ii'}^{jj'}(\tau) = \langle\langle T_\tau \hat{\sigma}_{ii'}(\tau)\hat{\sigma}_{jj'}\rangle\rangle \tag{4.38}$$

with $\tilde{H} = H_0$. Direct calculations yield

$$\Phi_{ii'}^{jj'}(\tau) = \sigma(\mathbf{a})\sigma(\mathbf{b}) \exp\left(\frac{1}{N}\sum_{\mathbf{q}} \gamma^2(\mathbf{q}) f_{\mathbf{q}} \frac{\cosh\left[\omega_{\mathbf{q}}\left(\frac{1}{2T} - |\tau|\right)\right]}{\sinh\frac{\omega_{\mathbf{q}}}{2T}}\right) \tag{4.39}$$

where $2f_{\mathbf{q}} = \cos(\mathbf{q}\cdot[\mathbf{c}-\mathbf{a}]) + \cos(\mathbf{q}\cdot[\mathbf{c}+\mathbf{b}]) - \cos(\mathbf{q}\cdot\mathbf{c}) - \cos(\mathbf{q}\cdot[\mathbf{c}-\mathbf{a}+\mathbf{b}])$ with $\mathbf{a} = \mathbf{m}-\mathbf{m}', \mathbf{b} = \mathbf{n}-\mathbf{n}'$ and $\mathbf{c} = \mathbf{n}'-\mathbf{m}'$.

To simplify Eq.(4.36) further one can neglect all terms, containing a small exponent $e^{-g^2} \ll 1$. Omitting small terms the nelf-energy is diagonal, $\Sigma_{ij} \simeq \Sigma\delta_{i,j}$ where

$$\Sigma = T\sum_{\omega_{n'}}\sum_{\mathbf{a}} \frac{\tilde{\Phi}_{\mathbf{a}}(\omega_n - \omega_{n'})}{i\omega_{n'} + \mu} \tag{4.40}$$

and

$$\tilde{\Phi}_{\mathbf{a}}(\Omega_n) = \frac{1}{2}\int_{-1/T}^{1/T} d\tau e^{i\Omega_n\tau}\tilde{\Phi}_{ii'}^{i'i}(\tau) \tag{4.41}$$

with $\Omega_n = 2\pi nT; n = 0, \pm1, \pm2, \ldots$. This Fourier component is readily calculated in the case of dispersionless phonons $\omega_{\mathrm{q}} = \omega$ expanding the exponent in Eq.(4.39)

$$\tilde{\Phi}_{\mathbf{a}}(\Omega_n) = \frac{2\sigma^2(\mathbf{a})}{\omega}\sum_{k=1}^{\infty}\sum_{p=0}^{k}\binom{k}{p}\frac{\sinh[(k-2p)\omega/2T]}{2^k k!\sinh^k(\omega/2T)}\frac{1}{N}\sum_{\mathbf{q}'}\gamma^2(\mathbf{q}')\left[1-\cos(\mathbf{q}'\cdot\mathbf{a})\right]^k\frac{(k-2p)\omega^2}{(k-2p)^2\omega^2+\Omega_n^2} \tag{4.42}$$

The main frequency independent contribution is

$$\tilde{\Phi}_{\mathbf{a}}(\Omega_n) \simeq \frac{T^2(\mathbf{a})}{g^2(\mathbf{a})\omega_0} \tag{4.43}$$

Summation over frequencies in Eq.(4.40) yields

$$-T\sum_{\omega_{n'}}\frac{1}{i\omega_{n'}+\mu} = \frac{1}{2}\tanh\frac{\mu}{2T} \tag{4.44}$$

The chemical potential is determined via the atomic density of carriers n

$$\frac{2}{N}\sum_{\mathbf{k}} n_{\mathbf{k}} = n \tag{4.45}$$

with the Fermi-Dirac distribution function

$$n_{\mathbf{k}} = \frac{1}{\exp\left[(\epsilon_{\mathbf{k}}-\mu)/T\right]+1} \simeq \frac{1}{2}\left(1+\tanh\frac{\mu}{2T}\right) \tag{4.46}$$

By the use of Eq.(4.45) one obtains

$$\tanh\frac{\mu}{2T} \simeq n-1 \tag{4.47}$$

and

$$\Sigma \simeq -(1-n)\sum_{\mathbf{a}}\frac{T^2(\mathbf{a})}{2\omega_0 g^2(\mathbf{a})} \tag{4.48}$$

or in the nearest neighbor approximation with the definition $D = z|T(\mathbf{a})|$

$$\Sigma \simeq -\frac{(1-n)E_p}{2z\lambda^2} \tag{4.49}$$

This expression is a result of the summation of the second order in H_{p-ph} multiphonon diagrams as shown in Fig.4.2a. The contribution of the second order being negative lowers the polaron energy and increases the effective mass further (to show this one should calculate the frequency derivative of $\Sigma(\omega)$). Gogolin (1982) in the framework of a single polaron problem estimated also the third and higher order contributions to Σ, Fig. 4.2 b

$$\Sigma^{(3)} \sim +\frac{E_p}{\lambda^3} \tag{4.50}$$

The third order contribution is positive and leads to the reduction of the effective mass. Because the dispersion is exponentially small one can sum all diagrams, including the crossing ones. These results show that the consistent perturbation expansion in $1/\lambda$ exists with the small parameter

$$\frac{1}{2z\lambda^2} \ll 1 \tag{4.51}$$

where z is the nearest neighbor number. Therefore if the coupling constant $\lambda > 1/\sqrt{2z}$, small polarons are stable and they tunnel in a narrow band, Eq.(4.26). This condition of the small polaron formation is independent of the adiabatic ratio ω/D. However, the term in front of the exponent in the bandwidth depends on this parameter. For the adiabatic small polaron ($\omega/D \ll 1$) it is different from D as follows from the numerical calculations, section 1.8.

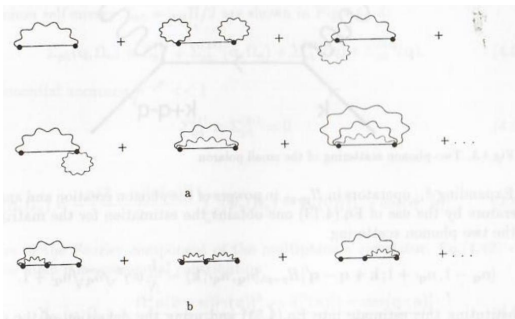

Fig.4.2. Polaron self-energy.

6.5.8 4.4 Temperature collapse of the polaron band

Theory

The self-energy effect is small at $T = 0$ if λ is of the order of unity or larger. However, the polaron bandwidth depends on the temperature according to Eq.(4.21). For high temperatures $T \gg \omega/2$ the band shrinks exponentially with increasing temperature

$$w \simeq D \exp\left(-\frac{2E_pT}{\omega^2}\right) \tag{4.52}$$

On the other hand the scattering of polarons within their narrow band becomes more important with the increasing temperature because of the simultaneous phonon emission and absorption. The absorption or emission of a single high-frequency phonon is forbidden by the energy

conservation for the nonadiabatic small polaron with the bandwidth $2w \leq \omega$. However, two-phonon processes, Fig.4.3 with the simultanecum emission and absorption of different phonons are allowed at finite temperatures. These incoherent events tend to destroy the coherent polaron tunneling in the band. the corresponding scattering rate is given by the Fermi-golden rule, which for dispersionless phonons is

$$\frac{1}{\tau} = 2\pi \left\langle \sum_{\mathbf{q},\mathbf{q}'} \left| \langle n_{\mathbf{q}} - 1, n_{\mathbf{q}'} + 1; \mathbf{k} + \mathbf{q} - \mathbf{q}' | \, H_{p-ph} \, | n_{\mathbf{q}}, n_{\mathbf{q}'}; \mathbf{k} \rangle \right|^2 \delta \left(\epsilon_{\mathbf{k}} - \epsilon_{\mathbf{k}+\mathbf{q}-\mathbf{q}'} \right) \right\rangle \tag{4.53}$$

where $|n_{\mathbf{q}}; \mathbf{k}\rangle$ is an eigenstate of a noninteracting small polaron propagating with momentum k and n_{q} phonons.

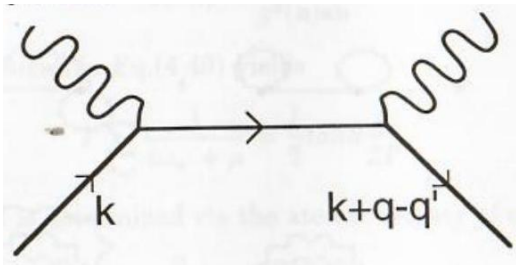

Fig.4.3. Two-phonon scattering of the small polaron.

Expanding $\hat{\sigma}_{ij}$ operators in H_{p-ph} in powers of the phonon creation and annihilation operators by the use of Eq.(4.13) one obtains the estimation for the matrix element of the two phonon scattering

$$\langle n_{\mathbf{q}} - 1, n_{\mathbf{q}'} + 1; \mathbf{k} + \mathbf{q} - \mathbf{q}' | \, H_{p-ph} \, | n_{\mathbf{q}}, n_{\mathbf{q}'}; \mathbf{k} \rangle \sim \frac{1}{N} w \gamma^2 \sqrt{n_{\mathbf{q}}} \sqrt{n_{\mathbf{q}'} + 1} \tag{4.54}$$

Substituting this estimate into Eq.(4.53) and using the definition of the density of states in the polaron band

$$N_p(\xi) \equiv \frac{1}{N} \sum_{\mathbf{k}} \delta \left(\xi - \epsilon_{\mathbf{k}} \right) \simeq \frac{1}{2w} \tag{4.55}$$

we have

$$\frac{1}{\tau} \simeq w \gamma^4 n_\omega \left(1 + n_\omega \right) \tag{4.56}$$

where $n_\omega = [\exp(\omega/T) - 1]^{-1}$ is the phonon distribution function. The matrix element γ is taken momentum independent. The polaron band is well defined if

$$\frac{1}{\tau} < w \tag{4.57}$$

which is the case in a wide temperature range

$$T \leq \frac{\omega}{\ln \gamma^4} \tag{4.58}$$

below *ca.* half of the characteristic phonon frequency for the reasonable values of $\gamma^2 \leq 5$.

At higher temperatures the incoherent thermally activated hopping dominates in the polaron motion. Then the polaronic states cannot be classified with the momen tum.

6.5.9 4.5 Phonons in a strong-coupling system

Theory

An essential question, which arises within the adiabatic Migdal approach is that of the phonon instability and the applicability of the Fröhlich hamiltonian. Taking into account the polaron formation we show in this section that the phonon frequency softening is small and therefore the Fröhlich hamiltonian is applicable also in the strong coupling regime. The first and different second order diagrams in H_{p-ph} contributing to the phonon self energy $\Sigma_{ph} = \omega_{\mathbf{q}}\Pi/2$ are shown in Fig.4.4a-d:

$$\Sigma_{ph}(\mathbf{q}, \Omega_n) = \Sigma_{ph}^{(1)} + \Sigma_{ph}^{(2a)}(\mathbf{q}, \Omega_n) + \Sigma_{ph}^{(2b)}(\mathbf{q}) + \Sigma_{ph}^{(2c)}(\mathbf{q}). \tag{4.59}$$

With exponential accuracy, $e^{-g^2} \ll 1$

$$\Sigma_{ph}^{(1)} = \Sigma_{ph}^{(2c)} = 0 \tag{4.60}$$

and

$$\Sigma_{ph}(\mathbf{q}, \Omega_n) = -\frac{n(2-n)|\gamma(\mathbf{q})|^2}{2} \sum_{\mathbf{a}} \left(\Phi_{\mathbf{a}}(\Omega_n) - \Phi_{\mathbf{a}}(0)\right)\left[1 - \cos(\mathbf{q}\cdot\mathbf{a})\right] \tag{4.61}$$

By the use of the Fourier component of the multiphonon correlator, Eq.(4.42) (reminder:

$$\tilde{\Phi}_{\mathbf{a}}(\Omega_n) = \frac{2\sigma^2(\mathbf{a})}{\omega} \sum_{k=1}^{\infty}\sum_{p=0}^{k} \binom{k}{p} \frac{\sinh[(k-2p)\omega/2T]}{2^k k! \sinh^k(\omega/2T)} \frac{1}{N} \sum_{\mathbf{q}'} \gamma^2(\mathbf{q}')\left[1 - \cos(\mathbf{q}'\cdot\mathbf{a})\right]^k \frac{(k-2p)\omega^2}{(k-2p)^2\omega^2 + \Omega_n^2} \tag{4.42}$$

) one obtains the main nonexponential contribution

$$\Sigma_{ph}(\mathbf{q}, \Omega_n) = \frac{\Omega_n^2 n(2-n)|\gamma(\mathbf{q})|^2}{2\omega^3} \sum_{\mathbf{a}} \frac{T^2(\mathbf{a})[1 - \cos(\mathbf{q}\cdot\mathbf{a})]}{g^6(\mathbf{a})}$$

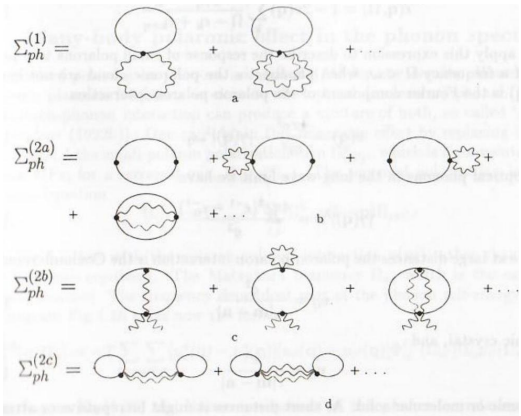

Fig. 4.4. Phonon self-energy in the strong-coupling limit.

The analytical continuation to the real frequencies is found by the simple substitution

$$i\Omega_n \to \tilde{\omega} + i0^+ \tag{4.63}$$

with the following result for the renormalised phonon frequency, which is a pole of the phonon GF:

$$\tilde{\omega}_{\mathbf{q}} \simeq \omega - \Delta(\mathbf{q}) \tag{4.64}$$

The phonon frequency softening

$$\Delta(\mathbf{q}) = \frac{n(2-n)|\gamma(\mathbf{q})|^2}{2\omega} \sum_{\mathbf{a}} \frac{T^2(\mathbf{a})[1-\cos(\mathbf{q}\cdot\mathbf{a})]}{g^6(\mathbf{a})} \tag{4.65}$$

(how to understand this formula???) is small compared with the frequency as $1/\lambda^2 \ll 1$. (why is it small???)

This result is consistent with the phonon frequency renormalisation in the two-site Holstein model, section 1.7. Phonons are stable in the strong-coupling regime. The ions change their equilibrium positions due to the electron-phonon coupling retaining their vibration frequencies practically unchanged.

6.5.10 4.6 Screening and polaronic plasmon

Theory

(what is the v that is used a lot below???)

Polarons are coupled not only with phonons via the residual interaction H_{p-ph} but also between themselves. At sufficiently high temperatures above the bipolaronic instability (see Chapter 5) the effect of H_{p-p} is described by the dielectric response function $\epsilon(\mathbf{q},\Omega)$, for which the canonical random phase approximation is adopted

$$\epsilon(\mathbf{q},\Omega) = 1 - 2v(\mathbf{q}) \sum_{\mathbf{k}} \frac{n_{\mathbf{k}+\mathbf{q}} - n_{\mathbf{k}}}{\Omega - \epsilon_{\mathbf{k}} + \epsilon_{\mathbf{k}+\mathbf{q}}} \tag{4.66}$$

One can apply this expression to describe the response of small polarons to a perturbation of a frequency $\Omega < \omega$, when phonons in the polaronic cloud are not excited. Here $v(\mathbf{q})$ is the Fourier component of the polaron-polaron interaction

$$v(\mathbf{q}) = \frac{4\pi e^2}{\epsilon q^2} - |\gamma(\mathbf{q})|^2 \omega_{\mathbf{q}} \tag{4.67}$$

For the optical phonons in the long-wave limit we have

$$|\gamma(\mathbf{q})|^2 \omega = \frac{4\pi e^2 \left(\epsilon^{-1} - \epsilon_0^{-1}\right)}{q^2} \tag{4.68}$$

Therefore at large distances the polaron-polaron interaction is the Coulomb repulsion,

$$v_{ij} = \frac{e^2}{\epsilon_0 |\mathbf{m} - \mathbf{n}|} \tag{4.69}$$

in an ionic crystal, and

$$v_{ij} = \frac{e^2}{\epsilon |\mathbf{m} - \mathbf{n}|} \tag{4.70}$$

in an atomic or molecular solid. At short distances it might be repulsive or attractive depending on the value of a short range ϵ.

In the static limit at large distances (or $q \to 0$) we obtain the usual Debye screening due to the repulsion with the static dielectric function

$$\epsilon(q,0) = 1 + \frac{q_s^2}{q^2} \tag{4.71}$$

where $q_s = \sqrt{2\pi e^2 n(2-n)/T\epsilon_0}$. This result is obtained for the temperature larger than the polaronic bandwidth using the expansion of the polaron distribution function:

$$n_{\mathbf{k}} \simeq \frac{n}{2}\left(1 - \frac{(2-n)\epsilon_{\mathbf{k}}}{2T}\right) \tag{4.72}$$

The polaron response becomes dynamic for a rather low frequency $\omega > w$,

$$\epsilon(\mathbf{q},\omega) = 1 - \frac{\omega_p^2(\mathbf{q})}{\omega^2} \tag{4.73}$$

with the temperature dependent plasma frequency

$$\omega_p^2(\mathbf{q}) = 2v(\mathbf{q})\sum_{\mathbf{k}} n_{\mathbf{k}}\left(\epsilon_{\mathbf{k}+\mathbf{q}} - \epsilon_{\mathbf{k}}\right) \tag{4.74}$$

which is proportional to the inverse temperature if $T \gg w$. This expression is applied to the polaronic plasmon with a frequency below or of the order of the characteristic phonon frequency, which is quite feasible due to a large value of the background dielectric constant and the enhanced effective mass. Otherwise, one should take into account the phonon shakeoff in the dielectric response function.

6.5.11 4.7 Many-body polaronic effect in the phonon spectrum

Theory

The effect of polarons on phonons is small as $1/\lambda^2$ for any density. However, if the polaronic plasmon frequency is close to the optical (molecular) phonon frequency the polaron-phonon interaction can produce a mixture of both, so called 'plasphon' (Alexandrov (1992b)). One can obtain this resonance effect by replacing in all diagrams Fig. 4.4 the small-polaron polarisation loop $\Pi^0_{iji'j'}$, which is a convolution of two polaron GFs, for a screened one, $\Pi_{iji'j'}(\Omega_n)$. The screened polarisation loop obeys the same equation

$$\Pi_{iji'j'} = \Pi^0_{iji'j'} + \sum_{l,p} \Pi^0_{ijll} v(\mathbf{l}-\mathbf{p}) \Pi_{ppi'j'} \tag{4.75}$$

as in Fig.3.2, but with the polaron-polaron interaction $v(\mathbf{m})$ rather than with the bare Coulomb repulsion. The Matsubara frequency Ω_n, which is the same in all terms is omitted. The frequency dependent part of the phonon self-energy given by the diagram Fig.4.4b takes now the form

$$\Sigma^{(2a)}_{ph}(\mathbf{q},\Omega_n) = -T\sum_{\Omega_{n'}}\sum_{iji'j'}\left[u_i^*(\mathbf{q}) - u_j^*(\mathbf{q})\right]\left[u_{i'}(\mathbf{q}) - u_{j'}(\mathbf{q})\right]\Phi^{i'j'}_{ij}(\Omega_{n'})\,\Pi_{iji'j'}(\Omega_{n'} - \Omega_n)\,. \tag{4.76}$$

According to Eq.(4.37) the Fourier component of the phonon correlation function comprises the part Φ, which is almost frequency independent for $\Omega_n \ll E_p$, and the exponentially small term, which is nonzero only for $\Omega_n = 0$. The contribution of this second term to the self-energy is enhanced, however, if the resonance condition $\omega_p \simeq \omega$ is met. By the use of Eq.(4.37) one obtains

$$\Sigma_{ph}(\mathbf{q},\Omega_n) = \Sigma^{res}_{ph}(\mathbf{q},\Omega_n) - \Delta(\mathbf{q}) \tag{4.77}$$

where
$\Sigma^{res}_{ph}(\mathbf{q},\Omega_n) = -\sum_{iji'j'}\left[u_i^*(\mathbf{q}) - u_j^*(\mathbf{q})\right]\left[u_{i'}(\mathbf{q}) - u_{j'}(\mathbf{q})\right]\sigma(\mathbf{m}-\mathbf{n})\sigma(\mathbf{m}'-\mathbf{n}')\,\Pi_{iji'j'}(-\Omega_n)$.

The solution to Eq.(4.75) is obtained with the Fourier transformation of the polarisation loop

$$\Pi_{iji'j'} = \frac{1}{N}\sum_{\mathbf{k},\mathbf{k}',\mathbf{g}} \Pi\left(\mathbf{k},\mathbf{k}',\mathbf{g}\right)\exp\left[-i\mathbf{k}\cdot\left(\mathbf{m}'-\mathbf{n}\right)+i\mathbf{k}\cdot\left(\mathbf{n}'-\mathbf{m}\right)+i\mathbf{g}\cdot\left(\mathbf{m}'-\mathbf{n}'\right)\right] \tag{4.79}$$

The Fourier transformation of Eq.(4.75) yields

$$\Pi\left(\mathbf{k},\mathbf{k}',\mathbf{g}\right) = \Pi^0\left(\mathbf{k},\mathbf{k}'\right)\left[N\delta_{\mathbf{g},0} + v\left(\mathbf{k}-\mathbf{k}'\right)\sum_{\mathbf{g}'}\Pi\left(\mathbf{k}+\mathbf{g}'-\mathbf{g},\mathbf{k}'+\mathbf{g}'-\mathbf{g},\mathbf{g}'\right)\right] \tag{4.80}$$

where

$$\Pi^0\left(\mathbf{k},\mathbf{k}'\right) = 2\frac{n_{\mathbf{k}}-n_{\mathbf{k}'}}{i\Omega_n+\epsilon_{\mathbf{k}}-\epsilon_{\mathbf{k}'}} \tag{4.81}$$

One can replace $\mathbf{k},\mathbf{k}'$ for $\mathbf{k}+\mathrm{g}$ and $\mathbf{k}'+\mathrm{g}$, respectively to obtain

$$\Pi\left(\mathbf{k}+\mathbf{g},\mathbf{k}'+\mathbf{g},\mathbf{g}\right) = \Pi^0\left(\mathbf{k}+\mathbf{g},\mathbf{k}'+\mathbf{g}\right)\left[N\delta_{\mathbf{g},0} + v\left(\mathbf{k}-\mathbf{k}'\right)A\left(\mathbf{k},\mathbf{k}'\right)\right] \tag{4.82}$$

where $A\left(\mathbf{k},\mathbf{k}'\right) \equiv \sum_{\mathbf{g}'}\Pi\left(\mathbf{k}+\mathbf{g},\mathbf{k}'+\mathbf{g}',\mathbf{g}'\right)$ is found by taking the sum in Eq.(4.80) over $\mathbf{g}$

$$A\left(\mathbf{k},\mathbf{k}'\right) = N\frac{\Pi^0\left(\mathbf{k},\mathbf{k}'\right)}{\epsilon\left(\mathbf{k}-\mathbf{k}',i\Omega_n\right)} \tag{4.83}$$

As a result we find

$$\Pi\left(\mathbf{k},\mathbf{k}',\mathbf{g}\right) = N\Pi^0\left(\mathbf{k},\mathbf{k}'\right)\left[\delta_{\mathbf{g},0} + v\left(\mathbf{k}-\mathbf{k}'\right)\frac{\Pi^0\left(\mathbf{k},\mathbf{k}'\right)}{\epsilon\left(\mathbf{k}-\mathbf{k}',i\Omega_n\right)}\right] \tag{4.84}$$

and
$\Sigma_{ph}^{res}\left(\mathbf{q},\Omega_n\right) = \frac{\gamma^2(\mathbf{q})}{2N^2}\sum_{\mathbf{k},\mathbf{g}}\left(\epsilon_{\mathbf{k}}\epsilon_{\mathbf{k}-\mathbf{q}-\mathbf{g}} + \epsilon_{\mathbf{k}-\mathbf{q}}\epsilon_{\mathbf{k}-\mathbf{g}} - \epsilon_{\mathbf{k}-\mathbf{g}}\epsilon_{\mathbf{k}-\mathbf{q}-\mathbf{g}} - \epsilon_{\mathbf{k}}\epsilon_{\mathbf{k}-\mathbf{g}}\right)\Pi(\mathbf{k},\mathbf{k}-\mathbf{q},\mathbf{g})$.

One can expand the unscreened polarisation $\Pi^0\left(\mathbf{k},\mathbf{k}'\right)$ in powers of a small parameter $w/\omega \ll 1$ as

$$\Pi^0\left(\mathbf{k},\mathbf{k}'\right) = 2\left(n_{\mathbf{k}}-n_{\mathbf{k}'}\right)\left[\frac{1}{i\Omega_n} + \frac{\epsilon_{\mathbf{k}}-\epsilon_{\mathbf{k}'}}{\Omega_n^2} + \ldots\right] \tag{4.86}$$

With this expansion we have

$$\Sigma_{ph}^{res}\left(\mathbf{q},\Omega_n\right) = -\frac{\beta(\mathbf{q})\omega_p^4(\mathbf{q})}{\omega\left[\Omega_n^2+\omega_p^2(\mathbf{q})\right]} \tag{4.87}$$

where $\beta(\mathbf{q}) = \omega|\gamma(\mathbf{q})|^2/v(\mathbf{q})$ is the dimensionless plasmon-phonon coupling constant. The dispersion relation for the plasmon-phonon mixture is obtained by carrying out the analytical continuation of $\Sigma_{ph}\left(\mathbf{q},\Omega_n\right)$ to real frequencies by the substitution $i\Omega_n \to \Omega$,

$$\Omega_{\mathbf{q}} = \omega - \Delta(\mathbf{q}) + \frac{\beta(\mathbf{q})\omega_p^4(\mathbf{q})}{\omega\left[\Omega_{\mathbf{q}}^2-\omega_p^2(\mathbf{q})\right]} \tag{4.88}$$

There are three solutions to Eq.(4.88)

$$\Omega_1 = \frac{\tilde{\omega}}{3} + \frac{2}{3}\cos\left(\frac{\alpha}{3}\right)\left[\tilde{\omega}^2 + \omega_p^2\right]^{1/2} \tag{4.89}$$

$$\Omega_{2,3} = \frac{\tilde{\omega}}{3} - \frac{2}{3}\cos\left(\frac{\alpha \pm \pi}{3}\right)\left[\tilde{\omega}^2 + \omega_p^2\right]^{1/2} \tag{4.90}$$

with $\tilde{\omega} = \omega - \Delta$ and $\cos\alpha = \left[\tilde{\omega}^3 - 9\tilde{\omega}\omega_p^2 + 27\beta\omega_p^4/2\omega\right] / \left[\tilde{\omega}^2 + 3\omega_p^2\right]^{3/2}$. The dependence on $\mathbf{q}$ of all parameters is assumed. Only two solutions, $\Omega_{1,2}$ are real and positive. Consequently, instead of a single phonon mode, strongly coupled to carriers there are two branches of excitations describing the propagation of coupled phonon and polaronic plasmon, so called 'plasphons'. If the plasmon-phonon coupling is weak, $\beta \ll 1$ their dispersion is described by

$$\Omega_{1,2} \simeq \frac{1}{2}\left[\tilde{\omega} + \omega_p \pm \sqrt{(\tilde{\omega} - \omega_p)^2 + 2\beta\omega_p^3/\omega}\right] \tag{4.91}$$

In the limit $\beta \to 0\Omega_{1,2}$ describe the renormalised phonon with the frequency $\tilde{\omega}$ and the polaronic plasmon ω_p. However, for a finite β and $\tilde{\omega} \simeq \omega_p$ they are mixed and both contribute to the phonon GF

$$D(\mathbf{q}, \Omega) = \sum_{i=1}^{3} \frac{P_i(\mathbf{q})}{\Omega - \Omega_i(\mathbf{q})} \tag{4.92}$$

The ratio of weights of two contributions is

$$\frac{P_2}{P_1} = \frac{\left(\Omega_2^2 - \omega_p^2\right)\left(\Omega_3 - \Omega_1\right)}{\left(\Omega_1^2 - \omega_p^2\right)\left(\Omega_3 - \Omega_2\right)} \tag{4.93}$$

It can be of the order of unity if the polaronic plasmon and phonon frequencies are close to each other.

6.5.12 4.8 Polaron thermodynamics

(what is the exact influence of polarons on thermodynamics???)

Heat capacity

In the normal state for sufficiently high temperatures the polaron-polaron correlations are not very important and in the first approximation the small polaron heat capacity as well as the magnetic susceptibility are those of narrow band fermions (same as for Fermi gas??).

Moreover in the temperature range $T < \omega/2$ (what is ω? maybe there should be w?) the polaron bandwidth is temperature independent.

(what is this w here??? and the n which is below???)

For a narrow band Fermi-gas one obtains the heat capacity C_p: (why limits are such???)

$$C_p = 2T\int_{-w-\mu}^{w-\mu} d\xi N_p(\xi)\frac{df}{d\xi}\left(\frac{\xi}{T}\frac{d\mu}{dT} - \frac{\xi^2}{T^2}\right) \tag{4.94}$$

where $f(\xi) = \left(\exp\left(\frac{\xi}{T}\right) + 1\right)^{-1}$. This expression yields a linear temperature dependence $C_p(T)$ for low temperatures $T < 0.4w$ if the polaron density of states is energy independent, $N_p = 1/2w$

$$C_p = \frac{\pi^2 T}{3w} \tag{4.95}$$

and a power law decrease ($\sim T^{-2}$) for $T > w$:

$$C_p = \frac{w^2 n(2-n)}{6T^2}. \tag{4.96}$$

The numerical calculations in the intermediate temperature region reveal only a small change in the position T_m of the maximum of $C_p(T)$ with the variation of the filling factor $n, T_m \simeq 0.4w$, and a gradual increase of the maximum value from $C_p^m = 0.2$ at $n = 0.2$ to $C_p^m = 0.6$ at $n = 1$. The temperature dependence of the heat capacity is similar to the Schottky anomaly except for the low temperature region with the linear C_p instead of the exponential one of two-level systems.

(where are the plots that compare predictions with experiment!!!???)

Magnetic susceptibility

In the polaronic system the narrow band includes all states of the Brillouin zone rather than a small part of them under a peak of the density of states as in a so-called 'van -Hove scenario' of high-T_c. (why??? what is 'van -Hove scenario'?)

(what is the idea of these formulas??? one magnetic moment per polaron, so we count polarons?)

This fact provides us with the possibility to get an absolute value of the spin susceptibility of polarons considerably higher than those of wide band electrons

$$\chi_s = -\frac{\mu_B^2}{w} \int_{-w-\mu}^{w-\mu} d\xi \frac{df}{d\xi} \tag{4.97}$$

where μ_B is the Bohr magneton. The chemical potential is determined through the density of polarons

$$\mu = T \ln \frac{\exp \frac{nw}{T} - 1}{\exp \frac{w}{T} - \exp \frac{(n-1)w}{T}}, \tag{4.98}$$

and

$$\chi_s = \frac{\mu_B^2}{w} \frac{\left(\exp \frac{nw}{T} - 1\right)\left(\exp \frac{(2-n)w}{T} - 1\right)}{\exp \frac{w}{T} - 1}. \tag{4.99}$$

Eq.(4.99) yields the Curie law in the high-temperature limit, $T \gg w$ (I can check it later, but it looks easy to reproduce)

$$\chi_s \simeq \frac{\mu_B^2 n(2-n)}{2T}, \tag{4.100}$$

and a temperature independent susceptibility enhanced due to the polaron narrowing of the band for $T < w$:

$$\chi_s = \frac{\mu_B^2}{w} \tag{4.101}$$

with w instead of D as in ordinary metals.

The enhancement is the same as that of the specific heat ratio $\gamma = C_p/T$, Eq.(4.95) in contrast with the ordinary metals, where only the electronic heat capacity is increased by the electron-phonon interaction while the magnetic susceptibility remains unaffected.

(where are the plots that compare predictions with experiment!!!???)

6.5.13 4.9 Polaron kinetics: hopping transport

Theory

Transport properties of polarons depend strongly on the temperature. For temperature lower than the Debye temperature (or the characteristic phonon energy) polarons tunnel through the narrow band, however at higher temperatures the polaronic band collapses as discussed in section 4.4 and their transport is diffusive via thermally activated hopping (see e.g. Mott and Davis (1979)). There is extensive literature on the hopping transport of small polarons, in particular, the excellent reviews by Appel (1969) and Firsov (1975) and books by Klinger (1979) and Böttger and Bryksin(1985). Böttger and Bryksin also discussed in detail the hopping polaron transport in a random potential. These and other studies elucidated the value of the activation energy of the conductivity as well as the sign and the temperature behavior of the Hall effect in the hopping regime, $T \gg \omega/2$. In this regime the transport is due to thermally activated jumps of polarons from site to site. For such processes the diffusion coefficient is given by $D \simeq a^2 W$, where W is the hopping probability. The only term in the polaronic Hamiltonian, which changes the phonon occupation numbers is the polaron-phonon interaction H_{p-ph}. Applying the perturbation theory with respect to this interaction up to the second order one estimates the nearest neighbor hopping probability with the Fermi golden rule as

$$W = 2\pi \left\langle \sum_j \left| \langle j|H_{p-ph}|i\rangle \right|^2 \delta\left(\sum_{\mathbf{q}} \omega_{\mathbf{q}} \left(n^j_{\mathbf{q}} - n^i_{\mathbf{q}} \right) \right) \right\rangle, \tag{4.102}$$

where $|i\rangle$ and $|j\rangle$ are the eigenstates of H_0 corresponding to the polaron on site i with n^i_{q} phonons in each phonon mode and the polaron on the neighboring site j with n^j_{q} phonons, respectively. Representing the δ function in Eq.(4.102) by the integral and using the definition of the Heisenbeg operators we obtain in the second order with respect to the bandwidth

$$W = \int_{-\infty}^{\infty} dt \left[\Phi^{\mathbf{n},\mathbf{m}}_{\mathbf{m},\mathbf{n}}(t) - \sigma^2(\mathbf{a}) \right] e^{-i0^+|t|} \tag{4.103}$$

A real time multiphonon correlation function $\Phi^{i'j'}_{ij}(t)$ is the same as the Matsubara one, Eq.(4.39) with the substitution $|\tau| \to it$. Thus, we have

$$\Phi^{\mathrm{n,m}}_{\mathrm{m,n}}(t) = \sigma^2(\mathbf{a}) \exp\left(\frac{1}{N} \sum_{\mathbf{q}} |\gamma(\mathbf{q})|^2 [1 - \cos(\mathbf{q}\cdot\mathbf{a})] \frac{\cosh\left[\omega_{\mathbf{q}}\left(\frac{i}{2T} + t\right)\right]}{\sinh \frac{\omega_{\mathbf{q}}}{2T}} \right). \tag{4.104}$$

Substituting this expression into Eq.(4.103) and shifting the integration contour one obtains

$$W = T^2(\mathbf{a}) e^{-2g^2(\mathbf{a})} \int_{-\infty}^{\infty} dt \left[\exp\left(\frac{1}{N} \sum_{\mathbf{q}} |\gamma(\mathbf{q})|^2 [1 - \cos(\mathbf{q}\cdot\mathbf{a})] \frac{\cos(\omega_{\mathbf{q}} t)}{\sinh \frac{\omega_{\mathbf{q}}}{2T}} \right) - 1 \right] e^{-i0^+|t|} \tag{4.105}$$

The integrand here is an oscillating function. The integration with respect to t is performed by the use of the saddle-point approximation. This approximation is jusiified if a finite dispersion of the phonon frequency $\delta\omega$ is taken into account and the lemperature is so high that $T > \omega^2/2\gamma^2\delta\omega$. If this inequality is satisfied the integrand
decreases rapidly with increasing time. Then one can expand in the exponent $\cos(\omega t)$ in powers with respect to t up to the second order term. The unity in the integrand, Eq.(4.105), which compensates the divergence for $t \to \infty$ can be neglected. As a result one finds

$$W \simeq T^2(\mathbf{a})e^{-E_a/T}\int_{-\infty}^{\infty} dte^{-\delta t^2} \tag{4.106}$$

where the activation energy is

$$E_a = \frac{T}{N}\sum_{\mathbf{q}} |\gamma(\mathbf{q})|^2[1-\cos(\mathbf{q}\cdot\mathbf{a})]\tanh\left(\omega_{\mathbf{q}}/4T\right), \tag{4.107}$$

and

$$\delta = \frac{1}{2N}\sum_{\mathbf{q}} |\gamma(\mathbf{q})|^2[1-\cos(\mathbf{q}\cdot\mathbf{a})]\frac{\omega_{\mathbf{q}}^2}{\sinh\left(\omega_{\mathbf{q}}/2T\right)} \tag{4.108}$$

The activation energy is half of the polaronic level shift E_p, Eq.(1.98) if there is no dispersion of $\omega_{\mathbf{q}}$ and $\gamma(\mathbf{q})$. The dispersion diminishes the value of E_a further. By means of the Einstein relation $\sigma = ne^2D/T$ the hopping conductivity in the hopping region $T \gg \omega/2$ is found to be

$$\sigma_h = ne^2a^2\frac{\sqrt{\pi}T^2(\mathbf{a})}{2T\sqrt{E_aT}}e^{-E_a/T} \tag{4.109}$$

The hopping mobility $\mu_h \equiv \sigma_h/ne \sim \exp\left(-E_a/T\right)$ can be below $ea^2 \simeq 1cm^2/Vs$, which is the lowest limit for the Boltzmann theory to be applied. Within the Boltzmann theory such a low mobility corresponds to the mean free path $l < a$, which is not a reasonable result.

To calculate the transverse conductivity σ_{xy} and the Hall coefficient $R_H = \sigma_{xy}/H\sigma_{xx}^2$ of polarons one can introduce the vector potential $\mathbf{A}(\mathbf{r})$ of the external field with the Peierls substitution (Peierls (1933))

$$T(\mathbf{m}-\mathbf{n}) \to T(\mathbf{m}-\mathbf{n})e^{-ie\mathbf{A}(\mathbf{m})\cdot(\mathbf{m}-\mathbf{n})} \tag{4.110}$$

which is a fair approximation if the magnetic field is weak compared with the atomic field

$$eHa^2 \ll 1. \tag{4.111}$$

Here $\mathbf{A}(\mathbf{r})$ is the vector potential which can be also time dependent. Within the Boltzmann theory the sign of the Hall coefficient $R_H \simeq \pm 1/en$ depends on the type of carriers (holes or electrons) and the Hall mobility $\mu_H \equiv R_H\sigma_{xx}$ is the same as the drift mobility μ_t up to numerical factor of the order of unity. The calculations of a hopping Hall current similar to those of the hopping conductivity (Friedman and Holstein (1963), Friedman (1995)) shows that the Hall mobility depends on the symmetry of the crystal lattice and has nothing in common with the hopping mobility, neither with respect to the temperature dependence and even nor with respect to the sign. Thus, for hexagonal lattices three -site hops yield

$$\mu_H = ea^2\frac{\sqrt{\pi}T(\mathbf{a})}{\sqrt{12E_aT}}e^{-E_a/3T} \tag{4.112}$$

with the same sign for electrons and holes. The activation energy of the Hall mobility is three times less than that of the hopping mobility. In cubic crystals, the hopping Hall effect is governed by four-site hops. For the four-site case calculations by Emin (1971) gave a Hall mobility even more temperature independent with the sign depending on the type of carriers.

6.5.14 4.10 MIR conductivity of polarons

Theory

One of the hallmarks of polarons is the frequency and temperature dependence of their mid-infrared (MIR) conductivity $\sigma(\nu)$. In the low frequency and low temperature region, where the tunneling band transport operates the conductivity has the canonical Drude form

$$\sigma(\omega) = \frac{ne\mu_t}{1+(\nu\tau)^2}, \tag{4.113}$$

where the transport relaxation time τ may be frequency dependent because of the narrow band. For high mid-infrared frequencies well above the polaron bandwidth but below the inter-band gap the Drude law breaks down. In this frequency region one can apply the generalised Einstein relation $\sigma(\nu) = eD(\nu)/\nu$, where $D(\nu) = a^2W(\nu)$ and $W(\nu)$ is the hopping probability of the absorption of the energy quantum ν. The number of nearest neighbor transitions per second with the absorption of photon of the energy ν is given by the Fermi-golden rule

$$W^- = 2\pi \left\langle \sum_j \left| \langle j|H_{p-ph}|i\rangle \right|^2 \delta\left(\sum_{\mathbf{q}} \omega_{\mathbf{q}} \left(n^j_{\mathbf{q}} - n^i_{\mathbf{q}}\right) - \nu\right)\right\rangle, \tag{4.114}$$

and with the photon emission

$$W^+ = 2\pi \left\langle \sum_j \left| \langle j|H_{p-ph}|i\rangle \right|^2 \delta\left(\sum_{\mathbf{q}} \omega_{\mathbf{q}} \left(n^j_{\mathbf{q}} - n^i_{\mathbf{q}}\right) + \nu\right)\right\rangle. \tag{4.115}$$

As a result one gets

$$\begin{aligned} W(\nu) = W^- - W^+ &= 2T^2(\mathbf{a})e^{-2g^2(\mathbf{a})}\sinh(\nu/2T) \\ &\times \int_{-\infty}^{\infty} dt e^{-i\nu t}\left[\exp\left(\frac{1}{N}\sum_{\mathbf{q}} |\gamma(\mathbf{q})|^2[1-\cos(\mathbf{q}\cdot\mathbf{a})]\frac{\cos(\omega t)}{\sinh\frac{\omega\mathbf{q}}{2T}}\right) - 1\right] \end{aligned} \tag{4.116}$$

An in the case of the dc hopping conductivity the integral over t is calculated using the saddle-point approximation (Böttger and Bryksin (1985)). The saddle point is lying on the imaginary axis, say, at $t = -iy$. Setting at this point the derivative of the exponent with respect to t equal zero one gets the following equation for y

$$\nu = \frac{1}{N}\sum_{\mathbf{q}} |\gamma(\mathbf{q})|^2[1-\cos(\mathbf{q}\cdot\mathbf{a})]\omega_{\mathbf{q}}\sinh\left(\omega_{\mathbf{q}}y\right). \tag{4.117}$$

If the frequency is not too high, $\nu \ll 4E_pT/\omega$ we can expand sinh in powers of ωy io find

$$y = \frac{\omega}{2\delta}, \tag{4.118}$$

where δ is defined by Eq.(4.108). Expanding the exponent in Eq.(4.116) in powers of t near the point $t = -iy$ and shifting the integration contour such that it passes through this point one obtains

$$\sigma(\nu) = \sigma_h \frac{T\sinh(\nu/2T)}{\nu} e^{\nu^2/4\delta}. \tag{4.119}$$

For high temperatures, $T \gg \omega/2$, this expression becomes

$$\sigma(\nu) = ne^2a^2\frac{\sqrt{\pi}T^2(\mathbf{a})\left[1-e^{-\nu/T}\right]}{2\nu\sqrt{E_aT}}\exp\left[-\frac{(\nu-4E_a)^2}{16E_aT}\right]. \tag{4.120}$$

Consequently, the frequency dependence of the MIR conductivity has a form of an asymmetric Gaussian peak centered at $\nu = 4E_a \simeq 2E_p$ with the half-width $4\sqrt{E_aT}$ (Eagles (1963), Klinger (1963), Reik (1963)), Fig.4.6. According to the Franckthe principle, the position of the ions is not changed during an optical transiion. Therefore the frequency dependence of the Mir conductivity can be understood Fig.1.3. The polaron, say in the left adiabatic levels on two-site holstein model, Fig.1.3. tical transition ange in the the the the photon energy required to the from the sum of $\sigma(\nu)$, Eq. (4.120). The main control the order of max(T then comes the thin lines near the bottom with the energy of he of $2E_p \pm \sqrt{\text{ines}}$ in Fig.4.5. The corresponding photon energies are lying in the interval $2E_p \pm \sqrt{8E_pT}$ in agreement with the obtained formula. For low temperatures $T < \omega/2$ the half-width of the MIR maximum is of the order $\sqrt{E_p\omega}$ rather than $\sim \sqrt{E_pT}$.

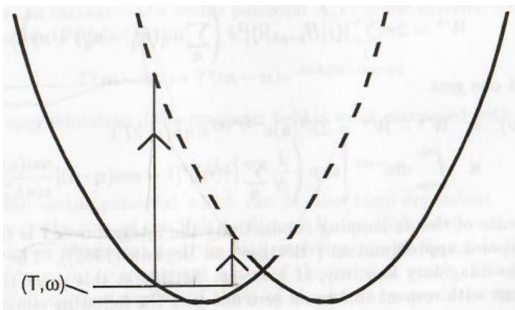

Fig.4.5. Optical transition between adiabatic levels of the two-site Holstein model.

The MIR absorption is due to the optical multiphonon transition within a single electron band. In the case of large polarons or electrons the MIR conductivity is much lower, if any. The analysis by Emin (1973, 1993) beyond the saddle-point approxima tion shows a more asymmetric and less temperature dependent MIR absorption of
large polarons compared with that of small polarons. Many perovskites have an intermediate value of the electron-phonon coupling $\lambda \sim 1$. It is, therefore, important to extend the theory of the MIR conductivity to the transition region from large to small polaron.

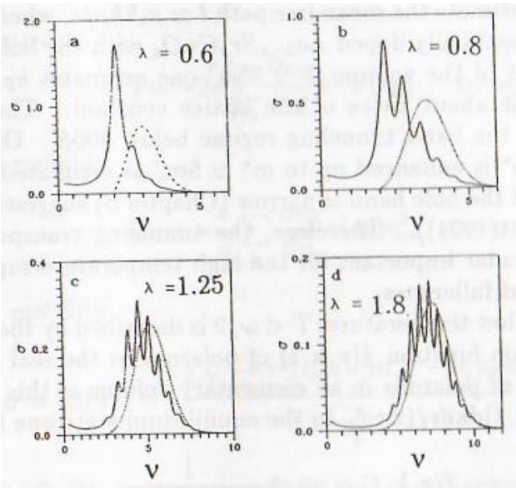

Fig.4.6. Small polaron MIR conductivity as a function of the frequency for different values of the electron-phonon coupling λ.

Such an extension is possible through the numerical calculations of $\sigma(\nu)$ of the finite size Holstein model by the exact diagonalisation procedure in the truncated space up to 50 excited phonons for the two site Holstein model and up to 20 phonons per each mode for the four site model (Alexandrov et al (1994b)). Conductivity occurs as energy is transferred between the electromagnetic field and the phonons via the charge carriers. The vibration energy must be capable of being dissipated. One has to introduce a continuous phonon density of states, which is not the case within the cluster model. However, one can avoid this problem introducing a lifetime τ_{ph} of phonons, which smears a δ-like density of their states, assuring the finite MIR conduclivity. The spectral shape of $\sigma(\nu)$ for the two-site Holstein model in the intermediate cegime ($\omega = 0.5J$) is shown in Fig.4.6 for $\tau_{ph}\omega = 2$. The main conclusions based on the numerical calculations are:

There is an agreement between the 'exact' $\sigma(\nu)$ and the analytical formula Eq.(4.119) in the strong coupling limit as far as the smooth part of the frequency dependence is concerned (dashed line).

The MIR conductivity is much more asymmetric in the intermediate coupling maion than that in the strong coupling regime;

The MIR conductivity shows an additional oscillating superstructure correspondling to a different spectral weight of the states with a different number of the virtual phanoms in the polaron cloud (section 4.12).

6.5.15 4.11 Polaron kinetics: band tunneling transport

Theory

The drift mobility μ_t along CuO 2 plane in high T_c copper oxides like $La_{2-x}Sr_xCuO_4$ is about 3 cm^2/Vs at room temperature. By the use of the transport relaxation time $\tau = \mu_t m^*/e$ one can estimate the mean free path $l \simeq \mu_t \hbar k_F/e$, where $\hbar k_F$ is the Fermi momentum. For the optimally doped $La_{2-x}Sr_xCuO_4$ with the hole density $n = x = 0.15$ per chemical unit of the volume $\Omega \simeq 95A^3$ one estimates $k_F \simeq 0.35 \times 10^8 A^{-1}$ and $l \simeq 6A$, which is about twice of the lattice constant. Therefore carriers in high T_c oxides are in the band tunneling regime below $300K$. On the other hand, their effective mass m^* is erhanced up to $m^* \simeq 5m_e$ as estimated from the London penetration depth and the hole band is narrow (Chapter 8) suggesting small polarons (Alexandrov and Mott(1994)). Therefore, the tunneling transport in

the narrow polaron band is particular important for the high temperature superconductors like copper oxides or doped fullerenes.

Polaron kinetics at low temperatures $T < \omega/2$ is described by the Boltzmann equation for the distribution function $f(\mathbf{r}, \mathbf{k}, t)$ of polarons in the real $\mathbf{r}$ and momentum k space. The number of polarons in an elementary volume of this space at time t is determined by $2f(\mathbf{r}, \mathbf{k}, t)d\mathbf{k}d\mathbf{r}/(2\pi)^3$. In the equilibrium state one has

$$f(\mathbf{r}, \mathbf{k}, t) = n_{\mathbf{k}} \equiv \frac{1}{\exp \frac{\epsilon_{\mathbf{k}} - \mu}{T} + 1} \tag{4.121}$$

The Boltzmann equation for polarons in an external electric $\mathbf{E}$ and magnetic $\mathbf{H}$ fields reads as

$$\frac{\partial f}{\partial t} + \mathbf{v}\frac{\partial f}{\partial \mathbf{r}} - e(\mathbf{E} + \mathbf{v} \times \mathbf{H})\frac{\partial f}{\partial \mathbf{k}} = \left(\frac{\partial f}{\partial t}\right)_c \tag{4.122}$$

where $\mathbf{v} = \partial\epsilon_{\mathbf{k}}/\partial\mathbf{k}$ is the group velocity. The collision integral for any elastic scattering is given by

$$\left(\frac{\partial f}{\partial t}\right)_c = 2\pi \sum_{\mathbf{q}} V_{sc}^2(\mathbf{q})\delta\left(\epsilon_{\mathbf{k}} - \epsilon_{\mathbf{k}+\mathbf{q}}\right)\left[f(\mathbf{r}, \mathbf{k}+\mathbf{q}, t) - f(\mathbf{r}, \mathbf{k}, t)\right] \tag{4.123}$$

where $V_{sc}(\mathrm{q})$ is the Fourier component of the scattering potential. The form of this integral does not depend on the statistics of particles because terms nonlinear in $f_{\mathbf{k}}$ are canceled. For a weak homogeneous electric and magnetic fields the Boltzmann equation can be solved by the substitution

$$f(\mathbf{r}, \mathbf{k}, t) = n_{\mathbf{k}} - \frac{\partial n_{\mathbf{k}}}{\partial \epsilon_{\mathbf{k}}}\mathbf{F}\left(\epsilon_{\mathbf{k}}\right) \cdot \mathbf{v} \tag{4.124}$$

We consider the case when the transport relaxation time defined as

$$\frac{1}{\tau\left(\epsilon_{\mathbf{k}}\right)} \equiv 2\pi \sum_{\mathbf{k}'} (1 - \cos\Theta) V_{sc}^2\left(\mathbf{k}' - \mathbf{k}\right)\delta\left(\epsilon_{\mathbf{k}'} - \epsilon_{\mathbf{k}}\right) \tag{4.125}$$

depends only on the energy. Here Θ is the angle between $\mathbf{v}'$ and $\mathbf{v}$. Then the Boltzmann equation for $\mathbf{F}(\epsilon)$ becomes

$$\mathbf{F}(\epsilon) \cdot \mathbf{v} = -e\tau(\epsilon)\left[\mathbf{E} \cdot \mathbf{v} - \mathbf{F}(\epsilon) \cdot \left(\mathbf{v} \times \mathbf{H} \cdot \nabla_{\mathbf{k}}\right)\mathbf{v}\right] \tag{4.126}$$

If the magnetic field is not too high, $\mu_t H \ll 1$, one can keep only terms linear in H with the following result for the nonequilibrium part of the distribution function

$$\mathbf{F}(\epsilon) \cdot \mathbf{v} = -e\tau(\epsilon)\left[\mathbf{E} \cdot \mathbf{v} + e\tau(\epsilon)\mathbf{E} \cdot \left(\mathbf{v} \times \mathbf{H} \cdot \nabla_{\mathbf{k}}\right)\mathbf{v}\right] \tag{4.127}$$

By the use of the current

$$\mathbf{j} = -2e \sum_{bfk} \frac{\partial n_{\mathbf{k}}}{\partial \epsilon_{\mathbf{k}}}\mathbf{v} \cdot \mathbf{F}\left(\epsilon_{\mathbf{k}}\right) \qquad \text{or cy7cis yer cnopu} \tag{4.128}$$

we obtain the drift mobility

$$\mu_t = -\frac{e}{n} \sum_{\mathbf{k}} \frac{\partial n_{\mathbf{k}}}{\partial \epsilon_{\mathbf{k}}}\tau\left(\epsilon_{\mathbf{k}}\right) v_x^2 \tag{4.129}$$

as well as the Hall mobility

$$\mu_H \equiv R_H \sigma_{xx} = e \frac{\sum_{\mathbf{k}} \frac{\partial n_{\mathbf{k}}}{\partial \epsilon_{\mathbf{k}}} \tau^2 \left(\epsilon_{\mathbf{k}}\right) \left(v_y^2 m_{xx}^{-1} - v_y v_x m_{yx}^{-1}\right)}{\sum_{\mathbf{k}} \frac{\partial n_{\mathbf{k}}}{\partial \epsilon_{\mathbf{k}}} \tau \left(\epsilon_{\mathbf{k}}\right) v_x^2} \tag{4.130}$$

Here $m_{\alpha\beta}^{-1} = \partial^2 \epsilon(\mathbf{k}) / \partial k_\alpha \partial k_\beta$ is the polaron effective mass tensor.
The temperature dependence of the mobilities is determined not only by the temperature dependence of the relaxation time but also by the energy dispersion $\epsilon_{\mathbf{k}}$ within the polaron band. At intermediate temperatures $w < T < \omega/2$ the finite bandwidth w becomes important. There are several (quasi)elastic scattering mechanisms, which normally restrict the relaxation time. In the strongly coupled electron-phonon sys1 cm the scattering due to the residual polaron-phonon interaction H_{p-ph} is primarily important. As we have discussed in section 4.4 two-phonon scattering due to the interaction with the high frequency phonons responsible for the polaron formadion becomes less effective at low temperatures $T \ll \omega/2$ because there are no such phonons available. On the other hand, impurities and thermal phonons contribute to Ule relaxation rate giving rise to the power temperature dependence of the polaronic mobilities rather than to the exponential one. Here we consider the scattering of twodimensional non-degenerate small polarons by the acoustical phonons (Alexandrov (1092c)). In this example, which is important for the normal state kinetics of high- T_c comper oxides the characteristic acoustic phonon frequency is $\omega_{\mathrm{q}} \leq s\sqrt{2m^* T}$ because Whe phonon momentum in the scattering is of the order of the polaron momentum $0\sqrt{2}m^* T$. The relevant phonon frequency turns out to be small compared with the temperature

$$\frac{\omega_{\mathrm{q}}}{T} \simeq \sqrt{\frac{m^* s^2}{T}} \ll 1 \tag{4.131}$$

Euri lor rather low temperatures of the order of $10K$ if $m^* < 10m_e$. Therefore the instituing is practically elastic with the square of the matrix element independent of line momentum and linear in temperature

$$V_{sc}^2(\mathbf{q}) = \frac{1}{2N} \left|\gamma_{ac}(\mathbf{q})\omega_{\mathbf{q}}\right|^2 n_{\omega_{\mathbf{q}}} \sim T \tag{4.132}$$

Here $n_{\omega\mathbf{q}} \simeq T/\omega_{\mathbf{q}} \gg 1$ is the distribution function of thermal phonons. By the use of the isotropic spectrum $\epsilon_{\mathbf{k}} = \epsilon_k$ one obtains

$$\frac{1}{\tau_{ac}} \sim Tk \frac{dk}{d\epsilon_k} \tag{4.133}$$

The $2D$ density of states is energy independent, $kdk/d\epsilon_k = m^*$ and so is τ_{ac}. As a result the drift mobility of $2D$ nondegenerate carriers scattered by acoustic phonons is inversely proportional to the temperature and the resistivity is linear in temperature

$$\rho \sim 1/\mu_t \sim T \tag{4.134}$$

if the number of polarons is temperature independent.
Consequently, there is a duality of the kinetic properties of small polarons. At high temperatures they behave as localised particles propagating through the crystal by the thermally activated hopping. On the other hand at low temperatures they are in the Bloch states with well defined momenta propagating by tunneling. This duality can be seen in the temperature dependence of resistivity. In particular, at high temperatures the activation exponential drop of resistivity is expected, while below some characteristic temperature resistivity follows the power law, which is sensitive to the scattering mechanism and the polaron band dispersion. In high T_c oxides and doped fullerenes the high temperature activation region is ill defined because the relevant phonon frequency and the activation energy are of the same order, ca. $500 - 1000K$. On

the other hand, in several nonsuperconducting oxides with the lower phonon frequencies the crossover between the band tunneling and the hopping is observed, Chapter 8.

6.5.16 4.12 Electron Green's function and ARPES of polaronic systems

Theory

The extended-localised duality of small polarons and the band narrowing effect can be seen in the electron spectral function (Alexandrov and Ranninger (1992b)). The intensity of the coherent (i.e. angle-dependent) contribution to the spectral weight is expected to be strongly reduced due to a factor $\exp(-g^2)$ which plays the role of a step ' Z ' of the Fermi distribution function, while the broad featureless incoherent background should appear due to the phonon cloud, which constitutes a small polaron. To see these features we calculate the temperature electron Green's function under the condition of the polaron band narrowing

$$g(\mathbf{k},\omega_n) = -\frac{1}{2}\sum_{\mathbf{m}}\int_{-1/T}^{1/T} d\tau e^{i\omega_n\tau + i\mathbf{k}\cdot\mathbf{m}}\langle\langle T_\tau c_0(\tau) c^\dagger_{\mathbf{m}}\rangle\rangle \tag{4.135}$$

For convenience we omit spin. Applying the Lang-Firsov canonical transformation and neglecting the residual polaron-phonon coupling H_{p-ph} one obtains

$$g(\mathbf{k},\omega_n) = \frac{T}{N}\sum_{\omega_{n'},\mathbf{m},\mathbf{k}'}\frac{\sigma(\mathbf{m},\omega_{n'}-\omega_n)\, e^{i(\mathbf{k}-\mathbf{k}')\cdot\mathbf{m}}}{i\omega_{n'}-\xi_{\mathbf{k}'}} \tag{4.136}$$

with the Fourier component $\sigma(\mathbf{m},\omega_n)$ of the correlation function, determined as

$$\sigma(\mathbf{m},\tau) = \exp\left(\frac{1}{2N}\sum_{\mathbf{q}}|\gamma(\mathbf{q})|^2 f_{\mathbf{q}}(\mathbf{m},\tau)\right), \tag{4.137}$$

with

$$f_{\mathbf{q}}(\mathbf{m},\tau) = [\cos(\mathbf{q}\cdot\mathbf{m})\cosh(\omega_{\mathbf{q}}|\tau|) - 1]\coth\frac{\omega_{\mathbf{q}}}{2T} + \cos(\mathbf{q}\cdot\mathbf{m})\sinh(\omega_{\mathbf{q}}|\tau|)$$

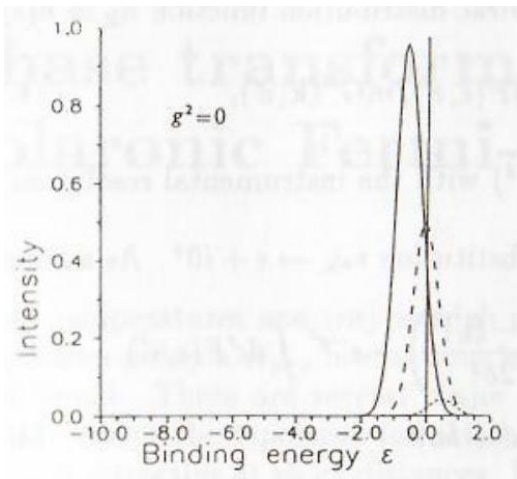

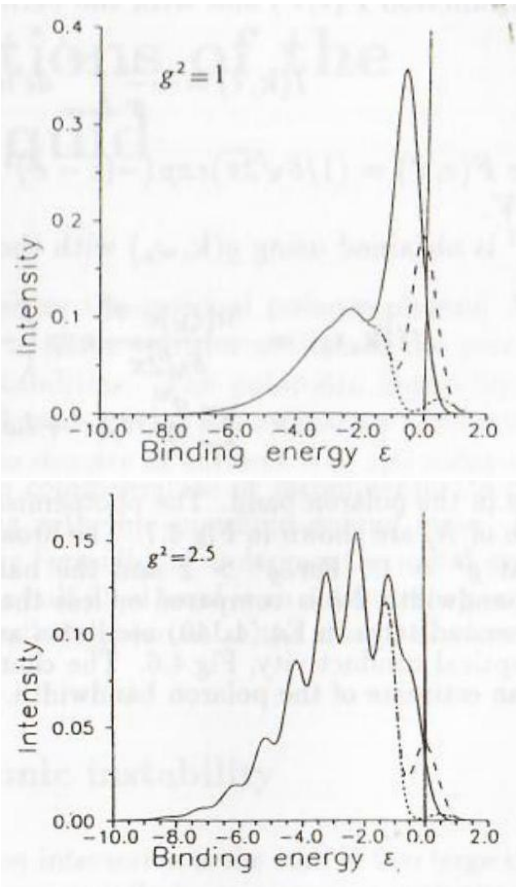

Fig 4.7 Polaron angle-resolved photoemission for three different angles and different coupling; ϵ is measured in units of ω.

Calculating the Fourier component of $\sigma(\mathbf{m},\tau)$ one obtains for the case of dispersiculess phonons ($\omega_{\mathbf{q}}=\omega$) and a constant $|\gamma(\mathbf{q})|^2=2g^2$

$$g\left(\mathbf{k},\omega_n\right)=\frac{e^{-g^2}}{i\omega_n-\xi_{\mathbf{k}}}+\frac{e^{-g^2}}{N}\sum_{l=1}^{\infty}\frac{g^{2l}}{l!}$$
$$\times\sum_{\mathbf{k}'}\left(\frac{n_{\mathbf{k}'}}{i\omega_n-\xi_{\mathbf{k}'}+l\omega}+\frac{1-n_{\mathbf{k}'}}{i\omega_n-\xi_{\mathbf{k}'}-l\omega}\right) \tag{4.138}$$

In the polaron regime the electron Green's function consists of two different contrihutiona. The first coherent term arises from the polaron band motion. The second is independent contribution describes the excitations accompanied by the emission
and absorption of phonons. It is this term which is responsible for the asymmetric background of the optical conductivity, Fig.4.6 and of the photoemission spectra (see below). We notice that the spectral density in the second term spreads over a wide frequency range of order of the polaron level shift $2g^2\omega$ or more. On the contrary the coherent term shows an angular dependence in a frequency range of order of the polaron bandwidth $2w$.

The angle-resolved photoemission spectroscopy (ARPES) measures the imaginary part of the retarded Green's function integrated with a Gaussian instrumental resolution function $F\left(\epsilon,\epsilon'\right)$ and with the Fermi-Dirac distribution function $n_{\mathbf{k}}\equiv n(\epsilon)$

$$I(\mathbf{k},\epsilon)=-\frac{1}{\pi}\int_{-\infty}^{\infty}d\epsilon' n\left(\epsilon'\right)F\left(\epsilon,\epsilon'\right)\operatorname{Im}G^R\left(\mathbf{k},\epsilon'\right) \tag{4.139}$$

where $F\left(\epsilon,\epsilon'\right)=\left(1/\delta\sqrt{2\pi}\right)\exp\left(-\left(\epsilon-\epsilon'\right)^2/2\delta^2\right)$ with the instrumental resolution $\delta\simeq 10$ meV.
G^R is obtained using $g\left(\mathbf{k},\omega_n\right)$ with the substitution $i\omega_n\to\epsilon+i0^+$. As a result

$$I(\mathbf{k},\epsilon) = \frac{n\left(\xi_{\mathbf{k}}\right)e^{-g^2}}{\delta\sqrt{2\pi}}\exp\left(-\frac{\left(\epsilon-\xi_{\mathbf{k}}\right)^2}{2\delta^2}\right) + e^{-g^2}\int d\epsilon' F\left(\epsilon,\epsilon'\right)$$
$$\times\sum_l \frac{g^{2l}}{l!}N_p\left(\epsilon'+l\omega\right)n\left(\epsilon'+l\omega\right) \tag{4.140}$$

with N_p the density of states in the polaron band. The photoemission spectra calculated with the Gaussian form of N_p are shown in Fig 4.7. The broadened asymmetric line shape occurs already at $g^2 = 1$. For $g^2 > 2$ and the bare half bandwidth $D = 200$meV the polaron bandwidth $2w$ is compared or less than the phonon frequency. In this regime the second term in Eq.(4.140) oscillates as a function of the binding energy just as the optical conductivity, Fig.4.6. The characteristic angular dispersion of ARPES gives an estimate of the polaron bandwidth.

6.6 2 Large and small bipolaron

6.6.1 2.1 Strong-coupling large bipolaron

Theory

Approaching the many polaron problem we first consider two carriers on a deformable lattice. As in the case of a single polaron we distinguish a strong and intermediatecoupling large bipolaron, formed by two large polarons in an ionic solid and a small bipolaron, formed by two small polarons in any solid if the electron-phonon interaction is sufficiently strong. A possibility of pairing of two large polarons was considered by Pekar (1951). He found that a large bipolaron does not exist for any value of the crystal parameters, ϵ and ϵ_0. Physically, one can reach this conclusion by scaling arguments (Emin (1995)) similar to those applied to a small polaron in the Introduction. The long range interaction with optical phonons is Coulomb like at large distances. Then the total energy, which must be minimised for a large polaron is

$$E_p(r) = \frac{\pi^2}{2mr^2} - \frac{e^2}{2\kappa r} \tag{2.1}$$

The first term in Eq.(2.1) is the minimum kinetic energy of a particle confined in a sphere of radius r, while the second term is the potential plus the deformation energy. Minimising Eq.(2.1) with respect to r one obtains the polaron radius

$$r_p = 2\pi^2 a_B$$

and the energy

$$E_p = -\frac{1}{4\pi^2}\alpha^2\omega. \tag{2.3}$$

The numerical coefficient in Eq.(2.3) ($\simeq -0.025$) should be compared with a more realistic variational estimation -0.109 , Eq.(1.42). For a state of two carriers sharing the same orbital state within a common potential well the corresponding functional is

$$E_b(r) = 2\frac{\pi^2}{2mr^2} - 4\frac{e^2}{2\kappa r} + \frac{e^2}{\epsilon r} \tag{2.4}$$

where the first term is twice the polaron kinetic energy, the second term is four times the corresponding term for a polaron because the polarisation is twice as large as that for a polaron, and the last term describes the Coulomb repulsion between two
carriers. Minimising Eq.(2.4) we obtain for the bipolaron radius

$$r_b = r_p \frac{\epsilon_0 - \epsilon}{\epsilon_0 - 2\epsilon} \tag{2.5}$$

with r_p determined by Eq.(2.2). Thus a large bipolaron can only form if $\epsilon_0 > 2\epsilon$. The ground state energy is

$$E_b = -\frac{1}{2\pi^2}\alpha^2\omega\left(\frac{\epsilon_0 - 2\epsilon}{\epsilon_0 - \epsilon}\right)^2 \tag{2.6}$$

The large bipolaron is energetically stable with respect to dissociation into two separate large polarons if the binding energy is positive:

$$\Delta \equiv 2E_p - E_b > 0 \tag{2.7}$$

This however is not the case because

$$\Delta = 2\left|E_p\right|\left[\left(1 - \frac{\epsilon}{\epsilon_0 - \epsilon}\right)^2 - 1\right] < 0 \tag{2.8}$$

While a large portion of the Coulomb repulsion is neutralised by the Fröhlich interaction, this long-range interaction alone remains insufficient to produce a bound state. Approaching the problem from the weak-coupling limit Takada (1982) reached the same conclusion for the three-dimensional case. He introduced the effective retarded interaction between electrons with the Fourier component $V(\mathbf{q}, \nu)$ determined as

$$V(\mathbf{q}, \nu) = \frac{4\pi e^2}{q^2\epsilon(\mathbf{q}, \nu)} \tag{2.9}$$

The dielectric function $\epsilon(\mathbf{q}, \nu) = \epsilon_0\left(\omega^2 - \nu^2\right)/\left(\omega^2 - \epsilon_0\nu^2/\epsilon\right)$ takes into account the retarded attraction, mediated by polar-optic phonons in a wide frequency region $\omega\epsilon/\epsilon_0 < \nu < \omega$. By the use of the two-particle vertex part one can derive the BetheSalpeter equation for the wave function $\phi_{\mathbf{p}}$, describing the relative motion of two electrons in the momentum representation

$$\left(\frac{p^2}{m} + \Delta\right)\phi_{\mathbf{p}} + \sum_{\mathbf{p}'} \frac{4\pi e^2}{\left|\mathbf{p} - \mathbf{p}'\right|^2 \epsilon} \frac{\left(p^2 + p'^2 + 2m\Delta + 2m\omega\epsilon/\epsilon_0\right)}{\left(p^2 + p'^2 + 2m\Delta + 2m\omega\right)}\phi_{\mathbf{p}'} = 0 \tag{2.10}$$

There are no solutions to this equation with a positive binding energy Δ in three dimensions. As is known from an elementary problem in quantum mechanics, a bound state can be formed more easily when the dimensionality is decreased. Since the state of the large bipolaron can be considered as the linear combination of longwave plane waves, the density of one-particle states near the bottom of the conduction band enters the problem. It should be large in order to bind two electrons. In a $3D$ system, however, the density of states vanishes at the bottom of the band and thus the bound state cannot be formed. Compared with a $3D$ system, a $2D$ system has a better chance to provide the bound state, because in a $2D$ system, the density of states is finite at the bottom of the band. In a $1D$ system, one can expect an even larger binding energy, because the density of states at the bottom of the band is infinite in this case. Takada found that in $1D$ and $2D$ system there is indeed a
bound solution of the Bethe-Salpeter equation with rather low binding energy. One can prove the absence of a bound state in three dimensions for any direct retarded interaction between electrons with the Fourier component of the form of Eq.(2.9) if the static dielectric function $\epsilon(\mathbf{q}, 0)$ is positive for all $\mathbf{q}$ (Khomskii (1995)). In the general case, however, the static electron-electron interaction can be attractive, which formally corresponds to the negative sign of $\epsilon(\mathbf{q}, 0)$ for finite q. This happens in some simple metals and, in particular, in complex compounds because

short-wave acoustic and local vibration modes contribute to the electron-electron interaction. There are arguments, that a negative short-wave static dielectric function does not necessarily lead to a global instability (Dolgov et al (1981)). Moreover in a strongly polarisible lattice with $\epsilon_0/\epsilon \gg 1$ the bipolaron radius, Eq.(2.5) is close to the polaron one. The absolute value of the binding energy $|\Delta|$ in units of twice the polaron binding energy calculated by scaling is very small

$$\frac{|\Delta|}{2\,|E_p|} \simeq 2\frac{\epsilon}{\epsilon_0} \ll 1 \tag{2.11}$$

Therefore one can expect that two polaron wave functions strongly overlap and the quantum exchange interaction can stabilise Pekar's bipolaron even without any other attraction except the Fröhlich one. This was first realised by Vinetskii and Giterman (1958). The functional, which must be minimised is now

$$\begin{aligned} J_b\left(\Psi\left(\mathbf{r}_1,\mathbf{r}_2\right)\right) = & \int d\mathbf{r}_1 \int d\mathbf{r}_2 \left[\frac{\left|\nabla_1\Psi\left(\mathbf{r}_1,\mathbf{r}_2\right)\right|^2}{2m} + \frac{\left|\nabla_2\Psi\left(\mathbf{r}_1,\mathbf{r}_2\right)\right|^2}{2m} + \frac{\left|\Psi\left(\mathbf{r}_1,\mathbf{r}_2\right)\right|^2}{\epsilon\left|\mathbf{r}_1-\mathbf{r}_2\right|}\right] \\ & - \frac{4}{2ma_B}\iint d\mathbf{r}_1 d\mathbf{r}_1' \iint d\mathbf{r}_2 d\mathbf{r}_2' \frac{\left|\Psi\left(\mathbf{r}_1,\mathbf{r}_2\right)\right|^2\left|\Psi\left(\mathbf{r}_1',\mathbf{r}_2'\right)\right|^2}{\left|\mathbf{r}_1-\mathbf{r}_1'\right|} \end{aligned} \tag{2.12}$$

The minimum of Eq.(2.12) should be compared with twice of the minimum of a polaron functional $J(\psi(\mathbf{r}))$, Eq.(1.9). Then the bipolaron binding energy is

$$\Delta = 2\min(J) - \min\left(J_b\right) \tag{2.13}$$

Vinetskii and Giterman selected the variational singlet function in a symmetric form similar to that of the hydrogen molecule

$$\psi\left(\mathbf{r}_1,\mathbf{r}_2\right) = A\left[\psi\left(\mathbf{r}_1-\mathbf{a}/2\right)\psi\left(\mathbf{r}_2+\mathbf{a}/2\right)+\psi\left(\mathbf{r}_2-\mathbf{a}/2\right)\psi\left(\mathbf{r}_1+\mathbf{a}/2\right)\right] \tag{2.14}$$

where A is the normalisation factor and $\psi(\mathbf{r})$ is a single polaron function. Correlations between polarons are taken into account by assuming a nonzero distance $|\mathbf{a}|$ between them. For a small distance the polarisation attraction force depends differently on the distance compared with the Coulomb repulsion. Therefore the separation of two polaron clouds can stabilise a bipolaron. The simplest form of $\psi(\mathbf{r})$ as for Pekar's polaron, section 1.1

$$\psi(\mathbf{r}) = \frac{1}{\sqrt{\pi r_p^3}} e^{-r/r_p} \tag{2.15}$$

yields a positive binding energy if

$$\frac{\epsilon}{\epsilon_0} \leq 0.05 \tag{2.16}$$

The maximum binding energy at $\epsilon/\epsilon_0 \to 0$ is small:

$$\frac{\Delta}{2\,|E_p|} = 0.08 \tag{2.17}$$

and the distance between two polarons is about 1.5 of the polaron radius r_p. Vinetskii and Pashitskii (1983) extended this approach to a crystal having two-dimensional or one-dimensional anisotropy of the carrier mass, either for easy movement in a plane $m_\parallel < m_\perp$ or for easy movement along an axis $m_\parallel > m_\perp$. Here $m_\parallel$is the in-plane and $m_\perp$ is the out-of-plane mass. A variational polaron wave function was taken in the Gaussian form

$$\psi(\mathbf{r}) = \beta^{1/2}\beta' \left(\frac{2}{\pi}\right)^{3/4} e^{-\beta^2 z^2 - \beta'^2 \rho^2} \tag{2.18}$$

where β, β' are variational parameters, z is the coordinate perpendicular to the plane and $\rho^2 = x^2 + y^2$. The effective mass anisotropy widens the range of existence of Pekar's bipolaron and increases its binding energy as shown in Fig.2.1 for the easy movement along the axis.

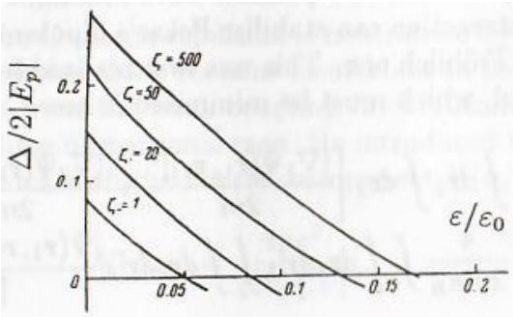

Fig.2.1. Dependence of the bipolaron binding energy on ϵ / ϵ_{0} for different values of the anisotropy

ξ, related to $m_{\parallel}/m_{\perp}$ by $2\xi^3 \left[\xi \ln\left(\sqrt{\xi^2-1}+\xi\right) - \sqrt{\xi^2-1}\right] / \left[\xi\sqrt{\xi^2-1} - \ln\left(\sqrt{\xi^2-1}+\xi\right)\right] = m_{\parallel}/m_{\perp}$.

It is seen from Fig.2.1 that when $m_{\parallel}/m_{\perp} \gg 1 (\xi \gg 1)$ a one - dimensional bipolaron can exist for a considerably larger ratio ϵ/ϵ_0 compared with the $3D$ case.

The variational approach to Pekar's bipolaron was improved by Mukhomorov (1982) and by Suprun and Moizhes (1982). Mukhomorov represented the two-particle wave function of the singlet state as a series of different polaron configurations including $|1s^2\rangle, |1s2p\rangle$ and $|2p^2\rangle$

$$\Psi(\mathbf{r}_1, \mathbf{r}_2) = A\left[\left|1s^2\right\rangle + C_1|1s2p\rangle + C_2\left|2p^2\right\rangle\right] \tag{2.19}$$

where different terms are symmetrised products of s-wave $\psi_s \sim (1+\beta r)\exp(-\beta r)$ and p-wave $\psi_p \sim rY_{10}(\Theta)\exp(-\beta' r)$ one-particle functions centered at the same site rather than at two different sites. This refinement of the variational wave function with four variational parameters $C_{1,2}, \beta$ and β' increases the binding energy up to $\Delta/2\,|E_p| = 0.195$ and the range of existence of the bipolaron up to $\epsilon/\epsilon_0 \leq 0.1$. Suprun and Moizhes found a simpler trial function with only two variational parameters β, β'

$$\Psi(\mathbf{r}_1, \mathbf{r}_2) \sim \psi_s(\mathbf{r}_1)\,\psi_s(\mathbf{r}_2)\,(1+\beta'\,|\mathbf{r}_1 - \mathbf{r}_2|)\,, \tag{2.20}$$

which gives a lower binding energy and a wider region $\epsilon/\epsilon_0 \leq 0.14$ than those determined with Eq.(2.19). It can thus be expected that, if the electron correlations are taken into account, a large bipolaron can exist with rather low binding energy.

6.6.2 2.2 Intermediate-coupling large bipolaron

Theory

As in the case of the large polaron the continuum approximation for the lattice polarisation is unacceptable for low and intermediate values of the electron-phonon coupling constant α. There is another problem with the variational estimation of the bipolaron binding energy in section 2.1 where the single-polaron energy E_p is estimated with the same shape of the polaron

trial function as for the bipolaron one. Adamowskii (1989) noticed that the values of $2\,|E_p|$ obtained by the Pekar strongcoupling method were much too low compared with the best estimates based on the path-integral approach. After recalculating the variational results for Δ of section 2.1 with the use of the best estimate of a single polaron ground state energy $|E_p|$ one obtains no binding of two polarons, with an exception of very large α. Consequently, there is no reliable conclusion concerning the existence of a large bipolaron within the strong-coupling variational analysis. A more reliable conclusion can be reached by applying the LLP and displacement canonical transformations as in the case of a single intermediate-coupling polaron, section 1.4 (Bassani et al (1991)).

Here two electrons in interaction with a phonon field are described by the following Hamiltonian

$$H = \sum_{j=1.2} \left[-\frac{\nabla_j^2}{2m} + \sum_{\mathbf{q}} \left(V_{\mathbf{q}} d_{\mathbf{q}} e^{i\mathbf{q}\cdot\mathbf{r}_j} + h.c. \right) \right] + \frac{e^2}{\epsilon\,|\mathbf{r}_1 - \mathbf{r}_2|} + \sum_{\mathbf{q}} \omega_{\mathbf{q}} \left(d_{\mathbf{q}}^\dagger d_{\mathbf{q}} + 1/2 \right) \tag{2.21}$$

Since the Hamiltonian commutes with the total linear momentum one can eliminate the center-of-mass coordinate and classify the relative motion of two polarons with the angular momentum L. Both linear and angular momenta include the phonon contribution. Their conservation constrains a possible shape of the trial functions. Introducing the relative coordinate $\mathbf{r} = \mathbf{r}_1 - \mathbf{r}_2$ and the position of the center of mass $\mathrm{R} = (\mathrm{r}_1 + \mathrm{r}_2)/2$ one can write the Hamiltonian in the form

$$II = -\frac{\nabla_{\mathbf{R}}^2}{4m} - \frac{\nabla_{\mathbf{r}}^2}{m} + 2\sum_{\mathbf{q}} \left[V_{\mathbf{q}} d_{\mathbf{q}} \cos(\mathbf{q}\cdot\mathbf{r}/2) e^{i\mathbf{q}\cdot\mathbf{R}} + h.c. \right] + \frac{e^2}{\epsilon r} + \sum_{\mathbf{q}} \omega_{\mathbf{q}} \left(d_{\mathbf{q}}^\dagger d_{\mathbf{q}} + 1/2 \right) \tag{2.22}$$

The unitary LLP transformation $\exp S_{LLP}$ with

$$S_{LLP} = i \sum_{\mathbf{q}} (\mathbf{q}\cdot\mathbf{R}) d_{\mathbf{q}}^\dagger d_{\mathbf{q}} \tag{2.23}$$

diminates the center of mass coordinate from the Hamiltonian. To classify the eigenstates by the total angular momentum one can introduce new phonon operators

$$d_{q,l,m} = \frac{q}{(2\pi)^{3/2}} \int d\Omega_{\mathbf{q}} Y_{l,m}^* \left(\Omega_{\mathbf{q}}\right) d_{\mathbf{q}} \tag{2.24}$$

where $d\Omega_q$ is the element of solid angle $\Omega_{\mathbf{q}}$ of $\mathbf{q}$ and $Y_{l,m}$ is a spherical harmonic. The variational trial state $|L, M\rangle$, which is an eigenstates of L and $M \equiv L_z$, is constructed by the use of the displacement operator $\exp S(\mathbf{r})$ as

$$|L, M\rangle = R_L(r) Y_{L,M} \left(\Omega_{\mathbf{r}}\right) \exp S(\mathbf{r}) \tag{2.25}$$

Here

$$S(\mathbf{r}) = \sum_{l.m} \int_0^\infty dq \left[g_{q,l}(r) Y_{l.m} \left(\Omega_{\mathbf{r}}\right) d_{q,l,m} - h.c. \right] \tag{2.26}$$

and

$$R_L(r) = A r^\beta e^{-r/r_b} \tag{2.27}$$

The energy $\langle L, M | e^{S_{LLP}} H e^{-S_{LLP}} | L, M \rangle$ is minimised with respect to the variational parameters r_b, β and the variational function $g_{q,l}(r)$. The latter can be expressed analytically

through the confluent hypergeometric functions. The total energy is calculated numerically and compared with twice the intermediate coupling polaron the two-dimensional case with the three-dimensional interaction $V_{\mathbf{q}} \sim 1/\sqrt{q}$ as well.

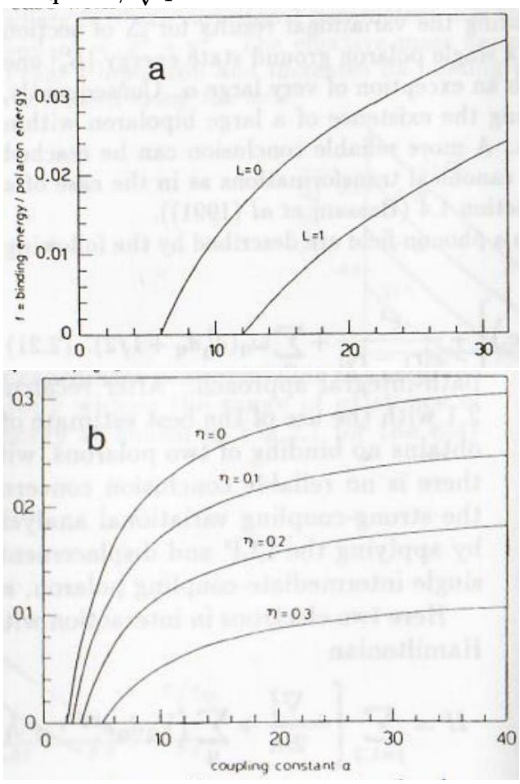

Fig.2.2 Dependence of the bipolaron binding energy on the coupling constant α in the threedimensional case for $\epsilon/\epsilon_0 = 0$ and $L = 0, 1(a)$ and in the two-dimensional case for different values of $\eta \equiv \epsilon/\epsilon_0(b)$.

Compared with the Pekar's variational approach there are several new features of the bipolaron formation in the intermediate coupling regime.

1. The large bipolaron exists ($\Delta > 0$) only if the electron-phonon coupling constant α is greater than a critical value α_c, which is ~ 6 in three dimensions and ~ 2 in two dimensions. The change in dimensionality increases the normalised binding energy by at least one order of magnitude as shown in Fig.2.2 a,b;

2. The largest value of ϵ/ϵ_0 for which $\Delta > 0$ depends on the coupling constant α being of the order of 0.05 in three dimensions and 0.4 in two dimensions.

3. The bipolaron radius is always of the order of a few polaron radii, i.e., in practical cases, of a few Å.

The latter means that a small bipolaron approach taking into account a finite bandwidth is more appropriate even in the case of the Fröhlich interaction.

6.6.3 2.3 Path integral approach to large bipolaron

Theory

A drawback of the variational formulation based on the canonical transformation is that it does not permit us to study well the bipolaron stability since the estimations of the single polaron energy are poor compared to the path integral calculations. The variational method in the form of the path integral applied to the Fröhlich polaron by Feynman (1955) is known to

give a very good variational estimates of the polaron ground state in the intermediate coupling regime. A large bipolaron problem was treated with path integrals by Kochetov et al (1977) in the $3D$ strong coupling limit, by Hiramoto and Toyozawa (1985) in three dimensions for optical and acoustic phonons and by Verbist et al (1991) for the whole coupling range in both two and three dimensions.

The path integral method allows for an exact elimination of the phonon coordinates. All thermodynamic quantities are known if one can calculate the partition function $Z = \mathrm{Tr}\left[e^{-\beta H}\right]$, where $\beta = 1/T$ is the inverse temperature in energy units ($k_B = 1$). The Hamiltonian at hand, Eq.(2.21) is the quadratic form with respect to the displacement (phonon) coordinates. Consequently, phonons can be eliminated exactly

$$Z = Z_b \prod_{\mathbf{q}} \left[2\sinh\left(\frac{\beta\omega_{\mathbf{q}}}{2}\right)\right]^{-1} \tag{2.28}$$

where the bipolaron partition sum Z_b is a path integral in only the electron coordinates

$$Z_b = \prod_{j=1.2} \int d\mathbf{x}_j \iint_{\mathbf{r}_j(0)=\mathbf{x}_j}^{\mathbf{r}_j(\beta)=\mathbf{x}_j} D\mathbf{r}_j(t) e^{S[\mathbf{r}_1(t),\mathbf{r}_2(t)]} \tag{2.29}$$

The bipolaron action $S\left[\mathbf{r}_1(t), \mathbf{r}_2(t)\right]$ includes the kinetic energies, the retarded self and inter-electron attractive interaction, mediated by phonons, and the Coulomb repulsion

$$\begin{aligned} S\left[\mathbf{r}_1(\tau), \mathbf{r}_2(\tau)\right] = &-\int_0^\beta d\tau \left(\frac{m}{2}\dot{\mathbf{r}}_1^2(\tau) + \frac{m}{2}\dot{\mathbf{r}}_2^2(\tau) + \frac{U}{|\mathbf{r}_1(\tau) - \mathbf{r}_2(\tau)|}\right) \\ &+ \sum_{j,l=1,2;\mathbf{q}} \omega_{\mathbf{q}}^{-1} \left|V_{\mathbf{q}}\right|^2 \int_0^\beta d\tau \int_0^\beta dsd\left(\omega_{\mathbf{q}}, \tau - s\right) e^{i\mathbf{q}\cdot[\mathbf{r}_j(\tau) - \mathbf{r}_l(s)]}, \end{aligned} \tag{2.30}$$

where $U = e^2/\epsilon$ is a measure for the repulsion strength, and

$$d(\omega, \tau) = \frac{\omega \cosh\left(\frac{\beta\omega}{2} - \omega|\tau|\right)}{2\sinh\left(\frac{\beta\omega}{2}\right)} \tag{2.31}$$

is the phonon Green's function, which Fourier component is defined in Chapter 3. The resulting path integral Z_b cannot be evaluated. However, the upper bound to the free energy $F_b = -T\ln Z_b$ can be estimated by the use of any trial quadratic action δ_0

$$F_b \leq F_0 - \frac{1}{\beta}\left\langle S - S_0\right\rangle, \tag{2.32}$$

where $F_0 = -T\ln Z_0$ is the free energy corresponding to the trial action S_0, and brackets denote an average with weight $\exp S_0$ defined as

$$\langle \ldots \rangle = Z_0^{-1} \prod_{j=1.2} \int d\mathbf{x}_j \iint_{\mathbf{r}_j(0)=\mathbf{x}_j}^{\mathbf{r}_j(\beta)=\mathbf{x}_j} D\mathbf{r}_j(t)(\ldots) e^{S_0[\mathbf{r}_1(t),\mathbf{r}_2(t)]} \tag{2.33}$$

While Hiramoto and Toyozawa used the quadratic action S_0 with four variational parameters, Verbist et al allowed two polarons to fluctuate around a mean distance
a from each other. The Coulomb repulsion was approximated by a quadratic one with strength K. In analogy with the Feynman trial action for a single polaron, each electron interacts quadratically with a fictitious particle of mass M and oscillator strength k. Furthermore, a quadratic interaction, with an oscillator strength k', between each electron and the oscillator of the other electron is also allowed. The Hamiltonian H_0 describing the model is

$$
\begin{aligned}
H_0 = & \sum_{j=1,2} \left[-\frac{\nabla_j^2}{2m} - \frac{\nabla_{\mathbf{R}_j}^2}{2M} + \frac{k}{2} \left(\mathbf{r}_j - \mathbf{R}_j \right)^2 \right] \\
& + \frac{k'}{2} \left[\left(\mathbf{r}_1 - \mathbf{R}_2 - \mathbf{a} \right)^2 + \left(\mathbf{r}_2 - \mathbf{R}_1 + \mathbf{a} \right)^2 \right] \\
& - \frac{K}{2} \left(\mathbf{r}_1 - \mathbf{r}_2 - \mathbf{a} \right)^2
\end{aligned} \tag{2.34}
$$

In analogy with the elimination of the phonon variables, the oscillator coordinates $\mathbf{R}_j$ can be eliminated to construct the trial action

$$
\begin{aligned}
S_0 \left[\mathbf{r}_1(t), \mathbf{r}_2(t) \right] = & - \sum_{j=1,2} \int_0^\beta d\tau \frac{m}{2} \dot{\mathbf{r}}_j^2(\tau) \\
& - \frac{(k^2 + k'^2)}{4M\nu^2} \sum_{j=1,2} \int_0^\beta d\tau \int_0^\beta ds d(\nu, \tau - s) \left[\mathbf{r}_j(\tau) - \mathbf{r}_j(s) \right]^2 \\
& - \int_0^\beta d\tau \int_0^\beta ds \left[\mathbf{r}_1(\tau) - \mathbf{r}_2(s) - \mathbf{a} \right]^2 \\
& \times \left[\frac{K}{2} \delta(\tau - s) - \frac{kk' d(\nu, \tau - s)}{M\nu^2} \right]
\end{aligned} \tag{2.35}
$$

where $\nu = \sqrt{(k + k')/M}$ is the frequency of the free oscillator. The electrons now exhibit a quadratic self-interaction, the second term in Eq.(2.35).

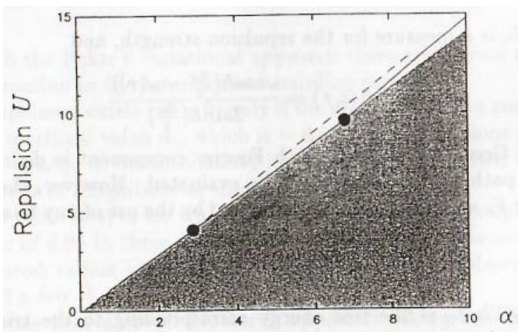

Fig.2.3. The stability region for large bipolaron formation in $3D$ and $2D$ (Verbist et al (1991)). Large bipolaron is formed below the curves, but above the shaded area.

They are bound together at an average distance $|\mathbf{a}|$ if the retarded attraction (the last term) is larger than the direct instanteneous repulsion, which is governed by the constant K. Minimising the right hand side of Eq.(2.34) with respect to the parameters M, k, k', K and $|\mathbf{a}|$ Verbist et al obtained a lower bipolaron energy
than with the canonical transformation method. The critical value of the coupling constant was found to be $\alpha_c \simeq 6.8$ in three dimensions. The path integral method gives not only a consistent description of a single polaron and bipolaron within the same physical picture, but also allows for a scaling relation for the free energy between different dimensions in the case when $\mathbf{a} = 0$

$$
F_{2D}(\alpha, U, \beta) = \frac{2}{3} F_{3D} \left(\frac{3\pi}{4} \alpha, \frac{3\pi}{4} U, \beta \right). \tag{2.36}
$$

This means that the free energy in two dimensions can be calculated from the free energy in three dimensions by scaling the coupling constant α as well as the repulsion strength U with a factor $3\pi/4$. As a result the critical value of α in two dimensions is about 2.9. The space $(\alpha, \epsilon/\epsilon_0)$ in which large bipolaron exists in two (dashed curve) and three (solid curve) dimensions is presented in Fig. 2.3, where the nonphysical part is shaded. Our general conclusion is that the Fröhlich interaction can lead to a bound state if the coupling constant is sufficiently large and the ratio ϵ/ϵ_0 is sufficiently small. This is rather surprising because the Fröhlich interaction never overscreens the Coulomb repulsion. Nevertheless, a bound state can be formed due to the quantum exchange.

One can expect that the interaction with acoustic phonons and local vibrations acts to help the bipolaron formation against the direct Coulomb repulsion. In fact it plays a dominant role giving rise to the total direct attraction of two electrons.

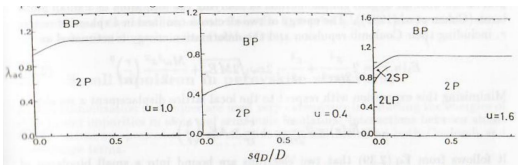

Fig.2.4 The critical acoustic phonon coupling constant for the small bipolaron formation as a function of the adiabatic ratio for three different values of the normalised Coulomb repulsion u.

As in the case of a single polaron, the deformation potential leads to the formation of small bipolarons rather than large bipolarons. By use of the path integral method and the effective mass (continuum) approximation for electrons Hiramoto and Toyozawa (1985) estimated the strength of the deformation potential, which binds two polarons. The continuum approach is sufficient for qualitative estimations if the Debye wave number $q_D \sim \pi/a$ is introduced as an upper limit cut-off in all sums in momentum space. The matrix element of the deformation potential depends on the momentum as $V_{\mathbf{q}} = E_d\sqrt{q/2NMs}$. The acoustic phonon frequency is $\omega_{\mathbf{q}} = sq$, where E_d the deformation potential, M the mass of a unit cell and s is the sound velocity. Applying the trial quadratic action similar to that with optical phonons Hiramoto and Toyozawa found the critical value of the acoustic phonon coupling

$$\lambda = \frac{E_p}{D}, \tag{2.37}$$

sufficient to form the small bipolaron. Here $E_p = E_d^2/2Ms^2$ is the polaron level shift calculated with Eq.(1.98) and $D = q_D^2/2m$ plays a role of the half bandwidth. When the characteristic Coulomb repulsion is small compared with the half bandwidth, $u \equiv 2e^2 q_D/\pi\epsilon D \ll 1$ the transition between two free electrons and a small bipolaron occurs at $\lambda \simeq 0.537$ that is a half of the critical value of λ_c at which the transition from large to small polaron takes place, $\lambda_c \simeq 1.075$ in the extreme adiabatic limit, $sq_D \ll D$. The effect of the adiabatic ratio sq_D/D on the critical value of λ was found to be small, Fig.2.4. The bipolaron mass was estimated to be enormous compared to the band mass in the extreme adiabatic limit while it is of the order of the band mass for $sq_D/D > 1$ as long as $\lambda = O(1)$. The deformation potential was found to be more effective for the bipolaron formation compared with the Fröhlich interaction. The mean distance between the two electrons in a bipolaron is usually about the lattice constant a. Consequently, the continuum approach does not work well in this type of problems. One would have to use a lattice small bipolaron model taking into account the finite bandwidth (Chapter 6).

6.6.4 2.4 Small bipolaron

Theory

Scaling arguments similar to those applied to the small polaron in the Introduction provide us with an elegant simple method of studying the formation of a small bipolaron (Cohen et al (1984)). The energy of two electrons confined in a sphere of radius r, including their Coulomb repulsion and the deformation energy is estimated as

$$E_b(u,r) = 2\frac{\pi^2}{2mr^2} + \frac{e^2}{\epsilon r} - 2x\omega\sqrt{2ME_p} + \frac{M\omega^2x^2}{2}\left(\frac{r}{a}\right)^3 \tag{2.38}$$

Minimising this expression with respect to the local lattice displacement x we obtain

$$E_b(r) = 2\frac{\pi^2}{2mr^2} + \frac{e^2}{\epsilon r} - 4E_p\left(\frac{a}{r}\right)^3 \tag{2.39}$$

It follows from Eq.(2.39) that two electrons are bound into a small bipolaron of radius $r = a\,(E_b(a) < 0)$ if the interaction with local and (or) acoustic vibrations is sufficiently strong

$$\lambda \geq 0.5 + u/8 \tag{2.40}$$

where $\lambda = 2ma^2E_p/\pi^2$ and u is the relative strength of the Coulomb repulsion, introduced in section 2.3. For sufficiently weak Coulomb interaction, the small bipolaron forms at twice lower coupling constant $\lambda \simeq 0.5$ than the small polaron, for which the critical value of λ estimated by scaling is about unity. This estimate is in perfect agreement with the path integral variational calculations, Fig.2.4. In ionic solids with a high value of the static dielectric constant $\epsilon_0 \gg 1$ polar optic phonons screen the Coulomb repulsion, rather than binds two electrons. Consequently, even the intermediate coupling, $\lambda > 0.5$ with acoustic phonons or (and) local vibrations is sufficient to form the small bipolaron in ionic solids, because u is replaced for $u\epsilon/\epsilon_0 \ll 1$.

Screening in solids and coupling with phonons are ill defined at large wave numbers of the order of the reciprocical lattice constant. Therefore, one has to postulate the existence of small bipolarons to explain some exotic properties of particular compounds rather than derive them from the first principles. Along this line Anderson
(1975) and Street and Mott (1975) introduced the concept of a small on-site localised bipolaron in glassy semiconductors (chalcogenide glasses) to explain their magnetic and electric properties. Though the ESR measurements did not reveal any considerable amount of localised states, other experiments showed their density about 10^{18} per cm^3. To explain these contradicting observations Street and Mott and Anderson proposed that the local lattice distortion is sufficiently strong for the reaction

$$2D^0 \rightarrow D^+ + D^- \tag{2.41}$$

to be exothermic. As a result in the ground state of chalcogenide glasses all donors are positively or negatively charged and D^0 are produced only by thermal excitation. The state D^-can be seen as a small bipolaron localised by the random potential.

Taking perturbatively into account the small polaron tunneling Alexandrov and Ranninger (1981a,b) introduced small bipolarons into the theory of superconductivity. This allowed for the prediction of the high T_c value about $100K$ (Alexandrov (1983), Alexandrov and Kabanov (1986)) and for the explanation of a number of kinetic and thermodynamic properties of high T_c superconducting oxides (Alexandov and Mott(1994), Chapter 8). The advantage of the perturbative approach is that in zero order the ground state can be studied without taking into account the electron kinetic energy, which is small perturbation due to the polaron band

narrowing (section 1.6 and Chapter 4). Consequently, one can obtain the binding energy and the size as well as geometry of the small bipolaron from the first principles by the use of the static lattice minimisation techniques (Catlow(1989)).

6.6.5 2.5 Small bipolaron in perovskite structures

Theory

Lattice minimisation techniques are used very extensively in modeling the energies of defects and impurities in ionic and semi-ionic insulators. Interactions between atoms in the lattice are presented by an effective potential including both Coulomb and short-range terms.

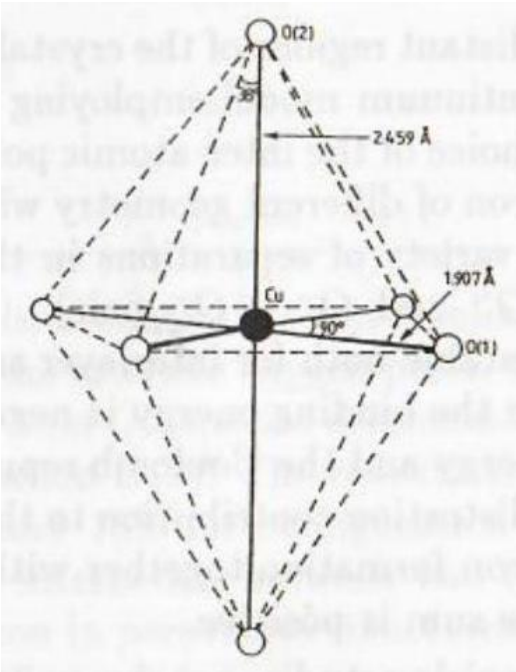

Fig. 2.5. CuO_{6} unit in La_2CuO_4.

This yields an equilibrium structure and phonon dispersion curves which are close to those observed experimentally. In their modeling of small bipolarons in doped Ca_3CuO_4 Zhang and Catlow (1991) treated holes as Cu^{3+} or O^{-}species placed in
the dielectric matrix with the CuO_6 unit, Fig.2.5. The energy of a region of the crystal surrounding the hole or the hole pair is then minimised with respect to the coordinates of the ions within the region containing ca. 200-300 ions.

Table 1$Cu^{3-} - Cu^{3+}$ pairs: configurations and energies				
configuration	number	separation of pair d/A	binding energy $-E_b$, eV	Coulomb
intralayer				
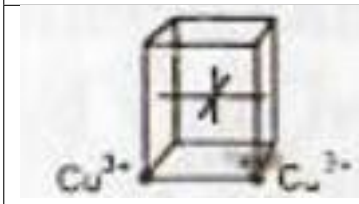	Cu(1)	3.81	0.414	0.135
Cu^{2-}	Cu(2)	5.41	0.254	0.095
c. $^{2+}$	Cu(4)	8.54	0.092	0.060
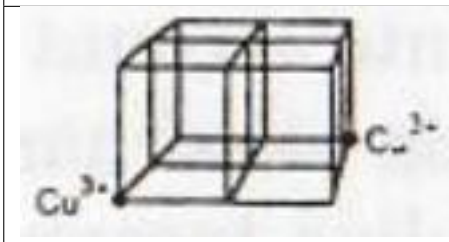	Cu(5)	10.81	0.120	0.048
interlayer				
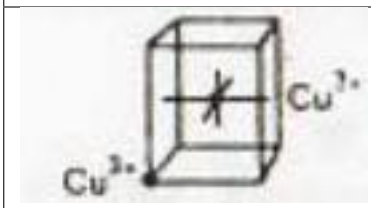	Cu(6)	7.10	0.046	0.073
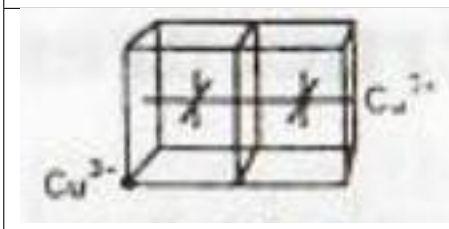	Cu(7)	10.74	0.036	0.058

The response of the more distant regions of the crystal is calculated using approximate procedures based on a continuum model employing the relative permittivity of the material. With a proper choice of the inter-atomic potentials one can find the binding energy of the small bipolaron of different geometry with accuracy within 0.01 eV. The pairing was studied for a variety of separations in three types of possible bipolaron ($Cu^{3+} - Cu^{3+}, Cu^{3+} - O^{-}$and $O^{-} - O^{-}$pair). Intercopper and copper-oxygen intersite bipolarons are unstable both for interlayer and intralayer pairing, as one can see from Tables 1-3, where the binding energy is negative for all separations studied. The sum of the binding energy and the Coulomb repulsive energy in the Tables yields an estimate of the lattice distortion contribution to the pairing. If the sum is negative the lattice opposes bipolaron formation together with the Coulomb repulsion, and it favors bipolarons when the sum is positive.

The results of $O^{-} - O^{-}$pairing studies are shown in Table 4. Three stable bipolaron configurations were found. For configuration $O(1)$, the bipolaron is bound by *ca.* 0.06 eV , whereas bipolaron configuration $O(2)$ is bound by *ca.*0.12eV. These two bound oxygen pairs are situated at the nearest-neighbor sites ($d = 2.66$Å) and next-nearest-neighbor sites ($d = 3.11$Å). There is also a lightly bound bipolaron $O(4)$
with a binding energy of 0.001 eV at $d = 3.58$Å. When d is larger than 3.81Å all the configurations are energetically unfavorable.

In order to distinguish pairing from the phase separation of holes one can calculate in addition to the binding energy of two holes Δ, the binding energy of four holes Δ_4 with respect to hole pairs. If Δ_4 is positive then phase separation would be expected. In the nearest-neighbor

site pair and next-nearest-neighbor site pair Zhang and Catlow found, however, a positive Δ and a negative Δ_4, which promote bipolaronic superconductivity (Chapter 6) without phase separation.

Table $2Cu^{3+} - O^{-}$pairs (intralayer): configurations and energies

configuration	number	separation of pair d/A	binding energy $-E_b$/eV	Co
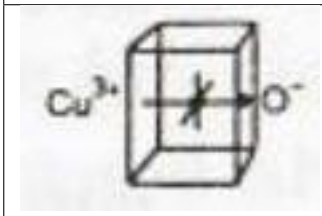	OCu(1)	1.91	1.010	0.2
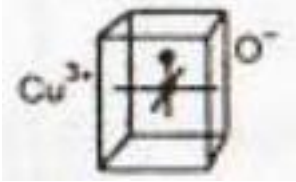	OCu(2)	2.46	0.228	0.2
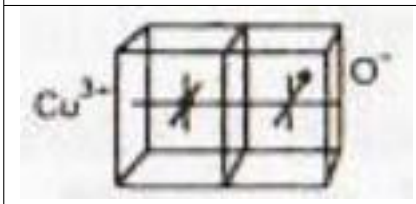	OCu(3)	4.31	0.237	0.1
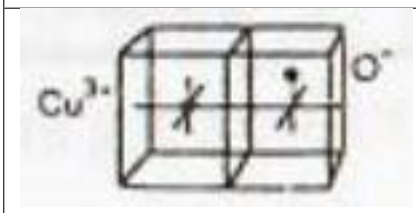	OCu(4)	4.64	0.129	0.1
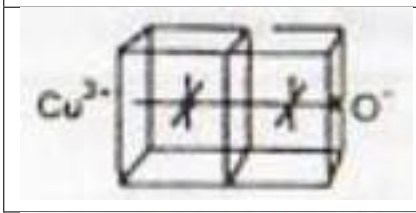	OCu(S)	5.72	0.114	0.0
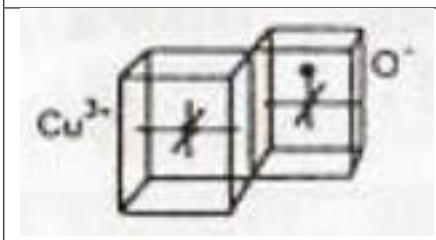	OCu(6)	5.79	0.053	0.0
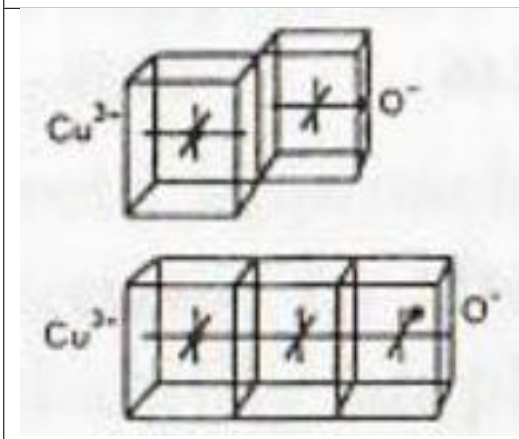	OCu(7)	6.89	0.145	0.0
	OCu(8)	7.87	0.078	0.0
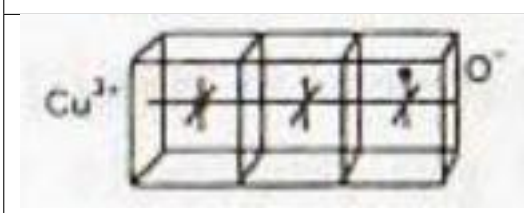	OCu(9)	7.89	0.137	0.0
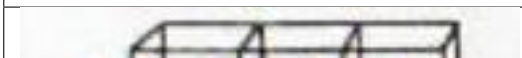				

Compared to the Coulomb repulsive energy the non-Coulombic lattice contribution is larger being ca. $0.2 - 0.3$eV for the intersite oxygen pairs. It was found that after latLice relaxation, the distance between O^-species decreases by 0.674Å in configuration $O(1)$ and by 0.564Å in configuration $O(2)$. The relative change of the pair distances in 25% for configuration $O(1)$ and 18% for configuration $O(2)$. This enhanced attraction is due to the covalent interaction between two O^-species. An important feature of the bipolaron formation in perovskite structures is that the bound state of the in-plane oxygen hole with the apex hole is more favorable. The binding energy of small bipolaron is strongly related not only to the distance of the pair but also to the detailed geometry of the site where the polaron is situated. Therefore, it is necessary to study the pairing mechanism of doped La_2CuO_4 using three-dimensional rather than two-dimensional models. The lattice contribution to the binding energy
is estimated to be larger than the characteristic antiferromagnetic exchange energy of the order of 0.1 eV. However, the latter is of the order of the binding energy Δ of the bipolaron and favors pairing further (Mott(1990)).

Table $3Cu^{3*} - O^+$pairs (interlayer): configurations and energies				
configuration	number	separation of pair d/A	binding energy $-E_b$/eV	Coulomb repulsive energy E_r, eV
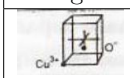	OCu(11)	4.92	0.061	0.105
	OCu(12)	6.75	0.006	0.076
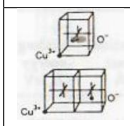	OCu(13)	7.23	0.096	0.071
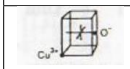	OCu(14)	7.76	0.079	0067
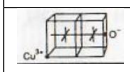	OCu(15)	10.17	0.041	0.060
configuration	number	separation of pair d/A	binding energy $-E_b$/eV	Coulomb repulsive energy E_r/eV
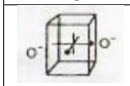	Ox($\hat{2}$)	2.66	-0.059	0.194
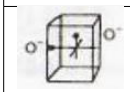	Ox(2)	3.11	-0.119	0.166
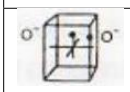	Ox(3)	3.17	0.036	0.163
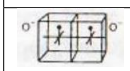	Ox(4)	3.58	-0.001	0.144
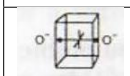	Ox(5)	3.81	0.228	0.135
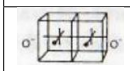	Ox(6)	3.81	0.127	0.135

In a similar study Allan and Mackrodt (1990) observed the difference in the bipolaron formation for Nd_2CuO_4 compared with La_2CuOO_4. They found no confining interactions in Nd_2CuO_4. It seems that the difference in bipolaron results for these two materials may arise from their structural difference (there is a $CuOO_6$ layer in La_2CuO_4 whereas there is a CuO_4 plane in Nd_2CuO_4). The detailed lattice structure may play an important role in the small bipolaron formation. As an example, the similar calculations performed on hole interactions in NiO revealed a much larger
repulsive interactions, and no configurations were found in which hole pairing might be ex-

pected. The lattice minimisation techniques show that the La_2CuO_4 structure is especially effective at screening of the Coulomb repulsion and the formation of intersite small bipolarons.

6.6.6 2.6 Effect of the kinetic energy on small-bipolaron formation

There is a finite probability for an electron to tunnel from one site of the lattice to the neighboring sites. The corresponding kinetic energy and the Coulomb repulsion oppose the small bipolaron formation. When the coupling constant is relatively large $\lambda > 1$, the hopping integrals are exponentially small as in the Holstein two-site model, section 1.6. Then the kinetic energy is a small perturbation and the static minimisation technique discussed above works perfectly well. However, in the intermediate coupling region $\lambda \leq 1$ the tunneling competes with the selftrapping and with the binding, trying to destroy both. The effect of the kinetic energy on the formation of small bipolaron depends on the lattice structure and geometry of the pair, because the binding energy is strongly related to them. In the case of a non-Bravais lattice such as the $CuOO_2$ plane of high T_c copper oxides some specific difficulties appear because of the multiband energy structure. A reasonable estimate of the kinetic energy effect on the small bipolaron can be obtained by solving a discrete Schrödinger equation for two electrons in the nearest neighbor approximation for a realistic crystal structure (Alexandrov and Kornilovitch (1993)). In this section we consider the solution of the two-particle problem on the CuO_2 plane modeling the repulsion by the positive Hubbard U term on copper, and the lattice mediated attraction by the negative term $-V$ on plane oxygen.

Within the discrete approach two electrons (holes) with opposite spins on the CuO_2 plane are described by the nine-component wave function $\phi_{\beta\gamma}(\mathbf{m}_1, \mathbf{m}_2)$. Each component is a probability amplitude to find one electron on a copper site ($\beta = 1$) or on two different plane oxygen sites ($\beta = 2, 3$) of the cell Fig.2.5 (the lattice vector $\mathbf{m}_1$), and the other electron on the site $\gamma = 1$ or 2,3 in the cell $\mathbf{m}_2$. The discrete Schrödinger equation is the infinite system of linear algebraic equations

$$\begin{aligned} E\phi_{\beta\gamma}(\mathbf{m}_1, \mathbf{m}_2) = &-\sum_{\alpha,1}(-1)^{l_x/2+l_y/2}\left[\phi_{\alpha\gamma}(\mathbf{m}_1+1, \mathbf{m}_2) + \phi_{\beta\alpha}(\mathbf{m}_1, \mathbf{m}_2+1)\right] \\ &+ U_\beta \delta_{\beta\gamma}\delta_{\mathbf{m}_1,\mathbf{m}_2}\phi_{\beta\gamma}(\mathbf{m}_1, \mathbf{m}_2) \end{aligned} \tag{2.42}$$

where $U_1 \equiv U > 0$ and $U_2 = U_3 \equiv -V < 0$ and all energies are measured in units of the copper-oxygen nearest neighbor hopping integral $\tilde{J}$ renormalised by the electron-phonon interaction according to Eq.(1.118). The energy levels of p oxygen and d copper orbitals are taken to be equal for simplicity. The coefficient $(-1)^{l_x/2+l_y/2}$ of the kinetic energy term is due to the symmetry of two different $p_{x,y}$ oxygen in-plane orbitals hybridised with the $d_{x^2-y^2}$ copper orbital. The nearest $Cu-O$ distance is conveniently taken as unity, so the size of the cell is 2×2. Then the Fourier transform of Eq. (2.42) is

$$\left(\hat{H}_0 - E\right)\hat{\phi}(\mathbf{k}_1, \mathbf{k}_2) = \hat{C}(\mathbf{K}) \tag{2.43}$$

where

$$\hat{\phi}(\mathbf{k}_1, \mathbf{k}_2) = \frac{1}{N^2}\sum_{\mathbf{m}_1,\mathbf{m}_2}\phi_{\beta\gamma}(\mathbf{m}_1, \mathbf{m}_2)\, e^{-i\mathbf{k}_1\cdot\mathbf{m}_1 - i\mathbf{k}_2\cdot\mathbf{m}_2} \tag{2.44}$$

is the nine-component Fourier component of the wave function,

$$\hat{C}(\mathbf{K}) = -U_\beta\delta_{\beta\gamma}\sum_{\mathbf{q}}\phi_{\gamma\gamma}(\mathbf{q}, \mathbf{K}-\mathbf{q}) \tag{2.45}$$

is the interaction term with $\mathbf{K} = \mathbf{k}_1 + \mathbf{k}_2$ being conserving total momentum of the bipolaron. The kinetic energy of two electrons is given by the 9×9 matrix

$$\hat{H}_0 = \begin{bmatrix} \hat{T}_2 & 2i\hat{I}\sin k_{1y} & -2i\hat{I}\sin k_{1x} \\ -2i\hat{I}\sin k_{1y} & \hat{T}_2 & 0 \\ 2i\hat{I}\sin k_{1x} & 0 & \hat{T}_2 \end{bmatrix} \tag{2.46}$$

with

$$\hat{T}_2 = \begin{bmatrix} 0 & 2i\sin k_{2y} & -2i\sin k_{2x} \\ -2i\sin k_{2y} & 0 & 0 \\ 2i\sin k_{2x} & 0 & 0 \end{bmatrix} \tag{2.47}$$

and $\hat{I}$ being a unitary 3×3 matrix. Substitution of a formal solution of Eq.(2.43) into Eq.(2.45) yields three coupled equations with respect to C_{11}, C_{22} and C_{33}. From their consistency we find the standard secular equation for the eigenvalues $E(\mathbf{K})$

$$\det \begin{vmatrix} Ud_1 - 1 & Vd_2 & Vd_3 \\ -Ud_2 & -Vd_5 - 1 & Vd_4 \\ -Ud_3 & Vd_4 & -Vd_6 - 1 \end{vmatrix} = 0, \tag{2.48}$$

where

$$d_1 = \frac{1}{4}\sum_{\mathbf{q}} [R_{11} + R_{33} + R_{13} + R_{31}]$$

$$d_2 = \sum_{\mathbf{q}} \frac{\sin q_y \sin(K_y - q_y)}{E_{\mathbf{q}} E_{\mathbf{K}-\mathbf{q}}} [R_{11} + R_{33} - R_{13} - R_{31}]$$

$d_3 = d_2(y \to x)$,

$$\begin{aligned} d_4 = 4\sum_{\mathbf{q}} & \frac{\sin q_x \sin(K_x - q_x) \sin q_y \sin(K_y - q_y)}{E_{\mathbf{q}}^2 E_{\mathbf{K}-\mathbf{q}}^2} \\ & \times [2(R_{12} + R_{32} + R_{23} + R_{21}) - R_{11} - R_{33} - R_{13} - R_{31} - 4R_{22}] \\ d_5 = \sum_{\mathbf{q}} & \frac{4\sin^2 q_y \sin^2(K_y - q_y)}{E_{\mathbf{q}}^2 E_{\mathbf{K}-\mathbf{q}}^2} (R_{11} + R_{33} + R_{13} + R_{31}) \\ & + \frac{8\sin^2 q_y \sin^2(K_x - q_x)}{E_{\mathbf{q}}^2 E_{\mathbf{K}-\mathbf{q}}^2} (R_{12} + R_{32}) \\ & + \frac{1}{E_{\mathbf{q}}^2 E_{\mathbf{K}-\mathbf{q}}^2} \left[8\sin^2 q_x \sin^2(K_y - q_y)(R_{21} + R_{23}) + 16\sin^2 q_x \sin^2(K_x - q_x) R_{22}\right] \end{aligned}$$

$d_6 = d_5(y \to x)$. The one-particle spectrum is determined by

$$-E_1(\mathbf{k}) = E_3(\mathbf{k}) \equiv E(\mathbf{k}) = 2\sqrt{\sin^2 k_x + \sin^2 k_y}; E_2(\mathbf{k}) = 0, \tag{2.49}$$

and by

$$R_{\beta\gamma} = \frac{1}{E - E_\beta(\mathbf{q}) - E_\gamma(\mathbf{K} - \mathbf{q})}, \tag{2.50}$$

which is a free two-particle propagator. The bipolaron forms if the binding energy

$$\Delta(\mathbf{K}) = \min\left[E_\beta(\mathbf{k}_1) + E_\gamma(\mathbf{k}_2] - E(\mathbf{K}) = -4\sqrt{2} - E(\mathbf{K}) > 0. \tag{2.51}$$

The numerical solution of the secular equation, Eq.(2.48) shows that the pairs with $\mathbf{K} = 0$ are more stable, Fig.(2.6). For the center of the Brillouin zone, $K = 0$, the bipolaron exists if

$$V \geq \frac{8\sqrt{2}U}{4\sqrt{2} + 3U} \tag{2.52}$$

Therefore, there is a critical value of the attraction $V \simeq 3.8$ above which the bound state exists for any repulsion U.

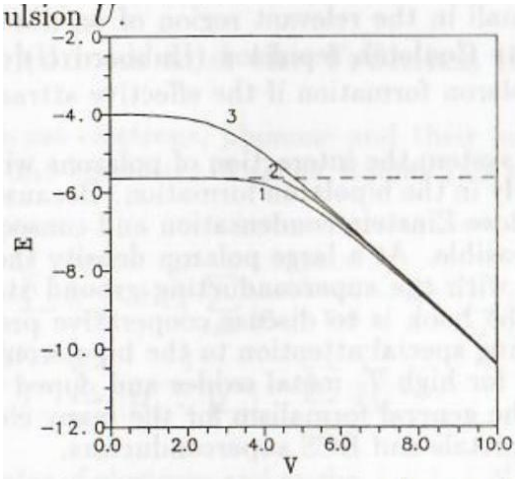

Fig.2.6. The energy of the bound state in units of the hopping integral versus the attractive potential V for (1) $K = U = 0$; (2) $K = 0, U = 1000$; (3) $K = (\pi/2, \pi/2)$ and U is arbitrary. The dashed line is the minimum of the kinetic energy of two electrons $(-4\sqrt{2})$.

The binding energy of a pair with the total momentum near the corners of the Brillouin zone does not depend on the repulsive potential at all, Fig.2.6. The reason for this is that near these points two particles interact on sites of only one and the wame type, so the repulsion on neighboring sites of another type does not affect the pairing.

The solution of the Schrödinger equation for two electrons enables us to calculate the bipolaron size r_b The space extension of the bipolaron wave function is determined by the sum

$$\phi_{\mathbf{K}}(\mathbf{r}_1, \mathbf{r}_2) \sim \sum_{\mathbf{q}} \frac{e^{i\mathbf{q}\cdot\mathbf{r}_1 + i(\mathbf{K}-\mathbf{q})\cdot\mathbf{r}_2}}{E^2 - [E_{\mathbf{q}} + E_{\mathbf{K}-\mathbf{q}}]^2}. \tag{2.53}$$

To derive the asymptotics at $\rho = \sqrt{x^2 + y^2} \to \infty$ one can apply the substitution

$$\frac{1}{E} = -i \int_0^\infty d\xi e^{(iE - 0^+)\xi} \tag{2.54}$$

to the sum, Eq.(2.53), which allows us to integrate over $\mathbf{q}$ with the following result for $K = 0$

$$\phi_0(x, y) \sim \int_0^\infty d\xi e^{\left(i\left[E^2/8 - 2\right] - 0^+\right)\xi} J_{x/2}(\xi) J_{y/2}(\xi). \tag{2.55}$$

Here $J_r(\xi)$ is the Bessel function and $x = x_1 - x_2, y = y_1 - y_2$. For the direction along $x = y$ we obtain

$$\phi_0(x, x) \sim Q_{x/2-1/2}\left(\left[E^2/8 - 2\right]^2/2 - 1\right) \tag{2.56}$$

where $Q_\nu(z)$ is the associated Legendre function with the exponential asymptotics for $\nu \to \infty$

$$\phi_0(x, x) \sim e^{-|x|/r_b} \tag{2.57}$$

The bipolaron radius is smaller than two lattice constants

$$r_b = \frac{2}{\operatorname{arccosh}\left([E^2/8-2]^2/2-1\right)} \leq 4 \tag{2.58}$$

if the binding energy is not extremely small, $\Delta = |E + 4\sqrt{2}| > 0.01$. Thus we conclude that the bipolaron is small in the relevant region of on-site correlations within the CuO_2 plane. The on-site Coulomb repulsion (Hubbard U), no matter how strong, cannot prevent the bipolaron formation if the effective attraction on oxygen sites is relatively large $V \simeq 3.8$.

In the multi-polaron system the interaction of polarons with each other and with the lattice results not only in the bipolaron formation. Because of the bosonic character of bipolarons their Bose-Einstein condensation and consequently, the bipolaronic superconductivity are feasible. At a large polaron density the charge and (or) magnetic ordering compete with the superconducting ground state. Our intention for the remaining part of the book is to discuss cooperative properties of self-trapped carriers on a lattice paying special attention to the bipolaronic superconductivity as the natural explanation for high T_c metal oxides and doped fullerenes. In the next Chapter we introduce the general formalism for the many electron-phonon problem Chapter we introduce the generar BCS and apply it to normal metals and BCS superconductors.

6.7 5 Phase transformations of the polaronic Fermi-liquid

At low temperatures and (or) at high densities the residual polaron-phonon H_{p-ph} and polaron-polaron H_{p-p} interactions lead to phase transformations of the polaronic Fermi-liquid. There are several major instabilities. The polaronic Fermi-liquid is unstable versus the bipolaron formation followed by the Bose-Einstein condensation if H_{p-p} is attractive at short distances. If the density of carriers is of the order of the atomic density the commensurate or incommensurate charge-density wave (CDW) develops competing with the superfluid ground state. If the Coulomb repulsion is atrong the polaronic Fermi liquid undergoes the metal-insulator Mott transition. The ground state for the half-filled band is an antiferromagnetic insulator, which, if doped, has spin-lattice small (bi)polarons as the charge carriers.

6.7.1 5.1 Bipolaronic instability

Theory

The polaron-polaron interaction is the sum of two large contributions of the opposite Aign, Eq.(4.14). It is generally large compared with the polaron bandwidth. This is just the opposite regime to that of the BCS superconductor where the Fermi energy in the largest one. In polar solids the Coulomb repulsion is perfectly screened by the lons. Then the acoustical and (or) molecular phonons make the short-range interaction between polarons to be attractive. As discussed in Chapter 2 two polarons furm a small bipolaron at intermediate value of the electron-phonon coupling $\lambda \geq 0.5$, practically independent off the value of the Coulomb potential. In the multi-polaron matem the formation of bipolarons is manifested as a pole in the two-particle vertex part at large q corresponding to the pairing of small polarons. For a short distance (large q) the Fourier component of the interaction $v(\mathbf{q}) \equiv U$ might be positive or (???)live. Because the polaron bandwidth is normally smaller than $|U|$ we can consider this static dielectric function defined by Eq.(4.66). For $(T \gg w)$ we have

$$\epsilon(\mathbf{q}, 0) = 1 + \frac{n(2-n)U}{2T} \tag{5.1}$$

A screened short-range interaction is given by

$$\tilde{U} = \frac{U}{\epsilon(\mathbf{q},0)} = \frac{UT}{T \pm T^{**}} \tag{5.2}$$

with the characteristic temperature

$$T^{**} = \frac{|U|n(2-n)}{2} \tag{5.3}$$

The upper sign corresponds to the repulsion $U > 0$ while the lower sign (-) to the attraction, $U < 0$. One can see that in the temperature region $w < T \ll T^{**}$ the short range repulsion is sufficiently suppressed by the screening. The two-body correlations lead to a modification of polaron trajectories, which reduces the Coulomb self-energy to a magnitude of the order of the polaronic bandwidth if $T \simeq w$. In the case of the attraction the pole occurs in the effective interaction $\tilde{U}$ at $T = T^{**}$. Therefore, in this case T^{**} is the critical temperature of the bipolaron formation. For a half-filled band $(n \simeq 1)T^{**}$ is of order of the attraction itself and might be as high as $10^3 K$, section 2.5.

6.7.2 5.2 Cooper pairing of nonadiabatic carriers

Theory

For an intermediate value of $\lambda \simeq 1$ the effective interaction of polarons can be comparable or even less than the polaron bandwidth, both being less or of the order of the characteristic phonon frequency. If a pair binding energy Δ is small compared with the renormalised bandwidth $2w$, polarons constituting a pair tunnel through many sites during the characteristic time $1/\Delta$. Therefore a pair spreads over a large number of sites. Such 'extended' bipolarons consisting of two small polarons are overlapped similar to Cooper pairs if their density is compared with the atomic one. This is a narrow region of the coupling where the BCS approach is applied to nonadiabatic carriers with a nonretarded attraction. Bipolarons are then Cooper pairs formed by two small polarons (Alexandrov (1983)). The appropriate Hamiltonian is the extended Hubbard Hamiltonian taking into account the polaron narrowing of the band

$$H_p = \sum_{i,j} \left(\sigma(\mathbf{m}-\mathbf{n}) - \mu\delta_{i,j}\right) c_i^\dagger c_j + \frac{1}{2} v_{ij} c_i^\dagger c_j^\dagger c_j c_i \Bigg) \tag{5.4}$$

where $\sigma(\mathbf{m})$ is determined with Eq.(4.17) for the nonadiabatic system ($\omega > D/z$), or with Eq.(1.135) $(\Delta E \simeq \sqrt{\frac{4E_p\omega}{\pi}} e^{-\tilde{g}^2})$ in the opposite case. For simplicity one can keep only the on-site v_0 and the nearest neighbor intersite v_1 interactions. At least one of them should be attractive to ensure the superconducting ground state. By introducing two order parameters

$$\Delta_0 = -v_0 \langle c_{\mathbf{m},\uparrow} c_{\mathbf{m},\downarrow} \rangle \tag{5.5}$$

$$\Delta_1 = -v_1 \langle c_{\mathbf{m},\uparrow} c_{\mathbf{m}+\mathbf{a},\downarrow} \rangle \tag{5.6}$$

and transforming to k -space one arrives at the usual BCS Hamiltonian

$$H_p = \sum_{\mathbf{k},s} \xi_{\mathbf{k}} c_{\mathbf{k},s}^\dagger c_{\mathbf{k},s} + \sum_{\mathbf{k}} \left[\Delta(\mathbf{k}) c_{\mathbf{k},\uparrow}^\dagger c_{-\mathbf{k},\downarrow}^\dagger + \text{ h.c. } \right] \tag{5.7}$$

where $\xi_{\mathbf{k}} = \epsilon_{\mathbf{k}} - \mu$ is the kinetic energy of the polaron tunneling with momentum $\mathbf{k}$ and

$$\Delta(\mathbf{k}) = \Delta_0 - \Delta_1 \frac{\xi_{\mathbf{k}} + \mu}{w} \tag{5.8}$$

is the order parameter corresponding to a singlet pairing. In general a triplet p-wave pairing is also possible with the Hamiltonian, Eq.(5.4).

Applying the standard diagonalisation procedure to the Hamiltonian one obtains for the order parameter

$$\langle c_{\mathbf{k},\uparrow} c_{-\mathbf{k},\downarrow} \rangle = \frac{\Delta(\mathbf{k})}{2\sqrt{\xi_{\mathbf{k}}^2 + \Delta(\mathbf{k})^2}} \tanh \frac{\sqrt{\xi_{\mathbf{k}}^2 + \Delta(\mathbf{k})^2}}{2T} \tag{5.9}$$

and with the definition Eq.(5.5,6)

$$\Delta_0 = -\frac{v_0}{N} \sum_{\mathbf{k}} \frac{\Delta(\mathbf{k})}{2\sqrt{\xi_{\mathbf{k}}^2 + \Delta(\mathbf{k})^2}} \tanh \frac{\sqrt{\xi_{\mathbf{k}}^2 + \Delta(\mathbf{k})^2}}{2T} \tag{5.10}$$

$$\Delta_1 = -\frac{v_1}{Nw} \sum_{\mathbf{k}} \frac{\Delta(\mathbf{k})\left(\xi_{\mathbf{k}} + \mu\right)}{2\sqrt{\xi_{\mathbf{k}}^2 + \Delta(\mathbf{k})^2}} \tanh \frac{\sqrt{\xi_{\mathbf{k}}^2 + \Delta(\mathbf{k})^2}}{2T} \tag{5.11}$$

The last two equations are equivalent to the BCS one for $\Delta(\mathbf{k}) = \Delta(\xi)$ with the potential depending on energy and with the half bandwidth w as a cutoff of the integral instead of the Debye temperature,

$$\Delta(\xi) = \int_{-w-\mu}^{w-\mu} d\xi' N_p\left(\xi'\right) V\left(\xi, \xi'\right) \frac{\Delta\left(\xi'\right)}{2\sqrt{\xi'^2 + \Delta\left(\xi'\right)^2}} \tanh \frac{\sqrt{\xi'^2 + \Delta\left(\xi'\right)^2}}{2T} \tag{5.12}$$

with $V\left(\xi, \xi'\right) = -v_0 - zv_1 \frac{(\xi+\mu)(\xi'+\mu)}{w^2}$. The polaron density of states is enhanced due to the polaron narrowing effect:

$$N_p(\xi) \equiv \frac{1}{N} \sum_{\mathbf{k}} \delta\left(\xi - \xi_{\mathbf{k}}\right) \tag{5.13}$$

luing of order of $1/2w$ instead of $1/2D$ for a bare band. The on-site and intersite interaction terms are both attractive (< 0) or one of them (on-site) may be repulsive.

6.7.3 5.3 High T_c polaronic superconductivity

Theory

The critical temperature T_c of a polaronic superconductor is determined from the Imo linearised equations in the limit $\Delta_{0,1} \to 0$:

$$\left(1 + A\left(\frac{v_0}{zv_1} + \frac{\mu^2}{w^2}\right)\right)\Delta - \frac{B\mu}{w}\Delta_1 = 0 \tag{5.14}$$

$$-\frac{A\mu}{w}\Delta + (1+B)\Delta_1 = 0 \tag{5.15}$$

where $\Delta = \Delta_0 - \Delta_1 \frac{\mu}{w}$ and

$$A = \frac{zv_1}{2w} \int_{-w-\mu}^{w-\mu} \frac{d\xi \tanh \frac{\xi}{2T_c}}{\xi} \tag{5.16}$$

$$B = \frac{zv_1}{2w} \int_{-w-\mu}^{w-\mu} \frac{d\xi \xi \tanh \frac{\xi}{2T_c}}{w^2} \tag{5.17}$$

These equations are applied only for a weak and intermediate polaron-polaron coupling $|v_{0,1}| < w$. In the limit of the weak coupling one obtains from Eq.(5.14,15)

$$T_c \simeq 1.14w\sqrt{1-\frac{\mu^2}{w^2}}\exp\left(\frac{2w}{v_0+zv_1\frac{\mu^2}{w^2}}\right) \tag{5.18}$$

The expression Eq.(5.18) plays the same role in the polaronic superconductivity as the BCS one for the low temperature superconductors. It predicts superconductivity even in the case of on-site repulsion $v_0 > 0$ if this repulsion is less than the total intersite attraction $z\,|v_1|$. It also predicts a nontrivial dependence of T_c on the doping. With the constant density of states within the polaron band the Fermi level μ is expressed through the number of polarons per atom n

$$\mu = w(n-1) \tag{5.19}$$

and

$$T_c \simeq 1.14w\sqrt{n(2-n)}\exp\left(\frac{2w}{v_0+zv_1(n-1)^2}\right) \tag{5.20}$$

T_c has two maxima as a function of n separated by a deep minimum for the half filled band ($n = 1$) when the nearest neighbor contributions to the pairing are mutually compensated.

The basic phenomenon that allows a high value of T_c is that the polaronic narrowing of the band, which eliminates the small exponential factor in the BCS or McMillan's formula Eq.(3.116). To show this we rewrite Eq.(5.20) in a slightly differ ent form separating the phonon mediated attraction and the Coulomb repulsion and taking explicitly into account the polaronic narrowing effect:

$$T_c \simeq \tilde{D}\exp\left(-g^2-\frac{\exp\left(-g^2\right)}{\lambda-\mu_c}\right) \tag{5.21}$$

where $\tilde{D} = 1.14D\sqrt{n(2-n)}$,

$$\lambda = \frac{2E_p + z(n-1)^2\sum_{\mathbf{m}=\mathbf{a}}\gamma^2(\mathbf{q})\omega_{\mathbf{q}}e^{i\mathbf{q}\cdot\mathbf{m}}}{2D} \tag{5,22}$$

and

$$\mu_c = \frac{U+z(n-1)^2V_c}{2D} \tag{5.23}$$

with U and V_c the onsite and intersite Coulomb repulsion, respectively. There are four independent parameters which determines the value of T_c, in particular the bare bandwidth D, the polaronic level shift E_p, the number of phonons g^2 in a polaronis
cloud, and the Coulomb repulsion μ_c. They correspond to the four independent parameters of the Fröhlich Hamiltonian: the electron kinetic energy $E_F \sim D$, the matrix element of the electron-phonon interaction $\gamma \sim g$, the characteristic phonon frequency $\omega = E_p/g^2$, and the Coulomb (pseudo)potential. Because only g^2 (or ω) depends on the ion mass one can determine the maximum value of T_c with respect to g^2 keeping D, λ and μ constant. Differentiating Eq.(5.21) with respect to g^2 we obtain for the maximum T_c^*

$$T_c^* = \tilde{D}\frac{\lambda-\mu_c}{e} \tag{5.24}$$

The applicability of this formula is restricted by the intermediate region of the interaction constant $\lambda - \mu_c < 1$ because of the formation of bipolarons in the large λ limit (Chapter 6).

However, if bipolarons are intersite and their effective mass is of the order of the polaron effective mass the expression Eq.(5.21) also describes the Bose-Einstein condensation of bipolarons, as we discuss in Chapter 6.

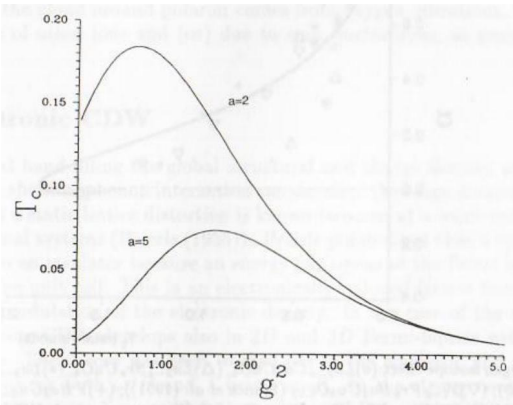

Fig.5.1. Critical temperature of a polaronic superconductor (in units of $\tilde{D}$) as a function of the interaction constant g^2 for two different values of the attraction between polarons, $a = 1/(\lambda - \mu_c)$.

T_8^* is limited by the condition of the small polaron formation $\lambda > 1/\sqrt{2z}$ (section (1)), which restricts the maximum value of D in Eq.(5.24). The value of g^2, at which I_c reaches its maximum is $g^2 = \ln(\lambda - \mu_c)^{-1}$, so

$$D < \sqrt{2z}\omega \ln(\lambda - \mu_c)^{-1} \tag{5.25}$$

and

$$T_c^* < \omega \frac{\sqrt{2z}(\lambda - \mu_c)\ln(\lambda - \mu_c)^{-1}}{e} \tag{5.26}$$

Une maximum value of the critical temperature of order of $\omega/3$ is reached in the Inimon of the intermediate coupling $g^2 \simeq 1$, Fig.5.1, where on the contrary the BCS superconductor has rather low T_c of order of 0.1ω. The absolute value depends on Wand can be as high as $200 - 300K$ depending on the value of the optical phonon
frequency. At large value of the coupling T_c of the bipolaronic superconductor drops because carriers become very heavy. Therefore we conclude that the highest T_c is in the transition region from polaronic to bipolaronic superconductivity. The fact that due to the polaron nonadiabaticity the short-range Coulomb pseudopotential μ_c is not suppressed contrary to the BCS case with μ_c^* rather than μ_c does not change this conclusion if $\lambda - \mu_c$ is positive.

With the formula for T_c, Eq.(5.21) interpolating between polaronic and bipolaronic superconductivity one can explain the unusual oxygen isotope effect in superconducting oxides, in particular its large value in low T_c oxides, an overall trend to lower value as T_c increases, and a negative α at high T_c, Fig.5.2. As it is shown below negative values of the isotope effect suggest that in some high- T_c oxides polaronic (rather than bipolaronic) superconductivity may exist.

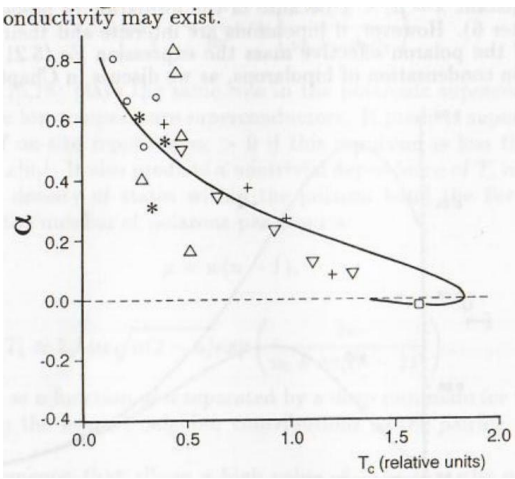

Fig.5.2. Oxygen isotope effect:(o) $La_{2-x}Ca_xCuO_4$, ($\triangle$)$La_{2-x}Sr_xCuO_4$, ($*$)$La_{2-x}Ba_xCuO_4$ (Craw ford et al. (1990)); (∇) $Y_{1-x}Pr_xBa_2Cu_3O_{6.92}$ (Franck et al. (1991)); ($+$) $YBa_2Cu_{4-x}Ni_xO_8$ (Bornemann et al. (1991a)); ($\square$) $Bi-Pb-Ca-Sr-Cu-O$ (Bornemann et al. (1991b)). Theoretical curve after Alexandrov (1992a).

As far as the oxygen mass dependence is concerned the formula Eq.(5.21) is applied both to the BCS-like polaronic superconductor and to the Bose-Einstein condensation of intersite bipolarons with the effective mass depending exponentially on the electron-phonon coupling $g : m^{**} \simeq m^* \sim \exp(g^2)$ (Chapter 6). As mentioned above the only quantity, which depends on the oxygen isotope mass M is g:

$$g^2 = \text{ const } \sqrt{M} + g_s^2 \tag{5.27}$$

where g_s^2 is a possible contribution to the mass renormalisation from the vibrations of other ions and from spin fluctuations. Differentiating Eq.(5.21) one obtains

$$\alpha = \frac{\beta g^2}{2}\left(1 - \frac{e^{-g^2}}{\lambda - \mu_c}\right), \tag{5.28}$$

where $\beta = 1 - g_s^2/g^2$ measures the relative contribution of oxygen to the small polaron cloud. Expressing T_c in units of $\tilde{D}$ we find

$$T_c = \exp\left(-g^2 - \frac{e^{-g^2}}{\lambda - \mu_c}\right) \tag{5.29}$$

With the equations (5.28, 29) one can analyse the correlation between the critical temperature and the isotope shift, Fig.5.2. It follows from our considerations that with the isotope effect one can distinguish the BCS like polaronic superconductivity $\alpha < 0$ from the Bose-Einstein condensation of small bipolarons $\alpha > 0$. With the increasing ion mass in the bipolaronic superconductor the bipolaron mass increases and the Bose-Einstein condensation temperature T_c decreases. On the contrary in polaronic superconductors the increase of the ion mass leads to the band narrowing and to the enhancement of the polaron density of states and therefore of T_c. The value of $\beta \simeq 1/3$ obtained from the fit to the experiment, Fig.5.2 shows that more than 30% of the cloud around polaron comes from oxygen vibrations, the rest is due to vibrations of other ions and (or) due to spin fluctuations, as proposed by Mott (1990).

6.7.4 5.4 Polaronic CDW

Theory

At substantial band-filling the global structural and charge density wave instability driven by the electron-phonon interaction can develop. A charge density wave (CDW) together with a static lattice distortion is known to occur at a wave vector $q = 2k_F$ in one-dimensional systems (Peierls (1955)). Peierls pointed out that a one-dimensional metal turns to an insulator because an energy gap opens at the Fermi level due to the doubling of the unit cell. This is an electronically induced lattice instability accompanied by a modulation of the electronic density. In the case of the weak electron-phonon coupling CDW develops also in $2D$ and $3D$ Fermi-liquids with the 'nested' Fermi surface. The theory has been worked out in the adiabatic and weak coupling approximations for both ω/D and λ being small. In the strong coupling limit the CDW ground state was discussed by Alexandrov and Ranninger (1981a). The central question is the electron excitation spectrum. The ground state is a charge ordered state of on-site small bipolarons. Taking into account the nonadiabatic corrections one should expect that the lowest charge excitation mode corresponds to the bipolaron conneling to the nearest neighbor site as discussed in Chapter 6. The dimerization of a half-filled Holstein chain of molecules in the strong coupling regime has been studied by Hirsch and Fradkin (1983) by means of the Monte-Carlo simulations. One of their conclusions is that the CDW order parameter is reduced gradually with the increasing adiabatic ratio ω/D due to the quantum fluctuations. Nasu (1985, 1991) and Zheng et al (1989) developed the variational approach to the Holstein $1D$ HamilImian describing the multi-electron system locally coupled to dispersionless phonons

$$\prime\prime = -t\sum_i \left(c_i^\dagger c_{i+1} + h.c.\right) - g\omega \sum_i \left(\hat{n}_i - 1/2\right)\left(d_i^\dagger + d_i\right) + \omega \sum_i \left(d_i^\dagger d_i + 1/2\right). \tag{5.30}$$

Here $\hat{n}_1 = c_1^\dagger c_i$ and t is the value of the nearest neighbor hopping integral. The muilibrium position of every oscillator is taken $\pm g\sqrt{2/M\omega}, 0$ if $n_{\mathbf{m}\uparrow} + n_{\mathbf{m}\downarrow} = 0, 2, 1,$
respectively. One can apply three successive unitary transformations with three variational parameters. The first one is a coherent state transformation for every phonon mode,

$$\exp S_1 = \exp\left[\sum_i (-1)^{i+1} m_0 \sqrt{M\omega/2}\left(d_i^\dagger - d_i\right)\right] \tag{5.31}$$

where m_0 is the first variational parameter, which measures the phonon-staggered ordering. As a result of the first transformation the equilibrium position of molecules becomes $(-1)^{i+1}m_0$ (for $\sum_s n_i = 1$). The second transformation is

$$\exp S_2 = \exp\left[\delta \sum_i g\left(\hat{n}_i - 1/2\right)\left(d_i^\dagger - d_i\right)\right] \tag{5.32}$$

which is an 'incomplete' Lang-Firsov polaronic transformation referring to the phononstaggered ordering state rather to the original homogeneous liquid. The variational parameter $\delta \leq 1$ measures the thickness of the phonon cloud around polaron, presumably allowing to consider the weak-coupling Migdal and polaron regimes within the same variational approach. However, differently from the displacement transformation of the Lee-Low-Pines theory (Chapter 1) or from the complete Lang-Firsov transformation, applied within the $1/\lambda$ expansion technique (Chapter 4), the 'incomplete' transformation, Eq.(5.32) leaves the substantial part ΔH_{e-ph} of the strong electron-phonon interaction in the transformed Hamiltonian

$$\Delta H_{e-ph} = -g\omega(1-\delta)\sum_i \left(\hat{n}_i - 1/2\right)\left(d_i^\dagger + d_i\right) \tag{5.33}$$

Finally, one can partly offset the polaronic narrowing effect, which is less favorable in the multi-polaron system compared with a single polaron one, by the third unitary transformation, the so-called 'squeezing' transformation (Zheng (1988))

$$\exp S_3 = \exp\left[\alpha \sum_i \left(d_i^\dagger d_i^\dagger - d_i d_i\right)\right] \tag{5.34}$$

This transformation generates a two-phonon coherent state with α being a third variational parameter. At this point Nasu and Zheng et al neglect the off-diagonal interaction ΔH_{e-ph} averaging the transformed Hamiltonian with respect to phonons. Thus the polaron and the phonon subsystems are decoupled with the effective Hamil tonian

$$\begin{aligned}\tilde{H}_{eff} \equiv \left\langle e^{S_3} e^{S_2} e^{S_1} H e^{-S_1} e^{-S_2} e^{-S_3}\right\rangle_{ph} = -\rho t \sum_i \left(c_i^\dagger c_{i+1} + h.c.\right) \\ + \sum_i \hat{n}_i \left[\left(2\delta - \delta^2\right) g^2\omega + (-1)^{i+1}(1-\delta) g\omega m_0 \sqrt{2M\omega}\right] \\ - 2\left(2\delta - \delta^2\right) g^2\omega \sum_i \hat{n}_{\mathbf{m}\uparrow}\hat{n}_{\mathbf{m}\downarrow} + NE_d\end{aligned} \tag{5.35}$$

where

$$\rho = \exp\left[-g^2\delta^2 e^{-4\alpha}\right] \tag{5.36}$$

is a new band narrowing factor and

$$E_d = \frac{\omega\cosh(4\alpha)}{2} + \frac{M\omega^2 m_0^2}{2} + \left(\delta^2 - 2\delta\right) g^2\omega \tag{5.37}$$

is the deformation energy per site. The effective Hamiltonian can be diagonalised with the Bloch representation for electrons. The ground state energy is minimised with respect to m_0, δ and α. It appears from the results of these calculations that because of the multi-polaron nature of the problem and the squeezing effect the band narrowing is not so dramatic as in a single polaron system. No order-disorder transition has been found and CDW ordering prevails for the half-filling for all values of the adiabatic ratio ω/D. This result is in agreement with the Monte Carlo simulations. However, the excitation spectrum is less reliable because the large off-diagonal interaction ΔH_{e-ph} is neglected in the effective variational Hamiltonian. It can have a drastic effect on the excitation spectrum.

As in the case of the polaronic Fermi-liquid the phonon excitation spectrum of the polaronic CDW state can be studied analytically by the use of the $1/\lambda$ expansion technique (Göbel et al (1994)). The CDW state of the half-filled chain of molecules in the strong coupling adiabatic regime has the following configuration

$$

$$

The phonon operators are now replaced by new operators describing the vibrations around the new equilibrium positions: $d_i \to d_i + \alpha_i$. After the substitution the Hamiltonian reads as

$$\begin{aligned}H = -t\sum_i \left(c_i^\dagger c_j + h.c.\right) - 2g\omega \sum_i \hat{n}_i\alpha_i - g\omega \sum_i \left(\hat{n}_i - \alpha_i/g\right)\left(d_i^\dagger + d_i\right) \\ + \omega \sum_i \left(d_i^\dagger d_i + 1/2 + \alpha_i^2\right)\end{aligned} \tag{5.38}$$

The last term represents the energy of the frozen distortion. The remaining terms give rise to the definition of two new electronic energy bands resulting from the broken symmetry of the ground state. The interaction terms are now supplemented by a term involving phonon operators only. The reason is that due to the buildup of CDW the occupation number n_i no longer has lattice periodicity. The supplemented term serves to cancel the expectation value of the interaction energy

$$n_i - \alpha_i/g = 0 \tag{5.39}$$

IIy defining $\alpha_{2i} \equiv \alpha$ and $\alpha_{2i+1} = \beta$ the new band structure is obtained by reverting to the reciprocical space shrinking the Brillouin zone from 2π to π (the lattice constant is taken as unity):

$$E_k^t = -g(\alpha - \beta) + \frac{t_k + t_{k+\pi}}{2} \pm \left[\frac{(t_k - t_{k+\pi})^2}{4} + g^2\omega^2(\alpha - \beta)^2 \right]^{1/2} \tag{5.40}$$

Where $t_h = -2$ tcos k and the momentum k has range $[-\pi/2, \pi/2]$. The parameters α, β Hacribing the distortion are now to be determined self-consistently. By minimising
the total energy with respect to α and β the lattice distortion depending on the coupling can be calculated. The contribution from the interaction term is expected to be small if Eq.(5.39) is satisfied. The amount of symmetry breaking is measured by $\Delta \equiv (\alpha - \beta)/g$. Introducing the familiar coupling constant $\lambda = g^2\omega/2t$ we obtain as a result of the minimisation of $\langle H \rangle$

$$\Delta = \frac{4}{\pi} \int_{-\pi/2}^{\pi/2} dk \frac{\lambda\Delta}{[\cos k + \lambda^2\Delta^2]^{1/2}} \tag{5.41}$$

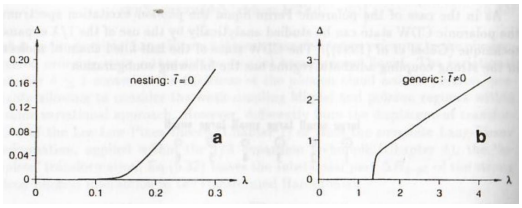

Fig.5.3. Distortion with (a) and without (b) nesting.

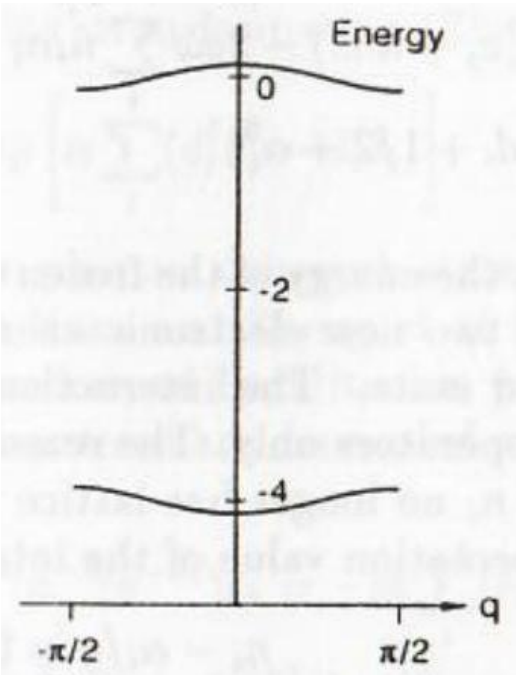

Fig.5.4. Electron energy bands of $1 D \mathrm{CDW}$ insulator for $\lambda \gg 1$.

Besides the trivial solution $\Delta = 0$ there is a nonvanishing one for every value of λ which gives the global minimum of the energy, Fig.5.3a. For large values of $\lambda > 1$ we have $\Delta \simeq 2 - 1/8\lambda^2$. In this range of λ the two energy bands become very flat and are separated by a huge 'Peierls' gap of the order of $4g^2\omega$, Fig.5.4. The immediate breaking of symmetry regardless of the value of λ, Fig.5.3a is an artificial feature particularly pertinent to one dimension. It is related to Fermi surface nesting and completely removed in higher dimensions with the realistic Fermi surface. To see the
general picture one can consider two dimensions with a pattern of symmetry breaking of the form

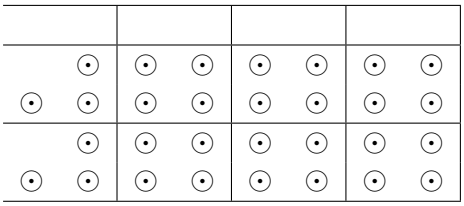

After symmetry breaking there will now arise four energy bands. However, the coupling must exceed a critical value λ_c for symmetry breaking to take place unless there is Fermi surface nesting. This can be verified with the bare kinetic energy dispersion of the form

$$E_{\mathbf{k}} = -2t\left(\cos k_x + \cos k_y\right) + \bar{t}\left(\cos 2k_x + \cos 2k_y\right) \tag{5.42}$$

For $\bar{t} = 0$ there is Fermi surface nesting and symmetry is broken for every value of the coupling, Fig.5.3a. On the other hand the general case $\bar{t} \neq 0$ shows no such pathological feature, Fig.5.3b. By expanding the static ground state energy about the equilibrium value of Δ up to the second order one finds for $\lambda > 1$ the renormalised phonon frequency $\tilde{\omega} = \omega\left(1 - O\left(1/\lambda^2\right)\right)$ similar to that of the two-site Holstein model, Eq.(1.129). With increasing λ the phonon frequency decreases to the left of the critical point $\lambda < \lambda_c$, vanishes at the phase transition and increases rapidly afterwards, as shown in Fig.5.5. This behavior of the phonon frequency is reminiscent of that of the finite size cluster, Fig.1.6. The spurious kink in the curve $\tilde{\omega}(\lambda)$

immediately after the phase transition, Fig.5.5 is due to a static approximation for the energy. Calculation done with the polarization loop (GF) smoothes out this part of the curve. The static energy result are then reproduced with the lowest order in the adiabatic parameter ω/t.

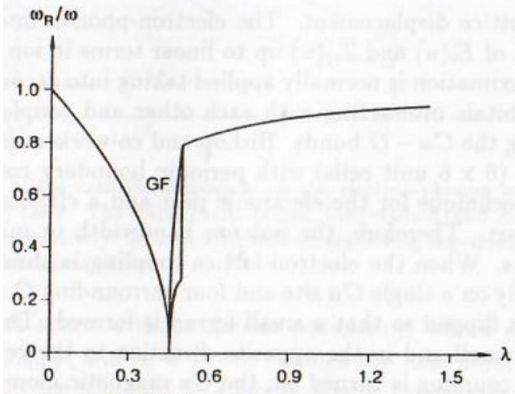

Iig.5.5. Renormalisation of the phonon frequency.

6.7.5 5.5 Small polarons in doped Mott insulators

Theory

I he formation and dynamics of polarons and bipolarons in strongly correlated narrow hand metals became fascinating topics because of renewed importance on account of its application to the high temperature superconductors. The behavior of a doped 'Mott' insulator - that is an antiferromagnetic material in which the moments have value $S = 1/2$ is still an unsolved problem; but we do not consider this to be the case for the antiferromagnetic materials in general. In magnetic materials the carriers in the conduction band form spin polarons - sometimes called ferrons (Nagaev (1979)); that is a group of moments oriented antiparallel to that of the carrier. This entity has a mass increasing exponentially with the number of moments it contains. One can assume that this remains so for the simple Mott insulator such as La_2CuO_4, if holes in the oxygen $2p$ band are introduced by doping with strontium. Then polarons must be of complex hybrid type. In the centre is a spin polaron, containing perhaps from 4 to 8 moments. But-in these highly dielectric materials, they will polarise the lattice. Both spin and lattice will contribute to the mass enhancement (Mott (1993)). Consequently, the problem combines aspects of coupled fields with distinct time scales (electrons, phonons and spin fluctuations), electron-electron interaction, lattice discreteness and, in real solids, competition between trapping in a random potential and the self-trapping.

The qualitative effects of the lattice- and spin-polaronic distortion upon doping into an antiferromagnetic stoichiometric background can be studied with the extended Peierls-Hubbard model (Bishop and Salkola (1995)). In particular case of CuO 2 plane of high- T_c copper oxides, Fig. 2.5 the model takes into account both the electron-phonon interaction (via the modulation of the atomic level E_i as well as the hopping integral T_{ij}) and the on-site (Hubbard U) and nearest-neighbor repulsion terms (V)

$$H = \sum_i E_i(u)\hat{n}_i + \sum_{\langle i\neq j\rangle} T_{ij}(u)c_i^\dagger c_j + \sum_{\mathbf{m}} U_{\mathbf{m}}\hat{n}_{\mathbf{m}\uparrow}\hat{n}_{\mathbf{m}\downarrow} + \sum_{\langle i\neq j\rangle} V_{ij}\hat{n}_i\hat{n}_j$$
$$+ \sum_{\mathbf{q}} \omega_{\mathbf{q}} \left(d_{\mathbf{q}}^\dagger d_{\mathbf{q}} + 1/2\right) \tag{5.43}$$

where u is the lattice displacement. The electron-phonon interaction is introduced by the expansion of $E_i(u)$ and $T_{ij}(u)$ up to linear terms in ion displacements u. The three-band approximation is normally applied taking into account holes in $Cud_{x^2-y^2}Op_x$ and Op_y orbitals

interacting with each other and coupled with the motion of oxygen ions along the $\mathrm{Cu}-\mathrm{O}$ bonds. Bishop and co-workers made their calculations on large clusters (6×6 unit cells) with periodic boundary conditions by the use of a Hartree-Fock technique for the electronic part and a classical adiabatic treatment for the lattice part. Therefore, the polaron bandwidth or mass remains outside of these calculations. When the electron-lattice coupling is absent, each added hole in localised primarily on a single Cu site and four surrounding O sites. The spin density at this Cu site is flipped so that a small ferron is formed. The spin densities at the four O sites are small and in the opposite direction to the central Cu spin. As the electron-phonon coupling is turned on, the Cu magnetic moment is reduced and the O atoms are displaced toward the central Cu. At the Cu site, where a small polaron resides, reduction of the magnetic moment results in strong mixing of the four O with the Cu. Then, substantially below a critical value of the electron-phonon coupling $\lambda \leq 1$ for destruction of the global antiferromagnetic state the magnetic moment of the central Cu collapses. Finally, above the critical value of λ the antiferromagnetic undoped ground state is replaced by a non-magnetic (lattice) small polaron state.

Under certain conditions the three-band Hubbard model discussed above in to
duced to a single-band $t-J$ model, in which the hole, constrained to a projected Hilbert space without double occupancy of sites, interacts with the spin density (for references see Dagotto (1994)). The formation of small polarons and bipolarons in the Holstein $t-J$ model was examined by Fehske et al (1995) by means of a variational diagonalisation technique on finite square lattices, up to 18 effective sites in size. The Hamiltonian of the $2D$ Holstein $t-J$ model is given by

$$H = -t \sum_{\langle i\neq j\rangle, s=s'} \left(c_i^\dagger c_j + h.c.\right) + J \sum_{\langle i\neq j\rangle} \left(\mathrm{S}_i \cdot \mathrm{S}_j - \frac{1}{4}\hat{n}_i\hat{n}_j\right)$$
$$- g\omega \sum_i h_i \left(d_i^\dagger + d_i\right) + \omega \sum_i \left(d_i^\dagger d_i + 1/2\right). \qquad (5.44))$$

0.04

Fig.5.6. Dependence of the transfer amplitude on the electron-phonon coupling for the onehole (a) and two- hole (b) cases. The solid, chain-dashed, long-dashed, and dashed curves refer to $\omega/l = 0.1, 0.8, 3.0, 10.0$, respectively. At $\omega = 0.1t$, the corresponding dependence for noncorrelated carriers is presented by the dotted curve.

II acts in a Hilbert space without double occupancy, where $\hat{n}_i = \sum_s c_{\mathbf{m},s}^\dagger c_{\mathbf{m},s}$, $\mathrm{H}_i = (1/2)\sum_{ss'} c_{\mathrm{m},s}^\dagger \tau_{ss'} c_{\mathrm{m},s'}$, and $h_i = 1-\hat{n}_i$ denotes the hole number operator. The linet two terms represent the standard $t-J$ model, where J measures the antiferromagnelic exchange interaction and t denotes hopping processes between nearest-neighbor colls on a square lattice. The third and fourth terms take the electron-phonon interaction and the phonon energy into account. The physics of the Holstein $t-J$ model 10 governed by two effects: the strong Coulomb correlations (due to J/t and the consiraint of no double occupancy), and the polaronic band renormalisation depending in $\lambda = g^2\omega/4t$ and ω/t. Including static displacement field, 'incomplete' polaron diccasing and squeezing effect and averaging over the transformed phonon vacuum as
described above, Fehske et al investigate numerically the ground state properties of the resulting polaronic $t-J$ model. As a measure of the phonon- induced band renormalisation the effective transfer amplitude

$$t_{eff} = \frac{E_t(g,J)}{E_t(0,J)} \qquad (5.45)$$

is introduced. Here

$$E_t = -\frac{\rho t}{N} \left\langle \sum_{\langle ij \rangle} \left(c_i^\dagger c_j + h.c. \right\rangle \tag{5.46}$$

denotes the kinetic energy with the reduction factor ρ, determined in Eq.(5.36). The effective transfer amplitude, calculated for $J/t = 0.4$ is shown in Fig 5.6a for the one hole case and in Fig.5.6b for the two hole case for different values of the adiabatic ratio ω/t. As in the noncorrelated system for low frequencies ($\omega < t$), one can distinguish the free hole if $\lambda \leq 0.2$ and the adiabatic small polaron for larger coupling with phonons. Increasing the electron-phonon interaction, the mobility of the hole ($\sim t_{eff}$) is strongly reduced when the small polaron is formed. To discuss the effect of the electronic correlations on the self-trapping transition, the noncorrelated case of spinless fermions is also considered. Obviously, the transition from large to small polaron is obtained at a much larger critical value of $\lambda_c \simeq 1$, which corresponds to the polaronic shift of the order of half the bare bandwidth, Fig.5.6a,b (dotted line). For the nonadiabatic case ($\omega \geq t$) there are small polarons at all values of λ, and the transfer amplitude decreases smoothly with increasing λ. As we have mentioned in section 5.4 the drawback of the variational approach is that a large part of the electron-phonon interaction is neglected because of the averaging with respect to phonons. However, the conclusion that the critical coupling strength λ for the selftrapping of the carriers in the doped Mott insulator is considerably reduced by the antiferromagnetic exchange interaction seems to be reasonable. Both lattice and spin distortions drive the system towards localisation. Therefore a rather weak electron-phonon interaction ($\lambda \geq 0.2$) can cause polaron band narrowing in strongly correlated phoriz electron system supporting a prominent role of the lattice degree of freedom in the cuprates.

6.8 6 Bipolaronic liquid

As we have mentioned in Chapter 5 the onsite or intersite attractive energy of two small polarons is generally larger than the polaron bandwidth. At this condition real space pairs of polarons i.e. small bipolarons form if temperature is not very high, $T < T^{**}$. Then the polaronic Fermi liquid transforms into a bipolaronic liquid. The latter is stable at low density of bipolarons because the effective bipolaron-bipolaron interaction is repulsive for all distances (see below). At large density the bipolaronic CDW state competes with the superfluid.

6.8.1 6.1 Coherent tunneling and repulsion of bipolarons

A small parameter $w/\Delta \ll 1$ where Δ is the bipolaron binding energy, of order of the attractive energy provides us with a consistent treatment of the bipolaronic systems (Alexandrov and Ranninger (1981a,b)). Under this condition the hopping term in the transformed Hamiltonian $\tilde{H}$ is a small perturbation to the ground state of immobile bipolarons and free phonons:

$$\tilde{H} = H_0 + H_{\text{pert}} \ , \tag{6.1}$$

where

$$H_0 = \frac{1}{2} \sum_{i,j} v_{ij} c_i^\dagger c_j^\dagger c_j c_i + \sum_{\mathbf{q}} \omega_{\mathbf{q}} \left(d_{\mathbf{q}}^\dagger d_{\mathbf{q}} + 1/2 \right) \tag{6.2}$$

and

$$H_{pert} = \sum_{i,j} \hat{\sigma}_{ij} c_i^\dagger c_j \tag{6.3}$$

Under the condition $\Delta \gg w$ there are no unbound polarons in the ground state, and the bipolaron motion can be described with a new canonical transformation $\exp(S_2)$. This transformation eliminates the first order of H_{pert} , which destroys the bipolaron and therefore has no diagonal contribution:

$$(S_2)_{f,p} = \sum_{i,j} \frac{\langle f|\hat{\sigma}_{ij} c_i^\dagger c_j|p\rangle}{E_f - E_p} \tag{6.4}$$

where $E_{f,p}$ and $|f\rangle, |p\rangle$ are the energy levels and the eigenstates of H_0. Neglecting the terms of higher order than $(w/\Delta)^2$ one obtains

$$(H_b)_{ff'} = \left(e^{S_2} \tilde{H} e^{-S_2}\right)_{ff'} \tag{6.5}$$

$$\begin{aligned}(H_b)_{ff'} \simeq (H_0)_{ff'} - \frac{1}{2} \sum_{\nu} \sum_{i,i';j,j'} \langle f|\hat{\sigma}_{ii'} c_i^\dagger c_{i'}|\nu\rangle\langle\nu|\hat{\sigma}_{jj'} c_j^\dagger c_{j'}|f'\rangle \\ \times \left(\frac{1}{E_\nu - E_{f'}} + \frac{1}{E_\nu - E_f}\right)\end{aligned} \tag{6.6}$$

The nonzero matrix elements of S_2 act between a localised bipolaron state and a state of two unpaired polarons localised in different cells or sites (in case of on-site pairs). The expression (6.6) determines the matrix elements of the transformed (bipolaronic) Hamiltonian H_b in the subspace $|f\rangle, |f'\rangle$ without unpaired polarons. On the other hand $|\nu\rangle$ refers to configurations involving two unpaired polarons, so that

$$E_f - E_\nu = -\Delta + \sum_{\mathbf{q}} \omega_{\mathbf{q}} \left(n_{\mathbf{q}}^f - n_{\mathbf{q}}^\nu\right) \tag{6.7}$$

where $n_{\mathrm{q}}^{f,\nu}$ are the phonon occupation numbers $(0, 1, 2, 3 \ldots)$. This equation is an explicit definition of the bipolaron binding energy Δ, which takes into account the interaction between bipolarons as well as between two unpaired polarons. The lowest eigenstates of H_b are in the subspace which involves only doubly occupied $c_{\mathbf{m},s}^\dagger c_{\mathbf{m},s'}^\dagger|0\rangle$ or empty $|0\rangle$ states. The bipolaron tunneling takes place via a transition to a virtual unpaired state implying a single polaron tunneling to the adjacent cell. The subsequent tunneling of a second polaron of a pair restores the initial energy state of the system. Because the bipolaron band is narrow (see below) there are no high-frequency phonons emitted or absorbed. Hence one can average H_b with the phonon density matrix

$$H_b = H_0 - i \sum_{i,i';j,j'} c_i^\dagger c_{i'} c_j^\dagger c_{j'} \int_0^\infty dt e^{-i\Delta t} \Phi_{ii'}^{jj'}(t) \tag{6.8}$$

with the real time t in the multiphonon correlator Φ determined in section 4.3. The difference between the 'exact' and averaged Hamiltonians can be treated perturbatively as the bipolaron-phonon interaction (section 6.3). Taking into account that there are only bipolarons in the subspace in which H_b operates one can rewrite the bipolaron Hamiltonian in terms of the creation $b_i^\dagger = c_{\mathbf{m}\uparrow}^\dagger c_{\mathbf{m},\downarrow}^\dagger$ and annihilation singlet bipolaron operators

$$H_b = -\sum_{\mathbf{m}} \left(\Delta + \frac{1}{2} \sum_{\mathbf{m}'} v^{(2)}_{\mathbf{m},\mathbf{m}'} \right) n_{\mathbf{m}} + \sum_{\mathbf{m}\neq\mathbf{m}'} \left(-t_{\mathbf{m},\mathbf{m}'} b^{\dagger}_{\mathbf{m}} b_{\mathbf{m}'} + \frac{1}{2} \bar{v}_{\mathbf{m},\mathbf{m}'} n_{\mathbf{m}} n_{\mathbf{m}'} \right) \tag{6.9}$$

where $n_{\mathrm{m}} = b^{\dagger}_{\mathrm{m}} b_{\mathrm{m}}$ is the bipolaron occupation number operator,

$$\bar{v}_{\mathrm{m},\ \mathrm{m}'} = 4v_{\mathrm{m},\ \mathrm{m}'} + v^{(2)}_{\mathrm{m},\ \mathrm{m}'} \tag{6.10}$$

is the bipolaron-bipolaron interaction including the direct (density-density) Coulomb repulsion (V_c), the attraction via phonons between two small polarons in different cells and a second order correction

$$v^{(2)}_{\mathbf{m},\mathbf{m}'} = 2i \int_0^{\infty} dt \Phi^{\mathbf{m}'\mathbf{m}}_{\mathbf{m}\mathbf{m}'}(t) \exp(-i\Delta t) \tag{6.11}$$

which is repulsive. The origin of this repulsion is that a virtual hop of one of the polarons of a pair is forbidden when the neighboring cell is occupied by another pair. The bipolaron transfer integral is of the second order in the electron kinetic energy $T(\mathbf{m})$

$$t_{\mathbf{m},\mathbf{m}'} = 2i \int_0^{\infty} dt \Phi^{\mathbf{m}\mathbf{m}'}_{\mathbf{m}\mathbf{m}'}(t) \exp(-i\Delta t) \tag{6.12}$$

To calculate t and $v^{(2)}$ one can use the explicit form of the multiphonon correlator, $\Phi^{m'm}_{mm'}$, Eq.(4.104). For $\Phi^{m'}_{mm'}$ the expression is the same, but with the opposite sign of the argument of the second exponent. If $T = 0$ and phonons are dispersionless the calculation yields (Alexandrov and Kabanov (1986))

$$t_{\mathbf{m},\mathbf{m}'} = \frac{2T^2(\mathbf{a})}{\Delta} e^{-2g^2} \sum_{k=0}^{\infty} \frac{(-2g^2)^k}{k!(1 + k\omega/\Delta)} \tag{6.13}$$

and

$$v^{(2)}_{\mathbf{m},\mathbf{m}'} = \frac{2T^2(\mathbf{a})}{\Delta} e^{-2g^2} \sum_{k=0}^{\infty} \frac{(+2g^2)^k}{k!(1 + k\omega/\Delta)} \tag{6.14}$$

with $\mathbf{a} = \mathbf{m} - \mathbf{m}'$. If $\Delta < \omega$ both the bipolaron hopping and the second order repulsion are about w^2/Δ. However, for large binding energy $\Delta \gg \omega$ the bipolaron bandwidth dramatically decreases being proportional to e^{-4g^2} in the limit $\Delta \to \infty$. This limit is, however, not realistic because $\Delta \simeq 2E_p - V_c \leq 2g^2\omega$. Therefore, a more realistic regime is $\omega < \Delta < 2g^2\omega$, where

$$t_{\mathbf{m},\mathbf{m}'} \simeq \frac{2\sqrt{2\pi}T^2(\mathbf{a})}{\sqrt{\omega\Delta}} \exp\left[-2g^2 - \frac{\Delta}{\omega} \left(1 + \ln \frac{2g^2\omega}{\Delta} \right) \right] \tag{6.15}$$

On the contrary the bipolaron-bipolaron repulsion increases, $v^{(2)} \sim D^2/\Delta$ in the limit $\Delta \to \infty$. For dispersionless molecular or optical phonons the intermolecular attraction via phonons (the second term in Eq.(4.14)) is zero. Therefore the direct Coulomb and the second order $v^{(2)}$ repulsive terms lead to a total repulsive interaction between bipolarons, preventing the formation of droplets. At finite temperatures the denominator of the second order terms of the bipolaronic Hamiltonian, Eq.(6.6) turns out to be zero if the resonance condition $N\omega = \Delta$ is met ($N = 1, 2, 3, \ldots$). This divergence is eliminated by taking into account the phonon frequency dispersion and (or) by including the higher terms of the $1/\lambda$ perturbation expansion.

The high temperature behavior of the bipolaron transfer integral is just opposite to that of the small polaron bandwidth. While the polaron band collapses with increasing temperature as described in section 4.4 the bipolaron band becomes wider [24] found by Bryksin and Gol'tsev (1988)

$$t_{\mathrm{m},\ \mathrm{m}'} \sim T^{-1/2} \exp\left[-\frac{E_p + \Delta}{2T}\right] \tag{6.16}$$

for $T > \omega$.
In the case of inter - site bipolarons, which are the bound states of two small polarons on neighboring sites, there are two additional points. First of all an intersite bipolaron can be formed with a nonzero spin $S = 1$ (triplet state) and with the energy $J \sim w^2/U$ above the singlet state $S = 0$. This should be taken into account by introducing additional spin quantum numbers $S = 1; l = 0, \pm 1$ in the definition of $b_{\mathbf{m}}$. The second point is that in a simple square or cubic lattice the inter-site bipolaron tunnels via the next neighbor hopping of a single polaron rather than via two-particle (Josephson-like) tunneling, described with Eq.(6.12). This 'crablike' tunneling results in a bipolaron bandwidth of the same order as the polaron one. In the perovskite structures the apex bipolaron is the ground state as discussed in section 2.5. Its band structure is described below. In general, H_b in the form of Eq.(6.9) is applied not only to on-site bipolarons but also to inter-site or more extended nonoverlapping pairs if $\mathbf{m}$ includes the spin, and $t_{\mathbf{m},\mathbf{m}'}$ is considered as a phenomenological parameter. The site index $\mathbf{m}$ should be generally considered as a position of the centre of mass of the bipolaron.

6.8.2 6.2 Bipolaron anisotropic flat bands in high- T_c copper oxides

Consideration of particular lattice structures shows that small inter-site bipolarons can be perfectly mobile even when the electron-phonon coupling is strong and the bipolaron binding energy is large (Alexandrov (1995)). Here we analyse the important case of copper based high-T_c oxides. The existence of the 'parent' Mott insulators suggest that high- T_c superconductors are in fact doped semiconductors with narrow electron bands. Therefore, different types of bipolarons can be found with computer simulation techniques based on the minimization of the ground state energy, Eq. (4.15) without the kinetic energy term, section 2.5. The intersite pairing of the in-plane oxygen hole with the apex one is energetically favorable in the perovskite structures with the binding energy $\Delta = 0.119$eV for La_2CuO_4, Table 4. Obviously, this apex bipolaron can tunnel from one cell to another via a direct single polaron tunneling from one apex oxygen to its apex neighbor as shown in Fig.6.1.

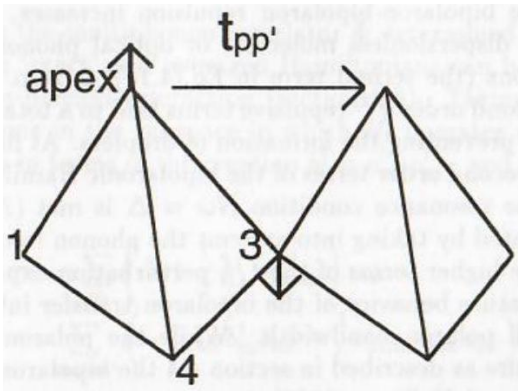

Fig.6.1. Apex bipolaron tunneling in perovskites.

To show this we consider the model Hamiltonian, including the oxygen-oxygen and oxygen-copper hopping integrals

$$H = \sum_{i,j} T_{ij} c_i^\dagger c_j + \sum_{\mathbf{q},j} \omega_{\mathbf{q}} \hat{n}_j \left(u_j(\mathbf{q}) d_{\mathbf{q}} + h.c. \right) + \sum_{\mathbf{q}} \omega_{\mathbf{q}} \left(d_{\mathbf{q}}^\dagger d_{\mathbf{q}} + 1/2 \right) + \sum_{i,j} V_{ij} \hat{n}_i \hat{n}_j \tag{6.17}$$

where T_{ij} determines the bare band structure in the site representation; c_i, c_j are hole annihilation operators for oxygen or copper sites $i, j; \hat{n}_j = c_j^\dagger c_j$ is the number operator, V_{ij} is the direct Coulomb repulsion, which does not include the on-site term $i = j$ for parallel spins. Oxides are strongly polarizable materials, so coupling with optical phonons dominates in the electron-phonon interaction

$$\gamma(\mathbf{q}) = -\frac{i\sqrt{8\pi\alpha}}{\sqrt{\Omega}(2m\omega)^{1/4} q} \tag{6.18}$$

The lattice polarization is coupled with the electron density, therefore the interaction is diagonal in the site representation and the coupling constant does not depend on the particular orbital. In doped oxides optical phonons are partially screened. Then molecular and acoustical phonons also contribute to the interaction. The canonical displacement transformation eliminates an essential part of the electron-phonon interaction. The transformed Hamiltonian is given by

$$\tilde{H} = SHS^{-1} = (T_p - E_p) \sum_{i(p)} n_{i(p)} + (T_d - E_d) \sum_{i(d)} n_{i(d)} + \sum_{i \neq j} \hat{\sigma}_{ij} c_i^\dagger c_j + \sum_{\mathbf{q}} \omega_{\mathbf{q}} \left(d_{\mathbf{q}}^\dagger d_{\mathbf{q}} + 1/2 \right) - \frac{1}{2} \sum_{\mathbf{q},i,j} \left(2\omega_{\mathbf{q}} u_i(\mathbf{q}) u_j^*(\mathbf{q}) - V_{ij} \right) \hat{n}_i \hat{n}_j \tag{6.19}$$

The first oxygen (p) and the second copper (d) diagonal terms include the polaronic level shift, which is the same for oxygen and copper ions

$$E_p = E_d = \sum_{\mathbf{q}} |u_j(\mathbf{q})|^2 \omega_{\mathbf{q}} \tag{6.20}$$

The transformed hopping term involves phonon operators

$$\hat{\sigma}_{ij} = T_{ij} \exp\left(\sum_{\mathbf{q}} u_i^*(\mathbf{q}) d_{\mathbf{q}}^\dagger - \text{ h.c. } \right) \exp\left(\sum_{\mathbf{q}} u_j(\mathbf{q}) d_{\mathbf{q}} - \text{ h.c. } \right). \tag{6.21}$$

There are two major effects of the electron-phonon interaction. The first one is the band narrowing due to a phonon cloud surrounding the hole. In case of a large charge Iransfer gap $E_g \gg \omega$ the bandwidth narrowing factor is the same for the direct $t_{pp'}$ and the second order via copper $t_{pp'}^{(2)}$ oxygen-oxygen transfer, Fig.6.2a,b

$$t_{pp'} \equiv \langle 0 | \hat{\sigma}_{pp'} | 0 \rangle = T_{pp'} e^{-g_{pp'}^2} \tag{6.22}$$

$$t_{pp'}^{(2)} \equiv \sum_{\nu} \frac{\langle 0 | \hat{\sigma}_{pd} | \nu \rangle \langle \nu | \hat{\sigma}_{dp'} | 0 \rangle}{E_0 - E_\nu} \simeq \frac{T_{pd}^2}{E_g} e^{-g_{pp'}^2}, \tag{6.23}$$

where $|\nu\rangle, E_\nu$ are eigenstates and eigenvalues of the transformed Hamiltonian, Eq.(6.19) without the third hopping term, $|0\rangle$ the phonon vacuum, and the reduction factor is

$$g_{pp'}^2 = \frac{1}{2N}\sum_{\mathbf{q}} |\gamma(\mathbf{q})|^2 \left(1 - \cos\left[\mathbf{q}\cdot(\mathbf{m}_p - \mathbf{m}_{p'})\right]\right) \tag{6.24}$$

These expressions are the result of the straightforward calculations described below. The direct hopping is given by

$$t_{pp'} = T_{pp'}\langle 0|\exp\left(\sum_{\mathbf{q}} u_p^*(\mathbf{q})d_{\mathbf{q}}^\dagger - \text{ h.c. }\right)\exp\left(\sum_{\mathbf{q}} u_{p'}(\mathbf{q})d_{\mathbf{q}} - \text{ h.c. }\right)|0\rangle \tag{6.25}$$

With the help of $e^{A+B} = e^A e^B e^{-[AB]/2}$ one obtains

$$t_{pp'} = T_{pp'}e^{-g_{pp'}^2}\langle 0|\exp\left(\sum_{\mathbf{q}} u_p^*(\mathbf{q})d_{\mathbf{q}}^\dagger\right)\exp\left(-\sum_{\mathbf{q}} u_{p'}(\mathbf{q})d_{\mathbf{q}}^\dagger\right)|0\rangle \tag{6.26}$$

where

$$g_{ij}^2 = \frac{1}{2}\sum_{\mathbf{q}}\left(|u_i(\mathbf{q})|^2 + |u_j(\mathbf{q})|^2 - 2u_i^*(\mathbf{q})u_j(\mathbf{q})\right) \tag{6.27}$$

The bracket in Eq.(6.26) is equal to unity. Then Eq.(6.22) follows from Eq.(6.26) using the definition of $u_j(\mathbf{q})$.

Taking into account that $E_\nu - E_0 = E_g + \sum_{\mathrm{q}} \omega_{\mathrm{q}} n_{\mathrm{q}}$ the second order indirect hopping Eq.(6.23) is written as

$$t_{pp'}^{(2)} = i\int_0^\infty dt e^{-iE_g t}\langle 0|\hat{\sigma}_{pd}(t)\hat{\sigma}_{dp'}|0\rangle \tag{6.28}$$

where

$$\hat{\sigma}_{pd}(t) = T_{pd}\exp\left(\sum_{\mathbf{q}} u_p^*(\mathbf{q},t)d_{\mathbf{q}}^\dagger - h.c.\right)\exp\left(\sum_{\mathbf{q}} u_d(\mathbf{q},t)d_{\mathbf{q}} - h.c.\right) \tag{6.29}$$

Here $u_j(\mathbf{q},t) \equiv u_j(\mathbf{q})\exp(i\omega_{\mathbf{q}}t)$ and $n_{\mathbf{q}} = 0, 1, 2, \ldots$ the phonon occupation numbers. Calculating the bracket in Eq.(6.28) one obtains

$$\langle\ldots\rangle = e^{-g_{pd}^2}e^{-g_{dp'}^2}\exp\left(-\sum_{\mathbf{q}}\left[u_p(\mathbf{q}) - u_d(\mathbf{q})\right]\left[u_d^*(\mathbf{q}) - u_{p'}^*(\mathbf{q})\right]e^{-i\omega\mathbf{q}^t}\right) \tag{6.30}$$

If $\omega_{\mathbf{q}}$ is $\mathbf{q}$-independent, the integral in Eq.(6.28) is calculated by the expansion of the exponent in Eq.(6.30):

$$t_{pp'}^{(2)} = \frac{T_{pd}^2}{E_g}e^{-g_{pd}^2}e^{-g_{dp'}^2}\sum_{k=o}^{\infty}\frac{(-1)^k\left(\sum_{\mathbf{q}}\left[u_p(\mathbf{q}) - u_d(\mathbf{q})\right]\left[u_d^*(\mathbf{q}) - u_{p'}^*(\mathbf{q})\right]\right)^k}{k!\,(1 + k\omega/E_g)} \tag{6.31}$$

Then Eq.(6.23) is obtained in the limit $E_g \gg \omega$.
Substitution of Eq.(6.18) into Eq.(6.24) yields

$$g_{pp'}^2, g^2 = \frac{E_p}{\omega}\left(1 - \frac{Si\,(q_d m)}{q_d m}\right) \tag{6.32}$$

if the Debye approximation for the Brillouin zone is applied. Here $\mathrm{Si}(x) = \int_0^x \sin(t)dt/t$, $m = a/\sqrt{2}$ and $m = a$ for the in-plane reduction factor $g^2_{pp'}$ and for the apex-reduction factor g^2, respectively. For $LSCO$ with $q_d \simeq 0.7\text{Å}^{-1}$ and $a \simeq 3.8\text{Å}$ one obtains $g^2_{pp'} \simeq 0.2E_p/\omega$ and $g^2 \simeq 0.3E_p/\omega$ where E_p is given by Eq.(1.99). Because the nearest neighbor oxygen-oxygen distance in copper oxides is less than the lattice constant the calculations yield a remarkably lower value of $g^2_{pp'} \simeq 0.2E_p/\omega$ than one can expect with a naive estimate ($\simeq E_p/\omega$).

The other effect of the electron-phonon coupling is the attraction between two polarons given by the last term in Eq.(6.19). For the Fröhlich interaction the polaron level shift in $La_{2-x}Sr_xCuO_4$ is estimated to be as large as $E_p \simeq 0.6$eV, section 1.5. Then with $\omega = 0.06$eV one obtains $g^2_{pp'} \simeq 2$. As a result a large attraction between two polarons of the order of $2E_p \geq 1$eV is possible accompanied by only one order of magnitude mass enhancement. Such a possibility is a result of the particular lattice structure and the phonon dispersion.

The bipolaron hopping integral t is obtained by projecting the Hamiltonian, Eq.(6.19) onto the reduced Hilbert space containing only empty or doubly occupied elementary cells. The wave function of the apex bipolaron localised, say in the cell $\mathbf{m}$ is written as

$$|\mathrm{m}\rangle = \sum_{i=1}^{4} A_i c_i^\dagger c_{apex}^\dagger |0\rangle \tag{6.33}$$

where i denotes the $p_{x,y}$ orbitals and spins of the four plane oxygen ions in the cell m , Fig. 2.5 and $c^\dagger_{\mathrm{apex}}$ is the creation operator for the hole on one of the three apex oxygen orbitals with the spin, which is same or opposite to the spin of the plane hole, depending on the total spin of the bipolaron. The probability amplitudes A_i are normalised by the condition $|A_i| = 1/2$ because only four plane orbitals p_{x1}, p_{y2}, p_{x3} and p_{y4} are relevant within the three band model. The matrix element of the Hamiltonian Eq.(6.19) of the first order with respect to the transfer integral responsible for the bipolaron tunneling to the nearest neighbor cell (m + a) is

$$t = \langle \mathbf{m}|\tilde{H}|\mathbf{m}+\mathbf{a}\rangle = \frac{1}{4} T^{apex}_{pp'} e^{-g^2} \tag{6.34}$$

where $T^{apex}_{pp'}$ is the single polaron hopping between two apex ions,

$$g^2 = \frac{1}{2N} \sum_{\mathbf{q}} |\gamma(\mathbf{q})|^2 \left[1 - \cos(q_x a)\right] \tag{6.35}$$

is the polaron narrowing factor, and a is the in-plane lattice constant, which is also the nearest neighbor apex-apex distance. As a result the hole bipolaron energy spectrum in the tight binding approximation consists of two bands $E^{x,y}$ formed by the overlap of p_s and p_y apex polaron orbitals, respectively, Fig.6.2b:

$$E^x_{\mathbf{k}} = -t\cos(k_x) + t'\cos(k_y) \tag{6.36}$$
$$E^y_{\mathbf{k}} = t'\cos(k_x) - t\cos(k_y) \tag{6.37}$$

where the in-plane lattice constant is taken to be $a = 1, t$ is the renormalized hopping integral, Eq.(6.34) between p orbitals of the same symmetry elongated in the direction of the hopping ($pp\sigma$) and t' is the renormalised hopping integral in the perpendicular direction ($pp\pi$). Their ratio $t/t' = T^{apex}_{pp'}/T^{appex}_{pp'} = 4$ as follows from the tables of hopping integrals in solids (Harrison (1989)).

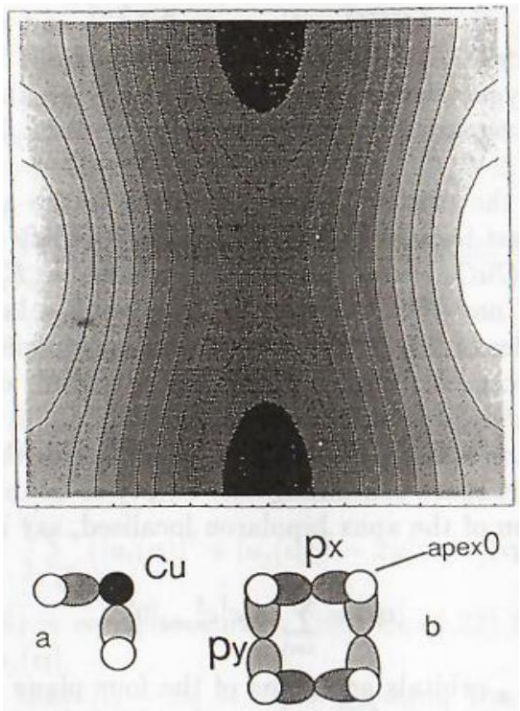

Fig.6.2. Counterplot of the 'x'-bipolaron dispersion $E_{\mathbf{k}}^{x}$. Dark regions correspond to the bottom of the band. $E_{\mathbf{k}}^{y}$ energy surfaces are obtained by $\pi/2$ rotation. Three-band model (a) and two-band

apex bipolaron model (b).

Two different bands are not mixed because $T_{p_x,p'_y}^{apex} = 0$ for the nearest neighbors. The random potential does not mix them either if it varies smoothly on the lattice scale. Consequently, we can distinguish ' x ' and ' y ' bipolarons with a lighter effective mass in x or y direction, respectively. The apex ' z ' bipolaron, if formed, is *ca.* four times less mobile than the x and y bipolarons. The bipolaron bandwidth is of the same order as the polaron one, which is a specific feature of the inter-site bipolaron discussed above. For a large part of the Brillouin zone near $(0, \pi)$ for ' x ' and $(\pi, 0)$ for ' y ' bipolaron, Fig.6.2 one can adopt the effective mass approximation

$$E_{\mathbf{k}}^{x,y} = \frac{k_x^2}{2m_{x,y}} + \frac{k_y^2}{2m_{y,x}} \tag{6.38}$$

with $k_{x,y}$ taken relative to the band bottom positions and $m_x = 1/t, m_y = 4m_x$. The bipolaron mass anisotropy has an important impact on the value of the Hall effect in high- T_c oxides (Chapter 8).

6.8.3 6.3 Bipolaron kinetics

As in the case of small polarons discussed in Chapter 4, bipolarons interact with phonons via the residual bipolaron-phonon interaction, which is a difference of the
exact and averaged with respect to phonons bipolaronic Hamiltonians

$$H_{b-ph} = \sum_{\mathbf{m}\neq\mathbf{m}'} \left(t_{\mathbf{m},\mathbf{m}'} - \hat{t}_{\mathbf{m},\mathbf{m}'}\right) b^{\dagger}_{\mathbf{m}} b_{\mathbf{m}'} + \frac{1}{2}\sum_{\mathbf{m}\neq\mathbf{m}'} \left(v^{(2)}_{\mathbf{m},\mathbf{m}'} - \hat{v}^{(2)}_{\mathbf{m},\mathbf{m}'}\right) n_{\mathbf{m}}\left(1 - n_{\mathbf{m}'}\right) \tag{6.39}$$

where

$$\hat{t}_{\mathbf{m},\mathbf{m}'} = i\int_0^{\infty} e^{-\left(i\Delta+0^+\right)t}\left[\hat{\sigma}_{\mathbf{m},\mathbf{m}'}(t)\hat{\sigma}_{\mathbf{m},\mathbf{m}'} + \hat{\sigma}_{\mathbf{m},\mathbf{m}'}\hat{\sigma}_{\mathbf{m},\mathbf{m}'}(-t)\right] \tag{6.40}$$

and

$$\hat{v}^{(2)}_{\mathbf{m},\mathbf{m}'} = i\int_0^{\infty} e^{-\left(i\Delta+0^+\right)t}\left[\hat{\sigma}_{\mathbf{m},\mathbf{m}'}(t)\hat{\sigma}_{\mathbf{m}',\mathbf{m}} + \hat{\sigma}_{\mathbf{m},\mathbf{m}'}\hat{\sigma}_{\mathbf{m}',\mathbf{m}}(-t)\right]. \tag{6.41}$$

The interaction is of the second order in the transfer integral $T(\mathbf{m})$, so it can be treated perturbatively by the $1/\lambda$ expansion technique. In particular, one can calculate the hopping conductivity of bipolarons in the high temperature regime $T > \omega/2$ (Bryksin and Gol'tsev (1988)). As in the case of small polarons the hopping bipolaron contribution to the conductivity is expressed in terms of the diffusion coefficient $D_b = 2a^2W_b$. Then the drift mobility is found from the Einstein relationship $\mu_b = 2eD_b/T$, where an additional 2 appears because the bipolaron charge is $2e$. The probability W_b of a jump to the nearest neighbor site per second in the lowest fourth order with respect to the hopping integral $T(\mathbf{m})$ is found by the use of the Fermi-golden rule with the interaction term H_{b-ph} rather than with H_{p-ph}

$$W_b = \int_{-\infty}^{\infty} dt\left[\left\langle\hat{t}_{\mathbf{m},\mathbf{n}}(t)\hat{t}_{\mathbf{n},\mathbf{m}}\right\rangle - t^2_{\mathbf{m},\mathbf{n}}\right] e^{-0^+|t|} \tag{6.42}$$

Here $|\mathbf{m}-\mathbf{n}| = a$ and $\hat{t}_{\mathbf{m},\mathbf{n}}(t) = \exp\left(iH_{ph}t\right)\hat{t}_{\mathbf{m},\mathbf{n}}\exp -iH_{ph}t$ is the Heisenberg hopping operator. If there is a phonon frequency dispersion, only the first saddle-point contributes to the integral in Eq.(6.42) with the following result

$$\mu_b \simeq ea^2\frac{64\pi^{3/2}T^4(\mathbf{a})}{\omega^2\sqrt{TE_a}\left(\Delta+4E_a\right)}\exp\left[\frac{-\left(\Delta+4E_a\right)^2}{16E_aT}\right], \tag{6.43}$$

where E_a is a single polaron activation energy, determined in Eq.(4.107). Because of the small exponential term in Eq.(6.43) the on-site bipolaron hopping mobility is lower compared with the contribution of the thermally excited polaron despite the fact that the polaron density is exponentially small ($\sim \exp(-\Delta/2T)$) compared with the bipolaron one. The on-site bipolaron contribution to the *dc* conductivity is small compared with the polaron contribution as $\sigma_b/\sigma_p \sim \exp\left(-\Delta^2/16E_aT\right)$. However, as the frequency of the electric field increases, the dominant role in conductivity is gradually transferred to bipolarons, as discussed in the next section. In the absence of the Coulomb repulsion the bipolaron binding energy is $\Delta \simeq 2E_p \simeq 4E_a$ and consequently, the bipolaron mobility obeys the law $\mu_b \sim \exp\left(-4E_a/T\right)$. This has a simple explanation because in this case the bipolaron jump is equivalent to a single polaron jump but with a double coupling constant with phonons. Of course, internite bipolarons with the activation energy of the same order as the single polaron activation energy dominate both in the *dc* and *ac* transport at all temperatures $T < T^{"}$. Also, at low temperatures $T < \omega/2$ we expect that the tunneling mechanism
will play the dominant role. In this temperature range bipolaron kinetics is that of charged bosons on a lattice, while the tunneling contribution of the thermally excited single polarons is frozen out. Low temperature bipolaron kinetics is discussed in Chapter 7.

6.8.4 6.4 MIR conductivity of small bipolarons

The frequency dependence of the MIR bipolaron conductivity can be estimated using the two-site Holstein model with two electrons and the Franck-Condon principle, which states that optical transitions take place instantaneously without any change in the nuclear configuration. Consequently, the optical transition between adiabatic levels takes place vertically as in the case of a single polaron, Fig.4.5. The corresponding qualitative analysis by Bryksin and Voloshin (1984) shows that the absorption coefficient of light by the on-site bipolaron has three Gaussian peaks located at frequencies $\nu_1 = 4E_a, 8E_a - U$ and $16E_a$. The lowest peak corresponds to the absorption by single thermally excited polarons. The highest peak is due to the shakeoff of phonons without dissociation of the bipolaron while the main central peak is the absorption involving dissociation. The value of the lowest single polaron peak is exponentially small ($\sim \exp(-2E_a/T)$) compared with the two high frequency absorption maxima, while the highest peak is smaller compared with the main central peak due to an additional factor $\sim J^2$. The width of the high-frequency peak, which is $\sim 8\sqrt{E_a T}$ is twice the width of the two low-frequency peaks. If the on-site Coulomb repulsion is absent, $U = 0$ the main maximum of the MIR conductivity is shifted relative to the maximum of the single polaron conductivity, section 4.10 by the value $\simeq 2E_p$ towards the high frequency region. The explanation is that the polaron shift of the atomic level is proportional to the square of the ion displacement, as is always the case in the harmonic approximation. Consequently, the polaron shift becomes $4E_p$ for two electrons on the same site compared with $2E_p$ when the electrons occupy different sites.

The exact diagonalisation of the two-site Holstein model in the truncated Hilbert space up to 50 phonons allows us to carry out the quantitative analysis of the bipolaronic MIR conductivity (Alexandrov et al (1994b)). In the case of two electrons in a two-site cluster the ground state changes essentially due to the formation of a bipolaron. If the electron-electron repulsion is weak optical properties will be determined by the excitation of a bipolaron in the state of two unpaired electrons. On the other hand, in the case of strong Hubbard U, the ground state corresponds to unpaired electrons and the main peak in $\sigma(\nu)$ is expected to be for $\nu \sim U$. The evolution of $\sigma(\nu)$ with increasing for two-site cluster with two electrons is shown in Fig.6.3 for $T = 0$. For $U = 0$ (Fig.6a) we found one peak in $\sigma(\nu)$ in the high energy region $\nu \simeq 4E_p$. This peak also shows the additional phonon superstructure, Other peaks are absent. If U increases, peak in $\sigma(\nu)$ shifts to the lower value of ν. This is due to the fact that the finite value of U reduces the binding energy of the the peak has well defined asymmetry (Fig. Further increase of U round

of U leads to the change of the ground state. A bipolaron is no longer the ground state. It leads to the appearance of an additional peak in $\sigma(\nu)$. These two peaks

state. It leads to the appearance of an additional peak in $\sigma(\nu)$. These two peak (Fig.6c,d) correspond to the excitation of an electron from the unpaired ground state to bonding and antibonding paired states $|\phi_\pm\rangle \sim \left(c^+_{1\uparrow}c^+_{2\downarrow} \pm c^+_{1\downarrow}c^+_{2\uparrow}\right)|0\rangle$. The lineshape in that case is also asymmetric. The observed spectral shape of the spectrum and the

phonon superstructure strongly suggest small lattice polarons as the common origin of the MIR conductivity in all perovskite materials, Chapter 8. If one accepts that the high energy MIR maximum at $\nu \simeq 0.7$eV in the high- $T_c YBCO$ is due to inter-site bipolarons and the gap, observed with the tunneling, IR reflectivity, photoemission, and with the electron energy loss spectroscopy $2\Delta \simeq 8T_c$ is the bipolaron binding energy one can estimate E_p and the characteristic inter-site Coulomb repulsion V_c. If we adopt in a qualitative analysis a similar shape of the on-site and the inter-site bipolaron absorption the position of the maximum of the inter-site bipolaron absorption is given by $\nu = 4E_p - V_c$ and $2\Delta = 2E_p - V_c$. With $\nu = 0.7$eV and $2\Delta = 0.07$eV we obtain $E_p \simeq 0.3$eV and $V_c = 0.5$eV. This value of E_p is close to that obtained with ther the appropriate electron-phonon interaction constant ($\lambda \sim 1 - 2$). The value of V_c is close to the estimation of the inter-site Coulomb repulsion with the high-frequency dielectric constant $\epsilon = 5$.

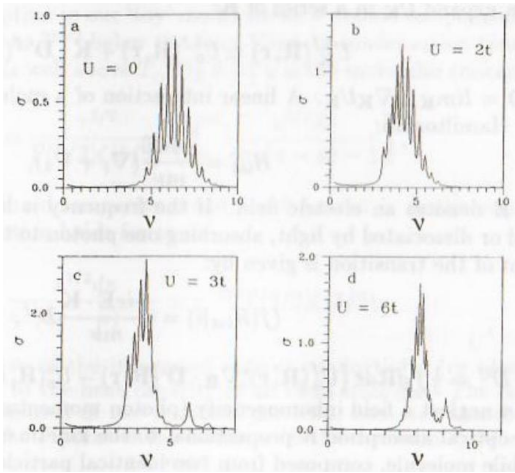

Fig.6.3. Two-site bipolaronic optical conductivity for different values of the on-site Hubbard repulsion $U, \omega = 0.5J$, and $\lambda = 0.8$.

6.8.5 6.5 Effect of superconducting phase transition on MIR conductivity

It is difficult to study the temperature dependence of the MIR conductivity on the temperature scale compared with the critical temperature of the superconducting phase transition T_c within the finite cluster model. Also, in the qualitative connideration of the preceding section the tunneling transport of bipolarons is ignored. Nevertheless, the temperature dependence of the integrated bipolaronic MIR conductivity can be studied by the use of the Kubo sum rule (Alexandrov et al (1993)). Let us discuss first a simple but rather general model which show a hundred percent decrease of the optical absorption while temperature changes from T_c to zero: an ideal gas of molecules, composed of two identical particles (electrons) on a lattice. To stabilize their bound state one should assume that the pair attraction operates, compensating the Coulomb repulsion. All molecules are in the ground internal state
with the binding energy being much higher than temperature. The periodic crystal field is assumed to be large compared with the binding energy, so all molecular states, including continuum, are built from the single-band single-electron Bloch wave functions.

Because of the translation symmetry the molecular wave function is a two-particle Bloch function described with the total quasi-momentum $\mathbf{K}$:

$$\Psi^{i,f}(\mathbf{r}_1, \mathbf{r}_2) = \exp(i\mathbf{K} \cdot \mathbf{R}) U_{\mathbf{K}}^{i,f}(\mathbf{R}, \mathbf{r}) \tag{6.44}$$

where $\mathbf{R} = (\mathbf{r}_1 + \mathbf{r}_2)/2, \mathbf{r} = \mathbf{r}_1 - \mathbf{r}_2$, and $U_{\mathbf{K}}(\mathbf{R}, \mathbf{r})$ is periodic with the lattice translations. At low temperatures only states with small K (near Γ point) are relevant, so one can expand $U_{\mathbf{K}}$ in a series of $\mathbf{K}$:

$$U_{\mathbf{K}}^{i,f}(\mathbf{R}, \mathbf{r}) \simeq U_0^{i,f}(\mathbf{R}, \mathbf{r}) + \mathbf{K} \cdot \mathbf{D}^{i,f}(\mathbf{R}, \mathbf{r}) \tag{6.45}$$

with $\mathbf{D} = \lim_{\mathbf{K} \to 0} \nabla_{\mathbf{K}} U_{\mathbf{K}}$. A linear interaction of a molecule with light is described by the Hamiltonian:

$$H_{int} = \frac{-ie\mathbf{E}}{m\nu} (\nabla_1 + \nabla_2) \tag{6.46}$$

where $\mathbf{E}$ denotes an electric field. If the frequency is high enough the molecule is excited or dissociated by light, absorbing one photon to the final state f. The matrix element of the transition is given by:

$$\langle f|H_{int}|i\rangle = \frac{-ie\mathbf{E}\cdot\mathbf{K}}{m\nu}D^{if} \tag{6.47}$$

where $D^{if} = \frac{1}{3}\int d\mathbf{R}d\mathbf{r}\left(U_0^f(\mathbf{R},\mathbf{r})^*\nabla_{\mathbf{R}}\cdot\mathbf{D}^i(\mathbf{R},\mathbf{r}) - U_0^i(\mathbf{R},\mathbf{r})\nabla_{\mathbf{R}}\cdot\mathbf{D}^f(\mathbf{R},\mathbf{r})^*\right)$. As usual one can neglect a field inhomogeneity (photon momentum). From Eq.(6.47) the rate of the optical absorption is proportional to the kinetic energy of a molecule, and an immobile molecule, composed from two identical particles cannot absorb, which is a trivial consequence of parity and spin conservation. The dipole matrix element for the Γ point is equal zero because all singlet states of a molecule with $\mathbf{K} = 0$ are even and all triplets are odd under the inversion transformation, $\mathbf{R},\mathbf{r} \to -\mathbf{R},-\mathbf{r}$, for a lattice with the inversion symmetry. This is similar to the dipole-forbidden singleelectron transitions in semiconductors. The matrix element, Eq.(6.47), increases with increasing K. It is now the essence of our argument that the occupancy at $K \neq 0$ is a thermodynamic function, which 'sees' the Bose condensation and, thus, allows us to measure the condensation directly via optical absorption. The Fermi-golden rule yields the optical conductivity:

$$\sigma(\nu) = \frac{4\pi e^2}{3m\nu}E_k\sum_f \left|D^{if}\right|^2\delta\left(\epsilon_f - \epsilon_i - \nu\right) \tag{6.48}$$

where $\epsilon_{i,f}$ is the energy spectrum of a single molecule, including its continuous part and

$$E_k = \sum_{\mathbf{K}}\frac{K^2}{4m}n(\mathbf{K}) \tag{6.49}$$

is the kinetic energy of all molecules, which obey the Bose-Einstein distribution with the chemical potential $\mu, n(\mathbf{K}) = \left(\exp\frac{K^2/4m-\mu}{T} - 1\right)^{-1}$. Integrating Eq.(6.48) over the frequency we obtain the conductivity sum rule for our system:

$$I(T) = \int_0^\infty d\nu\sigma(\nu) = \pi e^2 a^2 E_k \tag{6.50}$$

where

$$a^2 = \frac{4}{3m}\sum_f \frac{\left|D^{if}\right|^2}{\epsilon_f - \epsilon_i} \tag{6.51}$$

and a is a temperature independent characteristic length of the order of the molecular radius (a cubic lattice is assumed).

Thus the optical absorption in our 'toy' model shows a drastic temperature dependence, being proportional to $T^{5/2}$ below the Bose-Einstein condensation temperature $T_c = 3.3n^{2/3}/2m$ and linear well above T_c, Fig. 6.4 (n is the molecular concentration),

$$\frac{I(T)}{I\left(T_c\right)} = \frac{\tau^{5/2}}{\Gamma(5/2)\zeta(5/2)}\left(\int_0^\infty \frac{x^{3/2}dx}{\exp(x-\mu)-1}\right) \tag{6.52}$$

where $\tau = T/T_c$ is the reduced temperature and $\mu = 0$ for $\tau < 1$. In the normal state ($\tau > 1$) the following equation holds for μ:

$$\int_0^\infty \frac{x^{1/2}dx}{\exp(x-\mu)-1} = \tau^{-3/2}\Gamma(3/2)\zeta(3/2) \tag{6.53}$$

The temperature derivative of the integrated optical conductivity (or absorption), $dI(T)/dT$ is proportional to the heat capacity of an ideal Bose-gas. The condensed fraction of molecules,

composed of two identical particles, does not absorb light, if bosons are condensed at the Γ point of the lattice with the inversion symmetry.

Toy model

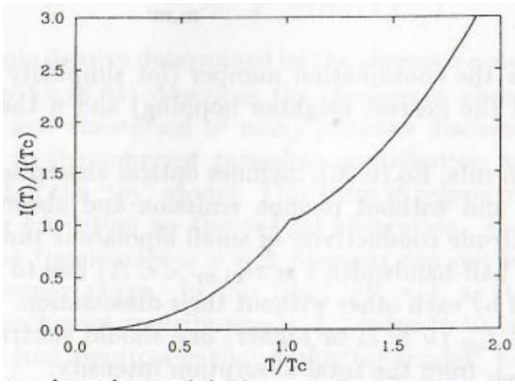

Fig.6.4. Temperature dependence of the integrated optical absorption of free bosons composed from two identical particles on a lattice.

To analyse the temperature dependence of the integrated MIR conductivity of bipolarons we apply the Kubo (1957) sum rule. The real part of the conductivity is

$$\sigma_{xx}(\nu) = \pi \sum_f |\langle 0|J_x|\, f\rangle|^2 \frac{\delta\left(\nu - E_f + E_0\right)}{E_f - E_0} \tag{6.54}$$

where $|0\rangle$ and $|f\rangle$ are the ground and excited states of the total Hamiltonian, including the electron-phonon interaction term. The current operator is

$$\mathbf{J} = ie \sum_{\mathbf{m},\mathbf{m}',s} (\mathbf{m}' - \mathbf{m})\, T\left(\mathbf{m} - \mathbf{m}'\right) c^{\dagger}_{\mathbf{m},s} c_{\mathbf{m}',s} \tag{6.55}$$

It satisfies the equation

$$\mathbf{J} = ie[H, \mathbf{X}] \tag{6.56}$$

where $\mathbf{X}$ is the sum of the position operators of the electrons:

$$\mathbf{X} = \sum_{\mathbf{m},s} \mathbf{m} c^{\dagger}_{\mathbf{m},s} c_{\mathbf{m},s} \tag{6.57}$$

Integrating over frequency Eq.(6.54) and using the identity Eq.(6.56) one obtains:

$$\int_0^{\infty} \sigma_{xx}(\nu) d\nu = \frac{ie\pi}{2} \langle 0| \left[X, J_x\right] |0\rangle \tag{6.58}$$

which yields after the direct substitution of Eq.(6.55,57)

$$I(T) = \frac{\pi e^2 a^2}{2} \left\langle - \sum_{\mathbf{m},\mathbf{m}',s} T\left(\mathbf{m} - \mathbf{m}'\right) c^{\dagger}_{\mathbf{m},s} c_{\mathbf{m}'s} \right\rangle \tag{6.59}$$

where a is the lattice constant. To calculate the kinetic energy of the strongly coupled electron-phonon system up to the second order in the transfer integral with the accuracy $\sim 1/\lambda^2$ one can apply the polaronic S and bipolaronic S_2 canonical transformations to Eq.(6.59) with the following result:

$$I(T) = \frac{\pi e^2 a^2}{2}\left(2v^{(2)}\left(n - \langle n_{\mathbf{m}} n_{\mathbf{m+a}}\rangle\right) + 2\left\langle \sum_{\mathbf{m},\mathbf{m}'} t_{\mathbf{m},\mathbf{m}'} b^{\dagger}_{\mathbf{m}} b_{\mathbf{m}'}\right\rangle\right) \tag{6.60}$$

with $v^{(2)} = zv^{(2)}_{\mathbf{m},\mathbf{m+a}}, z$ the coordination number (for simplicity we consider cubic or quadratic lattice and the nearest neighbor hopping) and n the bipolaron atomic density.

The conductivity sum rule, Eq.(6.60), includes optical absorption due to the bipolaron dissociation with and without phonon emission and absorption. It includes also the low-frequency Drude conductivity of small bipolarons tunneling in the bipolaron narrow band (the half-bandwidth $t = zt_{\mathbf{m},\mathbf{m}'} \ll \Delta$) due to their scattering by phonons, impurities and by each other without their dissociation. If one is interested only in the optical part I_{opt} ($\nu \simeq \Delta$ or higher) one should subtract the bipolaronic Drude contribution I_{Drude} from the total absorption intensity:

$$I(T) = I_{\text{opt}}(T) + I_{\text{Drude}}(T) \tag{6.61}$$

To derive the integrated bipolaronic Drude conductivity, I_{Drude} one can apply the sum rule to the bipolaronic Hamiltonian, Eq.(6.9), keeping in mind that bipolarons have charge $2e$

$$I_{\text{Drude}}(T) = \frac{4\pi e^2 a^2}{2}\left\langle \sum_{\mathbf{m},\mathbf{m}'} t_{\mathbf{m},\mathbf{m}'} b^{\dagger}_{\mathbf{m}} b_{\mathbf{m}'}\right\rangle \tag{6.62}$$

Subtracting Eq.(6.62) from Eq.(6.60) one obtains:

$$I_{opt} = \pi e^2 a^2\left[v^{(2)}\left(n - \langle n_{\mathbf{m}} n_{\mathbf{m+a}}\rangle\right) - \left\langle \sum_{\mathbf{m},\mathbf{m}'} t_{\mathbf{m},\mathbf{m}'} b^{\dagger}_{\mathbf{m}} b_{\mathbf{m}'}\right\rangle\right] \tag{6.63}$$

Let us consider a low-density regime. As we shall discuss in section 6.7 the ground state of our system is a homogeneous Bose-liquid, in which the tendency to charge order is suppressed by quantum fluctuations if $n < n_c$. The critical value of the dencity n_c above which the charge density wave develops turns out to be independent of the repulsion if the latter is strong $v + v^{(2)} \gg t$, where $t = zt(\mathbf{a})$ is the half width of the bipolaronic band. For a cubic lattice $n_c \simeq 0.08$. If the repulsion between bipolarons has a moderate value $v + v^{(2)} < 3t$ the homogeneous Bose-liquid is stable versus the charge ordering practically in the whole density region. In a homogeneous repulsive Bose-liquid the short range pair correlation function $g(r) = \langle n(0)n(r)\rangle/n^2$ is small. As example in liquid $He^4 g(r) < 0.2$ for $r < 2.5A$. The temperature dependent part of this correlator is even smaller. Thus the contribution to the conductivity sum rule, Eq.(6.63) of the term quadratic in the bipolaron density is practically temperature independent and negligible for the homogeneous strongly repulsive Bose-liquid. In the dilute limit one can also neglect the corrections to the free particle energy spectrum, which are small while the gas parameter is small. These simplifications yield:

$$I_{opt}(T) = \pi e^2 a^2\left[\left(v^{(2)} - t\right) n(T) + \int_0^{2t} \frac{\epsilon N_b(\epsilon) d\epsilon}{y^{-1}\exp(\epsilon/T) - 1}\right] \tag{6.64}$$

where $N_b(\epsilon)$ is the density of states in a narrow bipolaronic band, and

$$n(T) = \int_0^{2t} \frac{N_b(\epsilon) d\epsilon}{y^{-1}\exp(\epsilon/T) - 1} \tag{6.65}$$

is the bipolaron atomic density determined by the chemical potential $\mu, y = \exp(\mu/T)$. The first term in Eq.(6.64) describes the incoherent absorption of light accompanied by emission and absorption of many phonons discussed in section 6.4. The second term is due to the coherent tunneling contribution and is identical to that discussed above within the 'toy' model. This

term is responsible for the influence of the superconducting transition on the optical absorption. In the limit of very high diaracteristic phonon frequencies $\omega \gg \Delta$ phonons can not be emitted or absorbed in the relevant frequency range. In this limit $v^{(2)} = t$, as it was shown in section 6.1. If $v^{(2)} = t$ the incoherent contribution to I_{opt} turns to be zero, and the integrated optical absorption is just identical to that of the 'toy model', Eq.(6.52), at least in the low-temperature region, when the band energy dispersion is practically parabolic. In diis case $I_{\text{opt}}(0) = 0$. On the other hand if the phonon frequencies are comparable or leas than the bipolaron binding energy, $v^{(2)}$ does not contain the polaronic narrowing factor and is larger than t. In this more realistic case the absorption at $T = 0$ is finite and the coherent contribution is not very large, less than 10% of the total intensity.

To describe the temperature dependence of the infrared absorption in a wide temperature range in the normal state, compared with Δ one has to take into account the Inermal dissociation of the bipolaron on two small polarons. Restricting ourselves by
the quasi two-dimensional lattice with the constant density of polaronic and bipolaronic states within the polaronic and bipolaronic bands $N_p(\epsilon) = 1/2w, N_b(\epsilon) = 1/2t$ respectively, one obtains

$$\frac{I_{opt}(T)}{I_{opt}(0)} = \frac{2n(T)}{n_e} + \delta_c \frac{T^2}{T_c^2} \int_0^{2t/T} \frac{xdx}{y^{-1}\exp(x) - 1} \tag{6.66}$$

with

$$\delta_c = \frac{T_c^2}{t\,(v^{(2)} - t)\,n_e}. \tag{6.67}$$

The parameter δ_c determines the relative contribution of the coherent motion to the kinetic energy of the system and because normally $v^{(2)} \gg t > T_c/n_e$ this parameter is small, of the order of 0.1 or less. Here n_e is the electron (hole) atomic density, which is assumed to be temperature independent. Taking into account the upper polaronic band with the half bandwidth $w = tm^{**}/m^*$ one obtains the following equation for the chemical potential in the normal state ($T > T_c$):

$$\ln\left(\frac{1 - y\exp(-2t/T)}{1-y}\right) + \frac{m^*}{m^{**}} \ln\left(\frac{1 + \sqrt{y}\exp(-\Delta/2T)}{1 + \sqrt{y}\exp\left(-\Delta/2T - 2tm^{**}/m^*T\right)}\right) = \frac{tn_e}{T}. \tag{6.68}$$

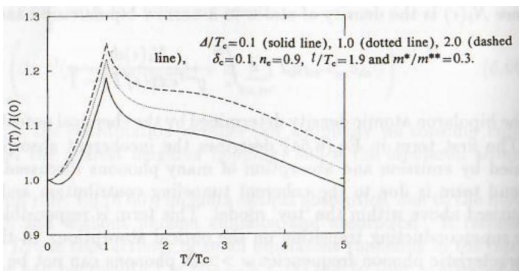

Fig.6.5. Temperature dependence of the integrated optical absorption of onsite small bipolarons

The ratio of the polaronic m^* and bipolaronic m^{**} effective masses is small in the case of onsite bipolarons. This fact enables us to neglect the polaronic contribu tion to the integrated optical absorption. The polaronic absorption is shifted to the low-frequency (Drude) region. In the superconducting phase $T < T_c$ the chemical potential is zero, so $y = 1$. The temperature dependence of the integrated intensity

$$\frac{I_{opt}(T)}{I_{opt}(0)} = 1 - \frac{m^*T}{2tm^{**}} \ln\left(\frac{1+\sqrt{y}\exp(-\Delta/2T)}{1+\sqrt{y}\exp\left(-\Delta/2T - 2tm^{**}/m^*T\right)}\right)$$
$$+\delta_c \frac{T^2}{T_c^2}\int_0^{2t/T} \frac{xdx}{y^{-1}\exp(x)-1} \tag{6.69}$$

calculated for three different values of the binding energy Δ/T_c is shown in Fig.6.5. Because the relative density of states in the polaronic band is small ($\sim m^*/m^{**}$) the temperature dependence of the on-site bipolaron concentration is weak except in the case of a very low binding energy.

It is well known that for frequencies much higher than the superconducting energy gap no change with temperature in optical absorption is expected within the BCS theory. However, a rather significant change with temperature of the MIR absorption is expected at the superconducting transition as a result of the Bose-Einstein condensation of small bipolarons in bipolaronic superconductors.

6.8.6 6.6 Pseudospin representation of the bipolaronic Hamiltonian

Bipolarons are not perfect bosons. In the subspace of pairs their commutation relations are those of Pauli matrices. Therefore, the 'pseudospin' representation of the bipolaronic Hamiltonian is convenient (Alexandrov and Ranninger (1981a)). We rewrite the bipolaronic Hamiltonian for a perfect lattice in the form

$$H_b = -\mu\sum_{\mathbf{m}} n_{\mathbf{m}} + \sum_{\mathbf{m}\neq\mathbf{m}'}\left(\frac{1}{2}\bar{v}_{\mathbf{mm}'}n_{\mathbf{m}}n_{\mathbf{m}'} - t_{\mathbf{mm}'}b^\dagger_{\mathbf{m}}b_{\mathbf{m}'}\right), \tag{6.70}$$

where the energy of a single localised bipolaron is included in the definition of the bipolaron chemical potential μ. The bipolaron operators obey the mixed commutation rules in a subspace of empty or doubly occupied sites (cells)

$$b_{\mathrm{m}}b^\dagger_{\mathrm{m}} + b^\dagger_{\mathrm{m}}b_{\mathrm{m}} = 1 \tag{6.71}$$

and

$$b_{\mathbf{m}}b^\dagger_{\mathbf{m}'} - b^\dagger_{\mathbf{m}'}b_{\mathbf{m}} = 0 \tag{6.72}$$

for $\mathbf{m}\neq\mathbf{m}'$. This makes useful the pseudospin analogy

$$b^\dagger_{\mathrm{m}} = S^x_{\mathrm{m}} - iS^y_{\mathrm{m}} \tag{6.73}$$

and

$$b^\dagger_{\mathrm{m}}b_{\mathrm{m}} = \frac{1}{2} - S^z_{\mathrm{m}} \tag{6.74}$$

with the spin(pseudo)1/2 operators $S^{x,y,z} = \frac{1}{2}\tau_{1,2,3}$. $S^z = 1/2$ corresponds to an empty cell and $S^z = -1/2$ to a cell occupied by a bipolaron. The spin operators preserve the bosonic character of bipolarons if they are on different cells and their fermionic (or hard core) internal structure. Replacing bipolarons for the spin operacore we transform the bipolaronic Hamiltonian into the familiar anisotropic Heisenberg Hamiltonian

$$H_b = \mu\sum_{\mathbf{m}} S^z_{\mathbf{m}} + \sum_{\mathbf{m}\neq\mathbf{m}'}\left(\frac{1}{2}\bar{v}_{\mathbf{mm}'}S^z_{\mathbf{m}}S^z_{\mathbf{m}'} - t_{\mathbf{mm}'}\left(S^x_{\mathbf{m}}S^x_{\mathbf{m}'} + S^y_{\mathbf{m}}S^y_{\mathbf{m}'}\right)\right) \tag{6.75}$$

with the bipolaron chemical potential playing the role of an external magnetic field. This Hamiltonian has been investigated in detail as a relevant form for magnetism and also for quantum solids like a lattice model for He^4. However, while in those cases the magnetic field is an independent thermodynamic variable, in our case it is fixed by the total 'magnetization' because the bipolaron density n is conserved

$$\frac{1}{N}\sum_{\mathrm{m}}\langle\langle S^z_{\mathrm{m}}\rangle\rangle = \frac{1}{2} - n \tag{6.76}$$

That leads to an important difference in the phase diagram and the excitation spectrum.

6.8.7 6.7 Superfluid versus charged ordered ground state

For the ground state one can apply a mean field approach introducing an average magnetic field $\mathbf{H_m}$ acting on a spin $\mathbf{m}$. In the nearest-neighbor approximation

$$\mathbf{H_m} = -\left(\mu + 2\bar{v}\left\langle S^z_{\mathbf{m}'}\right\rangle\right)\mathbf{e} + 2t\left\langle \mathbf{S}^{\perp}_{\mathbf{m}'}\right\rangle \tag{6.77}$$

where $\bar{v} = \frac{z}{2}\bar{v}_{\mathbf{mm}'}, t = zt_{\mathbf{mm}'}, \mathbf{m}' = \mathbf{m} + \mathbf{a}, \mathbf{e}$ is a unit vector in the z-direction, and $\mathbf{S}^{\perp}_{\mathbf{m}}$ is a spin component perpendicular to z. In the absence of the macroscopic current $\langle S^y\rangle = 0$ and at $T = 0$

$$\langle S^z_{\mathrm{m}}\rangle = \frac{1}{2}\cos\Theta \tag{6.78}$$

$$\langle S^x_{\mathrm{m}}\rangle = \frac{1}{2}\sin\Theta \tag{6.79}$$

where Θ is the angle between z-axis and spin. The ground state has $\langle\mathbf{S_m}\rangle$ parallel to $\mathbf{H_m}$ and we arrive at the following set of equations for Θ and μ

$$\sin\Theta = \frac{t\sin\Theta'}{\sqrt{\left(\mu + \bar{v}\cos\Theta'\right)^2 + t^2\sin^2\Theta'}} \tag{6.80}$$

$$\cos\Theta = -\frac{\mu + \bar{v}\cos\Theta'}{\sqrt{\left(\mu + \bar{v}\cos\Theta'\right)^2 + t^2\sin^2\Theta'}} \tag{6.81}$$

$$\cos\Theta + \cos\Theta' = 2(1 - 2n) \tag{6.82}$$

where Θ' is the angle for the nearest neighbors.
Two solutions to Eq.(6.80-82) are possible. The first one is a 'ferromagnetic' solution

$$\cos\Theta = \cos\Theta' = 1 - 2n \tag{6.83}$$

and

$$\mu = -(1 - 2n)(\bar{v} + t) \tag{6.84}$$

In the 'ferromagnetic' state bipolarons are distributed uniformly over the lattice willi the density per site n. The total energy of this state

$$\frac{E_f}{N} = -\frac{t}{4}\left(1 + (1 - 2n)^2\left(1 + \frac{\bar{v}}{t}\right)\right) \tag{6.85}$$

The second solution is an 'antiferromagnetic' one with two sublattices with different Θ and Θ',

$$\cos\Theta = 1 - 2n + \sqrt{1 + (1-2n)^2 - \frac{2(1-2n)\bar{v}}{\sqrt{\bar{v}^2 - t^2}}} \tag{6.86}$$

$$\cos\Theta' = 1 - 2n - \sqrt{1 + (1-2n)^2 - \frac{2(1-2n)\bar{v}}{\sqrt{\bar{v}^2 - t^2}}} \tag{6.87}$$

It exists if only $\bar{v} > t$ and the density is sufficiently high

$$n > n_c = \frac{1}{2}\left(1 - \sqrt{\frac{\bar{v} - t}{\bar{v} + t}}\right) \tag{6.88}$$

In the region of its existence the 'antiferromagnetic' state is a ground state because

$$E_a = -\frac{\bar{v}N}{4} < E_f \tag{6.89}$$

The conclusion is that the bipolarons exist at $T = 0$ in two states: as a homogeneous quantum liquid resembling He^4 or at high density as a mixture of an inhomogeneous Bose-Einstein condensate ($\sin\Theta \neq \sin\Theta' \neq 0$) and a charge density wave $\cos\Theta \neq \cos\Theta'$. At a very low density the Wigner crystallization of charged bipolarons is feasible because of their long-range Coulomb repulsion.

6.8.8 6.8 Excitation spectrum of the bipolaronic liquid

One can expect that the excitation spectrum is similar to that of a Heisenberg magnet and one-particle excitations are 'magnons'. At $T = 0$ one can write down the equation of the 'spin' motion

$$\frac{d\mathbf{S_m}}{dt} = \mathbf{H_m} \times \mathbf{S_m} \tag{6.90}$$

We allow each 'spin' besides its static component Eq. (6.78, 79) to have a small time and space dependent part

$$\delta\mathbf{S}\exp(i\mathbf{k}\cdot\mathbf{m} - i\omega t) \tag{6.91}$$

Irom Eq.(6.90) one obtains

$$-i\omega\delta S^x = -t\delta S^y \sin\Theta' \cot\Theta + (t - E_{\mathbf{k}})\,\delta S'^y \cos\Theta \tag{6.92}$$

$$-i\omega\delta S^y = t\delta S^x \sin\Theta' \cot\Theta - (t - E_{\mathbf{k}})\,\delta S'^x \cos\Theta$$
$$- t\delta S^z \sin\Theta' - \frac{\bar{v}}{t}(t - E_{\mathbf{k}})\,\delta S'^z \sin\Theta \tag{6.93}$$

$$-i\omega\delta S^z = t\delta S^y \sin\Theta' - (t - E_{\mathbf{k}})\,\delta S'^y \sin\Theta \tag{6.94}$$

Where $E_{\mathbf{k}} = \sum_{\mathbf{m}'} t_{\mathbf{m}\mathbf{m}'}\left[1 - \exp\left(i\mathbf{k}\cdot(\mathbf{m} - \mathbf{m}')\right)\right]$ is the energy dispersion of a single hipularon on a lattice. The condition of the existence of a nontrivial solution yields Hee excitation spectrum of the 'ferromagnetic' ground state $\omega = \epsilon_{\mathbf{k}}$:

$$\epsilon_{\mathbf{k}} = \sqrt{E_{\mathbf{k}}\left(t + [\bar{v} - (1-2n)^2(\bar{v} + t)]\left(1 - \frac{E_{\mathbf{k}}}{t}\right)\right)} \tag{6.95}$$

with $\mathbf{k}$ varying in the first Brillouin zone (for intersite bipolarons in a simple lattice it is half of the original one). In the long-wave limit $k \to 0$ this spectrum is sound-like like as in He^4, Fig.6.6f,

$$\epsilon_{\mathbf{k}} = sk \tag{6.96}$$

with the 'sound' velocity

$$s = 2a\sqrt{\frac{t(\bar{v}+t)n(1-n)}{z}} \tag{6.97}$$

The linear dispersion is, of course, the consequence of the nearest neighbor approximation, used here. The long-range Coulomb interaction yields the plasma gap in three dimensions and the square root dispersion in $2D$ (Chapter 7).

When the density is critical $n = n_c$, the spectrum is given by

$$\epsilon_{\mathbf{k}} = \sqrt{E_{\mathbf{k}}\,(2t - E_{\mathbf{k}})} \tag{6.98}$$

and the critical velocity $v_c = \min \frac{\epsilon_k}{k}$ is zero, Fig 6.6f.

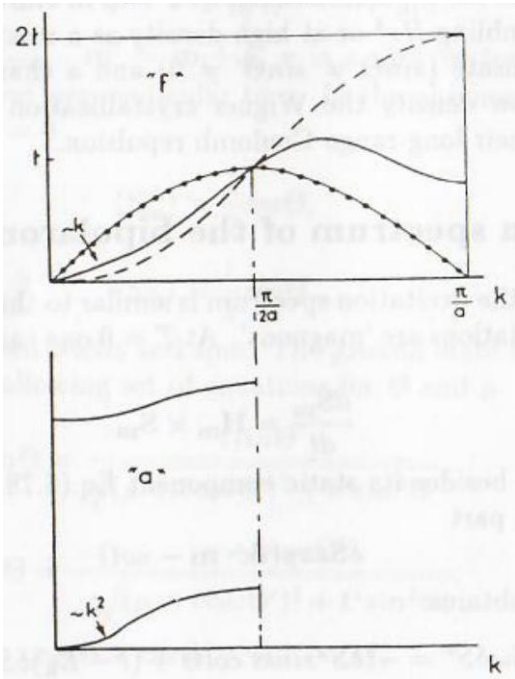

Fig.6.6. The excitation spectrum (solid lines) of $BS(f)$ and $M(a)$ ground states. Dashed line refers to a single bipolaron, dotted line to $n=n_{c}$.

Above n_c the charge density wave develops and the excitation spectrum consists of two branches

$$\epsilon^{\pm}_{\mathbf{k}} = \sqrt{\gamma^2 t^2 + E_{\mathbf{k}}\,(2t - E_{\mathbf{k}}) \pm \gamma t\sqrt{\gamma^2 t^2 + 2E_{\mathbf{k}}\,(2t - E_{\mathbf{k}})}} \tag{6,99}$$

with

$$\gamma^2 = 2\frac{\bar{v}^2 - t^2}{t^2}\left(1 + (1-2n)^2 - 2(1-2n)\frac{\bar{v}}{\sqrt{\bar{v}^2 - t^2}}\right) \tag{6.100}$$

and k varying in a new Brillouin zone, Fig.6.6a. In the long-wave limit

$$\epsilon^{+} = t\gamma\sqrt{2} \tag{6.101}$$

and

$$\epsilon^{-} \sim k^{2} \tag{6.102}$$

The gap in the spectrum is of order of $\bar{v}$ if $\bar{v} \gg t$.

6.8.9 6.9 $T - n$ phase diagram of the bipolaronic liquid

At finite temperatures thermal as well as quantum fluctuations are important. It is clear that under the condition $\bar{v} \gg t$ the off-diagonal long range order ($ODLRO$) (i.e. the Bose-Einstein condensate) disappears first with increasing temperature at $T \sim t$, followed by the disappearance of the charge ordered state ($DLRO$) at $T \sim \bar{v}$. At temperatures $\bar{v} < T < T^{**}$ an unusual metal of nondegenerate bipolarons exists with an elementary charge $2e$. As a result the $T - n$ phase diagram of a bipolaronic liquid consists of four phases. Two of them are the low-temperature phases: a bipolaronic superfluid (BS) and a mixed phase (M) with $ODLRO$, described above and two high-temperature phases, one of them is an unusual metal (N) and the other is a charge-ordered state (CO).

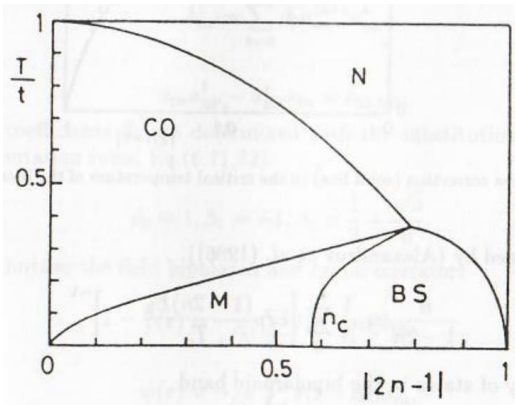

Fig.6.7. Mean-field $T - n$ phase diagram of bipolarons, $\bar{v} / t=2$.

In an extreme limit of a very high phonon frequency $\omega \gg \Delta$ the bipolaron liandwidth t and a short-range component of the repulsion $v^{(2)}$ are of the second under in the polaron bandwidth w for on-site bipolarons. In this limit the on-site hipolaron Hamiltonian can be mapped on the negative U Hubbard Hamiltonian if the long-range Coulomb interaction is screened. In a more realistic case of long-range butica and (or) $\omega < \Delta$ no such mapping is possible. Nevertheless in a qualitative analysis of the phase diagram we can use the finite temperature mean-field (MFA) anil random phase approximations (RPA), developed for the negative U Hubbard IInmiltonian by Robaszkiewicz et al (1981).

The MFA phase diagram is shown in Fig.6.7 for $\bar{v} = 2t$. Quantum fluctuations ('magnons'), which can be taken into account with the RPA equation of motion for the 'spin-spin' correlation function lead to a significant modification of the critical density n_c. Quantum fluctuations extend the region of the existence of the BS phase, which turns out to be the ground state ($T = 0$) even in the limit $\bar{v}/t \to \infty$ if the density is low,

$$n < 0.078 \tag{6.103}$$

for a simple cubic lattice.

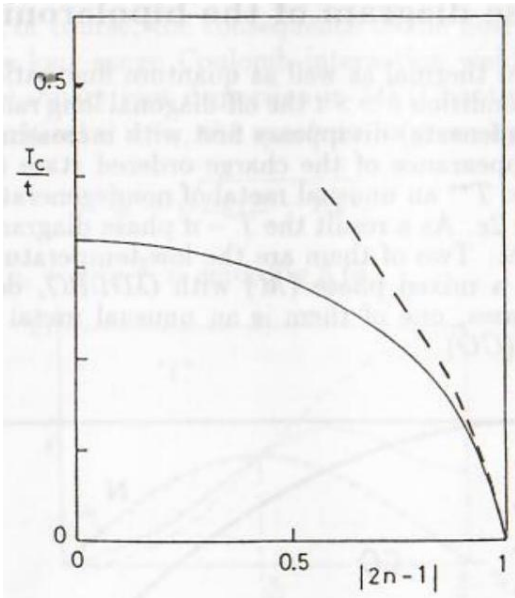

Fig.6.8. Hard-core correction (solid line) to the critical temperature of the ideal Bose gas (dashed line).
T_c is determined by (Alexandrov et al. (1986))

$$\frac{n}{1-2n} = \frac{1}{N}\sum_{\mathbf{k}}\left[\exp\frac{(1-2n)E_{\mathbf{k}}}{T_c} - 1\right]^{-1} \tag{6.104}$$

With the density of states in the bipolaronic band

$$N_b(E) = \frac{1}{N}\sum_{\mathbf{k}}\delta\left(E - E_{\mathbf{k}}\right)$$

this equation takes the form of the condition for the Bose-Einstein condensation of the ideal Bose gas if $n \ll 1$,

$$n = \int dE \frac{N_b(E)}{\exp\left(E/T_c\right) - 1} \tag{6.105}$$

At higher density a hard core correction appears, Fig.6.8,

$$T_c \simeq \frac{3.31 n^{2/3}}{m^{**}a^2}\left(1 - 0.54 n^{2/3}\right) \tag{6.100}$$

T_c is independent of the dynamical repulsion of bipolarons $\bar{v}$. This is an artifact of the random phase and nearest neighbor approximations.Taking into account the next neighbor interaction Kubo and Takada (1983) found two new phases of bipolaronic liquid: an incommensurate CO phase and an incommensurate M phase. A detailed study of the charge ordered bipolaronic states is given by Aubry (1995) in the adiabatic limit $\omega = 0$.

We believe, however, that in real solids the long range Coulomb repulsion of bipolarons is the only relevant term for low-energy kinetics and thermodynamics. That favors the homogeneous charged Bose-liquid for all realistic values of the Coulomb interaction and densities. A mapping of the bipolaronic Hamiltonian on a charged Bose gas is useful in this case.

6.8.10 6.10 Mapping on a charged Bose gas

One can transform the bipolaronic Hamiltonian to a representation containing only Bose operators $a_{\mathbf{m}}, a^{\dagger}_{\mathbf{m}}$

$$b_{\mathbf{m}} = \sum_{k=0}^{\infty} \beta_k a_{\mathbf{m}}^{\dagger k} a_{\mathbf{m}}^{k+1} \tag{6.107}$$

$$b_{\mathbf{m}}^{\dagger} = \sum_{k=0}^{\infty} \beta_k a_{\mathbf{m}}^{\dagger k+1} a_{\mathbf{m}}^{k} \tag{6.108}$$

with

$$a_{\mathbf{m}} a_{\mathbf{m}'}^{\dagger} - a_{\mathbf{m}'}^{\dagger} a_{\mathbf{m}} = \delta_{\mathbf{m},\mathbf{m}'} \tag{6.109}$$

The first few coefficients β_k are determined with the substitution of Eq.(6.107,108) into the commutation rules, Eq.(6.71,72)

$$\beta_0 = 1, \beta_1 = -1, \beta_2 = \frac{1}{2} + \frac{\sqrt{3}}{6} \tag{6.110}$$

We introduce further the field bipolaron and boson operators

$$\phi(\mathbf{r}) = \frac{1}{\sqrt{N}} \sum_{\mathbf{m}} \delta(\mathbf{r} - \mathbf{m}) b_{\mathbf{m}} \tag{6.111}$$

$$\psi(\mathbf{r}) = \frac{1}{\sqrt{N}} \sum_{\mathbf{m}} \delta(\mathbf{r} - \mathbf{m}) a_{\mathbf{m}} \tag{6.112}$$

where $\delta(\mathrm{r} - \mathrm{m})$ is the eigenfunction of the coordinate operator. The transformation for the field operators takes the form

$$\phi(\mathbf{r}) = \left(1 - \frac{\psi^{\dagger}(\mathbf{r})\psi(\mathbf{r})}{N} + \frac{(1/2 + \sqrt{3}/6)\psi^{\dagger}(\mathbf{r})\psi(\mathbf{r})\psi(\mathbf{r})}{N^2} + \ldots\right) \psi(\mathbf{r}) \tag{6.113}$$

The bipolaronic Hamiltonian is now

$$H_b = -\int d\mathbf{r} d\mathbf{r}' \psi^{\dagger}(\mathbf{r}) \left[t\left(\mathbf{r} - \mathbf{r}'\right) + \mu\right] \psi\left(\mathbf{r}'\right) + H_{int} \tag{6.114}$$

with

$$H_{int} = H_l + H_s \tag{6.115}$$

where H_l is the dynamic part of the interaction,

$$H_l = \frac{1}{2} \int d\mathbf{r} d\mathbf{r}' \bar{v}\left(\mathbf{r} - \mathbf{r}'\right) \psi^{\dagger}(\mathbf{r}) \psi^{\dagger}\left(\mathbf{r}'\right) \psi(\mathbf{r}) \psi\left(\mathbf{r}'\right) \tag{6.116}$$

H_s describes the kinematic hard-core effect,

$$\begin{aligned} H_s = \frac{2}{N} t\left(\mathbf{r} - \mathbf{r}'\right) \big(&\psi^{\dagger}(\mathbf{r}) \psi^{\dagger}\left(\mathbf{r}'\right) \psi\left(\mathbf{r}'\right) \psi\left(\mathbf{r}'\right) \\ &+ \psi^{\dagger}(\mathbf{r}) \psi^{\dagger}(\mathbf{r}) \psi(\mathbf{r}) \psi\left(\mathbf{r}'\right)\big) + H^{(3)} \end{aligned} \tag{6.117}$$

Here

$$t\left(\mathbf{r}-\mathbf{r}'\right)=\sum_{\mathbf{k}}\left(t-E_{\mathbf{k}}\right)e^{i\mathbf{k}\cdot\left(\mathbf{r}-\mathbf{r}'\right)} \tag{6.118}$$

$$\bar{v}\left(\mathbf{r}-\mathbf{r}'\right)=\frac{1}{N}\sum_{\mathbf{k}}\bar{v}_{\mathbf{k}}e^{i\mathbf{k}\cdot\left(\mathbf{r}-\mathbf{r}'\right)} \tag{6.119}$$

and $\bar{v}_{\mathbf{k}}=\sum_{\mathbf{m}'\neq\mathbf{m}}\bar{v}_{\mathbf{m},\mathbf{m}'}\exp(i\mathbf{k}\cdot\mathbf{m})$ is the Fourier component of the bipolaron repulsion. The term $H^{(3)}$ contains powers of the field operators higher than four. The essential physics of bipolarons is controlled by the two-particle interaction, which includes a short-range kinematic part $t\left(\mathbf{r}-\mathbf{r}'\right)$ as well. Because $\bar{v}$ contains also the short range part $v^{(2)}$ this kinematic contribution can be included in the definition of $\bar{v}$. As a result H_b is the Hamiltonian of the interacting charged bosons tunneling in a band.

6.8.11 6.11 Bipolaron electrodynamics

To describe electrodynamics of bipolarons one can take into account the vector potential $\mathbf{A}(\mathbf{r})$ of the external field with the Peierls substitution (Peierls (1933))

$$t_{\mathbf{m},\mathbf{m}'}\rightarrow t_{\mathbf{m},\mathbf{m}'}e^{-i2e\mathbf{A}(\mathbf{m})\cdot(\mathbf{m}-\mathbf{m}')} \tag{6.120}$$

which is a fair approximation if the magnetic field is weak compared with the atomic field

$$eHa^2\ll 1 \tag{6.121}$$

Here $\mathbf{A}(r)$ is a vector potential, which can be also time dependent. This yields in real space

$$t\left(\mathbf{r},\mathbf{r}'\right)=\sum_{\mathbf{k}}\left(t-E_{\mathbf{k}+2e\mathbf{A}}\right)e^{i\mathbf{k}\cdot\left(\mathbf{r}-\mathbf{r}'\right)} \tag{6.122}$$

If the condition Eq.(6.121) is satisfied one can expand $E_{\mathbf{k}}$ in the vicinity of $\mathbf{k}=0$ to obtain

$$t\left(\mathbf{r},\mathbf{r}'\right)\simeq\left(t+\frac{\left[\nabla-2ie\mathbf{A}(\mathbf{r})\right]^2}{2m^{**}}\right)\delta\left(\mathbf{r}-\mathbf{r}'\right) \tag{6,121}$$

where

$$\frac{1}{m^{**}}=\frac{d^2E_{\mathbf{k}}}{d\mathbf{k}^2}$$

at $k\rightarrow 0$. As a result the Hamiltonian of fermions strongly coupled with any bosonic field (i.e. phonons) reduces to

$$\begin{aligned}H_b=&-\int d\mathbf{r}\psi^{\dagger}(\mathbf{r})\left[\frac{(\nabla-2ie\mathbf{A}(\mathbf{r}))^2}{2m^{**}}+\mu\right]\psi(\mathbf{r})\\&+\frac{1}{2}\int d\mathbf{r}d\mathbf{r}'\bar{v}\left(\mathbf{r}-\mathbf{r}'\right)\psi^{\dagger}(\mathbf{r})\psi^{\dagger}\left(\mathbf{r}'\right)\psi(\mathbf{r})\psi\left(\mathbf{r}'\right)\end{aligned} \tag{6.124}$$

if three-body and higher order interactions are neglected. The hard core effect is taken into account by the definition of the repulsion $\bar{v}$ as described above, and the constant t in Eq.(6.122) is included in the chemical potential μ. At large distances the bipolaron-bipolaron interaction is the Coulomb one ($\bar{v}\sim 1/\epsilon r$ in the atomic solids or $\bar{v}\sim 1/\epsilon_0 r$ in the ionic compounds).

We have shown in this Chapter that the Fermi-liquid behavior is destroyed by the strong electron-phonon interaction. The ground state of carriers strongly coupled with phonons in a

doped band and Mott insulators is the bipolaronic charged Boseliquid. We proposed bipolarons as a key element for the understanding of the high- T_c phenomenon in metal oxides and doped fullerenes (Alexandrov and Mott (1994)). The key point for the bipolaronic mechanism of high- T_c superconductivity is the possibility of the coherent tunneling of (bi)polarons with a reasonable value of the effective mass. Several authors assert that their bandwidth should not exceed $10^{-4}-10^{-5}$eV, and then the maximal T_c attainable with small bipolarons should be a few K or less. However, we believe this is an erroneous conclusion based on an incorrect estimate of the bipolaron mass. For the intermediate value of the coupling constant $\lambda \simeq 1$ and the high-frequency phonons $\omega \simeq 0.1$eV. the polaron binding energy is large ($E_p = 0.2-0.6$eV) and the value of the bare electronic bandwidth compatible with the small polaron formation is large enough being of the order of 1.0 eV. In this case the estimate of the small polaron bandwidth yields the value of w as large as a few hundred K and the same for T_c. Taking into account the phonon frequency dispersion in the the perovskite crystal structure one can find the effective mass of intersite small bipolarons of the order of $10m_e$ as discussed in section 6.2. Of course, a short-range intersite Coulomb repulsion should be below $2E_p$ to ensure the formation of mobile intersite bipolarons. That is quite feasible because the highfrequency dielectric constant in metal oxides is large, normally $\epsilon \sim 5$ and larger. The low-frequency dielectric constant is extremely large in oxides. As a result, optical phonons perfectly screen the Coulomb repulsion. Then the deformation potential as well as molecular vibrations give rise into a net short-range attraction between small polarons as discussed in Chapter 2.

At low temperatures $T < \omega/2, T^{**}$ and low frequencies of an external field $\nu \ll \omega$ the internal structure of the bipolaron including its phonon cloud can not be observed. Therefore their low-temperature and low-frequency kinetics is that of charged bosons. An we have discussed (Alexandrov and Mott (1994)) the internal symmetry of the hipolaron should be distinguished from that of the macroscopic off-diagonal order parameter ψ_0(r) (see below). While the internal symmetry depends on the short-range allraction between two polarons and the unit cell geometry, the 'external' symmetry of 1/0 is determined by the long-range repulsion between bipolarons. Also the excitaIon spectrum of the superfluid bipolaronic liquid depends on the bipolaron-bipolaron mpulsion rather than on the internal bipolaron structure. Therefore, as an example, (lie nymmetry observed by the Josephson tunneling may be different from that observed with another technique. Low-energy physics of bipolarons can be studied within a simplified charged Bose-gas model. The Coulomb repulsion between bipolarons is significantly reduced in oxides by the ionic screening and the dimensionlees interaction r_s is not large even for heavy particles.

6.9 7 Charged Bose gas

A charged Coulomb Bose-gas (CBG) is a fundamental reference system in manyparticle physics with a superfluid phase transition. It has been studied by several authors and recently became of particular interest motivated by the bipolaron theory of high temperature superconductivity. As we have discussed in Chapter 6 the long-wave excitations of the bipolaronic liquid are those of charged bosons with the Coulomb repulsion between them. Schafroth (1955) demonstrated that an ideal gas of charged bosons exhibits the Meissner-Ochsenfeld effect (expulsion of a magnetic field) below the ideal Bose-gas condensation temperature. Later on the one-particle excitation spectrum at $T = 0$ was calculated by Foldy (1961), who worked at zero temperature using the Bogoliubov (1947) approach. The Bogoliubov method leads to the result that the ground state of the system has a negative correlation energy, whose magnitude increases with the density of bosons. Perhaps more interesting is the fact that the elementary excitations of the system have, for small momenta, energies characteristic of plasma oscillations which pass over smoothly for large momenta to the energies characteristic of single particle ex-

citations. Further investigations have been carried out at or near T_c, the transition temperature for the gas. These works has been concerned with the critical exponents (Bishop (1974)) and the change in the transition temperature from that of the ideal gas (Bishop (1974), Fetter (1971)). The RPA dielectric response function and screening in CBG have been studied in the high-density limit (Hore and Frankel (1975, 1976), including a low-dimensional ($2D$) CBG (Hines and Frankel (1979), Gold (1991)). In this Chapter we verify superfluid properties of charged bosons with the Bogoliubov-de Genes type equations derived for CBG by Alexandrov and Beere (1995) and discuss superconducting as well as normal state CBG kinetics.

6.9.1 7.1 Bogoliubov-de Gennes equations for CBG

The superfluid properties of charged bosons as well as their excitation spectrum and the response function can be studied by the use of the Bogoliubov-de Genes (BdG) type equations, fully taking into account the interaction of quasiparticles with the condensate. The Hamiltonian for a system of charged bosons on an oppositely charged liar ckround (to ensure charge neutrality) in an external field is given by

$$\begin{aligned} H = & \int d\mathbf{r}\psi^{\dagger}(\mathbf{r})\left[-\frac{(\nabla - i2e\mathbf{A})^2}{2m^{**}} + \mu\right]\psi(\mathbf{r}) \\ & + \frac{1}{2}\int d\mathbf{r}\int d\mathbf{r}' V\left(\mathbf{r}-\mathbf{r}'\right)\psi^{\dagger}(\mathbf{r})\psi(\mathbf{r})\psi^{\dagger}\left(\mathbf{r}'\right)\psi\left(\mathbf{r}'\right) \end{aligned} \tag{7.1}$$

For $3D$ charged bosons the Fourier component of the Coulomb potential $V(\mathbf{r})$ is $V(\mathbf{k}) = 16\pi e^2/k^2\epsilon_0$ with ϵ_0 a dielectric constant of the background and bosonic charge $2e$. For $2D$ system with a three dimensional interaction $V(\mathbf{k}) = 8\pi e^2/k\epsilon_0$. To respect electroneutrality one takes $V(\mathbf{k} \equiv 0) = 0$.

The equation of motion for the field operator, ψ, is derived using this Hamiltonian,

$$\begin{aligned} i\frac{\partial}{\partial t}\psi(\mathbf{r},t) = [H,\psi(\mathbf{r},t)] = & \left[-\frac{(\nabla - i2e\mathbf{A})^2}{2m^{**}} + \mu\right]\psi(\mathbf{r},t) \\ & + \int d\mathbf{r}' V\left(\mathbf{r}-\mathbf{r}'\right)\psi^{\dagger}\left(\mathbf{r}',t\right)\psi\left(\mathbf{r}',t\right)\psi(\mathbf{r},t) \end{aligned} \tag{7.2}$$

If the interaction is weak one can expect that the occupation numbers of one-particle states are not very much different from those in the ideal Bose-gas. In particular the state with zero momentum $k = 0$ remains to be macroscopically occupied and the corresponding Fourier component of the field operator $\psi(\mathbf{r})$ has anomalously large matrix element between the ground states of the system containing $N + 1$ and N bosons. It is convenient to consider a grand canonical ansamble, introducing a chemical potential μ. In this case the quantum state is a superposition of states $|N\rangle$ with slightly different total numbers of bosons. The weight of each state is a smooth function of N which is practically constant near the average number $\bar{N}$ on the scale $\pm\sqrt{N}$. Because ψ changes the number of particles only by one its diagonal matrix element coincides with the off-diagonal, calculated for the states with fixed $N = N + 1$ and $N = \bar{N}$. Following Bogoliubov (1947) one can separate the large diagonal matrix element ψ_0 from ψ by treating the rest ψ as a small fluctuation

$$\psi(\mathbf{r},t) = \psi_0(\mathbf{r},t) + \tilde{\psi}(\mathbf{r},t). \tag{7.3}$$

The anomalous average $\psi_0(\mathrm{r},t) = \langle\psi(\mathrm{r},t)\rangle$ is equal to $\sqrt{n_0}$ in a homogeneous system, where n_0 is the condensate density.

Substituting the Bogoliubov displacement transformation, Eq.(7.3) into the equa tion of motion and collecting c - number terms of ψ_0, and supracondensate boson operators $\tilde{\psi}$ we obtain a set of the BdG-type equations. The macroscopic condensale wave function, which plays the role of the order parameter obeys to the following equation

$$\begin{aligned} i\frac{\partial}{\partial t}\psi_0(\mathbf{r},t) &= \left[-\frac{(\nabla - i2e\mathbf{A})^2}{2m^{**}} + \mu\right]\psi_0(\mathbf{r},t) \\ &+ \int d\mathbf{r}' V(\mathbf{r}-\mathbf{r}')\, n(\mathbf{r}',t)\,\psi_0(\mathbf{r},t) + \int d\mathbf{r}' V(\mathbf{r}-\mathbf{r}') \\ &\times \left[\left\langle \tilde{\psi}^\dagger(\mathbf{r}',t)\,\tilde{\psi}(\mathbf{r},t)\right\rangle \psi_0(\mathbf{r}',t) + \left\langle \tilde{\psi}(\mathbf{r}',\mathbf{t})\,\tilde{\psi}(\mathbf{r},\mathbf{t})\right\rangle \psi_0^*(\mathbf{r}',\mathbf{t})\right] \end{aligned} \tag{7.4}$$

Taking explicitly into account the interaction of supracondensate bosons with the con densate and applying the Hartree approximation for the interaction between super condensate particles we obtain

$$\begin{aligned} i\frac{\partial}{\partial t}\tilde{\psi}(\mathbf{r},t) &= \left[-\frac{(\nabla - i2e\mathbf{A})^2}{2m^{**}} + \mu\right]\tilde{\psi}(\mathbf{r},t) + \int d\mathbf{r}' V(\mathbf{r}-\mathbf{r}')\, n(\mathbf{r},t)\tilde{\psi}(\mathbf{r},t) \\ &+ \int d\mathbf{r}' V(\mathbf{r}-\mathbf{r}')\left[\psi_0^*(\mathbf{r}',t')\,\psi_0(\mathbf{r},t) + \left\langle \tilde{\psi}^\dagger(\mathbf{r}',t)\,\tilde{\psi}(\mathbf{r},t)\right\rangle\right]\tilde{\psi}(\mathbf{r}',t) \\ &+ \int d\mathbf{r}' V(\mathbf{r}-\mathbf{r}')\left[\psi_0(\mathbf{r}',t)\,\psi_0(\mathbf{r},t) + \left\langle \tilde{\psi}(\mathbf{r}',t)\,\tilde{\psi}(\mathbf{r},t)\right\rangle\right]\tilde{\psi}^\dagger(\mathbf{r}',t) \\ &+ \int d\mathbf{r}' V(\mathbf{r}-\mathbf{r}')\left[\tilde{\psi}^\dagger(\mathbf{r}',t)\,\tilde{\psi}(\mathbf{r}',t) - \left\langle \tilde{\psi}^\dagger(\mathbf{r}',t)\,\tilde{\psi}(\mathbf{r}',t)\right\rangle\right]\psi_0(\mathbf{r},t) \\ &+ \int d\mathbf{r}' V(\mathbf{r}-\mathbf{r}')\left[\tilde{\psi}^\dagger(\mathbf{r}',t)\,\tilde{\psi}(\mathbf{r},t) - \left\langle \tilde{\psi}^\dagger(\mathbf{r}',t)\,\tilde{\psi}(\mathbf{r},t)\right\rangle\right]\psi_0(\mathbf{r}',t) \\ &+ \int d\mathbf{r}' V(\mathbf{r}-\mathbf{r}')\left[\tilde{\psi}(\mathbf{r}',t)\,\tilde{\psi}(\mathbf{r},t) - \left\langle \tilde{\psi}(\mathbf{r}',t)\,\tilde{\psi}(\mathbf{r},t)\right\rangle\right]\psi_0^*(\mathbf{r}',t) \end{aligned} \tag{7.5}$$

Here

$$n(\mathbf{r},t) = |\psi_0(\mathbf{r},t)|^2 + \left\langle \tilde{\psi}^\dagger(\mathbf{r},t)\tilde{\psi}(\mathbf{r},t)\right\rangle \tag{7.6}$$

is the boson density.
In the high density limit $r_s \ll 1$ for the temperature close to zero the number of bosons $\tilde{n}$ pushed up from the condensate by the repulsion is small. Therefore the contribution of terms nonlinear in $\tilde{\psi}$ is negligible. Applying a linear Bogoliubov transformation for $\tilde{\psi}$

$$\tilde{\psi}(\mathbf{r},t) = \sum_n u_n(\mathbf{r},t)\alpha_n + v_n^*(\mathbf{r},t)\alpha_n^\dagger \tag{7.7}$$

where α_n and $\alpha_n^\dagger$ are bosonic quasiparticle operators for the one-particle quantum state n, and omitting nonlinear terms we obtain two coupled Schrödinger equations for the wave functions $u(\mathbf{r},t)$ and $v(\mathbf{r},t)$

$$\begin{aligned} i\frac{\partial}{\partial t}u(\mathbf{r},t) &= \left[-\frac{(\nabla - i2e\mathbf{A})^2}{2m^{**}} + \mu\right]u(\mathbf{r},t) \\ &+ \int d\mathbf{r}' V(\mathbf{r}-\mathbf{r}')\left[|\psi_0(\mathbf{r}',t)|^2 u(\mathbf{r},t) + \psi_0^*(\mathbf{r}',t)\,\psi_0(\mathbf{r},t)u(\mathbf{r}',t)\right] \\ &+ \int d\mathbf{r}' V(\mathbf{r}-\mathbf{r}')\,\psi_0(\mathbf{r}',t)\,\psi_0(\mathbf{r},t)v(\mathbf{r}',t) \end{aligned} \tag{7.8}$$

and

$$
\begin{aligned}
-i\frac{\partial}{\partial t}v(\mathbf{r},t) = & \left[-\frac{(\nabla+i2e\mathbf{A})^2}{2m^{**}}+\mu\right]v(\mathbf{r},t) \\
& + \int d\mathbf{r}'V\left(\mathbf{r}-\mathbf{r}'\right)\left[\left|\psi_0\left(\mathbf{r}',t\right)\right|^2 v(\mathbf{r},t)+\psi_0\left(\mathbf{r}',t\right)\psi_0^*(\mathbf{r},t)\right]v\left(\mathbf{r}',t\right) \\
& + \int d\mathbf{r}'V\left(\mathbf{r}-\mathbf{r}'\right)\psi_0^*\left(\mathbf{r}',t\right)\psi_0^*(\mathbf{r},t)u\left(\mathbf{r}',t\right)
\end{aligned} \tag{7.9}
$$

There is also the sum rule,

$$
\sum_n \left[u_n(\mathbf{r},t)u_n^*\left(\mathbf{r}',t\right)-v_n(\mathbf{r},t)v_n^*\left(\mathbf{r}',t\right)\right]=\delta\left(\mathbf{r}-\mathbf{r}'\right), \tag{7.10}
$$

which retain the Bose commutation relations for all operators. The set of BdG equadions (7.4,8-10) plays the same role as the time-dependent Ginzburg-Landau equations for the BCS superconductors.

6.9.2 7.2 Excitation spectrum and ground state energy of CBG

For the homogeneous case and $\mathbf{A}=0$ the excitation wave functions are plane waves

$$
u_{\mathbf{k}}(\mathbf{r},t)=u_{\mathbf{k}}e^{i\mathbf{k}\cdot\mathbf{r}-i\epsilon_{\mathbf{k}}t} \tag{7.11}
$$

and

$$
v_{\mathbf{k}}(\mathbf{r},t)=v_{\mathbf{k}}e^{i\mathbf{k}\cdot\mathbf{r}-i\epsilon_{\mathbf{k}}t} \tag{7.12}
$$

The condensate wave function is (r,t) independent, $\psi_0=\sqrt{n_0}$, so the solution to Eq.(7.4) is

$$
\mu=0 \tag{7.13}
$$

Substitution of Eqs.(7.11-13) into the BdG set yields

$$
\epsilon_{\mathbf{k}}u_{\mathbf{k}}=\frac{k^2}{2m^{**}}u_{\mathbf{k}}+n_0V(\mathbf{k})\left[u_{\mathbf{k}}+v_{\mathbf{k}}\right] \tag{7.14}
$$

$$
-\epsilon_{\mathbf{k}}v_{\mathbf{k}}=\frac{k^2}{2m^{**}}v_{\mathbf{k}}+n_0V(\mathbf{k})\left[u_{\mathbf{k}}+v_{\mathbf{k}}\right] \tag{7.15}
$$

and from Eq.(7.10)

$$
\left|u_{\mathbf{k}}\right|^2-\left|v_{\mathbf{k}}\right|^2=1. \tag{7.16}
$$

As a result we find

$$
u_{\mathbf{k}}^2=\frac{1}{2}\left(1+\frac{\xi_{\mathbf{k}}}{\epsilon_{\mathbf{k}}}\right) \tag{7.17}
$$

$$
v_{\mathbf{k}}^2=-\frac{1}{2}\left(1-\frac{\xi_{\mathbf{k}}}{\epsilon_{\mathbf{k}}}\right) \tag{7.18}
$$

$$
u_{\mathbf{k}}v_{\mathbf{k}}=-\frac{V(\mathbf{k})n_0}{2\epsilon_{\mathbf{k}}} \tag{7.19}
$$

where $\xi_{\mathbf{k}} = k^2/2m^{**} + V(\mathbf{k})n_0$. The elementary excitation energy is

$$\epsilon_{\mathbf{k}} = \sqrt{\frac{k^4}{4\left(m^{**}\right)^2} + \frac{k^2 V(\mathbf{k})n_0}{m^{**}}}. \tag{7,20}$$

With the Fourier component of the Coulomb interaction this makes (Foldy (1961))

$$\epsilon_{\mathbf{k}} = \sqrt{\frac{k^4}{4\left(m^{**}\right)^2} + \omega_{p0}^2} \tag{7,21}$$

with a gap $\omega_{p0} = \sqrt{16\pi e^2 n_0/\epsilon_0 m^{**}}$, which is the classical plasma frequency for 4 plasma of density n_0, Fig.7.1a. In a two-dimensional system $V(\mathbf{k}) = 8\pi e^2/c_0 k$ and the Bogoliubov spectrum is gapless, Fig.7.1b,

$$\epsilon_{\mathbf{k}} = E_s\sqrt{k/q_s + k^4/q_s^4} \tag{7,\mu}$$

with $E_s = q_s^2/2m^{**}, q_s = \left(32\pi e^2 n_0/\epsilon_0\right)^{1/3}$ a two-dimensional screening wave-number and n_0 is the $2D$ density. The density of bosons pushed up from the condensate by the Coulomb repulsion at $T = 0$ is

$$\tilde{n} = \left\langle \tilde{\psi}^\dagger(\mathbf{r})\tilde{\psi}(\mathbf{r})\right\rangle = \sum_{\mathbf{k}} v_{\mathbf{k}}^2 \tag{7.23}$$

which is small compared with the total density n,

$$\frac{\tilde{n}}{n} \simeq 0.2 r_s^{3/4} \sim 1 \quad r_s = \frac{s}{a_0}$$

if the latter is high, so $r_s \ll 1$.

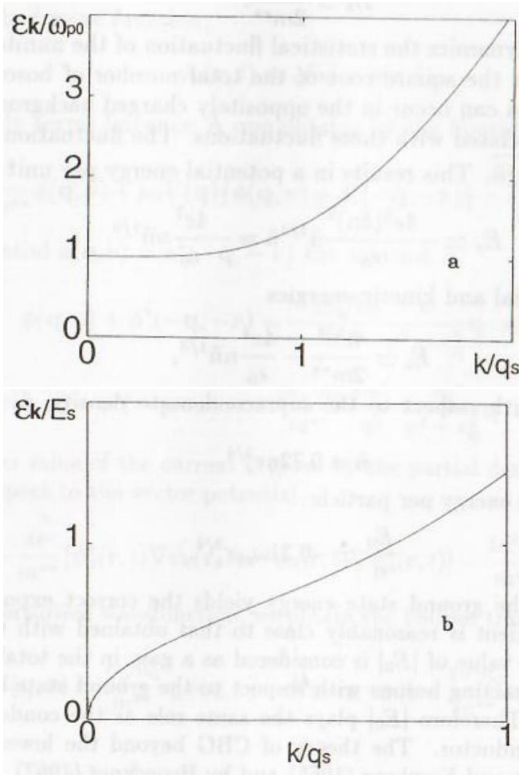

Fig.7.1. Excitation spectrum of a $3D(a)$ and $2D(b)$ charged Bose gas at $T = 0$.

The ground state $|0\rangle$ is a vacuum for the elementary excitations, $\alpha_{\mathbf{k}}|0\rangle = 0$. The ground state energy E_0 is obtained by substitution of Eq.(7.7) into the Hamiltonian and neglecting higher order terms than quadratic in α,

$$E_0 \equiv \langle 0|H|0\rangle = \frac{1}{2}\sum_{\mathbf{k}} (\epsilon_{\mathbf{k}} - \xi_{\mathbf{k}}) \tag{7.25}$$

This can be written per particle in terms of the plasma frequency ω_{p0}

$$\frac{E_0}{n} = \frac{2^{3/2}}{3^{1/4}\pi}\omega_{p0} r_s^{3/4} \int_0^\infty dk k^2 \left[\sqrt{k^4+1} - k^2 - 1/2k^2\right] \simeq -0.23\omega_{p0} r_s^{3/4} \tag{7.26}$$

The negative value of the ground state energy is due to the oppositely charged background. That can be shown by a simple estimation. The ground state energy is estimated as the zero-point energy of supracondensate bosons plus the potential energy arising from statistical fluctuations of their density. The zero-point energy is calculated as the kinetic energy of a single supracondensate boson confined to the average volume occupied of each of them ($\sim 1/\tilde{n}$). This produces an energy per unit volume of

$$E_k \simeq \frac{\tilde{n}^{5/3}}{2m^{**}} \tag{7.27}$$

From classical thermodynamics the statistical fluctuation of the number of bosons in a given volume goes as the square root of the total number of bosons within that volume. No fluctuations can occur in the oppositely charged background, producing a potential energy associated with these fluctuations. The fluctuation in the number of particles is $\delta n = \sqrt{n/\tilde{n}}$. This results in a potential energy per unit volume of

$$E_p \simeq -\frac{4e^2(\delta n)^2}{\epsilon_0}\tilde{n}^{1/3}\tilde{n} = -\frac{4e^2}{\epsilon_0} n\tilde{n}^{1/3} \tag{7.28}$$

The sum of the potential and kinetic energies

$$E_0 \simeq \frac{\tilde{n}^{5/3}}{2m^{**}} - \frac{4e^2}{\epsilon_0} n\tilde{n}^{1/3} \tag{7.29}$$

is then minimised with respect to the supracondensate density, $\tilde{n}$, producing the solution

$$\tilde{n} = 0.72 n r_s^{3/4} \tag{7.30}$$

and the ground state energy per particle

$$\frac{E_0}{n} \simeq -0.31\omega_{p0} r_s^{3/4} \tag{7.31}$$

This estimation of the ground state energy yields the correct exponent of r_s and the numerical coefficient is reasonably close to that obtained with the Bogoliubov transformation. The value of $|E_0|$ is considered as a gain in the total energy due to condensation of interacting bosons with respect to the ground state energy ($= 0$) of an ideal Bose gas. Therefore $|E_0|$ plays the same role as the condensation energy of the BCS superconductor. The theory of CBG beyond the lowest order in $r_0^{3/4}$ was discussed by Lee and Feenberg (1965) and by Brueckner (1967). They obtained the next order correction to the ground state energy. Woo and Ma (1967) found numerically the correction to the Bogoliubov excitation spectrum.

6.9.3 7.3 Linear-response function

The linear response function is defined as

$$J_m(\mathbf{q},\omega) = K^{mn}(\mathbf{q},\omega) a_n(\mathbf{q},\omega) \tag{7.32}$$

where $\mathbf{J}(\mathbf{q},\omega)$ and $\mathbf{a}(\mathbf{q},\omega)$ are the Fourier transforms of the current and vector potential, respectively. It is important that the vector potential $\mathbf{A}$ is defined as an external vector potential. The internal Coulomb field is explicitly taken into account by the Bogoliubov transformation. The use of the effective internal field $\mathbf{A}$ rather than the external one results in reducible diagrams for the polarisation, and thus in the double counting of the Coulomb interaction. To calculate the response to the leading order of the condensate density, n_0, we need only consider equation Eq.(7.4) with $\hat{\psi} = \mu = 0$

$$i\frac{\partial}{\partial t}\psi_0(\mathbf{r},t) = -\frac{(\nabla - i2e\mathbf{A})^2}{2m^{**}}\psi_0(\mathbf{r},t) + \int d\mathbf{r}' v\left(\mathbf{r}-\mathbf{r}'\right)\left|\psi_0^*\left(\mathbf{r}',t\right)\right|^2\psi_0(\mathbf{r},t) \tag{7.33}$$

Using a perturbed wave function,

$$\psi_0(\mathbf{r},t) = \sqrt{n_0} + \phi(\mathbf{r},t) \tag{7.34}$$

and keeping only terms linear in $\mathbf{A}$ one obtains by the Fourier transformation

$$\nu\phi(\mathbf{q},\nu) = \frac{q^2}{2m^{**}}\phi(\mathbf{q},\nu) + n_0 V(\mathbf{q})\left\{\phi(\mathbf{q},\nu) + \phi^*(-\mathbf{q},-\nu)\right\} - \frac{2e\sqrt{n_0}}{2m^{**}}\mathbf{q}\cdot\mathbf{a}(\mathbf{q},\nu) \tag{7.35}$$

For a real potential $\mathbf{a}(\mathbf{q},\nu) = \mathbf{a}^*(-\mathbf{q},-\nu)$ the solution is

$$\phi(\mathbf{q},\nu) + \phi^*(-\mathbf{q},-\nu) = -\frac{2e\sqrt{n_0}}{m^{**}}\frac{\nu}{\nu^2-\epsilon_{\mathbf{q}}^2}\mathbf{q}\cdot\mathbf{a}(\mathbf{q},\omega) \tag{7.36}$$

$$\phi(\mathbf{q},\nu) - \phi^*(-\mathbf{q},-\nu) = -\frac{2e\sqrt{n_0}}{m^{**}}\frac{2m^{**}}{q^2}\frac{\epsilon_{\mathbf{q}}^2}{\nu^2-\epsilon_{\mathbf{q}}^2}\mathbf{q}\cdot\mathbf{a}(\mathbf{q},\omega) \tag{7.37}$$

The expectation value of the current is given by the partial derivative of the Hamiltonian with respect to the vector potential,

$$\mathbf{J}(\mathbf{r},t) = -\frac{ie}{m^{**}}\left[\psi_0^*(\mathbf{r},t)\nabla\psi_0(\mathbf{r},t) - \psi_0(\mathbf{r},t)\nabla\psi_0^*(\mathbf{r},t)\right] - \frac{4e^2n_0}{m^{**}}\mathbf{A}(\mathbf{r},t) \tag{7.38}$$

Applying the perturbed wavefunction, we obtain the Fourier transform of the current as,

$$\mathbf{J}(\mathbf{q},\nu) = \frac{e\sqrt{n_0}}{m^{**}}\mathbf{q}\left[\phi(\mathbf{q},\nu) - \phi^*(-\mathbf{q},-\nu)\right] - \frac{4e^2n_0}{m^{**}}\mathbf{a}(\mathbf{q},\nu) \tag{7.39}$$

Hence

$$K^{mn}(\mathbf{q},\nu) = \frac{4e^2n_0}{m^{**}}\left[\delta^{mn}\frac{\nu^2}{\epsilon_{\mathbf{q}}^2-\nu^2} + \left(q^mq^n - \delta^{mn}q^2\right)\frac{\epsilon_{\mathbf{q}}^2}{q^2\left(\epsilon_{\mathbf{q}}^2-\nu^2\right)}\right] \tag{7.40}$$

This response function has been split into a longitudinal $K_l \sim \delta^{mn}$ and transverse $K_1 \sim (q^mq^n - \delta^{mn}q^2)$ parts.

The longitudinal response to the field $(\mathbf{D}\|\mathbf{q})$ is expressed in terms of the so-called external conductivity σ_{ex} as

$$\mathbf{J}_l(\mathbf{q},\nu) = \sigma_{ex}(\mathbf{q},\nu)\mathbf{D}(\mathbf{q},\nu) \tag{7.41}$$

where $\mathbf{D}$ is the external electric field. By the use of Eq.(7.40) we find

$$\sigma_{ex}(\mathbf{q},\nu) = \frac{K_l}{i\nu} = \frac{i\epsilon_0 \nu \omega_{p0}^2}{4\pi\left(\nu^2 - \epsilon_{\mathbf{q}}^2\right)} \tag{7.42}$$

The Kubo conductivity sum rule is satisfied

$$\int_0^\infty d\nu \mathrm{Re}\ \sigma_{ex}(\nu) = \frac{\pi e^2 n_0}{2m^{**}} \tag{7.43}$$

The conductivity in the transverse electromagnetic field ($\mathbf{D} \perp \mathbf{q}$) is

$$\sigma_t = \frac{i}{4\pi\lambda_H^2 \nu} \tag{7.44}$$

where

$$\lambda_H = \left[\frac{m^{**}}{16\pi e^2 n_0}\right]^{1/2} \tag{7.45}$$

This expression is the same as that for the BCS superconductor. Combined with the Maxwell equation it describes the Meissner-Ochsenfeld effect in CBG with the London penetration depth λ_H. Consequently, a charged Bose gas is a superconductor.

6.9.4 7.4 Collective excitations and screening

The dielectric response function $\epsilon(\mathbf{q},\nu)$ is defined as

$$\frac{1}{\epsilon(\mathbf{q},\nu)} = 1 + \frac{\rho(\mathbf{q},\nu)}{\rho_{ex}(\mathbf{q},\nu)} \tag{7.46}$$

The Fourier component of the boson charge density $\rho_b(\mathbf{q},\nu)$ obeys the continuity equation

$$qJ_l(\mathbf{q},\nu) - \nu\rho_b(\mathbf{q},\nu) = 0 \tag{7.47}$$

Combining the Maxwell

$$iqD(\mathbf{q},\nu) = 4\pi\frac{\rho_{ex}}{\epsilon_0} \tag{7.48}$$

and continuity equations we find the total density $\rho = \rho_{ex} + \rho_b$ and the dielectric function of CBG

$$\frac{1}{\epsilon(\mathbf{q},\nu)} = 1 - 4\pi\frac{K_l(\mathbf{q},\nu)}{\nu^2} \tag{7,49}$$

or

$$\epsilon(\mathbf{q},\nu) = 1 - \frac{\omega_{p0}^2}{\nu^2 - q^4/4\left(m^{**}\right)^2} \tag{7.50}$$

This expression is the same as derived for an ideal charged Bose gas by Hore and Frankel (1975).

The zeros of $\epsilon(\mathbf{q},\nu)$ describe collective excitations of the system. These turn out to be the same as the Bogoliubov single-particle excitations in agreement with the general arguments (Pines (1961)). The screening in the condensed CBG goes like $\epsilon(q,0) \sim 1/q^4$ in the long-wave limit. It produces a screened potential, which goes as

$$\tilde{V}(r) \sim \frac{\cos\left(q_s r/\sqrt{2}\right.}{r} e^{-q_s r/\sqrt{2}} \tag{7.51}$$

where $q_s = \sqrt{2m^{**}\omega_{p0}}$ is the inverse screening length.
For two-dimensional condensed bosons ($T = 0$) the dielectric response function can easily be derived in the same way,

$$\epsilon(\mathbf{q}, \nu) = 1 - \frac{E_s^2 q/q_s}{\nu^2 - E_s^2 q^4/q_s^4} \tag{7.52}$$

Zeros of $\epsilon(\mathbf{q}, \omega)$ yield the gapless collective branch, which is the same as the Bogoliubov mode, Eq.(7.22).

There is a direct analogy between excitations of CBG and of the BCS superconductor. The only difference is that in the former the plasmon mode is identical with the Bogoliubov quasiparticle, while in the BCS superconductor the collective plasmon mode lies well above the BCS quasiparticle gap.

6.9.5 7.5 Superconducting kinetics of CBG: $2D$ heat superconductor

The long-wave excitations are responsible for the kinetic properties of CBG at low temperatures differently from normal metals or BSC superconductors where the characteristic wavelength is of the order of the lattice constant. As we have discussed above the condensate screens perfectly well the scattering potential. Therefore, in CBG one can expect a strong enhancement of the scattering rate below T_c. For near $2D$ bosons this leads to an infinite thermal conductivity (Alexandrov and Mott (1993)).

The elastic scattering of excitations is described by the Hamiltonian:

$$H_s = \sum_{\mathbf{k},\mathbf{k}'} v\left(\mathbf{k}, \mathbf{k}'\right) \alpha_{\mathbf{k}'}^{\dagger} \alpha_{\mathbf{k}} \tag{7.53}$$

with

$$v\left(\mathbf{k}, \mathbf{k}'\right) = \frac{v_0\left(\mathbf{k} - \mathbf{k}'\right)\left(u_{\mathbf{k}} u_{\mathbf{k}'} + v_{\mathbf{k}} v_{\mathbf{k}'}\right)}{\epsilon\left(\mathbf{k} - \mathbf{k}', 0\right)} \tag{7.54}$$

a screened scattering potential and the coherence factors $u_{\mathbf{k}}, v_{\mathbf{k}}$ determined by Eq.(7.1719). Here $v_0(\mathbf{q})$ is the Fourier component of a bare (unscreened) boson -impurity or boson- acoustic phonon interactions. Because the characteristic excitation energy is of the order of temperature the boson-acoustic phonon scattering is practically elastic if the temperature is not extremely low, $T > m^{**}s^2/2$ as we have discussed in section 4.11. The static dielectric function of $2D$ charged bosons $\epsilon(q, 0)$ depends on q at low temperatures as

$$\epsilon(q, 0) = 1 + \left(\frac{q_s}{q}\right)^3 \tag{7.55}$$

With the Fermi golden rule and the Boltzmann equation one obtains the elastic transport relaxation rate for excitations in the usual way:

$$1/\tau(k) = 2\pi \sum_{\mathbf{k}'} \frac{k_x - k_x'}{k_x} v^2\left(\mathbf{k}, \mathbf{k}'\right) \delta\left(\epsilon_{\mathbf{k}} - \epsilon_{\mathbf{k}'}\right) \tag{7.56}$$

or

$$1/\tau(k) = \frac{k}{\pi} \frac{dk}{d\epsilon_{\mathbf{k}}} \left(u_{\mathbf{k}}^2 + v_{\mathbf{k}}^2\right)^2 \int_0^{\pi} d\phi (1 - \cos(\phi)) \frac{v_0^2(k\sqrt{2(1 - \cos(\phi))})}{\epsilon^2(k\sqrt{2(1 - \cos(\phi)}, 0)} \tag{7.57}$$

For the scattering by acoustic phonons (or by point defects) v_0 is independent of q. For charged impurities $v_0^2(q) \sim 1/q^2$.

By the use of the spectrum of low-energy $2D$ Bogoliubov excitations with $k < q_s$, $\epsilon_{\mathbf{k}} = E_s\sqrt{k/q_s}$ we obtain for the acoustic phonon

$$\tau^s_{ac}(k) \sim \left(\frac{q_s}{k}\right)^{9/2} \tag{7.58}$$

and

$$\tau^s_{im}(k) \sim \left(\frac{q_s}{k}\right)^{5/2} \tag{7.59}$$

for the impurity scattering. Both τ_{ac} and τ_{im} are infinite in the long-wave limit $k \to 0$ because of screening and of a large group velocity of the $2D$ Bogoliubov mode, $d\epsilon/dk$, which is divergent as $k^{-1/2}$ in this limit. Due to this singularity of the group velocity, which is a common feature of surface waves, and the due to the screening by the condensate the $2D$ Bogoliubov mode is a perfect heat carrier. In fact, the thermal conductivity is infinite. To show this we write the expression for the heat flow, taking into account that in the superconducting state both the chemical and the electrical potentials are zero:

$$\mathbf{Q} = -\sum_{\mathbf{k}} \frac{d\epsilon_{\mathbf{k}}}{d\mathbf{k}}\epsilon_{\mathbf{k}}\frac{\partial n(\mathbf{k})}{\partial T}\tau^s(k)\left(\frac{d\epsilon_{\mathbf{k}}}{d\mathbf{k}}\nabla T\right) \tag{7.60}$$

where $n(\mathbf{k})$ is the Bose-Einstein distribution function with zero chemical potential and

$$\tau^s = \frac{\tau^s_{ac}\tau^s_{im}}{\tau^s_{ac} + \tau^s_{im}} \tag{7.61}$$

Substitution of Eq.(7.61) into Eq.(7.60) yields the superconducting-state thermal conductivity:

$$K_s \sim \frac{1}{T^8}\int_0^{E_s/T} dx \frac{1}{x^2\sinh^2(x)\left(x^4 + \eta/T^5\right)} = \infty \tag{7,62}$$

where η is a temperature independent constant, proportional to the ratio of the iii purity and phonon scattering cross-sections. The infinite thermal conductivity it $2D + \epsilon$CBG is quite unexpected compared with the usual s-wave BCS supercon ductor, which has exponentially suppressed thermal conductivity due to a gap the excitation spectrum. Three-dimensional corrections to the spectrum cancel ii
'infrared' divergence of K_s. As a result the temperature shape of the thermal conductivity curve of near $2D$ bosons below their condensation temperature is controlled by the simultaneous increase of 'diffusivity' of the Bogoliubov excitations due to the screening of the scattering potential as well as due to the long-wave singularity of the group velocity and by the decrease of the heat capacity, $C_b \sim T^4$. This shape is in global qualitative agreement with the experimental data for high- T_c copper oxides which show the in-plane thermal conductivity enhancement in the superconducting state.

6.9.6 7.6 BEC of charged bosons in a random potential

Kinetic properties of charged bosons in real solids depend on their localization in a random potential. The intuitive picture of hard - core bosons filling up all localized single-particle states and Bose-condensing into the first extended state is known in the literature. To calculate the density of localised bosons $n_L(T)$ one should take into account the repulsion between them. One cannot ignore the fact that the localization length ξ generally varies with energy and diverges at the mobility edge. One would expect that the number of hard - core bosons in a localized state near the mobility edge diverges in a way similar to the localization length. Therefore,

it is still not clear how the hard-core bosons form a true (extended) Bose-Einstein condensate (BEC) in the random field.

However, in the case of CBG the Coulomb repulsion restricts the number of bosons in each localised state, so that the distribution function will show a mobility edge E_c (Mott (1993)). The number of bosons in a single potential well is determined by the competition between their long-range Coulomb repulsion $\simeq 4e^2/\xi$ and the binding energy $E_c - \epsilon$. If the localization length diverges with the critical exponent $\nu < 1$: $\left(\xi \sim (E_c - \epsilon)^{-\nu}\right)$, one can apply a 'single well-single particle' approximation assuming that one can place only one boson in each potential well. In doped semiconductors the exponent ν depends on the degree of compensation varying from $\nu = 0.5$ in SiP to $\nu \simeq 1.0$ in amorphous $NbSi$. In an extreme case of the hydrogen atom the average clectron-nucleus distance is proportional to the inverse binding energy, i.e. $\nu = 1$.

In two dimensions any random potential yields localised states, independent of its strength. Here we consider BEC of quasi-two dimensional bosons by the use of the 'single well-single particle' approximation (Alexandrov et al (1994)). Within this approximation localized charged bosons obey the Fermi-Dirac statistics:

$$n_L(T) = \int_{-\infty}^{E_c} \frac{N_L(\epsilon) d\epsilon}{\exp\left(\frac{\epsilon-\mu}{T}\right) + 1} \tag{7.63}$$

where $N_L(\epsilon)$ is the density of localized states. Near the mobility edge it remains constant $N_L(\epsilon) \simeq \frac{n_L}{\gamma}$ with γ of order of a binding energy in a single random potential well and n_L the total number of localized states per unit cell. We chose the position of the mobility edge as zero, $E_c = 0$. Then for $n \geq n_L$ the number of empty localised states turns out to be linear as a function of temperature in a wide temperature range $T < \gamma, 2t$ because the chemical potential is pinned in this temperature region to the mobility edge, $\mu \simeq E_c = 0$ ($2t$ is the bandwidth). This follows from the conservation
of the total number of bosons $n = n_b(T) + n_L(T)$, which yields for the chemical potential:

$$\frac{T}{2t} \ln \frac{1}{1-y} - \frac{n_L T}{\gamma} \ln\left(1 + y^{-1}\right) = n - n_L \tag{7.64}$$

If $T \ll (\gamma, 2t)$, the solution of this equation is $y \simeq 1$ with an exception of a very narrow region of concentration $n - n_L \ll T/2t$, where y decreases to about 0.6. The density of extended bosons n_b depends on y logarithmically,

$$n_b(T) = \frac{T}{2t} \ln\left(\frac{1 - ye^{-2t/T}}{1-y}\right) \tag{7.65}$$

Therefore its temperature dependence remains practically linear up to $T \simeq \gamma$:

$$n_b(T) = n - n_L + n_L bT, \tag{7.66}$$

with temperature independent $b = \ln 2/\gamma$.
It turns out that the decrease of the density of extended bosons with the temperature lowering (up to zero for $T = 0$ and $n_L = n$) does not prevent the Bose-Einstein condensation. There is no true Bose condensate in two dimensions. Therefore we introduce a three-dimensional correction to the free boson energy spectrum as

$$E_{\mathbf{k}} = \frac{k_{\parallel}^2}{2m^{**}} + 2t_{\perp}\left(1 - \cos\left(k_{\perp} d\right)\right) \tag{7.67}$$

Then the density of the extended states $N(\epsilon)$ is given by

$$N(\epsilon) = \frac{1}{2t\pi} \arccos\left(1 - \frac{\epsilon}{2t_{\perp}}\right) \tag{7.68}$$

for $0 < \epsilon < 4t_\perp$ and $N(\epsilon) = 1/2t$ for $4t_\perp < \epsilon < 2t$ with $t_\perp \ll t$ the inter-plane hopping, d the interplane distance, and $m^{**} \simeq \pi/ta^2$ the in-plane effective mass.

The BEC temperature is found by the use of

$$n_b(T) = \int_0^\infty dE \frac{N(E)}{\exp(E/T) - 1}, \tag{7.69}$$

which for $T_c \ll 2t$ can be written as

$$\frac{T_c}{2t\pi} \int_0^{4t_\perp/T_c} dx \frac{\arccos\left(1 - xT_c/2t_\perp\right)}{\exp(x) - 1} - \frac{T_c}{2t} \ln\left[1 - \exp\left(-\frac{4t_\perp}{T_c}\right)\right] = n - n_L + \frac{T_c n_L \ln 2}{\gamma}$$

This equation is simplified if $T_c \gg t_\perp$:

$$\frac{T_c}{2t} \ln\left[\frac{T_c \exp\left(1 - 2n_L t \ln 2/\gamma\right.}{2t_\perp}\right] = n - n_L \tag{7.71}$$

Depending on the 'compensation', $n - n_l, T_c$ changes from

$$T_c = \frac{2t\left(n - n_L\right)}{L} \tag{7.72}$$

for

$$n - n_L \gg \frac{t_\perp \exp\left(\frac{2n_L t \ln 2}{\gamma} - 1\right)}{t} \tag{7.73}$$

with

$$L = \ln\left[\frac{(n - n_L)\,\mathrm{texp}\left(1 - \frac{2n_L t \ln 2}{\gamma}\right)}{t_\perp}\right] \tag{7.74}$$

to

$$T_c \simeq 2t_\perp \exp\left(\frac{2n_L t \ln 2}{\gamma} - 1\right) \tag{7.75}$$

if $n = n_L.T_c$ depends on the compensation $n - n_L$ practically linearly, Fig.7.2.

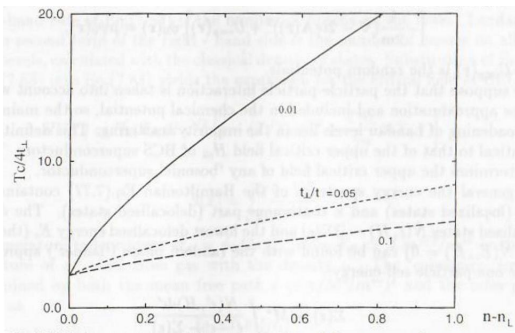

Fig.7.2. T_{c} of CBG in a random potential as a function of the compensation $n - n_L$.

In general, statistics of localised bosons is different from both the Fermi and BoseEinstein statistics. The shallow potential wells can accommodate more than one boson, so the profile of

the density of states just below the mobility edge is important for the low temperature CBG kinetics.

Charged bosons like ordinary carriers in doped semiconductors screen the random potential. The screening radius at $T = 0$ is given by the value $q_s^{-1} = \sqrt{2m^{**}\omega_{po}}$. Therefore, we would expect that the Mott criterion for the metal-insulator transition

$$n_{im}^{1/3} a_B \simeq 0.26, \tag{7.76}$$

to be valid with $2n_{im}$ instead of n_{im} and $a_B \simeq \epsilon_0/m^{**}(2e)^2$. With $\epsilon_0 \sim 100$ and $m^{**} \sim 10m_e$ this yields $n_{im} \sim 10^{22}$ cm^{-3}.

6.9.7 7.7 BEC of charged bosons in a magnetic field

As noted by Schafroth(1955) an ideal charged Bose-gas in a magnetic field cannot be condensed because of the one-dimensional character of particle motion within the
lowest Landau level. However, the interacting charged Bose-gas is condensed in a field lower than a certain critical value H^* because the interaction with impurities or between bosons broadens the Landau levels and thereby eliminates the one-dimensional singularity of the density of states (Alexandrov (1993)). As we discuss below the critical field of BEC has an unusual positive curvature near $T_{c0}, H^*(T) \sim (T_c - T)^{3/2}$. At low impurity concentration it diverges at $T \to 0$. The localization can drastically change the low-temperature behavior of $H^*(T)$, so at high concentration of impurities the re-entry effect to the normal state occurs.
H^* is determined as the field in which the first nonzero solution of the linearized stationary equation for the macroscopic condensate wave function $\psi_0(\mathbf{r}) = \langle N|\hat{\psi}(\mathbf{r},\tau) \mid N+1\rangle, (N \to \infty, N/V = n = \text{const})$ appears:

$$\left[-\frac{1}{2m}(\nabla - 2ie\mathbf{A}(\mathbf{r}))^2 + U_{imp}(\mathbf{r})\right]\psi_0(\mathbf{r}) = \mu\psi_0(\mathbf{r}) \tag{7.77}$$

where $U_{imp}(\mathbf{r})$ is the random potentials.
We suppose that the particle-particle interaction is taken into account within the Hartree approximation and included in the chemical potential, so the main origin of the broadening of Landau levels lies in the impurity scattering. This definition of H^* is identical to that of the upper critical field H_{c2} of BCS superconductors. Therefore H^* determines the upper critical field of any 'bosonic' superconductor.

In general the energy spectrum of the Hamiltonian Eq.(7.77) contains discrete levels (localized states) and a continuous part (delocalised states). The density of delocalised states $\tilde{N}(\epsilon, H) \sim \text{Im}\,\Sigma(\epsilon)$ and the lowest delocalised energy E_c (the mobility edge, $\tilde{N}(E_c, H) = 0$) can be found with the random phase ('ladder') approximation for the one-particle self-energy:

$$\Sigma(\epsilon) = M^2 \int \frac{N(\epsilon', H)\, d\epsilon'}{\epsilon - \epsilon' - \Sigma(\epsilon)} \tag{7.78}$$

where M^2 is the squared matrix element for the boson-impurity scattering multiplied by the impurity density, and

$$N(\epsilon, H) = \frac{\sqrt{2}\,(m^{**})^{3/2}\,\omega}{4\pi^2}\text{Re}\sum_{N=0}^{\infty}\frac{1}{\sqrt{\epsilon - \omega(N+1/2)}} \tag{7.79}$$

is the density of states for a noninteracting system with $\omega = 2eH/m^{**}$.
The solution of Eq.(7.78) yields for the lowest Landau level ($N = 0$)

$$\tilde{N}_0(\epsilon, H) = \frac{\sqrt{6}\,(m^{**})^{3/2}\,\omega}{8\pi^2\sqrt{\Gamma_0}}\left[\left(\frac{\tilde{\epsilon}^3}{27}+\frac{1}{2}+\sqrt{\frac{\tilde{\epsilon}^3}{27}+\frac{1}{4}}\right)^{1/3}-\left(\frac{\tilde{\epsilon}^3}{27}+\frac{1}{2}-\sqrt{\frac{\tilde{\epsilon}^3}{27}+\frac{1}{4}}\right)^{1/3}\right] \tag{7.80}$$

and

$$E_c = \frac{\omega}{2} - \frac{3\Gamma_0}{2^{2/3}} \tag{7,81}$$

Here $\Gamma_0 = 0.5\left(2M^2 eH\sqrt{m^{**}}/\pi\right)^{2/3}$ is the characteristic broadening of the lowest Lan dau level and $\tilde{\epsilon} = (\epsilon - \omega/2)/\Gamma_0$.

Because the singularity of the density of states is integrated out for all levels except $N = 0$, one can neglect their quantization using the zero field density of states for $\epsilon > \omega$,

$$N(\epsilon) \simeq \frac{(m^{**})^{3/2}\sqrt{\epsilon}}{\sqrt{2}\pi^2} \tag{7.82}$$

The first nontrivial extended solution of Eq.(7.77) appears at $\mu = E_c$. Thus the critical curve $H^*(T)$ is determined from the conservation of the number of particles n_b under the condition that the chemical potential coincides with the mobility edge:

$$\int_{E_c}^{\infty} \frac{\tilde{N}_0\,(\epsilon, H^*)\,d\epsilon}{\exp\left(\frac{\epsilon - E_c}{T}\right) - 1} = n\left[1 - (T/T_{c0})^{3/2} - \frac{n_L(T)}{n}\right] \tag{7.83}$$

The left-hand side of Eq.(7.83) is the number of bosons on the lowest Landau level, while the second term of the right - hand side is the number of bosons on all upper Landau levels, calculated with the classical density of states. Substitution of Eq.(7.80) and Eq.(7.63) into Eq.(7.83) yields the expression for the critical field of BEC:

$$H^*(T) = H_d\,(T_{c0}/T)^{3/2}\left[1 - (T/T_{c0})^{3/2} - \frac{T n_L}{\gamma n}\beta(T/\gamma)\right]^{3/2} \tag{7.84}$$

with

$$\beta(x) = \sum_{k=0}^{\infty}\frac{(-1)^k}{x+k} \tag{7.85}$$

and temperature independent $H_d = \phi_0/2\pi\xi_0^2$. Here $T_{c0} \simeq 3.3n^{2/3}/m^{**}$ is the BEC temperature of an ideal Bose gas with the density n. The 'coherence' length ξ_0 is determined by both the mean free path $l = \pi/M^2\,(m^{**})^2$ and the inter-particle distance as

$$\xi_0 \simeq 0.8(l/n)^{1/4} \tag{7.86}$$

Here $\phi_0 = \pi/e$ is the flux quantum.
Using the asymptotic $\beta(x) \simeq (2x)^{-1}$ at temperature $T > \gamma$ one obtains:

$$H^* = H_d\sqrt{1 - \frac{n_L}{2n}}\left(\frac{1}{\tau} - \sqrt{\tau}\right)^{3/2} \tag{7.87}$$

where $\tau \equiv T/T_c$ is the reduced temperature and

$$T_c = T_{c0}\left(1 - \frac{n_L}{2n}\right)^{2/3} \tag{7.88}$$

is the critical temperature of BEC in a random potential for zero magnetic field.
Thus $H^*(T)$ has the positive ' 3/2 ' curvature near T_c. This curvature is a universal feature of CBG, which does not depend on a particular scattering mechanism and on approximations made. The number of bosons at the lowest Landau level is proportional to the density of states near the mobility edge $\tilde{N}_0 \sim H/\sqrt{\Gamma(H)}$, where the 'width' of the Landau level is also proportional to the same density of states $\Gamma(H) \sim H/\sqrt{\Gamma(H)}$. Hence $\Gamma(H) \sim H^{2/3}$ and the number of condensed bosons is proportional to $H^{2/3}$. On the other hand this number in the vicinity of T_c should
be proportional to $T_c - T$ (the total number minus the number of thermally excited bosons). That gives the ' 3/2 ' law for $H^*(T)$.

At low temperatures $T \ll \gamma$ the temperature dependence of H^* turns to be different for different impurity concentration. If $0 < n_L < n$ the critical field diverges at $T \to 0$,

$$H^* \simeq H_d \left(T_{co}/T\right)^{3/2} \left(1 - \frac{n_L}{n}\right)^{3/2} \tag{7.89}$$

because the number of localized states is smaller then the number of bosons. In this case only the paramagnetic limit restricts the value of $H^*(0)$ if bosons are composed from two fermions with the opposite spins. If $n_L = n$ the critical field reaches its maximum at $T = 0$:

$$H^* \simeq H_d \left(T_{c0} \ln 2/\gamma\right)^{3/2} \left(1 - \frac{\pi^2 T}{8\gamma \ln 2}\right). \tag{7.90}$$

And finally, if $n < n_L < 2n$ there is a re-entry effect to the normal state at temperature below some T^*, so $H^* = 0$ for $T < T^*$, Fig.7.3.

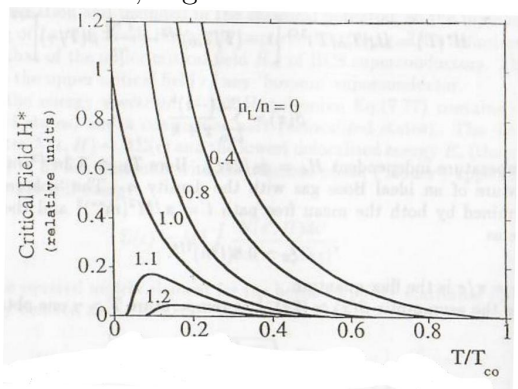

If the number of localized states is large, $n_L > 2n$ Bose condensation is impossible: $T_c = 0$.

Deriving Eq.(7.84) for H^* we expand the exponent in the left hand side of Eq.(7.83) and assume that the scattering amplitude is energy independent. The ultra-low ($T \ll \Gamma_0$) temperature behavior of H^* depends on these assumptions. In this temperature regime one can expect $T^{-9/2}$ behavior of H^* rather than $T^{-3/2}$. It depends also on the shape of the localised level distribution $N_L(\epsilon)$ as we shall discuss in Chap ter 8. However, the gross features like the divergent behavior at $T \to 0$ and the re-entry effect for the sufficiently large impurity density ($n_L > n$) are independent of the model and approximation made.

In contrast to the Fermi liquid, in which the long-range Coulomb interaction in screened and high-energy plasmons are not relevant for the low-frequency kinetic,
allowance for the Coulomb interaction at finite temperatures in CBG is a more complicated matter because plasmon and one particle excitation are essentially the same in the long-wave limit. However, the residual interaction between low-energy excitations of CBG is also screened, if we integrate out the high-energy excitations from the action. Therefore, one can assume that the mixed state of CBG in an external magnetic field can be described by the equation similar to that of the Ginsburg-Landau (GL) theory for the BCS superconductors, which is obtained from

the BdG set if we replace the long-range Coulomb potential for a short-range one $v_0(\mathbf{r}) \simeq v_{\mathrm{q}}\delta(\mathbf{r})$ and neglect fluctuations of the order of $\tilde{\psi}^2$ (Alexandrov et al (1987))

$$\left[-\frac{1}{2m}(\nabla - 2ie\mathbf{A}(\mathbf{r}))^2 - \mu + v_0\left|\psi_0(\mathbf{r})\right|^2\right]\psi_0(\mathbf{r}) = 0 \tag{7.91}$$

This equation is supplemented by the expression for the superfluid current, Eq.(7.38) and by the Maxwell equation. Recognizing that the chemical potential of a homogeneous system is $\mu = nv_0$, the characteristic lengths in the problem are

$$\lambda_H = \sqrt{\frac{m^{**}}{16\pi ne^2}}, \tag{7.92}$$

which is the field penetration depth and

$$\xi = \frac{1}{\sqrt{2m^{**}nv_0}} \tag{7.93}$$

the GL coherence length. The GL ratio is $\kappa \equiv \lambda_H/\xi = m^{**}\left(v_0/8\pi e^2\right)^{1/2}$. Because $\left(v_0/16\pi e^2\right)^{1/2}$ is of the order of the screening radius q_s^{-1} the GL ratio is very large

$$\kappa \sim \frac{m^{**}c}{q_s} \gg 1, \tag{7.94}$$

where c is the light velocity. Therefore CBG is the extreme type -II superconductor. The lower critical field, in which a first normal vortex appears is given by the canonical Abrikosov (1957) expression

$$H_{c1}(0) \simeq \frac{\phi_0 \ln\kappa}{4\pi\lambda_H^2} \tag{7.95}$$

In particular, for $T = 0$ we estimate

$$H_{c1}(0) \simeq \frac{4\pi en}{m^{**}}\ln\kappa \tag{7.96}$$

In order to calculate the thermodynamic critical field H_c, in which the homogeneous superconducting state is in the thermal equilibrium with the normal phase, we assume that the ground state energy E_0 is determined by the interaction energy in both phases. The normal state is a homogeneous phase, in which bosons are on the lowest Landau level. Allowance for only the interaction energy in this state is equivalent to neglecting of small diamagnetism. The kinetic energy of the superconducting phase is small because the supracondensate density is small. Thus for the normal state we obtain per unit volume

$$E_0^n = n^2 v_0 \tag{7.97}$$

and

$$E_0^s = \frac{1}{2}n^2 v_0 \tag{7.98}$$

for the superconducting state. Doubling the energy of the normal state compared with the superconducting state is explained by the exchange contribution in the normal state, which is positive, in contrast to the Fermi gas. As a result, the thermodynamic critical field is

$$H_c(0) \equiv \sqrt{8\pi\left(E_0^n - E_0^s\right)} = \left(4\pi v_0\right)^{1/2} n \tag{7.99}$$

One can compare H_c of CBG with that of noninteracting charged bosons, calculated by Schafroth (1955), $H_0 = 2\pi ne/m^{**}$. Their ratio is

$$\frac{H_c}{H_0} \sim \kappa \gg 1 \tag{7.100}$$

Thus the diamagnetic energy is negligible.

6.9.8 7.8 Normal state kinetics of CBG

Above T_c the boson gas is nondegenerate. Therefore their kinetic properties are those of the nondegenerate carriers in doped semiconductors and can be studied by solving the Boltzmann equation taking into account the scattering by acoustical phonons, by each other and by unscreened random potential. As a result one obtains the canonical expressions for the Hall coefficient R_H and the resistivity ρ:

$$R_H = \frac{\langle \tau^2 \rangle}{2en_b(T)\langle \tau \rangle^2} \tag{7.101}$$

$$\rho = \frac{m^{**}}{4e^2 n_b(T)\langle \tau \rangle} \tag{7.102}$$

where $\langle \ldots \rangle$ means an average with energy and the derivative of the Bose-Einstein distribution function

$$\langle A(E) \rangle \equiv \frac{\int dEN(E)EA(E)n'(E)}{\int dEN(E)En'(E)} \tag{7.103}$$

for the simplest case of isotropic energy spectrum with the density of states $N(E)$. Here $n'(E) = \partial n(E)/\partial E$.

The case of quasi-two dimensional bosons is important for high- T_c copper oxides. In the normal state the characteristic boson momentum is large compared with the inverse screening length $q > q_s$ and therefore the scattering potential is not screened, $\epsilon(q, 0) = 1$. The transport relaxation rate due to the two-dimensional acoustic phonon scattering is energy independent and linear in temperature (Section 4.11)

$$\frac{1}{\tau_{b-ac}} = m^{**} C_{ac} T \tag{7.104}$$

where the constant C_{ac} is proportional to the deformation potential.

In case of the classical statistics umklapp scattering can be neglected, so the scattering between bosons in extended states does not contribute to the resistivity. However, in the random potential the inelastic scattering of an extended boson by localised bosons makes a contribution because the momentum is not conserved in two-particle collisions. Therefore the boson-boson scattering contributes to the transport relaxation rate in disordered solids. In a 'single well-single particle approximation' the role of the Pauli exclusion principle is played by the dynamical repulsion between bosons. That is why the boson-boson relaxation rate has the same temperature dependence as the fermion-fermion scattering. In particular, the relaxation rate is proportional to the temperature squared because only localized bosons within the energy shell of the order of T near the mobility edge contribute to the scattering and because the number of the final states is proportional to temperature,

$$\frac{1}{\tau_{b-b}} = \frac{\alpha e^2 b n_L}{m^{**}} T^2 \tag{7.105}$$

with α a constant.
As a result one obtains

$$R_H = \frac{1}{2e\left(n - n_L + bn_L T\right)} \tag{7.106}$$

$$\rho = \left[\left(m^{**}\right)^2 C_{ac}/4e^2\right] \frac{T + \sigma_b T^2}{n - n_L + bn_L T} \tag{7.107}$$

where $\sigma_b = \alpha e^2 bn_L / \left(m^{**}\right)^2 C_{ac}$ is the relative boson-boson scattering cross-section. The density of extended bosons is temperature dependent as discussed in section 7.6, which leads to the temperature dependent Hall constant and to the linear resistivity. The boson-phonon scattering is mainly responsible for the linear temperature dependence of ρ at low temperatures while the boson-boson scattering and the temperature dependent density $n_b(T)$ are responsible for the linear ρ at higher temperatures. The residual resistivity is taken to be zero. Any nondegenerate carriers on a two-dimensional lattice have the same temperature and doping dependencies of their kinetic properties, so decomposition of the boson into two fermions at high temperatures does not change the temperature dependencies of R_H and ρ. As regards the Hall angle Θ_H above T_c the number of carriers increases linearly with T, while the boson-boson scattering gives the relaxation rate $1/\tau \sim nT$, so that $\rho \sim 1/n\tau \sim T$ and $\cot\Theta_H \sim 1/\tau \sim T^2$ in full agreement with many experimental observations in highT_c copper oxides (Alexandrov and Mott (1994)). At high temperatures ($T \gg \gamma$) the density of extended bosons eventually saturates, as measurements of the Hall coefficient in several copper oxides show.

Finally, we calculate the thermal conductivity K_n of $2D$ bosons in the normal state applying the standard kinetic theory, developed for metals and semiconductors, by replacing the Fermi distribution function for the Bose function. As a result one obtains the Wiedemann-Franz law

$$K_n = L_B \sigma T \tag{7.108}$$

where σ is the normal state conductivity, and

$$L_B = \left(\frac{k_B}{2e}\right)^2 \frac{3B_0(z)B_2(z) - 4B_1^2(z)}{B_0^2(z)} \tag{7.109}$$

is a bosonic Lorentz number with

$$B_\nu(z) = \int_0^\infty \frac{x^\nu dx}{\exp(x - z) - 1} \tag{7.110}$$

Here zT is the chemical potential and k_B is the Boltzmann constant. The transport relaxation time is assumed to be energy independent. In the classical high-temperature limit, $T \gg T_c$ we obtain:

$$L_B = 2\left(\frac{k_B}{2e}\right)^2 \tag{7.111}$$

The boson Lorentz number, Eq.(7.109), should be compared with the electron one, $L_e = \pi^2 k_B^2/3e^2$, which does not depend on the scattering mechanism or on the dimensionality for degenerate carriers. Their ratio is very small mainly due to the double elementary charge of a boson. It is given by

$$\frac{L_B}{L_e} = \frac{6}{4\pi^2} \tag{7.112}$$

which is approximately 0.152. Taking this into account one can explain the near equality of the thermal conductivity of superconducting and insulating crystals of $YBCO$ in the temperature range above 100 K (Alexandrov and Mott (1993)).

6.10 8 Evidence for mobile small polarons and bipolarons

6.10.1 8.1 Small versus large polarons

Over the last decades many materials with rather high density of carriers $n \geq 10^{20}$ cm^{-3} and low mobility of the order or even less than the Mott-Ioffe-Regel limit ($ea^2/\hbar \sim 1cm^2/Vs$) were discovered. In our book we have put forward the multipolaron theory of low-mobility solids, which cannot be understood within the framework of the canonical theory of metals. This Chapter is intended to discuss several experiments supporting the theory.

There is some confusion in the literature, particularly about the use of the terms 'large' and 'small' polarons and bipolarons. Some authors define the 'large polaron' as a mobile electron moving together with the self-induced extended polarization in an ionic crystal and the 'small polaron' as an immobile object completely localised within a unit cell (site). This is physically and historically incorrect. It has been known for four decades starting from pioneering work by Tjablikov (1952) and Holstein (1959) that the small polaron can tunnel in a narrow band because of the translational symmetry. Now a clear 'borderline' between large and small polarons and bipolarons is established with the scaling analysis, Monte-Carlo, cluster, variational and analytical calculations as we have discussed in Chapters 1,2 and 4. If one determines a dimensionless coupling constant

$$\lambda = \frac{E_p}{D} \tag{8.1}$$

which is essentially the same as the BCS one, large bipolarons can exist in ionic crystals at

$$\lambda \leq 0.5 \tag{8.2}$$

and small bipolarons exist in all crystals at

$$\lambda \geq 0.5 \tag{8.3}$$

Here $E_p \equiv g^2\hbar\omega$ is the Frank-Condon (or polaronic) shift, D is a bare half-bandwidth and ω is the characteristic phonon frequency. Therefore, $1/\lambda$ characterises the size of a polaron. The second dimensionless constant $g^2 = E_p/\hbar\omega$, which is the number of
phonons in a cloud around the polaron, determines the small polaron half-bandwidth w

$$w \sim D \exp\left(-g^2\right) \tag{8.4}$$

This is definitely nonzero and can be as high as several hundred K if high frequency phonons $\omega_0 \sim 0.05 - 0.1$eV are involved in the polaron formation and the bare adiabatic ratio $D/\hbar\omega$ is not very large: $D/\hbar\omega < 10$. Moreover, the calculations of the bandwidth beyond the Holstein model show that the narrowing factor g^2 is considerably reduced compared with a naive estimate ($\simeq E_p/\omega$) because of the dispersion. As we have discussed in section 6.2, $g^2 \sim 0.2E_p/\omega$ is quite feasible in copper based oxides.

As stressed by Shluger and Stoneham (1993) much of the single polaron theory is based on highly idealised models, often essentially a continuum description with a single vibrational frequency. These models ignore much of the wealth of the experimental data, which find interpretation in many atomistic simulations. The continuum description leads to the collapse of large polarons at an intermediate value of the coupling $\lambda \sim 1$. As a result, one can discuss

large polarons in ionic crystals only if the coupling with phonons is not large. The carrier density should also be small to avoid the overlap of the extended deformation fields as well as their screening. We believe that when the density of carriers is about 10^{21} cm^{-3} or higher, so the number of polarons per unit cell is above few percent, large bipolarons cannot survive because of screening. A simple estimation of the screening length r_s yields for the quasi-two dimensional Fermi gas

$$r_s \simeq \frac{\hbar}{2}\sqrt{\frac{\epsilon_0 d}{m^* e^2}} < 4\text{Å} \tag{8.5}$$

with the static dielectric constant $\epsilon_0 \sim 100, m^* = 5m_e$ and the interplane distance $d \sim 5A$. This estimate remains valid also for three dimensions if the carrier density $n \geq 10^{21}$ cm^{-3}. Therefore any extended lattice distortion and large polarons are ruled out by screening. In this case the many body effects including superconductivity should be described by the Migdal-Eliashberg theory, so the superconducting state at $\lambda \leq 0.5$ is the BCS superconductor.

On the other hand small mobile polarons form in the strong coupling regime $\lambda > 0.5$ at any doping. Their hallmarks are

- a low but finite mobility,
- the coherent band motion at temperatures below the characteristic phonon frequency and the activated mobility above it,
- a mid-infrared maximum of optical conductivity with a descrete multiphonon structure,
- the polaron band narrowing.

Being rather heavy they readily form small bipolarons if a short range attraction due to the local lattice deformation overcomes the Coulomb repulsion. Because in ionic solids the essential part of the Coulomb repulsion is screened by optical phonons, the deformation potential and molecular vibrations can easily bind two small polarons at a short distance. The hallmarks of small bipolarons are those of small polarons, plus

- superfluid phase transition similar to that of He^4,
- spin gap in the magnetic susceptibility, that is $\chi_s \to 0$ at $T \to 0$ if a singlet is the ground state ,
- electrodynamics of the charged Coulomb Bose gas,
- double elementary charge $2e$ in the normal state.

However, the absence of some of these properties does not tell us that carriers are not small (bi)polarons. As an example, proceeding from the absence of the activated mobility in doped copper oxides and from an estimation of the effective mass based on a Drude-like fit to the optical conductivity some workers interpret kinetic and optical data for copper oxides in terms of large polarons with $m^* \simeq 2m_e$ or free electrons. However, the value of the effective mass itself cannot be used to distinguish large and small polarons. In case of small polarons the mass enhancement is the same as the band narrowing factor, and is generally larger than an increase of the band mass due to the large polaron formation. However, in both cases the band mass can be and often is significantly smaller than the free electron mass m_e as discussed in section 3.5. Therefore, the absolute value of the effective mass does not yield the value of the band mass renormalisation. Moreover, a low effective mass of the order of $2m_e$ might be, in our view, an artifact of the Drude-like fit to the optical conductivity which definitely fails to describe

the multiphonon midinfrared maxima. The Drude formula is meaningless if the effective mass as well as the relaxation rate are frequency dependent. Their frequency dependence is itself a small polaronic feature. Low field measurements of the London penetration depth in high-T_c superconductors consistently yield larger m^* for polarons($\simeq 5m_e$) and $m^{**} \geq 10m_e$ for bipolarons. With a low value of the effective mass ($\sim 2m_e$) one fails to explain a low value of the *dc* mobility. Also the absence of the activation law in oxides at high temperatures is compatible with small polarons because the characteristic phonon frequency is very high ($\sim 1000K$), of the order of the activation energy, so the activation hopping can not be verified.

Here we present a discriminating selection of kinetic, optical, and photoemission experimental data, which unequivocally show that carriers in different insulating and superconducting oxides are small polarons and small bipolarons.

6.10.2 8.2 Small-polaron transport in TiO_2 and NiO

The comprehensive investigation of the small polaron transport has been performed in rutile TiO_2 by Bogomolov et al (1967). The small polaron transport mechanism was also proposed for NiO (Appel (1968), Austin and Mott (1969)). From experimental investigation of the drift and Hall mobilities, the infrared absorption, the thermoelectric power and comparison with the small polaron theory one gets quite convincing evidence for the small polaron transport in TiO_2. Figure 8.1 shows the drift and Hall mobilities for lightly reduced rutile above $100K$. The small value of the mobility is the most characteristic feature of TiO_2. For conduction perpendicular to the c axis the drift mobility shows an increase above room temperature with an activation energy of 0.13 eV. For conduction along the c axis the activation energy is 0.07 eV. The curve of the drift mobility has a minimum around room temperature, which is characteristic of small polarons if the activation region of parameters, $\omega < T \ll E_0$ is realised. The Hall depends depends on temperature, which is also characterister agreement with that in the high temperature region $\mu_H/\mu_d < 1$ is in agreement with that expected for
the adiabatic small polaron (Böttger and Bryksin (1985)). Normally, the activated behaviour of μ_H sets in at higher temperatures than for μ_d with a smaller activation energy. Thus the absence of an activated temperature dependence of μ_d only indicates that its activation region is not reached in the experiment. A striking feature in TiO_2 is that the Hall mobility is very small (~ 1 cm$^2/Vs$) above room temperature but rises to large value at temperatures below about $50K$. The drift mobility increases also with the temperature lowering up to the value about 50 cm$^2/Vs$ at 30 K , which also with the which, he explanation was given by Austin and Mott (1969). As we have discussed in Chapter 4 the polaron behaves like a heavy particle in a narrow band below $T \sim \omega_D/2$, and the relaxation time is determined by phonon and impurity scattering. The estimated polaron bandwidth is very small in rutile (see below), therefore single-phonon optical scattering is prohibited and twophonon contribution is frozen out. Thus a large increase in mobility is predicted at low temperatures, if the impurity scattering is not too strong.

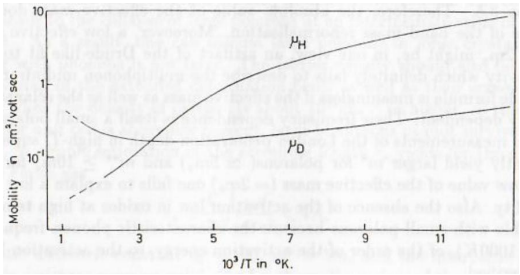

Fig.8.1. Hall μ_{H} and drift μ_d mobilities in TiO_2 as a function of the inverse temperature.

Semiconducting samples of TiO_2 show an absorption peak at $\sim$ 0.8eV which correlates in intensity with the magnitude of the conductivity. At temperatures above 50 K a single peak in the absorption is independent of the nature of the donor centres and attributed to small free polarons. Below $10K$, a single peak is observed at $\sim$ 1eV, the exact position depending on the nature of the donor centres, and this is attributed to bound polarons. The frequency and temperature dependence of the absorption coefficient of TiO_2 doped with Nb , measured by Kudinov et al (1969) agrees well with the MIR conductivity of small polarons (Böttger and Bryksin (1985)). From the analysis of the optical data the estimated characteristics of the small polaron are

$$E_p \simeq 0.4\text{eV}; E_a \simeq 0.2\text{eV}; g^2 = 4. \tag{8.6}$$

With the value of the transfer integral $T(\mathbf{a}) \simeq 0.1$eV estimated from band structure calculations one obtains by the use of the non-adiabatic small polaron theory (Chapter 4)

$$\sigma(\mathbf{a}) = T(\mathbf{a})e^{-g^2} \simeq 2meV, \tag{8.7}$$

and the effective mass enhancement

$$\frac{m^*}{m_e} \simeq 150 \tag{8.8}$$

The measurements of the line width of ESR on defect centres in TiO_2 for different carrier densities confirmed this estimation of the effective mass (Bogomolov et al (1968)).

As it was discussed by Austin and Mott (1969) nickel oxide is a Mott insulator, which becomes a p-type semiconductor when doped with lithium or partially reduced. The measured values of the drift and Hall mobilities are below 1 cm^2/V s at room temperature. However, because $\omega_D/2$ is rather high (about $400K$) the thermally activated hopping is hardly expected. Nevertheless, there is some evidence of hopping conduction to the thermally activated polaron hopping in Li-doped NiO. The estimated value of the polaronic level shift is $\sim$ 0.7eV, the polaron radius is 1Å, the bare transfer integral $T(\mathbf{a})$ is estimated at 0.3 eV contrasted with 0.1 eV for TiO_2. The polaron transfer integral is $\sigma(\mathbf{a}) < 12$meV which corresponds to $m^* > 30m_e$. The study of the polaronic transport in doped nickel oxide is complicated by the magnetic fluctuations. In NiO, μ_H shows an anomalous behaviour near the Neel point and the Hall constant changes sign. It seems certain that the sign reversal is associated with the onset of magnetic disorder cal absorption measurements are complicated by the state between 1 and 5 eV. An observed NIR absorptions

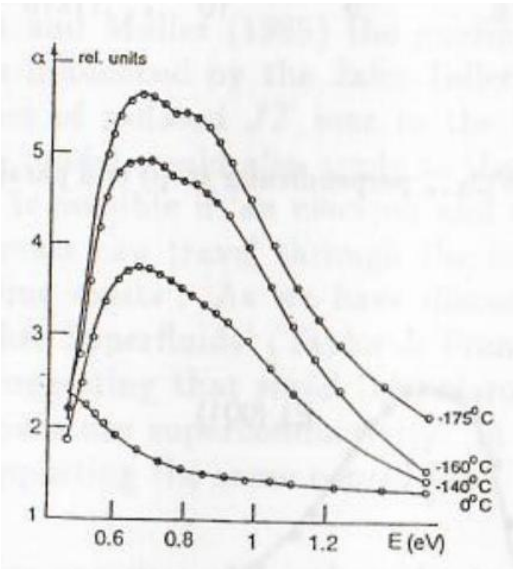

Fig.8.2. The absorbance of WO_{3-x} at low temperatures. Upon cooling poor metal $\delta - \mathrm{WO}_{3-x}$ transforms into (bi)polaronic semiconductor $\epsilon - WO_{3-x}$.

6.10.3 8.3 Mobile polarons and bipolarons in WO_{3-x}

Tungsten oxide, WO_{3-x}, studied in detail by a Cambridge group (Salje (1995)) shows properties of charge carrier transport, which cannot be described by those of free electrons. It is an almost ideal model compound for studies of polaronic transport because carriers can easily be generated or destroyed by chemical reactions or doping of WO_3 with $\mathrm{H}, \mathrm{V}, \mathrm{Mo}$ or implantation/removal of oxygen. They are not pinned to structural defects in crystals with reduced oxygen content because point defects are locally compensated. Formation of small polarons is specific for some structural
phases of WO_{3-x} but not for all. At room temperature and above $\delta - WO_{3-x}$ behaves as a poor metal. Its electronic transport is due to carriers with slightly enhanced mass and the Hall coefficient well in agreement with the predictions of almost free carriers with weak electron-phonon coupling, i.e. large polarons.

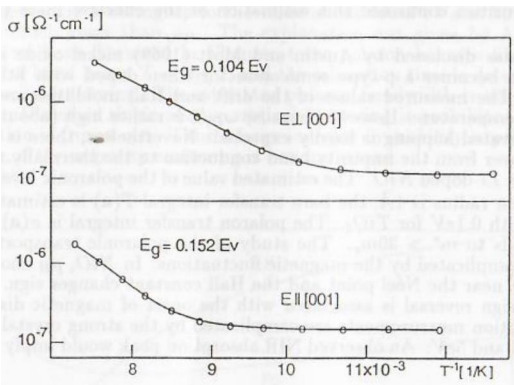

Fig.8.3. The conductivity of $\epsilon-W O_{3-x}$ perpendicular (top) and parallel (bottom) to the c-axis.

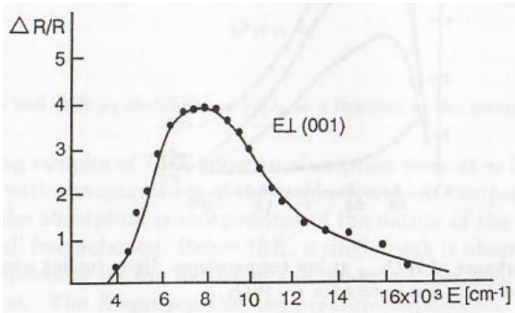

Fig.8.4. The energy dependence of the ESR photoeffect. $\Delta R/R$ is the relative change in ESR signal generated by illumination through splitting of bipolarons into pairs of small polarons ($T = 20K$).

The optical properties are dominated by Drude absorption and a fundamental absorption edge with $E_g = 2.77$eV, Fig.8.2. At temperatures close to 250 K , the crystal transforms on cooling into $\epsilon - WO_{3-x}$, which is insulating with a larger gap $E_g = 3.05$eV. The Drude absorption disappears. Instead, the optical absorption spectra display the (bi)polaronic profile, as shown in Fig.8.2. The experimentally observed profile shows a maximum at 0.71 eV , which corresponds to $E_p \simeq 0.3$eV, if
the IR conductivity is due to small polarons. The phonon energy results from the linewidth (section 4.11) and $\omega = 0.07$eV, i.e. in the expected spectral range of phonon modes of the WO_6 octahedra. The dc conductivity of $\epsilon - WO_{3-x}$ clearly shows the small (bi)polaron characteristics. The transport is thermally activated at $T \geq 100K$ with the activation energy $ca.E_p/2$ and tunneling in a (bi)polaronic band appears to occur at lower temperatures, Fig.8.3. When WO_3 is cooled in the dark, no ESR signal is observed in the ϵ-phase. This experimental result shows that all spins are paired in the ground state. The optical absorption shows a signal similar to that of polarons but shifted to higher energies about 1 eV. Single polarons are either generated thermally or, more conveniently, by photoexcitation of bipolarons. The fingerprint of single polarons is a strong ESR signal under illumination of $\epsilon - WO_{3-x}$ with the spectral dependence shown in Fig.8.4. The maximum efficiency occurs near 1 eV. The close similarity between the low-temperature absorption spectra and the spectral dependence of the ESR photoeffect suggests that the optical absorption is due to excitation of bipolarons. As the transport properties are highly two-dimensional ($\sigma_{ab} > 100\sigma_c$), it appears that bipolarons are confined to the $a - b$ plane, favoring the idea of disc-shaped bipolarons rather than spherical ones.

6.10.4 8.4 Small polarons in high- T_c oxides

According to Bednorz and Müller (1988) the guiding idea in searching for high- T_c superconductivity was influenced by the Jahn-Teller polaron model. Based on the experience from studies of isolated JT ions in the perovskite insulators, their assumption was that the model would also apply to the oxides, if they could be turned into conductors. This is possible if 'an electron and a surrounding lattice distortion with a high effective mass can travel through the lattice as a whole, and a strong electron-phonon coupling exists'. As we have discussed in 'High Temperature Superconductors and Other Superfluids' (Taylor & Francis (1994)) there is now a large body of experiments suggesting that small (bi)polarons are responsible for the phenomenon of high temperature superconductivity. In this section we discuss several recent observations supporting the same conclusion.

6.10.5 8.4.1 High- T_c oxides are doped semiconductors

The existence of 'parent' Mott insulators, which are spin ' 1/2 ' antiferromagnets suggest that high- T_c superconductors are, in fact, doped semiconductors. There is now a growing consensus that the dopant-induced charge carriers in high T_c oxides exhibit a significant dressing due to spin and lattice distortion. Studies of strongly correlated models like the Holstein $t-J$ model show that the critical electron-phonon coupling strength for polaron formation is considerably reduced by an antiferromagnetic exchange interaction compared to that in the uncorrelated model (section 5.5).

On the other hand, it has been suggested that optimally doped and overdoped oxides are metals with a large Fermi surface as follows from $ARPES$, the T^2 temperature dependence of resistivity, and from the small value of the Hall constant. However, the progress in elucidating the normal state of the prototypical cuprate $La_{2-x}Sr_xCuO4$ (Batlogg et al (1995), Hwang et al (1994)) leads us to the conclusion that optimally doped and overdoped copper oxides remain to be semiconductors. In
particular, semiconductor-like scaling with x of dc conductivity in $La_{2-x}Sr_xCuO_4$ for a wide temperature and doping region, Fig.8.5, has been observed.

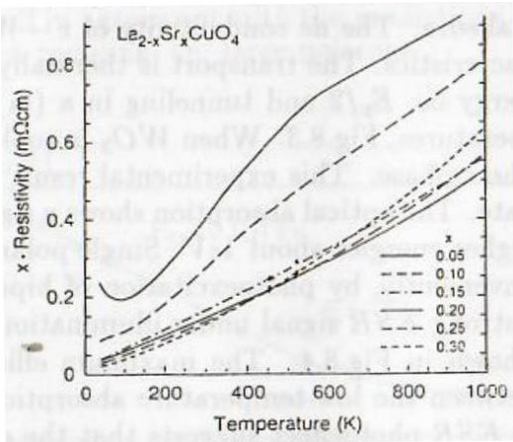

Fig.8.5. Resistivity of $\mathrm{La}{2-x} \mathrm{Sr}{x} \mathrm{CuO}_{4}$ multiplied by x covering the wide span of hole concentration from under to overdoping (Batlogg et al (1995)).

A plot of resistivity ρ multiplied by x brings $\rho(T)$ for various values of x on a similar scale, suggesting that the in-plane conductivity is dominated by holes, introduced with Sr, and that copper electrons remain localized even in overdoped oxides because of the large Hubbard U on copper and the local lattice deformation, which prevents their hopping.

Sometimes it is argued that unusual features of overdoped high- T_c oxides can be understood as a result of a strong magnetic pair-breaking if the spin-flip mean free path l_s is shorter than the coherence length ξ_0. However high- T_c oxides are at a 'clean' limit, the mean free path l is larger than ξ_0. This makes the magnetic pair breaking irrelevant for high- T_c because the strong inequality $l_s \ll l$ is unrealistic; normally $l_s \gg l$.

6.10.6 8.4.2 Low mobility

A low value of the in-plane mobility in high- T_c copper oxides is now well established. The Hall coefficient, dc conductivity, and hence the mobility in the CuO 2 planes were reported by MIT group (Chen et al (1995)) for single crystals of the prototypical cuprate La_2CuO_4 containing a few holes ($\sim 0.2\%$ per mole). In particular, they presented transport measurements

for current in the CuO 2 planes for two crystals. One of them, La_2CuO_{4+y}, referred to as $LCO-1$ in Fig.8.6, contained only enough oxygen accet a acce istic of undoped La_2CuO_4. The other, $La_{1.998}Sr_{0.002}CuO_4$ labeled as LSCO(295 K), has been reduced after growth to eliminate all excess oxygen. It contained about the same density of acceptors as $LCO-1$ and had almost the same Néel temperature. The in-plane mobilities are shown in Fig.8.6. Despite the different magnitudes of the mobilities the temperature dependencies are very similar and the absolute values are about 1 cm^2/Vs in the relevant temperature range near the superconducting transition in doped samples. A low effective mass of the oxygen-induced hole of only $\sim 2m_e$, as suggested by the Drude-like fit to the optical conductivity requires a surprisingly short scattering time and the concentration of ionized acceptors ten times larger than expected. Therefore, we believe that the effective mass of (bi)polarons in $LSCO$ should be enhanced up to $10m_e$ or more and (bi)polarons are small. This
conclusion is confirmed by the observation of an oxygen isotope effect on the Néel temperature in the insulating La_2CuO_4 suggesting the oxygen-mass dependence of the superexchange J (Zhao et al (1994))

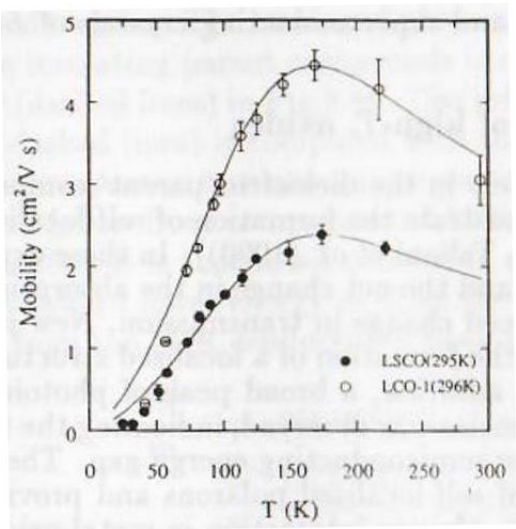

Fig.8.6. The in-plane mobilities of $LCO-1$ and $LSCO(295K)$ determined from Hall and conductivity measurements by Chen et al (1995).

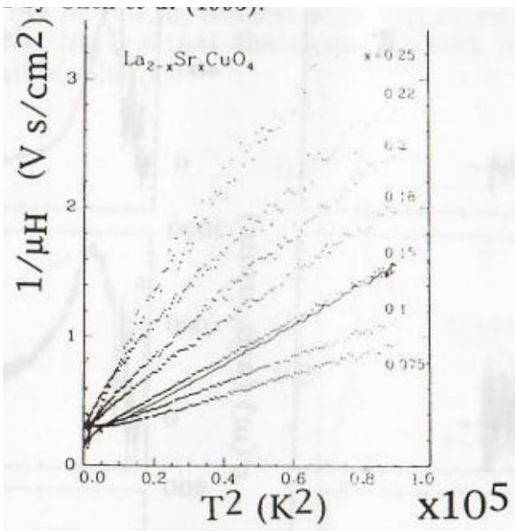

The latter is determined by the bandwidth and because of the small polaron band narrowing it depends on the phonon spectrum. This clear-cut experiment verified the crucial role of apex oxygen ions for the bipolaron formation in $LSCO$ in agreement with the first-principles calculations by Zhang and Catlow (1991), section 2.5. On the other hand, Mott (1995) has argued, that the polarons will necessarily produce also excited holes, which could be observed as light carriers.

The Hall mobilities of superconducting poly and single-crystals of $L_{2-x}Sr_xCuO_4$ were measured by Hwang et al (1994) over a wide temperature ($4-500$ K) and composition ($0 < x < 0.35$) range, Fig.8.7. For $x \leq 0.15$, the data follows a T^2 fit for $T > 100K$, with the systematic trend that the coefficient of the T^2 term increases with doping. This is in line with the bipolaron $2D$ kinetics as discussed in
section 7.8. The mobility value is between 1 cm$^2/Vs$ and 5 cm$^2/Vs$ for all measured temperatures and compositions. The Mott-Ioffe-Regel limit for the in-plane CuO_2 mobility is $ea^2/\hbar \simeq 2.5$ cm$^2/Vs(a \simeq 3.8$Å$)$. Therefore carriers are small polarons or bipolarons both in insulating and superconducting crystals of $LSCO$.

6.10.7 8.4.3 MIR conductivity of high- T_c oxides

Studies of photoinduced carriers in the dielectric 'parent' compounds like La_2CuO_4, $YBa_2Cu_3O_6$ and others demonstrate the formation of self-localised small polarons or bipolarons (Kim et al. (1988), Taliani et al. (1990)). In these experiments the sample was pumped by a laser beam and the net change in the absorption coefficient was determined from the photoinduced change in transmission. New photoinduced phonon modes were found indicating the formation of a localised structural distortion around a photogenerated carrier. In addition, a broad peak of photoinduced absorption in the electronic region of frequencies was observed, indicating the formation of localised electron states deep inside the semiconducting energy gap. These two aspects of the data confirm the formation of self-localised polarons and provide direct evidence of the importance of the electron-phonon interaction in metal oxides.

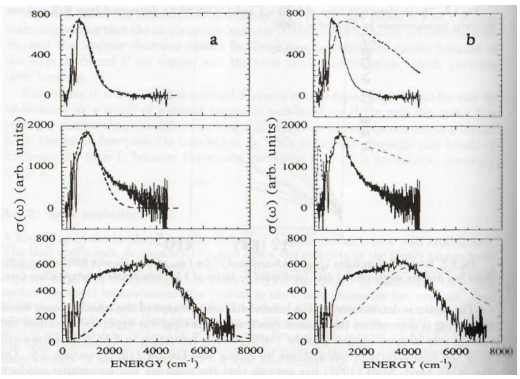

Fig.8.8 The photoinduced MIR conductivity in the insulator precursors for $\mathrm{Tl}{2} \mathrm{Ba}{2} \mathrm{CaCu}{2} \mathrm{O}{8}$ (top), $YBa_2Cu_3O_7$ (middle), and $La_{2-x}Sr_xCuO_4$ (bottom) compared with the polaron MIR conductivity (dashed line) (a); b: superconducting samples (dashed lines) compared with (a).

Mihailovic et al. (1990) described the spectral shape of the photoconductivity with the small polaron transport theory. They also argued that the similar spectral shape and systematic trends in both photoconductivity of optically doped dielectric samples and infrared conductivity of chemically doped high- T_c oxides indicate that carriers in the concentrated (metallic) regime retain much of the character of carriers in the dilute (photoexcited) regime. The measured photoinduced infrared conductivity $\sigma(\nu)$ (solid lines) in the insulating parent compounds is compared with the small-polaron MIR conductivity (dashed lines) in Fig.8.8a. The infrared conductivity of the high- T_c superconductors (dashed lines) is compared with the photoinduced infrared conductivity (solid lines) in respective insulator precursors in Fig.8.8b. One of the qualitative observations, which follow from comparison of MIR conductivities of insulating and superconducting materials is that in all perovskite exhibiting superconductivity, the peak energy shifts toward lower energy as T_c of the material increases. The polaron masses estimated from the MIR conductivity peak are

$$\begin{aligned} \frac{m^*}{m_e} &= 23(LSCO) \\ &= 13(YBCO) \\ &= 11\,(Tl_2Ba_2CaCu_2O_8) \end{aligned} \tag{8.9}$$

The critical temperature of the superconducting transition turns out to be inversely proportional to m^* in full agreement with the bipolaron theory of high- T_c superconductivity. That implies that the charge carriers in the normal state of high- T_c cuprates are small bipolarons.

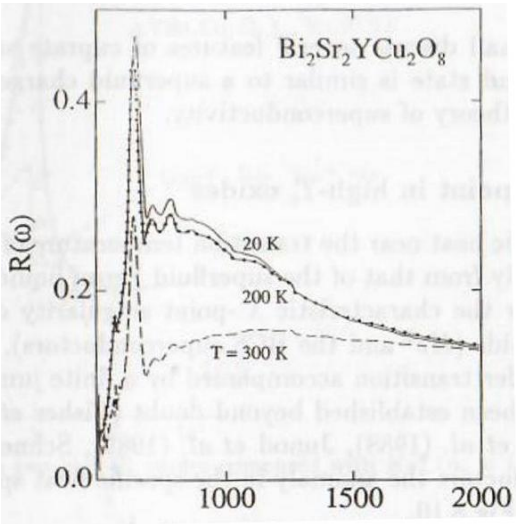

Photon Energy (cm^{-1})

Fig.8.9. MIR reflectivity $R(\nu)$ for BSYCO single crystal at three different temperatures.

It follows from two upper curves of Batlogg's scaling of resistivity with x, Fig. 8.7 that the self-trapped (bi)polarons can be trapped by impurities. Falk et al (1993) measured the temperature dependence of the MIR reflectivity of lightly-doped La_2CuO_4. They found the large difference between the optical 0.13 eV and thermal 0.035 eV ionization energy. This observation as well as the line shape and the temperature dependence of the MIR peak are consistent with absorption from polaronic impurity states.

Calvani et al (1994, 1995) in a series of papers reported a fine structure of the MIR conductivity in several copper oxides, as predicted by the numerical calculations of the optical conductivity of the Holstein clusters (Alexandrov et al (1994b)), Fig.4.6. As an example, the MIR reflectivity of a single crystal of insulating $Bi_2Sr_2YCu_2O_8(BSYCO)$ is shown in Fig. 8.9 for three different temperatures. Therein, a strong infra-red band is observed, with a clear and T - dependent fine structure, together with the phonon peak at 610 cm^{-1}. Starting from $300K$, the amplitude of the IR band increases by a factor of two for T decreasing to $200K$, then it saturates. For the same temperature variation, the phonon peak at 640 cm^{-1} increases by less than 20%. The fine structure has been explained in terms of overtones of additional modes, which strongly depend on doping and temperature. These modes correspond to vibration of the locally perturbed lattice and are quite general features, as they appear also in the metallic phases of several high- T_c oxides. The finding that in the metallic phases of many cuprates the polaron band in the optical absorption is superimposed on a normal Drude term, implies that the carriers, responsible for superconductivity could represent either a normal Fermi liquid coexisting with a substrate of small polarons, or the coherent part of a small-polaron fluid. The correlation of the position of the MIR peak with the value of T_c favors the second scenario.

6.10.8 8.5 Small bipolarons in high- T_c oxides

We now shall discuss several features of cuprate superconductors which show that their ground state is similar to a superfluid charged Bose gas, as predicted by the bipolaron theory of superconductivity.

6.10.9 8.5.1 λ-point in high- T_c oxides

The specific heat near the transition temperature of the superfluid Bose liquid differs significantly from that of the superfluid Fermi liquid. Bose liquids (or more precisely He^4) show the characteristic λ-point singularity of their specific heat. Superfluid Fermi liquids (He^3 and the BCS superconductors), on the contrary, exhibit a sharp second order transition accompanied by a finite jump in the specific heat.

It has been established beyond doubt (Fisher et al. (1988), Loram et al. (1988), Inderhees et al. (1988), Junod et al. (1989), Schnelle et al. (1990)) that in high T_c superconductors the anomaly in the specific heat spreads to about $|T - T_c| / T_c \sim 0.1$ or larger, Fig.8.10.

The estimations with the canonical gaussian fluctuations yield an unusually small coherence volume, Table 8.1, comparable with the unit cell volume, $\Omega \simeq 167\text{Å}^3$ in $YBCO$ (Loram et al. (1992)). That means that the overlap of pairs is small (if any). Moreover it was stressed by Salamon et al (1990) that the heat capacity anomaly is logarithmic, and consequently, cannot be adequately treated by gaussian corrections to the mean field BCS heat capacity.

On the other hand one can rescale the absolute value of the specific heat and the temperature to compare the experimentally determined specific heat of He^4 with that of high- T_c oxides (Alexandrov and Ranninger (1992a)), Fig.8.10. The specific heat per boson in the two high T_c oxides practically coincides with that of He^4 ($n_b = 1$) in the entire region of the λ singularity. In fact for the 2223 compound the λ shape is experimentally better verified than in He^4 itself because of the fifty times larger value

Table 8.1: The coherence volume Ω in $\dot{A}^{3}$, the in-plane ξ_{ab} and out- of- plane ξ_c coherence lengths derived from a Ginzburg-Landau analysis of the specific heat (Loram et al. (1992)).

Compound	Ω	$\xi_{ab}^2, \left(\text{Å}^2\right)$	$\xi_c, (\text{Å})$
$YBa_2Cu_3O_7$	400	125	3.2
$YBa_2Cu_3O_{7-0.025}$	309	119	2.6
$YBa_2Cu_3O_{7-0.05}$	250	119	2.1
$YBa_2Cu_3O_{7-0.1}$	143	119	1.2
$Ca_{0.8}Y_{0.2}Sr_2Tl_{0.5}Pb_{0.5}Cu_2O_7$	84	70	1.2
$Tl_{1.8}Ba_2Ca_{2.2}Cu_3O_{10}$		40	< 0.9

of the critical temperature. The density of nonlocalised bosons $n_b(T_c)$ determined from the heat capacity fit to He^4 is very close to that determined from the Hall measurements:

$$n_b \simeq 1.8 \times 10^{21} \text{ cm}^{-3} \tag{8.10}$$

in the optimally doped $YBCO$. The specific heat of a single crystal of $YBa_2Cu_3O_7$ was measured with the magnetic fields up to $8T$ providing strong evidence for the critical exponents consistent with those observed in He^4 (Overend et al. (1994)).

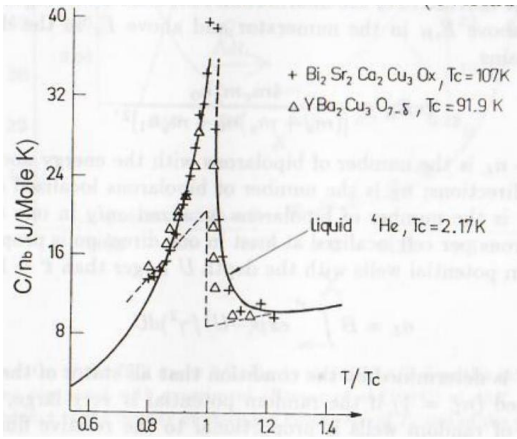

Fig.8.10. Heat capacity anomaly in two high- T_{c} oxides compared with He^4 $(n_b = 1)$, solid line

and with the BCS curve, dashed line.

6.10.10 8.5.2 Doping dependence of R_H, T_c and λ_H

The two-band bipolaron model discussed in section 6.2 allows us to explain an outstanding problem of the metal-semiconductor duality of overdoped copper oxides and the doping dependence of the critical temperature and the London penetration depth (Alexandrov (1995)).

It is well known that the effective mass anisotropy of energy ellipsoids in a square (or cubic) lattice diminishes the value of the Hall constant as in Si or Ge. In the presence of disorder an ' x ' -bipolaron can be localized in the y direction tunneling
practically freely along x and a ' y '-bipolaron can be localized in the x direction remaining free along y. That gives a very low metallic-like R_H, which presumably is due to bipolarons with the energy above the Hall mobility edge, $E > E_{cH}$. At the same time the dc conductivity remains proportional to the number of bipolarons above the mobility edge, which lies below, $E_c < E_{cH}$. To support this conclusion quantitatively one can adopt the effective mass approximation, Fig. 6.2

$$E_{\mathbf{k}}^{x,y} = \frac{k_x^2}{2m_{x,y}} + \frac{k_y^2}{2m_{y,x}} \tag{8.11}$$

with $m_x = 1/t$ and $m_y = 4m_x$. The Boltzmann equation in the relaxation time approximation yields (section 4.11)

$$R_H \sim \frac{\sum_{\mathbf{k},n=x,y} n'\left(E_{\mathbf{k}}^n\right)\left(\frac{\partial^2 E_{\mathbf{k}}^n}{\partial k_x^2}\left(\frac{\partial E_{\mathbf{k}}^n}{\partial k_y}\right)^2 - \frac{\partial E_{\mathbf{k}}^n}{\partial k_y}\frac{\partial E_{\mathbf{k}}^n}{\partial k_x}\frac{\partial^2 E_{\mathbf{k}}^n}{\partial k_y \partial k_x}\right)}{\left(\sum_{\mathbf{k},n} n'\left(E_{\mathbf{k}}^n\right)\left(\frac{\partial E_{\mathbf{k}}^n}{\partial k_x}\right)^2\right)^2}, \tag{8.12}$$

where $n'\left(E_{\mathbf{k}}^n\right)$ is the derivative of the distribution function. Counting bipolarons (n_0), with the energy above E_{cH} in the numerator and above E_c in the denominator of Eq.(8.12) one obtains

$$2eR_H = \frac{4m_x m_y n_0}{\left[\left(m_x + m_y\right) n_0 + m_y n_1\right]^2} \tag{8.13}$$

where $n_0 = x/2 - n_L$ is the number of bipolarons with the energy above E_{cH}, which are free in both directions; n_L is the number of bipolarons localized at least in one direction, and

n_1 is the number of bipolarons localized only in one direction. The number of bipolarons per cell localized at least in one direction is proportional to the number of random potential wells with the depth U larger than $t' \sim 1/m_y$

$$n_L = B \int_{-\infty}^{-t'} \exp\left(-U^2/\gamma^2\right) dU \tag{8.14}$$

The coefficient B is determined by the condition that all states of the Brillouin zone should be localized ($n_L = 1$) if the random potential is very large, $\gamma \gg t'$. The average depth γ of random wells is proportional to the relative fluctuation of the dopant density, which is the square root of the mean density x

$$\gamma = \gamma_0 \sqrt{x}. \tag{8.15}$$

Here γ_0 is the characteristic binding energy independent of the dopant density. That yields $B = \frac{2}{\gamma\sqrt{\pi}}$ and

$$n_0 = x/2 + \mathrm{erf}(\kappa/\sqrt{x}) - 1 \tag{8.16}$$

with $\kappa = t'/\gamma_0$. The number of bipolarons, $n_0 + n_1$, above the mobility edge E_c contributing to the longitudinal conductivity remains practically equal to the chemical density $x/2$ in a wide range of κ which can be verified with Eq.(8.14) replacing t' for $t = 4t'$. As a result, the Hall density $n_H = 1/2eR_H$ to the chemical density ratio is given by

$$\frac{n_H}{x/2} = \frac{[5x + 2\,\mathrm{erf}(\kappa/\sqrt{x}) - 2]^2}{16x[x + 2\,\mathrm{erf}(\kappa/\sqrt{x}) - 2]} \tag{8.17}$$

with $\mathrm{erf}(z) = \frac{2}{\sqrt{\pi}} \int_0^z \exp\left(-\xi^2\right) d\xi$. The agreement with the experiment is almost perfect for $\kappa = 0.57$, Fig.8.11. Due to the mass anisotropy the low temperature 'physical' density n_H remains c.1.6 times larger than the chemical $x/2$ even for low doping when $n_L \ll x/2$. The dc conductivity scales with x in overdoped samples as observed, Fig.8.5. because $n_0 + n_1 \simeq x/2$ for all x. On the contrary, the density n_0 of carriers extended in both directions falls rapidly in overdoped samples, Fig.8.11 (inset), due to increasing random potential fluctuations, proportional to $\sqrt{x}$. The mass anisotropy of the order of 4 can be seen commonly in doped semiconductors. However the anisotropy increases rapidly in overdoped samples. In fact, we believe that the large Hall to chemical density ratio, Fig.8.11 is a measure of this anisotropy and has nothing to do with a large Fermi surface.

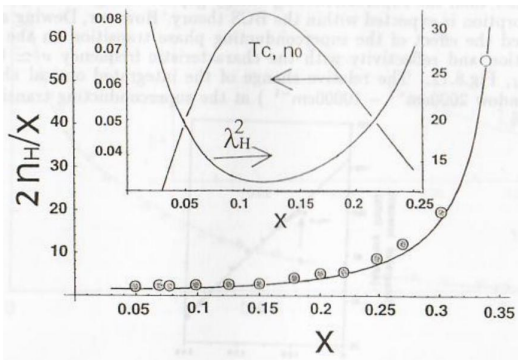

Fig.8.11. The ratio of the Hall $n_{H} =1 / 2 e R_{H}$ to chemical $x/2$ densities in $La_{2-x}Sr_xCuO_4$ as a function of doping compared with experiment (Hwang et al (1994)) at $40K$. Inset represents the theoretical dependence of the density of extended bosons n_0, of T_c and of the penetration depth (in relative units).

The critical temperature for the condensation of CBG is proportional and the London penetration depth squared is inversely proportional to the density n_0 of delocalised bosons in $2+\epsilon$ dimensions. Therefore

$$T_c \sim x + 2\,\mathrm{erf}(\kappa/\sqrt{x}) - 2$$

and

$$\lambda_H^2(0) \sim \frac{1}{x + 2\,\mathrm{erf}(\kappa/\sqrt{x}) - 2} \tag{8.19}$$

With these equations one can easily explain the doping dependence of $T_c(x)$ in superconducting oxides as well as the so-called 'Uemura' plot $T_c \sim 1/\lambda_H^2$ verified experimentally in underdoped and overdoped samples (Uemura (1995)), Fig.8.11 (insert).

As a result the metallic value of the Hall effect and the semiconducting scaling of *dc* conductivity in overdoped high- T_c oxides as well as the doping dependence of the critical temperature and of the London penetration depth can be explained by taking into account the localization of bipolarons in a random potential. Then both underdoped and overdoped high- T_c oxides are doped semiconductors with oxygen bipolarons as carriers partly localized by disorder.

6.10.11 8.5.3 NIR absorption in $YBCO$

Another piece of evidence for bipolarons in high - T_c oxides and their Bose-Einstein condensation comes from the near infrared (NIR) absorption in the high frequency region ($\nu \sim 0.5-0.7$eV) (Afexandrov et al. (1993)). It is well known that for frequencies much higher than the superconducting energy gap no change with temperature in optical absorption is expected within the BCS theory. However, Dewing and Salje (1992) observed the effect of the superconducting phase transition on the near infrared absorption and reflectivity with the characteristic frequency $\nu \simeq 0.7$eV in $YBa_2Cu_3O_{7-\delta}$, Fig.8.12. The relative change of the integrated optical absorption (frequency window 2000 cm^{-1} – 10000 cm^{-1}) at the superconducting transition was as high as 10%.

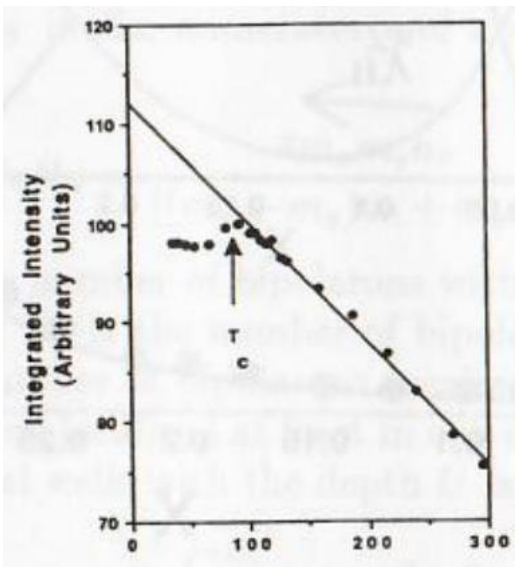

Temperature (K)

Fig.8.12. The temperature dependence of the NIR absorption near 5000 cm^{-1} in $YBa_2Cu_3O_7$.

This observation is in line with the temperature dependence of the optical bipolaronic conductivity, as discussed in section 6.5. The effect of the superconducting phase transition on NIR absorption is explained by the Bose-Einstein condensation of small bipolarons. Triplet intersite bipolarons, which are thermally activated, are responsible for the temperature dependence of the NIR conductivity in the normal state. The temperature dependence of the MIR and NIR reflectance and transmittance of thin Y *BCO* films was found to be consistent with the powder absorbance measurements (Yagil et al (1995)). In these regimes the optical energy is much higher than both temperature and superconducting energy gap, therefore the temperature dependence in the normal and in the superconducting states is anomalous and cannot be explained within a normal Fermi liquid approach.

6.10.12 8.5.4 Upper critical field of high- T_c oxides

The superconducting transition in a magnetic field for a wide temperature range starting from mK-level up to T_c has been reported by Mackenzie et al. (1993) in overdoped Tl-based cuprate. Resistively determined H_{c2} values from $T/T_c = 0.0025$ to $T/T_c = 1$ in a $T_c = 20$ K single crystal of $Tl_2Ba_2CuO_{6+\delta}$ follow the temperature dependence that is in good qualitative agreement with the type of curve for CBG, Fig.7.3 for $n_L/n \simeq 1$.

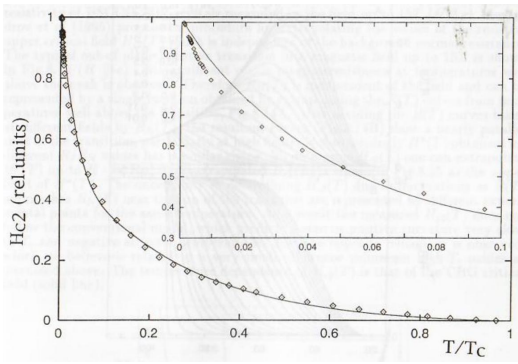

Fig.8.13. The upper critical field of $\mathrm{Tl}*{2}* *\mathrm{Ba}*{2}* \mathrm{CuO}_{6+\delta}$ compared with the critical field $H^*(T)$ of CBG.

Osofsky et al. (1993) also observed the divergent upward temperature dependence of the upper critical field $H_{c2}(T)$ for thin *BSCO* films, which was 5 times that expected for a conventional superconductor at the lowest temperature. The observed dependencies of $H_{c2}(T)$ are remarkably different from that predicted with the canonical Ginzburg-Landau theory, $H_{c2} \sim T_c - T$. The unusual temperature dependence of H_{c2} of a 'low T_c ' overdoped $Tl_2Ba_2CuO_{6+\delta}$ can be quantitatively described by the formula for the BEC critical field, derived in section 7.7 ,

$$H^*(T) = \text{ constant } \times \left(\frac{1 - 2n_L(\tau)/x}{\tau\,[1 - 2n_L(1)/x]} - \sqrt{\tau} \right)^{3/2} \tag{8.20}$$

Here $\tau = T/T_c$ with T_c the experimental critical temperature, x is the chemical polaron density determined in $Tl_2Ba_2CuO_{6+\delta}$ by the excess oxygen content $\delta, x = 2\delta$, and $n_L(\tau)$ is the number of localized bipolarons. $x/2 - n_L$ should be very small. In fact, at zero temperature the condition $2n_L(0)/x = 1$ is satisfied because each bipolaron is localised on the excess oxygen ion. In the 'single well-single particle' approximation
the number of localised bipolarons is determined by

$$n_L(\tau) = \int_{-\infty}^{0} d\epsilon \frac{N_L(\epsilon)}{\exp(\epsilon/T) + 1} \tag{8.21}$$

where $N_L(\epsilon)$ is the density of localised states.

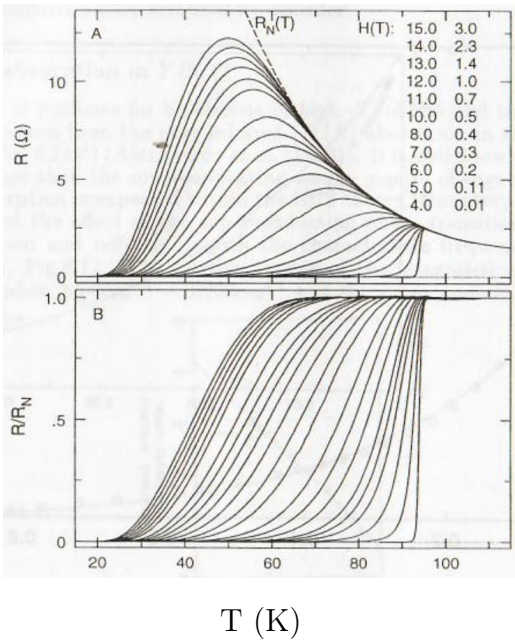

Fig.8.14. C-axis resistivity of single -crystal $Bi_2Sr_2CaCu_2O_8$ in a magnetic field (A) normalised with respect to the normal state resistivity (B).

The positive curvature of $H^*(T)$ on the temperature scale of the order of T_c does not depend on the particular shape of $N_L(\epsilon)$. However, at mK temperatures shallow potential wells are important. Therefore the low-temperature behaviour of $H^*(T)$ is sensitive to the shape of $N_L(\epsilon)$ just below the mobility edge. One can model

$$N_L(\epsilon) = 0.5 n_L(0) \left[\frac{e^{\epsilon/\gamma}}{\gamma} + \delta\left(\epsilon + E_0\right) \right] \tag{8.22}$$

to imitate both the discrete levels with the energy E_0 and the exponential shallow tail due to the randomness of the impurity potential. Then one can quantitatively describe the experimental curve $H_{c2}(T)$ with Eq.(8.20) and $\gamma/T_c = 0.13$ and $E_0/T_c = 0.3$ for three decades of temperature, Fig.8.13. This equation was also applied by Osofsky et al (1993, 1994) to describe H_{c2}(T) of $Bi_2Sr_2CuO_y$ with an excellent agreement for the critical temperature.

However, in the highest T_c cuprates the in-plane superconducting transition is known to display pronounced broadening in a magnetic field, with the top of the
transition having a much weaker field dependence than in the region near the bottom. This together with the high values of H_{c2} have made an experimental determination of H_{c2} very difficult in materials with $T_c > 60K$, with the consequence that widely varying values of $H_{c2}(0)$ have been estimated based on different models. The out-of-plane resistive transition shows a different behaviour in a magnetic field. An increasingly pronounced maximum (peak) developes below T_c and shifts to lower temperature rather than broadened with increasing field. By the use of the out-of-plane resistivity of BSCCO-2212 crystals measured in the field up to $15T(H\|c)$ Alexandrov et al (1995) proposed a procedure for extrapolating the values of the resistive upper critical field $H_{c2}(T)$ which is independent of the background normal resistance. The typical out-of-plane resistive transition in a magnetic field up to $15T$ is shown in Fig.8.14 ($H\|c$). No significant c -axis magnetoresistance at temperatures well above the peak is observed. Therefore $R_N(T)$ is independent of the field and can be represented by a single function obtained by extrapolating the $R(T)$ curves from temperatures well above the transition, Fig.8.14A. After dividing the $R(T)$ curves taken at different fields by $R_N(T)$, the resultant curves (Fig.8.14B)

show a nearly parallel shift of the transition, particularly at high fields. Not surprisingly $H^*(T)$ obtained for different R/R_N values has a similar shape. To determine $H_{c2}(T)$ one can extrapolate $H^*(T)$ up to $R \longrightarrow R_N$. The extrapolated $H_{c2}(T)$ is shown in Fig.8.15 as the upper limit of $H^*(T)$. The uncertainty in determining $H_{c2}(T)$ due to fluctuations as $R(T)$ approaches $R_N(T)$ near the top of the transition are represented by different experimental points for the same temperature. As a result the measured $H_{c2}(T)$ does not follow the conventional model, which predicts a zero or positive curvature very close to T_c and negative at lower temperatures. Just the opposite behaviour is observed, which we believe is related to a very small coherence volume in high- T_c oxides as discussed above. The temperature dependence of $H_{c2}(T)$ is that of the CBG critical field (solid line).

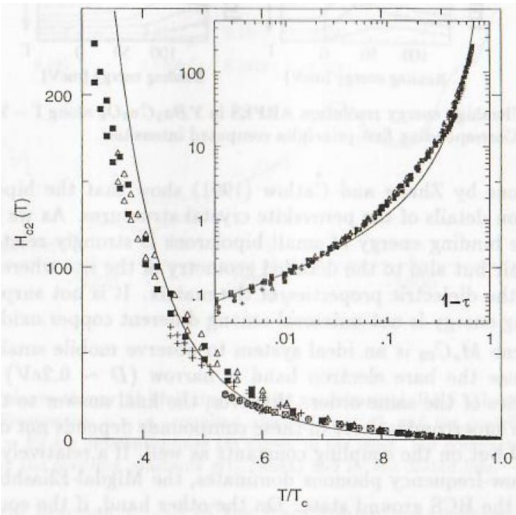

Fig.8.15. Resistive upper critical field of high- T_{c} BSCCO - 2212 single crystals.

6.10.13 8.6 Polaronic ARPES in high- T_c oxides and fullerene

Small- polaron features of the energy spectrum and the formation of bipolarons can be verified by the angle resolved photoemission spectra (ARPES) as discussed in section 4.12. We believe that the high resolution ARPES (Gofron et al (1994)) shows such features, Fig.8.16. The extremely flat anisotropic bands have been measured in several copper high- T_c oxides which display at least an order of magnitude less dispersion than the first-principles band structure methodology can provide (Fig.8.16b). This flatness is due to the polaron narrowing of the band, and the anisotropy is due to the remarkable difference of p_x overlaps in x and y direction, respectively. If bipolarons are formed the spectral weight is shifted down by half of the bipolaron binding energy with respect to the chemical potential. This could provide an explanation why the flat band observed with $ARPES$ in $Y\mathrm{Ba_2Cu_4O_8}$ does not cross the Fermi level. It lies approximately 20 meV below the chemical potential which means that the bipolaron binding energy is about $\Delta \simeq 40$meV in this material.

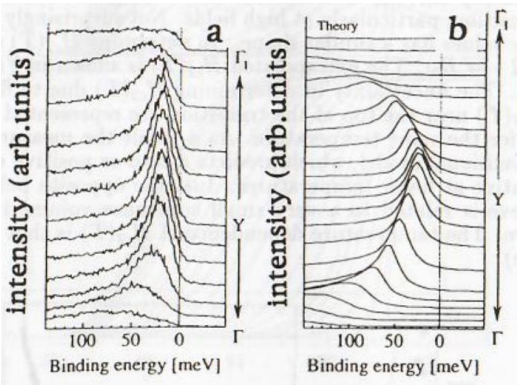

Fig.8.16. (a) Ultrahigh energy resolution ARPES in $\mathrm{YBa}{2} \mathrm{Cu}{4} \mathrm{O}_{8}$ along $\Gamma - Y$ direction of the Brillouin zone. (b) Corresponding first-principles computed intensities.

The calculations by Zhang and Catlow (1991) show that the bipolaron binding energy depends on details of the perovskite crystal structures. As we have discussed in Chapter 2 the binding energy of small bipolarons is strongly related not only to the size of the pair but also to the detailed geometry of the site where the polaron is situated and to the dielectric properties of the matrix. It is not surprising that the bipolaron binding energy is not universal among different copper oxides.

Doped fullerene M_xC_{60} is an ideal system to observe mobile small polarons and bipolarons because the bare electron band is narrow ($D \sim 0.2$eV) and there are phonon frequencies of the same order. However, the final answer to the question on the nature of the superconductivity in these compounds depends not only on the adiabatic ratio ω/D but on the coupling constants as well. If a relatively weak coupling ($\lambda \leq 0.5$) with low-frequency phonons dominates, the Migdal-Eliashberg theory can be applied with the BCS ground state. On the other hand, if the coupling is strong or high-frequency phonons are involved, our bipolaron theory should be applied. The photoemission spectroscopy of a molecule C_{60}^{-}(Gunnarsson et al (1995)) allows us to estimate the relative contribution of different phonon modes to the electron-phonon interaction (Alexandrov et al (1995b)). The Hamiltonian at hand, describing three degenerate t_{1u} electron states coupled with phonons, is diagonalised with respect to the coupling with the A_{g2}-vibration mode using the canonical Lang-Firsov displacement transformation $\exp(S)$ with the following result

$$\tilde{H} = -E_p^{A_{g2}} \sum_{m=1}^{3} \psi_m^\dagger \psi_m + \sum_{\nu=1}^{8} g^\nu \omega_\nu \sum_{n,m=1}^{3} \psi_n^\dagger M_{nm}^\nu \psi_m + \sum_{\nu}^{8} \sum_{\mu=1}^{5} \omega_\nu n_{\nu,\mu} \tag{8.23}$$

where $E_p^{A_{g2}} = \left(g^{A_{g2}}\right)^2 \omega_{A_{g2}}$ is the polaron shift due to the A_{g2} mode, $\hat{M}^\nu$ is the Hermitian dimensionless coupling matrix (of order of unity) for the five-fold degenerate H_g modes, and $n_{\nu,\mu}$ are the phonon occupation numbers for H_g modes.

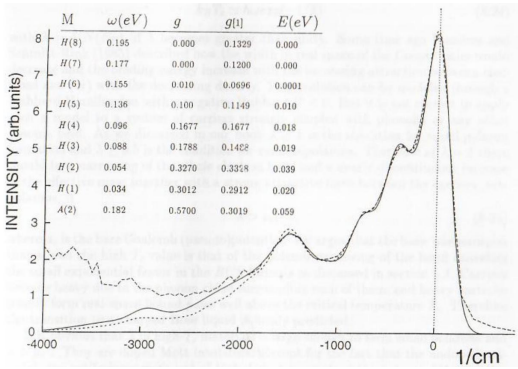

Fig.8.17. Polaron theory fit (full line) to the experimental PES (Gunnarsson et al (1995)) (dashed line). Frequencies $\omega= \omega_{\nu}$, coupling constants $g = g^{\nu}$, and the contribution to the ground state energy $E = E_p^{\nu}$ for different modes are shown in the inset. For comparison the variational fit is represented by the coupling constants g[1], (inset) and by the dotted line.

The spectral function $I_{pol}(\omega)$ of the Hamiltonian is calculated by the numerical diagonalisation in truncated Hilbert space for the H_g modes and integrated with the Gaussian instrumental resolution function of width $\sim$ 41meV as described in section 4.12. Thus one can fit the PES in a wide energy region as shown in Fig.8.17 with
g^{ν} being the fitting parameters. Due to an exact treatment of $A_g(2)$ mode the highenergy part of PES including the maximum at ca.3000 cm^{-1} is better represented compared with the variational analysis by Gunnarsson et al. The coupling with high frequency phonons $\omega_{\nu} \geq 0.096$eV dominates in the electron-phonon interaction as one can see in the inset of Fig.8.17, where the coupling to the $A_g(2)$ high-frequency mode turns out to be most important. This fact as well as the observation of the phononsided bands in PES by itself suggest that the nonadiabatic small polaron theory of this book rather than the adiabatic Migdal-Eliashberg approach should be applied to M_xC_{60}.

6.11 Conclusion

In this book we have put forward a multi-polaron theory of low-mobility solids. We believe that this theory is the only possibility for a description of what happens to the BCS model for superconductivity, in which

$$k_B T_c \simeq \hbar\omega \exp(-1/\lambda) \tag{8.24}$$

with $\lambda = VN(E_F)$, if λ becomes greater than unity. Some time ago Noziéres and Schmitt-Rink (1985) described how the width in real space of the Cooper pairs would decrease and the binding energy increase with the increasing attraction between electrons and (or) with the decreasing density. This evolution can be modeled through a Hubbard Hamiltonian with a negative Hubbard $U < 0$. But it is not correct to apply such a model to a system of carriers strongly coupled with phonons or any other bosonic field. As we discussed in our book $\lambda \geq 1$ is the condition for small polaron formation and $\lambda \geq 0.5$ is the condition for small bipolarons. Therefore at $\lambda \sim 1$ there should be a narrowing of the whole electron band and a nearly discontinuous increase in the effective mass together with a strong attractive force between the carriers, now polarons, if

$$\lambda > \mu_c \tag{8.25}$$

where μ_c is the bare Coulomb (pseudo)potential. We argue that the basic phenomenon that allows the high T_c value is that of the polaron narrowing of the band canceling the small exponential factor in the BCS formula as discussed in section 5.3. Carriers become heavy due to the phonon cloud surrounding each of them, and heavy particles readily form real-space bound pairs well above the critical temperature T_c. Therefore the transition to a charged Bose liquid is firmly predicted.

Is it obvious that λ in high- T_c materials is large enough to form small polarons and $\lambda > \mu_c$? They are doped Mott insulators. Except for the fact that the undoped materials are antiferromagnets and of high dielectric constant the nature of the carriers will be similar to that in $Si : B$: holes tunneling in a narrow band. The strong correlations will further decrease the bandwidth and therefore increase the bare $N(E)$ in a rigid lattice - just the condition for large λ. This conclusion is perfectly confirmed by the numerical calculations within the Holstein $t - J$ model, as discussed in section 5.5. One can argue that the Coulomb repulsion is not suppressed in narrow bands because there is no retardation contrary to the wide-band BCS superconductors. But it is well established for some simple metals that $\lambda > \mu_c$ even without retardation and the static dielectric constant $\epsilon(q, 0)$ is negative for finite q. Many models with a pure 'electronic' mechanism of pairing have been discussed in the literature during the last decade. To the best of our knowledge none of them has explained how to
overcome the direct Coulomb repulsion by the exchange Coulomb attraction. This is quite unlikely at the small distance of the order of two lattice constants, which is the characteristic size of pairs in high- T_c oxides. In contrast, the question does not arise for the electron-phonon interaction. The Coulomb repulsion in ionic solids is screened by polar optical phonons and the deformation potential rather easily makes $\lambda > \mu_c$.

We take the point of view that the carriers in a doped Mott insulator are small bipolarons surrounded by the spin and lattice polarised region. Both spin and lattice polarisation contribute to the high effective mass $m^{**} > 10m_e$, but only the latter to the isotope effect. In general, bosons and unbound electrons (or holes) can coexist, but trapping of bosons in a random field explains alone the metal-semiconductor duality of overdoped copper oxides.

According to the Fermi liquid (FL) scenario high- T_c superconductors are metals with a large Fermi surface of copper electrons. Within this scenario the pronounced deviation from the canonical FL behavior are due to the Fermi surface anisotropy and a large damping. We believe that the existence of the Mott parent insulators suggests just the opposite scenario according to which high- T_c superconductors are doped semiconductors with hole carriers bound into small bipolarons. All thermodynamic and kinetic properties favor this model.

Some direct evidence that these materials contain a charged $2e$ Bose liquid would be highly desirable. We have discussed the thermal conductivity; the contribution from the carriers given by the Wiedemann-Franz ratio depends strongly on the elementary charge as $\sim (e^*)^{-2}$ and should be significantly suppressed in case of $e^* = 2e$ compared with the Fermi-liquid contribution. The evidence for $e^* = 2e$ is strong, but perhaps not entirely convincing because one has to subtract the much larger phonon contribution to the heat transport. Stronger evidence comes from the measurements by Dewing and Salje (1992) of the temperature dependent infrared absorption band, centered at $\sim 0.5 - 0.7$eV as discussed in section 8.5.3. The intensities of absorption and transmission show a pronounced change of the slope of the temperature dependence at $T = T_c$, which is unusual at frequencies as high as 20 times of an estimated BCS gap. We have explained this observation assuming that below T_c a macroscopic proportion of singlets are condensed into the state with zero total momentum and hence with zero dipole moment. Possibly the most striking evidence for the charged Bose-liquid in high- T_c oxides comes from the unusual temperature dependence of the upper critical field H_{c2} as discussed in section 8.5.4. The direct experiment could be the classical Aharonov-Bohm interference above T_c in a mesoscopic oxide with low T_c at low temperatures where the inelastic mean free path is

large.

In using this model, we have to realise that the insulating properties of a Mott insulator do not depend on the ordering of the spins; they persist above the Neel temperature, and arise because the on-site Coulomb repulsion is larger than the polaron bandwidth. From the observation by Morris and co-workers (Zhao et al (1994)) of the oxygen isotope effect on the Néel temperature in La_2CuO_4 we know that the polaron band narrowing takes place also in the Mott insulators.

The problem of low-mobility conductors became a challenging problem about half a century ago, when the low mobility was observed in transition-metal oxides. The explanation was found with polarons. With the discovery of high- T_c superconductors this problem received renewed attention. We believe that bipolarons are the explanation.

7 Fröhlich Polarons: Lecture course including detailed theoretical derivations by Devreese. Single polaron

Abstract

Based on a course presented by the author at the International School of Physics Enrico Fermi, CLXI Course,."Polarons in Bulk Materials and Systems with Reduced Dimensionality", Varenna, Italy, 21.6. - 1.7.2005, including further developments since 2005.

In the present course, an overview is presented of the fundamentals of continuum-polaron physics, which provide the basis of the analysis of polaron effects in ionic crystals and polar semiconductors. These Lecture Notes deal with “large”, or “continuum”, polarons, as described by the Fröhlich Hamiltonian. The emphasis is on the polaron optical absorption, with detailed mathematical derivations.

Appendix A treats optical conductivity of a strong-coupling polaron.

Appendix B considers Feynman’s path-integral polaron treatment approached using time-ordered operator calculus.

Appendix C is devoted to the many-body large polaron optical conductivity in Nb doped strontium titanate.

Appendix D contains summary of the present state of the problem of the polaron mobility. **It is remarkable that the theory of the polaron mobility developed by Kadanoff [65], which was recognized during a long time, needs a correction factor as found in Ref. [151] and independently confirmed in the recent work [153].**

Appendix E lists recent publications on Fröhlich polarons in Nature, Science and Physical Review Letters appeared from 2005 to 2015.

Preface to the 5th edition

Since 2005, when the first edition of the present Lecture Course was prepared, polaron physics continued to intensely develop, involving new areas and testing new powerful methods. In subsequent editions, these new developments are included in order to emphasize which of them we consider important. (I’ll write what exactly was discovered later)

Renewed interest in large (Fröhlich) polarons has been inspired by recent experimental advances in the determination of the band structure of highly polar oxides [1]. The optical response of complex oxides clearly reveals the polaron features and can shed light on the band structure of a crystal and its polaron characteristics. The interpretation of the measured data is essential to achieve a comprehensive understanding and to optimize practical application of functional materials. In particular, the question whether the polarons are large or small is often a subject of intense discussions, for example, in the case of $SrTiO_3$ and TiO_2, key materials in many technological sectors.

In the recent ARPES measurements [1] no clear signatures of small-polaron phenomena in n-doped strontium titanate were found, and the conclusion was reached that small polarons are not formed in strontium titanate. The electron-phonon coupling strength in strontium titanate $\alpha \approx 3.6$ obtained in Ref. [2] is typical for a rather moderate coupling that makes the formation of small polarons in the conduction band of $SrTiO_3$ hardly possible. On the contrary, recent density functional calculations [3, 4] show that excess electrons form small polarons if the density of electronic carriers is sufficiently high. This opens the interesting possibility to study an interplay of small and large polarons in $SrTiO_3$ and other oxides. In Ref. [5], the many-large-polaron model gives then a convincing interpretation of the experimentally observed mid-infrared band of $SrTi_{1-x}Nb_xO_3$.

The polaron theory is a testing field for new powerful theoretical quantum field methods, such as the Diagrammatic Quantum Monte Carlo (DQMC) method. Applied first to the calculation of the ground-state energy of a Fröhlich polaron [6], DQMC has been successful in the calculation of the optical conductivity of the Fröhlich polaron [7]. This inspired attempts to develop analytical methods for the polaron optical response. The recent work on the strong-coupling large-polaron optical conductivity [8] shows a good agreement with DQMC in the strong-coupling limit. In Ref. [9], the momentum average approximation is applied to derive an analytic expression for the optical conductivity of a small polaron, that very well matches the DQMC data.

The polaron theory has found recently several new interesting applications. One of them is the theoretical interpretation of the physics of an impurity immersed in an atomic Bose-Einstein condensate. In Refs. [10, 11], the ground-state energy of the BEC polaron has been studied on the basis of a Fröhlich type Hamiltonian using the Feynman variational technique and the DQMC method. In Ref. [12], the problem of the BEC polaron has been treated using the renormalization group method. It successfully retrieves the DQMC results in the whole (available for the comparison) range of the particle-phonon coupling strength.

In summary, polaron physics recently demonstrated new fascinating developments, that makes the present lecture course timely and relevant.

7.1 Introduction. The "standard" theories

7.1.1 The polaron concept

(I skipped this for now)

A charge placed in a polarizable medium is screened. Dielectric theory describes the phenomenon by the induction of a polarization around the charge carrier. The idea of the autolocalization of an electron due to the induced lattice polarization was first proposed by L. D. Landau [1]. In the further development of this concept, the induced polarization can follow the charge carrier when it is moving through the medium. The carrier together with the induced polarization is considered as one entity (see Fig. 7.1). It was called a *polaron* by S. I. Pekar [2, 3]. The physical properties of a polaron differ from those of a band-carrier. A polaron is characterized by its *binding (or self-) energy* E_0, an *effective mass* m^* and by its characteristic *response* to external electric and magnetic fields (e. g. dc mobility and optical absorption coefficient).

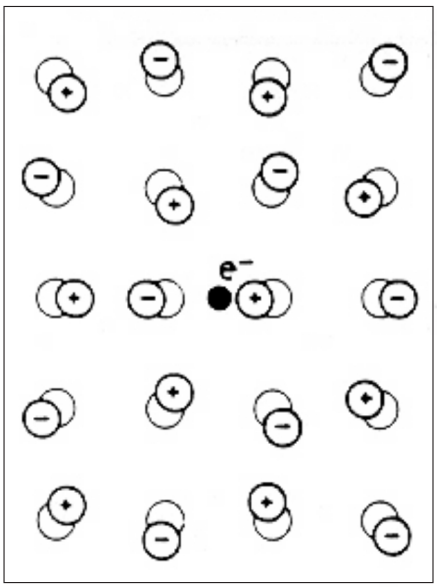

Figure 7.1: Artist view of a polaron. A conduction electron in an ionic crystal or a polar semiconductor repels the negative ions and attracts the positive ions. A self-induced potential arises, which acts back on the electron and modifies its physical properties. (From [4].)

If the spatial extension of a polaron is large compared to the lattice parameter of the solid, the latter can be treated as a polarizable continuum. This is the case of a *large (Fröhlich)* polaron. When the self-induced polarization caused by an electron or hole becomes of the order of the lattice parameter, a *small (Holstein)* polaron can arise [136]. As distinct from large polarons, small polarons are governed by short-range interactions.

7.1.2 Intuitive concepts

The polaron radius. Large polarons vs small polarons

Consider the LO (why exactly LO?) phonon field with frequency $\omega_{\rm LO}$ interacting with an electron. Denote by $\Delta\nu$ the quadratic mean square deviation of the electron velocity (it is not a frequency). In the electron-phonon interaction is weak, the electron can travel a distance

$$\Delta x \approx \frac{\Delta\nu}{\omega_{\rm LO}} \tag{7.1}$$

during a time $\omega_{\rm LO}^{-1}$, characteristic for the lattice period,because it is the distance within which the electron can be localized using the phonon field as measuring device. From the uncertainty relations it follows

$$\begin{aligned}
\Delta p \Delta x &= \frac{m}{\omega_{\rm LO}} \left(\Delta\nu\right)^2 \approx \hbar \\
\Delta\nu &\sim \sqrt{\frac{\hbar\omega_{\rm LO}}{m}}, \\
\Delta x &\sim \sqrt{\frac{\hbar}{m\omega_{\rm LO}}}.
\end{aligned} \tag{7.2}$$

At weak coupling Δx is a measure of the polaron radius r_p. To be consistent, the polaron radius r_p must be considerably larger than the lattice parameter a.(this is a criterion of a “large

polaron"). Experimental evaluation of the polaron radius leads to the follwing typical values: $r_p \approx 10\mathring{A}$ for alkali halides, $r_p \approx 20\mathring{A}$ for silver halides, $r_p \approx 100\mathring{A}$ for II-VI, II-V semiconductors. The continuum approximation is not satisfied for transition metal oxides (NiO, CaO, MnO), in other oxides (UO_2, NbO_2...). For those solids the "small polaron" concept is used. In some substances (e.g. perovskites) some intermediate region between large and small polarons is realized.

The coupling constant [5]

Consider the case of *strong electron-phonon interaction* in a polar crystal. The electron of mass m is then localized and can - to a first approximation - be considered as a static charge distribution within a sphere with radius l_1. The medium is characterized by an average dielectric constant $\bar{\varepsilon}$, which will be defined below.

The potential energy of a sphere of radius $l_1$uniformly charged with the charge e in a vacuum is (see Eq. (8.6) of Ref. [6])

$$U_{vac} = \frac{3}{5}\frac{e^2}{l_1}. \tag{7.3}$$

The potential energy of a uniformly charged sphere in a medium with the high-frequency dielectric constant ε_∞ is

$$U_1 = \frac{3}{5}\frac{e^2}{\varepsilon_\infty l_1}. \tag{7.4}$$

This is the potential energy of the *self-interaction* of the charge e uniformly spread over the sphere of radius l_1 in a medium with the dielectric constant ε_∞. In a medium with an inertial polarization field (due to LO phonons), the potential energy of the uniformly charged sphere is

$$U_2 = \frac{3}{5}\frac{e^2}{\varepsilon_0 l_1}, \tag{7.5}$$

where ε_0 is the static dielectric constant. The polaron effect is then related to the change of the potential energy of the interaction of the charged sphere due to the inertial polarization field. This change is the potential energy U_2 of the uniformly charged sphere in the presence of the inertial polarization field minus the potential energy of the *self-interaction* $U_1$of the charge e uniformly spread over the sphere in a medium without the inertial polarization:

$$U_{pol} \equiv U_2 - U_1 = \frac{3}{5}\frac{e^2}{l_1}\left(\frac{1}{\varepsilon_0} - \frac{1}{\varepsilon_\infty}\right) = -\frac{3}{5}\frac{e^2}{\bar{\varepsilon} l_1}, \tag{7.6}$$

with

$$\frac{1}{\bar{\varepsilon}} = \frac{1}{\varepsilon_\infty} - \frac{1}{\varepsilon_0}.$$

The electron distribution in a sphere may be non-uniform, what may influence the numerical coefficient in Eqs. (7.4) to (7.6). In this connection one can use the estimate [5]

$$U_{pol} \sim -\frac{e^2}{\bar{\varepsilon} l_1}. \tag{7.7}$$

The restriction of the electron in space requires its de Broglie wave length to be of the order l_1, so that its kinetic energy is of the order $4\pi^2\hbar^2/2ml_1^2$.Minimizing the total energy with respect to $l_1$leads to

$$\frac{\partial}{\partial l_1}\left(-\frac{e^2}{l_1\bar{\varepsilon}} + \frac{4\pi^2\hbar^2}{2ml_1^2}\right) = 0 \Longrightarrow \frac{1}{l_1} = \frac{e^2 m}{4\pi^2\hbar^2\bar{\varepsilon}},$$

wherefrom the binding energy is

$$U_1 = -\frac{e^4 m}{8\pi^2\hbar^2\bar{\varepsilon}^2}. \tag{7.8}$$

For *weak coupling*, one can neglect the kinetic energy of the electron. Taking the polaron radius according to (7.2), $r_p = \sqrt{2\hbar/m\omega_{\rm LO}}$, the binding energy is

$$U_2 = -\frac{e^2}{r_p\bar{\varepsilon}} = -\frac{e^2}{\bar{\varepsilon}}\sqrt{\frac{m\omega_{\rm LO}}{2\hbar}}. \tag{7.9}$$

We note that

$$\frac{U_1}{\hbar\omega_{\rm LO}} = -\frac{e^4 m}{8\pi^2\hbar^3\bar{\varepsilon}^2\omega_{\rm LO}} = -\frac{1}{4\pi^2}\left(\frac{U_2}{\hbar\omega_{\rm LO}}\right)^2. \tag{7.10}$$

Following the conventions of the field theory, the self energy at weak coupling is written as

$$U_2 = -\alpha\hbar\omega_{\rm LO}.$$

Therefore the so-called Fröhlich polaron coupling constant is

$$\begin{aligned}\alpha &= \frac{e^2}{\bar{\varepsilon}}\sqrt{\frac{m}{2\hbar^3\omega_{\rm LO}}}\\ &\equiv \frac{e^2}{\hbar c}\sqrt{\frac{mc^2}{2\hbar\omega_{\rm LO}}}\frac{1}{\bar{\varepsilon}}.\end{aligned} \tag{7.11}$$

For the average dielectric constant one shows that

$$\frac{1}{\bar{\varepsilon}} = \frac{1}{\varepsilon_\infty} - \frac{1}{\varepsilon_0},$$

where ε_∞ and ε_0 are, respectively, the electronic and the static dielectric constant of the polar crystal. The difference $1/\varepsilon_\infty - 1/\varepsilon_0$ arises because the ionic vibrations occur in the infrared spectrum and the electrons in the shells can follow the conduction electron adiabatically.

Polaron mobility

[1]

Here we give a simple derivation leading to the gross features of the mobility behaviuor, especially its temperature dependence. The key idea is that the mobility will change because the number of phonons in the lattice, with which the polaron interacts, is changing with temperature.

The phonon density is given by

$$n = \frac{1}{e^{\frac{\hbar\omega_{\rm LO}}{kT}} - 1}.$$

The mobility for large polaron is proportional to the inverse of the number of phonons:

$$\mu \approx \frac{1}{n} = e^{\frac{\hbar\omega_{\rm LO}}{kT}} - 1$$

and for low temperatures $kT \ll \hbar\omega_{\rm LO}$

[1] **See also Appendix D "Notes on the polaron mobility".**

$$\mu \approx e^{\frac{\hbar\omega_{\rm LO}}{kT}}. \tag{7.12}$$

The mobility of continuum poarons decreases with increasing temperature following an exponential law. The slope of the straight line in $\ln\mu$ vs $1/T$ is characterized by the LO phonon frequesncy. Systematic study performed, in particular, by Fröhlich and Kadanoff, gives

$$\mu = \frac{e}{2m\omega_{\rm LO}} e^{\frac{\hbar\omega_{\rm LO}}{kT}}. \tag{7.13}$$

The small polaron will jump from ion to ion under the influence of optical phonons. The lerger the numver of phonons, the lerger the mobility. The behaviuor of the small polaron is the opposite of that of the large polaron. One expects:

$$\mu \approx n = \frac{1}{e^{\frac{\hbar\omega_{\rm LO}}{kT}} - 1}.$$

For low temperatures $kT \ll \hbar\omega_{\rm LO}$ one has:

$$\mu \approx e^{-\frac{\hbar\omega_{\rm LO}}{kT}} : \tag{7.14}$$

the mobility of small polaron is thermally activated. Systematic analysis within the small-polaron theory shows that

$$\mu \approx e^{-\gamma\frac{\hbar\omega_{\rm LO}}{kT}} : \tag{7.15}$$

with $\gamma \sim 5$.

7.1.3 The Fröhlich Hamiltonian

Fröhlich proposed a model Hamiltonian for the "large" polaron through which its dynamics is treated quantum mechanically ("Fröhlich Hamiltonian"). The polarization, carried by the longitudinal optical (LO) phonons, is represented by a set of quantum oscillators with frequency $\omega_{\rm LO}$, the long-wavelength LO-phonon frequency, and the interaction between the charge and the polarization field is linear in the field [5]:

$$H = \frac{\mathbf{p}^2}{2m_b} + \sum_{\mathbf{k}} \hbar\omega_{\rm LO} a^+_{\mathbf{k}} a_{\mathbf{k}} + \sum_{\mathbf{k}} (V_k a_{\mathbf{k}} e^{i\mathbf{k}\cdot\mathbf{r}} + V_k^* a^\dagger_{\mathbf{k}} e^{-i\mathbf{k}\cdot\mathbf{r}}), \tag{7.16}$$

where $\mathbf{r}$ is the position coordinate operator of the electron with band mass m_b, $\mathbf{p}$ is its canonically conjugate momentum operator; $a^\dagger_{\mathbf{k}}$ and $a_{\mathbf{k}}$ are the creation (and annihilation) operators for longitudinal optical phonons of wave vector $\mathbf{k}$ and energy $\hbar\omega_{\rm LO}$. The V_k are Fourier components of the electron-phonon interaction

$$V_k = -i\frac{\hbar\omega_{\rm LO}}{k}\left(\frac{4\pi\alpha}{V}\right)^{\frac{1}{2}}\left(\frac{\hbar}{2m_b\omega_{\rm LO}}\right)^{\frac{1}{4}}. \tag{7.17}$$

The strength of the electron–phonon interaction is expressed by a dimensionless coupling constant α, which is defined as:

$$\alpha = \frac{e^2}{\hbar}\sqrt{\frac{m_b}{2\hbar\omega_{\rm LO}}}\left(\frac{1}{\varepsilon_\infty} - \frac{1}{\varepsilon_0}\right). \tag{7.18}$$

In this definition, ε_∞ and ε_0 are, respectively, the electronic and the static dielectric constant of the polar crystal.

In Table 2 the Fröhlich coupling constant is given for a few solids[2].

In deriving the form of V_k, expressions (7.17) and (7.18), it was assumed that (i) the spatial extension of the polaron is large compared to the lattice parameter of the solid ("continuum" approximation), (ii) spin and relativistic effects can be neglected, (iii) the band-electron has parabolic dispersion, (iv) in line with the first approximation it is also assumed that the LO-phonons of interest for the interaction, are the long-wavelength phonons with constant frequency $\omega_{\rm LO}$.

The model, represented by the Hamiltonian (7.16) (which up to now could not been solved exactly) has been the subject of extensive investigations, see, e. g., Refs. [23, 24, 25, 26, 27, 28, 29, 30]. In what follows the key approaches of the Fröhlich-polaron theory are briefly reviewed with indication of their relevance for the polaron problems in nanostructures.

7.1.4 Infinite mass model ["shift"–operators]

Here some insight will be given in the type of transformation that might be useful to study the Fröhlich Hamiltonian (7.16). For this purpose the Hamiltonian will be treated for a particle with infinite mass $m_b \to \infty$, (which is at $\mathbf{r} = 0$) :

$$H^{\infty} = \sum_{\mathbf{k}} \hbar\omega_{\rm LO} a^{+}_{\mathbf{k}} a_{\mathbf{k}} + \sum_{\mathbf{k}} (V_k a_{\mathbf{k}} + V_k^* a^{\dagger}_{\mathbf{k}}), \tag{7.19}$$

which can be transformed into the following expression with "shifted" phonon operators:

$$H^{\infty} = \sum_{\mathbf{k}} \hbar\omega_{\rm LO} \left(a^{\dagger}_{\mathbf{k}} + \frac{V_k}{\hbar\omega_{\rm LO}} \right) \left(a_{\mathbf{k}} + \frac{V_k^*}{\hbar\omega_{\rm LO}} \right) - \sum_{\mathbf{k}} \frac{|V_k|^2}{\hbar\omega_{\rm LO}}. \tag{7.20}$$

To determine the eigenstates of this Hamiltonian, one can perform a unitary transformation which produces the following "shift" of the phonon operators:

$$a_{\mathbf{k}} \to b_{\mathbf{k}} = a_{\mathbf{k}} + \frac{V_k^*}{\hbar\omega_{\rm LO}}, \qquad a^{\dagger}_{\mathbf{k}} \to b^{\dagger}_{\mathbf{k}} = a^{\dagger}_{\mathbf{k}} + \frac{V_k}{\hbar\omega_{\rm LO}}.$$

The transformation

$$S = \exp\left[-\sum_{\mathbf{k}} a^{\dagger}_{\mathbf{k}} \frac{V_k^*}{\hbar\omega_{\rm LO}} + \sum_{\mathbf{k}} \frac{V_k}{\hbar\omega_{\rm LO}} a_{\mathbf{k}} \right] \tag{7.21}$$

is canonical:

$$S^{\dagger} = \exp\left[-\sum_{\mathbf{k}} a_{\mathbf{k}} \frac{V_k}{\hbar\omega_{\rm LO}} + \sum_{\mathbf{k}} \frac{V_k^*}{\hbar\omega_{\rm LO}} a^{\dagger}_{\mathbf{k}} \right] = S^{-1}$$

and has the desired property:

$$S^{-1} a_{\mathbf{k}} S = a_{\mathbf{k}} - \frac{V_k^*}{\hbar\omega_{\rm LO}}, \qquad S^{-1} a^{\dagger}_{\mathbf{k}} S = a^{\dagger}_{\mathbf{k}} - \frac{V_k}{\hbar\omega_{\rm LO}}.$$

The transformed Hamiltonian is now:

$$S^{-1} H^{\infty} S = \sum_{\mathbf{k}} \hbar\omega_{\rm LO} a^{\dagger}_{\mathbf{k}} a_{\mathbf{k}} - \sum_{\mathbf{k}} \frac{|V_k|^2}{\hbar\omega_{\rm LO}}.$$

[2]In some cases, due to lack of reliable experimental data to determine the electron band mass, the values of α are not well established.

The eigenstates of the Hamiltonian contain an integer number of phonons ($|n_{\mathbf{k}}\rangle$) .The eigenenergies are evidently:

$$E = \sum_{\mathbf{k}} n_{\mathbf{k}} \hbar\omega_{\mathrm{LO}} - \sum_{\mathbf{k}} \frac{|V_k|^2}{\hbar\omega_{\mathrm{LO}}}.$$

This expression is divergent at it is often the case in field theory of point charges are considered. A transformation of the type S has been of great interest in developing weak coupling theory as shown below.

7.1.5 The "standard" theories

Weak coupling via a perturbation theory

For actual crystals α-values typically range from $\alpha = 0.02$ (InSb) up to $\alpha \sim 3$ to 4 (alkali halides, some oxides), see Table 1. A weak-coupling theory of the polaron was developed originally by Fröhlich [5] (check this paper! did he really obtain them earlier than others?). He derived the first weak-coupling perturbation-theory results:

$$E_0 = -\alpha\hbar\omega_{\mathrm{LO}} \tag{7.22}$$

and

$$m^* = \frac{m_b}{1 - \alpha/6}. \tag{7.23}$$

Expressions (7.22) and (7.23) are rigorous to order α.

Weak coupling via a canonical transformation [“shift”-operators]

Inspired by the work of Tomonaga on quantum electrodynamics (Q. E. D.), Lee, Low and Pines (LLP) [31] analyzed the properties of a weak-coupling polaron starting from a formulation based on canonical transformations (cp. the results of the subsection 7.1.4).As hown by them, the unitary transformation

$$U = \exp\left\{\frac{i}{\hbar}\left(\mathbf{P} - \sum_{\mathbf{k}} \hbar\mathbf{k} a_{\mathbf{k}}^{\dagger} a_{\mathbf{k}}\right) \cdot \mathbf{r}\right\}, \tag{7.24}$$

where $\mathbf{P}$ is a "c"-number representing the *total system momentum* allows to eliminate the electron co-ordinates from the system. Intuitively one might guess this transformation by writing the exact wave function in the form

$$\Psi_{\text{total } H} = \exp\left(\frac{i}{\hbar}\mathbf{p} \cdot \mathbf{r}\right) |\Phi\rangle .$$

It is plausible that the “Bloch” factor $\exp\left(i/\hbar\mathbf{p} \cdot \mathbf{r}\right)$ attaches the system to the electron as origin of the co-ordinates. After this transformation the Hamiltonian (7.16) becomes:

$$\mathcal{H} = U^{-1}HU = \frac{\left(\mathbf{P} - \sum_{\mathbf{k}} \hbar\mathbf{k} a_{\mathbf{k}}^{\dagger} a_{\mathbf{k}}\right)^2}{2m_b} + \sum_{\mathbf{k}} \hbar\omega_{\mathrm{LO}} a_{\mathbf{k}}^{\dagger} a_{\mathbf{k}} + \sum_{\mathbf{k}} (V_k a_{\mathbf{k}} + V_k^* a_{\mathbf{k}}^{\dagger}). \tag{7.25}$$

If, for the sake of simplicity, the case of total momentum equal to zero is considered, this expression becomes:

$$\mathcal{H} = \sum_{\mathbf{k},\mathbf{k}'} \frac{\hbar^2 \mathbf{k} \cdot \mathbf{k}' a_{\mathbf{k}}^{\dagger} a_{\mathbf{k}'}^{\dagger} a_{\mathbf{k}} a_{\mathbf{k}'}}{2m_b} + \sum_{\mathbf{k}} \left(\hbar\omega_{\mathrm{LO}} + \frac{\hbar^2 k^2}{2m_b}\right) a_{\mathbf{k}}^{\dagger} a_{\mathbf{k}} + \sum_{\mathbf{k}} (V_k a_{\mathbf{k}} + V_k^* a_{\mathbf{k}}^{\dagger}). \tag{7.26}$$

The first term of this Hamiltonian is the correlation energy term involving different values for $\mathbf{k}$ and $\mathbf{k}'$.If one diagonalizes the second and the trird term of the Hamiltonian (7.26) (this can be done exactly by means of the "shifted-oscillator canonical transformation" S (7.21)), the result of LLP is found. The expectation value of the first term is zero for the wave function $S\,|0\rangle$. Therefore one is sure to obtain a variational result. It is remarkable that merely extracting the $\mathbf{k} = \mathbf{k}'$ term from the expression

$$\sum_{\mathbf{k},\mathbf{k}'} \frac{\hbar^2 \mathbf{k}\cdot\mathbf{k}' a^\dagger_{\mathbf{k}} a^\dagger_{\mathbf{k}'} a_{\mathbf{k}} a_{\mathbf{k}'}}{2m_b} \tag{7.27}$$

eliminates the divergency from the problem (cp. with the case $m_b \to \infty$) and is equivalent to the sophisticated theory by Lee, Low and Pines (LLP), which corresponds thus to neglect of the term (7.27). The details of the LLP theory are given in Appendix 1. The explicit form for the energy is now

$$E = -\sum_{\mathbf{k}} \frac{|V_k|^2}{\hbar\omega_{\mathrm{LO}} + \frac{\hbar^2 k^2}{2m_b}} = -\alpha\hbar\omega.$$

This self energy is no longer divergent. The divergence is elmininated by the quantum cut-off occurring at $k = \sqrt{2m_b\omega_{\mathrm{LO}}}/\hbar$.

For the self energy the LLP result is equivalent to the perturbation result. The effective mass however is now given by

$$m^* = m_b\left(1 + \frac{\alpha}{6}\right),$$

a result, which follows if one considers the case $\mathbf{P} \neq 0$ and which is also exact for $\alpha \to 0$. However, the LLP effective mass is different from the perturbation result if α insreases.

The LLP approximation has often been called “intermediate-coupling approximation”. However its range of validity is the same as that of perturbation theory to order α. The significance of the LLP approximation consists of the flexibility of the canonical transformations together with the fact that it puts the Fröhlich result on a variational basis.

To order α^2, the analytical expressions for the coefficients are α^2: $2\ln(\sqrt{2}+1) - \frac{3}{2}\ln 2 - \frac{\sqrt{2}}{2} \approx -0.01591962$ for the energy and $\frac{4}{3}\ln(\sqrt{2}+1) - \frac{2}{3}\ln 2 - \frac{5\sqrt{2}}{8} + \frac{7}{36} \approx 0.02362763$ for the polaron mass [32].

At present the following weak-coupling expansions are known: for the energy [33, 34]

$$\frac{E_0}{\hbar\omega_{\mathrm{LO}}} = -\alpha - 0.0159196220\alpha^2 - 0.000806070048\alpha^3 - \ldots, \tag{7.28}$$

and for the polaron mass [32]

$$\frac{m^*}{m_b} = 1 + \frac{\alpha}{6} + 0.02362763\alpha^2 + \ldots \tag{7.29}$$

Strong coupling via a canonical transformation [“shift”-operators]

Historically, the strong coupling limit was studied before all other treatments (Landau, Pekar [23, 35]). Although it is only a formal case because the actual crystals seems to have α values smaller than 5, it is very interesting because it contains some indication of the intermediate coupling too: approach the excitations from the strong coupling limit and extrapolate to intermediate coupling is interesting because it is expected that some specific strong coupling properties “survive” at intermediate coupling. In what follows, a treatment, equivalent to that of Pekar, but in second quantization and written with as much analogy to the LLP treatment as possible is given.

We start from the Fröhlich Hamiltonian (7.16). At strong coupling one makes the assumption (a "Produkt-Ansatz") for the polaron wave-function

$$|\Phi\rangle = |\varphi\rangle|f\rangle \tag{7.30}$$

where $|\varphi\rangle$ is the "electron-component" of the wave function ($\langle\varphi|\varphi\rangle = 1$).The "field-component" of the wave function $|f\rangle$ ($\langle f|f\rangle = 1$) parametrically depends on $|\varphi\rangle$. The Produkt-Ansatz (7.30) — or Born-Oppenheimer approximation — implies that the electron adiabatically follows the motion of the atoms, while the field cannot follow the instantaneous motion of the electron. Fröhlich showed that the approximation (7.30) leads to results, which are only valid for sufficiently large $\alpha \to \infty$, i. e. in the strong-coupling regime. A more systematic analysis of strong-coupling polarons based on canonical transformations applied to the Hamiltonian (7.16) was performed in Refs. [36, 37, 38].

The expectation value for the energy is now:

$$\langle H\rangle = \langle\varphi|\frac{\mathbf{p}^2}{2m_b}|\varphi\rangle + \langle f|\left[\sum_{\mathbf{k}}\hbar\omega_{\mathrm{LO}}a_{\mathbf{k}}^{+}a_{\mathbf{k}} + \sum_{\mathbf{k}}(V_k a_{\mathbf{k}}\rho_{\mathbf{k}}e^{i\mathbf{k}\cdot\mathbf{r}} + V_k^* a_{\mathbf{k}}^{\dagger}\rho_{\mathbf{k}}^*)\right]|f\rangle$$

with

$$\rho_{\mathbf{k}} = \langle\varphi|\, e^{i\mathbf{k}\cdot\mathbf{r}}\,|\varphi\rangle\,.$$

We wish to minimize $\langle H\rangle$, but also

$$\langle f|\left[\sum_{\mathbf{k}}\hbar\omega_{\mathrm{LO}}a_{\mathbf{k}}^{+}a_{\mathbf{k}} + \sum_{\mathbf{k}}(V_k a_{\mathbf{k}}\rho_{\mathbf{k}}e^{i\mathbf{k}\cdot\mathbf{r}} + V_k^* a_{\mathbf{k}}^{\dagger}\rho_{\mathbf{k}}^*)\right]|f\rangle$$

has to be minimized. This expression will be minimized if $|f\rangle$ is the ground state wave function of the "shifted" oscullator-type Hamiltonian. As we can diagonalize this Hamiltonian exactly:

$$\sum_{\mathbf{k}}\hbar\omega_{\mathrm{LO}}a_{\mathbf{k}}^{+}a_{\mathbf{k}} + \sum_{\mathbf{k}}(V_k a_{\mathbf{k}}\rho_{\mathbf{k}}e^{i\mathbf{k}\cdot\mathbf{r}} + V_k^* a_{\mathbf{k}}^{\dagger}\rho_{\mathbf{k}}^*) \tag{7.31}$$

$$= \sum_{\mathbf{k}}\hbar\omega_{\mathrm{LO}}\left(a_{\mathbf{k}}^{\dagger} + \frac{V_k\rho_{\mathbf{k}}}{\hbar\omega_{\mathrm{LO}}}\right)\left(a_{\mathbf{k}} + \frac{V_k^*\rho_{\mathbf{k}}^*}{\hbar\omega_{\mathrm{LO}}}\right) - \sum_{\mathbf{k}}\frac{|V_k|^2\,|\rho_{\mathbf{k}}|^2}{\hbar\omega_{\mathrm{LO}}}, \tag{7.32}$$

we can apply a canonical transformation similar to (7.21):

$$S = \exp\left[\sum_{\mathbf{k}}\left(\frac{V_k\rho_{\mathbf{k}}}{\hbar\omega_{\mathrm{LO}}}a_{\mathbf{k}} - \frac{V_k^*\rho_{\mathbf{k}}^*}{\hbar\omega_{\mathrm{LO}}}a_{\mathbf{k}}^{\dagger}\right)\right], \tag{7.33}$$

which has the property:

$$S^{-1}a_{\mathbf{k}}S = a_{\mathbf{k}} - \frac{V_k^*\rho_{\mathbf{k}}}{\hbar\omega_{\mathrm{LO}}}, S^{-1}a_{\mathbf{k}}^{\dagger}S = a_{\mathbf{k}}^{\dagger} - \frac{V_k\rho_{\mathbf{k}}^*}{\hbar\omega_{\mathrm{LO}}}.$$

The transformed Hamiltonian is now:

$$S^{-1}\left[\sum_{\mathbf{k}}\hbar\omega_{\mathrm{LO}}a_{\mathbf{k}}^{+}a_{\mathbf{k}} + \sum_{\mathbf{k}}(V_k a_{\mathbf{k}}\rho_{\mathbf{k}}e^{i\mathbf{k}\cdot\mathbf{r}} + V_k^* a_{\mathbf{k}}^{\dagger}\rho_{\mathbf{k}}^*)\right]S$$
$$= \sum_{\mathbf{k}}\hbar\omega_{\mathrm{LO}}a_{\mathbf{k}}^{\dagger}a_{\mathbf{k}} - \sum_{\mathbf{k}}\frac{|V_k|^2\,|\rho_{\mathbf{k}}|^2}{\hbar\omega_{\mathrm{LO}}}.$$

The phonon vacuum $|0\rangle$ provides a minimum:

$$\langle 0| S^{-1} \left[\sum_{\mathbf{k}} \hbar\omega_{\mathrm{LO}} a_{\mathbf{k}}^{+} a_{\mathbf{k}} + \sum_{\mathbf{k}} (V_k a_{\mathbf{k}} \rho_{\mathbf{k}} e^{i\mathbf{k}\cdot\mathbf{r}} + V_k^* a_{\mathbf{k}}^{\dagger} \rho_{\mathbf{k}}^*) \right] S |0\rangle = -\sum_{\mathbf{k}} \frac{|V_k|^2 |\rho_{\mathbf{k}}|^2}{\hbar\omega_{\mathrm{LO}}}.$$

Hence, the Hamiltonian (7.31) is minimized by the ground state wave function

$$S|0\rangle = \exp\left[\sum_{\mathbf{k}} \left(\frac{V_k \rho_{\mathbf{k}}}{\hbar\omega_{\mathrm{LO}}} a_{\mathbf{k}} - \frac{V_k^* \rho_{\mathbf{k}}^*}{\hbar\omega_{\mathrm{LO}}} a_{\mathbf{k}}^{\dagger} \right) \right] |0\rangle . \tag{7.34}$$

It gives the ground state energy

$$E_0 = \langle\varphi| \frac{\mathbf{p}^2}{2m_b} |\varphi\rangle - \sum_{\mathbf{k}} \frac{|V_k|^2 |\rho_{\mathbf{k}}|^2}{\hbar\omega_{\mathrm{LO}}}, \tag{7.35}$$

which is still a functional of $|\varphi\rangle$. The functionals $\rho_{\mathbf{k}}$ are different for differerent excitations.

Ground state of strong-coupling polarons

For the ground state one considers a Gaussian wave function:

$$|\varphi_{"1s"}\rangle = C \exp\left(-\frac{m_b \Omega_0}{2\hbar} r^2 \right)$$

with a variational parameter Ω_0.

$$\begin{aligned}
\langle\varphi_{"1s"}|\varphi_{"1s"}\rangle &= C^2 \int d^3r \exp\left(-\frac{m_b\Omega_0}{\hbar} r^2 \right) = C^2 \left[\int_{-\infty}^{\infty} dx \exp\left(-\frac{m_b\Omega_0}{\hbar} x^2 \right) \right]^3 \\
&= C^2 \left(\frac{\sqrt{\pi}}{\frac{m_b\Omega_0}{\hbar}} \right)^3 = C^2 \left(\frac{\pi\hbar}{m_b\Omega_0} \right)^{3/2} = 1 \Rightarrow C^2 = \left(\frac{m_b\Omega_0}{\pi\hbar} \right)^{3/2}
\end{aligned}$$

$$|\varphi_{"1s"}\rangle = \left(\frac{m_b\Omega_0}{\pi\hbar} \right)^{3/4} \exp\left(-\frac{m_b\Omega_0}{2\hbar} r^2 \right).$$

For the further use, we introduce a notation $C_1^2 = \left(\frac{m_b\Omega_0}{\pi\hbar}\right)^{1/2}$. Such a wave function is consistent with the localization of the electron, which we expect for large α. The kinetic energy in (7.35) for this function is calculated using the representation of the operator $\mathbf{p}^2 = -\hbar^2\nabla^2 = -\hbar^2 (\nabla_x^2 + \nabla_x^2 + \nabla_x^2)$:

$$\begin{aligned}
\langle\varphi_{"1s"}| \frac{\mathbf{p}^2}{2m_b} |\varphi_{"1s"}\rangle &= -\frac{\hbar^2}{2m_b} C^2 \int d^3r \exp\left(-\frac{m_b\Omega_0}{2\hbar} r^2 \right) \\
&\times \left(\nabla_x^2 + \nabla_x^2 + \nabla_x^2 \right) \exp\left(-\frac{m_b\Omega_0}{2\hbar} r^2 \right) \\
&= -3\frac{\hbar^2}{2m_b} C^2 \int_{-\infty}^{\infty} dx \exp\left(-\frac{m_b\Omega_0}{2\hbar} x^2 \right) \nabla_x^2 \exp\left(-\frac{m_b\Omega_0}{2\hbar} x^2 \right) \\
&\times \int_{-\infty}^{\infty} dy \exp\left(-\frac{m_b\Omega_0}{\hbar} y^2 \right) \int_{-\infty}^{\infty} dz \exp\left(-\frac{m_b\Omega_0}{\hbar} z^2 \right)
\end{aligned}$$

$$
\begin{aligned}
&= -3\frac{\hbar^2}{2m_b}C_1^2\int_{-\infty}^{\infty}dx\exp\left(-\frac{m_b\Omega_0}{2\hbar}x^2\right)\\
&\times\nabla_x\left[-\frac{m_b\Omega_0}{\hbar}x\exp\left(-\frac{m_b\Omega_0}{2\hbar}x^2\right)\right]\\
&= 3\frac{\hbar^2}{2m_b}C_1^2\frac{m_b\Omega_0}{\hbar}\int_{-\infty}^{\infty}dx\left(1-\frac{m_b\Omega_0}{\hbar}x^2\right)\exp\left(-\frac{m_b\Omega_0}{\hbar}x^2\right)\\
&== 3\frac{\hbar^2}{m_b}C_1^2\frac{m_b\Omega_0}{\hbar}\int_{0}^{\infty}dx\left(1-\frac{m_b\Omega_0}{\hbar}x^2\right)\exp\left(-\frac{m_b\Omega_0}{\hbar}x^2\right)\\
&= 3\frac{\hbar^2}{m_b}C_1^2\frac{m_b\Omega_0}{\hbar}\left[\frac{\sqrt{\pi}}{2\sqrt{\frac{m_b\Omega_0}{\hbar}}}-\frac{m_b\Omega_0}{\hbar}\frac{\sqrt{\pi}}{4\sqrt{\left(\frac{m_b\Omega_0}{\hbar}\right)^3}}\right]\\
&= 3\frac{\hbar\Omega_0}{4}C_1^2\sqrt{\frac{\pi\hbar}{m_b\Omega_0}} = 3\frac{\hbar\Omega_0}{4}\sqrt{\frac{m_b\Omega_0}{\pi\hbar}}\sqrt{\frac{\pi\hbar}{m_b\Omega_0}} = \frac{3}{4}\hbar\Omega_0.
\end{aligned}
$$

The functional

$$
\begin{aligned}
\rho_{\mathbf{k}"1s"} &= \langle\varphi_{"1s"}|\,e^{i\mathbf{k}\cdot\mathbf{r}}\,|\varphi_{"1s"}\rangle = C^2\int d^3r\exp\left(-\frac{m_b\Omega_0}{\hbar}r^2+i\mathbf{k}\cdot\mathbf{r}\right)\\
&= C^2\int d^3r\exp\left(-\frac{m_b\Omega_0}{\hbar}\left[r^2+i\frac{\hbar}{m_b\Omega_0}\mathbf{k}\cdot\mathbf{r}-\frac{\hbar^2k^2}{4m_b^2\Omega_0^2}+\frac{\hbar^2k^2}{4m_b^2\Omega_0^2}\right]\right)\\
&= C^2\exp\left(-\frac{m_b\Omega_0}{\hbar}\frac{\hbar^2k^2}{4m_b^2\Omega_0^2}\right)\int d^3r\exp\left(-\frac{m_b\Omega_0}{\hbar}\left[\mathbf{r}+i\frac{\hbar}{2m_b\Omega_0}\mathbf{k}\right]^2\right)\Rightarrow\\
\rho_{\mathbf{k}"1s"} &= \exp\left(-\frac{\hbar k^2}{4m_b\Omega_0}\right).
\end{aligned}
\tag{7.36}
$$

The second term in (7.35) is then

$$
\begin{aligned}
-\sum_{\mathbf{k}}\frac{|V_k|^2\,|\rho_{\mathbf{k}"1s"}|^2}{\hbar\omega_{\mathrm{LO}}} &= -\frac{V}{(2\pi)^3}\int d^3k\frac{\hbar\omega_{\mathrm{LO}}}{k^2}\frac{4\pi\alpha}{V}\left(\frac{\hbar}{2m_b\omega_{\mathrm{LO}}}\right)^{\frac{1}{2}}\exp\left(-\frac{\hbar k^2}{2m_b\Omega_0}\right)\\
&= -\frac{\alpha\hbar\omega_{\mathrm{LO}}}{2\pi^2}.4\pi\left(\frac{\hbar}{2m_b\omega_{\mathrm{LO}}}\right)^{\frac{1}{2}}\int_0^{\infty}dk\exp\left(-\frac{\hbar k^2}{2m_b\Omega_0}\right)\\
&= -\frac{2\alpha\hbar\omega_{\mathrm{LO}}}{\pi}\left(\frac{\hbar}{2m_b\omega_{\mathrm{LO}}}\right)^{\frac{1}{2}}\frac{\sqrt{\pi}}{2}\sqrt{\frac{2m_b\Omega_0}{\hbar}} = -\frac{\alpha\hbar}{\sqrt{\pi}}\sqrt{\Omega_0\omega_{\mathrm{LO}}}.
\end{aligned}
\tag{7.37}
$$

The variational energy (7.35) thus becomes

$$
E_0 = \frac{3}{4}\hbar\Omega_0 - \frac{\hbar\omega_{\mathrm{LO}}\alpha}{\sqrt{\pi}}\sqrt{\frac{\Omega_0}{\omega_{\mathrm{LO}}}}. \tag{7.38}
$$

Putting

$$
\frac{\partial E_0}{\partial\Omega_0} = 0,
$$

one obtains

$$
\begin{aligned}
&\frac{3}{4} = \frac{\alpha}{2\sqrt{\pi}}\sqrt{\frac{\omega_{\mathrm{LO}}}{\Omega_0}} \Longrightarrow \sqrt{\frac{\Omega_0}{\omega_{\mathrm{LO}}}} = \frac{2\alpha}{3\sqrt{\pi}} \Longrightarrow \frac{\Omega_0}{\omega_{\mathrm{LO}}} = \frac{4}{9}\frac{\alpha^2}{\pi} \Longrightarrow\\
&\Omega_0 = \frac{4}{9}\frac{\alpha^2}{\pi}\omega_{\mathrm{LO}}.
\end{aligned}
\tag{7.39}
$$

Substituting (7.39) in (7.38), we find the ground state energy of the polaron E_0 (calculated with the energy of the uncoupled electron-phonon system as zero energy):

$$E_0 = \frac{3}{4}\hbar\frac{4}{9}\frac{\alpha^2}{\pi}\omega_{\rm LO} - \frac{\hbar\omega_{\rm LO}\alpha}{\sqrt{\pi}}\frac{2\alpha}{3\sqrt{\pi}} = \left(\frac{1}{3} - \frac{2}{3}\right)\frac{\alpha^2}{\pi}\hbar\omega_{\rm LO} \Longrightarrow$$

$$E_0 = -\frac{1}{3}\frac{\alpha^2}{\pi}\hbar\omega_{\rm LO} = -0.106\alpha^2\hbar\omega_{\rm LO}. \tag{7.40}$$

The strong-coupling mass of the polaron, resulting again from the approximation (7.30), is given [39] as:

$$m_0^* = 0.0200\alpha^4 m_b. \tag{7.41}$$

More rigorous strong-coupling expansions for E_0 and m^* have been presented in the literature [40]:

$$\frac{E_0}{\hbar\omega_{\rm LO}} = -0.108513\alpha^2 - 2.836, \tag{7.42}$$

$$\frac{m_0^*}{m_b} = 1 + 0.0227019\alpha^4. \tag{7.43}$$

The strong-coupling ground state energy (7.40) is lower than the LLP ground state energy for $\alpha > 10$.

The excited states of the polaron: SS, FC, RES

In principle, excited states of the polaron exist at all coupling. In the general case, and for simplicity for $\mathbf{P} = 0$, a continuum of states starts at $\hbar\omega_{\rm LO}$ above the ground state of the polaron. This continuum physically corresponds to the scattering of free phonons on the polaron. Those "scattering.states" (SS) were studied in [41] anf for the first time more generally in [39] are not the only excitations of the polaron. There are also *internal* excitation states corresponding to the excitations of the electron in the potential it created itself. By analogy with the excited states of colour centers, the following terminology is used.

(i) The states where the electron is excited in the potential belonging to the ground state configuration of the lattice are called *Franck-Condon* (FC) states

(ii) Excitations of the electron in which the lattice polarization is adapted to the electronic configuration of the excited electron (which itself then adapts its wave function to the new potential, etc. ... leading to a self-consistent final state), are called *relaxed excited state* (RES) [23].

Calculation of the lowest FC state

The formalism used until now is well adapted to treat the polaron excitations at strong coupling. The field dependence of the wave function is (7.34). For the FC state the $\rho_{\mathbf{k}}$ are the same as for the ground state (7.36). Physically $\rho_{\mathbf{k}}$ tells us, to what electronic distribution the field is adapted. The electronic part of the excited wave function is $2p$-like:

$$|\varphi_{"2p"}\rangle = C_{"2p"}\, z \exp\left(-\frac{m_b\Omega_p}{2\hbar}r^2\right) \tag{7.44}$$

with a parameter Ω_p, which is equal to Ω_0 :

$$\begin{aligned}\langle\varphi_{"2p"}|\varphi_{"2p"}\rangle &= C^2_{"2p"}\int_{-\infty}^{\infty} dz z^2 \exp\left(-\frac{m_b\Omega_p}{\hbar}z^2\right)\left[\int_{-\infty}^{\infty} dx \exp\left(-\frac{m_b\Omega_p}{\hbar}x^2\right)\right]^2 \\ &= C^2_{"2p"}\left(\frac{\sqrt{\pi}}{\frac{m_b\Omega_p}{\hbar}}\right)^2 \frac{\sqrt{\pi}}{2\left(\frac{m_b\Omega_p}{\hbar}\right)^{3/2}} = C^2_{"2p"}\left(\frac{\pi\hbar}{m_b\Omega_p}\right)^{3/2}\frac{\hbar}{2m_b\Omega_p} = 1 \Rightarrow \\ C^2_{"2p"} &= \left(\frac{m_b\Omega_p}{\pi\hbar}\right)^{3/2}\frac{2m_b\Omega_p}{\hbar}\end{aligned}$$

$$|\varphi_{"2p"}\rangle = \left(\frac{m_b\Omega_0}{\pi\hbar}\right)^{3/4}\left(\frac{2m_b\Omega_p}{\hbar}\right)^{1/2} z\exp\left(-\frac{m_b\Omega_0}{2\hbar}r^2\right).$$

We introduce still a notation

$$C_2^2 = \frac{2}{\sqrt{\pi}}\left(\frac{m_b\Omega_p}{\hbar}\right)^{3/2}$$

The FC state energy is, similarly to (7.35),

$$E_{FC} = \langle\varphi_{"2p"}|\frac{\mathbf{p}^2}{2m_b}|\varphi_{"2p"}\rangle - \sum_{\mathbf{k}}\frac{|V_k|^2|\rho_{\mathbf{k}"1s"}|^2}{\hbar\omega_{\mathrm{LO}}}. \tag{7.45}$$

The kinetic energy term is

$$
\begin{aligned}
\left\langle \varphi_{"2p"} \right| \frac{\mathbf{p}^2}{2m_b} \left| \varphi_{"2p"} \right\rangle &= -\frac{\hbar^2}{2m_b} C^2_{"2p"} \int d^3r z \exp\left(-\frac{m_b\Omega_p}{2\hbar} r^2\right) \\
&\times \left(\nabla_x^2 + \nabla_x^2 + \nabla_x^2\right) \left[z \exp\left(-\frac{m_b\Omega_p}{2\hbar} r^2\right)\right] \\
&= -\frac{\hbar^2}{2m_b} C^2_{"2p"} \int_{-\infty}^{\infty} dz z \exp\left(-\frac{m_b\Omega_p}{2\hbar} z^2\right) \nabla_z^2 \left[z \exp\left(-\frac{m_b\Omega_p}{2\hbar} z^2\right)\right] \\
&\times \int_{-\infty}^{\infty} dy \exp\left(-\frac{m_b\Omega_p}{\hbar} y^2\right) \int_{-\infty}^{\infty} dz \exp\left(-\frac{m_b\Omega_p}{\hbar} z^2\right) + \frac{2}{4}\hbar\Omega_p \\
&= -\frac{\hbar^2}{2m_b} C_2^2 \int_{-\infty}^{\infty} dz z \exp\left(-\frac{m_b\Omega_p}{2\hbar} z^2\right) \\
&\times \nabla_z \left[\left(1 - \frac{m_b\Omega_p}{\hbar} z^2\right) \exp\left(-\frac{m_b\Omega_p}{2\hbar} z^2\right)\right] + \frac{1}{2}\hbar\Omega_p \\
&= \frac{\hbar^2}{2m_b} C_2^2 \int_{-\infty}^{\infty} dz z \exp\left(-\frac{m_b\Omega_p}{2\hbar} z^2\right) \\
&\times \left[\frac{2m_b\Omega_p}{\hbar} z + \left(1 - \frac{m_b\Omega_p}{\hbar} z^2\right) \frac{m_b\Omega_p}{\hbar} z\right] \exp\left(-\frac{m_b\Omega_p}{2\hbar} z^2\right) \\
+\frac{1}{2}\hbar\Omega_p &= \frac{\hbar^2}{2m_b} C_2^2 \int_{-\infty}^{\infty} dz \left(3 - \frac{m_b\Omega_p}{\hbar} z^2\right) \frac{m_b\Omega_p}{\hbar} z^2 \exp\left(-\frac{m_b\Omega_p}{\hbar} z^2\right) \\
+\frac{1}{2}\hbar\Omega_p &= \frac{\hbar\Omega_p}{2} C_2^2 \left[\frac{3\sqrt{\pi}}{2\left(\frac{m_b\Omega_p}{\hbar}\right)^{3/2}} - \frac{m_b\Omega_p}{\hbar} \frac{3\sqrt{\pi}}{4\left(\frac{m_b\Omega_p}{\hbar}\right)^{5/2}}\right] + \frac{1}{2}\hbar\Omega_p \\
&= \frac{\hbar\Omega_p}{2} C_2^2 \frac{3\sqrt{\pi}}{4\left(\frac{m_b\Omega_p}{\hbar}\right)^{3/2}} + \frac{1}{2}\hbar\Omega_p \\
&= \frac{\hbar\Omega_p}{2} \frac{2}{\sqrt{\pi}} \left(\frac{m_b\Omega_p}{\hbar}\right)^{3/2} \frac{3\sqrt{\pi}}{4\left(\frac{m_b\Omega_p}{\hbar}\right)^{3/2}} + \frac{1}{2}\hbar\Omega_p \\
&= \frac{3}{4}\hbar\Omega_p + \frac{1}{2}\hbar\Omega_p = \frac{5}{4}\hbar\Omega_p. \qquad (7.46)
\end{aligned}
$$

For the FC state, $\Omega_p = \Omega_0$. The second term in (7.45) is precisely (7.37),

$$
-\sum_{\mathbf{k}} \frac{|V_k|^2 \left|\rho_{\mathbf{k}"1s"}\right|^2}{\hbar\omega_{\mathrm{LO}}} = -\frac{\hbar}{\sqrt{\pi}} \sqrt{\Omega_0 \omega_{\mathrm{LO}}},
$$

and the FC energy (7.45) becomes

$$
\begin{aligned}
E_{FC} &= \frac{5}{4}\hbar\Omega_0 - \frac{\hbar\omega_{\mathrm{LO}}\alpha}{\sqrt{\pi}} \sqrt{\frac{\Omega_0}{\omega_{\mathrm{LO}}}} \\
&= \frac{5}{4}\hbar\frac{4}{9}\frac{\alpha^2}{\pi}\omega_{\mathrm{LO}} - \frac{2}{3}\frac{\alpha^2}{\pi}\hbar\omega_{\mathrm{LO}} = \left(\frac{5}{9} - \frac{2}{3}\right)\frac{\alpha^2}{\pi}\hbar\omega_{\mathrm{LO}} \Longrightarrow
\end{aligned}
$$

The energy of the lowest FC state is, within the Produkt-Ansatz [42]:

$$
E_{\mathrm{FC}} = \frac{\alpha^2}{9\pi}\hbar\omega_{\mathrm{LO}} = 0.0354\alpha^2\hbar\omega_{\mathrm{LO}}. \qquad (7.47)
$$

The fact that this energy is positive, is presumably due to the choice of a harmonic potential. The real potential the electron sees is anharmonic, and a bound state may be expected.

Calculation of RES

The electronic part of the excited wave function is (7.44) with a variational parameter Ω_p, which is determined below. The variational RES energy is, similarly to (7.35),

$$E_{RES} = \langle \varphi_{"2p"} | \frac{\mathbf{p}^2}{2m_b} | \varphi_{"2p"} \rangle - \sum_{\mathbf{k}} \frac{|V_k|^2 |\rho_{\mathbf{k}"2p"}|^2}{\hbar\omega_{\mathrm{LO}}}. \tag{7.48}$$

Here the kinetic energy term is given by Eq. (7.46). The functional, which is now needed, is

$$\begin{aligned}
\rho_{\mathbf{k}"2p"} &= \langle \varphi_{"2p"} | e^{i\mathbf{k}\cdot\mathbf{r}} | \varphi_{"2p"} \rangle = C^2_{"2p"} \int d^3r z^2 \exp\left(-\frac{m_b\Omega_p}{\hbar} r^2 + i\mathbf{k}\cdot\mathbf{r}\right) \\
&= C^2_{"2p"} \int d^3r z^2 \exp\left(-\frac{m_b\Omega_p}{\hbar}\left[r^2 + i\frac{\hbar}{m_b\Omega_p}\mathbf{k}\cdot\mathbf{r} - \frac{\hbar^2k^2}{4m_b^2\Omega_p^2} + \frac{\hbar^2k^2}{4m_b^2\Omega_p^2}\right]\right) \\
&= C^2_{"2p"}\ exp\left(-\frac{m_b\Omega_p}{\hbar}\frac{\hbar^2k^2}{4m_b^2\Omega_p^2}\right) \int d^3r z^2 \exp\left(-\frac{m_b\Omega_p}{\hbar}\left[\mathbf{r} + i\frac{\hbar}{2m_b\Omega_p}\mathbf{k}\right]^2\right) \Rightarrow
\end{aligned}$$

$$\begin{aligned}
\rho_{\mathbf{k}"2p"} &= \exp\left(-\frac{\hbar k^2}{4m_b\Omega_p}\right) C_2^2 \int_{-\infty}^{\infty} dz z^2 \exp\left(-\frac{m_b\Omega_p}{\hbar}\left[z + i\frac{\hbar}{2m_b\Omega_p}k_z\right]^2\right) \\
&= .\exp\left(-\frac{\hbar k^2}{4m_b\Omega_p}\right) C_2^2 \int_{-\infty}^{\infty} dz \left(z - i\frac{\hbar}{2m_b\Omega_p}k_z\right)^2 \exp\left(-\frac{m_b\Omega_p}{\hbar}z^2\right) \\
&= \exp\left(-\frac{\hbar k^2}{4m_b\Omega_p}\right) C_2^2 \int_{-\infty}^{\infty} dz \left[z^2 - \left(\frac{\hbar}{2m_b\Omega_p}k_z\right)^2\right]^2 \exp\left(-\frac{m_b\Omega_p}{\hbar}z^2\right) \\
&= \exp\left(-\frac{\hbar k^2}{4m_b\Omega_p}\right) C_2^2 \left\{\frac{\sqrt{\pi}}{2\left(\frac{m_b\Omega_p}{\hbar}\right)^{3/2}} - \left(\frac{\hbar}{2m_b\Omega_p}k_z\right)^2 \frac{\sqrt{\pi}}{\left(\frac{m_b\Omega_p}{\hbar}\right)^{1/2}}\right\} \\
&= \left(1 - \frac{\hbar k_z^2}{2m_b\Omega_p}\right) \exp\left(-\frac{\hbar k^2}{4m_b\Omega_p}\right).
\end{aligned} \tag{7.49}$$

Further, we substitute (7.49) in the second term in the r.h.s. of Eq. (7.48):

$$
\begin{aligned}
-\sum_{\mathbf{k}} \frac{|V_k|^2 \left|\rho_{\mathbf{k}"1s"}\right|^2}{\hbar\omega_{\mathrm{LO}}} &= -\frac{V}{(2\pi)^3}\int d^3k \frac{\hbar\omega_{\mathrm{LO}}}{k^2}\frac{4\pi\alpha}{V}\left(\frac{\hbar}{2m_b\omega_{\mathrm{LO}}}\right)^{\frac{1}{2}} \\
&\times \left(1-\frac{\hbar k_z^2}{2m_b\Omega_p}\right)^2 \exp\left(-\frac{\hbar k^2}{2m_b\Omega_p}\right) \\
&= -\frac{\alpha\hbar\omega_{\mathrm{LO}}}{2\pi^2}\left(\frac{\hbar}{2m_b\omega_{\mathrm{LO}}}\right)^{\frac{1}{2}} 2\pi\int_{-1}^{1} dx \\
&\times \int_0^\infty dk \left(1-\frac{\hbar k^2 x^2}{m_b\Omega_p}+\frac{\hbar^2 k^4 x^4}{4m_b^2\Omega_p^2}\right)\exp\left(-\frac{\hbar k^2}{2m_b\Omega_p}\right) \\
&= -\frac{\alpha\hbar\omega_{\mathrm{LO}}}{\pi}\left(\frac{\hbar}{2m_b\omega_{\mathrm{LO}}}\right)^{\frac{1}{2}} \\
&\times \int_0^\infty dk \left(2-\frac{2}{3}\frac{\hbar k^2}{m_b\Omega_p}+\frac{2}{5}\frac{\hbar^2 k^4}{4m_b^2\Omega_p^2}\right)\exp\left(-\frac{\hbar k^2}{2m_b\Omega_p}\right) \\
&= -\frac{\alpha\hbar\omega_{\mathrm{LO}}}{\pi}\left(\frac{\hbar}{2m_b\omega_{\mathrm{LO}}}\right)^{\frac{1}{2}} \\
&\times \left[\frac{\sqrt{\pi}}{\left(\frac{\hbar}{2m_b\Omega_p}\right)^{1/2}}-\frac{1}{3}\frac{\hbar}{m_b\Omega_p}\frac{\sqrt{\pi}}{2\left(\frac{\hbar}{2m_b\Omega_p}\right)^{3/2}}+\frac{1}{5}\frac{\hbar^2}{4m_b^2\Omega_p^2}\frac{3\sqrt{\pi}}{4\left(\frac{\hbar}{2m_b\Omega_p}\right)^{5/2}}\right]
\end{aligned}
$$

$$
\begin{aligned}
&= -\frac{\alpha\hbar}{\sqrt{\pi}}\sqrt{\omega_{\mathrm{LO}}\Omega_p}\left[1-\frac{1}{3}+\frac{3}{20}\right] \\
&= -\frac{\alpha\hbar}{\sqrt{\pi}}\sqrt{\omega_{\mathrm{LO}}\Omega_p}\frac{60-20+9}{60} = -\frac{49}{60}\frac{\alpha\hbar}{\sqrt{\pi}}\sqrt{\omega_{\mathrm{LO}}\Omega_p}
\end{aligned}
$$

The variational energy (7.48) becomes

$$
E_{RES} = \frac{5}{4}\hbar\Omega_p - \frac{49}{60}\frac{\alpha\hbar}{\sqrt{\pi}}\sqrt{\omega_{\mathrm{LO}}\Omega_p}.
$$

Putting

$$
\frac{\partial E_{RES}}{\partial \Omega_p} = 0,
$$

one obtains

$$
\frac{5}{4} = \frac{49\alpha}{120\sqrt{\pi}}\sqrt{\frac{\omega_{\mathrm{LO}}}{\Omega_p}} \Longrightarrow \sqrt{\frac{\Omega_p}{\omega_{\mathrm{LO}}}} = \frac{49\alpha}{150\sqrt{\pi}} \Longrightarrow \frac{\Omega_p}{\omega_{\mathrm{LO}}} = \left(\frac{49}{150}\right)^2\frac{\alpha^2}{\pi} \Longrightarrow
$$

$$
\begin{aligned}
E_{RES} &= \frac{5}{4}\hbar\left(\frac{49}{150}\right)^2\frac{\alpha^2}{\pi}\omega_{\mathrm{LO}} - \frac{\hbar\omega_{\mathrm{LO}}\alpha}{\sqrt{\pi}}\frac{49}{60}\frac{49\alpha}{150\sqrt{\pi}} = \left(\frac{5}{4}-\frac{5}{2}\right)\left(\frac{49}{150}\right)^2\frac{\alpha^2}{\pi}\hbar\omega_{\mathrm{LO}} \\
&= -\frac{5}{4}\left(\frac{49}{150}\right)^2\frac{\alpha^2}{\pi}\hbar\omega_{\mathrm{LO}} = -\frac{49^2}{120\times 150}\frac{\alpha^2}{\pi}\hbar\omega_{\mathrm{LO}} \Longrightarrow
\end{aligned}
$$

The energy of the RES is (see Refs. [41, 39]):

$$
E_{\mathrm{RES}} = -0.042\alpha^2\hbar\omega_{\mathrm{LO}}. \tag{7.50}
$$

The effective mass of the polaron in the RES is given [39] as:

$$m^*_{RES} = 0.621\frac{\alpha^4}{81\pi^2}m_b = 0.0200\alpha^4 m_b. \tag{7.51}$$

The structure of the energy spectrum of the strong-coupling polaron is shown in Fig. 7.2.

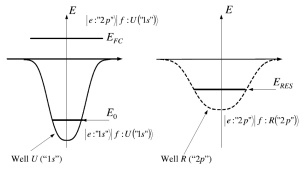

Figure 7.2: Structure of the energy spectrum of a polaron at strong coupling: E_0 — the ground state, $E_{\rm RES}$ — the (first) relaxed excited state; the Franck-Condon states ($E_{\rm FC}$). In fact, both the Franck-Condon states and the relaxed excited states lie in the continuum and, strictly speaking, are resonances.

The significance of the strong-coupling large polaron theory is formal only: it allows to test "all-coupling" theories in the limit $\alpha \to \infty$. Remarkably, the effective electron-phonon coupling strength significantly increases in systems of low dimension and low dimensionality.

All-coupling theory. The Feynman path integral

Feynman developed a superior all-coupling polaron theory using his path-integral formalism [43]. He studied first the self-energy E_0 and the effective mass m^* of polarons [43].

Feynman got the idea to formulate the polaron problem into the Lagrangian form of quantum mechanics and then eliminate the field oscillators, "... in exact analogy to Q. E. D. ... (resulting in) ... a sum over all trajectories ...". The resulting path integral (here limited to the ground-state properties) is of the form (Ref. [43]):

$$\langle 0,\beta|0,0\rangle = \int \mathcal{D}\mathbf{r}(\tau)\exp\left[-\frac{1}{2}\int_0^\beta \dot{\mathbf{r}}^2 d\tau + \frac{\alpha}{2^{\frac{3}{2}}}\int_0^\beta\int_0^\beta \frac{e^{-|\tau-\sigma|}}{|\mathbf{r}(\tau)-\mathbf{r}(\sigma)|}d\tau d\sigma\right], \tag{7.52}$$

where $\beta = 1/(k_B T)$. (7.52) gives the amplitude that an electron found at a point in space at time zero will appear at the same point at the (imaginary) time β. This path integral (7.52) has a great intuitive appeal: it shows the polaron problem as an equivalent one-particle problem in which the interaction, non-local in time or "retarded", occurs between the electron and itself. Subsequently Feynman showed how the variational principle of quantum mechanics could be adapted to the path-integral formalism and he introduced a quadratic trial action (non-local in time) to simulate (7.52).

Applying the variational principle for path integrals then results in an upper bound for the polaron self-energy at all α, which at weak and strong coupling gives accurate expressions. Feynman obtained smooth interpolation between a weak and strong coupling (for the ground state energy). The weak-coupling expansions of Feynman for the ground-state energy and the effective mass of the polaron are:

$$\frac{E_0}{\hbar\omega_{\rm LO}} = -\alpha - 0.0123\alpha^2 - 0.00064\alpha^3 - \ldots \ (\alpha \to 0), \tag{7.53}$$

$$\frac{m^*}{m_b} = 1 + \frac{\alpha}{6} + 0.025\alpha^2 + \ldots \ (\alpha \to 0). \tag{7.54}$$

In the strong-coupling limit Feynman found for the ground-state energy energy:

$$\frac{E_0}{\hbar\omega_{\rm LO}} \equiv \frac{E_{3D}(\alpha)}{\hbar\omega_{\rm LO}} = -0.106\alpha^2 - 2.83 - \ldots \quad (\alpha \to \infty) \tag{7.55}$$

and for the polaron mass:

$$\frac{m^*}{m_b} \equiv \frac{m^*_{3D}(\alpha)}{m_b} = 0.0202\alpha^4 + \ldots \quad (\alpha \to \infty). \tag{7.56}$$

Over the years the Feynman model for the polaron has remained the most successful approach to this problem. The analysis of an exactly solvable ("symmetrical") 1D-polaron model [41, 44], Monte Carlo schemes [30, 45] and other numerical schemes [46] demonstrate the remarkable accuracy of Feynman's path-integral approach to the polaron ground-state energy. Experimentally more directly accessible properties of the polaron, such as its mobility and optical absorption, have been investigated subsequently. Within the path-integral approach, Feynman et al. studied later the mobility of polarons [47, 48]. Subsequently the path-integral approach to the polaron problem was generalized and developed to become a powerful tool to study optical absorption, magnetophonon resonance and cyclotron resonance [49, 50, 51, 52, 53].

In Ref. [54], a self-consistent treatment for the polaron problem at all α was presented, which is based on the Heisenberg equations of motion starting from a trial expression for the electron position. It was used to derive the effective mass and the optical properties of the polaron at arbitrary coupling. A variational justification of the approximation used in Ref. [54] (through a Stiltjes continuous fraction) is reproduced in Appendix 2.

On Monte Carlo calculations of the polaron free energy

In Ref. [55], using a Monte Carlo calculation, the ground-state energy of a polaron was derived as $E_0 = \lim_{\beta\to\infty} \Delta F$, where $\Delta F = F_\beta - F^0_\beta$ with F_β the free energy per polaron and $F^0_\beta = [3/(2\beta)] \ln(2\pi\beta)$ the free energy per electron. The value $\beta\hbar\omega_{\rm LO} = 25$, used for the actual computation in Ref. [55], corresponds to $T/T_D = 0.04$ ($T_D = \hbar\omega_{\rm LO}/k_B$; $\hbar\omega_{\rm LO}$ is the LO phonon energy). So, as pointed out in Ref. [56], the authors of Ref. [55] actually calculated the *free energy* ΔF, rather than the polaron *ground-state energy*.

To investigate the importance of temperature effects on ΔF, the authors of Ref. [56] considered the polaron energy as obtained by Osaka [57], who generalized the Feynman [43] polaron theory to nonzero temperatures:

$$\frac{\Delta F}{\hbar\omega} = \frac{3}{\beta} \ln\left(\frac{w}{v}\frac{\sinh\frac{\beta_0 v}{2}}{\sinh\frac{\beta_0 w}{2}}\right) - \frac{3}{4}\frac{v^2 - w^2}{v}\left(\coth\frac{\beta_0 v}{2} - \frac{2}{\beta_0 v}\right)$$
$$- \frac{\alpha}{\sqrt{2\pi}}\left[1 + n(\omega_{\rm LO})\right]\int_0^{\beta_0} du \frac{e^{-u}}{\sqrt{D(u)}}, \tag{7.57}$$

where $\beta_0 = \beta\hbar\omega_{\rm LO}$, $n(\omega) = 1/\left(e^{\beta\hbar\omega} - 1\right)$, and

$$D(u) = \frac{w^2}{v^2}\frac{u}{2}\left(1 - \frac{u}{\beta_0}\right) + \frac{v^2 - w^2}{2v^3}\left(1 - e^{-vu} - 4n(v)\sinh^2\frac{vu}{2}\right). \tag{7.58}$$

This result is variational, with variational parameters v and w, and gives an upper bound to the exact polaron free energy.

The results of a numerical-variational calculation of Eq. (7.57) are shown in Fig. 7.3, where the free energy $-\Delta F$ is plotted (in units of $\hbar\omega_{\rm LO}$) as a function of α for different values of the lattice temperature. As seen from Fig. 7.3, (i) $-\Delta F$ increases with increasing temperature and (ii) the effect of temperature on ΔF increases with increasing α.

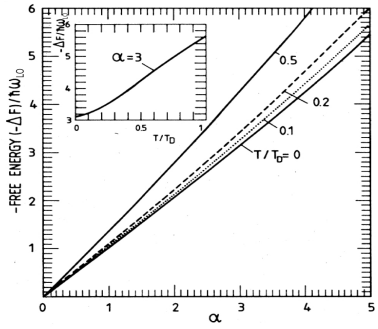

Figure 7.3: Contribution of the electron-phonon interaction to the free energy of the Feynman polaron as a function of the electron-phonon coupling constant α for different values of the lattice temperature. Inset: temperature dependence of the free energy for $\alpha = 3$. (From Ref. [56].)

In Table 3, the Monte Carlo results [55], $(\Delta F)_{\rm MC}$, are compared with the free energy of the Feynman polaron, $(\Delta F)_{\rm F}$, calculated in [56]. The values for the free energy obtained from the Feynman polaron model are *lower* than the MC results for $\alpha \lesssim 2$ and $\alpha \geq 4$ (but lie within the 1% error of the Monte Carlo results). Since the Feynman result for the polaron free energy is an upper bound to the exact result, we conclude that for $\alpha \lesssim 2$ and $\alpha \geq 4$ the results of the Feynman model are closer to the exact result than the MC results of [55].

On the contributions of the N-phonon states to the polaron ground state

The analysis of an exactly solvable ("symmetric") 1D-polaron model was performed in Refs. [58, 41, 59]. The model consists of an electron interacting with two oscillators possessing the opposite wave vectors: **k** and -**k**.The parity operator, which changes $a_{\mathbf{k}}$ and $a_{-\mathbf{k}}$ (and also $a^{\dagger}_{\mathbf{k}}$ and $a^{\dagger}_{-\mathbf{k}}$), commutes with the Hamiltonian of the system. Hence, the polaron states are classified

Table 2: *Electron-phonon coupling constants* (After Ref. [4])

Material	α	Ref.	Material	α	Ref.
InSb	0.023	[7]	AgCl	1.84	[13]
InAs	0.052	[7]	KI	2.5	[7]
GaAs	0.068	[7]	TlBr	2.55	[7]
GaP	0.20	[7]	KBr	3.05	[7]
CdTe	0.29	[8]	$Bi_{12}SiO_{20}$	3.18	[21]
ZnSe	0.43	[7]	CdF_2	3.2	[7]
CdS	0.53	[7]	KCl	3.44	[7]
α-Al_2O_3	1.25	[9]	CsI	3.67	[7]
AgBr	1.53	[13]	$SrTiO_3$	3.77	[22]
α-SiO_2	1.59	[14]	RbCl	3.81	[7]

Table 3: Comparison between the free energy of the Feynman polaron theory, $-(\Delta F)_{\rm F}$, and the Monte Carlo results of Ref. [55], $-(\Delta F)_{\rm MC}$, for $T/T_D = 0.04$. The relative difference is defined as $\Delta = 100 \times [(\Delta F)_{\rm F} - (\Delta F)_{\rm MC}]/(\Delta F)_{\rm MC}$. (From Ref. [56])

α	$-(\Delta F)_{\rm F}$	$-(\Delta F)_{\rm MC}$	Δ (%)
0.5	0.50860	0.505	0.71
1.0	1.02429	1.020	0.42
1.5	1.54776	1.545	0.18
2.0	2.07979	2.080	−0.010
2.5	2.62137	2.627	−0.21
3.0	3.17365	3.184	−0.32
3.5	3.73814	3.747	−0.24
4.0	4.31670	4.314	0.063

into the even and odd ones with the eigenvalues of the parity operator $+1$ and -1, respectively. For the lowest even and odd states, the phonon distribution functions W_N are plotted in Fig. 7.4, upper panel, at some values of the effective coupling constant λ of the "symmetric" model. The value of the parameter

$$\varkappa = \sqrt{\frac{(\hbar k)^2}{m_b \hbar \omega_{\mathrm{LO}}}}$$

for these graphs was taken 1, while the total polaron momentum $\mathbf{P} = 0$. In the weak-coupling case ($\lambda \approx 0.6$) W_N is a decaying function of N. When increasing λ, W_N acquires a maximum, e.g. at $N = 8$ for the lowest even state at $\lambda \approx 5.1$. The phonon distribution function W_N has the same character for the lowest even and the lowest odd states at all values of the number of the virtual phonons in the ground state. (as distinct from the higher states). This led to the conclusion that the lowest odd state is an internal excited state of the polaron.

In Ref [30], the structure of the polaron cloud was investigated using the diagrammatic quantum Monte Carlo (DQMC) method. In particular, partial contributions of N-phonon states to the polaron ground state were found as a function of N for a few values of the coupling constant α, see Fig. 7.4, lower panel. It was shown to gradually evolve from the weak-coupling case ($\alpha = 1$) into the strong-coupling regime ($\alpha = 17$). Comparion of the lower panel to the upper panel in Fig. 7.4 clearly shows that the evolution of the shape and the scale of the distribution of the N-phonon states with increasing α as derived for a large polaron within DQMC method [30] is *in remarkable agreement* with the results obtained within the "symmetric" 1D polaron model [58, 41, 59].

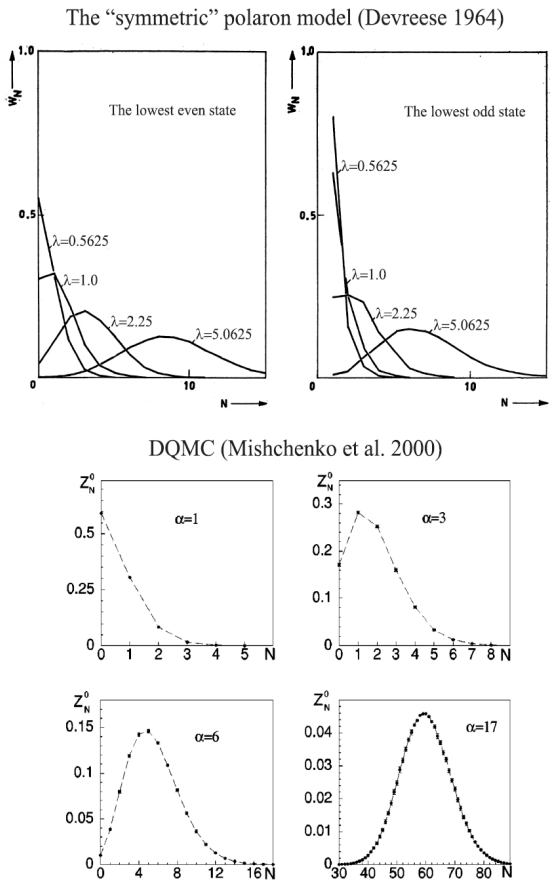

Figure 7.4: *Upper panel*: The phonon distribution functions W_N in the "symmetric" polaron model for various values of the effective coupling constant λ at $\kappa = 1, \mathbf{P} = 0$ (from [58], Fig. 23). *Lower panel*: Distribution of multiphonon states in the polaron cloud within DQMC method for various values of α (from [30], Fig. 7).

7.1.6 Polaron mobility

[3]

The mobility of large polarons was studied within various theoretical approaches(see Ref. [60] for the detailed references). Fröhlich [61] pointed out the typical behavior of the large-polaron mobility

$$\mu \propto \exp(\hbar\omega_{\mathrm{LO}}\beta), \tag{7.59}$$

which is characteristic for weak coupling. Here, $\beta = 1/k_B T$, T is the temperature. Within the weak-coupling regime, the mobility of the polaron was then derived, e. g., using the Boltzmann equation in Refs. [62, 63] and starting from the LLP-transformation in Ref. [64].

[3] **See also Appendix D "Notes on the polaron mobility".**

A nonperturbative analysis was embodied in the Feynman polaron theory, where the mobility μ of the polaron using the path-integral formalism was derived by Feynman et al. (usually referred to as FHIP) as a static limit starting from a frequency-dependent impedance function. For sufficiently low temperature T the mobility then takes the form [47]

$$\mu = \left(\frac{w}{v}\right)^3 \frac{3e}{4m_b\hbar\omega_{\rm LO}^2\alpha\beta} e^{\hbar\omega_{\rm LO}\beta} \exp\{(v^2 - w^2)/w^2 v\} \ , \tag{7.60}$$

where v and w are (variational) functions of α obtained from the Feynman polaron model.

Using the Boltzmann equation for the Feynman polaron model, Kadanoff [65] found the mobility, which for low temperatures can be represented as follows:

$$\mu = \left(\frac{w}{v}\right)^3 \frac{e}{2m_b\omega_{\rm LO}\alpha} e^{\hbar\omega_{\rm LO}\beta} \exp\{(v^2 - w^2)/w^2 v\} \ , \tag{7.61}$$

The weak-coupling perturbation expansion of the low-temperature polaron mobility as found using the Green's function technique [66] has confirmed that the mobility derived from the Boltzmann equation is exceedingly exact for weak coupling ($\alpha/6 \ll 1$) and at low temperatures ($k_B T \ll \hbar\omega_{\rm LO}$). As shown in Ref. [65], the mobility of Eq. (7.60) differs by the factor of $3/(2\beta\hbar\omega_{\rm LO})$ from that derived using the polaron Boltzmann equation as given by Eq. (7.61).

In the limit of weak electron-phonon coupling and low temperature, the FHIP polaron mobility of Eq. (7.60) differs by the factor of $3/(2\beta\hbar\omega_{\rm LO})$ from the previous result [62, 64, 63], which, as pointed out in Ref. [47] and in later publications (see, e.g., Refs.[65, 66, 60]), is correct for $\beta \gg 1$. As follows from this comparison, the result of Ref. [47] is not valid when $T \to 0$. As argued in Ref. [47] and later confirmed, in particular, in Ref. [67] the above discrepancy can be attributed to an interchange of two limits in calculating the impedance. In FHIP, for weak electron-phonon coupling, one takes $\lim_{\Omega\to 0}\lim_{\alpha\to 0}$, whereas the correct order is $\lim_{\alpha\to 0}\lim_{\Omega\to 0}$ (Ω is the frequency of the applied electric field). It turns out that for the correct result the mobility at low temperatures is predominantly limited by the absorption of phonons, while in the theory of FHIP it is the emission of phonons which gives the dominant contribution as T goes to zero [67].

The analysis based on the Boltzmann equation takes into account the phonon emission processes whenever the energy of the polaron is above the emission threshold. The independent-collision model, which underlies the Boltzmann-equation approach, however, fails in the "strong coupling regime" of the large polaron, when the thermal mean free path becomes less than the de Broglie wavelength; in this case, the Boltzmann equation cannot be expected to be adequate [47, 68].[4]

In fact, the expression (7.60) for the polaron mobility was reported to adequately describe the experimental data in several polar materials (see, e.g., Refs. [69, 68, 70]). Experimental work on alkali halides and silver halides indicates that the mobility obtained from Eq. (7.60) describes the experimental results quite accurately [69]. Measurements of mobility as a function of temperature for photoexcited electrons in cubic n-type $Bi_{12}SiO_{20}$ are explained well in terms of large polarons within the Feynman approach [68]. The experimental findings on electron transport in crystalline TiO_2 (rutile phase) probed by THz time-domain spectroscopy are quantitatively interpreted within the Feynman model [70]. One of the reasons for the agreement between theory based on Eq. (7.60) and experiment is that in the path-integral approximation to the polaron mobility, a Maxwellian distribution for the electron velocities is assumed, when applying the adiabatic switching on of the Fröhlich interaction. Although such a distribution is not inherent in the Fröhlich interaction, its incorporation tends to favor agreement with experiment because other mechanisms (interaction with acoustic phonons etc.) cause a Gaussian distribution.

[4]**For the polaron mobility in the weak- and strong-coupling regimes, see also Appendix D "Notes on the polaron mobility".**

7.2 Optical Absorption. Weak coupling

7.2.1 Optical absorption at weak coupling [within the perturbation theory]

At zero temperature and in the weak-coupling limit, the optical absorption is due to the elementary polaron scattering process, schematically shown in Fig. 7.5.

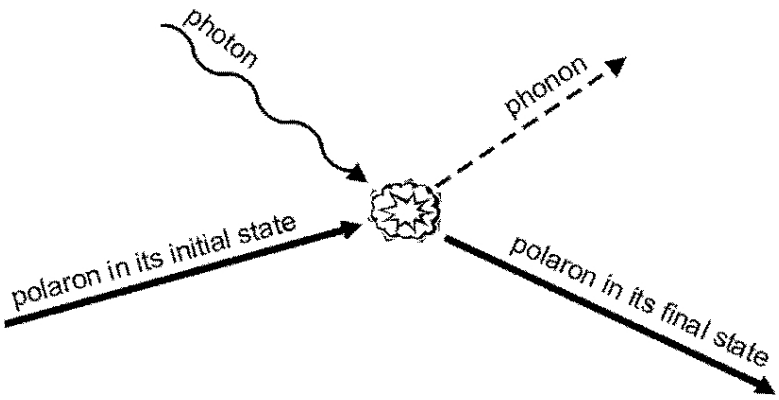

Figure 7.5: Elementary polaron scattering process describing the absorption of an incoming photon and the generation of an outgoing phonon.

In the weak-coupling limit ($\alpha \ll 1$) the polaron absorption coefficient was first obtained by V. Gurevich, I. Lang and Yu. Firsov [71], who started from the Kubo formula. Their optical-absorption coefficient is equivalent to a particular case of the result of J. Tempere and J. T. Devreese (Ref. [53]), with the dynamic srtucture factor $S(\mathbf{q},\omega)$ corresponding to the Hartree-Fock approximation (see also [72], p. 585). At zero temperature, the absorption coefficient for absorption of light with frequency Ω can be expressed in terms of elementary functions in two limiting cases: in the region of comparatively high polaron densities ($\hbar(\Omega-\omega_{\rm LO})/\zeta \ll 1$)

$$\Gamma(\omega) = \frac{1}{\epsilon_0 nc}\frac{2^{1/2}N^{2/3}\alpha}{(3\pi^2)^{1/3}}\frac{e^2}{(\hbar m_b\omega_{\rm LO})^{1/2}}\frac{\omega-1}{\omega^3}\Theta(\omega-1), \tag{7.62}$$

and in the low-concentration region ($\hbar(\Omega-\omega_{\rm LO})/\zeta \gg 1$)

$$\Gamma(\omega) = \frac{1}{\epsilon_0 nc}\frac{2Ne^2\alpha}{3m_b\omega_{\rm LO}}\frac{(\omega-1)^{1/2}}{\omega^3}\Theta(\omega-1), \tag{7.63}$$

where $\omega = \Omega/\omega_{\rm LO}$, ϵ_0 is the dielectric permittivity of the vacuum, n is the refractive index of the medium, N is the concentration of polarons and ζ is the Fermi level for the electrons. A step function

$$\Theta(\omega-1) = \begin{cases} 1 & \text{if} \quad \omega > 1, \\ 0 & \text{if} \quad \omega < 1 \end{cases}$$

reflects the fact that at zero temperature the absorption of light accompanied by the emission of a phonon can occur only if the energy of the incident photon is larger than that of a phonon ($\omega > 1$). In the weak-coupling limit, according to Eqs. (7.62), (7.63), the absorption spectrum consists of a "one-phonon line".

At nonzero temperature, the absorption of a photon can be accompanied not only by emission, but also by absorption of one or more phonons.

A simple derivation in Ref. [73] using a canonical transformation method gives the absorption coefficient of free polarons, which coincides with the result (7.63) of Ref. [71].

7.2.2 Optical absorption at weak coupling [within the canonical-transformation method [73] (DHL)]

The optical absorption of large polarons as a function of the frequency of the incident light is calculated using the canonical-transformation formalism by Devreese, Huybrechts and Lemmens (DHL) Ref. [73]. A simple calculation, which is developed below in full detail, gives a result for the absorption coefficient, which is exact to order α.

We start from the Hamiltonian of the electron-phonon system interacting with light is written down using the vector potential of an electromagnetic field $\mathbf{A}(t)$:

$$H = \frac{1}{2m_b}\left(\mathbf{p} + \frac{e}{c}\mathbf{A}(t)\right)^2 + \sum_{\mathbf{k}} \omega_{\mathrm{LO}} a_{\mathbf{k}}^{+} a_{\mathbf{k}} + \sum_{\mathbf{k}} \left(V_{\mathbf{k}} a_{\mathbf{k}} e^{i\mathbf{k}\cdot\mathbf{r}} + V_{\mathbf{k}}^{*} a_{\mathbf{k}}^{+} e^{-i\mathbf{k}\cdot\mathbf{r}}\right). \tag{7.64}$$

The electric field is related to the vector potential as

$$\mathbf{E}(t) = -\frac{1}{c}\frac{\partial \mathbf{A}(t)}{\partial t}. \tag{7.65}$$

Within the electric dipole interaction the electric field with frequency Ω is

$$\mathbf{E}(t) = \mathbf{E}\cos(\Omega t) \Rightarrow \tag{7.66}$$

$$\mathbf{A} = -\frac{c}{\Omega}\mathbf{E}\sin(\Omega t). \tag{7.67}$$

When expanding $\frac{1}{2m_b}\left(\mathbf{p} + \frac{e}{c}\mathbf{A}(t)\right)^2$ in the Hamiltonian, we find

$$\frac{1}{2m_b}\left(\mathbf{p} + \frac{e}{c}\mathbf{A}(t)\right)^2 = \frac{\mathbf{p}^2}{2m_b} + \frac{e}{m_b c}\mathbf{A}(t)\cdot\mathbf{p} + \frac{e^2}{2m_b c^2}A^2(t) \tag{7.68}$$

where the first term is the kinetic energy of the electron, and the second term describes the interaction of the electron-phonon system with light

$$V_t = \frac{e}{m_b c}\mathbf{A}(t)\cdot\mathbf{p} = -\frac{e}{m_b\Omega}\mathbf{E}\cdot\mathbf{p}\sin\Omega t \tag{7.69}$$

$$V_t \equiv V\sin\Omega t, \tag{7.70}$$

$$V \equiv -\frac{e}{m_b\Omega}\mathbf{E}\cdot\mathbf{p}. \tag{7.71}$$

Since $\mathbf{A}(t)$ does not depend on the electron coordinates, the term $\frac{e^2}{2m_b c^2}A^2(t)$ in (7.68) does not play a role in our description of the optical absorption. The total Hamiltonian for the system of a continuum polaron interacting with light is thus

$$H_{tot} = H_{pol} + V_t,$$

where H_{pol} is Fröhlich's Hamiltonian (7.16).

The absorption coefficient for absorption of light with frequency Ω by free polarons is proportional to the probability $P(\Omega)$ that a photon is absorbed by these polarons in their ground state,

$$\Gamma_p(\Omega) = \frac{N}{\varepsilon_0 c n 2E^2}\Omega P(\Omega). \tag{7.72}$$

Here N is number of polarons, which are considered as independent from each other, ε_0 is the permittivity of vacuum, c is the velocity of light, n is the refractive index of the medium in

which the polarons move, E is the modulus of the electric field vector of the incident photon. If the incident light can be treated as a perturbation, the transition probability $P(\Omega)$ is given by the Golden Rule of Fermi:

$$P(\Omega) = 2\pi \sum\nolimits_f \langle \Phi_0 | V | f \rangle \langle f | V | \Phi_0 \rangle \delta(E_0 + \Omega - E_f). \tag{7.73}$$

V is the amplitude of the time-dependent perturbation given by (7.71). The ground state wave function of a free polaron is $|\Phi_0\rangle$ and its energy is E_0. The wave functions of all possible final states are $|f\rangle$ and the corresponding energies are E_f. The possible final states are all the excited states of the polaron. The main idea of the present calculation is to avoid the explicit summation over the final polaron states, which are poorly known, by eliminating all the excited state wave functions $|f\rangle$ from the expression (7.73).

With this aim, the representation of the δ-function is used:

$$\delta(x) = \frac{1}{\pi} \operatorname{Re} \int_{-\infty}^{0} dt \exp\left[-i\left(x + i\varepsilon\right) t\right].$$

This leads to:

$$\begin{aligned} P(\Omega) &= 2 \operatorname{Re} \sum\nolimits_f \int_{-\infty}^{0} dt \langle \Phi_0 | V | f \rangle \langle f | V | \Phi_0 \rangle \exp\left[-i(\Omega + i\varepsilon + E_0 - E_f)t\right] \\ &= 2 \operatorname{Re} \sum\nolimits_f \int_{-\infty}^{0} dt \exp\left[-i(\Omega + i\varepsilon)t\right] \langle \Phi_0 | V | f \rangle \left\langle f \left| e^{iHt} V e^{-iHt} \right| \Phi_0 \right\rangle. \end{aligned}$$

Using the fact that

$$\sum\nolimits_f |f\rangle \langle f| = 1$$

and the notation

$$\begin{aligned} e^{iHt} V(0) e^{-iHt} &= V(t), \\ \frac{dV(t)}{dt} &= i\left[H, V(t)\right] \end{aligned}$$

we find

$$P(\Omega) = 2 \operatorname{Re} \int_{-\infty}^{0} dt \exp\left[-i(\Omega + i\varepsilon)t\right] \langle \Phi_0 | V(0) V(t) | \Phi_0 \rangle. \tag{7.74}$$

Defining

$$R(\Omega) = \int_{-\infty}^{0} dt \exp\left[-i(\Omega + i\varepsilon)t\right] \langle \Phi_0 | V(0) V(t) | \Phi_0 \rangle, \tag{7.75}$$

one has

$$P(\Omega) = 2 \operatorname{Re} R(\Omega). \tag{7.76}$$

Substituting (7.71) to (7.75), we find that

$$R(\Omega) = \left(\frac{e}{m_b \Omega}\right)^2 \int_{-\infty}^{0} dt e^{-i(\Omega + i\varepsilon)t} \langle \Phi_0 | (\mathbf{E} \cdot \mathbf{p}(0)) (\mathbf{E} \cdot \mathbf{p}(t)) | \Phi_0 \rangle \tag{7.77}$$

and hence

$$P(\Omega) = 2 \left(\frac{e}{m_b \Omega}\right)^2 \operatorname{Re} \int_{-\infty}^{0} dt e^{-i(\Omega + i\varepsilon)t} \langle \Phi_0 | (\mathbf{E} \cdot \mathbf{p}(0)) (\mathbf{E} \cdot \mathbf{p}(t)) | \Phi_0 \rangle. \tag{7.78}$$

It is convenient to apply the first LLP transformation S_1(7.271), which eliminates the electron operators from the polaron Hamiltonian:

$$
\begin{aligned}
&H \longrightarrow \mathcal{H} = S_1^{-1} H_{pol} S_1 = \mathcal{H}_0 + \mathcal{H}_1 : \\
&\mathcal{H}_0 = \frac{\mathbf{P}^2}{2m_b} + \sum_{\mathbf{k}} \left(\omega_{\mathrm{LO}} + \frac{k^2}{2m_b} - \frac{\mathbf{k}\cdot\mathbf{P}}{m_b} \right) a_{\mathbf{k}}^\dagger a_{\mathbf{k}} + \sum_{\mathbf{k}} (V_k a_{\mathbf{k}} + V_k^* a_{\mathbf{k}}^\dagger), \\
&\mathcal{H}_1 = \frac{1}{2m_b} \sum_{\mathbf{k}} \mathbf{k}\cdot\mathbf{k}' a_{\mathbf{k}}^\dagger a_{\mathbf{k}'}^\dagger a_{\mathbf{k}} a_{\mathbf{k}'},
\end{aligned}
$$

where $\mathcal{H}_0$ can be diagonalized exactly and gives rise to the self-energy $E = -\alpha\omega_{\mathrm{LO}}$, and $\mathcal{H}_1$ contains the correlation effects between the phonons. The optical absorption will be calculated here for the total momentum of the system $\mathbf{P} = \mathbf{0}$.

In the LLP approximation the explicit form of the matrix element in (7.77) is

$$
\langle \Phi_0 | (\mathbf{E}\cdot\mathbf{p}(0)) (\mathbf{E}\cdot\mathbf{p}(t)) | \Phi_0 \rangle = \left\langle 0 \left| S_2^{-1} S_1^{-1} \mathbf{E}\cdot\mathbf{p} S_1 S_1^{-1} \mathbf{E}\cdot\mathbf{p}(t) S_1 S_2 \right| 0 \right\rangle, \tag{7.79}
$$

where $S_1$and S_2 are the first (7.271) and the second (7.280) LLP transformations. The application of S_1 gives:

$$
S_1^{-1}\mathbf{p}(t) S_1 = S_1^{-1} e^{iHt} \mathbf{p} e^{-iHt} S_1 = S_1^{-1} e^{iHt} S_1 S_1^{-1} \mathbf{p} S_1 S_1^{-1} e^{-iHt} S_1.
$$

Using $\mathcal{H} = S_1^{-1} H S_1$, we arrive at $S_1^{-1} e^{iHt} S_1 = e^{i\mathcal{H}t}$.Further we recall $S_1^{-1}\mathbf{p}S_1 = \mathbf{P} - \sum_{\mathbf{k}} \hbar\mathbf{k} a_{\mathbf{k}}^\dagger a_{\mathbf{k}} + \mathbf{p}$, where $\mathbf{P} = \mathbf{0}$ and $\mathbf{p}$ is set 0 (see Appendix 1). This results in

$$
S_1^{-1}\mathbf{p}(t) S_1 = e^{i\mathcal{H}t} \mathbf{p} e^{-i\mathcal{H}t} = -\sum_{\mathbf{k}} \hbar\mathbf{k} e^{i\mathcal{H}t} a_{\mathbf{k}}^\dagger a_{\mathbf{k}} e^{-i\mathcal{H}t} = -\sum_{\mathbf{k}} \hbar\mathbf{k} a_{\mathbf{k}}^\dagger(t) a_{\mathbf{k}}(t).
$$

Then (7.79) takes the form

$$
\langle \Phi_0 | (\mathbf{E}\cdot\mathbf{p}(0)) (\mathbf{E}\cdot\mathbf{p}(t)) | \Phi_0 \rangle = \left\langle 0 \left| S_2^{-1} \left(\sum_{\mathbf{k}} \mathbf{E}\cdot\mathbf{k} a_{\mathbf{k}}^\dagger a_{\mathbf{k}} \right) \left(\sum_{\mathbf{k}} \mathbf{E}\cdot\mathbf{k} a_{\mathbf{k}}^\dagger(t) a_{\mathbf{k}}(t) \right) S_2 \right| 0 \right\rangle. \tag{7.80}
$$

Here the second LLP transformation is given by (7.280) with

$$
f_k = -\frac{V_k^*}{\omega_{\mathrm{LO}} + \frac{k^2}{2m_b}} \tag{7.81}
$$

and the vacuum is defined by $a_{\mathbf{k}} |0\rangle = 0$. The calculation of the matrix element (7.80) proceeds as follows:

$$
\begin{aligned}
&\left\langle 0 \left| S_2^{-1} \left(\sum_{\mathbf{k}} \mathbf{E}\cdot\mathbf{k} a_{\mathbf{k}}^\dagger a_{\mathbf{k}} \right) \left(\sum_{\mathbf{k}} \mathbf{E}\cdot\mathbf{k} a_{\mathbf{k}}^\dagger(t) a_{\mathbf{k}}(t) \right) S_2 \right| 0 \right\rangle \\
&= \left\langle 0 \left| S_2^{-1} \left(\sum_{\mathbf{k}} \mathbf{E}\cdot\mathbf{k} a_{\mathbf{k}}^\dagger a_{\mathbf{k}} \right) S_2 S_2^{-1} e^{i\mathcal{H}t} S_2 S_2^{-1} \left(\sum_{\mathbf{k}} \mathbf{E}\cdot\mathbf{k} a_{\mathbf{k}}^\dagger a_{\mathbf{k}} \right) S_2 S_2^{-1} e^{-i\mathcal{H}t} S_2 \right| 0 \right\rangle \\
&= \left\langle 0 \left| S_2^{-1} \left(\sum_{\mathbf{k}} \mathbf{E}\cdot\mathbf{k} a_{\mathbf{k}}^\dagger a_{\mathbf{k}} \right) S_2 e^{iS_2^{-1}\mathcal{H}S_2 t} S_2^{-1} \left(\sum_{\mathbf{k}} \mathbf{E}\cdot\mathbf{k} a_{\mathbf{k}}^\dagger a_{\mathbf{k}} \right) S_2 e^{-iS_2^{-1}\mathcal{H}S_2 t} \right| 0 \right\rangle.
\end{aligned} \tag{7.82}
$$

Further on, we calculate

$$
S_2^{-1} \mathcal{H} S_2 = H_0 + H_1
$$

where

$$H_0 = S_2^{-1}\mathcal{H}_0 S_2 = S_2^{-1}\left[\sum_{\mathbf{k}}\left(\omega_{\mathrm{LO}} + \frac{k^2}{2m_b}\right)a_{\mathbf{k}}^\dagger a_{\mathbf{k}} + \sum_{\mathbf{k}}(V_k a_{\mathbf{k}} + V_k^* a_{\mathbf{k}}^\dagger)\right]S_2$$

Further we use $S_2^{-1}a_{\mathbf{k}}S_2 = a_{\mathbf{k}} + f_{\mathbf{k}}$:

$$\begin{aligned}
H_0 &= \sum_{\mathbf{k}}\left(\omega_{\mathrm{LO}} + \frac{k^2}{2m_b}\right)a_{\mathbf{k}}^\dagger a_{\mathbf{k}} + \sum_{\mathbf{k}}\left(\omega_{\mathrm{LO}} + \frac{k^2}{2m_b}\right)|f_{\mathbf{k}}|^2 \\
&+ \sum_{\mathbf{k}}\left(\omega_{\mathrm{LO}} + \frac{k^2}{2m_b}\right)\left(a_{\mathbf{k}}^\dagger f_{\mathbf{k}} + a_{\mathbf{k}} f_{\mathbf{k}}^*\right) + \sum_{\mathbf{k}}\left[V_k\left(a_{\mathbf{k}} + f_{\mathbf{k}}\right) + V_k^*\left(a_{\mathbf{k}}^\dagger + f_{\mathbf{k}}^*\right)\right] \\
&= \sum_{\mathbf{k}}\left(\omega_{\mathrm{LO}} + \frac{k^2}{2m_b}\right)a_{\mathbf{k}}^\dagger a_{\mathbf{k}} + \sum_{\mathbf{k}}\frac{|V_k|^2}{\left(\omega_{\mathrm{LO}} + \frac{k^2}{2m_b}\right)} - 2\sum_{\mathbf{k}}\frac{|V_k|^2}{\left(\omega_{\mathrm{LO}} + \frac{k^2}{2m_b}\right)} \\
&= \sum_{\mathbf{k}}\left(\omega_{\mathrm{LO}} + \frac{k^2}{2m_b}\right)a_{\mathbf{k}}^\dagger a_{\mathbf{k}} - \sum_{\mathbf{k}}\frac{|V_k|^2}{\left(\omega_{\mathrm{LO}} + \frac{k^2}{2m_b}\right)}.
\end{aligned}$$

The last term can be calculated analytically:

$$\begin{aligned}
\sum_{\mathbf{k}}\frac{|V_k|^2}{\omega_{\mathrm{LO}} + \frac{k^2}{2m_b}} &= \frac{V}{(2\pi)^3}\int d^3k\left(\frac{\omega_{\mathrm{LO}}}{k}\right)^2\frac{4\pi\alpha}{V}\left(\frac{1}{2m_b\omega_{\mathrm{LO}}}\right)^{\frac{1}{2}}\cdot\frac{1}{\omega_{\mathrm{LO}} + \frac{k^2}{2m_b}} \\
&= \frac{\alpha\omega_{\mathrm{LO}}}{2\pi^2}4\pi\int_0^\infty dk\left(\frac{1}{2m_b\omega_{\mathrm{LO}}}\right)^{\frac{1}{2}}\frac{1}{1 + \frac{k^2}{2m_b\omega_{\mathrm{LO}}}} \\
&= \frac{2\alpha\omega_{\mathrm{LO}}}{\pi}\int_0^\infty d\kappa\frac{1}{1+\varkappa^2} = \frac{2\alpha\omega_{\mathrm{LO}}}{\pi}\arctan\varkappa\big|_0^\infty = \alpha\omega_{\mathrm{LO}},
\end{aligned}$$

$$H_0 = -\alpha\omega_{\mathrm{LO}} + \sum_{\mathbf{k}}\left(\omega_{\mathrm{LO}} + \frac{k^2}{2m_b}\right)a_{\mathbf{k}}^\dagger a_{\mathbf{k}}.$$

The term

$$H_1 = S_2^{-1}\mathcal{H}_1 S_2$$

will be neglected:

$$e^{iS_2^{-1}\mathcal{H}S_2 t} \approx e^{iH_0 t}.$$

Neglecting H_1, consistent with the LLP description, introduces no error in order α. Therefore (7.82) becomes

$$\left\langle 0 \left| \begin{array}{c} \sum_{\mathbf{k}}\mathbf{E}\cdot\mathbf{k}\left(a_{\mathbf{k}}^\dagger a_{\mathbf{k}} + f_{\mathbf{k}}a_{\mathbf{k}}^\dagger + f_{\mathbf{k}}^* a_{\mathbf{k}} + f_{\mathbf{k}}f_{\mathbf{k}}^*\right)e^{iH_0 t} \\ \times\sum_{\mathbf{k}}\mathbf{E}\cdot\mathbf{k}\left(a_{\mathbf{k}}^\dagger a_{\mathbf{k}} + f_{\mathbf{k}}a_{\mathbf{k}}^\dagger + f_{\mathbf{k}}^* a_{\mathbf{k}} + f_{\mathbf{k}}f_{\mathbf{k}}^*\right)e^{-iH_0 t} \end{array} \right| 0 \right\rangle. \tag{7.83}$$

For $\mathbf{P} = 0$ there is no privileged direction and $\sum_{\mathbf{k}}\mathbf{E}\cdot\mathbf{k}f_{\mathbf{k}}f_{\mathbf{k}}^* = 0$, (7.83) reduces to:

$$\left\langle 0 \left| \sum_{\mathbf{k}}\mathbf{E}\cdot\mathbf{k}f_{\mathbf{k}}^* a_{\mathbf{k}}e^{iH_0 t}\sum_{\mathbf{k}}\mathbf{E}\cdot\mathbf{k}f_{\mathbf{k}}a_{\mathbf{k}}^\dagger e^{-iH_0 t} \right| 0 \right\rangle.$$

From the equation of motion for $a_{\mathbf{k}}^\dagger$:

$$\frac{da_{\mathbf{k}}^\dagger(t)}{dt} = i\left[H_0, a_{\mathbf{k}}^\dagger\right] = i\left(\omega_{\mathrm{LO}} + \frac{k^2}{2m_b}\right)a_{\mathbf{k}}^\dagger,$$

it is easy now to calculate

$$e^{iH_0t}a_{\mathbf{k}}^{\dagger}e^{-iH_0t} = a_{\mathbf{k}}^{\dagger}\exp\left[i\left(\omega_{\mathrm{LO}}+\frac{k^2}{2m_b}\right)t\right].$$

The matrix element (7.80) now becomes

$$\langle\Phi_0|(\mathbf{E}\cdot\mathbf{p}(0))(\mathbf{E}\cdot\mathbf{p}(t))|\Phi_0\rangle = \sum_{\mathbf{k}}(\mathbf{E}\cdot\mathbf{k})^2 f_{\mathbf{k}}^* f_{\mathbf{k}}\exp\left[i\left(\omega_{\mathrm{LO}}+\frac{k^2}{2m_b}\right)t\right]+O(\alpha^2).$$

The transition probability (7.74) is then given by the expression

$$\begin{aligned}P(\Omega) &= 2\,\mathrm{Re}\,\frac{e^2}{m_b^2\Omega^2}\sum_{\mathbf{k}}(\mathbf{E}\cdot\mathbf{k})^2 f_{\mathbf{k}}^* f_{\mathbf{k}}\int_{-\infty}^{0}dt\exp\left[-i\left(\Omega+i\varepsilon-\omega_{\mathrm{LO}}-\frac{k^2}{2m_b}\right)t\right]\\ &= 2\pi\frac{e^2}{m_b^2\Omega^2}\sum_{\mathbf{k}}(\mathbf{E}\cdot\mathbf{k})^2|f_{\mathbf{k}}|^2\delta\left(\Omega-\omega_{\mathrm{LO}}-\frac{k^2}{2m_b}\right).\end{aligned}$$

Using (7.81), we obtain

$$\begin{aligned}P(\Omega) &= \frac{2\pi e^2}{m_b^2\Omega^2}\sum_{\mathbf{k}}\frac{(\mathbf{E}\cdot\mathbf{k})^2}{\left(\omega_{\mathrm{LO}}+\frac{k^2}{2m_b}\right)^2}|V_k|^2\delta\left(\Omega-\omega_{\mathrm{LO}}-\frac{k^2}{2m_b}\right)\\ &= \frac{2\pi e^2}{m_b^2\Omega^2}\frac{V}{(2\pi)^3}\int d^3k\left(\frac{\omega_{\mathrm{LO}}}{k}\right)^2\frac{4\pi\alpha}{V}\left(\frac{1}{2m_b\omega_{\mathrm{LO}}}\right)^{\frac{1}{2}}\\ &\times\frac{(\mathbf{E}\cdot\mathbf{k})^2}{\left(\omega_{\mathrm{LO}}+\frac{k^2}{2m_b}\right)^2}\delta\left(\Omega-\omega_{\mathrm{LO}}-\frac{k^2}{2m_b}\right)\\ &= \frac{e^2\alpha E^2}{m_b^2\Omega^2\pi}2\pi\int_{-1}^{1}dx x^2\int_0^{\infty}dk\left(\frac{1}{2m_b\omega_{\mathrm{LO}}}\right)^{\frac{1}{2}}\\ &\times\frac{k^2}{\left(1+\frac{k^2}{2m_b\omega_{\mathrm{LO}}}\right)^2}\frac{1}{\omega_{\mathrm{LO}}}\delta\left(\frac{\Omega}{\omega_{\mathrm{LO}}}-1-\frac{k^2}{2m_b\omega_{\mathrm{LO}}}\right)\\ &= \frac{8e^2\alpha E^2}{3m_b\Omega^2}\int_0^{\infty}d\kappa\frac{\varkappa^2}{(1+\varkappa^2)^2}\delta\left(\frac{\Omega}{\omega_{\mathrm{LO}}}-1-\varkappa^2\right)\\ &= \frac{4e^2\alpha E^2}{3m_b\Omega^2}\int_0^{\infty}d\zeta\frac{\sqrt{\zeta}}{(1+\zeta)^2}\delta\left(\frac{\Omega}{\omega_{\mathrm{LO}}}-1-\zeta\right)\\ &= \frac{4e^2\alpha E^2}{3m_b\Omega^2}\Theta\left(\frac{\Omega}{\omega_{\mathrm{LO}}}-1\right)\frac{\sqrt{\frac{\Omega}{\omega_{\mathrm{LO}}}-1}}{\left(\frac{\Omega}{\omega_{\mathrm{LO}}}\right)^2} = \frac{4e^2\alpha E^2\omega_{\mathrm{LO}}^2}{3m_b\Omega^4}\sqrt{\frac{\Omega}{\omega_{\mathrm{LO}}}-1}\quad\Theta\left(\frac{\Omega}{\omega_{\mathrm{LO}}}-1\right),\end{aligned}$$

where

$$\Theta\left(\frac{\Omega}{\omega_{\mathrm{LO}}}-1\right) = \begin{cases}1 & \text{if} \quad \frac{\Omega}{\omega_{\mathrm{LO}}}>1\\ 0 & \text{if} \quad \frac{\Omega}{\omega_{\mathrm{LO}}}<1\end{cases}.$$

The absorption coefficient (7.72) for absorption by free polarons for $\alpha\longrightarrow 0$ finally takes the form

$$\Gamma_p(\Omega) = \frac{1}{\varepsilon_0 cn}\frac{2Ne^2\alpha\omega_{\mathrm{LO}}^2}{3m_b\Omega^3}\sqrt{\frac{\Omega}{\omega_{\mathrm{LO}}}-1}\quad\Theta\left(\frac{\Omega}{\omega_{\mathrm{LO}}}-1\right). \tag{7.84}$$

The behaviuor of $\Gamma_p(\Omega)$ (7.84) as a function of Ω is as follows. For $\Omega<\omega_{\mathrm{LO}}$ there is no absorption. The threshold for absorption is at $\Omega=\omega_{\mathrm{LO}}$.From $\Omega=\omega_{\mathrm{LO}}$ up to $\Omega=\frac{6}{5}\omega_{\mathrm{LO}}, \Gamma_p$

increases to a maximum and for $\Omega > \frac{6}{5}\omega_{\rm LO}$ the absorption coefficient decreases slowly with increasing Ω.

Experimentally, this one-phonon line has been observed for free polarons in the infrared absorption spectra of CdO-films, see Fig. 7.6. In CdO, which is a weakly polar material with $\alpha \approx 0.74$, the polaron absorption band is observed in the spectral region between 6 and 20 μm (above the LO phonon frequency). The difference between theory and experiment in the wavelength region where polaron absorption dominates the spectrum is due to many-polaron effects.

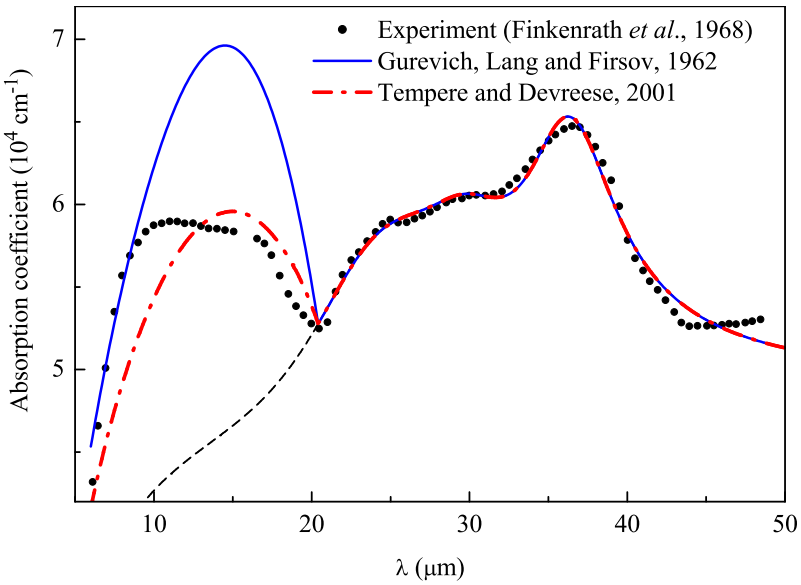

Figure 7.6: Optical absorption spectrum of a CdO-film with the carrier concentration $n = 5.9 \times 10^{19}$ cm^{-3} at $T = 300$ K. The experimental data (solid dots) of Ref. [74] are compared to different theoretical results: with (solid curve) and without (dashed line) the one-polaron contribution of Ref. [71] and for many polarons (dash-dotted curve) of Ref. [53].

7.3 Optical absorption. Strong coupling

The absorption of light by free large polarons was treated in Ref. [49] using the polaron states obtained wihtin the adiabatic strong-coupling approximation, which was considered above in subsection 7.1.5.

It was argued in Ref. [49], that for sufficiently large α ($\alpha > 3$), the (first) RES of a polaron is a relatively stable state, which can participate in optical absorption transitions. This idea was necessary to understand the polaron optical absorption spectrum in the strong-coupling regime. The following scenario of a transition, which leads to a *"zero-phonon" peak* in the absorption by a strong-coupling polaron, can then be suggested. If the frequency of the incoming photon is equal to

$$\Omega_{\rm RES} \equiv \frac{{\rm E}_{\rm RES}\text{-}E_0}{\hbar} = 0.065\alpha^2\omega_{\rm LO},$$

then the electron jumps from the ground state (which, at large coupling, is well-characterized by "s"-symmetry for the electron) to an excited state ("$2p$"), while the lattice polarization in the final state is adapted to the "$2p$" electronic state of the polaron. In Ref. [49] considering the decay of the RES with emission of one real phonon it is demonstrated, that the "zero-phonon" peak can be described using the Wigner-Weisskopf formula valid when the linewidth of that peak is much smaller than $\hbar\omega_{\rm LO}$.

For photon energies larger than

$$\Omega_{\rm RES} + \omega_{\rm LO},$$

a transition of the polaron towards the first scattering state, belonging to the RES, becomes possible. The final state of the optical absorption process then consists of a polaron in its lowest RES plus a free phonon. A "one-phonon sideband" then appears in the polaron absorption spectrum. This process is called *one-phonon sideband absorption.*

The one-, two-, ... K-, ... phonon sidebands of the zero-phonon peak give rise to a broad structure in the absorption spectrum. It turns that the *first moment* of the phonon sidebands corresponds to the FC frequency $\Omega_{\rm FC}$:

$$\Omega_{\rm FC} \equiv \frac{E_{\rm FC} - E_0}{\hbar} = 0.141\alpha^2\omega_{\rm LO}.$$

To summarize, the polaron optical absorption spectrum at strong coupling is characterized by the following features ($T = 0$):

a) An intense absorption peak ("zero-phonon line") appears, which corresponds to a transition from the ground state to the first RES at $\Omega_{\rm RES}$.

b) For $\Omega > \Omega_{\rm RES} + \omega_{\rm LO}$, a phonon sideband structure arises. This sideband structure peaks around $\Omega_{\rm FC}$.

The qualitative behaviour predicted in Ref. [49], namely, an intense zero-phonon (RES) line with a broader sideband at the high-frequency side, was confirmed after an all-coupling expression for the polaron optical absorption coefficient at $\alpha = 5, 6, 7$ had been studied [50].

In what precedes, the low-frequency end of the polaron absorption spectrum was discussed; at higher frequencies, transitions to higher RES and their scattering states can appear. The two-phonon sidebands in the optical absorption of free polarons in the strong-coupling limit were numerically studied in Ref. [75].

The study of the optical absorption of polarons at large coupling is mainly of formal interest because all reported coupling constants of polar semiconductors and ionic crystals are smaller than 5 (see Table 1).

7.4 Arbitrary coupling

7.4.1 Impedance function of large polarons: An alternative derivation of FHIP [76]

Definitions

We derive here the linear response of the Fröhlich polaron, described by the Hamiltonian

$$H = \frac{\mathbf{p}^2}{2m_b} + \sum_{\mathbf{k}} \hbar\omega_{\mathbf{k}} a^+_{\mathbf{k}} a_{\mathbf{k}} + \sum_{\mathbf{k}} (V_k a_{\mathbf{k}} e^{i\mathbf{k}\cdot\mathbf{r}} + V_k^* a^\dagger_{\mathbf{k}} e^{-i\mathbf{k}\cdot\mathbf{r}}), \tag{7.85}$$

to a spatially uniform, time-varying electric field

$$\mathbf{E}_\Omega(t) = E_0 \exp(i\Omega t)\, \mathbf{e}_x. \tag{7.86}$$

This field induces a current in the x-direction

$$j_\Omega(t) = \frac{1}{Z(\Omega)} E_\Omega(t). \tag{7.87}$$

The complex function $Z(\Omega)$ is called the impedance function. The frequency-dependent mobility is defined by

$$\mu(\Omega) = \mathrm{Re}\,\frac{1}{Z(\Omega)}. \tag{7.88}$$

For nonzero frequencies (in the case of polarons the frequencies of interest are in the infrared) one defines the absorption coefficient [50]

$$\Gamma(\Omega) = \frac{1}{n\epsilon_0 c}\,\mathrm{Re}\,\frac{1}{Z(\Omega)}, \tag{7.89}$$

where ϵ_0 is the dielectric constant of the vacuum, n the refractive index of the crystal, and c the velocity of light. In the following the amplitude of the electric field E_0 is taken sufficiently small so that linear-response theory can be applied.

The impedance function can be expressed via a frequency-dependent conductivity of a single polaron in a unit volume

$$\frac{1}{Z(\Omega)} = \sigma(\Omega) \tag{7.90}$$

using *the standard Kubo formula* (cf. Eq. (3.8.8) from Ref. [72]):

$$\sigma(\Omega) = i\frac{e^2}{Vm_b\Omega} + \frac{1}{V\hbar\Omega}\int_0^\infty e^{i\Omega t}\,\langle[j_x(t), j_x]\rangle\,dt. \tag{7.91}$$

In order to introduce a convenient representation of the impedance function, we give in the next subsection a definition and discuss properties of a scalar product of two operators [cf. [77], Chapter 5].

Definition and properties of the scalar product

For two operators A and B (i.e., elements of the Hilbert space of operators) the scalar product is defined as

$$(A, B) = \int_0^\beta d\lambda\,\left\langle\left(e^{\lambda\hbar L}A^\dagger\right)B\right\rangle. \tag{7.92}$$

The notation $\left(e^{\lambda\hbar L}A^\dagger\right)$ is used in order to indicate that the operator $e^{\lambda\hbar L}$ acts on the operator $A^\dagger$. The time evolution of the operator A is determined by the Liouville operator L:

$$-i\frac{\partial A}{\partial t} = LA \equiv \frac{1}{\hbar}\,[H, A] \tag{7.93}$$

with a commutator $[H, A]$, wherefrom

$$A(t) = e^{iLt}A(0) \equiv e^{iHt/\hbar}A(0)e^{-iHt/\hbar}. \tag{7.94}$$

The expectation value in (7.92) is taken over the Gibbs' ensemble:

$$\langle A\rangle = \mathrm{Tr}(\rho_0(H)A) \tag{7.95}$$

with the equilibtium density matrix when the electric field is absent

$$\rho_0(H) = e^{-\beta H}/\mathrm{Tr}(e^{-\beta H}). \tag{7.96}$$

One can show that (7.92) defines a positive definite scalar product with the following properties

$$\text{(i)} \qquad (A, B) = (B^\dagger, A^\dagger), \tag{7.97}$$

$$\text{(ii)} \qquad (A, LB) = (LA, B), \tag{7.98}$$

$$\text{(iii)} \qquad (A, LB) = \frac{1}{\hbar}\left\langle\left[A^\dagger, B\right]\right\rangle, \tag{7.99}$$

and [cf. Eq. (5.11) of [77]]

$$\text{(iv)} \qquad (A, B)^* = (B, A) \tag{7.100}$$

Demonstration of the property (7.97).

Starting from the definition (7.92) and using (7.94), we obtain

$$(A,B) = \int_0^\beta d\lambda \left\langle e^{\lambda H} A^\dagger e^{-\lambda H} B \right\rangle . \tag{7.101}$$

Substituting here (7.95) with (7.96), one finds

$$(A,B) = \int_0^\beta d\lambda \mathrm{Tr}\left[e^{-(\beta-\lambda)H} A^\dagger e^{-\lambda H} B\right] / \mathrm{Tr}(e^{-\beta H}).$$

Change of the variable $\lambda' = \beta - \lambda$ allows us to represnt this integral as

$$(A,B) = \int_0^\beta d\lambda' \mathrm{Tr}\left[e^{-\lambda' H} A^\dagger e^{-(\beta-\lambda')H} B\right] / \mathrm{Tr}(e^{-\beta H}).$$

Further, a cyclic permutation of the operators under the trace Tr sign gives

$$\begin{aligned}(A,B) &= \int_0^\beta d\lambda \mathrm{Tr}\left[e^{-(\beta-\lambda)H} B e^{-\lambda H} A^\dagger\right] / \mathrm{Tr}(e^{-\beta H}) \\ &= \int_0^\beta d\lambda \left\langle e^{\lambda H} B e^{-\lambda H} A^\dagger \right\rangle = \int_0^\beta d\lambda \left\langle \left(e^{\lambda \hbar L} B\right) A^\dagger \right\rangle \\ &= \int_0^\beta d\lambda \left\langle \left[e^{\lambda \hbar L} \left(B^\dagger\right)^\dagger\right] A^\dagger \right\rangle .\end{aligned}$$

According to the definition (7.92), this finalizes the demonstration of (7.97).

Demonstration of the property (7.98).

Starting from (7.101) and using (7.93), we obtain

$$\begin{aligned}(A,LB) &= \int_0^\beta d\lambda \left\langle e^{\lambda H} A^\dagger e^{-\lambda H} LB \right\rangle \\ &= \frac{1}{\hbar}\int_0^\beta d\lambda \left\langle e^{\lambda H} A^\dagger e^{-\lambda H} \left(HB - BH\right) \right\rangle .\end{aligned}$$

A cyclic permutation of the operators under the average $\langle \bullet \rangle$ sign gives

$$(A,LB) = \frac{1}{\hbar}\int_0^\beta d\lambda \left\langle e^{\lambda H} A^\dagger e^{-\lambda H} HB - H e^{\lambda H} A^\dagger e^{-\lambda H} B \right\rangle . \tag{7.102}$$

Using the commutation of H and $e^{\pm\lambda H}$, one finds

$$(A,LB) = \frac{1}{\hbar}\int_0^\beta d\lambda \left\langle e^{\lambda H} A^\dagger H e^{-\lambda H} B - e^{\lambda H} H A^\dagger e^{-\lambda H} B \right\rangle \tag{7.103}$$

$$= \frac{1}{\hbar}\int_0^\beta d\lambda \left\langle e^{\lambda H} \left(A^\dagger H - H A^\dagger\right) e^{-\lambda H} B \right\rangle \tag{7.104}$$

$$= \frac{1}{\hbar}\int_0^\beta d\lambda \left\langle e^{\lambda H} \left(HA - AH\right)^\dagger e^{-\lambda H} B \right\rangle \tag{7.105}$$

$$= \int_0^\beta d\lambda \left\langle e^{\lambda H} \left(\frac{1}{\hbar}[H,A]\right)^\dagger e^{-\lambda H} B \right\rangle . \tag{7.106}$$

With the definition (7.93), this gives

$$(A,LB) = \int_0^\beta d\lambda \left\langle e^{\lambda H} \left(LA\right)^\dagger e^{-\lambda H} B \right\rangle = . \int_0^\beta d\lambda \left\langle \left[e^{\lambda \hbar L} \left(LA\right)^\dagger\right] B \right\rangle .$$

According to the definition (7.92), this finalizes the demonstration of (7.98).

Demonstration of the property (7.99).

Starting from (7.104) and performing a cyclic permutation of the operators under the average $\langle\bullet\rangle$, we find

$$(A, LB) = \frac{1}{\hbar}\int_0^\beta d\lambda \left\langle e^{\lambda H}\left(A^\dagger H - HA^\dagger\right)e^{-\lambda H}B\right\rangle$$

Further we notice that

$$e^{\lambda H}\left(A^\dagger H - HA^\dagger\right)e^{-\lambda H} = -\frac{d\left(e^{\lambda H}A^\dagger e^{-\lambda H}\right)}{d\lambda},$$

consequently,

$$\begin{aligned}
(A, LB) &= -\frac{1}{\hbar}\int_0^\beta d\lambda \left\langle \frac{d\left(e^{\lambda H}A^\dagger e^{-\lambda H}\right)}{d\lambda}B\right\rangle \\
&= -\frac{1}{\hbar}\left\langle \int_0^\beta d\lambda \frac{d\left(e^{\lambda H}A^\dagger e^{-\lambda H}\right)}{d\lambda}B\right\rangle \\
&= -\frac{1}{\hbar}\left\langle e^{\lambda H}A^\dagger e^{-\lambda H}B\Big|_0^\beta\right\rangle = \frac{1}{\hbar}\left\langle\left(A^\dagger B - e^{\beta H}A^\dagger e^{-\beta H}B\right)\right\rangle \\
&= \frac{1}{\hbar}\mathrm{Tr}\left[e^{-\beta H}\left(A^\dagger B - e^{\beta H}A^\dagger e^{-\beta H}B\right)\right]/\mathrm{Tr}(e^{-\beta H}) \\
&= \frac{1}{\hbar}\mathrm{Tr}\left[e^{-\beta H}A^\dagger B - A^\dagger e^{-\beta H}B\right]/\mathrm{Tr}(e^{-\beta H}).
\end{aligned} \tag{7.107}$$

Further, a cyclic permutation of the operators in the second term under the trace Tr sign gives

$$\begin{aligned}
(A, LB) &= \frac{1}{\hbar}\mathrm{Tr}\left[e^{-\beta H}A^\dagger B - e^{-\beta H}BA^\dagger\right]/\mathrm{Tr}(e^{-\beta H}) \\
&= \frac{1}{\hbar}\mathrm{Tr}\left[e^{-\beta H}\left(A^\dagger B - BA^\dagger\right)\right]/\mathrm{Tr}(e^{-\beta H}) \\
&= \frac{1}{\hbar}\left\langle A^\dagger B - BA^\dagger\right\rangle = \frac{1}{\hbar}\left\langle\left[A^\dagger, B\right]\right\rangle.
\end{aligned}$$

Thus, the property (7.99) has been demonstrated.

Demonstration of the property (7.100).

We start from the represntation of the scalar product (7.101) and take a complex conjugate:

$$(A, B)^* = \int_0^\beta d\lambda \left\langle e^{\lambda H}A^\dagger e^{-\lambda H}B\right\rangle^* = \int_0^\beta d\lambda \left\langle B^\dagger e^{-\lambda H}Ae^{\lambda H}\right\rangle.$$

A cyclic permutation of the operators under the average $\langle\bullet\rangle$ sign gives then

$$\begin{aligned}
(A, B)^* &= \int_0^\beta d\lambda \left\langle e^{\lambda H}B^\dagger e^{-\lambda H}A\right\rangle = \int_0^\beta d\lambda \left\langle e^{\lambda H}B^\dagger e^{-\lambda H}A\right\rangle \\
&= \int_0^\beta d\lambda \left\langle\left(e^{\lambda\hbar L}B^\dagger\right)A\right\rangle.
\end{aligned} \tag{7.108}$$

According to the definition (7.92), this finalizes the demonstration of (7.100).

The above scalar product allows one to represent different dynamical quantities in a rather simple way. For example, let us consider a scalar product

$$\Phi_{AB}(z) = \left(A, \frac{1}{z-L}B\right) \tag{7.109}$$

$$= \int_0^\beta d\lambda \left\langle \left(e^{\lambda\hbar L}A^\dagger\right)\frac{1}{z-L}B\right\rangle$$

$$= -i\int_0^\beta d\lambda \left\langle e^{\lambda\hbar L}A^\dagger\left[\int_0^\infty dt e^{i(z-L)t}\right]B\right\rangle \tag{7.110}$$

$$= -i\int_0^\infty dt e^{izt}\int_0^\beta d\lambda \left\langle e^{\lambda\hbar L}A^\dagger e^{-iLt}B\right\rangle$$

$$= -i\int_0^\infty dt e^{izt}\int_0^\beta d\lambda \left\langle e^{\lambda H}A^\dagger e^{-\lambda H}e^{-iHt/\hbar}Be^{iHt/\hbar}\right\rangle$$

$$= -i\int_0^\infty dt e^{izt}\int_0^\beta d\lambda \left\langle e^{iHt/\hbar+\lambda H}A^\dagger e^{-iHt/\hbar-\lambda H}B\right\rangle$$

$$= -i\int_0^\infty dt e^{izt}\int_0^\beta d\lambda \left\langle e^{iH(t-i\lambda\hbar)/\hbar}A^\dagger e^{-iH(t-i\lambda\hbar)/\hbar}B\right\rangle$$

$$= -i\int_0^\infty dt e^{izt}\int_0^\beta d\lambda \left\langle e^{iL(t-i\lambda\hbar)}A^\dagger B\right\rangle \tag{7.111}$$

$$= -i\int_0^\infty dt e^{izt}\int_0^\beta d\lambda \left\langle A^\dagger(t-i\hbar\lambda)B(0)\right\rangle. \tag{7.112}$$

Representation of the impedance function in terms of the relaxation function

The impedance function is related to the relaxation function

$$\Phi(z) \equiv \Phi_{\dot{x}\dot{x}}(z) = \left(\dot{x}, \frac{1}{z-L}\dot{x}\right), \tag{7.113}$$

where $\dot{x}$ is the velocity operator, by the following expression:

$$\frac{1}{Z(\Omega)} = ie^2\lim_{\epsilon\to 0}\Phi(\Omega+i\epsilon) \tag{7.114}$$

$(z = \Omega + i\epsilon, \epsilon > 0)$.

Demonstration of the representation (7.113).

Apply (7.111) to the relaxation function entering (7.114):

$$\Phi(z) = -i\int_0^\beta d\lambda\int_0^\infty dt e^{izt}\left\langle\left(e^{i(t-i\hbar\lambda)L}\dot{x}\right)\dot{x}\right\rangle$$

and perform the integration by parts using the formula

$$\int_0^\infty e^{izt}f(t)\,dt = -\frac{i}{z}f(t)\,e^{izt}\Big|_{t=0}^{\infty} + \frac{i}{z}\int_0^\infty \frac{\partial f(t)}{\partial t}e^{izt}dt$$

$$= \frac{i}{z}f(0) + \frac{i}{z}\int_0^\infty \frac{\partial f(t)}{\partial t}e^{izt}dt:$$

$$\int_0^\infty e^{izt}\left\langle\left(e^{i(t-i\hbar\lambda)L}\dot{x}\right)\dot{x}\right\rangle dt = \frac{i}{z}\left\langle\left(e^{\hbar\lambda L}\dot{x}\right)\dot{x}\right\rangle + \frac{i}{z}\int_0^\infty e^{izt}\frac{\partial}{\partial t}\left\langle\left(e^{i(t-i\hbar\lambda)L}\dot{x}\right)\dot{x}\right\rangle dt$$
$$= \frac{i}{z}\left\langle\left(e^{\hbar\lambda L}\dot{x}\right)\dot{x}\right\rangle - \frac{1}{z}\int_0^\infty e^{izt}\left\langle L\left(e^{i(t-i\hbar\lambda)L}\dot{x}\right)\dot{x}\right\rangle dt.$$

This allows us to represent the relaxation function in the form

$$\Phi(z) = -i\int_0^\beta d\lambda\left(\frac{i}{z}\left\langle\left(e^{\hbar\lambda L}\dot{x}\right)\dot{x}\right\rangle - \frac{1}{z}\int_0^\infty e^{izt}\left\langle L\left(e^{i(t-i\hbar\lambda)L}\dot{x}\right)\dot{x}\right\rangle dt\right)$$
$$= \frac{1}{z}\int_0^\beta d\lambda\left\langle\left(e^{\hbar\lambda L}\dot{x}\right)\dot{x}\right\rangle + \frac{i}{z}\int_0^\beta d\lambda\int_0^\infty e^{izt}\left\langle L\left(e^{i(t-i\hbar\lambda)L}\dot{x}\right)\dot{x}\right\rangle dt$$
$$= \frac{1}{m_b z} + \frac{i}{z}\int_0^\beta d\lambda\int_0^\infty e^{izt}\left\langle L\left(e^{i(t-i\hbar\lambda)L}\dot{x}\right)\dot{x}\right\rangle dt,$$

where the expression (7.139) is inserted in the first term. Further on, the integral over λ is taken as follows:

$$\int_0^\beta d\lambda\left\langle L\left(e^{i(t-i\hbar\lambda)L}\dot{x}\right)\dot{x}\right\rangle = \left\langle\left(L\int_0^\beta e^{i(t-i\hbar\lambda)L}d\lambda\dot{x}\right)\dot{x}\right\rangle$$
$$= \frac{1}{\hbar}\left\langle\left(e^{iLt}\left(e^{\hbar\beta L}-1\right)\dot{x}\right)\dot{x}\right\rangle$$
$$= \frac{1}{\hbar}\left\langle e^{iLt}\left(e^{\hbar\beta L}\dot{x}-\dot{x}\right)\dot{x}\right\rangle$$
$$= \frac{1}{\hbar}\left\langle\left(e^{\hbar\beta L}\dot{x}(t)-\dot{x}(t)\right)\dot{x}\right\rangle$$
$$= \frac{1}{\hbar}\left\langle\left(e^{\beta H}\dot{x}(t)e^{-\beta H}-\dot{x}(t)\right)\dot{x}\right\rangle$$
$$= \frac{1}{\hbar\mathrm{Tr}e^{-\beta H}}\mathrm{Tr}\left[e^{-\beta H}\left(e^{\beta H}\dot{x}(t)e^{-\beta H}-\dot{x}(t)\right)\dot{x}\right]$$
$$= \frac{1}{\hbar\mathrm{Tr}e^{-\beta H}}\mathrm{Tr}\left[\left(\dot{x}(t)e^{-\beta H}-e^{-\beta H}\dot{x}(t)\right)\dot{x}\right]$$
$$= \frac{1}{\hbar\mathrm{Tr}e^{-\beta H}}\mathrm{Tr}\left[e^{-\beta H}\left(\dot{x}\dot{x}(t)-\dot{x}(t)\right)\dot{x}\right]$$
$$= \frac{1}{\hbar}\left\langle\dot{x}\dot{x}(t)-\dot{x}(t)\dot{x}\right\rangle = -\frac{1}{\hbar}\left\langle\dot{x}(t),\dot{x}\right\rangle.$$

Hence,

$$\Phi(z) = \frac{1}{m_b z} - \frac{i}{\hbar z}\int_0^\infty dt e^{izt}\left\langle[\dot{x}(t),\dot{x}]\right\rangle. \tag{7.115}$$

When setting $z = \Omega + i\varepsilon$ with $\varepsilon \to +0$, we have

$$\Phi(\Omega+i\varepsilon) = \frac{1}{m_b}\frac{1}{\Omega+i\varepsilon} - \frac{i}{\hbar(\Omega+i\varepsilon)}\int_0^\infty e^{i(\Omega+i\varepsilon)t}\left\langle[\dot{x}(t),\dot{x}]\right\rangle dt. \tag{7.116}$$

For $\Omega \neq 0$, we can set

$$\Phi(\Omega+i\varepsilon) = \frac{1}{m_b}\frac{1}{\Omega} - \frac{i}{\hbar\Omega}\int_0^\infty e^{i(\Omega+i\varepsilon)t}\left\langle[\dot{x}(t),\dot{x}]\right\rangle dt. \tag{7.117}$$

Multiplying $\Phi(\Omega+i\varepsilon)$ by ie^2, we find that

$$\begin{aligned} ie^2\Phi(\Omega+i\varepsilon) &= ie^2\left(\frac{1}{m_b}\frac{1}{\Omega}-\frac{i}{\hbar\Omega}\int_0^\infty e^{i(\Omega+i\varepsilon)t}\left\langle[\dot{x}(t),\dot{x}]\right\rangle dt\right) \\ &= i\frac{e^2}{m_b\Omega}+\frac{e^2}{\hbar\Omega}\int_0^\infty e^{i(\Omega+i\varepsilon)t}\left\langle[\dot{x}(t),\dot{x}]\right\rangle dt \\ &= i\frac{e^2}{m_b\Omega}+\frac{1}{\hbar\Omega}\int_0^\infty e^{i(\Omega+i\varepsilon)t}\left\langle[j_x(t),j_x]\right\rangle dt, \end{aligned} \tag{7.118}$$

where the electric current density is

$$j_x=-e\dot{x}.$$

Substituting further (7.118) in (7.114), we arrive at

$$\frac{1}{Z(\Omega)}=i\frac{e^2}{m_b\Omega}+\lim_{\epsilon\to 0}\frac{1}{\hbar\Omega}\int_0^\infty e^{i(\Omega+i\varepsilon)t}\left\langle[j_x(t),j_x]\right\rangle dt,$$

what coincides with the expression of the impedance function (7.90) through a frequency-dependent conductivity given by the Kubo formula (7.91), q.e.d.

Application of the projection operator technique

Using the Mori-Zwanzig projection operator technique (cf. [77], Chapter 5), the relaxation function (7.113)

$$\Phi(z)=\left(\dot{x},\frac{1}{z-L}\dot{x}\right)$$

can be represented in a form, which is especially convenient for the application in the theory of the optical absorption of polarons.

The projection operator P $(Q=1-P)$ is defined as

$$PA=\frac{\dot{x}(\dot{x},A)}{\chi} \tag{7.119}$$

with A an operator and

$$\chi=(\dot{x},\dot{x}). \tag{7.120}$$

The projection operator $Q=1-P$ projects an operator onto the space orthogonal to the space containing $\dot{x}$. Here we give some examples of the action of the projection operators:

$$P\dot{x}=\dot{x},\qquad Q\dot{x}=(1-P)\dot{x}=0; \tag{7.121}$$

$$Px=\frac{\dot{x}(\dot{x},x)}{\chi}=\frac{\dot{x}(iLx,x)}{\chi}=-\frac{i\dot{x}(x,Lx)}{\chi}=-\frac{i\dot{x}}{\chi}\left\langle[x,x]\right\rangle=0, \tag{7.122}$$

$$Qx=(1-P)x=x. \tag{7.123}$$

$$Pa_{\mathbf{k}}=\frac{\dot{x}(\dot{x},a_{\mathbf{k}})}{\chi}=\frac{\dot{x}(iLx,a_{\mathbf{k}})}{\chi}=-\frac{i\dot{x}(a_{\mathbf{k}},Lx)}{\chi}=-\frac{i\dot{x}}{\chi}\left\langle\left[a_{\mathbf{k}}^\dagger,x\right]\right\rangle=0, \tag{7.124}$$

$$Qa_{\mathbf{k}}=(1-P)a_{\mathbf{k}}=a_{\mathbf{k}} \tag{7.125}$$

The projection operators P and Q are idempotent:

$$\begin{aligned} P^2A &= \frac{\dot{x}\left(\dot{x},\frac{\dot{x}(\dot{x},A)}{\chi}\right)}{\chi}=\frac{\dot{x}(\dot{x},A)}{\chi}=PA; \\ Q^2 &= (1-P)^2=1-2P+P^2=1-P=Q. \end{aligned}$$

The Liouville operator can be identiaclly represented as $L = LP + LQ$. Then the operator $\frac{1}{z-L}$in the relaxation function (7.113) can be represented as follows:

$$\frac{1}{z-L} = \frac{1}{z-LQ-LP}.$$

We use the algebraic operator identity:

$$\frac{1}{x+y} = \frac{1}{x} - \frac{1}{x}y\frac{1}{x+y}$$

with $x = z - LQ$ and $y = -LP$:

$$\frac{1}{z-L} = \frac{1}{z-LQ} + \frac{1}{z-LQ}LP\frac{1}{z-L}.$$

Consequently, the relaxation function (7.113) takes the form

$$\Phi(z) = \left(\dot{x}, \frac{1}{z-LQ}\dot{x}\right) + \left(\dot{x}, \frac{1}{z-LQ}LP\frac{1}{z-L}\dot{x}\right). \tag{7.126}$$

The first term in the r.h.s. of (7.126) simplifies as follows:

$$\left(\dot{x}, \frac{1}{z-LQ}\dot{x}\right) = \left(\dot{x}, \left[\frac{1}{z} + \frac{1}{z^2}LQ + \frac{1}{z^3}LQLQ + ...\right]\dot{x}\right) = \left(\dot{x}, \frac{1}{z}\dot{x}\right)$$

because $Q\dot{x} = 0$. Using the quantity (7.120) we obtain:

$$\left(\dot{x}, \frac{1}{z-LQ}\dot{x}\right) = \frac{\chi}{z}. \tag{7.127}$$

The second term in the r.h.s. of (7.126) contains the operator

$$P\frac{1}{z-L}\dot{x}$$

which according to the definition of the projection operator P (7.119) can be transformed as

$$P\frac{1}{z-L}\dot{x} = \frac{\dot{x}}{\chi}\left(\dot{x}, \frac{1}{z-L}\dot{x}\right) = \frac{\dot{x}}{\chi}\Phi(z). \tag{7.128}$$

It is remarkable that this term is exactly expressed in terms of the sought relaxation function (7.113). Substituting (7.127) and (7.128) in (7.126), we find

$$\begin{aligned}
\Phi(z) &= \frac{\chi}{z} + \left(\dot{x}, \frac{1}{z-LQ}L\frac{\dot{x}}{\chi}\right)\Phi(z) \Rightarrow \\
z\Phi(z) &= \chi + \left(\dot{x}, \frac{z}{z-LQ}L\frac{\dot{x}}{\chi}\right)\Phi(z) \\
&= \chi + \left(\dot{x}, \frac{z-LQ+LQ}{z-LQ}L\frac{\dot{x}}{\chi}\right)\Phi(z) \\
&= \chi + \left(\dot{x}, \left[1 + \frac{LQ}{z-LQ}\right]L\frac{\dot{x}}{\chi}\right)\Phi(z) \Rightarrow \\
z\Phi(z) &= \chi + \left[\frac{(\dot{x}, L\dot{x})}{\chi} + \frac{1}{\chi}\left(\dot{x}, \frac{LQ}{z-LQ}L\dot{x}\right)\right]\Phi(z).
\end{aligned} \tag{7.129}$$

Introducring the quantity

$$O = \frac{(\dot{x}, L\dot{x})}{\chi} \tag{7.130}$$

and the function called the *memory function*

$$\Sigma(z) = \frac{1}{\chi}\left(\dot{x}, LQ\frac{1}{z - LQ}L\dot{x}\right), \tag{7.131}$$

we represent (7.129) in the form of the equation

$$[z - O - \Sigma(z)]\,\Phi\,(z) = \chi.$$

A solition of this equation gives the relaxation function $\Phi(z)$ represented within the Mori-Zwanzig projection operator technique:

$$\Phi(z) = \frac{\chi}{z - O - \Sigma(z)}. \tag{7.132}$$

The memory function (7.131) can be still transformed to another useful form.First of all, we apply the property of a scalar product (7.98):

$$\Sigma(z) = \frac{1}{\chi}\left(L\dot{x}, Q\frac{1}{z - LQ}L\dot{x}\right) \tag{7.133}$$

$$= \frac{1}{\chi}\left((P + Q)L\dot{x}, Q\frac{1}{z - LQ}L\dot{x}\right) \tag{7.134}$$

$$= \frac{1}{\chi}\left(PL\dot{x}, Q\frac{1}{z - LQ}L\dot{x}\right) + \frac{1}{\chi}\left(QL\dot{x}, Q\frac{1}{z - LQ}L\dot{x}\right). \tag{7.135}$$

For any two operators A and B

$$\begin{aligned}(PA, QB) &= \left(\frac{\dot{x}\,(\dot{x}, A)}{\chi}, \left[B - \frac{\dot{x}\,(\dot{x}, B)}{\chi}\right]\right)\\ &= \frac{(\dot{x}, A)}{\chi}\left[(\dot{x}, B) - \frac{(\dot{x}, \dot{x})\,(\dot{x}, B)}{\chi}\right]\\ &= \frac{(\dot{x}, A)}{\chi}\left[(\dot{x}, B) - (\dot{x}, B)\right] = 0,\end{aligned}$$

therefore the first term on the r.h.s. in (7.133) vanishes, and we obtain

$$\Sigma(z) = \frac{1}{\chi}\left(QL\dot{x}, Q\frac{1}{z - LQ}L\dot{x}\right). \tag{7.136}$$

In this expression, the operator $Q\frac{1}{z-LQ}$ can be represented in the following form, using the fact that Q is the idempotent operator:

$$\begin{aligned}Q\frac{1}{z - LQ} &= Q\left[\frac{1}{z} + \frac{1}{z^2}LQ + \frac{1}{z^3}LQLQ + ...\right]\\ &= \frac{1}{z}Q + \frac{1}{z^2}QLQ + \frac{1}{z^3}QLQLQ + ...\\ &= \frac{1}{z}Q + \frac{1}{z^2}QLQ^2 + \frac{1}{z^3}QLQ^2LQ^2 + ...\\ &= \left[\frac{1}{z} + \frac{1}{z^2}QLQ + \frac{1}{z^3}QLQQLQ + ...\right]Q \Rightarrow\\ Q\frac{1}{z - LQ} &= \frac{1}{z - QLQ}Q.\end{aligned} \tag{7.137}$$

A new Liouville operator can be defined, $\mathcal{L} = QLQ$, which describes the time evolution in the Hilbert space of operators, which is orthogonal complement of $\dot{x}$. Substituting then (7.137) with the operator $\mathcal{L}$ into (7.136), we bring it to the form, which will be used in what follows.

$$\Sigma(z) = \frac{1}{\chi}\left(QL\dot{x}, \frac{1}{z-\mathcal{L}}QL\dot{x}\right). \tag{7.138}$$

For the Hamiltonian (7.16) we obtain the following quantities:

$$\chi = (\dot{x}, \dot{x}) = \left(\frac{p_x}{m_b}, iLx\right) = \frac{i}{m_b\hbar}(p_x, Lx)$$

Using (7.99), we find

$$\chi = \frac{i}{m_b\hbar}\langle[p_x, x]\rangle = \frac{i}{m_b\hbar}\langle(-i\hbar)\rangle = \frac{1}{m_b} \tag{7.139}$$

and

$$O = \frac{(\dot{x}, L\dot{x})}{\chi} = m_b\frac{1}{\hbar}\langle[\dot{x}, \dot{x}]\rangle = 0. \tag{7.140}$$

Substituting (7.139) and (7.140) in (7.132), one obtains

$$\Phi(z) = \frac{1}{m_b}\frac{1}{z-\Sigma(z)}. \tag{7.141}$$

The operator

$$\begin{aligned}
L\dot{x} &= L\frac{p_x}{m_b} = \frac{1}{m_b\hbar}[H, p_x] = \\
&= -\frac{1}{m_b\hbar}\left[p_x, \sum_{\mathbf{k}}(V_k a_{\mathbf{k}} e^{i\mathbf{k}\cdot\mathbf{r}} + V_k^* a_{\mathbf{k}}^\dagger e^{-i\mathbf{k}\cdot\mathbf{r}})\right] \\
&= \frac{i}{m_b}\sum_{\mathbf{k}} ik_x(V_k a_{\mathbf{k}} e^{i\mathbf{k}\cdot\mathbf{r}} - V_k^* a_{\mathbf{k}}^\dagger e^{-i\mathbf{k}\cdot\mathbf{r}}) \Rightarrow \\
L\dot{x} &= -\frac{1}{m_b}\sum_{\mathbf{k}} k_x(V_k a_{\mathbf{k}} e^{i\mathbf{k}\cdot\mathbf{r}} - V_k^* a_{\mathbf{k}}^\dagger e^{-i\mathbf{k}\cdot\mathbf{r}})
\end{aligned} \tag{7.142}$$

does not depend on the velocities. Therefore, multiplying both parts of (7.142) with Q and taking into account (7.123) and (7.125), we obtain

$$QL\dot{x} = -\frac{1}{m_b}\sum_{\mathbf{k}} k_x(V_k a_{\mathbf{k}} e^{i\mathbf{k}\cdot\mathbf{r}} - V_k^* a_{\mathbf{k}}^\dagger e^{-i\mathbf{k}\cdot\mathbf{r}}),$$

what allows us to represent the memory function in the form

$$\begin{aligned}
\Sigma(z) &= \frac{1}{\chi}\left(QL\dot{x}, \frac{1}{z-\mathcal{L}}QL\dot{x}\right) \\
&= \frac{1}{m_b}\sum_{\mathbf{k}}\sum_{\mathbf{k}'}\begin{pmatrix} k_x(V_k a_{\mathbf{k}} e^{i\mathbf{k}\cdot\mathbf{r}} - V_k^* a_{\mathbf{k}}^\dagger e^{-i\mathbf{k}\cdot\mathbf{r}}), \\ \frac{1}{z-\mathcal{L}}k'_x(V_{k'} a_{\mathbf{k}'} e^{i\mathbf{k}'\cdot\mathbf{r}} - V_{k'}^* a_{\mathbf{k}'}^\dagger e^{-i\mathbf{k}'\cdot\mathbf{r}}) \end{pmatrix} \\
&= \frac{1}{m_b}\sum_{\mathbf{k}}\sum_{\mathbf{k}'} k_x k'_x V_k V_{k'}^* \begin{pmatrix} (a_{\mathbf{k}} e^{i\mathbf{k}\cdot\mathbf{r}} + a_{\mathbf{k}}^\dagger e^{-i\mathbf{k}\cdot\mathbf{r}}), \\ \frac{1}{z-\mathcal{L}}(a_{\mathbf{k}'} e^{i\mathbf{k}'\cdot\mathbf{r}} + a_{\mathbf{k}'}^\dagger e^{-i\mathbf{k}'\cdot\mathbf{r}}) \end{pmatrix}.
\end{aligned} \tag{7.143}$$

In transition to (7.143) we have used the property of the amplitude (7.17): $V_k^* = -V_k$ and taken into account that according to the definition (7.92), the first operator enters a scalar product in the hermitian conjugate form. Introducing the operators

$$b_{\mathbf{k}} = a_{\mathbf{k}} e^{i\mathbf{k}\cdot\mathbf{r}}; b_{\mathbf{k}}^\dagger = a_{\mathbf{k}}^\dagger e^{-i\mathbf{k}\cdot\mathbf{r}},$$

we represent the memory function as

$$\Sigma(z) = \frac{1}{m_b} \sum_{\mathbf{k}} \sum_{\mathbf{k}'} k_x k_x' V_k V_{k'}^* \left((b_{\mathbf{k}} + b_{\mathbf{k}}^\dagger), \frac{1}{z - \mathcal{L}} (b_{\mathbf{k}'} + b_{\mathbf{k}'}^\dagger) \right). \tag{7.144}$$

We notice that $Qb_{\mathbf{k}} = Q(a_{\mathbf{k}} e^{i\mathbf{k}\cdot\mathbf{r}}) = a_{\mathbf{k}} e^{i\mathbf{k}\cdot\mathbf{r}} = b_{\mathbf{k}}$. It will be represented through the four relaxation functions:

$$\Sigma(z) = \frac{1}{m_b} \sum_{\mathbf{k}} \sum_{\mathbf{k}'} k_x k_x' V_k V_{k'}^* \left[\Phi_{\mathbf{kk}'}^{++}(z) + \Phi_{\mathbf{kk}'}^{--}(z) + \Phi_{\mathbf{kk}'}^{+-}(z) + \Phi_{\mathbf{kk}'}^{-+}(z) \right], \tag{7.145}$$

$$\Phi_{\mathbf{kk}'}^{++}(z) = \left(b_{\mathbf{k}}^\dagger, \frac{1}{z - \mathcal{L}} b_{\mathbf{k}'}^\dagger \right), \tag{7.146}$$

$$\Phi_{\mathbf{kk}'}^{--}(z) = \left(b_{\mathbf{k}}, \frac{1}{z - \mathcal{L}} b_{\mathbf{k}'} \right), \tag{7.147}$$

$$\Phi_{\mathbf{kk}'}^{+-}(z) = \left(b_{\mathbf{k}}^\dagger, \frac{1}{z - \mathcal{L}} b_{\mathbf{k}'} \right), \tag{7.148}$$

$$\Phi_{\mathbf{kk}'}^{-+}(z) = \left(b_{\mathbf{k}}, \frac{1}{z - \mathcal{L}} b_{\mathbf{k}'}^\dagger \right). \tag{7.149}$$

There exist relations between the above relaxation functions. For example, the relaxation function (7.147), takes the form

$$\begin{aligned} \Phi_{\mathbf{kk}'}^{--}(z) &= \left(b_{\mathbf{k}}, \frac{1}{z - \mathcal{L}} b_{\mathbf{k}'} \right) \\ &= -i \int_0^\infty dt e^{izt} \left(e^{i\mathcal{L}t} b_{\mathbf{k}}(0), b_{\mathbf{k}'}(0) \right). \end{aligned}$$

Then the complex conjugate of this relaxation function:

$$\begin{aligned} \left[\Phi_{\mathbf{kk}'}^{--}(z) \right]^* &= i \int_0^\infty dt e^{-iz^*t} \left(e^{i\mathcal{L}t} b_{\mathbf{k}}(0), b_{\mathbf{k}'}(0) \right)^* \\ &= i \int_0^\infty dt e^{-iz^*t} \left(b_{\mathbf{k}'}(0), e^{i\mathcal{L}t} b_{\mathbf{k}}(0) \right), \end{aligned}$$

where the property (7.100) has been used. The property (7.97) gives

$$\begin{aligned} \left[\Phi_{\mathbf{kk}'}^{--}(z) \right]^* &= i \int_0^\infty dt e^{-iz^*t} \left(b_{\mathbf{k}'}(0), e^{i\mathcal{H}t/\hbar} b_{\mathbf{k}}(0) e^{-i\mathcal{H}t/\hbar} \right) \\ &= i \int_0^\infty dt e^{-iz^*t} \left(e^{i\mathcal{H}t/\hbar} b_{\mathbf{k}}^\dagger(0) e^{i\mathcal{H}t/\hbar}, b_{\mathbf{k}'}^\dagger(0) \right) \\ &= i \int_0^\infty dt e^{-iz^*t} \left(e^{i\mathcal{L}t} b_{\mathbf{k}}^\dagger(0), b_{\mathbf{k}'}^\dagger(0) \right) \\ &= i \int_0^\infty dt e^{-iz^*t} \left(b_{\mathbf{k}}^\dagger(t), b_{\mathbf{k}'}^\dagger(0) \right) = -\Phi_{\mathbf{kk}'}^{++}(-z^*), \end{aligned}$$

wherefrom it follows that

$$\Phi^{--}_{\mathbf{k}\mathbf{k}'}(z) = -\left[\Phi^{++}_{\mathbf{k}\mathbf{k}'}(-z^*)\right]^* . \tag{7.150}$$

Similarly, the relation

$$\Phi^{-+}_{\mathbf{k}\mathbf{k}'}(z) = -\left[\Phi^{+-}_{\mathbf{k}\mathbf{k}'}(-z^*)\right]^* \tag{7.151}$$

is proven.

Memory function

In this subsection we indicate which approximations must be made in the calculation of the relaxation functions in order to obtain the FHIP results for the impedance function. Consider the relaxation function (7.146):

$$\begin{aligned}\Phi^{++}_{\mathbf{k}\mathbf{k}'}(z) &= \left(b^\dagger_{\mathbf{k}}, \frac{1}{z-\mathcal{L}} b^\dagger_{\mathbf{k}'}\right) \\ &= -i\int_0^\infty dt e^{izt}\left(e^{i\mathcal{L}t} b^\dagger_{\mathbf{k}}(0), b^\dagger_{\mathbf{k}'}(0)\right) = -i\int_0^\infty dt e^{izt}\left(b^\dagger_{\mathbf{k}}(t), b^\dagger_{\mathbf{k}'}(0)\right),\end{aligned}$$

where $b^\dagger_{\mathbf{k}}(t) = e^{i\mathcal{L}t} b^\dagger_{\mathbf{k}}(0)$, and perform a partial integration:

$$\begin{aligned}\Phi^{++}_{\mathbf{k}\mathbf{k}'}(z) &= -\frac{1}{z}\int_0^\infty d\left(e^{izt}\right)\left(b^\dagger_{\mathbf{k}}(t), b^\dagger_{\mathbf{k}'}(0)\right) \\ &= -\frac{1}{z} e^{izt}\left(b^\dagger_{\mathbf{k}}(t) b^\dagger_{\mathbf{k}'}(0)\right)\Big|_0^\infty + \frac{1}{z}\int_0^\infty dt e^{izt}\left(\frac{db^\dagger_{\mathbf{k}}(t)}{dt}, b^\dagger_{\mathbf{k}'}(0)\right) \\ &= \frac{1}{z}\left(b^\dagger_{\mathbf{k}}(0), b^\dagger_{\mathbf{k}'}(0)\right) + \frac{1}{z}\int_0^\infty dt e^{izt}\left(i\mathcal{L} b^\dagger_{\mathbf{k}}(t), b^\dagger_{\mathbf{k}'}(0)\right) \\ &= \frac{1}{z}\left(b^\dagger_{\mathbf{k}}(0), b^\dagger_{\mathbf{k}'}(0)\right) - \frac{i}{z}\int_0^\infty dt e^{izt}\left(\mathcal{L} b^\dagger_{\mathbf{k}}(t), b^\dagger_{\mathbf{k}'}(0)\right).\end{aligned} \tag{7.152}$$

Here we supposed that

$$\lim_{t\longrightarrow\infty} e^{izt}\left(b^\dagger_{\mathbf{k}}(t), b^\dagger_{\mathbf{k}'}(0)\right) = 0.$$

In the second term in (7.152),

$$\begin{aligned}\left(\mathcal{L} b^\dagger_{\mathbf{k}}(t), b^\dagger_{\mathbf{k}'}(0)\right) &= \left(\mathcal{L} e^{i\mathcal{L}t} b^\dagger_{\mathbf{k}}, b^\dagger_{\mathbf{k}'}\right) = \left(QLQ e^{iQLQt} b^\dagger_{\mathbf{k}}, b^\dagger_{\mathbf{k}'}(0)\right) \\ &= \left(QLQ e^{iQHQt/\hbar} b^\dagger_{\mathbf{k}} e^{-iQHQt/\hbar}, b^\dagger_{\mathbf{k}'}\right) \\ &= \left(QL e^{iQHQt/\hbar} b^\dagger_{\mathbf{k}} e^{-iQHQt/\hbar}, b^\dagger_{\mathbf{k}'}\right)\end{aligned}$$

because $Qb^\dagger_{\mathbf{k}} = b^\dagger_{\mathbf{k}}$ and $Q^2 = Q$. Further on, we have

$$\begin{aligned}\left(\mathcal{L} b^\dagger_{\mathbf{k}}(t), b^\dagger_{\mathbf{k}'}(0)\right) &= \int_0^\beta d\lambda \left\langle e^{\lambda\hbar L} e^{iQHQt/\hbar} b_{\mathbf{k}} e^{-iQHQt/\hbar} LQ b^\dagger_{\mathbf{k}'}\right\rangle \\ &= \int_0^\beta d\lambda \left\langle e^{\lambda\hbar L} e^{iQHQt/\hbar} b_{\mathbf{k}} e^{-iQHQt/\hbar} L b^\dagger_{\mathbf{k}'}\right\rangle \\ &= \left(L e^{iQHQt/\hbar} b^\dagger_{\mathbf{k}} e^{-iQHQt/\hbar}, b^\dagger_{\mathbf{k}'}\right) \\ &= \left(L b^\dagger_{\mathbf{k}}(t), b^\dagger_{\mathbf{k}'}(0)\right).\end{aligned}$$

So, we find from (7.152)

$$\begin{aligned}\Phi^{++}_{\mathbf{k}\mathbf{k}'}(z) &= \frac{1}{z}\left(b^\dagger_{\mathbf{k}}(0), b^\dagger_{\mathbf{k}'}(0)\right) - \frac{i}{z}\int_0^\infty dt e^{izt}\left(Lb^\dagger_{\mathbf{k}}(t), b^\dagger_{\mathbf{k}'}(0)\right)\\ &= \frac{1}{z}\left(b^\dagger_{\mathbf{k}}(0), b^\dagger_{\mathbf{k}'}(0)\right) - \frac{i}{z}\int_0^\infty dt e^{izt}\left(b^\dagger_{\mathbf{k}}(t), Lb^\dagger_{\mathbf{k}'}(0)\right)\\ &= \frac{1}{z}\left(b^\dagger_{\mathbf{k}}(0), b^\dagger_{\mathbf{k}'}(0)\right) - \frac{i}{z\hbar}\int_0^\infty dt e^{izt}\left\langle\left[b_{\mathbf{k}}(t), b^\dagger_{\mathbf{k}'}(0)\right]\right\rangle. \end{aligned} \tag{7.153}$$

The first term in the r.h.s. of this expression can be represented as follows:

$$\begin{aligned}\frac{1}{z}\left(b^\dagger_{\mathbf{k}}(0), b^\dagger_{\mathbf{k}'}(0)\right) &= \frac{1}{z}\int_0^\beta d\lambda\left\langle\left(e^{\lambda\hbar L}b_{\mathbf{k}}\right)b^\dagger_{\mathbf{k}'}\right\rangle = \frac{1}{z}\left\langle\int_0^\beta d\lambda\left(e^{\lambda\hbar L}b_{\mathbf{k}}\right)b^\dagger_{\mathbf{k}'}\right\rangle\\ &= \frac{1}{z}\left\langle\left(\frac{e^{\beta\hbar L}-1}{\hbar L}b_{\mathbf{k}}\right)b^\dagger_{\mathbf{k}'}\right\rangle = \frac{1}{z\hbar}\left\langle e^{\beta H}\frac{1}{L}b_{\mathbf{k}}e^{-\beta H}b^\dagger_{\mathbf{k}'} - \frac{1}{L}b_{\mathbf{k}}b^\dagger_{\mathbf{k}'}\right\rangle\\ &= \frac{1}{z\hbar}\frac{1}{\mathrm{Tr}e^{-\beta H}}\mathrm{Tr}\left\{e^{-\beta H}\left[e^{\beta H}\frac{1}{L}b_{\mathbf{k}}e^{-\beta H}b^\dagger_{\mathbf{k}'} - \frac{1}{L}b_{\mathbf{k}}b^\dagger_{\mathbf{k}'}\right]\right\}\\ &= \frac{1}{z\hbar}\frac{1}{\mathrm{Tr}e^{-\beta H}}\mathrm{Tr}\left\{b^\dagger_{\mathbf{k}'}\frac{1}{L}b_{\mathbf{k}}e^{-\beta H} - e^{-\beta H}\frac{1}{L}b_{\mathbf{k}}b^\dagger_{\mathbf{k}'}\right\}\\ &= \frac{1}{z\hbar}\left\langle b^\dagger_{\mathbf{k}'}\frac{1}{L}b_{\mathbf{k}} - \frac{1}{L}b_{\mathbf{k}}b^\dagger_{\mathbf{k}'}\right\rangle\\ &= \frac{i}{z\hbar}\left\langle b^\dagger_{\mathbf{k}'}\frac{1}{iL}b_{\mathbf{k}} - \frac{1}{iL}b_{\mathbf{k}}b^\dagger_{\mathbf{k}'}\right\rangle\\ &= \frac{i}{z\hbar}\left\langle\int_0^\infty dt e^{iLt}b_{\mathbf{k}}b^\dagger_{\mathbf{k}'} - \int_0^\infty dt b^\dagger_{\mathbf{k}'}e^{iLt}b_{\mathbf{k}}\right\rangle\\ &= \frac{i}{z\hbar}\left\langle\int_0^\infty dt b_{\mathbf{k}}(t)b^\dagger_{\mathbf{k}'} - \int_0^\infty dt b^\dagger_{\mathbf{k}'}b_{\mathbf{k}}(t)\right\rangle\\ &= \frac{i}{z\hbar}\int_0^\infty dt\left\langle\left[b_{\mathbf{k}}(t), b^\dagger_{\mathbf{k}'}(0)\right]\right\rangle. \end{aligned}$$

Substituting it in the r.h.s. of (7.153), we find

$$\begin{aligned}\Phi^{++}_{\mathbf{k}\mathbf{k}'}(z) &= \frac{i}{z\hbar}\int_0^\infty dt\left\langle\left[b_{\mathbf{k}}(t), b^\dagger_{\mathbf{k}'}(0)\right]\right\rangle - \frac{i}{z\hbar}\int_0^\infty dt e^{izt}\left\langle\left[b_{\mathbf{k}}(t), b^\dagger_{\mathbf{k}'}(0)\right]\right\rangle\\ &= \frac{i}{z\hbar}\int_0^\infty dt\left(1-e^{izt}\right)\left\langle\left[b_{\mathbf{k}}(t), b^\dagger_{\mathbf{k}'}(0)\right]\right\rangle. \end{aligned} \tag{7.154}$$

In a similar way one obtains

$$\Phi^{+-}_{\mathbf{k}\mathbf{k}'}(z) = \frac{i}{z\hbar}\int_0^\infty dt\left(1-e^{izt}\right)\left\langle\left[b_{\mathbf{k}}(t), b_{\mathbf{k}'}(0)\right]\right\rangle. \tag{7.155}$$

Inserting the relaxation functions (7.154), (7.155), (7.150) and (7.151), we find the memory

function (7.145)

$$\begin{aligned}\Sigma(z) &= \frac{1}{m_b}\sum_{\mathbf{k}}\sum_{\mathbf{k}'} k_x k'_x V_k V^*_{k'} \frac{i}{z\hbar}\int_0^\infty dt\left(1-e^{izt}\right)\\ &\times\left[\begin{array}{c}\left\langle\left[b_{\mathbf{k}}(t), b^\dagger_{\mathbf{k}'}(0)\right]\right\rangle + \langle[b_{\mathbf{k}}(t), b_{\mathbf{k}'}(0)]\rangle\\ -\left\langle\left[b_{\mathbf{k}}(t), b^\dagger_{\mathbf{k}'}(0)\right]\right\rangle^* - \langle[b_{\mathbf{k}}(t), b_{\mathbf{k}'}(0)]\rangle^*\end{array}\right]\\ &= -\frac{1}{m_b}\sum_{\mathbf{k}}\sum_{\mathbf{k}'} k_x k'_x V_k V^*_{k'} \frac{2}{z\hbar}\int_0^\infty dt\left(1-e^{izt}\right)\\ &\times \operatorname{Im}\left[\left\langle\left[b_{\mathbf{k}}(t), b^\dagger_{\mathbf{k}'}(0)\right]\right\rangle + \langle[b_{\mathbf{k}}(t), b_{\mathbf{k}'}(0)]\rangle\right],\end{aligned}$$

wherefrom

$$\Sigma(z) = \frac{1}{z}\int_0^\infty dt\left(1-e^{izt}\right)\operatorname{Im} F(t) \tag{7.156}$$

with

$$F(t) = -\frac{2}{m_b\hbar}\sum_{\mathbf{k}}\sum_{\mathbf{k}'} k_x k'_x V_k V^*_{k'}\left\{\left\langle\left[b_{\mathbf{k}}(t), b^\dagger_{\mathbf{k}'}(0)\right]\right\rangle + \langle[b_{\mathbf{k}}(t), b_{\mathbf{k}'}(0)]\rangle\right\}. \tag{7.157}$$

Derivation of the memory function

To calculate the expectation values in Eq. (7.157), we shall make the following approximations (cf. Ref. [78]). The Liouville operator $\mathcal{L}$, which determines the time evolution of the operator $b^\dagger_{\mathbf{k}}(t) = e^{i\mathcal{L}t}b^\dagger_{\mathbf{k}}(0)$, is replaced by $L_{ph} + L_F$, where L_{ph} is the Liouville operator for free phonons and L_F is the Liouville operator for the Feynman polaron model [43]. The Fröhlich Hamiltonian appearing in the statistical average $\langle\bullet\rangle$ is imilarly replaced by $H_{ph} + H_F$, with H_{ph} the Hamiltonian of free phonons and H_F the Hamiltonian of the Feynman polaron model. With this approximation, e.g., the average

$$\left\langle b_{\mathbf{k}}(t)b^\dagger_{\mathbf{k}'}(0)\right\rangle = \left\langle a_{\mathbf{k}}(t)a^\dagger_{\mathbf{k}'}(0)\right\rangle\left\langle e^{i\mathbf{k}\cdot\mathbf{r}(t)}e^{-i\mathbf{k}'\cdot\mathbf{r}}\right\rangle = \delta_{\mathbf{k},\mathbf{k}'}\left\langle a_{\mathbf{k}}(t)a^\dagger_{\mathbf{k}}(0)\right\rangle\left\langle e^{i\mathbf{k}\cdot\mathbf{r}(t)}e^{-i\mathbf{k}\cdot\mathbf{r}}\right\rangle. \tag{7.158}$$

The time evolution of the free-phonon annihilation operator (7.94),

$$a_{\mathbf{k}}(t) = e^{iH_{ph}t/\hbar}a_{\mathbf{k}}e^{-iH_{ph}t/\hbar} = \exp\left(i\omega_{\mathbf{k}}a^+_{\mathbf{k}}a_{\mathbf{k}}t\right)a_{\mathbf{k}}\exp\left(-i\omega_{\mathbf{k}}a^+_{\mathbf{k}}a_{\mathbf{k}}t\right)$$

accorting to (7.93) is

$$\begin{aligned}-i\frac{da_{\mathbf{k}}(t)}{dt} &= \omega_{\mathbf{k}}\exp\left(i\omega_{\mathbf{k}}a^+_{\mathbf{k}}a_{\mathbf{k}}t\right)\left[a^+_{\mathbf{k}}a_{\mathbf{k}}, a_{\mathbf{k}}\right]\exp\left(-i\omega_{\mathbf{k}}a^+_{\mathbf{k}}a_{\mathbf{k}}t\right)\\ &= \omega_{\mathbf{k}}\exp\left(i\omega_{\mathbf{k}}a^+_{\mathbf{k}}a_{\mathbf{k}}t\right)\left[a^+_{\mathbf{k}}, a_{\mathbf{k}}\right]a_{\mathbf{k}}\exp\left(-i\omega_{\mathbf{k}}a^+_{\mathbf{k}}a_{\mathbf{k}}t\right)\\ &= -\omega_{\mathbf{k}}\exp\left(i\omega_{\mathbf{k}}a^+_{\mathbf{k}}a_{\mathbf{k}}t\right)a_{\mathbf{k}}\exp\left(-i\omega_{\mathbf{k}}a^+_{\mathbf{k}}a_{\mathbf{k}}t\right)\Rightarrow\\ a_{\mathbf{k}}(t) &= \exp\left(-i\omega_{\mathbf{k}}t\right)a_{\mathbf{k}}.\end{aligned}$$

Similarly,

$$a^\dagger_{\mathbf{k}}(t) = \exp\left(i\omega_{\mathbf{k}}t\right)a^\dagger_{\mathbf{k}}.$$

Hence, we have

$$\left\langle a_{\mathbf{k}}(t)a^\dagger_{\mathbf{k}}\right\rangle = \exp\left(-i\omega_{\mathbf{k}}t\right)\left\langle a_{\mathbf{k}}a^\dagger_{\mathbf{k}}\right\rangle = \exp\left(-i\omega_{\mathbf{k}}t\right)\left\langle 1 + a^\dagger_{\mathbf{k}}a_{\mathbf{k}}\right\rangle = \exp\left(-i\omega_{\mathbf{k}}t\right)\left[1 + n(\omega_{\mathbf{k}})\right],$$

where $n(\omega_{\mathbf{k}}) = [\exp(\beta\hbar\omega_{\mathbf{k}}) - 1]^{-1}$ is the average number of phonons with energy $\hbar\omega_{\mathbf{k}}$.

The calculation of the Fourier component of the electron density-density correlation function $\left\langle e^{i\mathbf{k}\cdot\mathbf{r}(t)}e^{-i\mathbf{k}\cdot\mathbf{r}}\right\rangle$ in Eq. (7.158) for an electron described by the Feynman polaron model is given below following the approach of Ref. [78].

We calculate the correlation function

$$\left\langle e^{i\mathbf{k}\cdot\mathbf{r}(t)}e^{-i\mathbf{k}\cdot\mathbf{r}(\tau)}\right\rangle = \frac{\mathrm{Tr}\left(e^{-\beta H_F}e^{i\mathbf{k}\cdot\mathbf{r}(t)}e^{i\mathbf{k}\cdot\mathbf{r}(\tau)}\right)}{\mathrm{Tr}\left(e^{-\beta H_F}\right)} \tag{7.159}$$

with the Feynman trial Hamiltonian

$$H_F = \frac{\mathbf{p}^2}{2m} + \frac{\mathbf{p}_f^2}{2m_f} + \frac{1}{2}\chi\left(\mathbf{r}-\mathbf{r}_f\right)^2. \tag{7.160}$$

Here, $\mathbf{r}(t)$ denotes the operator in the Heisenberg representation

$$\mathbf{r}(t) = e^{\frac{it}{\hbar}H_F}\mathbf{r}e^{-\frac{it}{\hbar}H_F}. \tag{7.161}$$

We show that the correlation function $\left\langle e^{i\mathbf{k}\cdot\mathbf{r}(t)}e^{-i\mathbf{k}\cdot\mathbf{r}(\tau)}\right\rangle$ depends on $(\tau - t)$ rather than on t and τ independently:

$$\begin{aligned}\left\langle e^{i\mathbf{k}\cdot\mathbf{r}(t)}e^{-i\mathbf{k}\cdot\mathbf{r}(\tau)}\right\rangle &= \frac{\mathrm{Tr}\left(e^{-\beta H_F}e^{\frac{it}{\hbar}H_F}e^{i\mathbf{k}\cdot\mathbf{r}}e^{-\frac{it}{\hbar}H_F}e^{\frac{i\tau}{\hbar}H_F}e^{i\mathbf{k}\cdot\mathbf{r}}e^{-\frac{i\tau}{\hbar}H_F}\right)}{\mathrm{Tr}\left(e^{-\beta H_F}\right)} \\ &= \frac{\mathrm{Tr}\left(e^{-\beta H_F}e^{i\mathbf{k}\cdot\mathbf{r}}e^{\frac{i(\tau-t)}{\hbar}H_F}e^{i\mathbf{k}\cdot\mathbf{r}}e^{-\frac{i(\tau-t)}{\hbar}H_F}\right)}{\mathrm{Tr}\left(e^{-\beta H_F}\right)} \\ &= \left\langle e^{i\mathbf{k}\cdot\mathbf{r}}e^{-i\mathbf{k}\cdot\mathbf{r}(\tau-t)}\right\rangle = \left\langle e^{i\mathbf{k}\cdot\mathbf{r}}e^{-i\mathbf{k}\cdot\mathbf{r}(\sigma)}\right\rangle,\end{aligned} \tag{7.162}$$

where $\sigma = \tau - t$.

The normal coordinates are the center-of-mass vector $\mathbf{R}$ and the vector of the relative motion ρ:

$$\begin{cases} \mathbf{R} = \frac{m\mathbf{r}+m_f\mathbf{r}_f}{m+m_f} \\ \rho = \mathbf{r}-\mathbf{r}_f \end{cases} \tag{7.163}$$

The inverse transformation is:

$$\begin{cases} \mathbf{r} = \mathbf{R} + \frac{m_f}{m+m_f}\rho \\ \mathbf{r}_f = \mathbf{R} - \frac{m}{m+m_f}\rho \end{cases} \tag{7.164}$$

The same transformation as (7.163) takes place for velocities:

$$\begin{cases} \dot{\mathbf{r}} = \dot{\mathbf{R}} + \frac{m_f}{m+m_f}\dot{\rho} \\ \dot{\mathbf{r}}_f = \dot{\mathbf{R}} - \frac{m}{m+m_f}\dot{\rho} \end{cases} \tag{7.165}$$

From (7.163) we derive the transformation for moments

$$\begin{cases} \frac{\mathbf{p}}{m} = \frac{\mathbf{P}}{m+m_f} + \frac{m_f}{m+m_f}\frac{\mathbf{p}_\rho}{\frac{mm_f}{m+m_f}} \\ \frac{\mathbf{p}_f}{m_f} = \frac{\mathbf{P}}{m+m_f} - \frac{m}{m+m_f}\frac{\mathbf{p}_\rho}{\frac{mm_f}{m+m_f}} \end{cases}$$

$$\Downarrow$$

$$\begin{cases} \mathbf{p} = \frac{m}{m+m_f}\mathbf{P} + \mathbf{p}_\rho \\ \mathbf{p}_f = \frac{m_f}{m+m_f}\mathbf{P} - \mathbf{p}_\rho \end{cases} \tag{7.166}$$

The Hamiltonian (7.160) then takes the form

$$H_F = \frac{\mathbf{P}^2}{2M} + \frac{\mathbf{p}_\rho^2}{2\mu} + \frac{1}{2}\mu\bar{\Omega}^2\rho^2 \tag{7.167}$$

with the masses

$$M = m + m_f,\ \mu = \frac{mm_f}{m + m_f} \tag{7.168}$$

and with the frequency

$$\bar{\Omega} = \sqrt{\frac{\chi}{\mu}}. \tag{7.169}$$

The Cartesian coordinates and moments corresponding to the relative motion can be in the standard way expressed in terms of the second quantization operators:

$$\begin{aligned} \rho_j &= \left(\frac{\hbar}{2\mu\bar{\Omega}}\right)^{1/2}\left(C_j + C_j^\dagger\right), \\ p_{\rho,j} &= -i\left(\frac{\mu\hbar\bar{\Omega}}{2}\right)^{1/2}\left(C_j - C_j^\dagger\right). \\ &(j = 1, 2, 3) \end{aligned} \tag{7.170}$$

In these notations, the Hamiltonian (7.167) takes the form

$$H_F = \frac{\mathbf{P}^2}{2M} + \sum_{j=1}^{3}\hbar\bar{\Omega}\left(C_j^\dagger C_j + \frac{1}{2}\right). \tag{7.171}$$

Using (7.171), we find the operators in the Heisenberg representation, (i) for the center-of mass coordinates

$$\begin{aligned} X_j(\sigma) &= e^{\frac{i\sigma}{\hbar}H_F}X_j e^{-\frac{i\sigma}{\hbar}H_F} = e^{i\frac{\sigma}{2M\hbar}P_j^2}X_j e^{-i\frac{\sigma}{2M\hbar}P_j^2} \\ &= X_j + i\frac{\sigma}{2M\hbar}\left[P_j^2, X_j\right] \\ &= X_j + i\frac{\sigma}{2M\hbar}\left(P_j^2X_j - P_jX_jP_j + P_jX_jP_j - X_jP_j^2\right) \\ &= X_j + i\frac{\sigma}{2M\hbar}\left(P_j\left[P_j, X_j\right] + \left[P_j, X_j\right]P_j\right) \\ &= X_j + i\frac{\sigma}{2M\hbar}P_j(-2i\hbar) = X_j + \frac{\sigma}{M}P_j, \end{aligned}$$

$$X_j(\sigma) = X_j + \frac{\sigma}{M}P_j, \tag{7.172}$$

(ii) for the operators C_j and $C_j^\dagger$

$$C_j(\sigma) = C_j e^{-i\bar{\Omega}\sigma},\ C_j^\dagger(\sigma) = C_j^\dagger e^{i\bar{\Omega}\sigma}. \tag{7.173}$$

Using the first formula of (7.164) we find

$$\mathbf{r}(\sigma) = \mathbf{R}(\sigma) + \frac{m_f}{m + m_f}\rho(\sigma)$$

$$\Downarrow$$

$$\mathbf{r}(\sigma) = \mathbf{R} + \frac{\sigma}{M}\mathbf{P} + \frac{m_f}{M}\left(\frac{\hbar}{2\mu\bar{\Omega}}\right)^{1/2}\left(\mathbf{C}e^{-i\bar{\Omega}\sigma} + \mathbf{C}^\dagger e^{i\bar{\Omega}\sigma}\right). \tag{7.174}$$

We denote

$$a \equiv \frac{m_f}{M}\left(\frac{\hbar}{2\mu\bar{\Omega}}\right)^{1/2} = \left(\frac{\hbar m_f^2}{2M^2\mu\bar{\Omega}}\right)^{1/2}$$
$$= \left(\frac{\hbar m_f^2}{2\left(m+m_f\right)^2 \frac{mm_f}{m+m_f}\bar{\Omega}}\right)^{1/2} = \left(\frac{\hbar m_f}{2mM\bar{\Omega}}\right)^{1/2}$$

$$\mathbf{r}\left(\sigma\right) = \mathbf{R} + \frac{\sigma}{M}\mathbf{P} + a\left(\mathbf{C}e^{-i\bar{\Omega}\sigma} + \mathbf{C}^\dagger e^{i\bar{\Omega}\sigma}\right). \tag{7.175}$$

Therefore, we obtain

$$e^{i\mathbf{k}\cdot\mathbf{r}} = \exp\left(i\mathbf{k}\cdot\mathbf{R}\right)\exp\left(ia\mathbf{k}\cdot\mathbf{C} + ia\mathbf{k}\cdot\mathbf{C}^\dagger\right)$$
$$= \prod_{j=1}^{3}\exp\left(ik_jX_j\right)\exp\left(iak_jC_j - iak_jC_j^\dagger\right)$$

$$e^{-i\mathbf{k}\cdot\mathbf{r}(\sigma)} = \exp\left[-i\mathbf{k}\cdot\mathbf{R} - i\frac{\sigma}{M}\mathbf{k}\cdot\mathbf{P} - ia\mathbf{k}\cdot\left(\mathbf{C}e^{-i\bar{\Omega}\sigma} + \mathbf{C}^\dagger e^{i\bar{\Omega}\sigma}\right)\right]$$
$$= \exp\left(-i\mathbf{k}\cdot\mathbf{R} - i\frac{\sigma}{M}\mathbf{k}\cdot\mathbf{P}\right)\exp\left(-ia\mathbf{k}\cdot\mathbf{C}e^{-i\bar{\Omega}\sigma} - ia\mathbf{k}\cdot\mathbf{C}^\dagger e^{i\bar{\Omega}\sigma}\right)$$
$$= \prod_{j=1}^{3}\exp\left(-ik_jX_j - i\frac{\sigma}{M}k_jP_j\right)\exp\left(-iak_jC_je^{-i\bar{\Omega}\sigma} - iak_jC_j^\dagger e^{i\bar{\Omega}\sigma}\right). \tag{7.176}$$

The disentangling of the exponents is performed using the formula

$$e^{A+B} = e^A T\exp\left(\int_0^1 d\lambda e^{-\lambda A}Be^{\lambda A}\right). \tag{7.177}$$

In the case when $[A,B]$ commutes with both A and B, this formula is reduced to

$$e^{A+B} = e^Ae^Be^{-\frac{1}{2}[A,B]}. \tag{7.178}$$

We perform the necessary commutations:

$$-\frac{1}{2}\left[-ik_jX_j, -i\frac{\sigma}{M}k_jP_j\right] = \frac{1}{2}k_j^2\frac{\sigma}{M}\left[X_j,P_j\right] = i\frac{\hbar k_j^2}{2M}\sigma,$$
$$-\frac{1}{2}\left[iak_jC_j^\dagger, iak_jC_j\right] = \frac{1}{2}a^2k_j^2\left[C_j^\dagger, C_j\right] = -\frac{1}{2}a^2k_j^2$$
$$-\frac{1}{2}\left[-iak_jC_j^\dagger e^{i\Omega\sigma}, -iak_jC_je^{-i\Omega\sigma}\right] = \frac{1}{2}a^2k_j^2\left[C_j^\dagger, C_j\right] = -\frac{1}{2}a^2k_j^2$$
$$\Downarrow$$

$$e^{i\mathbf{k}\cdot\mathbf{r}} = e^{i\mathbf{k}\cdot\mathbf{R}}e^{ia\mathbf{k}\cdot\mathbf{C}^\dagger}e^{ia\mathbf{k}\cdot\mathbf{C}}e^{-\frac{1}{2}a^2k^2},$$
$$e^{-i\mathbf{k}\cdot\mathbf{r}(\sigma)} = e^{-i\mathbf{k}\cdot\mathbf{R}}e^{-i\frac{\sigma}{M}\mathbf{k}\cdot\mathbf{P}}e^{-ia\mathbf{k}\cdot\mathbf{C}^\dagger e^{i\bar{\Omega}\sigma}}e^{-ia\mathbf{k}\cdot\mathbf{C}e^{-i\bar{\Omega}\sigma}}e^{i\frac{\hbar k^2}{2M}\sigma-\frac{1}{2}a^2k^2}$$

$$\Downarrow$$

$$e^{i\mathbf{k}\cdot\mathbf{r}}e^{-i\mathbf{k}\cdot\mathbf{r}(\sigma)} = e^{-i\frac{\sigma}{M}\mathbf{k}\cdot\mathbf{P}}e^{ia\mathbf{k}\cdot\mathbf{C}^\dagger}e^{ia\mathbf{k}\cdot\mathbf{C}}e^{-ia\mathbf{k}\cdot\mathbf{C}^\dagger e^{i\bar{\Omega}\sigma}}e^{-ia\mathbf{k}\cdot\mathbf{C}e^{-i\bar{\Omega}\sigma}}e^{i\frac{\hbar k^2}{2M}\sigma-a^2k^2}.$$

It follows from Eq. (7.178) that when $[A, B]$ commutes with both A and B,

$$e^A e^B = e^B e^A e^{[A,B]}. \tag{7.179}$$

Using (7.179), we find

$$\begin{aligned} e^{iak_j\cdot C_j} e^{-iak_j\cdot C_j^\dagger e^{i\bar{\Omega}\sigma}} &= e^{-iak_j\cdot C_j^\dagger e^{i\bar{\Omega}\sigma}} e^{iak_j\cdot C_j} e^{\left[iak_j\cdot C_j, -iak_j\cdot C_j^\dagger e^{i\bar{\Omega}\sigma}\right]} \\ &= e^{-iak_j\cdot C_j^\dagger e^{i\bar{\Omega}\sigma}} e^{iak_j\cdot C_j} e^{a^2 k_j^2 e^{i\bar{\Omega}\sigma}}. \end{aligned}$$

Herefrom, we find

$$e^{i\mathbf{k}\cdot\mathbf{r}} e^{-i\mathbf{k}\cdot\mathbf{r}(\sigma)} = e^{-i\frac{\sigma}{M}\mathbf{k}\cdot\mathbf{P}} e^{ia\mathbf{k}\cdot\mathbf{C}^\dagger\left(1-e^{i\bar{\Omega}\sigma}\right)} e^{ia\mathbf{k}\cdot\mathbf{C}\left(1-e^{-i\bar{\Omega}\sigma}\right)} e^{i\frac{\hbar k^2}{2M}\sigma - a^2k^2\left(1-e^{i\bar{\Omega}\sigma}\right)}. \tag{7.180}$$

The correlation function then is

$$\left\langle e^{i\mathbf{k}\cdot\mathbf{r}} e^{-i\mathbf{k}\cdot\mathbf{r}(\sigma)}\right\rangle = \left\langle e^{-i\frac{\sigma}{M}\mathbf{k}\cdot\mathbf{P}}\right\rangle \left\langle e^{ia\mathbf{k}\cdot\mathbf{C}^\dagger\left(1-e^{i\bar{\Omega}\sigma}\right)} e^{ia\mathbf{k}\cdot\mathbf{C}\left(1-e^{-i\bar{\Omega}\sigma}\right)}\right\rangle e^{i\frac{\hbar k^2}{2M}\sigma - a^2k^2\left(1-e^{i\bar{\Omega}\sigma}\right)}, \tag{7.181}$$

since the variables of the center-of mass motion and of the relative motion are averaged independently.

$$\begin{aligned} \left\langle e^{ia\mathbf{k}\cdot\mathbf{C}^\dagger\left(1-e^{i\bar{\Omega}\sigma}\right)} e^{ia\mathbf{k}\cdot\mathbf{C}\left(1-e^{-i\bar{\Omega}\sigma}\right)}\right\rangle &= \left\langle e^{i\mathbf{Q}\cdot\mathbf{C}^\dagger} e^{i\mathbf{Q}^*\cdot\mathbf{C}}\right\rangle \\ &= \frac{\mathrm{Tr}\left(e^{-\beta\hbar\bar{\Omega}\mathbf{C}^\dagger\cdot\mathbf{C}} e^{i\mathbf{Q}\cdot\mathbf{C}^\dagger} e^{i\mathbf{Q}^*\cdot\mathbf{C}}\right)}{\mathrm{Tr}\left(e^{-\beta\hbar\bar{\Omega}\mathbf{C}^\dagger\cdot\mathbf{C}}\right)} \end{aligned}$$

with

$$\mathbf{Q} = a\left(1 - e^{i\bar{\Omega}\sigma}\right)\mathbf{k}.$$

Let us consider the auxiliary expectation value

$$\begin{aligned} \left\langle e^{iQC^\dagger} e^{iQ^*C}\right\rangle &\equiv \frac{\mathrm{Tr}\left(e^{-\beta\hbar\bar{\Omega}C^\dagger C} e^{iQC^\dagger} e^{iQ^*C}\right)}{\mathrm{Tr}\left(e^{-\beta\hbar\bar{\Omega}C^\dagger C}\right)} \\ &= \frac{1}{\mathrm{Tr}\left(e^{-\beta\hbar\bar{\Omega}C^\dagger C}\right)} \sum_{n=0}^{\infty} \frac{(iQ)^n}{n!} \sum_{m=0}^{\infty} \frac{(iQ^*)^m}{m!} \mathrm{Tr}\left(e^{-\beta\hbar\bar{\Omega}C^\dagger C} \left(C^\dagger\right)^n C^m\right) \\ &= \frac{1}{\mathrm{Tr}\left(e^{-\beta\hbar\bar{\Omega}C^\dagger C}\right)} \sum_{n=0}^{\infty} \frac{(-1)^n |Q|^{2n}}{(n!)^2} \mathrm{Tr}\left(e^{-\beta\hbar\bar{\Omega}C^\dagger C} \left(C^\dagger\right)^n C^n\right). \end{aligned}$$

$$\begin{aligned} \mathrm{Tr}\left(e^{-\beta\hbar\bar{\Omega}C^\dagger C} \left(C^\dagger\right)^n C^n\right) &= \sum_{m=0}^{\infty} \left\langle m \left| e^{-\beta\hbar\bar{\Omega}C^\dagger C} \left(C^\dagger\right)^n C^n \right| m\right\rangle \\ &= \sum_{m=0}^{\infty} e^{-\beta\hbar\bar{\Omega}m} \left\langle m \left| \left(C^\dagger\right)^n C^n \right| m\right\rangle, \end{aligned}$$

where $|m\rangle$ are the eigenstates of $\left(C^\dagger C\right)$. The operators C act on these states as follows:

$$\begin{aligned} C|m\rangle &= \sqrt{m}\,|m-1\rangle, \\ C|0\rangle &= 0. \end{aligned}$$

Therefore, we find

$$\left\langle m \left| \left(C^\dagger\right)^n C^n \right| m \right\rangle = m\left(m-1\right)\ldots\left(m-n+1\right) = \frac{m!}{\left(m-n\right)!} \text{ for } n \leq m,$$
$$\left\langle m \left| \left(C^\dagger\right)^n C^n \right| m \right\rangle = 0 \text{ for } n > m.$$

$$\Downarrow$$

$$Tr\left(e^{-\beta\hbar\bar{\Omega}C^\dagger C}\left(C^\dagger\right)^n C^n\right) = \sum_{m=n}^{\infty} e^{-\beta\hbar\Omega m}\frac{m!}{\left(m-n\right)!},$$

and

$$\begin{aligned}
\mathrm{Tr}\left(e^{-\beta\hbar\Omega C^\dagger C}e^{iQC^\dagger}e^{iQ^*C}\right) &= \sum_{n=0}^{\infty}\frac{\left(-1\right)^n\left|Q\right|^{2n}}{\left(n!\right)^2}\sum_{m=n}^{\infty}e^{-\beta\hbar\bar{\Omega}m}\frac{m!}{\left(m-n\right)!} \\
&= \sum_{n=0}^{\infty}\frac{\left(-1\right)^n\left|Q\right|^{2n}}{n!}\sum_{m=n}^{\infty}e^{-\beta\hbar\bar{\Omega}m}\binom{m}{n} \\
&= \sum_{n=0}^{\infty}\frac{\left(-1\right)^n\left|Q\right|^{2n}}{n!}e^{-\beta\hbar\bar{\Omega}n}\sum_{k=0}^{\infty}e^{-\beta\hbar\bar{\Omega}k}\binom{k+n}{n} \\
&= \sum_{n=0}^{\infty}\frac{\left(-1\right)^n\left|Q\right|^{2n}}{n!}e^{-\beta\hbar\bar{\Omega}n}\frac{1}{\left(1-e^{-\beta\hbar\bar{\Omega}}\right)^{n+1}} \\
&= \frac{1}{1-e^{-\beta\hbar\bar{\Omega}}}\sum_{n=0}^{\infty}\frac{\left(-1\right)^n\left|Q\right|^{2n}}{n!}\frac{1}{\left(e^{\beta\hbar\bar{\Omega}}-1\right)^n} \\
&= \frac{1}{1-e^{-\beta\hbar\bar{\Omega}}}\exp\left(-\frac{\left|Q\right|^2}{e^{\beta\hbar\bar{\Omega}}-1}\right).
\end{aligned}$$

In particular, for $Q = Q^* = 0$, we have

$$Tr\left(e^{-\beta\hbar\Omega C^\dagger C}\right) = \frac{1}{1-e^{-\beta\hbar\Omega}}. \tag{7.182}$$

As a result, the expectation value $\left\langle e^{iQC^\dagger}e^{iQ^*C}\right\rangle$ is

$$\left\langle e^{iQC^\dagger}e^{iQ^*C}\right\rangle = \exp\left[-n\left(\Omega\right)\left|Q\right|^2\right], \tag{7.183}$$

with

$$n\left(\Omega\right) \equiv \frac{1}{e^{\beta\hbar\Omega}-1}.$$

Using this result, we obtain the expression

$$\begin{aligned}
\left\langle e^{i\mathbf{Q}\cdot\mathbf{C}^\dagger}e^{i\mathbf{Q}^*\cdot\mathbf{C}}\right\rangle &= \exp\left[-n\left(\Omega\right)\mathbf{Q}\cdot\mathbf{Q}^*\right] \\
&= \exp\left[-n\left(\Omega\right)a^2k^2\left(1-e^{i\bar{\Omega}\sigma}\right)\left(1-e^{-i\bar{\Omega}\sigma}\right)\right] \\
&= \exp\left[-4n\left(\Omega\right)a^2k^2\sin^2\left(\frac{1}{2}\Omega\sigma\right)\right].
\end{aligned}$$

The expectation value $\left\langle e^{-i\frac{\sigma}{M}\mathbf{k}\cdot\mathbf{P}}\right\rangle$ is

$$\begin{aligned}\left\langle e^{-i\frac{\sigma}{M}\mathbf{k}\cdot\mathbf{P}}\right\rangle &= \frac{\int d\mathbf{P}\exp\left(-\beta\frac{P^2}{2M}-i\frac{\sigma}{M}\mathbf{k}\cdot\mathbf{P}\right)}{\int d\mathbf{P}\exp\left(-\beta\frac{P^2}{2M}\right)}\\ &= \frac{\int d\mathbf{P}\exp\left(\frac{(-i\mathbf{P}\beta+\mathbf{k}\sigma)^2}{2M\beta}-\frac{k^2\sigma^2}{2M\beta}\right)}{\int d\mathbf{P}\exp\left(-\beta\frac{P^2}{2M}\right)}\\ &= \exp\left(-\frac{k^2\sigma^2}{2M\beta}\right).\end{aligned}$$

Collecting all factors in Eq. (7.181) together, we find

$$\left\langle e^{i\mathbf{k}\cdot\mathbf{r}}e^{-i\mathbf{k}\cdot\mathbf{r}(\sigma)}\right\rangle = \exp\left[i\frac{\hbar k^2}{2M}\sigma-\frac{k^2\sigma^2}{2M\beta}-4n\left(\bar{\Omega}\right)a^2k^2\sin^2\left(\frac{1}{2}\bar{\Omega}\sigma\right)-a^2k^2\left(1-e^{i\bar{\Omega}\sigma}\right)\right]\Rightarrow.$$

$$\left\langle e^{i\mathbf{k}\cdot\mathbf{r}(t)}e^{-i\mathbf{k}\cdot\mathbf{r}(\sigma+t)}\right\rangle = e^{-k^2D(\sigma)} \tag{7.184}$$

with the function

$$D(t) = \frac{\hbar}{2M}\left(-it+\frac{t^2}{\beta\hbar}\right)+a^2\left[1-\exp(i\bar{\Omega}t)+4n\left(\bar{\Omega}\right)\sin^2\left(\frac{\bar{\Omega}t}{2}\right)\right], \tag{7.185}$$

where

$$M = \left(\frac{v}{w}\right)^2 m_b, \bar{\Omega} = v\omega_{\mathrm{LO}}, a^2 = \frac{\hbar}{2m_b\omega_{\mathrm{LO}}}\frac{v^2-w^2}{v^3}. \tag{7.186}$$

According to (7.162),

$$\left\langle e^{i\mathbf{k}\cdot\mathbf{r}(t)}e^{-i\mathbf{k}\cdot\mathbf{r}(\sigma+t)}\right\rangle = \left\langle e^{i\mathbf{k}\cdot\mathbf{r}}e^{-i\mathbf{k}\cdot\mathbf{r}(\sigma)}\right\rangle.$$

Taking $\sigma=-t$ in (7.184) we finally find the Fourier component of the electron density-density correlation function $\left\langle e^{i\mathbf{k}\cdot\mathbf{r}(t)}e^{-i\mathbf{k}\cdot\mathbf{r}}\right\rangle$ which enters Eq. (7.158):

$$\left\langle e^{i\mathbf{k}\cdot\mathbf{r}(t)}e^{-i\mathbf{k}\cdot\mathbf{r}}\right\rangle = \exp\left[-k^2D(-t)\right] \tag{7.187}$$

Finally, the correlation functions in (7.157) reduce to

$$\begin{aligned}\left\langle b_{\mathbf{k}}(t)b_{\mathbf{k}}^{\dagger}(0)\right\rangle &= \left[1+n(\omega_{\mathbf{k}})\right]\exp\left(-i\omega_{\mathbf{k}}t\right)\exp\left[-k^2D(-t)\right],\\ \left\langle b_{\mathbf{k}}^{\dagger}(0)b_{\mathbf{k}}(t)\right\rangle &= n(\omega_{\mathbf{k}})\exp\left(-i\omega_{\mathbf{k}}t\right)\exp\left[-k^2D(t)\right],\\ \left\langle b_{\mathbf{k}}(t)b_{\mathbf{k}}(0)\right\rangle &= 0,\\ \left\langle b_{\mathbf{k}}(0)b_{\mathbf{k}}(t)\right\rangle &= 0.\end{aligned}$$

Inserting these equations into Eqs. (7.156) and (7.157), one obtains

$$\Sigma(z) = \frac{1}{z}\int_0^{\infty}dt\left(1-e^{izt}\right)\operatorname{Im}S(t) \tag{7.188}$$

with

$$\operatorname{Im}S(t) = \frac{2}{m_b\hbar}\sum_{\mathbf{k}}k_x^2\left|V_k\right|^2\operatorname{Im}\left\{\begin{array}{c}-\left[1+n(\omega_{\mathbf{k}})\right]\exp\left(-i\omega_{\mathbf{k}}t\right)\exp\left[-k^2D(-t)\right]\\ +n(\omega_{\mathbf{k}})\exp\left(-i\omega_{\mathbf{k}}t\right)\exp\left[-k^2D(t)\right]\end{array}\right\}.$$

Using the property $D(-t)^* =^2 D(t)$ for real vaues of t, one obtains

$$\begin{aligned}-\operatorname{Im}\exp\left(-i\omega_{\mathbf{k}}t\right)\exp\left[-k^2D(-t)\right]\} &= \operatorname{Im}\exp\left(i\omega_{\mathbf{k}}t\right)\exp\left[-k^2D(-t)^*\right]\}\\ &= \operatorname{Im}\exp\left(i\omega_{\mathbf{k}}t\right)\exp\left[-k^2D(t)\right]\}\end{aligned}$$

and consequently

$$S(t) = \frac{2}{m_b\hbar}\sum_{\mathbf{k}} k_x^2 \left|V_k\right|^2 \exp\left[-k^2 D(t)\right]\left\{\left[1+n(\omega_{\mathbf{k}})\right]\exp\left(i\omega_{\mathbf{k}}t\right)+n(\omega_{\mathbf{k}})\exp\left(-i\omega_{\mathbf{k}}t\right)\right\}. \quad (7.189)$$

Owing to the rotational invariance of $|V_k|^2$ and $\omega_{\mathbf{k}}$, we can substitute in (7.189)

$$k_x^2 \to \frac{k^2}{3}.$$

The resulting expression for

$$S(t) = \frac{2}{3m_b\hbar}\sum_{\mathbf{k}} k^2 \left|V_k\right|^2 \exp\left[-k^2 D(t)\right]\left\{\left[1+n(\omega_{\mathbf{k}})\right]\exp\left(i\omega_{\mathbf{k}}t\right)+n(\omega_{\mathbf{k}})\exp\left(-i\omega_{\mathbf{k}}t\right)\right\} \quad (7.190)$$

is identical with Eq. (35) of FHIP [47]. In the case of Fröhlich polarons, taking into account (7.17), Eq. (7.190) simplifies to

$$S(t) = \left(\frac{\hbar\omega_{\mathrm{LO}}}{m_b}\right)^{3/2}\frac{\alpha}{3\sqrt{2\pi}}\left\{\begin{array}{c}\left[1+n(\omega_{\mathrm{LO}})\right]\exp\left(i\omega_{\mathrm{LO}}t\right)\\ +n(\omega_{\mathrm{LO}})\exp\left(-i\omega_{\mathrm{LO}}t\right)\end{array}\right\}\left[D(t)\right]^{-3/2}. \quad (7.191)$$

7.4.2 Calculation of the memory function (Devreese *et. al.* [50])

Upon substituion of (7.114) and (7.141) into Eq. (7.89), we find the absorption coefficient

$$\begin{aligned}\Gamma(\Omega) &= \frac{1}{n\epsilon_0 c}\,\mathrm{Re}\left[\frac{ie^2}{m_b}\frac{1}{\Omega-\Sigma(\Omega)}\right] = -\frac{1}{n\epsilon_0 c}\frac{e^2}{m_b}\,\mathrm{Im}\left[\frac{1}{\Omega-\Sigma(\Omega)}\right]\\ &= -\frac{1}{n\epsilon_0 c}\frac{e^2}{m_b}\,\mathrm{Im}\left\{\frac{\Omega-\Sigma^*(\Omega)}{\left[\Omega-\mathrm{Re}\,\Sigma(\Omega)\right]^2+\left[\mathrm{Im}\,\Sigma(\Omega)\right]^2}\right\}\\ &= \frac{1}{n\epsilon_0 c}\frac{e^2}{m_b}\frac{\mathrm{Im}\,\Sigma^*(\Omega)}{\left[\Omega-\mathrm{Re}\,\Sigma(\Omega)\right]^2+\left[\mathrm{Im}\,\Sigma(\Omega)\right]^2} \Rightarrow\end{aligned}$$

$$\Gamma(\Omega) = -\frac{1}{n\epsilon_0 c}\frac{e^2}{m_b}\frac{\mathrm{Im}\,\Sigma(\Omega)}{\left[\Omega-\mathrm{Re}\,\Sigma(\Omega)\right]^2+\left[\mathrm{Im}\,\Sigma(\Omega)\right]^2}\ . \quad (7.192)$$

This general expression was the strating point for a derivation of the theoretical optical absorption spectrum of a single large polaron, at *all electron-phonon coupling strengths* by Devreese et al. in Ref. [50]. The memory function $\Sigma(\Omega)$ as given by Eq. (7.188) with (7.191) contains the dynamics of the polaron and depends on α, temperature and Ω.Following the notation, introduced in Ref. [47],

$$\Sigma(\Omega) = \frac{\chi^*(\Omega)}{\Omega} \quad (7.193)$$

we reresent Eq. (7.192) in the form used in Ref. [50]:

$$\Gamma(\Omega) = \frac{1}{n\epsilon_0 c}\frac{e^2}{m_b}\frac{\Omega\,\mathrm{Im}\,\chi(\Omega)}{\left[\Omega^2-\mathrm{Re}\,\chi(\Omega)\right]^2+\left[\mathrm{Im}\,\chi(\Omega)\right]^2}. \quad (7.194)$$

According to (7.188) and (7.193),

$$\mathrm{Im}\,\chi(\Omega) = \mathrm{Im}\int_0^\infty dt\,\sin(\Omega t)S(t), \quad \mathrm{Re}\,\chi(\Omega) = \mathrm{Im}\int_0^\infty dt\,\left[1-\cos(\Omega t)\right]S(t). \quad (7.195)$$

In the present Notes we limit our attention to the case $T = 0$ ($\beta \to \infty$). It was demonstrated in Ref.[50] that the exact zero-temperature limit arises if the limit $\beta \to \infty$ is taken directly in the expressions (7.195) (see Appendices A and B of Ref.[50]). As follows from (7.191),

$$S(t) = \left(\frac{\hbar\omega_{\rm LO}}{m_b}\right)^{3/2} \frac{\alpha}{3\sqrt{2}\pi} \exp\left(i\omega_{\rm LO}t\right) \left[D(t)\right]^{-3/2} \qquad (\beta \to \infty). \tag{7.196}$$

Accorting to (7.185)

$$D(t) = -i\frac{\hbar t}{2M} + a^2\left[1 - \exp(i\bar{\Omega}t)\right] \qquad (\beta \to \infty).$$

Using the Feynman units (where $\hbar = 1, \omega_{\rm LO} = 1$ and $m_b = 1$), we obtain from (7.186):

$$M = \left(\frac{v}{w}\right)^2, \bar{\Omega} = v, a^2 = \frac{1}{2}\frac{v^2 - w^2}{v^3},$$

and consequently

$$D(t) = \frac{1}{2}\frac{v^2 - w^2}{v^3}(1 - e^{ivt}) - i\frac{1}{2}\left(\frac{w}{v}\right)^2 t = \frac{1}{2}\left(\frac{w}{v}\right)^2 \left\{R(1 - e^{ivt}) - it\right\} \qquad (\beta \to \infty) \tag{7.197}$$

with

$$R = \frac{v^2 - w^2}{w^2 v}.$$

and according to (7.196)

$$S(t) = \frac{2\alpha}{3\sqrt{\pi}}\left(\frac{v}{w}\right)^3 e^{it}\left[R(1 - e^{ivt}) - it\right]^{-3/2} \qquad (\beta \to \infty). \tag{7.198}$$

From (7.195) one obtains immediately

$$\operatorname{Im}\chi(\Omega) = \frac{2\alpha}{3\sqrt{\pi}}\left(\frac{v}{w}\right)^3 \operatorname{Im}\int_0^\infty dt \frac{\sin(\Omega t)e^{it}}{\left[R(1 - e^{ivt}) - it\right]^{3/2}}, \tag{7.199}$$

$$\operatorname{Re}\chi(\Omega) = \frac{2\alpha}{3\sqrt{\pi}}\left(\frac{v}{w}\right)^3 \operatorname{Im}\int_0^\infty dt \frac{\left[1 - \cos(\Omega t)\right]e^{it}}{\left[R(1 - e^{ivt}) - it\right]^{3/2}}. \tag{7.200}$$

In the limit $\beta \to \infty$ the function $\operatorname{Im}\chi(\Omega)$ was calculated by FHIP [47]. However, to study the optical absorption to the same approximation as FHIP's treatment of the impedance, we have also to calculate $\operatorname{Re}\chi(\Omega)$ and use this result in (7.194). The calculation of $\operatorname{Re}\chi(\Omega)$, which is a Kramers-Kronig-type transform of $\operatorname{Im}\chi(\Omega)$, is a key ingredient in Ref. [50]. The details of those calculations are presented in the Appendices A, B and C to Ref. [50].

Developing the denominator of both integrals on the right-hand side of (7.199) and (7.200), the calculations are reduced to the evaluation of a sum of integrals of the type

$$\operatorname{Im}\int_0^\infty dt \frac{\sin(\Omega t)e^{i(1+nv)t}}{(R - it)^{3/2+n}}, \qquad \operatorname{Im}\int_0^\infty dt \frac{\cos(\Omega t)e^{i(1+nv)t}}{(R - it)^{3/2+n}}. \tag{7.201}$$

In Appendix B to Ref. [50] it is shown how such integrals are evaluated using a recurrence formula. For $\operatorname{Im}\chi(\Omega)$ a very convenient result was found in [50]:

$$\operatorname{Im}\chi(\Omega) = \frac{2\alpha}{3}\left(\frac{v}{w}\right)^3 \sum_{n=0}^{\infty} C^n_{-3/2}(-1)^n \frac{R^n 2^n}{(2n+1)...3\cdot 1}$$
$$\times \left|\Omega - 1 - nv\right|^{n+1/2} e^{-|\Omega-1-nv|R} \frac{1 + \operatorname{sgn}(\Omega - 1 - nv)}{2}. \tag{7.202}$$

This expression is a finite sum and not and infinite series. FHIP gave the first two terms of (7.202) explicitly.

Using the same recurrence relation it is seen the analytical expression (see Appendix B to Ref. [50]), which was found for $\mathrm{Re}\,\chi(\Omega)$ is far more complicated. To circumwent the difficulty with the numerical treatment of $\mathrm{Re}\,\chi(\Omega)$, the corresponding integrals in (7.201) have been transformed in [50] to integrals with rapildy convergent integrands:

$$\begin{aligned}
&\mathrm{Im}\int_0^\infty dt\frac{[1-\cos(\Omega t)]\,e^{i(1+nv)t}}{(R-it)^{3/2+n}}\\
&=-\frac{1}{\Gamma(n+\frac{3}{2})}\int_0^\infty dx\left[(n+\frac{1}{2})x^{n-1/2}e^{-Rx}-Rx^{n+1/2}e^{-Rx}\right]\\
&\times\ln\left|\left(\frac{(1+nv+x)^2}{\Omega^2-(1+nv+x)^2}\right)\right|^{1/2}.
\end{aligned}\tag{7.203}$$

The integral on the right-hand side of (7.203) is adequate for computer calculations. In Appendix C to Ref. [50] some supplementary details of the computation of (7.203) are given. Another analytical representation for the memory function (7.188) was derived in Ref. [76].

7.4.3 Discussion of optical absorption of polarons at arbitrary coupling

At weak coupling, the optical absorption spectrum (7.192) of the polaron is determined by the absorption of radiation energy, which is reemitted in the form of LO phonons. For $\alpha \gtrsim 5.9$, the polaron can undergo transitions toward a relatively stable RES (see Fig. 7.7). The RES peak in the optical absorption spectrum also has a phonon sideband-structure, whose average transition frequency can be related to a FC-type transition. Furthermore, at zero temperature, the optical absorption spectrum of one polaron exhibits also a zero-frequency "central peak" [$\sim \delta(\Omega)$]. For non-zero temperature, this "central peak" smears out and gives rise to an "anomalous" Drude-type low-frequency component of the optical absorption spectrum.

For example, in Fig. 7.7 from Ref. [50], the main peak of the polaron optical absorption for $\alpha = 5$ at $\Omega = 3.51\omega_{\mathrm{LO}}$ is interpreted as due to transitions to a RES. A "shoulder" at the low-frequency side of the main peak is attributed to one-phonon transitions to polaron-"scattering states". The broad structure centered at about $\Omega = 6.3\omega_{\mathrm{LO}}$ is interpreted as a FC band. As seen from Fig. 7.7, when increasing the electron-phonon coupling constant to α=6, the RES peak at $\Omega = 4.3\omega_{\mathrm{LO}}$ stabilizes. It is in Ref. [50] that the all-coupling optical absorption spectrum of a Fröhlich polaron, together with the role of RES-states, FC-states and scattering states, was first presented.

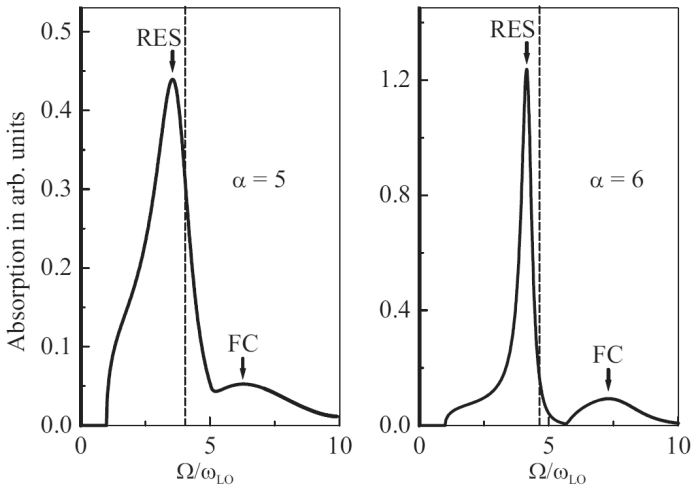

Figure 7.7: Optical absorption spectrum of a polaron calculated by Devreese *et al.* [50] $\alpha = 5$ and 6. The RES peak is very intense compared with the FC peak. The frequency $\Omega/\omega_{\rm LO} = v$ is indicated by the dashed lines.)

Recent interesting numerical calculations of the optical conductivity for the Fröhlich polaron performed within the diagrammatic Quantum Monte Carlo method [79], see Fig. 7.8, fully confirm the essential analytical results derived by Devreese et al. in Ref. [50] for $\alpha \lesssim 3$. In the intermediate coupling regime $3 < \alpha < 6$, the low-energy behavior and the position of the RES-peak in the optical conductivity spectrum of Ref. [79] follow closely the prediction of Ref. [50]. There are some minor qualitative differences between the two approaches in the intermediate coupling regime: in Ref. [79], the dominant ("RES") peak is less intense in the Monte-Carlo numerical simulations and the second ("FC") peak develops less prominently. There are the following qualitative differences between the two approaches in the strong coupling regime: in Ref.[79], the dominant peak broadens and the second peak does not develop, giving instead rise to a flat shoulder in the optical conductivity spectrum at $\alpha = 6$. This behavior has been tentatively attributed to the optical processes with participation of two [75] or more phonons.

The above differences can arise also due to the fact that, within the Feynman polaron model, one-phonon processes are assigned more oscillator strength and the RES tends to be more stable as compared to the Monte-Carlo result. The nature of the excited states of a polaron needs further study. An independent numerical simulation might be called for.

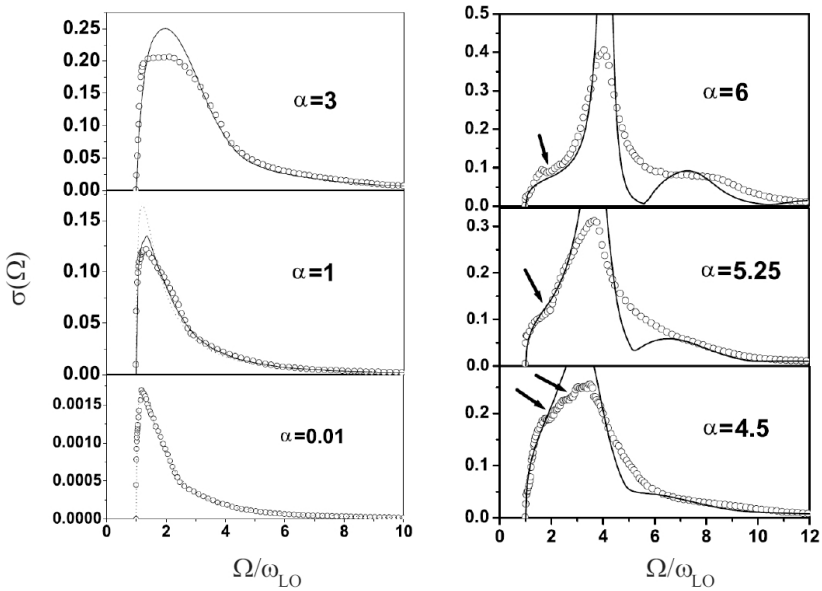

Figure 7.8: *Left-hand panel*: Monte Carlo optical conductivity spectra of one polaron for the weak-coupling regime (open circles) compared to the second-order perturbation theory (dotted lines) for $\alpha = 0.01$ and $\alpha = 1$ and to the analytical DSG calculations [50] (solid lines). *Right-hand panel*: Monte Carlo optical conductivity spectra for the intermediate coupling regime (open circles) compared to the analytical DSG approach [50] (solid lines). Arrows point to the two- and three-phonon thresholds. (From Ref. [79].)

In Fig. 7.9, Monte-Carlo optical conductivity spectrum of one polaron for $\alpha = 1$ compares well with that obtained in Ref. [80] within the canonical-transformation formalism taking into account correlation in processes involving two LO phonons. The difference between the results of these two approaches becomes less pronounced when decreasing the value of $\alpha = 1$ and might be indicative of a possible precision loss, which requires an independent check.

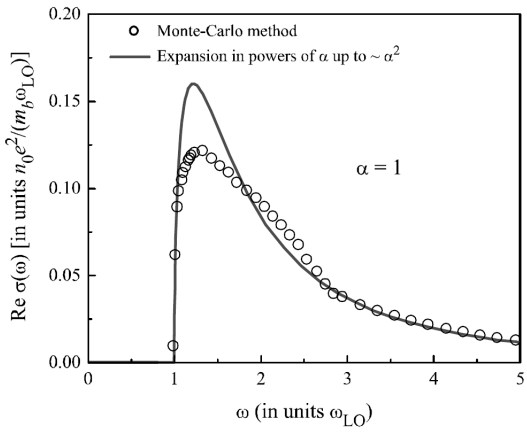

Figure 7.9: One-polaron optical conductivity $\mathrm{Re}\,\sigma(\omega)$ for $\alpha = 1$ calculated within the Monte Carlo approach [79] (open circles) and derived using the expansion in powers of α up to α^2 [80] (solid curve).

The coupling constant α of the known ionic crystals is too small ($\alpha < 5$) to allow for the experimental detection of sharp RES peaks, and the resonance condition $\Omega = Re\Sigma(\Omega)$ cannot be satisfied for $\alpha \lesssim 5.9$ as shown in Ref, [50]. Nevertheless, for $3 \lesssim \alpha \lesssim 5.9$ the development of RES is already reflected in a broad optical absorption peak. Such a peak, predicted in Ref. [50], was identified, e. g., in the optical absorption of $Pr_2NiO_{4.22}$ in Ref. [81]. Also, the resonance condition can be fulfilled if an external magnetic field is applied; the magnetic field stabilizes

the RES, which then can be detected in a cyclotron resonance peak.

Sum rules for the optical conductivity spectra

In this section, we analyze the sum rules for the optical conductivity spectra obtained within the DSG approach [50] with those obtained within the diagrammatic Monte Carlo calculation [79]. The values of the polaron effective mass for the Monte Carlo approach are taken from Ref. [30]. In Tables 3 and 4, we represent the polaron ground-state E_0 and the following parameters calculated using the optical conductivity spectra:

$$M_0 \equiv \int_1^{\omega_{\max}} \operatorname{Re}\sigma(\omega)\, d\omega, \tag{7.204}$$

$$M_1 \equiv \int_1^{\omega_{\max}} \omega \operatorname{Re}\sigma(\omega)\, d\omega, \tag{7.205}$$

where $\omega_{\max}$ is the upper value of the frequency available from Ref. [79],

$$\tilde{M}_0 \equiv \frac{\pi}{2m^*} + \int_1^{\omega_{\max}} \operatorname{Re}\sigma(\omega)\, d\omega, \tag{7.206}$$

where m^* is the polaron mass, the optical conductivity is calculated in units $\frac{n_0 e^2}{m_b \omega_{\mathrm{LO}}}$, m^* is measured in units of the band mass m_b, and the frequency is measured in units of ω_{LO}. The values of $\omega_{\max}$ are: $\omega_{\max} = 10$ for $\alpha = 0.01$, 1 and 3, $\omega_{\max} = 12$ for $\alpha = 4.5$, 5.25 and 6, $\omega_{\max} = 18$ for $\alpha = 6.5$, 7 and 8.

Table 3. Polaron parameters obtained within the diagrammatic Monte Carlo approach

α	$M_0^{(\mathrm{MC})}$	$m^{*(\mathrm{MC})}$	$\tilde{M}_0^{(\mathrm{MC})}$	$M_1^{(\mathrm{MC})}/\alpha$	$E_0^{(\mathrm{MC})}$
0.01	0.00249	1.0017	1.5706	0.634	−0.010
1	0.24179	1.1865	1.5657	0.65789	−1.013
3	0.67743	1.8467	1.5280	0.73123	−3.18
4.5	0.97540	2.8742	1.5219	0.862	−4.97
5.25	1.0904	3.8148	1.5022	0.90181	−5.68
6	1.1994	5.3708	1.4919	0.98248	−6.79
6.5	1.30	6.4989	1.5417	1.1356	−7.44
7	1.3558	9.7158	1.5175	1.2163	−8.31
8	1.4195	19.991	1.4981	1.3774	−9.85

Table 4. Polaron parameters obtained within the path-integral approach

α	$M_0^{(\mathrm{DSG})}$	$m^{*(\mathrm{Feynman})}$	$\tilde{M}_0^{(\mathrm{DSG})}$	$M_1^{(\mathrm{DSG})}/\alpha$	$E_0^{(\mathrm{Feynman})}$
0.01	0.00248	1.0017	1.5706	0.633	−0.010
1	0.24318	1.1957	1.5569	0.65468	−1.0130
3	0.69696	1.8912	1.5275	0.71572	−3.1333
4.5	1.0162	3.1202	1.5196	0.83184	−4.8394
5.25	1.1504	4.3969	1.5077	0.88595	−5.7482
6	1.2608	6.8367	1.4906	0.95384	−6.7108
6.5	1.3657	9.7449	1.5269	1.1192	−7.3920
7	1.4278	14.395	1.5369	1.2170	−8.1127
8	1.4741	31.569	1.5239	1.4340	−9.6953

The parameters corresponding to the Monte Carlo calculation are obtained using the numerical data kindly provided by A. Mishchenko. The comparison of the zero frequency moments $\tilde{M}_0^{(\mathrm{MC})}$ and $\tilde{M}_0^{(\mathrm{DSG})}$ with each other and with the value $\pi/2$ corresponding to the sum rule [82]

$$\frac{\pi}{2m^*} + \int_1^\infty \mathrm{Re}\,\sigma(\omega)\,d\omega = \frac{\pi}{2} \tag{7.207}$$

shows that $\left|\tilde{M}_0^{(\mathrm{MC})} - \tilde{M}_0^{(\mathrm{DSG})}\right|$ is smaller than each of the differences $\frac{\pi}{2} - \tilde{M}_0^{(\mathrm{MC})}$, $\frac{\pi}{2} - \tilde{M}_0^{(\mathrm{DSG})}$, which appear due to a finite interval of the integration in (7.204), (7.205).

We analyze also the fulfilment of the ground-state theorem [83]

$$E_0(\alpha) - E_0(0) = -\frac{3}{\pi}\int_0^\alpha \frac{d\alpha'}{\alpha'}\int_0^\infty \omega\,\mathrm{Re}\,\sigma(\omega,\alpha')\,d\omega \tag{7.208}$$

using the first-frequency moments $M_1^{(\mathrm{MC})}$ and $M_1^{(\mathrm{DSG})}$. The results of this comparison are presented in Fig. 7.10. The dots indicate the polaron ground-state energy calculated using the Feynman variational principle. The solid curve is the value of $E_0(\alpha)$ calculated numerically using the optical conductivity spectra and the ground-state theorem with the DSG optical conductivity [50] for a polaron,

$$E_0^{(\mathrm{DSG})}(\alpha) \equiv -\frac{3}{\pi}\int_0^\alpha \frac{d\alpha'}{\alpha'}\int_0^\infty \omega\,\mathrm{Re}\,\sigma^{(\mathrm{DSG})}(\omega,\alpha')\,d\omega. \tag{7.209}$$

The dashed and the dot-dashed curves are the values obtained using $M_1^{(\mathrm{DSG})}(\alpha)$ and $M_1^{(\mathrm{MC})}(\alpha)$, respectively:

$$\tilde{E}_0^{(\mathrm{DSG})}(\alpha) \equiv -\frac{3}{\pi}\int_0^\alpha \frac{d\alpha'}{\alpha'}\int_0^{\omega_{\max}} \omega\,\mathrm{Re}\,\sigma^{(\mathrm{DSG})}(\omega,\alpha')\,d\omega = -\frac{3}{\pi}\int_0^\alpha d\alpha'\frac{M_1^{(\mathrm{DSG})}(\alpha')}{\alpha'}, \tag{7.210}$$

$$\tilde{E}_0^{(\mathrm{MC})}(\alpha) \equiv -\frac{3}{\pi}\int_0^\alpha \frac{d\alpha'}{\alpha'}\int_0^{\omega_{\max}} \omega\,\mathrm{Re}\,\sigma^{(\mathrm{MC})}(\omega,\alpha')\,d\omega = -\frac{3}{\pi}\int_0^\alpha d\alpha'\frac{M_1^{(\mathrm{MC})}(\alpha')}{\alpha'}. \tag{7.211}$$

As seen from the figure, $E_0^{(\mathrm{DSG})}(\alpha)$ to a high degree of accuracy coincides with the variational polaron ground-state energy. Both $\tilde{E}_0^{(\mathrm{DSG})}(\alpha)$ and $\tilde{E}_0^{(\mathrm{MC})}(\alpha)$ differ from $E_0^{(\mathrm{DSG})}(\alpha)$ due to the integration over a finite interval of frequencies. However, $\tilde{E}_0^{(\mathrm{DSG})}(\alpha)$ and $\tilde{E}_0^{(\mathrm{MC})}(\alpha)$ are very close to each other. Herefrom, a conclusion follows that for integrals over the finite frequency region characteristic for the polaron optical absorption (i. e., except the "tails"), the function $\tilde{E}_0^{(\mathrm{MC})}(\alpha)$ (7.211) reproduces very well the function $\tilde{E}_0^{(\mathrm{DSG})}(\alpha)$.

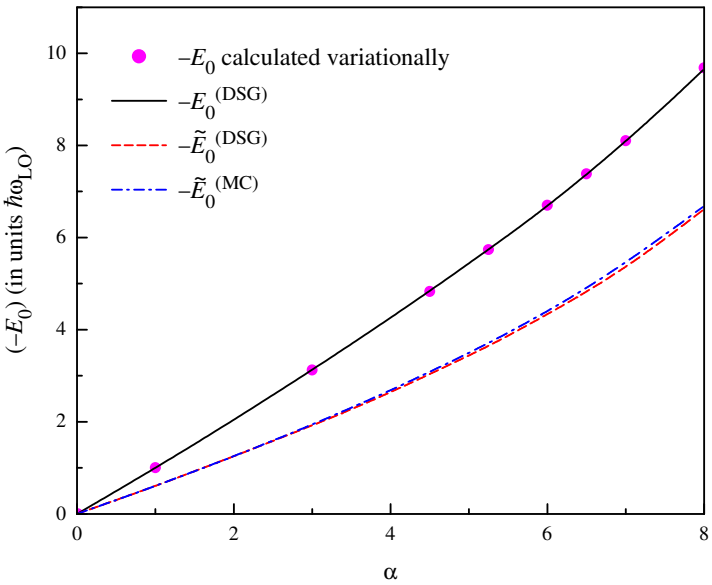

Figure 7.10: The ground-state theorem for a polaron using different data for the optical conductivity spectra, DSG from Ref. [50] and MC from Ref. [79]. The notations are explained in the text.

7.4.4 Scaling relations

Derivation of the scaling relations

The form of the Fröhlich Hamiltonian in n dimensions is the same as in 3D,

$$H = \frac{\mathbf{p}^2}{2m_b} + \sum_{\mathbf{k}} \hbar\omega_{\mathbf{k}} a_{\mathbf{k}}^\dagger a_{\mathbf{k}} + \sum_{\mathbf{k}} \left(V_{\mathbf{k}} a_{\mathbf{k}} e^{i\mathbf{k}\cdot\mathbf{r}} + V_{\mathbf{k}}^* a_{\mathbf{k}}^\dagger e^{-i\mathbf{k}\cdot\mathbf{r}} \right), \tag{7.212}$$

except that now all vectors are n-dimensional. In this subsection, dispersionless longitudinal phonons are considered, i.e., $\omega_{\mathbf{k}} = \omega_{\mathrm{LO}}$, and units are chosen such that $\hbar = m_b = \omega_{\mathrm{LO}} = 1$.

The electron-phonon interaction is a representation in second quantization of the electron interaction with the lattice polarization, which in 3D is essentially the Coulomb potential $1/r$. $|V_{\mathbf{k}}|^2$ is proportional to the Fourier transform of this potential, and as a consequence we have in n dimensions

$$|V_{\mathbf{k}}|^2 = \frac{A_n}{L_n k^{n-1}}, \tag{7.213}$$

where L_n is the volume of the n-dimensional crystal. Note that $|V_{\tilde{\mathbf{k}}}|^2$, where $\tilde{\mathbf{k}}$ is an $(n-1)$-dimensional vector, can be obtained from $|V_{\mathbf{k}}|^2$, where $\mathbf{k} = \left(\tilde{\mathbf{k}}, k_n\right)$ is an n-dimensional vector, by summing out one of the dimensions explicitly:

$$|V_{\tilde{\mathbf{k}}}|^2 = \sum_{k_n} |V_{\mathbf{k}}|^2 . \tag{7.214}$$

Inserting Eq. (7.213) into Eq. (7.214), we have

$$\frac{A_{n-1}}{L_{n-1}\tilde{k}^{n-2}} = \sum_{k_n} \frac{A_n}{L_n \left(\tilde{k}^2 + k_n^2\right)^{(n-1)/2}}. \tag{7.215}$$

Replacing the sum in Eq. (7.215) by an integral, i.e.,

$$\frac{L_{n-1}}{L_n} \sum_{k_n} \longrightarrow \frac{1}{2\pi} \int dk_n, \tag{7.216}$$

we obtain

$$\frac{A_{n-1}}{\tilde{k}^{n-2}} = \frac{A_n}{2\pi} \int_{-\infty}^{\infty} \frac{dk_n}{\left(\tilde{k}^2 + k_n^2\right)^{(n-1)/2}}. \tag{7.217}$$

Since

$$\int_{-\infty}^{\infty} \frac{dx}{\left(z^\mu + x^\mu\right)^\rho} = z^{1-\mu\rho} \frac{\Gamma\left(\frac{1}{\mu}\right)\Gamma\left(\rho - \frac{1}{\mu}\right)}{\Gamma(\rho)}, \tag{7.218}$$

we have

$$\int_{-\infty}^{\infty} \frac{dk_n}{\left(\tilde{k}^2 + k_n^2\right)^{(n-1)/2}} = \frac{1}{\tilde{k}^{n-2}} \frac{\Gamma\left(\frac{1}{2}\right)\Gamma\left(\frac{n-2}{2}\right)}{\Gamma\left(\frac{n-1}{2}\right)} = \frac{\sqrt{\pi}}{\tilde{k}^{n-2}} \frac{\Gamma\left(\frac{n-2}{2}\right)}{\Gamma\left(\frac{n-1}{2}\right)}, \tag{7.219}$$

where $\Gamma(x)$ is eh Γ function. Inserting Eq. (7.219) into Eq. (7.217), we obtain

$$A_n = \frac{2\sqrt{\pi}\Gamma\left(\frac{n-1}{2}\right)}{\Gamma\left(\frac{n-2}{2}\right)} A_{n-1}. \tag{7.220}$$

In 3D the interaction coefficient is well known, $|V_{\mathbf{k}}|^2 = 2\sqrt{2}\pi\alpha/L_3k^2$, so that

$$A_3 = 2\sqrt{2}\pi\alpha. \tag{7.221}$$

Inserting Eq. (7.221) into Eq. (7.220), we immediately obtain

$$A_2 = 2\sqrt{2}\pi\alpha \frac{\Gamma\left(\frac{1}{2}\right)}{2\sqrt{\pi}\Gamma(1)} = \sqrt{2}\pi\alpha. \tag{7.222}$$

Applying Eq. (7.220) $n-2$ times, we further obtain for $n > 3$

$$\begin{aligned} A_n &= \frac{\left(2\sqrt{\pi}\right)^{n-2} \prod_{j=2}^{n-1} \Gamma\left(\frac{j}{2}\right)}{\prod_{j=1}^{n-2} \Gamma\left(\frac{j}{2}\right)} A_2 = \frac{\left(2\sqrt{\pi}\right)^{n-2} \left(\frac{n-1}{2}\right)}{\Gamma\left(\frac{1}{2}\right)} A_2 = 2^{n-2}\pi^{(n-3)/2}\Gamma\left(\frac{n-1}{2}\right) A_2 \\ &= 2^{n-3/2}\pi^{(n-1)/2}\Gamma\left(\frac{n-1}{2}\right)\alpha. \end{aligned} \tag{7.223}$$

So, the interaction coefficient in n dimensions becomes [84]

$$|V_{\mathbf{k}}|^2 = \frac{2^{n-3/2}\pi^{(n-1)/2}\Gamma\left(\frac{n-1}{2}\right)\alpha}{L_n k^{n-1}}. \tag{7.224}$$

Following the Feynman approach [43], the upper bound for the polaron ground-state energy can be written down as

$$E = E_0 - \lim_{\beta\to\infty} \frac{1}{\beta} \langle S - S_0 \rangle_0, \tag{7.225}$$

where S is the exact action functional of the polaron problem, while S_0 is the trial action functional, which corresponds to a model system where an electron is coupled by an elastic force to a fictitious particle (i.e., the model system describes a harmonic oscillator). E_0 is the ground-state energy of the above model system, and

$$\langle F \rangle_0 \equiv \frac{\int F e^{S_0} \mathcal{D}\mathbf{r}(t)}{\int e^{S_0} \mathcal{D}\mathbf{r}(t)}. \tag{7.226}$$

As indicated above, the Fröhlich Hamiltonian in n dimensions is the same as in 3D, except that now all vectors are n-dimensional [and the coupling coefficient $|V_{\mathbf{k}}|^2$ is modified in accordance with Eq. (7.224)]. Similarly, the only difference of the model system in n dimensions from the model system in 3D is that now one deals with an n-dimensional harmonic oscillator. So, directly following [43], one can represent $\lim_{\beta\to\infty}\langle S-S_0\rangle_0/\beta$ as

$$\lim_{\beta\to\infty}\frac{1}{\beta}\langle S-S_0\rangle_0 = A+B, \tag{7.227}$$

where

$$A=\sum_{\mathbf{k}}|V_{\mathbf{k}}|^2\int_0^\infty\left\langle e^{i\mathbf{k}\cdot[\mathbf{r}(t)-\mathbf{r}(0)]}\right\rangle_0 e^{-t}dt, \tag{7.228}$$

$$B=\frac{w\left(v^2-w^2\right)}{4}\int_0^\infty\left\langle[\mathbf{r}(t)-\mathbf{r}(0)]^2\right\rangle_0 e^{-wt}dt, \tag{7.229}$$

w and v are variational parameters, which should be determined by minimizing E of Eq. (7.225). Since the averaging $\langle ...\rangle_0$ in Eq. (7.228) is performed with the trial action, which corresponds to a harmonic oscillator, components of the electron coordinates, r_j $(j=1,...,n)$, in $\left\langle e^{i\mathbf{k}\cdot[\mathbf{r}(t)-\mathbf{r}(0)]}\right\rangle_0$ separate [43]:

$$\left\langle e^{i\mathbf{k}\cdot[\mathbf{r}(t)-\mathbf{r}(0)]}\right\rangle_0=\prod_{j=1}^{n}\left\langle e^{ik_j[r_j(t)-r_j(0)]}\right\rangle_0. \tag{7.230}$$

For the average $\left\langle e^{ik_j[r_j(t)-r_j(0)]}\right\rangle_0$, Feynman obtained [43]

$$\left\langle e^{ik_j[r_j(t)-r_j(0)]}\right\rangle_0=e^{-k_j^2D_0(t)}, \tag{7.231}$$

where

$$D_0(t)=\frac{w^2}{2v^2}t+\frac{v^2-w^2}{2v^3}\left(1-e^{-vt}\right). \tag{7.232}$$

Inserting Eq. (7.230) with Eq. (7.231) into Eq. (7.228), we obtain

$$A=\int_0^\infty e^{-t}dt\sum_{\mathbf{k}}|V_{\mathbf{k}}|^2e^{-k^2D_0(t)}. \tag{7.233}$$

Inserting expression (7.224) for $|V_{\mathbf{k}}|^2$ into Eq. (7.233) and replacing the sum over $\mathbf{k}$ by an integral [see (7.216)], we have

$$\begin{aligned}A&=2^{n-3/2}\pi^{(n-1)/2}\Gamma\left(\frac{n-1}{2}\right)\alpha\int_0^\infty e^{-t}dt\int\frac{e^{-k^2D_0(t)}}{k^{n-1}}\frac{d\mathbf{k}}{(2\pi)^n}\\&=2^{n-3/2}\pi^{(n-1)/2}\Gamma\left(\frac{n-1}{2}\right)\alpha\int_0^\infty e^{-t}dt\int d\Omega_n\int_0^\infty\frac{e^{-k^2D_0(t)}}{k^{n-1}}\frac{k^{n-1}dk}{(2\pi)^n},\end{aligned} \tag{7.234}$$

where $d\Omega_n$ is the elemental solid angle in n dimensions. Since the integrand in Eq. (7.234) depends only on the modulus k of $\mathbf{k}$, one have simply $\int d\Omega_n=\Omega_n$ with

$$\Omega_n=\frac{2\pi^{n/2}}{\Gamma\left(\frac{n}{2}\right)}. \tag{7.235}$$

So, we obtain for A the result

$$\begin{aligned}A&=\frac{2^{-1/2}\pi^{-1/2}\Gamma\left(\frac{n-1}{2}\right)\alpha}{\Gamma\left(\frac{n}{2}\right)}\int_0^\infty e^{-t}dt\int_0^\infty e^{-k^2D_0(t)}dk=\frac{2^{-1/2}\pi^{-1/2}\Gamma\left(\frac{n-1}{2}\right)\alpha}{\Gamma\left(\frac{n}{2}\right)}\int_0^\infty\frac{\sqrt{\pi}e^{-t}}{2\sqrt{D_0(t)}}dt\\&=\frac{2^{-3/2}\Gamma\left(\frac{n-1}{2}\right)\alpha}{\Gamma\left(\frac{n}{2}\right)}\int_0^\infty\frac{e^{-t}}{\sqrt{D_0(t)}}dt.\end{aligned} \tag{7.236}$$

Like in Ref. [43], B can be easily calculated by noticing that

$$\left\langle [\mathbf{r}(t)-\mathbf{r}(0)]^2 \right\rangle_0 = \sum_{j=1}^{n} \left\langle [r_j(t)-r_j(0)]^2 \right\rangle_0 = \sum_{j=1}^{n} \left[-\frac{\partial^2}{\partial k_j^2} \left\langle e^{i\mathbf{k}\cdot[\mathbf{r}(t)-\mathbf{r}(0)]} \right\rangle_0 \right] \Bigg|_{\mathbf{k}=0}$$
$$= \sum_{j=1}^{n} 2D_0(t) = 2nD_0(t), \tag{7.237}$$

so that

$$\begin{aligned} B &= \frac{nw(v^2-w^2)}{2} \int_0^\infty D_0(t)\, e^{-wt} dt \\ &= \frac{nw(v^2-w^2)}{2} \int_0^\infty \left[\frac{w^2}{2v^2} t e^{-wt} + \frac{v^2-w^2}{2v^3} \left(e^{-wt} - e^{-(v+w)t} \right) \right] dt \\ &= \frac{nw(v^2-w^2)}{2} \left[\frac{w^2}{2v^2} \frac{1}{v^2} + \frac{v^2-w^2}{2v^3} \left(\frac{1}{w} - \frac{1}{v+w} \right) \right] \\ &= \frac{n(v^2-w^2)}{4v}. \end{aligned} \tag{7.238}$$

Inserting Eq. (7.224) with A and B, given by Eqs. (7.236) and (7.238), together with the ground-state energy of the model system [43] (an isotropic n-dimensional harmonic oscillator),

$$E_0 = \frac{n(v-w)}{2}, \tag{7.239}$$

into Eq. (7.225), we obtain

$$\begin{aligned} E &= \frac{n(v-w)}{2} - \frac{n(v^2-w^2)}{4v} - \frac{2^{-3/2}\Gamma\left(\frac{n-1}{2}\right)\alpha}{\Gamma\left(\frac{n}{2}\right)} \int_0^\infty \frac{e^{-t}}{\sqrt{D_0(t)}} dt \\ &= \frac{n(v-w)^2}{4v} - \frac{\Gamma\left(\frac{n-1}{2}\right)\alpha}{2\sqrt{2}\Gamma\left(\frac{n}{2}\right)} \int_0^\infty \frac{e^{-t}}{\sqrt{D_0(t)}} dt. \end{aligned} \tag{7.240}$$

In order to make easier a comparison of E for n dimensions with the Feynman result [43] for 3D,

$$E_{3\mathrm{D}}(\alpha) = \frac{3(v-w)^2}{4v} - \frac{1}{\sqrt{2\pi}} \alpha \int_0^\infty \frac{e^{-t}}{\sqrt{D_0(t)}} dt, \tag{7.241}$$

it is convenient to rewrite Eq. (7.240) in the form

$$E_{n\mathrm{D}}(\alpha) = \frac{n}{3} \left[\frac{3(v-w)^2}{4v} - \frac{1}{\sqrt{2\pi}} \frac{3\sqrt{\pi}\Gamma\left(\frac{n-1}{2}\right)}{2n\Gamma\left(\frac{n}{2}\right)} \alpha \int_0^\infty \frac{e^{-t}}{\sqrt{D_0(t)}} dt \right]. \tag{7.242}$$

It is worth recalling that the parameters w and v must be determined by minimizing E. Thus, in the case of Eq. (7.242) one has to minimize the expression in the square brackets. The only difference of this expression from the r.h.s. of Eq. (7.241) is that α is multiplied by the factor

$$a_n = \frac{3\sqrt{\pi}\Gamma\left(\frac{n-1}{2}\right)}{2n\Gamma\left(\frac{n}{2}\right)}. \tag{7.243}$$

This means that the minimizing parameters w and v in nD at a given α will be exactly the same as those calculated in 3D for the Fröhlich constant as large as $a_n\alpha$:

$$v_{n\mathrm{D}}(\alpha) = v_{3\mathrm{D}}(a_n\alpha), \; w_{n\mathrm{D}}(\alpha) = w_{3\mathrm{D}}(a_n\alpha). \tag{7.244}$$

Therefore, comparing Eq. (7.242) to Eq. (7.241), we obtain the scaling relation [84, 85, 86]

$$E_{n\mathrm{D}}(\alpha) = \frac{n}{3} E_{3\mathrm{D}}(a_n \alpha), \tag{7.245}$$

where a_n is given by Eq. (7.243). As discussed in Ref. [84], the above scaling relation is not an exact relation. It is valid for the Feynman polaron energy and also for the ground-state energy to order α. The next-order term (i.e., α^2) no longer satisfies Eq. (7.245). The reason is that in the exact calculation (to order α^2) the electron motion in the different space directions is coupled by the electron-phonon interaction. No such a coupling appears in the Feynman polaron model [see, e.g., Eq. (7.230)]; and this is the underlying reason for the validity of the scaling relation for the Feynman approximation.

In Refs. [84, 86], scaling relations are obtained also for the impedance function, the effective mass and the mobility of a polaron. The inverse of the impedance function $Z(\omega)$ is given by

$$\frac{1}{Z(\omega)} = \frac{i}{\omega - \Sigma(\omega)}, \tag{7.246}$$

where the memory function $\Sigma(\omega)$ can be expressed as [87]

$$\Sigma(z) = \frac{1}{z} \int_0^\infty dt \left(1 - e^{izt}\right) \mathrm{Im} S(t), \tag{7.247}$$

with $z = \omega + i0^+$ and

$$S(t) = \sum_{\mathbf{k}} 2k_1^2 |V_{\mathbf{k}}|^2 e^{-k^2 D(t)} T(t), \tag{7.248}$$

$$T(t) = [1 + n(1)] e^t + n(1) e^{-it}, \tag{7.249}$$

$$D(t) = \frac{w^2}{2v^2}\left(-it + \frac{t^2}{\beta}\right) + \frac{v^2 - w^2}{2v^3}\left[1 - e^{-ivt} + 4n(v)\sin^2\left(\frac{vt}{2}\right)\right]. \tag{7.250}$$

Here, β is the inverse temperature and $n(\omega)$ is the occupation number of phonons with frequency ω (recall that in our units $\omega_{\mathrm{LO}} = 1$).

As implied from Eqs. (7.246) and (7.247), scaling of $\Sigma(\omega)$ and $Z(\omega)$ is determined by scaling of $S(t)$. For an isotropic crystal, since $|V_{\mathbf{k}}|^2$, $D(t)$ and $T(t)$ do not depend on the direction of $\mathbf{k}$, one can write $\sum_{\mathbf{k}} k_1^2 |V_{\mathbf{k}}|^2 e^{-k^2 D(t)} T(t) = \sum_{\mathbf{k}} k_2^2 |V_{\mathbf{k}}|^2 e^{-k^2 D(t)} T(t) = \ldots = \sum_{\mathbf{k}} k_n^2 |V_{\mathbf{k}}|^2 e^{-k^2 D(t)} T(t)$, so that

$$S(t) = \frac{2}{n} \sum_{\mathbf{k}} k^2 |V_{\mathbf{k}}|^2 e^{-k^2 D(t)} T(t). \tag{7.251}$$

Inserting expression (7.224) for $|V_{\mathbf{k}}|^2$ and replacing the sum over $\mathbf{k}$ by an integral, we have

$$\begin{aligned} S(t) &= \frac{2}{n} \frac{2^{n-3/2} \pi^{(n-1)/2} \Gamma\left(\frac{n-1}{2}\right) \alpha}{(2\pi)^n} \int d\Omega_n \int_0^\infty k^2 e^{-k^2 D(t)} T(t)\, dk \\ &= \frac{2}{n} \frac{2^{n-3/2} \pi^{(n-1)/2} \Gamma\left(\frac{n-1}{2}\right) \alpha}{(2\pi)^n} \frac{2\pi^{n/2}}{\Gamma\left(\frac{n}{2}\right)} \int_0^\infty k^2 e^{-k^2 D(t)} T(t)\, dk \\ &= \sqrt{\frac{2}{\pi}} \frac{\Gamma\left(\frac{n-1}{2}\right) \alpha}{n \Gamma\left(\frac{n}{2}\right)} \int_0^\infty k^2 e^{-k^2 D(t)} T(t)\, dk. \end{aligned} \tag{7.252}$$

In particular, for 3D one has from Eq. (7.252)

$$S_{3\mathrm{D}}(\alpha; t) = \frac{2\sqrt{2}}{3\pi} \alpha \int_0^\infty k^2 e^{-k^2 D(t)} T(t)\, dk. \tag{7.253}$$

For nD, Eq. (7.252) can be rewritten is the form

$$\begin{aligned} S_{n\mathrm{D}}(\alpha;t) &= \frac{2\sqrt{2}}{3\pi}\frac{3\sqrt{\pi}\Gamma\left(\frac{n-1}{2}\right)}{2n\Gamma\left(\frac{n}{2}\right)}\alpha\int_0^\infty k^2 e^{-k^2 D(t)}T(t)\,dk \\ &= \frac{2\sqrt{2}}{3\pi}a_n\alpha\int_0^\infty k^2 e^{-k^2 D(t)}T(t)\,dk. \end{aligned} \tag{7.254}$$

So, the only difference of the expression for $S_{3\mathrm{D}}(t)$ from $S_{3\mathrm{D}}(t)$ is that α is multiplied by a_n. Since for the minimizing parameters w and v, which enter $D(t)$, scaling is determined by the same product α with a_n [see Eq. (7.244)], we can write

$$S_{n\mathrm{D}}(\alpha;t) = S_{3\mathrm{D}}(a_n\alpha;t), \tag{7.255}$$

so that [86]

$$\Sigma_{n\mathrm{D}}(\alpha;\omega) = \Sigma_{3\mathrm{D}}(a_n\alpha;\omega), \tag{7.256}$$

and

$$Z_{n\mathrm{D}}(\alpha;\omega) = Z_{3\mathrm{D}}(a_n\alpha;\omega). \tag{7.257}$$

The polaron mass at zero temperature can be obtained from the impedance function as [87, 88]

$$\frac{m^*}{m_b} = 1 - \lim_{\omega\to 0}\frac{\mathrm{Re}\Sigma(\omega)}{\omega}, \tag{7.258}$$

so that from the scaling relation (7.256) for the memory function we also have a scaling relation for the polaron mass [86]:

$$\frac{m^*_{n\mathrm{D}}(\alpha)}{(m_b)_{n\mathrm{D}}} = \frac{m^*_{3\mathrm{D}}(a_n\alpha)}{(m_b)_{3\mathrm{D}}}. \tag{7.259}$$

Since the mobility can be obtained from the memory function as [89]

$$\frac{1}{\mu} = -\frac{m_b}{e}\lim_{\omega\to 0}\frac{\mathrm{Im}\Sigma(\omega)}{\omega}, \tag{7.260}$$

fulfilment of the scaling relation (7.256) implies also a scaling relation for the mobility [86]:

$$\mu_{n\mathrm{D}}(\alpha) = \mu_{3\mathrm{D}}(a_n\alpha). \tag{7.261}$$

In the important particular case of 2D, the above scaling relations take the form [84, 85, 86]:

$$E_{2\mathrm{D}}(\alpha) = \frac{2}{3}E_{3\mathrm{D}}\left(\frac{3\pi}{4}\alpha\right), \tag{7.262}$$

$$Z_{2\mathrm{D}}(\alpha;\omega) = Z_{3\mathrm{D}}\left(\frac{3\pi}{4}\alpha;\omega\right), \tag{7.263}$$

$$\frac{m^*_{2\mathrm{D}}(\alpha)}{(m_b)_{n\mathrm{D}}} = \frac{m^*_{3\mathrm{D}}\left(\frac{3\pi}{4}\alpha\right)}{(m_b)_{3\mathrm{D}}}, \tag{7.264}$$

$$\mu_{2\mathrm{D}}(\alpha) = \mu_{3\mathrm{D}}\left(\frac{3\pi}{4}\alpha\right). \tag{7.265}$$

Check of the scaling relation for the path integral Monte Carlo result for the polaron free energy

The fulfilment of the PD-scaling relation [86] is checked for the path integral Monte Carlo results [45] for the polaron free energy.

The path integral Monte Carlo results of Ref.[45] for the polaron free energy in 3D and in 2D are given for a few values of temperature and for some selected values of α. For a check of the scaling relation, the values of the polaron free energy at $\beta = 10$ are taken from Ref. [45] in 3D (Table I, for 4 values of α) and in 2D (Table II, for 2 values of α) and plotted in Fig. 7.11, upper panel, with squares and open circles, correspondingly.

The PD-scaling relation for the polaron ground-state energy as derived in Ref. [86] reads:

$$E_{2D}(\alpha) \equiv \frac{2}{3} E_{3D}\left(\frac{3\pi\alpha}{4}\right). \tag{7.266}$$

In Fig. 7.11, lower panel, the available data for the free energy from Ref [45] are plotted in the following form *inspired by the l.h.s. and the r.h.s parts of Eq. (1)*: $F_{2D}(\alpha)$ (squares) and $\frac{2}{3}F_{3D}\left(\frac{3\pi\alpha}{4}\right)$(open triangles). As follows from the figure, t*he path integral Monte Carlo results for the polaron free energy in 2D and 3D very closely follow the PD-scaling relation of the form given by Eq. (7.266):*

$$F_{2D}(\alpha) \equiv \frac{2}{3} F_{3D}\left(\frac{3\pi\alpha}{4}\right). \tag{7.267}$$

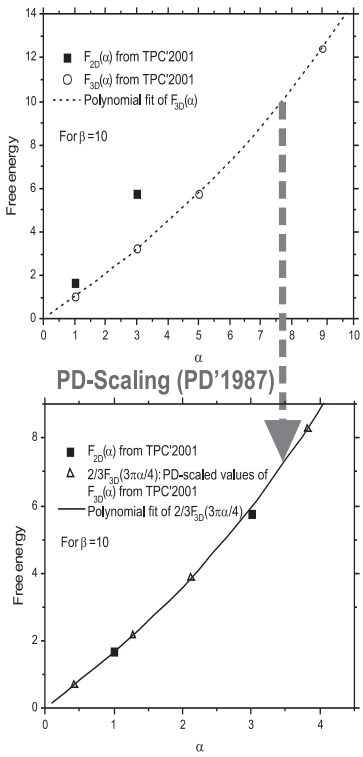

Figure 7.11: *Upper panel:* The values of the polaron free energy in 3D (squares) and 2D (open circles) obtained by Ciuchi'2001 [45] for $\beta = 10$. The data for $F_{3D}(\alpha)$ are interpolated using a polynomial fit to the available four points (dotted line). *Lower panel:* Demonstration of the PD-scaling cf. PD'1987: the values of the polaron free energy in 2D obtained by Ciuchi'2001 [45] for $\beta = 10$ (squares) are very close to the **PD-scaled** according to PD'1987 [86] values of the polaron free energy in 3D from Ciuchi'2001 for $\beta = 10$ (open triangles). The data for $\frac{2}{3}F_{3D}\left(\frac{3\pi\alpha}{4}\right)$ are interpolated using a polynomial fit to the available four points (solid line).

7.4.4 Appendix 1. Weak coupling: LLP approach

Inspired by the work of Tomonaga on quantum electrodynamics (Q. E. D.), Lee, Low and Pines (L.L.P.) [31] derived (7.22) and $m^* = m_b(1 + \alpha/6)$ from a canonical transformation formulation, which establishes (7.22) as a variational upper bound for the ground-state energy.

The wave equation corresponding to the Fröhlich Hamiltonian (7.16) is

$$H\Phi = E\Phi. \tag{7.268}$$

We shall take advantage of the fact that the total momentum of the system

$$\mathbf{P}_{op} = \sum_{\mathbf{k}} \hbar \mathbf{k} a_{\mathbf{k}}^{\dagger} a_{\mathbf{k}} + \mathbf{p} \tag{7.269}$$

(where $\mathbf{p} = -i\hbar\nabla$ is the momentum of the electron) is a constant of motion because it commutes with the Hamiltonian (7.16)

Indeed,

$$[\mathbf{p}, H] = [\mathbf{p}, \sum_{\mathbf{k}} (V_k a_{\mathbf{k}} e^{i\mathbf{k}\cdot\mathbf{r}} + V_k^* a_{\mathbf{k}}^\dagger e^{-i\mathbf{k}\cdot\mathbf{r}})] = \sum_{\mathbf{k}} (V_k a_{\mathbf{k}} \left[\mathbf{p}, e^{i\mathbf{k}\cdot\mathbf{r}}\right] + V_k^* a_{\mathbf{k}}^\dagger \left[\mathbf{p}, e^{-i\mathbf{k}\cdot\mathbf{r}}\right])$$
$$= \sum_{\mathbf{k}} \hbar\mathbf{k}(V_k a_{\mathbf{k}} e^{i\mathbf{k}\cdot\mathbf{r}} - V_k^* a_{\mathbf{k}}^\dagger e^{-i\mathbf{k}\cdot\mathbf{r}});$$

$$\begin{aligned}
\left[\sum_{\mathbf{k}} \hbar\mathbf{k} a_{\mathbf{k}}^\dagger a_{\mathbf{k}}, H\right] &= \left[\sum_{\mathbf{k}} \hbar\mathbf{k} a_{\mathbf{k}}^\dagger a_{\mathbf{k}}, \sum_{\mathbf{k}'} (V_{k'} a_{\mathbf{k}'} e^{i\mathbf{k}'\cdot\mathbf{r}} + V_{k'}^* a_{\mathbf{k}'}^\dagger e^{-i\mathbf{k}'\cdot\mathbf{r}})\right] = \\
&= \sum_{\mathbf{k}} \hbar\mathbf{k} \left[a_{\mathbf{k}}^\dagger a_{\mathbf{k}}, (V_k a_{\mathbf{k}} e^{i\mathbf{k}\cdot\mathbf{r}} + V_k^* a_{\mathbf{k}}^\dagger e^{-i\mathbf{k}\cdot\mathbf{r}})\right] = \\
&= \sum_{\mathbf{k}} \hbar\mathbf{k} \left\{V_k \left[a_{\mathbf{k}}^\dagger a_{\mathbf{k}}, a_{\mathbf{k}}\right] e^{i\mathbf{k}\cdot\mathbf{r}} + V_k^* \left[a_{\mathbf{k}}^\dagger a_{\mathbf{k}}, a_{\mathbf{k}}^\dagger\right] e^{-i\mathbf{k}\cdot\mathbf{r}}\right\} = \\
&= -\sum_{\mathbf{k}} \hbar\mathbf{k} \left(V_k a_{\mathbf{k}} e^{i\mathbf{k}\cdot\mathbf{r}} - V_k^* a_{\mathbf{k}}^\dagger e^{-i\mathbf{k}\cdot\mathbf{r}}\right);
\end{aligned}$$

$$[\mathbf{P}_{op}, H] = \left[\sum_{\mathbf{k}} \hbar\mathbf{k} a_{\mathbf{k}}^\dagger a_{\mathbf{k}} + \mathbf{p}, H\right] = 0. \tag{7.270}$$

Because of the commutation (7.270), the operators H and $\mathbf{P}_{op}$ have a common set of basis functions: $H\Phi = E\Phi$ and $\mathbf{P}_{op}\Phi = \mathbf{P}\Phi$.

It is possible to transform to a representation in which $\mathbf{P}_{op}$ becomes a "c" number $\mathbf{P}$, and in which the Hamiltonian no longer contains the electron coordinates. The unitary (canonical) transformation required is $\Phi = S_1\psi$, where

$$S_1 = \exp\left[\frac{i}{\hbar}(\mathbf{P} - \sum_{\mathbf{k}} \hbar\mathbf{k} a_{\mathbf{k}}^\dagger a_{\mathbf{k}})\cdot\mathbf{r}\right]. \tag{7.271}$$

Derivation of the transformations of the operators.

$$\begin{aligned}
&\mathbf{p} \longrightarrow S_1^{-1}\mathbf{p}S_1 = \\
&= \exp\left[-\frac{i}{\hbar}(\mathbf{P} - \sum_{\mathbf{k}} \hbar\mathbf{k} a_{\mathbf{k}}^\dagger a_{\mathbf{k}})\cdot\mathbf{r}\right] \mathbf{p} \exp\left[\frac{i}{\hbar}(\mathbf{P} - \sum_{\mathbf{k}} \hbar\mathbf{k} a_{\mathbf{k}}^\dagger a_{\mathbf{k}})\cdot\mathbf{r}\right] \\
&= \exp\left[-\frac{i}{\hbar}(\mathbf{P} - \sum_{\mathbf{k}} \hbar\mathbf{k} a_{\mathbf{k}}^\dagger a_{\mathbf{k}})\cdot\mathbf{r}\right] (-i\hbar\nabla) \exp\left[\frac{i}{\hbar}(\mathbf{P} - \sum_{\mathbf{k}} \hbar\mathbf{k} a_{\mathbf{k}}^\dagger a_{\mathbf{k}})\cdot\mathbf{r}\right] \\
&= \exp\left[-\frac{i}{\hbar}(\mathbf{P} - \sum_{\mathbf{k}} \hbar\mathbf{k} a_{\mathbf{k}}^\dagger a_{\mathbf{k}})\cdot\mathbf{r}\right] \left\{ \begin{array}{c} (\mathbf{P} - \sum_{\mathbf{k}} \hbar\mathbf{k} a_{\mathbf{k}}^\dagger a_{\mathbf{k}}) \exp\left[\frac{i}{\hbar}(\mathbf{P} - \sum_{\mathbf{k}} \hbar\mathbf{k} a_{\mathbf{k}}^\dagger a_{\mathbf{k}})\cdot\mathbf{r}\right] \\ + \exp\left[\frac{i}{\hbar}(\mathbf{P} - \sum_{\mathbf{k}} \hbar\mathbf{k} a_{\mathbf{k}}^\dagger a_{\mathbf{k}})\cdot\mathbf{r}\right] (-i\hbar\nabla) \end{array} \right\} \\
&= \mathbf{P} - \sum_{\mathbf{k}} \hbar\mathbf{k} a_{\mathbf{k}}^\dagger a_{\mathbf{k}} + \mathbf{p},
\end{aligned} \tag{7.272}$$

$$
\begin{aligned}
\mathbf{P}_{op} &\longrightarrow S_1^{-1}\mathbf{P}_{op}S_1 = \\
&= \exp\left[-\frac{i}{\hbar}(\mathbf{P}-\sum_{\mathbf{k}}\hbar\mathbf{k}a_{\mathbf{k}}^{\dagger}a_{\mathbf{k}})\cdot\mathbf{r}\right]\left(\sum_{\mathbf{k}}\hbar\mathbf{k}a_{\mathbf{k}}^{\dagger}a_{\mathbf{k}}+\mathbf{p}\right)\exp\left[\frac{i}{\hbar}(\mathbf{P}-\sum_{\mathbf{k}}\hbar\mathbf{k}a_{\mathbf{k}}^{\dagger}a_{\mathbf{k}})\cdot\mathbf{r}\right] \\
&= \exp\left[\frac{i}{\hbar}\sum_{\mathbf{k}}\hbar\mathbf{k}a_{\mathbf{k}}^{\dagger}a_{\mathbf{k}}\cdot\mathbf{r}\right]\sum_{\mathbf{k}}\hbar\mathbf{k}a_{\mathbf{k}}^{\dagger}a_{\mathbf{k}}\exp\left[-\frac{i}{\hbar}\sum_{\mathbf{k}}\hbar\mathbf{k}a_{\mathbf{k}}^{\dagger}a_{\mathbf{k}}\cdot\mathbf{r}\right]+S_1^{-1}\mathbf{p}S_1 \\
&= \sum_{\mathbf{k}}\hbar\mathbf{k}a_{\mathbf{k}}^{\dagger}a_{\mathbf{k}}+\mathbf{P}-\sum_{\mathbf{k}}\hbar\mathbf{k}a_{\mathbf{k}}^{\dagger}a_{\mathbf{k}}+\mathbf{p}=\mathbf{P}+\mathbf{p},
\end{aligned}
\tag{7.273}
$$

$$
\begin{aligned}
a_{\mathbf{k}} &\longrightarrow S_1^{-1}a_{\mathbf{k}}S_1 = \\
&= \exp\left[-\frac{i}{\hbar}(\mathbf{P}-\sum_{\mathbf{k}}\hbar\mathbf{k}a_{\mathbf{k}}^{\dagger}a_{\mathbf{k}})\cdot\mathbf{r}\right]a_{\mathbf{k}}\exp\left[\frac{i}{\hbar}(\mathbf{P}-\sum_{\mathbf{k}}\hbar\mathbf{k}a_{\mathbf{k}}^{\dagger}a_{\mathbf{k}})\cdot\mathbf{r}\right] \\
&= \exp\left[\frac{i}{\hbar}\sum_{\mathbf{k}}\hbar\mathbf{k}a_{\mathbf{k}}^{\dagger}a_{\mathbf{k}}\cdot\mathbf{r}\right]a_{\mathbf{k}}\exp\left[-\frac{i}{\hbar}\sum_{\mathbf{k}}\hbar\mathbf{k}a_{\mathbf{k}}^{\dagger}a_{\mathbf{k}}\cdot\mathbf{r}\right] \\
&= \exp\left[i\mathbf{k}a_{\mathbf{k}}^{\dagger}a_{\mathbf{k}}\cdot\mathbf{r}\right]a_{\mathbf{k}}\exp\left[-i\mathbf{k}a_{\mathbf{k}}^{\dagger}a_{\mathbf{k}}\cdot\mathbf{r}\right] \\
&= \exp\left[i\mathbf{k}a_{\mathbf{k}}^{\dagger}a_{\mathbf{k}}\cdot\mathbf{r}\right]a_{\mathbf{k}}\sum_{n=0}^{\infty}\frac{1}{n!}\left(-i\mathbf{k}a_{\mathbf{k}}^{\dagger}a_{\mathbf{k}}\cdot\mathbf{r}\right)^n \\
&= \exp\left[i\mathbf{k}a_{\mathbf{k}}^{\dagger}a_{\mathbf{k}}\cdot\mathbf{r}\right]\sum_{n=0}^{\infty}\frac{1}{n!}a_{\mathbf{k}}\left(-i\mathbf{k}a_{\mathbf{k}}^{\dagger}a_{\mathbf{k}}\cdot\mathbf{r}\right)^n \\
&= \exp\left[i\mathbf{k}\cdot\mathbf{r}a_{\mathbf{k}}^{\dagger}a_{\mathbf{k}}\right]\sum_{n=0}^{\infty}\frac{1}{n!}\left(-i\mathbf{k}\cdot\mathbf{r}\right)^n a_{\mathbf{k}}\left(a_{\mathbf{k}}^{\dagger}a_{\mathbf{k}}\right)^n \overset{\text{see}(*)}{=} \\
&= \exp\left[i\mathbf{k}\cdot\mathbf{r}a_{\mathbf{k}}^{\dagger}a_{\mathbf{k}}\right]\sum_{n=0}^{\infty}\frac{1}{n!}[-i\mathbf{k}\cdot\mathbf{r}\left(a_{\mathbf{k}}^{\dagger}a_{\mathbf{k}}+1\right)]^n a_{\mathbf{k}} \\
&= \exp\left[i\mathbf{k}\cdot\mathbf{r}a_{\mathbf{k}}^{\dagger}a_{\mathbf{k}}\right]\exp\left[-i\mathbf{k}\cdot\mathbf{r}(a_{\mathbf{k}}^{\dagger}a_{\mathbf{k}}+1)\right]a_{\mathbf{k}} \\
&= a_{\mathbf{k}}\exp\left(-i\mathbf{k}\cdot\mathbf{r}\right).
\end{aligned}
\tag{7.274}
$$

Here the property was used:

$$
a_{\mathbf{k}}\left(a_{\mathbf{k}}^{\dagger}a_{\mathbf{k}}\right)^n = \left(a_{\mathbf{k}}^{\dagger}a_{\mathbf{k}}+1\right)^n a_{\mathbf{k}}. \tag{*}
$$

It is evident for $n=0$.For $n=1$ it is demonstrated as follows:

$$
a_{\mathbf{k}}a_{\mathbf{k}}^{\dagger} = a_{\mathbf{k}}^{\dagger}a_{\mathbf{k}}+1 \Longrightarrow a_{\mathbf{k}}a_{\mathbf{k}}^{\dagger}a_{\mathbf{k}} = (a_{\mathbf{k}}^{\dagger}a_{\mathbf{k}}+1)a_{\mathbf{k}};
$$

then for $n\geq 2$ the validity of (*) is straightforwardly demonstrated by induction.

Finally,

$$
a_{\mathbf{k}}^{\dagger} \longrightarrow S_1^{-1}a_{\mathbf{k}}^{\dagger}S_1 = [S_1^{-1}a_{\mathbf{k}}S_1]^{\dagger} = a_{\mathbf{k}}^{\dagger}\exp\left(i\mathbf{k}\cdot\mathbf{r}\right). \tag{7.275}
$$

Using (7.272), (7.273), (7.274) and (7.275), one arrives at

$$
H \longrightarrow \mathcal{H} = S_1^{-1}HS_1 = \frac{\left(\mathbf{P}-\sum_{\mathbf{k}}\hbar\mathbf{k}a_{\mathbf{k}}^{\dagger}a_{\mathbf{k}}\right)^2}{2m_b}+\sum_{\mathbf{k}}\hbar\omega_{\mathrm{LO}}a_{\mathbf{k}}^{\dagger}a_{\mathbf{k}}+\sum_{\mathbf{k}}(V_k a_{\mathbf{k}}+V_k^{*}a_{\mathbf{k}}^{\dagger}), \tag{7.276}
$$

where $\mathbf{p}$ is set 0. [5] The wave equation (7.268) takes the form

$$HS_1\psi = ES_1\psi \Longrightarrow \mathcal{H}\psi = E\psi. \tag{7.277}$$

Our aim is to calculate for a given momentum $\mathbf{P}$ the lowest eigenvalue $E(P)$ of the Hamiltonian (7.276). For the low-lying energy levels of the electron $E(P)$ may be well represented by the first two terms of a power series expansion in $P^2 : E(P) = E_0 + P^2/2m_p + O(P^4)$, where m_p is the effective mass of the polaron.

The canonical transformation (7.271) formally eliminates the electron operators from the Hamiltonian. LLP use further a variational method of calculation. The trial wave function is chosen as

$$\psi = S_2\psi_0 \tag{7.278}$$

where ψ_0 is the eigenstate of the unperturbed Hamiltonian with no phonons present (vacuum state). Specifically, ψ_0 is defined by

$$a_{\mathbf{k}}\psi_0 = 0, \qquad (\psi_0, \psi_0) = 1 \tag{7.279}$$

and the second canonical transformation:

$$S_2 = \exp\left[\sum_{\mathbf{k}}(a^\dagger_{\mathbf{k}} f_{\mathbf{k}} - a_{\mathbf{k}} f^*_{\mathbf{k}})\right], \tag{7.280}$$

where $f_{\mathbf{k}}$ are treated as variational functions and will be chosen to minimize the energy. The physical significance of Eq. (7.280) is that it "dresses" the electron with the virtual phonon field, which describes the polarization. Viewed as a unitary transformation, S_2 is a *displacement* operator on $a_{\mathbf{k}}$ and $a^\dagger_{\mathbf{k}}$:

$$\begin{aligned}
a_{\mathbf{k}} &\longrightarrow S_2^{-1} a_{\mathbf{k}} S_2 = \\
&= \exp\left[-\sum_{\mathbf{k}}(a^\dagger_{\mathbf{k}} f_{\mathbf{k}} - a_{\mathbf{k}} f^*_{\mathbf{k}})\right] a_{\mathbf{k}} \exp\left[\sum_{\mathbf{k}}(a^\dagger_{\mathbf{k}} f_{\mathbf{k}} - a_{\mathbf{k}} f^*_{\mathbf{k}})\right] \\
&= \exp\left[-(a^\dagger_{\mathbf{k}} f_{\mathbf{k}} - a_{\mathbf{k}} f^*_{\mathbf{k}})\right] a_{\mathbf{k}} \exp\left[(a^\dagger_{\mathbf{k}} f_{\mathbf{k}} - a_{\mathbf{k}} f^*_{\mathbf{k}})\right] \overset{\text{see}(**)}{=} \\
&= a_{\mathbf{k}} + \left[a_{\mathbf{k}}, (a^\dagger_{\mathbf{k}} f_{\mathbf{k}} - a_{\mathbf{k}} f^*_{\mathbf{k}})\right] + \frac{1}{2}\left[\left[a_{\mathbf{k}}, (a^\dagger_{\mathbf{k}} f_{\mathbf{k}} - a_{\mathbf{k}} f^*_{\mathbf{k}})\right], (a^\dagger_{\mathbf{k}} f_{\mathbf{k}} - a_{\mathbf{k}} f^*_{\mathbf{k}})\right] + ... \\
&= a_{\mathbf{k}} + f_{\mathbf{k}},
\end{aligned} \tag{7.281}$$

$$a^\dagger_{\mathbf{k}} \longrightarrow S_2^{-1} a\dagger_{\mathbf{k}} S_2 = a^\dagger_{\mathbf{k}} + f^*_{\mathbf{k}}. \tag{7.282}$$

Here the relation was used

$$\exp[-V]\, a \exp[V] = a + [a, V] + \frac{1}{2}[[a, V], V] + \frac{1}{3!}[[[a, V], V], V] + ... \tag{**}$$

Further we seek to minimize the expression for the energy,

$$E = (\psi, H\psi) = \left(\psi_0, S_2^{-1}\mathcal{H}S_2\psi_0\right). \tag{7.283}$$

In virtue of (7.281) and (7.282), we obtain:

[5] Transformation of the equation $\mathbf{P}_{op}\Phi = \mathbf{P}\Phi$ leads to $S_1^{-1}\mathbf{P}_{op}S_1\psi = \mathbf{P}\psi$.At the same time, applying Eq. (7.273), we obtain $S_1^{-1}\mathbf{P}_{op}S_1 = \mathbf{P} + \mathbf{p}$.Setting the gauge $\mathbf{p}\psi = 0$ eliminates the operator $\mathbf{p}$ from the problem.

$$
\begin{aligned}
S_2^{-1}\mathcal{H}S_2 &= \frac{\left[\mathbf{P} - \sum_{\mathbf{k}} \hbar\mathbf{k}\left(a_{\mathbf{k}}^\dagger + f_{\mathbf{k}}^*\right)(a_{\mathbf{k}} + f_{\mathbf{k}})\right]^2}{2m_b} \\
&+ \sum_{\mathbf{k}} \hbar\omega_{\mathrm{LO}}\left(a_{\mathbf{k}}^\dagger + f_{\mathbf{k}}^*\right)(a_{\mathbf{k}} + f_{\mathbf{k}}) + \sum_{\mathbf{k}}\left[V_k(a_{\mathbf{k}} + f_{\mathbf{k}}) + V_k^*\left(a_{\mathbf{k}}^\dagger + f_{\mathbf{k}}^*\right)\right] \\
&= \frac{\left[(\mathbf{P} - \sum_{\mathbf{k}} \hbar\mathbf{k}a_{\mathbf{k}}^\dagger a_{\mathbf{k}}) - \sum_{\mathbf{k}} \hbar\mathbf{k}\,|f_{\mathbf{k}}|^2 - \sum_{\mathbf{k}} \hbar\mathbf{k}\left(a_{\mathbf{k}}^\dagger f_{\mathbf{k}} + a_{\mathbf{k}} f_{\mathbf{k}}^*\right)\right]^2}{2m_b} \\
&+ \sum_{\mathbf{k}} \hbar\omega_{\mathrm{LO}}\left(a_{\mathbf{k}}^\dagger a_{\mathbf{k}} + |f_{\mathbf{k}}|^2 + a_{\mathbf{k}}^\dagger f_{\mathbf{k}} + a_{\mathbf{k}} f_{\mathbf{k}}^*\right) \\
&+ \sum_{\mathbf{k}}\left[V_k(a_{\mathbf{k}} + f_{\mathbf{k}}) + V_k^*\left(a_{\mathbf{k}}^\dagger + f_{\mathbf{k}}^*\right)\right] \\
&= H_0 + H_1,
\end{aligned}
$$

where

$$
\begin{aligned}
H_0 &= \frac{\left[(\mathbf{P} - \sum_{\mathbf{k}} \hbar\mathbf{k}a_{\mathbf{k}}^\dagger a_{\mathbf{k}})\right]^2 + \left[\sum_{\mathbf{k}} \hbar\mathbf{k}\,|f_{\mathbf{k}}|^2\right]^2}{2m_b} + \sum_{\mathbf{k}}\left[V_k f_{\mathbf{k}} + V_k^* f_{\mathbf{k}}^*\right] \\
&+ \sum_{\mathbf{k}} |f_{\mathbf{k}}|^2\left\{\hbar\omega_{\mathrm{LO}} - \frac{\hbar\mathbf{k}\cdot\mathbf{P}}{m_b} + \frac{\hbar^2k^2}{2m_b}\right\} + \frac{\hbar^2}{m_b}\sum_{\mathbf{k}} \mathbf{k}a_{\mathbf{k}}^\dagger a_{\mathbf{k}} \cdot \sum_{\mathbf{k}'} \mathbf{k}'\,|f_{\mathbf{k}'}|^2 \\
&+ \sum_{\mathbf{k}} a_{\mathbf{k}}\left\{V_k + f_{\mathbf{k}}^*\left[\hbar\omega_{\mathrm{LO}} - \frac{\hbar\mathbf{k}\cdot\mathbf{P}}{m_b} + \frac{\hbar^2k^2}{2m_b} + \frac{\hbar^2\mathbf{k}}{m_b}\cdot\sum_{\mathbf{k}'} \mathbf{k}'\,|f_{\mathbf{k}'}|^2\right]\right\} \\
&+ \sum_{\mathbf{k}} a_{\mathbf{k}}^\dagger\left\{V_k^* + f_{\mathbf{k}}\left[\hbar\omega_{\mathrm{LO}} - \frac{\hbar\mathbf{k}\cdot\mathbf{P}}{m_b} + \frac{\hbar^2k^2}{2m_b} + \frac{\hbar^2\mathbf{k}}{m_b}\cdot\sum_{\mathbf{k}'} \mathbf{k}'\,|f_{\mathbf{k}'}|^2\right]\right\} \\
&+ \sum_{\mathbf{k}} \hbar\omega_{\mathrm{LO}} a_{\mathbf{k}}^\dagger a_{\mathbf{k}};
\end{aligned}
\tag{7.284}
$$

$$
\begin{aligned}
H_1 &= \sum_{\mathbf{k},\mathbf{k}'} \frac{\hbar^2\mathbf{k}\cdot\mathbf{k}'}{2m_b}\left\{a_{\mathbf{k}}a_{\mathbf{k}'}f_{\mathbf{k}}^*f_{\mathbf{k}'}^* + 2a_{\mathbf{k}}^\dagger a_{\mathbf{k}'}f_{\mathbf{k}}f_{\mathbf{k}'}^* + a_{\mathbf{k}}^\dagger a_{\mathbf{k}'}^\dagger f_{\mathbf{k}}f_{\mathbf{k}'}\right\} + \\
&+ \sum_{\mathbf{k},\mathbf{k}'} \frac{\hbar^2\mathbf{k}\cdot\mathbf{k}'}{2m_b}\left\{a_{\mathbf{k}}^\dagger a_{\mathbf{k}}a_{\mathbf{k}'}f_{\mathbf{k}'}^* + a_{\mathbf{k}'}^\dagger a_{\mathbf{k}}^\dagger a_{\mathbf{k}}f_{\mathbf{k}'}\right\}.
\end{aligned}
$$

Using (7.279), we obtain from (7.283) that

$$
\begin{aligned}
E = H_0 &= \frac{P^2 + \left[\sum_{\mathbf{k}} \hbar\mathbf{k}\,|f_{\mathbf{k}}|^2\right]^2}{2m_b} + \sum_{\mathbf{k}}\left[V_k f_{\mathbf{k}} + V_k^* f_{\mathbf{k}}^*\right] \\
&+ \sum_{\mathbf{k}} |f_{\mathbf{k}}|^2\left\{\hbar\omega_{\mathrm{LO}} - \frac{\hbar\mathbf{k}\cdot\mathbf{P}}{m_b} + \frac{\hbar^2k^2}{2m_b}\right\}.
\end{aligned}
\tag{7.285}
$$

We minimize (7.285) by imposing

$$
\frac{\delta E}{\delta f_{\mathbf{k}}} = 0, \qquad \frac{\delta E}{\delta f_{\mathbf{k}}^\dagger} = 0.
$$

This results in

$$V_k + f_{\mathbf{k}}^* \left\{ \hbar\omega_{\mathrm{LO}} - \frac{\hbar\mathbf{k}\cdot\mathbf{P}}{m_b} + \frac{\hbar^2 k^2}{2m_b} + \frac{\hbar^2}{m_b}\left[\sum_{\mathbf{k}'} \hbar\mathbf{k}' \left|f_{\mathbf{k}'}\right|^2\right]\cdot\mathbf{k} \right\} = 0 \tag{7.286}$$

and the appropriate complex conjugate equation for $f_{\mathbf{k}}$. Upon comparing (7.286) and (7.284), we see that the linear terms in $a_{\mathbf{k}}^\dagger$ and $a_{\mathbf{k}}$ are identically zero if (7.286) is satisfied, and hence that H_0 is diagonal in a representation in which $a_{\mathbf{k}}^\dagger a_{\mathbf{k}}$ is diagonal. So, the variational calculation by LLP is equivalent to the use of (7.284) as the total Hamiltonian provided $f_{\mathbf{k}}^*$ satisfies (7.286). An estimate of the accuracy of the LLP variational procedure was obtained by an estimate of the effect of H_1 using a perturbation theory.

Now we evaluate the energy of the ground state of the system, which is given by Eq. (7.285) with $f_{\mathbf{k}}^*$ satisfying Eq. (7.286). The only preferred direction in this problem is $\mathbf{P}$. Therefore one may introduce the parameter η defined as

$$\eta\mathbf{P} = \sum_{\mathbf{k}} \hbar\mathbf{k}\left|f_{\mathbf{k}}\right|^2. \tag{7.287}$$

Then Eq. (7.286) leads to

$$f_{\mathbf{k}}^* = -V_k \Bigg/ \left[\hbar\omega_{\mathrm{LO}} - \frac{\hbar\mathbf{k}\cdot\mathbf{P}}{m_b}(1-\eta) + \frac{\hbar^2 k^2}{2m_b}\right], \tag{7.288}$$

and we obtain the following implicit equation for η:

$$\begin{aligned}\eta\mathbf{P} &= \sum_{\mathbf{k}} \hbar\mathbf{k}\left|V_k\right|^2 \Bigg/ \left[\hbar\omega_{\mathrm{LO}} - \frac{\hbar\mathbf{k}\cdot\mathbf{P}}{m_b}(1-\eta) + \frac{\hbar^2 k^2}{2m_b}\right]^2 \\ &= \frac{V}{(2\pi)^3}\int d^3k\hbar\mathbf{k}\left(\frac{\hbar\omega_{\mathrm{LO}}}{k}\right)^2 \frac{4\pi\alpha}{V}\left(\frac{\hbar}{2m_b\omega_{\mathrm{LO}}}\right)^{\frac{1}{2}} \Bigg/ \left[\hbar\omega_{\mathrm{LO}} - \frac{\hbar\mathbf{k}\cdot\mathbf{P}}{m_b}(1-\eta) + \frac{\hbar^2 k^2}{2m_b}\right]^2.\end{aligned}$$

Let us introduce spherical coordinates with a polar axis along $\mathbf{P}$ and denote $x = \cos(\mathbf{k}\hat{\ }\mathbf{P})$:

$$\begin{aligned}\eta P &= \frac{\alpha\hbar^3\omega_{\mathrm{LO}}^2}{2\pi^2}\left(\frac{\hbar}{2m_b\omega_{\mathrm{LO}}}\right)^{\frac{1}{2}} 2\pi\int_{-1}^{1} dx x \int_0^\infty dk k \Bigg/ \left[\hbar\omega_{\mathrm{LO}} - \frac{\hbar k P x}{m_b}(1-\eta) + \frac{\hbar^2 k^2}{2m_b}\right]^2 \\ &= \frac{\alpha\hbar}{2\pi^2}\left(\frac{\hbar}{2m_b\omega_{\mathrm{LO}}}\right)^{\frac{1}{2}} 2\pi\int_{-1}^{1} dx x \int_0^\infty dk k \Bigg/ \left[1 - 2\frac{\hbar k P x}{2m_b\hbar\omega_{\mathrm{LO}}}(1-\eta) + \frac{\hbar^2 k^2}{2m_b\hbar\omega_{\mathrm{LO}}}\right]^2.\end{aligned}$$

Further, we introduce the parameter

$$q = \frac{P}{(2m_b\hbar\omega_{\mathrm{LO}})^{1/2}}(1-\eta) \tag{7.289}$$

and a new variable

$$\kappa = \frac{\hbar k}{(2m_b\hbar\omega_{\mathrm{LO}})^{1/2}}.$$

This gives

$$
\begin{aligned}
\eta &= \frac{\alpha\hbar}{\pi}\left(\frac{\hbar}{2m_b\omega_{\rm LO}}\right)^{\frac{1}{2}}\frac{2m_b\hbar\omega_{\rm LO}}{\hbar^2 P}\int_{-1}^{1}dxx\int_0^\infty d\kappa\kappa\Big/\left[1-2q\kappa x+\kappa^2\right]^2\\
&= \frac{\alpha}{\pi}\frac{\left(2m_b\hbar\omega_{\rm LO}\right)^{1/2}}{P}\int_{-1}^{1}dxx\int_0^\infty d\kappa\kappa\Big/\left[(\kappa-qx)^2+(1-q^2x^2)\right]^2\\
&= \frac{\alpha}{\pi}\frac{\left(2m_b\hbar\omega_{\rm LO}\right)^{1/2}}{P}\int_{-1}^{1}dxx\int_{-qx}^\infty d\kappa\,(\kappa+qx)\Big/\left[\kappa^2+(1-q^2x^2)\right]^2\\
&= \frac{\alpha}{\pi}\frac{\left(2m_b\hbar\omega_{\rm LO}\right)^{1/2}}{P}\int_{-1}^{1}dxx\left\{\begin{array}{c}-\frac{1}{2[\kappa^2+(1-q^2x^2)]}\\ +qx\left[\frac{\kappa}{2(1-q^2x^2)[\kappa^2+(1-q^2x^2)]}+\frac{1}{2(1-q^2x^2)^{3/2}}\arctan\left(\frac{\kappa}{[1-q^2x^2]^{1/2}}\right)\right]\end{array}\right\}_{-qx}^{\infty}\\
&= \frac{\alpha}{\pi}\frac{\left(2m_b\hbar\omega_{\rm LO}\right)^{1/2}}{P}\int_{-1}^{1}dxx\left\{\frac{1}{2}+\frac{qx\pi}{4(1-q^2x^2)^{3/2}}+\frac{q^2x^2}{2(1-q^2x^2)}+\frac{qx}{2(1-q^2x^2)^{3/2}}\arcsin(qx)\right\}.
\end{aligned}
$$

$$\Downarrow$$

$$
\begin{aligned}
\eta &= \frac{\alpha}{\pi}\frac{\left(2m_b\hbar\omega_{\rm LO}\right)^{1/2}}{P}\frac{q\pi}{4}\int_{-1}^{1}\frac{x^2}{(1-q^2x^2)^{3/2}}dx\\
&= \frac{\alpha}{4}(1-\eta)\int_{-1}^{1}\frac{x^2}{(1-q^2x^2)^{3/2}}dx\\
&= \frac{\alpha}{2}(1-\eta)\frac{q-\sqrt{1-q^2}\arcsin(q)}{q^3\sqrt{1-q^2}}\\
&= \frac{\alpha(1-\eta)}{2\left(\frac{P}{(2m_b\hbar\omega_{\rm LO})^{1/2}}(1-\eta)\right)^3}\left(\frac{q}{\sqrt{1-q^2}}-\arcsin(q)\right)\\
&= \frac{\alpha}{2(1-\eta)^2}\left(\frac{2m_b\hbar\omega_{\rm LO}}{P^2}\right)^{3/2}\left(\frac{q}{\sqrt{1-q^2}}-\arcsin(q)\right)
\end{aligned}
$$

So, we have arrived at the equation

$$\eta(1-\eta)^2=\frac{\alpha}{2}\left(\frac{2m_b\hbar\omega_{\rm LO}}{P^2}\right)^{3/2}\left(\frac{q}{\sqrt{1-q^2}}-\arcsin(q)\right), \tag{7.290}$$

or equivalently, using the definition (7.289),

$$\frac{\eta}{1-\eta}=\frac{\alpha}{2q^3}\left(\frac{q}{\sqrt{1-q^2}}-\arcsin(q)\right). \tag{7.291}$$

Using Eqs. (7.287) and (7.288), we can simplify the energy (7.285) as follows:

$$
\begin{aligned}
E &= \frac{P^2+(\eta\mathbf{P})^2}{2m_b}-2\sum_{\mathbf{k}}\frac{|V_k|^2}{\hbar\omega_{\rm LO}-\frac{\hbar\mathbf{k}\cdot\mathbf{P}}{m_b}(1-\eta)+\frac{\hbar^2k^2}{2m_b}}\\
&\quad+\sum_{\mathbf{k}}\frac{|V_k|^2}{\left(\hbar\omega_{\rm LO}-\frac{\hbar\mathbf{k}\cdot\mathbf{P}}{m_b}(1-\eta)+\frac{\hbar^2k^2}{2m_b}\right)^2}\left(\hbar\omega_{\rm LO}-\frac{\hbar\mathbf{k}\cdot\mathbf{P}}{m_b}+\frac{\hbar^2k^2}{2m_b}\right)
\end{aligned}
$$

$$= \frac{(1+\eta^2)\,P^2}{2m_b} - 2\sum_{\mathbf{k}} \frac{|V_k|^2}{\hbar\omega_{\mathrm{LO}} - \frac{\hbar\mathbf{k}\cdot\mathbf{P}}{m_b}(1-\eta) + \frac{\hbar^2k^2}{2m_b}}$$
$$+ \sum_{\mathbf{k}} \frac{|V_k|^2}{\left(\hbar\omega_{\mathrm{LO}} - \frac{\hbar\mathbf{k}\cdot\mathbf{P}}{m_b}(1-\eta) + \frac{\hbar^2k^2}{2m_b}\right)^2} \left(\hbar\omega_{\mathrm{LO}} - \frac{\hbar\mathbf{k}\cdot\mathbf{P}}{m_b}(1-\eta+\eta) + \frac{\hbar^2k^2}{2m_b}\right)$$

$$= \frac{(1+\eta^2)\,P^2}{2m_b} - 2\sum_{\mathbf{k}} \frac{|V_k|^2}{\hbar\omega_{\mathrm{LO}} - \frac{\hbar\mathbf{k}\cdot\mathbf{P}}{m_b}(1-\eta) + \frac{\hbar^2k^2}{2m_b}}$$
$$+ \sum_{\mathbf{k}} \frac{|V_k|^2}{\left(\hbar\omega_{\mathrm{LO}} - \frac{\hbar\mathbf{k}\cdot\mathbf{P}}{m_b}(1-\eta) + \frac{\hbar^2k^2}{2m_b}\right)^2} \left(\hbar\omega_{\mathrm{LO}} - \frac{\hbar\mathbf{k}\cdot\mathbf{P}}{m_b}(1-\eta) + \frac{\hbar^2k^2}{2m_b}\right)$$
$$- \sum_{\mathbf{k}} \frac{|V_k|^2}{\left(\hbar\omega_{\mathrm{LO}} - \frac{\hbar\mathbf{k}\cdot\mathbf{P}}{m_b}(1-\eta) + \frac{\hbar^2k^2}{2m_b}\right)^2} \left(\frac{\hbar\mathbf{k}\cdot\mathbf{P}}{m_b}\eta\right)$$

$$= \frac{(1+\eta^2)\,P^2}{2m_b} - 2\sum_{\mathbf{k}} \frac{|V_k|^2}{\hbar\omega_{\mathrm{LO}} - \frac{\hbar\mathbf{k}\cdot\mathbf{P}}{m_b}(1-\eta) + \frac{\hbar^2k^2}{2m_b}}$$
$$+ \sum_{\mathbf{k}} \frac{|V_k|^2}{\hbar\omega_{\mathrm{LO}} - \frac{\hbar\mathbf{k}\cdot\mathbf{P}}{m_b}(1-\eta) + \frac{\hbar^2k^2}{2m_b}}$$
$$- \left(\frac{\mathbf{P}}{m_b}\eta\right) \cdot \sum_{\mathbf{k}} \frac{\hbar\mathbf{k}\,|V_k|^2}{\left(\hbar\omega_{\mathrm{LO}} - \frac{\hbar\mathbf{k}\cdot\mathbf{P}}{m_b}(1-\eta) + \frac{\hbar^2k^2}{2m_b}\right)^2}$$

$$= \frac{(1+\eta^2)\,P^2}{2m_b} - \sum_{\mathbf{k}} \frac{|V_k|^2}{\hbar\omega_{\mathrm{LO}} - \frac{\hbar\mathbf{k}\cdot\mathbf{P}}{m_b}(1-\eta) + \frac{\hbar^2k^2}{2m_b}} - \left(\frac{\mathbf{P}}{m_b}\eta\right) \cdot \sum_{\mathbf{k}} \hbar\mathbf{k}\,|f_{\mathbf{k}}|^2$$
$$= \frac{(1+\eta^2)\,P^2}{2m_b} - \left(\frac{\mathbf{P}}{m_b}\eta\right) \cdot \eta\mathbf{P} - \sum_{\mathbf{k}} \frac{|V_k|^2}{\hbar\omega_{\mathrm{LO}} - \frac{\hbar\mathbf{k}\cdot\mathbf{P}}{m_b}(1-\eta) + \frac{\hbar^2k^2}{2m_b}}$$
$$\Downarrow$$
$$E = \frac{P^2}{2m_b}\left(1-\eta^2\right) - \sum_{\mathbf{k}} \frac{|V_k|^2}{\hbar\omega_{\mathrm{LO}} - \frac{\hbar\mathbf{k}\cdot\mathbf{P}}{m_b}(1-\eta) + \frac{\hbar^2k^2}{2m_b}}. \tag{7.292}$$

The sum over $\mathbf{k}$ in Eq. (7.292) is calculated as follows:

$$\sum_{\mathbf{k}} \frac{|V_k|^2}{\hbar\omega_{\mathrm{LO}} - \frac{\hbar\mathbf{k}\cdot\mathbf{P}}{m_b}(1-\eta) + \frac{\hbar^2k^2}{2m_b}}$$
$$= \frac{V}{(2\pi)^3} \int d\mathbf{k} \frac{\left(\frac{\hbar\omega_{\mathrm{LO}}}{k}\left(\frac{4\pi\alpha}{V}\right)^{\frac{1}{2}}\left(\frac{\hbar}{2m_b\omega_{\mathrm{LO}}}\right)^{\frac{1}{4}}\right)^2}{\hbar\omega_{\mathrm{LO}} - \frac{\hbar\mathbf{k}\cdot\mathbf{P}}{m_b}(1-\eta) + \frac{\hbar^2k^2}{2m_b}}$$
$$= \frac{V}{(2\pi)^3}\hbar^2\omega_{\mathrm{LO}}^2 \left(\frac{4\pi\alpha}{V}\right)\left(\frac{\hbar}{2m_b\omega_{\mathrm{LO}}}\right)^{\frac{1}{2}} \int d\mathbf{k} \frac{1}{k^2\left[\hbar\omega_{\mathrm{LO}} - \frac{\hbar\mathbf{k}\cdot\mathbf{P}}{m_b}(1-\eta) + \frac{\hbar^2k^2}{2m_b}\right]}$$
$$= \frac{m_b\omega_{\mathrm{LO}}^2\alpha}{\pi^2}\left(\frac{\hbar}{2m_b\omega_{\mathrm{LO}}}\right)^{\frac{1}{2}} \int d\mathbf{k} \frac{1}{k^2\left(k^2 - 2\frac{\mathbf{k}\cdot\mathbf{P}}{\hbar}(1-\eta) + \frac{2m_b\omega_{\mathrm{LO}}}{\hbar}\right)}.$$

For the calculation of this integral, we can use the auxiliary identity

$$\frac{1}{ab} = \int_0^1 \frac{1}{\left[ax + b\left(1-x\right)\right]^2}. \tag{7.293}$$

Setting

$$\begin{aligned} a &= k^2 - 2\frac{\mathbf{k}\cdot\mathbf{P}}{\hbar}(1-\eta) + \frac{2m_b\omega_{\mathrm{LO}}}{\hbar}, \\ b &= k^2, \end{aligned}$$

we find

$$\begin{aligned}
&\sum_{\mathbf{k}} \frac{\left|V_k\right|^2}{\hbar\omega_{\mathrm{LO}} - \frac{\hbar\mathbf{k}\cdot\mathbf{P}}{m_b}(1-\eta) + \frac{\hbar^2k^2}{2m_b}} \\
&= \frac{m_b\omega_{\mathrm{LO}}^2\alpha}{\pi^2}\left(\frac{\hbar}{2m_b\omega_{\mathrm{LO}}}\right)^{\frac{1}{2}} \int_0^1 dx \int d\mathbf{k} \frac{1}{\left[x\left(k^2 - 2\frac{\mathbf{k}\cdot\mathbf{P}}{\hbar}(1-\eta) + \frac{2m_b\omega_{\mathrm{LO}}}{\hbar}\right) + \left(1-x\right)k^2\right]^2} \\
&= \frac{m_b\omega_{\mathrm{LO}}^2\alpha}{\pi^2}\left(\frac{\hbar}{2m_b\omega_{\mathrm{LO}}}\right)^{\frac{1}{2}} \int_0^1 dx \int d\mathbf{k} \frac{1}{\left(k^2 - 2\frac{\mathbf{k}\cdot\mathbf{P}}{\hbar}(1-\eta)x + \frac{2m_b\omega_{\mathrm{LO}}}{\hbar}x\right)^2} \\
&= \frac{m_b\omega_{\mathrm{LO}}^2\alpha}{\pi^2}\left(\frac{\hbar}{2m_b\omega_{\mathrm{LO}}}\right)^{\frac{1}{2}} \int_0^1 dx \int d\mathbf{k} \frac{1}{\left(\left(\mathbf{k}-\frac{\mathbf{P}}{\hbar}(1-\eta)x\right)^2 + \frac{2m_b\omega_{\mathrm{LO}}}{\hbar}x - \frac{P^2}{\hbar^2}(1-\eta)^2x^2\right)^2} \\
&= \frac{m_b\omega_{\mathrm{LO}}^2\alpha}{\pi^2}\left(\frac{\hbar}{2m_b\omega_{\mathrm{LO}}}\right)^{\frac{1}{2}} \int_0^1 dx \int d\mathbf{k} \frac{1}{\left(k^2 + \frac{2m_b\omega_{\mathrm{LO}}}{\hbar}x - \frac{P^2}{\hbar^2}(1-\eta)^2x^2\right)^2}
\end{aligned}$$

As long as $P^2/\left(2m_b\right)$ is sufficiently small so that no spontaneous emission can occur (roughly $P^2/\left(2m_b\right) \lesssim \hbar\omega_{\mathrm{LO}}$), the quantity

$$A \equiv \frac{2m_b\omega_{\mathrm{LO}}}{\hbar}x - \frac{P^2}{\hbar^2}(1-\eta)^2x^2$$

is supposed to be positive for $0 < x < 1$. Therefore, we can use the integral

$$\int \frac{1}{\left(k^2+A\right)^2} d\mathbf{k} = \frac{\pi^2}{\sqrt{A}},$$

what gives

$$\begin{aligned}
&\sum_{\mathbf{k}} \frac{\left|V_k\right|^2}{\hbar\omega_{\mathrm{LO}} - \frac{\hbar\mathbf{k}\cdot\mathbf{P}}{m_b}(1-\eta) + \frac{\hbar^2k^2}{2m_b}} \\
&= \frac{m_b\omega_{\mathrm{LO}}^2\alpha}{\pi^2}\left(\frac{\hbar}{2m_b\omega_{\mathrm{LO}}}\right)^{\frac{1}{2}} \int_0^1 dx \frac{\pi^2}{\sqrt{\frac{2m_b\omega_{\mathrm{LO}}}{\hbar}x - \frac{P^2}{\hbar^2}(1-\eta)^2x^2}} \\
&= \frac{1}{2}\alpha\hbar\omega_{\mathrm{LO}} \int_0^1 dx \frac{1}{\sqrt{x - \frac{(1-\eta)^2P^2}{2m_b\hbar\omega_{\mathrm{LO}}}x^2}} \\
&= \frac{1}{2}\alpha\hbar\omega_{\mathrm{LO}} \int_0^1 dx \frac{1}{\sqrt{x - q^2x^2}}.
\end{aligned}$$

We change the variable $x = t^2$, what gives

$$\int_0^1 \frac{1}{\sqrt{x - q^2 x^2}} dx = 2 \int_0^1 \frac{1}{\sqrt{1 - q^2 t^2}} dt = \frac{2}{q} \arcsin q,$$

and hence

$$\sum_{\mathbf{k}} \frac{|V_k|^2}{\hbar\omega_{\mathrm{LO}} - \frac{\hbar \mathbf{k}\cdot\mathbf{P}}{m_b}(1-\eta) + \frac{\hbar^2 k^2}{2m_b}} = \frac{\alpha\hbar\omega_{\mathrm{LO}}}{q} \arcsin q. \tag{7.294}$$

As a result, the energy (7.292) is expressed in a closed form

$$E = \frac{P^2}{2m_b}\left(1-\eta^2\right) - \frac{\alpha\hbar\omega_{\mathrm{LO}}}{q} \arcsin q. \tag{7.295}$$

Further, we expand the r.h.s. of Eq. (7.291) to the second order in powers of P (or, what is the same, in powers of q) using the relation

$$\frac{q}{\sqrt{1-q^2}} - \arcsin(q) = \frac{1}{3}q^3 + O\left(q^5\right) \tag{7.296}$$

what results in

$$\frac{\eta}{1-\eta} = \frac{\alpha}{2q^3}\left[\frac{1}{3}q^3 + O\left(q^5\right)\right] = \frac{\alpha}{6} + O\left(q^2\right).$$

Solving this equation for η, we find

$$\eta = \frac{\alpha/6}{1+\alpha/6} + O\left(\frac{P^2}{2m_b\hbar\omega_{\mathrm{LO}}}\right). \tag{7.297}$$

We also apply the expansion in powers of q up to $\sim q^2$ to the energy (7.295):

$$\begin{aligned}
E &= \frac{P^2}{2m_b}\left(1-\eta^2\right) - \frac{\alpha\hbar\omega_{\mathrm{LO}}}{q}\left(q + \frac{1}{6}q^3 + O\left(q^5\right)\right) \\
&= \frac{P^2}{2m_b}\left(1-\eta^2\right) - \alpha\hbar\omega_{\mathrm{LO}} - \frac{1}{6}\alpha\hbar\omega_{\mathrm{LO}} q^2 + \hbar\omega_{\mathrm{LO}} O\left(q^4\right) \\
&= -\alpha\hbar\omega_{\mathrm{LO}} + \frac{P^2}{2m_b}\left(1-\eta^2\right) - \frac{\alpha P^2 (1-\eta)^2}{12m_b} + \hbar\omega_{\mathrm{LO}} O\left(q^4\right) \\
&= -\alpha\hbar\omega_{\mathrm{LO}} + \frac{P^2}{2m_b}\left(1-\eta^2\right) - \frac{\alpha P^2 (1-\eta)^2}{12m_b} + \hbar\omega_{\mathrm{LO}} O\left(q^4\right) \\
&= -\alpha\hbar\omega_{\mathrm{LO}} + \frac{P^2}{12m_b}(1-\eta)\left((6+\alpha)\eta - \alpha + 6\right) + \hbar\omega_{\mathrm{LO}} O\left(q^4\right) \\
&= -\alpha\hbar\omega_{\mathrm{LO}} + \frac{P^2}{12m_b}\left(1 - \frac{\alpha/6}{1+\alpha/6}\right)\left((6+\alpha)\frac{\alpha/6}{1+\alpha/6} - \alpha + 6\right) + \hbar\omega_{\mathrm{LO}} O\left(q^4\right) \\
&= -\alpha\hbar\omega_{\mathrm{LO}} + \frac{P^2}{2m_b(1+\alpha/6)} + \hbar\omega_{\mathrm{LO}} O\left(q^4\right).
\end{aligned}$$

Finally, we have arrived at the LLP polaron energy

$$E = -\alpha\hbar\omega_{\mathrm{LO}} + \frac{P^2}{2m_b(1+\alpha/6)} + \hbar\omega_{\mathrm{LO}} O\left(\left(\frac{P^2}{2m_b\hbar\omega_{\mathrm{LO}}}\right)^2\right). \tag{7.298}$$

7.4.4 Appendix 2. Expansion in Stieltjes continuous fractions [54]

In this derivation it is shown that the approximation used in the evaluation of the function, which determines the polaron mass [see Eqs. (40) and (B1) from Ref. [54]]

$$g(k,z) = \int_{-\infty}^{0} d\tau e^{iz\tau} \exp\left[-k^2 C(0)\right] \exp\left[k^2 C(\tau)\right] \tag{7.299}$$

with

$$C(\tau) = \frac{1}{3}\sum_{k'} \frac{k'^2}{m^2} \left|f_{k'}\right|^2 \frac{e^{i\gamma_{k'}\tau}}{\gamma_{k'}^2} \tag{7.300}$$

is equivalent to an expansion in a continued fraction limited to the first step. Moreover, it is proved that the choice of the coefficients of the continued fraction can be justified by a variational principle, at least when z is real and positive.

Expanding the last exponential of Eq. (7.299) in a power series leads to

$$\begin{aligned} g(k,z) &= \exp\left[-k^2 C(0)\right] \int_{-\infty}^{0} d\tau e^{iz\tau} \sum_{n=0}^{\infty} \frac{1}{n!} \left(\frac{1}{3m^2}\right)^n \\ &\times \sum_{\vec{k}_1,\ldots,\vec{k}_n} \frac{k_1^2 k_2^2 \ldots k_n^2 \left|f_{k_1}\right|^2 \left|f_{k_2}\right|^2 \ldots \left|f_{k_n}\right|^2}{\gamma_{k_1}^2 \gamma_{k_2}^2 \cdots \gamma_{k_n}^2} \\ &\times \exp\left[i(\gamma_{k_1} + \gamma_{k_2} + \ldots \gamma_{k_n}^2)\tau\right] \\ &= -i \exp\left[-k^2 C(0)\right] \sum_{n=0}^{\infty} \frac{(3m^2)^{-n}}{n!} \\ &\times \sum_{\vec{k}_1,\ldots,\vec{k}_n} \frac{k_1^2 k_2^2 \ldots k_n^2 \left|f_{k_1}\right|^2 \left|f_{k_2}\right|^2 \ldots \left|f_{k_n}\right|^2}{\gamma_{k_1}^2 \gamma_{k_2}^2 \cdots \gamma_{k_n}^2} \frac{1}{\gamma_{k_1} + \gamma_{k_2} + \ldots + \gamma_{k_n} + z}. \end{aligned} \tag{7.301}$$

The multiple sum over the k's is in fact an integral with 3n variables. It is possible to change the variables in that one of the new variables is

$$x_n = \gamma_{k_1} + \gamma_{k_2} + \ldots + \gamma_{k_n}. \tag{7.302}$$

Then the multiple sum which appears in the last term of Eq. (7.301) is of the following type:

$$J(z) = \int_{n\omega}^{\infty} \frac{L(x_n)}{x_n + z} dx_n, \tag{7.303}$$

where

$$L(x_n) = 0$$

is the result of the integration over the $n-1$ other variables. An expansion of integrals of the type (7.303) into Stieltjes continued fractions is known to give good results when z is real and not located on the cut of $J(z)$, i.e., when

$$z > -n\omega. \tag{7.304}$$

The first nontrivial step in the continued fraction expansion is

$$J(z) = \frac{a_0}{a_1 + z} \tag{7.305}$$

with

$$a_0 = \int_{n\omega}^{\infty} L(x_n) dx_n, \tag{7.306}$$

$$a_1 = \frac{\int_{n\omega}^{\infty} x_n L(x_n) dx_n}{\int_{n\omega}^{\infty} L(x_n) dx_n}. \tag{7.307}$$

A *variational principle* can be established, which gives a rather strong argument in favour of the approximation (7.305). Let us introduce a variational parameter $\bar{x}$ writing

$$J(z) = \int_{n\omega}^{\infty} \frac{L(x_n)}{(x_n - \bar{x}) + (z + \bar{x})} dx_n. \tag{7.308}$$

Performing two steps of the division, this relation becomes

$$\begin{aligned} J(z) = & \frac{1}{z + \bar{x}} \int_{n\omega}^{\infty} L(x_n) dx_n \\ & - \frac{1}{(z + \bar{x})^2} \int_{n\omega}^{\infty} (x_n - \bar{x}) L(x_n) dx_n + K(z, \bar{x}) \end{aligned} \tag{7.309}$$

with

$$K(z, \bar{x}) = \frac{1}{(z + \bar{x})^2} \int_{n\omega}^{\infty} \frac{(x_n - \bar{x})^2 L(x_n)}{x_n + z} dx_n. \tag{7.310}$$

The approximation consists of neglecting the term $K(z, \bar{x})$ in Eq. (7.309). As this term is positive [cf. (7.304)], the best approximation is obtained when it is minimum. Therefore let us use the freedom in the choice of $\bar{x}$ to minimize the expression (7.310),

$$\begin{aligned} \frac{\partial K(z, \bar{x})}{\partial \bar{x}} &= -2 \frac{K(z, \bar{x})}{z + \bar{x}} \\ -2 \frac{1}{(z + \bar{x})^2} \int_{n\omega}^{\infty} \frac{(x_n - \bar{x})^2 L(x_n)}{x_n + z} dx_n &= 0, \end{aligned} \tag{7.311}$$

which gives

$$-2 \frac{1}{(z + \bar{x})^2} \int_{n\omega}^{\infty} \left(\frac{x_n - \bar{x}}{z + \bar{x}} + 1 \right) \frac{x_n - \bar{x}}{x_n + z} L(x_n) dx_n = 0 \tag{7.312}$$

or

$$-2\frac{1}{(z+\bar{x})^3}\int_{n\omega}^{\infty}(x_n-\bar{x})L(x_n)dx_n=0. \tag{7.313}$$

This provides us with the best value of the variational parameter

$$\bar{x}=\frac{\int_{n\omega}^{\infty}x_nL(x_n)dx_n}{\int_{n\omega}^{\infty}L(x_n)dx_n}, \tag{7.314}$$

which is a_1 [cf. Eq. (7.307)].

With this value of $\bar{x}$ and neglecting $K(z,\bar{x})$, the expression (7.309) of the calculated quantity $J(z)$ becomes

$$J(z)=\frac{1}{z+\bar{x}}\int_{n\omega}^{\infty}L(x_n)dx_n=J(z)=\frac{a_0}{a_1+z}, \tag{7.315}$$

which is the first step (7.305) of a Stieltjes continued fraction.

To prove that this value of $\bar{x}$ gives a minimum of $K(z,\bar{x})$, let us calculate the second derivative

$$\begin{aligned}\frac{\partial^2K(z,\bar{x})}{\partial\bar{x}^2}&=\frac{6}{(z+\bar{x})^3}\int_{n\omega}^{\infty}(x_n-\bar{x})L(x_n)dx_n\\&+\frac{2}{(z+\bar{x})^3}\int_{n\omega}^{\infty}L(x_n)dx_n.\end{aligned} \tag{7.316}$$

Now the parameter $\bar{x}$ is replaced by its expression (7.314). The relation (7.316) becomes

$$\frac{\partial^2K(z,\bar{x})}{\partial\bar{x}^2}=\frac{2}{(z+a_1)^3}\int_{n\omega}^{\infty}L(x_n)dx_n, \tag{7.317}$$

which is positive of $z\geqslant -n\omega$, since it follows from relation (7.314) that $a_1>n\omega$.

Our approximation is related to that used by Feynman which is based on the following inequality:

$$\left\langle e^{-sx}\right\rangle\geqslant e^{-s\langle x\rangle}, \tag{7.318}$$

where the brackets denote the expectation value of the random variable x. For instance,

$$\left\langle e^{-sx}\right\rangle=\frac{\int_a^{\infty}L(x)e^{-sx}dx}{\int_a^{\infty}L(x)ds}, \tag{7.319}$$

where L(x) is the non-normalized probability density of x. The Laplace transform of Eq. (7.318) gives

$$\int_0^\infty e^{-sz}\left\langle e^{-sx}\right\rangle ds \geqslant \int_0^\infty e^{-sz}e^{-s\langle x\rangle}ds, \tag{7.320}$$

which after integration becomes

$$\int_a^\infty \frac{L(x)}{x+z}dx \geqslant \frac{\int_a^\infty L(x)ds}{\langle x\rangle + z} = \frac{a_0}{a_1+z}. \tag{7.321}$$

The last inequality shows the relation with our procedure.

8 Fröhlich Polarons: Lecture course including detailed theoretical derivations by Devreese. Many polarons

8.1 Optical conductivity of an interacting many-polaron gas

8.1.1 Kubo formula for the optical conductivity of the many-polaron gas

The derivations in the present section are based on Ref. [53]. The Hamiltonian of a system of N interacting continuum polarons is given by:

$$\begin{aligned} H_0 = &\sum_{j=1}^N \frac{p_j^2}{2m_b} + \sum_{\mathbf{q}} \hbar\omega_{\mathrm{LO}} b_{\mathbf{q}}^+ b_{\mathbf{q}} \\ &+ \sum_{\mathbf{q}}\sum_{j=1}^N \left(e^{i\mathbf{q}\cdot\mathbf{r}_j} b_{\mathbf{q}} V_{\mathbf{q}} + e^{-i\mathbf{q}\cdot\mathbf{r}_j} b_{\mathbf{q}}^+ V_{\mathbf{q}}^*\right) + \frac{e^2}{2\varepsilon_\infty}\sum_{j=1}^N \sum_{\ell(\neq j)=1}^N \frac{1}{|\mathbf{r}_i - \mathbf{r}_j|}, \end{aligned} \tag{8.1}$$

where $\mathbf{r}_j, \mathbf{p}_j$ represent the position and momentum of the N constituent electrons (or holes) with band mass m_b; $b_{\mathbf{q}}^+, b_{\mathbf{q}}$ denote the creation and annihilation operators for longitudinal optical (LO) phonons with wave vector $\mathbf{q}$ and frequency ω_{LO}; $V_{\mathbf{q}}$ describes the amplitude of the interaction between the electrons and the phonons; and e is the elementary electron charge. This Hamiltonian can be subdivided into the following parts:

$$H = H_e + H_{e-e} + H_{ph} + H_{e-ph} \tag{8.2}$$

where

$$H_e = \sum_{j=1}^N \frac{p_j^2}{2m_b} \tag{8.3}$$

is the kinetic energy of electrons,

$$H_{e-e} = \frac{e^2}{2\varepsilon_\infty}\sum_{j=1}^N \sum_{\ell(\neq j)=1}^N \frac{1}{|\mathbf{r}_i - \mathbf{r}_j|} \tag{8.4}$$

is the potential energy of the Coulomb electron-electron interaction,

$$H_{ph} = \sum_{\mathbf{q}} \hbar\omega_{\mathrm{LO}} b_{\mathbf{q}}^+ b_{\mathbf{q}} \tag{8.5}$$

is the Hamlitonian of phonons, and

$$H_{e-ph} = \sum_{\mathbf{q}} \sum_{j=1}^{N} \left(e^{i\mathbf{q}\cdot\mathbf{r}_j} b_{\mathbf{q}} V_{\mathbf{q}} + e^{-i\mathbf{q}\cdot\mathbf{r}_j} b_{\mathbf{q}}^{+} V_{\mathbf{q}}^{*} \right) \tag{8.6}$$

is the Hamiltonian of the electron-phonon interaction. Further on, we use the second quantization formalism for electrons, in which the terms H_e, H_{e-e} and H_{e-ph} are

$$H_e = \sum_{\mathbf{k},\sigma} \frac{\hbar^2 k^2}{2m_b} a_{\mathbf{k},\sigma}^{+} a_{\mathbf{k},\sigma}, \tag{8.7}$$

$$H_{e-e} = \frac{1}{2} \sum_{\mathbf{q}\neq 0} v_{\mathbf{q}} \sum_{\substack{\mathbf{k},\sigma \\ \mathbf{k}',\sigma'}} a_{\mathbf{k}+\mathbf{q},\sigma}^{+} a_{\mathbf{k}'-\mathbf{q},\sigma'}^{+} a_{\mathbf{k}',\sigma'} a_{\mathbf{k},\sigma} = \frac{1}{2} \sum_{\mathbf{q}\neq 0} v_{\mathbf{q}} : \rho_{\mathbf{q}} \rho_{-\mathbf{q}} :, \tag{8.8}$$

$$H_{e-ph} = \sum_{\mathbf{q}} \left(V_{\mathbf{q}} b_{\mathbf{q}} \rho_{\mathbf{q}} + V_{\mathbf{q}}^{*} b_{\mathbf{q}}^{+} \rho_{-\mathbf{q}} \right), \tag{8.9}$$

where : ... : is the symbol of the normal product of operators,

$$v_{\mathbf{q}} = \frac{4\pi e^2}{\varepsilon_\infty q^2 V} \tag{8.10}$$

is the Fourier component of the Coulomb potential, and

$$\rho_{\mathbf{q}} = \sum_{j=1}^{N} e^{i\mathbf{q}\cdot\mathbf{r}_j} = \sum_{\mathbf{k},\sigma} a_{\mathbf{k}+\mathbf{q},\sigma}^{+} a_{\mathbf{k},\sigma} \tag{8.11}$$

is the Fourier component of the electron density.

The ground state energy of the many-polaron Hamiltonian (8.1) has been studied by L. Lemmens, J. T. Devreese and F. Brosens (LDB) [91], for weak and intermediate strength of the electron-phonon coupling. They introduce a variational wave function:

$$|\psi_{\mathrm{LDB}}\rangle = U\,|\phi\rangle \left|\psi_{el}^{(0)}\right\rangle, \tag{8.12}$$

where $\left|\psi_{el}^{(0)}\right\rangle$ represents the ground-state many-body wave function for the electron (or hole) system and $|\phi\rangle$ is the phonon vacuum, U is a many-body unitary operator which determines a canonical transformation for a fermion gas interacting with a boson field:

$$U = \exp\left\{ \sum_{j=1}^{N} \sum_{\mathbf{q}} \left(f_{\mathbf{q}} a_{\mathbf{q}} e^{i\mathbf{q}\cdot\mathbf{r}_j} - f_{\mathbf{q}}^{*} a_{\mathbf{q}}^{+} e^{-i\mathbf{q}\cdot\mathbf{r}_j} \right) \right\}. \tag{8.13}$$

In Ref. [91], this canonical transformation was used to establish a many-fermion theory. The $f_{\mathbf{q}}$ were determined variationally [91] resulting in

$$f_{\mathbf{q}} = \frac{V_{\mathbf{q}}}{\hbar\omega_{\mathrm{LO}} + \dfrac{\hbar^2 q^2}{2m_b S(\mathbf{q})}}, \tag{8.14}$$

for a system with total momentum $\mathbf{P} = \sum_j \mathbf{p}_j = 0$. In this expression, $S(\mathbf{q})$ represents the static structure factor of the constituent interacting many electron or hole system :

$$NS(\mathbf{q}) = \left\langle \sum_{j=1}^{N} \sum_{j'=1}^{N} e^{i\mathbf{q}\cdot(\mathbf{r}_j - \mathbf{r}_{j'})} \right\rangle. \tag{8.15}$$

The angular brackets $\langle ... \rangle$ represent the expectation value with respect to the ground state.

The many-polaron optical conductivity is the response of the current-density, in the system described by the Hamiltonian (8.1), to an applied electric field (along the x-axis) with frequency ω. This applied electric field introduces a perturbation term in the Hamiltonian (8.1), which couples the vector potential of the incident electromagnetic field to the current-density. Within linear response theory, the optical conductivity can be expressed through the Kubo formula as a current-current correlation function:

$$\sigma(\omega) = i\frac{Ne^2}{Vm_b\omega} + \frac{1}{V\hbar\omega}\int_0^\infty e^{i\omega t}\left\langle [J_x(t), J_x(0)]\right\rangle dt. \tag{8.16}$$

In this expression, V is the volume of the system, and J_x is the x-component of the current operator $\mathbf{J}$, which is related to the momentum operators of the charge carriers:

$$\mathbf{J} = \frac{q}{m_b}\sum_{j=1}^{N}\mathbf{p}_j = \frac{q}{m_b}\mathbf{P}, \tag{8.17}$$

with q the charge of the charge carriers ($+e$ for holes, $-e$ for electrons) and $\mathbf{P}$ the total momentum operator of the charge carriers. The real part of the optical conductivity at temperature zero, which is proportional to the optical absorption coefficient, can be written as a function of the total momentum operator of the charge carriers as follows :

$$\mathrm{Re}\,\sigma(\omega) = \frac{1}{V\hbar\omega}\frac{e^2}{m_b^2}\,\mathrm{Re}\left\{\int_0^\infty e^{i\omega t}\left\langle [P_x(t), P_x(0)]\right\rangle dt\right\}. \tag{8.18}$$

8.1.2 Force-force correlation function

Let us integrate over time in (8.18) twice by parts as follows:

$$\begin{aligned}
&\int_0^\infty dt\,\langle [P_x(t), P_x]\rangle\, e^{i\omega t-\delta t}\\
&= \frac{1}{i\omega-\delta}\left\{\langle [P_x(t), P_x]\rangle\, e^{i\omega t-\delta t}\Big|_{t=0}^{\infty} - \int_0^\infty dt\left\langle\left[\frac{d}{dt}P_x(t), P_x\right]\right\rangle e^{i\omega t-\delta t}\right\}\\
&= -\frac{1}{i\omega-\delta}\int_0^\infty dt\left\langle\left[\frac{d}{dt}\left(e^{\frac{it}{\hbar}H}P_x e^{-\frac{it}{\hbar}H}\right), P_x\right]\right\rangle e^{i\omega t-\delta t}\\
&= -\frac{1}{i\omega-\delta}\int_0^\infty dt\left\langle\left[\left(e^{\frac{it}{\hbar}H}\frac{i}{\hbar}[H, P_x]\, e^{-\frac{it}{\hbar}H}\right), P_x\right]\right\rangle e^{i\omega t-\delta t}\\
&= -\frac{1}{i\omega-\delta}\int_0^\infty dt\left\langle\left[\frac{i}{\hbar}[H, P_x], e^{-\frac{it}{\hbar}H}P_x e^{\frac{it}{\hbar}H}\right]\right\rangle e^{i\omega t-\delta t}\\
&= -\frac{1}{i\omega-\delta}\int_0^\infty dt\left\langle\left[F_x(0), e^{-\frac{it}{\hbar}H}P_x e^{\frac{it}{\hbar}H}\right]\right\rangle e^{i\omega t-\delta t}\\
&= -\left(\frac{1}{i\omega-\delta}\right)^2\left\{\left\langle\left[F_x(0), e^{-\frac{it}{\hbar}H}P_x e^{\frac{it}{\hbar}H}\right]\right\rangle e^{i\omega t-\delta t}\Big|_{t=0}^{\infty}\right.\\
&\left.-\int_0^\infty dt\left\langle\left[F_x(0), \frac{d}{dt}e^{-\frac{it}{\hbar}H}P_x e^{\frac{it}{\hbar}H}\right]\right\rangle e^{i\omega t-\delta t}\right\}
\end{aligned}$$

$$
\begin{aligned}
&= -\left(\frac{1}{i\omega-\delta}\right)^2\left\{-\langle[F_x,P_x]\rangle+\int_0^\infty dt\left\langle\left[F_x(0),e^{-\frac{it}{\hbar}H}\left(\frac{i}{\hbar}[H,P_x]\right)e^{\frac{it}{\hbar}H}\right]\right\rangle e^{i\omega t-\delta t}\right\}\\
&= -\left(\frac{1}{i\omega-\delta}\right)^2\left\{-\langle[F_x,P_x]\rangle+\int_0^\infty dt\left\langle\left[F_x(0),e^{-\frac{it}{\hbar}H}F_x(0)e^{\frac{it}{\hbar}H}\right]\right\rangle e^{i\omega t-\delta t}\right\}\\
&= -\left(\frac{1}{i\omega-\delta}\right)^2\left\{-\langle[F_x,P_x]\rangle+\int_0^\infty dt\left\langle\left[e^{\frac{it}{\hbar}H}F_x(0)e^{-\frac{it}{\hbar}H},F_x(0)\right]\right\rangle e^{i\omega t-\delta t}\right\}\\
&= \frac{1}{(\omega+i\delta)^2}\left\{-\langle[F_x,P_x]\rangle+\int_0^\infty dt\,\langle[F_x(t),F_x(0)]\rangle e^{i\omega t-\delta t}\right\},
\end{aligned}
$$

where $\mathbf{F}\equiv\frac{i}{\hbar}[H,\mathbf{P}]$ is the operator of the force applied to the center of mass of the electrons.

Since both F_x and P_x are hermitian operators, the average $\langle[F_x,P_x]\rangle$ is imaginary. Hence, for $\omega\neq 0$, this term does not give a contribution into $\operatorname{Re}\sigma(\omega)$. As a result, integrating by parts twice, the real part of the optical conductivity of the many-polaron system is written with a force-force correlation function:

$$
\operatorname{Re}\sigma(\omega)=\frac{1}{V\hbar\omega^3}\frac{e^2}{m_b^2}\operatorname{Re}\left\{\int_0^\infty e^{i\omega t}\langle[F_x(t),F_x(0)]\rangle\,dt\right\}. \tag{8.19}
$$

The force operator is determined as

$$
F_x=\frac{i}{\hbar}[H,P_x]=\frac{i}{\hbar}[H_e+H_{e-e}+H_{ph}+H_{e-ph},P_x].
$$

Further, we use the commutators:

$$
\begin{aligned}
\left[a^+_{\mathbf{k+q},\sigma}a_{\mathbf{k},\sigma},P_x\right]&=\sum_{\mathbf{k}'}\hbar k'_x\left[a^+_{\mathbf{k+q},\sigma}a_{\mathbf{k},\sigma},a^+_{\mathbf{k}',\sigma}a_{\mathbf{k}',\sigma}\right]\\
&=\sum_{\mathbf{k}'}\hbar k'_x\begin{pmatrix} a^+_{\mathbf{k+q},\sigma}a_{\mathbf{k},\sigma}a^+_{\mathbf{k}',\sigma}a_{\mathbf{k}',\sigma}+a^+_{\mathbf{k+q},\sigma}a^+_{\mathbf{k}',\sigma}a_{\mathbf{k},\sigma}a_{\mathbf{k}',\sigma}\\ -a^+_{\mathbf{k}',\sigma}a^+_{\mathbf{k+q},\sigma}a_{\mathbf{k}',\sigma}a_{\mathbf{k},\sigma}-a^+_{\mathbf{k}',\sigma}a_{\mathbf{k}',\sigma}a^+_{\mathbf{k+q},\sigma}a_{\mathbf{k},\sigma}\end{pmatrix}\\
&=\sum_{\mathbf{k}'}\hbar k'_x\left(\delta_{\mathbf{kk}'}a^+_{\mathbf{k+q},\sigma}a_{\mathbf{k}',\sigma}-\delta_{\mathbf{k}',\mathbf{k+q}}a^+_{\mathbf{k}',\sigma}a_{\mathbf{k},\sigma}\right)\\
&=\sum_{\mathbf{k}'}\hbar k'_x\left(\delta_{\mathbf{kk}'}a^+_{\mathbf{k+q},\sigma}a_{\mathbf{k},\sigma}-\delta_{\mathbf{k}',\mathbf{k+q}}a^+_{\mathbf{k+q},\sigma}a_{\mathbf{k},\sigma}\right)\\
&=a^+_{\mathbf{k+q},\sigma}a_{\mathbf{k},\sigma}\sum_{\mathbf{k}'}\hbar k'_x\left(\delta_{\mathbf{kk}'}-\delta_{\mathbf{k}',\mathbf{k+q}}\right)=-\hbar q_x a^+_{\mathbf{k+q},\sigma}a_{\mathbf{k},\sigma},
\end{aligned}
$$

$$
[\rho_{\mathbf{q}},P_x]=-\hbar q_x\rho_{\mathbf{q}}.
$$

Hence, $[H_e,P_x]=0$, $[H_{e-e},P_x]=0$,

$$
\begin{aligned}
[H_{e-ph},P_x]&=\sum_{\mathbf{q}}\left(V_{\mathbf{q}}b_{\mathbf{q}}[\rho_{\mathbf{q}},P_x]+V^*_{\mathbf{q}}b^+_{\mathbf{q}}[\rho_{-\mathbf{q}},P_x]\right)\\
&=-\hbar\sum_{\mathbf{q}}q_x\left(V_{\mathbf{q}}b_{\mathbf{q}}\rho_{\mathbf{q}}-V^*_{\mathbf{q}}b^+_{\mathbf{q}}\rho_{-\mathbf{q}}\right),
\end{aligned}
$$

So, the commutator of the Hamiltonian (8.1) with the total momentum operator of the charge carriers leads to the expression for the force

$$
\mathbf{F}=-i\sum_{\mathbf{q}}\mathbf{q}\left(V_{\mathbf{q}}b_{\mathbf{q}}\rho_{\mathbf{q}}-V^*_{\mathbf{q}}b^+_{\mathbf{q}}\rho_{-\mathbf{q}}\right). \tag{8.20}
$$

This result for the force operator clarifies the significance of using the force-force correlation function rather than the momentum-momentum correlation function. The operator product $F_x(t)F_x(0)$ is proportional to $|V_{\mathbf{k}}|^2$, the charge carrier - phonon interaction strength. This will be a distinct advantage for any expansion of the final result in the charge carrier - phonon interaction strength, since one power of $|V_{\mathbf{k}}|^2$ is factored out beforehand. Substituting (8.20) into (8.19), the real part of the optical conductivity then takes the form:

$$\operatorname{Re}\sigma(\omega) = \frac{1}{V\hbar\omega^3}\frac{e^2}{m_b^2}\operatorname{Re}\int_0^\infty dt e^{i\omega t-\delta t}\sum_{\mathbf{q},\mathbf{q}'} q_x q'_x$$
$$\times\left\langle\left[\left[V_{\mathbf{q}}b_{\mathbf{q}}(t)+V^*_{-\mathbf{q}}b^+_{-\mathbf{q}}(t)\right]\rho_{\mathbf{q}}(t),\left(V_{-\mathbf{q}'}b_{-\mathbf{q}'}+V^*_{\mathbf{q}'}b^+_{\mathbf{q}'}\right)\rho_{-\mathbf{q}'}\right]\right\rangle. \tag{8.21}$$

Up to this point, no approximations other than *linear response theory* have been made.

8.1.3 Canonical transformation

The expectation value appearing in the right hand side of expression (8.21) for the real part of the optical conductivity is calculated now with respect to the LDB many-polaron wave function (8.12). The unitary operator (8.13) can be written as

$$U = \exp\sum_{\mathbf{q}} A_{\mathbf{q}}\rho_{\mathbf{q}}, \quad A_{\mathbf{q}} = f_{\mathbf{q}}b_{\mathbf{q}} - f^*_{-\mathbf{q}}b^+_{-\mathbf{q}}, \tag{8.22}$$

The transformed Hamiltonian (8.2) is denoted as

$$\tilde{H} = U^{-1}HU. \tag{8.23}$$

The momentum operator of an electron $\mathbf{p}_j$, the operator of the total momentum of electrons $\mathbf{P}$ and the phonon creation and annihilation operators are transformed by the unitary transformation (8.22) as follows:

$$U^{-1}\mathbf{p}_jU = \mathbf{p}_j + \sum_{\mathbf{q}}\hbar\mathbf{q}A_{\mathbf{q}}e^{i\mathbf{q}\cdot\mathbf{r}_j}, \tag{8.24}$$

$$U^{-1}\mathbf{P}U = \mathbf{P} + \sum_{\mathbf{q}}\hbar\mathbf{q}A_{\mathbf{q}}\rho_{\mathbf{q}}, \tag{8.25}$$

$$U^{-1}b_{\mathbf{q}}U = b_{\mathbf{q}} - f^*_{\mathbf{q}}\rho_{-\mathbf{q}}, \quad U^{-1}b^+_{\mathbf{q}}U = b^+_{\mathbf{q}} - f_{\mathbf{q}}\rho_{\mathbf{q}}. \tag{8.26}$$

As a result, after the transformation (8.22), the Hamiltonian takes the form (see Ref. [91]):

$$\tilde{H} = H_e + \tilde{H}_{e-e} + H_{ph} + \tilde{H}_{e-ph} + H_N + H_{ppe}, \tag{8.27}$$

where the terms are

$$\tilde{H}_{e-e} = \frac{1}{2}\sum_{\mathbf{q}\neq 0}\tilde{v}_{\mathbf{q}} : \rho_{\mathbf{q}}\rho_{-\mathbf{q}} :, \quad \tilde{v}_{\mathbf{q}} = v_{\mathbf{q}} + 2\left(\hbar\omega_{\mathrm{LO}}|f_{\mathbf{q}}|^2 - V_{\mathbf{q}}f^*_{\mathbf{q}} - V^*_{\mathbf{q}}f_{\mathbf{q}}\right), \tag{8.28}$$

$$\tilde{H}_{e-ph} = \sum_{\mathbf{q}}\left[\left(V_{\mathbf{q}} - \hbar\omega_{\mathrm{LO}}f_{\mathbf{q}}\right)b_{\mathbf{q}}\rho_{\mathbf{q}} + \left(V^*_{\mathbf{q}} - \hbar\omega_{\mathrm{LO}}f^*_{\mathbf{q}}\right)b^+_{\mathbf{q}}\rho_{-\mathbf{q}}\right]$$
$$+\frac{\hbar^2}{2m_b}\sum_{\mathbf{q}}A_{\mathbf{q}}\sum_{\mathbf{k},\sigma}\left(\mathbf{q}^2 + 2\mathbf{k}\cdot\mathbf{q}\right)a^+_{\mathbf{k}+\mathbf{q},\sigma}a_{\mathbf{k},\sigma}, \tag{8.29}$$

$$H_N = \hat{N} \sum_{\mathbf{q}} \left(\hbar\omega_{\mathrm{LO}} \left| f_{\mathbf{q}} \right|^2 - V_{\mathbf{q}} f_{\mathbf{q}}^* - V_{\mathbf{q}}^* f_{\mathbf{q}} \right), \quad \left(\hat{N} \equiv \sum_{\mathbf{k},\sigma} a_{\mathbf{k},\sigma}^+ a_{\mathbf{k},\sigma} \right), \tag{8.30}$$

$$H_{ppe} = \frac{\hbar^2}{2m_b} \sum_{\mathbf{q}\mathbf{q}'} \mathbf{q} \cdot \mathbf{q}' A_{\mathbf{q}} A_{\mathbf{q}'} \rho_{\mathbf{q}+\mathbf{q}'}. \tag{8.31}$$

The exact expression for the real part of the conductivity (8.21) after the replacement of $|\Psi_0\rangle$ by $|\Psi_{LDB}\rangle = U|\phi\rangle \left|\psi_{el}^{(0)}\right\rangle$ is transformed to the approximate one

$$\begin{aligned}
&\mathrm{Re}\,\sigma(\omega) \\
&= \frac{1}{V\hbar\omega^3} \frac{e^2}{m_b^2} \mathrm{Re} \int_0^\infty dt e^{i\omega t - \delta t} \sum_{\mathbf{q},\mathbf{q}'} q_x q_x' \\
&\times \left\langle \psi_{el}^{(0)} \middle| \left\langle \phi \middle| U^{-1} \begin{bmatrix} e^{\frac{it}{\hbar}H} \left[V_{\mathbf{q}} b_{\mathbf{q}} + V_{-\mathbf{q}}^* b_{-\mathbf{q}}^+ \right] \rho_{\mathbf{q}} e^{-\frac{it}{\hbar}H}, \\ \left(V_{-\mathbf{q}'} b_{-\mathbf{q}'} + V_{\mathbf{q}'}^* b_{\mathbf{q}'}^+ \right) \rho_{-\mathbf{q}'} \end{bmatrix} U \middle| \phi \right\rangle \middle| \psi_{el}^{(0)} \right\rangle \\
&= \frac{1}{V\hbar\omega^3} \frac{e^2}{m_b^2} \mathrm{Re} \int_0^\infty dt e^{i\omega t - \delta t} \sum_{\mathbf{q},\mathbf{q}'} q_x q_x' \\
&\times \left\langle \psi_{el}^{(0)} \middle| \left\langle \phi \middle| \begin{bmatrix} e^{\frac{it}{\hbar}\tilde{H}} U^{-1} \left[V_{\mathbf{q}} b_{\mathbf{q}} + V_{-\mathbf{q}}^* b_{-\mathbf{q}}^+ \right] U \rho_{\mathbf{q}} e^{-\frac{it}{\hbar}\tilde{H}}, \\ U^{-1} \left(V_{-\mathbf{q}'} b_{-\mathbf{q}'} + V_{\mathbf{q}'}^* b_{\mathbf{q}'}^+ \right) U \rho_{-\mathbf{q}'} \end{bmatrix} \middle| \phi \right\rangle \middle| \psi_{el}^{(0)} \right\rangle \\
&= \frac{1}{V\hbar\omega^3} \frac{e^2}{m_b^2} \mathrm{Re} \int_0^\infty dt e^{i\omega t - \delta t} \sum_{\mathbf{q},\mathbf{q}'} q_x q_x' \\
&\times \left\langle \psi_{el}^{(0)} \middle| \left\langle \phi \middle| \left[e^{\frac{it}{\hbar}\tilde{H}} \left(V_{\mathbf{q}} \left(b_{\mathbf{q}} - f_{\mathbf{q}}^* \rho_{-\mathbf{q}} \right) + V_{-\mathbf{q}}^* \left(b_{-\mathbf{q}}^+ - f_{-\mathbf{q}} \rho_{-\mathbf{q}} \right) \right) \rho_{\mathbf{q}} e^{-\frac{it}{\hbar}\tilde{H}}, \right.\right. \\
&\left.\left. \left(V_{-\mathbf{q}'} \left(b_{-\mathbf{q}'} - f_{-\mathbf{q}'}^* \rho_{\mathbf{q}'} \right) + V_{\mathbf{q}'}^* \left(b_{\mathbf{q}'}^+ - f_{\mathbf{q}'} \rho_{\mathbf{q}'} \right) \right) \rho_{-\mathbf{q}'} \right] \middle| \phi \right\rangle \middle| \psi_{el}^{(0)} \right\rangle.
\end{aligned}$$

So, we have arrived at the expression

$$\begin{aligned}
\mathrm{Re}\,\sigma(\omega) &= \frac{1}{V\hbar\omega^3} \frac{e^2}{m_b^2} \mathrm{Re} \int_0^\infty dt e^{i\omega t - \delta t} \sum_{\mathbf{q},\mathbf{q}'} q_x q_x' \\
\times \left\langle \psi_{el}^{(0)} \middle| \left\langle \phi \middle| \left[e^{\frac{it}{\hbar}\tilde{H}} \left(V_{\mathbf{q}} \left(b_{\mathbf{q}} - f_{\mathbf{q}}^* \rho_{-\mathbf{q}} \right) + V_{-\mathbf{q}}^* \left(b_{-\mathbf{q}}^+ - f_{-\mathbf{q}} \rho_{-\mathbf{q}} \right) \right) \rho_{\mathbf{q}} e^{-\frac{it}{\hbar}\tilde{H}}, \right.\right. \\
\left.\left. \left(V_{-\mathbf{q}'} \left(b_{-\mathbf{q}'} - f_{-\mathbf{q}'}^* \rho_{\mathbf{q}'} \right) + V_{\mathbf{q}'}^* \left(b_{\mathbf{q}'}^+ - f_{\mathbf{q}'} \rho_{\mathbf{q}'} \right) \right) \rho_{-\mathbf{q}'} \right] \middle| \phi \right\rangle \middle| \psi_{el}^{(0)} \right\rangle.
\end{aligned}$$

Since $\rho_{\mathbf{q}} \rho_{-\mathbf{q}} = \rho_{-\mathbf{q}} \rho_{\mathbf{q}}$, and $V_{\mathbf{q}} f_{\mathbf{q}}^* = V_{-\mathbf{q}} f_{-\mathbf{q}}^*$, the terms proportional to $\rho_{-\mathbf{q}} \rho_{\mathbf{q}}$ vanish after the summation over $\mathbf{q}$:

$$\sum_{\mathbf{q}} q_x V_{\mathbf{q}} f_{\mathbf{q}}^* \rho_{-\mathbf{q}} \rho_{\mathbf{q}} \overset{\mathbf{q} \to -\mathbf{q}}{=} - \sum_{\mathbf{q}} q_x V_{\mathbf{q}} f_{\mathbf{q}}^* \rho_{-\mathbf{q}} \rho_{\mathbf{q}} = 0. \tag{8.32}$$

Hence we obtain the real part of the optical conductivity in the form

$$\begin{aligned}
\mathrm{Re}\,\sigma(\omega) = \frac{1}{V\hbar\omega^3} \frac{e^2}{m_b^2} \mathrm{Re} \int_0^\infty dt e^{i\omega t - \delta t} \sum_{\mathbf{q},\mathbf{q}'} q_x q_x' \\
\times \left\langle \psi_{el}^{(0)} \middle| \left\langle \phi \middle| \left[e^{\frac{it}{\hbar}\tilde{H}} \left(V_{\mathbf{q}} b_{\mathbf{q}} + V_{-\mathbf{q}}^* b_{-\mathbf{q}}^+ \right) \rho_{\mathbf{q}} e^{-\frac{it}{\hbar}\tilde{H}}, \right.\right. \\
\left.\left. \left(V_{-\mathbf{q}'} b_{-\mathbf{q}'} + V_{\mathbf{q}'}^* b_{\mathbf{q}'}^+ \right) \rho_{-\mathbf{q}'} \right] \middle| \phi \right\rangle \middle| \psi_{el}^{(0)} \right\rangle.
\end{aligned} \tag{8.33}$$

Introducing the factor

$$\mathcal{J}(\mathbf{q},\mathbf{q}') = \left\langle \psi_{el}^{(0)} \middle| \left\langle \phi \middle| \left[e^{\frac{it}{\hbar}\tilde{H}} \left(V_{\mathbf{q}} b_{\mathbf{q}} + V_{-\mathbf{q}}^{*} b_{-\mathbf{q}}^{+} \right) \rho_{\mathbf{q}} e^{-\frac{it}{\hbar}\tilde{H}}, \right.\right.$$
$$\left.\left. \left(V_{-\mathbf{q}'} b_{-\mathbf{q}'} + V_{\mathbf{q}'}^{*} b_{\mathbf{q}'}^{+} \right) \rho_{-\mathbf{q}'} \right] \middle| \phi \right\rangle \middle| \psi_{el}^{(0)} \right\rangle, \tag{8.34}$$

the optical conductivity can be written as

$$\operatorname{Re}\sigma(\omega) = \frac{1}{V\hbar\omega^3} \frac{e^2}{m_b^2} \operatorname{Re} \int_0^\infty dt e^{i\omega t - \delta t} \sum_{\mathbf{q},\mathbf{q}'} q_x q_x' \mathcal{J}(\mathbf{q},\mathbf{q}'). \tag{8.35}$$

In the case of a weak electron-phonon coupling, we can neglect in the exponent $e^{-\frac{it}{\hbar}\tilde{H}}$ of (8.33) the terms $\tilde{H}_{e-ph}$ and H_{ppe} [i. e., the renormalized Hamiltonian of the electron-phonon interaction (8.28) and (8.31)]. Namely, we replace $\tilde{H}$ in Eq. (8.33) by the Hamiltonian

$$\tilde{H}_0 = H_e + \tilde{H}_{e-e} + H_{ph} + H_N. \tag{8.36}$$

In this case, we find

$$\mathcal{J}(\mathbf{q},\mathbf{q}') = \left\langle \psi_{el}^{(0)} \middle| \left\langle \phi \middle| \left[e^{\frac{it}{\hbar}\tilde{H}_0} \left(V_{\mathbf{q}} b_{\mathbf{q}} + V_{-\mathbf{q}}^{*} b_{-\mathbf{q}}^{+} \right) \rho_{\mathbf{q}} e^{-\frac{it}{\hbar}\tilde{H}_0}, \right.\right.$$
$$\left.\left. \left(V_{-\mathbf{q}'} b_{-\mathbf{q}'} + V_{\mathbf{q}'}^{*} b_{\mathbf{q}'}^{+} \right) \rho_{-\mathbf{q}'} \right] \middle| \phi \right\rangle \middle| \psi_{el}^{(0)} \right\rangle$$

$$= |V_{\mathbf{q}}|^2 \delta_{\mathbf{q}\mathbf{q}'} \left\langle \psi_{el}^{(0)} \middle| \left\langle \phi \middle| e^{i\tilde{H}_0 t/\hbar} \rho_{\mathbf{q}} b_{\mathbf{q}} e^{-i\tilde{H}_0 t/\hbar} \rho_{-\mathbf{q}} b_{\mathbf{q}}^{+} \right.\right.$$
$$\left.\left. - \rho_{\mathbf{q}} b_{\mathbf{q}} e^{i\tilde{H}_0 t/\hbar} \rho_{-\mathbf{q}} b_{\mathbf{q}}^{+} e^{-i\tilde{H}_0 t/\hbar} \middle| \phi \right\rangle \middle| \psi_{el}^{(0)} \right\rangle$$
$$= 2i|V_{\mathbf{q}}|^2 \delta_{\mathbf{q}\mathbf{q}'} \operatorname{Im} \left[\left\langle \psi_{el}^{(0)} \middle| \left\langle \phi \middle| e^{i\tilde{H}_0 t/\hbar} \rho_{\mathbf{q}} b_{\mathbf{q}} e^{-i\tilde{H}_0 t/\hbar} \rho_{-\mathbf{q}} b_{\mathbf{q}}^{+} \middle| \phi \right\rangle \middle| \psi_{el}^{(0)} \right\rangle \right].$$

The time-dependent phonon operators are

$$e^{i\tilde{H}_0 t/\hbar} b_{\mathbf{q}} e^{-i\tilde{H}_0 t/\hbar} = b_{\mathbf{q}} e^{-i\omega_{\mathrm{LO}} t},$$

so that we have

$$\mathcal{J}(\mathbf{q},\mathbf{q}') = 2i|V_{\mathbf{q}}|^2 \delta_{\mathbf{q}\mathbf{q}'} \operatorname{Im} \left[e^{-i\omega_{\mathrm{LO}} t} \left\langle \psi_{el}^{(0)} \middle| \left\langle \phi \middle| e^{i\tilde{H}_0 t/\hbar} \rho_{\mathbf{q}} e^{-i\tilde{H}_0 t/\hbar} \rho_{-\mathbf{q}} b_{\mathbf{q}} b_{\mathbf{q}}^{+} \middle| \phi \right\rangle \middle| \psi_{el}^{(0)} \right\rangle \right]$$
$$= 2i|V_{\mathbf{q}}|^2 \delta_{\mathbf{q}\mathbf{q}'} \operatorname{Im} \left[\left\langle \psi_{el}^{(0)} \middle| e^{i\tilde{H}_e t/\hbar} \rho_{\mathbf{q}} e^{-i\tilde{H}_e t/\hbar} \rho_{-\mathbf{q}} \middle| \psi_{el}^{(0)} \right\rangle \left\langle \phi \middle| b_{\mathbf{q}} b_{\mathbf{q}}^{+} \middle| \phi \right\rangle \right],$$

where $\tilde{H}_e = H_e + \tilde{H}_{e-e} + H_N$.

Taking the expectation value with respect to the phonon vacuum, we find

$$\mathcal{J}(\mathbf{q},\mathbf{q}') = 2i|V_{\mathbf{q}}|^2 \delta_{\mathbf{q}\mathbf{q}'} \operatorname{Im} \left[e^{-i\omega_{\mathrm{LO}} t} \left\langle \psi_{el}^{(0)} \middle| e^{i\tilde{H}_e t/\hbar} \rho_{\mathbf{q}} e^{-i\tilde{H}_e t/\hbar} \rho_{-\mathbf{q}} \middle| \psi_{el}^{(0)} \right\rangle \right]. \tag{8.37}$$

The optical conductivity (8.33) then takes the form:

$$\operatorname{Re}\sigma(\omega) = -\frac{2e^2}{V\hbar m_b^2 \omega^3} \operatorname{Im} \int_0^\infty dt e^{i\omega t - \delta t} \sum_{\mathbf{q}} q_x^2 |V_{\mathbf{q}}|^2$$
$$\times \operatorname{Im} \left[e^{-i\omega_{\mathrm{LO}} t} \left\langle \psi_{el}^{(0)} \middle| e^{i\tilde{H}_e t/\hbar} \rho_{\mathbf{q}} e^{-i\tilde{H}_e t/\hbar} \rho_{-\mathbf{q}} \middle| \psi_{el}^{(0)} \right\rangle \right] \tag{8.38}$$

For an isotropic electron-phonon system, q_x^2 in 3D can be replaced by $\frac{1}{3}\left(q_x^2+q_y^2+q_z^2\right)=\frac{1}{3}q^2$, what gives us the result

$$\operatorname{Re}\sigma_{3\mathrm{D}}(\omega)=-\frac{2}{3V\hbar\omega^3}\frac{e^2}{m_b^2}\sum_{\mathbf{q}}q^2\left|V_{\mathbf{q}}\right|^2\operatorname{Im}\int_0^\infty dte^{i\omega t-\delta t}\operatorname{Im}\left[e^{-i\omega_{\mathrm{LO}}t}F(\mathbf{q},t)\right], \tag{8.39}$$

where the two-point correlation function is

$$F(\mathbf{q},t)=\left\langle\psi_{el}^{(0)}\left|e^{\frac{it}{\hbar}\tilde{H}_e}\rho_{\mathbf{q}}e^{-\frac{it}{\hbar}\tilde{H}_e}\rho_{-\mathbf{q}}\right|\psi_{el}^{(0)}\right\rangle. \tag{8.40}$$

The same derivation for the 2D case, provides the expression

$$\operatorname{Re}\sigma_{2\mathrm{D}}(\omega)=-\frac{1}{A\hbar\omega^3}\frac{e^2}{m_b^2}\sum_{\mathbf{q}}q^2\left|V_{\mathbf{q}}\right|^2\operatorname{Im}\int_0^\infty dte^{i\omega t-\delta t}\operatorname{Im}\left[e^{-i\omega_{\mathrm{LO}}t}F(\mathbf{q},t)\right], \tag{8.41}$$

where A is the surface of the 2D system.

8.1.4 Dynamic structure factor

To find the formula for the real part of the optical conductivity in its final form, we introduce the standard expression for the dynamic structure factor of the system of charge carriers interacting through a Coulomb potential,

$$S(\mathbf{q},\omega)=\frac{1}{2N}\int_{-\infty}^{\infty}\left\langle\psi_{el}^{(0)}\left|\sum_{j,\ell}e^{i\mathbf{q}\cdot(\mathbf{r}_j(t)-\mathbf{r}_\ell(0))}\right|\psi_{el}^{(0)}\right\rangle e^{i\omega t}dt. \tag{8.42}$$

The dynamic structure factor is expressed in terms of the two-point correlation function as follows:

$$\begin{aligned}S(\mathbf{q},\omega)&=\frac{1}{2N}\int_{-\infty}^{\infty}\left\langle\psi_{el}^{(0)}\left|e^{\frac{it}{\hbar}\tilde{H}_e}\rho_{\mathbf{q}}e^{-\frac{it}{\hbar}\tilde{H}_e}\rho_{-\mathbf{q}}\right|\psi_{el}^{(0)}\right\rangle e^{i\omega t}dt\\&=\frac{1}{2N}\int_{-\infty}^{\infty}F(\mathbf{q},t)\,e^{i\omega t}dt=\frac{1}{2N}F(\mathbf{q},\omega)\end{aligned}$$

$$\Downarrow$$

$$S(\mathbf{q},\omega)=\frac{1}{2N}F(\mathbf{q},\omega), \tag{8.43}$$

where $F(\mathbf{q},\omega)$ is the Fourier image of $F(\mathbf{q},t)$:

$$F(\mathbf{q},\omega)=\int_{-\infty}^{\infty}F(\mathbf{q},t)\,e^{i\omega t}dt. \tag{8.44}$$

The function $F(\mathbf{q},t)$ obeys the following property:

$$\begin{aligned}F^*(\mathbf{q},t)&=\left\langle\psi_{el}^{(0)}\left|\rho_{-\mathbf{q}}^{+}e^{\frac{it}{\hbar}\tilde{H}_e}\rho_{\mathbf{q}}^{+}e^{-\frac{it}{\hbar}\tilde{H}_e}\right|\psi_{el}^{(0)}\right\rangle\\&=\left\langle\psi_{el}^{(0)}\left|\rho_{\mathbf{q}}e^{\frac{it}{\hbar}\tilde{H}_e}\rho_{-\mathbf{q}}e^{-\frac{it}{\hbar}\tilde{H}_e}\right|\psi_{el}^{(0)}\right\rangle\\&=\left\langle\psi_{el}^{(0)}\left|\rho_{\mathbf{q}}e^{\frac{it}{\hbar}\tilde{H}_e}\rho_{-\mathbf{q}}\right|\psi_{el}^{(0)}\right\rangle e^{-\frac{it}{\hbar}\tilde{E}_0},\end{aligned}$$

where $\tilde{E}_0$ is the eigenvalue of the Hamiltonian $\tilde{H}_e$:

$$\tilde{H}_e \left|\psi_{el}^{(0)}\right\rangle = \tilde{E}_0 \left|\psi_{el}^{(0)}\right\rangle .$$

Herefrom, we find that

$$\begin{aligned} F^*(\mathbf{q},t) &= e^{-\frac{it}{\hbar}\tilde{E}_0} \left\langle \psi_{el}^{(0)} \left| \rho_{\mathbf{q}} e^{\frac{it}{\hbar}\tilde{H}_e} \rho_{-\mathbf{q}} \right| \psi_{el}^{(0)} \right\rangle \\ &= \left\langle \psi_{el}^{(0)} \left| e^{-\frac{it}{\hbar}\tilde{H}_e} \rho_{\mathbf{q}} e^{\frac{it}{\hbar}\tilde{H}_e} \rho_{-\mathbf{q}} \right| \psi_{el}^{(0)} \right\rangle = F(\mathbf{q},-t) . \end{aligned} \tag{8.45}$$

From (8.45), for the function

$$B(\mathbf{q},t) \equiv \operatorname{Im}\left[e^{-i\omega_{\mathrm{LO}}t} F(\mathbf{q},t)\right] \tag{8.46}$$

the following equality is derived:

$$\begin{aligned} B(\mathbf{q},-t) &= \operatorname{Im}\left[e^{i\omega_{\mathrm{LO}}t} F(\mathbf{q},-t)\right] \\ &= \operatorname{Im}\left[e^{i\omega_{\mathrm{LO}}t} F^*(\mathbf{q},t)\right] \\ &= -\operatorname{Im}\left[e^{-i\omega_{\mathrm{LO}}t} F(\mathbf{q},t)\right] = -B(\mathbf{q},t) , \end{aligned}$$

$$B(\mathbf{q},-t) = -B(\mathbf{q},t) . \tag{8.47}$$

The integral in Eq. (8.39)

$$\operatorname{Im}\int_0^\infty dt e^{i\omega t-\delta t} \operatorname{Im}\left[e^{-i\omega_{\mathrm{LO}}t} F(\mathbf{q},t)\right] = \operatorname{Im}\int_0^\infty dt e^{i\omega t-\delta t} B(\mathbf{q},t)$$

is then transformed as follows:

$$\begin{aligned} \operatorname{Im}\int_0^\infty dt e^{i\omega t-\delta t} B(\mathbf{q},t) &= \frac{1}{2i}\left[\int_0^\infty dt e^{i\omega t-\delta t} B(\mathbf{q},t) - \int_0^\infty dt e^{-i\omega t-\delta t} B(\mathbf{q},t)\right] \\ &= \frac{1}{2i}\left[\int_0^\infty dt e^{i\omega t-\delta t} B(\mathbf{q},t) - \int_{-\infty}^0 dt e^{i\omega t+\delta t} B(\mathbf{q},-t)\right] \\ &= \frac{1}{2i}\left[\int_0^\infty dt e^{i\omega t-\delta t} B(\mathbf{q},t) + \int_{-\infty}^0 dt e^{i\omega t+\delta t} B(\mathbf{q},t)\right] \\ &= \frac{1}{2i}\int_{-\infty}^\infty dt e^{i\omega t-\delta|t|} B(\mathbf{q},t) \\ &= \frac{1}{2i}\int_{-\infty}^\infty dt e^{i\omega t-\delta|t|} \frac{1}{2i}\left[e^{-i\omega_{\mathrm{LO}}t} F(\mathbf{q},t) - e^{i\omega_{\mathrm{LO}}t} F^*(\mathbf{q},t)\right] \\ &= -\frac{1}{4}\int_{-\infty}^\infty dt e^{i\omega t-\delta|t|} \left[e^{-i\omega_{\mathrm{LO}}t} F(\mathbf{q},t) - e^{i\omega_{\mathrm{LO}}t} F(\mathbf{q},-t)\right] . \end{aligned}$$

We can show that, as far as $\left|\psi_{el}^{(0)}\right\rangle$ is the *ground* state, the integral $\int_{-\infty}^\infty dt e^{i\omega t-\delta|t|} F(\mathbf{q},-t)$ for positive ω is equal to zero. Let $\left\{\left|\psi_{el}^{(n)}\right\rangle\right\}$ is the total basis set of the eigenfunctions of the Hamiltonian $\tilde{H}_e$. Using these functions we expand $F(\mathbf{q},t)$:

$$\begin{aligned} F(\mathbf{q},t) &= \sum_n \left\langle \psi_{el}^{(0)} \left| e^{\frac{it}{\hbar}\tilde{H}_e} \rho_{\mathbf{q}} e^{-\frac{it}{\hbar}\tilde{H}_e} \right| \psi_{el}^{(n)} \right\rangle \left\langle \psi_{el}^{(n)} \left| \rho_{-\mathbf{q}} \right| \psi_{el}^{(0)} \right\rangle \\ &= \sum_n \left| \left\langle \psi_{el}^{(n)} \left| \rho_{-\mathbf{q}} \right| \psi_{el}^{(0)} \right\rangle \right|^2 e^{\frac{it}{\hbar}\left(\tilde{E}_0-\tilde{E}_n\right)}, \end{aligned}$$

$$\int_{-\infty}^{\infty} dt e^{i\omega t-\delta|t|} F(\mathbf{q},-t) = \sum_n \left|\left\langle \psi_{el}^{(n)} \left|\rho_{-\mathbf{q}}\right| \psi_{el}^{(0)} \right\rangle\right|^2 \int_{-\infty}^{\infty} dt e^{i\omega t+\frac{i}{\hbar}\left(\tilde{E}_n-\tilde{E}_0\right)t-\delta|t|}$$
$$= \sum_n \left|\left\langle \psi_{el}^{(n)} \left|\rho_{-\mathbf{q}}\right| \psi_{el}^{(0)} \right\rangle\right|^2 2\pi\delta\left(\omega+\frac{\tilde{E}_n-\tilde{E}_0}{\hbar}\right) = 0,$$

because for $\omega > 0$, $\omega + \frac{\tilde{E}_n-\tilde{E}_0}{\hbar}$ is never equal to zero.

So, rewriting expression (8.39) with the dynamic structure factor of the electron (or hole) gas results in:

$$\operatorname{Re}\sigma_{3\mathrm{D}}(\omega) = \frac{1}{6V\hbar\omega^3}\frac{e^2}{m_b^2}\sum_{\mathbf{q}} q^2 |V_{\mathbf{q}}|^2 \int_{-\infty}^{\infty} dt e^{i(\omega-\omega_{\mathrm{LO}})t-\delta|t|} F(\mathbf{q},t),$$
$$\operatorname{Re}\sigma_{2\mathrm{D}}(\omega) = \frac{1}{4A\hbar\omega^3}\frac{e^2}{m_b^2}\sum_{\mathbf{q}} q^2 |V_{\mathbf{q}}|^2 \int_{-\infty}^{\infty} dt e^{i(\omega-\omega_{\mathrm{LO}})t-\delta|t|} F(\mathbf{q},t),$$

and we obtain

$$\operatorname{Re}\sigma_{3\mathrm{D}}(\omega) = \frac{n_0}{3\hbar\omega^3}\frac{e^2}{m_b^2}\sum_{\mathbf{q}} q^2|V_{\mathbf{q}}|^2 S(\mathbf{q},\omega-\omega_{\mathrm{LO}}), \tag{8.48a}$$
$$\operatorname{Re}\sigma_{2\mathrm{D}}(\omega) = \frac{n_0}{2\hbar\omega^3}\frac{e^2}{m_b^2}\sum_{\mathbf{q}} q^2|V_{\mathbf{q}}|^2 S(\mathbf{q},\omega-\omega_{\mathrm{LO}}), \tag{8.48b}$$

where

$$n_0 = \begin{cases} N/V \text{ in 3D}, \\ N/A \text{ in 2D} \end{cases}$$

is the density of charge carriers.

For an isotropic medium, the dynamic structure factor does not depend on the direction of $\mathbf{q}$, so that $S(\mathbf{q},\omega) = S(q,\omega)$, where $q = |\mathbf{q}|$. Let us simplify the expression (8.48a) using explicitly the amplitudes of the Fröhlich electron-phonon interaction. The modulus squared of the Fröhlich electron-phonon interaction amplitude is given by

$$|V_{\mathbf{q}}|^2 = \begin{cases} \dfrac{(\hbar\omega_{\mathrm{LO}})^2}{q^2}\dfrac{4\pi\alpha}{V}\left(\dfrac{\hbar}{2m_b\omega_{\mathrm{LO}}}\right)^{1/2} & \text{in 3D} \\ \dfrac{(\hbar\omega_{\mathrm{LO}})^2}{q}\dfrac{2\pi\alpha}{A}\left(\dfrac{\hbar}{2m_b\omega_{\mathrm{LO}}}\right)^{1/2} & \text{in 2D}, \end{cases} \tag{8.49}$$

where α is the (dimensionless) Fröhlich coupling constant determining the coupling strength between the charge carriers and the longitudinal optical phonons [85, 86]. In 3D and 2D, respectively, the sums over $\mathbf{q}$ is transformed to the integrals as follows:

$$\text{3D: } \sum_{\mathbf{q}} \ldots = \frac{V}{(2\pi)^3}\int d\mathbf{q}\ldots$$
$$\text{2D: } \sum_{\mathbf{q}} \ldots = \frac{A}{(2\pi)^2}\int d\mathbf{q}\ldots$$

$$\Downarrow$$

$$\operatorname{Re}\sigma_{3\mathrm{D}}(\omega) = \frac{n_0}{3\hbar\omega^3}\frac{e^2}{m_b^2}\frac{V}{(2\pi)^3}\int d\mathbf{q} q^2 \left|\frac{\hbar\omega_{\mathrm{LO}}}{iq}\left(\frac{4\pi\alpha}{V}\right)^{1/2}\left(\frac{\hbar}{2m_b\omega_{\mathrm{LO}}}\right)^{1/4}\right|^2 S(q,\omega-\omega_{\mathrm{LO}})$$

$$\Downarrow$$

$$\mathrm{Re}\,\sigma_{3\mathrm{D}}(\omega) = \frac{n_0 e^2}{m_b^2}\frac{2\alpha}{3\pi}\frac{\hbar\omega_{\mathrm{LO}}^2}{\omega^3}\left(\frac{\hbar}{2m_b\omega_{\mathrm{LO}}}\right)^{1/2}\int_0^\infty q^2 S(q,\omega-\omega_{\mathrm{LO}})dq. \tag{8.51}$$

In the same way, we transform $\mathrm{Re}\,\sigma_{2\mathrm{D}}(\omega)$:

$$\mathrm{Re}\,\sigma_{2\mathrm{D}}(\omega) = \frac{n_0 e^2}{m_b^2}\frac{\alpha}{2}\frac{\hbar\omega_{\mathrm{LO}}^2}{\omega^3}\left(\frac{\hbar}{2m_b\omega_{\mathrm{LO}}}\right)^{1/2}\int_0^\infty q^2 S(q,\omega-\omega_{\mathrm{LO}})dq.$$

Using the Feynman units ($\hbar = 1$, $m_b = 1$, $\omega_{\mathrm{LO}} = 1$), $\mathrm{Re}\,\sigma(\omega)$ is

$$\mathrm{Re}\,\sigma_{3\mathrm{D}}(\omega) = n_0 e^2\frac{\sqrt{2}\alpha}{3\pi}\frac{1}{\omega^3}\int_0^\infty q^2 S(q,\omega-1)dq, \tag{8.52}$$

$$\mathrm{Re}\,\sigma_{2\mathrm{D}}(\omega) = n_0 e^2\frac{\alpha}{2\sqrt{2}}\frac{1}{\omega^3}\int_0^\infty q^2 S(q,\omega-1)dq. \tag{8.53}$$

From these expressions, it is clear that the scaling relation

$$\mathrm{Re}\,\sigma_{2\mathrm{D}}(\omega,\alpha) = \mathrm{Re}\,\sigma_{3\mathrm{D}}(\omega,\frac{3\pi}{4}\alpha) \tag{8.54}$$

which holds for the one-polaron case introduced in ref. [85, 86], is also valid for the many-polaron case if the corresponding 2D or 3D dynamic structure factor is used.

Calculation of the dynamic structure factor using the retarded Green's functions

The dynamic structure factor $S(\mathbf{q},\omega)$ is expressed through the two-point correlation function by Eq. (8.43). The correlation function $F(\mathbf{q},\omega)$ can be found using the retarded Green's function of the density operators

$$G^R(\mathbf{q},t) = -i\Theta(t)\left\langle\psi_{el}^{(0)}\left|\left[e^{\frac{it}{\hbar}\tilde{H}_0}\rho_{\mathbf{q}}e^{-\frac{it}{\hbar}\tilde{H}_0},\rho_{-\mathbf{q}}\right]\right|\psi_{el}^{(0)}\right\rangle, \tag{8.55}$$

where $\Theta(t)$ is the step function. Let us consider the more general case of a finite temperature,

$$G^R(\mathbf{q},t) = -i\Theta(t)\left\langle\left[e^{\frac{it}{\hbar}\tilde{H}_0}\rho_{\mathbf{q}}e^{-\frac{it}{\hbar}\tilde{H}_0},\rho_{-\mathbf{q}}\right]\right\rangle, \tag{8.56}$$

where the average is

$$\langle\ldots\rangle \equiv \frac{Tr\left(e^{-\beta\tilde{H}_0}\ldots\right)}{Tr\left(e^{-\beta\tilde{H}_0}\right)},\ \beta = \frac{1}{k_B T}. \tag{8.57}$$

The Fourier image $G^R(\mathbf{q},\omega)$ of the retarded Green's function $G^R(\mathbf{q},t)$ is

$$\begin{aligned}
G^R(\mathbf{q},\omega) &= \int_{-\infty}^{\infty} G^R(\mathbf{q},t)\,e^{i\omega t}dt \\
&= -i\int_0^\infty\left\langle\left[e^{\frac{it}{\hbar}\tilde{H}_0}\rho_{\mathbf{q}}e^{-\frac{it}{\hbar}\tilde{H}_0},\rho_{-\mathbf{q}}\right]\right\rangle e^{i\omega t}dt \\
&= -i\int_0^\infty\left(\left\langle e^{\frac{it}{\hbar}\tilde{H}_0}\rho_{\mathbf{q}}e^{-\frac{it}{\hbar}\tilde{H}_0}\rho_{-\mathbf{q}}\right\rangle - \left\langle\rho_{-\mathbf{q}}e^{\frac{it}{\hbar}\tilde{H}_0}\rho_{\mathbf{q}}e^{-\frac{it}{\hbar}\tilde{H}_0}\right\rangle\right)e^{i\omega t}dt
\end{aligned}$$

The imaginary part of $G^R(\mathbf{q},\omega)$ then is

$$\begin{aligned}
\operatorname{Im} G^R(\mathbf{q},\omega) &= -\operatorname{Re}\int_0^\infty \left(\left\langle e^{\frac{it}{\hbar}\tilde{H}_0}\rho_{\mathbf{q}}e^{-\frac{it}{\hbar}\tilde{H}_0}\rho_{-\mathbf{q}}\right\rangle - \left\langle \rho_{-\mathbf{q}}e^{\frac{it}{\hbar}\tilde{H}_0}\rho_{\mathbf{q}}e^{-\frac{it}{\hbar}\tilde{H}_0}\right\rangle\right)e^{i\omega t}dt \\
&= -\frac{1}{2}\int_0^\infty \left(\left\langle e^{\frac{it}{\hbar}\tilde{H}_0}\rho_{\mathbf{q}}e^{-\frac{it}{\hbar}\tilde{H}_0}\rho_{-\mathbf{q}}\right\rangle - \left\langle \rho_{-\mathbf{q}}e^{\frac{it}{\hbar}\tilde{H}_0}\rho_{\mathbf{q}}e^{-\frac{it}{\hbar}\tilde{H}_0}\right\rangle\right)e^{i\omega t}dt \\
&- \frac{1}{2}\int_0^\infty \left(\left\langle \rho_{\mathbf{q}}e^{\frac{it}{\hbar}\tilde{H}_0}\rho_{-\mathbf{q}}e^{-\frac{it}{\hbar}\tilde{H}_0}\right\rangle - \left\langle e^{\frac{it}{\hbar}\tilde{H}_0}\rho_{-\mathbf{q}}e^{-\frac{it}{\hbar}\tilde{H}_0}\rho_{\mathbf{q}}\right\rangle\right)e^{-i\omega t}dt \\
&= -\frac{1}{2}\int_{-\infty}^\infty \left\langle e^{\frac{it}{\hbar}\tilde{H}_0}\rho_{\mathbf{q}}e^{-\frac{it}{\hbar}\tilde{H}_0}\rho_{-\mathbf{q}}\right\rangle e^{i\omega t}dt + \frac{1}{2}\int_{-\infty}^\infty \left\langle \rho_{-\mathbf{q}}e^{\frac{it}{\hbar}\tilde{H}_0}\rho_{\mathbf{q}}e^{-\frac{it}{\hbar}\tilde{H}_0}\right\rangle e^{i\omega t}dt.
\end{aligned}$$

In the second integral here, we replace t by $(t' + i\hbar\beta)$:

$$\begin{aligned}
&\int_{-\infty}^\infty \frac{Tr\left(e^{-\beta\tilde{H}_0}\rho_{-\mathbf{q}}e^{\frac{it}{\hbar}\tilde{H}_0}\rho_{\mathbf{q}}e^{-\frac{it}{\hbar}\tilde{H}_0}\right)}{Tr\left(e^{-\beta\tilde{H}_0}\right)}e^{i\omega t}dt \\
&= \int_{-\infty-i\hbar\beta}^{\infty-i\hbar\beta} \frac{Tr\left(e^{-\beta\tilde{H}_0}\rho_{-\mathbf{q}}e^{\frac{it'}{\hbar}\tilde{H}_0-\beta\tilde{H}_0}\rho_{\mathbf{q}}e^{-\frac{it'}{\hbar}\tilde{H}_0+\beta\tilde{H}_0}\right)}{Tr\left(e^{-\beta\tilde{H}_0}\right)}e^{i\omega(t'+i\hbar\beta)}dt' \\
&= e^{-\beta\hbar\omega}\int_{-\infty-i\hbar\beta}^{\infty-i\hbar\beta} \frac{Tr\left(e^{\frac{it'}{\hbar}\tilde{H}_0-\beta\tilde{H}_0}\rho_{\mathbf{q}}e^{-\frac{it'}{\hbar}\tilde{H}_0}\rho_{-\mathbf{q}}\right)}{Tr\left(e^{-\beta\tilde{H}_0}\right)}e^{i\omega t'}dt'.
\end{aligned}$$

As far as the integral over t converges (i. e., $\left\langle e^{\frac{it}{\hbar}\tilde{H}_0}\rho_{\mathbf{q}}e^{-\frac{it}{\hbar}\tilde{H}_0}\rho_{-\mathbf{q}}\right\rangle$ tends to zero at $|t| \to \infty$), we can shift the integration contour to the real axis, what gives us the result

$$\begin{aligned}
&\int_{-\infty}^\infty \frac{Tr\left(e^{-\beta\tilde{H}_0}\rho_{-\mathbf{q}}e^{\frac{it}{\hbar}\tilde{H}_0}\rho_{\mathbf{q}}e^{-\frac{it}{\hbar}\tilde{H}_0}\right)}{Tr\left(e^{-\beta\tilde{H}_0}\right)}e^{i\omega t}dt \\
&= e^{-\beta\hbar\omega}\int_{-\infty}^\infty \frac{Tr\left(e^{\frac{it}{\hbar}\tilde{H}_0-\beta\tilde{H}_0}\rho_{\mathbf{q}}e^{-\frac{it}{\hbar}\tilde{H}_0}\rho_{-\mathbf{q}}\right)}{Tr\left(e^{-\beta\tilde{H}_0}\right)}e^{i\omega t}dt, \\
&\Updownarrow \\
&\int_{-\infty}^\infty \left\langle \rho_{-\mathbf{q}}e^{\frac{it}{\hbar}\tilde{H}_0}\rho_{\mathbf{q}}e^{-\frac{it}{\hbar}\tilde{H}_0}\right\rangle e^{i\omega t}dt \\
&= e^{-\beta\hbar\omega}\int_{-\infty}^\infty \left\langle e^{\frac{it}{\hbar}\tilde{H}_0}\rho_{\mathbf{q}}e^{-\frac{it}{\hbar}\tilde{H}_0}\rho_{-\mathbf{q}}\right\rangle e^{i\omega t}dt.
\end{aligned}$$

Herefrom, we find that

$$\operatorname{Im} G^R(\mathbf{q},\omega) = -\frac{1}{2}\left(1 - e^{-\beta\hbar\omega}\right)\int_{-\infty}^\infty \left\langle e^{\frac{it}{\hbar}\tilde{H}_0}\rho_{\mathbf{q}}e^{-\frac{it}{\hbar}\tilde{H}_0}\rho_{-\mathbf{q}}\right\rangle e^{i\omega t}dt$$

$$\Downarrow$$

$$\operatorname{Im} G^R(\mathbf{q},\omega) = -\frac{1}{2}\left(1 - e^{-\beta\hbar\omega}\right)F(\mathbf{q},\omega).$$

So, the equation follows from the analytical properties of the Green's functions:

$$F(\mathbf{q},\omega) = -\frac{2\operatorname{Im} G^R(\mathbf{q},\omega)}{1 - e^{-\beta\hbar\omega}}. \tag{8.58}$$

The formula (8.58) is related to arbitrary temperatures. In the zero-temperature limit ($\beta \to \infty$), the factor $\left(1 - e^{-\beta\hbar\omega}\right)^{-1}$ (8.58) turns into the Heavicide step function $\Theta(\omega)$, what leads to the formula

$$F(\mathbf{q},\omega)|_{T=0} = -2\Theta(\omega)\,\mathrm{Im}\,G^R(\mathbf{q},\omega)\big|_{T=0} \tag{8.59}$$

$$\Downarrow$$

$$S(\mathbf{q},\omega)|_{T=0} = -\frac{1}{N}\Theta(\omega)\,\mathrm{Im}\,G^R(\mathbf{q},\omega)\big|_{T=0} \tag{8.60}$$

The retarded Green function is related to the dielectric function of the electron gas by the following equation:

$$G^R(\mathbf{q},\omega) = \frac{1}{v_{\mathbf{q}}}\left[\frac{1}{\varepsilon(\mathbf{q},\omega)} - 1\right]. \tag{8.61}$$

Within the random phase approximation (RPA), following [72], the expression for $G^R(\mathbf{q},\omega)$ is

$$G^R(\mathbf{q},\omega) = \left[1 - v_{\mathbf{q}}P(\mathbf{q},\omega)\right]^{-1}\hbar P(\mathbf{q},\omega), \tag{8.62}$$

where the polarization function $P(\mathbf{q},\omega)$ is (see, e. g., p. 434 of [72])

$$P(\mathbf{q},\omega) = \frac{1}{\hbar}\sum_{\mathbf{k},\sigma}\frac{f_{\mathbf{k}+\mathbf{q},\sigma} - f_{\mathbf{k},\sigma}}{\omega - \frac{\hbar\mathbf{k}^2}{2m_b} + \frac{\hbar(\mathbf{k}+\mathbf{q})^2}{2m_b} + i\delta}, \quad \delta \to +0 \tag{8.63}$$

with the Fermi distribution function of electrons $f_{\mathbf{k},\sigma}$.

For a finite temperature, the explicit analytic expression for the imaginary part of the structure factor $P_{3\mathrm{D}}(\mathbf{q},\omega)$ is obtained (see [72]),

$$\begin{aligned}\mathrm{Im}\,P_{3\mathrm{D}}(\mathbf{q},\omega) &= \frac{Vm_b^2}{2\pi\hbar^4\beta q}\ln\frac{1+\exp\left\{\beta\left[\mu - E^{(+)}(q,\omega)\right]\right\}}{1+\exp\left\{\beta\left[\mu - E^{(-)}(q,\omega)\right]\right\}},\\ E^{(\pm)}(q,\omega) &\equiv \frac{\left(\hbar\omega \pm \frac{\hbar^2q^2}{2m_b}\right)^2}{4\frac{\hbar^2q^2}{2m_b}},\end{aligned} \tag{8.64}$$

with the chemical potential μ. The real part of the structure factor is obtained using the Kramers-Kronig dispersion relation:

$$\mathrm{Re}\,P(\mathbf{q},\omega) = \frac{1}{\pi}\int_{-\infty}^{\infty}\mathcal{P}\left(\frac{1}{\omega'-\omega}\right)\mathrm{Im}\,P(\mathbf{q},\omega')\,d\omega'. \tag{8.65}$$

Analytical expressions for both real and imaginary parts of $P(\mathbf{q},\omega)$ can be written down for the zero temperature (see [72]),

$$\begin{aligned}\mathrm{Re}\,P_{3\mathrm{D}}(q,\omega) &= -\frac{Vm_b}{4\pi^2\hbar^2q}\left\{\begin{array}{c}\left[k_F^2 - \frac{m_b^2}{\hbar^2q^2}\left(\omega - \frac{\hbar q^2}{2m_b}\right)^2\right]\ln\left|\frac{\omega - \frac{\hbar q^2}{2m_b} - \frac{\hbar k_F q}{m_b}}{\omega - \frac{\hbar q^2}{2m_b} + \frac{\hbar k_F q}{m_b}}\right|\\ + \left[k_F^2 - \frac{m_b^2}{\hbar^2q^2}\left(\omega + \frac{\hbar q^2}{2m_b}\right)^2\right]\ln\left|\frac{\omega + \frac{\hbar q^2}{2m_b} + \frac{\hbar k_F q}{m_b}}{\omega + \frac{\hbar q^2}{2m_b} - \frac{\hbar k_F q}{m_b}}\right|\\ +2k_Fq\end{array}\right\},\\ \mathrm{Im}\,P_{3\mathrm{D}}(q,\omega) &= -\frac{Vm_b}{4\pi\hbar^2q}\left\{\begin{array}{c}\left[k_F^2 - \frac{m_b^2}{\hbar^2q^2}\left(\omega - \frac{\hbar q^2}{2m_b}\right)^2\right]\Theta\left(k_F^2 - \frac{m_b^2}{\hbar^2q^2}\left(\omega - \frac{\hbar q^2}{2m_b}\right)^2\right)\\ -\left[k_F^2 - \frac{m_b^2}{\hbar^2q^2}\left(\omega + \frac{\hbar q^2}{2m_b}\right)^2\right]\Theta\left(k_F^2 - \frac{m_b^2}{\hbar^2q^2}\left(\omega + \frac{\hbar q^2}{2m_b}\right)^2\right)\end{array}\right\},\end{aligned} \tag{8.66}$$

where $k_F = \left(3\pi^2N/V\right)^{1/3}$ is the Fermi wave number.

After substituting into Eq. (8.58) the retarded Green's function (8.62) in terms of the polarization function we arrive at the formula

$$F(\mathbf{q},\omega) = -\frac{2\hbar}{1-e^{-\beta\hbar\omega}}\,\mathrm{Im}\,\frac{P(\mathbf{q},\omega)}{1-v_{\mathbf{q}}P(\mathbf{q},\omega)}$$

$$\Downarrow$$

$$S(\mathbf{q},\omega) = -\frac{\hbar}{N\left(1-e^{-\beta\hbar\omega}\right)}\frac{\mathrm{Im}\,P(\mathbf{q},\omega)}{\left[1-v_{\mathbf{q}}\,\mathrm{Re}\,P(\mathbf{q},\omega)\right]^2+\left[v_{\mathbf{q}}\,\mathrm{Im}\,P(\mathbf{q},\omega)\right]^2}, \tag{8.67}$$

$$S(\mathbf{q},\omega)|_{T=0} = -\frac{\hbar}{N}\Theta(\omega)\frac{\mathrm{Im}\,P(\mathbf{q},\omega)}{\left[1-v_{\mathbf{q}}\,\mathrm{Re}\,P(\mathbf{q},\omega)\right]^2+\left[v_{\mathbf{q}}\,\mathrm{Im}\,P(\mathbf{q},\omega)\right]^2}. \tag{8.68}$$

With this dynamic structure factor, the optical conductivity (8.52) (in the Feynman units) takes the form

$$\mathrm{Re}\,\sigma_{3\mathrm{D}}(\omega) = -e^2\frac{\sqrt{2}\alpha}{3\pi V}\frac{1}{\omega^3}\Theta(\omega-1) \times\int_0^\infty \frac{\mathrm{Im}\,P_{3\mathrm{D}}(q,\omega-1)}{\left[1-v_q\,\mathrm{Re}\,P_{3\mathrm{D}}(q,\omega-1)\right]^2+\left[v_q\,\mathrm{Im}\,P_{3\mathrm{D}}(q,\omega-1)\right]^2}q^2dq. \tag{8.69}$$

Correspondingly, in the 2D case we obtain the expression

$$\mathrm{Re}\,\sigma_{2\mathrm{D}}(\omega) = -e^2\frac{\alpha}{2\sqrt{2}V}\frac{1}{\omega^3}\Theta(\omega-1) \times\int_0^\infty \frac{\mathrm{Im}\,P_{2\mathrm{D}}(q,\omega-1)}{\left[1-v_q\,\mathrm{Re}\,P_{2\mathrm{D}}(q,\omega-1)\right]^2+\left[v_q\,\mathrm{Im}\,P_{2\mathrm{D}}(q,\omega-1)\right]^2}q^2dq. \tag{8.70}$$

Plasmon-phonon contribution

The RPA dynamic structure factor for the electron (or hole) system can be separated in two parts, one related to continuum excitations of the electrons (or holes) S_{cont}, and one related to the undamped plasmon branch:

$$S_{\mathrm{RPA}}(q,\omega) = A_{\mathrm{pl}}(q)\delta\left(\omega-\omega_{\mathrm{pl}}(q)\right)+S_{\mathrm{cont}}(q,\omega), \tag{8.71}$$

where $\omega_{\mathrm{pl}}(q)$ is the wave number dependent plasmon frequency and A_{pl} is the strength of the undamped plasmon branch.

In Eqs. (8.69), (8.70), the contribution of the continuum excitations corresponds to the region (q,ω) where $\mathrm{Im}\,P(q,\omega)\neq 0$. The contribution related to the undamped plasmons is provided by a region of (q,ω), where the equations

$$\begin{cases} \mathrm{Im}\,P(q,\omega)=0 \\ 1-v_q\,\mathrm{Re}\,P(q,\omega)=0 \end{cases}. \tag{8.72}$$

are fulfilled simultaneously. Using (8.61), we find that Eqs. (8.73) are equivalent to

$$\mathrm{Im}\,\frac{1}{\varepsilon(q,\omega)}=0,\quad \mathrm{Re}\,\frac{1}{\varepsilon(q,\omega)}=0. \tag{8.73}$$

In the region where $\mathrm{Im}\,P(\mathbf{q},\omega)=0$, the expression $\frac{\mathrm{Im}\,P(q,\omega)}{\left[1-v_q\,\mathrm{Re}\,P(q,\omega)\right]^2+\left[v_q\,\mathrm{Im}\,P(q,\omega)\right]^2}$ is proportional to the delta function, which gives a finite contribution to the memory function after the

integration over q:

$$\left.\frac{\operatorname{Im} P(q,\omega)}{\left[1-v_q \operatorname{Re} P(q,\omega)\right]^2+\left[v_q \operatorname{Im} P(q,\omega)\right]^2}\right|_{\operatorname{Im} P(q,\omega)=0}$$
$$=\frac{1}{\pi v_q}\delta\left(1-v_q \operatorname{Re} P(q,\omega)\right). \tag{8.74}$$

Using Eq. (8.74), the coefficients $A_{\mathrm{pl}}(q)$ in Eq. (8.71) can be expressed in terms of the polarization function $P(q,\omega)$ as follows:

$$\left.\frac{\operatorname{Im} P(q,\omega)}{\left[1-v_q \operatorname{Re} P(q,\omega)\right]^2+\left[v_q \operatorname{Im} P(q,\omega)\right]^2}\right|_{\operatorname{Im} P(q,\omega)=0}$$
$$=\left.\frac{1}{\pi v_q^2\left|\frac{\partial}{\partial\omega}\operatorname{Re} P(q,\omega)\right|}\right|_{\omega=\omega_{\mathrm{pl}}(q)}\delta\left(\omega-\omega_{\mathrm{pl}}(q)\right)$$
$$\Downarrow$$
$$A_{\mathrm{pl}}(q)=\left.\frac{1}{\pi v_q^2\left|\frac{\partial}{\partial\omega}\operatorname{Re} P(q,\omega)\right|}\right|_{\omega=\omega_{\mathrm{pl}}(q)}. \tag{8.75}$$

The contribution derived from the undamped plasmon branch $A_{\mathrm{pl}}(q)\delta\left(\omega-\omega_{\mathrm{pl}}(q)\right)$ is denoted in Ref. [53] as the *'plasmon-phonon' contribution*. The physical process related to this contribution is the emission of both a phonon and a plasmon in the scattering process.

8.1.5 Comparison to the infrared spectrum of $Nd_{2-x}Ce_xCuO_{2-y}$

Calvani and collaborators have performed doping-dependent measurements of the infrared absorption spectra of the high-T_c material $Nd_{2-x}Ce_xCuO_{2-y}$ (NCCO). The region of the spectrum examined by these authors (50-10000 cm^{-1}) is very rich in absorption features: they observe is a "Drude-like" component at the lowest frequencies, and a set of sharp absorption peaks related to phonons and infrared active modes (up to about 1000 cm^{-1}) possibly associated to small (Holstein) polarons. Three distinct absorption bands can be distinguished: the 'd-band' (around 1000 cm^{-1}), the Mid-Infrared band (MIR, around 5000 cm^{-1}) and the Charge-Transfer band (around 10^4 cm^{-1}). Of all these features, the d-band and, at a higher temperatures, the Drude-like component have (hypothetically) been associated with large polaron optical absorption [92].

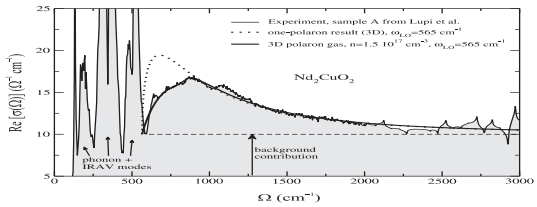

Figure 8.1: The infrared absorption of $Nd_2CuO_{2-\delta}$ ($\delta < 0.004$) is shown as a function of frequency, up to 3000 cm^{-1}. The experimental results of Calvani and co-workers [92] is represented by the thin black curve and by the shaded area. The so-called 'd-band' rises in intensity around 600 cm^{-1} and increases in intensity up to a maximum around 1000 cm^{-1}. The dotted curve shows the single polaron result. The full black curve represents the theoretical results obtained in the present work for the interacting many-polaron gas with $n_0 = 1.5 \times 10^{17}$ cm^{-3}, $\alpha = 2.1$ and $m_b = 0.5\ m_e$. (From Ref. [53].)

For the lowest levels of Ce doping, the d-band can be most clearly distinguished from the other features. The experimental optical absorption spectrum (up to 3000 cm^{-1}) of $Nd_2CuO_{2-\delta}$ ($\delta < 0.004$), obtained by Calvani and co-workers [92], is shown in Fig. 8.1 (shaded area) together with the theoretical curve obtained by the present method (full, bold curve) and, for reference, the one-polaron optical absorption result (dotted curve). At lower frequencies (600-1000 cm^{-1}) a marked difference between the single polaron optical absorption and the many-polaron result is manifest. The experimental d-band can be clearly identified, rising in intensity at about 600 cm^{-1}, peaking around 1000 cm^{-1}, and then decreasing in intensity above that frequency. At a density of $n_0 = 1.5 \times 10^{17}$ cm^{-3}, we found a remarkable agreement between our theoretical predictions and the experimental curve.

8.1.6 Experimental data on the optical absorption in manganites: interpretation in terms of a many-polaron response

In Refs. [93, 94], the experimental results on the optical spectroscopy of $La_{2/3}Sr_{1/3}MnO_3$ (LSMO) and $La_{2/3}Ca_{1/3}MnO_3$ (LCMO) thin films in the mid-infrared frequency region are presented. The optical conductivity spectra of LCMO films are interpreted in [93, 94] in terms of the optical response of small polarons, while the optical conductivity spectra of LSMO films are explained using the large-polaron picture (see Fig. 8.2).

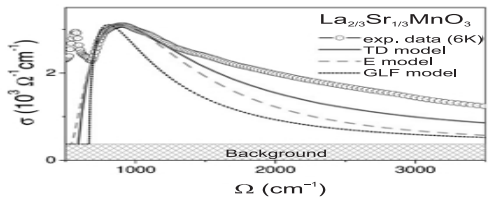

Figure 8.2: Comparison of the low-temperature MIR optical conductivity to $\sigma(\omega)$ from various model calculations: the solid line refers to the weak-coupling approach of Tempere and Devreese [53] modified for an on-site Hubbard interaction, the dashed line is the result of the phenomenological approach for self-trapped large polarons by Emin [95], the dotted curve is the weak-coupling single-polaron result [71]. (From Ref. [93].)

The real part of the optical conductivity $\operatorname{Re}\sigma(\omega)$ is expressed in Ref. [94] by the formula

$$\operatorname{Re}\sigma(\omega) = \alpha n_p \frac{2}{3}\frac{e^2}{m^2}\frac{(\hbar\omega_0)^2}{\pi\hbar\omega^3}\sqrt{\frac{\hbar}{2m\omega_0}}\int_0^\infty q^2 S^{(\mathrm{H})}(q,\omega-\omega_0)dq, \tag{8.76a}$$

where α is the electron-phonon coupling constant, n_p is the polaron density, m is the electron band mass, ω_0 is the LO-phonon frequency, and $S^{(\mathrm{H})}(q,\omega)$ is the dynamic structure factor, determined in Ref. [94] through the dielectric function of an electron gas $\varepsilon(\mathbf{q},\omega)$:

$$S^{(\mathrm{H})}(\mathbf{q},\omega) = \frac{\hbar}{n_p}\frac{q^2}{4\pi e^2}\operatorname{Im}\left[-\frac{1}{\varepsilon(\mathbf{q},\omega)}\right]. \tag{8.77}$$

In Ref. [53], the other definition for the dynamic structure factor is used, which is equivalent to that given by (8.77) (see Ref. [72]) with the factor N (the number of electrons)

$$S^{(\mathrm{TD})}(\mathbf{q},\omega) = \frac{1}{2}\int_{-\infty}^{+\infty}\langle\varphi_{\mathrm{el}}|\rho_{\mathbf{q}}(t)\,\rho_{-\mathbf{q}}(0)|\,\varphi_{\mathrm{el}}\rangle\, e^{i\omega t}dt = NS^{(\mathrm{H})}(\mathbf{q},\omega). \tag{8.78}$$

Here, φ_{el} denotes the ground state of the electron subsystem (without the electron-phonon interaction), $\rho_{\mathbf{q}} = \sum_{j=1}^{N} e^{i\mathbf{q}\cdot\mathbf{r}_j}$ is the Fourier component of the electron density.

In Ref. [53], the dynamic structure factor is calculated within the random-phase approximation (RPA) taking into account the Coulomb interaction between electrons with the Fourier component of the Coulomb potential

$$v_{\mathbf{q}} = \frac{4\pi e^2}{q^2\varepsilon_\infty}, \tag{8.79}$$

where ε_∞ is the high-frequency dielectric constant of the crystal. In Refs. [93, 94], the dynamic structure factor is calculated taking into account the local Hubbard electron-electron interaction instead of the Coulomb interaction. The local Hubbard interaction is used in the small-polaron formalism and describes the potential energy of two electrons on one and the same site (see, e. g., Refs. [96, 97]). In its simplest form the Hubbard interaction is (see Eq. (1) of Ref. [96])

$$V_H = U\sum_i n_{i\uparrow}n_{i\downarrow}, \tag{8.80}$$

where U is the coupling constant of the Hubbard interaction, $n_{i\uparrow}$ is the electron occupation number for the i-th site.

In Refs. [93, 94], there are no details of the calculation using the interaction term (8.80). The following procedure can be supposed. The transition from the summation over the lattice sites to the integral over the crystal volume V is performed taking into account the normalization condition

$$N_{\uparrow(\downarrow)} = \sum_i n_{i\uparrow(\downarrow)} = \int_V \tilde{n}_{\uparrow(\downarrow)}(\mathbf{r})\, d\mathbf{r},$$

where the density $\tilde{n}_{\uparrow(\downarrow)}(\mathbf{r})$ is to be determined through $n_{i\uparrow(\downarrow)}$. As far as the lattice cell volume $\Omega_0 \ll V$, the integral $\int_V n_{\uparrow(\downarrow)}(\mathbf{r})\, d\mathbf{r}$ can be written as the sum over the lattice sites:

$$\int_V n_{\uparrow(\downarrow)}(\mathbf{r})\, d\mathbf{r} = \Omega_0 \sum_i \tilde{n}_{\uparrow(\downarrow)}(\mathbf{r}_i),$$

where $\{\mathbf{r}_i\}$ are the vectors of the lattice. Therefore, from the equality

$$\sum_i n_{i\uparrow(\downarrow)} = \Omega_0 \sum_i \tilde{n}_{\uparrow(\downarrow)}(\mathbf{r}_i)$$

we find that

$$n_{i\uparrow(\downarrow)} = \tilde{n}_{\uparrow(\downarrow)}(\mathbf{r}_i).$$

The potential (8.80) is then transformed from the sum over sites to the integral:

$$V_H = \frac{U}{\Omega_0} \sum_i n_{i\uparrow} n_{i\downarrow} \Omega_0 = \int_V U\Omega_0 \delta(\mathbf{r} - \mathbf{r}')\, \tilde{n}_\uparrow(\mathbf{r})\, \tilde{n}_\downarrow(\mathbf{r}')\, d\mathbf{r} d\mathbf{r}'. \tag{8.81}$$

Consequently, in the continuum approach the Hubbard model is described by the δ-like interparticle potential $U\Omega_0\delta(\mathbf{r} - \mathbf{r}')$.

This development of the approach [53] performed in Refs. [93, 94] seems to be contradictory by the following reason. For a many-polaron system, both the electron-phonon and electron-electron interactions are provided by the electrostatic potentials. Therefore, it would be consistent to consider them both within one and the same approach. Namely, the Coulomb electron-electron interaction with the potential (8.79) is relevant for large and small polarons with the Fröhlich electron-phonon interaction, while the Hubbard electron-electron interaction is relevant for small Holstein polarons. Nevertheless, as recognized in Ref. [93], this model "reproduces the observed shape of the polaron peak quite convincingly" and provides a better agreement with the experiment [93, 94] than the phenomenological approach [95] and the one-polaron theory [71].

8.2 Interacting polarons in a quantum dot

8.2.1 The partition function and the free energy of a many-polaron system

We consider a system of N electrons with mutual Coulomb repulsion and interacting with the lattice vibrations following Ref. [98]. The system is assumed to be confined by a parabolic potential characterized by the frequency parameter Ω_0. The total number of electrons is represented as $N = \sum_\sigma N_\sigma$, where N_σ is the number of electrons with the spin projection $\sigma = \pm 1/2$. The electron 3D (2D) coordinates are denoted by $\mathbf{x}_{j,\sigma}$ with $j = 1, \cdots, N_\sigma$. The bulk phonons (characterized by 3D wave vectors $\mathbf{k}$ and frequencies $\omega_\mathbf{k}$) are described by the complex coordinates $Q_\mathbf{k}$, which possess the property [43]

$$Q^*_\mathbf{k} = Q_{-\mathbf{k}}. \tag{8.82}$$

The full set of the electron and phonon coordinates are denoted by $\bar{\mathbf{x}} \equiv \{\mathbf{x}_{j,\sigma}\}$ and $\bar{Q} \equiv \{Q_{\mathbf{k}}\}$.

Throughout the present treatment, the Euclidean time variable $\tau = it$ is used, where t is the real time variable. In this representation the Lagrangian of the system is

$$L\left(\dot{\bar{\mathbf{x}}}, \dot{\bar{Q}}; \bar{\mathbf{x}}, \bar{Q}\right) = L_e\left(\dot{\bar{\mathbf{x}}}, \bar{\mathbf{x}}\right) - V_C\left(\bar{\mathbf{x}}\right) - U_b\left(\bar{\mathbf{x}}\right) + L_{ph}\left(\dot{\bar{Q}}, \bar{Q}\right) + L_{e-ph}\left(\bar{\mathbf{x}}, \bar{Q}\right), \tag{8.83}$$

where $L_e\left(\dot{\bar{\mathbf{x}}}, \bar{\mathbf{x}}\right)$ is the Lagrangian of an electron with band mass m_b in a quantum dot:

$$L_e\left(\dot{\bar{\mathbf{x}}}, \bar{\mathbf{x}}\right) = -\sum_{\sigma=\pm 1/2} \sum_{j=1}^{N_\sigma} \frac{m_b}{2}\left(\dot{\mathbf{x}}_{j,\sigma}^2 + \Omega_0^2 \mathbf{x}_{j,\sigma}^2\right), \qquad \dot{\mathbf{x}} \equiv \frac{d\mathbf{x}}{d\tau}, \tag{8.84}$$

Ω_0 is the confinement frequency, $V_b\left(\bar{\mathbf{x}}\right)$ is the potential of a background charge (supposed to be static and uniformly distributed with the charge density en_b in a sphere of a radius R),

$$U_b\left(\bar{\mathbf{x}}\right) = \sum_{\sigma} \sum_{j=1}^{N} V_b\left(r_{j,\sigma}\right), \; r \equiv |\mathbf{x}|, \tag{8.85}$$

$$V_b\left(r\right) = -\frac{4\pi e^2 n_b}{3\varepsilon_0}\left[\Theta\left(r < R\right)\frac{3R^2 - r^2}{2} + \Theta\left(R \le r\right)\frac{R^3}{r}\right], \tag{8.86}$$

where ε_0 is the static dielectric constant of a crystal, $V_C\left(\bar{\mathbf{x}}\right)$ is the potential energy of the electron-electron Coulomb repulsion in the medium with the high-frequency dielectric constant ε_∞:

$$V_C\left(\bar{\mathbf{x}}\right) = \sum_{\substack{\sigma,\sigma'=\pm 1/2 \\ (j,\sigma)\neq(l,\sigma')}} \sum_{j=1}^{N_\sigma} \sum_{l=1}^{N_{\sigma'}} \frac{e^2}{2\varepsilon_\infty} \frac{1}{|\mathbf{x}_{j,\sigma} - \mathbf{x}_{l,\sigma'}|}, \tag{8.87}$$

$L_{ph}\left(\dot{\bar{Q}}, \dot{\bar{Q}}^*; \bar{Q}, \bar{Q}^*\right)$ is the Lagrangian of free phonons:

$$L_{ph}\left(\dot{\bar{Q}}, \bar{Q}\right) = -\frac{1}{2}\sum_{\mathbf{k}}(\dot{Q}_{\mathbf{k}}^* \dot{Q}_{\mathbf{k}} + \omega_{\mathbf{k}}^2 Q_{\mathbf{k}}^* Q_{\mathbf{k}}), \qquad \dot{Q} \equiv \frac{dQ}{d\tau}. \tag{8.88}$$

Further, $L_{e-ph}\left(\bar{\mathbf{x}}, \bar{Q}, \bar{Q}^*\right)$ is the Lagrangian of the electron-phonon interaction:

$$L_{e-ph}\left(\bar{\mathbf{x}}, \bar{Q}\right) = -\sum_{\mathbf{k}}\left(\frac{2\omega_{\mathbf{k}}}{\hbar}\right)^{1/2} V_{\mathbf{k}} Q_{-\mathbf{k}} \rho_{\mathbf{k}}, \tag{8.89}$$

where $\rho_{\mathbf{k}}$ is the Fourier transform of the electron density operator:

$$\rho_{\mathbf{k}} = \sum_{\sigma=\pm 1/2} \sum_{j=1}^{N_\sigma} e^{i\mathbf{k}\cdot\mathbf{x}_{j,\sigma}}. \tag{8.90}$$

$V_{\mathbf{k}}$ is the amplitude of the electron-phonon interaction. Here, we consider electrons interacting with the long-wavelength longitudinal optical (LO) phonons with a dispersionless frequency $\omega_{\mathbf{k}} = \omega_{\mathrm{LO}}$, for which the amplitude $V_{\mathbf{k}}$ is [26]

$$V_{\mathbf{k}} = \frac{\hbar\omega_{\mathrm{LO}}}{q}\left(\frac{2\sqrt{2}\pi\alpha}{V}\right)^{1/2}\left(\frac{\hbar}{m_b\omega_{\mathrm{LO}}}\right)^{1/4}, \tag{8.91}$$

where α is the electron-phonon coupling constant and V is the volume of the crystal.

We consider a *canonical* ensemble, where the numbers N_σ are fixed. The partition function $Z\left(\{N_\sigma\},\beta\right)$ of the system can be expressed as a path integral over the electron and phonon coordinates:

$$Z\left(\{N_\sigma\},\beta\right)=\sum_P\frac{(-1)^{\xi_P}}{N_{1/2}!N_{-1/2}!}\int d\bar{\mathbf{x}}\int_{\bar{\mathbf{x}}}^{P\bar{\mathbf{x}}}D\bar{\mathbf{x}}\left(\tau\right)\int d\bar{Q}\int_{\bar{Q}}^{\bar{Q}}D\bar{Q}\left(\tau\right)e^{-S\left[\bar{\mathbf{x}}(\tau),\bar{Q}(\tau)\right]},\tag{8.92}$$

where $S\left[\bar{\mathbf{x}}\left(\tau\right),\bar{Q}\left(\tau\right)\right]$ is the "action" functional:

$$S\left[\bar{\mathbf{x}}\left(\tau\right),\bar{Q}\left(\tau\right)\right]=-\frac{1}{\hbar}\int_0^{\hbar\beta}L\left(\dot{\bar{\mathbf{x}}},\dot{\bar{Q}};\bar{\mathbf{x}},\bar{Q}\right)d\tau.\tag{8.93}$$

The parameter $\beta\equiv 1/\left(k_BT\right)$ is inversely proportional to the temperature T. In order to take the Fermi-Dirac statistics into account, the integral over the electron paths $\{\bar{\mathbf{x}}\left(\tau\right)\}$ in Eq. (8.92) contains a sum over all permutations P of the electrons with the same spin projection, and ξ_P denotes the parity of a permutation P.

The action functional (8.93) is quadratic in the phonon coordinates $\bar{Q}$. Therefore, *the path integral over the phonon variables* in $Z\left(\{N_\sigma\},\beta\right)$ *can be calculated analytically* following Ref. [43]. Let us describe this path integration in detail. First, we introduce the real phonon coordinates through the real and imaginary parts of the complex phonon coordinates $Q'_{\mathbf{k}}\equiv\operatorname{Re}Q_{\mathbf{k}}$, $Q''_{\mathbf{k}}\equiv\operatorname{Im}Q_{\mathbf{k}}$. According to the symmetry property (8.82), they obey the equalities

$$Q'_{-\mathbf{k}}=Q'_{\mathbf{k}},\ Q''_{-\mathbf{k}}=-Q''_{\mathbf{k}}.\tag{8.94}$$

$$q_{\mathbf{k}}\equiv\begin{cases}\sqrt{2}Q'_{\mathbf{k}},\ k_x\geq 0,\\ \sqrt{2}Q''_{\mathbf{k}},\ k_x<0.\end{cases}\tag{8.95}$$

In this representation, the sum over phonon coordinates $\sum_{\mathbf{k}}\left|Q_{\mathbf{k}}\right|^2$ is transformed in the following way using the symmetry property (8.94):

$$\begin{aligned}\sum_{\mathbf{k}}\left|Q_{\mathbf{k}}\right|^2&=\sum_{\mathbf{k}}\left[\left(Q'_{\mathbf{k}}\right)^2+\left(Q''_{\mathbf{k}}\right)^2\right]\\&=2\sum_{\substack{\mathbf{k}\\(k_x\geq 0)}}\left(Q'_{\mathbf{k}}\right)^2+2\sum_{\substack{\mathbf{k}\\(k_x<0)}}\left(Q''_{\mathbf{k}}\right)^2\\&=\sum_{\substack{\mathbf{k}\\(k_x\geq 0)}}q_{\mathbf{k}}^2+\sum_{\substack{\mathbf{k}\\(k_x<0)}}q_{\mathbf{k}}^2=\sum_{\mathbf{k}}q_{\mathbf{k}}^2.\end{aligned}$$

Therefore, the phonon Lagrangian (8.88) with the real phonon coordinates is

$$L_{ph}=-\frac{1}{2}\sum_{\mathbf{k}}(\dot{q}_{\mathbf{k}}^2+\omega_{\mathbf{k}}^2q_{\mathbf{k}}^2).\tag{8.96}$$

The Lagrangian of the electron-phonon interaction (8.89) with the real phonon coordinates is transformed in the following way using (8.94):

$$\begin{aligned}L_{e-ph}&=-\sum_{\mathbf{k}}\left(\frac{2\omega_{\mathbf{k}}}{\hbar}\right)^{1/2}V_{\mathbf{k}}\rho_{\mathbf{k}}\left(Q'_{\mathbf{k}}-iQ''_{\mathbf{k}}\right)\\&=-\sum_{\substack{\mathbf{k}\\(k_x\geq 0)}}\left(\frac{2\omega_{\mathbf{k}}}{\hbar}\right)^{1/2}\left(V_{\mathbf{k}}\rho_{\mathbf{k}}+V_{-\mathbf{k}}\rho_{-\mathbf{k}}\right)Q'_{\mathbf{k}}\\&+i\sum_{\substack{\mathbf{k}\\(k_x<0)}}\left(\frac{2\omega_{\mathbf{k}}}{\hbar}\right)^{1/2}\left(V_{\mathbf{k}}\rho_{\mathbf{k}}-V_{-\mathbf{k}}\rho_{-\mathbf{k}}\right)Q''_{\mathbf{k}}.\end{aligned}$$

Let us introduce the real forces:

$$\gamma_{\mathbf{k}} \equiv \begin{cases} \frac{1}{\sqrt{2}}\left(\frac{2\omega_{\mathbf{k}}}{\hbar}\right)^{1/2}\left(V_{\mathbf{k}}\rho_{\mathbf{k}} + V_{-\mathbf{k}}\rho_{-\mathbf{k}}\right), \ k_x \geq 0, \\ \frac{1}{i\sqrt{2}}\left(\frac{2\omega_{\mathbf{k}}}{\hbar}\right)^{1/2}\left(V_{\mathbf{k}}\rho_{\mathbf{k}} - V_{-\mathbf{k}}\rho_{-\mathbf{k}}\right), \ k_x > 0. \end{cases} \tag{8.97}$$

This gives us the Lagrangian of the electron-phonon interaction in terms of the real forces and real phonon coordinates:

$$L_{e-ph} = -\sum_{\mathbf{k}} \gamma_{\mathbf{k}} q_{\mathbf{k}}. \tag{8.98}$$

So, the sum of the Lagrangians of phonons and of the electron-phonon interaction is expressed through ordinary real oscillator variables:

$$L_{ph} + L_{e-ph} = -\frac{1}{2}\sum_{\mathbf{k}}(\dot{q}_{\mathbf{k}}^2 + \omega_{\mathbf{k}}^2 q_{\mathbf{k}}^2 + \gamma_{\mathbf{k}} q_{\mathbf{k}}). \tag{8.99}$$

The path integration for each phonon mode with the coordinate $q_{\mathbf{k}}$ is performed independently as described in Sec. 2 of Ref. [43] and gives the result

$$\begin{aligned} &\int_{-\infty}^{\infty} dq_{\mathbf{k}} \int_{q_{\mathbf{k}}}^{q_{\mathbf{k}}} Dq_{\mathbf{k}}(\tau) \exp\left[-\frac{1}{\hbar}\int_0^{\hbar\beta} d\tau \frac{1}{2}(\dot{q}_{\mathbf{k}}^2 + \omega_{\mathbf{k}}^2 q_{\mathbf{k}}^2 + \gamma_{\mathbf{k}} q_{\mathbf{k}})\right] \\ &= \frac{1}{2\sinh\left(\frac{\beta\hbar\omega_{\mathbf{k}}}{2}\right)} \\ &\times \exp\left\{\frac{1}{4\hbar}\int_0^{\hbar\beta} d\tau \int_0^{\hbar\beta} d\tau' \frac{\cosh\left[\omega_{\mathbf{k}}\left(|\tau-\tau'| - \hbar\beta/2\right)\right]}{\omega_{\mathbf{k}}\sinh\left(\beta\hbar\omega_{\mathbf{k}}/2\right)} \gamma_{\mathbf{k}}(\tau)\gamma_{\mathbf{k}}(\tau'), \right\} \end{aligned}$$

where the exponential is the influence functional of a driven oscillator { [43], Eq. (3.43)}. Therefore, the path integral over all phonon modes is

$$\begin{aligned} &\int d\{q_{\mathbf{k}}\} \int_{\{q_{\mathbf{k}}\}}^{\{q_{\mathbf{k}}\}} D\{q_{\mathbf{k}}(\tau)\} \exp\left[-\frac{1}{\hbar}\int_0^{\hbar\beta} d\tau \sum_{\mathbf{k}} \frac{1}{2}(\dot{q}_{\mathbf{k}}^2 + \omega_{\mathbf{k}}^2 q_{\mathbf{k}}^2 + \gamma_{\mathbf{k}} q_{\mathbf{k}})\right] \\ &= \left(\prod_{\mathbf{k}} \frac{1}{2\sinh\left(\frac{\beta\hbar\omega_{\mathbf{k}}}{2}\right)}\right) \\ &\times \exp\left\{\frac{1}{4\hbar}\int_0^{\hbar\beta} d\tau \int_0^{\hbar\beta} d\tau' \sum_{\mathbf{k}} \frac{\cosh\left[\omega_{\mathbf{k}}\left(|\tau-\tau'| - \hbar\beta/2\right)\right]}{\omega_{\mathbf{k}}\sinh\left(\beta\hbar\omega_{\mathbf{k}}/2\right)} \gamma_{\mathbf{k}}(\tau)\gamma_{\mathbf{k}}(\tau'). \right\} \end{aligned}$$

Here, the product $\prod_{\mathbf{k}} \ldots$ is the partition function of free phonons, and the exponential is the influence functional of the phonon subsystem on the electron subsystem. This influence functional results from the above described *elimination of the phonon coordinates* and is usually written down as $e^{-\Phi}$, where Φ is

$$\Phi = -\frac{1}{4\hbar}\int_0^{\hbar\beta} d\tau \int_0^{\hbar\beta} d\tau' \sum_{\mathbf{k}} \frac{\cosh\left[\omega_{\mathbf{k}}\left(|\tau-\tau'| - \hbar\beta/2\right)\right]}{\omega_{\mathbf{k}}\sinh\left(\beta\hbar\omega_{\mathbf{k}}/2\right)} \gamma_{\mathbf{k}}(\tau)\gamma_{\mathbf{k}}(\tau'). \tag{8.100}$$

The sum over the phonon wave vectors $\mathbf{k}$ can be simplified as follows:

$$\begin{aligned}
&\sum_{\mathbf{k}} \frac{\cosh\left[\omega_{\mathbf{k}}\left(|\tau-\tau'|-\hbar\beta/2\right)\right]}{\omega_{\mathbf{k}}\sinh\left(\beta\hbar\omega_{\mathbf{k}}/2\right)}\gamma_{\mathbf{k}}\left(\tau\right)\gamma_{\mathbf{k}}\left(\tau'\right)\\
&=\frac{1}{\hbar}\sum_{\substack{\mathbf{k}\\(k_x\geq 0)}}\frac{\cosh\left[\omega_{\mathbf{k}}\left(|\tau-\tau'|-\hbar\beta/2\right)\right]}{\sinh\left(\beta\hbar\omega_{\mathbf{k}}/2\right)}\\
&\times\left[V_{\mathbf{k}}\rho_{\mathbf{k}}\left(\tau\right)+V_{-\mathbf{k}}\rho_{-\mathbf{k}}\left(\tau\right)\right]\left[V_{\mathbf{k}}\rho_{\mathbf{k}}\left(\tau'\right)+V_{-\mathbf{k}}\rho_{-\mathbf{k}}\left(\tau'\right)\right]\\
&-\frac{1}{\hbar}\sum_{\substack{\mathbf{k}\\(k_x<0)}}\frac{\cosh\left[\omega_{\mathbf{k}}\left(|\tau-\tau'|-\hbar\beta/2\right)\right]}{\sinh\left(\beta\hbar\omega_{\mathbf{k}}/2\right)}\\
&\times\left[V_{\mathbf{k}}\rho_{\mathbf{k}}\left(\tau\right)-V_{-\mathbf{k}}\rho_{-\mathbf{k}}\left(\tau\right)\right]\left[V_{\mathbf{k}}\rho_{\mathbf{k}}\left(\tau'\right)-V_{-\mathbf{k}}\rho_{-\mathbf{k}}\left(\tau'\right)\right]\\
&=\frac{2}{\hbar}\sum_{\substack{\mathbf{k}\\(k_x\geq 0)}}\frac{\cosh\left[\omega_{\mathbf{k}}\left(|\tau-\tau'|-\hbar\beta/2\right)\right]}{\sinh\left(\beta\hbar\omega_{\mathbf{k}}/2\right)}V_{\mathbf{k}}V_{-\mathbf{k}}\\
&\times\left[\rho_{\mathbf{k}}\left(\tau\right)\rho_{-\mathbf{k}}\left(\tau'\right)+\rho_{-\mathbf{k}}\left(\tau\right)\rho_{\mathbf{k}}\left(\tau'\right)\right]\\
&=\frac{2}{\hbar}\sum_{\mathbf{k}}\frac{\cosh\left[\omega_{\mathbf{k}}\left(|\tau-\tau'|-\hbar\beta/2\right)\right]}{\sinh\left(\beta\hbar\omega_{\mathbf{k}}/2\right)}\left|V_{\mathbf{k}}\right|^2\rho_{\mathbf{k}}\left(\tau\right)\rho_{-\mathbf{k}}\left(\tau'\right).
\end{aligned}$$

Herefrom, we find that

$$\Phi=-\sum_{\mathbf{k}}\frac{\left|V_{\mathbf{k}}\right|^2}{2\hbar^2}\int_0^{\hbar\beta}d\tau\int_0^{\hbar\beta}d\tau'\frac{\cosh\left[\omega_{\mathbf{k}}\left(|\tau-\tau'|-\frac{\hbar\beta}{2}\right)\right]}{\sinh\left(\frac{\beta\hbar\omega_{\mathbf{k}}}{2}\right)}\rho_{\mathbf{k}}\left(\tau\right)\rho_{-\mathbf{k}}\left(\tau'\right). \tag{8.101}$$

As a result, the partition function of the electron-phonon system (8.92) factorizes into a product

$$Z\left(\{N_\sigma\},\beta\right)=Z_p\left(\{N_\sigma\},\beta\right)\prod_{\mathbf{k}}\frac{1}{2\sinh\left(\beta\hbar\omega_{\mathbf{k}}/2\right)} \tag{8.102}$$

of the partition function of free phonons with a partition function $Z_p\left(\{N_\sigma\},\beta\right)$ of interacting polarons, which is a path integral over the electron coordinates only:

$$Z_p\left(\{N_\sigma\},\beta\right)=\sum_P\frac{(-1)^{\xi_P}}{N_{1/2}!N_{-1/2}!}\int d\bar{\mathbf{x}}\int_{\bar{\mathbf{x}}}^{P\bar{\mathbf{x}}}D\bar{\mathbf{x}}\left(\tau\right)e^{-S_p[\bar{\mathbf{x}}(\tau)]}. \tag{8.103}$$

The functional

$$S_p\left[\bar{\mathbf{x}}\left(\tau\right)\right]=-\frac{1}{\hbar}\int_0^{\hbar\beta}\left[L_e\left(\dot{\bar{\mathbf{x}}}\left(\tau\right),\bar{\mathbf{x}}\left(\tau\right)\right)-V_C\left(\bar{\mathbf{x}}\left(\tau\right)\right)\right]d\tau+\Phi\left[\bar{\mathbf{x}}\left(\tau\right)\right] \tag{8.104}$$

describes the phonon-induced retarded interaction between the electrons, including the retarded self-interaction of each electron.

Using (8.84) and (8.87) we write down $S_p\left[\bar{\mathbf{x}}\left(\tau\right)\right]$ explicitly:

$$\begin{aligned}
S_p\left[\bar{\mathbf{x}}\left(\tau\right)\right]=&\frac{1}{\hbar}\int_0^{\hbar\beta}\left[\sum_\sigma\sum_{j=1}^{N_\sigma}\frac{m_b}{2}\left(\dot{\mathbf{x}}_{j,\sigma}^2+\Omega_0^2\mathbf{x}_{j,\sigma}^2\right)+\sum_{\substack{\sigma,\sigma'\\(j,\sigma)\neq(l,\sigma')}}\sum_{j=1}^{N_\sigma}\sum_{l=1}^{N_{\sigma'}}\frac{e^2}{2\varepsilon_\infty\left|\mathbf{x}_{j,\sigma}-\mathbf{x}_{l,\sigma'}\right|}\right]d\tau\\
&-\sum_{\mathbf{q}}\frac{\left|V_{\mathbf{q}}\right|^2}{2\hbar^2}\int_0^{\hbar\beta}d\tau\int_0^{\hbar\beta}d\tau'\frac{\cosh\left[\omega_{\mathrm{LO}}\left(|\tau-\tau'|-\hbar\beta/2\right)\right]}{\sinh\left(\beta\hbar\omega_{\mathrm{LO}}/2\right)}\rho_{\mathbf{q}}\left(\tau\right)\rho_{-\mathbf{q}}\left(\tau'\right).
\end{aligned} \tag{8.105}$$

The free energy of a system of interacting polarons $F_p(\{N_\sigma\},\beta)$ is related to their partition function (8.103) by the equation:

$$F_p(\{N_\sigma\},\beta) = -\frac{1}{\beta}\ln Z_p(\{N_\sigma\},\beta). \tag{8.106}$$

At present no method is known to calculate the non-gaussian path integral (8.103) analytically. For *distinguishable* particles, the Jensen-Feynman variational principle [43] provides a convenient approximation technique. It yields a lower bound to the partition function, and hence an upper bound to the free energy.

It can be shown [99] that the path-integral approach to the many-body problem for a fixed number of identical particles can be formulated as a Feynman-Kac functional on a state space for N indistinguishable particles, by imposing an ordering on the configuration space and by the introduction of a set of boundary conditions at the boundaries of this state space. The resulting variational inequality for identical particles takes the same form as the Jensen-Feynman variational principle:

$$F_p \leqslant F_{var}, \tag{8.107}$$

$$F_{var} = F_0 + \frac{1}{\beta}\langle S_p - S_0\rangle_{S_0}, \tag{8.108}$$

where S_0 is a model action with the corresponding free energy F_0. The angular brackets mean a weighted average over the paths

$$\langle(\bullet)\rangle_{S_0} = \frac{\sum_P \frac{(-1)^{\xi_P}}{N_{1/2}!N_{-1/2}!}\int d\bar{\mathbf{x}}\int_{\bar{\mathbf{x}}}^{P\bar{\mathbf{x}}} D\bar{\mathbf{x}}(\tau)(\bullet)\, e^{-S_0[\bar{\mathbf{x}}(\tau)]}}{\sum_P \frac{(-1)^{\xi_P}}{N_{1/2}!N_{-1/2}!}\int d\bar{\mathbf{x}}\int_{\bar{\mathbf{x}}}^{P\bar{\mathbf{x}}} D\bar{\mathbf{x}}(\tau)\, e^{-S_0[\bar{\mathbf{x}}(\tau)]}}. \tag{8.109}$$

In the zero-temperature limit, the polaron ground-state energy

$$E_p^0 = \lim_{\beta\to\infty} F_p \tag{8.110}$$

obeys the inequality following from (8.107) with (8.108):

$$E_p^0 \leqslant E_{var}$$

with

$$E_{var} = E_0^0 + \lim_{\beta\to\infty}\left(\frac{1}{\beta}\langle S_p - S_0\rangle_{S_0}\right), \tag{8.111}$$

$$E_0^0 = \lim_{\beta\to\infty} F_0. \tag{8.112}$$

8.2.2 Model system

We consider a model system consisting of N electrons with coordinates $\bar{\mathbf{x}} \equiv \{\mathbf{x}_{j,\sigma}\}$ and N_f fictitious particles with coordinates $\bar{\mathbf{y}} \equiv \{\mathbf{y}_j\}$ in a harmonic confinement potential with elastic interparticle interactions as studied in Refs. [100, 98]. The Lagrangian of this model system takes the form

$$\begin{aligned} L_M(\dot{\bar{\mathbf{x}}},\dot{\bar{\mathbf{y}}};\bar{\mathbf{x}},\bar{\mathbf{y}}) = &-\frac{m_b}{2}\sum_\sigma\sum_{j=1}^{N_\sigma}\left(\dot{\mathbf{x}}_{j,\sigma}^2 + \Omega^2\mathbf{x}_{j,\sigma}^2\right) + \frac{m_b\omega^2}{4}\sum_{\sigma,\sigma'}\sum_{j=1}^{N_\sigma}\sum_{l=1}^{N_{\sigma'}}\left(\mathbf{x}_{j,\sigma} - \mathbf{x}_{l,\sigma'}\right)^2 \\ &-\frac{m_f}{2}\sum_{j=1}^{N_f}\left(\dot{\mathbf{y}}_j^2 + \Omega_f^2\mathbf{y}_j^2\right) - \frac{k}{2}\sum_\sigma\sum_{j=1}^{N_\sigma}\sum_{l=1}^{N_f}\left(\mathbf{x}_{j,\sigma} - \mathbf{y}_l\right)^2. \end{aligned} \tag{8.113}$$

The frequencies Ω, ω, Ω_f, the mass of a fictitious particle m_f, and the force constant k are variational parameters. Clearly, this Lagrangian is symmetric with respect to electron permutations. Performing the path integral over the coordinates of the fictitious particles in the same way as described above for phonons, the partition function $Z_0\left(\{N_\sigma\},\beta\right)$ of the model system of interacting polarons becomes a path integral over the electron coordinates:

$$Z_0\left(\{N_\sigma\},\beta\right)=\sum_P\frac{(-1)^{\xi_P}}{N_{1/2}!N_{-1/2}!}\int d\bar{\mathbf{x}}\int_{\bar{\mathbf{x}}}^{P\bar{\mathbf{x}}}D\bar{\mathbf{x}}\left(\tau\right)e^{-S_0[\bar{\mathbf{x}}(\tau)]},\tag{8.114}$$

with the action functional $S_0\left[\bar{\mathbf{x}}\left(\tau\right)\right]$ given by

$$\begin{aligned}S_0\left[\bar{\mathbf{x}}\left(\tau\right)\right]=&\frac{1}{\hbar}\int_0^{\hbar\beta}\sum_\sigma\sum_{j=1}^{N_\sigma}\frac{m_b}{2}\left[\dot{\mathbf{x}}_{j,\sigma}^2\left(\tau\right)+\Omega^2\mathbf{x}_{j,\sigma}^2\left(\tau\right)\right]d\tau\\&-\frac{1}{\hbar}\int_0^{\hbar\beta}\sum_{\sigma,\sigma'}\sum_{j=1}^{N_\sigma}\sum_{l=1}^{N_{\sigma'}}\frac{m_b\omega^2}{4}\left[\mathbf{x}_{j,\sigma}\left(\tau\right)-\mathbf{x}_{l,\sigma'}\left(\tau\right)\right]^2d\tau\\&-\frac{k^2N^2N_f}{4m_f\hbar\Omega_f}\int_0^{\hbar\beta}d\tau\int_0^{\hbar\beta}d\tau'\frac{\cosh\left[\Omega_f\left(|\tau-\tau'|-\hbar\beta/2\right)\right]}{\sinh\left(\beta\hbar\Omega_f/2\right)}\mathbf{X}\left(\tau\right)\cdot\mathbf{X}\left(\tau'\right),\end{aligned}\tag{8.115}$$

where $\mathbf{X}$ is the center-of-mass coordinate of the electrons,

$$\mathbf{X}=\frac{1}{N}\sum_\sigma\sum_{j=1}^{N_\sigma}\mathbf{x}_{j,\sigma}.\tag{8.116}$$

Analytical calculation of the model partition function

The partition function $Z_0\left(\{N_\sigma\},\beta\right)$ [Eq. (8.114)] for the model system of interacting polarons can be expressed in terms of the partition function $Z_M\left(\{N_\sigma\},N_f,\beta\right)$ of the model system of interacting electrons and fictitious particles with the Lagrangian L_M [Eq. (8.113)] as follows:

$$Z_0\left(\{N_\sigma\},\beta\right)=\frac{Z_M\left(\{N_\sigma\},N_f,\beta\right)}{Z_f\left(N_f,w_f,\beta\right)},\tag{8.117}$$

where $Z_f\left(N_f,w_f,\beta\right)$ is the partition function of fictitious particles,

$$Z_f\left(N_f,\beta\right)=\frac{1}{\left(2\sinh\frac{1}{2}\beta\hbar w_f\right)^{DN_f}},\tag{8.118}$$

with the frequency

$$w_f=\sqrt{\Omega_f^2+kN/m_f}\tag{8.119}$$

and D=3(2) for 3D(2D) systems. The partition function $Z_M\left(\{N_\sigma\},N_f,\beta\right)$ is the path integral for both the electrons and the fictitious particles:

$$\begin{aligned}Z_M\left(\{N_\sigma\},N_f,\beta\right)=&\sum_P\frac{(-1)^{\xi_P}}{N_{1/2}!N_{-1/2}!}\\&\int d\bar{\mathbf{x}}\int_{\bar{\mathbf{x}}}^{P\bar{\mathbf{x}}}D\bar{\mathbf{x}}\left(\tau\right)\int d\bar{\mathbf{y}}\int_{\bar{\mathbf{y}}}^{\bar{\mathbf{y}}}D\bar{\mathbf{y}}\left(\tau\right)e^{-S_M[\bar{\mathbf{x}}(\tau),\bar{\mathbf{y}}(\tau)]}\end{aligned}\tag{8.120}$$

with the "action" functional

$$S_M\left[\bar{\mathbf{x}}\left(\tau\right),\bar{\mathbf{y}}\left(\tau\right)\right]=-\frac{1}{\hbar}\int_0^{\hbar\beta}L_M\left(\dot{\bar{\mathbf{x}}},\dot{\bar{\mathbf{y}}};\bar{\mathbf{x}},\bar{\mathbf{y}}\right)d\tau, \tag{8.121}$$

where the Lagrangian is given by Eq. (8.113).

Let us consider an auxiliary "ghost" subsystem with the Lagrangian

$$L_g\left(\dot{\mathbf{X}}_g,\dot{\mathbf{Y}}_g,\mathbf{X}_g,\mathbf{Y}_g\right)=-\frac{m_bN}{2}\left(\dot{\mathbf{X}}_g^2+w^2\mathbf{X}_g^2\right)-\frac{m_fN_f}{2}\left(\dot{\mathbf{Y}}_g^2+w_f^2\mathbf{Y}_g^2\right) \tag{8.122}$$

with two frequencies w and w_f, where w is given by

$$w=\sqrt{\Omega^2-N\omega^2+kN_f/m_b}. \tag{8.123}$$

The partition function Z_g of this subsystem

$$Z_g=\int d\mathbf{X}_g\int d\mathbf{Y}_g\int\limits_{\mathbf{X}_g}^{\mathbf{X}_g}D\mathbf{X}_g\left(\tau\right)\int\limits_{\mathbf{Y}_g}^{\mathbf{Y}_g}D\mathbf{Y}_g\left(\tau\right)\exp\left\{-S_g\left[\mathbf{X}_g\left(\tau\right),\mathbf{Y}_g\left(\tau\right)\right]\right\}, \tag{8.124}$$

with the "action" functional

$$S_g\left[\mathbf{X}_g\left(\tau\right),\mathbf{Y}_g\left(\tau\right)\right]=-\frac{1}{\hbar}\int\limits_0^{\hbar\beta}L_g\left(\dot{\mathbf{X}}_g,\mathbf{X}_g,\dot{\mathbf{Y}}_g,\mathbf{Y}_g\right)d\tau \tag{8.125}$$

is calculated in the standard way, because its Lagrangian (8.122) has a simple oscillator form. Consequently, the partition function Z_g is

$$Z_g=\frac{1}{\left[2\sinh\left(\frac{\beta\hbar w}{2}\right)\right]^D}\frac{1}{\left[2\sinh\left(\frac{\beta\hbar w_f}{2}\right)\right]^D}. \tag{8.126}$$

The product Z_gZ_M of the two partition functions Z_g and $Z_M\left(\{N_\sigma\},N_f,\beta\right)$ is a path integral in the state space of N electrons, N_f fictitious particles and two "ghost" particles with the coordinate vectors $\mathbf{X}_g$ and $\mathbf{Y}_g$. The Lagrangian $\tilde{L}_M$ of this system is a sum of L_M and L_g,

$$\tilde{L}_M\left(\dot{\bar{\mathbf{x}}},\dot{\bar{\mathbf{y}}},\dot{\mathbf{X}}_g,\dot{\mathbf{Y}}_g;\bar{\mathbf{x}},\bar{\mathbf{y}},\mathbf{X}_g,\mathbf{Y}_g\right)\equiv L_M\left(\dot{\bar{\mathbf{x}}},\dot{\bar{\mathbf{y}}};\bar{\mathbf{x}},\bar{\mathbf{y}}\right)+L_g\left(\dot{\mathbf{X}}_g,\dot{\mathbf{Y}}_g,\mathbf{X}_g,\mathbf{Y}_g\right). \tag{8.127}$$

The "ghost" subsystem is introduced because the center-of-mass coordinates in $\tilde{L}_M$ can be explicitly separated much more transparently than in L_M. This separation is realized by the linear transformation of coordinates,

$$\left\{\begin{array}{l}\mathbf{x}_{j,\sigma}=\mathbf{x}'_{j,\sigma}+\mathbf{X}-\mathbf{X}_g,\\ \mathbf{y}_{j\sigma}=\mathbf{y}'_{j\sigma}+\mathbf{Y}-\mathbf{Y}_g,\end{array}\right. \tag{8.128}$$

where $\mathbf{X}$ and $\mathbf{Y}$ are the center-of-mass coordinate vectors of the electrons and of the fictitious particles, correspondingly:

$$\mathbf{X}=\frac{1}{N}\sum_\sigma\sum_{j=1}^{N_\sigma}\mathbf{x}_{j,\sigma},\quad \mathbf{Y}=\frac{1}{N_f}\sum_{j=1}^{N_f}\mathbf{y}_j. \tag{8.129}$$

Before the transformation (8.128), the independent variables are $\left(\bar{\mathbf{x}}, \bar{\mathbf{y}}, \mathbf{X}_g, \mathbf{Y}_g\right)$, with the center-of-mass coordinates $\mathbf{X}$ and $\mathbf{Y}$ determined by Eq. (8.129). When applying the transformation (8.128) to the centers of mass (8.129), we find that

$$\mathbf{X} = \frac{1}{N}\sum_{\sigma}\sum_{j=1}^{N_\sigma}\left(\mathbf{x}'_{j,\sigma} + \mathbf{X} - \mathbf{X}_g\right) = \frac{1}{N}\sum_{\sigma}\sum_{j=1}^{N_\sigma}\mathbf{x}'_{j,\sigma} + \mathbf{X} - \mathbf{X}_g, \tag{8.130}$$

$$\mathbf{Y} = \frac{1}{N_f}\sum_{j=1}^{N_f}\left(\mathbf{y}'_{j\sigma} + \mathbf{Y} - \mathbf{Y}_g\right) = \frac{1}{N_f}\sum_{j=1}^{N_f}\mathbf{y}'_{j\sigma} + \mathbf{Y} - \mathbf{Y}_g. \tag{8.131}$$

As seen from Eqs. (8.130), (8.131), after the transformation (8.128) the independent variables are $(\bar{\mathbf{x}}', \bar{\mathbf{y}}', \mathbf{X}, \mathbf{Y})$, while the coordinates $(\mathbf{X}_g, \mathbf{Y}_g)$ obey the equations

$$\mathbf{X}_g = \frac{1}{N}\sum_{\sigma}\sum_{j=1}^{N_\sigma}\mathbf{x}'_{j,\sigma}, \quad \mathbf{Y}_g = \frac{1}{N_f}\sum_{j=1}^{N_f}\mathbf{y}'_j. \tag{8.132}$$

In order to find the explicit form of the Lagrangian (8.127) after the transformation (8.128), we use the following relations for the quadratic sums of coordinates:

$$\begin{gathered}
\sum_{\sigma}\sum_{j=1}^{N_\sigma}\mathbf{x}^2_{j,\sigma} = \sum_{\sigma}\sum_{j=1}^{N_\sigma}\left(\mathbf{x}'_{j,\sigma}\right)^2 + N\left(\mathbf{X}^2 - \mathbf{X}_g^2\right), \quad \sum_{j=1}^{N_f}\mathbf{y}_j^2 = \sum_{j=1}^{N_f}\left(\mathbf{y}'_j\right)^2 + N_f\left(\mathbf{Y}^2 - \mathbf{Y}_g^2\right), \\
\sum_{\sigma,\sigma'}\sum_{j=1}^{N_\sigma}\sum_{l=1}^{N_{\sigma'}}\left(\mathbf{x}_{j,\sigma} - \mathbf{x}_{l,\sigma'}\right)^2 = 2N\sum_{\sigma}\sum_{j=1}^{N_\sigma}\left(\mathbf{x}'_{j,\sigma}\right)^2 - 2N_f^2\mathbf{X}_g^2, \\
\sum_{j=1}^{N_f}\sum_{l=1}^{N_f}\left(\mathbf{y}_j - \mathbf{y}_l\right)^2 = 2N_f\sum_{j=1}^{N_f}\left(\mathbf{y}'_j\right)^2 - 2N_f^2\mathbf{Y}_g^2, \\
\sum_{\sigma}\sum_{j=1}^{N_\sigma}\sum_{l=1}^{N_f}\left(\mathbf{x}_{j,\sigma} - \mathbf{y}_l\right)^2 = N_f\sum_{\sigma}\sum_{j=1}^{N_\sigma}\left(\mathbf{x}'_{j,\sigma}\right)^2 + N\sum_{j=1}^{N_f}\left(\mathbf{y}'_j\right)^2 + \\
NN_f\left(\mathbf{X}^2 + \mathbf{Y}^2 - 2\mathbf{X}\cdot\mathbf{Y} - \mathbf{X}_g^2 - \mathbf{Y}_g^2\right).
\end{gathered} \tag{8.133}$$

The substitution of Eq. (8.129) into Eq. (8.127) then results in the following 3 terms:

$$\tilde{L}_M\left(\dot{\bar{\mathbf{x}}}', \dot{\bar{\mathbf{y}}}', \dot{\mathbf{X}}, \dot{\mathbf{Y}}; \bar{\mathbf{x}}', \bar{\mathbf{y}}', \mathbf{X}, \mathbf{Y}\right) = L_w\left(\dot{\bar{\mathbf{x}}}', \bar{\mathbf{x}}'\right) + L_{w_f}\left(\dot{\bar{\mathbf{y}}}', \bar{\mathbf{y}}'\right) + L_C\left(\dot{\mathbf{X}}, \mathbf{X}; \dot{\mathbf{Y}}, \mathbf{Y}\right), \tag{8.134}$$

where $L_w\left(\dot{\bar{\mathbf{x}}}', \bar{\mathbf{x}}'\right)$ and $L_{w_f}\left(\dot{\bar{\mathbf{y}}}', \bar{\mathbf{y}}'\right)$ are Lagrangians of non-interacting identical oscillators with the frequencies w and w_f, respectively,

$$L_w\left(\dot{\bar{\mathbf{x}}}', \bar{\mathbf{x}}'\right) = -\frac{m_b}{2}\sum_{\sigma=\pm 1/2}\sum_{j=1}^{N_\sigma}\left[\left(\dot{\mathbf{x}}'_{j,\sigma}\right)^2 + w^2\left(\mathbf{x}'_{j,\sigma}\right)^2\right], \tag{8.135}$$

$$L_{w_f}\left(\dot{\bar{\mathbf{y}}}', \bar{\mathbf{y}}'\right) = -\frac{m_f}{2}\sum_{j=1}^{N_f}\left[\left(\dot{\mathbf{y}}'_{j,\sigma}\right)^2 + w_f^2\left(\mathbf{y}'_{j,\sigma}\right)^2\right]. \tag{8.136}$$

The Lagrangian $L_C\left(\dot{\mathbf{X}}, \mathbf{X}; \dot{\mathbf{Y}}, \mathbf{Y}\right)$ describes the combined motion of the centers-of-mass of the electrons and of the fictitious particles,

$$L_C\left(\dot{\mathbf{X}}, \mathbf{X}; \dot{\mathbf{Y}}, \mathbf{Y}\right) = -\frac{m_b N}{2}\left(\dot{\mathbf{X}}^2 + \tilde{\Omega}^2\mathbf{X}^2\right) - \frac{m_f N_f}{2}\left(\dot{\mathbf{Y}}^2 + w_f^2\mathbf{Y}^2\right) + kNN_f\mathbf{X}\cdot\mathbf{Y}, \tag{8.137}$$

with

$$\tilde{\Omega} = \sqrt{\Omega^2 + kN_f/m_b}. \tag{8.138}$$

The Lagrangian (8.137) is reduced to a diagonal quadratic form in the coordinates and the velocities by a unitary transformation for two interacting oscillators using the following replacement of variables:

$$\begin{aligned} \mathbf{X} &= \frac{1}{\sqrt{m_b N}} \left(a_1 \mathbf{r} + a_2 \mathbf{R}\right), \\ \mathbf{Y} &= \frac{1}{\sqrt{m_f N_f}} \left(-a_2 \mathbf{r} + a_1 \mathbf{R}\right) \end{aligned} \tag{8.139}$$

with the coefficients

$$a_1 = \left[\frac{1+\chi}{2}\right]^{1/2}, \quad a_2 = \left[\frac{1-\chi}{2}\right]^{1/2}, \tag{8.140}$$

$$\chi \equiv \frac{\tilde{\Omega}^2 - \tilde{\Omega}_f^2}{\left[\left(\tilde{\Omega}^2 - \tilde{\Omega}_f^2\right)^2 + 4\gamma^2\right]^{1/2}}, \quad \gamma \equiv k\sqrt{\frac{NN_f}{m_b m_f}}. \tag{8.141}$$

The eigenfrequencies of the center-of-mass subsystem are then given by the expression

$$\begin{cases} \Omega_1 = \sqrt{\frac{1}{2}\left[\tilde{\Omega}^2 + \tilde{\Omega}_f^2 + \sqrt{\left(\tilde{\Omega}^2 - \tilde{\Omega}_f^2\right)^2 + 4\gamma^2}\right]}, \\ \Omega_2 = \sqrt{\frac{1}{2}\left[\tilde{\Omega}^2 + \tilde{\Omega}_f^2 - \sqrt{\left(\tilde{\Omega}^2 - \tilde{\Omega}_f^2\right)^2 + 4\gamma^2}\right]}. \end{cases} \tag{8.142}$$

As a result, four independent frequencies Ω_1, Ω_2, w and w_f appear in the problem. Three of them (Ω_1, Ω_2, w) are the eigenfrequencies of the model system. Ω_1 is the frequency of the relative motion of the center of mass of the electrons with respect to the center of mass of the fictitious particles; Ω_2 is the frequency related to the center of mass of the model system as a whole; w is the frequency of the relative motion of the electrons with respect to their center of mass. The parameter w_f is an analog of the second variational parameter w of the one-polaron Feynman model. Further, the Lagrangian (8.137) takes the form

$$L_C = -\frac{1}{2}\left(\dot{\mathbf{r}}^2 + \Omega_1^2 \mathbf{r}^2\right) - \frac{1}{2}\left(\dot{\mathbf{R}}^2 + \Omega_2^2 \mathbf{R}^2\right), \tag{8.143}$$

leading to the partition function corresponding to the combined motion of the centers-of-mass of the electrons and of the fictitious particles

$$Z_C = \frac{1}{\left[2\sinh\left(\frac{\beta\hbar\Omega_1}{2}\right)\right]^D} \frac{1}{\left[2\sinh\left(\frac{\beta\hbar\Omega_2}{2}\right)\right]^D}. \tag{8.144}$$

Taking into account Eqs. (8.126) and (8.144), we obtain finally the partition function of the model system for interacting polarons

$$Z_0\left(\{N_\sigma\}, \beta\right) = \left[\frac{\sinh\left(\frac{\beta\hbar w}{2}\right)\sinh\left(\frac{\beta\hbar w_f}{2}\right)}{\sinh\left(\frac{\beta\hbar\Omega_1}{2}\right)\sinh\left(\frac{\beta\hbar\Omega_2}{2}\right)}\right]^D \tilde{\mathbb{Z}}_F\left(\{N_\sigma\}, w, \beta\right). \tag{8.145}$$

Here

$$\tilde{\mathbb{Z}}_F\left(\{N_\sigma\}, w, \beta\right) = \mathbb{Z}_F\left(N_{1/2}, w, \beta\right)\mathbb{Z}_F\left(N_{-1/2}, w, \beta\right) \tag{8.146}$$

is the partition function of $N = N_{1/2} + N_{-1/2}$ non-interacting fermions in a parabolic confinement potential with the frequency w. The analytical expressions for the partition function of N_σ spin-polarized fermions $\mathbb{Z}_F\left(N_\sigma, w, \beta\right)$ were derived in Ref. [101].

8.2.3 Variational functional

In order to obtain an upper bound to the free energy E_{var}, we substitute the model action functional (8.115) into the right-hand side of the variational inequality (8.107) and consider the limit $\beta \to \infty$:

$$
\begin{aligned}
&E_{var}\left(\{N_\sigma\}\right) \\
&= \mathbb{E}_F\left(\{N_\sigma\}, w\right) + \frac{m_b}{2}\left(\Omega_0^2 - \Omega^2 + N\omega^2\right)\left\langle \sum_{j=1}^{N} \mathbf{x}_j^2(0)\right\rangle_{S_0} \\
&- \frac{m_b\omega^2 N^2}{2}\left\langle \mathbf{X}^2(0)\right\rangle_{S_0} + \left\langle U_b(\bar{\mathbf{x}})\right\rangle_{S_0} + \sum_{\mathbf{q}\neq 0}\frac{2\pi e^2}{V\varepsilon_\infty q^2}\left[\mathcal{G}\left(\mathbf{q}, 0|\{N_\sigma\}, \beta\to\infty\right) - N\right] \\
&+ \lim_{\beta\to\infty}\frac{k^2N^2N_f}{4m_f\beta\hbar\Omega_f}\int_0^{\hbar\beta} d\tau \int_0^{\hbar\beta} d\tau' \frac{\cosh\left[\Omega_f\left(|\tau-\tau'| - \hbar\beta/2\right)\right]}{\sinh\left(\beta\hbar\Omega_f/2\right)}\left\langle \mathbf{X}(\tau)\cdot\mathbf{X}(\tau')\right\rangle_{S_0} \\
&- \lim_{\beta\to\infty}\sum_{\mathbf{q}}\frac{|V_{\mathbf{q}}|^2}{2\hbar^2\beta}\int_0^{\hbar\beta} d\tau \int_0^{\hbar\beta} d\tau' \frac{\cosh\left[\omega_{\mathrm{LO}}\left(|\tau-\tau'| - \hbar\beta/2\right)\right]}{\sinh\left(\beta\hbar\omega_{\mathrm{LO}}/2\right)}\mathcal{G}\left(\mathbf{q}, \tau-\tau'|\{N_\sigma\}, \beta\right).
\end{aligned}
\tag{8.147}
$$

Here, $\mathbb{E}_F(N, w)$ is the energy of N non-interacting fermions in a parabolic confinement potential with the confinement frequency w,

$$
\begin{aligned}
\mathbb{E}_F\left(\{N_\sigma\}, w\right) = \hbar w \sum_{\sigma=\pm 1/2}\Bigg\{&\sum_{n=0}^{L_\sigma-1}\left(n+\frac{3}{2}\right)g(n) \\
&+ \left(N_\sigma - N_{L_\sigma}\right)\left(L_\sigma + \frac{3}{2}\right)\Bigg\},
\end{aligned}
\tag{8.148}
$$

where σ is the spin of an electron, L_σ is the lower partly filled or empty level for N_σ electrons with the spin projection σ. The first term in the curly brackets of Eq. (8.175) (the upper line) is the number of electrons at fully filled energy levels, while the second term (square brackets) is the number of electrons at the next upper level (which can be empty or filled partially). The energy levels of a 3D oscillator are degenerate, so that

$$
g(n) = \frac{1}{2}(n+1)(n+2) \tag{8.149}
$$

is the degeneracy of the n-th energy level. The parameter

$$
N_{L_\sigma} = \frac{1}{6}L_\sigma\left(L_\sigma+1\right)\left(L_\sigma+2\right) \tag{8.150}
$$

is the number of electrons at all fully filled levels. The summation in Eq. (8.148) is performed explicitly, what gives us the result

$$
\mathbb{E}_F\left(\{N_\sigma\}, w\right) = \hbar w \sum_{\sigma}\left[\frac{1}{8}L_\sigma\left(L_\sigma+1\right)^2\left(L_\sigma+2\right) + \left(N_\sigma - N_{L_\sigma}\right)\left(L_\sigma + \frac{3}{2}\right)\right]. \tag{8.151}
$$

In Eq. (8.147), $\mathcal{G}\left(\mathbf{q}, \tau-\tau'|\{N_\sigma\}, \beta\right)$ is the two-point correlation function for the electron density operators:

$$
\mathcal{G}\left(\mathbf{q}, \tau|\{N_\sigma\}, \beta\right) = \left\langle \rho_{\mathbf{q}}(\tau)\,\rho_{-\mathbf{q}}(0)\right\rangle_{S_0}. \tag{8.152}
$$

The averages $\langle \mathbf{X}(\tau)\cdot\mathbf{X}(\tau')\rangle_{S_0}$ are calculated using the generating function method:

$$\langle X_k(\tau)X_k(\tau')\rangle_{S_0} = -\frac{\partial^2}{\partial\xi_k\partial\eta_k}\langle\exp\left[i\left(\xi\cdot\mathbf{X}(\tau)+\eta\cdot\mathbf{X}(\tau')\right)\right]\rangle_{S_0}\Big|_{\substack{\xi=0,\\ \eta=0}}, \tag{8.153}$$

$$\Longrightarrow \langle \mathbf{X}(\tau)\cdot\mathbf{X}(\tau')\rangle_{S_0} = \frac{3\hbar}{2mN}\sum_{i=1}^{2}\frac{a_i^2\cosh\left[\Omega_i\left(|\tau-\sigma|-\hbar\beta/2\right)\right]}{\Omega_i\sinh\left(\hbar\beta\Omega_i/2\right)}. \tag{8.154}$$

Substituting this expression into Eq. (8.147) and performing integrations over τ and σ analytically, we obtain the result

$$\frac{k^2N^2N_f}{4m_f\beta\hbar\Omega_f}\int_0^{\hbar\beta}d\tau\int_0^{\hbar\beta}d\tau'\frac{\cosh\left[\Omega_f\left(|\tau-\tau'|-\hbar\beta/2\right)\right]}{\sinh\left(\beta\hbar\Omega_f/2\right)}\langle\mathbf{X}(\tau)\cdot\mathbf{X}(\tau')\rangle_{S_0}$$
$$=\frac{3\hbar\gamma}{4}\sum_{i=1}^{2}\frac{a_i^2}{\Omega_f^2-\Omega_i^2}\left[\frac{\coth\left(\beta\Omega_i/2\right)}{\Omega_i}-\frac{\coth\left(\beta\Omega_f/2\right)}{\Omega_f}\right], \tag{8.155}$$

and in the zero-temperature limit we have

$$\lim_{\beta\to\infty}\frac{k^2N^2N_f}{4m_f\beta\hbar\Omega_f}\int_0^{\hbar\beta}d\tau\int_0^{\hbar\beta}d\tau'\frac{\cosh\left[\Omega_f\left(|\tau-\tau'|-\hbar\beta/2\right)\right]}{\sinh\left(\beta\hbar\Omega_f/2\right)}\langle\mathbf{X}(\tau)\cdot\mathbf{X}(\tau')\rangle_{S_0}$$
$$=\frac{3\hbar\gamma}{4}\sum_{i=1}^{2}\frac{a_i^2}{\Omega_f^2-\Omega_i^2}\left(\frac{1}{\Omega_i}-\frac{1}{\Omega_f}\right). \tag{8.156}$$

The average $\left\langle\sum_{j=1}^{N}\mathbf{x}_j^2\right\rangle_{S_0}$ is transformed, using the described above operations with the "ghost" subsystem,

$$\mathbf{x}_j=\mathbf{x}_j'+\mathbf{X}-\mathbf{X}_g, \tag{8.157}$$

and taking into account the first of equations (8.133)

$$\sum_{j=1}^{N}\mathbf{x}_j^2=\sum_{j=1}^{N}\left(\mathbf{x}_j'\right)^2+N\left(\mathbf{X}^2-\mathbf{X}_g^2\right). \tag{8.158}$$

Consequently, averaging the left-hand side of Eq. (8.158) on the model action functional S_0, one obtains

$$\left\langle\sum_{j=1}^{N}\mathbf{x}_j^2\right\rangle_{S_0}=\left\langle\sum_{j=1}^{N}\mathbf{x}_j^2\right\rangle_{S_M}=\left\langle\sum_{j=1}^{N}\mathbf{x}_j^2\right\rangle_{S_M+S_g}$$
$$=\left\langle\sum_{j=1}^{N}\mathbf{x}_j^2\right\rangle_{S_w}+N\left(\langle\mathbf{X}^2\rangle_{S_C}-\langle\mathbf{X}_g^2\rangle_{S_g}\right). \tag{8.159}$$

The term $\left\langle\sum_{j=1}^{N}\mathbf{x}_j^2\right\rangle_{S_w}$ is expressed using the virial theorem through the ground-state energy $\mathbb{E}_F(N,w)$ of N independent 3D fermion oscillators with the frequency w and with the mass m_b,

$$\left\langle\sum_{j=1}^{N}\mathbf{x}_j^2\right\rangle_{S_w}=\frac{\mathbb{E}_F(N,w)}{m_bw^2}=-\frac{1}{m_bw^2}\frac{\partial}{\partial\lambda}\ln\mathbb{Z}_I(N), \tag{8.160}$$

Two other terms in Eq. (8.159) are [cf. Eq. (8.154)]:

$$\left\langle \mathbf{X}^2 \right\rangle_{S_C} = \frac{3\hbar}{2m_b N} \sum_{i=1}^{2} \frac{a_i^2 \coth\left(\beta\Omega_i/2\right)}{\Omega_i},$$
$$\left\langle \mathbf{X}_g^2 \right\rangle_{S_g} = \frac{3\hbar}{2m_b N} \frac{\coth\left(\beta w/2\right)}{w}. \tag{8.161}$$

So, we obtain

$$\left\langle \sum_{j=1}^{N} \mathbf{x}_j^2 \right\rangle_{S_0} = \frac{\mathbb{E}_F\left(\{N_\sigma\}, w\right)}{m_b w^2} + \frac{3\hbar}{2m_b}\left(\sum_{i=1}^{2} \frac{a_i^2}{\Omega_i} - \frac{1}{w}\right). \tag{8.162}$$

The averaging of the background-charge potential gives us the result

$$\begin{aligned}\left\langle U_b\left(\bar{\mathbf{x}}\right)\right\rangle_{S_0} &= \frac{3\sqrt{2}\alpha\eta}{\pi\left(1-\eta\right)} \sum_{\sigma} \sum_{n=0}^{\infty} f_1\left(n,\sigma|\beta,N_\sigma\right)|_{\beta\to\infty} \sum_{k=0}^{n} \frac{\left(-1\right)^k}{k!} \binom{n+2}{n-k} \left(\frac{1}{2w}\right)^k \\ &\times \left\{ \frac{\Gamma\left(k-\frac{1}{2}\right)}{A^{k-1/2}} \left[{}_1F_1\left(k-\frac{1}{2};\frac{1}{2};-\frac{R^2}{4A}\right) - {}_1F_1\left(k-\frac{1}{2};\frac{3}{2};-\frac{R^2}{4A}\right)\right]\right\}, \\ \eta &\equiv \varepsilon_\infty/\varepsilon_0, \quad A \equiv \frac{\hbar}{4m_b N}\left(\sum_{i=1}^{2}\frac{a_i^2}{\Omega_i} + \frac{N-1}{w}\right),\end{aligned} \tag{8.163}$$

where $f_1\left(n,\sigma|\beta,N_\sigma\right)$ is the one-particle distribution function of fermions (the distribution functions are considered in more details in the next subsection).

Collecting all terms together, we arrive at the variational functional

$$\begin{aligned}E_{var}\left(\Omega_1,\Omega_2,w,\Omega_f\right) &= \hbar\left\{\frac{\Omega_0^2+w^2}{2w^2}\left[\frac{\tilde{E}\left(w,N\right)}{\hbar} - \frac{3}{2}w\right] + \frac{3}{2}\left(\Omega_1+\Omega_2-\Omega_f\right)\right. \\ &\left. + \frac{3}{4}\left(\Omega_0^2-\Omega_1^2-\Omega_2^2+\Omega_f^2\right)\sum_{i=1}^{2}\frac{a_i^2}{\Omega_i} + \frac{3\gamma^2}{4\Omega_f}\sum_{i=1}^{2}\frac{a_i^2}{\Omega_i\left(\Omega_i+\Omega_f\right)}\right\} \\ &+ \left\langle U_b\left(\bar{\mathbf{x}}\right)\right\rangle_{S_0} + E_C + E_{e-ph},\end{aligned} \tag{8.164}$$

where E_C and E_{e-ph} are the Coulomb and polaron contributions, respectively:

$$E_C = \frac{e^2}{4\pi^2\varepsilon_\infty}\int d\mathbf{q}\frac{1}{q^2}\left[\mathcal{G}\left(\mathbf{q},0|\left\{N_\sigma\right\},\beta\right)|_{\beta\to\infty} - N\right], \tag{8.165}$$

$$E_{e-ph} = -\frac{\sqrt{2}\alpha}{4\pi^2\hbar}\int d\mathbf{q}\frac{1}{q^2}\int_0^\infty d\tau \exp\left(-\omega_{\mathrm{LO}}\tau\right)\mathcal{G}\left(\mathbf{q},\tau|\left\{N_\sigma\right\},\beta\right)|_{\beta\to\infty}. \tag{8.166}$$

The correlation function (8.152) is calculated analytically in the next subsection. With this correlation function, the variational ground-state energy is calculated and minimized numerically.

8.2.4 Two-point correlation functions

The two-point correlation function (8.152) is represented as the following path integral:

$$\begin{aligned}\mathcal{G}\left(\mathbf{q},\tau|\left\{N_\sigma\right\},\beta\right) &= \frac{1}{Z_0\left(\left\{N_\sigma\right\},\beta\right)}\sum_P \frac{\left(-1\right)^{\xi_P}}{N_{1/2}!N_{-1/2}!} \\ &\times \int d\bar{\mathbf{x}}\int_{\bar{\mathbf{x}}}^{P\bar{\mathbf{x}}} D\bar{\mathbf{x}}\left(\tau\right)e^{-S_0[\bar{\mathbf{x}}(\tau)]}\rho_{\mathbf{q}}\left(\tau\right)\rho_{-\mathbf{q}}\left(0\right).\end{aligned} \tag{8.167}$$

We observe that $\mathcal{G}(\mathbf{q},\tau|\{N_\sigma\},\beta)$ can be rewritten as an average within the model "action" $S_M[\bar{\mathbf{x}}(\tau),\bar{\mathbf{y}}(\tau)]$ of interacting electrons and fictitious particles:

$$\begin{aligned}\mathcal{G}(\mathbf{q},\tau|\{N_\sigma\},\beta) = &\frac{1}{Z_M(\{N_\sigma\},N_f,\beta)}\sum_P \frac{(-1)^{\xi_P}}{N_{1/2}!N_{-1/2}!}\\ &\times\int d\bar{\mathbf{x}}\int_{\bar{\mathbf{x}}}^{P\bar{\mathbf{x}}} D\bar{\mathbf{x}}(\tau)\int d\bar{\mathbf{y}}\int_{\bar{\mathbf{y}}}^{\bar{\mathbf{y}}} D\bar{\mathbf{y}}(\tau)\, e^{-S_M[\bar{\mathbf{x}}(\tau),\bar{\mathbf{y}}(\tau)]}\\ &\times\rho_{\mathbf{q}}(\tau)\,\rho_{-\mathbf{q}}(0)\,. \end{aligned}\tag{8.168}$$

Indeed, one readily derives that the elimination of the fictitious particles in (8.168) leads to (8.167). The representation (8.168) allows one to calculate the correlation function $\mathcal{G}(\mathbf{q},\tau|\{N_\sigma\},\beta)$ in a much simpler way than through Eq. (8.167), using the separation of the coordinates of the centers of mass of the electrons and of the fictitious particles. This separation is performed for the two-point correlation function (8.168) by the same method as it has been done for the partition function (8.120). As a result, one obtains

$$\mathcal{G}(\mathbf{q},\tau|\{N_\sigma\},\beta) = \tilde{g}(\mathbf{q},\tau|\{N_\sigma\},\beta)\,\frac{\langle\exp[i\mathbf{q}\cdot(\mathbf{X}(\tau)-\mathbf{X}(\sigma))]\rangle_{S_C}}{\langle\exp[i\mathbf{q}\cdot(\mathbf{X}_g(\tau)-\mathbf{X}_g(\sigma))]\rangle_{S_g}},\tag{8.169}$$

where $\tilde{g}(\mathbf{q},\tau|\{N_\sigma\},\beta)$ is the time-dependent correlation function of N non-interacting electrons in a parabolic confinement potential with the frequency w,

$$\tilde{g}(\mathbf{q},\tau|\{N_\sigma\},\beta) = \langle\rho_{\mathbf{q}}(\tau)\,\rho_{-\mathbf{q}}(0)\rangle_{S_w}\,.\tag{8.170}$$

The action functional $S_w[\bar{\mathbf{x}}_\tau]$ is related to the Lagrangian $L_w(\dot{\bar{\mathbf{x}}},\bar{\mathbf{x}})$ [Eq. (8.135)]

$$S_w[\bar{\mathbf{x}}_\tau] = \frac{1}{\hbar}\int_0^{\hbar\beta} L_w(\dot{\bar{\mathbf{x}}},\bar{\mathbf{x}})\,d\tau.\tag{8.171}$$

The averages in (8.169) are calculated using Feynman's method of generating functions [43]. Namely, according to [43], the average

$$G[f(\tau)] \equiv \left\langle\exp\left\{\frac{i}{\hbar}\int_0^\beta f(\tau)\,x_\tau\,d\tau\right\}\right\rangle_{S_\omega},\tag{8.172}$$

where S_ω is the action functional of a one-dimensional harmonic oscillator with the frequency ω and with the mass m, results in

$$G[f(\tau)] = \exp\left\{-\frac{1}{4m\hbar\omega}\int_0^\beta d\tau\int_0^\beta d\sigma\frac{\cosh[\omega(|\tau-\sigma|-\beta/2)]}{\sinh(\beta\omega/2)}f(\tau)\,f(\sigma)\right\}.\tag{8.173}$$

The diagonalization procedure for the Lagrangian L_C (8.137) allows us to represent that Lagrangian as a sum of Lagrangians of independent harmonic oscillators, what gives the following explicit expressions for averages in Eq. (8.169):

$$\begin{aligned}&\langle\exp[i\mathbf{q}\cdot(\mathbf{X}(\tau)-\mathbf{X}(\sigma))]\rangle_{S_C}\\ &= \exp\left\{-\frac{\hbar q^2}{Nm_b}\left[\sum_{i=1}^2 a_i^2\frac{\sinh\left(\frac{\Omega_i|\tau-\sigma|}{2}\right)\sinh\left(\frac{\Omega_i(\hbar\beta-|\tau-\sigma|)}{2}\right)}{\Omega_i\sinh\left(\frac{\beta\hbar\Omega_i}{2}\right)}\right]\right\},\\ &\langle\exp[i\mathbf{q}\cdot(\mathbf{X}_g(\tau)-\mathbf{X}_g(\sigma))]\rangle_{S_g}\\ &= \exp\left[-\frac{\hbar q^2}{Nm_b}\frac{\sinh\left(\frac{w|\tau-\sigma|}{2}\right)\sinh\left(\frac{w(\hbar\beta-|\tau-\sigma|)}{2}\right)}{w\sinh\left(\frac{\beta\hbar w}{2}\right)}\right].\end{aligned}$$

The correlation function $\tilde{g}\left(\mathbf{q},\tau\right|\left\{N_\sigma\right\},\beta)$

As seen from the formula (8.170), $\tilde{g}\left(\mathbf{q},\tau\right|\left\{N_\sigma\right\},\beta)$ is the time-dependent correlation function of N non-interacting fermions in a parabolic confinement potential with the frequency w. Let us consider first of all a system of N identical spin-polarized oscillators with the Lagrangian

$$L=\frac{m}{2}\sum_{j=1}^{N}\left(\dot{\mathbf{x}}_j^2-\omega^2\mathbf{x}_j^2\right). \tag{8.174}$$

The corresponding Hamiltonian is

$$\hat{H}=\sum_{j=1}^{N}\left(\frac{\hat{\mathbf{p}}_j^2}{2m}+\frac{m\omega^2\hat{\mathbf{x}}_j^2}{2}\right), \tag{8.175}$$

$$\hat{H}=\sum_{j=1}^{N}\hat{h}_j,\quad \hat{h}\equiv\frac{\hat{\mathbf{p}}^2}{2m}+\frac{m\omega^2\hat{\mathbf{x}}^2}{2}. \tag{8.176}$$

A set of eigenfunctions of the one-particle Hamiltonian $\hat{h}$ is determined as follows:

$$\hat{h}\psi_{\mathbf{n}}\left(\mathbf{x}\right)=\varepsilon_n\psi_{\mathbf{n}}\left(\mathbf{x}\right), \tag{8.177}$$

where

$$\begin{aligned}&\mathbf{n}\equiv\left(n_1,n_2,n_3\right),\quad n\equiv n_1+n_2+n_3,\\ &\varepsilon_{\mathbf{n}}=\varepsilon_n=\hbar\omega\left(n+\frac{3}{2}\right),\quad \psi_{\mathbf{n}}\left(\mathbf{x}\right)=\varphi_{n_1}\left(x_1\right)\varphi_{n_2}\left(x_2\right)\varphi_{n_3}\left(x_3\right),\end{aligned} \tag{8.178}$$

$\varphi_n\left(x\right)$ is the n-th eigenfunction of a one-dimensional oscillator with the frequency ω.

The Hamiltonian (8.175) can be written down in terms of the annihilation ($\hat{a}_{\mathbf{n}}$) and creation ($\hat{a}_{\mathbf{n}}^+$) operators:

$$\hat{H}=\sum_{\mathbf{n}}\varepsilon_{\mathbf{n}}\hat{a}_{\mathbf{n}}^+\hat{a}_{\mathbf{n}}=\sum_{\mathbf{n}}\varepsilon_{\mathbf{n}}\hat{N}_{\mathbf{n}},\quad \hat{N}_{\mathbf{n}}\equiv\hat{a}_{\mathbf{n}}^+\hat{a}_{\mathbf{n}}. \tag{8.179}$$

The many-particle quantum states in the representation of "occupation numbers" are written down as $|\ldots N_{\mathbf{n}}\ldots\rangle$, where $N_{\mathbf{n}}$ is the number of particles in the $\mathbf{n}$-th one-particle quantum state. The states $|\ldots N_{\mathbf{n}}\ldots\rangle$ are defined as the eigenstates of the operator of the number of particles in the $\mathbf{n}$-th state $\hat{N}_{\mathbf{n}}$:

$$\hat{N}_{\mathbf{n}}\left|\ldots N_{\mathbf{n}}\ldots\right\rangle=N_{\mathbf{n}}\left|\ldots N_{\mathbf{n}}\ldots\right\rangle. \tag{8.180}$$

Let us determine a set of quantum states with a *finite* total number of particles

$$\sum_{\mathbf{n}}N_{\mathbf{n}}=N \tag{8.181}$$

as follows:

$$|\ldots N_{\mathbf{n}}\ldots\rangle|_{\sum_{\mathbf{n}}N_{\mathbf{n}}=N}\equiv\left|\Psi_{N,\{N_{\mathbf{n}}\}}\right\rangle. \tag{8.182}$$

Further on, we use the basis set of quantum states (8.182) for the derivation of the partition function, of the density function and of the two-point correlation function.

Partition function

The density matrix of the *canonical* Hibbs ensemble is

$$\hat{\rho} = \exp\left(-\beta\hat{H}\right), \quad \beta \equiv \frac{1}{k_B T}.$$

The partition function of this ensemble is the trace of the density matrix on the set of quantum states (8.182):

$$\begin{aligned}\mathbb{Z}_I(\beta|N) &= \sum_{\{N_{\mathbf{n}}\}} \left\langle \Psi_{N,\{N_{\mathbf{n}}\}} \middle| \exp\left(-\beta\hat{H}\right) \middle| \Psi_{N,\{N_{\mathbf{n}}\}} \right\rangle \\ &= \left[\sum_{\{N_{\mathbf{n}}\}} \exp\left(-\beta \sum_{\mathbf{n}} \varepsilon_{\mathbf{n}} N_{\mathbf{n}}\right)\right]_{\sum_{\mathbf{n}} N_{\mathbf{n}}=N}. \end{aligned} \tag{8.183}$$

This expression can be written down also in the form

$$\mathbb{Z}_I(\beta|N) = \sum_{\{N_{\mathbf{n}}\}} \exp\left(-\beta \sum_{\mathbf{n}} \varepsilon_{\mathbf{n}} N_{\mathbf{n}}\right) \delta_{N,\sum_{\mathbf{n}} N_{\mathbf{n}}}, \tag{8.184}$$

where

$$\delta_{j,k} = \begin{cases} 1, & j = k \\ 0, & j \neq k \end{cases}$$

is the delta symbol.

Let us introduce the generating function for the partition function in the same way as in Ref. [101]:

$$\begin{aligned}\Xi(\beta, u) &= \sum_{N=0}^{\infty} u^N \mathbb{Z}_I(\beta|N) = \sum_{N=0}^{\infty} u^N \sum_{\{N_{\mathbf{n}}\}} \exp\left(-\beta \sum_{\mathbf{n}} \varepsilon_{\mathbf{n}} N_{\mathbf{n}}\right) \delta_{N,\sum_{\mathbf{n}} N_{\mathbf{n}}} \\ &= \sum_{\{N_{\mathbf{n}}\}} \exp\left(-\beta \sum_{\mathbf{n}} \varepsilon_{\mathbf{n}} N_{\mathbf{n}}\right) \sum_{N=0}^{\infty} u^{\sum_{\mathbf{n}} N_{\mathbf{n}}} \delta_{N,\sum_{\mathbf{n}} N_{\mathbf{n}}} \\ &= \sum_{\{N_{\mathbf{n}}\}} \exp\left(-\beta \sum_{\mathbf{n}} \varepsilon_{\mathbf{n}} N_{\mathbf{n}}\right) u^{\sum_{\mathbf{n}} N_{\mathbf{n}}} \quad \Longrightarrow \end{aligned}$$

$$\Xi(\beta, u) = \prod_{\mathbf{n}} \left\{ \sum_{N_{\mathbf{n}}} \left[u \exp\left(-\beta\varepsilon_{\mathbf{n}}\right)\right]^{N_{\mathbf{n}}} \right\}. \tag{8.185}$$

Fermions

For fermions, the number $N_{\mathbf{n}}$ can take only values $N_{\mathbf{n}} = 0$ and $N_{\mathbf{n}} = 1$. Hence, for fermions (denoted by the index F), we obtain:

$$\Xi_F(\beta, u) = \prod_{\mathbf{n}} \left[1 + u \exp\left(-\beta\varepsilon_{\mathbf{n}}\right)\right].$$

Since the n-th level of a 3D oscillator is degenerate with the degeneracy

$$g(n) = \frac{(n+1)(n+2)}{2},$$

we find that the generating function $\Xi_F(\beta, u)$ is given by

$$\Xi_F(\beta, u) = \prod_{n=0}^{\infty} \left[1 + u \exp\left(-\beta\varepsilon_n\right)\right]^{g(n)}. \tag{8.186}$$

Bosons

For bosons (denoted by the index B), $N_{\mathbf{n}} = 0, 1, \ldots, \infty$. The summations over $\{N_{\mathbf{n}}\}$ in Eq. (8.185) gives:

$$\Xi_B(\beta, u) = \prod_{n=0}^{\infty} \left[\frac{1}{1 - u \exp(-\beta \varepsilon_n)} \right]^{g(n)}. \tag{8.187}$$

The results (8.185) and (8.187) prove (for the partition function) the equivalence of the path-integral approach for identical particles [101] and of the second-quantization method.

Integral representation

Let us use the Fourier representation for the delta symbol:

$$\delta_{N, \sum_{\mathbf{n}} N_{\mathbf{n}}} = \frac{1}{2\pi} \int_0^{2\pi} \exp\left[i \left(\sum_{\mathbf{n}} N_{\mathbf{n}} - N \right) (\theta - i\zeta) \right] d\theta, \tag{8.188}$$

where ζ is an arbitrary constant. Substituting Eq. (8.188) into Eq. (8.184) we obtain

$$\begin{aligned}
\mathbb{Z}_I(\beta|N) &= \sum_{\{N_{\mathbf{n}}\}} \exp\left(-\beta \sum_{\mathbf{n}} \varepsilon_{\mathbf{n}} N_{\mathbf{n}} \right) \frac{1}{2\pi} \int_0^{2\pi} \exp\left[i \left(\sum_{\mathbf{n}} N_{\mathbf{n}} - N \right) (\theta - i\zeta) \right] d\theta \\
&= \frac{1}{2\pi} \int_0^{2\pi} d\theta \exp\left[-iN(\theta - i\zeta) \right] \sum_{\{N_{\mathbf{n}}\}} \exp\left(-\beta \sum_{\mathbf{n}} \varepsilon_{\mathbf{n}} N_{\mathbf{n}} + i \sum_{\mathbf{n}} N_{\mathbf{n}} (\theta - i\zeta) \right) \\
&= \frac{1}{2\pi} \int_0^{2\pi} d\theta \exp(-iN\theta - N\zeta) \, \Xi\left(\beta, e^{i\theta + \zeta}\right) \quad \Longrightarrow
\end{aligned}$$

$$\mathbb{Z}_I(\beta|N) = \frac{1}{2\pi} \int_0^{2\pi} d\theta \exp\left[\ln \Xi\left(\beta, e^{i\theta+\zeta}\right) - N\zeta - iN\theta \right]. \tag{8.189}$$

The partition function for a finite number of particles can be obtained from the generation function also by the inversion formula [102]

$$\mathbb{Z}_I(\beta|N) = \frac{1}{2\pi i} \oint \frac{\Xi(\beta, z)}{z^{N+1}} dz \tag{8.190}$$

$$= \frac{1}{2\pi} \int_0^{2\pi} e^{\left[\ln \Xi\left(\beta, u e^{i\theta}\right) - N \ln u\right]} e^{-iN\theta} d\theta. \tag{8.191}$$

Let us denote in Eq. (8.189):

$$\zeta \equiv \ln u. \tag{8.192}$$

In these notations, Eqs. (8.189) and (8.191) are *identical*. For the numerical calculation, it is more convenient to choose in Eq. (8.188) the interval of the integration over θ as $[-\pi, \pi]$ instead of $[0, 2\pi]$, what gives:

$$\mathbb{Z}_I(\beta|N) = \frac{1}{2\pi} \int_{-\pi}^{\pi} \Phi_N(\theta) \, d\theta, \tag{8.193}$$

with the function

$$\Phi_N(\theta) = \exp\left[\ln \Xi\left(\beta, ue^{i\theta}\right) - N\ln u - iN\theta\right]. \tag{8.194}$$

The aforesaid method of derivation of the partition function [Eqs. (8.188) to (8.189)] is heuristically useful, because it allows a simple generalization to spin-mixed systems with various polarization distributions.

The two-point density-density correlation function in the operator formalism is

$$\tilde{g}\left(\mathbf{q}, \tau | \{N_\sigma\}, \beta\right) = \left\langle \hat{\rho}_{\mathbf{q}}(\tau)\, \hat{\rho}_{-\mathbf{q}}(0)\right\rangle, \tag{8.195}$$

where $\hat{\rho}_{\mathbf{q}}(t)$ is the density operator in the Heisenberg representation:

$$\hat{\rho}_{\mathbf{q}}(\tau) = \exp\left(\frac{\tau}{\hbar}\hat{H}\right)\rho_{\mathbf{q}}\exp\left(-\frac{\tau}{\hbar}\hat{H}\right). \tag{8.196}$$

In the "second-quantization" representation, $\hat{\rho}_{\mathbf{q}}(t)$ is

$$\begin{aligned}\hat{\rho}_{\mathbf{q}}(\tau) &= \sum_{\mathbf{n},\mathbf{n}'}\left(e^{i\mathbf{q}\cdot\hat{\mathbf{x}}}\right)_{\mathbf{n}\mathbf{n}'}\hat{a}^+_{\mathbf{n}}(\tau)\,\hat{a}_{\mathbf{n}'}(\tau)\\ &= \sum_{\mathbf{n},\mathbf{n}'}\left(e^{i\mathbf{q}\cdot\hat{\mathbf{x}}}\right)_{\mathbf{n}\mathbf{n}'}\hat{a}^+_{\mathbf{n}}\hat{a}_{\mathbf{n}'}\exp\left[\frac{\tau}{\hbar}\left(\varepsilon_{\mathbf{n}} - \varepsilon_{\mathbf{n}'}\right)\right].\end{aligned} \tag{8.197}$$

After substituting Eq. (8.197) into (8.195), we find that

$$\tilde{g}\left(\mathbf{q}, \tau | \{N_\sigma\}, \beta\right) = \sum_{\mathbf{n},\mathbf{n}'}\sum_{\mathbf{m},\mathbf{m}'}\left(e^{i\mathbf{q}\cdot\hat{\mathbf{x}}}\right)_{\mathbf{n}\mathbf{n}'}\left(e^{-i\mathbf{q}\cdot\hat{\mathbf{x}}}\right)_{\mathbf{m}\mathbf{m}'}\exp\left[\frac{\tau}{\hbar}\left(\varepsilon_{\mathbf{n}} - \varepsilon_{\mathbf{n}'}\right)\right]\left\langle \hat{a}^+_{\mathbf{n}}\hat{a}_{\mathbf{n}'}\hat{a}^+_{\mathbf{m}}\hat{a}_{\mathbf{m}'}\right\rangle. \tag{8.198}$$

The operator $\hat{a}^+_{\mathbf{n}}\hat{a}_{\mathbf{n}'}\hat{a}^+_{\mathbf{m}}\hat{a}_{\mathbf{m}'}$ has non-zero diagonal matrix elements in the basis of quantum states $\left|\Psi_{N,\{N_{\mathbf{n}}\}}\right\rangle$ only in the cases

$$\left\{\begin{array}{c}\mathbf{n} = \mathbf{n}'\\ \mathbf{m} = \mathbf{m}'\end{array}\right. \quad \text{or} \quad \left\{\begin{array}{c}\mathbf{n} = \mathbf{m}'\\ \mathbf{m} = \mathbf{n}'\end{array}\right. . \tag{8.199}$$

Hence, the average

$$\left\langle \hat{a}^+_{\mathbf{n}}\hat{a}_{\mathbf{n}'}\hat{a}^+_{\mathbf{m}}\hat{a}_{\mathbf{m}'}\right\rangle = \frac{1}{\mathbb{Z}_I(\beta|N)}\sum_{\{N_{\mathbf{n}}\}}\left\langle \Psi_{N,\{N_{\mathbf{n}}\}}\left|\exp\left(-\beta\hat{H}\right)\hat{a}^+_{\mathbf{n}}\hat{a}_{\mathbf{n}'}\hat{a}^+_{\mathbf{m}}\hat{a}_{\mathbf{m}'}\right|\Psi_{N,\{N_{\mathbf{n}}\}}\right\rangle \tag{8.200}$$

is not equal to zero only when the condition (8.199) is fulfilled. This allows us to write down the average (8.200) as

$$\begin{aligned}\left\langle \hat{a}^+_{\mathbf{n}}\hat{a}_{\mathbf{n}'}\hat{a}^+_{\mathbf{m}}\hat{a}_{\mathbf{m}'}\right\rangle &= \delta_{\mathbf{n}'\mathbf{n}}\delta_{\mathbf{m}'\mathbf{m}}\left(1-\delta_{\mathbf{m}\mathbf{n}}\right)\left\langle \hat{a}^+_{\mathbf{n}}\hat{a}_{\mathbf{n}}\hat{a}^+_{\mathbf{m}}\hat{a}_{\mathbf{m}}\right\rangle + \delta_{\mathbf{m}'\mathbf{n}}\delta_{\mathbf{n}'\mathbf{m}}\left(1-\delta_{\mathbf{m}\mathbf{n}}\right)\left\langle \hat{a}^+_{\mathbf{n}}\hat{a}_{\mathbf{m}}\hat{a}^+_{\mathbf{m}}\hat{a}_{\mathbf{n}}\right\rangle\\ &\quad + \delta_{\mathbf{n}'\mathbf{n}}\delta_{\mathbf{m}'\mathbf{m}}\delta_{\mathbf{m}\mathbf{n}}\left\langle \hat{a}^+_{\mathbf{n}}\hat{a}_{\mathbf{n}}\hat{a}^+_{\mathbf{n}}\hat{a}_{\mathbf{n}}\right\rangle\\ &= \delta_{\mathbf{n}'\mathbf{n}}\delta_{\mathbf{m}'\mathbf{m}}\left(1-\delta_{\mathbf{m}\mathbf{n}}\right)\left\langle \hat{N}_{\mathbf{n}}\hat{N}_{\mathbf{m}}\right\rangle + \delta_{\mathbf{m}'\mathbf{n}}\delta_{\mathbf{n}'\mathbf{m}}\left(1-\delta_{\mathbf{m}\mathbf{n}}\right)\left(\left\langle \hat{N}_{\mathbf{n}}\right\rangle - \left\langle \hat{N}_{\mathbf{n}}\hat{N}_{\mathbf{m}}\right\rangle\right)\\ &\quad + \delta_{\mathbf{n}'\mathbf{n}}\delta_{\mathbf{m}'\mathbf{m}}\delta_{\mathbf{m}\mathbf{n}}\bar{N}_{\mathbf{n}}\\ &= \delta_{\mathbf{n}'\mathbf{n}}\delta_{\mathbf{m}'\mathbf{m}}\left\langle \hat{N}_{\mathbf{n}}\hat{N}_{\mathbf{m}}\right\rangle + \delta_{\mathbf{m}'\mathbf{n}}\delta_{\mathbf{n}'\mathbf{m}}\left\langle \hat{N}_{\mathbf{n}}\left(1-\hat{N}_{\mathbf{m}}\right)\right\rangle.\end{aligned} \tag{8.201}$$

Here, the notation is used for the average occupation number $\bar{N}_{\mathbf{n}}$:

$$\left\langle \hat{N}_{\mathbf{n}}\right\rangle = \frac{1}{\mathbb{Z}_I(\beta|N)}\sum_{\{N_{\mathbf{n}}\}}\left\langle \Psi_{N,\{N_{\mathbf{n}}\}}\left|\exp\left(-\beta\hat{H}\right)\hat{N}_{\mathbf{n}}\right|\Psi_{N,\{N_{\mathbf{n}}\}}\right\rangle. \tag{8.202}$$

$$\mathbb{Z}_I(\beta|N) = \sum_{\{N_{\mathbf{n}}\}} \left\langle \Psi_{N,\{N_{\mathbf{n}}\}} \left| \exp\left(-\beta\hat{H}\right) \right| \Psi_{N,\{N_{\mathbf{n}}\}} \right\rangle$$
$$= \left[\sum_{\{N_{\mathbf{n}}\}} \exp\left(-\beta \sum_{\mathbf{n}} \varepsilon_{\mathbf{n}} N_{\mathbf{n}}\right) \right]_{\sum_{\mathbf{n}} N_{\mathbf{n}}=N}. \tag{8.203}$$

In the same way as Eq. (8.183), the average (8.202) can be written down in the form

$$\left\langle \hat{N}_{\mathbf{n}} \right\rangle = \frac{1}{\mathbb{Z}_I(\beta|N)} \left[\sum_{\{N_{\mathbf{n}'}\}} N_{\mathbf{n}} \exp\left(-\beta \sum_{\mathbf{n}'} \varepsilon_{\mathbf{n}'} N_{\mathbf{n}'}\right) \right]_{\sum_{\mathbf{n}'} N_{\mathbf{n}'}=N}.$$
$$\left\langle \hat{N}_{\mathbf{n}} \right\rangle = -\frac{1}{\beta \mathbb{Z}_I(\beta|N)} \frac{\delta \mathbb{Z}_I(\beta|N)}{\delta \varepsilon_{\mathbf{n}}},$$
$$\left\langle \hat{N}_{\mathbf{n}} \right\rangle = \frac{1}{2\pi \mathbb{Z}_I(\beta|N)} \int_{-\pi}^{\pi} \frac{\Phi_N(\theta)}{\exp(\beta\varepsilon_{\mathbf{n}} - \zeta - i\theta) + 1} d\theta. \tag{8.204}$$

Since $\varepsilon_{\mathbf{n}} = \varepsilon_n$, $\left\langle \hat{N}_{\mathbf{n}} \right\rangle$ depends only on n.

Using Eq. (8.192), we can write $\bar{N}_n$ as

$$\left\langle \hat{N}_{\mathbf{n}} \right\rangle = \frac{1}{2\pi \mathbb{Z}_I(\beta|N)} \int_{-\pi}^{\pi} \frac{\Phi_N(\theta)}{\frac{1}{u}\exp(\beta\varepsilon_n - i\theta) + 1} d\theta$$
$$= \frac{1}{2\pi \mathbb{Z}_I(\beta|N)} \int_{-\pi}^{\pi} \frac{\exp\left[\ln \Xi\left(\beta, ue^{i\theta}\right) - N\ln u - iN\theta\right]}{\frac{1}{u}\exp(\beta\varepsilon_n - i\theta) + 1} d\theta$$
$$= \frac{1}{2\pi \mathbb{Z}_I(\beta|N)} \int_{-\pi}^{\pi} \frac{\Xi\left(\beta, ue^{i\theta}\right)}{u^{N-1}} \frac{\exp\left[-i\theta(N-1) - \beta\varepsilon_n\right]}{1 + u\exp(i\theta - \beta\varepsilon_n)} d\theta. \tag{8.205}$$

The averages $\left\langle \hat{N}_{\mathbf{n}} \hat{N}_{\mathbf{m}} \right\rangle$ for $\mathbf{m} \neq \mathbf{n}$ can be also expressed in terms of the integral representation:

$$\left\langle \hat{N}_{\mathbf{n}} \hat{N}_{\mathbf{m}} \right\rangle \Big|_{\mathbf{m}\neq\mathbf{n}} = \frac{1}{\mathbb{Z}_I(\beta|N)} \sum_{\{N_{\mathbf{n}}\}} \left\langle \Psi_{N,\{N_{\mathbf{n}}\}} \left| \exp\left(-\beta\hat{H}\right) \hat{N}_{\mathbf{n}} \hat{N}_{\mathbf{m}} \right| \Psi_{N,\{N_{\mathbf{n}}\}} \right\rangle \Bigg|_{\mathbf{m}\neq\mathbf{n}}$$
$$= \frac{1}{\mathbb{Z}_I(\beta|N)} \left[\sum_{\{N_{\mathbf{n}'}\}} N_{\mathbf{n}} N_{\mathbf{m}} \exp\left(-\beta \sum_{\mathbf{n}'} \varepsilon_{\mathbf{n}'} N_{\mathbf{n}'}\right) \right]_{\sum_{\mathbf{n}'} N_{\mathbf{n}'}=N, \quad \mathbf{m}\neq\mathbf{n}}$$
$$= \frac{1}{\mathbb{Z}_I(\beta|N)\beta^2} \frac{\delta^2 \mathbb{Z}_I(\beta|N)}{\delta\varepsilon_{\mathbf{m}}\delta\varepsilon_{\mathbf{n}}}$$
$$= \frac{1}{\mathbb{Z}_I(\beta|N)\beta^2} \frac{\delta^2}{\delta\varepsilon_{\mathbf{m}}\delta\varepsilon_{\mathbf{n}}} \left(\frac{1}{2\pi} \int_0^{2\pi} d\theta \exp\left[\ln \Xi\left(\beta, e^{i\theta+\zeta}\right) - N\zeta - iN\theta\right] \right) \quad \Rightarrow$$

We obtain the integral representation for the average of the product of operators $\hat{N}_{\mathbf{n}}\hat{N}_{\mathbf{m}}$ for $\mathbf{m} \neq \mathbf{n}$:

$$\left\langle \hat{N}_{\mathbf{n}} \hat{N}_{\mathbf{m}} \right\rangle \Big|_{\mathbf{m}\neq\mathbf{n}} = \frac{1}{2\pi \mathbb{Z}_I(N)} \int_{-\pi}^{\pi} \frac{\Phi_N(\theta)}{\left[\exp(\beta\varepsilon_{\mathbf{n}} - \zeta - i\theta) + 1\right]\left[\exp(\beta\varepsilon_{\mathbf{m}} - \zeta - i\theta) + 1\right]} d\theta. \tag{8.206}$$

Let us introduce the notation

$$f(\varepsilon,\theta) \equiv \frac{1}{\exp(\beta\varepsilon - \zeta - i\theta) + 1}, \tag{8.207}$$

which formally coincides with the Fermi distribution function of the energy ε with the "chemical potential" $(\zeta + i\theta)/\beta$. Using this notation, the averages (8.204) and (8.206) can be written down in the form

$$\left\langle \hat{N}_{\mathbf{n}} \right\rangle = \frac{1}{2\pi \mathbb{Z}_I(\beta|N)} \int\limits_{-\pi}^{\pi} f(\varepsilon_{\mathbf{n}},\theta)\, \Phi_N(\theta)\, d\theta, \tag{8.208}$$

$$\left\langle \hat{N}_{\mathbf{n}} \hat{N}_{\mathbf{m}} \right\rangle\Big|_{\mathbf{m}\neq\mathbf{n}} = \frac{1}{2\pi \mathbb{Z}_I(N)} \int\limits_{-\pi}^{\pi} f(\varepsilon_{\mathbf{n}},\theta)\, f(\varepsilon_{\mathbf{m}},\theta)\, \Phi_N(\theta)\, d\theta. \tag{8.209}$$

We can develop the aforesaid procedure for the average of a product of any number of operators $\hat{N}_{\mathbf{n}_1}\hat{N}_{\mathbf{n}_2}\ldots\hat{N}_{\mathbf{n}_K}$, where all quantum numbers $\mathbf{n}_1, \mathbf{n}_2, \ldots, \mathbf{n}_K$ are *different*. The result is:

$$\left\langle \hat{N}_{\mathbf{n}_1}\hat{N}_{\mathbf{n}_2}\ldots\hat{N}_{\mathbf{n}_K} \right\rangle\Big|_{\mathbf{n}_j\neq\mathbf{n}_l} = \frac{1}{2\pi \mathbb{Z}_I(N)} \int\limits_{-\pi}^{\pi} f(\varepsilon_{\mathbf{n}_1},\theta)\, f(\varepsilon_{\mathbf{n}_2},\theta)\ldots f(\varepsilon_{\mathbf{n}_K},\theta)\, \Phi_N(\theta)\, d\theta. \tag{8.210}$$

It should be emphasized, that all expressions above [including Eq. (8.210)] are derived for a *canonical* Hibbs ensemble (i. e., for a fixed number of particles) and for both closed-shell and open-shell systems.

Let us substitute the average (8.201) into the correlation function $\tilde{g}(\mathbf{q},\tau|\{N_\sigma\},\beta)$:

$$\begin{aligned}\tilde{g}(\mathbf{q},\tau|\{N_\sigma\},\beta) = \sum_{\mathbf{n},\mathbf{n}'}\sum_{\mathbf{m},\mathbf{m}'} \left(e^{i\mathbf{q}\cdot\hat{\mathbf{x}}}\right)_{\mathbf{n}\mathbf{n}'} \left(e^{-i\mathbf{q}\cdot\hat{\mathbf{x}}}\right)_{\mathbf{m}\mathbf{m}'} \exp\left[\frac{\tau}{\hbar}(\varepsilon_{\mathbf{n}} - \varepsilon_{\mathbf{n}'})\right] \\ \times \left(\delta_{\mathbf{n}'\mathbf{n}}\delta_{\mathbf{m}'\mathbf{m}} \left\langle \hat{N}_{\mathbf{n}}\hat{N}_{\mathbf{m}} \right\rangle + \delta_{\mathbf{m}'\mathbf{n}}\delta_{\mathbf{n}'\mathbf{m}} \left\langle \hat{N}_{\mathbf{n}}\left(1 - \hat{N}_{\mathbf{m}}\right)\right\rangle\right)\end{aligned}$$

$\Longrightarrow$

$$\begin{aligned}\tilde{g}(\mathbf{q},\tau|\{N_\sigma\},\beta) = \sum_{\mathbf{n},\mathbf{m}} \left(e^{i\mathbf{q}\cdot\hat{\mathbf{x}}}\right)_{\mathbf{n}\mathbf{n}} \left(e^{-i\mathbf{q}\cdot\hat{\mathbf{x}}}\right)_{\mathbf{m}\mathbf{m}} \left\langle \hat{N}_{\mathbf{n}}\hat{N}_{\mathbf{m}} \right\rangle \\ + \sum_{\mathbf{n},\mathbf{m}} \left|\left(e^{i\mathbf{q}\cdot\hat{\mathbf{x}}}\right)_{\mathbf{n}\mathbf{m}}\right|^2 \exp\left[\frac{\tau}{\hbar}(\varepsilon_{\mathbf{n}} - \varepsilon_{\mathbf{m}})\right] \left\langle \hat{N}_{\mathbf{n}}\left(1 - \hat{N}_{\mathbf{m}}\right)\right\rangle.\end{aligned} \tag{8.211}$$

The matrix elements $\left(e^{i\mathbf{q}\cdot\hat{\mathbf{x}}}\right)_{\mathbf{n}\mathbf{m}}$ has the following form

$$\left(e^{i\mathbf{q}\cdot\hat{\mathbf{x}}}\right)_{\mathbf{n}\mathbf{m}} = \left\langle m_1 \left|e^{iq_1\hat{x}_1}\right| n_1\right\rangle \left\langle m_2 \left|e^{iq_2\hat{x}_2}\right| n_2\right\rangle \left\langle m_3 \left|e^{iq_3\hat{x}_3}\right| n_3\right\rangle,$$

where $\left\langle m \left|e^{iq\hat{x}}\right| n\right\rangle$ is the matrix element of a one-dimensional oscillator with the frequency w:

$$\begin{gathered}\left\langle m \left|e^{iq\hat{x}}\right| n\right\rangle = \exp\left(-\frac{\gamma^2}{2}\right)(i\gamma)^{n_> - n_<} \sqrt{\frac{n_<!}{n_>!}} L_{n_<}^{(n_> - n_<)}(\gamma^2), \\ \begin{cases} n_> \equiv \max(n,m); \\ n_< \equiv \min(n,m), \end{cases}\end{gathered} \tag{8.212}$$

$\gamma \equiv q\sqrt{\frac{\hbar}{2mw}}$, $|n\rangle$ are the quantum states of the one-dimensional oscillator with the frequency w, $L_n^{(\alpha)}(z)$ is the generalized Laguerre polynomial.

System with mixed spins

The correlation functions for a system with mixed spins can be explicitly derived by the generalization of Eqs. (8.193) and (8.210) to the case of the particles with the non-zero spin. We use the fact, that the derivation of Eqs. (8.193) and (8.210), performed in this section, does not depend on the concrete form of the energy spectrum $\varepsilon_{\mathbf{n}}$. Hence, in the formulae, derived above, the replacement should be made:

$$|\mathbf{n}\rangle \to |\mathbf{n},\sigma\rangle\,, \quad \hat{N}_{\mathbf{n}} \to \hat{N}_{\mathbf{n},\sigma} = a^{+}_{\mathbf{n},\sigma} a_{\mathbf{n},\sigma}, \tag{8.213}$$

where σ is the electron spin projection. Consequently, the matrix elements $\left(e^{i\mathbf{q}\cdot\hat{\mathbf{x}}}\right)_{\mathbf{mn}}$ are replaced by

$$\left(e^{i\mathbf{q}\cdot\hat{\mathbf{x}}}\right)_{\mathbf{mn}} \to \left\langle \mathbf{m},\sigma \left| e^{i\mathbf{q}\cdot\hat{\mathbf{x}}} \right| \mathbf{n},\sigma' \right\rangle = \delta_{\sigma\sigma'} \left(e^{i\mathbf{q}\cdot\hat{\mathbf{x}}}\right)_{\mathbf{mn}}. \tag{8.214}$$

Taking into account Eqs. (8.213) and (8.214), the two-point correlation function (8.211) becomes

$$\begin{aligned}\tilde{g}\left(\mathbf{q},\tau\right|\left\{N_\sigma\right\},\beta) = &\sum_{\mathbf{n},\mathbf{m}}\sum_{\sigma_1,\sigma_2}\left(e^{i\mathbf{q}\cdot\hat{\mathbf{x}}}\right)_{\mathbf{nn}}\left(e^{-i\mathbf{q}\cdot\hat{\mathbf{x}}}\right)_{\mathbf{mm}}\left\langle \hat{N}_{\mathbf{n},\sigma_1}\hat{N}_{\mathbf{m},\sigma_2}\right\rangle \\ &+\sum_{\mathbf{n},\mathbf{m}}\sum_{\sigma}\left|\left(e^{i\mathbf{q}\cdot\hat{\mathbf{x}}}\right)_{\mathbf{nm}}\right|^2 \exp\left[\frac{\tau}{\hbar}\left(\varepsilon_{\mathbf{n}}-\varepsilon_{\mathbf{m}}\right)\right]\left\langle \hat{N}_{\mathbf{n},\sigma}\left(1-\hat{N}_{\mathbf{m},\sigma}\right)\right\rangle.\end{aligned} \tag{8.215}$$

The averages $\left\langle \hat{N}_{\mathbf{n},\sigma}\right\rangle$ and $\left\langle \hat{N}_{\mathbf{n},\sigma_1}\hat{N}_{\mathbf{m},\sigma_2}\right\rangle$ are, respectively, one-particle and two-particle distribution functions,

$$\left\langle \hat{N}_{\mathbf{n},\sigma}\right\rangle \equiv f_1\left(n,\sigma|N_\sigma,\beta\right), \tag{8.216}$$

$$\left\langle \hat{N}_{\mathbf{n},\sigma}\hat{N}_{\mathbf{n}',\sigma'}\right\rangle \equiv f_2\left(n,\sigma;n',\sigma'\right|\left\{N_\sigma\right\},\beta). \tag{8.217}$$

The one-electron distribution function $f_1\left(n,\sigma|N_\sigma,\beta\right)$ is the average number of electrons with the spin projection σ at the n-th energy level, while the two-electron distribution function $f_2\left(n,\sigma;n',\sigma'\right|\left\{N_\sigma\right\},\beta)$ is the average product of the numbers of electrons with the spin projections σ and σ' at the levels n and n'. These functions are expressed through the following integrals [see (8.208), (8.209)]:

$$f_1\left(n,\sigma|N_\sigma,\beta\right) = \frac{1}{2\pi\mathbb{Z}_F\left(N_\sigma,w,\beta\right)}\int\limits_{-\pi}^{\pi} f\left(\varepsilon_n,\theta\right)\Phi\left(\theta,\beta,N_\sigma\right)d\theta, \tag{8.218}$$

$$f_2\left(n,\sigma;n',\sigma'\right|\left\{N_\sigma\right\},\beta) = \begin{cases} \frac{1}{2\pi\mathbb{Z}_F(N_\sigma,w,\beta)}\int\limits_{-\pi}^{\pi} f\left(\varepsilon_n,\theta\right)f\left(\varepsilon_{n'},\theta\right)\Phi\left(\theta,\beta,N_\sigma\right)d\theta, & \text{if } \sigma'=\sigma; \\ f_1\left(n,\sigma|N_\sigma,\beta\right)f_1\left(n,\sigma'|N_{\sigma'},\beta\right), & \text{if } \sigma'\neq\sigma \end{cases} \tag{8.219}$$

with the notations

$$\Phi\left(\theta,\beta,N_\sigma\right) = \exp\left[\sum_{n=0}^{\infty}\ln\left(1+e^{i\theta+\xi-\beta\varepsilon_n}\right) - N_\sigma\left(\xi+i\theta\right)\right], \tag{8.220}$$

$$f\left(\varepsilon,\theta\right) \equiv \frac{1}{\exp\left(\beta\varepsilon-\xi-i\theta\right)+1}. \tag{8.221}$$

The function $f\left(\varepsilon,\theta\right)$ formally coincides with the Fermi-Dirac distribution function of the energy ε with the "chemical potential" $\left(\xi+i\theta\right)/\beta$.

Here we consider the zero-temperature limit, for which the integrals (8.218) and (8.219) can be calculated analytically. The result for the one-electron distribution function is

$$f_1\left(n,\sigma|\beta,N_\sigma\right)|_{\beta\to\infty}=\left\{\begin{array}{cc}1, & n<L_\sigma;\\ 0, & n>L_\sigma;\\ \frac{N_\sigma-N_{L_\sigma}}{g_{L_\sigma}}, & n=L_\sigma.\end{array}\right. \tag{8.222}$$

According to (8.222), L_σ is the number of the lowest open shell, and

$$g_n=\left\{\begin{array}{cc}\frac{1}{2}\left(n+1\right)\left(n+2\right) & (3D)\,,\\ n+1 & (2D)\,.\end{array}\right.$$

is the degeneracy of the n-th shell. N_{L_σ} is the number of electrons in all the closed shells with the spin projection σ,

$$N_{L_\sigma}\equiv\sum_{n=0}^{L_\sigma-1}g_n=\left\{\begin{array}{cc}\frac{1}{6}L_\sigma\left(L_\sigma+1\right)\left(L_\sigma+2\right) & (3D)\,,\\ \frac{1}{2}L_\sigma\left(L_\sigma+1\right) & (2D)\,.\end{array}\right. \tag{8.223}$$

The two-electron distribution function $f_2\left(n,\sigma;n',\sigma'|\left\{N_\sigma\right\},\beta\right)$ at $T=0$ takes the form

$$\begin{aligned}&f_2\left(n,\sigma;n',\sigma'|\beta,\{N_\sigma\}\right)|_{\beta\to\infty}\\ &=\left\{\begin{array}{cc}f_1\left(n,\sigma|\beta,N_\sigma\right)|_{\beta\to\infty}\,f_1\left(n',\sigma'|\beta,N_{\sigma'}\right)|_{\beta\to\infty}\,, & n\neq n' \text{ or } \sigma\neq\sigma'\\ 1, & \sigma=\sigma' \text{ and } n=n'<L_\sigma;\\ 0, & \sigma=\sigma' \text{ and } n=n'>L_\sigma;\\ \frac{N_\sigma-N_{L_\sigma}}{g_{L_\sigma}}\frac{N_\sigma-N_{L_\sigma}-1}{g_{L_\sigma}-1}, & \sigma=\sigma' \text{ and } n=n'=L_\sigma.\end{array}\right.\end{aligned} \tag{8.224}$$

In summary, we have obtained the following expression for $\tilde{g}\left(\mathbf{q},\tau|\left\{N_\sigma\right\},\beta\right)$:

$$\begin{aligned}\tilde{g}\left(\mathbf{q},\tau|\left\{N_\sigma\right\},\beta\right)=&\sum_{\mathbf{n},\sigma,\mathbf{n}',\sigma'}\left(e^{i\mathbf{q}\cdot\mathbf{x}}\right)_{\mathbf{nn}}\left(e^{-i\mathbf{q}\cdot\mathbf{x}}\right)_{\mathbf{n}'\mathbf{n}'}f_2\left(n,\sigma;n',\sigma'|\left\{N_\sigma\right\},\beta\right)\\ &+\sum_{\mathbf{n},\mathbf{n}',\sigma}\left|\left(e^{i\mathbf{q}\cdot\mathbf{x}}\right)_{\mathbf{nn}'}\right|^2\exp\left[\frac{\tau}{\hbar}\left(\varepsilon_n-\varepsilon_{n'}\right)\right]\\ &\times\left[f_1\left(n,\sigma|\left\{N_\sigma\right\},\beta\right)-f_2\left(n,\sigma;n',\sigma|\left\{N_\sigma\right\},\beta\right)\right].\end{aligned} \tag{8.225}$$

This formula is valid for both closed and open shells. The correlation functions derived in this subsection are used both for the calculation of the ground-state energy and, a shown below, for the calculation of the optical conductivity of an N-polaron system in a quantum dot.

8.2.5 Many-polaron ground state in a quantum dot: extrapolation to the homogeneous limit and comparison to the results for a polaron gas in bulk [90]

The correlation function given by Eq. (8.225) can be subdivided as

$$\tilde{g}\left(\mathbf{q},\tau|\left\{N_\sigma\right\},\beta\right)=\tilde{g}_1\left(\mathbf{q},\tau|\left\{N_\sigma\right\},\beta\right)+\tilde{g}_2\left(\mathbf{q},\tau|\left\{N_\sigma\right\},\beta\right), \tag{8.226}$$

with

$$\begin{aligned}\tilde{g}_1\left(\mathbf{q},\tau|\left\{N_\sigma\right\},\beta\right)\equiv&\sum_{\mathbf{n},\mathbf{n}',\sigma}\left|\left(e^{i\mathbf{q}\cdot\mathbf{x}}\right)_{\mathbf{nn}'}\right|^2\exp\left[\frac{\tau}{\hbar}\left(\varepsilon_n-\varepsilon_{n'}\right)\right]\\ &\times\left[f_1\left(n,\sigma|\left\{N_\sigma\right\},\beta\right)-f_2\left(n,\sigma;n',\sigma|\left\{N_\sigma\right\},\beta\right)\right],\end{aligned} \tag{8.227}$$

$$\tilde{g}_2\left(\mathbf{q},\tau\right|\left\{N_\sigma\right\},\beta\right) \equiv \sum_{\mathbf{n},\sigma,\mathbf{n}',\sigma'} \left(e^{i\mathbf{q}\cdot\mathbf{x}}\right)_{\mathbf{nn}} \left(e^{-i\mathbf{q}\cdot\mathbf{x}}\right)_{\mathbf{n}'\mathbf{n}'} f_2\left(n,\sigma;n',\sigma'\right|\left\{N_\sigma\right\},\beta\right). \tag{8.228}$$

In accordance with the subdivision (8.226) of the correlation function, we subdivide the Coulomb and polaron contributions:

$$E_C = E_C^{(1)} + E_C^{(2)}, \tag{8.229}$$

$$E_{e-ph} = E_{e-ph}^{(1)} + E_{e-ph}^{(2)}. \tag{8.230}$$

We have numerically checked whether the polaron contribution per particle $E_{e-ph}^{(1)}/N$ tends to a finite value at $N \to \infty$. In Figs. 8.3 and 8.4, we have plotted the polaron contributions $E_{e-ph}^{(1)}/N$ as a function of N for a quantum dot in ZnO and in a polar medium with $\alpha = 5$, $\eta = 0.3$, respectively. [6] As seen from Fig. 8.3, the polaron contribution $E_{e-ph}^{(1)}/N$ in ZnO as a function of N oscillates taking expressed maxima for N corresponding to the closed shells $N = 2, 8, 20, 40, \ldots$. There exist kinks of $E_{e-ph}^{(1)}/N$ at N corresponding to the half-filled shells, but these kinks are extremely small. In the case of the medium with $\alpha = 5$, $\eta = 0.3$, for $r_s^* = 20$ (what corresponds to the density $n_0 \approx 1.14 \times 10^{18}$ cm^{-3}), the polaron contribution $E_{e-ph}^{(1)}/N$ oscillates taking maximal values at the numbers of fermions, which correspond to the closed shells for a spin-polarized system with parallel spins.

In Figs. 8.3 and 8.4, the dashed curves are the envelopes for local maxima (closed shells) and local minima of $E_{e-ph}^{(1)}/N$.We see that when these envelopes are *extrapolated* to larger number of fermions, the distance between the envelopes decreases. Therefore, the magnitude of the variations of $E_{e-ph}^{(1)}/N$ related to the shell filling diminishes with increasing N, and it is safe to suppose that in the limit of large N, the envelopes tend to one and the same value. That value corresponds to the *homogeneous* ("bulk") limit $\lim_{N\to\infty}\left(E_{e-ph}^{(1)}/N\right)$.

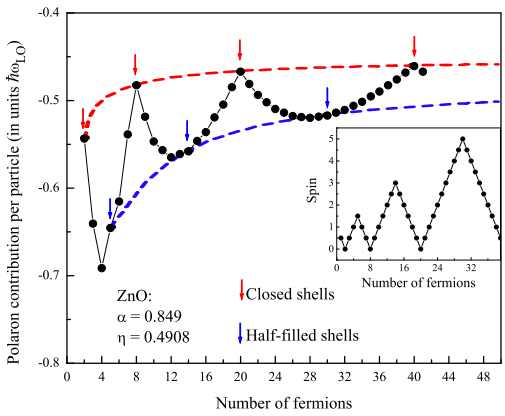

Figure 8.3: Polaron contribution $E_{e-ph}^{(1)}/N$ as a function of N for a ZnO quantum dot.The material parameters for ZnO are taken from Ref. [91]. The value $r_s^* = 2$ corresponds to $n_0 = 4.34 \times 10^{19}$ cm^{-2}. Inset: the total spin as a function of N.

[6] Since, as discussed above, for a single polaron only the whole polaron contribution $E_{e-ph} = E_{e-ph}^{(1)} + E_{e-ph}^{(2)}$ has a physical meaning, the plots for $E_{e-ph}^{(1)}$ in Figs. 3 and 4 start from $N = 2$. The total polaron contribution E_{e-ph} for $N = 1$ is plotted below, in Fig. 9.

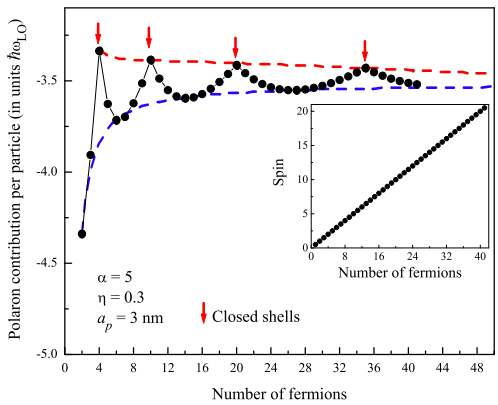

Figure 8.4: Polaron contribution $E^{(1)}_{e-ph}/N$ as a function of N for a quantum dot of a polar medium with $\alpha = 5$, $\eta = 0.3$. The value $r^*_s = 20$ corresponds to $n_0 = 1.14 \times 10^{18}$ cm^{-3}. Inset: the total spin as a function of N.

In Fig. 8.5, we compare the polaron contribution $E^{(1)}_{e-ph}/N$ calculated within our variational path-integral method for different numbers of fermions with the polaron contribution to the ground-state energy per particle for a polaron gas in bulk, calculated (i) in Ref. [103] within an intermediate-coupling approach (the thin solid curve), (ii) in Ref. [104], using a variational approach developed first in Ref. [91]. As seen from this figure, our all-coupling variational method provides lower values for the polaron contribution than those obtained in Refs. [103, 104]. The difference between the polaron contribution calculated within our method and that of Ref. [103] is smaller at low densities and increases in magnitude with increasing density. The difference between the polaron contribution calculated within our method and that of Ref. [104] very slightly depends on the density. The result of Ref. [104] becomes closer to our result only at high densities.

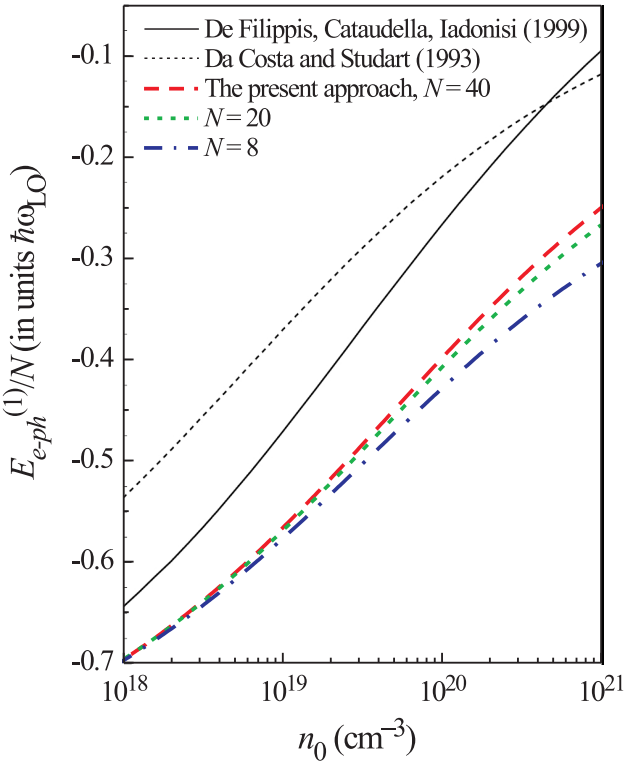

Figure 8.5: Polaron contribution to the polaron ground-state energy per particle $E_{e-ph}^{(1)}$ in an N-polaron quantum dot as a function of the effective density. The parameters are taken for ZnO (see Ref. [91]): $\alpha = 0.849$, $\varepsilon_0 = 8.15$, $\varepsilon_\infty = 4.0$, $\hbar\omega_{\rm LO} = 73.27$ meV, $m_b = 0.24 m_e$, where m_e is the electron mass in the vacuum. This polaron contribution is compared with the polaron contribution to the ground-state energy of a polaron gas in bulk calculated in Refs. [103, 104].

8.2.6 Optical conductivity

In Ref. [98] we have extended the memory-function approach to a system of arbitrary-coupling interacting polarons confined to a parabolic confinement potential. The optical conductivity relates the current $\mathbf{J}(t)$ per electron to a time-dependent uniform electric field $\mathbf{E}(t)$ in the framework of linear response theory. Further on, the Fourier components of the electric field are denoted by $\mathbf{E}(\omega)$:

$$\mathbf{E}(t) = \frac{1}{2\pi}\int_{-\infty}^{\infty} \mathbf{E}(\omega)\, e^{-i\omega t} d\omega, \tag{8.231}$$

and the similar denotations are used for other time-dependent quantities. The electric current per electron $\mathbf{J}(t)$ is related to the mean electron coordinate response $\mathbf{R}(t)$ by

$$\mathbf{J}(t) = -e\frac{d\mathbf{R}(t)}{dt}, \tag{8.232}$$

and hence

$$\mathbf{J}(\omega) = ie\omega\mathbf{R}(\omega). \tag{8.233}$$

Within the linear-response theory, both the electric current and the coordinate response are proportional to $\mathbf{E}(\omega)$:

$$\mathbf{J}(\omega) = \sigma(\omega)\,\mathbf{E}(\omega), \quad \mathbf{R}(\omega) = \frac{\sigma(\omega)}{ie\omega}\mathbf{E}(\omega), \tag{8.234}$$

where $\sigma(\omega)$ is the conductivity per electron. Because we treat an isotropic electron-phonon system, $\sigma(\omega)$ is a scalar function. It is determined from the time evolution of the center-of-mass coordinate:

$$\mathbf{R}(t) \equiv \frac{1}{N}\left\langle\left\langle \sum_{j=1}^{N} \mathbf{x}_j(t) \right\rangle\right\rangle_S . \tag{8.235}$$

The symbol $\langle\langle(\bullet)\rangle\rangle_S$ denotes an average in the *real-time* representation for a system with action functional S:

$$\langle\langle(\bullet)\rangle\rangle_S \equiv \int d\bar{\mathbf{x}} \int d\bar{\mathbf{x}}_0 \int d\bar{\mathbf{x}}_0' \int_{\bar{\mathbf{x}}_0}^{\bar{\mathbf{x}}} D\bar{\mathbf{x}}(t) \int_{\bar{\mathbf{x}}_0'}^{\bar{\mathbf{x}}} D\bar{\mathbf{x}}'(t)\, e^{\frac{i}{\hbar}S[\bar{\mathbf{x}}(t),\bar{\mathbf{x}}'(t)]} (\bullet) \left\langle \bar{\mathbf{x}}_0 \left|\hat{\rho}(t_0)\right| \bar{\mathbf{x}}_0' \right\rangle\Big|_{t_0\to-\infty} , \tag{8.236}$$

where $\left\langle \bar{\mathbf{x}}_0 \left|\hat{\rho}(t_0)\right| \bar{\mathbf{x}}_0' \right\rangle$ is the density matrix before the onset of the electric field in the infinite past ($t_0 \to -\infty$). The corresponding action functional is

$$S[\bar{\mathbf{x}}(t), \bar{\mathbf{x}}'(t)] = \int_{-\infty}^{t} \left[L_e\left(\dot{\bar{\mathbf{x}}}(t), \bar{\mathbf{x}}(t), t\right) - L_e\left(\dot{\bar{\mathbf{x}}}'(t), \bar{\mathbf{x}}'(t), t\right)\right] dt' - i\hbar\Phi[\bar{\mathbf{x}}(t), \bar{\mathbf{x}}'(t)] , \tag{8.237}$$

where $L_e\left(\dot{\bar{\mathbf{x}}}, \bar{\mathbf{x}}, t\right)$ is the Lagrangian of N interacting electrons in a time-dependent uniform electric field $\mathbf{E}(t)$

$$L_e\left(\dot{\bar{\mathbf{x}}}, \bar{\mathbf{x}}, t\right) = \sum_{\sigma}\sum_{j=1}^{N_\sigma}\left(\frac{m_b\dot{\mathbf{x}}_{j,\sigma}^2}{2} - \frac{m_b\Omega_0^2\mathbf{x}_{j,\sigma}^2}{2} - e\mathbf{x}_{j,\sigma}\cdot\mathbf{E}(t)\right) - \sum_{\substack{\sigma,\sigma'\\(j,\sigma)\neq(l,\sigma')}}\sum_{j=1}^{N_\sigma}\sum_{l=1}^{N_{\sigma'}}\frac{e^2}{2\varepsilon_\infty\left|\mathbf{x}_{j,\sigma}-\mathbf{x}_{l,\sigma'}\right|}. \tag{8.238}$$

The influence phase of the phonons

$$\begin{aligned}\Phi[\bar{\mathbf{x}}(s), \bar{\mathbf{x}}'(s)] = &-\sum_{\mathbf{q}}\frac{|V_{\mathbf{q}}|^2}{\hbar^2}\int_{-\infty}^{t} ds \int_{-\infty}^{s} ds' \left[\rho_{\mathbf{q}}(s) - \rho_{\mathbf{q}}'(s)\right] \\ &\times\left[T_{\omega_{\mathbf{q}}}^*(s-s')\,\rho_{\mathbf{q}}(s') - T_{\omega_{\mathbf{q}}}(s-s')\,\rho_{\mathbf{q}}'(s')\right]\end{aligned} \tag{8.239}$$

describes both a retarded interaction between different electrons and a retarded self-interaction of each electron due to the elimination of the phonon coordinates. This functional contains the free-phonon Green's function:

$$T_\omega(t) = \frac{e^{i\omega t}}{1-e^{-\beta\hbar\omega}} + \frac{e^{-i\omega t}}{e^{\beta\hbar\omega}-1}. \tag{8.240}$$

The equation of motion for $\mathbf{R}(t)$ is

$$m_b\frac{d^2\mathbf{R}(t)}{dt^2} + m_b\Omega_0^2\mathbf{R}(t) + e\mathbf{E}(t) = \mathbf{F}_{ph}(t) , \tag{8.241}$$

where $\mathbf{F}_{ph}(t)$ is the average force due to the electron-phonon interaction,

$$\mathbf{F}_{ph}(t) = -\operatorname{Re}\sum_{\mathbf{q}}\frac{2|V_{\mathbf{q}}|^2\mathbf{q}}{N\hbar}\int_{-\infty}^{t} ds\, T_{\omega_{\mathrm{LO}}}^*(t-s)\,\langle\langle\rho_{\mathbf{q}}(t)\,\rho_{-\mathbf{q}}(s)\rangle\rangle_S . \tag{8.242}$$

The two-point correlation function $\langle\langle\rho_{\mathbf{q}}(t)\,\rho_{-\mathbf{q}}(s)\rangle\rangle_S$ should be calculated from Eq. (8.236) using the exact action (8.237), but like for the free energy above, this path integral cannot be calculated analytically. Instead, we perform an approximate calculation, replacing the two-point correlation function in Eq. (8.242) by $\langle\langle\rho_{\mathbf{q}}(t)\,\rho_{-\mathbf{q}}(s)\rangle\rangle_{S_0}$, where $S_0\left[\bar{\mathbf{x}}(t),\bar{\mathbf{x}}'(t)\right]$ is the action functional with the optimal values of the variational parameters for the model system considered in the previous section in the presence of the electric field $\mathbf{E}(t)$. The functional $S_0\left[\bar{\mathbf{x}}(t),\bar{\mathbf{x}}'(t)\right]$ is quadratic and describes a system of coupled harmonic oscillators in the uniform electric field $\mathbf{E}(t)$. This field enters the term $-e\mathbf{E}(t)\cdot\sum_\sigma\sum_{j=1}^{N_\sigma}\mathbf{x}_{j,\sigma}$ in the Lagrangian, which only affects the center-of-mass coordinate. Hence, a shift of variables to the frame of reference with the origin at the center of mass

$$\begin{cases}\mathbf{x}_n(t)=\tilde{\mathbf{x}}_n(t)+\mathbf{R}(t),\\ \mathbf{x}'_n(t)=\tilde{\mathbf{x}}'_n(t)+\mathbf{R}(t),\end{cases}\tag{8.243}$$

results in

$$\langle\langle\rho_q(t)\,\rho_{-q}(s)\rangle\rangle_{S_0}=\langle\langle\rho_q(t)\,\rho_{-q}(s)\rangle\rangle_{S_0}\big|_{E=0}\,e^{i\mathbf{q}\cdot[\mathbf{R}(t)-\mathbf{R}(s)]}.\tag{8.244}$$

This result (8.244) is valid for any *quadratic* model action S_0.

The applicability of the parabolic approximation is confirmed by the fact that a self-induced polaronic potential, created by the polarization cloud around an electron, is rather well described by a parabolic potential whose parameters are determined by a variational method. For weak coupling, our variational method is at least of the same accuracy as the perturbation theory, which results from our approach at a special choice of the variational parameters. For strong coupling, an interplay of the electron-phonon interaction and the Coulomb correlations within a confinement potential can lead to the assemblage of polarons in multi-polaron systems. Our choice of the model variational system is reasonable because of this trend, apparently occurring in a many-polaron system with arbitrary N for a finite confinement strength.

The correlation function $\langle\rho_{\mathbf{q}}(t)\,\rho_{-\mathbf{q}}(s)\rangle_{S_0}\big|_{\mathbf{E}=0}$ corresponds to the model system in the absence of an electric field. For $t>s$, this function is related to the imaginary-time correlation function $\mathcal{G}(\mathbf{q},\tau|\{N_\sigma\},\beta)$, described in the previous section:

$$\langle\langle\rho_{\mathbf{q}}(t)\,\rho_{-\mathbf{q}}(s)\rangle\rangle_{S_0}\big|_{\mathbf{E}=0,t>s}=\mathcal{G}(\mathbf{q},i(t-s)\,|\,\{N_\sigma\},\beta).\tag{8.245}$$

Using the transformation (8.243) and the relation (8.245), we obtain from Eq. (8.242)

$$\mathbf{F}_{ph}(t)=-\operatorname{Re}\sum_{\mathbf{q}}\frac{2\left|V_{\mathbf{q}}\right|^2\mathbf{q}}{N\hbar}\int\limits_{-\infty}^{t}T^*_{\omega_{\mathrm{LO}}}(t-s)\,\mathrm{e}^{i\mathbf{q}\cdot[\mathbf{R}(t)-\mathbf{R}(s)]}\mathcal{G}(\mathbf{q},i(t-s)\,|\,\{N_\sigma\},\beta)\,ds.\tag{8.246}$$

Within the linear-response theory, we expand the function $\mathrm{e}^{i\mathbf{q}\cdot[\mathbf{R}(t)-\mathbf{R}(s)]}$ in Eq. (8.246) as a Taylor series in $[\mathbf{R}(t)-\mathbf{R}(s)]$ up to the first-order term. The zeroth-order term gives no contribution into $\mathbf{F}_{ph}(t)$ due to the symmetry of $\left|V_{\mathbf{q}}\right|^2$ and of $f_{\mathbf{q}}(t-s)$ with respect to the inversion $\mathbf{q}\to-\mathbf{q}$. In this approach, the Cartesian coordinates of the force ($j=1,2,3$) become

$$\begin{aligned}\left(\mathbf{F}_{ph}(t)\right)_j=\sum_{k=1}^{3}\sum_{\mathbf{q}}\frac{2\left|V_{\mathbf{q}}\right|^2q_jq_k}{N\hbar}\int\limits_{-\infty}^{t}\left[R_k(t)-R_k(s)\right]\\ \times\operatorname{Im}\left[T^*_{\omega_{\mathrm{LO}}}(t-s)\,\mathcal{G}(\mathbf{q},i(t-s)\,|\,\{N_\sigma\},\beta)\right]ds.\end{aligned}\tag{8.247}$$

Further on, we perform the Fourier expansion:

$$\mathbf{R}(t)=\frac{1}{2\pi}\int_{-\infty}^{\infty}\mathbf{R}(\omega)\,e^{-i\omega t}d\omega.\tag{8.248}$$

In Eq. (8.247), we make the replacement

$$\tau \equiv t - s, \quad \Longrightarrow \quad s = t - \tau,$$

what gives

$$\begin{aligned}
\left(\mathbf{F}_{ph}(t)\right)_j &= \sum_{k=1}^{3}\sum_{\mathbf{q}} \frac{2\left|V_{\mathbf{q}}\right|^2 q_j q_k}{N\hbar} \int_0^\infty d\tau \ \left[R_k(t) - R_k(t-\tau)\right] \mathrm{Im}\left[T^*_{\omega_{\mathrm{LO}}}(\tau)\, \mathcal{G}\left(\mathbf{q}, it \middle| \{N_\sigma\}, \beta\right)\right] \\
&= \sum_{k=1}^{3}\sum_{\mathbf{q}} \frac{2\left|V_{\mathbf{q}}\right|^2 q_j q_k}{N\hbar} \frac{1}{2\pi} \int_{-\infty}^{\infty} d\omega R_k(\omega)\, e^{-i\omega t} \int_0^\infty d\tau \ \left(1 - e^{i\omega\tau}\right) \mathrm{Im}\left[T^*_{\omega_{\mathrm{LO}}}(\tau)\, f_{\mathbf{q}}(\tau)\right] \\
&= \frac{1}{2\pi} \int_{-\infty}^{\infty} d\omega F_j(\omega)\, e^{-i\omega t},
\end{aligned}$$

where the Fourier component of the force is

$$\left(\mathbf{F}_{ph}(\omega)\right)_j = \sum_{k=1}^{3}\sum_{\mathbf{q}} \frac{2\left|V_{\mathbf{q}}\right|^2 q_j q_k}{N\hbar} \int_0^\infty dt \ \left(1 - e^{i\omega t}\right) \mathrm{Im}\left[T^*_{\omega_{\mathrm{LO}}}(\tau)\, \mathcal{G}\left(\mathbf{q}, it \middle| \{N_\sigma\}, \beta\right)\right] R_k(\omega). \tag{8.249}$$

The expression (8.249) can be written down as

$$\left(\mathbf{F}_{ph}(\omega)\right)_j = -m_b \sum_{k=1}^{3} \chi_{jk}(\omega)\, R_k(\omega), \tag{8.250}$$

where $\chi_{jk}(\omega)$ are components of the tensor

$$\chi_{jk}(\omega) = \sum_{\mathbf{q}} \frac{2\left|V_{\mathbf{q}}\right|^2 q_j q_k}{N\hbar m_b} \int_0^\infty dt \ \left(e^{i\omega t} - 1\right) \mathrm{Im}\left[T^*_{\omega_{\mathrm{LO}}}(t)\, \mathcal{G}\left(\mathbf{q}, it \middle| \{N_\sigma\}, \beta\right)\right]. \tag{8.251}$$

In the abstract tensor form, Eq. (8.250) is

$$\mathbf{F}(\omega) = -\overleftrightarrow{\chi}(\omega)\, \mathbf{R}(\omega). \tag{8.252}$$

In particular, for the isotropic electron-phonon interaction and in the absence of the magnetic field, the tensor $\overleftrightarrow{\chi}(\omega)$ is proportional to the unity tensor $\mathbb{I}$,

$$\overleftrightarrow{\chi}(\omega) = \chi(\omega)\, \mathbb{I}, \tag{8.253}$$

where $\chi(\omega)$ is the scalar memory function:

$$\chi(\omega) = \sum_{\mathbf{q}} \frac{2\left|V_{\mathbf{q}}\right|^2 q^2}{3N\hbar m_b} \int_0^\infty dt \ \left(e^{i\omega t} - 1\right) \mathrm{Im}\left[T^*_{\omega_{\mathrm{LO}}}(t)\, \mathcal{G}\left(\mathbf{q}, it \middle| \{N_\sigma\}, \beta\right)\right]. \tag{8.254}$$

Let us perform the Fourier transformation of the equation of motion (8.241):

$$m_b\left(\Omega_0^2 - \omega^2\right) \mathbf{R}(\omega) + e\mathbf{E}(\omega) = \mathbf{F}_{ph}(\omega). \tag{8.255}$$

With Eq. (8.252), this equation takes the form

$$m_b\left(\Omega_0^2 - \omega^2\right) \mathbf{R}(\omega) + e\mathbf{E}(\omega) = -m_b \overleftrightarrow{\chi}(\omega)\, \mathbf{R}(\omega)$$

$$\Downarrow$$

$$m_b\left[\omega^2-\Omega_0^2-\overleftrightarrow{\chi}(\omega)\right]\mathbf{R}(\omega)=e\mathbf{E}(\omega)\,. \tag{8.256}$$

Comparing Eqs. (8.234) and (8.256) between each other, we find that

$$m_b\left[\omega^2-\Omega_0^2-\overleftrightarrow{\chi}(\omega)\right]\frac{\sigma(\omega)}{ie\omega}\mathbf{E}(\omega)=e\mathbf{E}(\omega)\,,$$

so that

$$\sigma(\omega)=\frac{ie^2\omega}{m_b}\left[\omega^2-\Omega_0^2-\overleftrightarrow{\chi}(\omega)\right]^{-1}.$$

In the case when Eq. (8.253) is valid, we obtain the conductivity in the scalar form

$$\sigma(\omega)=\frac{ie^2\omega}{m_b\left[\omega^2-\Omega_0^2-\chi(\omega)\right]}.$$

The real part of the conductivity is

$$\begin{aligned}\operatorname{Re}\sigma(\omega)&=\operatorname{Re}\frac{ie^2\omega\left[(\omega^2-\Omega_0^2)-\operatorname{Re}\chi(\omega)+i\operatorname{Im}\chi(\omega)\right]}{m_b\left\{\left[(\omega^2-\Omega_0^2)-\operatorname{Re}\chi(\omega)\right]^2+\left[\operatorname{Im}\chi(\omega)\right]^2\right\}}\\&=-\frac{e^2\omega}{m_b}\frac{\operatorname{Im}\chi(\omega)}{\left[(\omega^2-\Omega_0^2)-\operatorname{Re}\chi(\omega)\right]^2+\left[\operatorname{Im}\chi(\omega)\right]^2}.\end{aligned}$$

In summary, the optical conductivity can be expressed in terms of the memory function $\chi(\omega)$ (cf. Ref. [50]),

$$\operatorname{Re}\sigma(\omega)=-\frac{e^2}{m_b}\frac{\omega\operatorname{Im}\chi(\omega)}{\left[\omega^2-\Omega_0^2-\operatorname{Re}\chi(\omega)\right]^2+\left[\operatorname{Im}\chi(\omega)\right]^2}, \tag{8.257}$$

where $\chi(\omega)$ is given by

$$\chi(\omega)=\sum_{\mathbf{q}}\frac{2\left|V_{\mathbf{q}}\right|^2q^2}{3N\hbar m_b}\int_0^\infty dt\,\left(e^{i\omega t}-1\right)\operatorname{Im}\left[T^*_{\omega_{\mathrm{LO}}}(t)\,\mathcal{G}\left(\mathbf{q},it\middle|\{N_\sigma\},\beta\right)\right]. \tag{8.258}$$

It is worth noting that the optical conductivity (8.257) differs from that for a translationally invariant polaron system both by the explicit form of $\chi(\omega)$ and by the presence of the term Ω_0^2 in the denominator. For $\alpha\to0$, the optical conductivity tends to a δ-like peak at $\omega=\Omega_0$,

$$\lim_{\alpha\to0}\operatorname{Re}\sigma(\omega)=\frac{\pi e^2}{2m_b}\delta(\omega-\Omega_0)\,. \tag{8.259}$$

For a translationally invariant system $\Omega_0\to0$, and this weak-coupling expression (8.259) reproduces the "central peak" of the polaron optical conductivity [82].

The further simplification of the memory function (8.258) is performed in the following way. With the Fröhlich amplitudes of the electron-phonon interaction, we transform the summation over $\mathbf{q}$ to the integral and use the Feynman units ($\hbar=1$, $\omega_{\mathrm{LO}}=1$, $m_b=1$), in which $\left|V_{\mathbf{q}}\right|^2=\frac{2\sqrt{2}\pi\alpha}{q^2V}$. We also use the fact that in an isotropic crystal, $\mathcal{G}\left(\mathbf{q},it\middle|\{N_\sigma\},\beta\right)=\mathcal{G}\left(q,it\middle|\{N_\sigma\},\beta\right)$. As a result, we find

$$\begin{aligned}\chi(\omega)&=\frac{V}{(2\pi)^3}\int_0^\infty 4\pi q^2dq\frac{2q^2}{3N}\frac{2\sqrt{2}\pi\alpha}{q^2V}\\&\times\int_0^\infty dt\,\left(e^{i\omega t}-1\right)\operatorname{Im}\left[T^*_{\omega_{\mathrm{LO}}}(t)\,\mathcal{G}\left(q,it\middle|\{N_\sigma\},\beta\right)\right]\\&=\frac{2\sqrt{2}\alpha}{3\pi N}\int_0^\infty q^2dq\int_0^\infty dt\,\left(e^{i\omega t}-1\right)\operatorname{Im}\left[T^*_{\omega_{\mathrm{LO}}}(t)\,\mathcal{G}\left(q,it\middle|\{N_\sigma\},\beta\right)\right].\end{aligned}$$

In the zero-temperature case, $T^{*}_{\omega_{\rm LO}}(t) \to e^{-it}$, and we arrive at the expression

$$\chi(\omega) = \frac{2\sqrt{2}\alpha}{3\pi N}\int_0^\infty q^2 dq \int\limits_0^\infty dt\left(e^{i\omega t}-1\right)\mathrm{Im}\left[e^{-it}\mathcal{G}\left(q,it|\left\{N_\sigma\right\},\beta\right)\right]. \tag{8.260}$$

Substituting the two-point correlation function $\mathcal{G}\left(q,it|\left\{N_\sigma\right\},\beta\right)$ with the one-electron (8.222) and the two-electron (8.224) distribution functions into the memory function (8.260) and expanding $\mathcal{G}\left(q,it|\left\{N_\sigma\right\},\beta\right)$ in powers of e^{-iwt}, $e^{-i\Omega_1 t}$ and $e^{-i\Omega_2 t}$, the integrations over q and t in Eq. (8.260) are performed analytically. The similar transformations are performed also in the 2D case. As a result, the memory function (8.258) is represented in the unified form for 3D and 2D interacting polarons:

$$\begin{aligned}
\chi(\omega) = {} & \lim_{\varepsilon\to+0}\frac{2\alpha}{3\pi N}\left(\frac{3\pi}{4}\right)^{3-D}\left(\frac{\omega_{\rm LO}}{A}\right)^{3/2} \\
& \times\sum_{p_1=0}^{\infty}\sum_{p_2=0}^{\infty}\sum_{p_3=0}^{\infty}\frac{(-1)^{p_3}}{p_1!p_2!p_3!}\left(\frac{a_1^2}{N\Omega_1 A}\right)^{p_1}\left(\frac{a_2^2}{N\Omega_2 A}\right)^{p_2}\left(\frac{1}{NwA}\right)^{p_3} \\
& \times\left\{\left[\sum_{m=0}^{\infty}\sum_{n=0}^{\infty}\sum_{\sigma}\left[f_1\left(n,\sigma|\left\{N_\sigma\right\},\beta\right)-f_2\left(n,\sigma;m,\sigma|\left\{N_\sigma\right\},\beta\right)\right]\right|_{\beta\to\infty}\right. \\
& \times\left(\begin{array}{c}\frac{1}{\omega-\omega_{\rm LO}-[p_1\Omega_1+p_2\Omega_2+(p_3-m+n)w]+i\varepsilon}-\frac{1}{\omega+\omega_{\rm LO}+p_1\Omega_1+p_2\Omega_2+(p_3-m+n)w+i\varepsilon} \\ +\mathcal{P}\left(\frac{2}{\omega_{\rm LO}+p_1\Omega_1+p_2\Omega_2+(p_3-m+n)w}\right)\end{array}\right) \\
& \times\sum_{l=0}^{m}\sum_{k=n-m+l}^{n}\frac{(-1)^{n-m+l+k}\,\Gamma\left(p_1+p_2+p_3+k+l+\frac{3}{2}\right)}{k!l!}\left(\frac{1}{wA}\right)^{l+k} \\
& \left.\times\binom{n+D-1}{n-k}\binom{2k}{k-l-n+m}\right] \\
& +\left[\left(\begin{array}{c}\frac{1}{\omega-\omega_{\rm LO}-(p_1\Omega_1+p_2\Omega_2+p_3w)+i\varepsilon}-\frac{1}{\omega+\omega_{\rm LO}+p_1\Omega_1+p_2\Omega_2+p_3w+i\varepsilon} \\ +\mathcal{P}\left(\frac{2}{\omega_{\rm LO}+p_1\Omega_1+p_2\Omega_2+p_3w}\right)\end{array}\right)\right. \\
& \times\sum_{m=0}^{\infty}\sum_{n=0}^{\infty}\sum_{\sigma,\sigma'}f_2\left(n,\sigma;m,\sigma'|\left\{N_\sigma\right\},\beta\right)\Big|_{\beta\to\infty} \\
& \times\sum_{k=0}^{n}\sum_{l=0}^{m}\frac{(-1)^{k+l}\,\Gamma\left(p_1+p_2+p_3+k+l+\frac{3}{2}\right)}{k!l!}\left(\frac{1}{wA}\right)^{k+l} \\
& \left.\left.\times\binom{n+D-1}{n-k}\binom{m+D-1}{m-l}\right]\right\},
\end{aligned} \tag{8.261}$$

where $D=2,3$ is the dimensionality of the space, $\mathcal{P}$ denotes the principal value, A is defined as $A\equiv\left[\sum_{i=1}^{2}a_i^2/\Omega_i+(N-1)/w\right]/N$, Ω_1,Ω_2, and w are the eigenfrequencies of the model system, a_1 and a_2 are the coefficients of the canonical transformation which diagonalizes the model Lagrangian (8.113).

Selected results: the manifestations of the shell filling in optical conductivity

The shell filling schemes for an N-polaron system in a quantum dot can manifest themselves in the spectra of the optical conductivity. In Fig. 8.6, optical conductivity spectra for $N=20$

polarons are presented for a quantum dot with the parameters of CdSe: $\alpha = 0.46$, $\eta = 0.656$ [7] and with different values of the confinement energy $\hbar\Omega_0$. [7] In this case, the spin-polarized ground state changes to the ground state satisfying Hund's rule with increasing $\hbar\Omega_0$ in the interval $0.0421H^* < \hbar\Omega_0 < 0.0422H^*$.

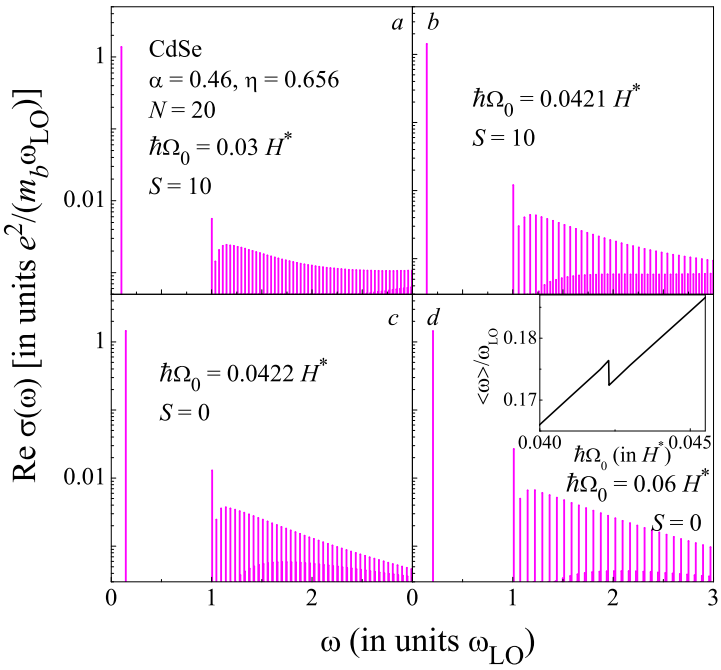

Figure 8.6: Optical conductivity spectra of $N = 20$ interacting polarons in CdSe quantum dots with $\alpha = 0.46$, $\eta = 0.656$ for different confinement energies close to the transition from a spin-polarized ground state to a ground state obeying Hund's rule. *Inset*: the first frequency moment $\langle\omega\rangle$ of the optical conductivity as a function of the confinement energy. (From Ref. [98].)

In the inset to Fig. 8.6, the first frequency moment of the optical conductivity

$$\langle\omega\rangle \equiv \frac{\int_0^\infty \omega \operatorname{Re}\sigma(\omega)\, d\omega}{\int_0^\infty \operatorname{Re}\sigma(\omega)\, d\omega}, \tag{8.262}$$

as a function of $\hbar\Omega_0$ shows a *discontinuity*, at the value of the confinement energy corresponding to the change of the shell filling schemes from the spin-polarized ground state to the ground state obeying Hund's rule. This discontinuity might be observable in optical measurements.

The shell structure for a system of interacting polarons in a quantum dot is clearly revealed when analyzing the addition energy and the first frequency moment of the optical conductivity in parallel. In Fig 8.7, we show both the function

$$\Theta(N) \equiv \langle\omega\rangle|_{N+1} - 2\langle\omega\rangle|_N + \langle\omega\rangle|_{N-1}, \tag{8.263}$$

and the addition energy

$$\Delta(N) = E^0(N+1) - 2E^0(N) + E^0(N-1). \tag{8.264}$$

for interacting polarons in a 3D CdSe quantum dot.

[7] For the numerical calculations, we use effective atomic units, where $\hbar$, the electron band mass m_b and $e/\sqrt{\varepsilon_\infty}$ have the numerical value of 1. This means that the unit of length is the effective Bohr radius $a_B^* = \hbar^2\varepsilon_\infty/(m_b e^2)$, while the unit of energy is the effective Hartree $H^* = m_b e^4/(\hbar^2\varepsilon_\infty^2)$.

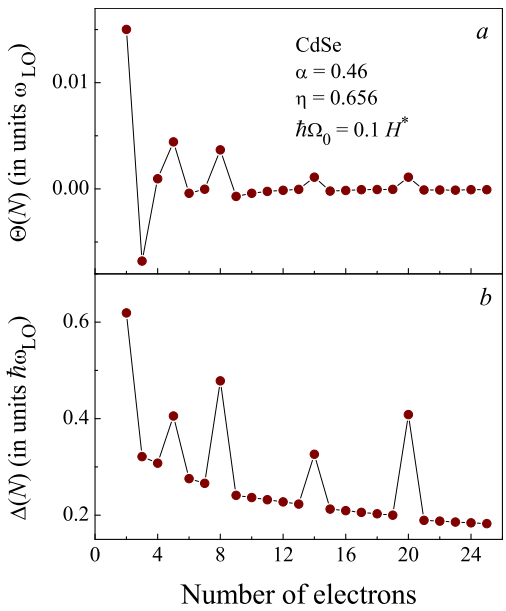

Figure 8.7: The function $\Theta(N)$ and the addition energy $\Delta(N)$ for systems of interacting polarons in CdSe quantum dots with $\alpha = 0.46$, $\eta = 0.656$ for $\hbar\Omega_0 = 0.1H^*$. (From Ref. [98].)

As seen from Fig 8.7, distinct peaks appear in $\Theta(N)$ and $\Delta(N)$ at the "magic numbers" corresponding to closed-shell configurations at $N = 8, 20$ and to half-filled-shell configurations at $N = 5, 14$. We see that each of the peaks of $\Theta(N)$ corresponds to a peak of the addition energy. The filling patterns for a many-polaron system in a quantum dot can be therefore determined from the analysis of the first moment of the optical absorption for different numbers of polarons.

8.3 Variational path-integral treatment of a translation invariant N-polaron system

8.3.1 The many-polaron system

In the present section, the ground-state properties of a translation invariant N-polaron system are theoretically studied in the framework of the variational path-integral method for identical particles, using a further development [105] of the model introduced in Refs. [100, 106, 98].

In order to describe a many-polaron system, we start from the translation invariant N-polaron Hamiltonian

$$H = \sum_{j=1}^{N} \frac{\mathbf{p}_j^2}{2m} + \frac{1}{2}\sum_{j=1}^{N}\sum_{l=1,\neq j}^{N} \frac{e^2}{\epsilon_\infty |\mathbf{r}_j - \mathbf{r}_l|} + \sum_{\mathbf{k}} \hbar\omega_{\mathrm{LO}} a_{\mathbf{k}}^\dagger a_{\mathbf{k}} + \left(\sum_{j=1}^{N}\sum_{\mathbf{k}} V_k a_{\mathbf{k}} e^{i\mathbf{k}\cdot\mathbf{r}_j} + H.c.\right), \quad (8.265)$$

where m is the band mass, e is the electron charge, ω_{LO} is the longitudinal optical (LO) phonon frequency, and V_k are the amplitudes of the Fröhlich electron-LO-phonon interaction

$$V_k = i\frac{\hbar\omega_{\mathrm{LO}}}{k}\left(\frac{4\pi\alpha}{V}\right)^{1/2}\left(\frac{\hbar}{2m\omega_{\mathrm{LO}}}\right)^{1/4}, \quad \alpha = \frac{e^2}{2\hbar\omega_{\mathrm{LO}}}\left(\frac{2m\omega_{\mathrm{LO}}}{\hbar}\right)^{1/2}\left(\frac{1}{\epsilon_\infty} - \frac{1}{\epsilon_0}\right), \quad (8.266)$$

with the electron-phonon coupling constant $\alpha > 0$, the high-frequency dielectric constant $\epsilon_\infty > 0$ and the static dielectric constant $\epsilon_0 > 0$, and consequently

$$\frac{e^2}{\epsilon_\infty} > \hbar\left(\frac{2\hbar\omega_{\mathrm{LO}}}{m}\right)^{1/2}\alpha \Longleftrightarrow \alpha\sqrt{2} < \left(\frac{H^*}{\hbar\omega_{\mathrm{LO}}}\right)^{1/2} \equiv U. \quad (8.267)$$

In the expression (8.267), H^* is the effective Hartree

$$H^* = \frac{e^2}{\epsilon_\infty a_B^*}, \quad a_B^* = \frac{\hbar^2}{me^2/\epsilon_\infty} \tag{8.268}$$

where a_B^* is the effective Bohr radius. The partition function of the system can be expressed as a path integral over all electron and phonon coordinates. The path integral over the phonon variables can be calculated analytically [43]. Feynman's phonon elimination technique for this system is well known and leads to the partition function, which is a path integral over the electron coordinates only:

$$Z = \left(\prod_{\mathbf{k}} \frac{e^{\frac{1}{2}\beta\hbar\omega_{\mathrm{LO}}}}{2\sinh\frac{1}{2}\beta\hbar\omega_{\mathrm{LO}}} \right) \oint e^S \mathcal{D}\bar{\mathbf{r}} \tag{8.269}$$

where $\bar{\mathbf{r}} = \{\mathbf{r}_1, \cdots, \mathbf{r}_N\}$ denotes the set of electron coordinates, and $\oint \mathcal{D}\bar{\mathbf{r}}$ denotes the path integral over all the electron coordinates, integrated over equal initial and final points, i.e.

$$\oint e^S \mathcal{D}\bar{\mathbf{r}} \equiv \int d\bar{\mathbf{r}} \int_{\bar{\mathbf{r}}(0)=\bar{\mathbf{r}}}^{\bar{\mathbf{r}}(\beta)=\bar{\mathbf{r}}} e^S \mathcal{D}\bar{\mathbf{r}}\,(\tau)\,.$$

Throughout this paper, imaginary time variables are used. The effective action for the N-polaron system is retarded and given by

$$\begin{aligned} S = &-\int_0^\beta \left(\frac{m}{2} \sum_{j=1}^N \left(\frac{d\mathbf{r}_j(\tau)}{d\tau} \right)^2 + \frac{1}{2} \sum_{j=1}^N \sum_{l=1,\neq j}^N \frac{e^2}{\epsilon_\infty \left|\mathbf{r}_j(\tau) - \mathbf{r}_l(\tau)\right|} \right) d\tau \\ &+ \frac{1}{2} \int_0^\beta \int_0^\beta \sum_{j,l=1}^N \sum_{\mathbf{k}} \left|V_k\right|^2 e^{i\mathbf{k}\cdot(\mathbf{r}_j(\tau)-\mathbf{r}_l(\sigma))} \frac{\cosh\hbar\omega_{\mathrm{LO}}\left(\frac{1}{2}\beta - |\tau-\sigma|\right)}{\sinh\frac{1}{2}\beta\hbar\omega_{\mathrm{LO}}} d\sigma d\tau. \end{aligned} \tag{8.270}$$

Note that the electrons are fermions. Therefore the path integral for the electrons with parallel spin has to be interpreted as the required antisymmetric projection of the propagators for distinguishable particles.

We below use units in which $\hbar = 1$, $m = 1$, and $\omega_{\mathrm{LO}} = 1$. The units of distance and energy are thus the effective polaron radius $[\hbar/(m\omega_{\mathrm{LO}})]^{1/2}$ and the LO-phonon energy $\hbar\omega_{\mathrm{LO}}$.

8.3.2 Variational principle

For distinguishable particles, it is well known that the Jensen-Feynman inequality [43] provides a lower bound on the partition function Z (and consequently an upper bound on the free energy F)

$$Z = \oint e^S \mathcal{D}\bar{\mathbf{r}} = \left(\oint e^{S_0} \mathcal{D}\bar{\mathbf{r}} \right) \left\langle e^{S-S_0} \right\rangle_0 \geq \left(\oint e^{S_0} \mathcal{D}\bar{\mathbf{r}} \right) e^{\langle S-S_0\rangle_0} \text{ with } \langle A\rangle_0 \equiv \frac{\oint A(\bar{\mathbf{r}})\, e^{S_0} \mathcal{D}\bar{\mathbf{r}}}{\oint e^{S_0} \mathcal{D}\bar{\mathbf{r}}}, \tag{8.271}$$

$$e^{-\beta F} \geq e^{-\beta F_0} e^{\langle S-S_0\rangle_0} \Longrightarrow F \leq F_0 - \frac{\langle S-S_0\rangle_0}{\beta} \tag{8.272}$$

for a system with real action S and a real trial action S_0.The many-body extension (Ref. [99, 107]) of the Jensen-Feynman inequality, requires that the potentials are symmetric with respect to all particle permutations, and that the exact propagator as well as the model propagator

are defined on the same state space. Within this interpretation we consider the following generalization of Feynman's trial action

$$S_0 = -\int_0^\beta \left(\frac{1}{2} \sum_{j=1}^N \left(\frac{d\mathbf{r}_j(\tau)}{d\tau} \right)^2 + \frac{\omega^2 + w^2 - v^2}{4N} \sum_{j,l=1}^N \left(\mathbf{r}_j(\tau) - \mathbf{r}_l(\tau) \right)^2 \right) d\tau$$
$$- \frac{w}{8} \frac{v^2 - w^2}{N} \sum_{j,l=1}^N \int_0^\beta \int_0^\beta \left(\mathbf{r}_j(\tau) - \mathbf{r}_l(\sigma) \right)^2 \frac{\cosh w \left(\frac{1}{2}\beta - |\tau - \sigma| \right)}{\sinh \frac{1}{2}\beta w} d\sigma d\tau \tag{8.273}$$

with the variational frequency parameters v, w, ω.

Using the explicit forms of the exact (8.270) and the trial (8.273) actions, the variational inequality (8.272) takes the form

$$F(\beta|N_\uparrow, N_\downarrow) \leq F_0(\beta|N_\uparrow, N_\downarrow) + \frac{U}{2\beta} \int_0^\beta \left\langle \sum_{j,l=1,\neq j}^N \frac{1}{|\mathbf{r}_j(\tau) - \mathbf{r}_l(\tau)|} \right\rangle_0 d\tau$$
$$- \frac{\omega^2 + w^2 - v^2}{4N\beta} \int_0^\beta \left\langle \sum_{j,l=1}^N \left(\mathbf{r}_j(\tau) - \mathbf{r}_l(\tau) \right)^2 \right\rangle_0 d\tau$$
$$- \frac{w}{8} \frac{v^2 - w^2}{N\beta} \int_0^\beta \int_0^\beta \left\langle \sum_{j,l=1}^N \left(\mathbf{r}_j(\tau) - \mathbf{r}_l(\sigma) \right)^2 \right\rangle_0 \frac{\cosh w \left(\frac{1}{2}\beta - |\tau - \sigma| \right)}{\sinh \frac{1}{2}\beta w} d\sigma d\tau$$
$$- \frac{1}{2\beta} \int_0^\beta \int_0^\beta \sum_{\mathbf{k}} |V_k|^2 \left\langle \sum_{j,l=1}^N e^{i\mathbf{k}\cdot(\mathbf{r}_j(\tau) - \mathbf{r}_l(\sigma))} \right\rangle_0 \frac{\cosh \omega_{\mathrm{LO}} \left(\frac{1}{2}\beta - |\tau - \sigma| \right)}{\sinh \frac{1}{2}\beta \omega_{\mathrm{LO}}} d\sigma d\tau. \tag{8.274}$$

In the zero-temperature limit ($\beta \to \infty$), we arrive at the following upper bound for the ground-state energy $E^0(N_\uparrow, N_\downarrow)$ of a translation invariant N-polaron system

$$E^0(N_\uparrow, N_\downarrow) \leq E_{var}(N_\uparrow, N_\downarrow | v, w, \omega),$$

with

$$E_{var}(N_\uparrow, N_\downarrow | v, w, \omega) = \frac{3}{4} \frac{(v-w)^2}{v} - \frac{3}{4}\omega + \frac{1}{2}\mathbb{E}_F(N_\downarrow) + \frac{1}{2}\mathbb{E}_F(N_\downarrow)$$
$$+ E_{C\|}(N_\uparrow) + E_{C\|}(N_\downarrow) + E_{C\uparrow\downarrow}(N_\uparrow, N_\downarrow)$$
$$+ E_{\alpha\|}(N_\uparrow) + E_{\alpha\|}(N_\downarrow) + E_{\alpha\uparrow\downarrow}(N_\uparrow, N_\downarrow), \tag{8.275}$$

where $\mathbb{E}_F(N)$ is the energy of N spin-polarized fermions confined to a parabolic potential with the confinement frequency ω, $E_{C\|}\left(N_{\uparrow(\downarrow)}\right)$ is the Coulomb energy of the electrons with parallel spins, $E_{C\uparrow\downarrow}(N_\uparrow, N_\downarrow)$ is the Coulomb energy of the electrons with opposite spins, $E_{\alpha\|}\left(N_{\uparrow(\downarrow)}\right)$ is the electron-phonon energy of the electrons with parallel spins, and $E_{\alpha\uparrow\downarrow}(N_\uparrow, N_\downarrow)$ is the electron-phonon energy of the electrons with opposite spins.

8.3.3 Results

Here, we discuss some results of the numerical minimization of $E_{var}(N_\uparrow, N_\downarrow | v, w, \omega)$ with respect to the three variational parameters v, w, and ω. The Fröhlich constant α and the Coulomb parameter

$$\alpha_0 \equiv \frac{U}{\sqrt{2}} \equiv \frac{\alpha}{1-\eta} \text{ with } \frac{1}{\eta} = \frac{\varepsilon_0}{\varepsilon_\infty} \tag{8.276}$$

characterize the strength of the electron-phonon and of the Coulomb interaction, obeying the physical condition $\alpha \geq \alpha_0$ [see (8.267)]. The optimal values of the variational parameters v, w, and ω are denoted v_{op}, w_{op}, and ω_{op}, respectively. The optimal value of the total spin was always determined by choosing the combination $(N_\uparrow, N_\downarrow)$ for fixed $N = N_\uparrow + N_\downarrow$which corresponds to the lowest value $E^0(N)$ of the variational functional

$$E^0(N) \equiv \min_{N_\uparrow} E_{var}(N_\uparrow, N - N_\uparrow | v_{op}, w_{op}, \omega_{op}) . \tag{8.277}$$

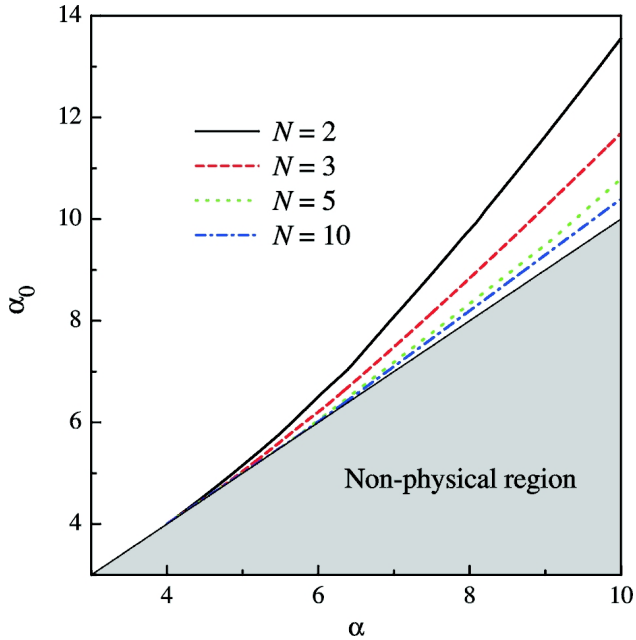

Figure 8.8: The "phase diagrams" of a translation invariant N-polaron system. The grey area is the non-physical region, for which $\alpha > \alpha_0$. The stability region for each number of electrons is determined by the equation $\alpha_c < \alpha < \alpha_0$. (From Ref. [105].)

In Fig. 8.8, the "phase diagrams" analogous to the bipolaron "phase diagram" of Ref. [108] are plotted for an N-polaron system in bulk with $N = 2, 3, 5$, and 10. The area where $\alpha_0 \leq \alpha$ is the non-physical region. For $\alpha > \alpha_0$, each sector between a curve corresponding to a well defined N and the line indicating $\alpha_0 = \alpha$ shows the stability region where $\omega_{op} \neq 0$, while the white area corresponds to the regime with $\omega_{op} = 0$. When comparing the stability region for $N = 2$ from Fig. 8.8 with the bipolaron "phase diagram" of Ref. [108], the stability region in the present work starts from the value $\alpha_c \approx 4.1$ (instead of $\alpha_c \approx 6.9$ in Ref. [108]). The width of the stability region within the present model is also larger than the width of the stability region within the model of Ref. [108]. Also, the absolute values of the ground-state energy of a two-polaron system given by the present model are smaller than those given by the approach of Ref. [108].

The difference between the numerical results of the present work and of Ref. [108] is due to the following distinction between the used model systems. The model system of Ref. [108] consists of two electrons interacting with two fictitious particles and with each other through quadratic interactions. But the trial Hamiltonian given by Eq. (6) of Ref. [108] is not symmetric with respect to the permutation of the electrons. It is only symmetric under the permutation of the pairs "electron + fictitious particle". As a consequence, this trial system is only applicable if the electrons are distinguishable, i.e. have opposite spin. In contrast to the model of Ref. [108], the model used in the present paper is described by the trial action (9), which is fully

symmetric with respect to the permutations of the electrons, as is required to describe identical particles.

The "phase diagrams" for $N > 2$ demonstrate the existence of stable multipolaron states (see Ref. [109]). As distinct from Ref. [109], here the ground state of an N-polaron system is investigated supposing that the electrons are fermions. As seen from Fig. 8.9, for $N > 2$, the stability region for a multipolaron state is narrower than the stability region for $N = 2$, and its width decreases with increasing N.

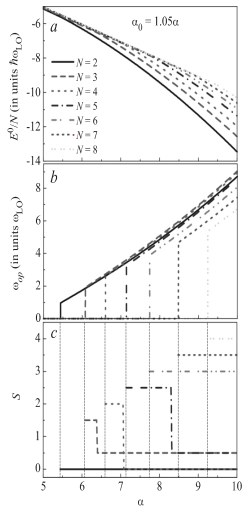

Figure 8.9: The ground-state energy per particle (a), the optimal value ω_{op} of the confinement frequency (b), and the total spin (c) of a translation invariant N-polaron system as a function of the coupling strength α for $\alpha_0/\alpha = 0.5$. The vertical dashed lines in the panel c indicate the critical values α_c separating the regimes of $\alpha > \alpha_c$, where the multipolaron ground state with $\omega_{op} \neq 0$ exists, and $\alpha < \alpha_c$, where $\omega_{op} = 0$. (From Ref. [105].)

A consequence of the Fermi statistics is the dependence of the polaron characteristics and of the total spin of an N-polaron system on the parameters (α, α_0, N). In Fig. 8.9, we present the ground-state energy per particle, the confinement frequency ω_{op} and the total spin S as a function of the coupling constant α for $\alpha_0/\alpha = 1.05$ and for a different numbers of polarons. The ground-state energy turns out to be a continuous function of α, while $\omega_{op}$and S reveal jumps. For $N = 2$ (the case of a bipolaron), we see from Fig. 8.9 that the ground state has a total spin $S = 0$ for all values of α, i. e., the ground state of a bipolaron is a singlet. This result is in agreement with earlier investigations on the large-bipolaron problem (see, e. g., [110]).

In summary, using the extension of the Jensen-Feynman variational principle to the systems of identical particles, we have derived a rigorous upper bound for the free energy of a translation

invariant system of N interacting polarons. The developed approach is valid for an arbitrary coupling strength. The resulting ground-state energy is obtained taking into account the Fermi statistics of electrons.

8.4 Ripplonic polarons in multielectron bubbles

8.4.1 Ripplon-phonon modes of a MEB

Spherical shells of charged particles appear in a variety of physical systems, such as fullerenes, metallic nanoshells, charged droplets and neutron stars. A particularly interesting physical realization of the spherical electron gas is found in multielectron bubbles (MEBs) in liquid helium-4. These MEBs are 0.1 μm – 100 μm sized cavities inside liquid helium, that contain helium vapor at vapor pressure and a nanometer-thick electron layer anchored to the surface of the bubble [112]. They exist as a result of equilibrium between the surface tension of liquid helium and the Coulomb repulsion of the electrons [113]. Recently proposed experimental schemes to stabilize MEBs [114] have stimulated theoretical investigation of their properties.

We describe the dynamical modes of an MEB by considering the motion of the helium surface ("ripplons") and the vibrational modes of the electrons together. In particular, we analyze the case when the ripplopolarons form a Wigner lattice [111].

First, we derive the Lagrangian of interacting ripplons and phonons within a continuum approach. The shape of the surface of a bubble is described by the function $R(\theta,\varphi) = R_\mathrm{b} + u(\theta,\varphi)$, where $u(\theta,\varphi)$ is the deformation of the surface from a sphere with radius R_b. The deformation can be expanded in a series of spherical harmonics $Y_{lm}(\theta,\varphi)$ with amplitudes Q_{lm},

$$u(\theta,\varphi) = \sum_{l=1}^{\infty}\sum_{m=-l}^{l} Q_{lm} Y_{lm}(\theta,\varphi)\,. \tag{8.278}$$

We suppose that the amplitudes are small in such a way that $\sqrt{l(l+1)}\,|Q_{lm}| \ll R_\mathrm{b}$.

The ripplon contribution (T_r) to the kinetic energy of an MEB, and the contributions to the potential energy due to the surface tension (U_σ) and due to the pressure (U_V) were described in Ref. [115]:

$$\begin{aligned} T_\mathrm{r} &= \frac{\rho}{2} R_\mathrm{b}^3 \sum_{l=1}^{\infty}\sum_{m=-l}^{l} \frac{1}{l+1}\left|\dot{Q}_{lm}\right|^2, \\ U_\sigma &= 4\pi\sigma R_\mathrm{b}^2 + \frac{\sigma}{2}\sum_{l=1}^{\infty}\sum_{m=-l}^{l}\left(l^2+l+2\right)|Q_{lm}|^2, \\ U_\mathrm{V} &= \frac{4\pi}{3} p R_\mathrm{b}^3 + p R_\mathrm{b}\sum_{l=1}^{\infty}\sum_{m=-l}^{l}|Q_{lm}|^2. \end{aligned} \tag{8.279}$$

Here $\rho \approx 145$ kg/m^3 is the density of liquid helium, $\sigma \approx 3.6\times 10^{-4}$ J/m^2 is its surface tension, and p is the difference of pressures outside and inside the bubble.

Expanding the surface electron density $n(\theta,\varphi)$ in a series of spherical harmonics with amplitudes n_{lm},

$$n(\theta,\varphi) = \sum_{l=0}^{\infty}\sum_{m=-l}^{l} n_{lm} Y_{lm}(\theta,\varphi)\,, \tag{8.280}$$

the kinetic energy of the motion of electrons can be written as

$$T_\mathrm{p} = \frac{1}{2}\sum_{l=1}^{\infty}\sum_{m=-l}^{l}\frac{4\pi m_\mathrm{e} R_\mathrm{b}^6}{l(l+1)N}\left|\dot{n}_{lm}\right|^2, \tag{8.281}$$

where m_{e} is the bare electron mass and N is the number of electrons. Finally, the electrostatic energy (U_{C}) of the deformed MEB with a non-uniform surface electron density (8.280) is calculated using the Maxwell equations and the electrostatic boundary conditions at the surface. The result is:

$$\begin{aligned} U_{\mathrm{C}} = & \frac{e^2 N^2}{2\varepsilon R_{\mathrm{b}}} + 2\pi e^2 R_{\mathrm{b}}^3 \sum_{l=1}^{\infty} \sum_{m=-l}^{l} \frac{|n_{lm}|^2}{l+\varepsilon(l+1)} \\ & - \frac{e^2 N^2}{8\pi\varepsilon R_{\mathrm{b}}^3} \sum_{l=1}^{\infty} \sum_{m=-l}^{l} \frac{l^2 - \varepsilon(l+1)}{l+\varepsilon(l+1)} |Q_{lm}|^2 \\ & - e^2 N \sum_{l=1}^{\infty} \sum_{m=-l}^{l} \frac{l+1}{l+\varepsilon(l+1)} n_{lm} Q_{lm}^*, \end{aligned} \tag{8.282}$$

with the dielectric constant of liquid helium $\varepsilon \approx 1.0572$. The last term in Eq. (8.282) describes the ripplon-phonon mixing. Only ripplon and phonon modes which have the same angular momentum couple to each other. After the diagonalization of the Lagrangian of this ripplon-phonon system, we arrive at the eigenfrequencies:

$$\begin{aligned} \Omega_{1,2}(l) = & \left\{ \frac{1}{2} \left[\omega_{\mathrm{p}}^2(l) + \omega_{\mathrm{r}}^2(l) \right.\right. \\ & \left.\left. \pm \sqrt{\left[\omega_{\mathrm{p}}^2(l) - \omega_{\mathrm{r}}^2(l)\right]^2 + 4\gamma^2(l)} \right] \right\}^{1/2}, \end{aligned} \tag{8.283}$$

where $\omega_{\mathrm{r}}(l)$ is the bare ripplon frequency,

$$\begin{aligned} \omega_{\mathrm{r}}(l) = & \left\{ \frac{l+1}{\rho R_{\mathrm{b}}^3} \left[\sigma \left(l^2 + l + 2\right) \right.\right. \\ & \left.\left. - \frac{e^2 N^2}{4\pi\varepsilon R_{\mathrm{b}}^3} \frac{l^2 - \varepsilon(l+1)}{l+\varepsilon(l+1)} + 2pR_{\mathrm{b}} \right] \right\}^{1/2}, \end{aligned} \tag{8.284}$$

while $\omega_{\mathrm{p}}(l)$ is the bare phonon frequency,

$$\omega_{\mathrm{p}}(l) = \left(\frac{e^2 N}{m_{\mathrm{e}} R_{\mathrm{b}}^3} \frac{l(l+1)}{l+\varepsilon(l+1)} \right)^{1/2}, \tag{8.285}$$

and $\gamma(l)$ describes the ripplon-phonon coupling:

$$\gamma(l) = \frac{e^2 N}{R_{\mathrm{b}}^3} \left(\frac{Nl}{4\pi m_{\mathrm{e}} \rho R_{\mathrm{b}}^3} \right)^{1/2} \frac{(l+1)^2}{l+\varepsilon(l+1)}. \tag{8.286}$$

8.4.2 Electron-ripplon interaction in the MEB

The interaction energy between the ripplons and the electrons in the multielectron bubble can be derived from the following considerations: (i) the distance between the layer electrons and the helium surface is fixed (the electrons find themselves confined to an effectively 2D surface anchored to the helium surface) and (ii) the electrons are subjected to a force field, arising from the electric field of the other electrons. For a spherical bubble, this electric field lies along the radial direction and equals

$$\mathbf{E} = -\frac{Ne}{2R_b^2} \mathbf{e_r}. \tag{8.287}$$

A bubble shape oscillation will displace the layer of electrons anchored to the surface. The interaction energy which arises from this, equals the displacement of the electrons times the force $e\mathbf{E}$ acting on them. Thus, we get for the interaction Hamiltonian

$$\hat{H}_{int} = \sum_j e|\mathbf{E}| \times u(\hat{\Omega}_j). \tag{8.288}$$

Here $u(\Omega)$ is the radial displacement of the surface in the direction given by the spherical angle Ω; and $\hat{\Omega}_j$ is the (angular) position operator for electron j. The displacement can be rewritten using (8.278) and we find

$$\hat{H}_{int} = \sum_j e|\mathbf{E}| \sum_{\ell,m} \hat{Q}_{\ell m} Y_{\ell m}(\hat{\Omega}_j). \tag{8.289}$$

Using the relation

$$\hat{Q}_{\ell,m} = (-1)^{(m-|m|)/2} \sqrt{\tfrac{\hbar(\ell+1)}{2\rho R_b^3 \omega_\ell}} (\hat{a}_{\ell,m} + \hat{a}^+_{\ell,-m}), \tag{8.290}$$

the interaction Hamiltonian can be written in the suggestive form

$$\hat{H}_{int} = \sum_{\ell,m} \sum_j M_{\ell,m} Y_{\ell,m}(\hat{\Omega}_j)(\hat{a}_{\ell,m} + \hat{a}^+_{\ell,-m}), \tag{8.291}$$

with the electron-ripplon coupling amplitude for a MEB given by

$$M_{\ell,m} = (-1)^{(m-|m|)/2} \frac{Ne^2}{2R_b^2} \sqrt{\frac{\hbar(\ell+1)}{2\rho R_b^3 \omega_\ell}} \tag{8.292}$$

8.4.3 Locally flat approximation

Substituting $M_{\ell,m}$ into (8.291), we get

$$\hat{H}_{int} = \sum_{\ell,m} \sum_j \frac{Ne^2}{2R_b^2} \sqrt{\frac{\hbar(\ell+1)}{2\rho R_b^3 \omega_\ell}} \times \left[(-1)^{(m-|m|)/2} \frac{Y_{\ell,m}(\hat{\Omega}_j)}{R_b} \right] (\hat{a}_{\ell,m} + \hat{a}^+_{\ell,-m}). \tag{8.293}$$

In this expression, we consider the limit of a bubble so large that the surface becomes flat on all length scales of interest. Hence we let $R_b \to \infty$ but keep $\ell/R_b = q$ a constant. This means we have to let $\ell \to \infty$ as well. In this limit,

$$\lim_{\ell\to\infty} Y_{\ell,0}(\theta) = \frac{i^\ell}{\pi\sqrt{\sin\theta}} \sin[(\ell + 1/2)\theta + \pi/4], \tag{8.294}$$

and $Y_{\ell,0}(\theta)$ varies locally as a plane wave with wave vector $q = \ell/R_b$. The wave function $Y_{\ell,m}(\hat{\Omega}_j)/R_b$ is furthermore normalized with respect to integration over the surface (with total area $4\pi R_b^2$). Thus, we get in the locally flat approximation

$$\hat{H}_{int} = \sum_{\mathbf{q}} \sum_j \frac{Ne^2}{2R_b^2} \sqrt{\frac{\hbar q}{2\rho\omega(q)}} e^{i\mathbf{q}.\hat{\mathbf{r}}_j} (\hat{a}_{\mathbf{q}} + \hat{a}^+_{-\mathbf{q}}), \tag{8.295}$$

or

$$\hat{H}_{int} = \sum_{\mathbf{q}} \sum_j M_q e^{i\mathbf{q}.\hat{\mathbf{r}}_j} (\hat{a}_{\mathbf{q}} + \hat{a}^+_{-\mathbf{q}}),$$

$$M_q = e|\mathbf{E}| \sqrt{\frac{\hbar q}{2\rho\omega(q)}}. \tag{8.296}$$

This corresponds in the limit of large bubbles to the interaction Hamiltonian expected for a flat surface.

8.4.4 Ripplopolaron in a Wigner lattice: the mean-field approach

In their treatment of the electron Wigner lattice embedded in a polarizable medium such as a semiconductors or an ionic solid, Fratini and Quémerais [116] described the effect of the electrons on a particular electron through a mean-field lattice potential. The (classical) lattice potential V_{lat} is obtained by approximating all the electrons acting on one particular electron by a homogenous charge density in which a hole is punched out; this hole is centered in the lattice point of the particular electron under investigation and has a radius given by the lattice distance d.

Within this particular mean-field approximation, the lattice potential can be calculated from classical electrostatics and we find that for a 2D electron gas it can be expressed in terms of the elliptic functions of first and second kind, $E(x)$ and $K(x)$,

$$V_{lat}(\mathbf{r}) = -\frac{2e^2}{\pi d^2}\left\{|d-r|\,E\left[-\frac{4rd}{(d-r)^2}\right] + (d+r)\,\mathrm{sgn}\,(d-r)\,K\left[-\frac{4rd}{(d-r)^2}\right]\right\}. \tag{8.297}$$

Here, $\mathbf{r}$ is the position vector measured from the lattice position. We can expand this potential around the origin to find the small-amplitude oscillation frequency of the electron lattice:

$$\lim_{r\ll d} V_{lat}(\mathbf{r}) = -\frac{2e^2}{d} + \frac{1}{2}m_e\omega_{lat}^2 r^2 + \mathcal{O}\left(r^4\right), \tag{8.298}$$

with the confinement frequency

$$\omega_{lat} = \sqrt{\frac{e^2}{m_e d^3}}. \tag{8.299}$$

In the mean-field approximation, the Hamiltonian for a ripplopolaron in a lattice on a *locally flat* helium surface is given by

$$\hat{H} = \frac{\hat{p}^2}{2m_e} + V_{lat}(\hat{\mathbf{r}}) + \sum_{\mathbf{q}} \hbar\omega(q)\hat{a}_{\mathbf{q}}^{+}\hat{a}_{\mathbf{q}} + \sum_{\mathbf{q}} M_q e^{-i\mathbf{q}.\mathbf{r}}\left(\hat{a}_{\mathbf{q}} + \hat{a}_{-\mathbf{q}}^{+}\right), \tag{8.300}$$

where $\hat{\mathbf{r}}$ is the electron position operator.

Now that the lattice potential has been introduced, we can move on and include effects of the bubble geometry. If we restrict our treatment to the case of large bubbles (with $N > 10^5$ electrons), then both the ripplopolaron radius and the inter-electron distance d are much smaller than the radius of the bubble R_b. This gives us ground to use the locally flat approximation using the auxiliary model of a ripplonic polaron in a planar system described by (8.300), but with a modified ripplon dispersion relation and an modified pressing field. We find for the modified ripplon dispersion relation in the MEB:

$$\omega(q) = \sqrt{\frac{\sigma}{\rho}q^3 + \frac{p}{\rho R_b}q}, \tag{8.301}$$

where R_b is the equilibrium bubble radius which depends on the pressure and the number of electrons. The bubble radius is found by balancing the surface tension and the pressure with

the Coulomb repulsion. The modified electron-ripplon interaction amplitude in an MEB is given by

$$M_{\mathbf{q}} = e|\mathbf{E}|\sqrt{\frac{\hbar q}{2\rho\omega(q)}}. \tag{8.302}$$

The effective electric pressing field pushing the electrons against the helium surface and determining the strength of the electron-ripplon interaction is

$$\mathbf{E} = -\frac{Ne}{2R_b^2}\mathbf{e}_{\mathbf{r}}. \tag{8.303}$$

8.4.5 Ripplopolaron Wigner lattice at finite temperature

To study the ripplopolaron Wigner lattice at finite temperature and for any value of the electron-ripplon coupling, we use the variational path-integral approach [43]. This variational principle distinguishes itself from Rayleigh-Ritz variation in that it uses a trial action functional S_{trial} instead of a trial wave function.

The action functional of the system described by Hamiltonian (8.300), becomes, after elimination of the ripplon degrees of freedom,

$$S = -\frac{1}{\hbar}\int_0^{\hbar\beta} d\tau \left\{\frac{m_e}{2}\dot{r}^2(\tau) + V_{lat}[r(\tau)]\right\} + \sum_{\mathbf{q}} |M_q|^2$$
$$\times \int_0^{\hbar\beta} d\tau \int_0^{\hbar\beta} d\sigma G_{\omega(q)}(\tau-\sigma) e^{i\mathbf{q}\cdot[\mathbf{r}(\tau)-\mathbf{r}(\sigma)]}, \tag{8.304}$$

with

$$G_\nu(\tau-\sigma) = \frac{\cosh[\nu(|\tau-\sigma| - \hbar\beta/2)]}{\sinh(\beta\hbar\nu/2)}. \tag{8.305}$$

In preparation of its customary use in the Jensen-Feynman inequality, the action functional (8.304) is written in imaginary time $t = i\tau$ with $\beta = 1/(k_B T)$ where T is the temperature. We introduce a quadratic trial action of the form

$$S_{trial} = -\frac{1}{\hbar}\int_0^{\hbar\beta} d\tau \left[\frac{m_e}{2}\dot{r}^2(\tau) + \frac{m_e\Omega^2}{2}r^2(\tau)\right]$$
$$- \frac{Mw^2}{4\hbar}\int_0^{\hbar\beta} d\tau \int_0^{\hbar\beta} d\sigma G_w(\tau-\sigma)\mathbf{r}(\tau)\cdot\mathbf{r}(\sigma). \tag{8.306}$$

where M, w, and Ω are the variationally adjustable parameters. This trial action corresponds to the Lagrangian

$$\mathcal{L}_0 = \frac{m_e}{2}\dot{r}^2 + \frac{M}{2}\dot{R}^2 - \frac{\kappa}{2}r^2 - \frac{K}{2}(\mathbf{r}-\mathbf{R})^2, \tag{8.307}$$

from which the degrees of freedom associated with $\mathbf{R}$ have been integrated out. This Lagrangian can be interpreted as describing an electron with mass m_e at position $\mathbf{r}$, coupled through a spring with spring constant κ to its lattice site, and to which a fictitious mass M at position $\mathbf{R}$ has been attached with another spring, with spring constant K. The relation between the spring constants in (8.307) and the variational parameters w, Ω is given by

$$w = \sqrt{K/m_e}, \tag{8.308}$$

$$\Omega = \sqrt{(\kappa+K)/m_e}. \tag{8.309}$$

Based on the trial action S_{trial}, Feynman's variational method allows one to obtain an upper bound for the free energy F of the system (at temperature T) described by the action functional S by minimizing the following function:

$$F = F_0 - \frac{1}{\beta} \langle S - S_{trial} \rangle \,, \tag{8.310}$$

with respect to the variational parameters of the trial action. In this expression, F_0 is the free energy of the trial system characterized by the Lagrangian $\mathcal{L}_0$, $\beta = 1/(k_b T)$ is the inverse temperature, and the expectation value $\langle S - S_{trial} \rangle$ is to be taken with respect to the ground state of this trial system. The evaluation of expression (8.310) is straightforward though lengthy. We find

$$\begin{aligned} F = & \frac{2}{\beta} \ln \left[2 \sinh \left(\frac{\beta \hbar \Omega_1}{2} \right) \right] + \frac{2}{\beta} \ln \left[2 \sinh \left(\frac{\beta \hbar \Omega_2}{2} \right) \right] \\ & - \frac{2}{\beta} \ln \left[2 \sinh \left(\frac{\beta \hbar w}{2} \right) \right] - \frac{\hbar}{2} \sum_{i=1}^{2} a_i^2 \Omega_i \coth \left(\frac{\beta \hbar \Omega_i}{2} \right) \\ & - \frac{\sqrt{\pi} e^2}{D} e^{-d^2/(2D)} \left[I_0 \left(\frac{d^2}{2D} \right) + I_1 \left(\frac{d^2}{2D} \right) \right] \\ & - \frac{1}{2\pi \hbar \beta} \int_{1/R_b}^{\infty} dq q |M_q|^2 \int_0^{\hbar\beta/2} d\tau \frac{\cosh[\omega(q)(\tau - \hbar\beta/2)]}{\sinh[\beta \hbar \omega(q)/2]} \\ & \times \exp \left[- \frac{\hbar q^2}{2m_e} \sum_{j=1}^{2} a_j^2 \frac{\cosh(\hbar \Omega_j \beta/2) - \cosh[\hbar \Omega_j (\tau - \beta/2)]}{\Omega_j \sinh(\hbar \Omega_j \beta/2)} \right] . \end{aligned} \tag{8.311}$$

In this expression, I_0 and I_1 are Bessel functions of imaginary argument, and

$$D = \frac{\hbar}{m_e} \sum_{j=1}^{2} \frac{a_j^2}{\Omega_j} \coth \left(\hbar \Omega_j \beta / 2 \right) , \tag{8.312}$$

$$a_1 = \sqrt{\frac{\Omega_1^2 - w^2}{\Omega_1^2 - \Omega_2^2}} ; a_2 = \sqrt{\frac{w^2 - \Omega_2^2}{\Omega_1^2 - \Omega_2^2}} . \tag{8.313}$$

Finally, Ω_1 and Ω_2 are the eigenfrequencies of the trial system, given by

$$\Omega_{1,2}^2 = \frac{1}{2} \left[\Omega^2 + w^2 \pm \sqrt{(\Omega^2 - w^2)^2 + 4K/(M m_e)} \right] . \tag{8.314}$$

Optimal values of the variational parameters are determined by the numerical minimization of the variational functional F as given by expression (8.311).

8.4.6 Melting of the ripplopolaron Wigner lattice

The Lindemann melting criterion [117] states in general that a crystal lattice of objects (be it atoms, molecules, electrons, or ripplopolarons) will melt when the average motion of the objects around their lattice site is larger than a critical fraction δ_0 of the lattice parameter d. It would be a strenuous task to calculate from first principles the exact value of the critical fraction δ_0, but for the particular case of electrons on a helium surface, we can make use of an experimental determination. Grimes and Adams [118] found that the Wigner lattice melts when $\Gamma = 137 \pm 15$, where Γ is the ratio of potential energy to the kinetic energy per electron. At temperature T the average kinetic energy in a lattice potential V_{lat} is

$$E_{kin} = \frac{\hbar \omega_{lat}}{2} \coth \left(\frac{\hbar \omega_{lat}}{2 k_B T} \right) , \tag{8.315}$$

and the average distance that an electron moves out of the lattice site is determined by

$$\left\langle \mathbf{r}^2 \right\rangle = \frac{\hbar}{m_e \omega_{lat}} \coth\left(\frac{\hbar\omega_{lat}}{2k_B T}\right) = \frac{2E_{kin}}{m_e \omega_{lat}^2}. \tag{8.316}$$

From this we find that for the melting transition in Grimes and Adams' experiment [118], the critical fraction equals $\delta_0 \approx 0.13$. This estimate is in agreement with previous (empirical) estimates yielding $\delta_0 \approx 0.1$ [119], and we shall use it in the rest of this section.

Within the approach of Fratini and Quémerais [116], the Wigner lattice of (ripplo)polarons melts when at least one of the two following Lindemann criteria are met:

$$\delta_r = \frac{\sqrt{\langle \mathbf{R}_{cms}^2 \rangle}}{d} > \delta_0, \tag{8.317}$$

$$\delta_\rho = \frac{\sqrt{\langle \rho^2 \rangle}}{d} > \delta_0. \tag{8.318}$$

where ρ and $\mathbf{R}_{cms}$ are, respectively, the relative coordinate and the center of mass coordinate of the model system (8.307): if $\mathbf{r}$ is the electron coordinate and $\mathbf{R}$ is the position coordinate of the fictitious ripplon mass M, this is

$$\mathbf{R}_{cms} = \frac{m_e \mathbf{r} + M\mathbf{R}}{m_e + M}; \rho = \mathbf{r} - \mathbf{R}. \tag{8.319}$$

The appearance of two Lindemann criteria takes into account the composite nature of (ripplo)polarons. As follows from the physical sense of the coordinates ρ and $\mathbf{R}_{cms}$, the first criterion (8.317) is related to the melting of the ripplopolaron Wigner lattice towards a ripplopolaron liquid, where the ripplopolarons move as a whole, the electron together with its dimple. The second criterion (8.318) is related to the dissociation of ripplopolarons: the electrons shed their dimple.

The path-integral variational formalism allows us to calculate the expectation values $\langle \mathbf{R}_{cms}^2 \rangle$ and $\langle \rho^2 \rangle$ with respect to the ground state of the variationally optimal model system. We find

$$\begin{aligned}\left\langle \mathbf{R}_{cms}^2 \right\rangle = & \frac{\hbar w^4}{m_e \left[w^2(\Omega_1^2 + \Omega_2^2) - \Omega_1^2\Omega_2^2\right](\Omega_1^2 - \Omega_2^2)} \\ & \times \left[\Omega_2^4(\Omega_1^2 - w^2)\coth(\hbar\Omega_1\beta/2)/\Omega_1 \right. \\ & \left. + \Omega_1^4(w^2 - \Omega_2^2)\coth(\hbar\Omega_2\beta/2)/\Omega_2\right],\end{aligned} \tag{8.320}$$

$$\begin{aligned}\left\langle \rho^2 \right\rangle = & \frac{\hbar}{m_e (\Omega_1^2 - \Omega_2^2)(\Omega_1^2 - w^2)(w^2 - \Omega_2^2)} \\ & \times \left[\Omega_1^3(w^2 - \Omega_2^2)\coth(\hbar\Omega_1\beta/2) \right. \\ & \left. + \Omega_2^3(\Omega_1^2 - w^2)\coth(\hbar\Omega_2\beta/2)\right].\end{aligned} \tag{8.321}$$

Numerical calculation shows that for ripplopolarons in an MEB the inequality $\Omega_1 \gg w$ is fulfilled ($w/\Omega_1 \approx 10^{-3}$ to 10^{-2}) so that the strong-coupling regime is realized. Owing to this inequality, we find from Eqs. (8.320),(8.321) that

$$\left\langle \mathbf{R}_{cms}^2 \right\rangle \ll \left\langle \rho^2 \right\rangle. \tag{8.322}$$

So, the destruction of the ripplopolaron Wigner lattice in an MEB occurs through the dissociation of ripplopolarons, since the second criterion (8.318) will be fulfilled before the first (8.317). The results for the melting of the ripplopolaron Wigner lattice are summarized in the phase diagram shown in Fig. 8.10.

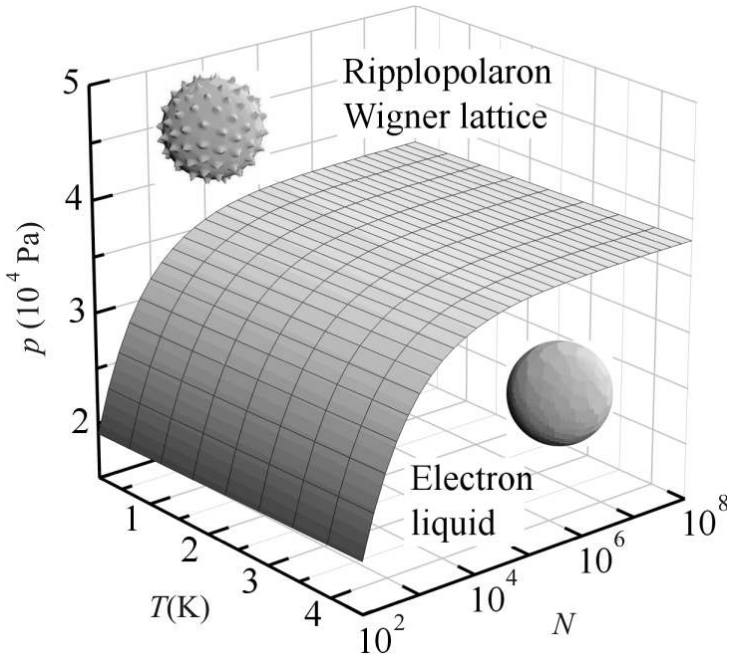

Figure 8.10: The phase diagram for the spherical 2D layer of electrons in the MEB. Above a critical pressure, a ripplopolaron solid (a Wigner lattice of electrons with dimples in the helium surface underneath them) is formed. Below the critical pressure, the ripplopolaron solid melts into an electron liquid through dissociation of ripplopolarons. (From Ref. [111].)

For every value of N, pressure p and temperature T in an experimentally accessible range, this figure shows whether the ripplopolaron Wigner lattice is present (points above the surface) or molten (points below the surface). Below a critical pressure (on the order of 10^4 Pa) the ripplopolaron solid will melt into an electron liquid. This critical pressure is nearly independent of the number of electrons (except for the smallest bubbles) and is weakly temperature dependent, up to the helium critical temperature 5.2 K. This can be understood since the typical lattice potential well in which the ripplopolaron resides has frequencies of the order of THz or larger, which correspond to ~ 10 K.

The new phase that we predict, the ripplopolaron Wigner lattice, will not be present for electrons on a flat helium surface. At the values of the pressing field necessary to obtain a strong enough electron-ripplon coupling, the flat helium surface is no longer stable against long-wavelength deformations [120]. Multielectron bubbles, with their different ripplon dispersion and the presence of stabilizing factors such as the energy barrier against fissioning [121], allow for much larger electric fields pressing the electrons against the helium surface. The regime of N, p, T parameters suitable for the creation of a ripplopolaron Wigner lattice lies within the regime that would be achievable in recently proposed experiments aimed at stabilizing multielectron bubbles [114]. The ripplopolaron Wigner lattice and its melting transition might be detected by spectroscopic techniques [118, 122] probing for example the transverse phonon modes of the lattice [123].

9 Fröhlich Polarons: Lecture course including detailed theoretical derivations by Devreese. Appendix

9.1 Optical conductivity of a strong-coupling Fröhlich polaron

[*S. N. Klimin and J. T. Devreese, Phys. Rev. B 89, 035201 (2014)*]

9.1.1 Introduction

The optical conductivity of the Fröhlich polaron model attracted attention for years [125]. In the regime of weak coupling, the optical absorption of a polaron was calculated using different methods, e. g., Green's function method [71], the Low-Lee-Pines formalism [73, 80], perturbation expansion of the current-current correlation function [126]. The strong-coupling polaron optical conductivity was calculated taking into account one-phonon [49] and two-phonon [75] transitions from the polaron ground state to the polaron relaxed excited state (RES). In fact the present work finalizes the project started in Ref. [49]. Using the path integral response formalism, the impedance function of an all-coupling polaron was calculated by FHIP [47] on the basis of the Feynman polaron model [43]. Developing further the FHIP approach, the optical conductivity was calculated in the path-integral formalism at zero temperature [50] and at finite temperatures [76]. In Ref. [127], the extension of the method of Ref. [50] accounting for the polaron damping (for the polaron coupling constant $\alpha \lesssim 8$) and the asymptotic strong-coupling approach using the Franck-Condon (FC) picture for the optical conductivity (for $\alpha \gtrsim 8$) have given reasonable results for the polaron optical conductivity at all values of α. The concept of the RES and FC polaron states played a key role in the understanding of the mechanism of the polaron optical conductivity [49, 75, 41, 50, 7, 76].

Recently, the Diagrammatic Quantum Monte Carlo (DQMC) numerical method has been developed [30, 79], which provides accurate results for the polaron characteristics in all coupling regimes. The analytic treatment [50] was intended to be valid at all coupling strengths. However, it is established in [50, 7, 75] that the linewidth of the obtained spectra [50] is unreliable for $\alpha \gtrapprox 7$. Nevertheless, the position of the peak attributed to RES in Ref. [50] is close to the maximum of the polaron optical conductivity band calculated using DQMC up to very large values of α (see Fig. 1).

An extension of the path-integral approach [50] performed in Ref. [127] gives a good agreement with DQMC for weak and intermediate coupling strengths. In the strong-coupling limit, in Ref. [127] the adiabatic strong-coupling expansion was applied. That expansion, however, is not exact in the strong-coupling limit because of a parabolic approximation [35] for the adiabatic potential.

In the present work, the strong-coupling approach of Ref. [127] is extended in order to obtain the polaron optical conductivity which is *asymptotically exact in the strong-coupling limit*. We develop the multiphonon strong-coupling expansion using numerically accurate in the strong-coupling limit polaron energies and wave functions and accounting for non-adiabaticity.

9.1.2 Optical conductivity

We consider the electron-phonon system with the Hamiltonian written down in the Feynman units ($\hbar = 1$, the carrier band mass $m_b = 1$, and the LO-phonon frequency $\omega_{\rm LO} = 1$)

$$H = \frac{\mathbf{p}^2}{2} + \sum_{\mathbf{q}} \left(b^+_{\mathbf{q}} b_{\mathbf{q}} + \frac{1}{2} \right) + \frac{1}{\sqrt{V}} \sum_{\mathbf{q}} \frac{\sqrt{2\sqrt{2}\pi\alpha}}{q} \left(b_{\mathbf{q}} + b^+_{-\mathbf{q}} \right) e^{i\mathbf{q}\cdot\mathbf{r}}. \tag{9.1}$$

where $\mathbf{r}, \mathbf{p}$ represent the position and momentum of an electron, $b^+_{\mathbf{q}}, b_{\mathbf{q}}$ denote the creation and annihilation operators for longitudinal optical (LO) phonons with wave vector $\mathbf{q}$, and $V_{\mathbf{q}}$ describes the amplitude of the interaction between the electrons and the phonons. For the Fröhlich electron-phonon interaction, the amplitude of the electron – LO-phonon interaction is

$$V_{\mathbf{q}} = \frac{1}{\sqrt{V}} \frac{\sqrt{2\sqrt{2}\pi\alpha}}{q} \tag{9.2}$$

with the crystal volume V, and the electron-phonon coupling constant α.

The polaron optical conductivity describes the response of the system with the Hamiltonian (8.2) to an applied electromagnetic field (along the z-axis) with frequency ω. This optical response is expressed using the Kubo formula with a dipole-dipole correlation function:

$$\operatorname{Re}\sigma(\omega) = \frac{n_0\omega}{2}\left(1 - e^{-\beta\omega}\right)\int_{-\infty}^{\infty} e^{i\omega t}\left\langle d_z(t)\, d_z\right\rangle\, dt, \tag{9.3}$$

where $\mathbf{d} = -e_0\mathbf{r}$ is the electric dipole moment, e_0 is the unit charge, $\beta = \frac{1}{k_B T}$, n_0 is the electron density. In the zero-temperature limit, the optical conductivity (9.3) measured in units of e_0^2 becomes

$$\operatorname{Re}\sigma(\omega) = \frac{\omega}{2}\int_{-\infty}^{\infty} e^{i\omega t} f_{zz}(t)\, dt, \tag{9.4}$$

with the correlation function

$$f_{zz}(t) \equiv \langle z(t)\, z(0)\rangle = \left\langle \Psi_0 \left| e^{itH} z e^{-itH} z \right| \Psi_0 \right\rangle, \tag{9.5}$$

where $|\Psi_0\rangle$ is the ground-state wave function of the electron-phonon system.

Within the strong-coupling approach, the ground-state wave function is chosen as the product of a trial wave function of an electron $\left|\psi_0^{(e)}\right\rangle$ and of a trial wave function of a phonon subsystem $|\Phi_{ph}\rangle$:

$$|\Psi_0\rangle = \left|\psi_0^{(e)}\right\rangle |\Phi_{ph}\rangle. \tag{9.6}$$

The phonon trial wave function is written as the strong-coupling unitary transformation applied to the phonon vacuum

$$|\Phi_{ph}\rangle = U\,|0_{ph}\rangle. \tag{9.7}$$

with the unitary operator

$$U = e^{\sum_{\mathbf{q}}\left(f_{\mathbf{q}} b_{\mathbf{q}} - f_{\mathbf{q}}^* b_{\mathbf{q}}^+\right)}, \tag{9.8}$$

and the variational parameters $\{f_{\mathbf{q}}\}$. The transformed Hamiltonian $\tilde{H} \equiv U^{-1} H U$ takes the form

$$\tilde{H} = \tilde{H}_0 + W \tag{9.9}$$

with the terms

$$\tilde{H}_0 = \frac{\mathbf{p}^2}{2} + \sum_{\mathbf{q}} |f_{\mathbf{q}}|^2 + V_a(r) + \sum_{\mathbf{q}}\left(b_{\mathbf{q}}^+ b_{\mathbf{q}} + \frac{1}{2}\right), \tag{9.10}$$

$$W = \sum_{\mathbf{q}}\left(W_{\mathbf{q}} b_{\mathbf{q}} + W_{\mathbf{q}}^* b_{\mathbf{q}}^+\right). \tag{9.11}$$

Here, $W_{\mathbf{q}}$ are the amplitudes of the renormalized electron-phonon interaction

$$W_{\mathbf{q}} = \frac{\sqrt{2\sqrt{2}\pi\alpha}}{q\sqrt{V}}\left(e^{i\mathbf{q}\cdot\mathbf{r}} - \rho_{\mathbf{q}}\right), \tag{9.12}$$

where $\rho_{\mathbf{q}}$ is the expectation value of the operator $e^{i\mathbf{q}\cdot\mathbf{r}}$ with the trial electron wave function $\left|\psi_0^{(e)}\right\rangle$:

$$\rho_{\mathbf{q}} = \left\langle \psi_0^{(e)} \left| e^{i\mathbf{q}\cdot\mathbf{r}} \right| \psi_0^{(e)} \right\rangle, \tag{9.13}$$

and $V_a(r)$ is the self-consistent potential energy for the electron,

$$V_a(r) = -\sum_{\mathbf{q}} \frac{4\sqrt{2}\pi\alpha}{q^2 V}\rho_{-\mathbf{q}} e^{i\mathbf{q}\cdot\mathbf{r}}. \tag{9.14}$$

Averaging the Hamiltonian (9.9) with the phonon vacuum $|0\rangle$ and with the trial electron wave function $|\psi_0\rangle$, we arrive at the following variational expression for the ground-state energy

$$E_0 = \langle \Psi_0 | H | \Psi_0 \rangle = \left\langle \psi_0 \left| \frac{\mathbf{p}^2}{2} \right| \psi_0 \right\rangle + \sum_{\mathbf{q}} |f_{\mathbf{q}}|^2 - \sum_{\mathbf{q}} \left(V_{\mathbf{q}} f_{\mathbf{q}}^* \rho_{\mathbf{q}} + V_{\mathbf{q}}^* f_{\mathbf{q}} \rho_{-\mathbf{q}} \right), \tag{9.15}$$

After minimization of the polaron ground-state energy (9.15), the parameters $f_{\mathbf{q}}$ acquire their optimal values

$$f_{\mathbf{q}} = V_{\mathbf{q}} \rho_{\mathbf{q}}. \tag{9.16}$$

The ground-state energy with $\{f_{\mathbf{q}}\}$ given by Eq. (9.16) takes the form

$$E_0 = \left\langle \psi_0 \left| \frac{\mathbf{p}^2}{2} \right| \psi_0 \right\rangle - \sum_{\mathbf{q}} |V_{\mathbf{q}}|^2 |\rho_{\mathbf{q}}|^2 . \tag{9.17}$$

With the strong-coupling Ansatz (9.6) for the polaron ground-state wave function and after the application of the unitary transformation (9.8), the correlation function (9.5) takes the form

$$f_{zz}(t) = \left\langle 0_{ph} \left| \left\langle \psi_0 \left| e^{it\tilde{H}} z e^{-it\tilde{H}} z \right| \psi_0 \right\rangle \right| 0_{ph} \right\rangle . \tag{9.18}$$

This correlation function can be expanded using a complete orthogonal set of intermediate states $|j\rangle$ and the completeness property:

$$\sum_j |j\rangle \langle j| = 1. \tag{9.19}$$

In the present work, we use the intermediate basis of the Franck-Condon (FC) states. The FC states correspond to the equilibrium phonon configuration for the ground state. Thus the FC wave functions are the exact eigenstates of the Hamiltonian $\tilde{H}_0$. Further on, the FC wave functions are written in the spherical-wave representation as $|\psi_{n,l,m}\rangle = R_{n,l}(r) Y_{l,m}(\theta, \varphi)$ where $R_{n,l}(r)$ are the radial wave functions, and $Y_{l,m}(\theta, \varphi)$ are the spherical harmonics, l is the quantum number of the angular momentum, m is the z-projection of the angular momentum, and n is the radial quantum number[8]. The energy levels for the eigenstates of the Hamiltonian $\tilde{H}_0$ are denoted $E_{n,l}$.

Using (9.19) with that complete and orthogonal basis , we transform (9.18) to the expression

$$f_{zz}(t) = \sum_{\substack{n,l,m,\\ n',l',m',\\ n'',l'',m''}} \langle \psi_{n,l,m} | z | \psi_{n'',l'',m''} \rangle \langle \psi_{n',l',m'} | z | \psi_0 \rangle \times \left\langle 0_{ph} \left| \left\langle \psi_0 \left| e^{it\tilde{H}} \right| \psi_{n,l,m} \right\rangle \left\langle \psi_{n'',l'',m''} \left| e^{-it\tilde{H}} \right| \psi_{n',l',m'} \right\rangle \right| 0_{ph} \right\rangle . \tag{9.20}$$

So far, the only approximation made in (9.20) is the strong-coupling Ansatz for the polaron ground-state wave function. However, in order to obtain a numerically tractable expression for the polaron optical conductivity, an additional approximation valid in the strong-coupling limit must be applied to the matrix elements of the evolution operator $e^{-it\tilde{H}}$ with the Hamiltonian of the electron-phonon system $\tilde{H}$ given by formula (9.9). According to Ref. [128], in the strong-coupling limit, the matrix elements of the Hamiltonian of the electron-phonon system between

[8] In this classification, the ground-state wave function is $|\psi_{0,0,0}\rangle \equiv |\psi_0\rangle$.

states corresponding to different energy levels are of order of magnitude α^{-4}. Therefore in the strong-coupling regime these matrix elements can be neglected; this is called the adiabatic or the Born-Oppenheimer (BO) approximation [128], because of its strict analogy with the Born-Oppenheimer adiabatic approximation in the theory of molecules and crystals ([129], p. 171). Consequently, in the further treatment we neglect the matrix elements $\left\langle \psi_{n,l,m} \left| e^{-it\tilde{H}} \right| \psi_{n',l',m'} \right\rangle$ for the FC states with different energies, $E_{n,l} \neq E_{n',l'}$. The same scheme was used in the theory of the multi-phonon optical processes for bound electrons interacting with phonons [23, 130].

Strictly speaking, the summation over the excited polaron states in Eq. (9.20) must involve the transitions to both the discrete and continuous parts of the polaron spectrum. A transition to the states of the continuous spectrum means that the electron leaves the polaron potential well. Therefore these transitions can be attributed to the "polaron dissociation". The transitions to the continuous spectrum are definitely beyond the adiabatic approximation. As shown in Ref. [23], the transition probability to the states of the continuous spectrum is very small compared with the transition probability between the ground and the first excited state (which belongs to the discrete part of the polaron energy spectrum). We neglect here the contribution to the polaron optical conductivity due to the transitions to the continuous spectrum.

The matrix elements neglected within the adiabatic approximation correspond to the transitions between FC states with different energies due to the electron-phonon interaction. Hence these transitions can be called non-adiabatic. The adiabatic approximation is related to the matrix elements of the evolution operator $e^{-it\tilde{H}}$. On the contrary, the matrix elements of the transitions between different FC states for the electric dipole moment are, in general, not equal to zero. Moreover, these transitions can be accompanied by the emission of phonons. The electron FC wave functions constitute a complete orthogonal set. However, the corresponding phonon wave functions can be non-orthogonal because of a different shift of phonon coordinates for different electron states. This makes multi-phonon transitions possible [130]. It is important to note that in our treatment we neglect only the non-adiabatic transitions between the electron states with *different* energies. On the contrary, the transitions within one and the same degenerate level can be non-adiabatic. This *internal non-adiabaticity* (i. e., the non-adiabaticity of the transitions within one and the same degenerate level) is taken into account in the subsequent treatment.

It is useful to stress the difference between the strong-coupling Ansatz and the adiabatic approximation. The strong-coupling Ansatz consists of the choice of the trial variational ground state wave function for the electron-phonon system in the factorized form (9.6). The adiabatic approximation means neglecting the matrix elements of the evolution operator between internal polaron states with different energies. These two approximations are not the same, but they both are valid in the strong-coupling regime and consistent with each other.

The correlation function (9.20) is transformed in the following way. The exponents $e^{it\tilde{H}}$ and $e^{-it\tilde{H}}$ are disentangled:

$$e^{-it\tilde{H}} = e^{-it\tilde{H}_0} \mathrm{T} \exp\left(-i \int_0^t ds W(s)\right), \tag{9.21}$$

$$e^{it\tilde{H}} = e^{it\tilde{H}_0} \mathrm{T} \exp\left(i \int_0^t ds W(-s)\right) \tag{9.22}$$

where $W(s)$ is the renormalized electron-phonon interaction Hamiltonian W in the interaction representation,

$$W(s) \equiv e^{is\tilde{H}_0} W e^{-is\tilde{H}_0}. \tag{9.23}$$

This gives us the result

$$f_{zz}(t) = \sum_{\substack{n,l,m,\\ n',l',m',\\ n'',l'',m''}} \langle \psi_{n,l,m} | z | \psi_{n'',l'',m''} \rangle \langle \psi_{n',l',m'} | z | \psi_0 \rangle e^{it\left(E_0 - E_{n'',l''}\right)}$$
$$\times \left\langle 0_{ph} \middle| \left\langle \psi_0 \middle| \mathrm{T}\exp\left(i\int_0^t dsW(-s)\right) \middle| \psi_{n,l,m} \right\rangle$$
$$\times \left\langle \psi_{n'',l'',m''} \middle| \mathrm{T}\exp\left(-i\int_0^t dsW(s)\right) \middle| \psi_{n',l',m'} \right\rangle \middle| 0_{ph} \right\rangle . \tag{9.24}$$

Within the adiabatic approximation, the optical conductivity is simplified. The full details of the derivation are described in the Appendix A. First, using the selection rules for the dipole matrix elements, the spherical symmetry of the Hamiltonian $\tilde{H}$ and the adiabatic approximation, the correlation function (9.24) is reduced to the form

$$f_{zz}(t) = \sum_n D_n e^{-i\Omega_{n,0}t}$$
$$\times \left\langle \psi_{n,1,0} \middle| \left\langle 0_{ph} \middle| \mathrm{T}\exp\left[-i\int_0^t dsW(s)\right] \middle| 0_{ph} \right\rangle \middle| \psi_{n,1,0} \right\rangle \tag{9.25}$$

where $\Omega_{n,0}$ is the FC transition frequency

$$\Omega_{n,0} \equiv E_{n,1} - E_0, \tag{9.26}$$

and D_n is the squared modulus of the dipole transition matrix element

$$D_n = \left| \langle \psi_0 | z | \psi_{n,1,0} \rangle \right|^2 . \tag{9.27}$$

Within the adiabatic approximation, the partial (with the electron wave functions) averaging of the operator T-exponent in (9.25) can be exactly performed (see details in Appendix A). As a result, the optical conductivity is transformed to the expression

$$\mathrm{Re}\,\sigma(\omega) = \frac{\omega}{6}\sum_n D_n \int_{-\infty}^{\infty} e^{i(\omega-\Omega_{n,0})t}$$
$$\times \left\langle 0_{ph} \middle| \mathrm{Tr}\left(\mathrm{T}\exp\left[-i\int_0^t ds\mathbb{W}^{(n)}(s)\right]\right) \middle| 0_{ph} \right\rangle dt. \tag{9.28}$$

The T-exponent in (9.28) contains the finite-dimensional matrix $\mathbb{W}^{(n)}(s)$ depending on the phonon coordinates:

$$\left(\mathbb{W}^{(n)}_{k,l,m}\right)_{m_1,m_2} = \langle \psi_{n,1,m_1} | W_{k,l,m} | \psi_{n,1,m_2} \rangle \tag{9.29}$$

where $W_{k,l,m}$ are the amplitudes of the electron-phonon interaction in the basis of spherical wave functions.

Because the kinetic energy of the phonons is of order α^{-4} compared to the leading term of the Hamiltonian [128], we neglect this kinetic energy in the present work, because the treatment is related to the strong-coupling regime. As a result, $Q_{k,l,m}$ commute with the Hamiltonian $\tilde{H}_0$, so that in (9.28), $\mathbb{W}^{(n)}(s) = \mathbb{W}^{(n)}$. Furthermore, in a finite-dimensional basis $\{|\psi_{n,l,m}\rangle\}$ for a given level (n,l), all eigenvalues of the Hamiltonian $\tilde{H}_0$ are the same. Therefore the T-exponent entering (9.28) in that finite-dimensional basis turns into a usual exponent. As a result, the strong-coupling polaron optical conductivity (9.28) takes the form

$$\mathrm{Re}\,\sigma(\omega) = \frac{\omega}{6}\sum_n D_n \int_{-\infty}^{\infty} e^{i(\omega-\Omega_{n,0})t} \left\langle 0_{ph} \middle| \mathrm{Tr}\exp\left(-i\mathbb{W}^{(n)}t\right) \middle| 0_{ph} \right\rangle dt. \tag{9.30}$$

The matrix interaction Hamiltonian (9.29) depends on the phonon coordinates, and the matrices $\mathbb{W}^{(n)}_{k,l,m}$ with different m for one and the same degenerate energy level do not commute with each other. According to the Jahn – Teller theorem [131], for a degenerate level there does not exist a unitary transformation which simultaneously diagonalizes all matrices $\mathbb{W}^{(n)}_{k,l,m}$ in a basis that does not depend on the phonon coordinates. The manifestations of that theorem are attributed to the Jahn – Teller effect. Therefore, because we neglect the non-commutation of the matrices $\mathbb{W}^{(n)}_{k,l,m}$, the Jahn – Teller effect is omitted.

In fact, neglecting the Jahn – Teller effect is not necessary. The averaging in Eq. (9.30) is performed exactly using the effective phonon modes similarly to Ref. [133] (see the details in Appendix B). As a result, we arrive at the following expression for the strong-coupling polaron optical conductivity

$$\begin{aligned}\operatorname{Re}\sigma(\omega) = \frac{\omega}{3\pi^2}\sum_n \frac{D_n}{a_0^{(n)}}\int_{-\infty}^{\infty}dx_0\int_{-\infty}^{\infty}dx_1\int_{-\infty}^{\infty}dx_2\int_{-\infty}^{\infty}dy_1\int_{-\infty}^{\infty}dy_2 \\ \times\sum_{j=1}^{3}\exp\left\{-\frac{1}{2}\left[x_0^2+\sum_{m=1,2}\left(x_m^2+y_m^2\right)+\frac{\left(\omega-\Omega_{n,0}-\frac{a_2^{(n)}}{2\sqrt{5\pi}}\lambda_j\left(Q_2\right)\right)^2}{\left(a_0^{(n)}\right)^2}\right]\right\}.\end{aligned} \tag{9.31}$$

Here, $\lambda_j\left(Q_2\right)$ are the eigenvalues for the matrix interaction Hamiltonian, which are explicitly determined in the Appendix B by the formula (9.74). The coefficients $a_0^{(n)}$ and $a_2^{(n)}$ are given by (9.65) and (9.66), respectively. The polaron optical conductivity given by the expression (9.31), is in fact an envelope of the multiphonon polaron optical conductivity band with the correlation function (9.28) provided by the phonon-assisted transitions from the polaron ground state to the polaron RES. This result is consistent with Ref. [49], where the same paradigm of the phonon-assisted transitions to the polaron RES was exploited, but the calculation was limited to the one-phonon transition.

In order to reveal the significance of the Jahn – Teller effect for the polaron, we alternatively calculate $\left\langle 0_{ph}\left|\operatorname{Tr}\exp\left(-i\mathbb{W}^{(n)}t\right)\right|0_{ph}\right\rangle$ neglecting the non-commutation of the matrices $\mathbb{W}^{(n)}_{k,l,m}$, as described in the Appendix B. 2. The resulting expression for the polaron optical conductivity is much simpler than formula (9.31) and is similar to the expression (3) of Ref. [127]:

$$\operatorname{Re}\sigma(\omega) = \omega\sum_n\sqrt{\frac{\pi}{2\omega_s^{(n)}}}D_n\exp\left(-\frac{\left(\omega-\Omega_{n,0}\right)^2}{2\omega_s^{(n)}}\right), \tag{9.32}$$

with the parameter (often called the Huang-Rhys factor)

$$\omega_s^{(n)} = \frac{1}{2}\left(a_0^{(n)}\right)^2+\frac{1}{4\pi}\left(a_2^{(n)}\right)^2. \tag{9.33}$$

The strong-coupling electron energies and wave functions in Eq. (9.28) can be calculated using different approximations. For example, within the Landau-Pekar (LP) approximation [35], the trial wave function $|\psi_0\rangle$ is chosen as the ground state of a 3D oscillator. Within the Pekar approximation [23], $|\psi_0\rangle$ is chosen in the form

$$|\psi_0(r)\rangle = Ce^{-ar}\left(1+ar+br^2\right) \tag{9.34}$$

with the variational parameters a and b. Finally, the trial ground state wave function can be determined numerically exactly following Miyake [40] (see also [132], Chap. 5.22). Within the LP approximation, formula (9.32) reproduces the polaron optical conductivity obtained in Ref. [127].

In the LP approximation, the matrix elements $\langle \psi_0 | z | \psi_{n,1,0} \rangle$ are different from zero only for $n = 1$, i. e. only for the $1s \to 2p$ transition. Beyond the LP approximation, also the transitions to other excited states are allowed because of the nonparabolicity of the self-consistent potential $V_a(r)$. The use of exact strong-coupling wave functions, instead of the LP wave functions, may significantly influence the optical conductivity. In the present treatment we use the numerically exact electron energies and wave functions of both ground and first excited states according to Ref. [40]. The FC transition energies $\Omega_{n,0}$ to leading order of the strong-coupling approximation are determined according to (9.26). In order to account for the corrections of the FC energy with accuracy up to α^0, we add to $\Omega_{n,0}$ the correction $\Delta\Omega_{\rm FC} \approx -3.8$ from Ref. [127]. Because we use the numerically accurate strong-coupling wave functions and energies corresponding to Miyake [40], the formula (9.24) *is asymptotically exact in the strong-coupling limit, at least in its leading term in powers of* α^{-2}.

9.1.3 Results and discussion

In Figs. 2 to 3, we have plotted the polaron optical conductivity spectra calculated for different values of the coupling constant α. The optical conductivity spectra calculated within the present strong-coupling approach taking into account the Jahn – Teller effect are shown by the solid curves. The optical conductivity derived neglecting the Jahn – Teller effect is shown by the dashed curves. It is worth mentioning that there is little difference in the optical conductivity spectra between those calculated with and without the Jahn – Teller effect. The optical conductivity obtained in Ref. [127] with the Landau-Pekar (LP) adiabatic approximation is plotted with dash-dotted curves. The full dots show the numerical Diagrammatic Quantum Monte Carlo (DQMC) data [79, 127]. The FC transition frequency for the transition to the first excited FC state $\Omega_{1,0} \equiv \Omega_{\rm FC}$ and the RES transition frequency $\Omega_{\rm RES}$ are explicitly indicated in the figures.

The polaron optical conductivity spectra calculated within the present strong-coupling approach are shifted to lower frequencies with respect to the optical conductivity spectra calculated within the LP approximation of Ref. [127]. This shift is due to the use of the numerically accurate strong coupling energy levels and wave functions of the internal polaron states, and of the numerically accurate self-consistent adiabatic polaron potential.

According to the selection rules for the matrix elements of the electron-phonon interaction, there is a contribution to the polaron optical conductivity from the phonon modes with angular momentum $l = 0$ (s-phonons) and with angular momentum $l = 2$ (d-phonons). The s-phonons are fully symmetric, therefore they do not contribute to the Jahn – Teller effect, while the d-phonons are active in the Jahn – Teller effect. The contribution of the d-phonons to the optical conductivity spectra is not small compared to the contribution of the s-phonons. However, the distinction between the optical conductivity spectra calculated with and without the Jahn – Teller effect is relatively small.

For $\alpha = 8$ and $\alpha = 8.5$, the maxima of the polaron optical conductivity spectra, calculated within the present strong-coupling approach are positioned to the low frequency side of the maxima of those calculated using the DQMC method. The agreement between our strong-coupling polaron optical conductivity spectra and the numerical DQMC data improves with increasing alpha. This is in accordance with the fact that the present strong-coupling approach for the polaron optical conductivity is asymptotically exact in the strong-coupling limit.

The total polaron optical conductivity must satisfy the sum rule [82]

$$\int_0^\infty \mathrm{Re}\,\sigma(\omega)\,d\omega = \frac{\pi}{2}. \tag{9.35}$$

In the weak- and intermediate-coupling regimes at $T = 0$, there are two contributions to the left-hand side of that sum rule: (1) the contribution from the polaron optical conductivity for

$\omega > \omega_{\rm LO}$ and (2) the contribution from the "central peak" at $\omega = 0$, which is proportional to the inverse polaron mass [82]. In the asymptotic strong-coupling regime, the inverse to the polaron mass is of order α^{-4}, and hence the contribution from the "central peak" to the polaron optical conductivity is beyond the accuracy of the present approximation (where we keep the terms $\propto \alpha^{-2}$ and $\propto \alpha^0$).

As discussed above, in the present work the transitions from the ground state to the states of the continuous part of the polaron energy spectrum are neglected. Therefore the integral over the frequency [the left-hand side of (9.35)] for the optical conductivity calculated within the present strong-coupling approximation can be (relatively slightly) smaller than $\pi/2$. The relative contribution of the transitions to the continuous part of the polaron spectrum, Δ_c, can be therefore estimated as

$$\Delta_c \equiv 1 - \frac{2}{\pi}\int_0^\infty \mathrm{Re}\,\sigma(\omega)\,d\omega, \tag{9.36}$$

where the right-hand side is obtained by a numerical integration of $\mathrm{Re}\,\sigma(\omega)$ calculated within the present strong-coupling approach. This numeric estimation shows that for $\alpha > 8$, $\Delta_c < 0.01$. Moreover, with increasing α, the relative contribution of the transitions to the continuous part of the polaron spectrum falls down. This confirms the accuracy of the present strong-coupling approach.

In Refs. [95, 134], the optical conductivity of a strong-coupling polaron was calculated assuming that in the strong-coupling regime the polaron optical response is provided mainly by the transitions to the continuous part of the spectrum (these transitions are called there "the polaron dissociation"). This concept is in contradiction both with the early estimation by Pekar [23] discussed above and with the very small weight of those transitions shown in Fig. 4. The approach of Ref. [95] in fact takes into account only a small part of the strong-coupling polaron optical conductivity – namely, the high-frequency "tail" of the optical conductivity spectrum.

When comparing the polaron optical conductivity spectra calculated in the present work with the DQMC data [79, 127], we can see that the present approach, with respect to DQMC, underestimates the high-frequency part of the polaron optical conductivity. This difference, however, gradually diminishes with increasing α, in accordance with the fact that the present method is an asymptotic strong-coupling approximation.

Because the optical conductivity spectra calculated in the present strong-coupling approximation using the expressions (9.31) and (9.32) represent the envelopes of the RES peak with the multi-phonon satellites, the separate peeks are not explicitly seen in those spectra. The FC and RES peaks are indicated in the figures by the arrows. The FC transition frequency $\Omega_{1,0}$ in the strong-coupling case is positioned close to the maximum of the polaron optical conductivity band (both calculated within the present approach and within DQMC). The RES transition frequency is positioned one $\omega_{\rm LO}$ below the onset of the LO-sidebands. Note that the strong-coupling polaron optical conductivity derived in Refs. [135] contains only the zero-phonon (RES) line and no phonon satellites at all. In contrast, in the present calculation, the maximum of the polaron optical conductivity spectrum shifts to higher frequencies with increasing α, so that the multiphonon processes invoking large number of phonons become more and more important, in accordance with predictions of Refs. [49, 50].

It is worth noting the following important point: the maximum of the polaron optical conductivity band can be hardly interpreted as a broadened transition to an FC state on the following reasons. Formula (9.28) describes a set of multi-phonon peaks. In the simplifying approximation which neglects the Jahn – Teller effect (see Ref. [127]), those peaks are positioned at the frequencies $\omega = \tilde{\Omega}_{n,0} + k$, where k is the number of emitted phonons and is the frequency of the zero-phonon line. The frequencies $\tilde{\Omega}_{n,0}$ do not coincide with the FC transition frequencies but are determined by

$$\tilde{\Omega}_{n,0} = \Omega_{n,0} - \omega_s^{(n)}, \tag{9.37}$$

where the Huang-Rhys factor $\omega_s^{(n)}$ describes the energy shift due to lattice relaxation. The physical meaning of the parameters $\omega_s^{(n)}$ obviously implies that the peaks at $\omega = \tilde{\Omega}_{n,0} + k$ should be attributed to transitions to the RES with emission of k phonons. So, the so-called "FC transition" is realized as the envelope of a series of phonon sidebands of the polaron RES but not as a transition to the FC state. The account of the Jahn-Teller effects in general makes the multiphonon peak series non-equidistant, but it changes nothing in the concept of the internal polaron states which is discussed above.

9.1.4 Conclusions

We have derived the polaron optical conductivity which is asymptotically exact in the strong-coupling limit. The strong-coupling polaron optical conductivity band is provided by the multiphonon transitions from the polaron ground state to the polaron RES and has the maximum positioned close to the FC transition frequency. With increasing the electron-phonon coupling constant α, the polaron optical conductivity band shape gradually tends to that provided by the Diagrammatic Quantum Monte Carlo (DQMC) method. This agreement demonstrates the importance of the multiphonon processes for the polaron optical conductivity in the strong-coupling regime.

The obtained polaron optical conductivity with a high accuracy satisfies the sum rule [82], what gives us an evidence of the fact that in the strong-coupling regime the dominating contribution to the polaron optical conductivity is due to the transitions to the *internal* polaron states, while the contribution due to the transitions to the continuum states is negligibly small.

Accurate numerical results, obtained using DQMC method [79], – modulo the linewidths for sufficiently large α – and the analytically exact in the strong-coupling limit polaron optical conductivity of the present work, as well as the analytical approximation of Ref. [127] confirm the essence of the mechanism for the optical absorption of Fröhlich polarons, which were proposed in Refs. [50, 7].

9.1.5 Appendix 1. Correlation function

The dipole-dipole correlation function $f_{zz}(t)$ given by (9.24) is further simplified within the adiabatic approximation and using the selection rules for the dipole transition matrix elements and the symmetry properties of the polaron Hamiltonian. First, according to the selection rules, the matrix element $\langle \psi_0 | z | \psi_{n,l,m} \rangle$ is

$$\langle \psi_{n',l',m'} | z | \psi_0 \rangle = \delta_{l',1} \delta_{m',0} \langle \psi_{n',1,0} | z | \psi_0 \rangle \tag{9.38}$$

Second, the interaction Hamiltonian W (and hence, also the evolution operator which involves W) is a scalar of the rotation symmetry group. The matrix elements $\langle \psi_{n,l,m} | W(s) | \psi_{n,l',m'} \rangle$ for $l \neq l'$ and $m \neq m'$ are then exactly equal to zero. Therefore, in the adiabatic approximation and due to the symmetry of the Hamiltonian $\tilde{H}$, we obtain the relations

$$\begin{aligned} &\left\langle \psi_0 \left| \mathrm{T} \exp\left(i \int_0^t ds W(-s) \right) \right| \psi_{n,l,m} \right\rangle \\ &\approx \delta_{n,0} \delta_{l,0} \delta_{m,0} \left\langle \psi_0 \left| \mathrm{T} \exp\left(-i \int_0^t ds W(s) \right) \right| \psi_0 \right\rangle, \end{aligned} \tag{9.39}$$

$$\left\langle \psi_{n'',l'',m''} \left| \mathrm{T}\exp\left(-i\int_0^t dsW(s)\right) \right| \psi_{n',l',m'} \right\rangle$$
$$\approx \delta_{n'',n'}\delta_{l'',l'} \left\langle \psi_{n',l',m'} \left| \mathrm{T}\exp\left(-i\int_0^t dsW(s)\right) \right| \psi_{n',l',m'} \right\rangle. \tag{9.40}$$

Furthermore, because the ground state ψ_0 is non-degenerate, we find that

$$\left\langle \psi_0 \left| \mathrm{T}\exp\left(-i\int_0^t dsW(s)\right) \right| \psi_0 \right\rangle \approx 1,$$

because within the adiabatic approximation, for any $n \geq 1$ the averages $\langle \psi_0 | W^n | \psi_0 \rangle = 0$.

The correlation function (9.24) using (9.38) to (9.40) takes the form

$$f_{zz}(t) = \sum_n D_n e^{-i\Omega_{n,0}t}$$
$$\times \left\langle \psi_{n,1,0} \left| \left\langle 0_{ph} \left| \mathrm{T}\exp\left[-i\int_0^t dsW(s)\right] \right| 0_{ph} \right\rangle \right| \psi_{n,1,0} \right\rangle \tag{9.41}$$

with the squared matrix elements of the dipole transitions

$$D_n \equiv |\langle \psi_{n,1,0} | z | \psi_0 \rangle|^2 = \frac{1}{3}\left(\int_0^\infty R_{n,1}(r) R_{0,0}(r) r^3 dr\right)^2, \tag{9.42}$$

and the FC transition frequencies

$$\Omega_{n,0} \equiv E_{n,1} - E_0. \tag{9.43}$$

Further on, the interaction Hamiltonian is expressed in terms of the complex phonon coordinates $Q_{\mathbf{k}}$:

$$W = \sqrt{2}\sum_{\mathbf{k}} W_{\mathbf{k}} Q_{\mathbf{k}}, \quad Q_{\mathbf{k}} = \frac{b_{\mathbf{k}} + b^+_{-\mathbf{k}}}{\sqrt{2}} \tag{9.44}$$

Here, we use the spherical-wave basis for phonon modes:

$$\varphi_{k,l,m}(\mathbf{r}) \equiv (-1)^{\frac{m-|m|}{2}} \phi_{k,l}(r) Y_{l,m}(\theta,\varphi), \tag{9.45}$$

where the radial part of the basis function is expressed through the spherical Bessel function $j_l(kr)$:

$$\phi_{k,l}(r) = \left(\frac{2}{R}\right)^{1/2} k\, j_l(kr), \; R = \left(\frac{3V}{4\pi}\right)^{1/3}. \tag{9.46}$$

The factor $(-1)^{\frac{m-|m|}{2}}$ is chosen in order to fulfil the symmetry property

$$\varphi^*_{k,l,m}(\mathbf{r}) = \varphi_{k,l,-m}(\mathbf{r}).$$

In the spherical-wave basis, the interaction Hamiltonian is

$$W = \sqrt{2}\sum_{k,l,m} W_{k,l,m} Q_{k,l,m}, \tag{9.47}$$

with the complex phonon coordinates

$$Q_{k,l,m} = \frac{b_{k,l,m} + b^+_{k,l,-m}}{\sqrt{2}} \tag{9.48}$$

and with the interaction amplitudes

$$W_{k,l,m} = \frac{\sqrt{2\sqrt{2}\pi\alpha}}{k} \left(\varphi_{k,l,m}\left(\mathbf{r}\right) - \rho_{k,l,m}\right), \ \rho_{k,l,m} \equiv \left\langle \psi_0 \left| \varphi_{k,l,m} \right| \psi_0 \right\rangle . \tag{9.49}$$

The dipole-dipole correlation function (9.41) is then

$$f_{zz}\left(t\right) = \sum_n D_n e^{-i\Omega_{n,0}t} \times \left\langle \psi_{n,1,0} \left| \left\langle 0_{ph} \left| \mathrm{T}\exp\left[-i\sqrt{2}\int_0^t ds \sum_{k,l,m} W_{k,l,m}\left(s\right) Q_{k,l,m}\left(s\right)\right] \right| 0_{ph} \right\rangle \right| \psi_{n,1,0} \right\rangle . \tag{9.50}$$

The operators $W_{k,l,m}\left(s\right)$ in (9.50) are equivalent to the $(2l+1)$-dimensional matrices $\mathbb{W}^{(n)}_{k,l,m}$ determined in the basis of the level (n,l). The matrix elements of these matrices are

$$\left(\mathbb{W}^{(n)}_{k,l,m}\right)_{m_1,m_2} = \left\langle \psi_{n,1,m_1} \left| W_{k,l,m} \right| \psi_{n,1,m_2} \right\rangle . \tag{9.51}$$

In these notations, $f_{zz}\left(t\right)$ given by (9.50) can be written down as

$$f_{zz}\left(t\right) = \sum_n D_n e^{-i\Omega_{n,0}t} \left\langle 0_{ph} \left| \left(\mathrm{T}\exp\left[-i\int_0^t ds \mathbb{W}^{(n)}\left(s\right)\right]\right)_{0,0} \right| 0_{ph} \right\rangle . \tag{9.52}$$

where $\mathbb{W}^{(n)}$ is the matrix electron-phonon interaction Hamiltonian expressed through the phonon complex coordinates in the spherical-wave representation as follows:

$$\mathbb{W}^{(n)} = \sqrt{2}\sum_{k,l,m} \mathbb{W}^{(n)}_{k,l,m} Q_{k,l,m}. \tag{9.53}$$

Here, $\mathbb{W}^{(n)}_{k,l,m}$ is a (3×3) matrix in a basis of a level $(n,l)_{l=1}$ of the Hamiltonian $\tilde{H}_0$.

Because $\mathbb{W}^{(n)}$ is a scalar of the rotation group, we can replace the diagonal matrix element of the T-exponent in (9.52) with the trace in the aforesaid-finite-dimensional basis. As a result, we obtain for the polaron optical conductivity (9.4) with (9.52) the expression

$$\mathrm{Re}\,\sigma\left(\omega\right) = \frac{\omega}{6}\sum_n D_n \int_{-\infty}^{\infty} e^{i(\omega-\Omega_{n,0})t} \times \left\langle 0_{ph} \left| \mathrm{Tr}\left(\mathrm{T}\exp\left[-i\int_0^t ds \mathbb{W}^{(n)}\left(s\right)\right]\right) \right| 0_{ph} \right\rangle dt. \tag{9.54}$$

9.1.6 Appendix 2. Effective phonon modes

In order to perform the averaging in Eq. (9.30) analytically, we introduce the effective phonon modes $Q_{0,0}$ and $Q_{2,m}$ similarly to Ref. [133]. The Hamiltonian $\mathbb{W}^{(n)}$ in terms of these effective phonon modes is expressed as

$$\mathbb{W}^{(n)} = \sqrt{2}\sum_{l,m} \tilde{\mathbb{W}}^{(n)}_{l,m} Q_{l,m} \tag{9.55}$$

where the matrices $\tilde{\mathbb{W}}^{(n)}_{l,m}$ (depending on the vibration coordinates $Q_{l,m}$) are explicitly given by the expressions (cf. Ref. [133]),

$$\mathbb{W}^{(n)} = a_0^{(n)}\mathbb{I}Q_{0,0} + a_2^{(n)}\sum_{m=-2}^{2} \mathbb{B}_m Q_{2,m} \tag{9.56}$$

with the matrices $\mathbb{B}_j$

$$\mathbb{B}_0 = \frac{1}{2\sqrt{5\pi}} \begin{pmatrix} -1 & 0 & 0 \\ 0 & 2 & 0 \\ 0 & 0 & -1 \end{pmatrix}, \tag{9.57}$$

$$\mathbb{B}_1 = \mathbb{B}_{-1}^{+} = \frac{1}{2}\sqrt{\frac{3}{5\pi}} \begin{pmatrix} 0 & 0 & 0 \\ -1 & 0 & 0 \\ 0 & 1 & 0 \end{pmatrix}, \tag{9.58}$$

$$\mathbb{B}_2 = \mathbb{B}_{-2}^{+} = \sqrt{\frac{3}{10\pi}} \begin{pmatrix} 0 & 0 & 0 \\ 0 & 0 & 0 \\ -1 & 0 & 0 \end{pmatrix}. \tag{9.59}$$

The coefficients $a_0^{(n)}$ and $a_2^{(n)}$ in Eq. (9.56) are

$$a_0^{(n)} = \left(\sqrt{2}\alpha \sum_k \frac{1}{k^2} \left[\langle \phi_{k,0} \rangle_{n,1} - \langle \phi_{k,0} \rangle_{0,0} \right]^2 \right)^{1/2}, \tag{9.60}$$

$$a_2^{(n)} = \left(4\sqrt{2}\pi\alpha \sum_k \frac{1}{k^2} \langle \phi_{k,2} \rangle_{n,1}^2 \right)^{1/2}. \tag{9.61}$$

Here $\phi_{k,l}$ is the radial part of the basis function expressed through the spherical Bessel function $j_l(kr)$:

$$\phi_{k,l}(r) = \left(\frac{2}{R}\right)^{1/2} k\, j_l(kr), \; R = \left(\frac{3V}{4\pi}\right)^{1/3}, \tag{9.62}$$

V is the volume of the crystal, and $\langle f(r) \rangle_{n,l}$ is the average

$$\langle f(r) \rangle_{n,l} = \int_0^\infty f(r) R_{n,l}^2(r) r^2 dr. \tag{9.63}$$

The normalization of the phonon wave functions corresponds to the condition

$$\int_0^R \phi_{k,l}(r) \phi_{k',l}(r) r^2 dr = \delta_{k,k'}. \tag{9.64}$$

After the straightforward calculation using (9.64), we express the coefficients $a_0^{(n)}$ and $a_2^{(n)}$ through the integrals with the radial wave functions:

$$a_0^{(n)} = \left(2\sqrt{2}\alpha \int_0^\infty dr \int_0^r dr'\, r (r')^2 \left[R_{n,1}^2(r) - R_{0,0}^2(r) \right] \left[R_{n,1}^2(r') - R_{0,0}^2(r') \right] \right)^{1/2}, \tag{9.65}$$

$$a_2^{(n)} = \left(\frac{8\sqrt{2}\pi\alpha}{5} \int_0^\infty dr \int_0^r dr' \frac{(r')^4}{r} R_{n,1}^2(r) R_{n,1}^2(r') \right)^{1/2}. \tag{9.66}$$

Exact averaging

Let us substitute the matrix interaction Hamiltonian (9.56) to the dipole-dipole correlation function (9.30), what gives us the result

$$f_{zz}(t) = \frac{1}{3} \sum_n D_n e^{-i\Omega_{n,0}t} \left\langle 0_{ph} \left| \exp\left(-ita_0^{(n)} Q_0\right) \mathrm{Tr} \exp\left(-it \frac{a_2^{(n)}}{2\sqrt{5\pi}} \mathbb{V}(Q_2) \right) \right| 0_{ph} \right\rangle. \tag{9.67}$$

Here, we use the matrix depending on the phonon coordinates,

$$\mathbb{V}\left(Q_2\right) \equiv 2\sqrt{5\pi} \sum_{m=-2}^{2} \mathbb{B}_m Q_{2m}, \tag{9.68}$$

whose explicit form is

$$\mathbb{V}\left(Q_2\right) = \begin{pmatrix} -Q_{2,0} & -\sqrt{3}Q_{2,-1} & -\sqrt{6}Q_{2,-2} \\ -\sqrt{3}Q_{2,1} & 2Q_{2,0} & \sqrt{3}Q_{2,-1} \\ -\sqrt{6}Q_{2,2} & \sqrt{3}Q_{2,1} & -Q_{2,0} \end{pmatrix}. \tag{9.69}$$

The matrix $\mathbb{V}\left(Q_2\right)$ is analytically diagonalized. The equation for the eigenvectors $\left|\chi\left(Q_2\right)\right\rangle$ and eigenvalues $\lambda\left(Q_2\right)$ of $\mathbb{V}\left(Q_2\right)$ is

$$\mathbb{V}\left(Q_2\right)\left|\chi\left(Q_2\right)\right\rangle = \lambda\left(Q_2\right)\left|\chi\left(Q_2\right)\right\rangle. \tag{9.70}$$

The eigenvalues are found from the equation

$$\det\left(\mathbb{V}\left(Q_2\right) - \lambda\left(Q_2\right)\mathbb{I}\right) = 0. \tag{9.71}$$

We make the transformation to the real phonon coordinates,

$$\begin{aligned} &Q_{2,0} \equiv x_0, \\ &Q_{2,m} \equiv \frac{x_m + iy_m}{\sqrt{2}}, \quad Q_{2,-m} = Q_{2,m}^* = \frac{x_m - iy_m}{\sqrt{2}}. \end{aligned}$$

Five variables x_0, x_1, x_2, y_1, y_2 are the independent real phonon coordinates. The l.h.s. of Eq. (9.71) is expressed in terms of these coordinates as

$$\det\left(\mathbb{V}\left(Q_2\right) - \lambda\left(Q_2\right)\mathbb{I}\right) = -\lambda^3 + 3p\lambda + 2q \tag{9.72}$$

with the coefficients

$$\begin{aligned} p &= x_0^2 + x_1^2 + x_2^2 + y_1^2 + y_2^2, \\ q &= x_0^3 + \frac{3}{2}x_0\left(x_1^2 + y_1^2\right) + \frac{3\sqrt{3}}{2}x_2\left(x_1^2 - y_1^2\right) - 3x_0\left(x_2^2 + y_2^2\right) + 3\sqrt{3}x_1y_1y_2. \end{aligned}$$

So, we have the cubic equation for λ:

$$\lambda^3 - 3p\lambda - 2q = 0. \tag{9.73}$$

Because the matrix $\mathbb{V}\left(Q_2\right)$ is Hermitian, all its eigenvalues are real. Therefore, $\frac{|q|}{p^{3/2}} \leq 1$ (otherwise, $\sin\left(3\varphi\right)$ is not real). Herefrom, we have three explicit eigenvalues:

$$\begin{aligned} \lambda_1\left(Q_2\right) &= 2\sqrt{p}\sin\left[\frac{\pi}{3} + \frac{1}{3}\arcsin\left(\frac{q}{p^{3/2}}\right)\right], \\ \lambda_2\left(Q_2\right) &= -2\sqrt{p}\sin\left[\frac{1}{3}\arcsin\left(\frac{q}{p^{3/2}}\right)\right], \\ \lambda_3\left(Q_2\right) &= -2\sqrt{p}\sin\left[\frac{\pi}{3} - \frac{1}{3}\arcsin\left(\frac{q}{p^{3/2}}\right)\right]. \end{aligned} \tag{9.74}$$

The trace in (9.67) is invariant with respect to the choice of the basis. Consequently, after the diagonalization $f_{zz}\left(t\right)$ takes the form

$$f_{zz}\left(t\right) = \frac{1}{3}\sum_n D_n e^{-i\Omega_{n,0}t} \sum_{j=1}^{3} \left\langle 0_{ph}\left|\exp\left(-it\left[a_0^{(n)}Q_0 + \frac{a_2^{(n)}}{2\sqrt{5\pi}}\lambda_j\left(Q_2\right)\right]\right)\right|0_{ph}\right\rangle. \tag{9.75}$$

After inserting $f_{zz}(t)$ given by (9.75) into (9.4), the integration over time gives the delta function multiplied by 2π, and we arrive at the result

$$\operatorname{Re}\sigma(\omega) = \frac{\pi\omega}{3}\sum_n D_n \sum_{j=1}^{3}\left\langle 0_{ph}\left|\delta\left(\omega - \Omega_{n,0} - a_0^{(n)}Q_0 - \frac{a_2^{(n)}}{2\sqrt{5\pi}}\lambda_j(Q_2)\right)\right|0_{ph}\right\rangle. \tag{9.76}$$

The ground-state wave function for the effective phonon modes is

$$|0_{ph}\rangle \equiv \Phi_0(Q) = \Phi_0^{(0)}(Q_0)\,\Phi_0^{(2)}(Q_2). \tag{9.77}$$

$\Phi_0^{(0)}(Q_0)$ is the one-oscillator ground-state wave function:

$$\Phi_0^{(0)}(Q_0) = \pi^{-1/4}\exp\left(-\frac{Q_0^2}{2}\right). \tag{9.78}$$

The ground-state wave function of phonons with $l = 2$ is:

$$\Phi_0^{(2)}(Q_2) = \pi^{-5/4}\exp\left[-\frac{1}{2}\left(x_0^2 + \sum_{m=1,2}\left(x_m^2 + y_m^2\right)\right)\right]. \tag{9.79}$$

The phonon ground-state wave function (9.77) is then

$$\Phi_0(Q) = \frac{1}{\pi^{3/2}}\exp\left[-\frac{1}{2}\left(x_0^2 + \sum_{m=1,2}\left(x_m^2 + y_m^2\right) + Q_0^2\right)\right]. \tag{9.80}$$

With these phonon wave functions, Eq. (9.76) results in the following expression for the polaron optical conductivity

$$\begin{aligned}\operatorname{Re}\sigma(\omega) = {} & \frac{\omega}{3\pi^2}\sum_n \frac{D_n}{a_0^{(n)}}\int_{-\infty}^{\infty}dx_0\int_{-\infty}^{\infty}dx_1\int_{-\infty}^{\infty}dx_2\int_{-\infty}^{\infty}dy_1\int_{-\infty}^{\infty}dy_2 \\ & \times\sum_{j=1}^{3}\exp\left\{-\frac{1}{2}\left[x_0^2 + \sum_{m=1,2}\left(x_m^2 + y_m^2\right) + \frac{\left(\omega - \Omega_{n,0} - \frac{a_2^{(n)}}{2\sqrt{5\pi}}\lambda_j(Q_2)\right)^2}{\left(a_0^{(n)}\right)^2}\right]\right\}.\end{aligned} \tag{9.81}$$

Averaging neglecting the Jahn-Teller effect

In order to perform the phonon averaging explicitly, we disentangle the exponent $\exp\left(-it\sqrt{2}\sum_{l,m}\tilde{\mathbb{W}}_{l,m}^{(n)}Q_{l,m}\right)$ as follows.

$$\begin{aligned}&\exp\left(-it\sqrt{2}\sum_{l,m}\tilde{\mathbb{W}}_{l,m}^{(n)}Q_{l,m}\right) = \exp\left(-it\sum_{l,m}\tilde{\mathbb{W}}_{l,-m}^{(n)}b_{l,m}^{+}\right) \\ &\times \mathrm{T}\exp\left(-i\int_0^t ds\sum_{l,m}e^{is\sum_{l',m'}\tilde{\mathbb{W}}_{l',-m'}^{(n)}b_{l',m'}^{+}}\tilde{\mathbb{W}}_{l,m}^{(n)}b_{l,m}e^{-is\sum_{l',m'}\tilde{\mathbb{W}}_{l',-m'}^{(n)}b_{l',m'}^{+}}\right).\end{aligned} \tag{9.82}$$

Neglecting non-commutation of matrices $\tilde{\mathbb{W}}_{l,m}^{(n)}$ we find that

$$\begin{aligned}&\sum_{l,m}e^{is\sum_{l',m'}\tilde{\mathbb{W}}_{l',-m'}^{(n)}b_{l',m'}^{+}}\tilde{\mathbb{W}}_{l,m}^{(n)}b_{l,m}e^{-is\sum_{l',m'}\tilde{\mathbb{W}}_{l',-m'}^{(n)}b_{l',m'}^{+}} \\ &= \sum_{l,m}\tilde{\mathbb{W}}_{l,m}^{(n)}b_{l,m} - is\sum_{l,m}\tilde{\mathbb{W}}_{l,-m}^{(n)}\tilde{\mathbb{W}}_{l,m}^{(n)}.\end{aligned} \tag{9.83}$$

The sum $\sum_{l,m} \tilde{\mathbb{W}}^{(n)}_{l,-m} \tilde{\mathbb{W}}^{(n)}_{l,m}$ in the basis (l,m) for a definite n is proportional to the unity matrix. Therefore, $\exp\left(-it\sqrt{2}\sum_{l,m} \tilde{\mathbb{W}}^{(n)}_{l,m} Q_{l,m}\right)$ is

$$\begin{aligned} & e^{-it\sqrt{2}\sum_{l,m} \tilde{\mathbb{W}}^{(n)}_{l,m} Q_{l,m}} \\ & = e^{-it\sum_{l,m} \tilde{\mathbb{W}}^{(n)}_{l,-m} b^{+}_{l,m}} e^{-it\sum_{l,m} \tilde{\mathbb{W}}^{(n)}_{l,m} b_{l,m} - \frac{t^2}{2}\sum_{l,m} \tilde{\mathbb{W}}^{(n)}_{l,-m} \tilde{\mathbb{W}}^{(n)}_{l,m}}, \end{aligned} \tag{9.84}$$

that gives us the result

$$\left\langle 0_{ph} \left| e^{-it\sqrt{2}\sum_{l,m} \tilde{\mathbb{W}}^{(n)}_{l,m} Q_{l,m}} \right| 0_{ph} \right\rangle = e^{-\frac{t^2}{2}\sum_{l,m} \tilde{\mathbb{W}}^{(n)}_{l,-m} \tilde{\mathbb{W}}^{(n)}_{l,m}}. \tag{9.85}$$

Using the explicit formulae for the matrices $\tilde{W}^{(n)}_{l,m}$, the matrix sum takes the form

$$\sum_{l,m} \tilde{\mathbb{W}}^{(n)}_{l,-m} \tilde{\mathbb{W}}^{(n)}_{l,m} = \omega^{(n)}_s \mathbb{I} \tag{9.86}$$

with the parameter

$$\omega^{(n)}_s = \frac{1}{2}\left(a^{(n)}_0\right)^2 + \frac{1}{4\pi}\left(a^{(n)}_2\right)^2. \tag{9.87}$$

Using (9.86), the optical conductivity (9.30) is transformed to the expression

$$\operatorname{Re}\sigma(\omega) = \omega \sum_n \sqrt{\frac{\pi}{2S_n}} D_n \exp\left(-\frac{(\omega - \Omega_{n,0})^2}{2S_n}\right). \tag{9.88}$$

Figures to Appendix A

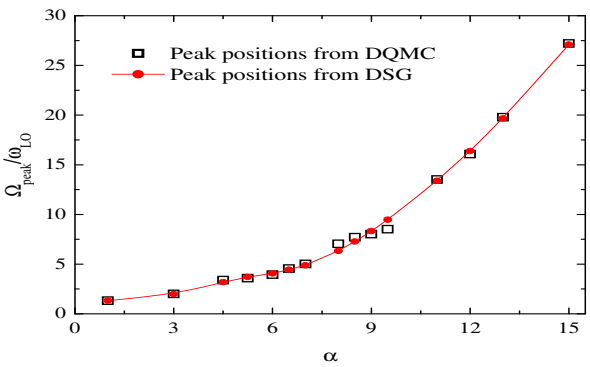

Fig. 1

Frequency of the main peak in the optical conductivity spectra calculated within the model of Ref. [50] (red dots) and the main-peak energy extracted from the DQMC data [79, 127] (black squares).

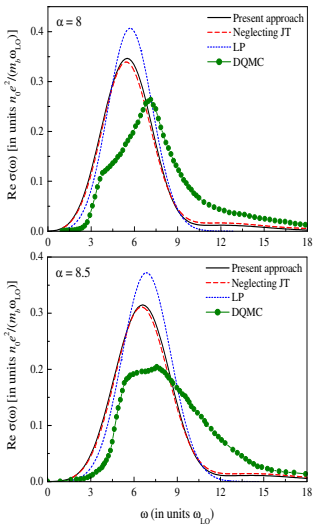

Fig. 2

The strong-coupling polaron optical conductivity calculated within the rigorous strong-coupling approach of the present work (black solid curves), within the present approach but neglecting the dynamic Jahn-Teller effect (red dashed curves), within the adiabatic approximation of Ref. [127] (blue dot-dashed curves), and the numerical Diagrammatic Monte Carlo data (full dots) for $\alpha = 8$ and 8.5.

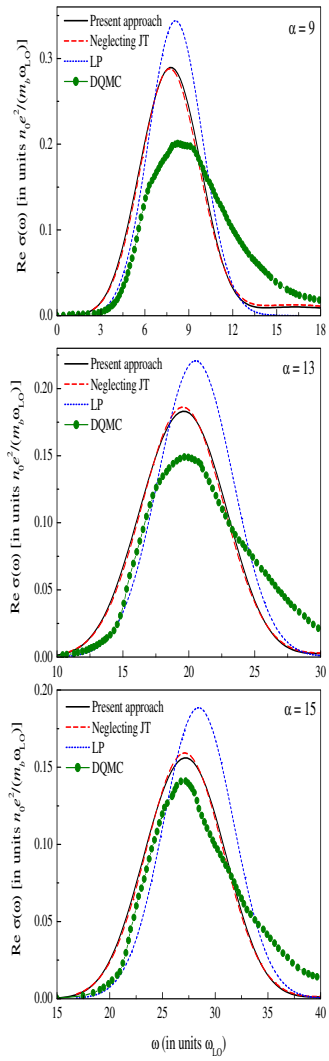

Fig. 3

The strong-coupling polaron optical conductivity calculated within the rigorous strong-coupling approach of the present work (black solid curves), within the present approach but neglecting the dynamic Jahn-Teller effect (red dashed curves), within the adiabatic approximation of Ref. [127] (blue dot-dashed curves), and the numerical Diagrammatic Monte Carlo data (full dots) for $\alpha = 9$, 13 and 15.

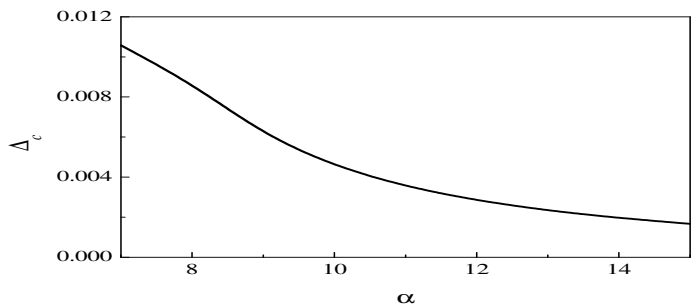

Fig. 4

Relative contribution of the transitions to the continuum polaron states to the zeroth frequency moment of the strong-coupling polaron optical conductivity as a function of the coupling constant α.

.

9.2 Feynman's path-integral polaron treatment approached using time-ordered operator calculus

[*S. N. Klimin and J. T. Devreese, Solid State Communications 151, 144 (2011)*]

Several studies have been devoted to the search of a Hamiltonian formalism equivalent to Feynman's path integral approximation to polaron theory. Bogolubov [138] reproduced the Feynman result for the polaron free energy [43] using time-ordering T-products . Yamazaki [139] introduced two kinds of auxiliary vector fields to derive Feynman's ground state polaron energy expression with the operator technique, however he found no proof of the variational nature of this result. Cataudella *et al.* [140] formally re-obtained Feynman's polaron ground-state energy expression by introducing additional degrees of freedom, but again their result could not be proved to constitute an upper bound for the polaron ground state energy.

The study of the excited polaron states is of interest i. a. for its application to the polaron response properties. In [47] a path-integral based response-formalism was introduced that was applied to derive polaron optical absorption spectra in [7]. The results for the polaron response obtained in [7] were re-derived with a Hamiltonian technique (Mori- formalism) in [76].

To the best of our knowledge, no explicit description of the polaron excited states has been derived within the "all coupling-" Feynman approach. Only for the limiting cases of weak and strong coupling approximations (and for a 1D-model system) such excitation spectra were derived [39, 125, 41].

In principle, the spectrum of the polaron excited states can be derived indirectly – using a Laplace transform of the finite-temperature partition function. However, it is not clear how to realize this program in practice.

The polaron excitation spectrum is interesting by itself. E.g. the existence and the nature of "relaxed excited states", "Franck-Condon states", "scattering states" is understood from the mathematical structure of corresponding eigenstates.

In the present letter we first present a re-derivation of the original Feynman variational path integral polaron model [43] for the ground state, using a Hamiltonian formalism, and we do provide a proof of the upper bound nature of the obtained ground state energy. Furthermore, using Feynman's (Hamiltonian-) time-ordered operator calculus (and an *ad hoc* unitary transformation) we obtain explicitly – and for the first time – the excited polaron states that correspond to the Feynman polaron model.

The novelty of the present approach consists (a) in the *direct calculation of the energies and the lifetimes of the excited polaron states* (within a Hamiltonian all-coupling approach – developed in this work – equivalent to the Feynman path integral polaron model) and (b) in the extension of the Feynman variational technique to non-parabolic trial potentials. Although the time-ordered operator calculus is formally equivalent to the path-integral formalism, it is not obvious how to directly calculate the excited polaron states using path integrals.

The present work, formulated with the (Hamiltonian) time ordered operator calculus, thus provides an (equivalent) tool complementary with respect to the Feynman path integral approach to the polaron, to study the polaron problem. Additionally we directly study the excited polaron states.

Consider an electron-phonon system with the Fröhlich Hamiltonian

$$H = \frac{\mathbf{p}^2}{2} + H_{ph} + H_{e-ph}, \tag{9.89}$$

$$H_{ph} = \sum_{\mathbf{q}} \left(a^+_{\mathbf{q}} a_{\mathbf{q}} + \frac{1}{2} \right), \tag{9.90}$$

$$H_{e-ph} = \frac{1}{\sqrt{V}} \sum_{\mathbf{q}} \frac{\sqrt{2\sqrt{2}\pi\alpha}}{q} \left(a_{\mathbf{q}} + a^+_{-\mathbf{q}} \right) e^{i\mathbf{q}\cdot\mathbf{r}}. \tag{9.91}$$

Here, the Feynman units are used: $\hbar = 1$, the band mass $m_b = 1$, the LO-phonon frequency $\omega_{\mathrm{LO}} = 1$.

The polaron partition function after exact averaging over phonon states is

$$Z_{pol} = \mathtt{Tr} \left[\mathtt{T} \exp \left(- \int_0^\beta \frac{\mathbf{p}_\tau^2}{2} d\tau + \hat{\Phi} \left[\mathbf{r}_\tau \right] \right) \right], \tag{9.92}$$

where $\beta = \frac{1}{k_B T}$. The "influence phase" of the phonons $\hat{\Phi} \left[\mathbf{r}_\tau \right]$ in the the time-ordered operator calculus has the same form as in the path-integral representation. The polaron free energy is determined as

$$F_{pol} = -\frac{1}{\beta} \ln Z_{pol}. \tag{9.93}$$

The trial Hamiltonian describes the electron interacting with a fictitious particle of the mass m_f through an attractive potential V_f:

$$H_{tr} = \frac{\mathbf{p}^2}{2} + \frac{\mathbf{p}_f^2}{2m_f} + V_f \left(\mathbf{r} - \mathbf{r}_f \right). \tag{9.94}$$

The trial potential V_f is, in general, non-parabolic. The parabolic potential with frequency parameter w corresponds to the Feynman polaron model.

Consider the "extended" partition function of the electron-phonon system

$$Z_{ext} = Z_f Z_{pol} \tag{9.95}$$

where Z_f is the partition function of a fictitious particle,

$$Z_f \equiv \mathtt{Tr}\left[\mathtt{T}\exp\left(-\int_0^\beta d\tau H_{f,\tau}\right)\right], \tag{9.96}$$

with Hamiltonian

$$H_f = \frac{\mathbf{p}_f^2}{2m_f} + V_f\left(\mathbf{r}_f\right). \tag{9.97}$$

The polaron free energy is expressed as the difference

$$F_{pol} = F_{ext} - F_f, \tag{9.98}$$

where F_f is the free energy of the fictitious particle confined to the potential $V\left(\mathbf{r}_f\right)$. The free energies F_{ext} and F_f are determined similarly to (9.93), with corresponding partition functions. In the zero-temperature limit, the free energies F_{pol}, F_{ext} and F_f become, respectively, the ground-state energies E_{pol}^0, E_{ext}^0 and E_f^0.

The key element of the present approach is the unitary transformation

$$U = e^{-i\mathbf{p}_f\cdot\mathbf{r}}. \tag{9.99}$$

Application of this canonical transformation results in the transformed "extended" Hamiltonian $H'_{ext} = UH_{ext}U^{-1}$,

$$\begin{aligned} H'_{ext} = &\frac{\left(\mathbf{p}+\mathbf{p}_f\right)^2}{2} + \frac{\mathbf{p}_f^2}{2m_f} + V_f\left(\mathbf{r}_f - \mathbf{r}\right) \\ &+ H_{ph} + H_{e-ph}. \end{aligned} \tag{9.100}$$

This Hamiltonian can be represented as a sum of an unperturbed Hamiltonian

$$H_0 \equiv H_{tr} + H_{ph} \tag{9.101}$$

and an interaction term

$$V \equiv \frac{1}{2}\mathbf{p}_f^2 + \mathbf{p}\cdot\mathbf{p}_f + H_{e-ph}. \tag{9.102}$$

Further we use the variational principle for the ground-state energy in terms of the time-ordered operators following Ref. [141]. The exact ground state $|0\rangle$ of the system with the Hamiltonian (9.100) can be written in the interaction representation starting from the unperturbed ground state $|-\infty\rangle$:

$$|0\rangle = \mathcal{U}\left(\infty, -\infty\right)|-\infty\rangle \tag{9.103}$$

where $\mathcal{U}\left(\infty, -\infty\right)$ is the time-evolution operator,

$$\mathcal{U}\left(t_2, t_1\right) = \mathcal{T}\exp\left(-i\int_{t_1}^{t_2} e^{-\delta|t|}e^{iH_0t}Ve^{-iH_0t}\right). \tag{9.104}$$

Here, $\delta \to +0$ and $\mathcal{T}$ denotes time ordering.

In the exact expectation value for the ground state energy $E^0_{ext} \equiv \langle 0 | H'_{ext} | 0 \rangle$, the phonons are eliminated using the time ordered-operator calculus as in Ref. [141]. The average of the interaction term becomes then

$$\begin{aligned}
&\langle 0 | H_{e-ph} | 0 \rangle \\
&= -i \frac{\sqrt{2}\pi\alpha}{V} \int_{-\infty}^{\infty} dt e^{-i|t|-\delta|t|} \\
&\times \sum_{\mathbf{q}} \frac{1}{q^2} \left\langle \infty \left| \mathcal{T} \left[\mathcal{U}(\infty, -\infty) e^{i\mathbf{q}\cdot[\mathbf{r}(t)-\mathbf{r}(0)]} \right] \right| -\infty \right\rangle .
\end{aligned} \tag{9.105}$$

This means that the polaron ground state energy is exactly described using a retarded potential in the interaction representation, cf. Eq. (2.16) of Ref. [141].

The ground state energy satisfies the Ritz variational principle with a trial state. Choosing the trial state as the ground state of the Hamiltonian (9.101), the variational principle can be written as [141]

$$\begin{aligned}
E^0_{ext} &\leq E^0_{tr} \\
&+ \langle \infty | \mathcal{T} \{ \mathcal{U}_{tr}(\infty, -\infty) [H'_{ext}(0) - H_0(0)] \} | -\infty \rangle ,
\end{aligned} \tag{9.106}$$

where $\mathcal{U}_{tr}(\infty, -\infty)$ is the time-evolution operator corresponding to the trial Hamiltonian (9.94).

The exact polaron ground state energy is denoted here as $E^0(\mathbf{k})$, where $\mathbf{k}$ is the polaron translation momentum. We find an upper bound for $E^0(\mathbf{k})$ substituting (9.105) in (9.106) and using the exact wave functions and energy levels of the trial Hamiltonian. The trial Hamiltonian (9.94) can be rewritten in terms of the coordinates $(\mathbf{R}, \boldsymbol{\rho})$ and momenta $(\mathbf{P}, \vec{\pi})$ of the center-of-mass and relative (internal) motions of the trial system with the masses $M = 1 + m_f$ and $\mu = m_f/(1 + m_f)$ using the frequency $v = wM$. The energy spectrum of the trial system is the sum of the translation- and oscillation contributions,

$$E_{\mathbf{k},n} = \frac{\mathbf{k}^2}{2M} + \varepsilon_n, \ \varepsilon_n = v\left(n + \frac{3}{2}\right). \tag{9.107}$$

The eigenfunctions of the Hamiltonian (9.94) are products of translational- and oscillatory wave functions:

$$\psi_{\mathbf{k};l,n,m}(\mathbf{R}, \boldsymbol{\rho}) = \frac{1}{\sqrt{V}} e^{i\mathbf{k}\cdot\mathbf{R}} \varphi_{l,n,m}(\boldsymbol{\rho}), \tag{9.108}$$

where $\varphi_{l,n,m}(\boldsymbol{\rho})$ is the 3D harmonic-oscillator wave function with a given angular momentum. The result is

$$E^0(\mathbf{k}) \leq \mathcal{E}_p^{(0,0)}(\mathbf{k}), \tag{9.109}$$

$$\begin{aligned}
\mathcal{E}_p^{(0,0)}(\mathbf{k}) &= \frac{3}{4}\frac{(v-w)^2}{v} \\
&+ \frac{1}{2}\left(1 - \frac{1}{(1+m_f)^2}\right)\mathbf{k}^2 - \frac{\sqrt{2}\alpha}{4\pi^2}\int \frac{d\mathbf{q}}{q^2} \\
&\times \sum_{\mathbf{k}',l',n',m'} \frac{\left|\langle \psi_{\mathbf{k};0,0,0} | e^{i\mathbf{q}\cdot\mathbf{r}} | \psi_{\mathbf{k}';l',n',m'} \rangle\right|^2}{\frac{1}{2(m_f+1)}\left((\mathbf{k}')^2 - \mathbf{k}^2\right) + vn' + 1},
\end{aligned} \tag{9.110}$$

where $v > w$ are the Feynman variational frequencies. The functional (9.110) can be reduced to the known Feynman result for the polaron ground-state energy. In the r.h.s. of (9.110 at

the polaron momentum $\mathbf{k} = 0$, we introduce the integral over the Euclidean time:

$$\frac{1}{\frac{(\mathbf{k}')^2}{2\left(m_f+1\right)} + vn' + 1} = \int_0^\infty e^{-\left(\frac{(\mathbf{k}')^2}{2\left(m_f+1\right)}+vn'+1\right)\tau} d\tau. \tag{9.111}$$

After this, the summations and integrations in (9.113) are performed analytically, and we arrive at the Feynman variational expression for the polaron ground-state energy:

$$\begin{aligned} E^0(\mathbf{k})\big|_{\mathbf{k}=0} \leq & \frac{3}{4}\frac{(v-w)^2}{v} \\ & - \frac{\alpha v}{\sqrt{\pi}} \int_0^\infty \frac{e^{-\tau}}{\sqrt{w^2\tau + \frac{v^2-w^2}{v}\left(1-e^{-v\tau}\right)}} d\tau. \end{aligned} \tag{9.112}$$

The electron-phonon contribution in (9.110) is structurally similar to the second-order perturbation correction to the polaron ground-state energy due to the electron-phonon interaction (using states of the Feynman model $\psi_{\mathbf{k};l,n,m}$ as the zero-order approximation). Therefore we can estimate the energies of the excited polaron states when averaging the difference between exact and unperturbed Hamiltonians in (9.106) with an excited trial state. We then arrive at the following extension for the r.h.s. of (9.110):

$$\begin{aligned} \mathcal{E}_p^{(l,n)}(\mathbf{k}) = & \frac{v^2+w^2}{2v}\left(n+\frac{3}{2}\right) - \frac{3}{2}w \\ & + \frac{1}{2}\left(1 - \frac{1}{(1+m_f)^2}\right)\mathbf{k}^2 - \frac{\sqrt{2}\alpha}{4\pi^2}\int \frac{d\mathbf{q}}{q^2} \\ & \times \sum_{\mathbf{k}',l',n',m'} \frac{\left|\left\langle \psi_{\mathbf{k};l,n,m}\left|e^{i\mathbf{q}\cdot\mathbf{r}}\right|\psi_{\mathbf{k}';l',n',m'}\right\rangle\right|^2}{\frac{1}{2\left(m_f+1\right)}\left((\mathbf{k}')^2 - \mathbf{k}^2\right) + v\left(n'-n\right)+1}. \end{aligned} \tag{9.113}$$

In the same approach, we obtain the inverse lifetimes for the excited states of the polaron:

$$\begin{aligned} \Gamma_{l,n}(\mathbf{k}) = & \frac{\sqrt{2}\alpha}{4\pi} \sum_{\mathbf{k}',l',n',m'} \int d\mathbf{q}\frac{1}{q^2} \\ & \times \left|\left\langle \psi_{\mathbf{k};l,n,m}\left|e^{i\mathbf{q}\cdot\mathbf{r}}\right|\psi_{\mathbf{k}';l',n',m'}\right\rangle\right|^2 \\ & \times \delta\left(\frac{q^2}{2\left(m_f+1\right)} + v\left(n'-n\right)+1\right). \end{aligned} \tag{9.114}$$

The broadening of the excited polaron "non-scattering" states must be taken into account for an analytical study of the polaron optical conductivity.

Using the above expressions, we determine the transition energies for the transitions between the ground and the first excited state $\hbar\Omega_{0\to 1exc} \equiv E_p^{(1exc)} - E_p^{(0)}$. Let us first consider the transition energies in which $E_p^{(1exc)}$ are calculated using optimal values of the parameters of the Feynman model obtained from the minimization of the variational ground-state energy $E_p^{(0)}$. This method formally leads to the Franck-Condon (FC) excited states, with the "frozen" phonon configuration corresponding to the ground state of the polaron. Note that the existence of Franck-Condon states as eigenstates of the Fröhlich polaron Hamiltonian has not been proved: Ref [41] suggests their non-existence as eigenstates for a simplified polaron model. Nevertheless the Franck-Condon concept can be significant, e. g. for approximate treatments using a basis of Franck-Condon states, as indicative for the frequency of the maxima of phonon-sidebands, etc.

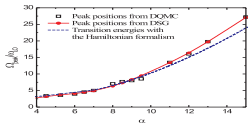

Fig. 1. Franck-Condon transition energies as a function of the coupling constant compared to the lowest-energy peak position of the polaron optical conductivity from Ref. [7] and the maximum of the polaron optical conductivity band from Ref. [79].

In Fig. 1, the FC transition energies calculated with the approach introduced in the present work for polaron momentum $\mathbf{k} = 0$ are plotted as a function of the coupling constant α. They are compared with the peak energies of the polaron optical conductivity calculated using the diagrammatic Monte Carlo method (DQMC) [79, 127] and with the peak energies attributed to polaron "relaxed excited states" (RES) in Ref. [7] ("DSG"). The DQMC and DSG main-peak energies are close to each other in the whole range of the coupling strength. In the range $4 \lessapprox \alpha \lessapprox 10$, the present result for the transition energy is close to the DQMC and the DSG peak energies. Furthermore, in this range of α, the non-monotonous behavior of the curvature is remarkably the same for the DQMC and DSG peak energies and for the present result.

There is a remarkable agreement between the peaks attributed to the RES in Ref. [7], the peak positions obtained within the strong-coupling approach, Eq. (3) of Ref. [127], and the positions of the maximum of the optical conductivity band calculated in Ref. [79] using DQMC. It is reasonable that the three aforesaid peaks must be interpreted in one and the same way. In order to clarify this, we can refer to Ref. [79]. In the strong-coupling regime, the dominant broad peak of the polaron optical conductivity spectrum can be considered as a "Franck-Condon sideband" of the "groundstate to RES-transition", even if this latter transition can have a negligible oscillator strength (see also [49]). The optical conductivity spectra of Ref. [127] in the strong-coupling approximation have been calculated taking into account the polaronic shift of the energy levels. The polaronic shift in Ref. [127] has been calculated with the Franck-Condon wave functions (i. e., with the strong-coupling wave functions corresponding to the "frozen" lattice configuration for the ground state). Note that the exact excitation spectrum of the Fröhlich-Hamiltonian might be devoid of Franck-Condon eigenstates, cf. Ref. [41]). It should be remarked that the maxima of the FC-sideband structures of Ref. [7] are positioned at the frequency $\Omega = v$, i. e., at the transition frequency for the model system without the polaron shift.

The Franck-Condon peak energies calculated in the present work also take into account the polaron shift. As follows from the above analysis, in the strong-coupling limit they must correspond to the Franck-Condon peak energies of the strong-coupling expansion of Ref. [127]. The agreement of the position of the maxima of these peaks with those attributed to transitions to the RES in Ref. [7] shows that in the strong-coupling range of α, the latter should be associated to the Franck-Condon sidebands rather than to the RES.

Another approach, in which the parameters of the first excited state are determined self-consistently (Ref. [49]), was used i. a. to calculate (in the strong-coupling case) the (lowest)

energy level of the relaxed excited state (RES). The transitions from the polaron ground state to the RES correspond to a zero-phonon peak in the optical conductivity.

For the study of the energies of excited states of the polaron, a variational approach requires special care, because the excited states of the polaron are not stable. A variational approach, strictly speaking, is only valid for excited states when the variational wave function of the excited state is orthogonal to the exact ground-state wave function.

For the estimation of the energy of the first RES with our present formalism, we determine a minimum of the expression (9.113) in a physically reasonable range of the variational parameters. In order to determine that range, we refer to Ref. [142], where the energy of the polaron RES is calculated variationally within the Green's function formalism.

The expression for the RES energy in Ref. [142] contains the electron-phonon contribution corresponding to the second-order perturbation formula. It differs, however, from the weak-coupling second-order perturbation expression by the choice of the unperturbed states: in Ref.[142] those are variational states rather than free-electron states. There exists some analogy between our approach and that of Ref. [142]. The latter, however, does not take into account the translation invariance of the polaron problem.

In Ref. [142], the energy of the polaron RES is calculated variationally. The unperturbed wave function of the RES is chosen orthogonal (due to symmetry) to the unperturbed ground state wave function. In the present approach, this orthogonality is also exactly satisfied because of symmetry.

The expressions for the polaron RES energy of Ref. [142] contain singularities, which occur when the energies of the unperturbed ground state and that of the first excited states are in resonant with the LO-phonon energy. These singularities are related to the instability of the excited polaron with respect to the emission of LO-phonons. Using the same reasoning as in Ref. [142] we search for a local minimum of the polaron RES energy in the range where the confinement frequency v of the Feynman model satisfies the inequality $v > 1$. The instability of the excited polaron state is then avoided.

The resulting numerical values of the transition energy to the first RES as a function of α are shown in Fig. 2. They are compared with the numerical-DQMC peak energies of the polaron optical conductivity band [79, 127], with the FC transition energies obtained in the present work, and with the leading term of the strong-coupling approximation for the RES transition energy from Ref. [49].

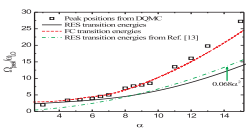

Fig. 2. The transition energy for the transition from the polaron ground state to the first RES(*solid black curve*) and to the first excited FC state (*dashed red curve*) as a function of α obtained in the present work, compared with the maximum of the polaron optical conductivity band from numerical DQMC (*black squares*, Ref. [79]). *The dashed-dot green curve*: the strong-coupling result for this transition energy as given in Ref. [49].

For $\alpha \lesssim 2.5$, there exists no minimum of $E_p^{(1exc)}$ in the range $v > 1$. We can interpret this result as a manifestation of the fact that for decreasing coupling strength, the RES is suppressed at sufficiently weak coupling. We see that for sufficiently small α ($\alpha \lesssim 6$), the RES transition energies show good agreement with the DQMC peak energies, what confirms the concept of RES developed in Refs. [7, 49]. For higher coupling strengths, the DQMC data appear to be closer to the FC (rather than to RES) transition energies. This result can be an indication of the fact that with increasing α, the mechanism of the polaron optical absorption changes its nature as suggested in Ref. [127], from a regime with dynamic lattice relaxation (for which the RES are relevant) at weak and intermediate coupling to the Franck-Condon ("LO-phonon sidebands"-) regime at strong coupling.

In summary, we have re-formulated the Feynman all-coupling path integral method for the polaron problem within a Hamiltonian formalism using time-ordered operator calculus. This reformulation allows us to describe not only the free energy and the ground state, but also to directly determine – for the first time – the excited polaron states that correspond to the Feynman all-coupling polaron model. A variational procedure for the polaron RES energy has been developed, within the formalism presented in this work, which provides results i.a. in agreement with the strong-coupling limit of Ref. [49]. The present treatment offers the prospect of further elucidation of the nature of the polaron resonances ("relaxed excited states" versus "Franck-Condon sidebands" [127]) at intermediate coupling.

9.3 Many-body large polaron optical conductivity in $SrTi_{1-x}Nb_xO_3$

[*J. T. Devreese, S. N. Klimin, J. L. M. van Mechelen, and D. van der Marel, Phys. Rev. B* ***81****, 125119 (2010)*]

9.3.1 Introduction

The infrared optical absorption of perovskite-type materials, in particular, of copper oxide based high-T_c superconductors and of the manganites has been the subject of intensive investigations [1, 2, 8, 3, 4, 7, 5, 6, 9, 10]. Insulating $SrTiO_3$ has a perovskite structure and manifests a metal–insulator transition at room temperature around a doping of 0.002% La or Nb per unit cell [11]. At low doping concentrations, between 0.003% and 3%, strontium titanate reveals a superconducting phase transition [12] below 0.7 K. Various optical experiments [16, 11, 13, 17, 14, 15] show a mid-infrared band in the normal state optical conductivity of doped $SrTiO_3$ which is often explained by polaronic behavior. In the recently observed optical conductivity spectra of Ref. [15], shown in Fig. 1, there is a broad mid-infrared optical conductivity band starting at a photon energy of $\hbar\Omega \sim 100$ meV, which is within the range of the LO-phonon energies of $SrTi_{1-x}Nb_xO_3$. The peaks/shoulders of the experimental optical conductivity band at $\hbar\Omega \sim 200$ to 400 meV resemble the peaks provided by the mixed plasmon-phonon excitations as described in Ref. [18]. Based on the experimental data, the authors deduce a coupling constant $3 < \alpha < 4$ and conclude the mid-infrared peaks to originate from large polaron formation. The high and narrow peaks positioned at the lower frequencies with respect to the mid-infrared band are attributed in Ref. [15] to the optical absorption of the TO-phonons.

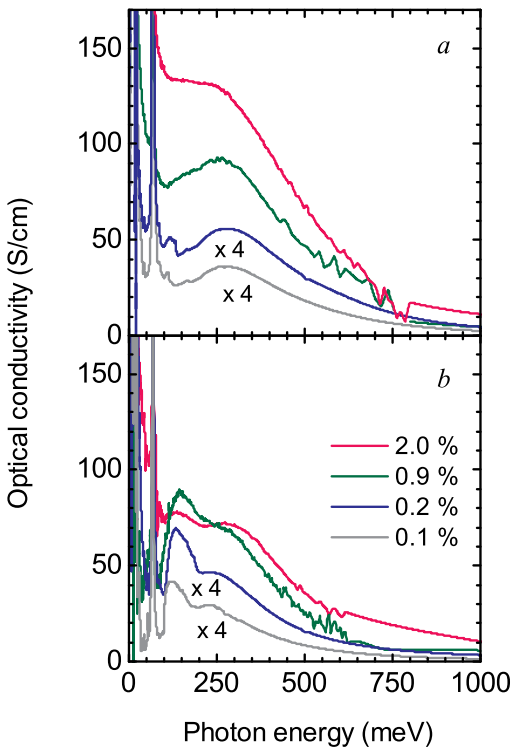

Figure 9.1: Optical conductivity of $SrTi_{1-x}Nb_xO_3$ for 0.1% (grey curves), 0.2% (blue curves), 0.9% (green curves) and 2% (pink curves) at 300 K (panel a) and 7 K (panel b). For clarity, the mid-infrared conductivities of $x = 0.1\%$ and 0.2% are magnified by a factor 4. (From Ref. [15].)

There are different types of polaron states in solids. In the effective mass approximation for the electron placed in a continuum polarizable medium, a so-called large or continuum polaron can exist. Large polaron wave functions and the corresponding lattice distortions spread over many lattice sites. Due to the finite phonon frequencies the ion polarizations can follow the polaron motion if the motion is sufficiently slow. Hence, large polarons with a low kinetic energy propagate through the lattice as free electrons but with an enhanced effective mass. When the polaron binding energy is larger than the half bandwidth of the electron band, all states in the Bloch bands are 'dressed' by phonons. In this strong-coupling regime, the finite electron bandwidth becomes important, so the continuum approximation cannot be applied. In this case the carriers are described as "small" or discrete (lattice) polarons that can hop between different states localized at lattice sites. A key distinction between large and small polarons is then the radius of the polaron state. For large polarons, that radius substantially exceeds the lattice constant, while for small polarons it is comparable to the lattice constant. A review of the properties of large and small polarons can be found, e. g., in Refs. [19, 20]. In the theory of "mixed" polarons [21, 22, 23, 24] the states of the electron-phonon system are composed of a mixture of large and small polaron states.

Polaron states are formed due to the electron-phonon interaction, which is different in the cases of large and small polarons. For a large polaron, the electron-phonon interaction is provided by a macroscopic (continuum) polarization of the lattice. This interaction is characterized by the coupling constant α introduced by Fröhlich [25],

$$\alpha = \frac{1}{2}\left(\frac{1}{\varepsilon_\infty} - \frac{1}{\varepsilon_0}\right)\frac{e^2}{\hbar\omega_L}\left(\frac{2m_b\omega_L}{\hbar}\right)^{1/2}, \tag{9.115}$$

where ε_∞ and ε_0 are, respectively, the high-frequency and the static dielectric constants, e is the electron charge, ω_L is the longitudinal optical (LO) phonon frequency in the Brillouin zone

centre, and m_b is the band electron (or hole) mass. The large-polaron coupling constant is thus expressed through macroscopic observable parameters of a polarizable medium. On the contrary, the electron-phonon interaction for a small polaron is described through microscopic parameters.

The nature of the polaron states in $SrTi_{1-x}Nb_xO_3$ is not yet clear. Previous optical measurements on strontium titanate were interpreted in terms of small polarons [26, 24]. However, that assumption contradicts the interpretation of transport measurements [27], which rather support the large-polaron picture. Also the heat capacity measurements [28], provide effective masses similar to those of large polarons. In Ref. [13], the experimental results of Ref. [16] on the temperature-dependent plasma frequencies in $SrTi_{1-x}Nb_xO_3$ were interpreted within the theory of mixed polarons [21, 22, 23, 24]. Thermoelectric power measurements [27] have shown that the density-of-states masses increase with increasing temperature, which can be explained by a theory of mixed polarons [21]. It has been supposed [14] that the polaron optical conductivity in $SrTi_{1-x}Nb_xO_3$ is probably provided by mixed polarons. A possible coexistence of large and small mass polarons has been suggested in Ref. [29]. In Ref. [30], coexistence of small and large polarons in the same solid is invoked to interpret experimental data on the optical absorption in oxides.

The key question is to determine the type of polarons that provide the mechanism of the polaron optical conductivity in $SrTi_{1-x}Nb_xO_3$. The optical response of large polarons in various approximations was studied, e. g., in Refs. [32, 33, 34, 31]. The same problem for the small polaron was investigated in [26, 35]. In the large-polaron theory, the optical absorption is provided by transitions (with $0, 1, \ldots$ phonon emission) between different continuum electron states. In the small-polaron theory, the optical absorption occurs when the self-trapped carrier is induced to transfer from its localized state to a localized state at an adjacent site, with emission of phonons. Because of the different physical mechanisms involved, the optical conductivity spectra of large and small polarons are different from each other. In the large-polaron theory the polaron optical conductivity behaves at high frequencies Ω as a power function $\left(\propto \Omega^{-5/2}\right)$. In the small-polaron theory, the polaron optical conductivity at high frequencies decreases much faster than for large polarons: as a Gaussian exponent. Therefore the analysis of optical measurements can shed some light on the aforesaid question on the type of polarons responsible for the optical conductivity in $SrTi_{1-x}Nb_xO_3$.

The polaron optical conductivity band of $SrTi_{1-x}Nb_xO_3$ occupies the mid-infrared range of the photon energies $\hbar\Omega \lesssim 1$ eV, and the threshold for interband electron-hole transitions lies at the band gap energy, which is around 3.3 eV in $SrTi_{1-x}Nb_xO_3$ [15]. Therefore interband transitions do not interfere with the polaron optical conductivity. Other mechanisms of electron intraband scattering (for example, electron-phonon interaction with acoustic phonons and/or electron or hole transitions from impurity centers) may be manifested together with the polaron mechanism in the energy range $\hbar\Omega \lesssim 1$ eV. The treatment of those mechanisms is, however, beyond the scope of the present investigation.

We can make some preliminary suggestions concerning the dominating mechanism of the mid-infrared optical conductivity in the Nb doped strontium titanate. The low-frequency edge of the mid-infrared band in $SrTi_{1-x}Nb_xO_3$ at a low temperature ($T = 7$ K) lies in the range of the LO-phonon energies obtained in [16]. The maximum of the mid-infrared band lies relatively close to this low-frequency edge (the difference in frequency between the low-frequency edge and the maximum of the mid-infrared band is comparable to the LO-phonon frequencies in $SrTi_{1-x}Nb_xO_3$). This behavior is characteristic of large-polaron optical conductivity rather than of small-polaron optical conductivity. Indeed, the maximum of the small polaron optical conductivity band is expected to be shifted to considerably higher frequencies with respect to the low-frequency edge of the polaron optical conductivity band (see, e.g., Ref. [35]). Also, at sufficiently high frequencies, the experimental mid-infrared band from Ref. [15] decreases with

increasing Ω rather slowly, which is characteristic for large-polaron optical conductivity rather than for small-polaron optical conductivity. We therefore can suggest that the large-polaron picture is the most appropriate for the interpretation of the mid-infrared band of $SrTi_{1-x}Nb_xO_3$ observed in Ref. [15].

In order to interpret the mid-infrared band of the experimental optical conductivity spectra of $SrTi_{1-x}Nb_xO_3$ [15] in terms of polarons, we calculate the large-polaron optical conductivity spectra for $SrTi_{1-x}Nb_xO_3$ using the model for the optical conductivity of a large-polaron gas developed in Ref. [18], adapted to take into account multiple LO-phonon branches [36]. The degeneracy and the anisotropy of the conduction band in $SrTi_{1-x}Nb_xO_3$ are taken into account.

9.3.2 Optical conductivity of a gas of large polarons

The optical absorption spectra of $SrTi_{1-x}Nb_xO_3$ are sensitive to the doping level [15]. Therefore a many-polaron description is in order. In our context, "many-polaron description" means an account of many-electron effects on the optical conductivity of a polaron gas. These effects include the influence of the electron-electron Coulomb interaction (which leads to screening effects) and of the Fermi statistics of the polaron gas on the optical conductivity spectra. In the low-density limit, those many-body effects are not important, and the optical conductivity of a polaron gas is well described by the optical conductivity of a single polaron multiplied by the electron density. The scope of the present study embraces a wide range of electron densities for which the single-polaron approach is, in general, insufficient. As shown below, even at the lowest electron density involved in the experiment [15], the shape and magnitude of the optical conductivity spectrum is strongly affected by many-body effects.

We wish to compare the experiments of Ref. [15], in particular the observed mid-infrared band, to the theoretical optical conductivity of a gas of large polarons. For that purpose we use the many-body large polaron approach of Refs. [18, 36], which takes into account the electron-electron interaction and the Fermi statistics of polarons.

Refs. [18, 36] are limited to the study of weak-coupling polarons. Up to $\alpha \approx 3$, which includes the case of $SrTi_{1-x}Nb_xO_3$, the weak coupling approximation can be expected to describe the main characteristics of the many-polaron optical response (see, e.g., Refs. [18, 19, 20]). In Ref. [36] a generalization of Ref. [18] is presented that takes into account the electron-phonon interaction with *multiple LO-phonon branches* as they exist, e. g., in complex oxides. For a single polaron, effects related to multiple LO-phonon branches were investigated in Ref. [38]. The starting point for the treatment of a many-polaron system is the Fröhlich Hamiltonian

$$H = \sum_{\mathbf{k}} \sum_{\sigma=\pm 1/2} \frac{\hbar^2 k^2}{2m_b} c^+_{\mathbf{k},\sigma} c_{\mathbf{k},\sigma} + \sum_{\mathbf{q}} \sum_{j=1}^{n} \hbar\omega_{L,j} a^+_{\mathbf{q},j} a_{\mathbf{q},j} + U_{e-e}$$
$$+ \frac{1}{\sqrt{V}} \sum_{\mathbf{q}} \sum_{j=1}^{n} \left(V_{\mathbf{q},j} a_{\mathbf{q},j} \sum_{\mathbf{k}} \sum_{\sigma=\pm 1/2} c^+_{\mathbf{k}+\mathbf{q},\sigma} c_{\mathbf{k},\sigma} + \mathrm{h.c.} \right), \tag{9.116}$$

where $c^+_{\mathbf{k},\sigma}$ ($c_{\mathbf{k},\sigma}$) are the creation (annihilation) operators for an electron with momentum $\mathbf{k}$ and with the spin z-projection σ, $a^+_{\mathbf{q},j}$ ($a_{\mathbf{q},j}$) are the creation (annihilation) operators for a phonon of the j-th branch with the momentum q, $\omega_{L,j}$ are the LO-phonon frequencies (approximated here as non-dispersive), and V is the volume of the crystal. The polaron interaction amplitude $V_{\mathbf{q},j}$ is [38]

$$V_{\mathbf{q},j} = \frac{\hbar\omega_{L,j}}{q} \left(\frac{4\pi\alpha_j}{V}\right)^{1/2} \left(\frac{\hbar}{2m_b\omega_{L,j}}\right)^{1/4}, \tag{9.117}$$

where α_j is a dimensionless partial coupling constant characterizing the interaction between an electron and the j-th LO-phonon branch. The electron-electron interaction is described by the

Coulomb potential energy

$$U_{e-e} = \frac{1}{2}\sum_{\mathbf{q}\neq 0}\frac{4\pi e^2}{\varepsilon_\infty q^2}\sum_{\mathbf{k},\mathbf{k}',\sigma,\sigma'} c^+_{\mathbf{k}+\mathbf{q},\sigma}c^+_{\mathbf{k}'-\mathbf{q},\sigma'}c_{\mathbf{k}',\sigma'}c_{\mathbf{k},\sigma}. \tag{9.118}$$

Optical phonons in $SrTiO_3$ show a considerable dispersion (see, e. g., Ref. [39] and references therein). The effect of the phonon dispersion is a broadening of features of the polaron optical conductivity band. The magnitude of the broadening is characterized by the dispersion parameter $\Delta\omega$ of the optical phonons, that contribute to the integrals over $\mathbf{q}$ entering the polaron optical conductivity. In a polar crystal with a single LO-phonon branch, that range of convergence is approximately $q_0 = (m_b\omega_{LO}/\hbar)^{1/2}$. For $SrTiO_3$, taking $\omega_{LO} = \max\{\omega_{L,j}\}$, we obtain $q_0 \approx 1.02\times 10^9\,\mathrm{m}^{-1}$. The boundary of the Brillouin zone π/a_0 in $SrTiO_3$ (where the lattice constant $a_0 \approx 0.3905$ nm) is at $8\times 10^9\,\mathrm{m}^{-1}$. Therefore the integration domain for the relevant integrals is one order smaller than the size of the Brillouin zone. In the region $0 < q < q_0$, the dispersion parameter of the LO-phonon frequencies, $\Delta\omega$, is a few percent of $\omega_{L,j}$. Consequently, $\Delta\omega$ is very small compared with the characteristic width of the polaron band. Therefore, in the present treatment, we apply the approximation of non-dispersive phonons.

For a description of a polarizable medium with n optical-phonon branches, we use the model dielectric function [40, 41]

$$\varepsilon(\omega) = \varepsilon_\infty\prod_{j=1}^{n}\left(\frac{\omega^2-\omega_{L,j}^2}{\omega^2-\omega_{T,j}^2}\right), \tag{9.119}$$

whose zeros (poles) correspond to the LO(TO) phonon frequencies $\omega_{L,j}$ ($\omega_{T,j}$). This dielectric function is the result of the straightforward extension of the Born-Huang approach [42] to the case where more than one optical-phonon branch exists in a polar crystal. The Born-Huang approach and its extension [40] generate expressions for the macroscopic polarization induced by the polar vibrations, and for the corresponding electrostatic potential. This electrostatic potential is a basis element of the Hamiltonian of the electron-phonon interaction. In Ref. [40], the Hamiltonian of the electron-phonon interaction has been explicitly derived with the amplitudes

$$V_{\mathbf{q}j} = \frac{1}{\sqrt{V}}\frac{e}{iq}\left(\frac{4\pi\hbar}{\left.\frac{\partial\varepsilon(\omega)}{\partial\omega}\right|_{\omega=\omega_{L,j}}}\right)^{1/2}. \tag{9.120}$$

Using Eqs. (9.117) and (9.120) with the dielectric function (9.119), we arrive at the following set of linear equations for the coupling constants α_j ($j = 1,\ldots,n$):

$$\sum_{k=1}^{n}\hbar\omega_{L,k}^3\left(\frac{\hbar}{2m_b\omega_{L,k}}\right)^{1/2}\frac{\alpha_k}{\omega_{L,k}^2-\omega_{T,j}^2} = \frac{e^2}{2\varepsilon_\infty}. \tag{9.121}$$

Knowledge of the band mass, of the electronic dielectric constant ε_∞ and of the LO- and TO-phonon frequencies is sufficient to determine the coupling constants α_j taking into account mixing between different optical-phonon branches. In the particular case of a single LO-phonon branch, Eq. (9.121) is reduced to (9.115).

In order to describe the optical conductivity of a polaron gas, we refer to the work [44], where the Mori-Zwanzig projection operator technique has been used to rederive the path-integral result of Ref. [43] and the impedance of Ref. [31]. We repeat the derivations of Ref. [44] with the replacement of single-electron functions by their many-electron analogs. For example, $e^{i\mathbf{q}\cdot\mathbf{r}}$ in the Hamiltonian of the electron-phonon interaction is replaced by the Fourier

component of the electron density for an N-electron system,

$$\rho(\mathbf{q}) \equiv \sum_{s=1}^{N} e^{i\mathbf{q}\cdot\mathbf{r}_s} = \sum_{\mathbf{k},\sigma} c^{+}_{\mathbf{k}+\mathbf{q},\sigma} c_{\mathbf{k},\sigma}. \tag{9.122}$$

As a result, we arrive at a formula which is structurally similar to the single-polaron optical conductivity [31, 44],

$$\sigma(\Omega) = \frac{e^2 n_0}{m_b} \frac{i}{\Omega - \chi(\Omega)/\Omega}, \tag{9.123}$$

where $n_0 = N/V$ is the carrier density, and $\chi(\Omega)$ is the memory function. The same many-electron derivation as in the present work, to the best of our knowledge, was first performed for the polaron gas in 2D in Ref. [45] in the weak electron-phonon coupling limit.

In Refs. [31, 44] the single-polaron memory function was calculated starting from the all-coupling Feynman variational principle [46]. For a many-polaron system, an effective all-coupling extension of that variational principle has not been worked out yet. In the present treatment, we restrict ourselves to the weak-coupling approximation for the electron-phonon interaction to derive the memory function. In this approximation, the memory function $\chi(\Omega)$ is similar to that of Ref. [45], with two distinctions: (1) the electron gas in the present treatment is three-dimensional, (2) several LO phonon branches are taken into account. The resulting form of the memory function is

$$\chi(\Omega) = \frac{4}{3\hbar m_b n_0 V} \sum_{\mathbf{q},j} q^2 |V_{\mathbf{q},j}|^2 \int_0^\infty dt \left(e^{i\Omega t} - 1\right) \times \mathrm{Im}\left[\frac{\cos\left[\omega_{L,j}\left(t + i\hbar\beta/2\right)\right]}{\sinh\left(\beta\hbar\omega_{L,j}/2\right)} S(\mathbf{q},t)\right], \tag{9.124}$$

where $\beta = 1/(k_B T)$. The dynamical structure factor $S(\mathbf{q},t)$ is proportional to the two-point correlation function (cf. Ref. [18]),

$$S(\mathbf{q},t) \equiv \frac{1}{2}\left\langle \sum_{i,j=1}^{N} e^{i\mathbf{q}\cdot[\mathbf{r}_j(t) - \mathbf{r}_k(0)]} \right\rangle = \frac{1}{2}\left\langle \rho(\mathbf{q},t)\, \rho(-\mathbf{q},0)\right\rangle. \tag{9.125}$$

To obtain $\chi(\Omega)$ to order α it is sufficient to perform the averaging in the correlation function (9.125) using the Hamiltonian (9.116) without the electron-phonon interaction and keeping the electron-electron interaction term U_{e-e}.

We calculate the dynamical structure factor (9.125) extending the method [18] to nonzero temperatures. In Ref. [18], the key advantage of the many-polaron variational approach [47] is exploited: the fact that the many-body effects are entirely contained in the dynamical structure factor $S(\mathbf{q},t)$. The structure factor can be calculated using various approximations. Terms of order of $|V_{\mathbf{q},j}|^2$ are automatically taken into account in the memory function (9.124). Consequently, up to order α for $\sigma(\Omega)$, it is sufficient to calculate $S(\mathbf{q},t)$ without the electron-phonon coupling. In Ref. [18], $S(\mathbf{q},t)$ was calculated within two different approximations: (i) the Hartree-Fock approximation, (ii) the random-phase approximation (RPA). As shown in Ref. [18], the RPA dynamical structure factor, contrary to the Hartree-Fock approximation, takes into account the effects both of the Fermi statistics and of the electron-electron interaction on the many-polaron optical-absorption spectra.

The dynamical structure factor is expressed through the density-density Green's functions defined as

$$\mathcal{G}(\mathbf{q},\Omega) \equiv -i \int_0^\infty e^{i\Omega t} \left\langle \rho(\mathbf{q},t)\, \rho(-\mathbf{q},0)\right\rangle dt, \tag{9.126}$$

$$G^R(\mathbf{q},\Omega) \equiv -i \int_0^\infty e^{i\Omega t} \left\langle \left[\rho(\mathbf{q},t), \rho(-\mathbf{q},0)\right]\right\rangle dt. \tag{9.127}$$

In terms of $G(\mathbf{q},\Omega)$ and $G^R(\mathbf{q},\Omega)$, the memory function (9.124) takes the form:

$$\begin{aligned}\chi(\Omega) = &\sum_j \frac{\alpha_j \hbar\omega_{L,j}^2}{6\pi^2 N m_b}\left(\frac{\hbar}{2m_b\omega_{L,j}}\right)^{1/2} \\ &\times \int d\mathbf{q}\,\{\mathcal{G}(\mathbf{q},\Omega-\omega_{L,j}) + \mathcal{G}^*(\mathbf{q},-\Omega-\omega_{L,j}) - \mathcal{G}(\mathbf{q},-\omega_{L,j}) - \mathcal{G}^*(\mathbf{q},-\omega_{L,j}) \\ &+ \frac{1}{e^{\beta\hbar\omega_{L,j}}-1}\left[G^R(\mathbf{q},\Omega-\omega_{L,j}) + \left(G^R(\mathbf{q},-\Omega-\omega_{L,j})\right)^* \right. \\ &\left. -G^R(\mathbf{q},-\omega_{L,j}) - \left(G^R(\mathbf{q},-\omega_{L,j})\right)^*\right]\}\,. \end{aligned} \tag{9.128}$$

Taking into account the Coulomb electron-electron interaction within RPA, the retarded Green's function $G^R(\mathbf{q},\Omega)$ is given by

$$G^R(\mathbf{q},\Omega) = \frac{\hbar V P^{(1)}(\mathbf{q},\Omega)}{1-\frac{4\pi e^2}{\varepsilon_\infty q^2}P^{(1)}(\mathbf{q},\Omega)}, \tag{9.129}$$

where $P^{(1)}(\mathbf{q},\Omega)$ is the polarization function of the free electron gas, see, e.g., [48]

$$P^{(1)}(\mathbf{q},\Omega) = \frac{1}{V}\sum_{\mathbf{k},\sigma}\frac{f_{\mathbf{k}+\mathbf{q},\sigma}-f_{\mathbf{k},\sigma}}{\hbar\Omega+\frac{\hbar^2(\mathbf{k}+\mathbf{q})^2}{2m_b}-\frac{\hbar^2k^2}{2m_b}+i\delta}, \quad \delta\to+0 \tag{9.130}$$

with the electron average occupation numbers $f_{\mathbf{k},\sigma}$. The function $\mathcal{G}(\mathbf{q},\Omega)$ is obtained from $G^R(\mathbf{q},\Omega)$ using the exact analytical relation

$$\left(1-e^{-\beta\hbar\Omega}\right)\operatorname{Im}\mathcal{G}(\mathbf{q},\Omega) = \operatorname{Im}G^R(\mathbf{q},\Omega) \tag{9.131}$$

and the Kramers-Kronig dispersion relations for $\mathcal{G}(\mathbf{q},\Omega)$.

The above expressions are written for an isotropic conduction band. However, the conduction band of $SrTi_{1-x}Nb_xO_3$ is strongly anisotropic and triply degenerate. The electrons are doped in three bands: d_{xy}, d_{yz} and d_{xz}, which all have their minima at $\mathbf{k}=0$. Each of these bands has light masses along two direction (x and y for d_{xy}, etc.) and a heavy mass along the third direction. While each electron has a strongly anisotropic mass, the electronic transport remains isotropic due to the fact that 2 light masses and 1 heavy mass contribute along each crystallographic axis.

The anisotropy of the electronic effective mass of the conduction band can be approximately taken into account in the following way. We use the averaged inverse band mass

$$\frac{1}{\bar{m}_b} = \frac{1}{3}\left(\frac{1}{m_x}+\frac{1}{m_y}+\frac{1}{m_z}\right) \tag{9.132}$$

and the density-of-states band mass

$$m_D = (m_x m_y m_z)^{1/3}\,. \tag{9.133}$$

The mass m_D appears in the prefactor of the linear term of the specific heat. Comparing the mass m_D obtained from the experimental specific heat [28, 49] with the mass $\bar{m}_b$ obtained using optical spectral weights [15] reveals the mass ratio of the heavy and light bands to be about 27. The expression (9.132) replaces the bare mass m_b in the optical conductivity (9.123) and in the memory function (9.128). The polarization function of the free electron gas (9.130) is calculated with the density-of-states mass m_D instead of m_b. The band degeneracy is taken into account through the degeneracy factor which is equal to 3, both in the polarization function and in the normalization equation for the chemical potential. The reduction of the polaron optical conductivity band due to screening with band degeneracy turns out to be less significant than without band degeneracy.

Theory and experiment

Material parameters

Several experimental parameters characterizing $SrTi_{1-x}Nb_xO_3$ are necessary for the calculation of the large-polaron optical conductivity (see, e.g., Refs. [14, 16]): the LO- and TO-phonon frequencies, the electron band mass, and the electronic dielectric constant ε_∞.

The electronic dielectric constant can be obtained using reflectivity spectra of $SrTi_{1-x}Nb_xO_3$. At $T = 10$ K, the reflectivity of $SrTi_{1-x}Nb_xO_3$ is $R \approx 0.16$ for $\Omega \approx 5000$ cm^{-1}. The electronic dielectric constant can be approximated using the expression

$$R(\Omega) = \left| \frac{\sqrt{\varepsilon(\Omega)} - 1}{\sqrt{\varepsilon(\Omega)} + 1} \right|^2 \tag{9.134}$$

and assuming that $\Omega = 5000$ cm^{-1} is a sufficiently high frequency to characterize the electronic response. From (9.134) it follows that for $SrTi_{1-x}Nb_xO_3$, $\varepsilon_\infty \approx 5.44$.

In order to determine the optical-phonon frequencies, we use the experimental data from available sources [15, 16]. In Ref. [15], three infrared active phonon modes are observed at room temperature: at 11.0 meV, 21.8 meV and 67.6 meV. With decreasing temperature, the lowest-frequency infrared-active phonon mode shows a strong red shift upon cooling, and saturates at about 2.3 meV at 7 K. Those infrared-active phonon modes are associated with the polar TO-phonons. The TO-phonon frequencies determined in Ref. [16] for $SrTi_{1-x}Nb_xO_3$ with $x = 0.9\%$ at $T = 300$ K are 100 cm^{-1}, 175 cm^{-1} and 550 cm^{-1}. The corresponding TO-phonon energies are 12.4 meV, 21.7 meV and 68.2 meV.

Refs. [15] and [16] are used as sources for phonon parameters. In Ref. [16], the TO-phonon frequencies are calculated on the basis of reflectivity measurements using a model dielectric function to fit experimental data. In Ref. [15], the TO-phonon frequencies are obtained from an analysis of both reflectivity and transmission spectra, using inversion of the Fresnel equations of reflection and transmission coefficients and the Kramers-Kronig transformation of the reflectivity spectra. The TO-phonon energies reported in Refs. [15] and [16] are in close agreement. This confirms the reliability of both experimental data sources [15, 16]. The values of the TO-phonon frequencies used in our calculation are taken from the experiment [15] because they are directly related to the samples of $SrTi_{1-x}Nb_xO_3$ for which the comparison of theory and experiment is made in the present work.

The TO phonon frequencies from Ref. [15] can be used when they are complemented with corresponding LO phonon frequencies. However, Ref. [15] does not contain data of the LO-phonon frequencies. In the present calculation we use the LO phonon frequencies from Ref. [16].

The averaged band mass (9.132) is taken to be $\bar{m}_b = 0.81 m_e$ (where m_e is the electron mass in vacuum) according to experimental data from Ref. [50]. Using the ratio of the heavy mass (m_z) to the light mass ($m_x = m_y$), $m_z/m_x = 27$, we find the density-of states band mass $m_D \approx 1.65 m_e$.

The TO- and LO- phonon frequencies and the resulting partial coupling constants calculated using the mass $\bar{m}_b$ are presented in Table 1.

Table 4: Optical-phonon frequencies and partial coupling constants of doped strontium titanate

x T	$x = 0.1\%$ $T = 7$ K	$x = 0.1\%$ $T = 300$ K	$x = 0.2\%$ $T = 7$ K	$x = 0.2\%$ $T = 300$ K	$x = 0.9\%$ $T = 7$ K	$x = 0.9\%$ $T = 300$ K	$x = 2\%$ $T = 7$ K	$x =$ $T =$
$\hbar\omega_{T,1}$ (meV)	2.27	11.5	2.63	11.5	6.01	12.1	8.51	13.0
$\hbar\omega_{L,1}$ (meV)	21.2	21.2	21.2	21.2	21.2	21.2	21.2	21.2
α_1	0.021	0.013	0.021	0.013	0.017	0.013	0.017	0.01
$\hbar\omega_{T,2}$ (meV)	21.2	21.8	21.2	21.8	21.2	21.8	21.2	21.8
$\hbar\omega_{L,2}$ (meV)	58.4	58.4	58.4	58.4	58.4	58.4	58.4	58.4
α_2	0.457	0.414	0.457	0.414	0.452	0.414	0.447	0.40
$\hbar\omega_{T,3}$ (meV)	67.6	67.1	67.6	67.1	67.6	67.1	67.6	67.1
$\hbar\omega_{L,3}$ (meV)	98.7	98.7	98.7	98.7	98.7	98.7	98.7	98.7
α_3	1.582	1.582	1.582	1.580	1.576	1.578	1.570	1.57
α_{eff}	2.06	2.01	2.06	2.01	2.05	2.01	2.03	2.01

The effective coupling constant in Table 1 is determined following Ref. [38], as a sum of partial coupling constants α_j,

$$\alpha_{\text{eff}} \equiv \sum_j \alpha_j \tag{9.135}$$

The result $\alpha_{\text{eff}} \sim 2$ shows that the electron-phonon coupling strength in $SrTi_{1-x}Nb_xO_3$ lies in the intermediate to weak coupling range, and the conditions for small polaron formation are not fulfilled. This analysis indicates that the large-polaron picture – rather than the small-polaron description is suitable for the interpretation of the mid-infrared band of the optical conductivity of $SrTi_{1-x}Nb_xO_3$.

We use the actual electron densities for the samples studied in Ref. [15] based on the unit cell volume (59.5 cubic angstrom) and the chemical composition (x is the doping level). These carrier densities (see Table 2) are confirmed by measurements of the Hall constants.

Table 5: Electron densities of $SrTi_{1-x}Nb_xO_3$

x (%)	n_0 (cm^{-3})
0.1	1.7×10^{19}
0.2	3.4×10^{19}
0.9	1.5×10^{20}
2.0	3.4×10^{20}

9.3.3 Optical conductivity spectra

We calculate the large-polaron optical conductivity spectra for $SrTi_{1-x}Nb_xO_3$ using the approach of Ref. [18] as adapted in Ref. [36] to take into account multiple LO-phonon branches. We also include in the numerical calculation the TO-phonon contribution to the optical conductivity, described by an oscillatory-like model dielectric function (see, e.g., Ref. [16]):

$$\operatorname{Re}\sigma_{TO}(\Omega) = \sum_j \sigma_{0,j} \frac{\gamma_j^2}{(\Omega - \omega_{T,j})^2 + \gamma_j^2}, \tag{9.136}$$

where the weight coefficients $\sigma_{0,j}$ and the damping parameters γ_j for each j-th TO-phonon branch are extracted from the experimental optical conductivity spectra of Ref. [15]. The polaron-and the TO-phonon optical responses are treated as independent of each other. Consequently the polaron-(9.123) and TO-phonon (9.136) contributions enter the optical conductivity additively.

Following the procedure described above using the material parameters discussed above, we obtain the theoretical large-polaron optical conductivity spectra of $SrTi_{1-x}Nb_xO_3$ shown in Fig. 2 and Fig. 3 at 7 K and 300 K, respectively. In each graph also the experimental optical conductivity spectra of Ref. [15] are shown. It should be emphasized that *in the present calculation, there is no fitting of material constants for the polaron contribution to* $\mathrm{Re}\,\sigma\,(\Omega)$. *Even the magnitude of the optical conductivity, which is often arbitrarily scaled in the literature, follows from first principles.*

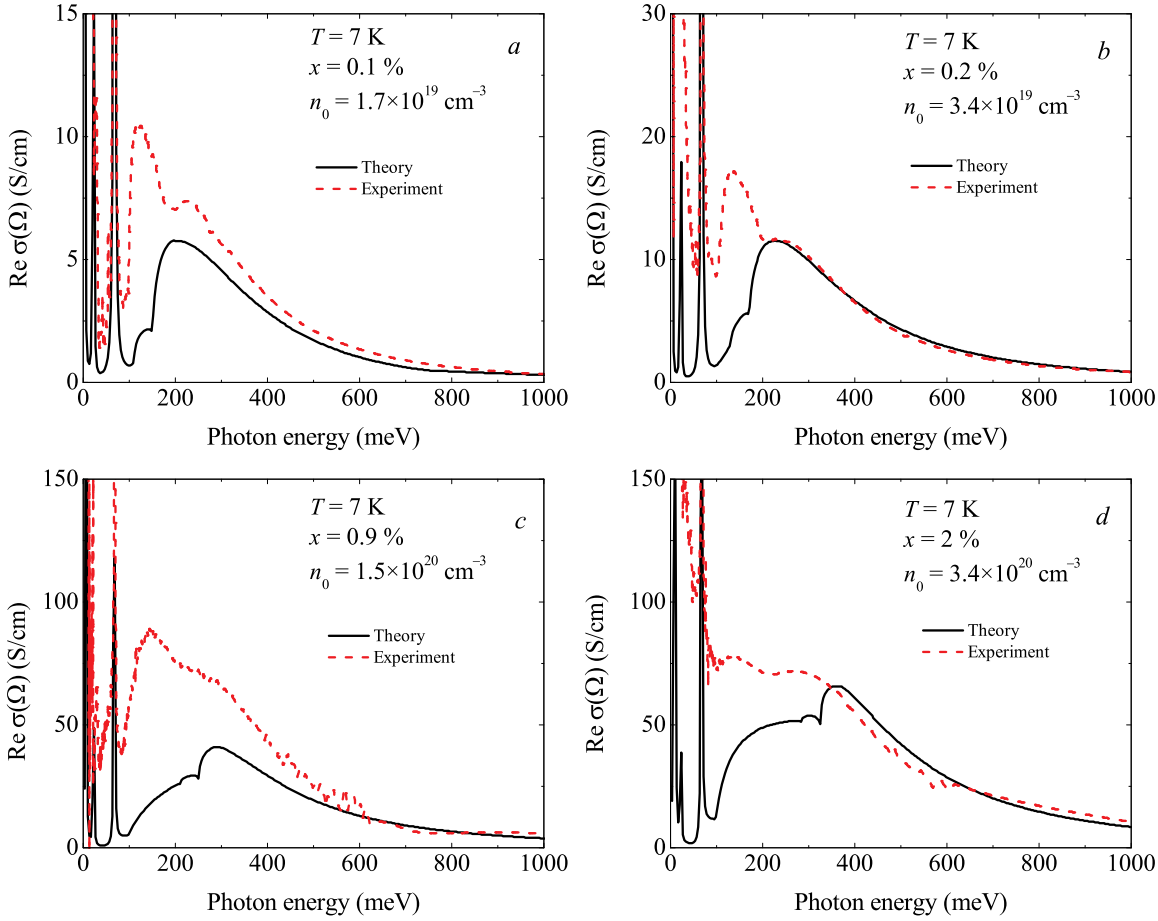

Figure 9.2: The many-large-polaron optical conductivity compared with the experiment [15] at $T = 7$ K. The doping level is $x = 0.1\%$ (a), 0.2% (b), 0.9% (c) and $2\%(d)$.

At 7 K, the calculated optical conductivity based on the Fröhlich model and extended for a gas of large polarons as described in the present paper, shows convincing agreement with the behavior of the experimental optical conductivity for the high energy part of the spectra, i.e., $\hbar\Omega \gtrapprox 300$ meV. The experimental polaron optical conductivity of $SrTi_{1-x}Nb_xO_3$ falls down at high frequencies following the power law (derived in the present work and typical for large polarons) rather than as a Gaussian exponent that would follow from the small-polaron theory. At lower photon energies $\hbar\Omega \lessapprox 200$ meV, the experiment shows distinct peaks that are not explained within the polaron theory. They can be due to other scattering mechanisms as discussed below.

The minor deviations between theoretical and experimental $\mathrm{Re}\,\sigma\,(\Omega)$ in the frequency range $\hbar\Omega \gtrapprox 300$ meV may be attributed to the difference between the actual electron densities and the densities calculated on the basis of the unit cell volume and the chemical composition. However, we prefer not to fit of the density.

The optical conductivity calculated for a single large-polaron absorption [31] predicts an

intensity 3-4 times larger than the experimental data for the lowest doping level $x = 0.1\%$, and therefore cannot explain those data. For higher dopings, the overestimation of the magnitude of the optical conductivity within the single-polaron theory is even larger than for $x = 0.1\%$. Therefore the many-polaron approach, used in the present work, is essential.

At 300 K, in Fig. 3 (a, b ,d), the agreement between theory and experiment is qualitative. Both experimental and theoretical spectra show a maximum at the room-temperature optical conductivity spectra in the range $\hbar\Omega \sim 250$ meV. For the doping level $x = 0.9\%$ the calculated optical conductivity spectrum underestimates the experimental data, as also observed at 7 K.

Many-body effects considerably influence the optical conductivity spectra of a polaron gas. First, features related to the emission of a plasmon together with a LO phonon [18] are manifested in the optical conductivity spectra of the many-polaron gas at $T = 7$ K as separate peaks whose positions shift to higher energies with increasing doping level. At room temperature, those peaks are strongly broadened and smoothened, and only a broad plasmon feature is apparent. Second, the mid-infrared optical conductivity (per particle) in $SrTi_{1-x}Nb_xO_3$ is decreasing at higher doping levels due to the screening of the polar interactions, which is accounted for in the present approach in which $S(\mathbf{q}, t)$ is based on RPA. The effect of screening can be illustrated by the fact that for $n_0 \sim 10^{20}$ cm^{-3}, the many-polaron optical conductivity *per particle* is reduced by about an order of magnitude compared to the single-polaron optical conductivity. The reduction in intensity of the polaron optical conductivity band can be interpreted as a decrease of the overall electron-phonon coupling strength due to many-body effects. Correspondingly, at high doping levels, the polaron mass m^*, determined by the sum rule introduced in Ref. [51]

$$\frac{\pi e^2 n_0}{2m^*} + \int_{\omega_L}^{\infty} \mathrm{Re}\,(\Omega)\, d\Omega = \frac{\pi e^2 n_0}{2\bar{m}_b} \tag{9.137}$$

is reduced, compared to the single-polaron effective mass. As shown in Refs. [18, 52], the sum rule [51] remains valid for an interacting polaron gas.

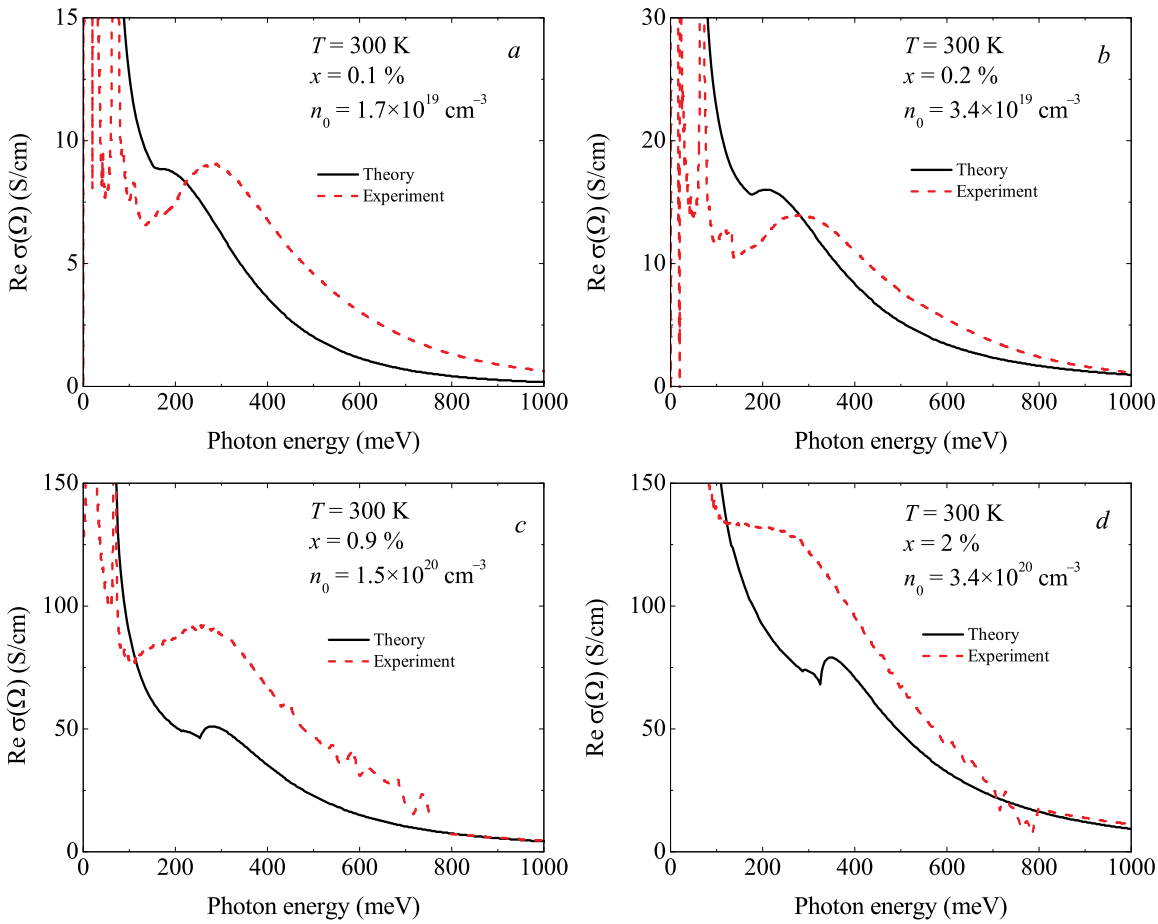

Figure 9.3: The many-large-polaron optical conductivity compared with the experiment [15] at $T = 300$ K. The doping level is $x = 0.1\%$ (a), 0.2% (b), 0.9% (c) and 2% (d).

The large-polaron theory of the optical absorption based on Ref. [18] explains without any fitting parameters the main characteristics and trends of the observed spectra of Ref. [15] in $SrTi_{1-x}Nb_xO_3$, including doping- and temperature dependence. Nevertheless, some features of the experimental spectra remain to be explained. In particular, at $T = 7$ K, the pronounced peak at $\hbar\Omega \sim 130$ meV in the experimental optical conductivity is not accounted for by the present theoretical analysis. In the theoretical spectra, peaks of much smaller intensity appear at about the same frequency. In the large-polaron theory, those peaks are provided by the interaction between electrons and the LO-phonon branch with energy $\hbar\omega_{L,2} \approx 58.4$ meV, accompanied by the emission of a plasmon as described in Ref. [18].

The intensity of the experimentally observed absorption peak at $\hbar\Omega \sim 130$ meV is considerably higher than described by the large-polaron theory. In the low density limit, the experimental optical data more rapidly approach the single polaron limit [31] than the theoretical predictions based on Eq. (9.124). This absorption peak at $\hbar\Omega \sim 130$ meV may be provided by other mechanisms, not controlled in the present study. E. g., electron-phonon interaction with low-frequency non-polar (e. g., acoustic) phonons may contribute to the optical conductivity. The squared modulus $|V_q|^2$, which characterizes the coupling strength, for the deformation electron-phonon interaction is $|V_{\mathbf{q}}|^2 \propto q$ [53], while for the Fröhlich interaction, $|V_{\mathbf{q}}|^2 \propto q^{-2}$. Consequently, for the deformation electron-phonon interaction, the short-wavelength phonons may provide non-negligible contributions to the optical conductivity. Also, at sufficiently large q, Umklapp scattering processes with acoustic phonons can play a role. The treatment of contributions due to acoustic phonons (and other mechanisms) is the subject of the future work. Another possible explanation of the absorption peak at $\hbar\Omega \sim 130$ meV is weakened screening

in the corresponding energy range due to dynamical-exchange [54].

9.3.4 Conclusions

Many-polaron optical conductivity spectra, calculated (based on Ref. [18]) within the large-polaron picture without adjustment of material constants, explain essential characteristics of the experimental optical conductivity [15]. The intensities of the calculated many-polaron optical conductivity spectra and the intensities of the experimental mid-infrared bands of the optical conductivity spectra of $SrTi_{1-x}Nb_xO_3$ (from Ref. [15]) are comparable for all considered values of the doping parameter. The doping dependence of the intensity of the mid-infrared band in the theoretical large-polaron spectra is similar to that of the experimental data of Ref. [15]. In the high-frequency range, the theoretical absorption curves describe well the experimental data (especially at low temperature). A remarkable difference between the present theoretical approach and experiment is manifested on the low frequency side of the mid-infrared range, where the experimental optical conductivity shows a sharp and pronounced peak for $\hbar\Omega \sim 130$ meV at 7 K. Although the theoretical curve also shows a feature around the same frequency, its intensity is clearly underestimated. This peak in the absorption spectrum at $\hbar\Omega \sim 130$ meV remains to be explained. The value of the effective electron-phonon coupling constant obtained in the present work ($\alpha_{eff} \approx 2$) corresponds to the intermediate coupling strength of the large-polaron theory.

The alternative small-polaron and mixed-polaron models for the optical conductivity require several fitting parameters. Furthermore, we find that the mixed-polaron model would need a major adjustment of the overall intensity in order to fit experimental spectra.

Contrary to the case of the large polaron, the small-polaron parameters cannot be extracted from experimental data. Moreover, the small-polaron model, for any realistic choice of parameters, shows a frequency dependence in the high-frequency range which is different from that of the experimental optical conductivity. Both the experimental and the theoretical large-polaron optical conductivity decrease as a power function at high frequencies, while the small-polaron optical conductivity falls down exponentially for sufficiently high Ω.

In summary, the many-body large-polaron model based on the Fröhlich interaction accounts for the essential characteristics (except – interestingly – for the intensity of a prominent peak at $\hbar\Omega \sim 130$ meV, that constitutes an interesting challenge for theory) of the experimental mid-infrared optical conductivity band in $SrTi_{1-x}Nb_xO_3$ without any adjustment of material parameters. The large-polaron model gives then a convincing interpretation of the experimentally observed mid-infrared band of $SrTi_{1-x}Nb_xO_3$.

References

[1] S. Lupi, P. Maselli, M. Capizzi, P. Calvani, P. Giura, and P. Roy, Phys. Rev. Lett. **83**, 4852 (1999).

[2] L. Genzel, A. Wittlin, M. Bayer, M. Cardona, E. Schonherr, and A. Simon, Phys. Rev. B **40**, 2170 (1989).

[3] P. Calvani, M. Capizzi, S. Lupi, P. Maselli, A. Paolone, and P. Roy, Phys. Rev. B **53**, 2756 (1996).

[4] S. Lupi, M. Capizzi, P. Calvani, B. Ruzicka, P. Maselli, P. Dore, and A. Paolone, Phys. Rev. B **57**, 1248 (1998).

[5] J.-G. Zhang, X.-X. Bi, E. McRae, P. C. Ecklund, B. C. Sales, M. Mostoller, Phys. Rev. B **43**, 5389 (1991).

[6] C. C. Homes, B. P. Clayman, J. L. Peng, R. L. Greene, Phys. Rev. B **56**, 5525 (1997).

[7] M. K. Crawford, G. Burns, G. V. Chandrashekhar, F. H. Dacol, W. E. Farneth, E. M. McCarron, III, and R. J. Smalley, Phys. Rev. B **41**, 8933 (1990).

[8] J. P. Falck, A. Levy, M. A. Kastner, and R. J. Birgeneau, Phys. Rev. B **48**, 4043 (1993).

[9] H. M. Rønnow, Ch. Renner, G. Aeppli, T. Kimura and Y. Tokura, Nature **440**, 1025 (2006).

[10] Ch. Hartinger, F. Mayr, J. Deisenhofer, A. Loidl and T. Kopp, Phys. Rev. B **69** 100403R (2004); Ch. Hartinger, F. Mayr, and A. Loidl, Phys. Rev. B **73**, 024408 (2006).

[11] P. Calvani, M. Capizzi, F. Donato, S. Lupi, P. Maselli, and D. Peschiaroli, Phys. Rev. B **47**, 8917 (1993).

[12] J. F. Schooley, W. R. Hosler, and M. L. Cohen, Phys. Rev. Lett. **12**, 474 (1964).

[13] D. M. Eagles, M. Georgiev and P. C. Petrova, Phys. Rev. B **54**, 22 (1996).

[14] C. Z. Bi, J. Y. Ma, J. Yan, X. Fang, B. R. Zhao, D. Z. Yao and X. G. Qiu, J. Phys.: Condens. Matter **18**, 2553 (2006).

[15] J. L. M. van Mechelen, D. van der Marel, C. Grimaldi, A. B. Kuzmenko, N. P. Armitage, N. Reyren, H. Hagemann, and I. I. Mazin, Phys. Rev. Lett. **100**, 226403 (2008).

[16] F. Gervais, J. L. Servoin, A. Baratoff, J. G. Bednorz and G. Binnig, Phys. Rev. B **47**, 8187 (1993).

[17] C. Ang, Z. Yu, Z. Jing, P. Lunkenheimer and A. Loidl, Phys. Rev. B **61**, 3922 (2000).

[18] J. Tempere and J. T. Devreese, Phys. Rev. B **64**, 104504 (2001).

[19] J. T. Devreese and A. S. Alexandrov, Rep. Prog. Phys. **72**, 066501 (2009).

[20] A. S. Alexandrov and J. T. Devreese, *Advances In Polaron Physics* (Springer, 2009).

[21] D. M. Eagles, Phys. Rev. **181**, 1278 (1969).

[22] D. M. Eagles, J. Phys. C **17**, 637 (1984).

[23] D. M. Eagles and P. Lalousis, J. Phys. C **17**, 655 (1984).

[24] D. M. Eagles, in *Physics of Disordered Materials*, edited by D. Adler (Plenum, New York, 1985), p. 357.

[25] H. Fröhlich, Adv. Phys. **3**, 325 (1954).

[26] H. G. Reik, Z. Phys. **203**, 346 (1967); in *Polarons in Ionic Crystals and Polar Semiconductors* (North-Holland, Amsterdam, 1972).

[27] H. P. R. Frederikse, W. R. Thurber and W. R. Hosler, Phys. Rev. **134**, A442 (1964).

[28] E. Ambler, J. H. Colwell, W. R. Hosler and J. F. Schooley, Phys. Rev. **148**, 280 (1966).

[29] G. Iadonisi, V. Cataudella, G. De Filippis, and D. Ninno, Europhys. Lett., **41**, 309 (1998).

[30] D. M. Eagles, R. P. S. M. Lobo, and F. Gervais, Phys. Rev. B **52**, 6440 (1995).

[31] J. Devreese, J. De Sitter, and M. Goovaerts, Phys. Rev. B **5**, 2367 (1972).

[32] V. L. Gurevich, I. G. Lang, and Yu. A. Firsov, Sov. Phys. Solid State **4**, 918 (1962).

[33] J. Devreese, W. Huybrechts, and L. Lemmens, Phys. Status Solidi B **48**, 77 (1971).

[34] E. Kartheuser, R. Evrard, and J. Devreese Phys. Rev. Lett. **22**, 94-97 (1969).

[35] D. Emin, Phys. Rev. B **48**, 13691 (1993).

[36] S. N. Klimin, V. M. Fomin, and J. T. Devreese, *to be published.*

[37] S. N. Klimin, V. M. Fomin, F. Brosens, and J. T. Devreese, Phys. Rev. B **69**, 235324 (2004).

[38] G. Verbist, F. M. Peeters, J. T. Devreese, Ferroelectrics **130**, 27 (1992).

[39] N. Choudhury, E. J. Walter, A. I. Kolesnikov, and C.-K. Loong, Phys. Rev. B **77**, 134111 (2008).

[40] Y. Toyozawa, in: *Polarons in Ionic Crystals and Polar Semiconductors,* North-Holland, Amsterdam (1972), pp. 1 – 27.

[41] R. Zheng, T. Taguchi, and M. Matsuura, Phys. Rev. B **66**, 075327 (2002).

[42] M. Born and K. Huang, *Dynamical Theory of Crystal Lattices* (Clarendon, Oxford, 1954).

[43] R. P. Feynman, R. W. Hellwarth, C. K. Iddings, and P. M. Platzman, Phys. Rev. **127**, 1004 (1962).

[44] F. M. Peeters and J. T. Devreese, Phys. Rev. B **28**, 6051 (1983).

[45] X. Wu, F. M. Peeters, and J. T. Devreese, Phys. Rev. B **34**, 2621 (1986).

[46] R. P. Feynman, Phys. Rev. **97**, 660 (1955).

[47] L. F. Lemmens, J. T. Devreese, and F. Brosens, Phys. Stat. Sol. (b) **82**, 439 (1977).

[48] G. D. Mahan, *Many-Particle Physics*, second edition (Plenum Press, 1990).

[49] N.E. Phillips, B.B. Triplett, R.D. Clear, H.E. Simon, J.K. Hulm, C.K. Jones and R. Mazelsky, Physica **55**, 571 (1971).

[50] J.L.M. van Mechelen (*to be published*)

[51] J. T. Devreese, L. F. Lemmens, and J. Van Royen, Phys. Rev. B **15**, 1212 (1977).

[52] J. Tempere and J. T. Devreese, Eur. Phys. J. B **20**, 27 (2001).

[53] F. M. Peeters and J. T. Devreese, Phys. Rev. B **32**, 3515 (1985).

[54] J. T. Devreese, F. Brosens, and L. F. Lemmens, Phys. Rev. B **21**, 1349 (1980); Phys. Rev. B **21**, 1363 (1980).

9.4 Notes on the polaron mobility

J. T. Devreese and S. N. Klimin

Here, we are focused on some important issues related to the polaron mobility. First, we discuss the polaron mobility in the weak-coupling regime on the basis of Ref. [143]. Several theoretical methods have been applied to study the transport properties of the Fröhlich polaron. The polaron mobility was calculated using various approaches: the calculation of the scattering amplitude [64], the kinetic equation [65], the Green's function technique, the Kubo formula [66, 63], the path-integral formalism [47, 48, 150].

A challenging difficulty is that, even for weak coupling and in the ohmic regime, there is a remarkable difference in the mobility as obtained via a relaxation-time approximation [62, 64, 144, 63, 65], and as obtained via the path-integral formalism, worked out by Thornber and Feynman [48], and which is based on the Feynman polaron model [43].

At weak coupling and small electric field, the relaxation time result for the mobility [66] seems more reliable than the Thornber-Feynman result. This might be partly due to the deviation of the electron velocity distribution from a drifted Maxwellian as shown analytically [145] from the Boltzmann equation at weak electron-phonon coupling and low temperature in the steady state regime.

Because the Boltzmann equation is valid at weak electron-phonon coupling, and because of its intuitively transparent structure, this equation is an important tool to study transport properties of polarons for weak coupling. In Ref. [143], its solution is discussed in the ohmic regime and for the steady state. The mobility in the zero temperature limit from Ref. [143] is given by:

$$\mu|_{T\to 0} \to \frac{e}{2\alpha}\bar{N}^{-1}, \tag{9.138}$$

where $\bar{N}$ is the average number of phonons. This is equivalent to the result from the relaxation-time approximation [65], which therefore holds in the zero-temperature limit.

An analytical solution of the Boltzmann equation at $T = 0$ was obtained in Ref. [146]. In Fig. 9.4, the mobility of a polaron in the weak-coupling regime, calculated using the exact solution of the Boltzmann equation [146] is calculated for InSb at $T = 77$ K and compared to the mobility from Ref. [48]. For weak electric fields the result of Ref. [146] is quite close to that of the polaron theory with a relaxation time but differs by the factor $\frac{3}{2}\frac{k_B T}{\hbar\omega_0}\frac{1}{2.5}$ from [48]. These results seem to confirm the validity of a relaxation time approach for the electric field $E \to 0$ (at least for InSb at 77 K). Nevertheless, as pointed out in [147], a system of non-interacting polarons is not ergodic and this point should be examined carefully before definite conclusions can be drawn when $E \to 0$. In Ref. [148], arbitrary temperature and electric field are considered, and an exact recursion relation is obtained for the time-dependent expansion coefficients of the electron distribution function in terms of Legendre polynomials.

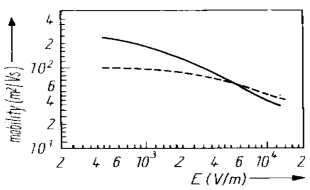

Figure 9.4: Mobility of weak-coupling polarons, obtained from the exact solution of the Boltzmann equation [146] (solid line) and from [48] (dashed line). (After Ref. [147].)

The DC mobility of a polaron in the strong-coupling regime was investigated by Volovik *et al.* [149]. They showed that the interaction Hamiltonian corresponding to scattering of a phonon by a polaron can be separated in the strong-coupling limit with the aid of the transformations of Bogoliubov and Tyablikov in conjunction with the LLP canonical transformation. In the leading order in powers of the inverse coupling constant α^{-1}, the principal role in the scattering is played by two-phonon processes. In the system of units with $\hbar = 1$, the following result for the strong-coupling polaron mobility has been obtained:

$$\mu = \frac{\gamma}{m\omega_{\mathrm{LO}}\alpha^2}\frac{T}{\omega_0}e^{\omega_0/T}, \tag{9.139}$$

with a numerical temperature-independent coefficient $\gamma \sim 1$.

The "$\frac{3}{2}k_BT$" problem reveals a key distinction between the polaron mobility obtained in Refs. [47, 48, 150] and the other approaches. Also the other problem is worth discussing. The results of the approaches [65, 66, 63] are in agreement with each other. Therefore during a long time they were recognized well-established. Several works appeared in which the polaron mobility at low temperatures differs from the Kadanoff result by the numerical factor 3, e. g., Refs. [151, 152]. However, they have not yet attract a proper attention.

In the work by V. F. Los [151], the polaron mobility was calculated on the basis of Kubo's formula using a Green's superoperator technique. As stated in Ref. [151], the relaxation-time approximation [65] does not take into account the change in the electron velocity in all the electron-phonon scattering processes allowed by the energy and momentum conservation laws. The polaron mobility obtained in Ref. [151] gives the correct temperature dependence of the polaron mobility but exceeds the expression obtained by Kadanoff exactly by a factor 3.

Recently, this "factor 3" has been again confirmed using a rigorous derivation. An approach to the polaron mobility has been proposed by F. Brosens and D. Sels [153], based on the dynamics of the Wigner distribution function, using the kinetic equations derived in Refs. [154, 155].

In the paper [153], the mobility of the Fröhlich polaron is calculated within approach, based on the dynamics of the Wigner distribution function. The approach proposed by the authors

is based on a path integral description of the Wigner distribution function. The time evolution of the electron distribution function $f(\mathbf{p},t)$ in the electron-phonon system under an external time-dependent uniform electric field $\mathbf{E}(t)$ is governed by the generalized kinetic equation

$$\begin{aligned}
&\left(\frac{\partial}{\partial t}+e\mathbf{E}(t)\cdot\frac{d}{d\mathbf{p}}\right)f(\mathbf{p},t)\\
&=\sum_{\mathbf{k}}\frac{2\left|\gamma(k)\right|^2}{\hbar^2}\iiint dt'd\mathbf{x}'d\mathbf{p}'\Theta(t'\leq t)\,f(\mathbf{p}',t')\\
&\times\left(\begin{array}{c}\left(\begin{array}{c}(n_B(\omega_k)+1)\cos(\mathbf{k}\cdot(\mathbf{x}-\mathbf{x}')+\omega_k(t-t'))\\+n_B(\omega_k)\cos(\mathbf{k}\cdot(\mathbf{x}-\mathbf{x}')-\omega_k(t-t'))\end{array}\right)\\ \times\left(K_0\left(\mathbf{x},\mathbf{p}-\frac{\hbar\mathbf{k}}{2},t|\mathbf{x}',\mathbf{p}'+\frac{\hbar\mathbf{k}}{2},t'\right)-K_0\left(\mathbf{x},\mathbf{p}+\frac{\hbar\mathbf{k}}{2},t|\mathbf{x}',\mathbf{p}'+\frac{\hbar\mathbf{k}}{2},t'\right)\right)\end{array}\right)
\end{aligned}\tag{9.140}$$

with the propagator

$$\begin{aligned}
K_0(\mathbf{x},\mathbf{p},t|\mathbf{x}',\mathbf{p}',t')&=\delta\left(\mathbf{p}-\mathbf{p}'-\int_{t'}^{t}e\mathbf{E}(\sigma)\,d\sigma\right)\\
&\times\delta\left(\mathbf{x}-\mathbf{x}'-\frac{\mathbf{p}'}{m}(t-t')-\int_{t'}^{t}\frac{e\mathbf{E}(\sigma)}{m}(t-\sigma)\,d\sigma\right).
\end{aligned}\tag{9.141}$$

Here, ω_k is the phonon frequency, $\gamma(k)$ is the amplitude of the electron-phonon interaction, and $n_B(\omega_k)$ is the free-phonon distribution function,

$$n_B(\omega_k)=\frac{1}{e^{\beta\hbar\omega_k}-1}.\tag{9.142}$$

The key result of Ref. [153] is the mobility of a weak-coupling polaron given by formula (IV.4):

$$\sigma_{DC}=\frac{3e^2}{2\alpha m\omega_{LO}}e^{\beta\hbar\omega_{LO}}.\tag{9.143}$$

This expression differs by the factor 3 from the result by Kadanoff and Osaka [65, 66, 63]. Also the critical re-derivation of the polaron optical conductivity on the basis of the Feynman polaron model results in the optical conductivity

$$\sigma_{DC}=\frac{3e^2}{2\alpha m^*\omega_{LO}}e^{\beta\hbar\omega_{LO}}\tag{9.144}$$

that differs by the factor $\frac{2\hbar\omega_{LO}}{k_BT}$ from the FHIP polaron mobility.

V. F. Los derived the polaron mobility [151] on the basis of the Kubo formula and the Bogoliubov technique of an exact elimination of the phonon operators. The mobility was obtained in Ref. [151] both in the weak-coupling approximation and using the Feynman polaron model. The weak-coupling expression given in Ref. [151] by formula (18) is the same as (9.140), i. e. three times larger than the Kadanoff polaron mobility.

The polaron mobility obtained in Ref. [151] using the Feynman polaron model, formula (36),

$$\mu^F=\frac{3e}{2\alpha}e^{\beta}\frac{e^{m_f/v}}{(m_f+1)^{3/2}}\tag{9.145}$$

differs from (9.144). However, the factor 3 with respect to the Kadanoff result is definitely present in (9.145).

The key distinction between the derivation of the polaron mobility in Refs. [151, 153], on the one hand, and in Refs. [65, 66, 63] is the relaxation-time approximation (RTA) (see Ref. [60]). The RTA consists in disregarding the contribution of the so called "re-population term"

(using terminology of Ref. [60]) in the kinetic equation. RTA is used in Refs. [65, 66, 63]. On the contrary, in Refs. [151, 153] there is no relaxation-time approximation. In Ref. [151], the parameter attributed to the relaxation time appears in a natural way quite rigorously. Moreover, in Ref. [153], the relaxation time does not appear at all.

The difference of the results by Los from the theory by Kadanoff and Osaka appears already at an intermediate stage. Los derived the evolution equation for the correlation function velocity-velocity $\langle v_\nu(0)\, v_\mu(\tau)\rangle$ [formula (9)], with the kernel function

$$\Gamma_\nu(\mathbf{p}) = 2\pi \sum_{\mathbf{k}} |V_{\mathbf{k}}|^2 \left(1 - \frac{v_\nu(\mathbf{p}-\mathbf{k})}{v_\nu(\mathbf{p})}\right) \times \{(1+N_{\mathbf{k}})\,\delta(T(\mathbf{p}) - T(\mathbf{p}-\mathbf{k}) - \omega_{\mathbf{k}}) + N_{\mathbf{k}}\delta(T(\mathbf{p}) - T(\mathbf{p}-\mathbf{k}) + \omega_{\mathbf{k}})\} \tag{9.146}$$

(the notations are in Ref. [151]).

The factor $[1 - v_\nu(\mathbf{p}-\mathbf{k})/v_\nu(\mathbf{p})]$ in the kernel function is an essential difference between the theory by Los and the theory by Osaka/Kadanoff. Without this factor, as checked in Ref. [151], the theory by Los would give the same result as the Kadanoff theory. This factor describes the change in the electron velocity in the electron-phonon scattering processes allowed by the energy and momentum conservation laws. It is important to note that in relaxation times of the kinetic equations corresponding to elastic scattering mechanisms (e. g., impurity scattering) or approximately elastic mechanisms (e. g., acoustic phonons), the factor $(1 - v'_\nu/v_\nu)$ is always present. In those kinetic equations, the second (subtracted) part, v'_ν/v_ν, comes from the aforesaid "re-population" term. This "re-population" term was neglected in Refs. [65, 66, 63]. It appears that the "re-population" term is in fact non-negligible. The analogous reasoning is developed in Ref. [153], where the "re-population" contribution to the kinetic equation is taken into account. It is shown in Ref. [153] that the neglect of the re-population term in the kinetic equation is an unwarranted approximation, because it *violates the particle number conservation*. The conclusions of Refs. [151, 153] are contrary to the assumption made in Refs. [65, 66, 63], where that term is neglected.

In Ref. [151], the expression (9.146) for $\Gamma_\nu(\mathbf{p})$ arises here from the rigorous microscopic treatment. It is important to note that such a relaxation time was introduced phenomenologically in 1939 in [156], but in subsequent studies the expression without the factor describing the change in the velocity was obtained.

In Ref. [156], the relaxation time has been phenomenologically defined by:

$$\frac{1}{\tau} = -\sum_{\mathbf{q}} \left(\frac{\Delta k}{k}\right)_x \phi_{\mathbf{q}}(\mathbf{k}) \tag{9.147}$$

where $\phi_{\mathbf{q}}(\mathbf{k})$ is the probability per unit time that an electron with the wave number $\mathbf{k}$ makes a collision with a lattice wave of wave number $\mathbf{q}$, and Δk is the average change of the x-component of the wave number k_x on each collision.

The factor

$$-\left(\frac{\Delta k}{k}\right)_x = \frac{k_x - k'_x}{k_x} = 1 - \frac{k'_x}{k_x}$$

entering (9.147) has exactly the same meaning as the factor $\left(1 - \frac{v_\nu(\mathbf{p}-\mathbf{k})}{v_\nu(\mathbf{p})}\right)$ which appears in the work by Los [151] and ensures the particle number conservation. Without this factor, the formula

$$\frac{1}{\tau} = \sum_{\mathbf{q}} W_{\mathbf{q}}(\mathbf{k}) \tag{9.148}$$

gives the result of Refs. [65, 66, 63]. With this factor, the derivation reproduced in Ref. [158] gives the same relaxation time and mobility as in Ref. [151].

In the paper by B. I. Davydov and I. M. Shmushkevich [157], the derivation of the mean free path and the electron mobility in ionic crystal is performed using the parameters of the medium which are not immediately measurable. Later, Born and Huang in their *Dynamical Theory of Crystal Lattices* [129] introduced the description of optical phonons and the electron-LO phonon interaction using only observable parameters, such as high-frequency and static dielectric constants. At present, these notations are of common use. In the monograph by A. Anselm [158], the theory by Davydov and Shmushkevich has been reproduced using these contemporary notations. The physics of the approach by Davydov and Shmushkevich is described in Ref. [158] in the following way.

"At low temperatures the scattering is inelastic, and, therefore, general the relaxation time cannot be introduced with the aid of Boltzmann equation ... However, as was demonstrated by B. I. Davydov and I. M. Shmushkevich in 1940, in the low-temperature case as well the relaxation time can be introduced, provided a correct calculation procedure is followed.

Qualitatively this can be explained as follows. At low temperatures, when $k_BT \ll \hbar\omega_0$ the absolute majority of the electrons are able only to absorb the phonons. Such absorption of a phonon results in the electron going over to the energy interval from $\hbar\omega_0$ to $2\hbar\omega_0$. Such an electron will immediately emit a phonon, because the ratio of the emission probability to the absorption probability is equal, according to (6.1), to $\frac{N_q+1}{N_q} \approx \exp\left(\frac{\hbar\omega_0}{k_BT}\right) \gg 1$. The variation of the electron energy in the result of such an absorption and an almost immediate emission of a phonon will be very small (only at the expense of the ω_0 vs q dependence), but the variation of wave vector will be substantial. This makes it possible to regard the electron scattering in a definite sense as elastic and to introduce the relaxation time."

Remarkably, the phenomenological definition (9.147) coincides with the Davydov-Shmushkevich formula for the inverse relaxation time. The resulting low-temperature relaxation time within the approach by Davydov and Shmushkevich is given by:

$$\tau = \frac{3\sqrt{2}}{2}\frac{\hbar^2\varepsilon^*}{e^2 m_b^{1/2}\left(\hbar\omega_0\right)^{1/2}}\exp\left(\frac{\hbar\omega_0}{k_BT}\right). \tag{9.149}$$

with ε^* defined through the high-frequency and static dielectric constants:

$$\frac{1}{\varepsilon^*} = \frac{1}{\varepsilon_\infty} - \frac{1}{\varepsilon_0}. \tag{9.150}$$

The mobility is expressed through the relaxation time in the standard way:

$$\mu = \frac{e}{m_b}\tau. \tag{9.151}$$

Hence the mobility is:

$$\mu = \frac{3\sqrt{2}}{2}\frac{\hbar^2\varepsilon^*}{e m_b^{3/2}\left(\hbar\omega_0\right)^{1/2}}\exp\left(\frac{\hbar\omega_0}{k_BT}\right). \tag{9.152}$$

Using the Fröhlich coupling constant α,

$$\alpha = \frac{1}{2\varepsilon^*}\frac{e^2}{\hbar\omega_0}\left(\frac{2m_b\omega_0}{\hbar}\right)^{1/2}, \tag{9.153}$$

the mobility is transformed to the expression

$$\mu = \frac{3e}{2m_b\alpha\omega_0}\exp\left(\frac{\hbar\omega_0}{k_BT}\right). \tag{9.154}$$

This result is three times larger than the mobility obtained by many authors, e. g., Kadanoff.

In the recent paper [159], the alternative representation has been found for the optical conductivity described by the Kubo formula. The treatment is based on the expression for the optical conductivity:

$$\sigma(z) = \frac{i}{zV}\left[\Pi(z) - e^2\Gamma\right] \qquad (z = \Omega + i\delta,\ \delta \to +0) \tag{9.155}$$

where V is the system volume, e is the electronic charge, $\Pi(z)$ is the current-current correlation function,

$$\Pi(z) = -i\int_0^\infty dt\ e^{izt}\left\langle\left[J(t), J(0)\right]\right\rangle \tag{9.156}$$

and the coefficient Γ is determined through the correlation function in the Euclidean time:

$$e^2\Gamma = -\int_0^\beta d\tau\left\langle J(\tau)\, J(0)\right\rangle, \qquad \beta = \frac{1}{k_B T}. \tag{9.157}$$

Here, the current operator is

$$J = -ev_x = -\frac{e}{m_b}p_x. \tag{9.158}$$

In the known expressions for the Kubo formula, Γ is given by explicit constants:

$$e^2\Gamma = -\frac{e^2}{m_b} \tag{9.159}$$

for a single electron with the band mass m_b (see, e. g., Ref. [50]).

In the memory-function representation, the polaron optical conductivity is given by formula (7) of Ref. [159]:

$$\sigma(z) = -\frac{i}{V}\frac{e^2\Gamma}{z + iM(z)}. \tag{9.160}$$

with the memory function $M(z)$. The equivalence relation (9.159) is important for the sum rule [82] due to the following reasons. On the one hand, it is easily checked by hand that the expression (8.77) explicitly satisfies the sum rule given by formula (6) of Ref. [159]:

$$\int_{-\infty}^{\infty}\mathrm{Re}\,\sigma(\Omega + i\delta)\, d\Omega = -\frac{\pi e^2\Gamma}{V}. \tag{9.161}$$

On the other hand, the polaron optical conductivity must satisfy the f-sum rule [82]:

$$\int_{-\infty}^{\infty}\mathrm{Re}\,\sigma(\Omega + i\delta)\, d\Omega = \frac{1}{V}\frac{\pi e^2}{m_b}. \tag{9.162}$$

Thus the relation (9.159) ensures the fulfilment of the f-sum rule for the polaron optical conductivity. When using exact polaron states, the integral in (9.157) gives analytically e^2/m_b. However, any approximation for the polaron states may violate (9.159) and consequently violate the f-sum rule.

The DC mobility of a Fröhlich polaron is obtained in Ref. [159] in the weak-coupling regime at low temperatures as $\mu = \frac{10}{3}\mu_{FHIP}$, i.e., the mobility differs by a numerical factor $10/3$ from the result of FHIP [47] and by $5k_BT/(\hbar\omega_0)$ from the value obtained by Kadanoff. Accounting for the above discussion, the fulfilment of the f-sum rule within the theory [159] and, consequently, the DC mobility need further verification.

In summary, the most reliable results for the mobility of a Fröhlich polaron are obtained in Refs. [151, 153]. It is proven in those works that the "re-population" term in the kinetic equation cannot be neglected, that leads to a significant change of the polaron mobility. Consequently, the results obtained in Refs. [151, 153] bring an important correction to the theory of the polaron response.

10 Pekar's Research in Electron Theory of Crystals, 1951

В монографии излагается новый метод теоретического рассмотрения электронов проводимости и локализованных электронов в ди9лектриках и полупроводниках с ионной кристаллической решёткой.

Монография рассчитана на читателя, владеющего основами квантовой механики и знакомого с электронной теорией кристаллов.

AUTHOR'S FOREWORD

В настоящей монографии даётся систематическое изложение работ автора по так называемой теории поляронов и теории локальных состояний электронов в полупроводниках и диэлектриках. Большая часть работ была выполнена в Институте Физики Академии наук УССР в период с 1944 г. по 1950 г. и публиковалась в виде кратких статей по мере их окончания. Некоторые же работы публикуются здесь впервые. В монографию включены также некоторые результаты сотрудников и аспирантов автора.

В монографии с единой точки зрения объясняется большой комплекс электрических, фотоэлектрических и оптических явлений, которые не получили удовлетворительного объяснения в обычной «зонной» теории электропроводности. Разработан новый математический аппарат, позволяющий в благоприятных случаях (когда параметры кристалла удовлетворяют определённым неравенствам) получать количественные результаты в численном согласии с опытом. Так, например, рассчитываются энергии тепловых диссоциаций носителей тока, форма спектра поглощения света и её температурная зависимость и пр. В неблагоприятных случаях, когда критерии применимости количественного рассмотрения нарушены, теория даёт лишь качественные результаты.

Предлагаемая теория приводит к представлениям, которые существенно отличаются от привычных представлений «зонной» теории. Например, инертная масса носителя тока оказывается зависящей от предельной частоты поляризационных колебаний ионов, от показателя преломления света в кристалле и от диэлектрической постоянной. Число колебательных степеней свободы ионов с появлением каждого носителя тока (полярона) сокращается на три. Свойства примесных

локальных состояний электронов с достаточно малой энергией тепловой диссоциации не зависят от природы примеси, а определяются параметрами полупроводника. Новые формулы получаются для подвижности носителей тока и т. д.

Сравнение теории с опытом оказалось благоприятным для теории. Однако оно должно быть распространено на гораздо большее число объектов и явлений. Этого пока не удалось сделать, поскольку полный комплект необходимых экспериментальных данных имеется всего лишь для десятка ионных кристаллов. Этот пробел должен быть восполнен работой экспериментаторов в тесном контакте с теоретиками.

В заключение считаю своим приятным долгом выразить глубокую благодарность Л. Д. Ландау за неоднократные весьма полезные дискуссии, постоянный интерес к работе и просмотр рукописи, А. Ф. Иоффе, И. В. Обреимову, Я. И. Френкелю, Н. Н. Боголюбову, И. Е. Тамму, Д. И. Блохинцеву за обсуждение отдельных результатов работы, а также коллективу моих сотрудников и аспирантов, имена которых указаны в тексте. Большое значение для меня имели замечания покойного акад. С. И. Вавилова.

10.1 I Introduction

10.1.1 1 Preliminary remarks

В течение последних двух-трёх десятков лет в технике широкое применение нашли кристаллы неметаллического типа - полупроводники и диэлектрики. Из электронных полупроводников изготовляются, например, твёрдые выпрямители тока, приборы, выполняющие функции многоэлектродных радиоламп, фотоэлементы и фотосопротивления с высокой чувствительностью в различных областях спектра, термоэлементы с большим коэффициентом полезного действия, люминофоры, кристаллические счётчики рентгеновских и радиоактивных лучей и пр. Интерес к полупроводниковым материалам в промышленности возрастает с каждым годом.

Применение неметаллических кристаллов в технике основано на использовании присущих им характерных свойств. Эти кристаллы обладают сравнительно большим электрическим сопротивлением, что даёт возможность создавать в них сильные электрические поля. В полупроводниках с пространственно неоднородным строением проводимость существенно зависит от величины и направления приложенного поля; на этом основано действие твёрдых выпрямителей. Сильная зависимость проводимости полупроводников от освещения и их еравнительно хорошая прозрачность позволяют изготовлять из них фотоэлементы и фотосопротивления. В то же время резкая зависимость электропроводности от температуры и большая термоэлектродвижущая сила дают возможность использовать полупроводники в термометрах и термоэлементах. Возрастание электропроводности под влиянием облучения кристалла рентгеновскими или радиоактивными лучами лежит

в основе действия кристаллических счётчиков. Окрашивание диэлектриков при облучении катодными лучами даёт возможность приготовлять осциллографические экраны «с памятью». В то время как в металлах вся поглощаемая световая энергия превращается в теплоту, многие диэлектрики возвращают значительную часть поглощённой световой энергии в виде люминесценции. Это даёт возможность изготовлять из них люминффоры. Широкое распространение получили полупроводниковые термоэлектронные катоды, обладающие малой термоэлектронной работой выхода и, следовательно, дающие большую эмиссию при сравнительно невысоких температурах. В отличие от металлов в полупроводниках концентрация свободных электронов проводимости мала; благодаря этому возникающий вблизи поверхности полупроводника в результате ионизации молекулы кристалла светом или катодными лучами быстрый электрон может со сравнительно малой потерей энергии доити до поверхности полупроводника и покинуть его. Этим объясняется наличие среди полупроводников эффективных фотокатодов и вторично-электронных эмиттеров. Светочувствительные соли, из которых изготовляются фотографические эмульсии, тоже принадлежат к числу диэлектриков. Приведённый выше перечень показывает, каково практическое значение кристаллов неметаллического типа, и объясняет всё возрастающий интерес к физике полупроводников и диэлектриков. Кроме того изучение этих кристаллов представляет большой научный интерес.

В течение последних тридцати с лишним лет накоплен огромный экспериментальный материал по электрическим, фотоэлектрическим, термоэлектрическим и оптическим явлениям в кристаллах. Раньше других и более полно были изучены щёлочно-галоидные кристаллы. Акад. А. Ф. Иоффе, совместно с В. К. Рентгеном была открыта фотопроводимость окрашенных щёлочно-галоидных кристаллов [30]. Вслед за этим Р. В. Полем и его школой, а также П. С. Тартаковским и его школой был подробно исследован внутренний фотоэффект в щёлочно-галоидных кристаллах. Эти работы пролили свет и на последующие исследования внутреннего фотоэффекта в

полупроводниках промышленного значения. Заслуги исследования люминесцентных и оптических свойств кристаллов принадлежат акад. С. И. Вавилову, И. В. Обреимову, В. Л. Лёвшину, Е. Ф. Гроссу, В. В. Антонову-Романовскому и др. Экспериментальному исследованию свойств полупроводников технического значения посвящено множество работ, в том числе работы А. Ф. Иоффе и А. В. Иоффе, В. Е. Лашкарёва, В. П. Жузе, Б. В. Курчатова, Н. Д. Маргулиса, С. М. Рывкина, В. И. Ляшенко, Ю. П. Маслаковца, И. К. Кикоина, Н. Д. Наследова, Б. М. Гохберга, С. Г. Калашникова, А. Н. Арсеньевой, Е. Г. Миселюка, Б. Т. Коломийца и др. Большое число исследований опубликовано и за границей.

Параллельно экспериментальным исследованиям развивалась теория. Современная теория электронных полупроводников может быть подразделена на две части: а) феноменологическую теорию и б) микротеорию состояний электронов в кристалле. Первая из них использует, например, общеизвестное уравнение электропроводности и диффузии «носителей тока»

$$I = -euN\frac{dV}{dx} - eD\frac{dN}{dx}, \tag{1.1}$$

где N-концентрация носителей тока, e - их заряд, u - подвижность, D - коэффициент диффузии, V - потенциал электрического поля, а I - плотность тока. Далее, характерным для феноменологической теории является уравнение Пуассона

$$\Delta V = -4\pi\rho(N), \tag{1.2}$$

где $p(N)$ - пространственная плотность заряда носителей тока. К феноменологической теории следует отнести зависимость концентрации носителе тока от температуры вида

$$N = Ae^{-\frac{W}{2kT}}, \tag{1.3}$$

где W - энергия тепловой диссоциации носителей тока (в случае теплового равновесия), и выражение для числа рекомбинаций носителей тока в единице объёма за секунду

$$z = \beta N N_1, \tag{1.4}$$

где β-коэффициент рекомбинации, а N_1 - концентрация центров рекомбинации. Приведённые выше уравнения можно назвать феноменологическими, поскольку при их обосновании

игнорируется механизм микропроцессов. Последнее видно уже из того, что эти уравнения имеют одинакоый вид, например для случая электронной и ионной проводимости, а также в случае газов, жидких и твёрдых тел. Лишь параметры теории u, D, A, W и β зависят от объекта.

Поскольку феноменологическая теория игнорирует механизм микропроцессов, она остаётся почти неизменной и в тех случаях, когда наши представления о микропроцессах терпят коренные изменения. Так, например, при появлении квантовомеханической электронной теории кристаллов вид уравнений (1.1)-(1.4) нисколько не изменился.

Феноменологическая теория полупроводников за последние 12 лет добилась значительных успехов. В 1938 г. Д. И. Блохинцевым и Б. И. Давыдовым было предложено качественное объяснение выпрямления тока в полупроводниках [1]. Почти одновременно С. И. Пекар дал количественную теорию выпрямителей с запирающими слоями [2]. Эта же теория была независимо предложена Н. Ф. Моттом в 1939 г. [3]. Теория довольно хорошо объяснила вольт-амперные характеристики выпрямителей с «химическими» запирающими слоями. Далее, на основе феноменологических уравнений (1.1)-(1.3) была построена теория контакта полупроводника с металлом как в случае

слабых токов (Б. И. Давыдов, Н. Ф. Мотт [4]), так и в случае сильных токов (С. И. Пекар, Шоттки и Шпенке [4]). Теория объяснила наблюдаемые на опыте приэлектродные сопротивления полупроводников и их вольт-амперные характеристики. Третьим примером использования феноменологических уравнений является теория кинетики фотопроводимости полупроводников, т. е. рассмотрение фотопроводимости и фото-э. д. с. в условиях импульсного освещения (С. М. Рывкин, В. П. Жузе, В. Е. Лашкарёв, К. Б. Толпыго [5]).

Однако только лишь феноменологическая теория совершенно недостаточна для полного и всестороннего изучения свойств кристаллов. Как мы уже указали, эта теория и круг ею описываемых явлений «не чувствительны» к механизму микропроцессов и, следовательно, не пригодны для изучения этих процессов. Кроме того феноменологическая теория обычно вынуждена вводить много материальных констант, например подвижность носителей тока, их коэффициент диффузии, энергию тепловой диссоциации носителей тока (а иногда и

несколько таковых), коэффициент рекомбинации, коэффициент поглощения света, квантовый выход внутреннего фотоэффекта и т. д. Эти константы не могут быть вычислены в рамках феноменологической теории. Поэтому они рассматриваются как неизвестные и взаимно независимые параметры, которые в лучшем случае определяются при сравнении теории с опытом. Иногда же число неизвестных параметров столь велико, что и согласие теории с опытом становится мало убедительным. В этих случаях роль феноменологической теории сводится лишь к схематизации и систематизации экспериментальных фактов.

Чтобы теоретически вычислить указанные выше материальные константы или установить связь между ними, необходимо глубоко вникнуть в механизм микропроцессов, протекающих в полупроводнике, в чём и заключается задача микротеории. Последняя развивалась на основе квантовой механики двадцать с лишним лет. Единственной популярной теорией является так называемая «зонная» теория, согласно которой состояния электронов проводимости в нулевом приближении описываются плоскими модулированными волнами, а энергетический спектр электронов состоит из чередующихся разрешённых и запрещённых зон. Ионы (атомы) кристаллической решётки в нулевом приближении совершают гармонические нормальные колебания, вид которых не зависит от присутствия в кристалле электронов проводимости. Таким образом, в нулевом приближении игнорируется взаимодействие между электронами и колебаниями решётки. Система распадается на две изолированные консервативные подсистемы: электроны проводимости и колебания решётки. Большинство явлений рассматривается в этом нулевом приближении. Лишь при вычислении коэффициента диффузии и подвижности электрона (которая в нулевом приближении оказывается бесконечной) вводится взаимодействие электронов проводимости с колебаниями ионов, как малое возмущение, что в первом приближении даёт рассеяние вышеупомянутых плоских модулированных волн.

«Зонная» теория несомненно является необходимым этапом в развитии электронной теории кристаллов. Однако следует признать, что за двадцать лет своего существования она не создала аппарата, позволяющего надёжно и достаточно точно вычислять материальные константы кристаллов и устанавливать

между ними связь. Удалось объяснить температурную зависимость подвижности электронов и порядок её величины. Что же касается энергий тепловых диссоциаций, формы спектра поглощения света примесями и основным веществом, квантового выхода внутреннего фотоэффекта, коэффициентов рекомбинации и пр., то теоретическое вычисление этих величин на основе зонной теории оказалось ненадёжным и очень часто даёт результаты, противоречащие опыту. Поэтому физики стараются не пользоваться

рассчитанными значениями указанных величин даже в тех случаях, когда отсутствуют опытные данные.

Не всегда от теории следует требовать точных количественных результатов. Иногда может представлять ценность и качественная теория, которая интерпретирует результаты экспериментов, вскрывает взаимную связь между явлениями и позволяет сознательно ставить дальнейшие опыты. Однако и с этими функциями зонная теория справляется плохо. Например, зонная теория не в состоянии интерпретировать тепловыделения при фотопереходе электрона (возбуждения большого числа квантов колебаний ионов при фотопереходе электрона). О количестве выделяющейся при этом теплоты можно судить на основании того факта, что наблюдающаяся энергия фотоперехода $h\nu$ иногда в полтора-два раза превышает энергию соответствующего теплового перехода W (см. § 31). Поскольку в зонной теории электроны и колебания решётки представляют собой две невзаимодействующие подсистемы, оптический переход электрона вовсе не должен был бы влиять на колебания решётки. Введение слабого взаимодействия между подсистемами, вызывающего рассеяние электронных волн, также не приводит теорию в согласие с опытом.

Руководствуясь зонной теорией, многие экспериментаторы стали на ложный путь построения энергетического спектра «электронной подсистемы» по частотам света, поглощаемого кристаллом. В действительности же энергия поглощаемого кванта света частично переходит в теплоту. На языке зонной теории это означает, что энергия поглощаемого кванта распределяется между двумя подсистемами. В качестве другого примера укажем на то, что зонная теория не объясняет зависимости спектра поглощения света в кристалле от температуры, а такая зависимость, и весьма значительная, наблюдается.

Следует также отметить, что с точки зрения зонной теории безизлучательные переходы электрона в кристалле, при которых энергия перехода, равная большому числу квантов колебаний решётки, выделяется в виде тепла, невероятны. Опыт же показывает, что такие переходы обладают значительной вероятностью.

Приведённые выше примеры далеко не исчерпывают трудностей, которые встречает обычная зонная теория при попытке качественного объяснения экспериментальных фактов. Таким образом, обычная зонная теория как количественная и даже как качественная теория не может быть признана удовлетворительпой. Укажем два её главных, принципиальных недостатка.

1. Многоэлектронная задача подменяется одноэлектронной (электрон рассматривается в периодическом потенциальном поле), что не во всех случаях может быть обосновано [10].

2. Взаимодействие электронов проводимости с колебаниями решётки рассматривается как малое возмущение. В действительности же у большинства кристаллов оно велико (больше других членов гамильтониана).

Касаясь первото из указанных недостатков, следует подчеркнуть, что в металлах замена многоэлектронной задачи одноэлектронной обычно оформляется как метод самосогласованного поля, применимость которого в условиях металла вызывает ряд сомнений [10]. Ниже, однако, речь идёт о движении «лишнего» электрона (электрона проводимости) в диэлектрике или полупроводнике. В этом случае, как будет показано в § 3 , при некоторых ограничивающих предположениях можно достаточно хорошо обосновать сведение задачи к рассмотрению одного электрона в периодическом поле.

Второй из указанных недостатков является существенным, особенно в кристаллах с ионной решёткой. Отмеченная выше несостоятельность обычной зонной теории при

попытке качественного объяснения тепловыделения при фотопереходе электрона, температурной зависимости спектра поглощения света, безизлучательных переходов электрона связана как раз со вторым, а не с первым недостатком.

В настоящей монографии рассматриваются состояния электронов проводимости в диэлектриках и полупроводниках с ионной кристаллической решёткой, а также локальные состояния электронов, играющие важную роль в электрических,

фотоэлектрических и оптических явлениях в этих кристаллах. Предлагаются новые методы рассмотрения электронов проводимости и локализованных электронов, которые позволяют существенно улучшить теорию и объяснить с елиной точки зрения большой комплекс явлений, не получивших удовлетворительной интерпретации в обычной зонной теории.

Излагаемая ниже теория учитывает диэлектрическую поляризацию ионного кристалла электрическим полем электрона проводимости. Возникающая при этом локальная поляризация связана со смещением ионов и, следовательно, инерционна. Она не может следовать за сравнительно быстро движущимся электроном и поэтому образует для электрона потенциальную яму. Глубина этой потенциальной ямы оказывается достаточной (для большинства кристаллов порядка $0,5-1$ эл.-в), чтобы в ней существовали дискретные энергетические уровни электрона. Электрон, находясь в локальном состоянии на одном из этих уровней, своим полем может поддерживать упомянутую выше локальную поляризацию кристалла. Вследствие свое инерционности ионы воспринимают не мгновенное, а среднее поле электрона. Последнее можно рассчитать как статическое поле $|\psi|^2$-облака электрона; оно создаёт статическую поляризационную потенциальную яму, которая в свою очередь стационарно поддерживает электрон в локальном состоянии. Такие состояния кристалла с поляризационной потенциальной ямой, в которой локализован электрон, были автором названы поляронами [12].

Потенциальная яма полярона вместе с осциллирующим в ней электроном может перемещаться по кристаллу в виде своеобразной поляризационной волны. Как показывают расчёты, у такой волны необычный закон дисперсии: энергия волны пропорциональна квадрату её скорости. В присутствии внешнего электрического поля полярон должен двигаться ускоренно, причём его ускорение пропорционально напряжению электрического поля (если последнее достаточно плавно изменяется в пространстве). Таким образом, полярон движется в кристалле подобно частице с зарядом электрона и с некоторой эффективной инертной массой, которая может во много раз отличаться от массы электрона.

Поляронные состояния системы оказались энергетически выгоднее, чем состояния с неполяризованным кристаллом и

свободным электроном, которые фигурируют в обычной зонной теории. Деполяризация кристалла и освобождение электрона могут произойти лишь в результате сравнительно редкой тепловой флуктуации. Поэтому подавляющее большинство электронов проводимости должно находиться в поляронном состоянии. Автор считает, что поляроны являются основными носителями тока в кристаллах [15], [17]. Утверждение, что электрон локализован в поляронной потенциальной яме, не означает, что этот электрон не принимает участия в электропроводности; оно означает только, что при каждой данной мгновенной конфигурации ионов, т. е. при каждом заданном положении поляризационной потенциальной ямы, электрон находится на дискретном энергетическом уровне и обладает ψ-функцией, отличной от нуля лишь в ограниченной области кристалла и экспоненциально затухающей по мере отдаления от этой области.

Следует подчеркнуть, что некоторые черты изложенной выше качественной картины отмечались и прежде советскими теоретиками в виде отдельных замечаний [6]. Так, в

1933 г. Л. Д. Ландау высказал важную идею об автолокализации электрона в идеальном кристалле в результате деформации решётки полем самого электрона. Эти локальные состояния предполагались неподвижными, и Л. Д. Ландау пытался их отождествить с F-центрами в окрашенных щёлочно-галоидных кристаллах. В 1936 г. Я. И. Френкель заметил, что электрон проводимости должен деформировать ближайшие к нему атомы кристалла и что эта локальная деформация должна перемещаться по кристаллу вслед за электроном. В 1936 г. Д. И. Блохинцев сделал попытку на основе приближения сильно связанных электронов выяснить, в каких кристаллах следует ожидать осуществления автолокализации электронов, указанной ранее Ландау. В то время не был найден правильный путь для рассмотрения автолокальных состояний, и поэтому не удалось доказать их существование и исследовать их свойства. Однако указанные статьи оказали определённое влияние на работы автора в этой области.

Данная выше качественная картина движения полярона в кристалле соответствует «полуклассическому» рассмотрению: движение электрона проводимости рассматривается квантовомеханически, а движение ионов - классически. В монографии

наряду с таким полуклассическим рассмотрением даётся и другое, в котором и движение ионов также рассматривается на основе квантовой механики. При этом получаются результаты, близкие к результатам полуклассического рассмотрения.

Тепловые колебания ионов приводят к небольшим деформационным колебаниям потенциальной ямы полярона около её равновесной формы. При этом локальное состояние электрона адиабатически «следует» за деформацией потенциальной ямы. Кроме того тепловые колебания ионов приводят к рассеянию упомянутых выше поляронных волн, в результате чего возникает конечный свободный пробег и постоянная подвижность поляронов (их движение подчиняется закону Ома).

Математический аппарат, развитый при рассмотрении электронов проводимости в I, II и III главах, затем легко обобщается и в IV и V главах применяется для рассмотрения локальных состояний электронов в F - и F'-центрах. Электроны взаимодействуют главным образом с продольными оптическими колебаниями ионов. В обычной зонной теории это взаимодействие предполагается малым возмущением, что было отмечено выше как основной недостаток этой теории, ибо в большинстве ионных кристаллов это взаимодействие велико. В поляронной же теории это взаимодействие не предполагается малым и включается в гамильтониан уже в нулевом приближении.

В монографии формулы нумеруются двумя цифрами: первая из них обозначает номер параграфа, вторая - номер формулы в пределах параграфа. Аналогично нумеруются рисунки и таблицы.

Изложение ведётся в терминах, соответствующих случаю полупроводников с электронной проводимостью. Однако все результаты могут быть дословно повторены для полупроводников с «дырочной» проводимостью.

10.1.2 § 2. Consequences arising from translational symmetry of crystals

В кристалле ядра атомов (или ионов) колеблются около некоторых положений равновесия. Для дальнейшего, однако, необходимо предварительно решить упрощённую абстрактную задачу. Именно, необходимо рассмотреть состояние электро-

нов в предположении, что ядра неподвижно закреплены в узлах кристаллической решётки. В этом случае в оператор энергии системы входят только координаты электронов. Введём обозначения для периодов решётки $\boldsymbol{a}_1, \boldsymbol{a}_2, \boldsymbol{a}_3$ и для «целочисленного вектора решётки»

$$m = m_1 a_1 + m_2 a_2 + m_3 a_3, \tag{2.1}$$

где m_1, m_2, m_3 - целые числа. Оператор энергии электронов H обладает трансляционной симметрией: он остаётся инвариантным, если к радиусам-векторам всех электронов одновременно прибавить $\boldsymbol{m}$. Трансляция какого-либо одного электрона не оставляет инвариантным оператор энергии вследствие наличия в нём энергии взаимодействия электронов

$$\sum_{i>j} \frac{e^2}{r_{ij}}.$$

Вышеупомянутую операцию трансляции всех электронов на вектор $\boldsymbol{m}$ обозначим $\mathbf{T}_{\boldsymbol{m}}$.

Совокупность таких операторов со всевозможными $\boldsymbol{m}$ образует коммутативную (абелеву) группу целочисленных трансляций. Применение оператора $\mathbf{T}_m$ к оператору энергии оставляет последний инвариантным, поэтому

$$\mathbf{T}_m \mathbf{H} = \mathbf{H} \mathbf{T}_m. \tag{2.2}$$

Таким образом, линейные операторы $\mathbf{T}_m$ коммутируют как между собой, так и с H. В этом случае, как известно, можно выбрать систему собственных функций оператора H так, чтобы они одновременно являлись собственными функциями всех операторов $\mathbf{T}_{\boldsymbol{m}}$. Если $\Psi_\alpha(\boldsymbol{r}_1, \ldots, \boldsymbol{r}_N)$ есть одна из таких функний, то

$$\mathbf{T}_m \Psi_\alpha = t_{m\alpha} \Psi_\alpha \tag{2.3}$$

где $t_{m\alpha}$ - собственное значение оператора $\mathbf{T}_m$. Иными словами, операция трансляции в применении к Ψ_α эквивалентна умножению на постоянный множитель. Нормировка Ψ_a при трансляционном преобразовании, очевидно, сохраняется, так как последнее эквивалентно параллельному переносу координатных осей в нормировочном интеграле. Поэтому

$$|t_{m\alpha}| = 1 \tag{2.4}$$

Не нарушая общности, можно собственные значения операторов

$$\mathbf{T}_{\boldsymbol{a}_1}, \mathbf{T}_{\boldsymbol{a}_2} \text{ и } \mathbf{T}_{\boldsymbol{a}_3} \tag{2.5}$$

записать соответственно в виде

$$e^{ik_\alpha \alpha_1}, e^{ik_\alpha \alpha_2} \text{ и } e^{ik_\alpha a_3}, \tag{2.6}$$

где $\boldsymbol{k}_\alpha$ - постоянный вектор, выбор которого можно ограничить неравенствами

$$\left.\begin{aligned} -\pi \leqslant \boldsymbol{k}_\alpha \boldsymbol{a}_1 \leqslant \pi, \\ -\pi \leqslant \boldsymbol{k}_\alpha \boldsymbol{a}_2 \leqslant \pi, \\ -\pi \leqslant \boldsymbol{k}_\alpha \boldsymbol{a}_3 \leqslant \pi. \end{aligned}\right\} \tag{2.7}$$

Произвольную трансляцию на вектор $\boldsymbol{m}$ можно осуществить рядом последовательных трансляций на векторы $\boldsymbol{a}_1, \boldsymbol{a}_2$ и $\boldsymbol{a}_3$:

$$\mathbf{T}_m = (\mathbf{T}_{\boldsymbol{a}_i})^{m_s} (\mathbf{T}_{\boldsymbol{a}_2})^{m_2} (\mathbf{T}_{\boldsymbol{a}_1})^{m_{i_1}}. \tag{2.8}$$

Собственное значение этого оператора является соответствующим произведением величин (2.6):

$$t_{m\alpha} = e^{it_\alpha m}. \tag{2.9}$$

Таким образом,

$$\mathbf{T}_m \Psi_\alpha = e^{ik_\alpha m} \Psi_\alpha. \tag{2.10}$$

Оператор $\mathbf{T}_{\boldsymbol{m}}$ не является самосопряжённым, тем не менее легко показать, что его собственные функции, принадлежащие различным собственным значениям, ортогональны.

Функция Ψ_α содержит столько квантовых чисел, сколько степеней свободы имеет система. В качестве трёх квантовых чисел удобно выбрать собственные значения (2.6) или же соответствующий вектор $\boldsymbol{k}$. Остальное множество квантовых чисел обозначим многомерным индексом β. При этом

$$\Psi_\alpha = \Psi_{\beta\kappa_\alpha}. \tag{2.11}$$

Рассмотрим функцию

$$e^{\frac{i}{\hbar}\sum_{j=1}^{N} p_j r_j} \tag{2.12}$$

с постоянными вещественными $\boldsymbol{p}_j$. Она является собственной функцией оператора $\mathbf{T}_m$ и принадлежит собственному значению e^{ikm}, где

$$k = \frac{1}{\hbar}\sum_{j=i}^{N} p_j + 2\pi g. \tag{2.13}$$

Вдесь $\boldsymbol{g}$ - целочисленный вектор обратной решётки, т. е. такой вектор, у которого произведения ga_1, ga_2 и ga_3 - целые числа. Его следует выбрать так, чтобы вектор $\boldsymbol{k}$ оказался в пределах (2.7).

Предполагая полноту системы функций $\Psi_{\beta k}$, можно положить

$$e^{\frac{i}{\hbar}\sum_{j=1}^{N} p_j r_j} = \sum_\beta C_\beta \Psi_{\beta k} \tag{2.14}$$

Здесь суммирование ведётся только по β, но не по $\boldsymbol{k}$, поскольку в это разложение входят только Ψ_β, принадлежащие, как и раскладываемая функция, собственному значению (2.13); другие $\Psi_{\beta s}$ в разложение войти не могут вследствие ортогональности собственных функций оператора $\mathbf{T}_m$. Из (2.13) и (2.14) вытекают следующие выводы:

1. Поскольку $\boldsymbol{p}_j$ могут быть произвольно выбраны, вектор $\boldsymbol{k}$ должен иметь обязательно непрерывный спектр значений в пределах (2.7).

2. В разложении (2.14) содержится, вообще говоря, бесконечное число членов. Следовательно, для каждого фиксированного k существует бесконечное число состояний с различными значениями энергии и других квантовых чисел.

Функция (2.12) является собственной функцией оператора импульса системы. Она принадлежит собственному значению импульса

$$P = \sum_{j=1}^{N} p_j. \tag{2.15}$$

Рассмотрим разложение

$$\Psi_{\beta k} = \sum_{p_1,\ldots,p_N} B_{p_1,\ldots,p_N} e^{\frac{i}{n}\sum_{j=1}^{N} p_j r_j}. \tag{2.16}$$

Здесь $|B_{p_1},\ldots,p_N|^3$ есть вероятность того, что в стационарном состоянии $\Psi_{\beta k}$ значения импульсов окажутся равными p_j. Левая часть (2.16) и каждый член правой части являются собственными функциями оператора $\mathbf{T}_m$ и должны принадлежать одному и тому же собственному значению этого оператора. Следовательно, в это разложение войдут только члены, для которых выполняется соотношение (2.13). Таким образом, в состоянии Фвь импульс не имеет определённого значения; его возможные значения образуют прогрессию

$$P = \hbar k - 2\pi\hbar g, \tag{2.17}$$

где g принимает значения, при которых ga_1, ga_2 и ga_3 целые числа.

10.1.3 § 3. Qualitative study of the states of electrons in a semiconductor with fixed ions

Как и в предыдущем параграфе, предположим, что ядра атомов закреплены в узлах решётки. Решение многоэлектронной задачи Шрёдингера в случае кристалла связано с огромными математическими трудностями. До сего времени эта задача не только не решена, но в общем случае не удаётся даже грубо схематизировать энергетический спектр электронов. Для дальнейшего, однако, понадобится лишь качественное исследование частного случая: диэлектрика, в который дополнительно введён один электрон. Этот электрон может быть введён в кристалл извне или же получен в результате ионизации одной из молекул диэлектрика (либо примеси, присутствующей в диэлектрике). В последнем случае предполагается, что электрон достаточно далеко удалился от покинутого им положительного иона и более с ним не взаимодействует. Появление таких лишних электронов в диэлектрике превращает его в полупроводник. Эти электроны и называются электронами проводимости. В дальнейшем предполагается, что концентрация электронов проводимости настолько мала, что можно пренебречь их кулоновским взаимодействием и считать, что все они движутся в идеальном диэлектрике независимо друг от друга.

Основное состояние диэлектрика, как известно, всегда соответствует дискретному уровню энергии системы. Предположим, что этот уровень лежит значительно ниже всех осталь-

ных уровней, т. е. для возбуждения диэлектрика необходима значительная энергия. При не слишком высоких температурах можно считать, что диэлектрик всегда находится в основном состоянии. Обычно основное состояние диэлектрика не вырождено. Изредка, однако, встречаются исключения из этого правила. Так, существуют кристаллы, вращающие плоскость поляризации света по часовой стрелке, и кристаллы того же вещества, вращающие плоскость поляризации против часовой стрелки (например, правовращающий и левовращающий кварцы). Здесь мы сталкиваемся, повидимому, с двумя совершенно равноправными симметричными состояниями кристалла, обладающими одинаковой энергией. Оба эти состояния являются основными. Переход целого кристалла из одного такого основного состояния в другое невероятен. Поэтому правовращающий и левовращающий кристаллы можно рассматривать как два разных кристалла, каждый из которых обладает одним единственным основным состоянием.

Приступая к исследованию энергетического спектра полупроводника, рассмотрим сначала два частных случая. Полученные при этом результаты значительно помогут ориентироваться и в общем случае.

Случай А. Предположим, что в диэлектрике электроны достаточно сильно связаны с ядрами и что их состояние адиабатически следует за сравнительно медленным движением электрона проводимости [7]. Иными словами, предположим, что для каждого мгновенного положения электрона проводимости r успевает установиться стационарное состояние остальных электронов диэлектрика. Очевидно, что как ψ-функция, так и энергия этих остальных электронов будут зависеть от $\boldsymbol{r}$, как от параметра. Электронная часть диэлектрической поляризации будет «безинерционно» следовать за движением электрона проводимости (критерий случая А будет приведён ниже).

В этом случае задача Шрёдингера решается в два этапа. Сначала находится состояние остальных электронов в предположении, что электрон проводимости закреплён в точке r. Для этого необходимо решить уравнение

$$\begin{aligned}\left[\mathrm{H}_a\left(r_1,\ldots,r_N\right)+U\left(r,|r_1-r| \ ,\ldots,|r_N-r|\right)\right]\Phi\left(r,r_1,\ldots,r_N\right)= \\ =W(r)\Phi\left(r,r_1,\ldots,r_N\right).\end{aligned}$$

Здесь r - параметр, $\mathbf{H}_d$ - оператор энергии диэлектрика в отсутствии электрона проводимости, U - энергия взаимодействия электрона проводимости со всеми остальными электронами и ядрами. В дальнейшем предполагается, что Φ есть основное состояние диэлектрика (возмущённое электроном проводимости, помещённым в точку r). $W(r)$ есть полная энергия кристалла, когда электрон проводимости зафиксирован в точке r.

При медленном перемещении электрона проводимости на расстояние $d\boldsymbol{r}$ необходимо затратить работу, которая согласно закону сохранения энергии должна быть равна изменению энергии системы

$$dW(r)=\nabla W dr. \tag{3.2}$$

Отсюда следует, что на электрон со стороны кристалла действует сила - ∇W и что $W(\boldsymbol{r})$ играет роль потенциальной энергии электрона проводимости в кристалле.

Если переместить электрон проводимости на целочисленный вектор решётки m, то в силу трансляционной симметрии кристалла его новое положение будет совершенно эквивалентно старому. При таком перемещении энергия кристалла не должна измениться:

$$W(r+m)=W(r). \tag{3.3}$$

Таким образом, потенциал электрона проводимости обладает периодами кристалла.

Вторым этапом решения задачи является рассмотрение движения электрона проводимости. Движение электрона проводимости описывается уравнением

$$\left[-\frac{\hbar^2}{2m}\Delta+W(\boldsymbol{r})\right]\psi(\boldsymbol{r})=E\psi(\boldsymbol{r}), \tag{3.4}$$

где E - полная энергия системы. Это есть уравнение движения электрона в поле с периодическим потенциалом $W(\boldsymbol{r})$.

В левой части уравнения (3.4) стоит оператор, который остаётся инвариантным при трансляции электрона на вектор $\boldsymbol{m}$. Из этого следует согласно § 2 , что его решения можно выбрать так, чтобы они одновременно являлись собственными функциями оператора $\mathbf{T}_{\boldsymbol{m}}$:

$$\mathbf{T}_m\psi_k(r)=e^{ikm}\psi_k(r) \tag{3,5}$$

(так называемая теорема Блоха). Не нарушая общности, можно положить

$$\psi_k=U_k(r)e^{ikr} \tag{3.6}$$

Из (3.5) следует, что $U_k(r)$ - периодическая функция и обладает периодами кристалла. Уравнение (3.4) точно решить не удаётся не только вследствие математических трудностей, но и потому, что функция $W(\boldsymbol{r})$ точно не известна.

В литературе опубликован ряд качественных исследований движения электрона в периодическом поле и рассмотрены различные частные случаи [8]. Обобщая результаты упомянутых исследований, можно заключить, что:
а) из всех квантовых чисел, входящих в $\psi_k(r)$, вектор k является единственным непрерывным квантовым числом; все остальные - дискретны;
б) как ψ_k, так- и соответствующая энергия E_k являются аналитическими функциями $\boldsymbol{k}$. Таким образом, каждая группа уровней, у которых все дискретные квантовые числа одинаковы, но различны k, образует непрерывную энергетическую зону.

Состояние всей системы в адиабатическом приближении [7] даётся произведением

$$\Psi_{\beta k} = \Phi\left(r, r_1, \ldots, r_N\right) U_{\beta k}(r) e^{ikr} \tag{3.7}$$

где β-совокупность дискретных квантовых чисел. Эту функцию, конечно, необходимо подвергнуть общеизвестным операциям симметризации и антисимметризации.

Функция Φ по соображениям, развитым в § 2 , тоже должна быть собственной функцией оператора $\mathbf{T}_{\boldsymbol{m}}$. Поскольку выше предполагалось, что основное состояние диэлектрика не вырождено, Φ должна быть вещественна (в противном случае Φ^* была бы вторым решением с той же энергией). Такая функция в результате действия оператора $\mathbf{T}_{\boldsymbol{m}}$ может умножаться лишь на $+1$ или на -1 . Следовательно, $\Psi_{\beta k}$ также является собственной функцией оператора $\mathbf{T}_m$ и принадлежит собственному значению

$$\pm e^{ikm}.$$

Для определённости положим здесь знак $+$. Таким обра-
зом, вектор k следует отождествить с соответствующим вектором, введённым в § 2.

Случай Б. Общеизвестное «предположение сильно связанных электронов» [8] заключается в том, что молекулы кристалла в нулевом приближении рассматриваются как молекулы соответствующего газа, взаимодействие между молекулами считается малым возмущением; ψ-функция кристалла в нулевом приближении задаётся как антисимметризованное произведение ψ-функций отдельных молекул.

Если в диэлектрический кристалл введён дополнительно «лишний» электрон, то предполагается, что он локализуется у одной из молекул, обрацая её в отрицательный ион. Если лишний электрон локализовался в молекуле, расположенной в начале координат, то ψ-функция нулевого приближения запишется в виде

$$\Psi_{0\beta} = \sum_{\lambda} (-1)^{\lambda} \mathbf{P}_{\lambda} \prod_{n \neq 0}^{\prime} \Psi_n\left(r_n\right) \varphi_{0\beta}\left(r_0\right), \tag{3.8}$$

где ψ_n - волновая функция основного состояния молекулы, расположенной в узле решётки с радиусом-вектором n, r_n - совокупность координат электронов, принадлежащих этой молекуле, эов - волновая функция β-состояния отрицательного иона, $\mathbf{P}_{\lambda}$ - оператор перестановки электронов.

Помещая лишний электрон в различные узлы решётки, можно построить множество аналогичных решений, которые все соответствуют одинаковой энергии системы. Все эти взаимно вырожденные решения можно получить, применяя оператор трансляции $\mathbf{T}_{\boldsymbol{m}}$ к $\Psi_{0\,\mathrm{o}}$: для случая, когда в ион превращается молекула, расположенная в узле $\boldsymbol{m}$, решение можно записать в виде

$$\Psi_{m\beta} = \mathbf{T}_m \Psi_{0\beta} \tag{3.9}$$

Тогда ψ-функция кристалла в нулевом приближении представляет собой линейные комбинации функций (3.9). Коэффициенты этих линейных комбинаций однозначно определяются из соотношений (2.3) и (2.9). В результате получается

$$\Psi_{\beta k} = C \sum_m e^{ikm} \Psi_{m\beta} \tag{3.10}$$

Используя эту функцию как ψ-функцию нулевого приближения, можно вычислить энергию системы в первом приближении. Ограничиваясь простейшим случаем ортогональной решётки, получим:

$$E_{\beta k} = \int \Psi^*_{\beta k} \mathbf{H} \Psi_{\beta k} d\tau d\tau_1 \ldots d\tau_N = E_\beta + \\ + \sum_{m=\boldsymbol{a}_k, \boldsymbol{a}_2, \boldsymbol{a}_s} 2\mathbf{H}_{m\beta} \cos k\boldsymbol{m}, \tag{3.11}$$

где

$$H_{m\beta} = \int \Psi_{m\beta} \mathbf{H} \Psi_{0\beta} d\tau d\tau_1 \ldots d\tau_N \tag{3.12}$$

а E_β - постоянная, не зависящая от $\boldsymbol{k}$. Здесь предполагается, что достаточно учесть взаимодействие лишь между соседними молекулами, т. е. что $H_{m\xi}$ значительно только, если $|m|_\dagger$ равен постоянной решётки.

Рассмотренные случаи А и Б являются, каждый в своём роде, предельными случаями. В реальных кристаллах они встречаются сравнительно редко. Однако, обобщая результаты, полученные в этих предельных случаях, можно сделать ряд важных для дальнейшего выводов качественного характера, которые, повидимому, будут справедливы для большинства реальных кристаллов. Именно:

1. Энергетический спектр диэлектрика, в который дополнительно введён электрон проводимости, начинается непрерывной зоной. Единственным непрерывно меняющимся квантовым числом в этой зоне является вектор k, введённый в § 2. Остальные квантовые числа β дискретны и зафиксированы на своих значениях, соответствующих самой нижней энергетической зоне.

2. $\Psi_{\beta k}$ и $E_{\beta k}$ являются аналитическими функциями k во всём интервале его изменения (2.7).

3. Предполагается, что в основном состоянии ток отсутствует и ψ-функция вещественна. В результате действия оператора трансляции на такую функцию она умножается на ± 1. Следовательно, в основном состоянии

$$\left.\begin{aligned} \boldsymbol{k}a_1 &= 0 \text{ или } \pi, \\ \boldsymbol{k}a_2 &= 0 \text{ или } \pi, \\ \boldsymbol{k}a_3 &= 0 \text{ или } \pi. \end{aligned}\right\} \tag{3.13}$$

4. $\Psi^*_{\beta k}$, так же как и $\Psi_{\beta k}$, является собственной функцией операторов $\mathbf{H}$ и $\mathbf{T}_{\boldsymbol{m}}$. В результате действия оператора $\mathbf{T}_{\boldsymbol{m}}$, $\Psi^*_{\boldsymbol{\beta k}}$ умножается на e^{-ikm}. Следовательно,

$$\Psi^*_{\beta k} = \Psi_{\beta, -k\bullet} \tag{3.14}$$

Эта функция принадлежит тому же собственному значению энергии, что и $\Psi_{\beta l}$. Таким образом,

$$E_{\beta k} = E_{\beta,-k}, \tag{3.15}$$

т. е. энергия является чётной функцией k.
5) $\Psi_{\beta j}$ представляет волнообразное движение в кристалле некоторого «ионного состояния», причём $\boldsymbol{k}$ играет роль волнового вектора плоской волны.

Следует иметь в виду, что выводы, сделанные в этом параграфе, справедливы лишь до тех пор, пока энергия возбуждения системы (кристалла с «лишним» электроном) остаётся меньше, чем энергия, необходимая для возбуждения соответствующего диэлектрика. В противном случае энергетические уровни рассмотренных выше состояний перекроются с уровнями других состояний кристалла, в которых молекулы диэлектрика возбуждены. При этом появится добавочное вырождение, которое нами не учитывалось и которое существенно усложняет даже качественное рассмотрение состояний. Речь идёт о случае, когда электрон проводимости обладает достаточной энергией, чтобы возбуждать молекулы диэлектрика, т. е. когда взаимодействие электрона проводимости с диэлектриком носит «неупругий» характер. В этом случае не может быть и речи о том, что состояние диэлектрика адиабатически «следует» за движением электрона проводимости (случай А). Метод возмущений, применённый в случае Б, также становится непригоден вследствие упомянутого перекрытия энергетических уровней.

10.1.4 § 4. Effective mass method

В дальнейшем предстоит неоднократно рассматривать состояния полупроводника, в котором присутствует добавочное внешнее электрическое поле. Волновое уравнение для кристалла с «лишним» электроном в отсутствие добавочного

поля имеет вид

$$\mathbf{H}\Psi_{\beta k} = E_{\beta k}\Psi_{\beta k}. \tag{4.1}$$

При наличии добавочного поля уравнение принимает вид

$$\left[\mathrm{H} + \sum_{j=i}^{N} V\left(\boldsymbol{r}_j\right) + V(\boldsymbol{r})\right]\Psi = E\Psi, \tag{4.2}$$

где V - потенциал добавочного поля. Предположим, что поле $V(\boldsymbol{r})$ значительно меньше микрополя, а также, что $V(\boldsymbol{r})$ есть плавная функция (относительно мало изменяющаяся на расстояниях порядка постоянной решётки). Точно решить это уравнение, рассматривая кристалл как многоэлектронную систему, практически невозможно. Решить уравнение (4.2) обычными методами теории возмущений (рассматривая его как возмущённое уравнение (4.1)) тоже нельзя. Дело в том, что функции $\Psi_{\beta t}$ принадлежат непрерывному спектру, что в данном случае делает метод «малых возмущений» непригодным. Кроме того решения невозмущённого уравнения (4.1) также неизвестны.

Развиваемый ниже метод эффективной массы даёт возможность, не зная решений уравнений (4.1) и (4.2), при некоторых ограничивающих предположениях получить ряд важнейших количественных результатов, рассмотрев другую, несравненно более простую задачу: движение одной частицы в поле $V(\boldsymbol{r})$.

Дадим обосиование этого метода в случае А (см. § 3), поскольку именно с этим случаем в дальнейшем придётся иметь дело. Как и в § 3, предположим, что состояние

электронов диэлектрика адиабатически «следует» за движением электрона проводимости. Первый этап решения задачи сводится к нахождению состояния электронов диэлектрика в предположении, что электрон проводимости закреплён в точке $\boldsymbol{r}$. Соответствующее волновое уравнение получается из (3.1), если в это уравнение в качестве малого возмущения добавить потенциал добавочного поля

$$\sum_{j=1}^{N} V\left(\boldsymbol{r}_j\right). \tag{4.3}$$

Поскольку невозмущённое основное состояние диэлектрика принадлежит дискретному энергетическому уровню, который

согласно сделанному предположению лежит значительно ниже всех остальных уровней, то в данном случае применим обычный метод малых возмущений. Возмущение (4.3) вызывает малую диэлектрическую поляризацию кристалла. Связанное с ней изменение энергии обозначим W_p. Поскольку $V\left(\boldsymbol{r}_j\right)$ - плавная функция, энергию поляризации можно рассчитать обычными методами макроскопической электростатики.

Благодаря сильной связи электронов с ядрами линейный закон поляризации справедлив в широких пределах. В этом случае энергия поляризации W_p будет такой же, как и в отсутствии закреплённого электрона проводимости. Следовательно, W_p не зависит от r (от положения точки закрепления электрона проводимости). Полная энергия системы в присутствии закреплённого электрона проводимости и внешнего поля имеет вид

$$W(\boldsymbol{r}) + W_p. \tag{4.4}$$

Здесь W_p - константа, а $W(r)$ - энергия кристалла, не возмущённого внешним полем; она представляет собой собственное значение энергии в уравнении (3.1) и обладает периодичностью кристалла (см. случай А в § 3).

Вторым этапом решения задачи в адиабатическом приближении является рассмотрение движения электрона проводимости, для которого энергия (4.4) играет роль потенциальной энергии. Состояние электрона проводимости определяется из уравнения

$$\left[-\frac{\hbar^2}{2m}\Delta + W_p + W(\boldsymbol{r}) + V(\boldsymbol{r})\right]\psi(\boldsymbol{r}) = E\psi(\boldsymbol{r}). \tag{4.5}$$

Это уравнение отличается от (3.4) добавочными членами W_p и $V(\boldsymbol{r})$. Добавочное поле $V(\boldsymbol{r})$ следует понимать уже ослабленным благодаря диэлектрической поляризации кристалла, т. е. уже делённым на диэлектрическую постоянную.

Прежде чем приступить к решению этого уравнения, необходимо провести некоторые предварительные исследования. В дальнейшем речь будет итти о самой низкой зоне энергий уравнения (3.4), и в этом случае индекс β будет опускаться. Как было отмечено в § 3 , собственное значение энергии

в уравнении (3.4) является аналитической чётной функцией k в области

$$-\frac{\pi}{a_i} \leqslant k_i \leqslant \frac{\pi}{a_i} \quad (i = 1, 2, 3) \tag{4.6}$$

(предполагается, что $\boldsymbol{a}_1, \boldsymbol{a}_2$ и $\boldsymbol{a}_3$ взаимно ортогональны).
Предположим, что функция $E_k = E(k)$ имеет минимум в точке $\boldsymbol{k} = 0$, что действительно имеет место во всех рассмотренных примерах [8]. Разложение такой функции по степеням k_i вблизи точки $k = 0$ должно иметь вид

$$E_k = E^0 + \frac{\hbar^2}{2\mu_1}k_1^2 + \frac{\hbar^2}{2\mu_2}k_2^2 + \frac{\hbar^2}{2\mu_3}k_3^2 + \ldots \tag{4.7}$$

где постоянные коэффициенты μ_1, μ_2 и μ_8 принято называть эффективными массами электрона соответственно в направлениях $\boldsymbol{a}_1, \boldsymbol{a}_2, \boldsymbol{a}_3$. Для кристаллов с кубической симметрией $\mu_1 = \mu_2 = \mu_B = \mu$.

Решение уравнения (3.4) согласно § 3 имеет вид

$$\psi_k = U_k(r)e^{ikr}, \tag{4.8}$$

где $U_k(r)$ - периодическая функция с периодами, равными периодам кристалла. Из условия нормировки ψ_k следует для U_v соотношение

$$\int U_k^* U_k d\tau = 1 \tag{4.9}$$

Наряду с уравнением (3.4) рассмотрим уравнение

$$\mathcal{H}\varphi(\boldsymbol{r}) = E'\varphi(\boldsymbol{r}), \tag{4.10}$$
$$\mathcal{H} = E^0 - \frac{\hbar^2}{2}\left(\frac{1}{\mu_1}\frac{\partial^2}{\partial x^2} + \frac{1}{\mu_2}\frac{\partial^2}{\partial y^2} + \frac{1}{\mu_3}\frac{\partial^2}{\partial z^2}\right),$$

где E^0 и μ_i те же, что и в формуле (4.7). Решение этого уравнения имеет вид

$$\varphi_k(r) = \frac{1}{L^{2/3}}e^{ikr},$$
$$E'_k = E^0 + \frac{\hbar^2}{2\mu_1}k_1^2 + \frac{\hbar^2}{2\mu_2}k_2^2 + \frac{\hbar^2}{2\mu_3}k_3^2, \tag{4.11}$$

где L^3 - объём «основной области», в которой ψ_k и φ_k нормированы. Спектры величин $\boldsymbol{k}$ и $\boldsymbol{E_k}$ удобно сделать квазидискретными, наложив на φ_k и ψ_k обычное условие периодичности с большими периодами L. Таким образом, спектры собственных значений энергии в уравнениях (3.4) и (4.10) при малых $\boldsymbol{k}$ совпадают с точностью до членов порядка $\boldsymbol{k}^4$.

Рассмотрим матричный элемент какой-либо плавной функции r (мало изменяющейся на расстояниях порядка постоянной решётки), например $V(\boldsymbol{r})$:

$$V_{k'k} \equiv \int \Psi_{k'}^* V(\boldsymbol{r})\Psi_k d\tau d\tau_1 \dots d\tau_N =$$
$$= \int \mid \Phi^2 d\tau_1 \dots d\tau_N \cdot \int U_{k'}^* U_k e^{i(k_k - k')r} V(\boldsymbol{r}) d\tau =$$
$$= \int U_{k'}^* U_k e^{i(k_k - k')r} V(\boldsymbol{r}) d\tau \tag{4.12}$$

Предположим, что вектор $\boldsymbol{k}$ - $\boldsymbol{k}'$ достаточно мал и экспоненциальная функция является такой же плавной, как и $V(\boldsymbol{r})$. В этом случае можно в (4.12) с большой точностью вынести периодическую быстро осциллирующую функцию $U_{k'}^* U_k$ за знак интеграла:

$$V_{k'k} \cong \overline{U_{k'}U_k} \int e^{i(k-k')r} V(\boldsymbol{r}) d\tau \tag{4.13}$$

$$\overline{U_{k'}U_k} = \frac{1}{L^3}\int_{I^3} U_{k'}^* U_k d\tau \tag{4.14}$$

Разложим эту величину в ряд по степеням $\boldsymbol{k}' - \boldsymbol{k}$:

$$\overline{U_{k'}U_k} = \frac{1}{L^3}\int_{L^s}\left[U_k^* + (k'-k)\,\nabla_k U_k^* + \ldots\right]U_k d\tau \tag{4.15}$$

∇_k означает градиент в k-пространстве. В этом разложении линейные члены после интегрирования должны исчезнуть. Действительно, заметим, что рассматриваемые кристаллы обладают центральной симметрией. Следовательно, оператор энергии в уравнении (3.4) остаётся инвариантным в результате центрального преобразования $\mathbf{C}$, заменяющего $\boldsymbol{r}$ на - $\boldsymbol{r}$. Применяя преобразование $\mathbf{C}$ к обеим частям уравнения (3.4), можно непосредственно убедиться в том, что если $\psi_k(\boldsymbol{r})$ есть решение этого уравнения, то

$$\mathrm{C}\psi_k(r) = \psi_k(-r) \tag{4.16}$$

также является решением уравнения (3.4) и принадлежит тому же собственному значению энергии, что и $\Psi_k(r)$.

Оператор $\mathbf{C}$ не коммутирует с оператором $\mathbf{T}_m$. Легко убедиться в том, что

$$\mathbf{T}_m\mathbf{C} = \mathbf{C}\mathbf{T}_{-m}. \tag{4.17}$$

Так как

$$\mathbf{T}_m\psi_k(\boldsymbol{r}) = e^{ikm}\psi_k(\boldsymbol{r}), \tag{4.18}$$

то с помощью (4.17) получается

$$\mathbf{T}_m\mathbf{C}\psi_k = \mathbf{C}\mathbf{T}_{-m}\psi_k = \mathbf{C}e^{-ikm}\psi_k = e^{-ikm}\mathbf{C}\psi_k. \tag{4.19}$$

Следовательно, C ψ_k является собственной функцией не только оператора энергии, стоящего в уравнении (3,4), но и оператора $\mathbf{T}_m$ и принадлежит собственному значению e^{-ikm}; её следует отождествить с $\psi - k$:

$$\mathrm{C}\psi_k = \psi_{-k} = \psi_k^* \tag{4.20}$$

(ср. (3.14)). Из (4.8) и (4.20) получается

$$\mathbf{C}U_k(r) = U_k^*(r). \tag{4.21}$$

Пользуясь правом замены переменных $\boldsymbol{r} \to -\boldsymbol{r}$ в определённом интеграле и используя (4.21), приходим к соотношению

$$\int\left(\nabla_k U_k^*\right)U_k d\tau = \int\left(\nabla_k \mathbf{C}U_k^*\right)\mathbf{C}U_k d\tau = \\ = \int\left(\nabla_k U_k\right)U_k^* d\tau \tag{4.22}$$

С другой стороны, дифференцируя (4.9) по $\boldsymbol{k}$, получим:

$$\int U_k^*\left(\nabla_k U_k\right)d\tau + \int\left(\nabla_k U_k^*\right)U_k d\tau = 0 \tag{4.23}$$

Из (4.22) и (4.23) очевидно, что

$$\int\left(\nabla_k U_k^*\right)U_k d\tau = 0 \tag{4.24}$$

Таким образом, линейные члены в разложении (4.15) исчезают.
Отбрасывая в (4.15) члены порядка $(k'-k)^2$ и выше и используя соотношение (4.9), получаем:

$$\overline{U^*_{k'}U_k} \cong \frac{1}{L^3}. \tag{4.25}$$

Для матричного элемента $V_{k'k}$ получается вместо выражение

$$V_{k'k} \cong \frac{1}{L^3}\int_{L^a} e^{i(k-k')r}V(r)d\tau = \int_{\dot{L}^s} \varphi^*_{k'}V(r)\varphi_k d\tau \tag{4.13}$$

Исследование показывает, что в разложениях (4.7) и можно пренебречь отброшенными членами, если

$$|k_i a_i| \leqslant \left\{ i = \left\{ \begin{array}{l} \pi \text{ в общеизвестном случае почти свобод-} \\ \text{ного электрона проводимости,} \end{array} \right\} \begin{array}{l} \text{в случае «сильно связанного» элек-} \\ \frac{\pi}{3} \text{ в слона проводимости [8].} \end{array} \right. \tag{4.15}$$

Если вектор $\boldsymbol{k}'$ - $\boldsymbol{k}$ недостаточно мал и это условие нарушается, разложение (4.15) сходится медленно. Однако в этом случае как в формуле (4.12), так и в формуле (4.26) интегралы быстро стремятся к нулю с ростом $|\boldsymbol{k}'-\boldsymbol{k}|$. Таким образом, формулу (4.26) можно применять при любых k и $\boldsymbol{k}'$, если только $V(\boldsymbol{r})$ - плавная функция.

Вернёмся теперь к решению уравнения (4.5). Основная идея излагаемого метода заключается в том, чтобы вместо этого уравнения сначала ренить более простое уравнение

$$[\mathfrak{H}(\boldsymbol{r}) + W_{\boldsymbol{p}} + V(\boldsymbol{r})]\,\varphi(\boldsymbol{r}) = E'\varphi(\boldsymbol{r}), \tag{4.28}$$

а затем с помощью полученного решения сконструировать приближённое решение уравнения (4.5) [11].

Этот метод будет пригоден лишь в тех случаях, когда дебройлевская длина волны квазичастицы, описываемой уравнением (4.28), значительно превосходит постоянную решётки. Точнее выражаясь, предполагается, что $\varphi(\boldsymbol{r})$ можно достаточно точно апроксимировать тригонометрическим многочленом вида

$$\varphi = \sum_k a_k\varphi_k(r). \tag{4.29}$$

где значительны лишь члены с такими k, для которых выполняется неравенство (4.27) (для φ_k см. (4.11)). Это ограничение понадобилось потому, что в дальнейшем придётся пользоваться разложениями (4.7) и (4.15), пренебрегая членами высшего порядка малости.

Заменяя уравнение (4.28) эквивалентным ему вариационным принципом, следует коэффициенты a_k выбрать из условия экстремума функционала

$$\begin{aligned} \overline{E'} = \int \varphi^*\left[\mathcal{H} + W_p + V(\boldsymbol{r})\right]\varphi d\tau \cong \\ \cong \sum_{k',k} a^*_{k'}, a_k\left[(E_k + W_p)\,\delta_{k'k} + V_{k'k}\right] \end{aligned} \tag{4.30}$$

при дополнительном условии нормировки

$$\int \varphi^*\varphi d\tau = \sum_k |a_k|^2 = 1 \tag{4.31}$$

(для E'_k см. (4.11)).
Совершенно аналогично можно поступить и с уравнением (4.5). Его решение следует апроксимировать многочленом вида

$$\psi = \sum_h b_k \psi_k(r), \tag{4.32}$$

$$|k_i a_i| \leqslant \frac{\pi}{3} \quad (i = 1, 2, 3), \tag{4.33}$$

причём ψ_k даётся формулой (4.8). Такая форма апроксимации выбирается на том основании, что не возмущённое внешним полем уравнение (3.4) имеет густой (квазидискретный) спектр собственных значений, а в таких случаях, как известно, в разложении ψ главную роль должны играть $\psi_{\xi k}$, принадлежащие уровням, расположенным вблизи E. Нас в дальнейшем будут интересовать случаи, когда E лежит вблизи дна зоны проводимости. Поэтому в разложение (4.32) и включены ξ_{se}, принадлежащие нижней части зоны проводимости.

Рассматривая соответствующую уравнению (4.5) вариационную задачу, следует коэффициенты b_k выбрать из условия экстремума функционала

$$\bar{E} = \int \psi^* \left[-\frac{\hbar^2}{2m}\Delta + W(\boldsymbol{r}) + W_p + V(\boldsymbol{r}) \right] \psi d\tau = \\ = \sum_{k',k} b^*_{k'} b_k \left[(E_k + W_p)\, \delta_{k'k} + V_{k'k} \right] \tag{4.34}$$

при дополнительном условии нормировки

$$\int \psi^* \psi d\tau = \sum_k |b_k|^2 = 1 \tag{4.35}$$

Здесь E_k должно совпадать с $\cdot E'_k$ формулы (4.30) с точностью до членов порядка k^4, как это следует из (4.7) и (4.11).

При сравнении выражений (4.30) и (4.34) становится очевидным, что функции $\bar{E}'\left(\ldots, a^*_{k'}, \ldots, a_k, \ldots\right)$ и $\bar{E}\left(\ldots, b^*_{k'}, \ldots, b_k, \ldots\right)$ одинаковы. Уравнения связей (4.31) и (4.35) тоже одинаковы. Следовательно, экстремальные значения $\bar{E}$ и $\overline{E'}$ совпадают. Соответствующие экстремуму значения a_k и b_k тоже должны совпадать.

Таким образом, доказано, что

1. энергетический спектр кристалла с электроном проводимости в присутствии добавочного поля $V(r)$ в адиабатическом приближении (случай А) определяется из уравнения (4.5);

2. энергетический спектр уравнения (4.5) в начальной своей части совпадает со спектром несравненно более простого уравнения (4.28);

3. если известно $\varphi(r)$-решение уравнения (4.28) и ψ_k - решения уравнения (3.4), то можно построить приближённое решение уравнения (4.5):

$$\psi(\boldsymbol{r}) = \sum_{\boldsymbol{k}} a_{\boldsymbol{k}} \psi_{\boldsymbol{k}}(\boldsymbol{r}), \tag{4.36}$$

где a_k - коэффициенты разложения (4.29). $\varphi(r)$ мы будем называть «сглаженной» волновой функцией, а $\psi(r)$ - «детальной» волновой функцией электрона;

4) ψ-функция всей системы в адиабатическом приближении, как известно [7], даётся произведением

$$\psi = \Phi\left(\boldsymbol{r}, \boldsymbol{r}_1, \ldots, \boldsymbol{r}_N\right) \psi(\boldsymbol{r}), \tag{4.37}$$

где Φ - функция, описывающая состояние остальных электронов диэлектрика в предноложении, что электрон проводимости закреплён в точке r, иными словами, Φ есть решение уравнения (3.1), возмущённого внешним полем

$$\sum_{j=1}^{N} V\left(r_j\right).$$

Мультипликативная запись состояния системы (4.37) позволяет приближённо говорить отдельно о состоянии элек-

трона проводимости $\psi(r)$ и о состоянии остальных электронов $\Phi\left(r, r_1, \ldots, r_N\right)$, где r - параметр.

Выше было показано, что энергетический спектр кристалла в присутствии внешнего поля даётся собственными значениями E' трёхмерного уравнения (4.28). Покажем теперь, что ряд других важных физических величин тоже можно вычислить, опираясь лишь на решение уравнения (4.28) и не прибегая к решению сложной многоэлектронной задачи.

Рассмотрим возмущение кристалла переменным полем, например световой волной. Предположим, что потенциал возмущения $V_1(r,t)$ является плавной функцией (длина волны света значительно больше постоянной решётки). Предположим, далее, что возмущение меняется со временем достаточно медленно, так что состояние электронов диэлектрика Φ адиабатически следует за возмущением. В случае световой волны это сводится к предположению, что частота света значительно меньше частот, поглощаемых электронами диэлектрика. Такая волна не способна возбудить диэлектрик; поэтому он в продолжение всего времени действия возмущения остаётся в основном состоянии.

На этот раз в уравнение (3.1) в качестве возмущения необходимо ввести добавочные члены

$$\sum_{j=1}^{N} \left[V\left(\boldsymbol{r}_j\right) + V_1\left(\boldsymbol{r}_j, t\right)\right]. \tag{4.38}$$

Под влиянием этого возмущения диэлектрик поляризуется. Как и в рассмотренном выше случае поляризации статическим полем, энергия поляризации будет той же, что и в отсутствии закреплённого электрона проводимости. Следовательно, она не зависит от координаты электрона проводимости $\boldsymbol{r}$. Обозначим энергию поляризации кристалла полем (4.38)

$$W_p + W_1(t) \tag{4.39}$$

Полная энергия кристалла, в котором электрон проводимости закреплён в точке $\boldsymbol{r}$, имеет вид

$$W(r) + W_p + W_1(t). \tag{4.40}$$

Эта энергия играет роль потенциальной энергии электрона проводимости. Состояние электрона проводимости определяется

из уравнения

$$i\hbar\frac{\partial\psi}{\partial t} = \left[-\frac{\hbar^2}{2m}\Delta + W(\boldsymbol{r}) + W_{\boldsymbol{p}} + \right.$$
$$\left. + W_1(t) + V(\boldsymbol{r}) + V_1(\boldsymbol{r},t)\right]\psi. \tag{4.41}$$

Сравнивая это уравнение с уравнением (4.5) для стационарного случая, легко заметить, что в нём появились дополнительные возмущающие члены

$$W_1(t) + V_1(r,t) \tag{4.42}$$

Это возмущение можно рассматривать обычным образом как причину переходов системы между стационарными состояниями, которые определяются из уравнения (4.5). Все физические следствия такого возмущения, в частности вероятности переходов, определяются матричными элементами вида

$$V_{1mn} = \int \psi_m^*(r)V_1(r,t)\psi_n(r)d\tau \tag{4.43}$$

где ψ_m и ψ_n - собственные функции уравнения (4.5).
Возмущение $W_1(t)$ не зависит от r и поэтому переходов не вызывает; его матричный элемент имеет вид

$$W_{1mn} = \delta_{mn}W_1(t). \tag{4.44}$$

Оказывается, что матричный элемент (4.43) можно вычислить, используя вместо ψ_m и ψ_n функции φ_m и φ_n (соответствующие решения уравнения (4.28)). Действительно, формулы (4.12) и (4.26) говорят о том, что для любой плавной функции $V_1(r,t)$

$$\int \psi_{k'}^* V_1 \psi_k d\tau \cong \int \varphi_{k'}^* V_1 \varphi_k d\tau \tag{4.45}$$

Следовательно, используя разложения (4.36) и (4.29), получаем:

$$V_{1mn} = \int \psi_m^* V_1 \psi_n d\tau \cong$$
$$\cong \sum_{k',k} a_{k'}^{*(m)} a_k^{(n)} \int \psi_{k'}^* V_1 \psi_k d\tau = \sum_{k',k} a_{k'}^{*(m)} a_{k_k}^{(n)} \times$$
$$\times \int \varphi_{k'}^* V_1 \varphi_k d\tau = \int \varphi_m^* V_1 \varphi_n d\tau \tag{4.46}$$

что и требовалось доказать. Следует иметь в виду, что таким методом можно вычислить лишь матричные элементы, у которых оба индекса (m и n) принадлежат состояниям с большой дебройлевской длиной волны, для которых разложение (4.29) можно ограничить членами с малыми $\boldsymbol{k}$ (см. критерий (4.27)). Как раз такие матричные элементы нам и понадобятся в дальнейшем.

Выше было показано, что энергетический спектр электрона проводимости в кристалле в присутствии внешнего поля, а также и ряд других физических свойств можно приближённо рассчитать, если удастся решить уравнение (4.28). В этом уравнении оператор $\mathcal{H}$ содержит параметры E^0 и μ_i, которые можно было бы определить, вообще говоря, только при решении исключительно сложных уравнений (3.1) и (3.4). При современном состоянии математики решение подобных уравнений невозможно.

Параметр E^0 входит в энергию только как аддитивная постоянная, а функция $\varphi(\boldsymbol{r})$ от него вообще не зависит. В дальнейшем, однако, предстоит иметь дело лишь с разностями энергий (вычисление энергий тепловых диссоциаций, частот поглощаемого света и т. п.), поэтому значение E^0 нам не понадобится.

Что касается эффективных масс μ_i, то они существенно входят в большинство результатов. В дальнейшем речь будет итти о кристаллах с кубической симметрией. В этом случае $\mu_1 = \mu_2 = \mu_3 = \mu$. Таким образом, теория будет содержать всего один неизвестный параметр μ, который будет определён при сравнении теории с экспериментом.

10.2 II Theory of Polarons with Classical Approach to Crystal Motion

10.2.1 § 5. Basic Equations

В предыдущей главе предполагалось, что ядра ионов неподвижно закреплены в узлах кристаллической решётки. В этом случае рассмотрение электрона проводимости в идеальном диэлектрическом кристалле свелось к задаче о движении электрона в периодическом поле с потенциалом $W(\boldsymbol{r})$ (уравнение (3.4)). В действительности, однако, ионы не закреплены в узлах решётки, а совершают тепловые колебания вблизи некоторых положений равновесия. Электрон проводимости своим полем диэлектрически поляризует кристалл. Поэтому в окрестности электрона проводимости упомянутые выше равновесные положения ионов смещены из узлов решётки. В результате электрон оказывается уже не в простом периодическом поле.

Рассмотрим подробнее изменение потенциала электрона проводимости, которое возникает благодаря смещениям ионов. Зафиксируем электрон проводимости в кристалле в точке $\boldsymbol{r}$ и проследим за изменением его потенциальной энергии, по мере того как ионы смещаются из узлов решётки. Сначала предположим, что один-два иона, ближайших к электрону, остаются неподвижными, а смещаются только остальные ионы. Смещение этих ионов вызовет такое же изменение потенциальной энергии электрона, как появление соответствующих идеальных диполей в узлах решётки. При этом в потенциальной энергии появляется добавочный член - потенциал поляризованной среды, который можно рассчитать по известной формуле макроскопической электростатики:

$$V(r) = e\int \frac{(r-r_1)\,p\,(r_1)}{|r-r_1|^3}d\tau_1 = -e\int \frac{\operatorname{div} P\,(r_1)}{|r-r_1|}d\tau_1. \tag{5.1}$$

Здесь $\boldsymbol{e}$ - заряд электрона, а $\boldsymbol{P}$ - дипольный момент единицы объёма диэлектрика, возникший благодаря смещению ионов; он слагается из дипольного момента, образованного самими смещёнными ионами, и из дополнительной поляризации связанных электронов диэлектрика, вызванной смещением ионов.

Макроскопическая формула (5.1) справедлива только в том случае, если удельная поляризация $\boldsymbol{P}\,(\boldsymbol{r}_1)$ является плавной функцией координат (относительно мало изменяется на расстоянии порядка постоянной решётки). Именно это и предполагается в дальнейшем. Критерии применимости макроскопического учёта поляризации будут подробно рассмотрены в § 7.

Предположим теперь, что упомянутые один-два ближайших иона тоже смещаются; их смещение вызовет дополнительное изменение потенциальной энергии электрона $V'(r)$. Таким образом, потенциальная энергия электрона проводимости равна

$$W(\boldsymbol{r}) + V(\boldsymbol{r}) + V'(\boldsymbol{r}). \tag{5.2}$$

Член $V'(\boldsymbol{r})$ в дальнейшем будет рассмотрен как малое возмущение, а пока, в нулевом приближении, он будет опущен.

Предположим, что массы ионов достаточно велики и их движение можно описывать классической механикой. Предположим, далее, что частоты колебаний ионов настолько малы, что состояние электрона проводимости адиабатически (безинерционно) следует за движением ионов [1]). Иначе говоря, для каждой мгновенной конфигурации ионов успевает установиться соответствующее стационарное состояние электрона проводимости. Если каким-либо путём (например, временным вмешательством внешних сил) создана данная конфигурация ионов и соответствующая поляризация $\boldsymbol{P}(\boldsymbol{r}_1)$, то в этот момент потенциальная энергия электрона равна $W(\boldsymbol{r})+V(\boldsymbol{r})$, а со-

стояние электрона определяется из уравнения

$$\left[-\frac{\hbar^2}{2m}\Delta+W(\boldsymbol{r})+V(\boldsymbol{r})\right]\psi(\boldsymbol{r})=E\psi(\boldsymbol{r}). \tag{5.3a}$$

Координаты ионов входят как параметры в $V(\boldsymbol{r}), \psi(\boldsymbol{r})$ и E.
Поскольку потенциал $V(r)$ является плавной функцией координат (мало меняется на расстоянии порядка постоянной решётки), можно воспользоваться методом эффективной массы (§ 4) и заменить уравнение (5.3а) более простым, в котором опускается периодический потенциал $W(\boldsymbol{r})$, а вместо m вводится эффективная масса μ. В результате получается уравнение

$$\left[-\frac{\hbar^2}{2\mu}\Delta+V(\boldsymbol{r})\right]\psi(\boldsymbol{r})=E\psi(\boldsymbol{r}). \tag{5.3}$$

Здесь опущена постоянная E^0 (см. формулу (4.7)). Это соответствует такому выбору начала отсчёта энергии электрона, при котором электрон, покоящийся на дне зоны проводимости, в отсутствии поля $V(\boldsymbol{r})$ имеет энергию, равную нулю.

Уравнение (5.3), строго говоря, описывает движение не электрона, а некоторой квазичастицы с массой μ. Однако в дальнейшем будет применяться более простая и привычная терминология: эта квазичастица будет называться «электроном с эффективной массой μ ».

Уравнение (5.3) определяет ψ-функцию электрона для произвольной конфигурации ионов. Рассмотрим теперь уравнения, определяющие движение самих ионов. Пусть $U_{\text{кин}}$ и $U_{\text{дот}}$ обозначают соответственно кинетическую и потенциальную энергию ионов диэлектрика в отсутствии электрона проводимости. Кинетическая энергия электрона и потенциальная энергия его взаимодействия с кристаллом в сумме равны энергии E, определяемой уравнением (5.3). Следовательно, полная энергия всей системы

$$H=E+U_{\text{пот}}+U_{\text{кии}} \tag{5.4}$$

Если здесь $U_{\text{кин}}$ выразить через импульсы ионов, а $U_{\text{пот}}$ и E - через координаты ионов, то H превратится в функцию Гамильтона, описывающую движение ионов.

Явное выражение $U_{\text{кин}}$ через импульсы ионов не представляет никакого труда. Что же касается $U_{\text{пот}}$ то, чтобы её вычислить, необходимо знать силы взаимодействия ионов.

Эти силы, однако, известны недостаточно точно. Обычно кристалл рассматривают как систему точек (ионов), совершающих малые гармонические колебания около положений равновесия. При этом $U_{\text{нот}}$ представляется квадратичной формой смещения ионов. Но

[81]) Это предположение может встретить возражения, если состояние электрона принадлежит непрерывному спектру энергий. В дальнейшем, однако, речь будет итти только о состояниях, принадлежащих дискретному спектру. В этом случае адиабатическое приближение применимо к кристаллу с таким же успехом, с каким оно обычно применяется к молекулам.

и в этом приближении в потенциальную энергию входит много неизвестных констант, и последующие расчёты движения ионов трудно довести до численных результатов.

В дальнейшем, однако, главную роль будет играть деформация специального типа: диэлектрическая поляризация, вызванная плавно меняющимся в пространстве и медленно меняющимся во времени электрическим полем. Такая деформация будет кратко называться поляризационной. В этом частном случае вычисление потенциальной энергии кристалла существенно облегчается, так как можно применить макроскопические методы расчёта, рассматривая кристалл как диэлектрический континуум. Потенциальную энергию поляризованного диэлектрика U_p можно рассчитать как работу, которая была затрачена на поляризацию. Зададимся какой-либо конфигурацией ионов и выберем такое внешнее электрическое поле, которое привело бы ионы в эту конфигурацию. Пусть $\boldsymbol{D}'(\boldsymbol{r})$ вектор индукции такого поля. При медленном включении этого поля ионы, смещаясь, примут заданную конфигурацию. Во время такой поляризации суммарный дипольный момент единицы объёма $\boldsymbol{P}$ связан с индукцией известным соотношением

$$P_{\text{сум}} = \frac{\varepsilon - 1}{4\pi\varepsilon} D, \tag{5.5}$$

где ε - диэлектрическая постоянная кристалла. Элементарная работа, совершённая внешним полем в единице объёма кристалла при бесконечно малом изменении поля, равна

$$D\delta P_{\text{оум}}$$

Суммарная работа, совершённая в результате поляризации в единице объёма, равна

$$\int_0^{D'} D\delta P_{\text{сум}_{\text{m}}} = \frac{\varepsilon - 1}{8\pi\varepsilon} D'^2. \tag{5.6}$$

Затем выключим поле настолько быстро, что ионы благодаря их большой инертности не успеют сдвинуться с места; а произойдёт лишь деполяризация связанных электронов диэлектрика. В результате кристалл окажется именно в том состоянии, для которого надлежит вычислить потенциальную энергию (состояние связанных электронов адиабатически соответствует [7] конфигурации ионов). При быстром выключении поля вместо статической диэлектрической постоянной ε следует пользоваться квадратом показателя преломления света n, точнее значением n на плато дисперсионной кривой с красной стороны от области собственного поглощения света связанными электронами. Быстрое выключение поля приводит к изменению поляризации, которое может быть вычислено по формуле, аналогичной (5.5):

$$\delta P = \frac{n^2 - 1}{4\pi n^2} \delta D. \tag{5.7}$$

При этом в единице объёма совершается работа

$$\int_{\dot{D}'}^{0} D\delta P_{\text{сум}} = -\frac{n^2 - 1}{8\pi n^2} D'^2 \tag{5.8}$$

Суммарная работа, затраченная на отклонение ионов в единице объёма, получается сложением работ (5.6) и (5.8), т. е. равна

$$\frac{1}{8\pi}\left(\frac{1}{n^2} - \frac{1}{\varepsilon}\right) D'^2. \tag{5.9}$$

Величина, стоящая в скобках, в дальнейшем явится основным параметром теории; поэтому введём для неё специальное обозначение

$$\frac{1}{n^2} - \frac{1}{\varepsilon} = c. \tag{5.10}$$

Потенциальная энергия поляризованного диэлектрика равна работе, затраченной на отклонение ионов во всём объёме кристалла:

$$U_p = \frac{c}{8\pi} \int D'^2(\boldsymbol{r}) d\tau \tag{5.11}$$

Здесь $\boldsymbol{D}'(\boldsymbol{r})$-индукция поля, которое удерживало бы в равновесии данную конфигурацию ионов.

Значительно удобнее потенциальную энергию выразить через дипольный момент, появляющийся в результате деформации. Пользуясь формулами (5.5) и (5.7), легко вычислить дипольный момент, который остаётся после быстрого выключения поля; он равен

$$P = \frac{c}{4\pi} D'. \tag{5.12}$$

В дальнейшем $\boldsymbol{P}$ будет называться инерционной частью поляризации. Она состоит из поляризации ионов и той части электронюй поляризации, которая стационарно поддерживается поляризованными ионами. Таким образом, этот вектор $\boldsymbol{P}$ совпадает с тем, который фигурирует в формуле (5.1). Формулу (5.11) теперь можно записать в виде

$$U_p = \frac{2\pi}{c} \int P^2(r) d\tau \tag{5.13}$$

В частном случае решёток, у которых элементарная ячейка состоит из одного положительного и одного отрицательного ионов (например, решётка каменной соли), произвольную плавную деформацию можно приближённо подразделить на две независимые части: 1) поляризацию, рассмотренную выше, и 2) упругую деформацию, при которой не возникает дипольный момент. К состоянию произвольной плавной деформации можно притти в два этапа: сначала поляризовать кристалл, затратив на это работу U_p, а затем подвергнуть кристалл упругой деформации, затратив на это дополнительную работу $U_{\text{упр.}}$. Последняя может быть рассчитана обычными методами макроскопической теории упругости. При этом можно в первом приближении пользоваться упругими константами неполяризованного кристалла, так как поляризация предполагается настолько малой, что вызванные ею изменения упругих констант ничтожны. Общая потенциальная энергия плавно деформированного кристалла в отсутствии электрона проводимости равна

$$U_{\text{пот}} = U_p + U_{\text{упр.}} \tag{5.14}$$

Явное выражение $U_{\text{упр}}$ нам пока что не понадобится, так как в ближайших параграфах рассматриваются явления, в которых существенную роль играет поляризация, а не упругая деформация.

При исследовании состояния кристалла без упругих деформаций в присутствии электрона проводимости удобно будет пользоваться следующим функционалом, зависящим от $\psi(\boldsymbol{r})$ и $\boldsymbol{P}(\boldsymbol{r})$:

$$F[\psi, \boldsymbol{P}] = \frac{\hbar^2}{2\mu} \int |\nabla\psi|^2 d\tau + \bar{V}[\psi, P] + \frac{2\pi}{c} \int P^2 d\tau, \tag{5.15}$$

где

$$\bar{V}[\psi, P] = \int V(r)|\psi|^2 d\tau_0 \tag{5.16}$$

Если воспользоваться для V выражением (5.1) и ввести обозначение

$$D\left[\psi, r_1\right] = -e \int |\psi(r)|^2 \frac{(r - r_1)}{|r - r_1|^3} d\tau \tag{5.17}$$

то (5.16) перепишется следующим образом:

$$\bar{V}[\psi, P] = -\int PD d\tau \tag{5.18}$$

Согласно формуле (5.17) $\boldsymbol{D}$ можно интерпретировать как индукцию электростатического поля, созданного облаком заряда с плотностью $e|\psi|^2$. Согласно (5.18) $\bar{V}$ представляет собой потенциальную энергию взаимодействия этого облака с поляризованной средой.

Для пояснения смысла функционала F и целесообразности его введения отметим следующие основные свойства этого функционала.

Если $\boldsymbol{P}(\boldsymbol{r})$ зафиксировать, а $\psi(\boldsymbol{r})$ найти из условия экстремума функционала F при дополнительном условии

$$\int |\psi|^2 d\tau = 1 \tag{5.19}$$

то согласно общеизвестному вариационному принципу квантовой механики полученные таким путём $\psi(\boldsymbol{r})$ являются стационарными квантовыми состояниями электрона в поле $V(\boldsymbol{r})$, т. е. решениями уравнения (5.3). Эти ?, следовательно, являются состояниями электрона, которые адиабатически соответствуют данной конфигурации ионов с поляризацией $\boldsymbol{P}(\boldsymbol{r})$. Если теперь подставить одно из таких ψ в функционал (5.15), то первый и второй члены в формуле (5.15) пред-

ставят, соответственно, кинетическую энергию электрона и потенциальную энергию взаимодействия электрона с кристаллом, а их сумма будет равна энергии E, фигурирующей в формулах (5.3) и (5.4). Третий член в (5.15) представляет потенциальную энергию поляризованного кристалла в отсутствии электрона проводимости. Таким образом, после минимизации функционала F путём вариации $\psi(r)$ он становится равен сумме первых двух членов формулы (5.4) и представляет собой потенциальную энергию ионов в присутствии электрона проводимости.

10.2.2 § 6. The Resting Polaron [12, 13]

Рассмотрим такое состояние кристалла с электроном проводимости, в котором энергия системы имеет минимальное возможное значение (абсолютная температура кристалла равна нулю). Это состояние будет в дальнейшем называться основным состоянием. Так как движение ионов описывается классической механикой, система будет обладать минимальной энергией, когда кинетическая энергия ионов равна нулю, а их потенциальная энергия имеет минимум.

Как было показано в предыдущем параграфе, потенциальная энергия ионов для заданной поляризации $P(r)$ даётся функционалом

$$F(\psi, P) = \frac{\hbar^2}{2\mu} \int |\nabla\psi|^2 d\tau - \int PD[\psi, r] d\tau + \frac{2\pi}{c} \int P^2 d\tau, \tag{6.1}$$

если в него подставлено такое $\psi(\boldsymbol{r})$, при котором функционал экстремален. Это ψ является стационарным состоянием электрона проводимости, которое адиабатически соответствует данной конфигурации ионов $\boldsymbol{P}(\boldsymbol{r})$. Однако ионы при этом, вообще говоря, не будут в равновесии. Чтобы притти к упомянутому выше минимуму потенциальной энергии ионов, необходимо $F[\psi, P]$ минимизировать ещё и по $P(r)$. Таким образом, в основном состоянии функционал (6.1) должен иметь абсолютный минимум, который получается в результате независимой вариации $\psi(\boldsymbol{r})$ и $\boldsymbol{P}(\boldsymbol{r})$ с сохранением нормировки ψ. Это минимальное значение F совпадает с полной энергие н системы в основном состоянии, так как в формуле (5.4) кинетическая энергия ионов равна нулю.

Если произвольно варьировать $\boldsymbol{P}(\boldsymbol{r})$ при фиксированном ψ, то соответствующая вариация F имеет вид

$$\delta_p F = -\int \delta P D d\tau + \frac{4\pi}{c}\int P\delta P d\tau \tag{6.2}$$

Приравнивая эту вариацию нулю, получаем:

$$P(r) = \frac{c}{4\pi} D[\psi, r]. \tag{6.3}$$

Сравнение этой формулы с формулой (5.12) показывает, что электрон будет стационарно поддерживать такую инерционную поляризацию кристалла, какую создало бы электростатическое поле с индукцие $\boldsymbol{D}[\psi, \boldsymbol{r}]$. Иными словами, ионы вследствие их инерционности не могут следовать за движением электрона и поляризуются так, как если бы на них действовало квантовомеханическое среднее значение поля электрона, определяемое формулой (5.17).

Подставляя $\boldsymbol{P}$ из формулы (6.3) в (6.1), приходим к функционалу, который зависит уже только от ψ:

$$J[\psi] \equiv F\left[\psi, \frac{c}{4\pi} D\right] = \frac{\hbar^2}{2\mu}\int |\nabla\psi|^2 d\tau - \frac{c}{8\pi}\int D^2[\psi, r] d\tau. \tag{6.4}$$

Необходимо теперь минимизировать этот функционал, варьируя ψ с сохранением её нормировки. Функционал (6.4) имеет абсолютный минимум, когда электрон находится не в свободном, а в локальном (связанном) состоянии, т. е. когда $|\psi|^2$ значительно лишь в ограниченной области кристалла и быстро стремится к нулю по мере отдаления от этой области. Действительно, отрицательный член в (6.4) только постоянным множителем отличается от энергии электростатического поля ψ-облака электрона. Если электрон находится в свободном состоянии, то плотность ψ-облака бесконечно мала $\left(\sim \frac{1}{L^3}\right)$ и отрицательный член в (6.4) также бесконечно мал; в этом случае $J[\psi] \geqslant 0$. Если же электрон находится в локальном состоянии, то в (6.4) отрицательный член обратно пропорционален эффективному радиусу ψ-облака, а положительный член обратно пропорционален квадрату радиуса; следовательно, при достаточно больших радиусах преобладать должен отрицательный член и $J[\psi] < 0$. Таким образом, в основном состоянии системы электрон локализован.

Рассматриваемое состояние системы замечательно тем, что поляризованный кристалл представляет для электрона потенциальную яму, которая стационарно поддерживает электрон в локальном состоянии, а электрон своим средним полем $\boldsymbol{D}$ в свою очередь стационарно поддерживает вышеупомянутую поляризацию кристалла. Таким образом, поляризационная потенциальная яма и ψ-функция электрона взаимно определяют друг друга. Такие самосогласованные состояния системы будут в дальнейшем кратко называться поляронами.

Перейдём теперь к минимизации функционала (6.4). Для отыскания абсолютного минимума функционала $J(\psi)$ был применён так называемый прямой вариационный

метод [13]. Именно, ψ апроксимировалась конкретной функцией, содержащей ряд параметров. Эта апроксимация подставлялась в (6.4), после чего $J[\psi]$ становился функцией упомянутых параметров. Затем параметры выбирались из условия минимума J. При выборе формы апроксимирующей функции следует учесть, что ψ имеет непрерывную производную, на бесконечности стремится к нулю, как e^{-ar}; благодаря известному свойству основных состояний в квантовой механике ψ не имеет узлов, наконец, в изотропно поляризующемся кристалле основное состояние должно быть сферически симметрично. Был испробован ряд апроксимирующих функций различного вида. Наиболее точные результаты (самое низкое значение минимума J) были получены с функцией вида

$$\psi_0 = A\left(1 + \alpha r + \beta r^2\right) e^{-\alpha r} \tag{6.5}$$

(в дальнейшем величины, относящиеся к основному состоянию обозначаются индексом «нуль»). A выражается через α и β из условия нормировки; α и β являются независимыми параметрами и выбираются из условия минимума J.

Функция, имеющая всего два независимых параметра (α и β), конечно, не способна сколько-нибудь точно апроксимировать состояние электрона. Однако, несмотря на это, интересующее нас минимальное значение $J[\psi]$, представляющее энергию основного состояния, получается с большой точностью. Объясняется это тем, что при определении минимума $J[\psi]$ требуется, чтобы апроксимирующая функция была способна апроксимировать не значения самой ψ, а лишь значения интегралов, фигурирующих в выражении $J[\Psi]$. Кроме того существенно,

что вблизи минимума вариация J равна нулю и, следовательно, $J[\psi]$ мало чувствителен к небольшим отступлениям ψ от точной минимали.

Погрешность такого прямого вариационного метода можно оценить, применяя его к различным задачам, для которых известно точное решение. Если, например, вычислить энергетический терм основного состояния трёхмерного гармонического осциллятора, пользуясь вариационным принципом квантовой механики и применяя апроксимацию (6.5), то оказывается, что даже при одном независимом параметре α (положив $\beta = 0$) получается величина, всего на 5% превосходящая точное значение терма. Если же использовать апроксимацию (6.5) с обоими параметрами, то погрешность при вычислении терма составляет уже доли процента. Такая высокая точность определения экстремального значения функционала не связана с благоприятной случайностью, а характерна для прямых вариационных методов вообще.

Вернёмся к вычислению минимума $J[\psi]$ с помощью апроксимации (6.5). Вместо переменной r удобно ввести безразмерную переменную

$$x = 2\alpha r. \tag{6.6}$$

Тогда вместо (6.5) получается

$$\psi_0 = A\left(1 + \frac{x}{2} + \gamma x^2\right) e^{-\frac{x}{2}}, \tag{6.7}$$

где

$$\gamma = \frac{\beta}{4\alpha^2}.$$

Подстановка этого выражения в формулы (5.17) и (6.4) и последующее интегрирование приводят к выражению

$$J = \frac{3}{2}\frac{\pi\hbar^2 A^2}{\mu\alpha}(1 + 4\gamma + 24\gamma^2) - \frac{ce^2\pi^2 A^4}{\alpha^5}(10,494 + 209,88\cdot\gamma + \\ +1884\cdot\gamma^2 + 8507,8\cdot\gamma^3 + 16727\cdot\gamma^4)\,. \tag{6.8}$$

Условие нормировки (5.19) после подстановки в него апроксимации (6.7) и интегрирования приобретает вид

$$\frac{\pi A^2}{2\alpha^3}\left(14 + 168\gamma + 720\gamma^2\right) = 1. \tag{6.9}$$

Согласно (6.8) J является функцией параметров A^2, а и ɣ. Необходимо найти его минимум при дополнительном условии связи (6.9). Обычный метод нахождения связанного экстремума приводит к системе трёх уравнений, из которых определяются значения A^2, а и ɣ. Если из этой системы уравнений исключить A^2 и α, выразив их через γ, то для γ получается уравнение

$$0,11196\gamma + 3,0396\gamma^2 + 6,7956\gamma^3 - \\ - 172,56\gamma^4 - 1411,6\gamma^5 - 3481,7\gamma^6 = 0. \tag{6.10}$$

Исследование показывает, что это уравнение имеет четыре вещественных корня и два комплексных.

Величины α и A^2 выражаются через ɣ однозначно с помощью соотношения

$$\alpha = \frac{\mu e^2 c}{\hbar^2}\cdot\frac{167,91 + 3358,1\gamma + 30143\gamma^2 + 136125\gamma^3 + 267637\gamma^4}{24\,(1 + 4\gamma + 24\gamma^2)\,(14 + 168\gamma + 720\gamma^2)} \tag{6.11}$$

и соотношения (6.9). В нижеследующей таблице приведены вещественные корни уравнения (6.10), а также соответствующие экстремальные значения J и α.

Таблица 6.1

i	i	$\frac{\alpha_i\hbar^2}{\mu e^2 c}$	$-\frac{J\hbar^2}{\mu e^4 c^2}$
1	$-0,1959$	0,1588	0,009807
2	$-0,0447$	0,4054	0,05395
3	0	0,5	0,05355
4	0,1129	0,6585	0,05432

Как известно из теории прямых вариационных методов, физический смысл следует придавать только самому нижнему из экстремальных значений J, т. е. четвёртому [1]). Оно представляет собой упоминавшийся выше абсолютный минимум функционала $F[\psi, P]$, т. е. полную энергию системы в основном состоянии:

$$J\left[\Psi_0\right] = H_0 = -0,0544\frac{\mu e^4}{\hbar^2}c^2 \tag{6.12}$$

(округление сделано в сторону понижения энергии). Выраженная в электрон-вольтах, эта энергия равна

[81]) Остальные экстремумы J могут оказаться результатом недостаточной «гибкости» апроксимирующей функции и могут исчезнуть при переходе к более общим апроксимациям.

$$H_0 = -1,47\frac{\mu}{m}c^2. \tag{6.13}$$

Здесь μ - эффективная масса электрона в кристалле, а m - масса свободного электрона.

Начало отсчёта энергии системы выбрано так, что $H = 0$, когда ионы неподвижны и находятся в узлах решётки, а электрон - на дне зоны проводимости. Поэтому энергия H_0 равна с обратным знаком энергии тепловой диссоциации полярона, в результате которой кристалл полностью деполяризуется и электрон переходит в свободное (зонное) состояние. Эта энергия настолько велика, что даже при высоких температурах преобладающее большинство «лишних» электронов (введённых в диэлектрик извне) должно находиться в поляронном состоянии.

Подставляя известные теперь параметры γ_4 и α_4, можно записать ψ-функцию основного состояния в виде

$$\Psi_0 = 0,1229\alpha_4^{3/2}\left(1 + \alpha_4 r + 0,4516\alpha_4^2 r^2\right)e^{-\alpha r}, \tag{6.14}$$

где

$$\alpha_4 = 0,6585\frac{\mu e^2}{\hbar^2}c. \tag{6.15}$$

Если вместо (6.5) применить апроксимацию только с одним независимым параметром α, положив $\beta = 0, \gamma = 0$, то получаются как раз результаты, приведённые в третьей строке таблицы 6.1. Интересно отметить, что соответствующее экстремальное значение J отличается от (6.12) менее чем на 2% Таким образом, добавление второго независимого параметра γ позволяет понизить энергию всего на 2%. Дальнейшее увеличение числа параметров позволяет понизить минимум J лишь на доли процента. Следовательно, погрешность выражения энергии (6.12) составляет лишь доли процента. Этот результат дополняет рассмотренный выше пример гармонического осциллятора, демонстрирующий высокую точность определения энергии прямым вариационным методом даже при небольшом числе параметров, но при разумном выборе формы апроксимирующей функции.

Для более грубых вычислений можно пользоваться апроксимацией с одним параметром α. В этом случае

$$\psi_0 \cong \frac{\alpha_3^{3/2}}{\sqrt{7\pi}}\left(1 + \alpha_3 r\right)e^{-\alpha_5 r}, \tag{6.16}$$

где

$$\alpha_B = \frac{\mu e^2}{2\hbar^2}c. \tag{6.17}$$

Зная ψ-функцию электрона (6.14), можно по формуле

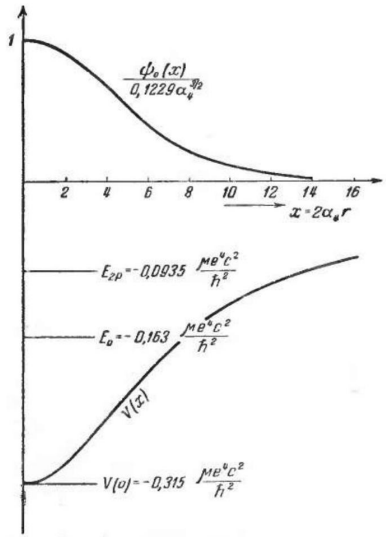

Рис. 6.1. Потенциальная яма, энергетические уровни и ψ-функция электрона в поляроне.

(5.17) вычислить соответствующую индукцию $\boldsymbol{D}_0$, по формуле (6.3) - поляризацию $\boldsymbol{P}_0(\boldsymbol{r})$, наконец, по формуле (5.1)

можно вычислить форму поляризационной потенциальной ямы $V_0(r)$, в которой движется электрон. Опуская детали вычисления, которые читатель может найти в соответствующих статьях [13], приведём лишь окончательное выражение для потенциала

$$V_0(r) = -2\alpha_4 ce^2 \left[\frac{1}{x} - e^{-x}\left(\frac{1}{x} + 0,7605 + 0,2605x + \right.\right.$$
$$\left.\left. +0,05087x^2 + 0,005703x^3 + 0,0003024x^4\right)\right] \tag{6.18}$$

где $x = 2\alpha_4$ r. Когда $x \gg 1$, экспоненциальный множитель очень мал, и потенциал стремится к кулоновскому:

$$V_0(r) \to -\frac{ce^2}{r}. \tag{6.19}$$

В точке $r = 0$ потенциал имеет минимум параболического типа, как показано на рис. 6.1.

10.2.3 § 7. Criteria for the applicability of the theory [12]

В предыдущих параграфах в процессе построения теории был сделан ряд ограничивающих предположений, благодаря которым удалось существенно упростить математический аппарат. В настоящем параграфе эти предположения будут последовательно рассмотрены и будут даны простые критерии, позволяющие легко установить, в какой мере эти предположения справедливы для того или иного конкретного кристалла.

В §§ 3 и 4 предполагалось, что состояние связанных электронов диэлектрика безинерционно следует за движением электрона проводимости (случай А). Благодаря этому удалось многоэлектронную задачу свести к рассмотрению движения одного электрона в периодическом поле с потенциалом $W(\boldsymbol{r})$. Это адиабатическое приближение справедливо в тех случаях, когда расстояние между энергетическими уровнями электрона проводимости в поляризационной потенциальной яме $V(\boldsymbol{r})$ значительно

меньше, чем энергия возбуждения связанных электронов диэлектрика [7], т. е. когда частоты света ω, поглощаемые и излучаемые электроном проводимости в поляроне, значительно меньше частот ω_e, поглощаемых связанными электронами диэлектрика:

$$\omega \ll \omega_e. \tag{7.1}$$

Далее, в § 4 при рассмотрении возмущения системы быстропеременным полем (например, светом) предполагалось, что это возмущение, вызывая переходы электрона проводимости из одного состояния в другое, однако не возбуждает связанных электронов диэлектрика. Соблюдение этого условия гарантируется тем же неравенством (7.1).

В § 5 предполагалось, что состояние электрона проводимости адиабатически следует за движением ионов. Это справедливо в тех случаях, когда ω значительно больше собственных частот колебаний ионов ω_i:

$$\omega \gg \omega_i. \tag{7.2}$$

Одновременное выполнение неравенств (7.1) и (7.2) означает, что электрон проводимости, находясь в поляронной потенциальной яме, должен поглощать свет в той области спектра, в которой данный диэлектрик прозрачен. В § 9 будет показано, что в основном состоянии полярон должен поглощать главным образом свет частоты

$$\hbar_\omega = 1,3\,|H_0|\,. \tag{7.3}$$

Поэтому упомянутые выше предположения справедливы, если соблюдается неравенство

$$\hbar\omega_i \ll 1,3\,|H_0| \ll \hbar\omega_{\omega_e}. \tag{7.4}$$

В § 5 предполагалось, что при взаимодействии электрона с поляризованным кристаллом главную роль должна играть поляризация сравнительно большого объёма кристалла, размеры которого превышают постоянную решётки. На этом основании энергия взаимодействия электрона с поляризованным кристаллом рассчитывалась макроскопическим путём. Для основного состояния эта энергия с помощью формул (5.18) и (6.3) может быть записана в следующем виде:

$$\bar{V}\left[\Psi_0, P_0\right] = -\int P_0 D_0 d\tau = -\frac{c}{4\pi}\int D_0^3 d\tau. \tag{7.5}$$

Чтобы получить представление о величине объёма кристалла, поляризация которого определяет главную часть энергии (7.5), полезно ввести понятие о поляризационном радиусе полярона r_p. Определим его условно как радиус сферы, центр которой совпадает с центром полярона и которая заключает

половину объёмного интеграла (7.5). В результате вычисления получается

$$r_p \cong \frac{10\hbar^2}{c\mu e^2} \tag{7.6}$$

Поляризацию можно рассматривать макроскопически при условии, что этот радиус превышает постоянную решётки, т. е. если

$$\frac{10\hbar^2}{c\mu e^2} > a. \tag{7.7}$$

При построении теории был использован метод эффективной массы. Как указывалось в § 4, этот метод справедлив лишь в том случае, когда дебройлевская длина волны

квазичастицы с эффективной массой μ превышает постоянную решётки, точнее говоря, если при разложении ψ-функции квазичастицы в ряд Фурье вида

$$\psi_0(r) = \frac{1}{L^{8/2}} \sum_{\boldsymbol{k}} a_{\boldsymbol{k}} e^{ikr} \tag{7.8}$$

главную роль будут играть гармоники с длиной волны, превышающей постоянную решётки. Если для $\psi_0(\boldsymbol{r})$ воспользоваться приближённым выражением (6.16), то коэффициент Фурье примет вид

$$a_k = \frac{32\sqrt{\frac{\pi}{7}}}{L^{2/2}\alpha_B^{2/2}} \frac{1}{\left(1 + \frac{k^2}{a_3^2}\right)^3}. \tag{7.9}$$

Эта формула показывает, что a_k имеет максимальное значение при $k = 0$; при $k = \alpha, a_k$ равен $\frac{1}{8}$ своего максимального значения, а с дальнейшим ростом k, a_k быстро стремится к нулю (как $\frac{1}{k^6}$). Таким образом, в разложении (7.8) главную роль играют гармоники с $k \leqslant \alpha_3$, т. е. с длинами волн

$$\lambda = \frac{2\pi}{k} \geqslant \frac{2\pi}{a_3} = \frac{4\pi}{c} \frac{\hbar^2}{\mu e^2}. \tag{7.10}$$

Метод эффективной массы применим, если

$$\frac{4\pi}{c} \frac{\hbar^2}{\mu e^2} > a. \tag{7.11}$$

К. Б. Толпыго [46] рассмотрел высшие приближения метода эффективной массы, получил соответствующие поправки к выражению энергии полярона и пришёл к критерию метода, совпадающему с (7.11). Этот критерий, оказывается, совпадает с критерием (7.7), определяющим законность макроскопического рассмотрения поляризации.

В § 5 предполагалось, что поляризационные смещения ионов малы по сравнению с постоянной решётки, и поэтому потенциал $V'(r)$ в (5.2) можно считать малым возмущением. Вычислим эти смещения в том месте кристалла, где индукция $\boldsymbol{D}_0(\boldsymbol{r})$ и поляризация максимальны. В этом расчёте можно воспользоваться упрощённым приближённым выражением для $\psi_0(\boldsymbol{r})$(6.16) и (6.17). Оказывается, что индукция достигает максимального значения на сфере радиуса

$$r = 2,8 \frac{\hbar^2}{\mu e^2 c}, \tag{7.12}$$

причём это максимальное значение равно

$$D_{0\ \text{мако}} = 0,035e \left(\frac{\mu e^2 c}{\hbar^2}\right)^2 \tag{7.13}$$

Удельный дипольный момент, созданный смещёнными ионами, $\boldsymbol{P}_i$ не следует смешивать с введённой выше инерционной поляризацией $\boldsymbol{P}$, так как последняя включает в себя и ту часть электронной поляризации $\boldsymbol{P}_e$, которую вызывают смещённые ионы. Если $\boldsymbol{P}_{\text{оум}}$ есть суммарная поляризация, то

$$P_i = P_{\text{оум}} - P_e = \frac{\varepsilon - n^2}{4\pi} \frac{D}{\varepsilon} = n^2 P. \tag{7.14}$$

Поскольку нас интересуют лишь порядки величин, предположим для простоты, что решётка кубическая и что все ионы, составляющие элементарную кристаллическую

ячейку, одновалентны и подвергаются одинаковым поляризационным смещениям Δ. Тогда

$$\Delta = \frac{a^3 P_i}{ev}, \tag{7.15}$$

где a - постоянная решётки, а v - число ионов в элементарной ячейке. В том месте, где индукция и поляризация макси-

мальны, с помощью формул (7.13-15) получаем:

$$\frac{\Delta}{a} = \frac{0,035}{4\pi\nu}\left(1 - \frac{n^2}{\varepsilon}\right)\left(a\frac{\mu e^2 c}{\hbar^2}\right)^2. \tag{7.16}$$

В § 5 предполагалось, что отношение $\frac{\Delta}{a}$ значительно меньше единицы. Как показывает формула (7.16), это ограничение слабее, чем ограничение (7.7), и вытекает из последнего.

Таким образом, критерии применимости теории сводятся к неравенству (7.4) и неравенству (7.7). Параметрами теории являются

$$c = \frac{1}{n^2} - \frac{1}{\varepsilon} \tag{7.17}$$

и эффективная масса μ. Параметр c для большинства ионных кристаллов колеблется между $\frac{1}{4}$ и $\frac{1}{10}$. Что же касается эффективной массы, то она бывает как больше, так и меньше массы свободного электрона. Например, у щёлочно-галоидных

$$r_p = \frac{10\hbar^2}{\mu e^2 c} = \frac{5,29}{\frac{\mu}{m}c}\text{Å}$$

Таблица 7.1

	Cu_2O	NaCl	NaBr	NaJ	KCl	KBr	KJ	RbCl	RbBr	RbJ	PbS
e	9	5,8	6,39	6,6	4,78	4,81	5,2	5,2	5,16	5,58	17,9
n^2	4	2,33	2,6	2,91	2,175	2,36	2,65	2,18	2,36	2,6	2,81
$\boldsymbol{c}$	0,139	0,257	0,229	0,192	0,251	0,217	0,185	0,265	0,23	0,206	0,3
$\frac{\mu}{m}$	1,81	2,78	2,96	3,25	1,85	1,87	2,11	1,78	1,7	1,89	0,46
r_p	Å21	7,4	7,85	8,5	11,4	13	13,6	11,3	13,5	13,6	38,3
aÅ		2,81	2,97	3,23	3,14	3,29	3,53	3,27	3,42	3,66	2,98

кристаллов эффективная масса в полтора-два с половиной раза превышает массу свободного электрона (см. табл. 7.1). У некоторых оксидов [14] эффективная масса, наоборот, меньше

массы свободного электрона. Поэтому в дальнейшем необходимо проверять критерии отдельно для каждого конкретного кристалла, с которым придётся иметь дело.

Здесь же в качестве примера рассмотрим случай, когда $\mu = m$ и $c = 0,25$. Неравенство (7.4) в этом случае выполняется, так как $\hbar\omega_i$ у большинства кристаллов не превышает двух-трёх сотых электрон-вольта, $|H_0|$ равна десятой элек-трон-вольта, а $\hbar\omega_e$ у диэлектриков составляет несколько электрон-вольт. Неравенство (7.7) также соблюдено, поскольку поляризационный радиус полярона r_p в рассматриваемом примере равен сорока водородным радиусам, что превышает постоянную решётки любого кристалла.

В табл. 7.1 приведены эффективные массы электронов и радиусы поляронов для некоторых конкретных кристаллов. Параметры теории для этих кристаллов взяты из §§ 30 , 31 и 36.

§ 8. Неустойчивость зонного состояния электрона. Процесс формирования полярона [15]. Теорема «1:2:3:4»

В § 6 было показано, что в идеальном ионном кристалле существуют поляроны, а также что энергия системы при поляронном состоянии значительно ниже, чем при свободном (зонном) состоянии электрона, и следовательно, большинство «лишних» электронов должно оказаться в поляронном состоянии. Рассмотрим теперь, в какой мере зонное состояние является метастабильным и каким образом электрон может из зонного состояния перейти в поляронное. В частности, интересно выяснить, нужна ли для формирования полярона предварительная тепловая флуктуация, образующая первоначальную поляризационную потенциальную яму достаточнoЙ глубины, чтобы в ней существовали дискретные уровни. Ниже будет показано, что такая предварительная флуктуация не требуется. Наоборот, можно указать такой ход поляризации кристалла, приводящий к локализации электрона, при котором потенциальная энергия ионов монотонно убывает.

Рассмотрим, например, поляризацию

$$P_\varphi = \frac{c}{4\pi} D[\varphi, r], \tag{8.1}$$

где функционал $\boldsymbol{D}$ определяется формулой (5.17), а

$$\varphi = k^{n/2}\psi_0(kr) \quad (0 \leqslant k \leqslant 1) \tag{8.2}$$

(ψ_0 - основное состояние полярона). ψ-функция электрона, адиабатически соответствующая данной поляризации, является минималью функционала

$$F\left[\psi, \boldsymbol{P}_\varphi\right] = \frac{\hbar^2}{2\mu}\int |\nabla\psi|^2 d\tau - \int \boldsymbol{P}_\varphi \boldsymbol{D}[\psi, \boldsymbol{r}] d\tau + \frac{2\pi}{c}\int P_\varphi^2 d\tau \tag{8.3}$$

(см. § 5), а сам функционал после минимизации его по ψ представляет собой потенциальную энергию ионов. Покажем, что минимальное значение F отрицательно: $F_{\text{мин}}\ [\psi, \boldsymbol{P}_\varphi] \leqslant F\left[\varphi, \boldsymbol{P}_\varphi\right] =$

$$= \frac{\hbar^2}{2\mu}\int |\nabla\varphi|^2 d\tau - \frac{c}{8\pi}\int D^2[\varphi, r] d\tau = J[\varphi]. \tag{8.4}$$

Далее, простой заменой переменных под знаком интеграла легко показать, что

$$\int |\nabla\varphi|^2 d\tau = k^2 \int |\nabla\psi_0|^2\, d\tau$$

и

$$D[\varphi, r] = k^2 D\left[\psi_0, kr\right], \tag{8.5}$$

поэтому

$$J[\varphi] = k^2 \frac{\hbar^2}{2\mu}\int |\nabla\psi_0|^2\, d\tau - k\frac{c}{8\pi}\int D^2\left|\psi_0, r\right| d\tau \tag{8.6}$$

При $k = 1$ эта величина переходит в $J\left[\psi_0\right]$, которое отрицательно (см. § 6). Если k убывает от единицы до нуля, $J[\varphi]$ остаётся всё время отрицательным, так как в (8.6) положительныи член убывает пропорционально k^2, а отрицательныйпропорционально k. Тогда из неравенства (8.4) очевидно, что $F_{\text{мин}}\ [\psi, \boldsymbol{P}_\varphi]$ тоже отрицателен для любого k в интервале от нуля до единицы. Полученное отрицательное значение $F_{\text{ми}}$ означает, что соответствующее состояние электрона ψ локальное.

Таким образом, уже при произвольно малой поляризации кристалла, соответствующей произвольно малому k в формулах (8.1) и (8.2), электрон попадает в локальное состояние, которое энергетически выгоднее, чем зонное. По мере

роста k и соответствующей поляризации потенциальная энергия ионов $F_{\text{ми}}$ монотонно убывает от нуля в сторону отрицательных значений.

Следовательно, неполяризованный кристалл не соответствует минимуму потенциальной энергии, т. е. он неустойчив. Поляризация будет стремиться расти, а за ней должно адиабатически «следовать» состояние локализованного электрона. В конце концов кинетическая энергия ионов, накопленная за время ускоренной поляризации, превратится в теплоту, и равновесие наступит при такой конфигурации ионов, при которой F достигнет минимума не только по ψ, но и по $\boldsymbol{P}$. Иными словами, система придёт в самосогласованное состояние полярона.

Очевидно, что процесс формирования полярона не требует никакой тепловой флуктуации и совершается за время порядка периода колебания ионов. Наоборот, зонное состояние электрона получается в результате диссоциации полярона, для чего требуется флуктуативная деполяризация кристалла.

Сделанные выше выводы о неустойчивости зонного состояния электрона и о стремлении системы «соскользнуть» в поляронное состояние опираются на исследование самых начальных этапов поляризации, при которых поляризационная яма ещё очень неглубока, а эффективный радиус ψ-функции электрона очень велик. На этих этапах процесса с предельной точностью можно пользоваться макроскопическим рассмотрением поляризации независимо от того, получится ли в конце концов у самосогласованного полярона поляризационный радиус больше постоянной решётки или нет. Следовательно, в кристалле должны существовать поляроны независимо от соблюдения неравенства (7.7). Последнее даёт лишь возможность упростить расчёт полярона путём макроскопического учёта поляризации.

Самосогласованных поляронных состояний в кристалле может быть несколько: согласно соображениям, развитым в § 6, каждый экстремум функционала $J[\psi]$ представляет самосогласованное состояние. В § 6 был подробно рассмотрен лишь самый низкий из экстремумов функционала $J[\psi]$ - основное состояние, так как оно представляет наибольший интерес. Докажем теперь общую теорему, относящуюся к любому самосогласованному состоянию и устанавливающую связь между

энергией системы H, средней кинетической энергией электрона $\bar{T}$, энергией поляризации кристалла U_p (формула (5.13)), собственным значением энергии E в уравнении (5.3) и средней потенциальной энергией взаимодействия электрона с поляризованным кристаллом $\bar{V}$ (формула (5.18)). В самосогласованном состоянии энергия системы H даётся экстремальным значением функционала

$$J[\psi] = \frac{\hbar^2}{2\mu}\int |\nabla\psi|^2 d\tau - \frac{c}{8\pi}\int D^2[\psi, r]d\tau. \tag{8.7}$$

Предположим, что ψ_0 является экстремалью этого функционала. Наряду с ψ_0 введём функцию φ согласно формуле (8.2). Функция φ остаётся нормированной при любом $k > 0.J[\varphi]$ должен иметь экстремум при $k = 1$, так как при этом φ переходит в Ψ_0. Дифференцируя выражение (8.6) по k и приравнивая в экстремальной точке производную нулю, получаем:

$$\frac{\hbar^2}{\mu}\int |\nabla\psi_0|^2 d\tau - \frac{c}{8\pi}\int D_0^3 d\tau = 0, \tag{8.8}$$

что можно записать в виде

$$2\bar{T} + \frac{1}{2}\bar{V} = 0. \tag{8.9}$$

Энергия H равна экстремальному значению функционала (8.7), т. е.

$$H = \bar{T} + \frac{1}{2}\bar{V}. \tag{8.10}$$

Из этих двух уравнений получается

$$\bar{T} = -H \text{ и } \bar{V} = 4H. \tag{8.11}$$

Собственное значение энергии E в уравнении Шрёдингера равно

$$E = \bar{T} + \bar{V} = 3H. \tag{8.12}$$

Наконец, согласно формулам (5.13) и (5.18) и формуле (6.3)

$$U_p = -\frac{1}{2}\bar{V}. \tag{8.13}$$

Таким образом, в любом самосогласованном состоянии

$$\left.\begin{array}{rl} \bar{T} & = -H, \\ U_p & = -2H, \\ -E & = -3H, \\ -\bar{V} & = -4H \end{array}\right\} \tag{8.14}$$

или

$$\bar{T} : U_p : -E : -\bar{V} = 1 : 2 : 3 : 4. \tag{8.15}$$

10.2.4 § 9. Photodissociation and photo-excitation of the polaron [12], [16]

При рассмотрении фотопереходов электрона согласно принципу Франка-Кондона следует предположить, что за малое время фотоперехода тяжёлые ионы не успевают заметно сместиться. Поэтому в течение всего фотоперехода поляризацию кристалла и потенциальную яму электрона можно считать фиксированными и соответствующими исходному состоянию электрона.

Под фотодиссоциацией полярона понимаются фотопереход электрона в зонное состояние (в область $E > 0$) и последующая деполяризация кристалла. Диссоциированное состояние существует недолго: как только освобождённый светом электрон затормозится, он немедленно снова поляризует кристалл и попадает в локальное состояние, которое затем переходит в самосогласованное поляронное состояние, порождая при этом поляризационные волны. Красная граница фотодиссоциации, как всегда, определяется соотношением

$$\hbar\omega = -E, \tag{9.1}$$

где E - шрёдингеровский энергетический уровень исходного самосогласованного состояния электрона, отсчитанный от начала непрерывного спектра (от дна зоны).

Замечательная особенность самосогласованных поляронов заключается в том, что порог их фотодиссоциации ровно в три раза больше, чем энергия тепловой диссоциации [12]. Согласно формуле (8.12) и формуле (9.1)

$$\hbar\omega = -3H, \tag{9.2}$$

где H есть энергия тепловой диссоциации полярона. Эта разница между энергией тепловой диссоциации и энергией фотодиссоциации может быть интерпретирована следующим образом. В исходном состоянии энергия системы равна H. При тепловой диссоциации кристалл флуктуативно деполяризуется, потенциальная яма электрона исчезает и электрон оказывается в зонном состоянии; если электрон оказывается на дне зоны, то при этом энергия всей системы в диссоциированном состоянии равна нулю. Таким образом, энергия тепловои диссоциации равна - H.

Иначе обстоит дело при фотодиссоциации: тотчас же после фотоэффекта поляризация ещё не успевает исчезнуть. Поэтому в диссоциированном состоянии (когда электрон находится на дне зоны) энергия системы равна энергии поляризации кристалла

$$U_p = -2H \tag{9.3}$$

(см. формулу (8.14)). Следовательно, энергия фотодиссоциации равна $-3H$. После фотоэффекта кристалл деполяризуется и при этом энергия (9.3) превращается в теплоту.

Для основного поляронного состояния, рассмотренного в § 6, энергия тепловой диссоциации даётся формулой (6.12), а красная граница фотодиссоциации определяется соотношением [12]

$$\hbar\omega_0 = -E_0 = -3H_0 = 0,163\frac{\mu e^4}{\hbar^2}c^2. \tag{9.4}$$

Рассмотрим теперь фотовозбуждение полярона. Ограничимся рассмотрением основного самосогласованного состояния (§ 6). В этом случае потенциальная яма электрона даётся формулоЙ (6.18) и представлена на рис. 6.1. Предположим согласно принципу Франка-Кондона, что фотопереход совершается при фиксированной потенциальной яме (6.18). Для этой потенциальной ямы должны быть рассчитаны все конечные состояния электрона, в которые он переходит при фотовозбуждении. Поскольку эта потенциальная яма обладает сферической симметрией, угловая часть ψ-функций всех состояний даётся обычными сферическими функциями; при этом существуют общеизвестные правила отбора для оптических переходов. Поскольку основное состояние является s-состоянием, то разрешены переходы только в p-состояния.

Итак, предположим, что поляризация кристалла фиксирована и соответствует основному поляронному состоянию, т. е. равна

$$P_0(r) = \frac{c}{4\pi}D\left[\psi_0, r\right]. \tag{9.5}$$

Соответствующие стационарные состояния электрона, как было показано в § 5 , являются минималями функционала

$$F\left[\psi, P_0\right] = \frac{\hbar^2}{2\mu}\int|\nabla\psi|^2 d\tau - \int P_0 D[\psi, r]d\tau + \frac{2\pi}{c}\int P_0^2 d\tau \tag{9.6}$$

($\boldsymbol{P}_0$ не варьируется).

Для минимизации этого функционала применим прямой вариационный метод, подобно тому как это уже делалось в § 6. Поскольку нас интересуют только p-состояния ($l = 1$), угловая часть ψ-функций может быть наперёд задана в виде сферической функции первого порядка $Y_1(\vartheta, \varphi)$.

Рассмотрим ψ-функцию самого нижнего из p-уровней. Ее радиальная часть, как известно, не имеет узлов (кроме точки $r = 0$). Учитывая известный асимптотический ход этой ψ-функции при больших и при малых r, мы можем апроксимировать её формой

$$\Psi_p^0 = CY_1(\vartheta, \varphi) x e^{-\beta x}, \tag{9.7}$$

где $x = 2\alpha_4 r$ (α_4-то же, что в § 6), а C и β - варьируемые параметры. Значок ^{0} сверху у ψ-функции напоминает о том, что состояние вычисляется при заданной поляризации $\boldsymbol{P}_0(\boldsymbol{r})$ (не самосогласованное). Из условия нормировки $\cup_p^0$ получается

$$C^2 = (2\alpha_4)^3 \frac{(2\beta)^5}{4!}. \tag{9.8}$$

функцию ψ_p^0 подставляем в функционал (9.6) и значение параметра β находим из условия минимума $F\left[\psi_p^0, P_0\right]$. В результате вычисления получается

$$2\beta = 0,5146. \tag{9.9}$$

Энергия электрона

$$E_p^0 = \frac{h^2}{2\mu} \int \left|\nabla \psi_p^0\right|^2 d\tau - \int \boldsymbol{P}_0 \boldsymbol{D}\left[\psi_p^0, \boldsymbol{r}\right] d\tau \tag{9.10}$$

В результате подстановки сюда $(9.7), (9.8)$ и $(9,9)$ получим:

$$E_p^0 = -0,0935 \frac{\mu e^4}{\hbar^2} c^2 \tag{9.11}$$

Полная энергия системы в рассматриваемом состоянии равна соответствующему экстремальному значению функционала (9.6):

$$H_p^0 = F\left[\psi_p^0, P_0\right] = E_p^0 + \frac{2\pi}{c} \int P_0^2 d\tau = 0,0153 \frac{\mu e^4}{\hbar^2} c^2 \tag{9.12}$$

Полная энергия системы оказалась положительной. Это, однако, ещё не значит, что произойдёт диссоциация полярона. Дело в том, что немедленно после фотоперехода $\psi_0 \to \psi_p^0$ получается несамосогласованное состояние: поляризация ещё соответствует основному состоянию ψ_0, тогда как электрон уже находится в состоянии Ψ_p^0. Тотчас же после фотоперехода ионы начнут ускоренно двигаться к своим новым равновесным положениям, возникнут поляризационные волны, энергия которых превратится в теплоту. Если из H_p^0 вычесть энергию этих поляризационных волн и таким образом получить энергию системы уже после тепловыделения, то она оказывается отрицательной. Следовательно, диссоциации полярона не произойдёт.

Частота света, поглощаемого при фотопереходе $\psi_0 \to \psi_p^0$, определяется соотношением

$$\hbar\omega_{p0} = E_p^0 - E_0 = 0,0697 \frac{\mu \cdot 4}{\hbar^2} c^2 \tag{9.13}$$

Сила осциллятора для этого перехода, вычисленная М. Ф. Дейгеном, равна

$$f_{p0} = 0,93. \tag{9.14}$$

Таким образом, для всех остальных фотопереходов как на дискретные уровни, так и в непрерывный спектр суммарная сила осциллятора составляет всего 0,07 . Это значит, что рассмотренный переход $\psi_0 \to \psi_p^0$ значительно более вероятен, чем все другие переходы.

Поляризационная потенциальная яма полярона на больших расстояниях r стремится к кулоновской форме

$$V \to -\frac{e^2}{r} c \tag{9.15}$$

Поэтому для возбуждённых состояний с большим эффективным радиусом энергия и ч-функция могут быть рассчитаны по формулам водородоподобного атома с эффективным зарядом ядра ес. Для p-состояний такое приближение пригодно уже, когда главное квантовое число равно четырём и более.

В этом параграфе применялся принцип Франка-Кондона, который справедлив, строго говоря, лишь в том случае, когда массы ионов бесконечно велики, а собственные частоты ионов бесконечно малы. В этом предельном случае спектр поглощения света поляроном должен был бы состоять из резких дискретных линий и сплошной части, подобно спектру атома. Однако в реальных кристаллах частоты ионов обладают конечной величиной, что должно привести к некоторым отступлениям от результатов настоящего параграфа (к эффекту конечной ширины линий поглощения). Этот вопрос будет рассмотрен в § 28 применительно к F-центрам.

10.2.5 § 10. Progressive motion of the polaron [17], [18]

Согласно § 5 функция Гамильтона, описывающая движение ионов кристалла, имеет вид

$$H = \frac{\hbar^2}{2\mu}\int |\nabla\psi|^2 d\tau - \int PD[\psi, r]d\tau + U_{\text{пот}} + U_{\text{кин}*} \tag{10.1}$$

Предполагается, что сюда уже подставлено ψ, приводящее величину (10.1) к экстремальному значению при фиксированном $\boldsymbol{P}$. Это ч представляет собой стационарное состояние электрона в кристалле с поляризацией $\boldsymbol{P}$. Оно удовлетворяет соотношению

$$\frac{\hbar^2}{2\mu}\delta\int |\nabla\psi|^2 d\tau - \int \boldsymbol{P}\delta\boldsymbol{D}d\tau = 0 \tag{10.2}$$

при дополнительном условии

$$\int |\psi|^2 d\tau = 1 \tag{10.3}$$

При этом ψ и $D[\,\psi, r]$ определяются конфигурацией ионов, т. е. зависят от координат ионов, как от параметров. Поляризация $\boldsymbol{P}$ есть линейная функция координат ионов. Последние два члена в формуле (10.1) представляют собой функцию Гамильтона для ионов в отсутствие электрона проводимости.

Первый и второй члены в формуле (10.1) появляются при введении в кристалл электрона проводимости; поскольку они зависят только от координат ионов, а не от их скоростей, то их следует рассматривать как добавочную потенциальную энергию ионов, которая появляется при введении в кристалл электрона проводимости. При этом появляются добавочные силы, действующие на ионы. Добавочная сила, действующая на ка-кой-либо ион, равна с обратным знаком градиенту добавочной потенциальной энергии, взятому по координатам данного иона. При дифференцировании первого и второго членов формулы (10.1) следует учесть соотношение (10.2), показывающее, что производная от первого члена сокращается с той частью производной второго члена, в которой дифференцируется $\boldsymbol{D}$ при фиксированном $\boldsymbol{P}$. Таким образом, остаётся лишь во втором члене дифференцировать $\boldsymbol{P}$ при фиксированном $\boldsymbol{D}$. В результате оказывается, что действующая на ионы добавочная сила равна $e\boldsymbol{D}$.

Попытка рассмотрения общего случая движения ионов наталкивается на непреодолимые математические трудности. Как известно, даже в отсутствии электрона проводимости и при рассмотрении лишь малых (нормальных) колебаний ионов расчёты

удалось довести до численных результатов только в предельном случае длинных поляризационных волн, т. е. когда длина волны значительно больше постоянной решётки. Рассматривая более сложную задачу - движение ионов в присутствии электрона проводимости, нам тем более придётся ограничиться случаем малых колебаний и плавных поляризационных деформаций.

В этом случае уравнения движения ионов будут состоять из линейных однородных частей, соответствующих собственным (нормальным) колебаниям ионов в отсутствии электрона проводимости и, кроме того, будут содержать добавочную силу $\boldsymbol{eD}$, связанную с присутствием электрона проводимости. $\boldsymbol{D}$, так же как и ч, зависит от координат ионов, но эту зависимость в общем случае трудно выразить явно. Поэтому уравнения движения ионов представляют собой сложную нелинейную бесконечную систему уравнений, которую в общем случае трудно не только решить, но даже записать. Существуют, однако, частные случаи движения, когда задача упрощается. Таковым является, например, рассмотренный в § 6 случай, когда ионы

покоятся в равновесных положениях. В этом параграфе будет рассмотрен несколько более общий случай, когда полярон прямолинейно и равномерно движется в кристалле.

Речь идёт о таком движении ионов, при котором поляризационная потенциальная яма электрона, а также ψ и $\boldsymbol{D}$ волнообразно перемещаются со скоростью v, сохраняя свою форму, т. е. когда

$$P = P(r - vt), \tag{10.4}$$

$$\psi = \psi(r - vt), \tag{10.5}$$

$$D = D(r - vt). \tag{10.6}$$

Прежде всего покажем, что уравнения движения обладают частными решениями типа (10.4), (10.5), (10.6). Предположим сначала без обоснования, что добавочная сила представляет собой волну типа (10.6), и разложим её в ряд Фурье

$$\left.\begin{array}{c} D(r - vt) = \sum_k D_k e^{ik(r-vt)} = \sum_k D_k e^{i(kr-\omega_k t)}, \\ \omega_k = kv. \end{array}\right\} \tag{10.7}$$

Рассмотрим вынужденные колебания ионов, вызванные силой (10.7). Они представляют собой простую суперпозицию колебаний, вызванных отдельными гармониками вида

$$D_k e^{i(kr-\omega_k t)}. \tag{10.8}$$

Основная идея автора [17] заключается в том, чтобы, не решая задачи о вынужденных колебаниях ионов, вызванных силой (10.8), заменить эту волнообразную силу эквивалентной электромагнитной волной, а затем, использовав экспериментальные данные о дисперсии электромагнитных волн в кристалле, найти непосредственно колебания удельного дипольного момента $\boldsymbol{P}$. Этот метод избавляет от необходимости явного введения нормальных координат ионов, что само по себе представило бы трудности. Волны (10.8) существенно отличаются от обычных электромагнитных: они не поперечны, не имеют магнитной компоненты, при данной частоте длина их волны меньше, чем у электромагнитных. Чтобы пояснить, о какой эквивалентности всё же идёт речь, рассмотрим этот вопрос несколько подробнее.

Волнообразная сила (10.8) способна вызывать поляризационные колебания ионов той же частоты ω_k и длины волны, какими обладает сама сила. Иначе говоря, вынужденное поляризационное колебание должно иметь вид

$$P_k e^{i(kr-\omega_k t)}, \tag{10.9}$$

где k и ω_k те же, что в формуле (10.8). Для того чтобы полностью определить поляризационное колебание, остаётся найти его амплитуду $\boldsymbol{P_k}$. В общем случае $\boldsymbol{P_k}$ зависит от $\boldsymbol{D_k}$, $\omega_{\boldsymbol{k}}$ и k. Однако, поскольку D является плавной функцией r (поляризационный радиус полярона превышает постоянную решётки, см. § 7), в разложении (10.7) главную роль играют волны, длина которых значительно больше постоянной решётки. В этом предельном случае бесконечно длинных волн $(k \to 0) P_k$ зависит только от $\boldsymbol{D}_k$ и ω_k, но не от $\boldsymbol{k}$.

Следовательно, амплитуда вынужденного поляризационного колебания определяется исключительно амплитудой и частотой внешнего поля, а длина волны поля и его поперечность не играют роли. Вот почему при вычислении P_k можно поле (10.8) заменить электромагнитной волной с той же амплитудой $\boldsymbol{D_k}$ и частотой ω_k. Такую электромагнитную волну мы будем называть эквивалентной.

После того как поле (10.8) заменено эквивалентной электромагнитной волной, можно $\boldsymbol{P_k}$ выразить через $\boldsymbol{D_k}$ с помощью диэлектрической постоянной $\varepsilon(\omega_k)$, определяющей дисперсию электромагнитных волн в кристалле. Учитывая, что $\boldsymbol{P_k}$ есть только инерционная часть поляризации кристалла аналогично выводу формулы (5.12) для статических полей, легко для гармонически колеблющихся полей получить формулу

$$P_k = \frac{c(\omega_k)}{4\pi} D_k, \tag{10.10}$$

где

$$c(\omega_k) = \frac{1}{n^2} - \frac{1}{\varepsilon(\omega_k)}.$$

Поляризация, вызванная добавочной силой (10.7), как уже упоминалось, представляет собой простую суперпозицию поляризационных колебаний, вызванных отдельными гармониками

вида (10.8):

$$P = \sum_k P_k e^{i(kr-\omega_k t)} = \frac{1}{4\pi} \sum_k c(\omega_k) D_k e^{i(kr-\omega_k t)}. \tag{10.11}$$

Предположим, что скорость поступательного движения полярона достаточно мала:

$$v \ll \omega_i r_p, \tag{10.12}$$

где ω_f - собственная частота колебания ионов, а r_p - поляризационный радиус полярона (см. формулу (7.6)). В этом случае в сумме (10.11) главную роль играют члены, у которых

$$\omega_k \ll \omega_i, \tag{10.13}$$

и $\varepsilon(\omega_k)$ и $c(\omega_k)$ можно считать вещественными, пренебрегая поглощением в кристалле электромагнитных волн с частотой ω_k. Разложение ε и c по степеням ω_k будет содержать лишь чётные члены:

$$c(\omega_k) = c_0 + c_2 \omega_k^2 + \ldots \tag{10.14}$$

Дальнейшие члены разложения можно отбросить на основании неравенства (10.13). Подставляя это разложение в (10.11) и учитывая, что

$$\omega_k^{2n} e^{i(kr-\omega_k t)} = (-1)^n \frac{\partial^{2n}}{\partial t^{2n}} e^{i(kr-\omega_k t)}, \tag{10.15}$$

удобно выражение для поляризации записать в просуммированном виде

$$\boldsymbol{P} = \frac{1}{4\pi}\left[c_0 \boldsymbol{D} - c_2 \frac{\partial^2 \boldsymbol{D}}{\partial t^2} + \ldots\right]. \tag{10.16}$$

Это есть частное решение уравнений вынужденных колебаний ионов под влиянием силы $\boldsymbol{D}$. Оно в дальнейшем заменит собой канонические уравнения движения ионов. Это решение соответствует случаю, когда отсутствуют тепловые колебания ионов ($T = 0$). Нетрудно убедиться в том, что соотношение (10.16) справедливо не только, когда сила $\boldsymbol{D}$ имеет вид (10.6), но и в общем случае, когда $\boldsymbol{D}$ является плавной функцией $\boldsymbol{r}$ и медленно меняется со временем.

Вернёмся теперь к вопросу о существовании частного решения типа (10.4-6). Три функции $P(r,t), \psi(r,t)$ и $D(r,t)$ определяются из трёх уравнений: $(10,16), (10,2)$ и (5.17). По

виду этих уравнений ясно, что все три одновременно можно удовлетворить функциями типа (10.4-6). Если, например, предположить, как это сделано выше, что $\boldsymbol{D}$ имеет вид волны (10.6), то из (10.16) следует, что P также имеет вид волны (10.4). Тогда из (10.2) следует, что ? имеет вид волны (10.5) (поляризационная потенциальная яма поступательно движется со скоростью $\boldsymbol{v}$, а ψ-функция адиабатически следует за ней, сохраняя свою форму). Отсюда в свою очередь следует согласно формуле (5.17), что $\boldsymbol{D}$ является волной типа (10.6), что подтверждает исходное предположение, принятое сначала без доказательства. Таким образом, форма решения (10.4-6) является самосогласованной.

В поисках частного решения типа (10.4-6) выберем систему координат так, чтобы направление оси x совпало с направлением скорости полярона v. В такой системе координат равенства (10.4-6) будут выглядеть следующим образом:

$$P = P(x - vt, y, z) \tag{10.17}$$
$$\psi = \psi(x - vt, y, z) \tag{10.18}$$
$$D = D(x - vt, y, z). \tag{10.19}$$

В применении к таким функциям операция $\frac{\partial}{\partial t}$ эквивалентна операции $-v\frac{\partial}{\partial x}$. Поэтому уравнение (10.16) можно переписать в виде

$$P = \frac{1}{4\pi}\left[c_0 D - c_2 v^2 \frac{\partial^2 D}{\partial x^2}\right]. \tag{10.20}$$

Если это P подставить в уравнение (10.2), то получится

$$\frac{\hbar^2}{2\mu}\delta \int |\nabla|^2\Big|^2 d\tau - \frac{1}{4\pi}\int \left(c_0 D - c_2 v^2 \frac{\partial^2 D}{\partial x^2}\right)\delta D d\tau = 0 \tag{10.21}$$

при дополнительном условии

$$\int |\psi|^2 d\tau = 1. \tag{10.3}$$

Здесь предполагается, что $\boldsymbol{D}$ выражено через ψ согласно формуле (5.17). Интегрируя в (10,21) последний член по частям,

это уравнение можно представить в виде

$$\delta J_v[\psi] = 0 \tag{10.22}$$

$$J_v[\psi] = \frac{\hbar^2}{2\mu}\int |\nabla\psi|^2 d\tau - \frac{c_0}{8\pi}\int D^2 d\tau - \frac{c_2 v^2}{8\pi}\int \left(\frac{\partial D}{\partial x}\right)^2 d\tau \tag{10.23}$$

Таким образом, искомое ψ является экстремалью функционала $J_v[\psi]$ при дополнительном условии (10.3). Этот функционал таков, что если $\psi(\boldsymbol{r})$ является его экстремалью, то экстремалью будет также и $\psi(r-\xi)$ при условии, что вектор ξ не зависит от x, y, z (ξ может зависеть от времени). Придавая вектору ξ различные значения, можно получить бесконечное множество экстремалей, которые все соответствуют одному и тому же значению функционала.

Все эти ψ удовлетворяют уравнениям (10.2) и (10.20), однако, вообще говоря, не удовлетворяют уравнению (10.16). Если же положить

$$\xi_x = vt, \quad \xi_y = \xi_z = 0, \tag{10.24}$$

то ψ и $\boldsymbol{D}$ приобретают вид (10.18-19). В этом случае уравнение (10.16) совпадает с уравнением (10.20) и также удовлетворяется. Следовательно, мы действительно приходим к решению первоначально поставленной задачи - к решению системы уравнений (10.16), (10.2) и (5.17).

Функционал $J_v[\psi]$ является обобщением функционала $J[\psi]$ (формула (6.4)) на случай движущегося полярона; при $\mathfrak{v} \to 0 J_v[\psi]$ переходит в $J[\psi]$. В случае покоящегося полярона его основное состояние описывалось ψ-функцией, которая являлась минималью $J[\Psi]$ и была сферически симметрична (§ 6). В случае же движущегося полярона соответствующая ψ-функция является абсолютной минималью функционала $J_v[\psi]$; она обладает не сферической, а лишь осевой симметрией, что связано с присутствием третьего члена в формуле (10.23). Ось симметрии параллельна оси Ox, т. е. направлению скорости v.

Выше предполагалось, что скорость v достаточно мала, чтобы соблюдалось неравенство (10.12). В этом случае третий член в формуле (10.23) значительно меньше предыдущих: он относится ко второму члену приблизительно, как $v^2/\omega_i^2 r_p^2$. Следовательно, третий член в формуле (10.23) можно считать малым возмущением, а функционал $J_v[\psi]$ рассматривать как

возмущённый функционал J $[\psi]$. В соответствии с этим уравнение (10.22) можно решать методами теории возмущений, приняв за нулевое приближение решение для покоящегося полярона ψ_0(§6) и раскладывая ψ по степеням «малого параметра» v^2:

$$\dot{\psi} = \psi_0 + v^2\psi_1 + \ldots \tag{10.25}$$

Не углубляясь в подробные вычисления методом возмущений, следует, однако, подчеркнуть вывод, существенный для дальнейшего: пока справедливо неравенство (10.12), разность между ψ и ψ_0 мала и порядка v^2.

Перейдём теперь к вычислению эффективной массы полярона в его поступательном движении. Эта масса была вычислена автором совместно с Л. Д. Ландау [18]. Необходимо определить зависимость энергии всей системы от скорости движения полярона с точностью до членов порядка v^2. Энергия всей системы даётся формулой (10.1). Необходимо в ней прежде всего найти конкретное выражение двух последних членов - потенциальной и кинетической энергий ионов. Предположим, что до прихода полярона в данную область кристалла ионы покоились, и примем энергию ионов в этом состоянии за начало отсчёта энергии. При движении полярона сквозь рассматриваемую область кристалла ионы начнут волнообразно смещаться под влиянием добавочной силы

eD, рассмотренной выше. Потенциальную и кинетическую энергии ионов в этом случае можно рассчитать как работу, совершённую силой eD над ионами. Используя формулу (10.16), можно работу, совершаемую в единице объёма за единицу времени, выразить следующим образом:

$$D\dot{P} = \frac{D}{4\pi}\left[c_0\dot{D} - c_2\ddot{D}\right]. \tag{10.26}$$

Если эту величину проинтегрировать по времени от момента, когда сила $\boldsymbol{D}$ ещё отсутствовала (полярон был далеко), до настоящего момента, когда в рассматриваемой точке присутствует сила $\boldsymbol{D}$, то в результате получится энергия ионов единицы объёма кристалла. Она оказывается равнои

$$\frac{c_0}{8\pi}D^2 - \frac{c_2}{4\pi}D\ddot{D} + \frac{c_2}{8\pi}\dot{D}^2. \tag{10.27}$$

Если теперь величину (10.27) проинтегрировать по объёму всего кристалла, то получится суммарная потенциальная и кинетическая энергия ионов кристалла:

$$U_{\text{пот}} + U_{\text{кии}} = \frac{c_0}{8\pi}\int D^2 d\tau + \frac{3c_2}{8\pi}\int \dot{D}^2 d\tau \tag{10.28}$$

При упомянутом интегрировании следует учесть, что в применении к функции $\boldsymbol{D}$ операция $\frac{\partial}{\partial t}$ эквивалентна операции $-v\frac{\partial}{\partial x}$. Это даёт возможность преобразовать интегрированием по частям интеграл от второго члена (10.27) и объединить его с третьим членом. Подставляя (10.28) и (10.16) в формулу (10.1), можно энергию системы представить в виде

$$\begin{aligned} H = \tfrac{\hbar^2}{2\mu}\int|\nabla\psi|^2 d\tau - \tfrac{c_0}{8\pi}\int D^2 d\tau + \tfrac{c_2}{8\pi}\int \dot{D}^2 d\tau = \\ = J_v|\psi| + \tfrac{c_2}{4\pi}\int \dot{D}^2 d\tau \end{aligned} \tag{10.29}$$

Для определения эффективной массы полярона необходимо эту энергию разложить в ряд по степеням v до членов порядка v^2 включительно. Для этого в формулу (10.29) следует подставить разложение (10.25).

Первые два члена в формуле (10.29) представляют собой функционал $J[\Psi]$, а Ψ_0 является его экстремалью. Соответствующее экстремальное значение функционала

$$J\left[\xi_0\right] = H_0 \tag{10.30}$$

даётся формулой (6.12); оно представляет собой энергию системы при неподвижном поляроне. Замену Ψ_0 на Ψ можно рассматривать как малую вариацию ψ:

$$\delta\psi = \psi - \psi_0 = v^2\psi_1 + \ldots \tag{10.31}$$

Поскольку эта вариация берётся в экстремальной точке, соответствующее изменение J будет порядка не $\delta\psi$, а $(\delta\psi)^2$, т. е. порядка $\boldsymbol{v}^4$. Следовательно,

$$J[\psi] = H_0 + \text{ const } \cdot v^4 + \ldots \tag{10.32}$$

Разложение третьего члена формулы $(10, 29)$ по степеням $\mathfrak{v}$
имеет вид

$$\frac{c_2}{8\pi}\int \dot{D}^2 d\tau = \frac{c_2 v^2}{8\pi}\int\left(\frac{\partial D\left[\Psi_0\right]}{\partial x}\right)^2 d\tau + \ldots \tag{10.33}$$

Таким образом, энергию системы с точностью до членов порядка v^2 можно записать в виде

$$H = H_0 + \frac{1}{2}Mv^2 \tag{10.34}$$
$$M = \frac{c_2}{4\pi}\int\left(\frac{\partial D\left[\psi_0\right]}{\partial x}\right)^2 d\tau$$

При вычислении M функция ψ_0 была нами взята в форме (6.16). В результате вычисления получилось:

$$M = 5,8\cdot 10^{-3}\left(\frac{\mu e^2}{\hbar^2}c_0\right)^3 e^2 c_2 = 9,08\cdot 10^3\left(\frac{\mu}{m}\right)^3 c_0^3 c_2 2. \tag{10.35}$$

Вычисление M с помощью аппроксимации (6.14) приводит к подобной формуле, в которой вместо коэффициента 5,8 стоит 5,2 [73].

Выше было показано, что полярон способен равномерно и прямолинейно двигаться в кристалле «по инерции». Если к кристаллу приложить внешнее электрическое поле, то полярон в таком поле будет двигаться ускоренно. Если это поле достаточно мало и однородно и не вызывает заметных деформаций полярона, то потенциальная энергия полярона по отношению к внешнему полю будет такой же, как потенциальная энергия точечного заряда, расположенного в центре полярона. Приравнивая мощность, развиваемую внешним полем $\boldsymbol{E}$, приращению энергии (10.34) за секунду, получаем:

$$M\dot{\boldsymbol{v}} = e\boldsymbol{E}. \tag{10.36}$$

Эта формула показывает, что полярон во внешнем поле будет двигаться как частица с зарядом e и массой M. Поэтому коэффициент M будет называться эффективной массой полярона. Обычно M оказывается значительно больше массы электрона. Например, для кристалла NaCl , если принять $\varepsilon = 5,8;\ n^2 = 2,33; \omega_i = 4,88\cdot 10^{13} 2\mu, \frac{\mu}{m} = 2,78$, то получается

$$\frac{M}{m} = 391.$$

В этом параграфе была вычислена эффективная масса полярона в предположении, что ионы движутся по законам классической механики. В § 16 даётся расчёт эффективной массы полярона с квантовомеханическим рассмотрением движения ионов, причём для M получается то же самое значение.

В 1950 г. была опубликована работа Н. Н. Боголюбова [47], в которой намечен путь вычисления энергии поступательно движущегося полярона в более общем случае, не прибегая к разложению по степеням v^2. В этой работе учитывается упомянутая выше зависимость ψ-функции электрона от v и её отступление от сферической симметрии. В частном случае малых скоростеи, раскладывая энергию системы по степеням v^2, Н. Н. Боголюбов получает для эффективной массы полярона выражение (10.34). В § 30 будет показано, что для кристаллов с решёткой типа каменной соли

$$c_2 = \frac{c_n}{\omega_i^2}, \tag{10.37}$$

где ω_i-предельная частота продольных поляризационных колебаний ионов. Согласно формулам (7.6), (10.35) и (10.37) критерий (10.12) можно записать в более удобном виде:

$$\frac{Mv^2}{2} \ll 0,29\frac{\mu e^4 c_0^2}{\hbar^2} = 5,33\left|H_0\right|, \tag{10.38}$$

где $|H_0|$-энергия тепловой диссоциации полярона. Если поляроны находятся в тепловом равновесии с кристаллом, то их кинетическая энергия порядка $\frac{3}{2}kT$. В этом случае неравенство (10.38) может нарушиться только при таких температурах, когда kT больше энергии тепловой диссоциации полярона $|H_0|$.

10.2.6 § 11. A new look at the electronic conductivity of ionic crystals [15], [17]

В течение последних двадцати лет развилась и завоевала себе популярность теория электронной проводимости кристаллов на основе квантовой механики. Для всех вариантов упомянутой теории характерна следующая постановка вопроса:

в нулевом приближении Ψ-функции электрона проводимости вычисляются в предположении, что ионы неподвижно закреплены в узлах решётки, как это делалось в § 3; задача сводится к рассмотрению электрона в периодическом поле $W(\boldsymbol{r})$; ψ-функции имеют вид плоских модулированных волн (см., например, формулу (3.6)). Такие состояния электрона выше назывались для краткости просто «зонными». Движение ионов в нулевом приближении рассматривается так, как если бы электрона проводимости вовсе не было, т. е. предполагается, что ионы совершают гармонические колебания около узлов решётки, причём эти колебания волнообразно распространяются по кристаллу. Таким образом, как мы уже указывали, в нулевом приближении игнорируется взаимодействие между электроном проводимости и колебаниями ионов. Это взаимодействие вводится в первом приближении как малое возмущение, вызывающее рассеяние вышеупомянутых плоских модулированных волн. В разных вариантах теории вычисляется в первом приближении вероятность рассеяния ψ-волн на колебаниях ионов, т. е. «свободный пробег» электрона.

В этой главе было показано, что наряду с зонными состояниями электрона проводимости существуют поляронные состояния, в которых ψ-функция электрона локализована в ограниченной части пространства (см., например, формулу (6.14)), а ионы колеблются не около узлов решётки, а около иных равновесных положений, которые смещены из узлов в результате диэлектрической поляризации кристалла полем электрона. Как было показано в предыдущем параграфе, поляроны могут поступательно двигаться и, следовательно, могут участвовать в электропроводности в качестве носителей тока наряду с зонными электронами.

Интересно выяснить, какой же из этих двух видов носителей тока играет главную роль в электропроводности? Как было показано в § 6, поляронное состояние энергетически значительно выгоднее, чем зонное состояние электрона. Энергия диссоциации полярона, при которой электрон переходит в зонное состояние, равна

$$-H_0 = 1,47\frac{\mu}{m}c^2 \ni \Omega. - B, \tag{11.1}$$

Эта энергия обычно порядка десятых электрон-вольта. Поэтому при не слишком высоких температурах преобладающее большинство электронов проводимости должно находиться в поляронном состоянии. С помощью обычной статистики можно вычислить концентрацию зонных электронов. Как известно, у полупроводников с малой концентрацией электронов проводимости, когда электронный газ не вырожден, равновесная концентрация зонных электронов даётся формулой

$$N_{\text{зон}} = \frac{2}{\hbar^3}\left(\frac{\mu kT}{2\pi}\right)^{3/2} e^{\frac{\zeta}{kT}}. \tag{11.2}$$

Здесь ζ - химический потенциал электронов ($\zeta < 0$); энергия электрона на дне зоны

проводимости попрежнему принимается за нуль. Равновесная концентрация поляронов грубо приблизительно определяется аналогичной формулой

$$N_p \cong \frac{2}{\hbar^3}\left(\frac{MkT}{2\pi}\right)^{3/2} e^{\frac{\zeta - H_0}{kT}} \tag{11.3}$$

Более точная формула для концентрации поляронов будет выведена в § 19 для идеального полупроводника и в § 29 для полупроводника с примесью (донором электронов).

Отношение концентрации поляронов к концентрации зонных электронов равно

$$\frac{N_p}{N_{30H}} \cong \left(\frac{M}{\mu}\right)^{3/2} e^{-\frac{H_0}{kT}}. \tag{11.4}$$

Это отношение может быть очень велико. Например, для щёлочно-галоидных кристаллов множитель $\left(\frac{M}{\mu}\right)^{3/2}$ порядка тысяч, а экспоненциальный множитель при $H_0 = -0,2$ эл.-в и $T = 300°$K равен ≈ 2500. Следовательно, отношение концентраций порядка нескольких миллионов. При понижении температуры это отношение экспоненциально растёт ($H_0 < 0$). Таким образом, концентрация поляронов подавляюще превосходит концентрацию зонных электронов.

Чтобы выяснить, какой из этих двух видов носителей тока играет главную роль в электропроводности, необходимо, помимо концентраций, сравнить ещё их подвижности. Поэтому надо оценить подвижность полярона во внешнем однородном

электрическом поле $\boldsymbol{E}$. Согласно уравнению (10.36) предыдущего параграфа полярон должен был бы в однородном поле двигаться равномерно ускоренно. Однако в предыдущем параграфе игнорировались тепловые колебания ионов, а также поглощение в кристалле «эквивалентных электромагнитных волн» ($\varepsilon(\omega_k)$ считалось вещественным). На самом деле оба эти фактора приводят к торможению поступательно движущегося полярона и определяют его подвижность.

Влияние тепловых колебаний ионов будет рассмотрено в следующей главе на основе квантовомеханического описания движения ионов (§ 20). Однако сейчас, несколько забегая вперёд, заметим, что учёт тепловых колебаний ионов приводит к подвижности полярона, температурная зависимость которой при низких температурах даётся множителем $e^{\hbar\omega_i/kT}$. При $T \to 0$ эта подвижность быстро стремится к бесконечности. Следовательно, при достаточно низких температурах тепловые колебания ионов играют второстепенную роль в торможении полярона; главную роль при низких температурах играет, повидимому, поглощение в кристалле «эквивалентных электромагнитных волн». Перейдём к его рассмотрению.

В предыдущем параграфе было показано, что с появлением в кристалле движущегося полярона ионы подвергаются действию добавочной силы eD. Для определения силы торможения полярона или же его подвижности необходимо вычислить энергию, которую за единицу времени движущийся полярон затрачивает на возбуждение колебаний ионов, иначе говоря, энергию, которую ионы приобретают в поле $\boldsymbol{D}$. Это поле согласно формуле (10.7) предыдущего параграфа может быть представлено как суперпозиция гармонических волн. Последние же можно заменить эквивалентными электромагнитными волнами, т. е. электромагнитными волнами той же амплитуды и частоты (см. § 10). Таким образом, влияние движущегося полярона на ионы заменяется действием на ионы пакета эквивалентных электромагнитных волн. Необходимо вычислить энергию, которую за единицу времени эти электромагнитные волны передают ионам. Задача, следовательно, сводится к рассмотрению поглощения эквивалентных электромагнитных волн в кристалле.

Если собственные колебания ионов кристалла строго гармоничны, то кристалл, как известно, должен поглощать только

электромагнитные волны, частоты которых совпадают с частотами собственных колебаний ионов ω_i. Если к тому же кристалл идеален (без дефектов), то оптически активными должны быть одни лишь предельные частоты колебаний ионов (частоты колебаний, у которых длина волны бесконечна). В этом случае кристалл совсем не должен поглощать упомянутые выше эквивалентные электромагнитные волны, так как их частоты ω_k, по предположению, значительно меньше частот собственных колебаний ионов ω_i (см. формулу (10.13)). Эквивалентная электромагнитная волна будет лишь стационарно поддерживать вынужденные колебания ионов, но не будет их генерировать, т. е. не будет передавать энергии ионам. В этом случае полярон движется по инерции без торможения, как показано в предыдущем параграфе.

Экспериментальные исследования [19], однако, показывают, что спектр поглощения электромагнитных волн ионами кристалла состоит не из нескольких резких линий, соответствующих предельным частотам ионов, а представляет собой широкую непрерывную область поглощения. Поглощение особенно интенсивно вблизи собственных частот ионов ω_i, но существенно (для интересующего нас вопроса) также и в области значительно меньших частот. Этот факт, повидимому, связан с ангармонизмом в колебаниях ионов и, возможно, в какой-то мере с дефектами кристалла.

Не углубляясь в объяснение вида спектра поглощения электромагнитных волн ионами кристалла, можно силу торможения и подвижность полярона выразить непосредственно через коэффициент поглощения кристалла.

Для этого вычислим энергию, которую упомянутый выше пакет эквивалентных электромагнитных волн передаёт ионам за елиницу времени. Рассмотрим электромагнитную волну, эквивалентную $\boldsymbol{k}$-й гармонике и ей комплексно сопряжённой в разложении (10.7). Вектор индукции этой волны равен

$$\boldsymbol{D}_{\boldsymbol{k}} e^{-i\omega_{\boldsymbol{k}} t} + \boldsymbol{D}_{-\boldsymbol{k}} e^{i\omega_{\boldsymbol{k}} \boldsymbol{k}} \tag{11.5}$$

Так как ω_k значительно меньше собственных частот колебаний ионов, то вещественная часть показателя преломления этой волны равна

$$n_0 = \sqrt{\mathrm{e}}. \tag{11.6}$$

(ε - статическая диэлектрическая постоянная), а его мнимая часть в первом приближении пропорциональна частоте:

$$n_0 x = b\omega_k. \tag{11.7}$$

Коэффициент поглощения кристалла τ связан с постоянной b следующим образом:

$$\tau = \frac{2n_0 z_k}{c_1}\omega_k = \frac{2b}{c_1}\omega_k^2, \tag{11.8}$$

где c_1 - скорость света в пустоте. Среднее по времени значение интенсивности электромагнитной волны (11.5) равно

$$\bar{S} = \frac{c_1}{2\pi\varepsilon^{3/2}} \left|D_k\right|^2 \tag{11.9}$$

Энергия электромагнитной волны, поглощаемая за единицу времени в единице объёма кристалла,

$$\tau\bar{S} = \frac{b}{\pi\varepsilon^{3/2}}\omega * \left|D_k\right|^2. \tag{11.10}$$

Совокупность волн (10.7) во всём объёме кристалла L^3 за единицу времени передаёт ионам энергию

$$W = \frac{L^3 b}{2\pi\varepsilon^{3/2}} \sum_k \omega_k^2 \left|D_k\right|^2 = \frac{b}{2\pi\varepsilon^{3/2}} \int_{L^3} [(\eta\Gamma)D]^2 d\tau. \qquad ((11.1)$$

Іосследнее равенство легко проверить, если $\boldsymbol{D}$ под интегралом разложить по формуле (10.7). Как было показано в предыдущем параграфе, при малых скоростях полярона $D[$ ч, $\boldsymbol{r}]$ мало отличается от D [Ψ_0, r]. Поэтому при вычислении интеграла функция ψ была нами взята из формулы (6.16). В результате вычисления получилось:

$$W = \frac{0,29 e^9 \alpha_3^3 v^2 b}{\pi\varepsilon^{8/2}} \tag{11.12}$$

$$\alpha_3 = 0,95 \cdot 10^8 \frac{\mu}{m} c_0 c M^{-1}. \tag{11.13}$$

В случае стационарного движения полярона во внешнем электрическом поле $\boldsymbol{E}$ энергию W, которую полярон передаёт ионам за единицу времени, следует приравнять мощности внешнего поля $ev\boldsymbol{E}$. Из такого равенства следует выражение

для подвижности полярона

$$u = \frac{v}{|E|} = \frac{\pi\varepsilon^{\varepsilon/2}}{0,29 e \alpha_3^3 b} \tag{11.14}$$

Подставляя сюда α_8 из формулы (11.13), получаем:

$$u = 2,62 \cdot 10^{-14} \frac{\varepsilon^{3/2}}{b\left(\frac{\mu}{m}\right)^3 \left(\frac{1}{n^2} - \frac{1}{\varepsilon}\right)^3} \text{ ед. CGSE.} \tag{11.15}$$

Эта формула выражает подвижность полярона через коэффициент поглощения электромагнитных волн, частоты которых значительно меньше собственных частот колебаний ионов.

Значение постоянной b следует взять из экспериментальных данных по поглощению электромагнитных волн в кристалле. Например, для кристалла NaCl$b \approx 2,7 \cdot 10^{-15}$ сек. [19], $n = 1,52$, $\varepsilon = 5,8$. Если для этого кристалла произвольно предположить $\mu = m$, то получается:

$$u = 8 \cdot 10^3 \text{ ед. CGSE} = 26,7 \frac{c^2}{сек \cdot} \tag{11.16}$$

В § 31 будет показано, что у NaCl$\mu = 2,78m$. Если принять это значение μ, то получается:

$$u = 372 \text{ ед. CGSE } = 1,24 \frac{c^2}{\cdot}. \tag{11.17}$$

После того как будет рассмотрени подвижность поляронов с учётом тепловых колебаний ионов, мы вернёмся к вопросу о том, какой из двух упомянутых видов носителей тока доминирует в электропроводности. Будет показано, что подвижность поляронов по порядку величины как раз совпадает с экспериментально определяемыми подвижностями носителей тока в кристаллах. Попытка отождествить экспериментально наблюдаемые носители тока с зонными электронами заставляет считать, что у зонных электронов и у поляронов подвижности одного порядка. Но тогда вследствие превосходства концентрации поляронов зонные электроны не могли бы играть сколько-нибудь значительной роли в электропроводности. Таким образом, приходится

предположить, что не зонные электроны, а поляроны являются основными носителями тока.

10.3 III. Polaron Theory with Quantum Mechanical Approach to Ion Motion

10.3.1 § 12. Basic Equations

В предыдущей главе движение ионов рассматривалось с помощью классической механики. Преимущества такого подхода заключаются в его наглядности и сравнительной простоте. Классическая механика применима, как известно, в тех случаях, когда дебройлевская длина волны частицы λ медленно меняется в пространстве:

$$\frac{d\lambda}{dx} \ll 2\pi. \tag{12.1}$$

Однако для ионов кристалла это неравенство выполняется плохо. Гоэтому результаты предыдущей главы, полученные на основе классической механики, нуждаются в проверке и уточнении путём квантовомеханического рассмотрения движения ионов. Это и будет сделано в настоящей главе. Кроме того, в предыдущем игнорировались тепловые колебания ионов (был рассмотрен случай $T = 0$). В этой главе тепловые колебания ионов будут учтены.

Как было показано в § 3, если ионы были бы закреплены в узлах решётки, то электрон проводимости оказался бы в периодическом поле с потенциалом $W(\boldsymbol{r})$. Благодаря смещениям ионов из узлов решётки в потенциальной энергии электрона проводимости появляются добавочные члены $V(r) + V'(r)$, которые были подробно рассмотрены в § 5. Таким образом, при произвольных положениях ионов потенциальная энергия электрона проводимости равна

$$W(r) + V(r) + V'(r). \tag{12.2}$$

Здесь $V(\boldsymbol{r})$ попрежнему обозначает потенциал электрона в поляризованном диэлектрическом континууме и предполагается плавной функцией $\boldsymbol{r}$, в то время как $V'(\boldsymbol{r})$ есть изменение потенциала электрона, происходящее от смещения одногодвух ионов, наиболее близких к электрону. Изменение потенциала $V'(\boldsymbol{r})$ выделяется в отдельное слагаемое, так как оно не может быть правильно учтено с помощью модели диэлектрического континуума и не является плавной функцией координат [1]).

Член $V'(r)$ в предыдущей главе не учитывался вовсе, так как там шла речь только о поляризационных смещениях ионов, вызванных силой $\boldsymbol{D}$; эти смещения очень малы (см. формулу (7.16)), а вместе с ними был мал и член $V'(r)$.

Напротив, в этой главе будут рассматриваться тепловые колебания и нулевые колебания ионов, амплитуды которых превосходят поляризационные смещения ионов. Поэтому член $V'(\boldsymbol{r})$ будет играть роль, большую чем в предыдущей главе, и учитывается как малое возмущение.

Предположим, что в отсутствии электрона проводимости колебания ионов могут быть описаны с помощью нормальных координат. Эти колебания, как известно [21], подразделяются на акустические, при которых волнообразно меняется плотность кристалла, и оптические, при которых волнообразно меняется дипольный момент. Все нормальные колебания взаимно независимы; функция Гамильтона системы состоит из отдельных слагаемых, каждое из которых является функцией Гамильтона для какого-либо одного нормального колебания. Предположим для простоты, что кристалл

обладает решёткой типа каменной соли. Пусть $H_{\text{ак}}$ обозначает гамильтониан всех акустических волн, $H_{0\|\|}$ - гамильтониан всех продольных оптических волн и $H_{0\,\text{п}\,\perp}$ - гамильтониан всех поперечных оптических волн. В присутствии электрона проводимости оператор энергии всей системы имеет вид

$$\mathcal{H} = -\frac{\hbar^2}{2m}\Delta + W(\boldsymbol{r}) + V(\boldsymbol{r}) + \\ + V'(\boldsymbol{r}) + H_{\text{on}\|} + H_{\text{on1}} + H_{\text{an}}. \tag{12.3}$$

Здесь первый член представляет кинетическую энергию электрона проводимости, второй, третий и четвёртый члены -энергию его взаимодействия с ионами, а последние три члена гамильтониан ионов в отсутствие электронов проводимости.

Согласно формуле (5.1)

$$V(r) = e\int \frac{P\left(r_1'\left(r - r_1\right)\right.}{\left|r - r_1\right|^3} d\tau_1. \tag{12.4}$$

Разложим удельную поляризацию в ряд Фурье [1]):

$$P(r) = \sum_x P_x \chi_x(r), \tag{12.5}$$

$$\gamma_x(r) = \sqrt{\frac{2}{L^3}} \begin{cases} \cos xr & \text{при} \quad x_x \leqslant 0, \\ \sin xr & \text{при} \quad x_x > 0. \end{cases}$$

Здесь, как обычно, введено условие цикличности с большими периодами $L; \chi_{\varkappa}$ нормированы в объёме основной области L^3. Три проекции $\boldsymbol{P}_x$: одна на направление $\boldsymbol{x}$ и две в плоскости, пергендикулярной к x, относятся соответственно к продольной и к двум поперечным поляризационным волнам. В отсутствие электрона проводимости эти проекции гармонически колеблются во времени; их удобно принять в качестве нормальных координат, описывающих оптические колебания ионов.

Удельную поляризацию можно подразделить на два слагаемых:

$$P(r) = P_{\|}(r) + P_{\perp}(r), \tag{12.6}$$

где первое слагаемое представляет собой сумму всех продольных волн, а второе слагаемое - сумму всех поперечных волн. Если разбиение (12.6) проделать в формуле (12.4) под интегралом и учесть, что

$$\operatorname{div} P_{\perp} \equiv 0, \tag{12.7}$$

то член с $P_{\perp}$ в результате интегрирования исчезает:

$$\int P_{\perp} \operatorname{grad} \frac{1}{|r - r_1|} d\tau_1 = \\ = \int \operatorname{div} \frac{P_{\perp}}{|r - r_1|} d\tau_1 - \int \frac{1}{|r - r_1|} \operatorname{div} P_{\perp} d\tau_1 = 0. \tag{12.8}$$

[81]) Это разложение представляет собой переход к поляризующемуся континууму. Смысл имеют только такие гармоники Фурье, у которых длина волны значительно больше постоянной решётки. Именно такие гармоники будут играть главную роль во взаимодействии колебаний ионов с поляроном.

Здесь первый член правой части исчезает после преобразования объёмного интеграла в поверхностный, а второй член равен нулю на основании (12.7). Таким образом,

$$V(r) = e \int \frac{P_{\parallel}(r_1)(r - r_1)}{|r - r_1|^3} d\tau_1. \tag{12.9}$$

Следовательно, потенциал $V(\boldsymbol{r})$ не зависит от нормальных координат поперечных поляризационных волн.

В формуле (12.3) член $V'(\boldsymbol{r})$ рассматривается как малое возмущение. Если его в нулевом приближении опустить, то нормальные координаты акустических и поперечных оптических колебаний будут входить только в последние два члена формулы (12.3). Так как эти члены не зависят от остальных координат системы, то, следовательно, акустические и поперечные оптические колебания полностью отделяются, как независимые замкнутые коисервативные подсистемы. Иначе говоря, акустические и поперечные оптические колебания в нулевом приближении не взаимодействуют с движением системы по другим степеням свободы. Значит, ψ-функция системы в нулевом приближении состоит из трёх множителей; один из них зависит только от координат акустических колебаний, другой - от координат поперечных оптических колебаний и третий - от координат продольных оптических колебаний и от координат электрона. Первые два множителя тривиальны: они выглядят так же, как если бы электрона проводимости в кристалле вовсе не было.

В ближайших параграфах будут рассмотрены в нулевом приближении движение электрона проводимости и продольные поляризационные колебзния. Это движение описывается оператором энергии

$$\mathbf{H}' = \mathbf{H} - \mathbf{H}_{\text{on}\perp} - \mathbf{H}_{\text{aK}} = -\frac{\hbar^2}{2m}\Delta + \\ + W(r) + V(r) + \mathbf{H}_{\text{on}\parallel}. \tag{12.10}$$

Ниже речь будет итти исключительно о продольных поляризационных колебаниях; поэтому символ « $\parallel$ » при $\boldsymbol{P}$ и $\boldsymbol{P}_{\varkappa}$ будет для простоты опускаться.

При решении волнового уравнения с оператором (12.10) можно воспользоваться методом эффективной массы, т. е. опустить периодический потенциал $W(\boldsymbol{r})$, одновременно заменив m на μ. Этот метод был обоснован в § 4 для случая одного электрона в заданном потенциальном поле. Рассматриваемый случай отличается тем, что здесь, помимо электрона, имеется ещё множество колебательных степеней свободы. Однако метод эффективной массы легко может быть обобщён и на этот случай [1]).

В результате (12.10) заменяется более простым оператором

$$\mathbf{H} = -\frac{\hbar^2}{2\mu}\Delta + V(\boldsymbol{r}) + \mathbf{H}_{0\pi}\|. \tag{12.11}$$

Как известно, гамильтониан всякой системы, совершающей малые гармонические колебания, представляет собой квадратичную форму нормальных координат и скоростей, причём в эту форму входят лишь квадраты этих величин, но не входят их смешанные произведения. В частности, гамильтониан продольных оптических колебаний может быть представлен в виде

$$H_{00\parallel} = \sum_x \frac{2\pi}{c_x}\left(P_x^2 + \frac{1}{\omega_x^2}\dot{P}_x^2\right). \tag{12.12}$$

Здесь P_x, как уже упоминалось, приняты в качестве нормальных координат, описывающих продольные поляризацион-

ные колебания, ω_x - собственные частоты нормальных колебаний, c_x - постоянные коэффициенты.

Если поляризация является плавной функцией координат (мало меняется на расстояниях порядка постоянной решётки), в разложении (12.5) и в сумме (12.12) главную роль играют члены с малыми $\boldsymbol{\varkappa}$. В этом случае $\omega_\varkappa$ и $c_\varkappa$ можно приближённо заменить соответствующими величинами для предельного колебания (колебания с бесконечной длиной волны). Эти предельные величины будут обозначаться просто ω и c. Гамильтониан продольных оптических колебаний в этом случае перепишется в виде

$$H_{01\|} = \frac{2\pi}{c}\sum_x \left(P_x^3 + \frac{1}{\omega^2}\dot{P}_x^2\right) = \\ = \frac{2\pi}{c}\int_{\dot{L}^3}\left[1^2(r) + \frac{1}{\omega^2}\dot{P}^2(r)\right]d\tau \tag{12.13}$$

Входящий сюда коэффициент c следует отождествить с коэффициентом (5.10); в этом легко убедиться, сравнив член потенциальной энергии колебаний в формуле (12.13) с выражением (5.13).

Для дальнейшего удобно ввести безразмерные канонические сопряжённые координаты

$$q_x = \sqrt{\frac{4\pi}{\hbar\omega_x c_x}}P_x \tag{12.14}$$

и импульсы

$$g_x = \sqrt{\frac{4\pi}{\hbar\omega_x^3 c_x}}\dot{P}_{x'} \tag{12.15}$$

При таких обозначениях формула (12.12) приобретает вид

$$H_{0\pi\|} = \frac{1}{2}\sum_x \hbar\omega_x\left(q_x^3 + g_x^2\right) \tag{12.16}$$

Классические уравнения движения ионов (при отсутствии электрона проводимости) имеют вид канонических уравнений

$$\left.\begin{aligned}\hbar\dot{q}_x &= \tfrac{\partial H_{0H\|}}{\partial g_x},\\ \hbar\dot{g}_x &= -\tfrac{\partial H_{0H\|}}{\partial q_x}\end{aligned}\right\} \tag{12.17}$$

Оператор энергии получается, как обычно, путём замены в формуле (12.16) $g_\varkappa$ на $-i\frac{\partial}{\partial q_\varkappa}$. Оператор энергии электрона и продольных оптических колебаний получается путём подстановки (12.9) и (12.16) в (12.11):

[81]) Для оператора (12.10) обоснование метода вполне аналогично тому, что дано в § 4, с той лишь разницей, что вместо разложения (4.29) следует вести разложение по собственным функциям оператора

$$-\frac{\hbar^2}{2\mu}\Delta + E^0 + \mathrm{H}_{0\mathrm{n}}$$

и вместо разложения (4.32) следует раскладывать по собственным функциям оператора

$$-\frac{\hbar^2}{2m}\Delta + W(\boldsymbol{r}) + \mathbf{H}_{\mathrm{on}\|}.$$

$$\mathbf{H} = -\frac{\hbar^2}{2\mu}\Delta + e\int \frac{\boldsymbol{P}_{\parallel}(\boldsymbol{r}_1)(\boldsymbol{r}-\boldsymbol{r}_1)}{|\boldsymbol{r}-\boldsymbol{r}_1|^3}d\tau_1 + \\ + \frac{1}{2}\sum_x \hbar\omega_x\left(q_x^2 - \frac{\partial^2}{\partial q_x^2}\right) \tag{12.18}$$

Здесь предполагается, что $\boldsymbol{P}_{\parallel}$разложено в ряд по формуле (12.5), а коэффициенты разложения выражены через q_x по формуле (12.14).

10.3.2 § 13. Properties of the wave function arising from the theory of groups

Рассмотрим оператор, действующий на координаты системы таким образом, что его действие эквивалентно перемещению электрона проводимости и поляризационной потенциальной ямы на расстояние ξ. Будем называть его оператором трансляции полярона и обозначим T_ξ. Этот оператор производит следующее преобразование координат:

$$r \to r' = r + \xi, \tag{13.1}$$

$$P_{\parallel}(r_1) \to P'_{\parallel}(r_1) = P_{\parallel}(r_1 - \xi). \tag{13.2}$$

Преобразование (13.2) можно выразить через нормальные координаты колебаний ионов:

$$P'_{\varkappa} = \int P'_{\parallel}(r_1)\chi_{\varkappa}(r_1)\,d\tau_1 = \int P_{\parallel}(r_1-\xi)\chi_{\varkappa}(r_1)\,d\tau_1 = \\ = \int P_{\parallel}(r_1)\chi_{\varkappa}(r_1+\xi)\,d\tau_1 \tag{13.3}$$

Но согласно формуле (12.5)

$$\chi_{\chi}(r_1+\xi) = \begin{cases} \chi_{\chi}(r_1)\cos\varkappa\xi - \chi_{-\chi}(r_1)\sin\varkappa\xi & (\chi_x \leqslant 0), \\ \chi_{\chi}(r_1)\cos\varkappa\xi + \chi_{-\chi}(r_1)\sin\varkappa\xi & (\chi_x > 0). \end{cases} \tag{13.4}$$

Подставляя это в (13.3), получаем:

$$P'_{\varkappa} = P_{\varkappa}\cos\varkappa\xi + P_{-\varkappa}\sin\varkappa\xi. \tag{13.5}$$

Это преобразование нормальных координат равносильно преобразованию (13.2).

Оператор энергии системы H выражается формулой (12.18). Очевидно, он является инвариантом трансляционного преобразования. Действительно, первый член в выражении H не меняется в результате трансляции, так как оператор Δ является инвариантом преобразования (13.1), второй член в выражении H тоже остаётся неизменным, так как преобразования (13.1) и (13.2) равносильны замене в определённом интеграле переменной интегрирования r_1 на $r_1 + \xi$. В третьем члене выражения $\mathbf{H}$ можно слагаемые объединить попарно, соединяя в одну пару члены с индексом $\boldsymbol{x}$ и с индексом - $\boldsymbol{x}$.

Так как

$$\omega_x = \omega_{-x}, \tag{13.6}$$

то каждая такая пара членов имеет вид

$$\frac{1}{2}\hbar\omega_x\left(q_x^2+q_{-x}^3+\frac{\partial^2}{\partial q_x^2}+\frac{\partial^2}{\partial q_{-x}^2}\right). \tag{13.7}$$

При трансляции согласно формуле (13.5) координаты $q_\varkappa$ и $q_{-\varkappa}$ преобразуются следующим образом:

$$\left.\begin{aligned} q'_x &= q_x\cos x\xi + q_{-x}\sin x\xi,\\ q'_{-x} &= -q_x\sin x\xi + q_{-x}\cos x\xi. \end{aligned}\right\} \tag{13.8}$$

Если рассматривать q_x и q_{-x} как декартовы координаты некоторой точки в илоскости, то преобразование (13.8) представляет собой поворот осей декартовых координат на угол $\boldsymbol{x}\ \xi$. При таком повороте формы

$$q_\varkappa^3+q_{-\varkappa}^2 \quad \text{и} \quad \frac{\partial^2}{\partial q_\varkappa^2}+\frac{\partial^2}{\partial q_{-\varkappa}^3} \tag{13.9}$$

остаются, как известно, инвариантными. Таким образом, выражение (13.7) и весь третий член в выражении H являются инвариантами трансляционного преобразования. Так как H является инвариантом преобразования $\mathbf{T}_\xi$, то эти операторы коммутируют:

$$\mathrm{T}_\xi\mathrm{H} = \mathrm{H}\mathrm{T}_\xi. \tag{13.10}$$

Совокупность операторов трансляции $\mathbf{T}_\xi$ со всевозмож-I ными $\boldsymbol{\xi}$ образует коммутативную группу. Эта группа изоморфно изображается группой перемещений точки в пространстве. Согласно известным теоремам теории групп можно выбрать полную систему собственных функций Ψ оператора $\mathbf{H}$ таким образом, чтобы они одновременно являлись собственными функциями всех операторов $\mathbf{T}_\xi$. Совершенно аналогично тому, как это было сделано в § 2 для оператора $\mathbf{T}_m$, можно показать, что собственные значения оператора $\mathbf{T}_\xi$ имеют вид $e^{ik\xi}$, т. е.

$$\mathrm{T}_\xi\Psi_k\left(\boldsymbol{r},\ldots,q_x,\ldots\right) = e^{ik\xi}\Psi_k\left(\boldsymbol{r},\ldots,q_x,\ldots\right), \tag{13.11}$$

где $\Psi_{\boldsymbol{k}}$ - собственная функция оператора $\mathbf{H}$ и всех операторов T_ξ. Легко показать, что оператор $\mathcal{H}$ (формула (12.3)) тоже коммутирует с $\mathbf{T}_\xi$ и его собственные функции также обладают свойством (13.11).

Формула (13.11) является аналогом и обобщением теоремы Блоха (см. (3.5)). Последняя относилась к электрону в заданном постоянном периодическом поле, тогда как формула (13.11) относится к системе со многими степенями свободы и получена уже в результате учёта взаимодействия электрона с колебаниями ионов. Из формулы (13.11) следует, что операторы $\mathcal{H}^{-}\mathbf{H}$ обладают непрерывным энергетическим спектром (k - непрерывное квантовое число).

10.3.3 § 14. Approximate determination of system energy

В § 12 было показано, что в нулевом приближении электрон проводимости и продольные поляризационные колебания представляют собо замкнутую консервативную подсистему, которая не взаимодействует с акустическими и поперечными оптическими колебаниями. Оператор энергии этой подсистемы даётся формулой (12.18). В этом параграфе будет приближённо вычислена энергия основного состояния полярона с помощью довольно грубого прямого вариационного метода. В следующих параграфах будет получено более точное и более общее решение задачи.

Вместо волнового уравнения с оператором (12.18) используем эквивалентный вариационный принцип:

$$\int \Psi^* \left(r, \ldots, q_x, \ldots\right) H \Psi \left(r, \ldots, q_x, \ldots\right) d\tau dq = \text{ мин.}, \quad (14.1)$$

где

$$dq = \prod_x dq_x$$

при дополнительном условии

$$\int |\Psi|^2 d\tau dq = 1 \quad (14.2)$$

Минимизация функционала (14.1) осуществлялась путём апроксимации состояния системы функцией вида

$$\Psi \left(r, \ldots, q_x, \ldots\right) = \Psi(r) \Phi \left(\ldots, q_x, \ldots\right). \quad (14.3)$$

Произвольно ограничивая выбор апроксимирующей функции мультипликативной формой (14.3), мы, конечно, уменьшаем её «гибкость»; вследствие этого точный минимум не будет достигнут, и получится завышенное значение энергии. Однако ошибка при этом получается небольшая [1]); убедиться в этом можно будет путём сравнения результата с более точным результатом § 16.

Переходя к минимизации функционала (14.1), удобно ввести предварительно следующие обозначения:

$$\bar{P}_\varkappa = \int P_\varkappa |\Phi|^2 dq \quad (14.4)$$

$$\bar{H}_{\text{о}\|} = \int \Phi^* \mathbf{H}_{\text{о}\pi} \Phi dq \quad (14.5)$$

$$D\left[\psi, r_1\right] = e \int |\psi(r)|^2 \frac{(r_1 - r)}{|r_1 - r|^3} d\tau \quad (14.6)$$

$$D_\varkappa[\psi] = \int D\left[\psi, r_1\right] \chi_\varkappa \left(r_1\right) d\tau_1 \quad (14.7)$$

Так как $\boldsymbol{D}$ - безвихревой вектор, то согласно формуле (14.7) $\boldsymbol{D_x}$ всегда параллелен $\boldsymbol{x}$, а следовательно, и $\boldsymbol{P_x}$ (поскольку речь идёт только о продольных поляризационных волнах).

Чтобы это показать, заметим, что $\boldsymbol{D}$ является градиентом:

$$\left.\begin{array}{ll} D & = -\operatorname{grad} \varphi, \\ \varphi\left(r_1\right) & = e \int |\psi(r)|^2 \frac{d\tau}{|r_1 - r|}. \end{array}\right\} \quad (14.8)$$

Поэтому интеграл в формуле (14.7) можно преобразовать следующим образом:

[81]) Заметим, что аналогичное мультипликативное ограничение накладывается на ψ-функцию в методе Хартри [23]-фока [24]. В большинстве прямых вариационных методов на апроксимирующую функцию накладываются ещё большие ограничеиия. И всё же в этих методах обычно получаются весьма точные значения знергии.

$$-\int \left[\nabla\varphi\left(\boldsymbol{r}_1\right)\right]\chi_{\varkappa}\left(\boldsymbol{r}_1\right)d\tau_1 =$$
$$= -\int \nabla\left(\varphi\chi_{\varkappa}\right)d\tau_1 + \int \varphi\left(\nabla\ell_{\varkappa}\right)d\tau_1 \tag{14.9}$$

Здесь в первом члене правой части интегрирование может быть непосредственно выполнено; после подстановки бесконечных пределов интегрирования этот интеграл обрацается в нуль. Второй член правой части параллелен вектору $\boldsymbol{x}$, так как согласно формуле (12.5)

$$\nabla\gamma_x = x_{\chi_{-x}}. \tag{14.10}$$

Таким образом, векторы $\boldsymbol{D}_x, \boldsymbol{x}$ и $\boldsymbol{P}_{\boldsymbol{x}}$ действительно параллельны.

Предположим, что в формуле (14.3) функции ? и Φ, каждая в отдельности, нормированы. Это предположение не является новым ограничением. Если в функционал (14.1) подставить H согласно формулам (12.18) и (12.5) и Ψ согласно формуле (14.3), то мы получим:

$$\bar{H} = \int \Psi^*\mathbf{H}\Psi d\tau dq =$$
$$= \frac{\hbar^2}{2\mu}\int |\nabla\Psi|^2 d\tau - \sum_x \bar{P}_x D_x[\Psi] + \bar{H}_{\text{оп}\,\|}. \tag{14.11}$$

Необходимо минимизировать этот функционал, варьируя независимо ψ и Φ, но сохраняя их нормировку. Варьируя Φ при произвольном фиксировании ψ и приравнивая соответствующую вариацию $\bar{H}$ нулю, мы приходим к уравнению Эйлера следующего вида:

$$\left(\sum_x \mathbf{H}_x\right)\Phi = \lambda\Phi, \tag{14.12}$$

где

$$\mathbf{H}_x = \frac{\hbar\omega_x}{2}\left[\left(q_x - q_{x0}\right)^2 - \frac{\partial^2}{\partial q_x^3}\right] - \frac{c_x}{8\pi}D_x^1[\Psi] \tag{14.13}$$

и

$$q_{\varkappa)} = \left(\frac{c_{\varkappa}}{4\pi\hbar\omega_{\varkappa}}\right)^{1/2} D_{\varkappa}[\psi]. \tag{14.14}$$

Уравнение (14.12) решается точно: подстановкой

$$\Phi = \prod_x \Phi_{n_x}\left(q_x - q_{x0}\right) \tag{14.15}$$

в нём разделяются переменные и оно распадается на независимые уравнения вида

$$\mathrm{H}_x\Phi_{n_x}\left(q_x - q_{x0}\right) = E_x\Phi_{n_x}\left(q_x - q_{x0}\right). \tag{14.16}$$

Каждое такое уравнение можно рассматривать как волновое уравнение для гармонического осциллятора, у которого положение равновесия смещено в точку q_{x0} под влиянием дополнительной постоянной силы. Его решение имеет вид

$$\Phi_{n_x}\left(q_x - q_{x0}\right) = e^{-\frac{1}{2}\left(q_x - q_{x0}\right)^2} H_{n_x}\left(q_x - q_{x0}\right) \tag{14.17}$$

$$E_x = \hbar\omega_x\left(n_x + \frac{1}{2}\right) - \frac{c_x}{8\pi} D_x^2. \tag{14.18}$$

Здесь n_x - квантовое число осциллятора, а H_{n_x} - полином Чебышева-Эрмита степени n_x.

Подставляя (14.15), (14.17) и (14.18) в функционал (14.11), получаем:

$$\bar{H} = \frac{\hbar^2}{2\mu}\int |\nabla\psi|^2 d\tau - \frac{1}{8\pi}\sum_x c_x D_x^2[\psi] + \\ + \sum_x \hbar\omega_x\left(n_x + \frac{1}{2}\right). \tag{14.19}$$

Теперь уже этот функционал зависит только от ψ и его следует минимизировать, варьируя ψ. Необходимо, однако, предварительно избавиться от бесконечного суммирования во втором члене формулы (14.19). Для этого следует использовать встречавшееся уже неоднократно предположение о том,

что поляризационный радиус полярона значительно больше постоянной решётки. В этом случае согласно формуле (14.7) значительны только такие D_x, у которых

$$x \ll \frac{2\pi}{a}, \tag{14.20}$$

где a - постоянная решётки.

В формуле (14.19) в сумме будут играть главную роль члены с малыми x, удовлетворяющими неравенству (14.20). Поэтому c_x можно приближённо заменить его предельным значением при $x = 0$. Последнее, как было показано в § 12 , совпадает с коэффициентом

$$c = \frac{1}{n^2} - \frac{1}{\varepsilon}, \tag{14.21}$$

введённым в § 5. Заменив $c_\varkappa$ на c и вынося его за знак суммы, можно остальную часть бесконечной суммы просуммировать [1]):

$$\sum_x D_x^2 = \int D^2[\psi, r] d\tau. \tag{14.22}$$

Это равенство может быть легко проверено путём разложения $\boldsymbol{D}$ под интегралом в ряд вида

$$D[\psi, r] = \sum_x D_x[\psi]\chi_x(r). \tag{14.23}$$

Таким образом, из формулы (14.19) получается:

$$\bar{H} = J[\psi] + \sum_x \hbar\omega_x\left(n_x + \frac{1}{2}\right), \tag{14.24}$$

где $J[\psi]$ - функционал, уже встречавшийся в предыдущей главе (см. формулу (6.4)). Этот функционал уже был минимизирован в § 6; поэтому сейчас остаётся использовать

уже известные результаты. Минимальное значение J и соответствующее ψ даются формулами (6.12), (6.14) и (6.15). Если подставить

эти результаты в формулу (14.24), то получится:

$$\left.\begin{array}{l} \bar{H}_{\text{мин}} = J\left[\psi_0\right] + \sum_x \hbar\omega_x \left(n_x + \frac{1}{2}\right), \\ J\left[\psi_0\right] = -0,0544 \frac{\mu e^4}{\hbar^2} c^2. \end{array}\right\} \tag{14.25}$$

Эта величина представляет собой энергию системы, если электрон находится в основном поляронном состоянии, а колебания ионов характеризуются набором квантовых чисел n_x. Здесь первый член совпадает с энергией основного состояния полярона, вычисленной в предыдущей главе. Второй член представляет энергию колебания ионов относительно смещённых под влиянием поля $\boldsymbol{D}$ положений равновесия; в предыдущей главе этот член, естественно, отсутствовал, так как там не рассматривались собственные колебания ионов. Такое совпадение результатов этого параграфа с результатами § 6 как в отношении ?-функции электрона, так и в отношении энергии объясняется тем, что мультипликативная апроксимация (14.3) не способна учесть корреляцию между движением электрона и движением ионов. Она даёт возможность электрону «почувствовать» лишь среднее поле колеблющихся ионов. Это среднее поле такое же, как если бы ионы покоились в смещённых равновесных положениях; именно этот случай и был рассмотрен в § 6 .

Из результатов этого параграфа следует, что не только при классическом, но и при квантовомеханическом рассмотрении движения ионов получаются поляронные состояния, которые устойчивы и энергетически более выгодны, чем зонные состояния электрона. Этот вывод не может быть опровергнут при точном решении волнового уравнения системы, так как уже упоминалось, что полученное здесь значение энергии является заведомо завышенным, точное же значение энергии основного состояния системы лежит ещё ниже.

Полученное выше выражение для Ψ соответствует случаю, когда полярон локализован в начале координат, т. е. когда центр полярона находится в точке $r = 0$. Согласно § 13 оператор энергии H обладает трансляционной симметрией, т. е.

$$\mathrm{T}_\xi \mathrm{H} = \mathrm{H}\mathrm{T}_\xi. \tag{14.26}$$

Отсюда следует, что если Ψ является собственной функцией оператора $\mathbf{H}$, то функция

$$\Psi_\xi = \mathbf{T}_\xi \Psi \tag{14.27}$$

тоже будет собственной функцией оператора H. Ψ_ξ соответствует полярону, локализованному в точке ξ; она принадлежит тому же собственному значению энергии системы, что и функция Ψ.

10.3.4 § 15. System energy operator in adiabatic approximation [22]

Более точные результаты могут быть получены с помощью адиабатического приближения. Частоты колебаний ионов предполагаются настолько малыми, что состояние электрона проводимости успевает адиабатически следовать за движением ионов. Это предположение уже было сделано во второй главе (см. § 5).

Преимущество адиабатического приближения заключается в том, что оно позволяет при рассмотрении состояния электрона учесть фактическое мгновенное значение поля

[81]) Возможно более точное суммирование без замены c_x на c [22].

колеблющихся ионов, тогда как метод, применённый в предыдущем параграфе, давал возможность электрону «почувствовать» лишь среднее значение поля ионов.

Предположим, что конфигурация ионов кристалла определяется нормальными координатами P_x или q_x. Состояние электрона, адиабатически соответствующее этой конфигурации ионов, определяется из уравнения

$$\left[-\frac{\hbar^2}{2\mu}\Delta + V(\boldsymbol{r})\right]\psi(\boldsymbol{r}) = E\psi(\boldsymbol{r}). \tag{15.1}$$

Если заменить это уравнение эквивалентным вариационным принципом и подставить $V(\boldsymbol{r})$ согласно формуле (12.9), то получится:

$$\begin{aligned} &E\left(\ldots, P_x, \ldots\right) = \\ &\quad = \mathrm{M}_{\mathrm{H}_\psi}\left\{\frac{\hbar^2}{2\mu}\int |\nabla\psi|^2 d\tau - \int P_\parallel\left(r_1\right) D\left[\psi, r_1\right] d\tau_1\right\}. \end{aligned} \tag{15.2}$$

Этот функционал следует минимизировать, варьируя ψ при фиксированной поляризации $P_\parallel\left(r_1\right)$, т. е. при фиксированных P_x.

Полная энергия электрона проводимости и продольных оптических колебаний ионов в адиабатическом приближении равна

$$H = E\left(\ldots, P_x, \ldots\right) + H_{\text{оп}\,\parallel}. \tag{15.3}$$

Если сюда подставить $H_{\text{оп}\,\parallel}$ из формулы (12.13), то получится

$$H = E\left(\ldots, P_x, \ldots\right) + \frac{2\pi}{c}\int\left[P_\parallel^2(r) + \frac{1}{\omega^2}\dot{P}_\parallel^2(r)\right] d\tau \tag{15.4}$$

Эта энергия есть гамильтониан, описывающий продольные поляризационные колебания ионов в присутствии электрона проводимости.

Точно решить задачу с таким гамильтонианом невозможно уже хотя бы потому, что неизвестно точное явное выражение $E\left(\ldots, P_x, \ldots\right)$: для определения $E\left(\ldots, P_x, \ldots\right)$ при произвольных P_x потребовалось бы найти решение уравнения (15.1) при произвольной поляризационной потенциальной яме $V(r)$, что практически невозможно. Можно, однако, приближённо решить задачу, если учесть, что при не слишком высоких температурах ионы колеблются преимущественно вблизи положений, при которых потенциальная энергия ионов минимальна. Согласно формулам (15.4) и (15.2) эта потенциальная энергия равна

$$\begin{aligned} &\text{мин}_{\,\psi} F[\psi, P] = \text{ мин}_{\,\psi}\left\{\frac{\hbar^2}{2\mu}\int |\nabla\psi|^2 d\tau - \right. \\ &\left. - \int P\left(r_1\right) D\left[\psi, r_1\right] d\tau_1\right\} + \frac{2\pi}{c}\int P^2(r) d\tau \end{aligned} \tag{15.5}$$

Чтобы найти упомянутые равновесные конфигурации ионов с минимальной потенциальной энергией, необходимо минимизировать (15.5) по $\boldsymbol{P}$, т. е. найти абсолютный минимум $\boldsymbol{F}$ как по §, так и по P. Именно такая минимизация F была проведена в § 6 при рассмотрении покоящегося полярона. Рассчитанные там величины

$$\psi_0(r), \quad D_0(r), \quad P_0(r) \quad \text{и} \quad V_0(r) \tag{15.6}$$

относятся к полярону, центр которого находится в начале координат. Однако следует подчеркнуть, что покоящийся полярон может с одинаковым успехом локализоваться в

любой точке кристалла, и во всех случаях потенциальная энергия ионов будет иметь одно и то же минимальное значение. Таким образом, существует бесконечное множество равновесных конфигураций ионов. Для полярона с центром в точке ξ равновесное решение получается простой трансляцией величин (15.6) на вектор ξ: это решение имеет вид

$$\psi_0(r-\xi), \quad D_0(r-\xi), \quad P_0(r-\xi) \quad \text{и} \quad V_0(r-\xi). \tag{15.7}$$

Если ионы колеблются вблизи конфигураций, при которых потенциальная энергия минимальна, то это значит, что поляризация всегда приближается к $\boldsymbol{P}_0(\boldsymbol{r}-\boldsymbol{\xi})$, если только всякий раз надлежащим образом выбирать ξ. Следовательно, поляризацию можно представить в виде

$$P(r) = P_0(r-\xi) + P'(r), \tag{15.8}$$

где $\boldsymbol{P}'(\boldsymbol{r})$ можно рассматривать как малое возмущение поляризации, когда речь идёт о той части пространства, где локализован полярон, т. е. где член $P_0(r-\xi)$ значителен. В остальном пространстве, вдали от точки ξ, член $P_0(r-\xi)$ исчезающе мал, и поляризация кристалла равна $P'(r)$. В уравнении (15.1) $\psi(r)$ определяется поляризацией и потенциалом $V(r)$ как раз в области, где локализован полярон.

В нулевом приближении член $P'(r)$ опускается, и тогда решением уравнения (15.1) будет $\psi_0(\boldsymbol{r}$ - $\xi)$. Далее, вводя член $P'(r)$ как малое возмущение и пользуясь обычной теорией возмущений, можно вычислить энергию электрона в первом приближении. Она оказывается равной

$$E\left(\ldots, P_x, \ldots\right) = \frac{\hbar^2}{2\mu}\int \left|\nabla\psi_0\right|^2 d\tau - \int P(r)D_0(r-\xi)d\tau. \tag{15.9}$$

Нетрудно подсчитать поправку к энергии второго порядка [45]. Эта поправка оказывается уже малой и может быть отброшена.

Если в формулу (15.4) поставить выражения (15.9) и (15.8) и учесть, что

$$P_0(r-\xi) = \frac{c}{4\pi}D_0(r-\xi), \tag{15.10}$$

то получается:

$$H = J\left[\psi_0\right] + \frac{2\pi}{c}\int P'^2(\boldsymbol{r})d\tau + \frac{2\pi}{c\omega^2}\int \dot{P}^2(\boldsymbol{r})d\tau \tag{15.11}$$

Раскладывая здесь поляризацию $P'(r)$ и $P(r)$ в тригонометрический ряд вида (12.5), переходя затем к безразмерным каноническим сопряжённым координатам q_x и импульсам g_x (см. (12.14) и (12.15)) и заменяя g_x на оператор $-i\frac{\partial}{\partial q_x}$, получим для энергии (15.11) оператор

$$\mathbf{H} = J\left[\xi_0\right] + \frac{1}{2}\hbar\omega\sum_x\left[\left(q_x - q_{x\xi}\right)^2 - \frac{\partial^2}{\partial q_x^3}\right]. \tag{15.12}$$

Здесь

$$\left.\begin{array}{l} q_{x\xi} = \sqrt{\frac{4\pi}{\hbar\omega c}}P_{x\xi}, \\ P_{x\xi} = \int P_0(r-\xi)\gamma_x(r)d\tau \end{array}\right\} \tag{15.13}$$

Возникает вопрос о том, как следует выбрать ξ в функциях $P_0(r-\xi)$ и $\psi_0(r-\xi)$, чтобы вектор $P_0(r-\xi)$ приближался к фактической поляризации $\boldsymbol{P}(\boldsymbol{r})$ в области, где локализован полярон. Очевидно, ξ должен зависеть от заданной поляризации $\boldsymbol{P}(\boldsymbol{r})$, при которой надлежит вычислить энергию $E\left(\ldots, P_x, \ldots\right)$.

Лучшим выбором ξ следует признать такой, при котором $E(\ldots, P_x, \ldots)$ точнее всего выражается формулой (15.9). Согласно вариационному принципу (15.2) наибольшую точность при вычислении $E(\ldots, P_x, \ldots)$ обеспечит такой выбор ξ, при котором энергия (15.9) минимальна. Условия минимума имеют вид

$$\frac{\partial E(\ldots, P_\varkappa, \ldots, \xi)}{\partial \xi_i} = \\ = -\int P(r) \frac{\partial D_0(r-\xi)}{\partial \xi_i} d\tau = 0 \quad (i = 1, 2, 3) \tag{15.14}$$

Из этих трёх уравнений определяются компоненты вектора ξ (ξ_1, ξ_2 и ξ_3) в зависимости от $P(r)$. Таким образом, в операторе (15.12) ξ является функционалом $P(r)$ или же функцией координат q_x, определяющих поляризацию.

Изложенный выше выбор $\boldsymbol{\xi}$ можно интерпретировать следующим образом. Предположим, что в инерционно поляризующейся среде с дипольным моментом $\boldsymbol{P}(\boldsymbol{r}, t)$ находится свободный невесомый и недеформируемый заряд, причём плотность заряда равна $e\left|\psi_0(r-\xi)\right|^2$ и, следовательно, электрическая индукция заряда $\boldsymbol{D}_0(\boldsymbol{r}-\boldsymbol{\xi})$ ($\boldsymbol{\xi}$ - координата центра заряда). Если рассматривать движение заряда на основе классической механики, то положение ξ такого невесомого заряда в любой момент времени определяется из условия минимума потенциальной энергии его взаимодействия с поляризованной средой:

$$-\int P(r,t) D_0(r-\xi) d\tau = \text{ мин.} \tag{15.15}$$

Это условие совпадает с (15.14).
Перейдём теперь к исследованию свойств функции $\xi(\ldots, q_x, \ldots)$, которая в неявном виде определяется тремя уравнениями (15.14). Эти свойства будут использованы в следующих параграфах. Раскладывая в формуле (15.14) $\boldsymbol{P}(\boldsymbol{r})$ и $\boldsymbol{D}_0(\boldsymbol{r}-\xi)$ в тригонометрический ряд по функциям $\gamma_x(\boldsymbol{r})$, осуществляя затем почленное интегрирование и учитывая соотношения (15.13) и (15.10), можно уравнения (15.14) переписать в виде

$$\sum_x q_x \frac{\partial q_{x\xi}}{\partial \xi_i} = 0 \quad (i = 1, 2, 3) \tag{15.16}$$

Решить эти уравнения относительно ξ_1, ξ_2 и ξ_3 не удаётся. Поскольку уравнения (15.16) линейны и однородны относительно q_x, очевидно, что при одновременном умножении всех q_x на произвольный множитель t корни уравнений ξ_i не меняются:

$$\xi_i(\ldots, tq_x, \ldots) \equiv \xi_i(\ldots, q_x, \ldots). \tag{15.17}$$

Следовательно, $\xi_i(\ldots, q_x, \ldots)$ являются однородными функциями q_x, причём порядок однородности равен нулю. Дифференцируя тождество (15.17) по t и затем полагая $t = 1$, получаем:

$$\sum_x \frac{\partial \tilde{s}_i}{\partial q_x} q_x \equiv 0 \tag{15.18}$$

Производные $\frac{\partial \xi_i}{\partial q_x}$ можно вычислить путём дифференцирования уравнений (15.16):

$$\sum_x \sum_{j=1}^{3} q_x \frac{\partial^2 q_{x\xi}}{\partial \xi_i \partial \xi_j} d\xi_j +$$
$$+ \sum_x \frac{\partial q_{x\xi}}{\partial \xi_i} dq_x = 0 \quad (i = 1, 2, 3) \tag{15.19}$$

Вводя обозначения
и

$$\left.\begin{aligned} a_{ij} &= -\textstyle\sum_x q_x \frac{\partial^2 q_{x\xi}}{\partial \xi_i \partial \xi_j} \\ b_i &= \textstyle\sum_x \frac{\partial q_{x\xi}}{\partial \xi_i} dq_x \end{aligned}\right\} \tag{15.20}$$

можно соотношения (15.19) переписать в виде

$$\sum_{j=1}^{3} a_{ij} d\xi_j = b_i \quad (i = 1, 2, 3) \tag{15.19a}$$

Эти три линейных уравнения легко разрешаются относительно $d\xi_j$. Например:
где

$$d\xi_1 = \frac{1}{\Delta} \begin{vmatrix} b_1 & a_{12} & a_{13} \\ b_2 & a_{22} & a_{23} \\ b_3 & a_{32} & a_{33} \end{vmatrix} \tag{15.21}$$
$$\Delta = \begin{vmatrix} a_{11} & a_{12} & a_{13} \\ a_{21} & a_{22} & a_{23} \\ a_{31} & a_{32} & a_{33} \end{vmatrix}$$

Аналогично выражаются $d\xi_2$ и $d\xi_3$. Если сюда подставить b_i согласно формуле (15.20), легко найти, что

$$\frac{\partial \xi_1}{\partial q_x} = \frac{1}{\Delta} \begin{vmatrix} \frac{\partial q_{x\xi}}{\partial \xi_1} & a_{12} & a_{13} \\ \frac{\partial q_{x\xi}}{\partial \xi_2} & a_{22} & a_{23} \\ \frac{\partial q_{x\xi}}{\partial \xi_2} & a_{32} & a_{33} \end{vmatrix}. \tag{15.22}$$

Принимая во внимание соотношения (12.14), (15.13) и (15.8), можно коэффициенты a_{ij} выразить следующим образом:

$$a_{ij} = -\sum_x q_x \frac{\partial^2 q_{x\xi}}{\partial \bar{\xi}_i \partial \bar{\xi}_j} = -\frac{4\pi}{\hbar\omega c} \sum_x P_x \frac{\partial^2 P_x \xi}{\partial \bar{\xi}_i \partial \bar{\xi}_j} =$$
$$= -\frac{4\pi}{\hbar\omega c} \int P(r) \frac{\partial^2 P_0(r-\xi)}{\partial \bar{\xi}_1 \partial \bar{\xi}_j} d\tau = -\frac{4\pi}{\hbar\omega c} \int [P_0(r-\xi) + P'(r)] \times$$
$$\times \frac{\partial^2 P_0(r-\xi)}{\partial x_i \partial x_j} d\tau = a_{ij}^0 + a'_{ij} \tag{15.23}$$

где

$$a_{ij}^0 = -\frac{4\pi}{\hbar\omega c} \int \boldsymbol{P}_0(\boldsymbol{r}) \frac{\partial^2 \boldsymbol{P}_0(\boldsymbol{r})}{\partial x_i \partial x_j} d\tau =$$
$$= \frac{4\pi}{\hbar\omega c} \int \frac{\partial \boldsymbol{P}_0}{\partial x_i} \frac{\partial \boldsymbol{P}_0}{\partial x_j} d\tau = \delta_{ij} \frac{4\pi}{\hbar\omega c} \int \left(\frac{\partial \boldsymbol{P}_0}{\partial x_i} \right)^2 d\tau \tag{15.24}$$

и

$$a'_{ij} = -\frac{4\pi}{\hbar\omega c}\int P'(r)\frac{\partial^2 P_0(r-\xi)}{\partial x_i \partial x_j}d\tau \tag{15.25}$$

Вследствие сферической симметрии вектора $\boldsymbol{P}_0(\boldsymbol{r})$

$$a^0_{11} = a^0_{32} = a^0_{33}, \tag{15.26}$$

поэтому в дальнейшем эти коэффициенты будем обозначать просто a^0. Таким образом,

$$a_{ij} = \delta_{ij}a^0 + a'_{ij} \tag{15.27}$$

Используя соотношение (15.10) и учитывая, что фигурирующий в формуле (10.34) коэффициент c_2 у кристаллов с решёткой типа каменной соли связан с c соотношением [1])

$$c_2 = \frac{c}{\omega^2}, \tag{15.28}$$

можно формулу (15.24) переписать в виде

$$a^0_{ij} = \delta_{ij}a^0, \quad a^0 = \frac{\omega M}{\hbar}. \tag{15.29}$$

Здесь M - эффективная масса полярона, введённая в предыдущей главе (см. формулу (10.34)).

Выше предполагалось, что в той части пространства, где локализован полярон, т. е. где $P_0(r-\xi)$ существенно отличается от нуля, $P'(r)$ является малым возмущением. В соответствии с этим предположением a'_{ij} являются величинами первого порядка малости, тогда как a^0 - нулевого порядка малости.

Если ограничиться величинами первого порядка малости, то

$$\Delta = a^{0^3} + a^{09}\left(a'_{11} + a'_{23} + a'_{33}\right) + \ldots \tag{15.30}$$

и

$$\frac{\partial \xi_i}{\partial q_x} = \frac{1}{a^0}\frac{\partial q_{x\xi}}{\partial \xi_i} - \frac{1}{a^{0^2}}\sum_{j=1}^{8} a'_{ij}\frac{\partial q_{x\xi}}{\partial \xi_j} + \ldots \tag{15.31}$$

Здесь многоточием обозначены члены высшего порядка малости. Легко показать, что

$$\sum_x \frac{\partial^{m_1+m_2+m_3} q_x \xi}{\partial \xi_1^{m_1}\partial \xi_3^{m_2}\partial \xi_3^{m_3}}\frac{\partial^{n_1+n_2+n_3} q_{x\xi}}{\partial \xi_1^{n_1}\partial \xi_2^{n_2}\partial \xi_3^{n_3}} =$$
$$= \frac{4\pi}{\hbar\omega c}\int \frac{\partial^{m_1+m_2+m_3} P_0(r-\xi)}{\partial \xi_1^{m_1}\partial \xi_3^{m_2}\partial \xi_3^{m_3}}\frac{\partial^{n_1+n_2+n_3} P_0(r-\xi)}{\partial \xi_1^{n_1}\partial \xi_2^{n_2}\partial \xi_3^{n_3}}d\tau. \tag{15.32}$$

8

1. c_2 по своему первоначальному определению есть коэффициент разложения в формуле (10.14) (см. также формулу (10.10)). В случае кристаллов с решёткой типа каменной соли гамильтониан продольных оптических колебаний для длинных волн имеет упрощённый вид (12.13). В этом случае легко рассмотреть вынужденные предельные колебания ионов (колебания с бесконечной длиной волны) под

Для доказательства этого равенства следует $P_0(r-\xi)$ под интегралом разложить в ряд по функциям $\chi_*(r)$ и затем почленно интегрировать. Если хотя бы одно из трёх чисел влиянием внешней периодической силы вида $\boldsymbol{D_k e^{i\omega_k t}}$. В результате получается формула вида (10.10), в которой

$$c\left(\omega_k\right)=\frac{c}{1-\frac{\omega_{10}^2}{\omega^2}}$$

(ω - собственная частота предельных колебаний ионов). Если $c\left(\omega_k\right)$ разложить в ряд вида (10.14), то для c_2 получится значение (15.28).
$m_i+n_i(i=1,2,3)$ нечётно, то интеграл в формуле (15.32) равен нулю, так как подинтегральное выражение является нечётной функцией соответствующей координаты ($\boldsymbol{P}_0(\boldsymbol{r})$ сферически симметричный вектор).

Опираясь на формулы (15.24-25) и (15.30-32), можно получить следующие соотношения:

$$\sum_x\left(\frac{\partial \xi_i}{\partial q_x}\right)^2=\frac{1}{a^0}\left(1-\frac{2a_{ii}'}{a^0}+\ldots\right) \tag{15.33}$$

и

$$\sum_x \frac{\partial^2 \xi_i}{\partial q_x^3}=-\sum_x \frac{\partial \xi_i}{\partial q_x}\frac{1}{\Delta}\frac{\partial \Delta}{\partial q_x}=-\frac{1}{a^{00}}\sum_x x^2 q_x \frac{\partial q_{x\xi}^{\xi}}{\partial \xi_i}+\ldots \tag{15.34}$$

Эти соотношения будут использованы в следующих параграфах.

10.3.5 § 16. Energy spectrum and ψ-functions of the system in adiabatic approximation

Попытка найти точные собственные значения и собственные функции оператора энергии (15.12) наталкивается на большие математические трудности не только потому, что в операторе (15.12) переменные q_x не разделяются, но в особенности потому, что не известна явная зависимость коэффициентов q_x s от $q_\varkappa$: зависимость ξ от $q_\varkappa$ задана лишь в неявном виде. В этом параграфе будут найдены приближённые собственные значения и собственные функции оператора (15.12).

Сначала рассмотрим не полную, а частную систему собственных функций, которуго будем искать в виде

$$\Psi\left(\ldots, q_x, \ldots\right)=e^{ik\varepsilon(\ldots,q_x,\cdots)} f(\eta), \tag{16.1}$$

где

$$\eta=\frac{1}{2}\sum_x\left(q_x-q_{x\xi}\right)^2 \tag{16.2}$$

Дифференцируя (16.2) по q_x, получим:

$$\frac{\partial \eta}{\partial q_x}=\left(q_x-q_{x\xi}\right)-\sum_{x_1}\sum_{i=1}^{3}\left(q_{x_1}-q_{x_1\xi}\right)\frac{\partial q_{x\xi}}{\partial \xi_i}\cdot\frac{\partial \xi_i}{\partial q_x}. \tag{16.3}$$

Здесь второй член в правой части равен нулю на основании уравнений (15.16), а также соотношения (15.32) и последующих замечаний. Следовательно,

$$\frac{\partial \eta}{\partial q_x} = q_x - q_{x\xi} \tag{16.4}$$

и

$$\frac{\partial^2 \eta}{\partial q_x^3} = 1 - \sum_{i=1}^{3} \frac{\partial q_{x\xi}}{\partial \xi_i} \frac{\partial \xi_i}{\partial q_x}. \tag{16.5}$$

Если подставить функцию (16.1) в уравнение

$$H\Psi = H\Psi \tag{16.6}$$

и учесть равенства (15.18) и (15.22), то для $f(\eta)$ получится уравнение

$$\begin{aligned} -\eta f'' - \frac{1}{2} f' \sum_x \left(1 - \sum_{j=1}^{3} \frac{\partial q_{x\xi}}{\partial \xi_j} \frac{\partial \xi_j}{\partial q_x}\right) + \\ + \left\{\eta + \frac{1}{2} \sum_x \left[\left(k \frac{\partial \xi}{\partial q_x}\right)^2 - ik \frac{\partial^2 \xi}{\partial q_x^2}\right]\right\} f = \lambda f, \end{aligned} \tag{16.7}$$

где

$$\lambda = \frac{H - J\left[\xi_0\right]}{\hbar\omega}. \tag{16.8}$$

Если в (16.7) подставить (15.31), (15.33-34) и отбросить члены первого порядка малости, сохранив лишь члены нулевого порядка, то для f получится уравнение

$$-\eta f'' - \frac{1}{2} f'(\nu - 3) + \left(\eta + \frac{k^2}{2a^0}\right) f = \lambda f, \tag{16.9}$$

где

$$v = \sum_x 1 \tag{16.10}$$

есть общее число поляризационных продольных нормальных колебаний диэлектрика в основной области (в объёме L^3).

Подстановкой

$$f = v(\eta) e^{-\eta} \tag{16.11}$$

уравнение (16.9) сводится к уравнению

$$\eta v'' + \left(\frac{v-3}{2} - 2\eta\right) v' + \left(\lambda - \frac{v-3}{2} - \frac{\boldsymbol{k}^2}{2a^0}\right) v = 0. \tag{16.12}$$

Решение этого уравнения будем искать в виде степенного ряда

$$v = \sum_{m=0}^{\infty} a_m \eta^m. \tag{16.13}$$

Подставляя этот ряд в уравнение (16.12) и приравнивая нулю приведённые коэффициенты при всех степенях η, получаем систему уравнений вида

$$a_{m+1} = a_m \frac{2m + \frac{\nu-3}{2} + \frac{\hbar^2}{2a^0} - \lambda}{(m+1)\left(m + \frac{\nu-3}{2}\right)} \quad (m = 0, 1, 2, \ldots). \tag{16.14}$$

Эти уравнения являются рекуррентными формулами, определяющими a_m через a_0. Ряд (16.13) сходится при любом η, так как

$$\lim_{m\to\infty} \frac{a_{m+1}}{a_m} = \frac{2}{m} \to 0 \tag{16.15}$$

Из этой формулы видно, что дальние члены («хвост») ряда (16.13) асимптотически совпадают с дальними членами разложения функции $e^{2\eta}$. При $\eta \to \infty$ в разложении (16.13) господствуют дальние члены (высокие степени η). Следовательно, при $\eta \to \infty v$ стремится к бесконечности, как $e^{2\eta}$. При этом $f = ve^{-\eta}$ и Ψ также стремятся к бесконечности. Конечные решения существуют только при таких значениях λ, при которых ряд (16.13) обрывается, вырождаясь в многочлен. Для этого необходимо, чтобы при некотором целочисленном $m = n$ обращался в нуль числитель в правой части формулы (16.14). При этом собственные значения λ должны быть равны

$$\lambda_{kn} = 2n + \frac{v-3}{2} + \frac{k^2}{2a^0}. \tag{16.16}$$

Согласно формулам (16.8) и (15.29)

$$H_{kn} = J\left[\psi_0\right] + \frac{\nu-3}{2}\hbar\omega + 2n\hbar\omega + \frac{\hbar^2 k^2}{2M}, \tag{16.17}$$

а соответствующие ψ-функции системы равны

$$\Psi_{kn} = e^{in\xi} f_n(\eta) = e^{ik\xi-\eta} v_n(\eta), \tag{16.18}$$

где $v_n(\eta)$ - многочлен n-и степени, коэффициенты которого определяются рекуррентной формулой (16.14).

Найденная выше система собственных функций, конечно, не является полной, так как решения искались в ограниченном классе функций (16.1-2). Однако основное состояние как раз содержится среди решений (16.18): полагая $n = 0$, $k = 0$, имеем:

$$\Psi_{\text{CO}} = Ae^{-\eta}. \tag{16.19}$$

Эта функция не имеет узлов и, следовательно, соответствует состоянию с наименьшей энергией.

Энергия основного состояния системы равна

$$H_{00} = J\left[\Psi_0\right] + \frac{\nu-3}{2}\hbar\omega. \tag{16.20}$$

Это значение эчергии основного состояния, как и следовало ожидать, лежит ниже (на $\frac{3}{2}\hbar\omega$), чем значение, вычисленное прямым вариационным методом (см. (14.25)); последний, как известно, приводит к завышенным величинам энергии.

Перейдём теперь к рассмотрению другого метода решения уравнения (16.6), который даёт возможность найти полную систему приближённых собственных функций оператора H. Вместо прежних переменных q_x введём новые переменные:

$$q'_x = q_x - q_{x\xi(\ldots,q_x,\ldots)} \tag{16.21a}$$

$$\cdots\cdots\cdots \tag{16.216}$$

$$q'_{x_l} = \sqrt{q^2_{x_l} + q^2_{-x_l}} \quad (l = 1, 2, 3)$$

и

$$\xi_j = \xi_j\left(\ldots, q_x, \ldots\right) \quad (j = 1, 2, 3). \tag{16.21b}$$

Новые ("штрихованные") переменные введены несколько несимметрично: из общего числа ν координат $\nu - 6$ координат определяются формулами (16.21a), три координаты определяются формулаии (16.21 б), наконец, в качестве последних трёх координат выбраны три компоненты вектора ξ. Из дальнейшего будет видно, что физические результаты не зависят от того, какие именно шесть старых координат входят в преобразование (16.21) особым образом в качестве координат $q_{\pm x_l}(l = 1, 2, 3)$.

Из преобразования (16.21) можно найти преобразования для производных

$$\frac{\partial}{\partial q_x} = \frac{\partial}{\partial q'_x} - \sum_{x_1}\sum_{j=1}^{3}\frac{\partial \xi_j}{\partial q_x}\frac{\partial q_{x_1\xi}}{\partial \xi_j}\frac{\partial}{\partial q'_{x_1}} + \sum_{j=1}^{3}\frac{\partial \xi_j}{\partial q_x}\frac{\partial}{\partial \xi_j} \tag{16.22}$$

$$\frac{\partial}{dq_{\pm x_l}} = \frac{q_{\pm x_l}}{\sqrt{q_{x_l}^3 + q_{-x_l}^2}}\frac{\partial}{\partial q'_{x_l}} - \sum_{x_1}''\sum_{j=1}^{3}\frac{\partial \xi_j}{\partial q_{\pm x_l}}\frac{\partial q_{x_{1,\xi}}}{\partial \xi_j}\frac{\partial}{\partial q'_{x_l}} + \\ + \sum_{j=1}^{8}\frac{\partial \xi_j}{\partial q_{\pm x_l}}\frac{\partial}{\partial \bar{\varsigma}_j} \tag{16.23}$$

Здесь и в дальнейшем $\sum_x$ " означает суммирование по всем значениям x за вычетом шести значений: $\pm x_l (l = 1, 2, 3)$, в то время как $\sum'_x$ означает суммирование по всем значениям x за вычетом трёх: $-x_l (l = 1, 2, 3)$.

Если оператор (15.12) преобразовать к новым переменным, пользуясь формулами (15.31), (15.33), а также формулой (15.32) и последующими замечаниями, и отбросить члены первого порядка малости ($\sim \boldsymbol{P}'(\boldsymbol{r})$), сохранив члены нулевого порядка, то получится [1]):

$$\mathbf{H} = J\left[\psi_0\right] + \frac{1}{2}\hbar\omega\boldsymbol{\Sigma}'_x\left(q'^2_x - \frac{\partial^2}{\partial q_x^2}\right) - \\ - \frac{\hbar^2}{2M}\sum_{j=1}^{3}\frac{\partial^2}{\partial \xi_j^2} + \mathbf{H}' + \mathbf{H}'' \tag{16.24}$$

где

$$H' = \frac{\hbar^2}{2M}\sum_{x}'\sum_{j=1}^{s}\frac{\partial^2 q_{x\xi}}{\partial \xi_j^2}\frac{\partial}{\partial q'_x} \tag{16.25}$$

и

$$\mathbf{H}'' = \frac{\hbar^2}{2M}\sum_{x,x_1}'\sum_{j=1}^{3}\frac{\partial q_{x\xi}}{\partial \tilde{\varsigma}_j}\frac{\partial q_{x,\xi}}{\partial \hat{\varsigma}_j}\frac{\partial^2}{\partial q'_x \partial q'_x} \tag{16.26}$$

Члены $\mathbf{H}'$ и $\mathbf{H}''$ будут учтены в следующем параграфе как малые возмущения. Здесь же, в нулевом приближении, мы эти члены опустим. В результате оператор энергии системы приобретает вид

[81]) При этом следует иметь в виду, что величины $q_{x\xi}$ бесконечно малы ($\sim 1/L^{\frac{3}{2}}$) и что некоторые $\sum''_x$, содержащие бесконечно большое число бесконечно малых слагаемых, можно заменить на $\sum_x$.

$$J\left[\psi_0\right]+\frac{1}{2}\hbar\omega\sum_x{}'\left(q_x'^2-\frac{\partial^2}{\partial q_x'^2}\right)-\frac{\hbar^2}{2M}\Delta_\varepsilon. \tag{16.27}$$

Волновое уравнение с таким оператором энергии решается точно благодаря полному разделению переменных. Решение имеет вид

$$\Psi_k,\ldots,n_x,\ldots=\frac{1}{L^{3/2}}e^{ik\xi}\Pi_x'\Phi_{nx}\left(q_x'\right). \tag{16.28}$$

Функции Φ_{nx} суть волновые функции гармонических осцилляторов; они определяются формулой (14.17). Собственные функции (16.28) образуют полную систему. Соответствующие собственные значения энергии системы равны

$$\mathbf{H}_k,\ldots,n_{x'}\ldots=J\left[\psi_0\right]+\hbar\omega\sum_x{}'\left(n_x+\frac{1}{2}\right)+\frac{\hbar^2\boldsymbol{k}^2}{2M}. \tag{16.29}$$

Сравнение этой формулы с формулой (16.17) показывает, что каждый из энергетических уровней (16.17), полученных выше, при рассмотрении ограниченного класса решений задачи точно совпадает с одним из уровней (16.29). В частности, энергия основного состояния системы согласно формуле (16.29) равна

$$H_0,\ldots,0,\ldots=J\left[\psi_0\right]+(v-3)\frac{\hbar\omega}{2}; \tag{16.30}$$

это выражение точно совпадает с (16.20) (следует иметь в виду, что $\sum_x'$ содержит $v-3$ слагаемых).

В формулах (16.28) и (16.29) штрихи у знаков произведения и суммы означают, что рассматриваемая система имеет колебательных степеней свободы на три меньше, чем диэлектрик без электрона проводимости. Это легко понять с помощью

следующих соображений: введение в кристалл электрона, состояние которого адиабатически «следует» за движением ионов, не должно изменить общего числа степеней свободы ионов. До введения электрона проводимости все v степеней свободы ионов были колебательными. После введения электрона проводимости и образования полярона появляются три степени свободы ионов ξ_1,ξ_2 и ξ_3, движение по которым носит не колебательный, а трансляционный характер. Эти новые три степени свободы могли появиться только за счёт уменьшения на три числа колебательных степеней свободы.

Состояния (16.28) и (16.18) будут в дальнейшем условно называться поляронными волнами. Формула (16.29) выражает зависимость энергии такой волны от волнового вектора k. Волновым пакетом будем называть суперпозицию волн (16.28) с близкими значениями k. Если ввести в каждую из этих волн, образующих пакет, временной множитель $e^{-iH_kt/\hbar}$, то совершенно обычным путём получается известная формула для групповой скорости пакета

$$v=\frac{1}{\hbar}\nabla_kH_k,\ldots,n_x,\ldots=\frac{\hbar\cdot k}{M}. \tag{16.31}$$

Классической скорости движения полярона соответствует групповая скорость волнового пакета v. С помощью формулы (16.31) последний член в выражении (16.29) можно записать в виде

$$\frac{\hbar^2k^2}{2M}=\frac{Mv^2}{2} \tag{16.32}$$

Эта величина представляет собой кинетическую энергию поступательного движения полярона. Формулу (16.31) можно рассматривать как соотношение де-Бройля для полярона; при этом Mv играет роль импульса полярона.

Центр полярона (точка с координатой э) движется в пространстве подобно свободной частице с массой M. Таким образом, при квантовомеханическом рассмотрении движения ионов эффективная масса полярона оказалась точно такой же, как в главе II, где движение ионов рассматривалось классически.

Общий электрический заряд, заключённый внутри волнового пакета, равен заряду электрона e. Движение такого

пакета представляет собой электрическиЙ ток. Интегральный ток (плотность тока, проинтегрированная по объёму основной области L^3) равен ev.

Упоминавшееся выше условие цикличности в применении $\Psi_k, \ldots, n_{\chi'}, \ldots$ означает, что $\Psi_k, \ldots, n_{\chi'}, \ldots$ должна быть периодической функцией ξ_1, ξ_2 и ξ_3, причём по каждому из этих аргументов она должна обладать периодом L. Из этого условия следует, что компоненты волнового вектора $\boldsymbol{k}$, а также векторов $*$ не могут быть произвольными, а могут принимать только следующие значения:

$$k_s = \frac{2\pi}{L} m_s, \quad x_s = \frac{2\pi}{L} \mu_s$$
$$(s = 1, 2, 3; m_s, \mu_s = 0, \pm 1, \pm 2, \pm 3, \ldots) \tag{16.33}$$

Выше коэффициенты a'_{ij} считались величинами первого порядка малости, а коэффициенты a^0 - нулевого порядка. Теперь, когда ψ-функции системы уже известны, необходимо проверить справедливость сделанных выше пренебрежений.

Прежде всего необходимо установить критерий случаев, когда a'_{ij} действительно значительно меньше a^0.

Согласно формулам (15.25), (15.13) и (16.21а)

$$a'_{ij} = -\sum_x (q_x - q_{x\xi}) \frac{\partial^2 q_{x\xi}}{\partial \xi_i \partial_{\xi j}} = -\sum_x{}' q'_x \frac{\partial^2 q_{x\xi}}{\partial \xi_i \partial \xi_j}. \tag{16.34}$$

Эта величина, вообще говоря, может принимать неограниченно большие значения, если только q'_x достаточно велики. Однако конфигурации ионов с большими q'_x мало вероятны, так как при этом очень мало

$$|\Psi_k, \ldots, n_{x'}, \ldots|^2 = \prod_x{}' \Phi^2_{\eta_x}(q'_x). \tag{16.35}$$

Для интересующей нас цели необходимо оценить a'_{ij} при таких конфигурациях ионов, при которых величина $\left|\Psi_{k,\ldots,n_{\chi'},\ldots}\right|^2$ значительна. Поскольку a'_{ij} - величина знакопеременная, в среднем равная нулю, удобнее всего оценивать её по среднему квадрату

$$\overline{a'^2_{ij}} = \int a'^2_{ij} |\Psi_k, \ldots, n_{x'}, \ldots|^2 dq' d\xi_1 d\xi_2 d\xi_3$$

где

$$dq' = \prod_x{}' dq'_x. \tag{16.36}$$

Подставляя сюда выражения (16.34-35) и принимая во внимание, что

$$\overline{q'_{x_1}q'_{x_2}} = \int q'_{x_1}q'_{x_2}\prod_x{}' \Phi^2_{n_x}\left(q'_x\right)dq' = \delta_{x_1x_2}\left(n_{x_1}+\frac{1}{2}\right), \tag{16.37}$$

получаем:

$$\begin{aligned}\overline{a^2_{ij}} = \sum\nolimits'_x \left(n_x+\tfrac{1}{2}\right)\left(\tfrac{\partial^2 q_{x\xi}}{\partial\bar{s}_i\partial\bar{s}_j}\right)^2 &= \left(\bar{n}+\tfrac{1}{2}\right)\tfrac{4\pi}{\hbar\omega c}\int\left(\tfrac{\partial^2 P_0(r)}{\partial x_i\partial x_j}\right)^2 d\tau = \\ &= \left(\bar{n}+\tfrac{1}{2}\right)\tfrac{c}{4\pi\hbar\omega}\int\left(\tfrac{\partial^2 D_0(r)}{\partial x_i\partial x_j}\right)^2 d\tau.\end{aligned} \tag{16.38}$$

Здесь предполагается, что колебания ионов находятся в тепловом равновесии, поэтому n_x вынесено за знак суммы при среднем планковском значении (см. § 19):

$$\bar{n} = \frac{1}{e^{n\omega/kT}-1}.$$

При вычислении интеграла (16.38) можно в функцию $\boldsymbol{D_0} = \boldsymbol{D}\left[\psi_0, \boldsymbol{r}\right]$ подставить $\psi_0(\boldsymbol{r})$ из (6.16). В результате вычисления получается:

$$\overline{a'^2_{ij}} = 0,011\left(\bar{n}+\frac{1}{2}\right)\frac{a_3^5e^2c}{\hbar\omega}\cdot\begin{cases}3, & \text{если } i=j,\\ 1, & \text{если } i\neq j.\end{cases} \tag{16.39}$$

Необходимо, чтобы $\overline{a'^2_{ij}}$ было значительно меньше, чем a^{0^2}. Используя формулы (15.29), (10.35) и (15.28), получаем:

$$a^{0^2} = 2,153\cdot 10^{-3}\frac{a_3^6e^4c^2}{(\hbar\omega)^2} \tag{16.40}$$

Неравенство $a^{0^2} \gg \overline{a^2_{ij}}$ можно записать в виде

$$0,098\frac{\mu e^4c^2}{\hbar^3\omega} \gg \left(\bar{n}+\frac{1}{2}\right)\cdot\begin{cases}3, & \text{если } i=j,\\ 1, & \text{если } i\neq j.\end{cases} \tag{16.41}$$

Выражая левую часть этого неравенства через $|H_0|$ согласно формуле (6.12), можно его переписать в виде

$$1,8\,|H_0| \gg \left(\bar{n}+\frac{1}{2}\right)\hbar\omega\cdot\begin{cases}3, & \text{если } i=j\\ 1, & \text{если } i\neq j.\end{cases} \tag{16.42}$$

При низких температурах ($\bar{n}<1$) условие (16.42) приблизительно совпадает с условием (7.4), лежащим в основе адиабатического приближения; в этом случае неравенство (16.42) не представляет собой нового ограничения теории.

Можно оценить погрешности, связанные с пренебрежением величинами первого порядка малости $\left(a'_{ij}\right)$. При переходе к новым переменным (16.21) оператор (15.12) преобразуется в оператор (16.24). Главные члены оператора (16.24) - первый и второй члены - получаются точно. Пренебрежение членами a'_{ij} вносит относительную ошибку порядка $a'_{ij,}a^0$ лишь в последние три члена оператора (16.24). Что касается членов $\mathbf{H}'$ и $\mathbf{H}''$, то они сами предполагаются малыми и в следующем параграфе будут рассмотрены как возмущение, вызывающее рассеяние поляронных волн. Третий член в операторе (16.24) представляет собой кинетическую энергию поступательного движения полярона и обычно порядка kT. Таким образом, в операторе (16.24) опущены члены порядка

$$\frac{Mv^2}{2}\frac{\sqrt{\overline{a'^2_{ij}}}}{a^0} = \frac{Mv^2}{2}\sqrt{\frac{\left(\bar{n}+\frac{1}{2}\right)\hbar\omega\cdot\begin{cases}3\\1\end{cases}}{1,8\mid H_0!}}. \tag{16.43}$$

10.3.6 § 17. Scattering of polaron waves by optical oscillations of ions

Точный оператор энергии системы обладает собственными функциями, которые представляют стационарные квантовые состояния системы.

Оказавшись в одном из таких состояний, система останется в нём сколь угодно долго (будучи, конечно, изолированной от внешних влияний). Стационарное состояние с не равной нулю плотностью тока есть состояние сверхпроводника. Действительно, при этом в отсутствии внешнего

электрического поля в кристалле течёт постоянный ток. Такие случаи в дальнейшем исключаются из рассмотрения.

Если в стационарном состоянии плотность тока равна нулю, то ток может быть создан путём включения внешнего электрического поля. В этом случае имеет смысл понятие удельной электропроводности и подвижности полярона во внешнем поле. Однако после включения внешнего поля состояние уже не будет стационарным в квантовомеханическом смысле, так как носитель тока будет непрерывно накоплять энергию в поле и передавать её колебаниям ионов; это значит, что будет увеличиваться температура кристалла.

Принципиально, вероятно, можно ввести внешнее электрическое поле в оператор энергии системы и с помощью временно́го уравнения Шрёдингера найти вышеупомянутые нестационарные состояния, вычислить плотность тока и подвижность. Однако практически этого сделать нельзя, по крайней мере при современном состоянии теории.

В настоящее время основным методом вычисления подвижности является кинетическое уравнение. Оно может быть применено, как известно, только в том случае, если гамильтониан системы распадается на две части: на гамильтониан движения «носителя тока» и гамильтониан движения «среды». Каждая из этих частей в отдельности должна описывать консервативную подсистему, обладающую определёнными энергетическими уровнями и стационарными состояниями. Слабое взаимодействие между указанными подсистемами должно вызывать в них квантовые переходы. Для получения функции распределения для скоростей носителя тока необходимо его волновые функции выбирать таким образом, чтобы они описывали состояния, в которых не только энергия, но и скорость носителя тока имела бы определённое значение.

Как раз такое разделение системы на две слабо взаимодействующие подсистемы было проделано выше: в формуле (16.24) второй член является гамильтонианом движения «среды», третий член - гамильтонианом движения «носителя тока» (полярона), а последние два члена $\mathbf{H}'$ и $\mathbf{H}''$ представляют собой взаимодействие между указанными подсистемами, вызывающее в них квантовые переходы. В нулевом приближении, пренебрегая взаимодействием $\mathbf{H}' + \mathbf{H}''$, получаем поляронные волны (16.28), которые как раз представляют собой

состояния, в которых скорость носителя тока имеет точное значение (16.31).

Для дальнейшего вычисления подвижности носителя тока методом кинетического уравнения необходимо определить вероятность рассеяния поляронных волн (16.28) членами возмущения $\mathbf{H}'$ и $\mathbf{H}''$. Вопрос о малости этого рассеяния и соответствующие критерии будут рассмотрены ниже.

Чтобы получить явное выражение для коэффициентов $q_{x\xi}$, следует исходить из формулы (15.13), причём $P_0(r)$ можно вычислить с помощью формул (6.3) и (6.16). В результате вычисления получается:

$$q_{x\xi} = q_x^0 \cdot \begin{cases} \cos x\xi \text{ при } x_x \geqslant 0, \\ \sin x\xi \text{ при } x_x < 0, \end{cases} \tag{17.1}$$

где

$$q_{\varkappa}^{0} = \sqrt{\frac{8\pi c}{\hbar\omega L^3}}\frac{e}{x}\frac{1+\frac{x^2}{28\alpha_3^3}}{\left(1+\frac{x^2}{4\alpha_3^2}\right)^4}, \quad \alpha_3 = \frac{\mu e^2}{2\hbar^2}c \tag{17.2}$$

и

$$\Delta_{\xi} q_{x\xi} = -x^2 q_{x\xi}. \tag{17.3}$$

Оператор $\mathbf{H}'$ теперь можно записать в виде

$$\mathbf{H}' = -\frac{\hbar^2}{2M}\sum_{x}{}' x^2 q_{x\xi}\frac{\partial}{\partial q'_x} \tag{17.4}$$

Согласно обычной теории возмущений квантовой механики вероятность рассеяния поляронной волны выражается через матричный элемент перехода

$$\begin{aligned} &H'_{k,\ldots}, n_{\varkappa}, \ldots; k', \ldots, n'_{x'}, \ldots = \\ &\quad = \int \Psi^*_{k,\ldots,n_{x'}}, \ldots \mathbf{H}'\Psi_{k',\ldots,n'_{x'}}, \ldots dq d\xi_1 d\xi_2 d\xi_{3'} \end{aligned} \tag{17.5}$$

Подстановка сюда $\Psi_k, \ldots, n_x, \ldots$ по формуле (16.28) и последующее интегрирование показывают, что матричный элемент (17.5) не равен нулю только для таких переходов $k, \ldots, n_x, \ldots \to k', \ldots, n'_x, \ldots$, при которых:

1. изменяется на единицу | только одно из осцилляторных квантовых чисел n_x;
2. это квантовое число n_x принадлежит одному из двух поляризационных колебаний с волновым вектором

$$x = \pm\left(k' - k\right). \tag{17.6}$$

При соблюдении обоих этих правил отбора модуль матричного элемента равен

$$\left|H'_{kn_{\varkappa}}; k' n_{\varkappa_x} \pm 1\right| = \frac{\hbar^2}{4M}\left|k'-k\right|^2 \sqrt{\frac{1}{2}\cdot\left\{\begin{array}{l} n_{\varkappa}+1 \\ n_{\varkappa} \end{array}\right. \cdot q^0_{k'-k}}. \tag{17.7}$$

Под корнем должно стоять $n_x + 1$ или n_x соответственно для переходов $n_x \to n_x + 1$ или $n_x \to n_x - 1$.

Аналогично при рассмотрении матрицы возмущения $\mathbf{H}''$ оказывается, что матричные элементы $H''_{k,\ldots,n_k}\kappa', \ldots, n'_x, \ldots$ отличны от нуля только для таких переходов, при которых либо
а) изменяются на единицу два осцилляторных квантовых числа n_{x_1} и n_{x_2}, причём волновые векторы этих колебаний удовлетворяют соотношению

$$k' - k = \pm x_1 \pm x_2, \tag{17.8}$$

либо
б) изменяется на двойку одно квантовое число n_x, причём

$$k' - k = \left\{\begin{array}{l} \pm 2x \\ 0 \end{array}\right. \tag{17.9}$$

либо, наконец,
в) осцилляторные квантовые числа не меняются.

Впоследствии мы увидим, что в пределе, когда размеры основной области неограниченно увеличиваются ($L \to \infty$), вероятность рассеяния, подчиняющегося правилам б) и в), стремится к нулю. При этом вероятность рассеяния по правилу а) остаётся конечной (см. ниже).

В случае а) с помощью формул (16.26), (16.28) и (17.1) получается:

$$| H''_{kn_{x_1}n_{x_2};k'n_{x_1}\pm 1,n_{x_2}\pm 1} = \frac{\hbar^2}{16M} |x_1 x_2| \, q^0_{x_1} q^0_{x_2} \times$$
$$\times \sqrt{\left\{ \begin{array}{l} n_{x_1}+1 \\ n_{x_1} \end{array} \right.} \sqrt{\left\{ \begin{array}{l} n_{x_2}+1 \\ n_{x_2} \end{array} \right.} . \tag{17.10}$$

Здесь x_1 и x_2 связаны соотношением (17.8). Под корнями должно стоять $n_{x_i}+1$ или $n_{x_i}(i=1,2)$ соответственно для переходов $n_{\varkappa_i} \to n_{\varkappa_i}+1$ и $n_{\varkappa_i} \to n_{\varkappa_i}-1$.

Вероятность перехода системы в течение единицы времени из состояния с волновым вектором k в состояние с волновым вектором $\boldsymbol{k}'$, который лежит внутри телесного угла $d\boldsymbol{Q}$, даётся общеизвестной формулой теории возмущений

$$W_{kn_{x'}k'n'_x} dQ = \frac{2\pi}{\hbar} \left| H'_{kn_{x'}k'n'_x} + H''_{kn_{x'},k'n'_x} \right|^2 \rho dQ. \tag{17.11}$$

Здесь ρ имеет следующий смысл: $dN = \rho d\mathbf{Q} dH_{k'n'_\alpha}$ есть число состояний системы, в которых волновой вектор $\boldsymbol{k}'$ лежит внутри телесного угла dQ, а энергия - в интервале между $H_{k'n'_x}$ и $H_{k'n'_x} + dH_{k'n'_x}$. Величина ρ легко вычисляется следующим образом. Дифференцирование (16.29) даёт:

$$dH_{k'n'_x} = \frac{h^2 k' dk'}{M}. \tag{17.12}$$

Необходимо найти число состояний системы, в которых волновой вектор $\boldsymbol{k}'$ лежит внутри телесного угла $d\mathrm{Q}$, а его модуль k'-в интервале dk'. Каждое состояние системы изображается фазовой точкой в k-пространстве. Искомое число состояний равно числу точек в элементе объёма

$$k'^2 dk' d\mathrm{Q}. \tag{17.13}$$

Согласно формуле (16.33) эти точки заполняют k-пространство с постоянной концентрацией $\left(\frac{L}{2\pi}\right)^3$. Поэтому, учитывая (17.12),

$$dN = \left(\frac{L}{2\pi}\right)^3 k'^2 dk' d\mathrm{Q} = \left(\frac{L}{2\pi}\right)^3 \frac{M}{\hbar^2} k' d\mathrm{Q} dH_{k'n'_x}. \tag{17.14}$$

Отсюда видно, что

$$\rho = \left(\frac{L}{2\pi}\right)^3 \frac{M}{\hbar^2} k'. \tag{17.15}$$

Как указывалось выше, матричный элемент $H'_{\mathrm{kn}\,\boldsymbol{n}'_{\boldsymbol{n}'},\boldsymbol{k}'\boldsymbol{n}'_{\boldsymbol{n}}}$ не равен нулю только для переходов, при которых одно из

осцилляторных квантовых чисел n_x изменяется на единицу; такие переходы будем в дальнейшем называть одноквантовыми. Матричный же элемент $H''_{kn_x,k'n'_x}$ отличен от нуля только для двухквантовых переходов. $H'_{kn_x,k'n'_x}$ и $H''_{kn_x,k'n'_x}$ для данного перехода не могут быть отличны от нуля одновременно. Поэтому, рассматривая одноквантовое

рассеяние, нужно в формуле (17.11) опустить член $H_{kn_{x'}s'n'_x}$ и наоборот, при рассмотрении двухквантового рассеяния следует игнорировать член $H'_{kn_\varkappa,k'n'_\varkappa}$).

Перейдём к рассмотрению одноквантового рассеяния. Подставляя в формулу (17.11) выражения (17.7), (17.2) и (17.15), получаем:

$$W'_{\boldsymbol{k}\boldsymbol{n}_{\boldsymbol{x}'}}\boldsymbol{k}'n_{\boldsymbol{x}^{\pm 1}}dQ = \\ = \frac{d\Omega ce^2\left|\boldsymbol{k}'-\boldsymbol{k}\right|^2\boldsymbol{k}'}{16\pi M\omega}\frac{\left(1+\frac{|\boldsymbol{k}'-\boldsymbol{k}|^2}{28\alpha_3^2}\right)^2}{\left(1+\frac{|\boldsymbol{k}'-\boldsymbol{k}|^2}{4\alpha_3^2}\right)^8}\cdot\begin{cases} n_\varkappa+1, \\ n_{\varkappa'}\end{cases} \tag{17.16}$$

Если колебания ионов находятся в тепловом равновесии, можно в формуле (17.16) заменить n_x средним планковским значением

$$\vec{n} = \frac{1}{e^{\frac{n_\omega}{kT}}-1} \tag{17.17}$$

В этом случае вероятность рассеяния полярона на колебаниях с индексами $\boldsymbol{x} = (\boldsymbol{k}'-\boldsymbol{k})$ и $\boldsymbol{x} = -(\boldsymbol{k}'-\boldsymbol{k})$ одинакова. Поэтому суммарная вероятность рассеяния $\boldsymbol{k}\to\boldsymbol{k}'$ на любом из

двух упомянутых колебаний равна удвоенной вероятности (17.16)

$$W'_{kk'}d\mathbf{Q} = 2W'_{kn_{x'},k'n_{\varkappa\pm 1}}d\mathbf{Q} = \\ = \frac{d\Omega ce^2\left|k'-k\right|^2k'}{8\pi M\omega}\frac{\left(1+\frac{|k'-k|^2}{28a_3^2}\right)^2}{\left(1+\frac{|k'-k|^2}{4a_3^2}\right)^8}\cdot\begin{cases} \bar{n}+1, \\ \bar{n}.\end{cases} \tag{17.18}$$

Полная энергия системы $H_{\text{к},}, \ldots, n_{\text{х}}, \ldots$. (см. (16.29)) при этом переходе должна сохраняться; поэтому

$$\frac{\hbar^2}{2M}\left(\boldsymbol{k}'^2-\boldsymbol{k}^2\right) = \begin{cases} -\hbar\omega, \\ +\hbar\omega.\end{cases} \tag{17.19}$$

Формула (17.18) упрощается в двух предельных случаях:

1. Предельный случай медленно движущегося полярона, когда

$$\frac{\hbar^2k^2}{2M} \ll \hbar\omega. \tag{17.20}$$

При этом рассеяние возможно только с поглощением, а не с излучением кванта колебаний $\hbar\omega$. Согласно формулам (17.19) и (17.20)

$$k \ll k' \cong \sqrt{\frac{2M\omega}{\hbar}} \tag{17.21}$$

8

1. Возмущение $\mathbf{H}'$ приводит к двухквантовому рассеянию во втором приближении. Расчёт показывает, что если $\hbar\omega \leqslant 3\left|H_0\right|$, вероятность этого рассеяния ничтожна по сравнению с вероятностью двухквантового рассеяния, которое даёт член H'' в первом приближенни. Отметим, что вышеуказанное неравенство должно соблюдаться, поскольку в основе адиабатического приближения лежит более жёсткое неравенство (см. (7.4)).

Поэтому

$$W'_{kk'}dQ = \frac{dQce^2}{4\pi\hbar^{3/2}}\sqrt{2M\omega}\frac{\left(1+\frac{1}{7}x\right)^2}{(1+x)^8} - \bar{n} \tag{17.22}$$

где

$$x = \frac{|\boldsymbol{k}' - \boldsymbol{k}|^2}{4a_{\mathbf{8}}^2} \tag{17.23}$$

При выполнении условия (17.20), принимая во внимание (10.35), имеем:

$$x \cong \frac{M\omega}{2\hbar\alpha_3^2} = 0,0116\frac{\mu e^4 c^2}{\hbar^3\omega} \tag{17.24}$$

Как видно из формул (17.22) и (17.24), для медленно движущегося полярона вероятность рассеяния не зависит ни от угла рассеяния, ни от скорости полярона.
2) Предельный случай быстро движущегося полярона, когда

$$\frac{\hbar^2 k^2}{2M} \gg \hbar\omega \tag{17.25}$$

В этом случае согласно формулам (17.19) и (17.25)

$$k' \cong k. \tag{17.26}$$

Поэтому

$$x = \frac{|\boldsymbol{k}' - \boldsymbol{k}|^2}{4a_3^2} \cong \frac{\boldsymbol{k}^2(1-\cos\vartheta)}{2\alpha_3^2}, \tag{17.27}$$

где ϑ - угол между направлениями $\boldsymbol{k}$ и $\boldsymbol{k}'$,

$$d\mathbf{Q} = 2\pi\sin\theta d\theta \cong \frac{4\pi\alpha_3^2}{k^2}dx \tag{17.28}$$

Подставляя в формулу (17.16) выражения (17.27-28) и (10.35), получаем:

$$W'_{kk'}dQ = 43,1\frac{\alpha_3\omega}{k}\frac{\left(1+\frac{1}{7}x\right)^2 xdx}{(1+x)^8}\cdot\begin{cases}\bar{n}+1,\\ \bar{n}.\end{cases} \tag{17.29}$$

Перейдём теперь к рассмотрению двухквантового рассеяния. Вероятность рассеяния, при котором $n_{\varkappa_1}$ возрастает на единицу, а $n_{\varkappa_2}$ убывает на единицу, даётся формулой (17.11), в которую следует подставить выражения (17.10) и (17.15). В результате получается:

$$\begin{aligned} &W_{k,n_{x_1},n_{x_3};k',n_{x_1}+1,n_{x_2}-1}d\Omega = \\ &\quad = \frac{\hbar L^3 k'}{(32\pi)^2 M}\left|x_1 x_2 q_{x_1}^0 q_{x_2}^0\right|^2 (n_{x_1}+1)\, n_{x_2} d\Omega. \end{aligned} \tag{17.30}$$

Рассеяние возможно только при соблюдении условий (17.8):

$$x_2 = \pm\left(k' - k \pm x_1\right).$$

Предполагая, что колебания ионов находятся в тепловом равновесии, снова можно в (17.30) n_{χ_1} и n_{x_2} заменить на планковское среднее $\bar{n}_1$

Формула (17.30) даёт вероятность рассеяния $k, n_{x_1}, n_{x_2} \to\to \boldsymbol{k}', n_{x_1}+1, n_{x_2}-1$ с участием двух заданных нормальных колебаний ионов с индексами $\varkappa_1$ и $\varkappa_2$. Однако в дальнейшем нас будет интересовать вероятность рассеяния $\boldsymbol{k} \to \boldsymbol{k}'$, причём нам безразлично, какие именно нормальные колебания участвуют в рассеянии. Вероятность такого рассеяния можно получить путём суммирования величины (17.30) по всем x_1 и x_2, удовлетворяющим условию (17.8):

$$W''_{k,k'} = \sum_{x_1} W''_{k,n_{x_1},n_{x_3};k',n_{x_1}+1,n_{x_2}-1;}; \tag{17.31}$$
$$x_2 = \pm\left(k' - k \pm x_1\right).$$

В уравнении (17.8) возможны четыре различные комбинации знаков и при каждой из них сумма (17.31) имеет одно и то же значение, поскольку суммируется чётная функция x_1 и x_2. Поэтому можно выбрать какую-нибудь одну комбинацию знаков, например положить

$$x_2 = k' - k - x_1, \tag{17.8a}$$

а затем результат суммирования умножить на 4 . Суммирование по x_1 можно заменить интегрированием, причём необходимо учесть, что вследствие условий цикличности в элементе x-пространства $dx_1dx_2dx_3$ имеется

$$\left(\frac{L}{2\pi}\right)^3 dx_1dx_2dx_3 \tag{17.32}$$

продольных поляризационных колебаний ионов.
Подставляя в (17.31) выражения (17.30), (17.2) и (10.35) и переходя от суммы к интегралу, получаем:

$$W''_{kk'}d\mathrm{Q} = 0,174\frac{ce^2k'}{\hbar}I(a)(\bar{n}+1)\bar{n}d\mathrm{Q}, \tag{17.33}$$

где

$$I(a) = \iiint_{-\infty}^{\infty} \frac{[r(a+r)]^2\left(1+\frac{1}{7}r^2\right)^2\left[1+\frac{1}{7}(a+r)^2\right]^2}{r^2(a+r)^2\left(1+r^2\right)^8\left[1+(a+r)^2\right]^8}\times \tag{17.34}$$

$Xdxdydz.$
Здесь

$$\frac{k'-k}{2\alpha_3} = a, \quad \frac{x_1}{2\alpha_3} = r, \tag{17,35}$$

а x, y, z-декартовы проекции вектора r.

Поскольку при рассмотренном выше двухквантовом рассеянии общая энергия колебаний ионов не меняется, то согласно закону сохранения энергии и кинетическая энергия полярона не меняется. Следовательно,

$$k' = k. \tag{17.36}$$

Совершенно аналогично можно рассмотреть двухквантовое рассеяние, при котором оба квантовых числа n_{x_1} и n_{x_9} убывают на единицу или оба возрастают на единицу. В первом случае получается формула (17.30), но в ней вместо $(n_{\varkappa_1}+1)\,n_{\varkappa_2}$ должно стоять $n_{\varkappa_1}n_{\varkappa_2}$; во втором случае вместо $(n_{\varkappa_1}+1)\,n_{\varkappa_2}$ следует поставить $(n_{x_1}+1)\,(n_{x_2}+1)$.

Суммарная вероятность рассеяния $k \to k'$ получается суммированием по всем $\boldsymbol{x}_1$ и $\boldsymbol{x}_2$, удовлетворяющим условию (17.8). Но при вычислении суммы, аналогичной (17.31), надо иметь в виду следующее: если выше каждая пара слагаемых, отличающихся друг от друга перестановкой индексов x_1 и x_2, соответствовала двум различным квантовым переходам (конечные состояния переходов различны), то в том случае, когда оба квантовых числа n_{x_1} и n_{x_2} одновременно убывают (возрастают) на единицу, слагаемые, отличающиеся перестановкой x_1 и x_2, соответствуют одному и тому же переходу (конечное состояние одинаково). Таким образом, вероятность каждого перехода в сумме фигурирует дважды и сумму следует разделить на 2 .

Учитывая это обстоятельство, вместо формулы (17.33) мы придём к формуле

$$W''_{kk'} d\mathrm{Q} = 0,174 \frac{ce^2 k'}{2\hbar} I(a) d\mathrm{Q} \cdot \begin{cases} \bar{n}^2 \\ (\bar{n}+1)^2. \end{cases} \tag{17.37}$$

Из закона сохранения энергии следует:

$$\frac{\hbar^2}{2M}\left(\boldsymbol{k}'^2 - k^2\right) = \begin{cases} 2\hbar\omega, \\ -2\hbar\omega. \end{cases} \tag{17.38}$$

В этих формулах следует брать верхние или нижние выражения, если при рассеянии полярона, соответственно, поглощаются или рождаются два кванта колебаний ионов. Рассеяние с рождением двух квантов колебаний возможно только, если кинетическая энергия полярона до рассеяния больше

чем $2\hbar\omega$. Легко убедиться в том, что вероятность рассеяния $k \to \boldsymbol{k}'$ с изменением квантового числа n_x на 2 , а также без изменения квантовых чисел стремится к нулю с ростом L, как $\frac{1}{L^3}$.

В заключение заметим, что все полученные выше выражения для вероятностей рассеяния справедливы только при условии, что рассеяние мало интенсивно; в противном случае сам метод возмущений неприменим. Очевидно, для медленных поляронов, у которых кинетическая энергия меньше $\hbar\omega$, возможно одноквантовое рассеяние лишь с поглощением кванта $\hbar\omega$ и двухквантовое рассеяние, при котором по меньшей мере один квант поглощается. При этом вероятности рассеяния пропорциональны $\bar{n}$ или $\overline{n^2}$, т. е. они действительно малы при достаточно низких температурах.

Для быстрых поляронов возможно также рассеяние с рождением колебательных квантов. Вероятности такого рассеяния содержат множители $(\bar{n}+1)$ и $(\bar{n}+1)^2$. Эти множители не могут быть сделаны произвольно малыми путём понижения температуры. В этом случае вероятности рассеяния могут оказаться малыми лишь при благоприятных численных значениях параметров кристалла. В § 20 будут рассмотрены количественные условия, определяющие границы применимости метода рассеяния.

10.3.7 § 18. Scattering of polaron waves by acoustic oscillations of the crystal

Если бы ионы кристалла были закреплены в узлах решётки, то электрон проводимости оказался бы в периодическом поле с потенциалом $W(\boldsymbol{r})$. Вследствие смещений ионов из узлов решётки в потенциальной энергии электрона проводимости появляются добавочные члены $V(\boldsymbol{r}) + V'(\boldsymbol{r})$, которые были подробно рассмотрены в § 5. Член $V(\boldsymbol{r})$ представляет собой поляризационную потеншиальную яму, которая выше рассчитывалась как потенциал поляризованного континуума. Член $V'(r)$ даёт то добавочное изменение потенциала, которое связано со смещением одного-двух ионов, наиболее близких к электрону проводимости; при расчёте $V'(r)$ нельзя исходить из

модели диэлектрического континуума, а следует учесть детальный ход микропотенциала в кристалле.

Выше, при рассмотрении квантовых состояний систем, член $V'(r)$ игнорировался. Введём его теперь как малое возмущение, вызывающее рассеяние поляронных волн. Очевидно, что $V'(\boldsymbol{r})$ является функцией смещений ионов той кристаллической ячейки, в которой находится электрон проводимости. Предполагая, что смещения ионов малы, можно разложить $V'(r)$ в ряд по степеням смещений и ограничиться линейными членами. Таким образом, $V'(r)$ можно считать линейной функцией смещений ионов. Смещения ионов в свою очередь являются линейными функциями всех нормальных координат ионов (как оптических, так и акустических колебаний). Следовательно, смещения ионов, а поэтому и $V'(r)$ можно разложить на два слагаемых. В одно из них линейно и однородно входят нормальные координаты акустических колебаний кристалла, в другое - нормальные координаты оптических колебаний:

$$V'(r) = V'_{\text{ak}}(r) + V_{\text{On}}(r). \tag{18.1}$$

Оператор энергии всей системы выражается формулой (12.3). Если в нулевом приближении опустить член $V'(\boldsymbol{r})$, то, как было показано в § 12 , оператор энергии распадается на три слагаемых. Первое из них зависит только от координат электрона r и от нормальных координат продольных поляризационных колебаний q_x; оно имеет вид (12.10). Второе слагаемое зависит только от координат поперечных поляризационных колебаний и третье - только от координат акустических колебаний. Таким образом, в нулевом приближении система распадается на три независимые замкнутые консервативные подсистемы и ψ-функция системы состоит из трёх соответствующих множителей. Первый из них является собственной функцией оператора (12.10). Второй и третий множители представляют собой ψ-функции поперечных оптических и акустических колебаний; они выглядят так же, как если бы электрона проводимости в кристалле вовсе не было.

Поскольку возмущение $V'(r)$ является линейной однородной формой нормальных координат, то, как всегда в подобных случаях, вызываются квантовые переходы, при которых только одно из осцилляторных квантовых чисел изменяется на единицу. В таких случаях рассеяние на различных нормальных колебаниях происходит независимо и может быть

рассмотрено отдельно [1]) (речь идёт о рассеянии первого порядка малости).

Пользуясь этим обстоятельством, можно рассмотреть сначала рассеяние поляронных волн акустическими колебаниями кристалла, у которых длина волны значительно больше постоянной решётки. Такое рассеяние было рассмотрено Ю. Е. Перлиным [27]. В случае длинноволновых акустических колебаний можно считать, что ионы, наиболее близкие к электрону проводимости, подвергаются одинаковым смещениям $\boldsymbol{u}$. При этом вся картина микропотенциала просто передвигается на расстояние $\boldsymbol{u}$. В результате этого в точке $\boldsymbol{r}$ получается такое значение микропотенциала, какое до смещения было в точке $\boldsymbol{r}$ - $\boldsymbol{u}$. Если до смещения ионов микропотенциал имел значение $W(\boldsymbol{r})$, то после смещения ионов микропотенциал в точке r будет равен

$$W_1(\boldsymbol{r}) = W(\boldsymbol{r} - \boldsymbol{u}) \cong W(\boldsymbol{r}) - \boldsymbol{u}\nabla W + \ldots \tag{18.2}$$

Отсюда следует, что

$$V'_{\text{aE}}(r) = -u\nabla W. \tag{18.3}$$

Смещение $\boldsymbol{u}$ можно разложить по собственным нормальным колебаниям кристалла [28]:

$$u = \sqrt{\frac{\bar{Q}}{L^3}} \sum_{qj} e_{qj} \left(a_{qj} e^{iqr} + a^*_{qj} e^{-iqr} \right). \tag{18.4}$$

Здесь $\mathbf{Q}$ - объём элементарной кристаллической ячейки, $\boldsymbol{q}$ - волновой вектор акустической волны. Данное значение $\boldsymbol{q}$ принадлежит, как известно, трём акустическим волнам; одна из них поляризована параллельно, а две другие - перпендикулярно к $\boldsymbol{q}$. Индекс $j = 1, 2, 3$ нумерует три упомянутые волны. Вектор $\boldsymbol{e_{qj}}$ является ортом, определяющим поляризацию. В качестве нормальных координат, описывающих акустические колебания кристалла, выберем амплитуды a_{qj}.

Формула (18.3) показывает, что $V'_{\text{ax}}(r)$ не является плавной функцией r ($V'_{\text{ac}}(r)$ существенно меняется на расстоянии

порядка постоянной решётки). Поэтому при вычислении матричного элемента перехода методом эффективной массы, развитым в § 4, следует пользоваться не «сглаженными» волновыми функциями электрона (4.29), а детальными волновыми функциями (4.36). Сглаженная волновая функция электрона в основном поляронном состоянии $\psi_0(\boldsymbol{r} - \xi)$ была определена выше. Следуя § 4, детальная волновая функция электрона равна

$$\psi_{0\ \text{дет}} = \sum_k A_k U_k(r) e^{ikr}. \tag{18.5}$$

Здесь A_k суть коэффициенты разложения «сглаженной» функции $\psi_0(\boldsymbol{r} - \boldsymbol{\xi})$ в ряд Фурье:

$$A_k = \frac{1}{L^{3/2}} \int \psi_0(r - \xi) e^{-ikr} d\tau = e^{-ik\xi} a_k \tag{18.6}$$

где коэффициенты

$$a_k = \frac{1}{L^{3/2}} \int \psi_0(\boldsymbol{r}) e^{-ikr} d\tau \tag{18.7}$$

уже встречались выше; они выражаются формулой (7.9).
Согласно общеизвестному методу адиабатического приближения [7] полная ψ-функция системы получается путём умножения ψ-функции ионов на ψ-функцию электрона; предполагается, что последняя адиабатически «следует» за медленным движением ионов и зависит от координат ионов, как от параметров. Используя результаты § 16 , в частности формулу (16.28), полную ψ-функцию системы можно записать следующим образом:

$$\begin{aligned} &\Phi_k, \ldots, n_x, \ldots, N_{qj} = \\ &\quad = \frac{1}{L^{3/2}} \psi_{0\ \text{дет}}(r\xi) e^{in\xi} \prod_x{}' \Phi_{n_x}(q'_x)\, \Psi_{\perp\ \text{оп}} \prod_{qj} \psi_{N_{qj}}(a_{qj}). \end{aligned} \tag{18.8}$$

Здесь $\Psi_{\perp\ \text{оп}}$ и $\prod_{qj} \Psi_{Njj}(a_{qj})$ являются волновыми функциями поперечных оптических и акустических колебаний; они имеют тривиальный вид (такой же, как если бы электрона проводимости в кристалле вовсе не было). $\psi_{N_{qj}}(a_{qj})$ есть волновая

функция гармонического осциллятора, описывающая колебание нормальной координаты $a_{qj} \cdot N_{qj}$ - осцилляторные квантовые числа акустических колебаний.

[81]) Это, очевидно, следуст из общего вида вероятности рассеяния, если учесть, что при каждом переходе отличен от нуля матричный элемент только одной из нормальных координат.

В состоянии (18.8) энергия системы равна

$$H_k, \ldots, n_x \ldots, N_{qj} = J\left[\psi_0\right] + \hbar\omega \sum_x{}' \left(n_x + \frac{1}{2}\right) + H_{0\pi\perp} + \\ + \sum_{qj} \hbar\omega_{qj} \left(N_{qj} + \frac{1}{2}\right) + \frac{\hbar^2 k^2}{2M}. \tag{18.9}$$

Вероятность рассеяния поляронных волн (18.8) акустическими колебаниями кристалла выражается через матричный элемент

$$\left(V'_{\text{nk}}\right)_k, \ldots, N_{qj}; k', \ldots, N'_{qj} = \int \Phi^*_{k,\ldots,N_{qj}} V'_{\text{ak}}\left(r, \ldots, a_{qj}, \ldots\right) \times \\ \times \Phi_{k',\ldots,N'_{qj}} d\tau d\xi_1 d\xi_2 d\xi_3 dq d\tau_{\text{oH}} \perp \prod_{qj} da_{qj}. \tag{18.10}$$

Сюда необходимо подставить выражения (18.3-8) и осуществить интегрирование. Из соображений ортогональности немедленно следует, что матричный элемент (18.10) отличен от нуля только для переходов, при которых n_x, а также осцилляторные квантовые числа поперечных оптических колебаний не изменяются. Квантовые числа N_{qj} при переходе должны оставаться неизменными за исключением одного, которое изменяется на единицу; координата a_{qj}, соответствующая этому квантовому числу, имеет отличные от нуля матричные элементы вида

$$\left(a_{qj}\right)_{N_{qj}}, N_{qj} + 1 = \sqrt{\frac{\hbar\left(N_{qj} + 1\right)}{2\gamma {\omega_{qj}}^2}}, \tag{18.11}$$

$$\left(a_{qj}\right)_{N_{qj}, N_{qj}-1} = \sqrt{\frac{\hbar N_{qj}}{2\gamma {\omega_{qj}}^2}}. \tag{18.12}$$

Здесь γ - плотность (удельный вес) кристалла. Явное выражение $\psi_{N_{qj}}\left(a_{qj}\right)$ и вывод формул (18.11) и (18.12) даются в [28] § 32.

В результате матричный элемент (18.10) можно записать в виде

$$\left(V'_{\text{aK}}\right)_{kN_{qj}:k',N_{qj}\pm 1} = \\ = -\frac{1}{L^{q/2}} \sum_{k_1 k_2} a^{*n}_{k_1} a_{k_2} \int_{L^3} e^{i(k_1 - k_2 + k' - k)\xi} d\xi_1 d\xi_2 d\xi_3 \times \\ \times \int_{L^2} U^*_{k_1}(r) U_{k_{\text{e}}}(r) e^{i(k_2 - k_1 \pm q)r} \left(\boldsymbol{e}_{qj} \nabla W\right) d\tau \times \\ \times \int \frac{\hbar}{2\gamma\omega_{qj}} \left\{ \begin{array}{l} N_{qj} + 1 \\ N_{qj} \end{array} \right. \tag{18.13}$$

Здесь для переходов $N_{qj} \to N_{qj} + 1$ следует брать всюду верхний знак и под корнем $N_{qj} + 1$; для переходов $N_{qj} \to N_{qj} - 1-$ нижний знак и под корнем N_{qj}.

Поскольку векторы $\boldsymbol{k}_1$ и $\boldsymbol{k}_2$, а также $\boldsymbol{k}$ и $\boldsymbol{k}'$ в силу условия цикличности образуют дисконтинуум вида (16.33),

$$\int_{L^a} e^{i(k_1 - k_2 + k' - k, \xi)} d\xi_1 d\xi_2 d\xi_3 = L^3 \delta_{k_1 - k_2 + k' - k} \tag{18.14}$$

Если учесть, что $U_l(r)$ и $W(r)$ обладают периодами решётки, то -

$$\int_{L^j} \boldsymbol{U}^*_{\boldsymbol{k}_1}(\boldsymbol{r}) U_{\boldsymbol{k}_2}(\boldsymbol{r}) e^{i(\boldsymbol{k}_2-\boldsymbol{k}_1\pm\boldsymbol{q})r} \left(\boldsymbol{e}_{\boldsymbol{q}_j}\Gamma W\right) d\tau =$$
$$= \delta_{\boldsymbol{k}_2-\boldsymbol{k}_1\pm\boldsymbol{q}} \int_{\boldsymbol{L}^j} U^*_{\boldsymbol{k}_1}(\boldsymbol{r}) U_{\boldsymbol{k}_2}(\boldsymbol{r}) \left(\boldsymbol{e}_{\boldsymbol{q}j}\Gamma W\right) d\tau \tag{18.15}$$

Именно такой интеграл встречается в старой теории электропроводности (см. [28] § 34); оценка показывает, что для поперечных волн, когда $\boldsymbol{e}_{qj} \perp \boldsymbol{q}$, он равен нулю, а для продольных волн, когда $\boldsymbol{e}_{qj} \| \boldsymbol{q} (j = 1)$,

$$\int_{L^3} U^*_{k_1}(r) U_{k_2}(r) \left(e_{q_1}\nabla W\right) d\tau \cong \pm\frac{2}{3} i \left|k_2 - k_1\right| G \tag{18.16}$$

где

$$G \cong \frac{\hbar^2}{2m} \int \left|\nabla U_0(r)\right|^2 d\tau \tag{18.17}$$

есть средняя кинетическая энергия электрона на дне зоны проводимости в «зонной» теории электропроводности. Таким образом, поляроны рассеиваются только продольными акустическими волнами. Поперечные волны более не будут рассматриваться, и индекс j в дальнейшем опускается.

Из равенств (18.14) и (18.15) следует, что в правой части формулы (18.13) отличны от нуля только члены, у которых

$$\boldsymbol{k}_2 - \boldsymbol{k}_1 = \boldsymbol{k}' - \boldsymbol{k} = \mp\boldsymbol{q}. \tag{18.18}$$

Последнее равенство выражает закон сохранения квазиимпульса при рассеянии.

Учитывая равенства (18.14-16), получаем:

$$\left(V'_{\text{ax}}\right)_{kN_q;k'N_q\pm1} = \pm\frac{2iqG}{3L^{3/2}} \sum_k a^*_{k\pm q} a_k \sqrt{\frac{\hbar}{2\gamma\omega_q}} \begin{cases} N_q + 1, \\ N_q. \end{cases} \tag{18.19}$$

Так как

$$\omega_0(r) = \frac{1}{L^{3/2}} \sum_{\hbar} a_k e^{ikr} \tag{18.20}$$

и
$\bigcup^*_0(r) e^{\pm iqr} = \frac{1}{L^{3/2}} \sum_{k_1} a^*_{k_1} e^{-i(k_1\mp q)r} = \frac{1}{L^{3/2}} \sum_k a^*_{k\pm q} e^{-ikr}$,

то, перемножая выражения (18.20) и (18.21) и затем интегрируя по объёму основной области, получаем:

$$\int \left|\psi_0(r)\right|^2 e^{\pm iqr} d\tau = \sum_k a^*_{k\pm\boldsymbol{q}'} a_k \tag{18.22}$$

Следовательно, сумма, фигурирующая в формуле (18.19), сводится к объёмному интегралу (18.22). Этот интеграл можно вычислить, используя для $\psi_0(r)$ выражение (6.16). В результате вычисления получается:

$$\int \left|\psi_0(r)\right|^2 e^{\pm\ell\alpha r} d\tau = \frac{1 + \frac{q^2}{28\alpha_3^2}}{\left(1 + \frac{q^2}{4\alpha_3^2}\right)^4} \tag{18.23}$$

Матричный элемент перехода может быть записан в виде

$$(V'_{\text{ax}})_{kN_{q'}k'N_q\pm1} = \\ = \pm\frac{2}{3}\frac{iG}{L^{3/2}}\sqrt{\frac{\hbar}{2\gamma\omega_q}\{N_q+1\frac{q\left(1+\frac{q^2}{28x_3^2}\right)}{\left(1+\frac{q^2}{4\alpha_3^2}\right)^4}} \tag{18.24}$$

.

Вероятность рассеяния в единицу времени вычисляется по обычной формуле

$$W^{\text{an}}_{kkk'}d\Omega = \frac{2\pi}{\hbar}\left|V'_{\text{ak}}\right|_{kN_q;k'N_q\pm1}\cdot\rho dQ, \tag{18.25}$$

где ρ выражается формулой (17.15). Если принять во внимание равенство (18.18), а также учесть, что

$$\frac{\omega_q}{q} = w \tag{18.26}$$

есть скорость звука в кристалле, то получается:

$$W^{\text{ax}}_{kk'}, dQ = \frac{MG^2k'\left|\boldsymbol{k}'-\boldsymbol{k}\right|\boldsymbol{d}Q}{18\pi^2\hbar^2\gamma w}\times \\ \times\frac{\left(1+\frac{|\boldsymbol{k}'-\boldsymbol{k}|^2}{28a_3^2}\right)^2}{\left(1+\frac{|\boldsymbol{k}'-\boldsymbol{k}|^2}{4a_3^2}\right)^8}\cdot\begin{cases} N_{\boldsymbol{k}'-\boldsymbol{k}}+1, \\ N_{\boldsymbol{k}'-\boldsymbol{k}'}\end{cases} \tag{18.27}$$

Полная энергия системы при квантовом нереходе должна сохраняться; поэтому

$$\frac{\hbar^2}{2M}\left(\boldsymbol{k}'^2-\boldsymbol{k}^2\right) = \mp\hbar\omega_q = \mp\hbar qw = \mp\hbar\left|\boldsymbol{k}'-\boldsymbol{k}\right|w. \tag{18.28}$$

Формула (18.27) была получена Ю. Е. Перлиным [27]. Сравнение её с формулой (17.18), выражающей вероятность одноквантового рассеяния полярона предельными оптическими колебаниями, показывает, что в этих формулах есть много общего. В частности, одинаковый вид имеет в обеих формулах вторая дробь. Эта дробь порядка единицы при $\frac{|k'-k|}{\alpha_3} < 1$, но с ростом отношения $\frac{|\boldsymbol{k}'-\boldsymbol{k}|}{\alpha_3}$ она начинает быстро убывать, стремясь

к нулю. Таким образом, интенсивно рассеивают поляроны лишь длинные волны решётки, у которых волновой вектор

$$q = \left|\boldsymbol{k}'-\boldsymbol{k}\right| \leqslant \alpha_\beta, \tag{18.29}$$

а длина волны

$$\lambda_{\text{ak}} \geqslant \frac{2\pi}{\alpha_3} > r_p, \tag{18.30}$$

где r_p - поляризационный радиус полярона (см. (7.6)), который сам, по предположению, должен быть больше постоянноЙ решётки.

В случае длинных воли, удовлетворяющих неравенству (18.30), справедлива формула (18.3) и следующие из неё (см. выше) результаты. Коротковолновые колебания кристалла рассеивают поляроны слабо и рассматриваться не будут.

Параметр теории G определяется формулой (18.17) и представляет собой квантовомеханическое среднее значение кинетической энергии электрона на дне зоны проводимости в старой зонной теории [8]. G можно численно оценить в двух предельных случаях:

1. В известном случае «почти свободных электронов» $u_k(r) = \text{const.}$ и, следовательно, $G = 0$. В этом случае рассеяния поляронов акустическими колебаниями вообще нет.

2. В случае «сильно связанных электронов» можно, как известно, оперировать с ψ-функциями изолированных атомов. Если для грубой оценки предположить, что в каждом атоме электрон проводимости находится в кулоновском поле, то согласно теореме вириала средняя кинетическая энергия электрона равна потенциалу ионизации атома. В ионном кристалле ψ-функция электрона проводимости значительна главным образом вблизи положительных ионов. Следовательно, G по порядку величины равен потенциалу ионизации элемента, образующего положительные ионы кристалла. Для щёлочно-галоидных кристаллов, например, $G \sim 4 - 5$ эл.-в.
   Ю. Е. Перлиным была произведена сравнительная оценка вероятности рассеяния поляронов оптическими и акустическими колебаниями ионов. Оказалось, что при комнатной температуре у всех кристаллов (для которых выполняются кри-

терии теории) главную роль играет рассеяние оптическими колебаниями. Однако вероятность рассеяния оптическими колебаниями пропорциональна

$$\bar{n} = \frac{1}{e^{\frac{n\omega}{kT}} - 1},$$

а вероятность рассеяния акустическими колебаниями пропорциональна

$$\bar{N}_q = \frac{1}{e^{\frac{n\omega_q}{kT}} - 1}.$$

Поскольку $\omega > \omega_q$, при понижении температуры $\bar{n}$ убывает быстрее, чем $\bar{N}_q$, и в конце концов сравнительно большую роль в рассеянии начинают играть акустические колебания. Однако у большинства кристаллов это наступает при столь низких температурах, когда оба механизма рассеяния уже не существенны, ибо подвижность полярона определяется уже «остаточным» сопротивлением, рассмотренным в § 11.

До сих пор игнорировался член $V'_{\text{оп}}(r)$ в формуле (18.1). Он приводит к добавочному рассеянию поляронов оптическими колебаниями ионов. Этот эффект следовало бы рассмотреть совместно с одноквантовым рассеянием в § 17; матричные элементы переходов надо было бы вычислять для суммы возмущений $\mathrm{H}' + V'_{\text{оп}}$. Однако легко убедиться в том, что это добавочное рассеяние сравнительно мало. При попытке его рассмотрения главная трудность заключается в том, что в случае оптических колебаний ионов возмущение микропотенциала $W(\boldsymbol{r})$ имеет сложный вид и не может быть представлено простой формулой (18.3). Но для оценки порядка величин всё же можно воспользоваться (18.3), подставляя вместо u смещение ближайшего к электрону иона (связанное с его оптическими колебаниями). В результате такого вычисления получается матричный элемент, напоминающий (18.24), но в нём вместо $\boldsymbol{q}$ стоит $\boldsymbol{x}$, вместо $\omega_{\boldsymbol{q}} - \omega$, вместо $N_{\boldsymbol{q}} - n_{\boldsymbol{x}}$. Этот матричный элемент оказывается всегда значительно меньшим, чем $H'_{k,\ldots}, n_{\varkappa'}k', \ldots, n_{\varkappa^{\pm 1}}$, и его можно опустить.

10.3.8 § 19. Application of statistics in case of thermal equilibrium

Согласно общеизвестному закону канонического распределения вероятность состояния с квантовыми числами $k, \ldots, n_x, \ldots$ равна

$$P\left(k, \ldots, n_x, \ldots\right) = Ae^{-\frac{H_k, \ldots, n_x, \ldots}{kT}}. \tag{19.1}$$

Здесь A - нормировочный коэффициент, не зависящий от квантовых чисел состояния, k - постоянная Больцмана

$$H_{k,\ldots,n_{x'}\ldots} = J\left[\psi_0\right] + \sum_x{}' \hbar\omega_x \left(n_x + \frac{1}{2}\right) + \frac{\hbar^2 k^2}{2M}. \tag{19.2}$$

Коэффициент A легко определяется из условия нормировки:

$$\sum_{k,\ldots,n_{x'},\ldots} P\left(k, \ldots, n_k, \ldots\right) = 1 \tag{19.3}$$

Подставляя сюда выражения (19.1-2), учитывая, что концентрация фазовых точек в k-пространстве равна $\left(\frac{L}{2\pi}\right)^3$ и проводя интегрирование по $\boldsymbol{k}$ и суммирование по n_x, находим:

$$A = \frac{1}{L^3}\left(\frac{2\pi\hbar^2}{M\mathrm{k}T}\right)^{3/2} e^{\frac{J[\psi_{\mathrm{L}}]+\sum_\chi' \frac{n\omega_\chi}{2}}{\mathrm{k}T}} \prod_\chi \left(1 - e^{-\frac{\hbar\omega_\chi}{\mathrm{k}T}}\right). \tag{19.4}$$

Вероятность состояния с данным значением k, но произвольными значениями n_α можно получить путём суммирования выражения (19.1) по всем возможным значениям n_x:

$$P(k) = \sum_{\ldots,n_{\varkappa'}\ldots} P\left(k, \ldots, n_{\varkappa'}, \ldots\right) = \frac{1}{L^3}\left(\frac{2\pi\hbar^2}{MkT}\right)^{a'} e^{-\frac{n^2k^2}{2MkT}} \cdot (\tag{19.5}$$

Таким образом, в случае теплового равновесия по отношению к поляронам справедливо максвелловское распределение по скоростям.

Вероятность состояния с данным значением n_x, но произвольными значениями остальных квантовых чисел получается

путём суммирования (19.1) по всем квантовым числам, за исключением n_x:

$$P\left(n_x\right) = \left(1 - e^{-\frac{\hbar\omega_x}{kT}}\right) e^{-\frac{\hbar\omega_x}{kT}}. \tag{19.6}$$

Отсюда непосредственно получается выражение для среднего значения $\bar{n}_x$, которым мы пользовались в §§ 16 – 18:

$$\bar{n}_x = \sum_{n_x=0}^{\infty} n_x P\left(n_x\right) = \frac{1}{e^{\frac{\hbar\omega_x}{\mathrm{k}T}} - 1}. \tag{19.7}$$

Перейдём теперь к вычислению равновесной концентрации электронов проводимости (поляронов) и «дырок», появляющихся в кристалле в результате теплового возбуждения. Следует различать два вида возбуждений диэлектрика: 1) возбуждения, в результате которых появляются носители тока, т. е. электронные и «дырочные» поляроны, и 2) возбуждения, в результате которых образуются так называемые экситоны, рассмотренные впервые Я. И. Френкелем [9], а затем Р. Пайерлсом [9], Ф. Моттом [25], А. С. Давыдовым [26] и др. Экситоны не являются носителями тока.

Предположим, что концентрация электронов проводимости дырок и экситонов настолько мала, что можно пренебречь взаимодействием между ними. В этом случае

можно говорить об энергии, необходимой для образования в кристалле электрона проводимости и дырки, причём эта энергия не зависит от количества уже имевшихся в кристалле носителей тока и экситонов. Выберем начало отсчёта энергии таким образом, чтобы энергия системы равнялась нулю, когда кристалл находится в основном состоянии, т. е. когда отсутствуют электроны проводимости, дырки и экситоны, а ионы совершают только нулевые колебания. Пусть совокупность экситонов, имеющихся в кристалле, характеризуется многомерным квантовым числом m, а суммарная энергия этих экситонов равна W_m (явное выражение W_m в дальнейшем не понадобится). Представим далее энергию, необходимую для образования электрона проводимости и дырки, в виде

$$W + \frac{\hbar^2 \boldsymbol{k}^2}{2M} + \frac{\hbar^2 \boldsymbol{k}^2}{2M'} \tag{19.8}$$

Предполагается, что как электрон проводимости, так и дырка находятся в поляронном состоянии; W есть энергия, необходимая для образования неподвижных, но достаточно удалённых друг от друга электронного и дырочного поляронов; k, M и k', M' суть волновые векторы и эффективные массы соответственно электронного и дырочного поляронов.

Энергия возбуждённого кристалла равна $H\left(\ldots, n_x, \ldots, m, N, \ldots, \boldsymbol{k}_i, \ldots, \boldsymbol{k}'_j, \ldots\right) =$

$$= \sum_{x}^{\pi''\cdots'} \hbar\omega_x n_x + W_m + NW + \sum_{i=1}^{N} \left(\frac{\hbar^2 k_i^2}{2M} + \frac{\hbar^2 k_i'^2}{2M'} \right). \tag{19.9}$$

Здесь первый член представляет собой энергию колебаний ионов; сумма имеет $2N$ штрихов, так как при появлении каждого электронного или дырочного полярона система приобретает три трансляционные степени свободы (ξ_1, ξ_2 и ξ_3) и утрачивает три колебательные степени свободы (см. § 16). Второй член в (19.9) представляет собой энергию экситонов, N - число электронов проводимости, а также число дырок. Третий и четвёртый члены формулы (19.9) представляют собой энергию, которую необходимо затратить для образования в кристалле электронных и дырочных поляронов. N является одним из квантовых чисел системы.

Согласно закону канонического распределения вероятность состояния с квантовыми числами $\ldots, n_x, \ldots, m, N, \ldots\ldots, \boldsymbol{k}_i, \ldots, \boldsymbol{k}_j, \ldots$ равна

$$P\left(\ldots, n_x, \ldots, m, N, k_i, \ldots, k'_j, \ldots\right) = \\ = A_1 e^{-\frac{H\left(\ldots, n_{x'}, \ldots, m, N, k_i \cdots, k'_j, \ldots\right)}{kT}}. \tag{19.10}$$

Нас будет интересовать вероятность определённого значения N при любых произвольных значениях прочих квантовых чисел. Эта вероятность получается путём суммирования вероятности (19.10) по всевозможным состояниям системы с дан-

$$P(N) = \frac{A_1 \left(gg'\right)^N}{(N!)^2} \sum_{\ldots, n_{x'} \ldots, m, n_{i'} \ldots, k'_j \ldots} e^{-\frac{H\left(\ldots, n_{x'} \ldots, m, N, k_i, \ldots, k'_j\right)}{\mathrm{k}T}}.$$

Здесь учтено, что, помимо квантовых чисел $n_\varkappa, m, N, \boldsymbol{k}_i, \boldsymbol{k}'_j$, входящих в выражение энергии, состояние характеризуется ещё спиновыми квантовыми числами N электронов и N дырок, от которых энергия не зависит. Если g и g' обозначают число возможных значений спина соответственно электрона и дырки ($g = g' = 2$), то кратность спинового вырождения равна $\left(gg'\right)^N$. Далее следует учесть, что в формуле (19.11) слагаемые, отличающиеся друг от друга простой перестановкой $\boldsymbol{k}_i$ или $\boldsymbol{k}'_j$. соответствуют не

разным, а одному и тому же квантовому состоянию системы (все электронные поляроны тождественны и все дырочные поляроны тождественны). Так как число перестановок волновых векторов $\boldsymbol{k}_i$ равно $N\,!$ и число перестановок $\boldsymbol{k}'_j$ равно тоже $N\,!$, то, следовательно, каждому квантовому состоянию системы соответствует $(\,N\,!)^{\,2}$ одинаковых слагаемых в сумме (19.11). Поэтому для получения правильного результата эту сумму нужно разделить на $(\,N\,!)^{\,2}$.

Переходя к вычислению суммы в формуле (19.11), введём следующие обозначения: сумма состояний колебаний ионов

$$\sum_{\ldots,n_{x'}\ldots} e^{-\frac{\sum_x^{N'''\ldots} n_{\omega_x n_x}^{2N}}{kT}} = \tag{19.12}$$

$$= \prod_x^{\overbrace{N'''}^{2N}} \frac{1}{1-e^{-\frac{n\omega_x}{kT}}} \cong Z_{\text{ион}}\,(T)\left(1-e^{-\frac{n_{0w}}{kT}}\right)^{6N}.$$

Здесь $Z_{\text{нон}}$ - сумма состояний колебаний ионов кристалла в отсутствии носителей тока; она зависит от температуры, но не зависит от квантовых чисел системы. Сумма состояний экситонов

$$\sum_m e^{-\frac{W_m}{\mathrm{kT}}} = Z_{\text{экс}}\,(T). \tag{19.13}$$

Далее

$$\sum_{k_i} e^{-\frac{\hbar^2 k_i^2}{2M\mathrm{k}T}} = \left(\frac{L}{2\pi}\right)^3 \int_0^\infty e^{-\frac{n^2 k_i^2}{2M\mathrm{k}T}} \cdot 4\pi k_i^2 dk_i = L^3\left(\frac{M\mathrm{k}T}{2\pi\hbar^2}\right)^{3/2}. \tag{19.14}$$

Используя формулы (19.12-14), можно формулу (19.11) представить в виде

$$P(N) = \frac{A_1 Z_{\text{нон}}\cdot Z_{\text{эко}}}{(N!)^2}\left[L^6 gg'\left(\frac{\sqrt{MM}\mathrm{k}T}{2\imath\hbar^2}\right)^3 \times\right.$$

$$\left.\times\left(1-e^{-\frac{\hbar\omega}{\mathrm{kT}}}\right)^6 e^{-\frac{W}{\mathrm{kT}}}\right]^N. \tag{19.15}$$

Чтобы определить наиболее вероятное число носителей тока N, следует найти максимум $P(N)$ (удобнее искать максимум логарифма этой функции). $P(N)$ имеет максимум при

$$N = L^3\sqrt{gg'}\left(\frac{\sqrt{MM'}\mathrm{k}T}{2\pi\hbar^2}\right)^{3/2}\left(1-e^{-\frac{\hbar\omega}{\mathrm{k}T}}\right)^3 e^{-\frac{W}{2\mathrm{k}T}}. \tag{19.16}$$

Эта формула отличается от соответствующей формулы зонной теории полупроводников, во-первых, тем, что здесь фигурируют эффективные массы электронного и дырочного поляронов, тогда как в старой теории фигурируют эффективные массы зонного электрона и зонной дырки; первые могут быть во много раз больше вторых. Таким образом, количественно формула (19.16) может существенно отличаться от аналогичной формулы старой теории. Во-вторых, формула (19.16) имеет множитель $\left(1-e^{-\frac{\hbar\omega}{\mathrm{kT}}}\right)^{\mathbf{s}}$, которого нет в старой формуле. Этот множитель появился в

результате учёта сокращения колебательных степеней свободы системы на шесть с появлением каждой пары носителей тока (см. § 16).

Случай, когда в кристалл введена примесь (донор или акцептор) и носители тока возникают в результате ионизации этой примеси, будет рассмотрен в главе V.

10.3.9 § 20. Mobility of Polarons

Как было показано в предыдущем параграфе, в случае теплового равновесия имеет место максвелловское распределение групповых скоростей поляронов. Если в кристалле создать небольшое однородное электрическое поле, то среднее значение скорости поляронов в направлении поля, а также

плотность электрического тока оказываются пропорциональными полю:

$$\vec{v} = uE, \tag{20.1}$$

где $\bar{v}$ - среднее значение скорости поляронов, $\boldsymbol{E}$ - напряжение электрического поля. Коэффициент пропорциональности u называется подвижностью.

В присутствии электрического поля, направленного параллельно оси Ox, функция распределения скоростей поляронов $f(\boldsymbol{v})$[1]) определяется из обычного кинетического уравнения

$$\frac{\partial f}{\partial t} + \frac{eE}{M}\frac{\partial f}{\partial v_{xx}} + (a-b)f = 0. \tag{20.2}$$

Член $(a-b)f$ представляет собой изменение за секунду функции распределения вследствие рассеяния поляронов колебаниями ионов. Вид этого члена существенно упрощается, если предположить, что при «столкновении» полярона его кинетическая энергия $\mathscr{E}$ изменяется относительно мало, а направление движения может измениться значительно. В этом случае, если положить, как это обычно делают,

$$\left.\begin{array}{c} f = f_0(\mathscr{E}) + f_1(\mathscr{E})\cos\beta; \\ f_1 \ll f_0; \quad \mathfrak{G} = \frac{Mv^2}{2} \end{array}\right\} \tag{20.3}$$

(β - угол между v и осью Ox), то получается следующий общеизвестный результат: за единицу времени из единичного объёма пространства скоростей уходит благодаря столкновениям поляронов

$$\begin{aligned} af &= \int f(\vartheta)W(\mathscr{E},\vartheta)dQ = \\ &= f_0(\mathscr{G})\int W(\mathscr{G},\vartheta)dQ + f_1(\mathscr{G})\cos\beta\int W(\mathscr{E},\vartheta)dQ. \end{aligned} \tag{20.4}$$

Здесь $W(\mathscr{E},\vartheta)dQ$ - вероятность рассеяния полярона (за единицу времени) в элемент сферического угла dQ с отклонением на угол ? от первоначального направления движения.

В вышеупомянутый единичный объём за единицу времени попадает поляронов

$$bf = f_0(\mathscr{E})\int W(\mathscr{E},\vartheta)d\mathbb{Q}' + f_1(\mathscr{E})\int W(\mathscr{E},\vartheta)\cos\beta' d\mathbb{Q}' \tag{20.5}$$

причём углы ϑ и β' показаны на рис. 20.1

[8 1]) $f(v)dv_xdv_ydv_z$ есть число поляронов в единице объёма кристалла, у которых компоненты скорости лежат в соответствующих дифференциальных интервалах.

$$\cos\beta' = \cos\vartheta\cos\beta + \sin\vartheta\sin\beta\cos\varphi. \tag{20.6}$$

Второй интеграл в правой части формулы (20.5) упрощается, если направление v принять за полярную ось и положить

$$d\mathrm{Q} = \sin\vartheta d\vartheta d\varphi. \tag{20.7}$$

В результате вычисления получается:

$$(a-b)f = f_1(\mathscr{E})\cos\beta\cdot 2\pi\times$$

$$\times\int_0^\pi W(\mathscr{B},\vartheta)(1-\cos\vartheta)\sin\vartheta d\vartheta. \tag{20.8}$$

Традиционное выражение «члена столкновений», возникшее ещё в классической электронной теории проводимости, имеет вид

$$(a-b)f = \frac{v}{l}f_1(\hat{b})\cos\beta, \tag{20.9}$$

где l - «свободный пробег» но-

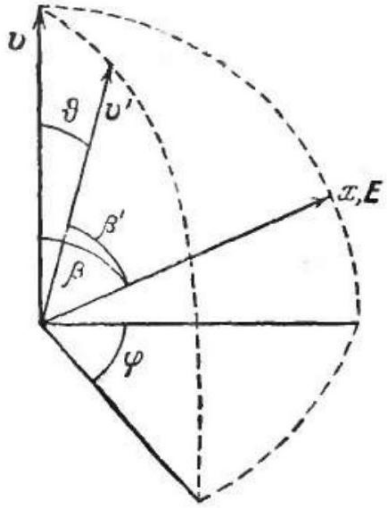

Рис. 20.1.

сителя тока.

Сопоставление формул (20.8) и (20.9) приводит к следующему определению свободного пробега l (&):

$$\frac{v}{l(\mathscr{B})} = 2\pi\int_0^\pi W(\mathscr{B},\vartheta)(1-\cos\vartheta)\sin\vartheta d\vartheta. \tag{20.10}$$

Отношение

$$\tau = \frac{l(\dot{\&})}{v} \tag{20.11}$$

мы будем условно называть средним временем свободного пробега.

Кинетическое уравнение (20.2) решается методом последовательных приближений; его решение раскладывается по степеням малого параметра $\boldsymbol{E}$. В нулевом приближении,

когда $\boldsymbol{E} = 0$, решение уравнения (20.2) сводится к члену f_0 (8), который согласно § 19 представляет собой максвелловскую функцию распределения скоростей. При включении поля $\boldsymbol{E}$ в функции распределения появляется член первого порядка $f_1(\&)\cos\beta$.

Если подставить (20.3) в (20.2) и учесть, что для максвелловской функции распределения

$$\frac{\partial f_0}{\partial v_x} = \frac{\partial f_0}{\partial \underset{\theta}{b}} Mv\cos\beta, \tag{20.12}$$

то получится:

$$f_1(\mathscr{B}) = -eEl(\mathscr{B})\frac{\partial f_0}{\partial \mathscr{G}}. \tag{20.13}$$

Средняя скорость полярона равна

$$\begin{aligned}\bar{v}_x &= \frac{1}{N}\int v_x f(v) v^2 dv dQ = \frac{4\pi}{3N}\int_0^\infty f_1(\mathfrak{B}) v^3 dv = \\ &= -\frac{4\pi eE}{3N}\int_0^\infty l(\mathscr{E})\frac{\partial f_0}{\partial \mathscr{B}} v^3 dv\end{aligned} \tag{20.14}$$

Здесь N-концентрация поляронов в кристалле. Таким образом, подвижность равна

$$u = \frac{\bar{v}_x}{E} = -\frac{4\pi e}{3N}\int_0^\infty l(\mathfrak{b})\frac{\partial f_0}{\partial \dot{c}_{\mathfrak{b}}} v^3 dv. \tag{20.15}$$

Сюда следует подставить максвелловскую функцию распределения в виде

$$f_0(\mathscr{E}) = N\left(\frac{M}{2\pi \mathrm{k}T}\right)^{2/2} e^{-\frac{\delta}{\mathrm{k}T}}. \tag{20.16}$$

Если известна вероятность рассеяния $W(\ \&,\ 0)$, то можно по формуле (20.10) вычислить $l(\ )$, а затем по (20.15) определить u.

В качестве примера рассмотрим случай, когда вероятность рассеяния не зависит ни от угла рассеяния, ни от энергии

полярона ($W\ (\&,\ \vartheta\ ) = W = \mathrm{const.}$). В этом случае согласно формулам (20.10-11) τ тоже постоянно:

$$\tau = \frac{1}{4\pi W}, \tag{20.17}$$

$$l = \tau v. \tag{20.18}$$

Іодставляя (20.16) и (20.18) в формулу (20.15) и осуществляя интегрирование, получаем:

$$u = \frac{e}{M}\tau. \tag{20.19}$$

Этот же результат может быть получен другим путём, без использования кинетического уравнения и предположения (20.3). Полярон движется почти прямолинейно во время своего свободного пробега; при столкновении с колебаниями ионов он скачкообразно меняет направление своего движения. Таким образом, его траектория представляет собой ломаную линию. Проследим за движением какого-либо полярона в течение достаточно большого промежутка времени, когда он совершает n

свободных пробегов ($n \gg 1$). Пусть $t_i (i = 1, 2, \ldots, n$) суть моменты времени, когда полярон терпит столкновения; время i-го пробега равно

$$\tau_i = t_i - t_{i-1}. \tag{20.20}$$

Если v_i есть скорость полярона в самом начале i-го свободного пробега, то

$$\bar{v} = \frac{1}{t_n} \int_0^{t_n} v(t) dt = \frac{1}{t_n} \sum_{i=1}^{n} \int_{t_{i-1}}^{t_i} \left| v_i + \frac{eE}{M} (t - t_{i-1}) \right| dt =$$
$$= \frac{1}{t_n} \sum_{i=1}^{n} \left[v_i \tau_i + \frac{eE}{M} \frac{\tau_i^2}{2} \right] \tag{20.21}$$

В том случае, когда вероятность рассеяния не зависит от угла рассеяния и от скорости полярона, все направления v_i равновероятны, а также нет никакой корреляции между $\boldsymbol{v}_i$ и τ_i. При этом

$$\lim_{n \to \infty} \frac{1}{t_n} \sum_{i=1}^{n} v_i \tau_i = 0 \tag{20.22}$$

Вводя для среднего времени пробега обозначение

$$\bar{\tau} = \frac{1}{n} \sum_{i=1}^{n} \tau_i = \frac{t_n}{n} \tag{20.23}$$

и для среднего квадрата времени пробега обозначение

$$\overline{\tau^2} = \frac{1}{n} \sum_{i=1}^{n} \tau_i^2, < \tag{20.24}$$

можно формулу (20.21) переписать в виде

$$\bar{v} = \frac{eE}{M} \frac{\overline{\tau^2}}{2\tau}.$$

Следовательно, подвижность полярона равна

$$u = \frac{e\overline{\tau^2}}{M \frac{1}{2\tau}} \tag{20.25}$$

Вероятность того, что время пробега окажется в пределах от t до $t + dt$, даётся хорошо известной формулой

$$W(t) dt = e^{-\frac{t}{\tau}} \frac{dt}{\tau}$$

Опираясь на эту формулу, легко показать, что

$$\overline{\tau^2} = 2\bar{\tau}^2, \quad \bar{\tau} = \tau \tag{20.26}$$

Подставляя это соотношение (20.25), получаем:

$$u = \frac{e}{M} \bar{\tau}, \tag{20.27}$$

что точно совпадает с (20.19).

Оба приведённых выше вывода формулы для подвижности существенно опираются на

представление о свободном пробеге полярона. Иными словами, предполагается, что столкиовения происходят сравнительно редко, а между столкновениями носитель тока консервативно движется во внешнем поле. Согласно соотношению неопределённостей квантовой механики, если время свободного пробега τ, то в энергии

полярона появляется неопределённость порядка

$$\Delta\dot{G} \sim \frac{\hbar}{\tau}. \tag{20.28}$$

Понятием свободного пробега и функцией распределения скоростей $f(v)$ можно пользоваться только в том случае, если Δ э значительно меньше средней кинетической энергии полярона $\left(\frac{3}{2}kT\right)$:

$$\frac{\hbar}{\tau} \ll \mathrm{k}T. \tag{20.29}$$

Это же условие должно соблюдаться для того, чтобы было законно рассмотрение рассеяния методом возмущений в §§ 17 и 18. Если ч выразить через u из (20.19) и подставить в условие (20.29), то последнее приобретает следующий вид:

$$\frac{e\hbar}{Mu} \ll \mathrm{k}T. \tag{20.30}$$

Все полученные выше формулы этого параграфа могут быть использованы как старой зонной теорией электропроводности, так и поляронной теорией. Разница заключается лишь в том, что в старой теории под массой носителя тока M следует понимать эффективную массу электрона μ, которая по порядку величины равна массе свободного электрона m. В поляронной же теории электропроводности под M следует понимать эффективную массу полярона; последняя определяется формулой (10.35) и может значительно (иногда в сотни раз) превышать массу свободного электрона. Поэтому для данного значения подвижности неравенство (20.30) будет в поляронной теории соблюдаться значительно лучше, чем в старой теории.

Оказывается, что это неравенство имеет место далеко не всегда. Если, например, задаться подвижностью $u = 50^2/\cdot$ (подвижности такого порядка наблюдаются экспериментально у многих полупроводников с ионной решёткой) и если положить массу носителя тока равной $M = m$, то левая часть критерия (20.30) равна 0,023 эл.-в, а $\mathrm{k}T$ при комнатной температуре равно 0,025 эл.-в. При достаточно низких температурах неравенство (20.30) должно непременно выполняться,

так как подвижность при охлаждении кристалла быстро растёт по закону

$$u = u_0\left(e^{\frac{\hbar\omega}{kT}} - 1\right). \tag{20.31}$$

Обоснование этого закона будет дано ниже.

Вернёмся теперь к вычислению подвижности полярона. Одновременный учёт одноквантового и двухквантового рассеяния полярона оптическими колебаниями и рассеяния акустическими колебаниями приводит к слишком сложному выражению для подвижности. Поэтому рассмотрим три упомянутых механизма рассеяния порознь в надежде на то, что в большинстве случаев какой-нибудь из них окажется доминирующим и остальные два можно будет игнорировать.

а) Учёт одноквантового рассеяния оптическими колебаниями

1. Низкие температуры [22], когда

$$cT \ll \hbar\omega. \tag{20.32}$$

В этом случае для подавляющего большинства поляронов выполняется неравенство (17.21) и справедлива формула (17.22). Вероятность рассеяния не зависит ни от угла рассеяния, ни от энергии полярона.

Выше при решении кинетического уравнения предполагалось, что при «столкновении» энергия полярона изменяется незначительно. Однако в случае (20.32) после поглощения кванта колебаний $\hbar\omega$ кинетическая энергия полярона возрастает во много раз. Эту трудность можно устранить, если условиться под кинетическим «столкновением» понимать двойной переход: упомянутое поглощение кванта и немедленно за ним следующее излучение кванта $\hbar\omega$, после которого кинетическая энергия полярона почти равна исходному значению (с точностью, с которой можно считать поглощённый и излучённый кванты энергии одинаковыми, пренебрегая дисперсией поляризационных волн). Приэтом следует иметь в виду, что согласно формуле (17.18) вероятность поглощения кванта пропорциональна $\bar{n}$, а вероятность излучения кванта - $(\bar{n}+1)$. Так как по (20.32) $\bar{n} \ll 1$, то вторая вероятность гораздо больше первой. Поэтому можно

пренебречь сравнительно малым временем, которое полярон проводит в быстром движении, и считать, что он немедленно излучает квант и возвращается к исходной энергии. Вероятность такого двойного «столкновения» сводится к вероятности менее вероятного из двух переходов, т. е. к вероятности поглощения кванта. Поскольку первый из двух переходов приводит к изотропному рассеянию полярона, то и всё двойное «столкновение» должно изотропно рассеивать полярон (равновероятно во всех направлениях).

В этом случае подвижность выражается формулой (20.19). Среднее время свободного пробега равно

$$\tau = \frac{1}{4\pi W'_{kkk'}}, \tag{20.33}$$

где $W'_{kk'}$ даётся формулами (17.22) и (17.24). В результате для подвижности полярона получается формула

$$u' = u'_0 \left(e^{\frac{\hbar\omega}{kT}} - 1\right), \tag{20.34}$$

где

$$u'_0 = \frac{\hbar^{3/2}}{M^{3/2}ce\sqrt{2\omega}} \frac{(1+x)^8}{\left(1+\frac{1}{7}x\right)^2}, \quad x = 0,0116\frac{\mu e^4 c^2}{\hbar^3\omega} \tag{20.35}$$

Если сюда подставить значение M из формулы (10.35), то получается:

$$u'_0 = 5,8\cdot 10^{-38} \frac{\omega^{5/2}(1+x)^8}{\left(\frac{\mu}{m}\right)^{1/2} c^7 \left(1+\frac{1}{7}x\right)^2} \text{ CGSE}. \tag{20.36}$$

Здесь ω в единицах сек. $^{-1}$

2) Высокие температуры, при которых удовлетворяется неравенство

$$\mathrm{k}T \gg \hbar\omega. \tag{20.37}$$

В этом случае для подавляющего большинства поляронов выполняется неравенство (17.25) и справедливы формулы (17.29) и (17.27). При высоких температурах $\bar{n} \cong \frac{\mathrm{k}T}{\hbar\omega} \gg 1$. Поэтому согласно формуле (17.29) вероятность рассеяния

на угол ϑ с поглощением кванта $\hbar\omega$ и с излучением кванта $\hbar\omega$ приблизительно одинакова. Суммарная вероятность рассеяния полярона с кинетической энергией & на угол ϑ равна

$$W'(\mathscr{E},\vartheta)2\pi\sin\vartheta d\vartheta = 43,1\frac{\alpha_3\Theta}{k}\frac{\left(1+\frac{1}{7}x\right)^2 xdx}{(1+x)^8}\cdot 2\bar{n}. \tag{20.38}$$

Вычисление свободного пробега по формулам (20.10), и (17.27) даёт:

$$\frac{1}{l} = 172,4\frac{a_3^8\omega\bar{n}}{vk^3}\int_0^{k^2/\alpha_3^2}\frac{\left(1+\frac{1}{7}x\right)^2 x^2dx}{(1+x)^8} \tag{20.39}$$

Предположим, что при высоких температурах у большинства поляронов k^2/α_3^2 порядка единицы или больше. Тогда в формуле (20.39) можно верхний предел интегрирования заменить бесконечностью

$$\int_0^\infty\frac{\left(1+\frac{1}{7}x\right)^2 x^2dx}{(1+x)^8} = 0,01174. \tag{20.40}$$

Выражая v и k через кинетическую энергию полярона & и принимая во внимание соотношения (10.35) и (20.40), можно формулу (20.39) переписать в следующем виде:

$$l(\mathscr{E}) = 0,0916\frac{e^2c}{\mathrm{k}T}\left(\frac{\mathscr{E}}{\hbar\omega}\right)^2. \tag{20.41}$$

Подвижность вычисляется по формуле (20.15), в которую следует подставить выражения (20.41) и (20.16). В результате вычисления получается:

$$u' = 0,733\frac{e^3c}{(\hbar\omega)^2}\sqrt{\frac{\overline{kT}^1}{2\pi M}}. \tag{20.42}$$

б) Учёт двухквантового рассеяния оптическими колебаниями

Рассмотрим рассеяние с излучением и поглощением одного кванта колебаний. В этом случае при рассеянии кинетическая энергия полярона остаётся почти неизменной, как это и требовалось при решении кинетического уравнения. Вероятность рассеяния определяется формулами (17.33 – 35). Изменение волнового вектора связано с углом рассеяния соотношением

$$1-\cos\vartheta = \frac{(k'-k)^3}{2k^2} = \frac{2\alpha_3^2a^2}{k^2} \tag{20.43}$$

$$\sin\vartheta d\vartheta = \frac{4\alpha_8^2}{k^2}ada \tag{20.44}$$

Согласно формуле (20.10) свободный пробег полярона в этом случае равен

$$\frac{1}{l(\mathscr{G})} = 47\left(\frac{\hbar\omega}{\mathscr{G}}\right)^2\alpha_3(\bar{n}+1)\bar{n}\int_0^{\frac{k}{x_\mathrm{S}}} I(a)a^3da \tag{20.45}$$

$I(a)$ имеет максимальное значение при $a = 0$ и быстро убывает к нулю, когда a превышает значение $\frac{1}{2}$. Поэтому, если

[81]) Эта формула отличается от ошибочной формулы опубликованной в статье [22].

$$\frac{k}{\alpha_3} > \frac{1}{2}, \tag{20.46}$$

можно верхний предел интеграла в формуле (20.45) заменить бесконечностью. При этом получается:

$$\int_0^\infty I(a)a^3 da \cong 0,00118 \tag{20.47}$$

$$l(\mathscr{G}) = \left(\frac{\mathscr{E}}{\hbar_\omega}\right)^2 \frac{18}{\alpha_3(n+1)n} \tag{20.48}$$

Вычисление подвижности по формулам (20.15-16) и подстановка выражения (6.17) для α_8 дают:

$$u'' = \frac{288(\mathrm{k}T)^{3/2}}{(2\pi M)^{1/2}\omega^2 \mu ec(\bar{n}+1)\bar{n}} \tag{20.49}$$

Подвижности, полученные в результате учёта одноквантового и двухквантового рассеяния, обозначаются соответственно u' и u''.

1. Случай низких температур

$$\mathrm{k}T \ll \hbar\omega. \tag{20.50}$$

При выполнении этого условия, подставляя в формулу (20.49) планковское выражение для $\bar{n}$, получаем:

$$\frac{1}{(\bar{n}+1)_{\bar{n}}} = e^{\frac{\hbar\omega}{\mathbf{k}T}} - 2 + \ldots \tag{20.51}$$

и

$$u'' = \frac{288(\mathrm{k}T)^{3/2}\left(e^{\frac{\hbar\omega}{\mathrm{K}T}} - 2 + \ldots\right)}{(2\pi M)^{1,\omega^2}\omega^2 \mu ec}. \tag{20.52}$$

Следует иметь в виду, что при весьма низких температурах для большинства поляронов может оказаться нарушенным неравенство (20.46). В этом случае замена верхнего предела интеграла формулы (20.45) бесконечностью приводит к заниженному значению свободного пробега, и следовательно, формула (20.52) даёт заниженное значение подвижности. Однако в случае низких температур подвижность u'', связанная с учётом двухквантового рассеяния, оказывается значительно больше подвижности u', полученной при учёте рассеяния одноквантового. Таким образом, двухквантовое рассеяние играет лишь второстепенную роль в торможении поляронов. Их подвижность определяется одноквантовым рассеянием и выражается формулами (20.34) и (20.36).

Выше было рассмотрено только такое двухквантовое рассеяние, при котором один квант колебаний ионов поглощается, а другой рождается. Наряду с этим возможен и другой вид двухквантового рассеяния поляронов, при котором поглоцаются оба кванта колебаний. Сравнение формул (17.33) и (17.37) показывает, что рассеяние второго типа гораздо менее вероятно, чем первого. Действительно, в первом случае вероятность пропорциональна $\bar{n}(\bar{n}+1)$, а во втором $-\bar{n}^2$; при низких температурах $\bar{n}(\bar{n}+1) \gg \bar{n}^2$. Кроме того, изменение волнового вектора $|\boldsymbol{k}' - \boldsymbol{k}|$ и величина $\boldsymbol{a}$ во втором слуае больше, чем в первом, и следовательно, $I(a)$, наоборот, во втором случае

значительно меньше. Таким образом, дополнительный учёт второго типа двухквантового рассеяния почти не изменяет значения u''.

Двухквантовое рассеяние с рождением двух квантов колебаний ионов возможно только у поляронов с кинетической энергией, превышающей $2\hbar\omega$. При низких температурах таких быстрых поляронов в кристалле почти нет. Поэтому такой вид рассеяния не играет существенной роли в явлении электропроводности.
2) Случай высоких температур

$$\mathrm{k}T \gg \hbar\omega. \tag{20.53}$$

При этом

$$\bar{n} \cong \frac{\mathrm{k}T}{\hbar_\omega} \gg 1, \tag{20.54}$$

и формулу (20.49) можно представить в виде

$$u'' = \frac{288\hbar^2}{\mu ec(2\pi M\mathrm{k}T)^{1/2}} \tag{20.55}$$

Для выяснения удельной роли двухквантового рассеяния в торможении полярона удобно пользоваться формулой

$$\frac{u'}{u''} = 0,00255\left(\frac{\mathrm{k}T}{\hbar\omega}\right)\cdot\frac{\mu e^4c^2}{\hbar^3\omega}. \tag{20.56}$$

Эта формула показывает, что при высоких температурах возможны случаи, когда $\frac{u'}{u''}$ окажется больше единицы, т. е. когда главную роль в торможении поляронов будет играть двухквантовое рассеяние. Это может случиться у кристаллов, для которых хорошо выполняется неравенство, лежащее в основе адиабатического приближения (если исключить нереально высокие температуры). Однако и в таких кристаллах, как показывает исследование, даже при высоких температурах рассеяние с рождением и поглощением двух колебательных квантов играет сравнительно малую роль.

Необходимо отметить, что результаты теории сохраняют силу лишь при не слишком высоких температурах, при которых справедливо предположение (§ 16) о том, что поляризационная

потенциальная яма полярона мало отличается от её равновесной формы $V_0(r-\xi)$. Это имеет место до тех пор, пока подТаблица 20.1

$$\varepsilon = 5, n = 1,58, \mu = m, \omega = 5\cdot 10^{13} сек^{-1}$$
$$(\hbar\omega = 0,033 \ni \Omega. - \varepsilon), c = 0,2$$

	Низкие температуры $\mathrm{k}T = \frac{1}{3}\hbar\omega$	Высокие температуры $\mathrm{k}T =$
	$1,9\cdot 10^4$	$1,2\cdot 10^4$
	$32\cdot 10^4$	$4,8\cdot 10^4$
	63	40
u' абс. ед. u'' абс. ед. u'^2/ - u''^2/ -	1070	160

коренное выражение в правой части формулы (16.43) значительно меньше единицы. Чтобы лучше представить себе вели-

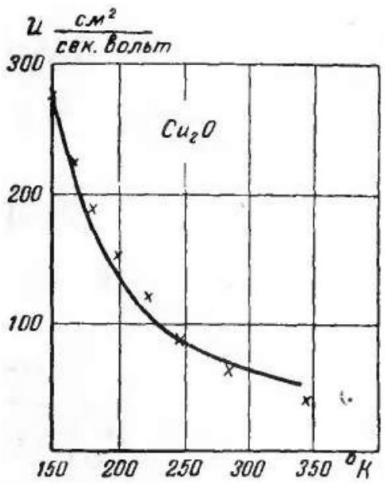

Рис. 20.2. - Кривая $u = 27\left(e^{363/T} - 1\right) \times -$ экспериментальные результаты Энгельгарда [54].

чины полученных выше подвижностей и их соотношение, рассмотрим численный пример, задавшись типичными средними значениями параметров кристалла (см. таблицу 20.1).

Из приведённой таблицы видно, что в рассмотренном примере как при низких, так и при высоких температурах $u' < u''$. Это значит, что подвижность поляронов определяется главным образом одноквантовым рассеянием. Однако при высоких температурах u' и u'' оказываются уже одного порядка.

Приведённые в таблице вычисленные значения подвижности поляронов по порядку величины совпадают с подвижностями носителей тока в полупроводниках, определёнными экспериментально по электропроводности и постоянной Холла.

Температурный ход подвижности при низких температурах даётся формулой (20.34), которая, повидимому, согласуется с опытом: на рис. 20.2 и 20.3 сплошные кривые соответствуют формуле (20.34), крестики - экспериментальным данным Энгельгарда для Cu_zO [54], а пунктир данным Дунаева и Маслаковца для PbS [65]. По температурному ходу подвижностей были определены частоты оптических колебаний ионов ω. У Cu_2O оказалось $\hbar\omega == 0,031$ эл.-в, а у PbS $\hbar\omega = 0,074$ эл.-в.

Точное численное сравнение с опытом коэффициента u_0', к сожалению, невозможно из-за неточного знания параметров c и μ в кристаллах Cu_2O и PbS . Формула (20.36) показывает,

$$u \frac{\text{см}^{\,2}}{\text{сек вольт}}$$

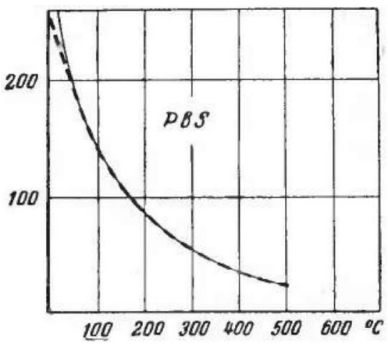

Рис. 20.3. - Кривая u = 14,7 ($e^{865/T}$ - 1), - - - экспериментальная кривая Дунаева и Маслаковца [65].

Гораздо более точно известны параметры теории в щёлоч-но-галоидных кристаллах (см. §§ 30 и 31). Вычисление подвижности по формулам (20.34) и (20.36), например для NaCl , при комнатной температуре приводит к значению $u' = 2,67^2/\cdot$. Эта подвижность оказывается больше, чем подвижность, обусловленная торможением полярона, рассмотренным в § 11 (см. формулу (11.17)). Таким образом, в NaCl одноквантовое рассеяние играет меньшую роль, чем вышеупомянутое торможение.

К сожалению, для щёлочно-галоидных кристаллов нет экспериментальных данных о подвижности носителей тока, так как не удалось измерить постоянную Холла. Попытки измерения эффекта Холла в окрашенных фотопроводящих щёлочно-галоидных кристаллах были сделаны Тартаковским [33] и Эвансом [20], но оказались безрезультатными вследствие исключительной малости эффекта. Эвансу удалось установить лишь верхний предел отношения поперечного (холловского) электрического поля к продольному. Отсюда можно установить верхний предел подвижности носителей тока, который для NaCl оказывается равным $8,3 \quad c^2/сек\cdot$. Таким образом, вычисленное значение подвижности не противоречит экспериментам Эванса. NaCl является кристаллом, в котором радиус полярона исключительно мал, что видно из таблицы 7.1. Рассмотренное в § 11 торможение полярона согласно формуле (11.15) обратно пропорционально кубу радиуса полярона; поэтому в NaCl это торможение особенно велико и может конкурировать с тепловым рассеянием поляронов даже при комнатной температуре. В большинстве же кристаллов это торможение меньше, чем в NACI. В этих кристаллах подвижность при комнатной температуре определяется рассеянием поляронов тепловыми поляризационными колебаниями ионов. Однако с понижением температуры вероятность всех видов теплового рассеяния поляронов экспоненциально стремится к нулю. Следовательно, при достаточно низких температурах торможение поляронов, рассмотренное в § 11, становится господствующим; оно сохраняет ко-

нечную величину даже при температуре абсолютного нуля. Мы будем его условно называть остаточным сопротивлением.

Вернёмся теперь к вопросу об основных носителях тока в ионном кристалле с электронной проводимостью. В § 8 было показано, что «зонные» состояния в смысле старой теории, когда ψ-функция электрона представляет собой плоскую незатухающую модулированную волиу, а ионы колеблются вблизи несмещённых поляризацией положений равновесия (узлов решётки), не являются устойчивыми, энергетически выгодными состояниями системы. Приблизительно такие состояния реализуются, когда в кристалл влетают быстрые электроны, не успевающие поляризовать ионы. Поэтому зонные состояния представляют интерес при рассмотрении, например, рассеяния быстрых электронов в кристалле, а также при рассмотрении внешнего фотоэффекта и вторично-электронной эмиссии из полупроводников, где нас интересует судьба быстрых электронов, способных преодолеть потенциал выхода из полупроводника в вакуум.

В случае теплового равновесия, как было показано в § 11 , подавляющее большинство электронов проводимости должно находиться в поляронном состоянии. Упомянутые выше зонные состояния могут возникнуть лишь в результате редкой тепловой флуктуации. Поэтому зонные электроны могли бы играть роль в электропроводности только, если бы их подвижность была на много порядков больше подвижности поляронов. Однако в этом параграфе было показано, что подвижность поляронов по

[81]) Формулы для подвижности были получены в предположении, что элементарная ячейка кристалла состоит только из двух ионов и что продольные поляризационные колебания характеризуются только одной единственной предельной частотой ω. В кристалле Cu_2O это не так. Поэтому здесь формулы для подвижности не могут претендовать на точность. Совпадение наблюдающегося температурного хода подвижности с формулой (20.34) может иметь место,

[8]если одна из ветвей продольных поляризационных колебаний рассеивает поляроны гораздо интенсивнее, чем другая, а также если предельные частоты у обеих ветвей близки друг к другу.

порядку величины как раз совпадает с экспериментально измеренными подвижностями носителей тока в кристаллах. Предположение, что зонные электроны обладают подвижностью гораздо большего порядка, означало бы, что не они являются носителями тока. Предположение же, что у зонных электронов и у поляронов подвижности одного порядка, приводит опять-таки к заключению, что вследствие концентрационного превосходства главными носителями тока должны быть поляроны,

10.4 IV Theory of F-centers and F'-centers with Classical Approach to Motion of Ions

10.4.1 § 21. Crystal Staining

Окрашивание кристаллов было раньше всего и наиболее подробно экспериментально исследовано в щёлочно-галоидных кристаллах. Впервые обнаружили фотопроводимость окрашенной каменной соли Иоффе и Рентген [30].

Подробный обзор всех экспериментальных фактов, накопленных в течение многих лет, может составить материал для большой книги и, конечно, выходит за рамки настоящей монографии. Читатель найдёт его в соответствующей литературе [55, 33, 34, 35, 31]. Многие из этих фактов будут рассмотрены ниже, в порядке их теоретического объяснения. В этом же параграфе будут даны минимальные сведения, необходимые для понимания дальнейшего.

Явление окрашивания криЕталлов заключается в следующем: если в зону проводимости нагретого щёлочно-галоидного кристалла любым путём ввести электроны, то в кристалле появляется новая полоса поглощения света в той области частот, где первоначально кристалл был прозрачен. При этом кристалл приобретает окраску. При последующем охлаждении кристалла новая полоса поглощения и окраска долго сохраняются (годы). Методы окрашивания кристаллов делятся на две группы:
А. Электроны возбуждаются в зону проводимости путём облучения кристалла ультрафиолетовым светом, рентгеновскими лучами, α-, β - или γ-лучами.
Б. Электроны вводятся в кристалл извне. Достигается это, например, путём помещения кристалла между металли-

ческими электродами и пропускания тока; при этом электроны поступают в кристалл из остроконечного катода. Другой способ введения в кристалл электронов заключается в прогревании кристалла в парах щелочного металла (не обязательно того же, который входит в химическую формулу кристалла); при этом атомы щелочного пара поглощаются кристаллом, ионизируются и освобождают электроны, поступающие в зону проводимости.

Концентрация вводимых в кристалл электронов может быть доведена до $10^{18} - 10^{20}$ в c^3. Поэтому введение электронов немыслимо без нейтрализации возникающего при этом пространственного заряда (в противном случае создалось бы недопустимо большое электрическое поле, способное разорвать кристалл и, конечно, препятствующее введению электронов). Нейтрализация пространственного заряда становится возможной, поскольку кристалл нагрет и обладает электролитической электропроводностью: по мере того как в какой-нибудь элемент объёма кристалла приходят электроны, из него уходят отрицательные ионы галоида. Химический анализ окрашенных кристаллов, действительно, обнаруживает в них избыток щёлочи.

Роль нагревания кристалла состоит не только в том, чтобы обеспечить возможность нейтрализации пространственного заряда. Это видно из того, что нагревание необходимо и при окрашивании методами А , например при облучении рентгеновскими лучами, когда нейтральность кристалла совсем не нарушается. Опыт показывает, что при всех методах окрашивания скорость окрашивания и максимальная густота окраски экспоненциально

растут с температурой ($\sim e^{-a/T}$). Объяснение этому факту будет дано в следующем параграфе.

Окрашенные кристаллы при низких температурах являются диэлектриками. Это свидетельствует о том, что введённые в кристалл электроны закрепляются на локальных энергетических уровнях, расположенных ниже зоны поляронной проводимости. При нагревании окрашенный кристалл становится обычным полупроводником донаторного типа: часть электронов, закреплённых на локальных уровнях, в результате теплового возбуждения возвращается в зону проводимости. При этом наблюдается электропроводность, экспоненциально растущая с температурой ($\sim e^{-W/2kT}$). Измерение соответствующей

энергии тепловой диссоциации (W) показывает, что в окрашенных щёлочно-галоидных кристаллах локальные уровни отстоят от дна зоны проводимости приблизительно на 1-2 эл.-в.

Окраска кристалла и новая полоса поглощения света, очевидно, вызваны появлением электронов в упомянутых выше локальных состояниях. Эти состояния были названы F-иентрами. Спектр поглощения света F-центрами изображается колоколообразной кривой, представленной на рис. 21.1. (T = 20°C).

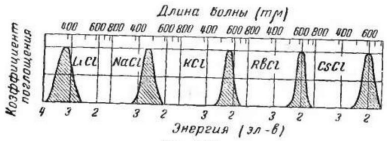

Рис. 21.1.

Поглощение света в F-полосе вызывает фотопроводимость кристалла. При окрашивании кристалла различными методами получаются F-центры с одинаковыми свойствами.

Если кристалл окрашен одним из методов группы А, т. е. если электроны перешли в зону проводимости вследствие облучения кристалла, то при этом в кристалле образуются «дырки» - покинутые электронами вакантные уровни. Такой кристалл постепенно обесцвечивается, по мере того как возбуждённые электроны рекомбинируют с дырками (возвращаюстя в основное состояние). Обесцвечивание можно существенно ускорить, нагревая или освещая кристалл, так как при этом активируются переходы электронов из F-центров в зону проводимости, где они могут свободно передвигаться но кристаллу и получают возможность рекомбинировать

Если кристалл окрашен одним из методов группы Б, т. е. электроны введены в кристалл извне, то упомянутых выше дырок нет, и рекомбинация невозможна. В этом случае окраска (F-центры) гораздо более устойчива. Для обесцвечивания необходимо удалить из кристалла электроны, а для этого нужно удалить из кристалла избыток ионов щёлочи -

компенсирующий пространственный заряд. Опыт показывает, что при прогревании кристалла, окрашенного методом Б, в вакууме кристалл обесцвечивается и вместе с тем на стенку вакуумной колбы садится щёлочь, испарённая кристаллом. Другой способ обесцвечивания заключается в том, чтобы соответствующей термической обработкой заставить избыток щёлочи коагулировать в коллоиды; электроны покидают F-центры и связываются с избыточными ионами щёлочи, образуя нейтральные атомы коллоидов. При этом F-полоса поглощения исчезает, а цвет кристалла изменяется-появляется коллоидная окраска, которая нас в дальнейшем не будет интересовать.

10.4.2 § 22. Critical review of existing hypotheses about the nature of F-centers

Согласно квантовой механике у электрона проводимости в строго идеальном кристалле существуют только такие состояния, в которых он может свободно двигаться во всём объёме кристалла. Следовательно, локальные состояния электрона могут появиться только вследствие нарушения периодичности кристалла. Настоящий параграф посвящён выяснению вопроса о том, что представляют собой те нарушения периодичности, вблизи которых локализуются электроны, образуя F-центры. Об этом разными авторами высказано много предположений. Однако почти все они в своём развитии сводятся к какому-нибудь из следующих четырёх основных предположений.

I. Л. Д. Ландау указал на принципиальную возможность локальной деформации кристаллической решётки полем самого электрона проводимости; в результате такой деформации нарушается периодичность кристалла, и электрон попадает в локальное состояние, стационарно поддерживая своим полем деформацию кристалла. Эти автолокализовавшиеся электроны согласно предположению Ландау и являются F-центрами [6].

II. Электроны, как известно, могут локализоваться вблизи нарушений периодичности кристалла [29, 32]. Ряд авторов предполагает, что F-центры суть электроны, локализовавшиеся вблизи внутренних трещин кристалла, полостей, атомов химической примеси, мест с механическими напряжениями и т. п.

III. Гильш и Поль [36] предположили, что F-центр представляет собой электрон, локализовавшийся вблизи лишнего иона щелочного металла, образуя нечто вроде нейтрального атома щелочного металла.

IV. Де-Бур [37] предположил, что F-центр есть электрон, который заместил в решётке отрицательный ион галоида.

Рассмотрим по порядку все эти предположения.

I. Исследования автора, изложенные во второй и третьей главах, подтвердили предположение о существовании автолокализованных состояний электрона. Таковыми являются рассмотренные выше поляроны. Однако поляроны не могут быть отождествлены с F-центрами по следующим соображениям:

1. Поляроны не могут быть названы локальными состояниями электрона в полном смысле этого слова: при каждой фиксированной конфигурации ионов Ψ-функция электрона действительно локальна, т. е. отлична от нуля в сравнительно малой области кристалла (см. § 6); однако электрон может свободно перелвигаться по всему объёму кристалла вместе с поляризационной потенциальной ямой (см. §§ 10 и 16). Поляроны обладают большой подвижностью (см. § 20) и, по мнению автора, являются носителями тока в кристалле. Что же касается F-центров, то они неподвижны. Опыт показывает, что даже густо окрашенный кристалл с концентрацией F-центров порядка $10^{20}c^{-3}$ при низких температурах является диэлектриком.

2. Если бы F-центры представляли собой поляроны, то процесс окрашивания методами А состоял бы из двух этапов: возбуждения электронов в зону проводимости облучением и торможения электронов и перехода их в поляронное состояние.

Второй процесс совершается гораздо быстрее первого. Поэтому скорость окрашивания определялась бы первым этапом и не должна была бы зависеть от температуры [1]). Опыт же показывает, что скорость окрашивания экспоненциально растёт с температурой.

3) Экспериментально установлено, что в кристаллах, окрашенных облучением, скорость обесцвечивания (рекомби-

нации) растёт при нагревании кристалла. Предельно достижимая концентрация F-центров определяется отношением скорости окрашивания к скорости обесцвечивания и, следовательно, при нагревании должна была бы убывать, если верна гипотеза I. Опыт, однако, показывает, что предельно достижимая концентрация экспоненциально ($\sim e^{-a/T}$) растёт с температурой.
4) Экспериментально твёрдо установлено, что при окрашивании методами Б в кристалле создаётся избыток положительных ионов щелочного металла, компенсирующий пространственный заряд введённых в кристалл электронов. В таком кристалле должны либо существовать лишние ионы щелочного металла, либо отсутствовать на своих местах некоторые ионы галоида; в обоих случаях указанные дефекты будут действовать как положительные заряды, стремясь своим кулоновским полем привлечь к себе поляроны. Учитывая, что выигрыш энергии при оседании полярона на такой положительно заряженный центр порядка 1 эл.-в. (см. § 29), а концентрация таких центров равна концентрации введённых электронов, т. е. достигает порядка $10^{18} - 10^{20} - 3$, и, применяя обычную статистику, легко убедиться в том, что при не слишком высокой температуре почти все поляроны сядут на положительные центры. Свободных поляронов остаётся так мало, что ими нельзя объяснить наблюдающегося интенсивного поглощения света.
II. В реальном кристалле безусловно могут существовать внутренние трещины, полости, механические напряжения, атомы примеси и т. п. дефекты. У этих нарушений периодичности потенциала, вообще говоря, могут образоваться локальные состояния электрона.

Особенность предположения II заключается в том, что обычно нет возможности количественно рассчитать свойства этих локальных состояний электрона вследствие большого разнообразия указанных дефектов кристалла и их недостаточной определённости.

Предположения II должны быть отвергнуты по следующим соображениям:

1. При окрашивании методами Б концентрация F-центров доходит до $10^{20}c^{-3}$, а в кристалле CaF_2 даже до $10^{22}c^{-3}$ [37]. Присутствие химической примеси в таком количестве заведомо

исключено даенными химических анализов и условиями выращивания кристаллов. Допустить непременное наличие трещин и т. п. в таком количестве и независимо от условий выращивания кристалла также невозможно.

Указанное число дефектов не можег заранее существовать в любом кристалле. Следовательно, они появляются лишь в процессе окрашивания. Они могут быть связаны только с излишком щелочного металла или дефицитом галоида (предположения III и IV); концентрация последних заведомо совплдает с указанной концентрацией F-центра (компенсация пространственного заряда).
2) Дефекты кристалла, перечисленные в предположении II, могут быть весьма разнообразны; столь же разнообразны должны быть и свойства соответствующих локальных состояний электронов. F-центры же, наоборот, довольно стандартны и идентичны даже для различно выращенных образцов кристалла.

III и IV. Предположения III и IV полностью согласуются с изложенными выше свойствами окрашенных кристаллов:

[81]) Речь идёт о скорости окрашивания, когда концентрация F-центров ещё значительно меньше своего предельного (асимптотического) значения и линейно растёт со временем.

1. В процессе окрашивания методами Б в кристалле создаётся избыток ионов щелочного металла в количестве, равном количеству введённых извне электронов (для компенсации пространственного заряда). Этот факт твёрдо установлен химическим анализом окрашенных кристаллов и другими прямыми экспериментами. Следовательно, в таких кристаллах заведомо существуют и как раз в нужных количествах лишние ионы щёлочи или вакансии ионов галоида. Естественно предположить, что именно у этих дефектов локализуются электроны, образуя F-центры. Опыт показывает, что в тех случаях, когда избыток щёлочи коагулирует в коллоиды, F-центры исчезают.

2. При окрашивании путём облучения А следует предположить, что лишние ионы щёлочи или вакансии ионов галоида образуются вследствие тепловой диссоциации (срыва) ионов из узлов решётки. С этой точки зрения вполне понятно, почему при окрашивании методами А необходимо нагревать кристалл, несмотря на то, что электролитической проводимости для компенсации пространственного заряда в этом случае не требуется. Понятно также, почему скорости окрашивания и предельная достижимая концентрация F-центров экспоненциально растут с температурой.

3. Облучая кристалл при низкой температуре, можно получить лишь ничтожную концентрацию F-центров. Но если неокрашенный кристалл нагреть до температуры, при которой появляется электролитическая проводимость, после этого быстро охладить (закалить) и затем облучить, то можно получить значительную концентрацию F-центров. Этот интересный факт вполне объясняется предположениями III и IV: холодный кристалл мало окрашивается потому, что в нём мало дефектов лишних ионов щёлочи в междуузлиях или вакантных галоидных узлов; нагревание до температуры электролитической проводимости вызывает диссоциацию ионов из узлов решётки, т. е. появление дефектов, которые фиксируются при быстром охлаждении (при медленном охлаждении ионы успели бы рекомбинировать, и решётка исправилась бы). Таким образом, получается холодный кристалл с большой концентрацией дефектов, который может быть сравнительно густо окрашен облучением.

4. В предположениях III и IV мы имеем дело со стандартными дефектами, что вполне объясняет стандартность и идентичность F-центров независимо от степени идеальности кристаллов, условий их выращивания и методов окрашивания.

5. Предположения III и IV подкрепляются вышеупомянутым выводом о том, что полярону энергетически выгодно сесть на избщточный ион щелочного металла или на вакансию иона галоида.

6. Как известно, кристалл окрашивается более интенсивно в тех местах, где имеются механические напряжения. Этот факт с точки зрения предположений III и IV объясняется тем, что в этих местах легче происходит тепловая диссоциация ионов.

Выше были рассмотрены факты, подтверждающие в равной мере как предположение III, так и предположение IV. Іерейдём теперь к рассмотрению фактов, позволяющих отдать предпочтение одному из них - предположению IV.

7) В кристалле CaF_2 путём окрашивания методами Б удаётся довести концентрацию F-центров до $10^{22}c^{-3}$, и при этом наблюдается значительное уменьшение плотности кристалла [37]. Последнее является подтверждением предположения IV и опровержением III.

8) Если в расплавленной щёлочно-галоидной соли растворить какой-нибудь щелочной

металл, то характерной F-полосы поглощения не получается, а появляется добавочное поглощение,

спектр которого определяется растворённым металлом, а не солью; этот спектр похож на спектр поглощения пара растворённого металла, но смещён и размазан. Нет сомнений в том, что поглощают атомы растворённого металла и что спектр несколько отличается от спектра паров вследствие небольшого возмущения энергетических уровней атомов диэлектрической жидкой средой. Именно такие центры поглощения имеются в виду в предположении III.

Однако оказывается, что при замерзании такого раствора исчезает упомянутый выше спектр поглощения щелочных атомов и появляется типичная F-полоса поглощения, вид которой характерен для данной соли и не зависит от свойств растворённого металла. Это значит, что при замерзании соли атомы растворённого металла ионизируются (при этом исчезает соответствующее поглощение), а освободившиеся при этом электроны образуют F-центры, локализуясь на стандартных дефектах, которые в жидкой фазе отсутствуют. Эти факты опровергают предположение III и легко согласуются с IV.
9) Анализ [35] ряда экспериментальных и теоретических исследований показывает, что если в ионном кристалле нарушено стехиометрическое соотношение компонент - имеется избыток одной компоненты, то энергетически более выгодной является структура с вакантными узлами решётки, а не с лишними ионами в междуузлиях. Это также является аргументом против предположения III и в пользу предположения IV.

Проделанное выше качественное исследование существующих гипотез и известных экспериментальных фактов заставляет остановиться на предположении IV, согласно которому F-центр есть электрон, заместивший ион галоида в узле решётки. Ниже будет показано, что предноложение IV приводит и к правильным количественным результатам.

Исторически термин « F-центр» возник при изучении окрашенных щёлочно-галоидных и земельно-щёлочно-галоидных кристаллов и до последнего времени применялся именно к этим кристаллам. Но, как будет показано ниже, локализация носителей тока (электронов или дырок) у вакантных узлов решётки имеет место и в других ионных кристаллах, не только в диэлектриках, например в кварце, но и в полупроводниках. Процесс образования таких локальных состояний аналогичен окрашиванию щёлочно-галоидных кристаллов, а их свойства подобны

свойствам F-центров в щёлочно-галоидных кристаллах. Подобные локальные состояния мы тоже будем называть F-центрами. В качестве примера приведём закись меди. Прогрев закиси меди в атмосфере кислорода создаёт в ней избыток кислорода совершенно так же, как прогрев щёлочно-галоидного кристалла в парах щёлочи создавал избыток щёлочи. С появлением избытка кислорода решётка закиси меди перестраивается, и образуются вакантные медные узлы решётки, вблизи которых локализуются дырки проводимости. Образование этих локальных состояний сопровождается появлением новой типичной колоколообразной полосы поглощения $-F$-полосы с максимумом в области 0,6 эл.-в. Поглощение света в F-полосе вызывает фотопроводимость. Отличие закиси меди от щёлочно-галоидных кристаллов заключается в том, что здесь F-полоса лежит в инфракрасной, а не в видимой части спектра и поэтому её появление не меняет цвета кристалла.

10.4.3 § 23. Basic equations for crystal with F-центром

Количественная теория F-центров, подобно теории поляронов, будет развита для случаев, когда

1. движение локализованного электрона можно рассматривать с помощью метода эффективной массы, т. е. когда средняя кинетическая энергия локализованного

электрона значительно меньше, чем ширина зоны проводимости в кристалле с ионами, фиксированными в узлах решётки (см. § 4);

2. поляризационный радиус F-центра достаточно велик, чтобы можно было диэлектрическую поляризацию кристалла вокруг F-центра рассчитывать макроскопическим путём.

Такой F-центр можно представить себе как полярон, севший на вакантный узел решётки, покинутый отрицательным ионом. Гамильтониан системы в этом случае составляется совершенно так же, как в § 12 , в случае полярона; следует лишь дополнительно ввести потенциальную энергию взаимодействия электрона с дефектом кристалла. Энергия статической поляризации кристалла полем дефекта войдёт в гамильтониан аддитивной постоянной, которую можно не учитывать. Под $\boldsymbol{P}(\boldsymbol{r})$ в дальнейшем понимается инерционная поляризация за вычетом вышеупомянутой статической. Если отрицательный

ион с зарядом ze (z - валентность иона) покидает узел решётки, расположенный в начале координат, то потенциальная энергия электрона, связанная с этим дефектом, равна

$$-\frac{ze^2}{\varepsilon r} \tag{23.1}$$

Выражение (23.1) справедливо на расстояниях r, превышающих радиус иона. На меньших расстояниях потенциальная энергия электрона выражается сложнее. Однако, поскольку размеры области, в которой ψ-функция электрона отлична от нуля, значительно превышают радиус иона, ход потенциала на малых расстояниях не имеет существенного значения.

Оператор энергии электрона и продольных оптических колебаний получается, если потенциал дефекта (23.1) просто добавить к оператору (12.11). В результате имеем:

$$\mathbf{H} = -\frac{\hbar^2}{2\mu}\Delta + V(\boldsymbol{r}) - \frac{ze^2}{sr} + \mathbf{H}_{0\mathrm{n}}\| \tag{23.2}$$

$$V(\boldsymbol{r}) = e\int \frac{(\boldsymbol{r}-\boldsymbol{r}_1)\,\boldsymbol{P}(\boldsymbol{r}_1)}{|\boldsymbol{r}-\boldsymbol{r}_1|^3} d\tau_1 \tag{23.3}$$

Ограничиваясь, как и в § 12, случаями, когда удельная поляризация является плавной функцией координат, можно для $H_{\text{оп}}$ воспользоваться формулой (12.13):

$$H_{0\mathrm{I}\|} = \frac{2\pi}{c}\int \left[P^2(r) + \frac{1}{\omega^2}\dot{P}^2(r)\right] d\tau \tag{23.4}$$

В $\boldsymbol{P}(\boldsymbol{r})$ не включается стационарная поляризация кристалла, вызванная кулоновским полем дефекта. Энергия системы полагается равной нулю, когда электрон покоится на дне зоны проводимости, а в кристалле существует только упомлнутая стационарная поляризация, вызванная полем дефекта ($\boldsymbol{P} = \mathbf{0}$).

Далее предполагается, так же как в § 5, что ионы движутся согласно классической механике, а состояние электрона $\Psi(r)$ адиабатически «следует» за движением ионов. Для каждой мгновенной конфигурации ионов $\boldsymbol{P}(\boldsymbol{r})$ адиабатически соответствующее состояние электрона определяется из уравнения

$$\left[-\frac{\hbar^2}{2\mu}\Delta + V(r) - \frac{ze^2}{\epsilon r}\right]\psi(r) = E\psi(r). \tag{23.5}$$

Подобно тому как это делалось в § 5, удобно ввести функционал

$$F[\psi, P] = \frac{\hbar^2}{2\mu}\int |\nabla\psi|^2 d\tau + \bar{V}[\psi, P] + \\ + \frac{2\pi}{c}\int P^2 d\tau - \frac{ze^2}{\varepsilon}\int \frac{|\psi|^2}{r} d\tau \tag{23.6}$$

где

$$\bar{V}[\psi, P] = \int V(r)|\psi(r)|^2 d\tau = -\int PD d\tau \tag{23.7}$$

Если задаться каким-нибудь фиксированным $\boldsymbol{P}(\boldsymbol{r})$ и искать экстремумы $F[\psi, P]$, варьируя ψ при дополнительном условии

$$\int |\psi|^2 d\tau = 1 \tag{23.8}$$

то полученные таким путём ψ согласно общеизвестному вариационному принципу квантовой механики являются собственными функциями уравнения (23.5). Если одно из этих экстремальных ψ подставить в F, то после этого F зависит уже только от $\boldsymbol{P}(\boldsymbol{r})$ и представляет собой потенциальную энергию ионов при наличии в кристалле F-центра.

Перейдём теперь к рассмотрению состояний системы, в которых ионы покоятся в равновесии. В этих состояниях кинетическая энергия ионов равна нулю, а их потенциальная энергия минимальна. Последнее означает, что функционал $F[\psi, P]$ должен быть не только экстремален в зависимости от ψ, но кроме того минимален в зависимости от $\boldsymbol{P}(\boldsymbol{r})$. Таким образом, для отыскания равновесных состояний необходимо искать экстремумы F, независимо варьируя $\psi(r)$ и $P(r)$.

В результате вариации $\boldsymbol{P}(\boldsymbol{r})$ при фиксированном $\psi(\boldsymbol{r})$ получается:

$$\delta_P F = -\int \delta P D d\tau + \frac{4\pi}{c}\int P\delta P d\tau \tag{23.9}$$

Приравнивая эту вариацию нулю, получаем:

$$P(r) = \frac{c}{4\pi} D[\psi, r], \tag{23.10}$$

а подставляя это выражение для $\boldsymbol{P}$ в (23.7) и (23.6), приходим к функционалу, который зависит уже только от ψ:

$$J_F[\psi] \equiv F\left[\psi, \frac{c}{4\pi}D\right] = \\ = \frac{\hbar^2}{2\mu}\int |\nabla\psi|^2 d\tau - \frac{c}{8\pi}\int D^2[\psi, r] d\tau - \frac{ze^2}{\varepsilon}\int \frac{|\psi|^2}{r} d\tau = \\ = J[\psi] - \frac{ze^2}{\varepsilon}\int \frac{|\psi|^2}{r} d\tau \tag{23.11}$$

Индекс F показывает, что данный функционал относится к F-центру в отличие от аналогичного функционала $J[\Psi]$ в задаче о поляроне (см. формулу (6.4)).

Необходимо теперь искать экстремуй $J_F[\psi]$, варьируя ψ с сохранением нормировки (23.8). Полученные таким путём равновесные состояния системы будут называться самосогласованными, так как в этих состояниях поляризационная потенциальная яма $V(\boldsymbol{r})$ и состояние электрона $\psi(\boldsymbol{r})$ взаимно определяют и обусловливают друг друга.

Найдя $\psi(r)$, которая является экстремалью $J_F[\psi]$, можно затем по формуле (23.10) найти соответствующую поляризацию кристалла $\boldsymbol{P}(\boldsymbol{r})$ и по формуле (23.3) вычислить

самосогласованную поляризационную потенциальную яму $V(\boldsymbol{r})$. Упомянутое выше $\psi(\boldsymbol{r})$ непременно является одной из собственных функций уравнения (23.5). Может оказаться, что эта функция принадлежит не самому нижнему энергетическому уровню в данной потенциальной яме. В этом случае возможен переход электрона на один из нижних уровней с излучением света. За короткое время фотоперехода тяжёлые ионы не успеют заметно сместиться; поэтому можно считать, что в течение фотоперехода поляризационная потенциальная яма остаётся почти неизменной (фиксированной). Однако в результате фотоперехода изменяется ψ-функция электрона, а вместе с неи и поле электронного облака $D[\psi, r]$, первоначальная конфигурация ионов оказывается неравновесной, и ионы начинают колебаться. Таким образом, в рассмотренном случае время жизни первоначального равновесного самосогласованного состояния системы равно оптическому времени жизни электрона на возбуждённом уровне,

Возможен и другой случай, когда экстремаль $J_F[\Psi]$ представляет собой собственную функцию самого нижнего энергетического уровня уравнения (23.5). В этом случае рассмотренное выше излучение света невозможно, и система будет находиться в равновесии бесконечное время.

Во всяком равновесном, т. е. самосогласованном, состоянии кинетическая энергия ионов равна нулю; следовательно, полная энергия системы совпадает с потенциальной энергией ионов F, которая в свою очередь совпадает со значением функционала $J_F[\psi]$ (см. формулу (23.11)).

10.4.4 § 24. Energy spectrum and ψ-functions of the electron in the F-center

Рассмотрим основное состояние кристалла с F-центром, т. е. такое состояние, в котором энергия системы имеет минимальное возможное значение. Абсолютная температура кристалла предполагается равной нулю. В этом состоянии кинетическая энергия ионов должна быть равна нулю, а потенциальная энергия должна иметь абсолютный минимум. Так как рассматриваемое состояние является равновесным, то полная и потенциальная энергии ионов равны $J_F[\Psi]$. Задача сводится, следовательно, к отысканию абсолютного минимума функционала $J_F[\psi]$.

Минимальное значение $J_F[\Psi]$ заведомо отрицательно. Чтобы это доказать, достаточно подставить в формулу (23.11) хотя бы ψ-функцию основного состояния полярона ψ_0 (см. § 6). В результате такой подстановки $J\left[\psi_0\right]$, а следовательно, и $J_F\left[\psi_0\right]$ окажутся отрицательными; ясно поэтому, что отрицательным должно быть и абсолютное минимальное значение $J_F\left[\psi_0\right]$.

Абсолютный минимум функционала $J_F[\psi]$ был найден прямым вариационным методом, подобно тому как это делалось в случае полярона. Расчёты были проделаны автором совместно с М. Ф. Дейгеном [16]. При этом ?-функция электрона апроксимировалась выражениями трёх видов:

1. $\psi_{1\ \mathrm{s}} = A(1+\alpha r)e^{-\alpha r}$,
2. $\psi_{1\ \mathrm{s}} = Ae^{-\alpha r}$,
3. $\psi_{1\ \mathrm{s}} = Ae^{-\alpha r^2}$,

где A и α - параметры апроксимации.

Ниже приведены соответствующие значения энергии основного состояния системы $J_F\left[\Psi_{18}\right]$ и собственные значения энергии электрона E_{18}, фигурирующие в уравнении (23.5):

$$1)\qquad \left.\begin{aligned} J_F\left[\psi_{1s}\right] &= -\tfrac{27}{56}\tfrac{\mu e^4}{\hbar^2}\left(\tfrac{z}{\varepsilon}+\tfrac{c}{3}\right)^2 \\ E_{1s} &= -\tfrac{27}{56}\tfrac{\mu e^4}{\hbar^2}\left(\tfrac{z^3}{\varepsilon^2}+\tfrac{4}{3}\tfrac{zc}{\varepsilon}+\tfrac{1}{3}c^2\right), \\ \alpha &= \tfrac{\mu e^2}{2\hbar^2}\left(\tfrac{3z}{\varepsilon}+c\right), \quad A=\tfrac{\alpha^{3/2}}{\sqrt{7\pi}}; \end{aligned}\right\} \tag{24.5}$$

$$2.\qquad \left.\begin{aligned} J_F\left[\psi_{1s}\right] &= -\tfrac{1}{2}\tfrac{\mu e^4}{\hbar^2}\left(\tfrac{z}{\varepsilon}+\tfrac{5c}{16}\right)^2, \\ E_{18} &= -\tfrac{\mu e^4}{2\hbar^2}\left(\tfrac{z^2}{\varepsilon^2}+\tfrac{5}{4}\tfrac{zc}{\varepsilon}+\tfrac{75}{256}c^2\right), \end{aligned}\right\}$$

$$\alpha=\frac{\mu e^2}{2\hbar^2}\left(\frac{2z}{\varepsilon}+\frac{5c}{8}\right), \quad A=\frac{\alpha^{3/2}}{\sqrt{\pi}}; \tag{24.7}$$

$$3.\qquad \left.\begin{aligned} J_F\left[3_{18}\right] &= -\tfrac{1}{2}\tfrac{\mu e^4}{\hbar^2}\left(\tfrac{2^{3/3}}{\sqrt{3\pi}}\tfrac{z}{\varepsilon}+\tfrac{c}{\sqrt{3\pi}}\right)^2, \\ E_{18} &= -\tfrac{\mu e^4}{2\hbar^2}\left(\tfrac{8}{3\pi}\tfrac{z^2}{\varepsilon^2}+\tfrac{8\sqrt{2}}{3\pi}\tfrac{zc}{\varepsilon}+\tfrac{c^2}{\pi}\right), \end{aligned}\right\}$$

$$\alpha=\frac{\mu^2 e^4}{9\pi\hbar^4}\left(2^{3/2}\cdot\frac{z}{\varepsilon}+c\right)^2, \quad A=\left(\frac{2\alpha}{\pi}\right)^{3/4}. \tag{24.9}$$

Во всех трёх случаях точность результата оценивалась путём сравнения полученного значения энергетического терма с его известными значениями в двух предельных случаях: в случае $c\to 0$, когда задача об F-центре переходит в задачу о водородоподобном атоме, и в случае $z\to 0$, когда мы приходим к задаче о поляроне, которая была решена весьма точно в § 6. Наиболее удачной оказалась апроксимация 1). Целесообразно остановиться на выражениях (24.4), несколько округлив их в сторону понижения терма:

$$\left.\begin{aligned} J_F\left[\psi_{1s}\right] &= -\tfrac{1}{2}\tfrac{\mu e^4}{\hbar^2}\left(\tfrac{z}{\varepsilon}+\tfrac{c}{3}\right)^2, \\ E_{1s} &= -\tfrac{\mu e^4}{2\hbar^2}\left(\tfrac{z^2}{\varepsilon^2}+\tfrac{4}{3}\tfrac{zc}{\varepsilon}+\tfrac{c^2}{3}\right). \end{aligned}\right\} \tag{24.10}$$

Погрешность этих формул не превышает 3% во всём интервале возможных значений c и ϵ. В дальнейшем мы будем пользоваться исключительно формулами (24.10).

Для рассмотрения поглощения света F-центром необходимо знать кроме основного также и возбуждённые состояния электрона. Выше уже предполагалось, что за малое время фотоперехода тяжёлые ионы не успевают заметно сместиться. Поэтому можно считать, что фотопереход совершается при неизменной фиксированной поляризационной потенциальной яме, согласованной с исходным состоянием электрона. Свет поглощается главным образом F-центрами, находящимися в основном состоянии, ибо таких большинство. Поэтому необходимо рассчитать энергетический спектр электрона в F-центре при потенциальной яме, согласованной с основным состоянием.

Поляризацию кристалла следует вычислять по формуле (23.10), в которую нужно подставить ψ основного состояния в виде (24.1), (24.5). Найденную поляризацию основного состояния $\boldsymbol{P}_{1s}(\boldsymbol{r})$ следует подставить в формулу (23.3) для вычисления соответствующей потенциальной ямы. Последняя, как легко заметить, получается сферически симметричной. Слеловательно, мы имеем дело с электроном, движущимся в центральном поле. Угловая часть ψ-функций электрона даётся, как обычно, сферическими функциями $Y_l(\vartheta,\varphi)$; состояния электрона можно обозначать индексами $s,p,d,\ldots$ в зависимости от значений азимутального квантового числа $\boldsymbol{l}$. Основное состояние является s-состоянием. Поэтому согласно известным правилам отбора оптический переход электрона разрешён только в p-состояния, рассмотрением которых мы и займёмся.

Следуя вариационному методу, изложенному в § 23 , необходимо в функционале $F[\psi, P]$ положить $P = P_{1s}(r)$ (самосогласованная поляризация основного состояния), а затем искать экстремумы $F[$ ч, $P_{18}]$, варьируя только ψ. Для определения самого нижнего из p-уровней был применён прямой вариационный метод, а именно ψ-функция электрона апроксимировалась формой

$$\psi_{2pF}^{1s} = CY_1(\theta, \varphi)2\alpha r e^{-2\alpha\beta r}, \tag{24.11}$$

α определялась формулой (24.5), а C и β представляли собои параметры апроксимации.

Выбор этой формы оправдывается теми же соображениями, какие были приведены в § 9, при апроксимации p-состояния полярона. Значок ^{1s} сверху у ψ-функции напоминает о том, что

состояние вычисляется при заданной поляризации $\boldsymbol{P}_{18}$ (несамосогласованное).

Нормировка функции ψ_{2pF}^{18} приводит к соотношению

$$C^2 = \frac{(2\alpha)^3(2\beta)^5}{4!}. \tag{24.12}$$

Далее ψ-функция в форме (24.11-12) была подставлена в функционал $F[\psi, P_{1s}]$. Условие минимума функционала $F\left[\psi_{2pF}^{1s}, P_{1s}\right]$ приводит к следующему уравнению для β:

$$\begin{gathered}\tfrac{1}{6\beta-1}\left\{1 - 2\beta - \tfrac{1}{7}\left(\tfrac{2\beta}{2\beta+1}\right)^4 \cdot \left[7 + \tfrac{2{,}8}{2\beta+1} + \right.\right. \\ \left.\left. + \tfrac{70}{(2\beta+1)^2} + \tfrac{120}{(2\beta+1)^3} + \tfrac{105}{(2\beta+1)^4}\right]\right\} = \tfrac{z}{\frac{\varepsilon}{n^2}-1}.\end{gathered} \tag{24.13}$$

Ниже даётся таблица величины β для различных значений отношения ε/n_2 при $z = 1$.

Таблица 24.1

E/$\boldsymbol{n}^2$	β	$\varepsilon/\boldsymbol{n}^2$	β	ε/n^2	β
1,00	0,1666	2,4096	0,2430	2,8290	0,2540
1,2766	0,1900	2,4267	0,2435	2,8696	0,2550
1,4144	0,2000	2,4433	0,2440	2,9871	0,2575
1,5926	0,2100	2.4606	0,2445	3,1097	0,2600
1,7909	0,22	2,4780	0,2450	3,2374	0,2625
2,0264	0,23	2,5136	0,2460	3,3779	0,2650
2,1622	0,235	2,5496	0,2470	3,5286	0,2675
2,3118	0,240	2,5866	0,2480	3,6897	0,2700
2,3436	0,241	2,6249	0,2490	3,8822	0,2725
2,3760	0,242	2,6639	0,2500	4,0522	0,2750
2,3929	0,2425	2,7438	0,2520	∞	0,3361

Собственное значение энергии электрона E, фигурирующее в уравнении (23.5), для нижнего p-уровня выражается формулой

$$\begin{gathered}E_{2pF}^{1s} = \frac{\mu e^4}{2\hbar^2} c\left(\frac{3z}{\varepsilon} + c\right)\left\{\left(\frac{3z}{\varepsilon c} + 1\right)\beta^2 - \beta + \right. \\ + \frac{(2\beta)^5}{14(2\beta+1)^7}\left[7(2\beta+1)^3 + 19(2\beta+1)^2 + \right. \\ \left. \left. +25(2\beta+1) + 15\right] - \frac{\beta}{\varepsilon c}\right\}.\end{gathered} \tag{24.14}$$

Потенциальная яма электрона при больших r имеет кулоновский вид

$$-\frac{e^2}{r}\left(c+\frac{z}{\varepsilon}\right). \tag{24.15}$$

Поэтому энергия возбуждённых состояний с большим эффективным радиусом может быть вычислена по формуле для водородоподобного атома с зарядом ядра $e\left(c+\frac{z}{\varepsilon}\right)$:

$$E_{npF}^{1s}=-\frac{\mu e^4}{2\hbar^2 n^2}\left(c+\frac{z}{\varepsilon}\right)^2. \tag{24.16}$$

Практически по этой формуле можно вычислять все p-уровни, кроме самого низкого, т. е. кроме уровня с $n=2$.

10.4.5 § 25. Absorption of light by F-centers [15]

Зная уровни энергии электрона, можно рассчитать частоты света, поглощаемого F-пентром, по формуле

$$\hbar\omega_n = E_{npF}^{1s} - E_{1sF}^{1s}. \tag{25.1}$$

Красная граница частот, вызывающих переходы в непрерывныи спектр, определяется по формуле

$$\hbar_{\omega_\infty} = -E_{1sF}^{1s} \quad \left(E_{\infty\neq F}^{1s}=0\right) \tag{25.2}$$

Согласно формулам (25.1-2) спектр поглощения F-центра должен был бы представлять собой серию линий. Частота ω_∞ является границей серии, за которой должно начинаться непрерывное поглощение.

Однако на опыте наблюдается только непрерывный спектр поглощения, изображённый на рис. 21.1, а дискретные линии поглощения не наблюдаются вообще. Не следует думать, что дискретный спектр превращается в непрерывный благодаря размытию линий вследствие тепловых колебаний ионов: F-полоса поглощения не обнаруживает линейчатой структуры даже при температуре абсолютного нуля. Здесь, на первый взгляд, имеется противоречие между теорией и экспериментом.

Чтобы выяснить этот вопрос и показать, что противоречия между теорией и экспериментом в действительности нет, необходимо прежде всего более точно установить, какого вида спектр поглощения следует ожидать, исходя из изло-

женной теории. Автором совместно с М. Ф. Дейгеном была вычислена «сила осциллятора» f_{21} перехода электрона из состояния ψ_{1s} в состояние ψ_{2pF}^{1s}. Результаты вычисления представлены на рис. 25.1.

Из приведённой кривой видно, что у большинства ионных кристаллов, в частности у щёлочно-галоидных кристаллов,

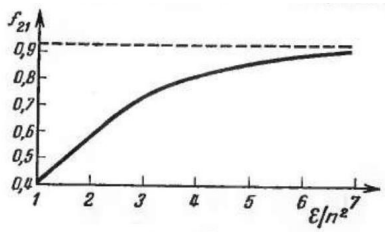

Рис. 25.1.

f_{21} порядка $0,7 - 0,8$. Сумма сил осцилляторов для переходов во все возможные возбуждённые состояния, как известно, равна единице. Следовательно, всё бесконечное множество переходов в состояния $3p, 4p, 5p, \ldots$, а также и в непрерывный спектр составляет в сумме сил осцилляторов всего $0,3 - 0,2$. Это значит, что в поглощении света господствующую роль играет переход $1s \to 2p$ и именно с этим переходом следует связывать F-полосу поглощения. Все же остальные переходы мало вероятны и поглощают свет несравненно слабее.

Оценим теперь естественную ширину спектральной линии, соответствующей переходу $1s \to 2p$. Как уже отмечалось выше, за малое время фотоперехода электрона поляризация кристалла не успевает измениться, и тотчас же после фотоперехода ионы начинают перемещаться в свои новые равновесные положения. При этом вид поляризационной потенциальной ямы меняется во времени, что приводит к некоторому расширению энергетического уровня конечного состояния электрона. Расширение уровня связано с малым «временем жизни» несамосогласованного конечного состояния Ψ^{1s}_{3pF}. Это время можно грубо оценить как время существенного изменения формы потенциальной ямы и считать его порядка

$$\Delta t = \frac{1}{\omega}, \tag{25.3}$$

где ω - частота колебаний ионов. Уширение уровня можно оценить из обычного соотношения

$$\Delta E \geqslant \frac{h}{\Delta t} = h\omega = 2\pi\hbar\omega \tag{25.4}$$

Согласно формуле (25.4) ΔE равно нескольким десятим электрон-вольта, что по порядку величины как раз совпадает с наблюдающейся шириной F-полосы поглощения.

Не только линия, соответствующая переходу $1s \to 2p$, но и остальные, гораздо менее интенсивные линии поглощения должны обладать аналогичной естественной шириной. В результате они перекрываются и образуют непрерывный спектр поглощения - «хвост» F-полосы, уходящий в коротковолновую сторону.

Рассмотренный выше механизм расширения линий действует и при температуре абсолютного нуля. При отличной от нуля температуре следует ожидать добавочного расширения F-полосы вследствие тепловых колебаний ионов, что действительно наблюдается на опыте.

Нариду с вышеизложенной интерпретацией F-полосы поглощения автором следует указать и на другую точку зрения, согласно которой F-полоса соответствует переходам электрона непосредственно в зону проводимости. Эту точку зрения обычно обосновывают теми двумя фактами, что поглощение света вызывает фотопроводимость кристалла и F-полоса поглощения даже при температуре абсолютного нуля не обнаруживает линейчатой структуры и сохраняет конечную ширину.

Эти два аргумента на первый взгляд кажутся убедительными, и поэтому некоторые физики до настоящего времени придерживались этой последней точки зрения. Чтобы выяснить этот вопрос, рассмотрим ряд соображений, опровергающих предположение о переходе электрона непосредственно в зону проводимости и подтверждающих предположение о переходе электрона на дискретный уровень.

А. Соображения, не связанные с принятой выше моделью F-центра.

1. При глубоком охлаждении окрашенных кристаллов квантовый выход внутреннего фотоэффекта (среднее число электронов, освобождаемых одним поглощённым квантом света) быстро (экспоненциально) стремится к нудю с понижением

температуры; вместе с ним стремится к нулю и фотопроводимость. Интенсивность поглощения света при этом остаётся почти неизменной. Этот факт противоречит предположению о фотопереходе электронов непосредственно в зону проводимости, так как в этом случае квантовый выход равнялся бы единице и не зависел бы от температуры. Указанный факт свидетельствует о том, что возбуждение электронов осуществляется в два этапа: сначала светом на дискретный уровень, затем термически в состояние свободного полярона. Первый этап определяет поглощение света и не зависит от температуры; второй этап - тепловая диссоциация возбуждённого светом F-центра - требует тепловой флуктуации, вероятность которой экспоненциально зависит от температуры.
2) Не представляется возможным предположить существование зоны проводимости настолько малой ширины, чтобы её можно было отождествить с шириной F-полосы поглощения. Ширина зоны проводимости, например в щёлочно-галоидных кристаллах, составляет несколько электрон-вольт. Экспериментальное исследование тонкой структуры спектров поглощения рентгеновских лучей [39] позволяет приближённо оценить ширину зоны проводимости; например, для KCl получается ширина зоны, приблизительно равная 5 эл.-в. Ширина же F-полосы поглощения у KCl порядка 0,4 эл.-в.
Б. Соображения, связанные с принятой выше моделью F-центра.
3) Экспериментально определённая [40] сила осциллятора для F-полосы поглощения (0,7 у $\mathrm{NaCl}, 0,8$ у KCl) весьма удовлетворительно согласуется с вычисленной силой осциллятора для перехода $1s \to 2p$ (рис. 25.1) и значительно превышает вычисленную силу осциллятора для переходов в непрерывный спектр. Поэтому F-полосу следует связывать с переходом $1s \to 2p$, а не с переходом в непрерывный спектр.
4) М. Ф. Дейген [41] рассчитал вид спектра поглощения F-нентра для фотопереходов электрона в зону проводимости. Этот спектр изображается несимметричной кривой, монотонно и медленно спадающей в сторону коротких волн, и совсем не похож на наблюдающуюся довольно симметричную и узкую F-полосу поглощения.
5) Естественная ширина линии поглощения, соответствующей переходу $1s \to 2p$, оценённая выше по порядку вели-

чины, согласуется с наблюдающейся шириной F-полосы поглощения.

В настоящем параграфе все количественные результаты получены в предположении, что фотопереход электрона совершается при неподвижных ионах, и только при помощи качественных соображений показано, что учёт движения ионов способен объяснить ширину и непрерывность F-полосы поглощения. Детальное объяснение характерной формы F-полосы поглощения, вычисление её полуширины и объяснение деформации F-полосы при изменении температуры будут даны в § 28 на основе квантовомеханического рассмотрения движения ионов.

10.4.6 § 26. Theory of F'-центров

Автором совместно с О. Ф. Томасевич было показано [42], что при благоприятных значениях в и n энергетически выгодно состояние, в котором F-центр присоединяет к себе второй электрон проводимости, образуя так называемый F'-центр. Оператор энергии в этом случае составляется так же, как и в случае F-центра (см. § 23), с той лишь разницей, что на этот раз не один, а два электрона движутся в инерционнополяризующейся среде в поле точечного положительного заряда. Вместо формулы (23.2) мы приходим к выражению

$$H = -\frac{\hbar^2}{2\mu}\left(\Delta_1 + \Delta_2\right) + V\left(\boldsymbol{r}_1\right) + V\left(\boldsymbol{r}_2\right) - \frac{ze^2}{\varepsilon}\left(\frac{1}{r_1} + \frac{1}{r_2}\right) + \\ + \frac{e^2}{n^2\left|\boldsymbol{r}_1 - \boldsymbol{r}_2\right|} + H_{\text{onll}}, \tag{26.1}$$

где

$$V(r) = e\int \frac{\left(r - r_1\right)P\left(r_1\right)}{\left|r - r_1\right|^3} d\tau_1. \tag{26.2}$$

Предпоследний член в формуле (26.1) представляет собой энергию взаимодействия электронов. Множитель n^2 в знаменателе играет роль диэлектрической постоянной, которая учитывает только безинерционную часть поляризации кристалла. Инерционная часть поляризации не следует за движением электронов; она выделена отдельно и учитывается членами V и $H_{\text{оп}\,\|}$.

Предположим, как это уже неоднократно делалось выше, что состояние электронов адиабатически следует за движе-

нием ионов. Используя вариационный принцип квантовой механики (аналогично §§ 5 и 23), можно показать, что волновая функция электронов $\Psi\left(\boldsymbol{r}_1, \boldsymbol{r}_2\right)$, адиабатически соответствующая конфигурации ионов $\boldsymbol{P}(\boldsymbol{r})$, является экстремалью функционала

$$F[\Psi, P] = \frac{\hbar^2}{2\mu}\int\left(\left|\nabla_1\Psi\right|^2 + \left|\nabla_2\Psi\right|^2\right) d\tau_1 d\tau_2 + \\ + \int\left|\Psi\right|^2\left[V\left(r_1\right) + V\left(r_2\right) - \frac{ze^2}{\varepsilon}\left(\frac{1}{r_1} + \frac{1}{r_2}\right) + \right. \\ \left. + \frac{e^2}{n^2\left|r_1 - r_2\right|}\right] d\tau_1 d\tau_2 + \frac{2\pi}{c}\int P^2 d\tau \tag{26.3}$$

Необходимо найти экстремум этого функционала путём вариации $\Psi\left(\boldsymbol{r}_1, \boldsymbol{r}_2\right)$ при фиксированном $\boldsymbol{P}(\boldsymbol{r})$, сохраняя нормировку Ψ. Экстремальное значение F будет зависеть от $P(r)$ и представит собой потенциальную энергию ионов кристалла в присутствии F'-центра.

Так как $\Psi\left(\boldsymbol{r}_1, \boldsymbol{r}_2\right)$ может быть только симметричной или антисимметричной, выражение (26.3) можно упростить:

$$F[\Psi, P] = \frac{\hbar^2}{\mu}\int\left|\nabla_1\Psi\right|^2 d\tau_1 d\tau_2 + \int\left|\Psi\right|^2\left[2V\left(r_1\right) - \right. \\ \left. - \frac{2ze^2}{\varepsilon r_1} + \frac{e^2}{n^2\left|r_1 - r_2\right|}\right] d\tau_1 d\tau_2 + \frac{2\pi}{c}\int P^2 d\tau \tag{26.4}$$

Можно показать, что в основном состоянии спины электронов антипараллельны, а $\boldsymbol{\Psi}\left(\boldsymbol{r}_1, \boldsymbol{r}_2\right)$ симметрична по отношению к координатам электронов. Подобно тому как это делается при решении задачи об атоме гелия, $\Psi\left(r_1, r_2\right)$ основного состояния мы будем апроксимировать мультипликативной симметричной формой вида

$$\Psi\left(\boldsymbol{r}_1, \boldsymbol{r}_2\right) = \psi\left(\boldsymbol{r}_1\right)\psi\left(\boldsymbol{r}_2\right). \tag{26.5}$$

Подставляя (26.5) в (26.4), член

$$\frac{e^2}{n^2}\int\frac{|\psi(\boldsymbol{r}_1)|^2|\psi(\boldsymbol{r}_2)|^2}{|\boldsymbol{r}_1-\boldsymbol{r}_2|}d\tau_1 d\tau_2 \tag{26.6}$$

можно интерпретировать как удвоенную электростатическую энергию облака заряда с плотностью $e|\Psi(\boldsymbol{r})|^2$. Эту энергию можно записать в виде

$$\frac{1}{4\pi n^2}\int D^2[\psi,r]d\tau, \tag{26.7}$$

где $\boldsymbol{D}$ - электростатическая индукция этого облака, уже определённая выше формулой (5.17). Результат подстановки (26.5) в (26.4) имеет вид

$$\begin{aligned} F=\tfrac{\hbar^2}{\mu}\textstyle\int|\nabla\psi|^2d\tau-2\int PDd\tau-\tfrac{2ze^2}{\varepsilon}\int\tfrac{|\psi|^2}{r}d\tau+\\ +\tfrac{1}{4\pi n^2}\textstyle\int D^2d\tau+\tfrac{2\pi}{c}\int P^2d\tau. \end{aligned} \tag{26.8}$$

Рассмотрим такое состояние кристалла с F'-центром, в котором энергия системы имеет наименьшее возможное значение. Это состояние в дальнейшем будет называться основным. Очевидно, что в этом состоянии кинетическая энергия ионов равна нулю, а их потенциальная энергия минимальна. Поскольку потенциальная энергия ионов даётся функционалом F, после того как он минимизирован по ψ, то, чтобы получить упомянутый минимум потенциальной энергии, необходимо функционал F минимизировать ещё и по $\boldsymbol{P}$. Таким образом, в основном состоянии функционал (26.8) должен иметь абсолютный минимум, который получается в результате произвольных и независимых вариаций $\psi(r)$ и $\boldsymbol{P}(r)$ (но с сохранением нормировки $\psi(r)$).

Варьируя $\boldsymbol{P}(\boldsymbol{r})$ при фиксированном $\Psi(\boldsymbol{r})$ и приравнивая нулю соответствующую вариацию F, получаем:

$$P(r)=\frac{c}{2\pi}D[\psi,r]. \tag{26.9}$$

Эта формула определяет «самосогласованную» поляризацию кристалла, которая стационарно поддерживается электростатическим полем облака заряда двух электронов. Она отличается от аналогичной формулы для случая F-центра (см. формулу (23.10)) множителем 2.

Подставляя (26.9) в (26.8), получим функционал

$$\begin{aligned} J_{F'}[\psi]\equiv F\left[\psi,\frac{c}{2\pi}D\right]=\frac{\hbar^2}{\mu}\int|\nabla\psi|^2d\tau-\\ -\frac{c'}{4\pi}\int D^2[\psi,r]d\tau-\frac{2ze^2}{\varepsilon}\int\frac{|\psi|^2}{r}d\tau, \end{aligned} \tag{26.10}$$

где

$$c'=2c-\frac{1}{n^2}=\frac{1}{n^2}-\frac{2}{\varepsilon}. \tag{26.11}$$

Этот функционал теперь необходимо экстремизировать, варьируя ψ. Здесь ${J_F}^5[\psi]$ представляет собой удвоенный функционал $J_F[\psi]$, встречавшийся в §§ 23 и 24 при рассмотрении F-центра, с той лишь разницей, что вместо прежнего коэффициента c здесь фигурирует c'. Благодаря этому совпадению можно просто использовать результаты § 24. Экстремаль функционала $J_{FF}[\psi]$ определяется формулами (24.1) и (24.5), если только в формуле (24.5) заменить c на c':

$$\psi_{F'} = A\left(1+\alpha_{F'}r\right)e^{-\alpha_{F'}r}, A = \frac{\alpha_{F'}^{\frac{\sigma^5}{}}}{(7\pi)^{1/2}}, \tag{26.12}$$

$$\alpha_{F'} = \frac{\mu e^2}{2\hbar^2}\left(c' + \frac{3z}{\varepsilon}\right). \tag{26.13}$$

Энергия основного состояния системы равна

$$J_{F'}\left[\psi_{F'}\right] = -\frac{\mu e^4}{\hbar^2}\left(\frac{z}{\varepsilon} + \frac{c'}{3}\right)^2. \tag{26.14}$$

Так как апроксимацию $\Psi\left(\boldsymbol{r}_1, \boldsymbol{r}_2\right)$ мы произвольно ограничили мультипликативной формой (26.5), то полученное таким образом минимальное значение $J_{F'}$, определяемое формулой (26.14), должно быть несколько завышено. Апроксимация (26.5), как известно, не учитывает взаимной корреляции положений электронов. Чтобы оценить ошибку, происходящую от мультипликативного ограничения (26.5), О. Ф. Томасевич применила функцию вида

$$\Psi = A\left(1+\alpha r_1\right)\left(1+\alpha r_2\right)\left(1+\beta\left|r_1 - r_2\right|\right)e^{-\alpha(r_1+r_2)}, \tag{26.15}$$

где A, а и β - параметры. При этом минимальное значение $J_{F'}$ оказалось всего на $1-2\%$ ниже, чем (26.14). Таким

образом, обобщая апроксимацию, не удаётся заметно понизить минимальное значение J_F; это свидетельствует о том, что значение (26.14) лежит близко к точному минимуму J_F.

В результате тепловой флуктуации поляризации F'-центр может диссоциировать, образуя свободный полярон и F-центр. Энергия такой тепловой диссоциации $W_{F'}$ получается путём прибавления к энергии полярона энергии F-центра и вычитания энергии F'-центра:

$$W_{F'} = H_{0,\ldots,0,\ldots} + J_{F'} - J_{F'}. \tag{26.16}$$

Используя формулы (16.20), (24.10) и (26.14), получаем:

$$W_{F'} = \frac{\mu e^4}{2\hbar^2}[\frac{1}{n^2}\left(\frac{2z}{3} - \frac{4}{9}\right) + \\ + \frac{1}{\varepsilon}\left(\frac{2}{3} + z^2 - 2z\right)\Bigg] - \frac{3}{2}\hbar\omega. \tag{26.17}$$

Если $W_{F'} > 0$, то F'-центр устойчив и для его диссоциации необходимо затратить энергию. Если же $W_{F'} < 0$, то в кристалле не существует F'-центров [1]).

В случае единичных положительных зарядов ($z = 1$)

$$W_{F'} = \frac{\mu e^4}{2\hbar^2\varepsilon}\left[\frac{2}{9}\frac{1}{n^2} - \frac{1}{3\varepsilon}\right] - \frac{3}{2}\hbar\omega. \tag{26.18}$$

Если можно здесь пренебречь последним членом, то условие существования F'-центров запишется в виде

$$\frac{\varepsilon}{n^2} > \frac{3}{2}. \tag{26.19}$$

Это неравенство выполняется для большинства ионных кристаллов.

Представляет интерес вопрос о том, могут ли в идеальном кристалле в отсутствии положительного заряда два электрона локализоваться в общей самосогласованной поляризационной потенциальной яме. Такое состояние естественно называть биполяроном. К этому случаю легко перейти,

полагая $z \to 0$ во всех формулах этого параграфа. При этом из формулы (26.17) получается:

$$W_6 = \frac{\mu e^4}{2\hbar_\varepsilon^2}\left[\frac{2}{3}\frac{1}{6} - \frac{4}{9}\frac{1}{n^2}\right] - \frac{3}{2}\hbar\omega. \tag{26.20}$$

Если можно пренебречь здесь последним членом, то условие $W_6 > 0$ сведётся к неравенству

$$\frac{\varepsilon}{n^2} < \frac{3}{2}. \tag{26.21}$$

Кроме этого неравенства, для существования биполярона необходимо, чтобы коэффициент $\alpha_{F''}$, определяемый формулой (26.13), при $z \to 0$ был положителен. Для этого должно быть

$$\frac{\varepsilon}{n^2} > 2. \tag{26.22}$$

Это неравенство несовместимо с (26.21). Следовательно, биполяронных состояний не существует в области применимости настоящей теории.

10.5 IV Theory of F-centers and F'-centers with Quantum Approach to Motion of Ions [38]

10.5.1 § 27. Energy spectrum and ψ-function of the crystal with F-center

В случае F-центра (аналогично случаю полярона) взаимодействие электрона с продольными поляризационными колебаниями ионов гораздо сильнее, чем взаимодействие с поперечными поляризационными и с акустическими колебаниями. Последние поэтому в первом приближении можно отделить как изолированную консервативную подсистему, подобно тому как это делалось в § 12.

Оператор энергии электрона и продольных оптических колебаний ионов при наличии F-центра проще всего можно получить, добавляя к знакомому уже нам оператору энергии полярона (12.18) энергию взаимодействия электрона с дефектом (23.1). В результате оператор энергии принимает вид

$$\mathbf{H} = -\frac{\hbar^2}{2\mu}\Delta + e\int\frac{(\boldsymbol{r}-\boldsymbol{r}_1)\,\boldsymbol{P}(\boldsymbol{r}_1)}{|\boldsymbol{r}-\boldsymbol{r}_1|^3}d\tau_1 - \\ - \frac{ze^2}{\epsilon\boldsymbol{r}} + \frac{1}{2}\sum_{\boldsymbol{x}} h\omega_{\varkappa}\left(q_{\varkappa}^2 - \frac{\partial^2}{\partial q_{\varkappa}^3}\right). \tag{27.1}$$

Энергия системы предполагается равной нулю; когда все ионы покоятся в равновесных положениях, в кристалле существует лишь поляризация, вызванная

[81]) Неравенство $W_{F'} < 0$ означает, что непрерывный энергетический спектр диссоциированных состояний системы (состояний с F-центром и свободным поляроном) простирается ниже рассчитанного уровня F'-центра. В этом случае незаконен вышеприведённый расчёт энергии F'-центра прямым вариационным методом.

«положительно заряженным дефектом», а электрон проводимости находится вдали от дефекта на дне зоны проводимости.

Для вычисления энергетических уровней системы вместо уравнения Шрёдингера был использован вариационный прин-

цип квантовой механики. Собственная функция системы апроксимировалась мультипликативной формой

$$\Psi\left(r,\ldots,q_x,\ldots\right)=\Psi(r)\Phi\left(\ldots,q_x,\ldots\right). \tag{27.2}$$

Дальнейший ход решения задачи аналогичен § 14, где рассматривался полярон.

Введём обозначения

$$\bar{P}_{\varkappa}=\int P_{\varkappa}|\Phi|^2dq,\quad dq=\prod dq_{\varkappa} \tag{27.3}$$

$$\bar{H}_{\text{on}}\|=\int \Phi^{*}\text{H}_{\text{on}}\|\Phi dq \tag{27.4}$$

$$D\left[\psi,r_1\right]=e\int|\psi(r)|^2\frac{(r_1-r)}{\left|r_1-r\right|^3}d\tau \tag{27.5}$$

$$D_{\varkappa}[\psi]=\int D\left[\psi,r_1\right]\chi_{\varkappa}\left(r_1\right)d\tau_1 \tag{27.6}$$

Волновые функции системы являются экстремалями функционала

$$\begin{aligned}\bar{H}=\textstyle\int\Psi^{*}\text{H}\Psi d\tau dq=\frac{\hbar^2}{2\mu}\int|\nabla\psi|^2d\tau-\sum_x\bar{P}_xD_x[\psi]-\\ -\frac{e^2}{\varepsilon}\int\frac{|\psi|^2}{r}d\tau+\bar{H}_{\text{oII}}\,\|\end{aligned} \tag{27.7}$$

Необходимо найти экстремумы этого функционала, варьируя независимо ψ и Φ, но сохраняя их нормировку.

Варьируя Φ при произвольном фиксированном ψ и приравнивая соответствующую вариацию $\vec{H}$ нулю, мы приходим к уравнению Эйлера следующего вида:

$$\left(\sum_x\mathbf{H}_x\right)\Phi=\lambda\Phi \tag{27.8}$$

$$\mathbf{H}_x=\frac{\hbar\omega_x}{2}\left[\left(q_x-q_{x0}\right)^2-\frac{\partial^2}{\partial q_x^3}\right]-\frac{c_x}{8\pi}D_x^2[\Psi] \tag{27.9}$$

$$q_{x0}=\sqrt{\frac{c_x}{4\pi\hbar\omega_x}}\cdot D_x[\Psi]. \tag{27.10}$$

При подстановке

$$\Phi=\prod_x\Phi_{n_x}\left(q_x-q_{x0}\right),\lambda=\sum_x\lambda_x \tag{27.11}$$

в уравнении (27.8) переменные разделяются. В результате получается:

$$\Phi_{n_{\varkappa}}\left(q_{\varkappa}-q_{\varkappa 0}\right)=e^{-\frac{1}{2}\left(q_{\varkappa}-q_{\varkappa 0}\right)^{2^2}}\cdot H_{n_{\varkappa}}\left(q_{\varkappa}-q_{\varkappa 0}\right) \tag{27.12}$$

$$\lambda_{\varkappa}=\hbar\omega_{\varkappa}\left(n_{\varkappa}+\frac{1}{2}\right)-\frac{c_{\varkappa}}{8\pi}D_{\varkappa}^3[\psi]. \tag{27.13}$$

Здесь H_{n_x} - полиномы Чебышева-Эрмита степени n_{x^*}. Подставляя (27.11-13) в функционал (27.7), получаем:

$$\bar{H}[\Psi] = \frac{\hbar^2}{2\mu}\int |\nabla\psi|^2 d\tau - \frac{1}{8\pi}\sum_x c_x D_x^2 - \frac{e^2}{\varepsilon}\int \frac{|\psi|^2}{r} d\tau +$$
$$+ \sum_x \hbar\omega_x \left(n_x + \frac{1}{2}\right) \tag{27.14}$$

Теперь уже этот функционал зависит только от ψ и его следует минимизировать, варьируя ψ. Пренебрегая дисперсией поляризационных волн в кристалле, будем в дальнейшем считать $\omega_\varkappa$ и $c_\varkappa$ не зависящими от $\boldsymbol{x}$ и равными своим предельным значениям ω и c, характерным для предельного случая $x \to 0$. Тогда, вынося в формуле (27.14) коэффициент c_z за знак суммы, подобно тому как это делалось в § 14 , получаем:

$$\bar{H}[\psi] = J_F[\psi] + \sum_x \hbar\omega \left(n_x + \frac{1}{2}\right) \tag{27.15}$$

$$J_F[\psi] = \frac{\hbar^2}{2\mu}\int |\nabla\psi|^2 d\tau - \frac{c}{8\pi}\int D^2[\psi, r] d\tau - \frac{e^2}{\varepsilon}\int \frac{|\psi|^2}{r} d\tau \tag{27.16}$$

Основное состояние электрона соответствует абсолютному минимуму функционала $J_F[\psi]$. Последний был найден в § 24; результаты вычислений представлены формулами (24.1), (24.5) и (24.10). Используя эти результаты, энергию системы в случае, когда электрон находится в основном состоянии, можно представить в виде

$$\left.\begin{array}{c} H_{1s,\ldots,n_x,\ldots} = -A\left(1 + \frac{\varepsilon c}{3}\right)^2 + \hbar\omega \sum_x \left(n_x + \frac{1}{2}\right), \\ A = \frac{\mu e^4}{2\hbar^2\varepsilon^2}. \end{array}\right\} \tag{27.17}$$

Соответствующая Ψ-функция системы имеет вид

$$\Psi_{1s,\ldots,n_x},\ldots = \psi_{18}(r)\prod_x \Phi_{n_x}. \tag{27.18}$$

Основное состояние системы получим, полагая в этих формулах $n_x = 0$.

Переходя к рассмотрению возбуждённых состояний системы, заметим прежде всего, что когда в вариационном принципе квантовой механики для апроксимации Ψ-функции применяется произвольно ограниченная форма (в данном случае имеется в виду произвольное мультипликативное ограничение (27.2)), то, вообще говоря, собственные значения энергии не совпадают даже приближённо с относительными экстремумами функционала $\bar{H}$. Согласно теории прямых вариационных методов, первый возбуждённый уровень энергии следует искать как абсолютный минимум функционала $\bar{H}$ при дополнительном условии ортогональности Ψ-функции к Ψ-функции предварительно найденного основного состояния; второй возбуждённый уровень энергии следует искать как абсолютный минимум функционала $\bar{H}$ при двух дополнительных условиях ортогональности Ψ-функции к предварительно найденным Ψ-функциям основного и первого возбуждённого состояния и т. д.

Легко проверить, что, задавая в (27.18) различные целочисленные значения n_x, мы получим как раз систему ортогональных функций, которые являются абсолютными минималями функционала $\bar{H}$ при вышеупомянутых дополнительных условиях ортогональности. Следовательно, этим функциям можно придавать физический смысл

и рассматривать их как состояния, в которых поляризационные колебания ионов возбуждены, а электрон находится в своём основном состоянии.

Наряду с рассмотренными выше состояниями (27.18), в которых электрон находился в основном состоянии, существуют и другие состояния системы с возбуждённым электроном. Эти состояния были рассмотрены тоже с помощью вариационного метода, причём Ψ-функция системы апроксимировалась мультипликативной формой (27.2). Первое из таких возбуждённых состояний является абсолютной минималью функционала $\bar{H}$ при дополнительном условии ортогональности $\psi(r)\psi_{18}(r)$. Задача снова сводится к минимизации

функционала $J_F[\psi]$, но на этот раз при дополнительном условии ортогональности ψ к Ψ_{18}. Исследования качественного характера заставили остановиться на апроксимации состояния электрона функцией вида

$$\psi_{2p} = \frac{8}{\sqrt{2\pi}}(\alpha\beta)^{5/2} r e^{-2\alpha\beta r}\cos\vartheta. \tag{27.19}$$

Здесь α-тот же параметр, который фигурировал в выражении функции ψ_{1s} (см. формулы (24.1), (24.5)), а β - параметр, подлежащий вариации. Функция (27.19) нормирована и ортогональна к функции ψ_{1s} -

Функция (27.19) была подставлена в функционал $J_F[\psi]$, после чего параметр β был определён из условия минимума этого функционала. Согласно вычислениям Г. Е. Зильбермана [43] получилось:

$$2\beta = \frac{1 + 0,3914\cdot\varepsilon c}{3+\varepsilon c}, \tag{27.20}$$

$$J_F\left[\psi_{2p}\right] = -\frac{1}{4}A(1+0,3914\cdot\varepsilon c)^2. \tag{27.21}$$

При этом энергия системы, определяемая формулой (27.15), равна

$$\begin{aligned} H'_{2p,\ldots,n'_x,\ldots} &= -\frac{1}{4}A(1+0,3914\cdot\varepsilon c)^2 + \\ &+ \hbar\omega\sum_x\left(n'_x + \frac{1}{2}\right). \end{aligned} \tag{27.22}$$

Были рассчитаны и некоторые другие возбуждённые состояния электрона [43], однако они в дальнейшем не понадобятся и здесь рассмотрены не будут.

Следует иметь в виду, что при различных состояниях электрона $\psi_{1s}, \psi_{3p}, \ldots$ будут соответственно различными электростатическая индукция $|\psi|^2$-облака элек грона $\boldsymbol{D}[\psi, \boldsymbol{r}]$ и равновесные положения ионов q_{x0} (см. формулы (27.5) и (27.10)). Чтобы различать эти величины для разных состояний электрона, снабдим их теми же индексами, что и ψ-функции электрона; так, в основном состоянии запишем $\boldsymbol{D}_{18}, \boldsymbol{D}_{218}$, $q_{\boldsymbol{x}1s}$, а в первом возбуждённом состоянии - $\boldsymbol{D}_{2p}, \boldsymbol{D}_{\boldsymbol{x}2p}, q_{\boldsymbol{x}2p}$.

10.5.2 § 28. Absorption of light by F-centers

В этом параграфе будет рассмотрен фотопереход электрона из состояния ψ_{18} в состояние ψ_{2p}. При этом будет принято во внимание и существенно отразится на результатах то обстоятельство, что электрон сильно взаимодействует с продольными поляризационными колебаниями ионов.

Перед фотопереходом система находится в исходном состоянии

$$\Psi_{18,\ldots,n_{x'}\cdots=} = \Psi_{1s}(r)\prod_x \Phi_{n_x}\left(q_x - q_{x18}\right). \tag{28.1}$$

В результате фотоперехода она оказывается в конечном состоянии

$$\Psi'_{2p,\ldots,n'_x,\ldots} = \xi'_{2p}(\boldsymbol{r})\prod_x \Phi_{n'_x}\left(q_x - q_{x2p}\right). \tag{28.2}$$

При фотопереходе поглощается свет, частота которого определяется соотношением

$$\begin{aligned}\hbar\omega_l &= H_{2p,\ldots,n'_x,\ldots} - H_{1s,\ldots,n'_x\ldots} = \\ &= A\left(0,75 + 0,471\cdot\varepsilon c + 0,0728\cdot\varepsilon^2 c^2\right) + t\hbar\omega,\end{aligned} \tag{28.3}$$

где

$$l = \sum_x \left(n'_x - n_x\right) \tag{28.4}$$

есть целое число - суммарное число квантов колебаний ионов, рождённых в результате фотоперехода.

Вероятность перехода в единицу времени равна

$$P_{12} = \frac{4\pi^2 e^2}{\hbar^2}\left|Z_{12}\right|^2 \frac{S\left(\omega_l\right)}{c_1 n\left(\omega_l\right)}. \tag{28.5}$$

Здесь S - спектральная плотность интенсивности света, c_1 скорость света в пустоте, Z_{12} - матричный элемент проекции радиуса-вектора электрона на направление электрического поля световой волны, которое предполагается направленным вдоль оси Oz . Формула (28.5) отличается от обычной формулы для атомов в вакууме [44] множителем $n\left(\omega_l\right)$ в знаменателе - показателем преломления света в кристалле.

Общее количество световой энергии, поглощаемой линией ω_l за единицу времени в 1 c^3 кристалла, равно

$$S\left(\omega_l\right)\tau_l \equiv \hbar\omega_l N\cdot\sum_{(l)} P_{12}. \tag{28.6}$$

Здесь N-концентрация $\dot{F}$-центров, а $\sum_{(l)}$ означает суммирование по всем переходам, при которых поглощается энергия $\hbar\omega_l$, т. е. суммирование по всем конечным состояниям, у которых квантовые числа n'_x удовлетворяют соотношению (28.4) при заданном l.

Приступая к вычислению матричного элемента

$$\begin{aligned}Z_{12} = \int \psi^*_{18}(r) z\psi_{2p}(r)d\tau \prod_x \int \Phi^*_{n_x}\left(q_x - q_{x18}\right)\times \\ \times\,\Phi_{n'_x}\left(q_x - q_{x2p}\right)dq_x\end{aligned} \tag{28.7}$$

введём следующие обозначения:

$$z_{12} = \int \psi^*_{1s} z\psi_{2p}d\tau = \frac{32}{\sqrt{7}}\frac{(2\beta)^{t/2}}{\alpha}\cdot\frac{2\beta+6}{(2\beta+1)^6} \tag{28.8}$$

и

$$s_\varkappa = \int \Phi^*_{n_\varkappa}\left(q_\varkappa - q_{\varkappa 1s}\right)\Phi_{n'_\varkappa}\left(q_\varkappa - q_{\varkappa 2p}\right)dq_\varkappa =$$

$$= \begin{cases} 1 - \frac{1}{2}\left(q_{\varkappa 18} - q_{\varkappa 2p}\right)^2\left(n_\varkappa + \frac{1}{2}\right) + \ldots \text{ при } n'_\varkappa = n_\varkappa, \\ \left(q_{\varkappa 18} - q_{\varkappa 2p}\right)\sqrt{\frac{n_\varkappa+1}{2}} + \ldots & \text{при } n'_\varkappa = n_\varkappa + 1, \\ -\left(q_{\varkappa 18} - q_{\varkappa 2p}\right)\sqrt{\frac{n_\varkappa}{2}} + \ldots & \text{при } n'_\varkappa = n_\varkappa - 1. \end{cases} \tag{28.9а}$$

Здесь q_{x1s} и q_{x2p} являются бесконечно малыми величинами: они пропорциональны $L^{-3/3}$, где L - длина ребра куба, представляющего собой основную область цикличности, в которой ортонормированы базисные функции $\chi_\varkappa(r)$ (см. § 12). Многоточием в формулах (28.9) обозначены члены высшего порядка малости.

Рассмотрим сначала «чисто электронный» переход, при котором осцилляторные квантовые числа не изменяются. В этом случае все s_x имеют значение (28.9а). Произведение, фигурирующее в формуле (28.7), имеет вид

$$s = \prod_\varkappa s_\varkappa = \prod_\varkappa \left[1 - \frac{1}{2}\left(q_{\varkappa 1s} - q_{\varkappa 2p}\right)^2 \times \right.$$
$$\left. \times \left(n_\varkappa + \frac{1}{2}\right) + \ldots\right]. \tag{28.10}$$

Здесь бесконечно большое число множителей: по мере того как L неограниченно увеличивается, плотность волновых чисел x так же стремится к бесконечности, как L^3. С другой стороны, каждый множитель стремится к единице, отличаясь от единицы на величину порядка L^{-3}. После раскрытия неопределённости получается:

$$s = \lim_{L\to\infty}\prod_x s_x = e^{-\frac{1}{2}\sum_x\left(q_{x1s}-q_{x2p}\right)^2\left(n_x+\frac{1}{2}\right)}. \tag{28.11}$$

Легко убедиться в том, что отброшенные члены высшего порядка малости в (28.9а) исчезают в предельном выражении (28.11).

Перейдём теперь к рассмотрению переходов, при которых осцилляторные квантовые числа n_x изменяются. Сначала рассмотрим переходы, при которых $\tilde{l}_1$ квантовых чисел n_{x_i} возрастает на единицу, а l_2 других квантовых чисел n_{x_j} убывает на единицу. Этот случай отличается от рассмотренного выше тем, что в произведении

$$\prod_\varkappa \int \Phi^*_{n_\varkappa}\left(q_\varkappa - q_{\varkappa 18}\right)\Phi_{n'_\varkappa}\left(q_\varkappa - q_{\varkappa 2p}\right)dq_\varkappa \tag{28.12}$$

l_1 множителей имеет значение не (28.9а), а (28.9б), тогда как l_2 других множителей имеет вместо (28.9а) значение (28.9в). Изъятие любого конечного числа множителей вида (28.9а) в пределе не изменит произведения (28.12), поэтому остаётся лишь ввести дополнительно соответствующее число множителей вида (28.9б) и (28.9в). Таким образом, для рассматри-

ваемых переходов, при которых l_1 колебательных квантов рождается и l_2 квантов поглощается,

$$\prod_x s_z = \pm s\prod_{i=1}^{l_1}\left(q_{x_i 18} - q_{x_i 2p}\right) \times$$
$$\times \sqrt{\frac{n_{x_i}+1}{2}}\prod_{j=1}^{l_2}\left(q_{x_j 18} - q_{xj2p}\right)\sqrt{\frac{n_{x_j}}{2}}. \tag{28.13}$$

Перейдём теперь к вычислению суммы, фигурирующей в формуле (28.6):

$$\sum_{(a)} P_{12} = \frac{4\pi e^2 \left|z_{12}\right|^2 S\left(\omega_l\right)}{\hbar^2 c_1 n\left(\omega_l\right)} R_l \tag{28.14}$$

где

$$R_l = \sum_{(l)} \left| \prod_x s_x \right|^2 . \tag{28.15}$$

Суммирование проведём в два этапа: сначала просуммируем по всем переходам, при которых поглощается l_2 осцилляторных квантов и рождается $l_1 = l_2 + l$ квантов; затем просуммируем по всем возможным положительным значениям числа l_2 при фиксированном l. Первая сумма имеет вид

$$R_{l_1 l_2} = \sum_{(l_1 l_2)} \left| \prod_{\varkappa} s_{\varkappa} \right|^2 = \frac{s^2}{l_1 l_2!} \underbrace{\ldots,\kappa_i,\ldots\ldots}_{1} \underbrace{\ldots,x_j\ldots}_{l_2} \prod_{i=1}^{l_1} \left(q_{x_i 1s} - q_{x_i 2p}\right)^2 \times$$

$$\times \frac{n_{x_i}+1}{2} \prod_{j=1}^{l_2} \left(q_{x_j 18} - q_{x_j 2p}\right)^2 \frac{n_{x_j}}{2}. \tag{28.16}$$

Это суммирование учитывает возможность многими способами выбрать l_1 осцилляторов повышающих и l_2 осцилляторов, понижающих свои квантовые числа на единицу. Деление на l_1 ! и l_2 ! связано с тем, что слагаемые, отличающиеся друг от друга перестановкой индексов $\boldsymbol{x}_i$, а также перестановкой индексов x_j, соответствуют не разным, а одному и тому же квантовому переходу и должны учитываться только один раз.

В формуле (28.16) имеется в виду суммирование членов, у которых все индексы x_i и x_j различны. Однако легко по-

казать, что члены, у которых совпадают два и более индексов x_i, x_j, составляют в сумме бесконечно малую величину, исчезающую при $L \to \infty$. Поэтому суммирование можно распространить на все без исключения комбинации индексов x_i и $\boldsymbol{x_j}$.

Наряду с рассмотренными выше переходами следовало бы рассмотреть и такие переходы, при которых квантовые числа осцилляторов изменяются больше, чем на единицу. Но вычисление показывает, что эти переходы дают в сумме (28.15) слагаемые высшего порядка малости, исчезающие в пределе $L \to \infty$.

В формуле (28.16) сумму произведений можно заменить произведением сумм вида

$$\left.\begin{array}{c} \sum_x \left(q_{x18} - q_{x2p}\right)^2 \left\{ \begin{array}{ll} n_x + 1, & \\ n_x & \end{array} \right. = a \left\{ \begin{array}{l} \bar{n}+1, \\ \bar{n}, \end{array} \right\} \\ a = \sum_x \left(q_{x18} - q_{x2p}\right)^2 . \end{array}\right\} \tag{28.17}$$

Здесь предполагается, что колебания ионов находятся в тепловом равновесии и среднее значение n_x выносится за знак суммы

$$\bar{n} = \frac{1}{e^{\frac{n\omega}{\mathrm{kT}}} - 1} \tag{28.18}$$

Из формул (28.17), (27.10), (27.6) и (27.5) получается:

$$a = \frac{c}{4\pi\hbar\omega} \sum_x \left(D_{x^{1s}} - D_{x^2p}\right)^2 = \frac{c}{4\pi\hbar\omega} \int \left(D_{1s} - D_{2p}\right)^2 d\tau \tag{28.19}$$

Если этот интеграл вычислить с помощью формул (27.5), (24.1), (24.5), (27.19) и (27.20), то получается:

$$a = \frac{A}{\hbar\omega}\varepsilon c(3+\varepsilon c)\left\{\frac{3}{7} - 2\beta\cdot 0,6086+\right.$$
$$\left.+\frac{1}{7}\left(\frac{2\beta}{2\beta+1}\right)^5\left[7(2\beta+1)+19+\frac{25}{2\beta+1}+\frac{15}{(2\beta+1)^2}\right]\right\}\cdot (\tag{28.20}$$

Для большинства ионных кристаллов $1 \leqslant \varepsilon c \leqslant 2$. В этом случае можно выражение (28.20) с точностью до трёх

десятичных знаков приближённо выразить с помощью простой формулы

$$a = \frac{A}{\hbar\omega}\left[-0,003+0,706\varepsilon c+0,201(\varepsilon c)^2\right]. \tag{28.21}$$

С помощью обозначений (28.17) можно формулу (28.16) записать в виде

$$R_{l_1 l_2} = \frac{s^2}{l_1 1 l_2 1}\left(a\frac{\bar{n}+1}{2}\right)^{l_1}\left(a\frac{\bar{n}}{2}\right)^{l_2} \tag{28.22}$$

а формулу (28.11) - в виде

$$s = e^{-\frac{1}{2}\left(\bar{n}+\frac{1}{2}\right)a}. \tag{28.23}$$

Для вычисления суммы (28.15) необходимо $R_{l_1 l_2}$ просуммировать по всем l_1 и l_2, разность которых равна заданному l:

$$R_l = \sum_{l_3=0}^{\infty} R_{l_2+l,l_9} = s^2\left(a\frac{\bar{n}+1}{2}\right)^l \sum_{l_3=0}^{\infty}\frac{\left(a^2\frac{(\bar{n}+1)\bar{n}}{4}\right)^{l_2}}{(l_2+l)!l_2!} =$$
$$= s^2\left(1+\frac{1}{n}\right)^{l/2} l_l(z) \tag{28.24}$$
$$z = a\sqrt{(\bar{n}+1)\bar{n}}$$

где $I_l(z)$ - бесселева функция порядка l от мнимого аргумента:

$$I_l(z) = \frac{1}{i^l}J_l(iz) \tag{28.25}$$

Общее количество световой энергии, поглощаемой линией ω_2 за единицу времени в $1c^3$ кристалла, согласно формулам (28.6) и (28.14) равно

$$\tau_l S(\omega_l) = \frac{4\pi e^2 |z_{12}|^2 N\omega_l}{\hbar c_1 n(\omega_l)} S(\omega_l) R_l \tag{28.26}$$

Спектр поглощения состоит из ряда эквидистантных линий, расстояние между которыми равно частоте колебаний ионов ω.

Формулы (28.24) и (28.26) показывают, что интенсивность поглощения плавно изменяется от линии к линии. Ниже будет показано, что наиболее интенсивные линии соответствуют фотопереходам, при которых рождается 20 - 30 квантов

колебаний ионов. Спектральная ширина области поглощения света порядка $0,4-1,0$ эл.-в, а расстояние между соседними линиями порядка $0,02-0,03$ эл.-в.

В принятой нами выше модели диэлектрического континуума все поляризационные (оптические) колебания ионов обладают одинаковыми собственными частотами. В действительности же в кристалле существует дисперсия, т. е. собственные частоты оптических колебаний ω_x являются непрерывными функциями $\boldsymbol{x}$ и с ростом $\boldsymbol{x}$ убывают, изменяясь в общем процентов на десять. Учёт этой дисперсии приводит к расширению упомянутых выше дискретных линий поглощения. Поскольку последние расположены весьма близко друг к другу, они перекрываются, образуя непрерывный спектр поглощения. В интервале световых частот $d\omega_l$ заключается

$$\frac{d\omega_l}{\omega} \tag{28.27}$$

линий поглощения, и следовательно, поглощается за единицу времени энергия, равная

$$\tau_l S\left(\omega_l\right) \frac{d\omega_l}{\omega}. \tag{28.28}$$

Таким образом, коэффициент поглощения равен

$$\tau\left(\omega_l\right) = \frac{\tau_l}{\omega} = \frac{4\pi e^2 \left|z_{12}\right|^2 N\omega_l}{\hbar n\left(\omega_l\right) c_1 \omega} s^2 \left(1+\frac{1}{\bar{n}}\right)^{l/2} I_l(z), \tag{28.29}$$
$$\omega_l = \omega_0 + l\omega, \quad z = a\sqrt{(\bar{n}+1)\bar{n}}.$$

Здесь ω_0 - частота света, поглощаемого при «чисто электронном» переходе, а l можно считать непрерывно меняющейся величиной.

Эту формулу можно упростить в двух предельных случаях, которые мы будем условно называть случаем высоких температур и случаем низких температур.

Случай высоких температур.
Мы имеем в виду случай

$$z = a\sqrt{(\bar{n}+1)\bar{n}} \gg 1, \tag{28.30}$$

когда для $l \leqslant z$ имеет место приближённое равенство

$$I_l(z) \approx \frac{1}{\sqrt{2\pi z}} e^{z-\frac{l^2}{2z}} \tag{28.31}$$

Погрешность этой асимптотической формулы уже при $z = 4$ составляет $4-6\%$, а при $z = 6-3-4\%$. Вместо частоты света удобно ввести энергию светового кванта $\mathrm{Q} = \hbar\omega_l$. Если далее ввести обозначения

$$\tau_{\mathrm{MakO}} = \frac{4\pi e^2 \left|z_{12}\right|^2 NQ}{n(\Omega) c_1 \hbar^2 \omega} \frac{s^2}{\sqrt{2\pi z}} e^{z\left[1+\frac{1}{8}\ln^2\left(1+\frac{1}{\bar{n}}\right)\right]} \tag{28.32}$$

и

$$\mathrm{Q}_{\mathrm{Mak}} = A\left(0,75 + 0,471\varepsilon c + 0,0728\varepsilon^2 c^2\right) +$$
$$+\frac{\hbar\omega a}{2}\sqrt{(\bar{n}+1)\bar{n}} \cdot \ln\left(1+\frac{1}{\bar{n}}\right) \tag{28.33}$$
$$\delta = 2\hbar\omega\sqrt{2z\ln 2} \tag{28.34}$$

то, подставляя (28.31) в (28.29), получим для коэффициента поглощения следующее выражение:

$$\tau = \tau_{\text{МАКО}} e^{-\frac{4\ln 2}{\delta^2}(\Omega-\Omega_{\text{МАКО}})^2} \tag{28.35}$$

Если в формулу (28.32) подставить s в экспоненциальном виде (28.23), то получится экспоненциальная функция, приведённый показатель которой равен

$$a\left\{\sqrt{(\bar{n}+1)\bar{n}}\cdot\left[1+\frac{1}{8}\ln^2\left(1+\frac{1}{\bar{n}}\right)\right]-\bar{n}-\frac{1}{2}\right\}. \tag{28.36}$$

Выражение, стоящее в фигурных скобках, с большой точностью равно нулю, когда $\bar{n}$ меняется от $\frac{1}{2}$ до ∞. Если исключить неестественно большие значения a, то экспоненциальную функцию можно опустить и формулу (28.32) переписать в виде

$$\tau_{\text{Маке}} = \frac{4\pi e^2 \left|z_{12}\right|^2 NQ}{n(\Omega)c_1\hbar^2\omega\sqrt{2\pi z}} \tag{28.37}$$

Пренебрегая в формуле (28.35) медленным изменением $\tau_{\text{маке}}$ при изменении частоты света по сравнению с быстрым

изменением экспоненциала, можно считать $\tau_{\text{маке}}$ постоянным коэффициентом, заменив в (28.37) Ω на $\Omega_{\text{мако}}$ -

При этом $Q_{\text{мако}}$ представляет собой частоту света (в энергетических единицах), при которой коэффициент поглощения достигает своего максимального значения $\tau_{\text{макс}}$. При достаточно высоких температурах, когда $\bar{n} \geqslant \frac{1}{2}$, выражение $\sqrt{(\bar{n}+1)\bar{n}} \times \times \ln\left(1+\frac{1}{n}\right)$ практически равно единице. В этом случае

$$\mathbf{Q}_{\text{мако}} = A\left(0,75+0,471\varepsilon c+0,0728\varepsilon^2c^2\right)+\frac{\hbar\omega a}{2}. \tag{28.38}$$

Для кристаллов, у которых $1 \leqslant \varepsilon c \leqslant 2$, можно воспользоваться приближением (28.21), и в результате получается:

$$\Omega_{\text{мако}} \cong A\left(0,749+0,824\varepsilon c+0,173\varepsilon^2c^2\right). \tag{28.39}$$

Параметр б является полушириной полосы поглощения, т. е. расстоянием между двумя точками, в которых функция (28.35) равна половине своего максимального значения. Произведение

$$\delta\tau_{\text{мако}} = 8\sqrt{\pi\ln 2}\frac{e^2\left|z_{12}\right|^2 NQ_{\text{мако}}}{n\left(Q_{\text{мако}}\right)c_1\hbar} \tag{28.40}$$

не зависит от температуры.

При достаточно высоких температурах, когда

$$\left.\begin{array}{l}\frac{\hbar\omega}{\mathrm{k}T}\leqslant 1,\\ \sqrt{(\bar{n}+1)\bar{n}}\cong\frac{\mathrm{k}T}{\hbar\omega}.\end{array}\right\} \tag{28.41}$$

В этом случае

$$\delta \cong 2\sqrt{2\ln 2}\sqrt{a\hbar\omega\mathrm{k}T}. \tag{28.42}$$

Случай низких температур.

Низкими температурами будем условно называть такие температуры, при которых

$$\frac{z^2}{4(l+1)} \ll 1 \text{ и } \bar{n} \ll 1. \tag{28.43}$$

В этом случае в формуле (28.29) можно $I_l(z)$ разложить в ряд по степеням z и ограничиться первым членом разложе-

ния. В результате получается:

$$\left.\begin{array}{c}\tau = \tau_{\text{мако}}\sqrt{2\pi z}\cdot e^{-\frac{a}{2}}\frac{\left(\frac{a}{2}\right)^l}{\Gamma(l+1)}\\ l = \frac{\omega_l-\omega_0}{\omega} > 0\end{array}\right\} \tag{28.44}$$

где $\tau_{\text{мако}}$ попрежнему определяется формулой (28.37), а Г-гаммафункция. Согласно формуле (28.44) $\tau(\omega_l)$ представляется колоколообразной кривой, форма которой не зависит от температуры. Кривая достигает максимума при

$$l_{\text{МаКС}} = \frac{a}{2}. \tag{28.45}$$

Следовательно, в рассматриваемом случае низких температур $\Omega_{\text{мако}}$ выражается теми же формулами (28.38-39), которые получались в случае высоких температур (однако численное значение $\mathbf{Q}_{\text{мако}}$ теперь будет несколько бобьшим, так как ε убывает при охлаждении кристалла). Максимальное значение коэффициента поглощения при низких температурах равно

$$\tau^0_{\text{мако}} = \tau_{\text{мако}}\,(2\sqrt{(\bar{n}+1)\bar{n}})^{1/2}. \tag{28.46}$$

Значок ^{0} показывает, что данная величина относится к температуре абсолютного нуля. Формула (28.46) получена в предположении, что $l_{\text{мако}} \gg 1$ и, следовательно, можно пользоваться асимптотическим представлением $\Gamma\,(l_{\text{мако}}+1)$.

Элементарное вычисление показывает, что полуширина полосы поглощения в случае низких температур равна

$$\delta^0 = 2\hbar\omega\sqrt{a\ln 2}. \tag{28.47}$$

Произведение полуширины на максимальное значение коэффициента поглощения получается тем же, что и для высоких температур:

$$\tau^0_{\text{мако}}\cdot\delta^0 = \tau_{\text{мако}}\,\delta. \tag{28.48}$$

10.5.3 § 29. Application of statistics in case of thermal equilibrium

В § 19 был рассмотрен идеальный кристалл, в котором электронные и дырочные поляроны возникали в результате тепловой ионизации молекул кристалла. Была вычислена равновесная концентрация поляронов. В этом параграфе будет рас-

смотрен так называемый примесный полупроводник, в котором большинство электронов проводимости (поляронов) возникает в результате тепловой ионизации локальных центров (доноров). Предполагается, что энергия тепловой диссоциации для локальных центров значительно меньше, чем для молекул основного вещества, и поэтому именно первые являются основными поставщиками электронов проводимости, несмотря на то, что их концентрация меньше, чем концентрация молекул основного вещества.

В этом параграфе будут вычислены равновесная концентрация носителей тока в примесном полупроводнике, а также концентрация электронов в локальных центрах. Определению этих величин посвящено очень много опубликованных работ, основанных на старой зонной теории кристаллов. Результаты всех этих вычислений неизменно совпадают и не вызывают дискуссий с точки зрения зонной теории. Если, однако, принять во внимание изложенные выше результаты автора по теории поляронов,

F-центров и F'-центров, то статистические расчёты должны быть модернизированы и приведут к формулам для концентраций, несколько отличным от формул зонной теории.

В следующей главе будет показано, что во многих примесных полупроводниках донорами электронов проводимости являются F-центры. Поэтому рассмотрим применение статистики к кристаллу с F-центрами. Пусть N_h-концентрация положительных зарядов, вблизи которых может локализоваться электрон, образуя F-центр; это могут быть лишние положительные ионы в междуузлиях или же чаще всего вакансии отрицательных ионов. Пусть далее N_0 - концентрация электронов, аддитивно введённых в кристалл; эти электроны при темнературе абсолютного нуля все локализованы в виде F-центров (предполагается, что $N_h \geqslant N_0$). Обозначим концентрацию F-центров, F'-центров и поляронов проводимости, соответственно, через $N_F, N_{F'}$ и N.

Энергию диссоциации F-центра, в результате которой электрон покидает положительный заряд и уходит в виде свободного полярона, получим, вычитая из энергии поляронного состояния (16.30) энергию основного состояния кристалла с F-центром.

Последняя даётся формулой (27.17), если в ней положить $n_\varkappa = 0$. Таким образом, энергия диссоциации F-центра - W_F

оказывается равной (при $z = 1$)

$$W_F = \frac{\mu e^4}{2\hbar^2\varepsilon^2}\left(1 + \frac{2}{3}\varepsilon c\right) - \frac{3}{2}\hbar\omega. \tag{29.1}$$

Аналогично можно вычислить энергию диссоциации F'-центра, в результате которой образуется F-центр и свободный полярон. Для этого следует вычесть из энергии кристалла с F-центром и поляроном энергию кристалла с F'-центром. При $z = 1$ получается (см. формулу (26.18)):

$$W_{F'} = \frac{\mu e^4}{2\hbar^2\varepsilon}\left[\frac{2}{9}\frac{1}{n^2} - \frac{1}{3\varepsilon}\right] - \frac{3}{2}\hbar\omega. \tag{29.2}$$

В остальном статистический расчёт вполне аналогичен расчёту, данному в § 19. Выберем начало отсчёта энергии таким образом, чтобы энергия системы равнялась нулю, когда кристалл находится в основном состоянии, т. е., когда электроны находятся в основных состояниях F-центров, экситонов нет, а ионы совершают лишь нулевые колебания. Пусть совокупность экситонов, имеющихся в кристалле, характеризуется многомерным квантовым числом m, а суммарная энергия этих экситонов равна W_m. К энергии возбуждённого состояния системы можно притти следующим образом: переведём N электронов из F-центров в состояние поляронов, затратив на это энергию

$$NW_F + \sum_{i=1}^{N}\frac{\hbar^2 k_i^2}{2M} \tag{29.3}$$

Здесь второй член представляет кинетическую энергию поляронов. Затем $N_{F'}$ других электронов переведём из F-центров в качестве вторых электронов в другие F-центры, из которых при этом образуются F'-центры. На это потребуется затратить энергию, равную

$$N_{F'}\left(W_F - W_{F'}\right). \tag{29.4}$$

Далее возбудим колебания ионов, затратив на это энергию

$$\sum_x \overbrace{\cdots'''}^{N} \hbar\omega_{x'} n_{x^*} \tag{29.5}$$

Здесь сумма имеет N штрихов, так как с появлением каждого полярона система утрачивает три колебательные степени свободы (см. § 16). Наконец, возбудим в кристалле экситоны, затратив на это энергию W_m. В результате энергия возбуждённого кристалла оказывается равной

$$\begin{aligned} H\left(\ldots, n_x, \ldots; m, N, N_{F'}, \ldots, k_i, \ldots\right) = \\ = \sum_{x}^{\pi''\ldots} \hbar_{\omega_x n_x} + W_m + \\ + N W_F + N_{F'}\left(W_F - W_{F'}\right) + \sum_{i=1}^{N} \frac{\hbar^2 k_i^2}{2M}. \end{aligned} \tag{29.6}$$

Согласно закону канонического распределения вероятность состояния с квантовыми числами $\ldots, n_{\varkappa}, \ldots, m, N, N_{F'}, \ldots, k_i, \ldots$ равна

$$P\left(n_{\varkappa}, m, N, N_{F'}, k_i\right) = A e^{-\frac{H\left(n_{x'}, m, N, N_{F^r}, k_i\right)}{\mathrm{k}T}}. \tag{29.7}$$

Нас будет интересовать вероятность определённых значений N и N_F, при произвольных значениях прочих квантовых чисел. Эта вероятность получается путём суммирования вероятности (29.7) по всем возможным состояниям системы с данными N и N_F:

$$\begin{aligned} P\left(N, N_{F'}\right) = & \frac{A g^{N_0 - 2N_{F'}}}{N!} \frac{N_h!}{N_{F'}! N_{F'}\left(N_h - N_F - N_{F'}\right)!} \times \\ & \times \sum_{\ldots, n_{x'}, \ldots, m, \ldots, n_i, \ldots} e^{-\frac{H}{\mathrm{k}T}}, \\ N_F = & N_0 - N - 2N_{F'}. \end{aligned} \tag{29.8}$$

Здесь множитель $g^{N_0 - 2N_F}$ представляет собой кратность спинового вырождения состояний ($g = 2$); его легко получить, если учесть, что все N_0 электронов, за вычетом $2N_{F'}$ электронов, локализованных в F'-центрах, могут иметь две ориентации спина. В F'-центре (в основном состоянии) согласно § 26 имеется два электрона, у которых $\Psi\left(r_1, r_2\right)$ - симметричная

функция координат; следовательно, спины электронов могут быть ориентированы только антипараллельно. Поэтому в F'-центрах нет спинового вырождения.

В формуле (29.8) дробь с факториалами представляет собой число распределений $N_F -$ F-центров и $N_{F'} - F'$-центров на N_h вакансиях. Слагаемые суммы, отличающиеся друг от друга простой перестановкой векторов $\boldsymbol{k}_i$, соответствуют не разным, а одному и тому же состоянию системы (все поляроны тождественны). Поэтому для получения правильного результата сумма делится на N !

Переходя к вычислению суммы в формуле (29:8), введём обозначения, аналогичные обозначениям § 19:

$$\begin{aligned} \sum_{\ldots, n_x, \ldots} e^{-\frac{1}{kT} \sum_x^{T''\ldots'} \hbar \omega_x n_x} = \prod_{x}^{N} \overbrace{\cdots}^{N} \frac{1}{1 - e^{\frac{\hbar\omega}{kT}}} = \\ = Z_{\text{нон}}(T) \left(1 - e^{-\frac{\hbar\omega}{kT}}\right) 3N \end{aligned} \tag{29.9}$$

где $Z_{\text{ион}}$ - сумма состояний колебаний ионов диэлектрика без аддитивно введённых электронов. Сумма состояний экситонов

$$\sum_m e^{-\frac{W_m}{\kappa T}} = Z_{\text{ако}}(T) \tag{29.10}$$

Далее

$$\sum_{\boldsymbol{k}} e^{-\frac{\hbar^2 k^2}{2M\mathrm{k}T}} \to \left(\frac{L}{2\pi}\right)^3 \int_0^\infty e^{-\frac{\hbar^2 k^2}{2M\mathrm{k}T}} \cdot 4\pi k^2 dk = L^3 \left(\frac{M\mathrm{k}T}{2\pi\hbar^2}\right)^{3/2} \tag{29.11}$$

Используя формулы (29.9-11), можно формулу (29.8) представить в виде

$$\begin{gathered} P(N, N_{F'}) = \frac{Ag^{N_0-3N_{F'}}}{N!} \frac{N_h! Z_{\text{ион}} \cdot Z_{\text{эко}}}{N_{F'}! N_{F'} (N_h - N_F - N_{F'})!} \times \\ \times \left(1 - e^{-\frac{n\omega}{\mathrm{k}T}}\right)^{3N} \times \\ \times \left[L^3 \left(\frac{M\mathrm{k}T}{2\pi\hbar^2}\right)^{3/2}\right]^N e^{-\frac{1}{\mathrm{k}T}[NW_F + N_{F'}(W_F - W_{F'})]} \\ N_F = N_0 - N - 2N_{F'} \end{gathered} \tag{29.12}$$

Чтобы найти наиболее вероятные значения N и $N_{F'}$, необходимо найти максимум $P(N, N_{F'})$ (удобнее искать максимум логарифма этой величины). Приравнивая нулю частные производные $\ln P(N, N_{F'})$ по N и $N_{F'}$, получаем два уравнения:

$$\begin{aligned} & N(N_h - N_0 + N + N_{F'}) = \\ & = (N_0 - N - 2N_{F'}) \left(1 - e^{-\frac{\hbar\omega}{\mathrm{k}T}}\right)^{\mathrm{B}}_{L^3} \left(\frac{M\mathrm{k}T}{2\pi\hbar^2}\right)^{3/2} e^{-\frac{W_F}{\mathrm{k}T}}, \end{aligned} \tag{29.13}$$

$$\begin{aligned} & N_{F'}(N_h - N_0 + N + N_{F'}) = \\ & = \frac{1}{g^2}(N_0 - N - 2N_{F'})^2 e^{-\frac{WF - W_{F'}}{\mathrm{k}T}}. \end{aligned} \tag{29.14}$$

Из этих уравнений определяются N и $N_{F'}$.
При не слишком высоких температурах, когда большая часть аддитивно введённых в кристалл электронов находится в невозбуждённом состоянии,

$$N \text{ и } N_{\bar{F}'} \ll N_{0^\circ} \tag{29.15}$$

В этом случае уравнения (29.13-14) могут быть упрощены и сведены к

$$\begin{aligned} & N(N_h - N_0 + N + N_{F'}) = \\ & = N_0 \left(1 - e^{-\frac{\hbar\omega}{\mathrm{k}T}}\right)^3 L^3 \left(\frac{M\mathrm{k}T}{2\pi\hbar^2}\right)^{3/3} e^{-\frac{W_F}{\mathrm{k}T}} \end{aligned} \tag{29.16}$$

$$N_{F'}(N_h - N_0 + N + N_{F'}) = \frac{N_0^3}{g^2} e^{-\frac{W_F - W_{F'}}{\mathrm{k}T}}. \tag{29.17}$$

Если ввести обозначение

$$Q = \left(1 - e^{-\frac{\hbar\omega}{\mathrm{k}T}}\right)^3 L^3 \left(\frac{M\mathrm{k}T}{2\pi\hbar^2}\right)^{\%/2}, \tag{29.18}$$

то решение уравнений (29.16) и (29.17) можно записать в виде

$$\frac{N_{F'}}{N} = \frac{N_0}{g^2 Q} e^{\frac{W_{F'}}{kT}}, \tag{29.19}$$

где

$$N = \frac{-\left(N_h - N_0\right) + \left[\left(N_h - N_0\right)^2 + 4\left(1 + \frac{N_0}{g^2 Q} e^{\frac{W_{F'}}{\mathrm{k}T}}\right) N_0 Q e^{-\frac{W_F}{\mathrm{k}T}}\right]^{1/2}}{2\left(1 + \frac{N_0}{g^2 Q} e^{\frac{W_{F'}}{\mathrm{k}T}}\right)} \tag{29.20}$$

Часто число аддитивно введённых электронов N_0 совпадает с числом положительных центров N_h. Это имеет место, например, если полупроводник нейтрален, в то время как, кроме электронов, никакие другие отрицательные заряды (ионы) в кристалл не вводились. В этом случае формула (29.20) переходит в

$$N = \left(\frac{N_0 Q e^{-\frac{W_F}{\mathrm{k}T}}}{1 + \frac{N_0}{g^2 Q} e^{\frac{W_{F'}}{\mathrm{k}T}}}\right)^{1/2}. \tag{29.21}$$

При достаточно низких температурах в знаменателе второй член непременно будет значительно больше единицы, что согласно формуле (29.19) означает $N_{F'} \gg N$. При этих температурах формула (29.21) переходит в

$$N = gQe^{-\frac{W_F + W_{F'}}{2\mathrm{k}T}}. \tag{29.22}$$

Интересно отметить, что в этом случае число носителей тока N не зависит от числа доноров $N_h\,(= N_0)$, а также, что в показателе экспоненциальной функции фигурирует энергия $W_F + W_{F'}$.

При более высоких температурах может оказаться, что в формуле (29.21) в знаменателе второй член значительно

меньше единицы, т. е. $N_{F'} \ll N$. Тогда эта формула сводится к

$$N = \sqrt{N_0 Q} e^{-\frac{W_F}{2kT}}. \tag{29.23}$$

Формулы (29.21-23) получаются из (29.20), если

$$N_h - N_0 \ll N \text{ и } N_{F'}. \tag{29.24}$$

Возможен также случай обратного неравенства:

$$N_h - N_0 \gg N \text{ и } N_{F'}. \tag{29.25}$$

В этом случае формула (29.20) приближённо переходит в формулу

$$N = \frac{N_0 Q}{N_h - N_0} e^{-\frac{W_F}{\mathbf{kT}}}. \tag{29.26}$$

Все полученные выше формулы показывают, что с ростом температуры N монотонно возрастает. Следовательно, неравенство (29.15) непременно будет нарушено при достаточно высоких температурах. (При этом полученные выше формулы уже не

[81]) Формула (29.20) была впервые получена Т. И. Либерберг, но не была опубликована.

справедливы.) Нарушение этого неравенства означает, что большая часть доноров уже отдала свои электроны; с дальнейшим ростом температуры рост N прекратится, если только не возникнет термоионизация молекул кристалла, рассмотренная в § 19.

Результаты этого параграфа могут значительно отличаться от соответствующих результатов зонной теории вследствие иного значения коэффициента Q.

10.6 VI Comparison of Theory with Experiments. Application of theory to Specific Crystals

10.6.1 § 30. Defining Theory Parameters

Развитая выше теория содержит четыре параметра: ε, n, ω и μ. Эти параметры не являются специфичными только для поляронов, F-центров и F'-центров, а характеризуют и идеальный кристалл, не содержащий локальных состояний электронов. Поэтому значения параметров могут быть определены независимо от рассмотренных выше явлений путём изучения различных свойств идеальных кристаллов.

В частности, параметры ε, n и ω существенным образом входят в формулу, выражающую закон дисперсии света в идеальном кристалле, и могут быть определены из экспериментальных дисперсионных кривых, если таковые известны. Выведем формулу дисперсии для ионных кристаллов с решёткой типа каменной соли в инфракрасной области, вдали от частот, поглощаемых связанными электронами диэлектрика. В этой области частот можно считать, что электронные оболочки поляризуются безинерционно, так что их поляризация характеризуется постоянной n^2, не зависящей от частоты. Пусть $\varepsilon(\omega_l)$ означает диэлектрическую постоянную для гармонически колеблющихся полей с частотой ω_l, а под ε попрежнему будем понимать статическую диэлектрическую постоянную ($\varepsilon = \varepsilon(0)$). Совершенно аналогично тому, как был получен гамильтониан продольных поляризационных колебаний (12.13), можно и для поперечных поляризационных колебаний с большой длиной волны получить гамильтониан

$$H_{\text{on}\perp} = \frac{2\pi}{c}\sum_x \left(P_x^2 + \frac{1}{\omega^2}\dot{P}_x^2\right) = \frac{2\pi}{c}\int_{\dot{L}^a}\left[P^2(r) + \frac{1}{\omega^2}\dot{P}^2(r)\right]d\tau. \quad (30.1)$$

Этот гамильтониан описывает собственные поперечные колебания ионов идеального кристалла. Здесь ω - предельная частота собственных колебаний, одинаковая как у продольных, так и у поперечных колебаний. Если ввести световую монохроматическую волну с индукцией

$$D' = D'_0 \cos\left[\omega_l t - kr\right], \quad (30.2)$$

то энергия взаимодействия поляризационных колебаний со световой волной равна

$$-\int_{L^s} PD' d\tau \quad (30.3)$$

Раскладывая здесь под интегралом $\boldsymbol{P}$ в тригонометрический ряд вида (12.5) и осуществляя почленное интегрирование, найдём явное выражение энергии взаимодействия через нормальные координаты ионов P_x. При этом оказывается, что в энергию взаимодействия (30.3) входят только две нормальные координаты с индексами

$$x = \pm k. \quad (30.4)$$

Следовательно, только с этими двумя нормальными колебаниями взаимодействует световая волна.

Если дополнить гамильтониан (30.1) членом (30.3) и рассмотреть вынужденные колебания ионов в поле световой волны, то элементарное вычисление показывает, что вынужденные колебания создают добавочный дипольный момент инерционной поляризации, равный

$$P' = \frac{c}{4\pi}\frac{D'}{1-\frac{\omega_l^2}{\omega^2}}. \tag{30.5}$$

Кроме этого световая волна индуцирует момент безинерционной поляризации, равный

$$P'_e = \frac{n^2-1}{4\pi n^2}D'. \tag{30.6}$$

Таким образом, полный удельный дипольный момент равен

$$P'_{\text{сум}} = P' + P'_e = \frac{1}{4\pi}\left(\frac{c}{1-\frac{\omega_l^2}{\omega^2}} + 1 - \frac{1}{n^2}\right)D', \tag{30.7}$$

$\varepsilon(\omega_l)$ определяется, как всегда, соотношением

$$P' = \frac{\varepsilon(\omega_l)-1}{4\pi\varepsilon(\omega_l)}D'. \tag{30.8}$$

Отождествляя коэффициенты в формулах (30.8) и (30.7), получаем: .

$$\varepsilon(\omega_l) = n^2 + \frac{\varepsilon - n^2}{1-\frac{\varepsilon}{n^2}\frac{\omega_l^2}{\omega^2}}. \tag{30.9}$$

Вводя обозначение

$$\omega_g^2 = \frac{n^2}{\varepsilon}\omega^2, \tag{30.10}$$

можно формуле (30.9) придать привычную форму

$$\varepsilon(\omega_l) = n^2 + \frac{\varepsilon - n^2}{1-\frac{\omega_l^3}{\omega_g^2}}. \tag{30.11}$$

Это и есть формула дисперсии в упомянутой выше инфракрасной области. Частота ω_g, при которой кривая дисперсии имеет разрыв гиперболического типа, не совпалает с частотой собственных колебаний ионов ω. Правильное соотношение между этими частотами даётся формулой (30.10) [1]).

Если экспериментально известна кривая дисперсии света в кристалле, то, апроксимируя её формулой (30.11), можно определить параметры ε, n и ω. При этом ε получается как предельное значение $\varepsilon(\omega_l)$ при $\omega_l^2 \ll \omega_g^2$, а n^2-как предельное значение $\varepsilon(\omega_l)$ при $\omega_l^2 \gg \omega_g^2$, причём ω_l должно оставаться всё же меньше, чем частоты, поглощаемые связанными электронами, т. е. должно соответствовать на экспериментальной дисперсионной кривой плато между областью дисперсии существенно ионной и областью существенно электронной. Зная ε и n, получаем ω из соотношения (30.10).

К. Б. Толпыго обобщил дисперсионную формулу (30.11) [48], распространив её дальше в область, где уже проявляется

электронная дисперсия: он получил трёхчленную формулу вида

$$\varepsilon\left(\omega_l\right)=1+\frac{n^2-1}{1-\frac{\omega_l^2}{\omega_g'^2}}+\frac{\varepsilon-n^2}{1-\frac{\omega_l^2}{\omega_g^2}}. \tag{30.12}$$

Здесь введён ещё один параметр ω_g', по порядку величины равный частотам света, поглощаемого связанными электронами. С помощью этой формулы К. Б. Толпыго апроксимировал экспериментальные дисперсионные кривые для кристаллов LIF, $\mathrm{NaF}, \mathrm{NaCl}, \mathrm{KCl}, \mathrm{KBr}$, KJ в более широком диапазоне частот, чем это позволила бы формула (30.11). Результаты представлены на рис. 30.1. Здесь сплошные кривые представляют теоретический ход дисперсии согласно формуле (30.12), а точки-экспериментальные данные.

При апроксимации оказалось, что n определяется весьма точно, в то время как ε - гораздо менее точно (поскольку отсутствуют экспериментальные данные в области $\omega_l < \omega_g$). Поэтому пришлось для каждого кристалла задаваться несколькими значениями ε, выбирая их в пределах разброса экспериментальных значений, полученных разными авторами при непосредственном статическом измерении ε. Для каждого выбранного значения в проводилась апроксимация путём подбора n, ω_g и ω_g'. Результаты вычислений приведены в табл. 30.1.

В последнем столбце таблицы для сравнения приведены частоты максимумов поглощения света в тонких пластинках кристалла ω_d, измеренные Барнесом [49]. Предпочтение отдавалось тому варианту апроксимации, при котором ω_g более всего приближалось ω_d. Соответствующие строки в табл. 30.1 подчёркнуты. На рис. 30.1 приведены кривые, соответствующие подчёркнутым строчкам таблицы.

Для других ионных кристаллов, в которых дисперсия не измерялась в достаточно широком спектральном интервале, пришлось ограничиться более грубым определением параметров: показатель преломления n брался в области, где кривая дисперсии имеет горизонтальное плато между областью ионной дисперсии и областью электронной дисперсии. Для ε бралось статическое значение. Для ε разные авторы приводят иногда различные значения. Так, для ε в закиси меди ряд авторов приводит значение около 10 , тогда как в новейшей статье

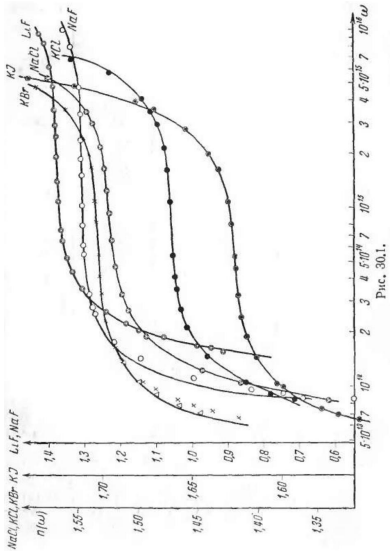

Рис. 30.1.

[81]) Следует подчеркнуть, что в литературе весьма распространено другое ошибочное соотношение между этими частотами.

Таблица 30.1

Кристалл	ε	n^2	$\omega_g \cdot 10^{-13}$	$\omega_d \cdot 10^{-13}$
	8,142	1,926	6,083	
LiF	8,726	1,926	5,864	5,782
	9,226	1,926	5,660	
NaF	5,26	1,748	4,416	4,642
	5,62	2,330	3,178	
NaCl	5,80	2,330	3,095	3,085
	6,00	2,330	3,011	
	6,29	2,330	2,898	
	4,50	2,175	2,828	
KCl	4,68	2,175	2,736	
	4,778	2,175	2,687	2,666
	4,30	2,358	2,406	
KBr	4,61	2,358	2,236	
	4,81	2,358	2,141	2,135
KJ	4,94	2,648	1,920	
	5,20	2,648	1,828	1,848

Гуддена и Хенингера [50] приводятся значения 7,88 и 8,75 . Ниже для закиси меди принимается округлённо $\varepsilon = 9$.

До последнего времени не существует сколько-нибудь надёжных методов определения эффективной массы электрона μ. Поэтому μ остаётся единственным неизвестным параметром теории. Ниже μ будет определяться путём совмещения вычисленной абсциссы (частоты) максимума F-полосы поглощения $\Omega_{\text{мако}}$ с соответствующей экспериментально измеренной величиной. Полученные таким образом значения μ приведены в табл. 31.1 .

10.6.2 § 31. Comparison with the experience of thermal dissociation energies of F-centers

Если щёлочно-галоидные кристаллы с F-центрами нагреть выше комнатноЙ температуры на несколько сот градусов, то в них появляется «темновая» электронная проводимость, зависящая от температуры по закону

$$\sigma = \sigma_0 e^{-\frac{W}{2kT}}, \tag{31.1}$$

где W у разных кристаллов колеблется между 1,3 и 2 эл.-в [51]. Таким образом, эти кристаллы превращаются в типичные полупроводники, в которых донорами электронов проводимости являются F-центры. Последнее следует из того, что аналогичное нагревание тех же кристаллов без F-центров не приводит к электронной проводимости.

Удельная электропроводность кристалла о связана с подвижностью u и концентранией поляронов N соотношением

$$\sigma = euN. \tag{31.2}$$

Как было показано в § 20 , подвижность зависит от температуры сравнительно мало (особенно при высоких температурах); поэтому наблюдающийся весьма быстрый рост

электропроводности с температурой (31.1) обусловлен температурной зависимостью концентрации поляронов N.

Равновесная концентрация поляронов в случае, когда донорами являются F-центры, была рассчитана в § 29. В рассматриваемых ниже случаях бóльшая часть аддитивно введённых в кристалл электронов находится в невозбуждённом состоянии. Кроме того в формуле (29.21) под корнем в знаменателе второй член значительно меньше единицы. Поэтому равновесная концентрация поляронов определяется формулой (29.23). Следовательно, энергия активации W, фигурирующая в формуле (31.1) и определяемая экспериментально по температурному ходу электропроводности, представляет собой энергию тепловой диссоциации F-центра.

В табл. 31.1 в четвёртой строке приведены значения $\Omega_{\text{мако}}/A$, вычисленные по формулам (28.38-39). В пятой строке приведены положения максимумов F-полос, измеренные экспериментально. Коэффициент $A = \mu e^4/2\hbar^2\varepsilon^2$ подбирался так, чтобы теоретическое значение $\mathbf{Q}_{\text{мако}}$, определяемое формулой (28.38), совпало с измеренным. Таким образом, определялись значения μ (седьмая строка таблицы) - единственного неизвестного параметра теории. Затем по формуле (29.1) вычислялись теоретические значения энергии тепловой диссоциации F-центра (восьмая строка). В девятой строке для сравнения приведены экснериментальные значения энергии тепловой диссоциации F-центра, определённые по температурному ходу электропроводности.

Таблица 31.1

	Cu_2O	NaCl	NaBr	NaJ	KCl	KBr	3	???	??	???
s	9	5,8	6,39	6,6	4,78	4,81	5,2	5,2	5,16	5,58
n^2	4	2,33	2,6	2,91	2,175	2,36	2,65	2,18	2,36	2,6
εc	1,25	1,49	1,46	1,27	1,2	1,04	0,96	1,38	1,185	1,15
$\frac{\Omega_{\text{мако}}}{A}$	2,05	2,36	2,32	2,08	1,99	1,79	1,7	2,22	1,97	1,93
$\Omega_{\text{мако}}^{(\text{вычу})} = \Omega_{\text{мако}}^{(\text{ивм})}$ (эл.-в)	0,62	2,65	2,29	2,1	2,19	1,96	1,8	1,98	1,71	1,59
A (эл.-в)	0,302	1,12	0,985	1,01	1,10	1,10	1,06	0,895	0,867	0,825
$\frac{\mu}{m}$	1,81	2,78	2,96	3,25	1,85	1,87	2,11	1,78	1,70	1,89
$W_F^{(\text{выч})}$ (эл.-в)	0,51	2,2	1,9	1,8	2,0	1,8	1,7	1,7	1,5	1,4
$W_F^{(\text{изм})}$ (эл.-в)	0,5-0,6	1,9	1,6	1,5	2,0	1,7	1,7	1,7	1,4	1,3

Для щёлочно-галоидных кристаллов использованы значения W_F, измеренные Смакулой [51] на кристаллах, равномерно окрашенных по всему объёму [1]).

В первом столбце табл. 31.1 приведены данные для закиси меди. Здесь F-центр представляет собой положительную «дырку проводимости», локализовавшуюся вблизи вакантного

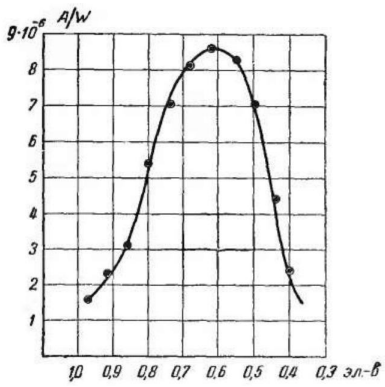

Рис. 31.1.

медного узла решётки. Спектр поглощения света F-центром в закиси меди лежит в инфракрасной области. Это поглощение сопровождается фотопроводимостью. Шенвальд [52] исследовал спектральное распределение этой фотопроводимости; его результаты представлены на рис. 31.1.

Максимум кривой соответствует энергии кванта света в 0,62 эл.-в. Кривая имеет типичную колоколообразную форму, характерную для F-центров также и в щёлочно-галоидных кристаллах [53].

Температурная зависимость электропроводности в закиси меди исследовалась многими авторами. Имеется некоторый разброс полученных значений энергии тепловой диссоциации. В табл. 31.1 использованы данные Энгельгарда [54], так как они получены на тех же образцах Cu_2O и относятся к тем же центрам, что и спектральные измерения Шенвальда.

Из сравнения двух последних строк табл. 31.1 видно, что вычисленные значения энергии тепловой диссоциации хорошо согласуются с измеренными. Согласие хуже у трёх натриевых солей, у которых поляризационный радиус F-центра оказывается меньше постоянной решётки и, следовательно, условия применимости теории нарушены [1]).

Наиболее характерной особенностью данной теории является превосходство энергии фотовозбуждения $G_{\text{мако}}$ над энергией тепловой диссоциации W_F, невзирая на то, что при фотопереходе электрон переводится на дискретный уровень, а при тепловой диссоциации - в непрерывный спектр. Объясняется это тем, что при фотопереходе рождается несколько десятков квантов колебаний ионов (см. § 28). Из табл. 31.1 видно, что вышеупомянутое превосходство энергии фотопере-

[81]) Известны опыты, в которых окрашивался не весь кристалл, а лишь его небольшая область, а затем под действием внешнего электрического поля это облако окраски двигалось по кристаллу. Перемещение такого облака происходит потому, что F-центры диссоциируют, освобождённые при этом электроны дрейфуют вдоль приложенного поля и локализуются в новых местах, образуя там F-центры. Хотя подвижность облака окраски экспоненциально зависит от температуры, не следует пытаться из этих опытов определять энергию тепловой диссоциации F-центров. Дело в том, что описанное выше

[8]движение облака сопряжено с перемещением в кристалле большого пространственного заряда и было бы немыслимо без токов нейтрализации, текущих в неокрашенной части кристалла. Поэтому подвижность облака лимитируется и определяется электропроводностью неокрашенного кристалла, которая тоже экспоненциально зависит от температуры.

[1]) Вообще щёлочно-галоидные кристаллы обладают исключительно малыми поляризационными радиусами F-центров, вследствие чего выполнение критериев теории F-центров (но не поляронов) здесь на пределе. Гораздо бобьшие радиусы F-центров должны быть в полупроводниках промышленного типа. Это видно из того, что в этих полупроводниках энергии тепловых диссоциаций F-центров порядка десятых электрон-вольта вместо $1,3-2$ эл.-в в щё-лочно-галоидных кристаллах (чем меньше энергия тепловой диссоциации F-центра, тем обычно больше его радиус). К сожалению, F-полосы поглощения в промышленных полупроводниках мало изучены, так как они лежат в инфракрасной области спектра.

хода над энергией тепловой диссоциации действительно наблюдается экспериментально.

Для краткости опустим сравнение с опытом изложенной в главе IV теории F-центров с классическим рассмотрением движения ионов; читатель найдёт его в соответствующей статье [15]. Там получены значения μ и W_F, близкие к тем, которые приведены в табл. 31.1.

Используя известные теперь значения μ, можно вычислить эффективную массу полярона M. Результаты вычисления представлены в следующей таблице:

Таблица 31.2

	NaCl	KCl	KBr	KJ	Cu_2O
$20\frac{M}{m} =$	391	160	155	167	9,69

10.6.3 § 32. Width, shape and temperature dependence of F absorption bands

Типичная форма F-полосы поглощения и её температурная зависимость изображены на рис. 32.1. На этом рисунке представлен экспериментально измеренный спектр поглощения света в кристалле KBr [55].

При дальнейшем охлаждении кристалла ниже температуры $-245°$C, вплоть до абсолютного нуля, форма F-полосы более не меняется. В случае высоких температур, когда выполняется неравенство (28.30), полуширина полосы поглощения даётся формулой (28.34). Для всех рассмотренных ниже кристаллов комнатные температуры относятся к случаю высоких температур. В табл. 32.1 дано сравнение полуширин, вычисленных по формуле (28.34), с измеренными полуширинами при комнатной температуре. При вычислении были использованы значения параметров ε, n, ω и μ, приведённые в табл. 30.1 и 31.1.

Экспериментальные значения полуширин для щёлочно-галоидных кристаллов взяты из книги П. С. Тартаковского [33], а для закиси меди - из данных Шенвальда (рис. 31.1). Поскольку для закиси меди отсутствуют экспериментальные исследования дисперсии света в инфракрасной области, не было возможности определить ω методом, изложенным в § 30 ; пришлось определить ω менее точно, по температурной зависимости подвижности электронов, как это было описано в § 20 .

$T = 293°$K

Кристалл	NaCl	KCl	KBr	KJ	Cu_2O
$\hbar\omega$(эл. $-$)	0,032	0,026	0,020	0,017	0,031
$\hbar\omega/kT$	1,28	1,04	0,795	0,675	1,24
$\sqrt{\bar{n}(\bar{n}+1)}$	0,73	0,92	1,22	1,45	0,76
$a = 2l_{\text{мако}}$	52	47,6	51,9	53,7	11,6
z	37	43,8	63,3	77,8	8,78
$\delta_{\text{выч}}$ (эл.-в)	0,47	0,40	0,37	0,35	0,22
$\delta_{\text{нам}}$ (эл.-в)	0,47	0,35	0,35	0,35	0,35

Табл. 32.1 показывает, что у щёлочно-галоидных кристаллов теоретические значения полуширин хорошо согласуются

Поэтому пока пришлось ограничиться случаем закиси меди.

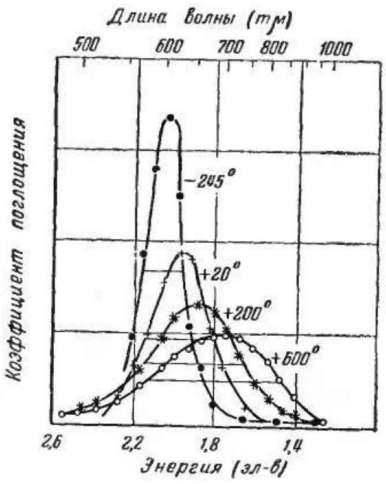

Рис. 32.1.

с опытом. У закиси меди измеренная полуширина на $0,1-0,15$ эл.-в больше, чем вычисленная, что можно объяснить следующим образом; отмеченный в предыдущем параграфе разброс экспериментальных значений энергии тепловой диссоциации F-центров в закиси меди связан с неидеальностью кристаллов и некоторой неидентичностью F-центров. Если допустить, что в упомянутых в предыдущем параграфе образцах Cu_2O энергетические уровни F-нентров имели разброс порядка $0,1-0,15$ эл.-в, то объяснятся одновременно и разброс энергий тепловой диссоциации и наблюдающееся добавочиое расширение F-полосы. Следует также иметь в виду, что теоретическая формула (28.34) выведена для кристаллов с решёткой типа каменной соли и в применении к закиси меди от неё нельзя требовать большой точности.

При нагревании кристалла ширина полосы поглощения растёт, как это видно из рис. 32.1. Для большинства кристаллов при комнатной и более высоких температурах справедлива формула (28.42), согласно которой ширина должна расти пропорционально квадратному корню из абсолютной температуры. Этот вывод теории хорошо согласуется с опытом. Так, например, в случае кристалла KBr по рис. 32.1 отношение $\delta/\sqrt{T}$ не зависит от температуры:

T	293°K	473°K	873°K
$\delta/\sqrt{T}$	0,76	0,78	0,78

(здесь б взято в условных единицах). Температура -245°C относится к случаю низких температур. В этом случае полуширина полосы определяется формулой (28.47). Для KBr вычисленное $\delta^\circ = 0,24$ эл.-в, а измеренное $\delta^\circ = 0,22$ эл.-в. у NaF$\delta^\circ_{\text{выч}} = 0,61$ эл.-в $, \delta^\circ_{\text{изм}} = 0,62$ эл.-в. Таким образом, и при низких температурах теоретическое значение полуширины согласуется с опытом.

Согласно формулам (28.40) и (28.48) произведение $\tau_{\text{мако}} \cdot \delta$ не зависит от температуры. Это свойство F-полосы действительно экспериментально наблюдается. Кроме того, поскольку теория даёт правильную температурную зависимость полуширины δ, а произведение $\tau_{\text{мако}} \cdot \delta$ не зависит от температуры, то очевидно, что теория даёт столь же правильную температурную зависимость $\tau_{\text{мако}}$ -

Не только основные параметры F-полосы (полуширина и высота), но и её характерная форма хорошо описываются в случае высоких температур формулой (28.35), а в случае низких температур - формулой (28.44). В частности, сходство F-полосы с «гауссовой кривой» (28.35) при высоких температурах отмечалось экспериментаторами ещё задолго до появления какой-либо теории F-полосы.

Независимость формы F-полосы от температуры при низких температурах, вытекающая из формулы (28.44), также наблюдается на опыте.

Опыт показывает, что при нагревании кристаллов максимумы F-полос поглощения смещаются в красную сторону [55]. Это смещение является сравнительно малым эффектом: yKBr, например, согласно рис. 32.1, при изменении абсолютной температуры от 28 до 873°K, когда полуширина и высота кривой меняются почти в четыре раза, $\Omega_{\text{мако}}$ уменьшается всего на 15%. Изложенная в главе V теория не претендует на объяснение этого малого температурного эффекта уже хотя бы потому, что при таком большом изменении температуры параметры теории ε и μ также могут заметно измениться. Интересно, однако, отметить, что формула (28.39) неожиданно хорошо описывает уменьшение $\mathbf{\Omega}_{\text{мако}}$ с температурой, если в ней учесть температурную зависимость є и пренебречь неизвестной нам температурной зависимостью μ: согласно формуле (28.39)

$$\frac{1}{Q_{\text{мако}}} \cdot \frac{dQ_{\text{мако}}}{dt} = \left[\frac{(0,824 + 2\varepsilon c \cdot 0,173)(\varepsilon c + 1)}{0,749 + \varepsilon c \cdot 0,824 + (\varepsilon c)^2 \cdot 0,173} - 2\right] \frac{1}{\varepsilon} \cdot \frac{d\varepsilon}{dt}. \tag{32.1}$$

Экспериментально найденное значение температурного коэффициента ε вблизи комнатных температур равно [56]

	NaCl	KCl
$\frac{1}{\varepsilon} \cdot \frac{d\varepsilon}{dt} =$	$3,4 \cdot 10^{-4}$	$3,03 \cdot 10^{-422 рад^{-1}}$

Если воспользоваться этими значениями и по формуле (32.1) вычислить температурную зависимость $\mathbf{\Omega}_{\text{мако}}$, то она оказывается в согласии с опытом [55]:

	NaCl	KCl
Вычисленное $\frac{1}{Q_{\text{мако}}} \cdot \frac{dQ_{\text{мако}}}{dt}$	$2,0 \cdot 10^{-4}$	$1,9 \cdot 10^{-4}$
Измеренное $\frac{1}{Q_{\text{мако}}} \cdot \frac{dQ_{\text{мако}}}{dt}$	$1,8 \cdot 10^{-4}$	$1,8 \cdot 10^{-4}$

Резюмируя изложенное в §§ 31 и 32 , следует признать, что теория не только качественно, но и количественно объясняет рассмотренные выше основные свойства F-центров.

10.6.4 § 33. On the theory of electron recombination in semiconductors [57]

Если полупроводник находится в тепловом равновесии, то среднее число электронов на различных энергетических уровнях легко вычисляется с помощью равновесной статистики. Для вычисления достаточно знать лишь энергии и кратности различных квантовых состояний электрона; не нужно знать ни механизма, ни вероятностей перехода электронов из одного состояния в другое.

Гораздо труднее рассмотреть случаи, когда тепловое равновесие нарушено, например, когда в полупроводнике создаётся добавочная проводимость путём облучения его светом, рентгеновскими лучами, γ-лучами или путём обстрела заряженными частицами. В этих случаях приходится пользоваться кинетическими уравнениями, а для этого необходимо знать вероятности рекомбинации электронов. Особенные трудности представляет теоретическое рассмотрение рекомбинации с переходом энергии в тепловую её форму, так как до последнего времени механизм тепловой рекомбинации не выяснен даже качественно. Некоторые качественные результаты в этой области получены Адировичем [71]. В кинетических уравнениях член рекомбинации обычно записывается в виде

$$\beta N' N,$$

где N - концентрация электронов проводимости, N'-концентрация центров рекомбинации, а β - коэффициент рекомбинации, который обычно определяется лишь при сравнении теории с опытом. В этом параграфе β вычисляется теоретически для некоторых важных частных случаев.

Нижеследующий расчёт коэффициента рекомбинации не опирается на предположение о том, что носителями тока являются непременно поляроны. Поэтому, хотя изложение и будет вестись в терминах поляронной теории проводимости, полученные результаты будут справедливы и для других видов носителей тока; в частности, результаты будут применимы к гомеополярным кристаллам, где носители тока имеют более сложную форму [58].

Центры рекомбинации предполагаются неподвижными (дефекты кристалла) или по крайней мере менее подвижными, чем поляроны (например, дырки проводимости, если они обладают большой эффективной массой). Если центры рекомбинации обладают положительными зарядами, то они привлекают к себе поляроны своим кулоновским полем. Если же они нейтральны, то диэлектрически поляризуются полем приблизившегося полярона, и в результате тоже возникает сила притяжения между поляроном и центром рекомбинации. В общем случае предположим, что эта сила притяжения описывается потенциалом $V(r)$ и простирается на значительное расстояние порядка нескольких свободных пробегов полярона.

Окружим мысленно центры рекомбинации сферическими поверхностями малого радиуса r и вычислим поток поляронов внутрь этих сфер. При этом предполагается, что r значительно меньше среднего расстояния между центрами, и при рассмотрении потока через данную сферу можно пренебречь силовым влиянием соседних центров. С другой стороны, предполагается, что r больше свободного пробега полярона, так что при вычислении потока можно пользоваться обычным уравнением электропроводности и диффузии. Число поляронов, втекающих за секунду внутрь упомянутых сфер в единице объёма полупроводника, равно

$$z = SNu\frac{dV}{dr} + SD\frac{dN}{dr}, \tag{33.1}$$

где u - подвижность поляронов, D - их коэффициент диффузии, а S - суммарная поверхность всех сфер в единице объёма

$$S = 4\pi r^2 N' \tag{33.2}$$

Под $N(r)$ следует понимать концентрашию вблизи многосвязной поверхности, состоящей из вышеупомянутых сфер. Эти сферы заключают в себе лишь ничтожную долю всего объёма кристалла. Поэтому электроны, возбуждённые в зону проводимости в результате облучения кристалла, после замедления и перехода в поляронное состояние чаще всего будут оказываться вне этих сфер и для рекомбинации должны будут пройти через сферы в виде потока (33.1). Последний весьма быстро приобретает квазистационарный характер: время релаксации порядка 10^{-12} сек. и меньше. Поскольку за такое малое время общее число электронов проводимости в кристалле не успевает заметно измениться, можно z считать квазистационарным потоком, не зависящим от r, и отождествить z с числом рекомбинаций, происходяцих за секунду в единице объёма.

Если из дифференциального уравнения (33.1) (считая z не зависящим от r) определить $N(r)$, концентрацию поляронов вдали от центров рекомбинации положить равной $N(\infty) = N_\infty$ и принять во внимание известное соотношение

$$\frac{D}{u} = \frac{\mathrm{k}T}{e}, \tag{33.3}$$

то получается:

$$N(r) = \left(N_\infty - \frac{z}{4\pi N' D}\int_0^\infty e^{\frac{eV}{kT}}dx\right)e^{-\frac{eV}{kT}}, \quad x = \frac{1}{r} \tag{33.4}$$

Когда полярон приближается к центру рекомбинации на расстояние r_0 - порядка радиуса полярона, то появляется некоторая вероятность теплового перехода электрона в связанное состояние. Вычислить эту вероятность исключительно трудно. Однако можно утверждать, что число электронов, переходящих в связанное состояние за одну секунду в единице объёма (число рекомбинаций), пропорционально числу центров N' и концентрации поляронов в непосредственной

окрестности центров $N(r_0)$. Таким образом, число рекомбинаций можно записать в виде

$$\beta_1 N' N(r_0),$$

где β_1 - неизвестный коэффипиент пропорциональности. Согласно формуле (33.4)

$$N(r_0) = \left(N_\infty - \frac{z}{4\pi N' D}\int_0^{\frac{1}{r_0}} e^{\frac{eV}{kT}}dx\right)e^{-\frac{eV(r_0)}{kT}} \tag{33.5}$$

Как уже упоминалось, в квазистационарном случае поток z следует приравнять числу рекомбинаций:

$$z = \beta_1 N' N(r_0). \tag{33.6}$$

Из уравнений (33.5-6) следует:

$$z = \frac{\beta_1 N' N_\infty e^{-\frac{eV(r_0)}{kT}}}{1 + \frac{\beta_1}{4\pi D}e^{-\frac{eV(r_0)}{kT}}\int_0^{\frac{1}{r_0}} e^{\frac{eV}{kT}}dx}. \tag{33.7}$$

Здесь возможны два предельных случая:

А. В знаменателе формулы (33.7) второй член значительно меньше единицы. Тогда, пренебрегая этим членом, получаем:

$$z = \beta N' N_\infty, \quad \beta = \beta_1 e^{-\frac{eV(r_0)}{kT}}. \tag{33.8}$$

Эти формулы показывают, что в коэффициент рекомбинации β входит больцмановский экспоненциальный множитель, учитывающий повышение концентрации поляронов вблизи центров рекомбинации, вызванное силовым полем $V(r)$. Однако значение β остаётся неизвестным, так как не известен коэффициент β_1.

Б. В знаменателе формулы (33.7) второй член значительно больше единицы. В этом случае

$$z = \beta N' N_\infty, \quad \beta = \frac{4\pi D}{\int_0^{\frac{1}{r_0}} e^{\frac{eV}{kT}}dx}. \tag{33.9}$$

Эти формулы представляют интерес, поскольку дают возможность вычислить коэффициент тепловой рекомбинации в различных конкретных случаях. Если неравенство случая Б не выполняется, то формула (33.9) выражает верхний предел коэффициента рекомбинации, так как она получена в результате пренебрежения единицей в знаменателе формулы (33.7).

Случаи А и Б могут быть интерпретированы следующим образом: в случае А «узким местом» процесса рекомбинации, определяющим его скорость, является не привлечение

поляронов к центрам рекомбинации, а переход электронов в связанное состояние. Поэтому коэффициент рекомбинации β не зависит от коэффициента диффузии D (или подвижности u), а определяется вероятностью перехода электрона в связанное состояние (β_1). В случае Б, наоборот, определяющим фактором для скорости рекомбинации является не переход электрона в связанное состояние, а привлечение поляронов к центрам рекомбинации. Поэтому β не зависит от β_1, а зависит от D (или u). Ниже речь будет итти только о случае Б.

Рекомбинация на положительно заряженных центрах. Потенциал взаимодействия полярона с центром имеет кулоновскую форму

$$V = -\frac{e}{\varepsilon r} = -\frac{e}{\varepsilon}x, \tag{33.10}$$

где ε - диэлектрическая постоянная. В формуле (33.9) интеграл от 0 до $\frac{1}{r_0}$ можно заменить интегралом от 0 до ∞, если

$$e^{-\frac{e^2}{\varepsilon r, kT}} \ll 1. \tag{33.11}$$

Таким образом,

$$\int_0^{\frac{1}{r_0}} \frac{eV}{e^{\mathrm{k}T}} dx \cong \int_0^{\infty} e^{-\frac{e^e x}{\varepsilon \mathrm{k}T}} dx = \frac{\varepsilon \mathrm{k}T}{e^2} \tag{33.12}$$

Подставляя это в формулу (33.9), получаем:

$$\beta = \frac{4\pi D e^2}{\varepsilon \mathrm{k}T} = \frac{4\pi e u}{\varepsilon}. \tag{33.13}$$

При таком коэффициенте рекомбинации для среднего времени
жизни электрона в свободном состоянии получается выражение

$$t = \frac{1}{\beta N'} = \frac{\varepsilon}{4\pi e u N'} \tag{33.14}$$

Средний сдвиг электрона под влиянием внешнего электрического поля $-\Delta^1$) получается умножением t на дрейфовую скорость полярона $\mathfrak{v} = uE$:

$$\Delta = tuE = \frac{\varepsilon E}{4\pi e N'} \tag{33.15}$$

В рассматриваемом частном случае сдвиг, оказывается, не зависит от подвижности и от температуры.

Если облучение кристалла за секунду в единице объёма возбуждает L электронов в зону проводимости, то в стационарном случае

$$L = \beta N' N_\infty. \tag{33.16}$$

Отсюда с помощью формулы (33.13) получается:

$$\sigma = euN_\infty = \frac{\epsilon L}{4\pi N'}. \tag{33.17}$$

Здесь σ есть удельная электропроводность кристалла, вызванная стационарным облучением. Формула (33.17) показывает, что при данном фиксированном N' о не зависит от подвижности и температуры.

Рекомбинация на нейтральных центрах. Нейтральный центр диэлектрически поляризуется полем приблизившегося полярона. Возникающий при этом дипольный момент равен

$$p = \gamma \frac{e}{\varepsilon r^2}, \tag{33.18}$$

где γ-коэффициент поляризации центра, а r-расстояние от полярона до центра. Этот диполь притягивает полярон полем

$$E = -\frac{2p}{\varepsilon r^3} = -\frac{2ye}{\varepsilon^2 r^5}.$$

Такому полю соответствует потенциал

$$V = -\frac{1}{2}\frac{\gamma e}{\varepsilon^2 r^4} = -ax^4, \quad a = \frac{\gamma e}{2\varepsilon^2}. \tag{33.19}$$

Если

$$\frac{ea}{r_0^4 \mathrm{k}T} > 1, \tag{33.20}$$

то можно в формуле (33.9) интеграл от 0 до $\frac{1}{r_0}$ заменить интегралом от 0 до ∞. В этом случае

$$\int_0^{\frac{1}{r_0}} e^{\frac{eV}{kT}} dx \cong \int_0^{\infty} e^{-\frac{eax^4}{kT}} dx = 0,9064 \left(\frac{kT}{ea}\right)^{1/4} \tag{33.21}$$

Подставляя это выражение в формулу (33.9), получаем:

$$\beta = 1,1 \frac{4\pi D}{\left(\frac{\mathrm{k}T}{ea}\right)^{1/4}} = 1,1 \cdot 4\pi u \left(\frac{(\mathrm{k}T)^3 a}{e^3}\right)^{1/4}. \tag{33.22}$$

Среднее время жизни электрона в свободном состоянии есть

$$t = \frac{1}{N'\beta} = \frac{0,9064}{4\pi u N'} \left(\frac{e^3}{(\mathrm{k}T)^3 a}\right)^{1/4}, \tag{33.23}$$

а средний сдвиг электрона

$$\Delta = tuE = \frac{0,9064E}{4\pi N'} \left(\frac{\epsilon^3}{a(\mathrm{k}T)^3}\right)^{1/4}. \tag{33.24}$$

При стационарном облучении полупроводника возникает электропроводность, равная

$$\sigma = \frac{0,9064eL}{4\pi N'} \left(\frac{e^3}{a(\mathrm{k}T)^3}\right)^{1/4}. \tag{33.25}$$

Применение теории рекомбинации к конкретным кристаллам и сравнение её с опытом даётся в следующем параграфе.

8

1. Средний путь, проходимый электроном по направлению приложенного поля до момента его рекомбинации.

10.6.5 § 34. Recombination of conduction electrons at F-centers. Comparison of theory with experience [59]

При поглощении света F-центрами в кристалле появляется фотопроводимость. Освобождённые светом электроны, образовав поляроны, дрейфуют по направлению электрического поля до тех пор, пока не прилипнут к «центрам рекомби-

нации». Среди этих центров рекомбинации очень часто господствующая роль принадлежит нейтральным F-центрам, которые способны присоединить к себе второй электрон. Так обстоит дело, например, в окрашенных щёлочно-галоидных кристаллах, где главная роль рекомбинации на F-центрах очевидна из следующих экспериментально установленных фактов.

1. Среднее время жизни фотоэлектрона в свободном состоянии и его сдвиг обратно пропорциональны концентрации нейтральных (не ионизированных светом) F-центров, что видно из рис. 34.1.

2. По мере поглощения света F-центрами F-полоса поглощения постепенно бледнеет, и одновременно появляется новая полоса поглощения в более длинноволновой части спектра. Это значит, что свет, ионизируя F-центры, разрушает F-полосу поглощения, освобождённые светом электроны долго не возвращаются в свои первоначальные состояния, а локализуются в других местах, образуя центры, дающие новую полосу поглощения. При последующем нагревании кристалла или при облучении его светом, поглощаемым новой полосой, новые центры диссоциируют: появляется электропроводность, новая полоса бледнеет, а F-полоса восстанавливается (электроны возвращаются в свои первоначальные состояния) [33].

Существенно, что при исчезновении каждого нового центра восстанавливаются два F-центра, и наоборот, при образовании одного нового центра исчезают два F-центра [60].

Объяснить это отношение «1:2» можно только, предположив, что новый центр представляет собой F-центр, присоединивший к себе «лишний» (второй) электрон, т. е. есть F'-центр, рассмотренный в § 26. При диссоциации F'-центра остаётся F-центр, а освобождённый электрон может либо локализоваться у галоидной вакансии, образовав второй F-центр (в результате исчезает один F'-центр и появляются два F-центра), либо попасть на нейтральный F-центр, превратив его в F'-центр (в результате общее число F - и F'-центров остаётся неизменным). При фотодиссоциации F-центра освобождённый электрон также имеет две возможности: он может локализоваться у галоидной вакансии, образовав F-центр (при этом общее число F - и F'-центров остаётся неизменным); он может также попасть на F-центр, превратив его

в F'-центр (в результате исчезают два F-центра и появляется один F'-центр).

Приведённые выше факты свидетельствуют о том, что электроны проводимости рекомбинируют главным образом на нейтральных F-центрах. Рекомбинация на ионизированных F-центрах, а также на других дефектах кристалла (трещины, примеси и т. п.) в вышеописанных опытах играла сравнительно малую роль. Эти факты подтверждают теоретический вывод (§ 26) о том, что в щёлочно-галоидных кристаллах, где энергия $W_{F'}$ (определяемая формулой (26.18)) положительна, энергетически выгодно присоединение к F-центру второго электрона.

В предыдущем параграфе был теоретически вычислен средний сдвиг фотоэлектрона во внешнем электрическом поле. В случае рекомбинации на нейтральных F-центрах согласно формулам (33.24) и (33.19) этот сдвиг равен

$$\Delta = \frac{0,9064E}{4\pi N_F}\left(\frac{2e^2\varepsilon^2}{\gamma(\mathrm{k}T)^3}\right)^{1/4}, \tag{34.1}$$

где $\boldsymbol{E}$ - напряжение электрического поля, приложенного к кристаллу, N_F - концентрация F-центров, а γ - поляризуемость F-центра. Последняя была рассчитана Ю. Е. Перлиным [61] на основе теории F-центров, изложенной в главе IV.

Таким образом, все параметры формулы (34.1) известны достаточно точно, и по ней можно вычислить сдвиг электрона при разных концентрациях F-центров и температурах. На рис. 34.1 прямая линия изображает вычисленнце сдвиги в единичном электрическом поле в зависимости от концентрации F-центров при температуре $-100°$C в KCl . Точками, крестами, треугольниками представлены результаты экспериментальных измерений Г. Гласера [62], относящиеся к различным образцам кристалла. Согласие теории с опытом следует признать хорошим. Температурную зависимость сдвига исследовали в щёлочно-галоидных кристаллах Гласер и Лефельд в лаборатории Поля [55]. На рис. 34.2 и 34.3 представлена полученная ими температурная зависимость произведения Δ/E на квантовый выход фотоэлектронов при фотоионизации F-центров $\eta(T)$. Чтобы установить из этих кривых температурную зависимость непосредственно сдвига Δ, необходимо независимым путём определить температурный ход $\eta(T)$.

Как указывалось в § 25, фотоионизация F-центра представляет собой двухступенчатый процесс: свет переводит электрон из основного состояния на возбуждённый уровень дискретного спектра, а затем тепловая флуктуация переводит электрон в непрерывный спектр, и он покидает F-центр. Поэтому квантовый выход фотоэлектронов $\eta(T)$ при глубоком охлаждении кристалла быстро стремится к нулю ($\sim e^{-a/T}$).

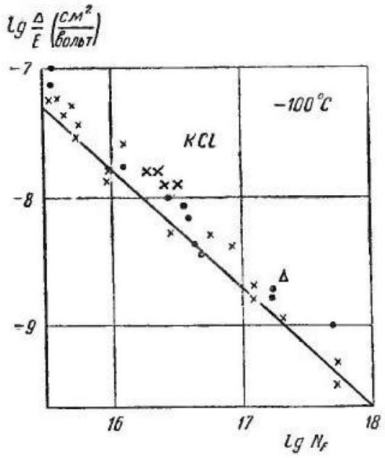

Рис. 34.1.

Сведения о температурном ходе $\eta(T)$ можно почерпнуть из измерений Пика [60], который исследовал фотодиссоциацию F-центров с образованием F'-центров. Из его измерений следует, что при низких температурах $\eta(T)$ сначала быстро растёт с температурой (этим объясняется крутой подъём кривых на рис. 34.2 и 34.3), а затем стремится к предельному значению, равному единице. Практически $\eta = 1$уKCl, начиная с температуры $-100°$C, а у NaCl $-$ 140°C. Таким образом, отрезки кривых справа от этих точек на рис. 34.2 и 34.3 изображают температурный ход Δ/E.

Наряду с экспериментальными значениями на рис. 34.2 и 34.3 пунктиром приведены теоретические кривые для Δ/E,

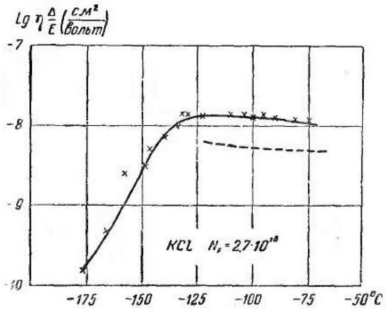

Рис. 34.2.

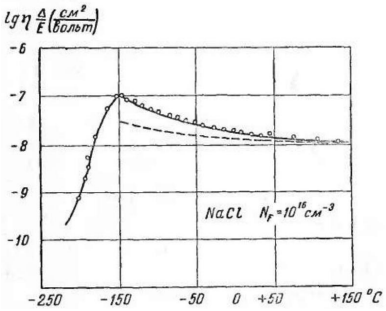

Рис. 34.3.

вычисленные по формуле (34.1). Сравнивая вычисленные значения сдвигов с измеренными, следует иметь в виду, что концентрации F-центров, указанные на обоих рисунках, известны лишь приблизительно; поэтому как на рис. 34.2 , так и на рис. 34.3 вычисленные абсолютные величины сдвигов следует считать совпадающими с опытом в пределах экспериментальной ошибки. Температурный ход теоретической кривой $\left(\Delta \sim T^{-3/4}\right)$ у KCl согласуется с опытом. у NaCl экспериментальная кривая сначала убывает с температурой несколько быстрее, чем теоретическая; начиная с температуры 40 или 50°C обе кривые почти совпадают. Возможно, что ниже температур $40-50$°C у NaCl ещё не выполняется неравенство случая Б § 33 (β_1 с температурой растёт), а в этом случае теория даёт только верхний предел коэффициента рекомбинации и, соответственно, нижний предел сдвига.

10.6.6 § 35. Quantum Output of Photodissociation F - and F'-центров

В любом электрически нейтральном центре (F-центре, атоме химической примеси, молекуле основного вещества кристалла) энергетический спектр электронов имеет бесконечное число дискретных уровней, сгущающихся по направлению к непрерывному спектру, т. е. к уровню $E=0$. Это становится очевидным, если представить себе один из электронов удалённым от «ионного остатка»: этот электрон окажется в кулоновском поле положительного ионного остатка, тогда его энергетический спектр и ψ-функции совпадут со спектром и ψ-функциями высоко возбуждённых состояний атома водорода.

Как было показано в § 9, в поляроне электрон также обладает энергетическим спектром с бесконечным числом дискретных уровней, сгущающихся при приближении к уровню $E=0$. Этот «водородоподобный» характер верхней части дискретного спектра сохранится и в том случае, когда полярон «сядет» на какой-либо нейтральный центр,

поскольку в этой части спектра ψ-функции электрона обладают большим эффективным радиусом и влияние нейтрального центра будет мало (его радиус значительно меньше «радиуса» ψ-функции электрона). В последнем случае получается уже не нейтральный, а отрицательно заряженный центр, но упомянутый характер

верхней части спектра сохраняется. Примером такого отрицательно заряженного центра является F'-центр при $z = 1$.

С точки зрения обычной зонной теории электропроводности диссоциация центра происходит только в том случае, когда энергия электрона положительна. Поэтому если световое излучение переводит электрон на дискретный уровень ($E < 0$), то для диссоциации всегда необходима ещё и тепловая флуктуация, чтобы выбросить электрон в зону проводимости. Квантовый выход фотодиссоциации, таким образьм, должен

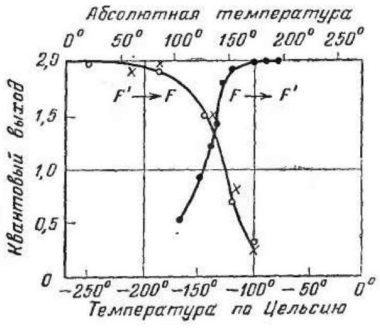

Phc. 35.1.

при глубоком охлаждении кристалла быстро (экспоненциально) стремиться к нулю. Однако опыт опровергает этот вывод зонной теории: при фотодиссоциации F'-центров в щёлочно-галоидных кристаллах наибольший квантовый выход $\eta' = 1$ наблюдается при температуре, близкой к абсолютному нулю [60], как показано на рис. 35.1.

Другой факт, указывающий на то, что при понижении температуры квантовый выход фотодиссоциации F'-центров не стремится к нулю, состоит в следующем: при поглощении света в F'-полосе возникает фотопроводимость, которая остаётся значительной вплоть до самых низких температур, как показано на рис. 35.2 [69].

Если предположить, что при поглощении света в F'-полосе электрон переходит не на дискретный уровень, а непосред-

ственно в зону проводимости, то отмеченный выше большой квантовый выход фотодиссоциации при низких температурах: был бы понятен. Но в этом случае возникает другая трудность: в F'-центре спектр энергии электронов имеет бесконечное число дискретных уровней. Наиболее интенсивное поглощение света, как показывает расчёт, связано не с переходами электронов в непрерывный спектр, а с их переходами на дискретные уровни, причём наиболее вероятным является переход одного из двух электронов на нижний p-уровень.

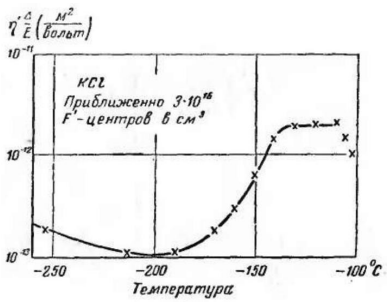

Рис. 25.2.

Таким образом, если предположить, что F'-полоса связана с переходами в непрерывный спектр, то с красной стороны от неё должна была бы наблюдаться гораздо более интенсивная полоса поглощения, соответствующая переходам на дискретные уровни. Такая полоса не наблюдается. Предположение, что наблюдающаяся экспериментально F'-полоса представляет собой перекрытие полос, соответствующих переходам на дискретные уровни и в непрерывный спектр, означало бы, что при поглощении света электроны переходят чаще всего на дискретные уровни; в этом случае при температуре, равной абсолютному нулю, квантовый выход фотодиссоциации должен быть значительно меньше единицы, что не наблюдается. Таким образом, обычная зонная теория электропроводности не даёт даже качественного объяснения наблюдающихся фактов.

Рассмотрим теперь эти факты с точки зрения поляронной теории проводимости, т. е. предположим, что в результате диссоциации F'-центра образуются F-центр и свободный полярон, а не зонный электрон. В этом случае энергия системы в диссоциированном состоянии будет ниже, чем по зонной теории, а энергия тепловой диссоциации как возбуждённого, так и невозбуждённого F'-центра соответственно меньше. Эта энергия тепловой диссоциации в результате расчёта оказывается отрицательной не только для возбуждённых состояний F'-центра, но иногда даже для основного состояния, как это отмечалось в § 26. Отрицательная энергия тепловой диссоциации означает (см. § 26), что соответствующее стационарное состояние F'-центра в действительности не существует.
С. Ф. Томасевич рассчитала энергетический спектр F'-центров в щёлочно-галоидных кристаллах [63]. Оказалось, что в этих кристаллах существуют основные состояния F'-центров и энергия их тепловой диссоциации порядка $+0,1 - 0,3$ эл.-в. Всё же возбуждённые состояния соответствуют уже диссоциации. Таким

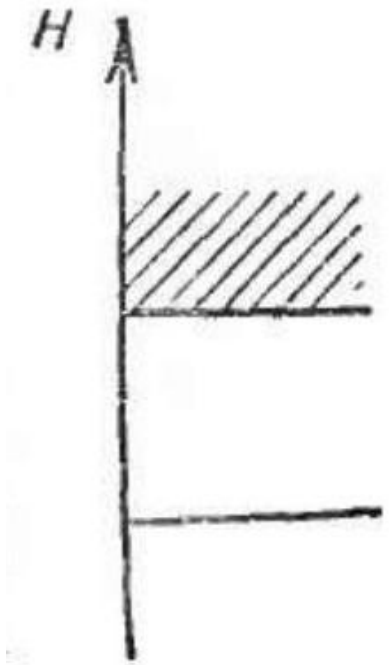

Рис. 35.3.

Поглощение света в F'-полосе переводит систему непосредственно в диссоциированное состояние; при этом никакой тепловой флуктуации для диссоциации не требуется. Квантовый выход фотодиссоциации должен быть равен единице независимо от температуры. Здесь при качественном объяснении экспериментальных фактов не возникает трудностей, подобных тем, что встретились в зонной теории.

Энергетический спектр F'-центра, изображённый на рис. 35.3, предлагался ещё Зейтцом [35], как хорошо объясняющий экспериментальные факты. Однако он не может быть обоснован в рамках зонной теории, предполагающей, что электрон, покидая F'-центр, может двигаться только в зоне проводимости, т. е. с положительной энергией. Действительно, в этом случае расчёт энергетического спектра F'-центра, проведённый

прямым вариационным методом [63], показывает, что, помимо основного уровня, существуют и другие дискретные уровни, в том числе p-уровни. Точное решение задачи, как известно, может дать более низкие значения термов, но не может опровергнуть их существование.

Рассмотрим теперь квантовый выход фотодиссоциации F-центров. У F-центров энергетические уровни электронов лежат ниже, чем у F'-центров при $z = 1$. Расчёт показывает, что кроме основного имеется ряд возбуждённых состояний системы, обладающих положительными энергиями диссоциации. Иначе говоря, энергетический спектр системы имеет ряд дискретных уровней, расположенных под непрерывной зоной диссоциированных состояний. При поглощении света в F-полосе электрон переходит чаще всего на $2p$-, а иногда на $3p$-уровень. Эти уровни обладают положительной энергией диссоциации. Поэтому после фотовозбуждения F-центра для его диссоциации необходима ещё и тепловая флуктуация. Так объясняется наблюдающееся падение квантового выхода фотодиссоциации F-центров при охлаждении кристалла.

Г. Е. Зильберман рассчитал возбуждённые состояния F-центров и энергии их тепловых диссоциаций в кристаллах NaCl и KCl , а также температурный ход квантового выхода $\eta(T)$ [64,43]. Последний оказался в качественном согласии с опытом и объяснил одновременно и температурную зависимость квантового выхода реакции $F \to F'$, представленную на рис. 35.1 , и крутое падение величины $\tau(T)\Delta/E$ при охлаждении

кристалла, представленное на рис. 34.2 и 34.3.

10.6.7 § 36. Metal-type electronic semiconductorsSulfurous lead

В большинстве электронных полупроводников электроны проводимости при абсолютном нуле температуры отсутствуют, и лишь при нагревании кристалла они появляются в результате термической ионизации атомов примеси или основного вещества кристалла. При этом концентрация электронов проводимости экспоненциально растёт с температурой ($\sim e^{-W/2\mathrm{k}T}$), что было объяснено в §§ 19 и 29.

Изредка, однако, встречаются полупроводники, в которых концентрация электронов проводимости значительна при абсо-

лютном нуле температуры и не зависит от температуры вплоть до температур порядка нескольких сот градусов. У таких полупроводников в вышеупомянутом интервале температур, где концентрация электронов проводимости постоянна, удельная электропроводность при нагревании убывает (как у металлов) за счёт уменьшения подвижности [65]. Такие полупроводники называются полупроводниками металлического типа. К этому типу полупроводников относится, например, сернистый свинец с избытком свинца и др.

Обычно вышеупомянутые свойства полупроводников металлического типа объясняются особенностями энергетического спектра электронов в этих кристаллах: предполагается, что локальные электронные уровни доноров (атомов примеси) лежат не под дном зоны проводимости, как у большинства примесных полупроводников, а выше дна зоны проводимости. Поэтому энергетически выгоден процесс передачи донором электрона в зону проводимости кристалла (энергия тепловой диссоциации «отрицательна»). При абсолютном нуле температуры электроны находятся в состояниях с наименьшей энергией, т. е. в зоне проводимости, а не на локальных уровнях доноров. Концентрация электронов проводимости определяется концентрацией доноров и, следовательно, не зависит от температуры. Лишь при достаточно высоких температурах, когда начинается термоионизация молекул основного вещества полупроводника или доноров с положительной энергией диссоциации, концентрация электронов проводимости начинает расти с температурой.

Такое объяснение свойств полупроводников металлического типа весьма популярно, но тем не менее неудовлетворительно с теоретической точки зрения. Действительно, из условия электрической нейтральности полупроводника очевидно следует, что наряду с электронами проводимости непременно должны существовать в таком же количестве положительные заряды. Это могут быть, например, ионизированные доноры, отдавшие свои электроны в зону проводимости. Каждый такой положительный заряд создаёт для электрона потенциальную яму, которая на достаточно больших расстояниях от заряда имеет кулоновский вид. В такой яме существует бесконечное число дискретных энергетических уровней для электрона, причём все они расположены под дном зоны проводимости.

Чтобы это показать, основываясь на «зонной» теории электропроводности, достаточно с помощью метода эффективной массы электрона исключить периодический потенциал, действующий на электрон в кристалле, а затем рассмотреть стационарные состояния электрона с большими эффективными радиусами. При этом задача сведётся к рассмотрению движения частицы с эффективной массой μ в кулоновском поле притяжения. Полученные при этом значения энергии представляют собой энергетические уровни электрона, отсчитанные от дна зоны проводимости (см. § 4). В вышеупомянутой задаче водородоподобного атома эти уровни, как известно, отрицательны, т. е. расположены под дном зоны проводимости. Этим методом нельзя

исследовать локальные состояния с малым радиусом, так как в этом случае непригоден метод эффективной массы и поле некулоновское. При исследовании же состояний с большими радиусами ни метод эффективной массы, ни кулоновский вид поля не вызывают сомнений.

Существование локальных состояний носителя тока вблизи любого положительного заряда можно доказать также, основываясь на поляронной теории электропроводности. Доказательство вполне аналогично предыдущему с той лишь разницей, что в этом случае следует рассматривать поступательное движение полярона в целом как частицы с эффективной массой M в кулоновском поле положительного заряда.

Наличие вблизи каждого положительного заряда дискретных уровней и локальных состояний носителя тока означает, что при абсолютном нуле температуры все носители тока локализуются на этих уровнях. Таким образом, следует отказаться от упомянутого выше предположения об энергетической выгодности покидания донора носителями тока и ухода их в зону проводимости.

Прежде чем приступить к объяснению металлической проводимости полупроводников, рассмотрим некоторые особенности полупроводников этого рода. Их типичным представителем является сернистый свинец с избытком свинца. Необходимость избытка свинца указывает на то, что металлическая проводимость является «примесной», причём в качестве донора электронов выступает избыточный свинец. Диэлектрическая постоянная PbS $\varepsilon = 17,9$ [66]. Что касается параметров n, μ и ω, то, к сожалению, из-за отсутствия необхо-

димых экспериментальных данных их не удалось определить методом, изложенным в §§ 30 и 31. Пришлось удовлетвориться менее точной оценкой. Параметр ω был определён в § 20 по температурному ходу подвижности. При этом получилось $\hbar\omega = 0,074$ эл.-в, $\iota_0' = 14\frac{c^2}{сек}$. Далее Дунаевым и Маслаковцем экспериментально исследована в PbS зависимость

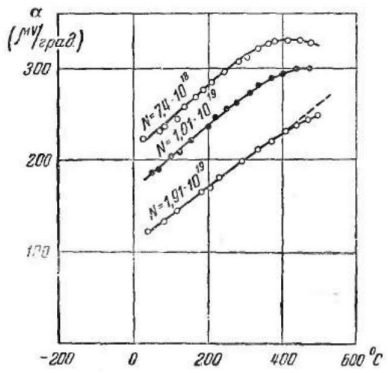

Рис. 36.1

термоэлектродвижущей силы от температуры и концентрации носителей тока N [65]. На рис. 36.1 и 36.2 к есть величина термоэлектродвижущей силы в микровольтах на градус разности температур.

Представленный на рисунках температурный и концентрационный ход α довольно хорошо согласуется с теоретической формулой Н. А. Писаренко

$$\alpha = \frac{k}{e}\left[2 + \ln\frac{2(2\pi MkT)^{3/2}}{h^8 N}\right]. \tag{36.1}$$

Здесь M - эффективная масса носителя тока - является единственным неизвестным параметром. Она была определена путём сравнения формулы (36.1) с опытом и оказалась рав-

ной $M = 0,6m$. На рис. 36.2 сплошная прямая изображает теоретическую зависимость (36.1) при $M = 0,6m$; пунктирная прямая соответствует формуле (36.1) при $M = m$. Приравнивая теоретические выражения для $M(c,\mu)$ и $u_0'(c,\mu)$ (см. формулы (10.35) и (20.35)) их значениям, найденным из опыта, получаем два уравнения для неизвестных и μ. Их совместное решение даёт $c = 0,3$ и $\mu = 0,46m$. При этих

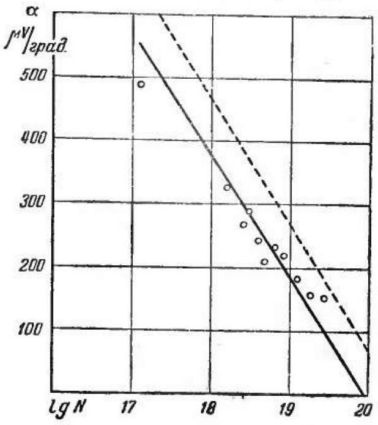

Рис. 36.2.

значениях параметров поляризационный радиус полярона, введённый в § 7, оказывается равным

$$r_p = \frac{10\hbar^2}{\mu e^2 c} = 38,3\text{Å}. \tag{36.2}$$

Такое большое значение радиуса связано с исключительно большим в и малыми M и μ в сернистом свинце.

При таких значениях параметров радиусы валентных электронов в атомах избыточного свинца столь велики, что рассмотрение движения этих электронов сводится к задаче об F'-центре. Положительный ионный остаток донора можно считать точечным зарядом с $z = 2$. Если предположить, что

введённые в кристалл лишние атомы свинца вызывают перестройку решётки, в результате которой они оказываются не в междуузельном пространстве, а становятся положительными узлами новой решётки, предварительно отдав свои валентные электроны, то в кристалле образуется дефицит отрицательных ионов серы, т. е. появляются вакантные отрицательные узлы решётки. Последние, подобно положительным зарядам, должны привлечь к себе электроны, освобождённые при ионизации доноров; при этом образуются опять-таки F'-центры.

Если вычислить энергию тепловой диссоциации такого F'-центра по формуле (26.17), то для неё получается значение $W_{F'} = 0,03$ эл.-в. Следует иметь в виду, что формула (26.17) в случае сернистого свинца не точна, так как полученное значение W_F, оказалось значительно меньшим, чем «энергия связи» полярона; эта последняя равна

$$-J[\psi_0] + \frac{3}{2}\hbar\omega = 0,173 \text{ эл.-в.}$$

Это значит, что в PbS вследствие аномальных значений параметров F'-центр следует представлять себе как два полярона, осциллирующие вместе со своими поляризационными потенциальными ямами с большой амплитудой около двоиного положительного заряда. Поле положительного заряда лишь слегка деформирует эти поляроны. Для описания такого движения апроксимация (26.12) плоха. Критерий

адиабатичности (16.41) в сернистом свинце тоже выполняется плохо, что заставляет с опасением относиться к приведённым выше значениям параметров c и μ. Поэтому полученное выше значение $W_{F'}$ неточно.

Возможна другая оценка энергии тепловой диссоциации F'-центра, в которой не используются значения параметров c и μ, а используется лишь значение M, взятое выше непосредственно из опыта. При этом предположение адиабатичности (16.41) тоже не понадобится. Эта оценка основана как раз на использовании малости W_F по сравнению с «энергией связи» полярона. Поэтому она хороша для PbS , но менее пригодна для щёлочно-галоидных кристаллов. Для этой второй оценки предположим, что оба электрона вместе со своими поляризационными потенциальными ямами движутся вокруг центрального положительного заряда как две квази-

частицы с эффективными массами M. Когда квазччастица находится на большом расстоянии от положительного заряда, потенциальная энергия её взаимодействия с этим зарядом имеет кулоновский вид. Но на расстояниях порядка и меньше чем «радиус» ψ-облака электрона в поляроне (13 A в PbS) форма потенциальной ямы отклоняется от кулоновской, при этом потенциальная яма имеет параболический минимум (а не полюс) в точке, где находится точечный положительный заряд (потенциальная энергия имеет такой вид, как если бы точечный положительный заряд взаимодействовал с размазанным твёрдым отрицательным облаком).

При оценке энергии диссоциации такого F'-центра сделаем два упрощения, дающие ошибки разных знаков, которые почти компенсируются: предположим, что потенциал поля везде кулоновский, а эффективный заряд положительного ядра положим $z_{\text{эф}} = 1$, а не $z_{\text{эф}} = 1,35$, как это имеет место в атоме гелия. Применяя формулу для водородоподобного атома, получаем:

$$W_{\boldsymbol{F}'} \sim \frac{M\boldsymbol{e}^1}{2\hbar^2\varepsilon^2} = 0,025 \text{ эл.-в}, \tag{36.3}$$

что почти совпадает с оценкой этой величины по формуле (26.17). Эффективный радиус ψ-функции, описывающей движение поляронов в F'-центре,

$$r \sim \frac{\hbar^2\varepsilon}{Me^2} = 16\text{Å}. \tag{36.4}$$

Вернёмся тенерь к объяснению «металлической» проводимости серкистого свинца. При указанных выше значениях ε и M и при концентрациях F'-центров порядка $10^{18}c^{-3}$ поляроны способны сравнительно легко переходить от одного F'-центра к другому сквозь потенциальный барьер (без тепловой диссоциации). Такая электропроводность вполне аналогична обычной электропроводности металлов с той лишь разницей, что здесь роль узлов решётки играют F'-центры, а роль постоянной решётки играет расстояние между ними. Соблюдение строгой периодичности расположения узлов здесь, как и в случае металлов, не имеет существенного значения. Это подтверждается совпадением порядка величины электропроводности твёрдого и жидкого металлов.

Лёгкость, с которой электроны способны переходить из узла в узел, определяется «перекрытием» ψ-функций соседних узлов. Последнее же определяется отношением эффективного радиуса «атомной» ψ-функции к постоянной решётки. Следовательно, в сернистом свинце при радиусе ψ-функции F'-центра порядка 16 A и при расстоянии между центрами порядка 70 A получается такое же «перекрытие», как в металле при радиусе атомной функции порядка 1Å и постоянной решётки порядка 4 A.

Можно ещё другим способом оценить степень связи электронов с узлами решётки «квазиметалла», использовав для этого одномерную модель Кронига [28], в которой междуузельные потенциальные барьеры выбираются прямоугольной формы. В этой модели, как известно, степень связи электронов определяется значением параметра

$$P = \frac{MV_0}{\hbar^2} b_1 b_2, \tag{36.5}$$

где V_0-высота междуатомного потенциального барьера, b_2 - его ширина, а b_1 - ширина междубарьерного про-

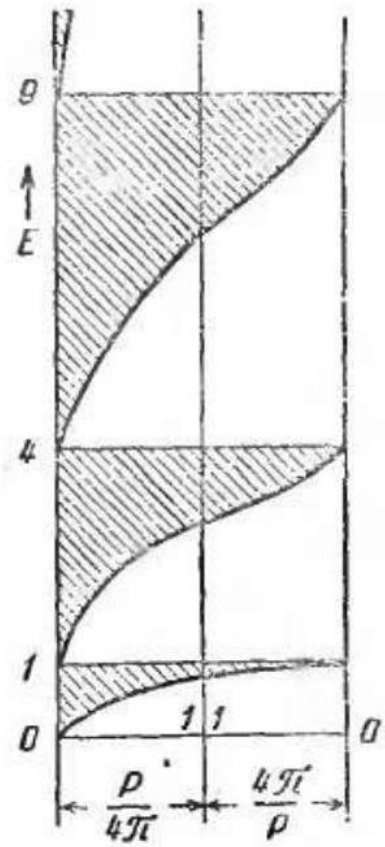

Рис. 36.3.

В рассмотренном выше примере кристалла сернистого свинца, в котором расстояние между F'-центрами равнялось 70Å, следует принять $b_1 = 30\text{Å}, b_2 = 40\text{Å}, V_0 = 0,025$ эл.-в. При этом получается $P = 2,4$. Из рис. 36.3 видно, что при таком значении P разрешённые зоны энергии оказываются шире, чем запрещённые, т. е. перед нами - случай слабой связи.

В этом случае не имеет смысла подразделение поляронов на свободные и связанные в F'-центрах, подобно тому как в металлах не имеет смысла подразделять валентные электроны

на свободные и связанные в атомах. Все поляроны могут свободно двигаться по всему объёму кристалла, обладая при этом эффективной массой порядка массы свободного полярона M.

В случае слабой связи ширина первой разрешённой энергетической зоны для кубической решётки, как известно, равна

$$\frac{3\hbar^2}{2M}\left(\frac{\pi}{a}\right)^2, \tag{36.6}$$

где a - постоянная решётки.

В случае «квазиметаллической» решётки сернистого свинца, полагая $M = 0,6m, a = 70$ А, для ширины первой энергетической зоны получаем 0,04 эл.-в. Эта ширина зоны оказалась больше энергетического расстояния между дискретными уровнями,

соответствующими орбитальному движению полярона как целого вокруг положительного заряда в изолированном F'-центре. Таким образом, энергетические зоны, соответствующие различным дискретным уровням F^2-центра, перекрываются. Поэтому квазирешётка, образованная F'-центрами, представляет собой аналог не диэлектрика, а металла.

Приведённое выше качественное рассмотрение показывает, что в сернистом свинце концентрация носителей тока не должна зависеть от температуры. Электропроводность должна убывать с температурой за счёт уменьшения подвижности, что и наблюдается.

Рассмотренный выше пример, где среднее расстояние между соседними F'-центрами равнялось 70Å, соответствует концентрации избыточного свинца $2,9 \cdot 10^{18} c^{-3}$. Посмотрим теперь, как должна изменяться картина по мере уменьшения концентрации избыточного свинца. Расстояние между F'-центрами будет расти, «перекрытие» ψ-функций соседних F'-центров будет уменьшаться, и постепенно случай слабои связи перейдёт в случай связи сильной. При этом энергетический спектр носителя тока в кристалле существенно изменится, подобно тому как изменился бы спектр электронов в металле при непрерывном увеличении постоянной решётки (при котором металл постепенно переходил бы в газ).

В этом случае энергетический спектр носителя тока можно разделить на две существенно различные части. Первая, нижняя, часть спектра состоит из зон, соответствующих дис-

кретным уровням энергии поляронов в F'-центрах. Чем больше расстояние между F'-центрами, тем эти зоны уже, а эффективная масса движения носителя тока в зоне - больше (эффективная масса экспоненциально убывает с ростом расстояния между F'-центрами). По мере уменьшения концентрации избыточного свинца электропроводность по этим зонам экспоненциально стремится к нулю. Вторая, верхняя, часть спектра соответствует ионизированным состояниям F'-центров. Здесь чем больше расстояния между F'-центрами, тем лучше соблюдаются условия предельного случая слабой связи (см. в [28] § II). Носитель тока будет двигаться как свободный полярон в идеальном беспримесном кристалле, обладая соответствующей подвижностью и эффективной массой M. Потенциальные ямы F-центров будут лишь слегка рассеивать поляроны, тем меньше, чем меньше концентрация этих центров.

Данное выше объяснение металлической проводимости сернистого свинца может быть распространено и на другие полупроводники металлического типа.

В основу экспериментальной проверки этого объяснения следует положить вытекающее из теории характерное изменение свойств полупроводника в зависимости от концентрации доноров. По мере уменьшения концентрации доноров следует ожидать последовательного осуществления трёх случаев:

1. При больших концентрациях примеси, когда ψ-функции соседних доноров сильно «перекрываются», состояния носителей тока и их энергетический спектр должны быть такими, как у «квазиметалла», у которого постоянная решётки равна расстоянию между донорами и в котором периодический потенциал имеет очень малую амплитуду осцилляции (например, в PbS - сотые эл.-в). Концентрация носителей тока не должна зависеть от температуры, а электропроводность должна падать с температурой за счёт уменьшения подвижности. Лишь при достаточно высоких температурах, когда начнётся термодиссоциация электронов в основном веществе кристалла, концентрация носителей тока начнёт расти с температурой.

2. При меньших концентрациях доноров их ψ-функции перекрываются мало. В этом случае энергетический спектр носителя тока разделяется на две части: нижнюю с узкими разрешёнными зонами и большими эффективными массами

носителя тока, экспоненциально зависящими от концентрации доноров, и верхнюю, в которой носитель тока движется как свободный полярон в идеальном беспримесном кристалле.

При не слишком высоких температурах, когда термодиссоциация электронов из основного вещества ещё незначительна, бобьшая часть носителей тока должна находиться в нижней части спектра: здесь их концентрация почти не должна зависеть от температуры. В верхней же части спектра, поскольку она расположена выше химического потенциала электронов, должна находиться лишь небольшая часть носителей тока, и их концентрация должна экспоненциально зависеть от температуры ($\sim e^{-b/T}$).

Подвижность носителей тока в верхней части спектра больше, чем в нижней. Поэтому при некоторых концентрациях доноров роль обеих частей спектра в электропроводности может оказаться сравнимой. При этом температурная зависимость электропроводности должна иметь вид

$$\sigma = A + Be^{-\frac{b}{T}}. \tag{36.7}$$

Здесь первый член представляет электропроводность нижней части спектра, а второй член - электропроводность верхней части спектра.

Зависимость вида (36.7) действительно наблюдалась в 1934 г. Курчатовым, Костиной и Русиновым в карборунде (SiC) [68]. Эти авторы объяснили её как раз предположением о существовании двух зон проводимости: первой «примесной» зоны проводимости, в которой концентрация электронов не зависит от температуры, и второй обычной зоны, в которой концентрация электронов экспоненциально зависит от температуры. Следует заметить, что такая своеобразная двузонная интерпретация зависимости (36.7) не однозначна: в случае 1), где имеется перекрытие всех зон и получается одна общая зона проводимости металлического типа, следует тоже ожидать температурной зависимости электропроводности вида (36.7), когда начнётся термоионизация основного вещества, как отмечалось выше. Пожалуй, наиболее убедительным доказательством «двузонной» проводимости было бы измерение зависимости A и B от концентрации доноров, показывающее, что A экспонен-

циально убывает с ростом расстояния между донорами, в то время как B мало зависит от концентрации доноров.

3) При дальнейшем уменьшении концентрации доноров перекрытие их функций становится бесконечно малым, ширины разрешённых зон в нижней части спектра стремятся к нулю, а соответствующие эффективные массы - к бесконечности. Движение носителей тока по этим зонам становится невозможным. В верхней же части спектра не происходит какихлибо существенных изменений.

В этом случае кристалл становится полупроводником не металлического, а обычного донорного типа. При абсолютном нуле температуры все электроны находятся в нижней части спектра, т. е. связаны в донорах. Никакой электропроводности в этом случае нет. При нагревании кристалла небольшая доля электронов возбуждается в верхнюю часть спектра, где они могут свободно двигаться по кристаллу в виде поляронов с эффективной массой M. Концентрация поляронов проводимости должна экспоненциально зависеть от температуры, как показано в § 29 .

Следует подчеркнуть, что в таких полупроводниках, как сернистый свинец, где половина энергии тепловой диссоциации донора меньше $\hbar\omega$, подвижность меняется с температурой быстрее, чем концентрация носителей тока. В этом случае электропроводность полупроводника будет всё-таки расти при охлаждении кристалла. Лишь при самых низких температурах, когда рассеяние поляронов тепловыми колебаниями станет незначительным, а подвижность будет определяться «остаточным»

сопротивлением, не зависящим от температуры, электропроводность, пройдя через максимум, начнёт убывать при дальнейшем охлаждении.

По мере уменьшения концентрации доноров «перекрытие» ослабится сначала у ψ-функций самых низких уровней F'-центров, у которых наиболее малы эффективные радиусы, а затем постепенно это будет происходить с ψ-функциями более высоких зон нижней части спектра. При этом электропроводность последовательно будет прекращаться во всё более высоко расположенных зонах нижней части спектра и в пределе, при очень малых концентрациях примеси, электропроводность сохранится лишь в верхней части спектра. Это должно на опыте выглядеть, как «рост энергии тепловой диссоциации»

полупроводника по мере уменьшения концентрации доноров. Такой рост действительно наблюдается во многих примесных полупроводниках с малой энергией тепловой диссоциации.

В литературе имеются указания на то, что всякий примесный полупроводник с ростом концентрации примеси превращается в полупроводник металлического типа [32] (если только примесь не коагулирует в коллоиды). Экспериментальный материал, однако, не достаточен для окончательных выводов. Для более полной проверки теории должны быть экспериментально исследованы зависимости электропроводности от температуры вплоть до самых низких температур и от концентрации доноров в широкой области концентраций. Для тех же полупроводников независимым путём должны быть определены параметры теории ε, n, μ и ω.

10.6.8 § 37. Conclusion

Развитая выше теория содержит четыре параметра: ε, n, ω и μ. Первые три для большинства рассмотренных кристаллов хорошо известны. Они измеряются непосредственно, независимо от рассмотренных выше явлений. Единственным неизвестным параметром оказывается эффективная масса электрона μ. Она определялась в § 31 при совмещении абсциссы максимума F-полосы поглощения $\Omega_{\text{мако}}$ с соответствующим экспериментальным значением. После этого теория уже не содержала неизвестных параметров, и все последующие вычисления ряда физических свойств кристаллов приводили к конкретным численным результатам. Сравнение последних с опытом явилось проверкой теории.

Так, были вычислены и оказались в хорошем согласии с опытом энергии тепловых диссоциаций F-центров в десяти ионных кристаллах (табл. 31.1). Дано количественное объяснение наблюдающемуся на опыте факту относительно большей величины энергии фотовозбуждения F-центра $Q_{\text{мако}}$ по сравнению с энергией термоионизации W_F.

Вычисленные значения сил осцилляторов, соответствующих поглощению света F-центрами для NaCl и KCl , согласуются с опытом в пределах точности экспериментальных данных (§ 25). Вычисленные значения полуширины F-полос поглощения для пяти рассмотренных кристаллов согласуются с опытом
(табл. 32.1). Зависимость этих полуширин от температуры также согласуется с опытом в большом интервале температур: от $\sim 0°$K до $873°$K. Теория объясняет типичную форму F-полос поглощения, их деформацию с изменением температуры при высоких температурах и независимость от температуры при низких (§ 32).

Теория приводит к правильному значению коэффициента рекомбинации поляронов на F-центрах с образованием F'-центров. Вычисленные значения средних сдвигов поляронов в окрашенных KCl и NaCl согласуются с опытом (рис. 34.1, 34.2, 34.3). Теория даёт условия существования в кристалле F'-центров (§ 26). В щёлочно-галоидных кристаллах это условие выполняется, и F'-центры в них

действительно наблюдаются. Теория объясняет температурную зависимость квантового выхода фотодиссоциации F - и F'-центров. В частности, объясняется, почему при глубоком охлаждении кристаллов квантовый выход фотодиссоциации у F-центров стремится к нулю, а у F'-центров - к единице (§ 35).

Оценка параметров теории в сернистом свинце показывает, что вследствие аномальных значений этих параметров ψ-функции электронов доноров сильно «перекрываются» уже при концентрациях доноров порядка $10^{18}c^{-3}$. Это приводит к качественному объяснению проводимости металлического типа, наблюдающейся в сернистом свинце (с избытком свинца).

Вычисленные значения подвижностей поляронов по порядку величины совпадают с измеренными подвижностями носителей тока в полупроводниках. В случае низких температур исследована экспериментально температурная зависимость подвижности, которая качественно согласуется с теоретической.

Таким образом, сравнение теории с опытом оказалось благоприятным для теории. Оно показало, что предлагаемая теория, несмотря на ряд упрощений и идеализаций, всё же правильно учитывает главные элементы поставленной задачи и объясняет с единой точки зрения большой комплекс электрических, фотоэлектрических и оптических явлений в кристаллах. В ряде случаев теория даёт количественные результаты в хорошем согласии с опытом. Это позволяет судить о точности, которую допускает развитый выше математический аппарат.

Однако следует признать, что сравнение предлагаемой микротеории с опытом находится пока только в начальной стадии. Необходимо рассмотреть гораздо большее число кристаллов и более широкий круг явлений. Это затруднено в настоящий момент тем, что, с одной стороны, экспериментально всесторонне изучены лишь немногие кристаллы (лишь для десятка кристаллов удалось определить параметры теории и т. д.), а с другой стороны, недостаточно развиты применения теории к многочисленным наблюдающимся явлениям.

Эти замечания относятся не только к микротеории, изложенной в этой книге, но в ещё большей степени к обычной зонной микротеории, где работа теоретиков ограничивалась пока главным образом вычислением энергетических зон и подвижности электрона. Подвижность электрона в ионных кристаллах была вычислена Фреилихом и Моттом [14]; она оказалась зависящей от эффективной массы электрона μ. Упомянутые авторы, повидимому, не нашли надёжных путей, позволяющих независимым путём определить μ, что затруднило сравнение вычисленной подвижности с опытом.

Рассмотренные выше применения теории к конкретным кристаллам и явлениям далеко не исчерпывают всех возможностей теории. В настоящий момент имеются результаты применения теории к явлениям люминесценции, собственного поглощения света в ионных кристаллах, к оптическим свойствам атомов, растворённых в жидком диэлектрике, и пр. Рассмотрено движение поляронов в жидких диэлектриках (А. С. Давыдов [70]).

Делаются также попытки уточнения теории путём обобщения и усовершенствования метода эффективной массы электрона и более точного рассмотрения неоднородной поляризации кристалла с учётом его ионной структуры (К. Б. Толпыго [46], [48]). Эти уточнения будут иметь большое значение в тех кристаллах, где радиус полярона окажется малым по сравнению с постоянной решётки.

10.6.9 Appendix. Attempt to Consider Polarons Under the Assumption of Weak Interaction of Electron with Polarization Oscillations

Среди откликов на публикации автора по теории поляронов в 1950 г. появилась работа Фрейлиха, Пельцера и Цинау «Свойства медленных электронов в полярных веществах» [72]. В этой работе поляроны рассматриваются с помощью другого математического приближения, в основе которого лежит неравенство, как раз обратное условию адиабатичности (7.2 – 3); таким образом, рассмотрен обратный предельный случай. Некоторые полученные результаты качественно совпадают с результатами §§ 16 и 17: электрон проводимости, окружённый локальной инерционной поляризацией, может свободно двигаться по кристаллу; тепловые колебания ионов вызывают рассеяние поляронов. Однако другие результаты даже качественно отличаются от изложенных в монографии. Так, например, совершенно иной характер имеет ψ-функция системы, масса носителя тока почти совпадает с эффективной массой электрона μ и пр. Количественные результаты совершенно отличны от изложенных в монографии, что вполне естественно.

В вышеупомянутой работе делается вывод о том, что полярон как целое может двигаться по кристаллу, причём этот вывод противопоставляется результатам работ, сделанных в СССР, где якобы предполагается, что полярон неподвижен. В действительности ещё в первой работе автора по теории поляронов, опубликованной в 1946 г. [12], указывалось, что полярон должен двигаться во внешнем электрическом поле, а в последующих работах 1947 г. [15] и 1948 г. [17, 18] полярон считался основным носителем тока.

Таким образом, полемическое замечание Фрейлиха, Пельцера и Цинау, высказанное в 1950 г., основано на недоразумении. Перейдём к рассмотрению основных пунктов упомянутой работы. Авторы исходят из гамильтониана (12.18). Его можно переписать в виде

$$\mathbf{H} = -\frac{\hbar^2}{2\mu}\Delta + \frac{1}{2}\sum_x \hbar\omega\left(q_x^2 - \frac{\partial^2}{\partial q_x^2}\right) + H' \tag{Д.1}$$

где

$$H' = e\int \frac{(r-r_1)\,P(r_1)}{|r-r_1|^3}d\tau_1 = -e\sqrt{4\pi\hbar\omega c}\times \\ \times\sum_x \frac{q_x}{x}\chi_{-x}(r). \tag{Д.2}$$

Далее, следуя методам обычной зонной теории, член H' считается малым возмущением (что не предполагается в настоящей монографии). В нулевом приближении член H' опускается, и тогда собственные функции оператора энергии имеют вид

$$\Psi_0(k,\ldots,n_x,\ldots) = \frac{1}{L^{s/2}}e^{ikr}\prod_x \Phi_{n_x}(q_x), \tag{Д.3}$$

где Φ_{n_x} - собственные функции уравнения для гармонического осциллятора, имеющие вид (14.17). Спектр энергии системы в нулевом приближении выражается формулой

$$E_0(k,\ldots,n_x,\ldots) = \frac{\hbar^2k^2}{2\mu} + \sum_x \hbar\omega\left(n_x + \frac{1}{2}\right). \tag{Д.4}$$

Затем вводится член H' как малое возмущение. Матрица возмущения равна

$$|H'_k, \ldots, n'_\varkappa; k, \ldots, n_\varkappa, \ldots| = \frac{e}{\varkappa}\sqrt{\frac{\pi\hbar\omega c}{L^3}}\times \\ \times \begin{cases} (n_\varkappa+1)^{1/2} & \text{при } n'_\varkappa = n_\varkappa + 1, \\ n_\varkappa^{1/2} & \text{при } n_\varkappa = n_\varkappa - 1. \end{cases} \tag{Д.5}$$

Элементы этой матрицы отличны от нуля только, если

$$\left.\begin{aligned} \boldsymbol{k}' - \boldsymbol{k} = \pm x_0 \\ n'_{x_1} = n_{x_1} \text{ для } x_1 \neq x, \\ n'_x = n_x \pm 1. \end{aligned}\right\} \tag{Д.7}$$

Не углубляясь в исследования законности применения теории возмущений к данной задаче, где спектр энергии непрерывен, следует по крайней мере ограничиться случаями, в которых вычисление не приводит к несобственным интегралам. Последние не появляются лишь при рассмотрении возмущения таких состояний системы, в которых

$$\text{все } n_\varkappa = 0 \text{ и } \frac{\hbar^2 k^2}{2\mu} < \hbar\omega. \tag{Д.8}$$

Вводя обозначения

$$E_0(k) = \frac{\hbar^2 k^2}{2^\mu}, \quad E_0(k,x) = \frac{\hbar^2(k-x)^2}{2\mu} + \hbar\omega, \frac{\hbar^2 u^2}{2\mu} = \hbar\omega \text{ (Д. 9)}$$

и опуская в дальнейшем энергию нулевых колебаний ионов, можно энергию системы во втором приближении записать в виде

$$E(\boldsymbol{k}) = E_0(\boldsymbol{k}) - 2\sum_x \frac{|H'_x|^2}{E_0(k,x) - E_0(k)} = \\ = \frac{\hbar^2 k^2}{2\mu} - \frac{4\mu e^2 \pi\omega c}{L^8\hbar}\sum_x \frac{1}{x^2\left[(k-x)^2 + u^2 - k^2\right]}. \tag{Д.10}$$

Волновая функция системы в первом приближении имеет вид

$$\Psi(k) = \Psi_0(k; 0, 0, \ldots) + \\ + \sum_x C_x \Psi_0\left(k - x; 0, 0, \ldots, 1_x, \ldots, 0, \ldots\right) \tag{Д.11}$$

где

$$C_x = -\frac{2\mu i e\sqrt{2\hbar\omega\pi c}}{\hbar^2 L^{3/2} x\left[(k-x)^2 + u^2 - k^2\right]}. \tag{Д.12}$$

Авторы вышеупомянутой работы используют результаты теории возмущений лишь для предварительной ориентации и стремятся получить более точные результаты прямым вариационным методом. Ψ-функция системы апроксимируется выражением (Д. 11), где коэффициенты $C_\varkappa$ являются параметрами апроксимации и определяются из условия минимума функционала

$$Q[\Psi] = \frac{\int \Psi^* H \Psi d\tau dq}{\int \Psi^* \Psi d\tau dq}. \tag{Д.13}$$

Энергия системы вычисляется как минимальное значение $Q(\Psi)$. В результате расчёта получается:

$$E(k) = E_0(k) - 2\sum_x \frac{|H'_x|^2}{E_0(k,x) - E(k)} = \frac{\hbar^2 k^2}{2\mu} - \frac{4\mu \cdot e^2 \pi \omega c}{L^3 \hbar} \times$$
$$\times \sum_x \frac{1}{x^2\left[(k-x)^2 + u^2 - \frac{2\mu}{\hbar^2}E(k)\right]} \tag{Д.14}$$

Это выражение превращается в соответствующее выражение теории возмущений (Д. 10), если энергия возмущения достаточно мала.

Чтобы решить уравнение (Д. 14) относительно $E(k)$, удобно ввести следующие безразмерные переменные:

$$x = \frac{k}{u}, \quad \alpha = \frac{c}{2}\frac{e^2 u}{\hbar\omega}, \quad y = \frac{E_0(k) - E(k)}{\hbar\omega}. \tag{Д.15}$$

При этом энергия системы может быть выражена в виде

$$E(k) = \hbar\omega\left(x^2 - y\right). \tag{Д.16}$$

Если подставить безразмерные переменные в формулу (Д. 14) и заменить суммирование интегрированием, получается:

$$y = \frac{\alpha u}{2\pi^2}\int_0^\infty d\varkappa \iint \frac{dQ}{(k-x)^2 + u^2(1+y) - k^2} =$$
$$= \frac{\alpha}{x}\arcsin\frac{x}{(1+y)^{1/2}} \tag{Д.17}$$

Неравенство (Д. 8) означает, что $x^2 < 1$. В этом случае знаменатель подинтегрального выражения не обращается в нуль.

Уравнение (Д. 17) можно переписать в более удобной форме:

$$\frac{x}{(1+y)^{2/2}} = \sin\frac{xy}{\alpha}. \tag{Д.18}$$

В состоянии с наименьшей энергией $k = 0$, т. е. $x = 0$. В этом случае (Д. 18) превращается в

$$y_0\left(1 + y_0\right)^{1/2} = \alpha. \tag{Д.19}$$

Если здесь $\alpha \ll 1$, то получается $y_0 \cong \alpha$, что соответствует предельному случаю малого взаимодействия и совпадает с результатом теории возмущений.

Перейдём теперь к сравнению результатов Фрейлиха, Пельцера и Цинау с нашими результатами и выясним, какой из методов вычисления и в каких случаях имеет преимущества. Выше в монографии энергия основного состояния системы была вычислена двумя способами. Грубо приближённое значение энергии было получено прямым вариационным методом в § 14. Оно выражается формулой (14.25):

$$J\left[\psi_0\right] = -0,544\frac{\mu e^4}{\hbar^2}c^2 = -0,109\alpha^2\hbar\omega. \tag{Д.20}$$

Здесь α - параметр, введённый формулой (Д.15). Другое более точное, вычисление в § 16 привело к формуле (16.20).

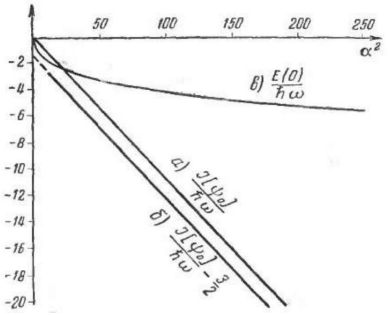

Рис. Д. 1.

Энергия основного состояния системы за вычетом энергии нулевых колебаний ионов в этом случае равна

$$J\left[\psi_0\right] - \frac{3}{2}\hbar\omega = -\left(0,109\alpha^2 + \frac{3}{2}\right)\hbar\omega. \tag{Д.21}$$

На рис. Д. 1 даны значения энергии основного состояния в единицах $\hbar\omega$ в зависимости от параметра α. Кривая а)

представляет формулу (Д. 20), кривая б) - формулу (Д. 21) и кривая в) - формулу (Д. 19). Сравнивая энергии, полученные прямыми вариационными методами, следует отдать предпочтение тому из них, который привёл к наиболее низкому значению энергии.

Из рисунка видно, что метод Фрейлиха, Пельцера и Цинау имеет преимущества в случае

$$\frac{\left|J\left[\psi_c\right]\right|}{\hbar_\omega} < 1, \tag{Д.22}$$

т. е. как раз тогда, когда нарушено условие адиабатичности (7.2-3), лежащее в основе нашего метода. В реальных ионных кристаллах это встречается редко.

Наш метод имеет преимущества в случае

$$\frac{J\left[\psi_0\right]}{\hbar\omega} > 1, \tag{Д.23}$$

который реализуется в большинстве кристаллов и, в частности, во всех кристаллах, рассмотренных в главе VI (кроме, может быть, кристалла PbS). Это видно из нижеследующей таблицы.

Таблица Д.1

	NaCl	KCl	KBr	KJ	Cu_2O
c	0,257	0,251	0,217	0,185	0,139
μ/m	2,78	1,85	1,87	2,11	1,81
$\left\|J\left[\frac{0}{0}\right]\right\| = 1,47\frac{\mu}{m}c^2 \ni .-$	0,270	0,172	0,129	0,106	0,0513
$\hbar_\omega$ эл.-в	0,0322	0,0262	0,02	0,017	0,0313
$\left\|J\left[\frac{6}{0}\right]\right\|/\hbar\omega$	8,39	6,56	6,45	6,24	1,64
$\alpha^2 = 9,18\frac{\left\|J[\psi_0]\right\|}{\hbar\omega}$	77	60,3	59,3	57,3	15,9

В промежуточной области, когда

$$\frac{|J\left[\psi_0\right]|}{\hbar_\omega} \sim 1, \tag{Д.24}$$

оба метода дают, повидимому, лишь качественные результаты.

Посмотрим теперь, в каких случаях можно взаимодействие электрона проводимости с поляризационными колебаниями ионов считать малым возмущением, как это делается в обычной зонной теории. Как показали Фрейлих, Пельцер и Цинау, для этого должно быть $\alpha \ll 1$, что означает согласно формуле (Д. 20)

$$\frac{|J|\psi_0||}{\hbar_\omega} \ll 0,1. \tag{Д.25}$$

Вряд ли найдутся кристаллы, для которых выполнялось бы это условие.

Part V
Old, Fundamental Theories

11 Old Articles that Derive Important Properties

11.1 Electrons in Lattice Fields by Frolich 1954

H. Fröhlich (1954): Electrons in lattice fields, Advances in Physics, 3:11, 325-361
(Viktor said that this article connects Pekar's model with Frolich's model, I'll check later)

11.1.1 § 2. Introduction

An electric point charge e brought into a dielectric medium polarizes its surroundings. If this point charge is static then the polarization is determined by the static dielectric constant (think, how exactly?).

For a moving point charge the polarization can only be determined if the dynamic properties of the medium (which dynamic properties?) are known.

If furthermore the point charge is replaced by a particle with a certain mass and charge, then the polarization produced by the particle reacts on it. A situation arises which can be described in terms of a field, the polarization field, which interacts with the particle; the latter then possesses a self energy in the field. A simple and interesting application of this idea is presented in the motion of a free electron in the conduction band of an ionic crystal with which the present article is mainly concerned.

The interest in discussing this question is twofold. Firstly, of course, a calculation of the properties of free electrons in ionic crystals has an intrinsic interest. Secondly, however, this case provides a very simple example for a non relativistic field theory, and in view of its simplicity it might be expected to lead to the discovery of a number of new features of such fields and to the development of new methods. In fact after the first application of the methods of field theory to electrons in ionic crystals (Fröhlich, Pelzer and Zienau 1950), the use of these methods in metals led to an important step in the theory of superconductivity and to the prediction of the isotope effect (Fröhlich 1950). Subsequent discussion has shown, however (Fröhlich 1953) that new methods are required to deal with all aspects of superconductivity, and at present it seems that a method which would combine the results of the two methods described in §4 and §5 might fit the requirements (cf. end of §6).

The methods of §4 and §5 can best be described as dynamic and static respectively. The static method is essentially an application of Hartree's self consistent field method. Thus an electron with mass m in an ionic lattice may be described by an electronic wave function giving rise to an average charge distribution ρ. Treating this ρ as a static charge, it establishes a polarization in the lattice which can be calculated from the laws of electrostatics. This polarization gives rise to an attractive force on the electron, and to a potential energy of the order $-e^2/l\epsilon^*$ if the charge ρ extends over a spherical range whose radius is of the order l; ϵ^* is an effective dielectric constant. The restriction of the electron in space requires its de Broglie wave length to be of the order l so that its
kinetic energy is of the order $4\pi^2\hbar^2/2ml^2$. Minimizing the total energy E_0 with regard to l leads to

$$\frac{\partial}{\partial l}\left(-\frac{e^2}{l\epsilon^*}+\frac{4\pi^2\hbar^2}{2ml^2}\right)=0;\quad \frac{1}{l}=\frac{e^2m}{4\pi^2\hbar^2\epsilon^*};\quad E_0\sim-\frac{1}{8\pi^2}\frac{e^4m}{\epsilon^{*2}\hbar^2}.. \tag{1.1}$$

A procedure of this kind can be correct only if the time the electron requires to travel the distance l is short compared with the period of the vibrations of the lattice; otherwise it is not permissible to treat ρ as a static charge distribution. This condition is not fulfilled in most cases of practical interest and it is necessary, therefore, to take account of the dynamic properties of the lattice. This is carried out in §4. To obtain a qualitative picture it should be noticed that if $\omega/2\pi$ denotes the frequency of the lattice vibrations giving rise to polarization a point charge moving with velocity v polarizes the lattice to its full static value only at distances large compared with v/ω. Thus for sufficiently large distances the polarization potential decreases like a Coulomb field ; for distances less than v/ω it remains nearly constant. The interaction with the point charge is thus of the order $-e^2\omega/v\epsilon^*$. For an electron this holds only if its velocity is sufficiently large to make its de Broglie wave length h/mv shorter than v/ω. One may expect, therefore, that the lowest value the potential energy can have on the dynamic model is of the order $-e^2/d\epsilon^*$ where d is the length at which $h/mv = v/\omega$, i.e. $d = (h/m\omega)^{1/2}$. In § 4 it is shown, in fact, that the self energy on the dynamic model is of the order $-e^2/d\epsilon^*$.

The range of validity of the two methods will be discussed in § 6; it will also be shown then that the linking up of the two methods has not succeeded so far in view of certain difficulties inherent in the Hartree method.

Finally in § 7 questions of mobility will be discussed.

11.1.2 § 2. Lattice Fields

The field of force acting on an electron brought into an insulating or semiconducting crystal can be derived from a periodic field of force. This latter will be defined as the field of force in an ideal crystal assuming that the atoms or ions of the lattice are undeformable and are rigidly fixed to the lattice points. F. Bloch (1928) has shown that an electron can move freely through such a periodic field of force though the connection between its energy and its momentum in general differs from that of a free electron in vacuum. In many cases, in particular for slow electrons in the conduction band, the electronic energy η_k is a quadratic function of the momentum $\hbar\mathbf{k}$ so that

$$\eta_k = \hbar^2 k^2/2m, \tag{2.1}$$

as for free electrons although the effective mass m in general differs from the electronic mass m_{el}. This case (2.1) will always be assumed for the following.

Such an electron for which the periodic field of force has already been taken into account is subject to further forces resulting from deviations of the field of force from strict periodicity. These are due to displacements and deformations of atoms or ions (lattice defects will be disregarded here). Such displacements can be described by attaching a displacement vector to each lattice point. Moreover for electrons with sufficiently low energy the electronic wave function changes only very little in one lattice distance. Therefore the lattice can be treated as a continuum. The displacement vectors then become a continuous function of position, i.e. they form a vector field.

The present article is mainly concerned with isotropic ionic crystals. Here displacements leading to electric polarization have a much stronger interaction with electrons than other types of displacements. The latter will, therefore, be disregarded though their influence on the mobility will be mentioned in § 7. Let $\mathbf{P}(\mathbf{r})$ be the electric polarization at the position $\mathbf{r}$. Its interaction with the magnetic field of a slow electron is negligible compared with the electrostatic interaction. Therefore the rotational part of $\mathbf{P}$ is irrelevant so that the condition

$$\operatorname{curl}\mathbf{P}(\mathbf{r}) = 0, \tag{2.2}$$

can be imposed. Hence if electric displacement $\mathbf{D}(\mathbf{r})$ and electric field $\mathbf{E}(\mathbf{r})$ are introduced in the usual way by

$$D(r) = E(r) + 4\pi P(r), \tag{2.3}$$

the only sources of $\mathbf{D}$ are free charges, i.e. in the case of a single free electron in the crystal,

$$\left.\begin{array}{ll} & \mathbf{D}\left(\mathbf{r}, \mathbf{r}_{el}\right) = -\operatorname{grad} \frac{e}{|\mathbf{r}-\mathbf{r}_{el}|}, \\ \text{i.e.} & \operatorname{curl} \mathbf{D} = \mathbf{0}; \quad \operatorname{div} \mathbf{D} = 4\pi e \delta\left(\mathbf{r} - \mathbf{r}_{el}\right), \end{array}\right\} \tag{2.4}$$

where $\mathbf{r}_{el}$ is the electronic coordinate and $+e$ the electronic charge. In the absence of electrons $D = 0$, therefore, so that $\mathbf{D}$ represents the 'external' field acting on the polarization of the crystal. Since $\mathbf{P}(\mathbf{r})d^3\mathbf{r}$ is the electric dipole moment of a volume $d^3\mathbf{r}$ around $\mathbf{r}$, clearly if a potential $\Phi(\mathbf{r})$ is defined by

$$4\pi \mathbf{P}(\mathbf{r}) = \operatorname{grad} \Phi(\mathbf{r}), \quad . \tag{2.5}$$

the interaction energy between electron and lattice displacements is given by (using (2.4))

$$-\int D\left(\mathbf{r}, \mathbf{r}_{el}\right) \mathbf{P}(\mathbf{r}) d^3\mathbf{r} = \frac{1}{4\pi} \int \operatorname{grad} \frac{e}{|\mathbf{r} - \mathbf{r}_{el}|} \operatorname{grad} \Phi(\mathbf{r}) d^3\mathbf{r} = e\Phi\left(\mathbf{r}_{el}\right). \tag{2.6}$$

Since the lattice polarization does not make any contribution to $\mathbf{D}$, it follows that -4πP represents the electric field due to the polarization, and $\Phi(\mathbf{r})$ is its potential.

It should be emphasized now that the polarization $\mathbf{P}$ is determined by the dynamic properties of the lattice. Thus while $\mathbf{D}$ is always given by (2.4) independent of the state of polarization of the lattice, the electric
field E depends on it, and can be found from (2.3) provided P has been determined from the dynamic equations. In reasonable approximation (cf. Fröhlich 1949, § 18) P can be considered as composed of two contributions

$$\mathbf{P}(\mathbf{r}) = \mathbf{P_0}(\mathbf{r}) + \mathbf{P}_{ir}(\mathbf{r}), \tag{2.7}$$

each of which satisfies a harmonic oscillator equation with frequencies $\omega_0/2\pi$ and $\omega/2\pi$ corresponding to optical absorption in the ultra violet ($\mathbf{P_0}$) and infra red ($\mathbf{P}_{ir}$) regions respectively. The former is mainly due to deformation and the latter due to displacement of ions. In the presence of an external field $\mathbf{D}$,

$$\ddot{\mathbf{P}}_{ir}(\mathbf{r}) + \omega^2 \mathbf{P}_{ir}(\mathbf{r}) = \mathbf{D}\left(\mathbf{r}, \mathbf{r}_{el}\right)/\gamma, \tag{2.8}$$

$$\ddot{\mathbf{P}}_{\mathbf{0}}(\mathbf{r}) + {\omega_{\mathbf{0}}}^2 \mathbf{P_0}(\mathbf{r}) = \mathbf{D}\left(\mathbf{r}, \mathbf{r}_{el}\right)/\delta, \tag{2.9}$$

where γ and δ are constants closely connected with the energy due to the respective displacements (cf. eqn. (2.20)). The frequency $\omega/2\pi$ is correlated to the frequency $\omega_r/2\pi$ of residual rays by

$$\omega = \left(\epsilon/\epsilon_\infty\right)^{1/2} \omega_r, \tag{2.10}$$

where ϵ is the static dielectric constant and ${\epsilon_\infty}^{1/2}$ is the refractive index in the optical region before onset of ultra violet absorption.

To find γ and δ, consider the static case in which $\mathbf{P} = 0$, i.e.

$$4\pi \mathbf{P}(\mathbf{r}) = (\epsilon - 1)\mathbf{E}(\mathbf{r}) = (1 - 1/\epsilon)\mathbf{D}(\mathbf{r}) \tag{2.11}$$

making use of the static relation $\mathbf{D} = \epsilon \mathbf{E}$. Furthermore, the high frequency dielectric constant ϵ_∞ is defined by $\mathbf{D} = \epsilon_\infty \mathbf{E}$ on the assumption that the frequency $\omega_\infty/2\pi$ of the external field satisfies the condition $\omega_0 \gg \omega_\infty \gg \omega_{ir}$. In this case equations (2.8) and (2.9) show immediately that the infra red polarization can no longer follow and hence is negligible, $\mathbf{P}_{ir} \simeq 0$, but that the optical polarization $\mathbf{P}_0$ can follow nearly adiabatically so that $\ddot{\mathbf{P}}_0$ can be neglected as compared with ${\omega_0}^2\mathbf{P}_0$. Hence $\mathbf{P}_0$ has nearly the same value as in a static field of equal strength,

$$4\pi P_0(r) = (1 - 1/\epsilon_\infty)\, D(r), \qquad \text{(static case)} \tag{2.12}$$

so that from (2.11), (2.12) and (2.7),

$$4\pi P_{ir}(r) = \left(\frac{1}{\epsilon_\infty} - \frac{1}{\epsilon}\right) D(r) \qquad \text{(static case)} \tag{2.13}$$

Comparison of (2.8) and (2.9), for the static case ($\ddot{\mathbf{P}}_{ir} = 0, \ddot{\mathbf{P}}_0 = 0$), with (2.12) and (2.13) respectively leads to

$$\begin{aligned} \frac{1}{\gamma} &= \frac{\omega^2}{4\pi}\left(\frac{1}{\epsilon_\infty} - \frac{1}{\epsilon}\right), \\ \frac{1}{\delta} &= \frac{\omega_0^2}{4\pi}\left(1 - \frac{1}{\epsilon_\infty}\right) \end{aligned} \tag{2.15}$$

The equations of motion (2.8) and (2.9) of the lattice field have to be supplemented by the equation of motion for the electron which follows immediately with the help of the interaction energy (2.6). Thus classically

$$m\ddot{\mathbf{r}}_{el} = -e \operatorname{grad} \Phi\left(\boldsymbol{r}_{el}\right) \tag{2.16}$$

All three equations of motion can be derived from the Lagrangian

$$\begin{aligned} L = \frac{1}{2}\gamma \int \left[\dot{\mathbf{P}}_{ir}{}^2(\mathbf{r}) - \omega^2 \mathbf{P}_{ir}{}^2(\mathbf{r})\right] d^3\mathbf{r} + \frac{1}{2}\delta \int \left[\dot{\mathbf{P}}_0{}^2(\mathbf{r}) - {\omega_0}^2 \mathbf{P}_0{}^2(\mathbf{r})\right] d^3\mathbf{r} \\ + \int \mathbf{D}\left(\mathbf{r}, \mathbf{r}_{el}\right)\left[\mathbf{P}_0(\mathbf{r}) + \mathbf{P}_{ir}(\mathbf{r})\right] d^3\mathbf{r} + \frac{1}{2} m \dot{\mathbf{r}}_{el}{}^2, \end{aligned} \tag{2.17}$$

by putting

$$\delta L = 0, \tag{2.18}$$

and treating the components of $\mathbf{r}_{el}, \mathbf{P_0}(\mathbf{r})$ and $\mathbf{P}_{ir}(\mathbf{r})$ as variables. † It will be noticed that in contrast to most other types of fields the spatial derivatives of the functions $\mathbf{P}_0(\mathbf{r})$ and $\mathbf{P}_{ir}(\mathbf{r})$ do not occur in the Lagrangian. Therefore in a straightforward way the components of these functions at different positions can be taken as different variables and (2.18) then yields immediately

$$\frac{d}{dt}\frac{\partial L}{\partial \dot{q}} - \frac{\partial L}{\partial q} = 0, . \tag{2.19}$$

if q represents any of these variables; the differentiations with respect to them follow by considering the integrals as limits of sums. Equations (2.19) then lead to eqns. (2.16), and to (2.8) and (2.9) for all $\mathbf{r}$.

The moment conjugate to q is defined as $\partial L/\partial \dot{q}$ so that $\gamma \mathbf{P}_{ir}(\mathbf{r}), m\dot{\mathbf{r}}_{el}$ and $\delta \dot{\mathbf{P}}_{\mathbf{0}}(\mathbf{r})$ are conjugate to $\mathbf{P}_{ir}(\mathbf{r}), \mathbf{r}_{el}$ and $\mathbf{P_0}(\mathbf{r})$ respectively. Hence the Hamiltonian is given by

$$H' = \sum_q \frac{\partial L}{\partial \dot{q}} \dot{q} - L = \frac{1}{2}\gamma \int \left[\dot{\mathbf{P}}_{ir}{}^2(\mathbf{r}) + \omega^2 \mathbf{P}_{ir}{}^2(\mathbf{r})\right] d^3\mathbf{r}$$
$$+ \frac{1}{2}\delta \int \left[\dot{\mathbf{P}}_0{}^2(\mathbf{r}) + \omega_0{}^2 \mathbf{P}_0{}^2(\mathbf{r})\right] d^3\mathbf{r}$$
$$- \int D\left(\mathbf{r}, \mathbf{r}_{el}\right) \left[\mathbf{P}_{ir}(\mathbf{r}) + \mathbf{P}_0(\mathbf{r})\right] d^3\mathbf{r} + \frac{1}{2} m \dot{\mathbf{r}}_{el}{}^2.. \tag{2.20}$$

In the classical case of an electron at rest, when $\mathbf{P_0}$ and $\mathbf{P}_{ir}$ are given by (2.12) and (2.13), and $\mathbf{D}$ by (2.4), H' becomes infinite because the integrands in (2.20) diverge as $\mathbf{r} \to \mathbf{r}_{el}$. This arises from the disregard of the atomic structure of the substance. In a rough way this can be remedied by developing the polarization vectors in a Fourier series, and omitting terms with wave lengths shorter than a critical one whose wave length is of the order of the lattice distance.

In the quantum mechanical treatment this divergency does not occur as will be seen in §§4 and 5. Nevertheless, for simplicity, a classical argument will be used to eliminate the contributions of $\mathbf{P_0}$ to the

Hamiltonian. For this purpose it will be noticed that the force acting on a classical electron at rest must vanish, so that $\Phi(\mathbf{r})$ has a minimum at $\mathbf{r} = \mathbf{r}_{el}$ (provided the above mentioned 'cut off' at short waves is used) and $\mathbf{P}\left(\boldsymbol{r}_{el}\right)$ vanishes. For a moving electron, however, $\mathbf{P}\left(\boldsymbol{r}_{el}\right)$ does not vanish because of the time dependent terms in the equations of motion for $\mathbf{P}_{\mathrm{ir}}\left(\mathbf{r}\right)$ and $\mathbf{P_0}(\mathbf{r})$. Inspection of eqns. (2.8) and (2.9) for a time dependent D shows that for slowly moving electrons $\mathbf{P}_0\left(\mathbf{r}_{el}\right)$ remains nearly zero and at any rate is much smaller than $\mathbf{P}_{ir}\left(\mathbf{r}_{el}\right)$ because $\omega_0{}^2$ is very large compared with $\omega_{ir}{}^2$. Physically it means that the deformation of the ions giving rise to $\mathbf{P}_0$ has a much smaller inertia than the displacement of ions (leading to $\mathbf{P}_{ir}$). It follows from the above that all terms in H' containing $\mathbf{P_0}(\mathbf{r})$ depend only very insensitively on the velocity of the electron. For small velocity the quantity

$$C = \int \left\{\frac{1}{2}\delta \left[\dot{\mathbf{P}}_0^2(\mathbf{r}) + \omega_0^2 \mathbf{P}_0^2(\mathbf{r})\right] - D\left(\mathbf{r}, \mathbf{r}_{el}\right) \mathbf{P}_0(\mathbf{r})\right\} d^3\mathbf{r} \tag{2.21}$$

can then be considered as a constant and the Hamiltonian of a slow electron in an ionic lattice field can then be written as

$$H = H' - C = \int \left\{\frac{1}{2}\gamma \left[\dot{\mathbf{P}}_{ir}{}^2(\mathbf{r}) + \omega^2 \mathbf{P}_{ir}{}^2(\mathbf{r})\right] - \mathbf{D}\left(\mathbf{r}, \mathbf{r}_{el}\right) \mathbf{P}_{ir}(\mathbf{r})\right\} d^3\mathbf{r} + \frac{1}{2} m \dot{\mathbf{r}}_{el}{}^2 \tag{2.22}$$

It is useful to introduce here a complex field vector $\mathbf{B}(\mathbf{r})$ such that

$$\mathbf{B}(\mathbf{r}) = \left(\frac{\gamma\omega}{2\hbar}\right)^{1/2} \left(\mathbf{P}_{ir}(\mathbf{r}) + \frac{i}{\omega}\dot{\mathbf{P}}_{ir}(\mathbf{r})\right), \tag{2.23}$$
$$\mathbf{B}^+(\mathbf{r}) = \left(\frac{\gamma\omega}{2\hbar}\right)^{1/2} \left(\mathbf{P}_{ir}(\mathbf{r}) - \frac{i}{\omega}\dot{\mathbf{P}}_{ir}(\mathbf{r})\right), \tag{+}$$
$$\operatorname{curl} \mathbf{B} = \operatorname{curl} \mathbf{B}^+ = 0, \tag{2,24}$$

or

[8]† In view of conditions (2.2), $\mathbf{P}_0$ and $\mathbf{P}_{ir}$ actually have only one available component each.

$$\mathbf{P}_{ir}(\mathbf{r}) = \left(\frac{\hbar}{2\gamma\omega}\right)^{1/2} [\mathbf{B} + (\mathbf{r}) + \mathbf{B}(\mathbf{r})], \tag{2.25}$$

$$\dot{\mathbf{P}}_{ir}(\mathbf{r}) = \left(\frac{\hbar\omega}{2\gamma}\right)^{1/2} i[\mathbf{B} + (\mathbf{r}) - \mathbf{B}(\mathbf{r})].\cdot \tag{2.26}$$

Then with (2.22),
$H = \hbar\omega \int \mathbf{B} + (\boldsymbol{r})\mathbf{B}(\boldsymbol{r})d^3\mathbf{r} - \left(\frac{\hbar}{2\gamma\omega}\right)^{1/2} \int \mathbf{D}\left(\mathbf{r}, \boldsymbol{r}_{el}\right)[\mathbf{B} + (\mathbf{r}) + \mathbf{B}(\mathbf{r})]d^3\mathbf{r} + \frac{\mathbf{p}_{el}{}^2}{2m}$,
where $\mathbf{p}_{el} = m\dot{\mathbf{r}}_{el}$. The constants in the definition of $\mathbf{B}$ have been chosen in view of the following quantization. For this purpose $\mathbf{B}(\mathbf{r})$ will be subjected to a periodic boundary condition over a cube of volume $V = L^3$, i.e. considering (2.24),

$$\mathbf{B}(\mathbf{r}) = \sum_{\mathbf{w}} \frac{\mathbf{w}}{w} b_{\mathbf{w}} \frac{\exp(i\mathbf{wr})}{V^{1/2}}, \quad \mathbf{B} + (\mathbf{r}) = \sum_{\mathbf{w}} \frac{\mathbf{w}}{w} b_{\mathbf{w}} + \frac{\exp(-i\mathbf{wr})}{V^{1/2}}, \tag{2.28}$$

where the coefficients w_i of the wave vector $\mathbf{w}$ satisfy

$$w_i = \frac{2\pi}{L} n_i, \quad n_i = 0, \pm 1, \pm 2, . \tag{2.29}$$

Also defining (cf. (2.5)) $\Phi_{ir}(\mathbf{r})$ by

$$4\pi \mathbf{P}_{ir}(\mathbf{r}) = \operatorname{grad} \Phi_{ir}(\mathbf{r}), \tag{2,30}$$

it follows that (cf. (2.6)) the interaction energy is given by

$$-\int \mathbf{D}\left(\mathbf{r}, \mathbf{r}_{el}\right) \mathbf{P}_{ir}(\mathbf{r}) d^3\mathbf{r} = e\Phi_{ir}\left(\mathbf{r}_{el}\right) \tag{2.31}$$

or using (2.30), (2.25) and (2.28), by
$e\Phi_{ir}\left(\mathbf{r}_{el}\right) = 4\pi i \left(\frac{e^2\hbar}{2\gamma\omega V}\right)^{1/2} \sum_{\mathbf{w}} \frac{1}{w} \left[b_{\mathbf{w}} + \exp\left(-i\mathbf{wr}_{el}\right) - b_{\mathbf{w}} \exp\left(i\mathbf{wr}_{el}\right)\right]$.
Hence with (2.27),

$$\begin{aligned} H =& \frac{p_{el}^2}{2m} + \hbar\omega\Sigma b_{\mathbf{w}} + b_{\mathbf{w}} \\ &+ 4\pi i \left(\frac{e^2\hbar}{2\gamma\omega V}\right)^{1/2} \sum_{\mathbf{w}} \frac{1}{w} \left[b_{\mathbf{w}} + \exp\left(-i\mathbf{wr}_{el}\right) - b_{\mathbf{w}} \exp\left(i\mathbf{wr}_{el}\right)\right]. \end{aligned} \tag{2.33}$$

It will be noticed that (2.32) holds only if $w \neq 0$, and in fact terms with $w = 0$ must be excluded from all the sums. To justify this it should be realized that strictly speaking the case of a single electron in an otherwise neutral lattice cannot be subjected to a periodic boundary condition. For the volume V contains an electron, i.e. the charge e, a situation which cannot be continued periodically in view of the long range of repulsive Coulomb interaction. To avoid this difficulty an opposite charge, -e, should be distributed homogeneously over the volume V. This just compensates the component $w = 0$ of the electronic charge, and hence there is no $w = 0$ term in the interaction energy.

For quantization it will be remembered that the components of $\mathbf{P}_{\mathbf{ir}}(\mathbf{r})$ and $\gamma\mathbf{P}_{ir}(\mathbf{r})$ are conjugate variables. Making use of (2.25), (2.26), (2.28) and (2.2), this means that $(\hbar/2\gamma\omega)^{1/2}\left(b_{\mathbf{w}}{}^{+} + b_{\mathbf{w}}\right)$ and $\gamma(\hbar\omega/2\gamma)^{1/2} i\left(b_{\mathbf{w}}{}^{+} - b_{\mathbf{w}}\right)$ are conjugate. Thus using the notation $[u, v] = uv - vu$, quantization according to Bose statistics demands that

$$\frac{1}{2}i\hbar\left[b_{\mathbf{w}}{}^{+}+b_{\mathbf{w}},b_{\mathbf{w}}{}^{+--}b_{\mathbf{w}}\right]=i\hbar, \tag{2.34}$$

and that commutators involving different ws vanish. It then follows that

$$[b_{\mathbf{w}},b_{\mathbf{w}'}+]=\delta_{\mathbf{w},\mathbf{w}'};\quad [b_{\mathbf{w}},b_{\mathbf{w}'}]=0.. \tag{2.35}$$

Also, in the Hamiltonian, the terms with $b_{\mathbf{w}}+b_{\mathbf{w}}$ should by symmetrized and hence be replaced by $\frac{1}{2}\left(b_{\mathbf{w}}+b_{\mathbf{w}}+b_{\mathbf{w}}b_{\mathbf{w}}{}^{+}\right)=b_{\mathbf{w}}+b_{\mathbf{w}}+\frac{1}{2}$, using (2.35). This means that (2.33) should be augmented by $\hbar\omega\Sigma_{\mathbf{w}}\frac{1}{2}$ which is a constant, representing the zero point energy of the oscillating ions. This term can be omitted, however, because it would simply change the zero of the total energy. Also, in the usual way, the components p_{jel} of $\mathbf{p}_{el}$ must be replaced by the operator $(\hbar/i)\partial/\partial r_{jel}$, i.e.

$$[p_{jel},r_{kel}]=-i\hbar\delta_{jk}, \tag{2.36}$$

It is useful at this stage to introduce dimensionless variables, because this shows that the problem presented by the Hamiltonian H, eqn. (2.33), essentially depends on a single parameter, the interaction parameter which is defined by

$$\alpha=\frac{2\pi e^2u}{\hbar\gamma\omega^3}=\frac{1}{2}\left(\frac{1}{\epsilon_\infty}-\frac{1}{\epsilon}\right)\frac{e^2u}{\hbar\omega} \tag{2.37}$$

Use has been made of (2.14); u is an inverse length defined by

$$\frac{\hbar^2u^2}{2m}=\hbar\omega,\qquad \text{i.e. } u=\left(\frac{2m\omega}{\hbar}\right)^{1/2} \tag{:.38}$$

Define now the dimensionless quantities

$$\mathbf{x}=u\mathbf{r}_{el},\quad \mathbf{v}=\mathbf{w}/u,\quad S=Vu^3, \tag{2.39}$$

and express the Hamiltonian in terms of $\hbar\omega$. Then from (2.33), using (2.37)-(2.39),

$$\begin{aligned}F&=\frac{H}{\hbar\omega}\\&=-\sum_{\mathbf{1}}^{\mathbf{3}}\frac{\partial^2}{\partial x_i{}^2}+\sum_{\mathbf{v}}b_{\mathbf{v}}+b_{\mathbf{v}}+i\left(\frac{\mathbf{4}\pi\alpha}{S}\right)^{1/2}\sum_{\mathbf{v}}\frac{1}{v}\left[b_{\mathbf{v}}+\exp(-i\mathbf{vx})-b_{\mathbf{v}}\exp(i\mathbf{vx})\right]\end{aligned} \tag{2.40}$$

where x_i are the components of $\mathbf{x}$.

11.1.3 §3. General Properties

The aim of the present section is to discuss some general properties of the polarization field $\mathbf{P}_{ir}(\mathbf{r})$ or $\mathbf{B}(\mathbf{r})$. Consider first the field in the absence of an electron. Its Hamiltonian H_{field} follows from (2.33) by omitting the electronic and the interaction terms, i.e.

$$H_{\text{field}}=\Sigma H_{\mathbf{w}};\quad H_{\mathbf{w}}=\hbar\omega b_{\mathbf{w}}+b_{\mathbf{w}} \tag{3.1}$$

Here $H_{\mathbf{w}}$ will be recognized as the Hamiltonian of a harmonic oscillator with frequency $\omega/2\pi$, coordinate $q_{\mathbf{w}}$ and momentum $p_{\mathbf{w}}$ where

$$q_{\mathbf{w}}=\left(\frac{\hbar}{2M\omega}\right)^{1/2}\left(b_{\mathbf{w}}++b_{\mathbf{w}}\right);\quad p_{\mathbf{w}}=i\left(\frac{M\hbar\omega}{2}\right)^{1/2}\left(b_{\mathbf{w}}{}^{+-}b_{\mathbf{w}}\right) \tag{3.2}$$

and M is its mass. For then

$$H_{\mathbf{w}} = \frac{p_{\mathbf{w}}^2}{2M} + \frac{1}{2}M\omega^2 q_{\mathbf{w}}^2 - \frac{1}{2}\hbar\omega \tag{3.3}$$

From the theory of the harmonic oscillator it follows that the eigenvalues of ${b_{\mathbf{w}}}^+ b_{\mathbf{w}}$ are positive integers, or zero, i.e.

$$b_{\mathbf{w}} + b_{\mathbf{w}} \left|n_{\mathbf{w}}\right\rangle = n \left|n_{\mathbf{w}}\right\rangle, \quad n = 0, 1, 2, , \tag{3.4}$$

where $\left|n_{\mathbf{w}}\right\rangle$ denotes a normalized eigenfunction. Also it is easily proved that (n is a positive integer)

$$b_{\mathbf{w}}^{+n} \left|0_{\mathbf{w}}\right\rangle = (n!)^{1/2} \left|n_{\mathbf{w}}\right\rangle, \tag{3.5}$$

and

$${b_w}^n \left|n_w\right\rangle = (n!)^{1/2} \left|0_w\right\rangle; \quad b_w \left|0_w\right\rangle = 0 \tag{3.6}$$

In view of these properties the operators $b_{\mathbf{w}}+$ and $b_{\mathbf{w}}$ are denoted as creation and annihilation operators, respectively.

The field is thus represented by a set of oscillators $\mathbf{w}$, all having the same frequency $\omega/2\pi$. Alternatively the field can be considered as represented by polarization quanta of different wave numbers $\mathbf{w}$, but all having the same energy $\hbar\bar{\omega}$, independent of w. The corresponding classical polarization waves have thus equal frequency, independent of the wave number, a property which follows also directly from eqn. (2.8). Hence

$$\partial\omega/\partial w = 0, \tag{3.7}$$

which means that the group velocity of polarization waves vanishes.
One would conclude from this that the field cannot transportmomentum. In field theory the quantity $\hbar w$ is, however, usually denoted as momentum of a quantum because in the presence of an electron the operator

$$h\mathbf{W} = \sum \hbar\mathbf{w} b_{\mathbf{w}} + b_{\mathbf{w}} + \mathbf{p}_{el} \tag{3.8}$$

is a constant of motion, i.e.

$$[\mathbf{W}, H] = 0 \quad \cdot \tag{3.9}$$

Equation (3.9) follows immediately from (3.8) and (2.33) using the commutators (2.35) and (2.36). For clearly ${p_{el}}^2$ and $b_{\mathbf{w}} + b_{\mathbf{w}}$ commute both with $\mathbf{W}$ whereas

$$\left[{b_{\mathbf{w}}}^+ b_{\mathbf{w}}, {b_{\mathbf{w}}}^+\right] = {b_{\mathbf{w}}}^+, \quad [p_{el}, \exp(-i\mathbf{w}\mathbf{r}_{el})] = -\hbar\mathbf{w}\exp(-i\mathbf{w}\mathbf{r}_{el}), \text{ etc.} \tag{3.10}$$

Hence the commutator of $\mathbf{p}_{el}$ with the interaction term in the Hamiltonian just cancels that of $\Sigma\hbar\mathbf{w}b_{\mathbf{w}} + b_{\mathbf{w}}$. In spite of (3.9) it will be shown presently that a polarization quantum does not carry any momentum. In fact through discussions with B. Szigeti and S. Zienau it was realized that in any lattice field the quanta cannot carry momentum because the individual atoms or ions of the lattice oscillate around their respective equilibrium positions, and hence on an average have zero momentum. The momentum of the lattice is always carried by its centre of gravity as will be demonstrated presently. Hence (3.9) does not represent the momentum law but the law of conservation of the total wave vector.

To show this it will be necessary to introduce the coordinate $\boldsymbol{r}_c$ of the centre of gravity of the lattice and treat it as a dynamic variable. This means that the developments of § 2 , in

particular the equations of motion, the Lagrangian and the Hamiltonian require modifications because in §2 it was tacitly assumed that the centre of gravity is at rest. To carry this through let $\mathbf{r}'$ be the positional vector in a fixed coordinate system relative to which the centre of gravity has the coordinate $\mathbf{r}_c$, and the electron has the coordinate $\mathbf{r}_{el}{}'$, i.e.

$$\mathbf{r}' = \mathbf{r} + \mathbf{r}_c, \quad \mathbf{r}'_{el} = \mathbf{r}_{el} + \mathbf{r}_c \tag{3.11}$$

Hence the polarization vector $\mathbf{P}_{ir}(\mathbf{r}, t)$ has to be replaced by

$$\mathbf{P}_{ir}\left(\mathbf{r}' - \mathbf{r}_c, t\right) = \mathbf{P}'\left(\mathbf{r}', t\right)$$

and

$$\frac{\partial \mathbf{P}_{ir}(\mathbf{r}, t)}{\partial t} \quad \text{by} \quad \frac{\partial \mathbf{P}'\left(\mathbf{r}', t\right)}{\partial t} + \left(\dot{\mathbf{r}}_c \frac{\partial}{\partial \mathbf{r}'}\right) \mathbf{P}'\left(\mathbf{r}', t\right) \tag{3.12}$$

With these replacements, the new Lagrangian L' is obtained from the field terms of (2.17) (the $\mathbf{P}_0$-terms will be omitted) by adding the kinetic energies of electron and centre of gravity. Thus introducing the operator

$$\partial = \partial\left(t, \mathbf{r}', \dot{\mathbf{r}}_c\right) = \frac{\partial}{\partial t} + \left(\dot{\mathbf{r}}_c \frac{\partial}{\partial \mathbf{r}'}\right), . \tag{3.13}$$

one finds (NM is the mass of the lattice)

$$L' = \int \left\{ \frac{1}{2}\gamma\left(\partial \mathbf{P}'\right)^2 - \frac{1}{2}\gamma\omega^2 \mathbf{P}'^2 + \mathbf{D}\mathbf{P}' \right\} d^3\mathbf{r}' + \frac{1}{2} m \dot{\mathbf{r}}'^2_{el} + \frac{1}{2} NM \dot{\mathbf{r}}_e^2 \tag{3.14}$$

It will be noted that $\mathbf{D}\left(\mathbf{r}, \mathbf{r}_{el}\right) = \mathbf{D}\left(\mathbf{r}', \mathbf{r}_{el}{}'\right)$ because this function depends on $|\mathbf{r} - \mathbf{r}_{el}|$ only. The variables in L' are the components of $\mathbf{r}_c, \mathbf{r}_{el}{}'$ and $\mathbf{P}'\left(\mathbf{r}', t\right)$ the latter for all value of $\mathbf{r}'$. The conjugate momenta are given by

$$p_{ci} = \frac{\partial L'}{\partial \dot{\mathbf{r}}_{ci}} = NM \dot{\mathbf{r}}_{ci} + \gamma \int \partial \mathbf{P}' \frac{\partial}{\partial r'_i} \mathbf{P}' d^3\mathbf{r}', \tag{3.15}$$

$$\mathbf{P}'_{el} = \frac{\partial L'}{\partial \dot{\mathbf{r}}_{el}} = m \dot{\mathbf{r}}'_{el} \quad \cdots\cdots \tag{3.16}$$

and

$$\mathbf{Q}' = \frac{\partial L'}{\partial \dot{\mathbf{p}}'} = \gamma \partial\left(t, \mathbf{r}', \dot{\mathbf{r}}_c\right) \mathbf{P}. \quad \cdots\cdots \tag{3.17}$$

The equations of motion follow with the help of (2.19). Since spatial derivatives of $\mathbf{P}'$ now occur under the integral, the Lagrangian derivative with regard to $\mathbf{P}'$ has to be taken, i.e.

$$\left(\frac{\partial}{\partial q}\right)_{q = P'_j} \to \frac{\partial}{\partial P'_j} - \sum_l \frac{\partial}{\partial r'_l} \frac{\partial}{\partial\left(\partial P'_j / \partial r'_l\right)}. \tag{3.18}$$

Hence one finds for $q \to \mathbf{r}_{el}{}'$, with (2.4),

$$\begin{aligned} m \ddot{\mathbf{r}}_{el}{}' &= \int \frac{\partial \mathbf{D}\left(|\mathbf{r}' - \mathbf{r}_{el}{}'|\right)}{\partial \mathbf{r}_{el}{}'} \mathbf{P}'\left(\mathbf{r}'\right) d^3\mathbf{r}' = -\int \frac{\partial \mathbf{D}'}{\partial \mathbf{r}'} \mathbf{P}' d^3\mathbf{r}' \\ &= -4\pi e \mathbf{P}'\left(\mathbf{r}_{el}{}'\right) = -e \operatorname{grad} \Phi'\left(\mathbf{r}_{el}{}'\right), \end{aligned} \tag{3.19}$$

where

$$e\Phi'\left(\mathbf{r}_{el}{}'\right) = -\int D\left(|\mathbf{r}' - \mathbf{r}_{el}{}'|\right)\mathbf{P}'\left(\mathbf{r}'\right)d^3\mathbf{r}',. \tag{3.20}$$

denotes the interaction energy between field and electron.
For $q \to r_{ci}$, (2.19) yields

$$NM\ddot{r}_{ci} + \gamma\frac{\partial}{\partial t}\int \partial\left(t, \mathbf{r}', \dot{\mathbf{r}}_c\right)\mathbf{P}'\left(\mathbf{r}'\right)\frac{\partial}{\partial r_i'}\mathbf{P}'\left(\mathbf{r}'\right)d^3\mathbf{r}' = 0, \tag{3.21}$$

and for $q \to \mathbf{P}'$,

$$\partial^2\left(t, \mathbf{r}', \dot{\mathbf{r}}_c\right)\mathbf{P}'\left(\mathbf{r}'\right) + \omega^2\mathbf{P}'\left(\mathbf{r}'\right) = \mathbf{D}\left(\mathbf{r}', \mathbf{r}_{el}'\right)/\gamma.. \tag{3.22}$$

The latter follows also directly from (2.8) with the replacement (3.13). Clearly if $\dot{\mathbf{r}}_{el}{}' = \dot{\mathbf{r}}_c$, then $\mathbf{P}' = \mathbf{D}\left(|\mathbf{r}' - \mathbf{r}_{el}{}'|\right)/\gamma\omega^2$ is a particular solution, as required. The solutions of the homogeneous equation (3.22) (i.e. of (3.22) with $\mathbf{D} = 0$), can be written as a superposition of plane waves such that for one of them

$$\mathbf{P}_{\mathbf{w}}' \propto \exp\left(i\mathbf{w}\mathbf{r}' - i\omega' t\right), \tag{3.23}$$

where

$$\omega' = \omega + \dot{\mathbf{r}}_i\mathbf{w} \quad \text{or} \quad \partial\omega'/\partial\mathbf{w} = \dot{\mathbf{r}}_0, \tag{3.24}$$

the latter with the use of (3.7). Thus the group velocity is now equal to the velocity of the centre of gravity, as required.

To discuss (3.21) it will be noticed that the integral occurring in this equation can be transformed. For with the use of (3.13),

$$\begin{aligned}&\frac{\partial}{\partial t}\int \partial\left(t, \mathbf{r}', \dot{\mathbf{r}}_e\right)\mathbf{P}'\left(\mathbf{r}'\right)\frac{\partial}{\partial r_i'}\mathbf{P}'\left(\mathbf{r}'\right)d^3\mathbf{r}\\ &= \int\left[\left\{\partial^2\mathbf{P}' - \left(\dot{\mathbf{r}}_c\frac{\partial}{\partial\mathbf{r}'}\right)\left(\dot{\mathbf{P}}' + \left(\dot{\mathbf{r}}_c\frac{\partial}{\partial\mathbf{r}'}\right)\mathbf{P}'\right)\right\}\frac{\partial\mathbf{P}'}{\partial r_i'} + \left(\dot{\mathbf{P}}' + \left(\dot{\mathbf{r}}_e\frac{\partial}{\partial\mathbf{r}'}\right)\mathbf{P}'\right)\frac{\partial\dot{\mathbf{P}}}{\partial r_i'}\right]d^3\mathbf{r}'\end{aligned} \tag{3.25}$$

Now through integration in parts it is found that
and

$$\begin{aligned}\int\dot{\mathbf{P}}'\tfrac{\partial\dot{\mathbf{P}}'}{\partial r_i'}d^3\mathbf{r}' = -\int\dot{\mathbf{P}}'\tfrac{\partial\dot{P}'}{\partial r_i'}d^3\mathbf{r}' = 0; \quad &\text{similarly } \int\mathbf{P}'\tfrac{\partial\dot{\mathbf{P}}'}{\partial r_i'}d^3\mathbf{r}' = 0\\ &\int\tfrac{\partial^2\mathbf{P}'}{\partial r_k'\partial r_j'}\tfrac{\partial\mathbf{P}'}{\partial r_i'}d^3\mathbf{r}' = 0, \cdots\end{aligned} \tag{3.26}$$

because all surface integrals vanish. For this reason, also

$$\int\left(\dot{\mathbf{r}}_o\frac{\partial}{\partial\mathbf{r}'}\right)\left(\mathbf{P}'\frac{\partial\dot{\mathbf{P}}'}{\partial r_i'} - \dot{\mathbf{P}}'\frac{\partial\mathbf{P}'}{\partial r_i'}\right)d^3\mathbf{r}' = 0 \tag{3.27}$$

Thus on the right-hand side of (3.25) all terms vanish except $\partial^2\mathbf{P}'$. Making use of (3.22) and again of (3.26), and of curl $\mathbf{P}' = 0$,

$$\begin{aligned}\int\partial^2\mathbf{P}'\frac{\partial\mathbf{P}'}{\partial r_i'}d^3\mathbf{r}' &= -\omega^2\int\mathbf{P}'\frac{\partial\mathbf{P}'}{\partial r_i'}d^3\mathbf{r}' + \frac{1}{\gamma}\int\mathbf{D}\frac{\partial\mathbf{P}'}{\partial r_i'}d^3\mathbf{r}' = \frac{1}{\gamma}\int\left(\mathbf{D}\frac{\partial}{\partial\mathbf{r}'}\right)P_i'd^3\mathbf{r}'\\ &= -\frac{1}{\gamma}\int\frac{\partial\mathbf{D}}{\partial\mathbf{r}'}\mathbf{P}_i' = -4\pi eP_i'\left(\mathbf{r}_{el}{}'\right),\end{aligned} \tag{3.28}$$

the latter with the use of (2.4). Thus from (3.21) and the above,

$$NM\ddot{\mathbf{r}}_c = 4\pi e\mathbf{P}'\left(\mathbf{r}_{el}{}'\right). \tag{3.29}$$

Comparison with (3.19) shows that

$$\frac{d\mathbf{p}}{dt} = 0, \quad \text{where} \quad \mathbf{p} = m\dot{\mathbf{r}}_{el} + NM\dot{\mathbf{r}}_c \tag{3.30}$$

which represents the momentum law on the usual definition of centre of gravity momentum by $NM\dot{\mathbf{r}}_c$. This definition differs from that of $\mathbf{p}_c$ by (3.15) ; this is a pure formality required by the Lagrangian formalism in view of the occurrence of $\dot{\mathbf{r}}_c$ in the field terms. In eqn. (3.30) all properties of polarization waves have been eliminated. This equation thus shows that any change of the electronic momentum by interaction with polarization waves is compensated by an opposite change in $NM\dot{\mathbf{r}}_c$, i.e. by the centre of gravity momentum (in the conventional definition) of the lattice.

The new Hamiltonian now follows in the usual way from (3.14) using (3.15)-(3.17), $H' = \sum_q \dot{q}\frac{\partial L'}{\partial \dot{q}} - L' = \frac{1}{2}NM\dot{\mathbf{r}}_c^2 + \frac{1}{2}m\dot{\mathbf{r}}_{el}^2 + \int\left\{\frac{1}{2}\gamma\left[\left(\partial\mathbf{P}'\right)^2 + \omega^2\mathbf{P}'^2\right] - \mathbf{D}\mathbf{P}'\right\}d^3\mathbf{r}'$.

Again a complex quantity $\mathbf{B}'\left(\mathbf{r}'\right)$ can be introduced similar to (2.23)-(2.26) and (2.28) by

$$\mathbf{B}'\left(\boldsymbol{r}'\right) = \left(\frac{\gamma\omega}{2h}\right)^{1/2}\left(\mathbf{P}' + \frac{i}{\omega}\partial\mathbf{P}'\right) = \sum_{\mathbf{w}}\frac{\mathbf{w}}{w}b_{\mathbf{w}}\frac{\exp\left(i\mathbf{w}\mathbf{r}'\right)}{V^{1/2}}, \tag{3.32}$$

or

$$\mathbf{P}'\left(\mathbf{r}'\right) = \left(\frac{\hbar}{2\gamma\omega}\right)^{1/2}\left[\mathbf{B}' + \left(\mathbf{r}'\right) + \mathbf{B}'\left(\mathbf{r}'\right)\right], \tag{3.33}$$

$$\partial\mathbf{P}'\left(\mathbf{r}'\right) = \left(\frac{\hbar\omega}{2\gamma}\right)^{1/2} i\left[\mathbf{B}' + \left(\mathbf{r}'\right) - \mathbf{B}'\left(\mathbf{r}'\right)\right]. \tag{3.34}$$

Introducing this into (3.15), the momentum $\mathbf{p}_c$ is found to be

$$\mathbf{p}_c = NM\mathbf{r}_c - \Sigma\hbar\mathbf{w}b_{\mathbf{w}}{}' + b_{\mathbf{w}}{}' \tag{3.35}$$

Hence from (3.31) using (3.35), (3.16) and (3.32)-(3.34) by a procedure similar to that leading to (2.33),

$$\begin{aligned} H' =& \frac{1}{2NM}\left(\mathbf{p}_c + \sum_{\mathbf{w}}\hbar\mathbf{w}_{\mathbf{w}}{}' + b_{\mathbf{w}}{}'\right)^2 + \frac{\mathbf{p}_{el}{}^2}{2m} + \hbar\omega\Sigma b_{\mathbf{w}}{}' + b_{\mathbf{w}}{}' \\ &+ 4\pi i\left(\frac{e^2\hbar}{2\gamma\omega V}\right)^{1/2}\sum_{\mathbf{w}}\frac{1}{w}\left[b_{\mathbf{w}}{}' + \exp\left(-i\mathbf{w}\mathbf{r}_{el}{}'\right) - b_{\mathbf{w}}{}'\exp\left(i\mathbf{w}\mathbf{r}_{el}{}'\right)\right]. \end{aligned} \tag{3.36}$$

Quantization can now be carried out in the usual way by introduction of the commutators

$$[b'_{\mathbf{w}}, b'_{\mathbf{w}}+] = \delta_{\mathbf{w},\mathbf{w}'}, \quad \left[p'_{elj}, r'_{elj}\right] = -i\hbar, \quad [p_{cj}, r_{cj}] = -i\hbar \tag{3.37}$$

Thus the conservation law for the total wave number holds as in (3.8) and (3.9), i.e.

$$[\mathbf{W}', H'] = \mathbf{0} \quad \text{with} \quad \hbar\mathbf{W}' = \mathbf{p}_{el}{}' + \sum_{\mathbf{w}}\hbar\mathbf{w}_{\mathbf{w}'}{}' + b_{\mathbf{w}}{}' \tag{3.38}$$

In addition, however, $\mathbf{p}_c$ is also conserved because

$$[\mathbf{p}_c, H'] = 0 \tag{3.39}$$

This follows because H' is independent of $\mathbf{r}_c$. It must be noted that

$$\dot{\mathbf{r}}_c = \frac{\hbar}{i}[H', \mathbf{r}_c] = \frac{!}{NM}\left(\mathbf{p}_c + \Sigma\hbar\mathbf{w}b_{\mathbf{w}}{}' + b_{\mathbf{w}}{}'\right), \tag{3.40}$$

so that with the use of (3.38), eqn. (3.39) is found to be equivalent with

$$[\mathbf{p}, H'] = 0 \quad \text{where} \quad \mathbf{p} = \mathbf{p}_{el} + NM\dot{\mathbf{r}}_c. \tag{3.41}$$

a conservation law already found previously (3.30) for the classical case.
On the usual definition, $\mathbf{p}$ represents the total momentum of the system. Its conservation is clearly a law different from the conservation of the total wave number $\mathbf{W}'$.

In all practical cases, NM is so large that the first term in the Hamiltonian can be neglected, i.e. it is sufficient to deal with (2.33) or (2.40). The main purpose of the above discussion was to clarify the physical meaning of the conservation laws, and to show how momentum is conserved even though polarization quanta do not carry momentum.

11.1.4 §4. Stationary Solutions I

The present section deals mainly with the derivation of approximate wave functions and eigenvalues of the Hamiltonian (2.33) or (2.40). The problem is one of finding the self energy of a single electron in the polarization field. The simplest method to find solutions is application of perturbation theory (cf. Fröhlich, Pelzer and Zienau 1950). This method holds only for weak interaction, i.e. when $\alpha < 1$.

4.1. Perturbation Theory

Consider first the solutions of the Hamiltonian

$$F_0 = -\sum_1^3 \frac{\partial^2}{\partial {x_i}^2} + \sum_{\mathbf{v}} b_{\mathbf{v}} + b_{\mathbf{v}} \tag{4.1}$$

obtained from (2.40) by omitting the interaction terms proportional to the interaction parameter α. The wave functions are products of a free electron wave function, and oscillator wave functions of the type defined in (3.4),

$$|\mathbf{k}; n_{\mathbf{v}_1}, n_{\mathbf{v}_2}, n_{\mathbf{v}}\rangle = S^{-1/2}\exp(i\mathbf{q}\mathbf{x})\Pi\,|n_{\mathbf{v}}\rangle \tag{4.2}$$

where (cf. (2.38))

$$\mathbf{k} = \mathbf{q} + \sum_{\mathbf{v}} \mathbf{v}n_{\mathbf{v}}; \quad u\mathbf{k} = \mathbf{W} \tag{4.3}$$

in dimensionless form (cf. (2.39)), and

$$b_{\mathbf{v}} + b_{\mathbf{v}}\,|n_{\mathbf{v}}\rangle = n_{\mathbf{v}}\,|n_{\mathbf{v}}\rangle \tag{4.4}$$

similar to (3.4). Clearly $\mathbf{q}$ is determined by (4.3) in terms of $\mathbf{k}$ and the n_v 's and need thus not be explicitly included in the parameters defining the wave function. The corresponding energy ϵ_0 (multiples of $\hbar\omega$) satisfying

$$F_0 \left|\mathbf{k}; n_{\mathbf{v}}\right\rangle = \epsilon_0 \left(\mathbf{k}; n_{\mathbf{v}}\right) \left|\mathbf{k}; n_{\mathbf{v}}\right\rangle . \tag{4.5}$$

is given by

$$\epsilon_0 \left(\mathbf{k}; n_{\mathbf{v}}\right) = q^2 + \sum_{\mathbf{v}} n_{\mathbf{v}} = \left(\mathbf{k} - \sum_{\mathbf{v}} \mathbf{v} n_{\mathbf{v}}\right)^2 + \sum_{\mathbf{v}} n_{\mathbf{v}} \tag{4.6}$$

The interaction term (cf. (2.40))

$$F_{\text{int}} = F - F_0 = i \left(\frac{4\pi\alpha}{S}\right)^{1/2} \sum_{\mathbf{v}} \frac{1}{v} \left[b_{\mathbf{v}} + \exp(-i\mathbf{v}\mathbf{x}) - b_{\mathbf{v}} \exp(i\mathbf{v}\mathbf{x})\right] . \tag{4.7}$$

will now be treated as perturbation. This can be done by straightforward use of perturbation theory provided the zero order energy of the system is less than $\hbar\omega$, i.e. the corresponding eigenvalue ϵ_0 of F_0 satisfies $\epsilon_0 < 1$, because then for given total wave vector $\mathbf{k}$ the system is not degenerate. For in this case no quantum is excited, hence $\mathbf{k} = \mathbf{q}$, and $k < 1$ the latter to satisfy $\epsilon_0 < 1$. Thus

$$\left|\mathbf{k}; 0_{\mathbf{v}}\right\rangle = S^{-1/2} \exp(i\mathbf{k}\mathbf{x})_{\chi}; \quad \chi = \Pi \left|0_{\mathbf{v}}\right\rangle ; \quad k < 1. \tag{4.8}$$

is the normalized zero order eigenfunction with wave vector $\mathbf{k}$, and

$$\epsilon_0 \left(\mathbf{k}, 0_v\right) = k^2 < 1 \tag{4.9}$$

is the corresponding zero order energy.
Now since according to (3.5) and (3.6)

$$b_{\mathbf{v}} \left|0_{\mathbf{v}}\right\rangle = 0; \quad b_{\mathbf{v}} + \left|0_{\mathbf{v}}\right\rangle = \left|1_{\mathbf{v}}\right\rangle , \tag{4,10}$$

and in view of the orthogonality of the wave functions

$$S^{-1} \int_S \exp\left(i\mathbf{k} - \mathbf{k}' \cdot \mathbf{x}\right) d^3\mathbf{k} = \delta_{\mathbf{k}\mathbf{k}'}; \quad \left\langle n_{\mathbf{v}} \mid n_{\mathbf{v}}\right\rangle = \delta_{\mathbf{v}\mathbf{v}'} \tag{4.11}$$

the interaction term F_{int} leads to transitions from a state described by (4.8) to states in which a single quantum is excited, provided the total wave vector remains unaltered. Their wave functions are thus of the type

$$\left|\mathbf{k}; 0_{\mathbf{v}_1} 1_{\mathbf{v}} 0_{\mathbf{v}'}\right\rangle = S^{-\mathbf{1/2}} \exp(i\mathbf{k} - \mathbf{v} \cdot \mathbf{x}) b_{\mathbf{v}}{}^{+} \chi \tag{4.12}$$

with an energy

$$\epsilon_0 \left(\mathbf{k}; 0_{\mathbf{v}_1} 1_{\mathbf{v}}\right) = \left(\mathbf{k} - \mathbf{v}\right)^2 + 1 \tag{4.13}$$

The non vanishing matrix elements are thus given by

$$\left\langle 1_{\mathbf{v}} 0_{\mathbf{v}_1}; \mathbf{k}\right| F_{\text{int}} \left|\mathbf{k}; 0_{\mathbf{v}_1} 1_{\mathbf{v}}\right\rangle = i(4\pi\alpha/S)^{1/2} \mathbf{1}/v \tag{4.14}$$

From second order perturbation theory, therefore,

$$E(\mathbf{k}) = \hbar\omega \left(k^2 - \frac{4\tau\alpha}{S} \sum_{\mathbf{v}} \frac{1}{v^2 \left[(\mathbf{k} - \mathbf{v})^2 + 1 - k^2\right]}\right) \tag{4.15}$$

is the perturbed energy (in ordinary units, hence the factor $\hbar\omega$), and, using (4.8), (4.9), (4.12)-(4.14),

$$\Psi(\mathbf{k}) = \frac{\exp(i\mathbf{kx})}{\delta^{1/2}} \left(1 - i\left(\frac{4-c}{s}\right)^{1/2} \sum_{\mathbf{v}} \frac{b_{\mathbf{v}} + \exp(-i\mathbf{vx})}{v\left[(\mathbf{k}-\mathbf{v})^2 + \mathbf{l} - k^2\right]}\right) \chi, . \tag{4.16}$$

the corresponding wave function.
The summation in (4.15) is easily carried out by transforming the sum into an integral,

$$\sum_{\mathbf{v}} \to \frac{S}{(20)^3} \int d^3\mathbf{v}, \tag{4.17}$$

which follows from (2.29) and (2.39). It will be observed that no restriction in the v-integration limits of the type mentioned in § 2 for the classical case is required because of the rapid convergence of the integral for $v > 1$. Thus

$$E(\mathbf{k}) = \hbar\omega \left(k^2 - \alpha \frac{\sin^{-1} k}{k}\right); \quad k < 1, \alpha < 1.. \tag{4.18}$$

Also since for $k < 1$,

$$\frac{\sin^{-1} k}{k} = k + \frac{1}{6}k^3 +, \quad k < 1 \tag{4.19}$$

we have

$$E(\mathbf{k}) = E(0) + \frac{\hbar^2}{2m^*}(uk)^2 +, , \tag{4.20}$$

where (c.f (2.38))

$$E(0) = -\alpha\hbar\omega = -\left(\frac{1}{\epsilon_\infty} - \frac{1}{\epsilon}\right) e^2 \left(\frac{m\omega}{2\hbar}\right)^{1/2}, \quad \alpha < 1. \tag{4.21}$$

is the energy of the lowest state ($k = 0$) and

$$m^* = m/(1 - \alpha/6) \simeq m(1 + \alpha/6), \quad \alpha < 1 \tag{4.22}$$

may be denoted as an effective mass. For uk is the wave number in usual units, and hence $(\hbar uk)^2/2m^*$ would represent the kinetic energy of a particle of mass m^* and momentum huk.

The perturbation method described above is restricted to weak interaction, $\alpha < 1$. It leads to wave functions of type (4.16) in which never more than a single quantum can be excited. It will be shown now that the range of validity of eqn. (4.21) goes far beyond $\alpha = 1$.

4.2. Gurari Method

Gurari has shown (1953) that a variational method can be applied in order to derive eqn. (4.21) for $E(0)$. In §5 with a different variational method another value for $E(0)$ will be derived which is proportional to α^2. This will permit us to estimate the α-range in which (4.21) holds with reasonable accuracy because variational methods never yield energies lower than the exact one. Gurari's results were derived independently by Lee and Pines (1952) who use a method by Tomonaga (1947) which is closely related to Gurari's method (cf. also Lee, Low and Pines 1953, and Zienau 1953).

In the general theory of quantum mechanics it is shown that the solutions of

$$F\Psi = E(\mathbf{k})\Psi, \quad . . \tag{4.23}$$

satisfy the variational principle

$$\delta J = 0 \quad \text{with} \quad \int \Psi + \Psi = 1, \tag{4.24}$$

where

$$J = \int \Psi + F\Psi \tag{4.25}$$

The integrations are to be extended over all variables. They are understood in a sufficiently general sense, e.g. if the b_w 's are represented by matrices then the corresponding sums must be taken.

The functions Ψ will now be chosen through a generalization of the wave functions in perturbation theory. Instead of using a linear superposition of wave functions (all with equal total wave vector $\mathbf{k}$) containing no more than one quantum, $\Psi(\mathbf{k})$ will now be chosen so as to lead to no more than a single quantum for each wave vector $\mathbf{v}$; any total number of quanta may be present, however, provided they belong to different wave vectors. Again let $\mathbf{k}$ be the total wave vector of the system, and define functions

$$\psi(\mathbf{k}, \mathbf{v}) = N(k, v, \xi) \left[1 + S^{-1/2} c(k, v, \xi) \exp(-i\mathbf{v}\mathbf{x}) b_{\mathbf{v}} +\right] \tag{4.26}$$

where

$$N(k, v, \xi) = \left[1 + S^{-1} |c(k, v, \xi)|^2\right]^{-1/2} \simeq 1. \tag{4.27}$$

The $c(k, v, \xi)$ are numerical constants, and ξ is the cosine of the angle between $\mathbf{k}$ and $\mathbf{v}$,

$$\xi = (\mathbf{k}\mathbf{v})/kv \tag{4.28}$$

The volume S (in reduced units) is supposed to be extended towards infinity-after completion of the calculation of $E(\mathbf{k})$; its occurrence thus defines orders of magnitudes and it will be assumed that the c 's do not contain S. Let then

$$\Psi(\mathbf{k}) = S^{-1/2} \exp(i\mathbf{k}\mathbf{x}) \prod_{\mathbf{v}} \psi(\mathbf{k}, \mathbf{v}) \chi, \tag{4.29}$$

and determine the c 's from the variational eqn. (4.24). It will be noticed that $\Psi(\mathbf{k})$ is already normalized. Also by development of the product into a sum it is easily seen that all terms occurring are of the form

$$|\mathbf{k}; n_{\mathbf{v}}\rangle = S^{-1/2} \exp\left[i\left(\mathbf{k} - \Sigma \mathbf{v} n_{\mathbf{v}}\right) \mathbf{x}\right] \Pi_{\mathbf{v}} \left|n_{\mathbf{v}}\right\rangle \tag{4.30}$$

thus, according to (4.2) and (4.3), belonging to the same total wave vector $\mathbf{k}$.

In calculating the integral J, (4.25) with the use of (2.40) and (4.29) consider first the pure field terms $\Sigma_{\mathbf{v}} b_{\mathbf{v}} + b_{\mathbf{v}}$. It will be noticed that all $\psi(\mathbf{k}, \mathbf{v})$ commute, and that $b_{\mathbf{v}} + b_{\mathbf{v}}$ commutes with all $\psi\left(\mathbf{k}, \mathbf{v}'\right)$'s $(\mathbf{v} \neq \mathbf{v}')$. Hence using χ from (4.8)

$$\begin{aligned} J_1 &= \int \Psi^+ \sum_{\mathbf{v}} b_{\mathbf{v}} + b_{\mathbf{v}} \Psi = S^{-1} \sum_{\mathbf{v}} \int_S d^3\mathbf{x} \left\langle 0_{\mathbf{v}}\right| \psi^+(\mathbf{k}, \mathbf{v}) b_{\mathbf{v}} + b_{\mathbf{v}} \psi(\mathbf{k}, \mathbf{v}) \left|0_{\mathbf{v}}\right\rangle \\ &= S^{-1} \sum_{\mathbf{v}} \int_S N^2(v, k, \xi) |c(k, v, \xi)|^2 S^{-1} d^3\mathbf{x} \simeq S^{-1} \sum_{\mathbf{v}} |c(k, v, \xi)|^2. \end{aligned} \tag{4.31}$$

Here use has been made of (4.10) and (4.11), and $N^2 \simeq 1$ has been introduced because $S \to \infty$. It must be observed that this is always possible in sums of the type occurring in (4.31) and in similar ones occurring below. In the wave function $\Psi(\mathbf{k})$, however, where a product

$\Pi_{\mathbf{v}} N(v,k,\xi)$ occurs in the denominator replacement of $N(v,k,\xi^*)$ by unity is not permissible because the number of factors in the product increases with S.

The interaction term in F reduces in a similar way to a sum when eqns. (4.10) and (4.11) are used. For then

$$\begin{aligned} J_2 &= i(4\pi\alpha/S)^{1/2} \int \Psi + \sum_{\mathbf{v}} \left[b_{\mathbf{v}} + \exp(-i\mathbf{vx}) - b_{\mathbf{v}} \exp(i\mathbf{vx})\right] \Psi \\ &= iS^{-3/2}(4\pi\alpha)^{1/2} \sum_{\mathbf{v}} \int_S d^3\mathbf{x} \left\langle 0_{\mathbf{v}} \right| \psi^+(\mathbf{k},\mathbf{v}) \left[b_{\mathbf{v}} + \exp(-i\mathbf{vx})\right. \\ &\left. -b_{\mathbf{v}} \exp(i\mathbf{vx})\right] \psi(\mathbf{k},\mathbf{v}) \left|0_{\mathbf{v}}\right\rangle \\ &= iS^{-1}(4\pi\alpha)^{1/2} \sum_{\mathbf{v}} \left[c^*(k,v,\xi) - c(k,v,\xi)\right]/v... \end{aligned} \tag{4.32}$$

Finally the electronic term is slightly more complicated,

$$\begin{aligned} J_3 = -\sum_1^3 \int \Psi + \frac{\partial^2}{\partial x_i^2}\Psi = \int \frac{\partial\Psi}{\partial\mathbf{x}} + \frac{\partial\Psi}{\partial\mathbf{x}} = k^2 - iS^{-1}\mathbf{k} \int \chi^+ \Pi_{\mathbf{v}} \psi^+(\mathbf{k},\mathbf{v}) \\ \times \frac{\partial}{\partial\mathbf{x}} \Pi_{\mathbf{v}} \psi(\mathbf{k},\mathbf{v})\chi + \text{ c.c. } + S^{-1} \int \chi^+ \left(\frac{\partial}{\partial\mathbf{x}} \Pi_{\mathbf{v}} \psi^+(\mathbf{k},\mathbf{v})\right) \left(\frac{\partial}{\partial\mathbf{x}} \Pi_{\mathbf{v}} \psi(\mathbf{k},\mathbf{v})\right) \chi. \end{aligned} \tag{4.33}$$

Here c.c. denotes the conjugate complex of the previous term. The second term in (4.33) is obtained by similar methods to the ones used to evaluate (4.31) and (4.32). Thus with χ from (4.8) and with use of (4.11),

$$\begin{aligned} &- iS^{-1}\mathbf{k} \int \chi^+ \Pi_{\mathbf{v}} \psi^+(\mathbf{k},\mathbf{v}) \frac{\partial}{\partial\mathbf{x}} \Pi_{\mathbf{v}} \psi(\mathbf{k},\mathbf{v})\chi \\ &= -iS^{-1}\mathbf{k} \sum_{\mathbf{v}} \int_S d^3\mathbf{x} \left\langle 0_{\mathbf{v}} \right| \psi^+(\mathbf{k},\mathbf{v}) \frac{\partial}{\partial\mathbf{x}} \psi(\mathbf{k},\mathbf{v}) \left|0_{\mathbf{v}}\right\rangle \\ &= -iS^{-1}\mathbf{k} \sum_{\mathbf{v}} \mathbf{v} |c(k,v,\xi)|^2.. \end{aligned} \tag{4.34}$$

In a similar way the last term is found, and one obtains

$$\begin{aligned} J_3 =& k^2 - 2S^{-1} \sum_{\mathbf{v}} (\mathbf{kv}) |c(k,v,\xi)|^2 + S^{-1} \sum_{\mathbf{v}} v^2 |c(k,v,\xi)|^2 \\ &+ S^{-2} \sum_{\mathbf{v}} \sum_{\mathbf{v}'} (\mathbf{vv}') \left|c(k,v,\xi)\right|^2 \left|c\left(k,v',\xi'\right)\right|^2. \end{aligned} \tag{4.35}$$

Here the factor ($\mathbf{v}'$) can be simplified because using (4.28)

$$\mathbf{vv}' = vv' \left(\xi\xi' + \sin(\mathbf{k},\mathbf{v}) \sin\left(\mathbf{k},\mathbf{v}'\right) \cos\left(\phi - \phi'\right)\right) \tag{4.36}$$

where ϕ and ϕ' are the polar angles of $\mathbf{v}$ and $\mathbf{v}'$ respectively. In the following summation (integration) over $\mathbf{v}$, the term with $\cos(\phi - \phi')$ vanishes because $c(k,v,\xi)$ is independent of ϕ, and

$$\int_0^{2\pi} \cos\left(\phi - \phi'\right) d\phi = 0$$

Thus $\mathbf{vv}'$ can be replaced by $vv'\xi\xi'$. Hence using (4.31), (4.32) and (4.35),

$$\begin{aligned} J =& J_1 + J_2 + J_3 = k^2 + S^{-1}\sum_{\mathbf{v}}\left(1 - 2\mathbf{kv} + v^2\right) c^*(k,v,\xi)c(k,v,\xi) \\ &+ i(4\pi\alpha)^{1/2}S^{-1}\sum_{\mathbf{v}}\left(c^*(k,v,\xi) - c(k,v,\xi)\right)/v + g^2\cdots \end{aligned} \tag{4.37}$$

where

$$g = S^{-1}\sum_{v} vc^*(k,v,\xi)c(k,v,\xi) \tag{4,38}$$

The variational principle $\delta J = 0$ requires that differentiation of J with regard to all $c(k,v,\xi)$ and $c^*(k,v,\xi)$ should vanish. Hence

$$0 = \left(1 - 2kv\xi + 2gv\xi + v^2\right) c(k,v,\xi) + i(4\pi\alpha)^{1/2}/v \tag{4.39}$$

It is useful to introduce here a vector $\mathbf{g}$ whose magnitude is g and whose direction is the same as that of $\mathbf{k}$, i.e.

$$\mathbf{g} = g\mathbf{k}/k. \tag{4.40}$$

Then from (4.39)

$$c(k,v,\xi) = -\frac{i(4\pi\alpha)^{1/2}}{v\left(1 - 2(\mathbf{k} - \mathbf{g}\cdot\mathbf{v}) + v^2\right)}, \tag{4.41}$$

and $c^*(k,v,\xi)$ is its conjugate complex.
The above solution holds only if $c(k,v,\xi)$ does not become infinite for and value of $\mathbf{v}$. To prevent this the condition

$$(k-g)^2 < 1 (4.42)$$

must be satisfied.
With the values (4.41) for the coefficients c the integral J, (4.25), represents the energy (in terms of $\hbar\omega$). Hence from (4.37) and (4.41), using (4.38) and (4.40),

$$\begin{aligned} E(\mathbf{k}) =& \hbar\omega\left\{k^2 + g^2 + 4\pi\alpha S^{-1}\sum_{\mathbf{v}}\left(\frac{1 - 2\mathbf{k} + v^2}{v^2\left[1 - 2(\mathbf{k} - \mathbf{g}\cdot\mathbf{v}) + v^2\right]^2}\right.\right. \\ &\left.\left. - \frac{2}{v^2\left[1 - 2(\mathbf{k} - \mathbf{g}\cdot\mathbf{v}) + v^2\right]}\right)\right\} \\ =& \hbar\omega\left\{k^2 - g^2 - 4\pi\alpha S^{-1}\sum_{\mathbf{v}}\frac{1}{v^2\left[1 - 2(\mathbf{k} - \mathbf{g}\cdot\mathbf{v}) + v^2\right]}\right\} \end{aligned} \tag{4.43}$$

and from (4.38) and (4.41), using (4.40),

$$g = \frac{4\pi\alpha}{k}S^{-1}\sum_{\mathbf{v}}\frac{(\mathbf{vk})}{v^2\left[\mathbf{I} - 2(\mathbf{k} - \mathbf{g}\cdot\mathbf{v}) + v^2\right]^2} \tag{4.44}$$

With (4.17) after integration one obtains

$$E(\mathbf{k}) = \hbar\omega\left\{k^2 - g^2 - \alpha\frac{\sin^{-1}(k-g)}{k-g}\right\}, . \tag{4.45}$$

and

$$g = \frac{1}{2}\alpha \left\{ -\frac{\sin^{-1}(k-g)}{(k-g)^2} + \frac{1}{(k-g)\left(1-(k-g)^2\right)^{1/2}} \right\} \tag{4.46}$$

i.e. two simultaneous equations for $E(k)$ and g. Again condition (4.42) must be observed. It will be noticed that eqn. (4.46) can also be written as

$$g = \frac{1}{2}\alpha \frac{d}{dk} \frac{\sin^{-1}(k-g)}{k-g}. \tag{4.47}$$

Now if $|k-g| \ll 1$, by development of $\left[\sin^{-1}(k-g)\right]/(k-g)$ (cf. (4.19)). eqn. (4.47) becomes

$$g = \alpha(k-g)/6, \text{ or } k = (k-g)(1+\alpha/6), \text{ or } g = \frac{k\alpha/6}{1+\alpha/6}. \tag{4.48}$$

Thus as $k \to 0$, also $g \to 0$. With the use of (4.48), and of a further development of the $\sin^{-1}$, finally

$$E(\mathbf{k}) = E(0) + \hbar^2(ku)^2/2m^*, \quad k \ll 1, . \tag{4.49}$$

where

$$E(0) = -\alpha\hbar\omega = -\left(\frac{1}{\epsilon_\infty} - \frac{1}{\epsilon}\right) e^2 \left(\frac{m\omega}{2\hbar}\right)^{1/2}, \tag{4.50}$$

and

$$m^* = m(1+\alpha/6). \tag{4.51}$$

Thus $E(0)$ is identical with the result (4.21) of perturbation theory, but it is no longer restricted to $\alpha < 1$. The limit of α up to which the result is reliable will be studied in §5 with the use of a variational method which gives the energy proportional to α^2. Also m^* is seen to agree with the result which perturbation theory yields for $\alpha \ll 1$. Again this value now holds for larger α.

Expression (4.49) had to be restricted to sufficiently small values of k to make use of the development of $\sin^{-1}(k-g)$. This would not restrict, however, the validity of eqns. (4.45) and (4.46) which have solutions for all k. In particular $E(k) \propto k\hbar\omega$ as $k \to \infty$. Such solutions, however, have no physical meaning because $E(\mathbf{k})$ has to be restricted to values for which

$$E(\mathbf{k}) - E(0) < \hbar\omega \tag{4.52}$$

which means that the energy of the system should be less than one quantum above the energy of the ground state. If this were not fulfilled then the trial wave functions (4.29) (with (4.26)) would not be the only ones leading to the energy $E(\mathbf{k})$ for given $\mathbf{k}$. Others would exist as well in which at least one of the $\psi(\mathbf{k}, \mathbf{v})$'s would be replaced by a function in which the state with one quantum is principally excited (and not the state without quantum as in (4.29)). A degeneracy would thus occur. It would require a new approach which has not been found yet.

Equation (4.49) suggests that the electric current carried by the system is given by $ej = e\hbar ku/m*$ where $\bar{j}$ represents the average electronic velocity. In fact with the use of (4.29), (4.26), (4.41), (4.48) and of the orthogonality relations,

$$
\begin{aligned}
e\bar{j} &= \frac{e\hbar u}{m}\int \Psi + \frac{\partial \Psi}{\partial \mathbf{x}} = \frac{e\hbar}{m}\left\{\mathbf{k} - 4\pi\alpha S^{-1}\sum_{\mathbf{v}} \frac{\mathbf{v}}{v^2\left(1-2(\mathbf{k}-\mathbf{g}\cdot\mathbf{v})+v^2\right)^2}\right\} \\
&= \frac{e\hbar u}{m}\frac{\mathbf{k}}{k}(k-g) = \frac{e\hbar u}{m^*}\mathbf{k}, \cdots\cdots\cdots
\end{aligned} \tag{4.53}
$$

as suggested. Use has been made of (4.44) and of the fact that the direction of the vector represented by the sum must be $\mathbf{k}/k$. In the last step (4.51) has been applied.

It is also of interest to calculate the polarization near an electron. For this purpose it is best to derive an appropriate expectation value of the polarization potential $\Phi_{ir}(\mathbf{r})$ defined in (2.30). Clearly with (2.25) and (2.28), using (2.37)-(2.39)

$$
\text{where} \quad e\Phi_{ir}(\mathbf{y}) = i(4\pi\alpha/S)^{1/2}\hbar\omega\Sigma_{\mathbf{v}}\left(b_{\mathbf{v}} + \exp(-i\mathbf{v}\mathbf{y}) - b_{\mathbf{v}}\exp(i\mathbf{v}\mathbf{y})\right)/v, \tag{4.54}
$$

$$
\mathbf{y} = ur \quad \cdots\cdots(4.5
$$

has been introduced. Let now the integration over all variables of the wave function Ψ be split into an electronic one, denoted by $\int d^3\mathbf{x}$. and one, denoted by the symbol $\langle\ \rangle$, referring to the field variables. Thus the integration over all variables introduced in (4.25) can be written as

$$
\int = \int d^3\mathbf{x}\langle\quad\rangle\cdot \tag{4.56}
$$

It follows then that $\langle\Psi+\Psi\rangle$ is the probability of finding the electron at a position $\mathbf{x}$ irrespective of the polarization, and $\langle\Psi+\Phi_{ir}(\mathbf{y})\Psi\rangle$ represents the expectation value of $\Phi_{ir}(\mathbf{y})$ at a position $\mathbf{y}$ and simultaneously finding the electron at $\mathbf{x}$.

Define now

$$
\Phi_{ir}(\mathbf{x},\mathbf{y}) = \langle\Psi+\Phi_{ir}(\mathbf{y})\Psi\rangle/\langle\Psi+\Psi\rangle = S\langle\Psi+\Phi_{ir}(\mathbf{y})\Psi\rangle \tag{4.57}
$$

which is the expectation value of the polarization potential at a position $\mathbf{y}$, provided the electron is at $\mathbf{x}$. For this purpose it will be noticed that from (4.29) and (4.26), with the use of (3.5), (4.10) and (4.11),

$$
\begin{aligned}
\left\langle\Psi^+ b_{\mathbf{v}'} + \Psi\right\rangle =& S^{-1}\left\langle\chi^+\Pi_{\mathbf{v}}\psi^+(\mathbf{k},\mathbf{v})b_{\mathbf{v}'} + \Pi_{\mathbf{v}}\psi(\mathbf{k},\mathbf{v})\chi\right\rangle \\
=& S^{-1}\left\langle 0_{\mathbf{v}'}\left[\mathbf{1} + S^{-1/2}c^*\left(k,v',\xi'\right)\exp\left(i\mathbf{v}'\mathbf{x}\right)b_{\mathbf{v}'}\right]\right. \\
& \left.\times b_{\mathbf{v}'} + \left[\mathbf{1} + S^{-1/2}c\left(k,v',\xi'\right)\exp\left(-i\mathbf{v}'\mathbf{x}\right)b_{\mathbf{v}'}+\right]0_{\mathbf{v}'}\right\rangle \\
=& S^{-\mathbf{3/2}}c^*\left(k,v',\xi'\right)\exp\left(i\mathbf{v}'\mathbf{x}\right)
\end{aligned} \tag{4.58}
$$

Hence from (4.54), (4.57) and (4.41)

$$
\begin{aligned}
e\Phi_{ir}(\mathbf{x},\mathbf{y}) =& i(4\pi\alpha)^{1/2}S^{-1}\hbar\omega\sum\left[c^*(k,v,\xi)\exp(i\mathbf{v}\cdot\mathbf{x}-\mathbf{y})\right. \\
& \left.- c(k,v,\xi)\exp(-i\mathbf{v}\cdot\mathbf{x}-\mathbf{y})\right]/v \\
=& -4\pi\alpha S^{-1}\sum_{\mathbf{v}}\frac{2\cos(\mathbf{v}\cdot\mathbf{k}-\mathbf{y})}{v^2\left[1-2(\mathbf{k}-\mathbf{g}\cdot\mathbf{v})+v^2\right]}\cdot.
\end{aligned} \tag{4.59}
$$

In the simplest case $k=0$ (i.e. also $g=0$) one has with (4.17),

$$\begin{aligned} S^{-1}\sum_{\mathbf{v}}\frac{2\cos(\mathbf{v}\cdot\mathbf{x}-\mathbf{y})}{v^2\left(1+v^2\right)} &= \frac{2}{4\pi^2}\int_0^\infty dv\int_{-1}^1\frac{\cos(v|\mathbf{x}-\mathbf{y}|\eta)}{1+v^2}d\eta \\ &= \frac{1}{\pi^2|\mathbf{x}-\mathbf{y}|}\int_0^\infty\frac{\sin(v|\mathbf{x}-\mathbf{y}|)}{v\left(1+v^2\right)}dv \\ &= \frac{1-\exp(-|\mathbf{x}-\mathbf{y}|)}{\pi|\mathbf{x}-\mathbf{y}|} \end{aligned} \tag{4.60}$$

Returning now to ordinary units with the help of (2.37)-(2.39) (denoting then $\Phi_{ir}(\mathbf{x},\mathbf{y})$ by $\Phi_{ir}\left(\boldsymbol{r}_{el},\mathbf{r}\right)$) eqns. (4.59) and (4.60) yield

$$e\Phi_{ir}\left(\mathbf{r}_{el},\mathbf{r}\right)=-\left(\frac{1}{\epsilon_\infty}-\frac{1}{\epsilon}\right)\frac{e^2}{|\mathbf{r}-\mathbf{r}_{el}|}\left[1-\exp\left(-u\left|\mathbf{r}-\mathbf{r}_{el}\right|\right)\right]. \tag{4.61}$$

Thus if $|\mathbf{r}-\mathbf{r}_{el}|\gg 1/u$, the polarization potential of a point charge is found. If $|\mathbf{r}-\mathbf{r}_{el}|\ll 1/u$, however, one finds

$$e\Phi_{ir}\left(\mathbf{r}_{el},\mathbf{r}\right)\simeq-\left(\frac{1}{\epsilon_\infty}-\frac{1}{\epsilon}\right)e^2u,\quad |\mathbf{r}-\mathbf{r}_{el}|\ll 1/u, \tag{4.62}$$

i.e. the polarization potential of a charge extended over a sphere whose radius is of the order $1/u$. The case that k is different from zero leads to a slight modification of (4.61).

11.1.5 §5. Stationary Solutions II

The eigenvalues of the Hamiltonian (2.40) derived in the previous section are linear in the interaction parameter α. In the present section a different method, originally due to Landau (1933) (cf. also Pekar 1946, 1949) will be used which has been discussed qualitatively in §1. It will be shown that it can be derived with the help of the variational principle (4.24) and will be found to yield eigenvalues which are quadratic in α.

For this purpose use the trial wave function Ψ as a product of an electronic wave function $\Omega(\mathbf{x})$ and a lattice wave function Φ,

$$\Psi=\Omega(\mathbf{x})\Phi,\ \ldots\ldots\ldots \tag{5.1}$$

where $\Omega(\mathbf{x})$ depends on the electronic coordinate $\mathbf{x}$ only, and Φ on the coordinates describing the polarization waves. It will be assumed that both are normalized, i.e. using the definition (4.56) for the respective integrations

$$\int_S d^3\mathbf{x}\Omega^+(\mathbf{x})\Omega(\mathbf{x})=1;\quad \left\langle\Phi^+\Phi\right\rangle=1 \tag{5.2}$$

Clearly with (4.1) and (4.56),

$$\int\Psi+F_0\Psi=-\sum_1^3\int_S\Omega^+(\mathbf{x})\frac{\partial^2}{\partial {x_i}^2}\Omega(\mathbf{x})d^3\mathbf{x}+\sum_{\mathbf{v}}\left\langle\Phi+b_{\mathbf{v}}+b_{\mathbf{v}}\Phi\right\rangle, \tag{5,3}$$

and with (4.7)

$$\begin{aligned}\textstyle\int\Psi^+F_{\text{int}}\Psi=i(4\pi\alpha/S)^{1/2}\left\langle\Phi^+\int_S d^3\mathbf{x}\Omega^+(\mathbf{x})\sum_{\mathbf{v}}\left[b_{\mathbf{v}}+\exp(-i\mathbf{v}\mathbf{x})\right.\right.\\ \left.\left.-b_{\mathbf{v}}\exp(i\mathbf{v}\mathbf{x})\right]\Omega(\mathbf{x})\Phi\right\rangle\end{aligned} \tag{5.4}$$

The conditions (5.2) can be satisfied with the use of the Lagrangian factors λ_1 and λ_2 so that the variational principle (4.24) requires

$$\delta\left\{\int \Psi + F\Psi - \lambda_1 \int_S \Omega^+\Omega d^3\mathbf{k} - \lambda_2\langle\Phi + \Phi\rangle\right\} = 0 \tag{5.5}$$

or using (5.3) and (5.4),

$$\delta\left\{-\int_S d^3\mathbf{x}\Omega^+(\mathbf{x})\left(\sum_{\mathbf{1}}^{3}\frac{\partial^2}{\partial {x_i}^2} + \lambda_{\mathbf{1}}\right)\Omega(\mathbf{x}) + \sum_{\mathbf{v}}\left\langle \Phi^+\left(\sum_{\mathbf{v}} {b_{\mathbf{v}}}^+ b_{\mathbf{v}} - \lambda_2\right)\Phi\right\rangle \right.$$
$$\left. + \left\langle \Phi + \int_S d^3\mathbf{x}\Omega^+(\mathbf{x})F_{\text{int}}\,\Omega(\mathbf{x})\Phi\right\rangle\right\} = 0, \tag{5.6}$$

where the functions Ω, Φ and their conjugates have to be varied. This is simplified because only the last term depends on both. Thus variation with respect to $\Omega^+(\mathbf{x})$ yields

$$-\sum_{1}^{3}\frac{\partial^2\Omega(\mathbf{x})}{\partial {x_i}^2} + \langle\Phi + F_{\text{int}}\Phi\rangle\,\Omega(\mathbf{x}) = \lambda_1\Omega\left(\mathbf{x}^*\right) \tag{5.7}$$

Similarly from variation of Φ^+,

$$\sum_{\mathbf{v}} b_{\mathbf{v}} + b_{\mathbf{v}}\Phi + \int_S d^3\mathbf{x}\Omega + (\mathbf{x})F_{\text{int}}\Omega(\mathbf{x})\Phi = \lambda_2\Phi \tag{5.8}$$

Variation of Ω and Φ leads to the conjugate equations. Equation (5.7) is the Schrödinger equation for an electron moving in a 'self consistent ' field $\langle\Phi + F_{\text{int}}\,\Phi\rangle$. Similarly (5.8) represents the motion of the field of polarization waves in a 'self consistent' source. Clearly in view of (5.4), Φ can be written as a product,

$$\Phi = \Pi_{\mathbf{v}}\Phi_{\mathbf{v}}; \qquad \text{also } \lambda_2 = \sum_{\mathbf{v}}\lambda_{\mathbf{v}}, \quad . \tag{5.9}$$

where Φ_v depends on the coordinates of the v-th field component only. It satisfies

$$\begin{aligned} b_{\mathbf{v}} + b_{\mathbf{v}}\Phi_{\mathbf{v}} + i(4\pi\alpha/S)^{\mathbf{1/2}}(1/v)\left(b_{\mathbf{v}} + \textstyle\int_S \Omega + (\mathbf{x})\exp(-i\mathbf{v}\mathbf{x})\Omega(\mathbf{x})d^3\mathbf{x}\right. \\ \left. -b_{\mathbf{v}}\textstyle\int_S \Omega^+(\mathbf{x})\exp(i\mathbf{v}\mathbf{x})\Omega(\mathbf{x})d^3\mathbf{x}\right)\Phi_{\mathbf{v}} = \lambda_{\mathbf{v}}\Phi_{\mathbf{v}} \end{aligned} \tag{5.10}$$

which is the equation of a displaced harmonic oscillator. Hence

$$\langle\Phi_{\mathbf{v}} + b_{\mathbf{v}} + \Phi_{\mathbf{v}}\rangle = i(4\pi\alpha/S)^{1/2}(1/v)\int_S \Omega^+(\mathbf{x})\exp(i\mathbf{v}\mathbf{x})\Omega(\mathbf{x})d^3\mathbf{x} \tag{5.1I}$$

With the use of (5.4) and (5.11), therefore, the self consistent potential energy of the electron becomes (use (4.17))

$$\begin{aligned} &\langle\Phi + F_{\text{int}}\,\Phi\rangle \\ &= -\frac{4\pi\alpha}{S}\sum_{v}\frac{1}{v^2}\int_S d^3\mathbf{x}'\Omega^+\left(\mathbf{x}'\right)\Omega\left(\mathbf{x}'\right)\left[\exp\left(i\mathbf{v}\cdot\mathbf{x}' - \mathbf{x}\right) + \exp\left(-i\mathbf{v}\cdot\mathbf{x}' - \mathbf{x}\right)\right] \\ &= \frac{4\pi\alpha}{(2\pi)^3}\int_S d^3\mathbf{x}'\int d^3\mathbf{v}\frac{2\cos\left(\mathbf{v}\cdot\mathbf{k}' - \mathbf{x}\right)}{v^2}\Omega^+\left(\mathbf{x}'\right)\Omega\left(\mathbf{x}'\right) \\ &= -2\alpha\int_S \frac{\Omega^+\left(\mathbf{x}'\right)\Omega\left(\mathbf{x}'\right)}{|\mathbf{x}' - \mathbf{x}|}d^3\mathbf{x}' \end{aligned} \tag{5.12}$$

It represents the energy of the charge e at $\mathbf{x}$ placed into the polarization potential due to the charge distribution $\Omega^{+}(\mathbf{x}')\,\Omega(\mathbf{x}')$. This is easily seen by going back to conventional units with the help of (2.37)-(2.39), i.e.

$$\hbar\omega\left\langle\Phi+F_{\text{int}}\Phi\right\rangle=-\left(\frac{1}{\epsilon_{\infty}}-\frac{1}{\epsilon}\right)e^{2}\int\frac{\Omega^{+}(\mathbf{r})\Omega(\mathbf{r})}{|\mathbf{r}-\mathbf{r}_{el}|}d^{3}\mathbf{r} \tag{5.13}$$

Introduction of (5.13) into (5.7) leads to an integral equation for $\Omega(\mathbf{x})$. Qualitatively, it is clear that $\Omega(\mathbf{x})$ must be a function which is large in a limited space only. For only in this way can the 'self consistent' potential energy have relatively large negative values. To find an approximative solution use will be made again of the variational method in its original form (4.24). For this purpose let

$$\Omega(\mathbf{x})=\left(\beta^{3}/8\pi\right)^{1/2}\exp\left(-\beta\left|\mathbf{x}-\mathbf{x}_{0}\right|/2\right), \tag{5.14}$$

where $\mathbf{x}_0$ is an arbitrary radius vector. Then with

$$J=\left\langle\int_{S}d^{3}\mathbf{x}\Phi^{+}\Omega^{+}(\mathbf{x})F\Omega(\mathbf{x})\Phi\right\rangle, \tag{5.15}$$

the variational method requires that

$$\partial J/\partial\beta=0, \tag{5.16}$$

provided Φ and Ω are normalized, and Φ is a solution of (5.8). As mentioned it is composed of displaced harmonic oscillator solutions.

Now using the expression for F according to (5.3) and (5.4), together with (5.8)-(5.10), the integral J, defined in (5.15) becomes

$$J=-\int_{S}\Omega^{+}(\mathbf{x})\sum_{1}^{3}\frac{\partial^{2}}{\partial x_{i}^{2}}\Omega(\mathbf{x})d^{3}\mathbf{x}+\sum_{\mathbf{v}}\lambda_{\mathbf{v}} \tag{5.17}$$

Also from (5.10) for the lowest states of the displaced harmonic oscillators,

$$\begin{aligned}\underset{\mathbf{v}}{\Sigma}\lambda_{\mathbf{v}}=&-(4\pi\alpha/S)\Sigma\left|\int_{\mathbf{v}}\Omega^{+}(\mathbf{x})\exp(-i\mathbf{v}\mathbf{x})\Omega(\mathbf{x})d^{3}\mathbf{x}\right|^{2}/v^{2}\\=&-(4\pi\alpha/S)\int_{S}d^{3}\mathbf{x}\left\{\Omega^{+}(\mathbf{x})\Omega(\mathbf{x})\frac{1}{2}\Sigma\left(1/v^{2}\right)\int_{S}d^{3}\mathbf{x}'\Omega^{+}(\mathbf{x}')\,\Omega(\mathbf{x}')\right.\\&\left.\times\left[\exp\left(i\mathbf{v}\cdot\mathbf{x}'-\mathbf{x}\right)+\exp\left(-i\mathbf{v}\mathbf{x}'-\mathbf{x}\right)\right]\right\}\\=&\frac{1}{2}\int_{S}\Omega^{+}(\mathbf{x})\Omega(\mathbf{x})\left\langle\Phi^{+}F_{\text{int}}\Phi\right\rangle d^{3}\mathbf{x},\quad\cdots\cdots\end{aligned} \tag{5.18}$$

where eqn. (5.12) has been used in the last step. Thus the potential energy $\Sigma\lambda_{\mathbf{v}}$ appearing in (5.17) is obtained by averaging the potential energy (5.12) over the density distribution $\Omega^{+}(\mathbf{x})\Omega(\mathbf{x})$ of the electron. and multiplying it by $\frac{1}{2}$. This reduction by a factor $\frac{1}{2}$ arises from the positive contributions in displacing the oscillators.

Introducing now $\Omega(\mathbf{x})$ from (5.14), one finds with (5.18) and (5.12),

$$\begin{aligned}\sum_{v}\lambda_{v}=&-\alpha\left(\beta^{3}/8\pi\right)^{2}\int_{S}d^{3}\mathbf{x}\int_{S}d^{3}\mathbf{x}'\frac{\exp\left(-\beta\left|\mathbf{x}'_{-}-\mathbf{x}_{0}\right|\right)\exp\left(-\beta\left|\mathbf{x}-\mathbf{x}_{0}\right|\right)}{|\mathbf{x}-\mathbf{x}'|}\\=&-\frac{5}{16}\alpha\beta.\cdots\cdots\cdots\cdots\cdots\cdots\cdots\end{aligned} \tag{5.19}$$

Furthermore,
Hence with (5.17)

$$-\int_S \Omega^+(\mathbf{x}) \sum_1^3 \frac{\partial^2}{\partial x_i^2} \Omega(\mathbf{x}) d^3\mathbf{x} = \frac{1}{4}\beta^2 \tag{5.20}$$

$$J = -\frac{5}{16}\alpha\beta + \frac{1}{4}\beta^2. \tag{5.21}$$

It will be noticed that the wave functions used here are all normalized so that from (5.16),

$$\beta = \frac{5}{8}\alpha, \quad \text{and hence} \quad J = -\frac{25}{256}\alpha^2. \tag{5.22}$$

In ordinary units, therefore, with the help of (2.37)-(2.39),

$$E(0) = \hbar\omega J = -\frac{25}{256}\alpha^2\hbar\omega = -\frac{25}{512}\left(\frac{1}{\epsilon_\infty} - \frac{1}{\epsilon}\right)^2 \frac{e^4 m}{\hbar^2} \tag{5.23}$$

The polarization potential $\Phi_{ir}(\boldsymbol{y})$ at a position $\boldsymbol{y}$ defined by (2.30) and (4.54) is an operator whose essential part is now, however, a c-number. For from (5.10) and (5.11),

$$b_{\mathbf{v}}{}^+ = i(4\pi\alpha/S)^{1/2}(1/v)\int_S \exp(i\mathbf{v}\mathbf{x})\Omega^+(\mathbf{x})\Omega(\mathbf{x})d^3\mathbf{k} + d_{\mathbf{v}}{}^+ \tag{5.24}$$

where d_v and $d_v{}^+$are operators satisfying a harmonic oscillator equation

$$d_{\mathbf{v}} + d_{\mathbf{v}}\left|n_{\mathbf{v}}\right\rangle = n_{\mathbf{v}}\left|n_{\mathbf{v}}\right\rangle \quad \text{i.e.} \quad \left\langle n_{\mathbf{v}}\right| d_{\mathbf{v}} + \left|n_{\mathbf{v}}\right\rangle = 0 \tag{5.25}$$

Hence from (4.54) and (5.24)

$$\begin{aligned} e\Phi_{ir}(\mathbf{y}) = -(4\pi\alpha/S)h\omega\Sigma_{\mathbf{v}}\,(1/v^2)\textstyle\int_S d^3\mathbf{x}\exp(i\mathbf{v}\cdot\mathbf{x}-\mathbf{y})\Omega^+(\mathbf{x})\Omega(\mathbf{x}) \\ + \text{c.c.} \;\; + e\Phi_{ir}{}'\cdots\cdots\cdots\cdots \end{aligned} \tag{0}$$

where $\Phi_{ir}{}'$ depends on the d_v 's in such a way that its expectation value vanishes. The main part is a c-number and is equal to expression (5.13) (cf. (5.12), replacing there $\mathbf{x}$ by $\mathbf{y}$ and $\mathbf{x}'$ by $\mathbf{x}$). Hence $\Phi_{ir}(\mathbf{y})$ is the polarization potential of the static charge distribution $\Omega + (\mathbf{x})\Omega(\mathbf{x})$, and the polarization $\mathbf{P}_{ir}$ can similarly be derived from the electric displacement $\mathbf{D}$ due to the charge distribution $\Omega^+(\mathbf{x})\Omega(\mathbf{x})$. Thus from (5.26) is is found that (c.c. leads to a factor two)

$$\sum_1^3 \frac{\partial^2}{\partial y_i^2}\Phi_{ir}(\mathbf{y}) = \frac{2}{e}4\pi\alpha\hbar\omega\Omega + (\mathbf{x})\Omega(\mathbf{x}) \tag{5.27}$$

or in ordinary units using (2.37)-(2.39),

$$\nabla_{\mathbf{r}}^2\Phi_{ir}(\mathbf{r}) = 4\pi\rho\left(|\mathbf{r}-\mathbf{r}_0|\right)\left(\frac{1}{\epsilon_\infty} - \frac{1}{\epsilon}\right), \quad .. \tag{5.28}$$

where

$$\rho\left(|\mathbf{r}-\mathbf{r}_0|\right) = eu^3\left(\frac{1}{\epsilon_\infty} - \frac{1}{\epsilon}\right)\Omega^+\left(|\mathbf{x}-\mathbf{x}_0|\right)\Omega\left(|\mathbf{x}-\mathbf{x}_0|\right) \tag{5.29}$$

is the electric charge density. Spherical symmetry of both Φ_{ir} and ρ around the point $\mathbf{r}_0 = \mathbf{x}_0/u$ has been indicated. Clearly using (2.30) and $\operatorname{div}\mathbf{D} = 4\pi\rho\left(|\mathbf{r}-\mathbf{r}_0|\right)$.(5.30) one finds with the appropriate boundary condition

$$\mathbf{P}_{ir} = \mathbf{D}/\gamma\omega^2 \tag{5.31}$$

using the definition (2.14).
This shows that the treatment of the polarization field in the present section is essentially a classical one based on the static charge distribution ρ. In fact in this case (5.31) follows immediately from (2.8) when $\dot{\mathbf{P}}_{ir} = 0$.

This classical approach can be used to estimate the effective mass of the system in the present modèl (Landau and Pekar 1948, Pelzer 1950). For this purpose the electron will be considered as a rigid charge distribution moving with a small velocity. This means that $\mathbf{r}_0$ is now a point moving through the field, i.e.

$$\mathbf{r}_0 = \dot{\mathbf{r}}_0 t$$

where $\dot{\mathbf{r}}_0$ is the constant velocity. Since now $\dot{\mathbf{P}}_{ir}$ no longer vanishes, (5.31) has to be replaced by (2.8), or (5.28) by

$$\nabla_{\mathbf{r}}^2 \left(\ddot{\Phi}_{ir}/\omega^2 + \Phi_{ir} \right) = 4\pi\rho \left(|\mathbf{r} - \dot{\mathbf{r}}_0 t| \right) \left(\frac{1}{\epsilon_\infty} - \frac{1}{\epsilon} \right). \tag{5.33}$$

Now if $\dot{\mathbf{r}}_0$ is sufficiently small then

$$\Phi_{ir} = \Phi_0 \left(|\mathbf{r} - \dot{\mathbf{r}}_0 t| \right) + \Phi_1 \tag{5.34}$$

where Φ_0 satisfies (5.28) with $\mathbf{r}_0$ from (5.32), and $|\Phi_1| \ll |\Phi_0|$. With this latter condition, and with

$$\dot{\Phi}_0 \left(|\mathbf{r} - \dot{\mathbf{r}}_0 t| \right) = \Phi_0' \dot{\mathbf{r}}_0; \quad \Phi_0' = \partial\Phi_0/\partial\mathbf{r}, \tag{5.35}$$

eqn. (5.33) leads immediately to

$$\Phi_1 = -\left(1/\omega^2\right) \ddot{\Phi}_0 = -\left(\mathbf{r}_0^2/\omega^2\right) \Phi_0''. \tag{5.36}$$

In this perturbation treatment the total energy of the system is equal to the energy in the static case, (5.23), augmented by terms proportional to $\dot{\mathbf{r}}_0{}^2$. These terms can be obtained from the classical Hamiltonian (2.22). Clearly from (2.30) and (5.34),

$$4\pi\mathbf{P}_{ir} = \operatorname{grad}\Phi_0 - \left(\dot{\mathbf{r}}_0^2/\omega^2\right) \operatorname{grad}\Phi_0{}'', \tag{5.37}$$

and using (5.35)

$$4\pi\dot{\mathbf{P}}_{ir} = \dot{\mathbf{r}}_0 \operatorname{grad}\Phi_0' - \left(\mathbf{r}_0{}^3/\omega^2\right) \operatorname{grad}\Phi_0'''. \tag{5.38}$$

Thus since with (5.30) and (2.30)

$$-\int \mathbf{D}\mathbf{P}_{ir} d^3\mathbf{r} = \int \rho\Phi_{ir} d^3\mathbf{r} \tag{5.39}$$

the terms of (2.22) which are proportional to $\dot{\mathbf{r}}_0{}^2$ are given by (definition of m^*)

$$\begin{aligned} \tfrac{1}{2}m^*\dot{\mathbf{r}}_0^2 = \tfrac{1}{2}m\dot{\mathbf{r}}_0^2 + \tfrac{1}{2}\left(\gamma/4\pi^2\right)\dot{\mathbf{r}}_0^2 \int \left\{ \left(\operatorname{grad}\Phi_0{}'\right)^2 - 2\operatorname{grad}\Phi_0 \operatorname{grad}\Phi_0{}'' \right\} \\ - \left(\dot{\mathbf{r}}_0^2/\omega^2\right) \int \rho\Phi_0{}''. \end{aligned} \tag{5.40}$$

A term $\frac{1}{2}m\dot{\mathbf{r}}_0{}^2$ for the additional kinetic energy of the electron has been added.

Both ρ and Φ_0 depend on $|\mathbf{r}_0 - \dot{\mathbf{r}}_0 t|$ only, and the integration is straightforward. Integration by parts and use of (2.14) and (5.28) yields

$$\frac{1}{2}m^* = \frac{1}{2}m + \frac{1}{2}\left(4\pi/\omega^2\right)\left(1/\epsilon_\infty - 1/\epsilon\right) \int \rho^2(\mathbf{r}) d^3\mathbf{r} \tag{5.41}$$

From (5.29), (5.14)

$$\int \rho^2(\boldsymbol{r})d^3\mathbf{r} = 4\pi e^2 u^3 \left(\beta^3/8\pi\right)^2 \int_0^\infty \exp(-2\beta x)x^2 dx = e^2u^3\beta^3/64\pi \tag{5.42}$$

so that

$$\frac{m^*}{m} = 1 + \frac{e^2u^3\beta^3}{8m\omega^2}\left(\frac{1}{\epsilon_\infty} - \frac{1}{\epsilon}\right). \tag{5.43}$$

Introducing β from (5.22), and using (2.37)-(2.39), finally

$$m^*/m = 1 + \frac{1}{2}(5/8)^3\alpha^4. \tag{5.44}$$

11.1.6 §6. Discussion of Solutions and of Methods

6.1. Results

The solutions for the lowest state of an electron in a polar crystal having a self energy $E(0)$ were derived in §§ 4 and 5 with the help of the variational method. Since the energy values obtained in this method are above the exact value (or equal to it) it follows that the lower of the two solutions (4.50) and (5.23) is the better one. Hence

$$E(0) = -\alpha\hbar\omega = -\left(\frac{1}{\epsilon_\infty} - \frac{1}{\epsilon}\right)e^2\left(\frac{m\omega}{2\hbar}\right)^{1/2} \quad \text{if} \quad \alpha < \frac{256}{25}, \tag{6.1}$$

and

$$E(0) = -\frac{25}{256}\alpha^2\hbar\omega = -\frac{25}{256}\left(\frac{1}{\epsilon_\infty} - \frac{1}{\epsilon}\right)\frac{e^4m}{\hbar^2} \quad \text{if} \quad \alpha > \frac{256}{25}. \tag{6.2}$$

In order to see which of the two solutions holds in practical cases consider sodium chloride (NaCl). Here approximately $\epsilon = 5.6$ and $\epsilon_\infty = 2 \cdot 3$. The wavelength of the residual rays is 61μ and the corresponding frequency is $\omega_r/2\pi \simeq \frac{1}{2} \times 10^{13}\text{sec}^{-1}$. Hence with eqn. (2.10), $\omega \simeq 4.9 \times 10^{13}\text{sec}^{-1}$. Using for m the electronic mass, $m = m_{\text{el}}$, eqns. (2.37) and (2.38) lead to $\alpha \simeq 6, u \simeq 10^7$ cm$^{-1}, \hbar\omega \simeq 0.03$ev. It follows then that (6.1) applies to this case leading to a self energy $E(0) \simeq 0 \cdot 18$ ev and to an effective mass (cf. (4.51)) of $m^* = m(1 + \alpha/6) \simeq 2m$. It will be noticed from (2.37) and (2.38) that $x \propto 1/\sqrt{\omega}$. Assuming $m = m_{el}$, this is the only factor which may vary substantially from substance to substance. In NaCl , the frequency ω is rather small so that for most substances smaller α-values than $\alpha = 6$ should be expected, i.e. in general (6.1) should hold and m^*/m should be nearly of order unity. The properties of an electron in such a substance are then not changed substantially through its interaction with the polarization field, at any rate as long as its energy is less than $\hbar\omega$ above the ground state (cf. (4.52)). It is also seen that $u^{-1} \simeq 10^{-7}$ cm is a length sufficiently larger than the lattice distance which justifies the approximation of the lattice as a continuum.

It is not easy to find actual substances for which α is so large as to make (6.2) the better solution. The possibility of large α might occur in conduction in impurity bands where m/m_{el} may be rather large, since $\alpha \propto (m/m_{el})^{1/2}$. Values of the effective mass of the order $100m_{el}$ are indicated by the work of Breckenridge and Hosler (1953) on titanium dioxide semiconductors, but even there it will be seen that the method of §4 gives better results. In this substance roughly $\epsilon \sim 110, \epsilon_\infty \sim 8, \omega \sim 10^{14}\text{sec}^{-1}$ and hence $u \sim 1.7 \times 10^7\,(m/m_{el})^{1/2}$ cm^{-1} and $\alpha \sim 2\,(m/m_{el})^{1/2}$; the estimate is very crude in particular since TiO_2 is not isotropic. To make here $\alpha = 256/25 \simeq 10$ requires $m/m_{el} \sim 25$. Hence from (4.51), $m^*/m = 1 + \alpha/6 \simeq 3$, or $m^*/m_{el} \sim 75$ which is of the correct order of magnitude. The method of § 4 might, therefore,

in this case just have reached its limit. To apply the method of § 5 would require $\alpha \geqslant 10$, i.e. $m/m_{el} \geqslant 25$. In this case according to (5.44), $m^*/m = 1 + \frac{1}{2}(5/8)^3\alpha^4 \gtrsim 1200$, and hence $m^*/m_{el} \gtrsim 30000$, a value which is much too large.

6.2. Method

Clearly it seems desirable to develop a method which leads to a continuous transition between the two methods, i.e. in which the energy $E(0)$ is of the form $-\hbar\omega\,(c_1\alpha + c_2\alpha^2)$. For this purpose a variational method which employs a combination of the wave functions used in §§4 and 5 might be successful. Buckingham (1954) has in fact carried through such a calculation. The transition has been found, however, not to be continuous; up to a value α_0 which is slightly smaller than 256/25 it was found that the results of § 4 are exactly reproduced. At $\alpha = \alpha_0$ there is an abrupt change in wave function and a discontinuity of $\partial E(0)/\partial\alpha$. At $\alpha > \alpha_0$ the results obtained in §5 are slightly modified. These unsatisfactory features are I think largely due to some unsatisfactory properties of the method used in § 5 connected with the concentration of the wave functions (5.1), (5.14) around an arbitrary point x_0 in space. The wave functions (4.29), (4.26) of §4 do not have this disadvantage. For on replacing there $\mathbf{x}$ in the wave function by $\mathbf{x}-\mathbf{x}_1$, where $\mathbf{x}_1$ is a constant vector, the wave function (4.29) is simply multiplied by a phase factor $\exp(i\mathbf{k}\mathbf{x}_1)$. To show this it must be proved that the functions $\psi(\mathbf{k},\mathbf{v})$ given by (4.26) are not changed when replacing there $\mathbf{x}$ by $\mathbf{x}-\mathbf{x}_1$ (without altering $\mathbf{x}$ in the Hamiltonian F). This means that in (4.26) $c(k,v,\xi)\exp(-i\mathbf{v}\mathbf{x})$ must be replaced by $c_1(k,v,\xi)\exp(-i\mathbf{v}.\mathbf{x}-\mathbf{x}_1)$ where the new coefficients $c_1(k,v,\xi)$ must be determined by the variational procedure. It is then found immediately that

$$c(k,v,\xi) = c_1(k,v,\xi)\exp(i\mathbf{v}\mathbf{x}_1)\,,. \tag{6.3}$$

so that $\psi(\mathbf{k},\mathbf{v})$ remains unaltered, as required.
The property of the total wave function Ψ, discussed above, namely

$$\Psi(\mathbf{x}-\mathbf{x}_1) = \exp(-i\mathbf{k}\mathbf{x}_1)\,\Psi(\mathbf{x}), \tag{6.4}$$

where $\mathbf{k}$ is the total wave vector can also be derived directly from the

Hamiltonian F as has been shown by Zienau (1954). It is closely connected with the conservation of the total wave vector. The wave functions used in §5 do not satisfy this requirement. Nevertheless they can of course be used as trial wave functions in a variational procedure, and in fact as has been shown, for very strong interaction ($\alpha > 256/25$) they lead to better energies than the wave functions used in § 4. One might think of modifying the trial wave functions used in §5 so as to satisfy the requirement (6.4). This is not possible, however, without completely changing the method of the self consistent field used in §5. The difficulty is closely connected with the fact that in this method the total wave vector is not on principal axes. Thus with its definition by (3.8), using the wave function (5.1),

$$\left(-i\frac{\partial}{\partial\mathbf{x}} + \sum_{\mathbf{v}}\mathbf{v}b_{\mathbf{v}} + b_{\mathbf{v}}\right)\Omega(\mathbf{x})\Phi \neq \mathbf{k}\Omega(\mathbf{x})\Phi, \tag{6.5}$$

where $\mathbf{k}$ is a constant vector ; with the wave function (4.29), however,

$$\left(-i\frac{\partial}{\partial\mathbf{x}} + \sum_{\mathbf{v}}\mathbf{v}b_{\mathbf{v}} + b_{\mathbf{v}}\right)\exp(i\mathbf{k}\mathbf{x})\Pi_{\mathbf{v}}\psi(\mathbf{k},\mathbf{v})\chi = \mathbf{k}\exp(i\mathbf{k}\mathbf{x})\Pi_{\mathbf{v}}\psi(\mathbf{k},\mathbf{v})\chi \tag{6.6}$$

as has been demonstrated with the help of (4.30).
The difficulty (6.5) encountered in the self consistent method in §5 arises always in the use of the Hartree method, e.g. when solving the problem of n interacting particles in terms of a product

of n wave functions each depending on the coordinates of a single particle (or an appropriately symmetrized combination of such wave functions). This can be demonstrated very simply in the case of two particles, e.g. a proton (coordinates $\mathbf{x}_p$) and an electron (coordinates $\mathbf{x}_e$) forming a hydrogen atom. The exact solution is of the form

$$\psi = \exp\left(i\mathbf{k}\mathbf{x}_c\right)\phi\left(\mathbf{x}_e - \mathbf{x}_p\right), \tag{6.7}$$

where $\mathbf{x}_c$ represents the centre of gravity coordinates, and ($\mathbf{x}_e - \mathbf{x}_p$) the relative coordinates. The total momentum operator is given by - $i\hbar\partial/\partial\mathbf{x}_c$ ($= \hbar\times$ total wave vector) and is on principal axes. In the ground state $\phi\left(\mathbf{x}_e - \mathbf{x}_p\right)$ is a function which is large only near $\mathbf{x}_e - \mathbf{x}_p = 0$. It means that the electron is found always near the proton, but this may be anywhere in the total space available.

In the Hartree approximation, on the other hand, one uses a trial function

$$\psi_{\boldsymbol{H}} = \psi_e\left(\mathbf{x}_e\right)\psi_p\left(\mathbf{x}_p\right), \tag{6.8}$$

where the functions $\psi_\epsilon\left(\mathbf{x}_e\right)$ and $\psi_p\left(\mathbf{x}_p\right)$ are to be determined from the variational method. This leads to a Schrödinger equation each for the electron and for the proton. The respective potential energies are obtained from the potentials of the average charge distributions of the proton and the electron, respectively. In order to obtain a satisfactory result for the ground state, both ψ_e and ψ_p must be spherically symmetrical functions centred at an arbitrary point $\mathbf{x}_0$ in space and being large in the neighbour-
hood of $\mathbf{x}_0$ only (ψ_e in a radius of the order of the Bohr radius, ψ_p in a correspondingly smaller radius). The energy of the ground state obtained in this way is a very good approximation to the correct value. The wave function of the whole system is, however, concentrated around an arbitrary point $\mathbf{x}_0$. In the exact solution the function $\phi\left(\mathbf{x}_e - \mathbf{x}_\eta\right)$ (6.7) is of course also concentrated around the point $\mathbf{x}_e - \mathbf{x}_p = 0$; the function $\exp\left(i\mathbf{k}\mathbf{x}_c\right)$ provides, however, for the atom to be with equal probability at any point in space. In the Hartree wave function (6.8) it would not be permissible to multiply ψ_H by $\exp\left(i\mathbf{k}\mathbf{x}_0\right)$ and to use $\mathbf{x}_0$ as a further available variable coordinate vector because all six degrees of freedom have already been used in $\psi_e\left(\mathbf{x}_e\right)$ and $\psi_p\left(\mathbf{x}_p\right)$. It is seen clearly now how this is connected with the fact that $\partial/\partial\mathbf{x}_c$ is now not on principal axes. This condition would restrict the relative motion of the electron and the proton just in such a way as to make three degrees of freedom available for the motion of the centre of gravity. In the Hartree approximation, however, there is no correlation between the motion of the proton and the electron, except on an average, binding both to the same point $\mathbf{x}_0$.

The wave functions used in §5 correspond to the case discussed above. Thus both, electron wave functions $\Omega(\mathbf{x})$ and polarization potential Φ_{ir} are centred around the same point x_0 as follows from eqns. (5.14) and (5.28).

A further difference in the use of the methods of §§ 4 and 5 can be seen in the behaviour of the polarization potential Φ_{ir}. In the Hartree method (cf. (5.28)) Φ_{ir} is essentially the classical potential of a static charge ρ. The value obtained in § 4, however, depends on the dynamic properties of the lattice (cf. (4.61), (4.62)). As a consequence the value of $E(0)$ according to the method of §4, i.e. (6.1), depends on the dynamic properties of the field, i.e. on ω, whereas (6.2) found from the method of § 5 is independent of ω.

A method of assessing the range of validity of the method used in § 4 has been developed by Lee, Low and Pines (1953), and independently by Zienau (1953). Essentially these authors find a Hamiltonian which is satisfied exactly by the wave functions (4.29) so that one can investigate the influence of the terms which have been neglected. Gurari (1953) had already indicated this possibility. The method applied is to transform the variables (operators) O occurring in the Hamiltonian F(2.40) in such a way,

$$O' = S_t O S_t^{-1}, \quad \cdots\cdots \tag{6.9}$$

that in the new variables O' the Hamiltonian F does no longer contain terms which are linear in the field variables. In (6.9) the operator S_t must be unitary.

It is of advantage to carry through the transformation in two stages, $S_t = S_2 S_1$, and choose

$$S_{\mathbf{1}} = \exp\left(-i\sum \mathbf{v}\mathbf{x}b_{\mathbf{v}} + b_{\mathbf{v}}\right). \tag{6.10}$$

This transforms the operator of the electronic wave vector, $-i\partial/\partial\mathbf{x}$, into the total wave vector for

$$\begin{aligned} -iS_1\frac{\partial}{\partial\mathbf{x}}S_1^{-1} &= -i\exp\left(-i\Sigma\mathbf{v}\mathbf{x}b_{\mathbf{v}} + b_{\mathbf{v}}\right)\frac{\partial}{\partial\mathbf{x}}\exp\left(i\Sigma\mathbf{v}\mathbf{x}b_{\mathbf{v}} + b_{\mathbf{v}}\right) \\ &= -i\frac{\partial}{\partial\mathbf{x}} + \Sigma\mathbf{v}b_{\mathbf{v}} + b_{\mathbf{v}} = \mathbf{k}. \quad \cdots\cdots\cdots \end{aligned} \tag{6.11}$$

By equating it to the constant vector $\mathbf{k}$ it has been indicated that it is a constant of motion as has been shown in § 3. Also
$b_{\mathbf{v}}' = S_1 b_{\mathbf{v}} S_1{}^{-1} = \exp\left(-i\mathbf{v}\mathbf{x}b_{\mathbf{v}} + b_{\mathbf{v}}\right) b_{\mathbf{v}} \exp\left(i\mathbf{v}\mathbf{x}b_{\mathbf{v}} + b_{\mathbf{v}}\right) = b_{\mathbf{v}}\exp(i\mathbf{v}\mathbf{x})$,
because using (2.35) (n is a positive integer),

$$b_{\mathbf{v}}b_{\mathbf{v}} + b_{\mathbf{v}} = \left(b_{\mathbf{v}} + b_{\mathbf{v}} + 1\right) b_{\mathbf{v}}; \quad b_{\mathbf{v}}\left(b_{\mathbf{v}} + b_{\mathbf{v}}\right)^n = \left(b_{\mathbf{v}} + b_{\mathbf{v}} + 1\right)^n b_{\mathbf{v}} \tag{6.13}$$

and similarly for $b_{\mathbf{v}}{}^+$. Hence $b_{\mathbf{v}}{}^+ b_{\mathbf{v}} = b_{\mathbf{v}}{}^+ b_{\mathbf{v}}'$. Thus inserting from (6.11) and (6.12) into expression (2.40) for F,

$$F = \left(\mathbf{k} - \sum_{\mathbf{v}} \mathbf{v}b_{\mathbf{v}}' + b_{\mathbf{v}}'\right)^2 + \sum_{\mathbf{v}} b_{\mathbf{v}}' + b_{\mathbf{v}}' + i(4\pi\alpha/S)^{1/2}\sum_{\mathbf{v}}\left(b_{\mathbf{v}}' + -b_{\mathbf{v}}'\right)/v \tag{6.14}$$

In this Hamiltonian the total wave vector of the system is $\mathbf{k}$, but $\mathbf{k}$ may have any value. In this way the number of available variables has been reduced by three in a similar way as the number of available variables of a system of interacting particles can be reduced by three by eliminating the centre of gravity motion.

Now choose

$$S_2 = \exp\left[-\sum_{\mathrm{v}} c(k, v, \xi)\left(b_{\mathrm{v}}'^{+} + b_{\mathrm{v}}'\right)\right], \tag{6.15}$$

and let the (imaginary) constants $c(k, v, \xi)$ be given by (4.41). Hence

$$\begin{aligned} \beta_{\mathbf{v}} = S_2 b_{\mathbf{v}}' S_2{}^{-1} = \exp\left[c(k, v, \xi)\left(b_{\mathbf{v}}'^{+} + b_{\mathbf{v}}'\right)\right] b_{\mathbf{v}}' \exp\left[c^*(k, v.\xi)\left(b_{\mathbf{v}}' + b_{\mathbf{v}}'\right)\right] \\ = b_{\mathbf{v}}' + c^*(k, v, \xi), \end{aligned} \tag{6.16}$$

since

$$c(k, v, \xi) = -c^*(k, v, \xi) \quad \text{and} \quad \left[b_{\mathbf{v}}', b_{\mathbf{v}}'^{+n}\right] = nb_{\mathbf{v}}'^{+n-1} \tag{6.17}$$

It will be seen that with the choice (4.41) for $c(k, v, \xi)$ the linear terms in $\beta_{\mathbf{r}}$ just cancel when (6.16) is inserted into (6.14). Making, therefore, use of the definition (4.43), (4.44) of $E(\mathbf{k})$, it is found that

$$\boldsymbol{F} = (E(\mathbf{k})/\hbar\omega) - k^2 + \left(\mathbf{k} - \Sigma\mathbf{v}\beta_{\mathbf{v}} + \beta_{\mathbf{v}}\right)^2 + F_1 + \boldsymbol{F}_2, \tag{6.18}$$

where

$$F_1 = S^{-1} \sum_{\mathbf{v},\mathbf{v}'} (\mathbf{v} \cdot \mathbf{v}')\, c(k, v, \xi) c^* (k, v', \xi') \left(2\beta_{\mathbf{v}} + \beta_{\mathbf{v}'} - \beta_{\mathbf{v}} + \beta_{\mathbf{v}'} + -\beta_{\mathbf{v}}\beta_{\mathbf{v}'}\right) \tag{6.19}$$

and

$$F_2 = -2S^{-1/2} \sum_{\mathbf{v},\mathbf{v}'} \left(c(k, v, \xi)\beta_{\mathbf{v}} + \beta_{\mathbf{v}'} + \beta_{\mathbf{v}'} + c^*(k, v, \xi)\beta_{\mathbf{v}'} + \beta_{\mathbf{v}'}\beta_{\mathbf{v}}\right) \tag{6.20}$$

The wave function now depends on the variables $\beta_{\mathbf{v}}, \beta_{\mathbf{v}}+$. In particular, it is seen that a product of oscillator wave functions $|n_v\rangle$ for the oscillators $\beta_v + \beta_v$ satisfies

$$\begin{aligned} &\left\{E(\mathbf{k})/\hbar\omega - k^2 + (\mathbf{k} - \Sigma\mathbf{v}\beta_{\mathbf{v}} + \beta_{\mathbf{v}})^2\right\} \prod_{\mathbf{v}} |n_{\mathbf{v}}\rangle \\ &= \left\{E(\mathbf{k})/\hbar\omega - k^2 + \left(\mathbf{k} - \sum_{\mathbf{v}} \mathbf{v} n_{\mathbf{v}}\right)^2\right\} \prod_{\mathbf{v}} |n_{\mathbf{v}}\rangle\,, \cdot \end{aligned} \tag{6.21}$$

and is, therefore, a solution for the Hamiltonian $F - F_1 - F_2$. Hence the wave function χ, cf. (4.8), satisfies

$$(F - F_1 - F_2)\,\chi = (E(\mathbf{k})/\hbar\omega)\chi..... \tag{6.22}$$

i.e. the solution of § 4 for a given $\mathbf{k}$ is identical with the lowest solution of $F - F_1 - F_2$.

To estimate the error committed in this approximation one can treat $F_1 + F_2$ as a perturbation. This will not be carried out here in detail. By second order perturbation including some numerical work, Lee, Low and Pines (1953) find a correction

$$\Delta E = -\left(0 \cdot 007\alpha^2 + 0 \cdot 01k^2\alpha^2/(1 + \alpha/6)^2\right)\hbar\omega. \tag{6.23}$$

Thus for $\mathbf{k} = 0$, one finds α^2 terms as in § 5, though with a much smaller factor. This means that when $\alpha = 256/25$, perturbation theory for $F_1 + F_2$ is no longer valid. The range of validity of perturbation theory for $F_1 + F_2$ should in fact be restricted to α-values for which

$$|\Delta E| \ll \hbar\omega, \text{ i.e. } \alpha^2 \ll 160 \tag{6.24}$$

At $\alpha = 256/25 \simeq 10, \alpha^2 \simeq 100$ which is not very small compared with 160 . For $\alpha = 6$, however the value for NaCl, $\alpha^2 = 36$, the correction (6.23) is sufficiently smaller than $\hbar\omega$ to make the results of § 4 reliable.

Equation (6.18) also shows that the case $E(\mathbf{k}) - E(0) > \hbar\omega$ leads to difficulties because then the solutions of $F - F_1 - F_2$ are then degenerate.

In conclusion, therefore, it has been found that the method of § 4 gives reliable solutions for energy and effective mass if the interaction parameter α satisfies $\alpha^2 \ll 100$ and provided $E(\mathbf{k}) - E(0) < \hbar\omega$. There is no obvious way in which this method can be extended beyond these limits. The method of § 5 should give reasonable energies $E(0)$ for $\alpha^2 > 100$ though in this case it may no longer be justifiable to treat the lattice as a continuum. This method leads to difficulties inherent in the Hartree method and connected with the motion of the centre of gravity of the system. The validity of the calculation of the effective mass in this method is, therefore, unclear.

It should finally be remarked that application of the method of §5 to metals has led to an understanding of the superconductive properties of a one dimensional superconductor (Fröhlich 1954) but does not yield the isotope effect which is obtained, however, by methods corresponding to those used in § 4. This agrees with the observation that the method of § 5 does not introduce the dynamic properties of the lattice. Thus in this case too development of a method linking the results of §4 and § 5 would be very desirable.

11.1.7 § 7. Mobility

If a weak external electric field is applied to the system consisting of an electron and the polarization field then an electric current is established. Its magnitude can be described in terms of the microscopic mobility μ
which is the average electronic velocity per unit field strength. By definition μ is connected with the average relaxation time $\bar{\tau}$ by

$$\mu = e\bar{\tau}/m \tag{7.1}$$

The methods for calculating μ or $\bar{\tau}$ are well established in the case of sufficiently weak interaction between electron and lattice vibrations, i.e. when perturbation theory holds ($\alpha < 1$). In this case the electron (or electrons) is considered as nearly independent of the polarization quanta. The electron is then accelerated by the field, and is scattered by occasional absorption or emission of a quantum. Assuming the quanta to be in thermal equilibrium, the electron carries an average electric current which is proportional to the strength of the field.

This procedure cannot be generalized in a straightforward manner to the case of stronger coupling ($\alpha > 1$). For this would require the possibility of separating the system into free quanta on the one hand, and the electron plus ' bound ' quanta on the other. The methods developed in previous sections, however, involved the assumption that the total energy (above the ground state) of the whole system is less than $\hbar\omega$ which excludes the presence of free quanta. The difficulties which one meets in attempts to go to higher total energies can be seen from the transformed Hamiltonian in.the form (6.18)-(6.20). There if $\alpha^2 \ll 100$, the terms $F_1 + F_2$ can be considered as negligibly small provided no ' free' quanta are present so that the wave function is given by χ and the energy by $E(\mathbf{k})$, as shown in (6.22). If, however, $n_{\boldsymbol{v}}$ quanta of wave vector $\mathbf{v}$ are excited, as considered in (6.21), then the previously neglected terms $F_1 + F_2$ may become extremely large so that the separation of free quanta achieved in the Hamiltonian $F - F_1 - F_2$ has no longer any physical significance.

In view of these difficulties application of perturbation theory only will be discussed in the present section. It may be hoped that some of the results obtained in this way have a validity beyond $\alpha = 1$, although no proof for this can be given at present. This hope arises from the calculation of the energy of the ground state in § 4 according to which perturbation theory happened to give good results up to $\alpha \simeq 10$. This means, of course, that electronic energies larger than $\hbar\omega$ have to be excluded because in this energy region none of our methods could be applied. Perturbation theory does yield satisfactory results, however, for electronic energies which are very large compared with $\hbar\omega$. This case was treated by the author (Fröhlich 1937) in a paper in which the idea of polarization waves was first introduced. The probability per second for absorption or emission of a quantum by the electron was found vsry small compared with ω so that no objections against the use of perturbation theory arise in this case. This no longer holds, however, when the results are extrapolated to electronic energies near $\hbar\omega$ in agreement with the conclusions of the present discussion. If the electronic energy is less than $\hbar\omega$, however, then quanta can no longer be emitted
but only be absorbed. If furthermore the temperature is so low that very few quanta only are present then the probability for this process is very small. It may be hoped then that perturbation theory may be applied to this case as also suggested above. The calculation of the mobility was carried out by Fröhlich and Mott (1937) and corrected for a more correct electron lattice interaction by Fröhlich, Pelzer and Zienau (1950). In this latter paper it was indicated that after absorption of a quantum the electron has an energy larger than $\hbar\omega$ above the ground state and hence can emit a quantum. The probability for this process in general is so large that perturbation theory cannot be applied, and this is the main reason for the uncertainty of the validity of perturbation theory even in the case of low temperatures and

average electronic energies below $\hbar\omega$. The fact that the probability of emission is very large suggests that the whole process of scattering should be treated similarly to that of resonance scattering of light. Thus a quantum $\hbar\omega$, wave vector $\mathbf{v}$ is absorbed by the electron and re-emitted with wave vector $\mathbf{v}'$. In this process the electron is scattered elastically, changing its wave vector by $\mathbf{v} - \mathbf{v}'$. This resonance scattering has been treated by Zienau (1950).† This process can also be treated by replacing the free electron wave function by a function of the type treated in § 4, but treating the quantum as free, as carried out by Low and Pines (1953). Their result suggests that perturbation theory does give satisfactory results in the case of low temperatures and electronic energies below $\hbar\omega$. Finally it should be mentioned that use of perturbation theory for both absorption and emission together with an appropriate treatment of the kinetic equation leads for low temperatures to the same result for the mobility as the method of resonance scattering. This follows from the paper by Howarth and Sondheimer (1953).

The above survey shows that in actual crystals where usually $1 < \alpha < 10$, there is some hope that application of perturbation theory for the calculation of the mobility should give reasonable results for temperatures $T \ll \hbar\omega/k$ and electronic energies sufficiently smaller than $\hbar\omega$ though as mentioned it has not been possible, so far, to prove this. In view of the theoretical uncertainties, it seems desirable not to involve the complicated theory of resonance scattering but to derive the result very simply by assuming right from the beginning that the probability per second for resonance scattering, i.e. for absorption and re-emission of a quantum is equal to that for absorption alone as would in fact follow from perturbation theory where the ratio of absorption to emission probabilities is very small, of the order $\bar{n}/(1+\bar{n}) \simeq \bar{n} \ll 1$. Here

$$\bar{n} = \frac{1}{\exp(\hbar\omega)/kT) - 1} \ll 1; \quad kT \ll \hbar\omega \tag{7.2}$$

is the average excitation probability of a quantum.

To derive this probability let the electron be in a state with wave vector $\mathbf{q}$, so that its energy is $\hbar\omega q^2$ and let

$$q^2 \ll 1 \tag{7.3}$$

Also let $n_{\mathbf{v}}$ describe the number of excited quanta with wave vector $\mathbf{v}$ so that the zero order wave functions are given by (4.2). Using $\hbar\omega F_{\text{int}}$ (4.7) as perturbation, transitions into electronic states q' are possible in which a single quantum is absorbed, conserving energy and the total wave vector, i.e.

$$\mathbf{q}' = \mathbf{q} + \mathbf{v}, \tag{7.4}$$

and

$$q'^2 = q^2 + v^2 + 2qv\cos\theta = q^2 + 1 \quad \text{or} \quad v^2 + 2vq\cos\theta = 1 \tag{7.5}$$

Here θ is the angle between $\mathbf{q}$ and $\mathbf{v}$. Since $|\cos\theta| < 1$, it follows immediately that v is restricted to the range

$$1 - q < v < 1 + q \tag{7.6}$$

Now since

$$\langle n_{\mathbf{v}} - 1|\, b_{\mathbf{v}}\, |n_{\mathbf{v}}\rangle = {n_{\mathbf{v}}}^{1/2}, \tag{7.7}$$

[8]† A mistake by a factor 2/3 in the final integration has been corrected by C. Herring (1952).

it follows from (4.7) and (4.2) that the absolute square of the matrix element for the absorption process is given by

$$|M|^2 = \frac{4\pi\alpha}{S}\frac{n_v}{v^2}(\hbar\omega)^2 \tag{7.8}$$

The transition probability per second is obtained in the usual way by multiplying (7.8) by $2\pi/\hbar$ and by the number of levels in the final state per unit final energy $q'^2\hbar\omega$. Since the final electronic state is exactly given by (7.4) the density of levels is equal to the density of levels for the quanta, i.e. per unit energy using (7.5) it is given by

$$\frac{S}{(2\pi)^3}\frac{v^2 dv d\cos\theta d\phi}{\hbar\omega d\left(q'^2\right)} = \frac{S}{(2\pi)^3}\frac{v^2 dv d\phi}{\hbar\omega 2qv} \tag{7.9}$$

Hence with (7.8) averaging $n_{\mathbf{v}}$ over a small $\mathbf{v}$ range,

$$dP_a = \frac{2\pi}{\hbar}\frac{4\pi\alpha}{(2\pi)^3}\frac{\hbar\omega}{2qv}\bar{n}dvd\phi \tag{7.10}$$

represents the probability of absorption of a quantum in a certain wave vector range by the electron in the state q. The wave vector range is such that the angle θ of $\mathbf{q}$ and $\mathbf{v}$ is exactly given by (7.5), the magnitude v has a range dv, and the azimuth ϕ with $\mathbf{q}$ as axis has a range $d\phi$.

It must be noticed now that conservation of energy requires that re-emission of a quantum by the electron in the state $\mathbf{q}'$ leads to a final state $\mathbf{q}''$ such that

$$q^2 = q''^2. \quad . . \tag{7.11}$$

The direction of the final state is arbitrary and the probability for reemission follows from (7.10) by replacing there $\bar{n}$ by $1+\bar{n}$. Now with (7.3) it follows from (7.6) that v has nearly the same value $v \simeq 1$ whatever
the direction of $\mathbf{q}''$ so that the probability for scattering into any of these directions is equal. Thus using (7.10), (7.6) and (7.3)

$$P_a = \int dP_a = \frac{\alpha\omega\bar{n}}{2\pi q}\int_0^{2\pi} d\phi \int_{1-q}^{1+q}\frac{dv}{v} = \frac{\alpha\omega\bar{n}}{q}\log\frac{1+q}{1-q} \simeq 2\pi\omega\bar{n} \tag{7.12}$$

is the probability per second for any absorption process, and hence since the probability for re-emission is very much larger (provided $\bar{n} \ll 1$) P_a is also the probability per second for resonance scattering. This latter involves elastic scattering of the electron with equal probability for any scattering angle. Hence

$$P_a d\Omega/4\pi = 2\alpha\omega\bar{n}d\Omega/4\pi \quad . . \tag{7.13}$$

is the probability per second for the elastic scattering of the electron in a solid angle $d\Omega$.

With the help of this transition probability the rate of change of an electronic distribution function $f(\mathbf{q})$ can be calculated. For clearly

$$\frac{\partial f(\mathbf{q})}{\partial t} = -P_a\int\left(f(\mathbf{q}) - f\left(\mathbf{q}''\right)\right)d\Omega''/4\pi, \quad q^2 = q''^2 \tag{7.14}$$

since P_a is independent of the direction of $\mathbf{q}''$; $d\Omega''$ represents the differential of the solid angle of $\mathbf{q}''$. In thermal equilibrium, $f(\mathbf{q})$ depends on the magnitude q only and hence $\partial f/\partial t = 0$ in this case. It will be noticed, of course. that elastic scattering cannot alter the magnitude of q and hence can establish equilibrium only if $ff(\mathbf{q})d\Omega$ has the equilibrium value. This is

assumed to hold in the theory of conductivity in weak fields where a distribution function $f(\mathbf{q})$ of the form

$$f(\mathbf{q}) = f_0(q) + (q_F/q)\, f_1(q) \tag{7.15}$$

is considered. Here q_F is the projection of $\mathbf{q}$ into the field direction, and both $f_0(q)$ and $f_1(q)$ depend on the magnitude of q only. Clearly then

$$\begin{aligned}\int (f(\mathbf{q}) - f(\mathbf{q}''))\, d\Omega'' &= (f_1(q)/q) \int (q_F - q_F'')\, d\Omega'' \\ &= \mathbf{4}\pi\, (q_F/q)\, f_1(q) = \mathbf{4}\pi\, (f(\mathbf{q}) - f_0(q))\end{aligned} \tag{7.16}$$

because $\int q_F{}'' d\Omega'' = 0$. From the definition of the relaxation time τ,

$$\frac{\partial f(\mathbf{q})}{\partial t} = -\frac{1}{\tau}\, (f(\mathbf{q}) - f_0(q))\,, \quad . \tag{7.17}$$

it follows with (7.16), (7.14) and (7.13) that

$$1/\tau = 2\alpha\omega\bar{n}. \tag{7.18}$$

Also since τ is independent of $\mathbf{q}, \tau = \bar{\tau}$.
It should be remarked that second order field effects change the average electronic energy. Equilibrium can then not be established through elastic scattering processes only.

The mobility μ now follows by introducing (7.18) into (7.1). Use of (7.2) and (2.37) leads to
$\mu = \frac{ea_0}{(2\hbar\omega m_{el})^{1/2}} \left(\frac{1}{\epsilon_\infty} - \frac{1}{\varsigma}\right)^{-1} \left(\frac{m_{el}}{m}\right)^{3/2} [\exp(\hbar\omega/kT) - \mathrm{I}], \quad kT <\leqslant \hbar\omega \quad .$
where

$$a_0 = \hbar^2/me^2 \simeq 0.5 \times 10^8 \text{ cm} \tag{7.20}$$

is the Bohr radius. Hence if

$$\Theta = \hbar\omega/k \tag{7.21}$$

is expressed in degrees absolute,

$$\mu \simeq 10 \left(\frac{1}{\epsilon_\infty} - \frac{1}{c}\right)^{-1} \left(\frac{m_{el}}{m}\right)^{3/2} \frac{\exp(\Theta/T) - 1}{\sqrt{\Theta}} \text{ cm}^2/\text{ volt sec }, \quad T \ll \Theta. \tag{7.22}$$

It will be recalled that $\omega/2\pi$ is the frequency of longitudinal vibrations which is connected with the frequency of residual rays by eqn. (2.10). Hence if c is the velocity of light and λ is the residual ray wave length then from (7.21) and (2.10),

$$\Theta = \frac{\hbar}{k}\frac{2\pi c}{\lambda}\sqrt{\frac{\epsilon}{\epsilon_\infty}}. \tag{7.23}$$

Before comparing the theoretical value (7.22) for the microscopic mobility μ with experimental results the above mentioned difficulties in the theory must be emphasized again. Furthermore it should be remembered that there will always be contributions to the scattering of electrons due to mechanisms of a different nature from the one discussed here. Thus scattering due to the so-called acoustic vibrations will make a contribution to μ proportional to $T^{-3/2}$ and should thus be decisive at very low temperatures. The magnitude of this type of scattering is in general very small, however (cf. Mayer and Polder 1953).

Experiments on NaCl have been carried out by Redfield (1953) who finds $\mu = 250 \pm 50$ cm^2/volt sec $T = 82 \pm 2°$K and $\mu \sim 40$ at $T = 200°$K. Theoretically with $\epsilon = 5 \cdot 6, \epsilon_\infty = 2 \cdot 3, \lambda = 61 \times 10^{-4}$ cm, one has $\Theta = 340°$ and hence $\mu = 280\,(m_{el}/m)^{3/2}$ and $\mu = 15\,(m_{el}/m)^{3/2}$ respectively. The agreement is very satisfactory (with $m \sim m_{el}$). Measurements on AgCl by Haynes and Shockley (1953) can be represented by $\mu = 30[\exp(290/T) - 1]$. Theoretically with $\epsilon = 12 \cdot 3, \epsilon_\infty = 4 \cdot 0$ and $\Theta = 290°$, the factor 30 is replaced by $4\,(m_{el}/m)^{3/2}$ which has also the correct magnitude. The measured temperature range is not wide enough, however, to exclude a $T^{-3/2}$ law. Agreement with the theoretical temperature dependence over a wide range was obtained by Breckenridge and Hosler (1953) on TiO_2. Their absolute values indicate very high electronic effective mass probably due to conduction in impurity bands.

Perturbation theory which was used in the derivation of expression (7.18) for τ is also valid for electronic energies which are very high compared with $\hbar\omega$. The actual expression in this case differs, however, from (7.18) for various reasons. This case will not be considered here because interaction with very short polarization waves is predominant in this case so that treatment of the lattice as a continuum is no longer permissible. This leads to some uncertainties concerned with the value of ω and with the correct form of the interaction, but on the other hand use of perturbation theory is well justified. In contrast to this case, however, use of perturbation theory for electronic energies of the order $\hbar\omega$ is quite unjustifiable in particular for alkali halides where $\alpha \simeq 6$.

Further experiments might help to overcome the theoretical difficulties encountered in this respect. This would require the measurement of electronic mobilities for electronic energies of the order of $\hbar\omega$ i.e. in the case of thermal equilibrium for temperatures of the order $T \simeq \Theta$.

11.1.8 References

Bloch, F., 1928, Z. Phys., 52, 555.
Breckenridge, R., and Hosler, W., 1953, Phys. Rev., 91, 793.
Buckingham, M. J., 1954, E.R.A. Report, to be published.
Fröhlich, H., 1937, Proc. Roy. Soc. A, 160, 280 ; 1949, Theory of Dielectrics (Oxford : Clarendon Press) ; 1950, Phys. Rev., 79, 845 and Proc. Phys. Soc. A, 63, 778; 1953, Physica, 19, 755 ; 1954, Proc. Roy. Soc. A, 223, 296.
Fröhlich, H., and Mott, N. F., 1939, Proc. Roy. Soc. A, 171, 496.
Fröhlich, H., Pelzer, H., and Zienau, S., 1950, Phil. Mag., 41, 221.
Gurari, M., 1953, Phil. Mag., 44, 329.
Haynes, J., and Shockley, W., 1951, Phys. Rev., 82, 935.
Herring, C., 1952, personal communication.
Howarth, D. J., and Sondheimer, E. H., 1953, Proc. Roy. Soc. A, 219, 53.
Landau, L., 1933, Phys. Z. Sowjetunion, 3, 664.
Landau, L., and Pekar, S., 1948, Journal of Physics, U.S.S.R., 18, 419.
Lee, T., and Pines, D., 1952, Phys. Rev., 88, 960.
Lee, T., Low, F., and Pines, D., 1953, Phys. Rev., 90, 297.
Low, F., and Pines, D., 1953, Phys. Rev., 91, 193.
Meyer, H., and Polder, D., 1953, Physica, 19, 255.
Pekar, S., 1946, Journal of Physics, U.S.S.R., 10, 341 ; 1949, Ibid., 19, 796.
Pelzer, H., 1950, E.R.A. Report L/T243.
Redfield, A., 1953, Phys. Rev., 91, 753.
Tomonaga, S., 1947, Progr. Theor. Phys., 2, 6.
Zienau, S., 1950, E.R.A. Report L/T236; 1953, E.R.A. Report L/T299 ; 1954, to be published.

11.2 Effective Mass of a Polaron by Landau, Pekar

Translated and reprinted from Zh. Eksp. Teor. Fiz. 18, No. 5, pp. 419-423 (1948)

Abstract

It is assumed that the current carrier in crystals with ionic lattice is a polaron rather than a conduction band electron. The conservative motion of a polaron as a whole is considered. The dependence of the system energy on the velocity of translational motion of a polaron and the equation of motion of a polaron in an external field are obtained.

Introduction

The available theory of the electron conduction in dielectrics and semiconductors assumes that the conduction electron moves within one of the "allowed" energy bands of a crystal, and the electron ш-function is a wave, whose amplitude is constant over the whole crystal bulk. The presence of forbidden gaps in crystals is experimentally confirmed: this is testified by the fact of the dielectric existence itself, data on the temperature dependence of the electric conduction, data on the internal photoeffect and the photoeffect from a metal into a dielectric, etc. Other features of the theory mentioned above did not find any direct confirmation, and they even contradict sometimes the experimental facts.

But first of all (at least in the case of ionic crystals), it is worth to indicate that the available theory includes an internal contradiction, namely: while considering the quantum states of conduction electrons, it is assumed, as usual, that ions are fixed at lattice sites; in this case, an electron appears to be in a periodic field. However, in reality, ions are moving, and the electron state adiabatically follows the ion motion. S.I. Pekar already considered this motion [1] and showed that the conduction electron polarizes dielectrically the ionic crystal with the own electric field. It turns out that, already at the very beginning of the process of polarization, the polarized crystal represents a potential well with discrete spectrum for the electron. The electron having spent a part of its energy to polarize the crystal goes to a discrete level into the local state; then the
crystal polarization increases, and the electron level and the energy of the whole system are lowered. The equilibrium will be reached when the energy of the system reaches its minimum. In this case, the polaron is created, as was considered by one of the authors in the previous works [2,3] in detail. Thus, the band state of a conduction electron does not correspond to an extremum of the system energy, i.e. it is unstable. Slow conduction electrons should constantly transfer into the polaron state. The decay time of a band state for the slow electron should be of the order of 10^{-13} s; hence, it is necessary to revise the foundations of the available conduction theory.
S.I. Pekar [1, 4] offered a new point of view concerning the electron conduction of ionic crystals. According to it, the current carrier is just a polaron, rather than a free electron in the conduction band. In an external electric field, the polaron should move like a negative charge. In this case, the local state should shift as a whole along the field direction (the inertial polarization of the crystal should follow the polaron movement). The calculated polaron mobility [4] is in good agreement, by the order of magnitude, with the mobility of a current carrier determined experimentally as a product of the electric conduction and the Hall constant.

In the present paper, we will calculate the effective mass of a polaron.

Effective Mass of a Polaron

The inertial and inertialess parts [2] may be separated within the dielectric polarization of ionic crystals. The inertialess part of the polarization is characterized by the square of the refraction index of light (within the range, where the dispersion curve has its plateau);

it is assumed that it fully follows the movement of a conduction electron. As a result of the inertialess polarization of crystal sites by the field of the electron, it undergoes the action of a supplementary force modulated with
lattice periods; this force will be introduced into the total periodic potential of the electron in the crystal. To solve the coming tasks, we may use the known method of electron effective mass [5]. That is, we can ignore the periodic potential and simultaneously change the electron mass with its effective mass μ.

The assumption that the electron state $\psi(\mathbf{r}, t)$ adiabatically follows the ion motion and the radius of the ψ-state exceeds the lattice constant results in the following expression for the energy H of the system:
$H = \frac{\hbar^2}{2\mu} \int |\nabla\psi|^2 d\tau - \int \mathbf{p}\mathbf{D}[\psi] d\tau + U_p$.

Here, $\mathbf{p}(\mathbf{r}, t)$ is the inertial part of the specific polarization of a dielectric [2],

$$\mathbf{D}[\psi] = e \int |\psi(\mathbf{r}_1)|^2 \left\{ (\mathbf{r} - \mathbf{r}_1) / |\mathbf{r} - \mathbf{r}_1|^3 \right\} d\tau \tag{2}$$

is the quantum-mechanical mean of the electrostatic induction of the electron. In formula (1), the first and second terms stand, respectively, for the kinetic energy of an electron and the interaction energy of the electron with the polarized crystal, and U_p is the total energy of the crystal under the assumption that the electron is suddenly moved away (the potential and kinetic energies of ions).

In accordance with the variation principle of quantum mechanics (it replaces the Schrödinger equation), for every given polarization $\mathbf{p}(\mathbf{r}, t), \psi(\mathbf{r}, t)$ is determined as a minimum of functional (1) with the additional condition

$$\int |\psi|^2 d\tau = 1; \tag{3}$$

hence,
$\frac{\hbar^2}{2\mu} \delta \int |\nabla\psi|^2 d\tau - \int \mathbf{p}\delta\mathbf{D}[\psi] d\tau = 0$.

In what follows, we assume that the ψ-function is already defined in this manner; then H is the Hamilton function describing the ion movement in the crystal.

We assume that the crystal is a system of ions performing small harmonic oscillations and express H via the corresponding normal coordinates and velocities of ions. The ion movement is determined with usual canonical Hamilton's equations (while differentiating H, expression (4) should be taken into account). Such equations are those for forced ion oscillations under the action of a force $\mathbf{D}(\mathbf{r}, t)$.

Let us consider a special case of motion when the polaron moves translationally as a whole with the velocity $\mathbf{v}$, i.e. when
$\psi = \psi(\mathbf{r} - \mathbf{v}t), \quad \mathbf{D} = \mathbf{D}(\mathbf{r} - \mathbf{v}t), \quad \mathbf{p} = \mathbf{p}(\mathbf{r} - \mathbf{v}t)$.

Expanding $\mathbf{D}$ and $\mathbf{p}$ in the Fourier series, one obtains:
$\mathbf{D} = \sum_k \mathbf{D}_\mathbf{k} e^{i\mathbf{k}(\mathbf{r}-\mathbf{v}t)} = \sum_k \mathbf{D}_\mathbf{k} e^{i(\mathbf{k}\mathbf{r}-\omega_\mathbf{k} t)}, \quad \omega_\mathbf{k} = \mathbf{k}\mathbf{v}$, (6)
$\mathbf{p} = \sum_k \mathbf{p}_\mathbf{k} e^{i(\mathbf{k}\mathbf{r}-\omega_\mathbf{k} t)}$.

We note that the forced ion oscillations caused by the force $\mathbf{D}$ can be obtained as a simple superposition of oscillations caused by separate harmonics of the form
$\mathbf{D}_\mathbf{k} e^{i(\mathbf{k}\mathbf{r}-\omega_\mathbf{k} t)}$.

Certainly, these harmonics are not usual electromagnetic waves (their velocity $v \neq c$, they are characterized by a different dispersion law, and they are not transverse). However, since the polaron size exceeds the lattice constant, dominating in expansion (6) are the harmonics, whose wavelengths also exceed the lattice constant. In this case, the task can be reduced to the known limiting case of long waves. So that, when considering the forced oscillations of ions, harmonics (8) can be replaced by electromagnetic waves, the induction vector of which has the

same amplitude and frequency. This change allows us to express the polarization of a dielectric via the dielectric constant $\varepsilon(\omega)$ defining the dispersion of electromagnetic waves in crystals as

$$\mathbf{p_k} = c\left(\omega_{\mathbf{k}}\right)/4\pi)\,\mathbf{D_k}, \quad c(\omega) = \left(1/n^2\right) - \left(1/\varepsilon(\omega)\right) \tag{9}$$

(when deducing the expression for $c(\omega)$, one should bear in mind that $\mathbf{p}$ is only the inertial part of the specific polarization [2]). It is assumed that the crystal is polarized in an isotropic manner.

Relations (9) are the solution of the equation for forced oscillations. Equations (2), (4), and (9) define the functions $\psi, \mathbf{D}$, and $\mathbf{p}$, respectively. It is obvious that all three these equations are simultaneously satisfied with functions of form (5).

To determine the effective mass of a polaron, it is necessary to calculate energy (1) to within terms of the order of v^2. In accordance with this and taking the parity of the function $\varepsilon(\omega)$ into account (we ignore the imaginary part of ε, i.e. the absorption), we represent $c(\omega)$ as the series

$$c\left(\omega_{\mathbf{k}}\right) = c_0 + c_2\omega_{\mathbf{k}}^2 + \ldots \tag{10}$$

$$c_0 = \left(1/n^2\right) - \left(1/\varepsilon(0)\right), \quad c_2 = c_0/\omega_1^2, \tag{11}$$

where ω_1 is the limiting frequency of optical oscillations of ions (it and the "dispersion frequency" should not be confused). Since
$\omega_{\mathbf{k}}^2 D_{\mathbf{k}} e^{i(\mathbf{kr}-\omega_{\mathbf{k}}t)} = -\left(\partial^2/\partial t^2\right)\mathbf{D_k} e^{i(\mathbf{kr}-\omega_{\mathbf{k}}t)}$,
it is convenient to write the equations for forced oscillations (9) in the summed form:

$$\mathbf{p}(\mathbf{r},t) = (1/4\pi)\left[c_0\mathbf{D}(\mathbf{r},t) - c_2\left(\partial^2\mathbf{D}/\partial t^2\right)\right]. \tag{12}$$

Now, it is easy to obtain the expression for the crystal energy U_p. Taking into account that the work performed in a unit volume of the crystal per unit time is

$$\mathbf{D}\dot{\mathbf{p}} = (\mathbf{D}/4\pi)\left[c_0\dot{\mathbf{D}} - c_2\dddot{\mathbf{D}}\right], \tag{13}$$

and setting the energy of a unit volume without field (a polaron is far away) to be equal to zero, we obtain

$$U_p = (c_0/8\pi)\int \mathbf{D}^2 d\tau + (3c_2/8\pi)\int \dot{\mathbf{D}}^2 d\tau. \tag{14}$$

Substituting (12) and (14) in formula (1) for the energy of the system, we get

$$H = \frac{\hbar^2}{2\mu}\int |\nabla\psi|^2 d\tau - \frac{c_0}{8\pi}\int \mathbf{D}^2[\psi]d\tau + \frac{c_2}{8\pi}\int \dot{\mathbf{D}}^2[\psi]d\tau. \tag{15}$$

The case of immovable polaron ($v = 0, \dot{\mathbf{D}} = 0$) was considered in detail by one of the authors in previous works [2, 3], where the ground-state wave function $\psi = \psi_0(\mathbf{r})$ of a polaron and the respective energy

$$H_0 = -0.0547\left(\mu e^4/\hbar^2\right)c_0^2 \tag{16}$$

were obtained. Taking this solution as a zero approximation and passing to the case of a uniformly moving polaron, it can be shown that the ψ-function and the energy acquire small corrections, if the velocity

$$v \ll r_m\omega_1, \tag{17}$$

where r_m is the polaron radius [2].
To within terms of the order of v^2, the energy can be written in the form
$H = H_0 + \frac{1}{2}Mv^2$,
$M = \frac{c_2}{3}\left[\int_0^\infty \left(\frac{\partial \mathbf{D}[\psi_0]}{\partial r}\right)^2 r^2 dr + 2\int_0^\infty \mathbf{D}^2\left[\psi_0\right] dr\right]$.

By substituting $D\left[\psi_0\right]$ from (3), we get that the effective mass of a polaron
$M = 5.8 \times 10^{-3}\left(\mu e^2/\hbar^2\right)^3 e^2 c_0^3 c_2 =$

$$= 9.08 \times 10^3 (\mu/m)^3 c_0^3 c_2 \text{ g}, \tag{19}$$

where m is the free electron mass, μ is the effective electron mass in the ordinary conduction band. As usual, M turns out to be considerably higher than the electron mass (in the case of NaCl , it is 432 times higher).

By considering the motion of a polaron in an external electric field $\mathbf{E}$ and equating the power developed by this field to the energy increment (18) per second, we obtain an ordinary equation of motion for the polaron:

$$M\dot{\mathbf{v}} = e\mathbf{E}. \tag{20}$$

It has been assumed above that the uniform motion of a polaron is conservative, i.e. harmonics (8) keep stationary forced oscillations of ions but do not generate natural oscillations of ions. However, in reality, the forced ion oscillations generate natural oscillations due to some anharmonism (heat is released). In this case, some deceleration of a polaron is observed. The energy given to the lattice by a polaron can be formally calculated as the absorption of above-mentioned electromagnetic waves equivalent to harmonics (8) in the crystal. The calculation has shown [4] that the braking force is proportional to the velocity, and the mobility of the polaron in an external field is

$$u = 0.262 \times 10^{-13} \frac{\varepsilon(0)^{3/2}}{b(\mu/m)^3 c_0^3} \text{ abs. un.} \tag{21}$$

The coefficient b is experimentally determined by measuring the absorption of electromagnetic waves in a crystal: namely, $b\omega$ is the imaginary part of the refraction index of a crystal for waves with frequency $\omega \ll \omega_1$. The braking force $\mathbf{R}$ can be expressed in terms of the mobility and the velocity of a polaron as

$$\mathbf{R} = -e\mathbf{v}/u. \tag{22}$$

Neglecting a weak braking and quantizing the motion of a polaron as a whole (without field), we can ascertain that the motion can be described by plane waves (like the motion of the mass center of any complex particle with internal degrees of freedom). Therefore, the dependence of the density of energy levels for the translational motion of a polaron on its kinetic energy has the same form as that in the case of a free particle with mass M and spin 1/2.

The thermodynamically equilibrium concentration of polarons is expressed by the usual formula
$n = (2/h^3)\left(2\pi MkT\right)^{3/2} e^{(\zeta - H_0)/kT}$,
where ζ is the chemical potential of electrons in a crystal. However, the coefficient of the exponential factor is usually by many orders higher than that in the case of electrons. Due to the interaction of polarons with thermal oscillations of ions, the Maxwell distribution for polaron velocities is established.

1. S.I. Pekar, Zh. Eksp. Teor. Fiz. 17, 868 (1947).

2. S.I. Pekar, Zh. Eksp. Teor. Fiz. 16, 341 (1946).

3. S.I. Pekar, Zh. Eksp. Teor. Fiz. 16, 335 (1946).

4. S.I. Pekar, Zh. Eksp. Teor. Fiz. 18, 105 (1948).

5. S.I. Pekar, Zh. Eksp. Teor. Fiz. 16, 933 (1946).

Received January 20, 1948

LANDAU LEV DAVIDOVICH (22.01.1908-01.04.1968)

Lev Davidovich Landau was the outstanding physicist-theorist of the XX century, Full Member of the Academy of Sciences of the USSR, the Nobel Prize winner in physics (1962) "For pioneer investigations in the theory of condensed matter and especially of liquid helium".

During 1932-1937, he was Head of the Department of Theoretical Physics at the Ukrainian Physical-Technical Institute in Kharkov (now NSC "Kharkov Institute of Physics and Technology" of NAS of Ukraine), L.D. Landau headed a chair at Kharkov State University also. Since 1937, he was Head of the Theoretical Department of the Institute for Physical Problems of the Academy of Sciences of the USSR in Moscow. He is a founder of the Kharkov's scientific school of theoretical physics.

L.D. Landau's investigations cover practically all branches of theoretical physics, ranging from fluid mechanics to quantum field theory [1]. L.D. Landau predicted the existence of neutron stars (W. Baade, F. Zwicky, L.D. Landau), he constructed a general theory of phase transitions of the second order (19361937). The Ginzburg-Landau equation is of great importance in the theory of superconductivity. The Landau levels, Landau diamagnetism, and Landau-Lifshits equation are well known

in physics. L.D. Landau constructed the theory of superfluid liquid helium-II [2] and the theory of the Fermi liquid [3-5]. L.D. Landau's investigations in plasma physics and in the theory of magnetism are of great importance. L.D. Landau formulated the theory of a two-component neutrino (independently of A. Salam, T. Lee, and C. Yang, 1957) and proposed the principle of conservation of the combined parity in the weak interactions of elementary particles [6].

A significant part in the L.D. Landau's heritage belongs to the world-famous "Course of Theoretical Physics" written jointly with E.M. Lifshits in many volumes.

1. L.D. Landau, Selected works (Nauka, Moscow, 1969), volumes 1, 2 (in Russian); Collected Papers of L.D. Landau, edited by D. ter Haar (Pergamon Press, London, 1965).

2. L.D. Landau, Zh. Eksp. Teor. Fiz. 11, 592 (1941) [J. Phys. USSR, 5, 71 (1941)].

3. L.D. Landau, Zh. Eksp. Teor. Fiz. 30, 1058 (1956).

4. L.D. Landau, Zh. Eksp. Teor. Fiz. 32, 59 (1957).

5. L.D. Landau, Zh. Eksp. Teor. Fiz. 35, 97 (1958).

6. L.D. Landau, Zh. Eksp. Teor. Fiz. 32, 407 (1957).

PEKAR SOLOMON ISAKOVYCH (16.03.1917-08.06.1985)

S.I. Pekar was born in Kyiv. He was graduated from Kyiv State University in 1938. At the age of 24 , he was conferred the Doctor degree for his candidate thesis "Studies on the Theory of Semiconductors". From 1941 up to his death, S.I. Pekar was working at the Academy of Sciences of UkrSSR as the Head of the Department of Theoretical Physics (1941-1960 - Institute of Physics, 1960-1985 - Institute of Semiconductors). Since 1946, he was Professor. S.I. Pekar

headed the Chair of Theoretical Physics at Kyiv State University in 1944-1949 and in 1953-1962. There, he founded the specialization "physicist-theorist" for students and postgraduates. In 1961, S.I. Pekar was elected Academician of the Academy of Sciences of UkrSSR without intermediate grade "Corresponding member". He is the author of several important discoveries in solid-state physics. Two of them are commonly recognized peaks of the world science: the theory of autolocalized states of electrons named polarons by him (1946) and the discovery of additional light waves in crystals (1957) plus a new theory of crystallooptics (the phenomenon was officially registered as a discovery).

11.3 Mobility of Slow Electrons in a Polar Crystal by Feynman, Hellwarth, et al.

Abstract

We have obtained an approximate expression for the impedance function at all frequencies, temperatures, and coupling strengths of an electron coupled to a polar lattice (a system commonly called a polaron). The starting point for the calculation is the quantum mechanical expression for the expected current. The phonon coordinates are eliminated from this expression by well-known fieldtheory techniques. The resulting exact "influence functional" is then approximated by a corresponding quadratic "influence functional" which, it is hoped, imitates the real polaron. Correction terms are computed to account for the difference between the approximate impedance and the exact polaron impedance in a manner closely analogous to Feynman's treatment of the polaron self-energy. In fact, the analytic evaluation of the expression for the impedance obtained here is carried out using the approximate

11.3.1 I. Introduction

A^{N}N electron in a polar crystal interacts with the surrounding crystal. The effect of this interaction is to surround the electron with a distorted lattice: a cloud of phonons. The nature of this system, "the polaron," has been extensively studied. [1–4] It is interesting as a phenomenon in solids, but it has an extended interest since it is one of the simplest examples of the interaction of a particle and a field. It is in many ways analogous to the problem of a nucleon interacting with a meson field. (The extra complications of spin and isotopic spin do not, however, permit direct use of the methods to be described here, without some extension of their power.) In cases of practical interest, the coupling between the electron and the longitudinal optical modes of vibration of the crystal is sufficiently strong that simple perturbation methods do not apply. It is the strong-coupling aspect of the problem which has aroused so much interest. For this reason, the "polaron problem" has generally been studied in a considerably idealized form.

It is assumed that in the undistorted lattice the electron would move as a free particle (with possibly an altered mass), that only the optical modes interact with the electron, that they do so in a very simple way, and

"influence functional" that was successfully employed in minimizing the binding (and free) energy of the polaron in earlier calculations. However, the accuracy obtained using this approximation, for the impedance calculation, is less satisfactory and its limitations are discussed. Nevertheless, beginning at intermediate coupling strengths, the approximate impedance produces a level structure of increasing complexity and narrowing resonances as the coupling

[81] R. P. Feynman, Phys. Rev. 97, 660 (1955), hereafter to be called I.
[2] H. Frohlich, Advances in Physics, edited by N. F. Mott (Taylor and Francis, Ltd., London, 1954), Vol. 3, p. 325.
[3] S. I. Pekar, Zhur. Eksp. i Teoret. Fiz. 19, 796 (1949).
[4] T. D. Schultz, Phys. Rev. 116, 526 (1960).

strengthens. This suggests that further refinements may be fruitful. Methods for finding a better quadratic influence functional for use in our impedance expression as well as ways of improving the expression further are suggested. A comparison of our results with those of the Boltzmann equation points up interesting differences which arise from reversing the order of taking limits of zero frequency and coupling.
that they all have the same frequency. These are quite drastic simplifications; however, sufficient data are not available to improve these assumptions so as to represent any actual crystal. The methods given here do not require these simplifications (except perhaps that the electron's kinetic energy is a quadratic function of its momentum); the same techniques can be readily applied to include variations of frequency and coupling of the optical modes with wave number, influences of other modes, etc., although some of the integrals done analytically here might have to be done numerically.

In discussing losses and mobility such idealization may alter completely the true behavior, because some essential loss mechanism such as lattice defects or interaction with acoustic phonons has been idealized away. It is important to appreciate, therefore, that in all the remaining analysis and discussion we shall be talking only about a strictly idealized problem.

One of us [1] has shown that the ground-state energy and effective mass of the polaron could be calculated with considerable accuracy from a variational principal obeyed by path integrals. Of more interest, experimentally, is the mobility of the polaron and, more generally, its response to weak, spatially uniform, time varying electric fields. This is a more complicated problem involving the rate at which a drifting electron loses momentum by phonon interactions, through emissions of phonons or collisions with phonons already present. In the practical situation at temperatures not too near the melting point of the crystal the density of
optical phonons is quite low as a result of the high energy required to excite them. In our idealized model losses can occur only through collisions with optical phonons, so that these collisions could be analyzed by first finding the collision cross section and then using the Boltzmann equation (or equivalently the usual formulas for transport cross section) to get the mobility. [5] This is the technique generally employed in transport problems. Yet there exists a class of transport problems in which this cannot be done. If many phonons are colliding simultaneously with an electron most of the time, and if there are possibly quantum interferences among these collisions (such that the cross section for scattering from one phonon depends on the presence and behavior of others), the collisions cannot be separated in time as required for the validity of the Boltzmann transport equation. What we need to calculate (the average position of an electron at time t, if at $t = 0$ a pulsed electric field was applied) can be easily written formally, but little has been done with such a form unless the coupling is weak or the collisions are well separated. [6,7]

A secondary interest which we had in this problem was to see if we could compute transport problems in cases when not only the perturbation theory, but also the Boltzmann equation is inadequate. Therefore, in spite of its lack of reality, we have analyzed the problem of the impedance of a polaron of arbitrary coupling strength in an oscillating electric field, for arbitrary temperatures (temperatures so high perhaps that the Boltzmann factor $e^{-\hbar\omega/kT}$ for the energy $\hbar\omega$ of the optical modes is not necessarily small).

In any specific range of conditions, such as low temperature, high temperature, or high frequency of external electric field, etc., special approximations might be made to obtain a better answer than is given by our general formula. However, it was of interest to see how well one could do in a general way for arbitrary values of the parameters.

11.3.2 II. Formulation of the Mobility Problem in Terms of Electron Coordinate Alone

If a weak alternating electric field $E = E_0 e^{i\nu t}$ is applied to the crystal in the x direction, the current induced (by motion of the electron) may be written as

$$j(\nu) = [z(\nu)]^{-1} E_0 e^{i\nu t}. \tag{1}$$

This defines the impedance function $z(\nu)$ which we wish to calculate. We will assume that the crystal is isotropic so that $j = \langle \dot{x} \rangle$, where $\langle x \rangle$ is the expectation of the electron displacement in the x direction (taking the electric charge as unity). The displacement $\langle x \rangle$ is $E/i\nu z(\nu)$.

Transformed to time variables, this implies that

$$\langle x(\tau) \rangle = -\int_{-\infty}^{\infty} iG(\tau - \sigma) E(\sigma) d\sigma \tag{2}$$

where $G(\tau), i$ times the electron displacement at time τ induced by a pulsed electric field at time zero, has the inverse transform

$$\int_{-\infty}^{\infty} G(\tau) e^{-i\nu\tau} d\tau = G(\nu) = [\nu z(\nu)]^{-1} \tag{3}$$

We take $G(\tau) = 0$ for $\tau < 0$.[8]
The effect of a perturbing field $\mathbf{E}(t)$ in the x direction is to add to the complete Hamiltonian of the system H, the term $-xE(t) \equiv -\mathbf{E} \cdot \mathbf{X}$ (where x is the component of the vector position of the electron $\mathbf{X}$ in the direction of the field). If at some time (a), long before the field is turned on [i.e., $\mathbf{E}(t) = 0$ for $t < a$] the state of the system is represented by the density matrix ρ_a, then the density matrix at time τ is $U(\tau, a)\rho_a U'^{-1}(\tau, a)$. Thus, the expected position at time τ is

$$\langle x(\tau) \rangle = \mathrm{Tr}\left[x U(\tau, a) \rho_a U'^{-1}(\tau, a) \right], \tag{4}$$

where

$$U(\tau, a) = \exp\left\{ -i \int_a^{\tau} \left[H_s - \mathbf{X}_s \cdot \mathbf{E}(s) \right] ds \right\} \tag{5}$$

is the unitary operator for the development of a state in time with the complete Hamiltonian $H - \mathbf{X} \cdot \mathbf{E}$.

We use a time-ordered operator notation; all unprimed operators are placed to the left, latest times farthest to the left, then the matrix ρ at the right and finally all primed operators on the right of ρ, with latest times farthest to the right. [9] Thus, primed operators are ordered oppositely to unprimed. We can, therefore, write

$$U'^{-1}(\tau, a) = \exp\left\{ i \int_a^{\tau} \left[H'_s - \mathbf{X}'_s \cdot \mathbf{E}'(s) \right] ds \right\} \tag{6}$$

The quantity E is not an operator but simply a function of s so that in (4), $E'(s) = E(s)$. However, as we shall see in a moment, it is convenient to handle a more general case where E and E' are different arbitrary functions of s.

For weak fields we expand (4) to first order in E and find an expression for $x(\tau)$ of the form (2). Evidently, $-iG(\tau - \sigma)$ is the response to a δ function E, so we may set $E(s) = \epsilon\delta(s - \sigma) =$

[85] J. Howarth and E. H. Sondheimer, Proc. Roy. Soc. (London) A219, 53 (1953).
[6] R. Kubo, J. Phys. Soc. Japan 12, 570, 1203 (1957).
[7] M. Lax, Phys. Rev. 109, 1921 (1958).

$E'(s)$, substitute into (4), and expand the exponential to first order in ϵ. However, we note that (4) itself may be considered to be $-i$ times the first functional derivative with respect to $E(\tau) - E'(\tau)$ of

$$g = \mathrm{Tr}\left[U(b,a)\rho_a U'^{-1}(b,a)\right], \tag{7}$$

as $b \to +\infty$, and $a \to -\infty$. That is to say, we calculate g from (5), (6), and (7) with

$$E(s) = \epsilon\delta(s-\sigma) + \eta\delta(s-\tau) \tag{8a}$$

and

$$E'(s) = \epsilon\delta(s-\sigma) - \eta\delta(s-\tau) \tag{8b}$$

The quantity we require is

$$G(\tau-\sigma) = \frac{1}{2}\left(\partial^2 g/\partial\eta\partial\epsilon\right)_{\eta=\epsilon=0} \tag{9}$$

If the initial state is one of a definite temperature T, then

$$\rho_a = \exp(-\beta H)/Q, \tag{10}$$

where $\beta = 1/kT$ and Q is a normalizing constant, which we eliminate by calculating $(1/2g)\left(\partial^2 g/\partial\eta\partial\epsilon\right)$ evaluated at $\epsilon = \eta = 0$.

The Hamiltonian representing an electron in interaction with the vibrational modes of a crystal is

$$\begin{aligned} H = \mathbf{P}^2/2m + \sum_{\mathrm{K}} \omega_{\mathrm{K}} a_{\mathrm{K}}{}^{\dagger} a_{\mathrm{K}} \\ + V^{-1/2} \sum_{\mathrm{K}} \left[C_{\mathrm{K}}{}^{*} a_{\mathrm{K}}{}^{\dagger} \exp(-i\mathbf{K}\cdot\mathbf{X}) \right. \\ \left. + C_{\mathrm{K}} a_{\mathrm{K}} \exp(i\mathbf{K}\cdot\mathbf{X})\right] \end{aligned} \tag{11}$$

In this expression, $a_{\mathrm{K}}, a_{\mathrm{K}}{}^{\dagger}$ are the annihilation and creation operation of phonons of momentum $\mathbf{K}$, frequency ω_{K}, coupled to the electron via the coupling coefficient C_{K}; $\mathbf{P}$ is the momentum of the electron; $\mathbf{X}$ is its coordinate; m is its effective mass calculateed in a fixed lattice; V is the crystal volume. We take $\hbar = 1, m = 1$.

As a specific example we shall take the simplified model of Fröhlich [2] in which $\omega_{\mathrm{K}} = 1$ independent of $\mathbf{K}$,
and $C_{\mathrm{K}} = i2^{3/4}\pi^{1/2}\alpha^{1/2}/|\mathbf{K}|$, where α is a constant related to the dielectric constant; intermediate coupling corresponds to $\alpha \approx 6$.

The quantity ρ_a, the initial distribution, should be $e^{-\beta H}$ for the full Hamiltonian H. If the time (a) is sufficiently far in the past we can just as well take ρ_a = const $\times \exp\left(-\beta \sum_{\mathrm{K}} \omega_{\mathrm{K}} a_{\mathrm{K}}{}^{\dagger} a_{\mathrm{K}}\right)$. That is, we may assume that in the past only the oscillators were in thermal equilibrium at temperature β^{-1}. As a result of the coupling, the entire system will come very quickly to thermal equilibrium at the same temperature. The energy of the single electron and its coupling are infinitesimal (of the order $1/V$) relative to the heat bath of the system of phonon oscillators, so that the exchange of energy between the electron and the lattice will bring everything to thermal equilibrium at the original lattice temperature.

[88] In our idealized model $\mathbf{X}$ and $\mathbf{E}$ will be in the same direction, although in general (in the presence of magnetic field or anisotropic crystalline fields), G and z will be tensors.
[9] R. P. Feynman, Phys. Rev. 84, 108 (1951).

With this choice of ρ_a the dependence of U, U', and ρ_a in (7) on the phonon oscillator coordinates is sufficiently simple so that the oscillator coordinates may be eliminated and the entire expression reduced to a double path integral involving the electrons coordinates only. This reduction, explained in Appendix A, is carried out by methods analogous to those used before by one of the authors on problems in electrodynamics. [9]

The result is (taking $a \to -\infty, b \to +\infty$)

$$g = \iint e^{i\Phi} \mathfrak{D}\mathbf{X}(t) D\mathbf{X}'(t) \tag{12}$$

where

$$\begin{aligned}\Phi = &\int_{-\infty}^{+\infty} \left[\frac{1}{2}\left(\frac{d\mathbf{X}(t)}{dt}\right)^2 - \frac{1}{2}\left(\frac{d\mathbf{X}'(t)}{dt}\right)^2\right] dt - \int_{-\infty}^{+\infty} \left[\mathbf{E}(t)\cdot\mathbf{X}(t) - \mathbf{E}'(t)\cdot\mathbf{X}'(t)\right] dt \\ &+ \frac{i}{2}\int \frac{d^3K}{(2\pi)^3} |C_{\mathrm{K}}|^2 \int_{-\infty}^{+\infty}\int_{-\infty}^{+\infty} \{\exp[i\mathbf{K}\cdot\mathbf{X}(t)] - \exp[i\mathbf{K}\cdot\mathbf{X}'(t)]\} \times [y(\omega_{\mathrm{K}}, t-s) \\ &\times \{\exp[-i\mathbf{K}\cdot\mathbf{X}(s)] + \exp[-i\mathbf{K}\cdot\mathbf{X}'(s)\} + ia(\omega_{\mathrm{K}}, t-s)\{\exp[-i\mathbf{K}\cdot\mathbf{X}(s)] - \exp[-i\mathbf{K}\cdot\mathbf{X}'(s)]\}]\end{aligned} \tag{13}$$

The functions $y(\omega, \tau)$ and $a(\omega, \tau)$ are given in Appendix A. In the special case of Fröhlich's Hamiltonian the integral on $\mathbf{K}$ can be performed to give

$$\begin{aligned}\Phi_F = &\int_{-\infty}^{+\infty} \left[\frac{1}{2}\left(\frac{d\mathbf{X}(t)}{dt}\right)^2 - \frac{1}{2}\left(\frac{d\mathbf{X}'(t)}{dt}\right)^2\right] dt + \int_{-\infty}^{+\infty} \left[\mathbf{E}(t)\cdot\mathbf{X}(t) - \mathbf{E}'(t)\cdot\mathbf{X}'(t)\right] dt \\ &+ i\alpha 2^{-3/2} \int_{-\infty}^{+\infty}\int_{-\infty}^{+\infty} \left[\frac{e^{-i|t-s|} + 2P(\beta)\cos(t-s)}{|\mathbf{X}(t) - \mathbf{X}(s)|} + \frac{e^{+i|t-s|} + 2P(\beta)\cos(t-s)}{|\mathbf{X}'(t) - \mathbf{X}'(s)|}\right. \\ &\left. - \frac{2\left[e^{-i(t-s)} + 2P(\beta)\cos(t-s)\right]}{|\mathbf{X}'(t) - \mathbf{X}(s)|}\right] dtds\end{aligned} \tag{14}$$

where $P(\beta) = \left[e^{\beta} - 1\right]^{-1}$.
The double integral $\mathfrak{D}\mathbf{X}(t)\mathfrak{D}\mathbf{X}'(t)$ is only over those paths which satisfy the boundary condition $\mathbf{X}(t) - \mathbf{X}'(t) = 0$ at times t approaching $\pm\infty$. The boundary conditions on the paths at large positive or negative times, reflects the arbitrariness of the initial electron state.

Thus, we have reduced the problem of find G via (7), (8), and (9) to that of finding the dependence of a path integral (12) on the forcing functions E and E'. This expression is exact [for the Hamiltonian (11)] but quite complicated. In the next section we discuss approximate methods of evaluation.

11.3.3 III. A Method of Approximation

In I, a path integral, similar to (14), had to be evaluated. It was argued there that in some rough approximation the "interaction of the charge with itself" represented there by a term in the action function $S, 2^{-3/2}\alpha e^{-|t-s|}|\mathbf{X}(t) - \mathbf{X}(s)|^{-1}$, might be imitated by a function S_0 in which this term is replaced by $1/2Ce^{-w|t-s|}[\mathbf{X}(t) - \mathbf{X}(s)]^2$. One may think of the interaction term in S as indicating that at time t the particle acts as though it were in a potential $2^{-1/2}\alpha \int_{-\infty}^{t} e^{-(t-s)} \times |\mathbf{X}(t) - \mathbf{X}(s)|^{-1} ds$ resulting from the electrostatic interaction of the electron with its mean charge density of its previous positions [the weight for different times being $e^{-(t-s)}$]. The assumption then is that such a potential may be roughly replaced by a parabolic

potential centered at the mean position of the electron in the past [the weight for different times being $e^{-w(t-s)}$]. In fact, the extra parameter w can be adjusted to compensate partly for the error of using a parabolic potential in place of the true potential form. This argument strongly suggests that the dynamical behavior of the electron, (its motion under an applied electric field) might be described approximately if we replace Φ by a Φ_0, where

$$\begin{aligned}\Phi_0 = \int_{-\infty}^{+\infty} \left[\frac{1}{2}\left(\frac{d\mathbf{X}(t)}{dt}\right)^2 - \frac{1}{2}\left(\frac{d\mathbf{X}'(t)}{dt}\right)^2\right] dt - \int_{-\infty}^{+\infty} \left[\mathbf{E}(t)\cdot\mathbf{X}(t) - \mathbf{E}'(t)\cdot\mathbf{X}'(t)\right] dt \\ -\frac{iC}{2}\int_{-\infty}^{+\infty}\int_{-\infty}^{+\infty} \left\{\left[\mathbf{X}(t)-\mathbf{X}(s)\right]^2\left[e^{-iw|t-s|} + 2P(\beta w)\cos w(t-s)\right]\right. \\ + \left[\mathbf{X}'(t)-\mathbf{X}'(s)\right]^2\left[e^{+iw|t-s|} + 2P(\beta w)\cos w(t-s)\right] \\ \left. -2\left[\mathbf{X}'(t)-\mathbf{X}(s)\right]^2\left[e^{-iw(t-s)} + 2P(\beta w)\cos w(t-s)\right]\right\} dtds \qquad (15)\end{aligned}$$

The parameters C and w are to be determined so as to approximate Φ as closely as possible. At zero temperature ($P = 0$), we shall fix C and w at the values given in I. The assumption that Φ_0 is a good approximation to Φ for computing the mobility at low temperatures is based on the supposition that the comparison Lagrangian, which gives a good fit to the groundstate energy at zero temperature, will also give the dynamical behavior of the system. In finding the ground-state energy, the parameters can be chosen by a variational principle but we know of no such principle for the mobility. At finite temperatures the parameters C and w can be determined from a variational principal for the free energy which is a direct extension of the method used in I for the ground-state energy, and reduces to it in the zero-temperature limit. Others [10,10a] have derived in detail the expressions from which the best C and w may be determined for finite β. Thus, C and w can be considered as known functions of α and β even though, unfortunately, no closed analytic form exists, and in any specific calculation they would have to be evaluated numerically.

Actually, we shall not be satisfied merely to replace Φ by Φ_0, but we shall obtain a first correction to $z(\nu)$ by studying, in the next section, the first term in an

expansion of $\exp\left[i\left(\Phi - \Phi_0\right)\right]$:

$$\begin{aligned} g = \iint e^{i\Phi}\mathfrak{D}\mathfrak{X}\mathbf{X}' \approx \int\int e^{i\Phi_0\mathfrak{D}}\mathbf{X}\mathfrak{D}\mathbf{X}' \\ + \int e^{i\Phi_0} i\left(\Phi - \Phi_0\right)\mathfrak{D}\mathbf{X}\mathbf{X}' \qquad (16)\end{aligned}$$

In this section, however, we will consider only the first term,

$$g_0 = \int e^{i\Phi_0 D}\mathbf{X}\mathfrak{D}\mathbf{X}' \qquad (17)$$

We can expect to evaluate the integral (17) exactly, because the expression for Φ_0 is a quadratic form in $\mathbf{X}(t)\mathbf{X}'(t)$ and all such "Gaussian" path integrals can be evaluated exactly. [9] There are several ways to perform the integration in (17). One way is to observe that the expression (15) is obtained by eliminating the variable $\mathbf{Y}$ from a system in which an electron interacts with a single particle described by the Lagrangian

$$L_0 = \frac{1}{2}(d\mathbf{X}/dt)^2 + \frac{1}{2}(d\mathbf{Y}/dt)^2 - \frac{1}{2}k(\mathbf{X}-\mathbf{Y})^2 + \mathbf{E}\cdot\mathbf{X} \qquad (18)$$

[810] Y. Osaka, Progr. Theoret. Phys. (Kyoto) 22, 437 (1959).

[10a] M. A. Krivologz and S. I. Pekar, Bull. Acad. Sci. U.S.S.R. 21, 1, 13, 29 (1957).

If we calculate the g for such a system by integrating over all the $\mathbf{Y}$ variables first, then (17) results; provided we choose $k = (v^2 - w^2)$ and $M = (v^2 - w^2)/w^2$, where $v^2 = w^2 + 4C/w$. However, L_0 can be re-analyzed as the
sum of two normal modes,

$$L_0 = \frac{1}{2}(M+1)\left(d\mathbf{X}_2/dt\right)^2 + \mathbf{E}\cdot\mathbf{X}_2 + \frac{M}{2(M+1)} \times \left[\left(d\mathbf{X}_1/dt\right)^2 - v^2\mathbf{X}_1{}^2\right] - \frac{M}{(M+1)}\mathbf{E}\cdot\mathbf{X}_1 \tag{19}$$

so that g_0 can be written as the product of two factors, one for each harmonic oscillator. For a single oscillator of mass m and frequency ω, coupled as $\mathbf{\Gamma}(t)\cdot\mathbf{X}$, the value of g is given in Appendix A. Here we have two oscillators, one of mass $m_1 = M + 1 = v^2/w^2$ and frequency $\omega_1 = 0$ coupled with a $\mathbf{\Gamma}(t) = \mathbf{E}(t)$, and a second oscillator with $m_2 = M/M+1, \omega_2 = v$, and $\mathbf{\Gamma}(t) = -(M/M+1)\mathbf{E}(t) = -\left[(v^2 - w^2)/v^2\right]\mathbf{E}(t)$. If the contributions of the two normal modes are combined, g_0 takes the form

$$g_0 = \exp\left(\tfrac{i}{4\pi}\int_{-\infty}^{+\infty}[f(-\nu) - f'(-\nu)]\left\{[f(\nu) + f'(\nu)]\,Y_0(\nu) + i\,[f(\nu) - f'(\nu)]\,A_0(\nu)\right\}d\nu\right), \tag{20}$$

where [11]

$$Y_0(\nu) = -\left(\nu^2 - w^2\right)/(\nu - i\varepsilon)^2\left[(\nu - i\varepsilon)^2 - v^2\right] \tag{21}$$

and

$$A_0(\nu) = \tfrac{\pi}{2}\left\{\tfrac{2w^2}{v^2\beta\varepsilon^2}[\delta(\nu+\varepsilon) + \delta(\nu-\varepsilon)] + [1 + 2P(\beta v)] \times \tfrac{(v^2-w^2)}{v^3}[\delta(\nu+v) + \delta(\nu-v)]\right\} \tag{22}$$

We have expressed $E(t)$ and $E'(t)$ by their Fourier transforms

$$f(\nu) = \int_{-\infty}^{+\infty} E(t)e^{-i\nu t}dt \tag{23}$$

To obtain $G_0(\tau - \sigma)$ we must evaluate g_0 for E and E' given in (8), that is to say, we must substitute

$$\begin{aligned} f(\nu) &= \epsilon e^{-i\nu\sigma} + \eta e^{i\nu\tau} \\ f'(\nu) &= \epsilon e^{-i\nu\sigma} - \eta e^{i\nu\tau} \end{aligned} \tag{24}$$

into (20), and find the term of order $\epsilon\eta$. Evidently

$$G_0(\tau - \sigma) = \frac{+i}{2\pi}\int_{-\infty}^{+\infty} Y_0(\nu)e^{+i\nu(\tau-\sigma)}d\nu \tag{25}$$

where $G_0(\tau - \sigma)$ is the zeroth order approximation to $G(\tau - \sigma)$ [Eq. (2)]. Therefore,

$$G_0(\nu) = +iY_0(\nu) \tag{26}$$

Since Y_0 is the classical response function for the comparison system L_0, the result has the immediate

[811] ε is a small positive quantity and the limit $\varepsilon \to 0$ is to be taken.

interpretation that $G_0(\nu)$ is the response we would have predicted for the system L_0 had we treated it classically. In addition, there is no temperature dependence in G_0 (except through the variation of the parameters v, w with temperature). Both of these well-known results follow from the linearity of L_0.[12,13]

For a particle of mass m, for low frequencies, $G \approx -i/m\nu^2$ so that a comparison of this expression with (21) and (26) gives an effective electron mass $m = v^2/w^2$. This value for m is not the same as the more accurate value given in I, but as Shultz [4] has shown, it is numerically not very different over a wide range of α. Thus, the reactive part of G_0 may be satisfactory, but the dissipative (real part) appearing as it does all at the single frequency v, must be only a very crude approximation.

In the next section we shall compute the corrections implied by the additional expansion terms in (16). We shall find that the mass is now exactly that given in I, and that the dissipatiion has a much more realistic behavior.

11.3.4 IV. First Corrected Term

To evaluate the second term on the right-hand side of (16) we shall have to integrate $e^{i\Phi_0}(\Phi - \Phi_0)$. In order to see what is involved, consider only one of the terms arising from $\Phi e^{i\Phi_0}$:

$$\begin{aligned} T = \int e^{i\Phi_0} \Bigg\{ \int \frac{d^3K}{(2\pi)^3} |C_{\mathrm{K}}|^2 \\ \times \int_{-\infty}^{+\infty} \int_{-\infty}^{\infty} \exp\{i\mathbf{K}\cdot[\mathbf{X}(t) - \mathbf{X}(s)]\} \\ \times [y(\omega_{\mathrm{K}}, t-s) + ia(\omega_{\mathrm{K}}, t-s)]\, dsdt\} \\ \times \mathfrak{D}\mathbf{X}(t)\mathfrak{D}\mathbf{X}'(t) \end{aligned} \tag{27}$$

Other terms from Φ are similar to (27) with some replacements of $\mathbf{X}$ by $\mathbf{X}'$, while the terms from Φ_0 we will consider later. Evaluation of (27) requires a knowledge of the path integral $R(K,t,s) = \int e^{i\Phi_0} \exp \mathfrak{J}\{i\mathbf{K}\cdot[\mathbf{X}(t) - \mathbf{X}(s)]\}\mathfrak{D}\mathfrak{X}\mathbf{X}'$.

Once $R(K,t,s)$ has been evaluated, (27) becomes an ordinary multiple integral:

$$\begin{aligned} T = \int \frac{d^3K}{(2\pi)^3} |C_{\mathrm{K}}|^2 \int_{-\infty}^{+\infty} \int_{-\infty}^{\infty} R(K,t,s) \\ \times [y(\omega_{\mathrm{K}}, t-s) + ia(\omega_{\mathrm{K}}, t-s)]\, dsdt \end{aligned} \tag{29}$$

The function R is easily evaluated. It is clearly given by our general formula (20) with

$$\mathbf{f}(\nu) = \left(\epsilon e^{-i\nu\sigma} + \eta e^{-i\nu\tau}\right)\hat{\imath} + \mathbf{K}\left(e^{-i\nu t} - e^{-i\nu s}\right) \tag{30}$$

and [14]

$$\mathbf{f}(\nu) = \left(\epsilon e^{-i\nu\sigma} - \eta e^{-i\nu\tau}\right)\hat{\imath} \tag{31}$$

Similarly, a term of the form (27) with $\mathbf{X}(t)$ replaced by $\mathbf{X}'(t)$ can be expressed in terms of our general path integral (20) by using the proper f 's,

[8,12] F. L. Vernon, Jr., Ph.D. thesis, California Institute of Technology, 1959 (unpublished).

[13] R. W. Hellwarth, Hughes Research Laboratories, Fourth Quarterly Progress Report, September 15, 1958 (unpublished).

$$\mathbf{f}(\nu) = \left(\epsilon e^{-i\nu\sigma} + \eta e^{-i\nu\tau}\right)\hat{\imath} - \mathbf{K}e^{-i\nu s} \tag{32}$$

and

$$\mathbf{f}'(\nu) = \left(\epsilon e^{-i\nu\sigma} - \eta e^{-i\nu\tau}\right)\hat{\imath} - \mathbf{K}e^{-i\nu t} \tag{33}$$

In this way, $\int e^{i\Phi_0}\Phi D\mathbf{X}\Phi\mathbf{X}'$ can be evaluated. Similarly the term $\int e^{i\Phi_0}\Phi_0\mathfrak{D}\mathbf{X}\mathfrak{D}\mathbf{X}'$ may be obtained. To get $\int e^{i\Phi_0}[\mathbf{X}(t)-\mathbf{X}(s)]^2\Phi\mathbf{X}\Phi\mathbf{X}'$, one can differentiate R with respect to K twice and evaluate it at $K=0$. (Details are given in Appendix B.)

The final result for the first-order change in G is

$$G_1 = -iY_0^2(\nu)\left[\chi(\nu) + (4C/w)\nu^2/\left(\nu^2 - w^2\right)\right] \tag{34}$$

where

$$\chi(\nu) = \int_0^\infty \left[1 - e^{i\nu u}\right] \operatorname{Im} S(u)du \tag{35a}$$

and

$$S(u) = \int \frac{d^3K}{(2\pi)^3}\,|C_{\mathbf{K}}|\frac{2K^2}{3}e^{-K^2D(u)/2} \left[\exp\left(i\omega_{\mathbf{K}}u\right) + 2P\left(\beta\omega_{\mathbf{K}}\right)\cos\left(\omega_{\mathbf{K}}u\right)\right] \tag{35b}$$

"Im" means the imaginary part and the function $D(u)$ is defined as

$$D(u) = \frac{w^2}{v^2}\left[\frac{v^2-w^2}{w^2v}\left[1 - e^{+ivu} + 4P(\beta v)\sin^2(vu/2)\right] - iu + u^2/\beta\right] \tag{35c}$$

For Fröhlich's Hamiltonian, the integration over $\mathbf{K}$ may be done to give

$$S(u) = 2\alpha/3\sqrt{\pi}\left\{[D(u)]^{-3/2}\left[e^{iu} + 2P(\beta)\cos u\right]\right\} \tag{36}$$

We have found an approximate form for $G(\nu)$:

$$G(\nu) = G_0(\nu) + G_1(\nu) \tag{37}$$

From it we may find the impedance to first order in $G_1(\nu)$:

$$\nu z(\nu) = 1/G(\nu) \sim 1/G_0(\nu) - \left[1/G_0(\nu)^2\right]G_1(\nu) \tag{38}$$

The question arises as to whether it is more accurate to expand in this way or to leave the formula as $\nu z(\nu)$

$= (G_0 + G_1)^{-1}$. Of course, if G_1 were truly small it would not matter. However, there are excellent reasons to believe that the expanded form is far more accurate. This is best explained by considering a simple example of a free particle to which we add a harmonic binding as a perturbation. The resulting G 's are [Φ_0 arising from $\frac{1}{2}m(d\mathbf{X}/dt)^2$ only],

$$G_0(\nu) = +iY_0(\nu) = -i/m\nu^2 \tag{39a}$$

[814] Equation (20) is a one-dimensional formula. For the case of vector forces the product of two f 's is to be interpreted as a dot product.

and

$$G_1(\nu) = -i\omega_0^2/m\nu^4 \tag{39b}$$

where ω_0 is the natural frequency of the oscillator. In this case the expanded form of $z(\nu)$ is

$$i\nu z(\nu) = m\left(\omega_0^2 - \nu^2\right) \tag{40}$$

The true $G(\nu)$ shows a structure (resonance at $\nu = \omega_0$) which is not reflected in an expanded form of G, but which is precisely duplicated (for this linear system) if one expands $z(\nu)$. Therefore, we substitute (34) into (38) to obtain the simple result,

$$-i\nu z(\nu) = \nu^2 - \chi(\nu) \tag{41}$$

With $\chi(\nu)$ given by (35), this is our final expression for the impedance of the polaron. It is Eqs. (41) and (35) which we will evaluate in various limits and discuss in the following sections.

The first term on the right-hand side of (41) is a pure free-particle term, while $\chi(\nu)$ contains all of the corrections due to the interaction with phonons. The entire dependence of our results (41) on the trial action Φ_0 is in $D(u)$, Eq. (35c). $D(u)$ in turn appears only in the exponential term in Eq. (35b). This exponential is an effect due to recoil as can be seen by expanding the $\exp(i\mathbf{K}\cdot\mathbf{X})$ term in the Hamiltonian as $1 + i\mathbf{K}\cdot\mathbf{X}$ (which we may call a dipole, or linear coupling approximation). If the expansion is made, then the exponential term $e^{-K^{2D}(u)/2}$ in (35b) will not appear. In other words, if we had any problem in which the field oscillators were coupled linearly to the electron's coordinate $\mathbf{X}$, then our method would give us the exact formula for the impedance irrespective of the choice made for the trial functional Φ_0.[15] This is fact in the best argument for treating the perturbation expansion (16) as an expansion for $z(\nu)$ in the manner of Eq. (38).

Therefore, insofar as the system of phonons behaves as though they were linearly coupled, so there were no recoil effects, (41) is exact. However, recoil effects are included in (41); it is only that they are not included precisely. They are approximated by finding their effect for the imitative functional Φ_0 rather than the true functional Φ. For this reason we expect (41) to be an excellent approximation to the true impedance of the polaron.

11.3.5 V. Behavior of the Impedance

For purposes of further analysis in which we shall change the contour of integration on the variable u, we list some properties of $S(u)$. For real $u, S^*(u) = S(-u)$ and $S(iu)$ is purely real. In addition $S(u) = S(i\beta - u)$ for complex u. The real part of $D(u)$ must be positive in order for the K integral to converge. Therefore, the region of u where this happens, namely the strip parallel to the real axis between the lines $u =$ real and $u =$ real $+i\beta$, is the region free of singularities for $S(u)$. In the limit of zero temperatures ($\beta \to \infty$) this strip, over which $S(u)$ is analytic, widens to include the entire upper half-plane.

1. Zero Temperature, $v < 1$; Effective Mass

For Fröhlich's case we consider first the case $\nu < 1$, $\beta = \infty$. Then the path of integration [in the integral for $\chi(\nu)$] along the real axis may be rotated to the path along the positive or negative imaginary axis $u \approx 0$ to $\pm i\infty$ (depending on the sign of e^{iu}). The resulting expression is

[815] Assuming that $\mathbf{\Phi}_0$ also implies a linear coupling and is a quadratic functional of $\mathbf{X}(t), \mathbf{X}'(t)$.

$$-i\nu z(\nu) = \nu^2 - \frac{2\alpha}{3\sqrt{\pi}} \int_0^\infty e^{-\tau}(1 - \cosh \nu\tau) \times \left[\frac{v^2 - w^2}{v^3} \left(1 - e^{-v\tau}\right) + \frac{w^2}{v^2}\tau \right]^{-3/2} d\tau \tag{42}$$

Therefore, z is purely imaginary for $\nu < 1$ and there is no dissipation at the absolute zero of temperature (a dc field will continue to accelerate the electrons indefinitely). The reason for this behavior is simply that there are no existing phonons for the electrons to scatter off and none can be created by the electrons until the frequency ν of the applied field is high enough to excite the electrons to a state of energy $\hbar\nu$ higher than the energy $\hbar\omega$ needed to create a phonon. If there is a range of frequencies ω down to zero (as for acoustic modes) then a resistance exists at any frequency of the applied field and at zero temperature. In the Fröhlich model it begins at $\nu = 1$. Of course, a dc field will eventually speed the electrons up until they can radiate phonons and dissipate energy. However, this is a nonlinear effect in the applied field strength and is not described by a theory of the impedance. For extremely low frequencies ν we can put $(1 - \cosh \nu\tau) = -\nu^2\tau^2/2$. The result is that

$$-i\nu z(\nu) = \nu^2 \left\{ 1 + \frac{\alpha}{3\sqrt{\pi}} \int_0^\infty u^2 e^{-u} \times \left[\left(\frac{v^2 - w^2}{v^3} \right) \left(1 - e^{-vu}\right) + \frac{w^2}{v^2} u \right]^{-3/2} du \right\} \tag{43}$$

The polaron behaves like a free particle with an effective mass. This mass is the same as the one derived in I, by a modification of the variational ground-state energy calculation.

2. General Expression for Dissipation

The analytic properties of $S(u)$ outlined at the beginning of this section allows one to rewrite the expression for the $\operatorname{Im}\chi(\nu)$ in a form more convenient for computation. We may write (35a) as

$$\operatorname{Im}\chi(\nu) = \operatorname{Im} \int_0^\infty \sin(\nu u) S(u) du \tag{44}$$

Using the fact that $S(u)$ is analytic between $u =$ real and $u =$ real $+i\beta$, we may change the contour of integration in (44) from along the real axis to one which goes first from 0 to $i\beta/2$ up the imaginary axis and then from $i\beta/2$ to $i\beta/2 + \infty$ parallel to the real axis. (The closing piece of the contour required at infinity does not contribute.) Because $S(iu)$ and $\sin(i\nu u)d(iu)$ are real, the leg of the contour up the imaginary axis contributes nothing to (44), which requires the imaginary part. The contribution from the remaining part of the contour (from $i\beta/2$ to $i\beta/2 + \infty$) gives

$$\operatorname{Im}\chi(\nu) = \sinh(\beta\nu/2) \int_0^\infty \cos(\nu u) \Sigma(u) du \tag{45a}$$

where $\Sigma(u) = S(u + i\beta/2)$ is given by

$$\Sigma(u) = \int \frac{d^3K}{(2\pi)^3} \Big| C_{\mathrm{K}}|^2 \times \frac{2}{3}K^2 \frac{\cos(\omega_{\mathrm{K}}u)\exp\left[-\frac{1}{2}K^2\Delta(u)\right]}{\sinh(\beta\omega_{\mathrm{K}}/2)} \tag{45b}$$

and $\Delta(u) \equiv D(u + i\beta/2)$.

$$\Delta(u) = \frac{w^2}{v^2}\left[\left(\frac{v^2 - w^2}{w^2 v}\right)\frac{\cosh(\beta v/2) - \cos(vu)}{\sinh(\beta v/2)} + \frac{u^2}{\beta} + \frac{\beta}{4}\right]. \tag{45c}$$

The dc mobility μ for the polaron is given by

$$\mu^{-1} = \lim_{\nu\to 0} \operatorname{Im}\chi(\nu)/\nu$$

Our results (44), therefore, gives

$$\mu^{-1} = \frac{1}{2}\beta\int_0^\infty \Sigma(u)du \tag{46}$$

For the case of Fröhlich's Hamiltonian, we find that

$$\operatorname{Im}\chi(\nu) = \frac{2\alpha}{3\sqrt{\pi}}\frac{\beta^{3/2}\sinh(\beta\nu/2)}{\sinh(\beta/2)}\left(\frac{v}{w}\right)^3 \times \int_0^\infty \frac{\cos(\nu u)\cos(u)du}{[u^2 + a^2 - b\cos(vu)]^{3/2}} \tag{47a}$$

where

$$a^2 \equiv \beta^2/4 + R\beta\coth(\beta v/2)$$
$$b \equiv R\beta/\sinh(\beta v/2) \tag{47b}$$

and

$$R \equiv \left(v^2 - w^2\right)/w^2 v \tag{47c}$$

3. Dissipation at Low Temperatures

For low temperatures $e^{-\beta}$ and, therefore, $e^{-\beta v}$ are very much less than one, so that (47a) may be expanded as a power series in b.

$$\operatorname{Im}\chi(\nu) = \frac{2\alpha}{3\sqrt{\pi}}\frac{\sinh(\beta\nu/2)}{\sinh(\beta/2)}\left(\frac{v}{w}\right)^3\int_0^\infty \frac{\cos(\nu u)\cos u}{(u^2+a^2)^{3/2}} \times \Big\{1 + \frac{3\beta R e^{-\beta v/2}\cos(vu)}{(u^2+a^2)} + \frac{15}{4}\frac{\beta^2 R^2 e^{-\beta v}}{(u^2+a^2)^2}[1 + \cos(2vu)] + \cdots\Big\}du \tag{48}$$

Now an integral like $\int \cos(\lambda u)du/\left(u^2 + a^2\right)^{3/2}$ falls off exponentially like $(2\pi|\lambda|)^{1/2}(a)^{-3/2}e^{-|\lambda|a}$ as λ increases. Thus, the smallest values of λ count, and these count with the smallest power $e^{-\beta}$ in front. This permits us to select the important terms for each ν. For example, the last term in brackets contributes when $\nu \approx 2v + 1$ for there is a contribution from $\cos(\nu u)\cos(u)\cos(2vu)$. The $e^{-\beta v}$ is compensated for by the $e^{\beta(\nu-1)/2}$ in front.

For $\nu < 1 + v$, and $|1 - \nu| > \beta^{-1}$, only the first term in the expansion contributes and we obtain

$$\begin{aligned}\operatorname{Im}\chi(\nu) \approx \frac{2}{3}\alpha\left(\frac{v}{w}\right)^3\left(1 - e^{-\beta\nu}\right)e^{\beta(\nu-1)/2} \\ \times\left[(|\nu-1|)^{1/2}e^{-\beta|\nu-1|/2}e^{-R|\nu-1|}\right. \\ \left.+(\nu+1)^{1/2}e^{-\beta(\nu+1)/2}e^{-R(\nu+1)}\right]\end{aligned} \tag{49}$$

As $\beta \to \infty$ this shows a threshold at $\nu = 1$. Below $\nu = 1$ the result is nearly zero; above, it is $\sim \frac{2}{3}\alpha(v/w)^3(v-1)^{1/2} \times \exp[-R(\nu-1)]$. This is the threshold to create one optical phonon from the energy quantum $\hbar\nu$ supplied by the external field. If we have an excess energy $\nu - 1$, the final electron has momentum proportional to $(\nu-1)^{1/2}$ and this appears as a factor because of the phase space available. The cross section depends in some way on the frequency above threshold; the factor $\exp[-R(\nu-1)]$ is a rough approximation to this, generated by our model Φ_0.

To study the dependence on β in a little more detail, in case $\nu < 1$, (49) can be rewritten as

$$\begin{aligned}\operatorname{Im}\chi(\nu) \approx \frac{2}{3}\alpha(\nu/w)^3\left[(1-\nu)^{1/2}e^{-\beta(1-\nu)}e^{-R(1-\nu)}\right. \\ + (1+\nu)^{1/2}e^{-R(1+\nu)}e^{-\beta} - (1-\nu)^{1/2}e^{-R(1-\nu)}e^{-\beta} \\ \left.-(1+\nu)^{1/2}e^{-R(1+\nu)}e^{-\beta(1+\nu)}\right]\end{aligned} \tag{50}$$

The terms are easily understood. In the first, an electron absorbs a quantum of energy ν to emit a phonon with energy one. The chance that the electron has enough energy, $1 - \nu$, to do this is $e^{-\beta(1-\nu)}$. In the second, the electron absorbs a quantum ν and also absorbs a phonon (they are present in number $e^{-\beta}$) so the outgoing electron momentum is $(1+\nu)^{1/2}$. The third corresponds to the electron absorbing a phonon and emitting a quantum $\hbar\nu$ to the electric field. This emission contributes negatively to the energy loss of the electric field. The fourth term results from a particularly energetic electron of energy exceeding $1+\nu$ radiating a phonon and emitting a quantum to the field.

Since the dc mobility is given by the $\operatorname{Im}\chi(\nu)/\nu$ as $\nu \to 0$ (50) gives an expression at low temperatures for the dc mobility of the Fröhlich model. Using our trial functional Φ_0, we find that

$$\mu = \left(\frac{w}{v}\right)^3(3/4\alpha\beta)e^{\beta}e^{\left(v^2-w^2\right)/w^2v} \tag{51}$$

The dependence of (51) on the coupling strength α is as α^{-1} for small α (and high β) because the "best" $w \approx v$ for small α (see I). This dependence on α is of course the same as is derived by perturbation theory. As α becomes large ($\alpha \gg 1$) the best parameters satisfy the relation $v/w \sim \alpha^2$. Therefore, the mobility μ becomes proportional to $\alpha^{-7}e^{\alpha^2}$ at high coupling strengths. The result (51) can not be compared directly with the results of previous calculations [4,5,16,17] because its temperature dependence is e^{β}/β rather than the e^{β} dependence found in the other approaches. At high β (where these previous calculations are valid), the different dependence on temperature would be experimentally unobservable. However, the origin and significance of this (incorrect) temperature dependence is interesting and will be discussed at some length in a later section.

Returning to our general expression for the $\operatorname{Im}\chi(\nu)$ (48), we see that there are other thresholds at higher frequencies coming from higher terms in the sum (48). For $\beta = \infty$ the next

threshold is at $\nu = v + 1$, the contribution above threshold being $(2\alpha/3)(v/w)^3(v - v - 1)^{3/2} \times \exp[-R(\nu - v - 1)]$. These higher thresholds correspond to exciting the electron to an excited state of energy v and emitting a phonon. The position of this excited state (at v) and the higher ones along with the selection rule that says these cannot be excited without the emission of a p-state phonon is a fiction supplied by our imitating action Φ_0.

Of course, for strong couplings, there will be such complicated excited states, with partial selection rules leading to a complex curve for $\operatorname{Im}\chi(\nu)$. For strong electron-phonon coupling, the electron is in effect bound in a potential which it makes by distorting the lattice in its neighborhood. If the lattice were held fixed in this distorted state, we would expect the electron to have various excited states in this potential. In fact, the lattice moves so that "states" are unstable, but for large α the excitation energies are of order α^2 larger than the lattice frequency so it cannot follow quickly enough.

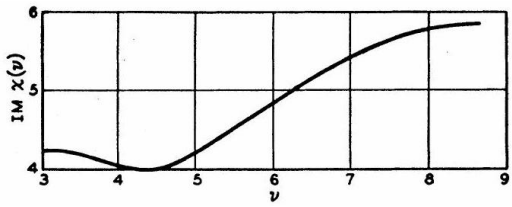

Fig. 1. Plot of $\operatorname{Im} \chi(\nu)$ for $\alpha = 3, w = 2.5, v = 3.4$ and $\beta = 100.\nu$ is plotted in units of the optical mode frequency ω and $\operatorname{Im}\chi(\nu)$ is plotted in units of (m/ω).

The $\operatorname{Im}\chi(\nu)$ should have a maximum when ν is equal to a frequency which can be absorbed in going to such an excited "state." The widths of these maxima reflect the lifetimes of these "states" for phonon emission. Naturally, we cannot expect our approximate formula (35a) to give such detailed results correctly. [18] It is reassuring, however, that our method gives such a realistic looking behavior, and strongly suggests that it represents a long step forward toward the correct $\operatorname{Im}\chi(\nu)$. In the last section we outline some ways of improving the $\operatorname{Im}\chi(\nu)$. When the coupling is not too strong ($\alpha \approx 3$), these thresholds are weak and hard to see, and the curves will have a "washed out" appearance. In Figs. 1-3 are given curves of $\operatorname{Im}\chi(\nu)$ vs ν for $\alpha = 3, \alpha = 5, \alpha = 7$ and for low temperatures ($\beta = 100$). These figures show the resonance effects very nicely. As a functon of frequency each curve consists of maxima of increasing width. As a function of α the curves show more maxima of decreasing width as α increases. All of the curves were computed numerically on an IBM 7090 computer, using an infinite power series expansion of (47a) in terms of K functions (Bessel functions of imaginary argument). The values of the parameters used were $w = 2.5, v = 3.4$ for $\alpha = 3, w = 2.1, v = 4.0$ for $\alpha = 5$, and $w = 1.6, v = 5.8$ for $\alpha = 7$.

[816] F. Low and D. Pines, Phys. Rev. 98, 414 (1955).

[17] Y. Osaka, Progr. Theoret. Phys. (Kyoto) 25, 4, 517 (1961).

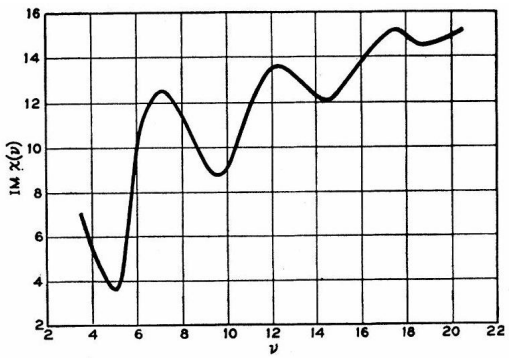

Fig. 2. Plot of $\operatorname{Im} \chi(\nu)$ for $\alpha = 5, w = 2.1, v = 4.0$, and $\beta = 100.\nu$ is plotted in units of the optical mode frequency ω and $\operatorname{Im} \chi(\nu)$ is plotted in units of (m/ω).

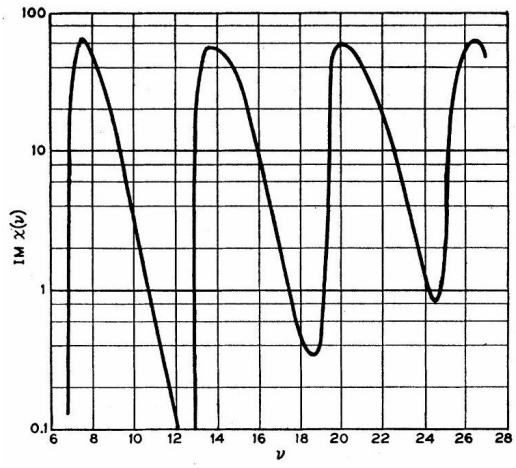

Fig. 3. Plot of $\operatorname{Im} \chi(\nu)$ for $\alpha = 7, w = 1.6, v = 5.8$, and $\beta = 100.\nu$ is plotted in units of the optical mode frequency ω and $\operatorname{Im} \chi(\nu)$ is plotted in units of (m/ω).

4. Behavior at High Temperatures

For high temperatures, β is small and (disregard for a moment the variation of w/v with temperature) $\Delta(u)$ varies like u^2/β. Therefore, only small u will be of importance in the exponent, and we can expand $\Delta(u)$ (45c) as

$$\begin{aligned}\Delta(u) = 1/\beta \Big[&\left(u^2 + \beta^2/4\right) \\ &- \left(v^2 - w^2/12\right)\left(u^2 + \beta^2/4\right)^2 + \cdots \Big] .\end{aligned} \tag{52}$$

The leading term is, therefore, that of perturbation theory, and our formula is insensitive to the trial functional Φ_0. Actually this is even more accurate than it appears, because as T rises the parameters v and w change in just such a way that $v^2 - w^2$ falls making the approximation (52) still better. [10,10a]

At very high temperatures the perturbation theory works because the electron has on the average, an energy high compared to the lattice frequency. In this case the effective polarization should fall to zero in the limit of infinite temperature. We, therefore, expect that the accuracy of our formula will increase as the temperature rises.

[818] Pekar, in the strong-coupling limit, using Gaussian trial wave functions for the electron, finds an excited state at precisely v.

11.3.6 VI. Weak-Coupling Limit, Boltzmann Equation

In the limit of weak coupling (C_{K} small or α small) the "best" model parameters are $v \approx w$ or $C \approx 0$. That is, the model of (15) becomes the bare free electron. Perturbation theory is also simply the expansion (16) but with Φ_0 just the free-electron influence functional [i.e., $D(u) = -iu + u^2/\beta$]. Therefore, our series $G_0 + G_1 + \cdots$ for the admittance agrees with perturbation theory in the weak-coupling limit.

One would expect then, that in the limit of weak coupling the mobility in constant fields obtained here
would be exactly that obtained from the Boltzmann equation using perturbation theory for the electronphonon scattering cross sections. This turns out to be not true; the question being whether the limit $\nu \to 0$ is taken before or after the limit of weak coupling $|C_{\mathbf{K}}|^2 \to 0$ is taken. A detailed comparison of our result to that of the Boltzmann equation for weak coupling is instructive.

The Boltzmann equation for a particle with momentum distribution $f(\mathbf{P})$ in an electric field $\mathbf{E}(t)$ in the x direction is

$$\partial f/\partial t + E\partial f/\partial P_x = -\int \left[\gamma\left(\mathbf{P} \to \mathbf{P}'\right) f(\mathbf{P}) - \gamma\left(\mathbf{P}' \to \mathbf{P}\right) f\left(\mathbf{P}'\right)\right] d^3P'/(2\pi)^3 \tag{53}$$

In (53), $\gamma\left(\mathbf{P} \to \mathbf{P}'\right)$ is the probability per second that an electron of momentum $\mathbf{P}$ is scattered to momentum $\mathbf{P}'$ by collisions with the phonon gas. This rate, using the usual perturbation theory, is

$$\gamma\left(\mathbf{P} \to \mathbf{P}'\right) = 2\pi \mid C_{\mathrm{K}}|^2 \left[\left(1 - e^{-\beta\omega_{\mathrm{K}}}\right)^{-1} \delta\left(\frac{1}{2}P'^2 - \frac{1}{2}P^2 + \omega_{\mathrm{K}}\right) + \left(e^{\beta\omega_{\mathrm{K}}} - 1\right)^{-1} \delta\left(\frac{1}{2}P'^2 - \frac{1}{2}P^2 - \omega_{\mathrm{K}}\right)\right]. \tag{54}$$

The first term in (54) is just the probability to emit a phonon of momentum $\mathbf{K} = \mathbf{P}' - \mathbf{P}$. The second term is the probability to absorb a phonon of momentum $\mathbf{K}$.

The Maxwell distribution, $f_0(P) = (2\pi/\beta)^{-3/2} e^{-\beta P^2/2}$, is a solution of (54) with no electric field since

$$\gamma\left(\mathbf{P} \to \mathbf{P}'\right) f_0(P) = \gamma\left(\mathbf{P}' \to \mathbf{P}\right) f_0\left(P'\right). \tag{55}$$

If E is a very weak, spatially uniform field varying as $E = E_0 e^{i\nu t}$, the deviation of f from equilibrium can be written as $f = f_0\left[1 + E_0 e^{i\nu t} P_x h(\mathbf{P})\right]$, where $h(\mathbf{P})$ is a function of P^2 satisfying [using (54)]

$$(i\nu h + \beta) P_x = -\int \gamma\left(\mathbf{P} \to \mathbf{P}'\right) \times \left[P_x h(\mathbf{P}) - P'_x h\left(\mathbf{P}'\right)\right] d^3P'/(2\pi)^3 \tag{56}$$

The current j is $-E_0 e^{i\nu t} \int {P_x}^2 h(\mathbf{P}) f_0(P) d^2P$, so the impedance is given by $1/z(\nu) = -\int {P_x}^2 h(\mathbf{P}) f_0(P) d^3P$. Multiplying (56) by $P_x h(\mathbf{P}) f_0(P)$ and integrating over all $\mathbf{P}$, we find another expression for the impedance:

$$z(\nu) = \frac{\frac{1}{2}\iint f_0(P)\gamma\left(\mathbf{P}\to\mathbf{P}'\right)\left[P_x h(\mathbf{P}) - P_x{}' h\left(\mathbf{P}'\right)\right]^2 d^3P' d^3P + i\nu\int P_x{}^2 h^2(\mathbf{P}) f_0(P) d^3P (2\pi)^3}{(2\pi)^3\beta\left[\int P_x{}^2 h(\mathbf{P}) f_0(P) d^3P\right]^2} \tag{57}$$

The integral equation is quite difficult to solve in general. We will content ourselves with an approximate analysis. The expression (57) has been written so that it is stationary [19] for variation of h about the true solution (56). That is, errors in h will appear only in second order in $z(\nu)$.

The simplest approximate solution to (56) is that $h(\mathbf{P})$ is a constant. Then (57) gives

$$z(\nu) - i\nu = \Gamma \tag{58}$$

where

$$\Gamma = \frac{\beta}{2}\iint f_0(P)\gamma(\mathbf{P}\to\mathbf{P}') \times \left(P_x - P_x'\right)^2 d^3P d^3P'/(2\pi)^3 \tag{59}$$

This represents a frequency-independent pure resistance Γ. Thus, $i\nu\Gamma$ should be compared to the $\chi(\nu)$ of (35a). To do so we substitute (54) into (59). One sees that the first term in brackets in (54) gives the same contribution as the second, so calling $\mathbf{P}' = \mathbf{P} \approx \mathbf{K}$ we get (replacing
$K_x{}^2$ by $K^2/3$)

$$\Gamma = \frac{\beta}{3(2\pi)^2}\iint K^2\left|C_{\mathbf{K}}\right|^2 P\left(\omega_{\mathbf{K}}\right) f_0(P) \times \delta\left[\frac{1}{2}(\mathbf{P}-\mathbf{K})^2 - \frac{1}{2}P^2 - \omega_{\mathbf{K}}\right] d^3P d^3K \tag{60}$$

Next we replace the δ function by $\delta(x) = \int_{-\infty}^{\infty} e^{iux} du/2\pi$. The $\mathbf{P}$ integral is then readily evaluated to give

$$\Gamma = \beta\int d^3K (2\pi)^{-3}\left|C_{\mathrm{K}}\right|^{2\frac{1}{3}} K^2 \int_{-\infty}^{\infty} du P\left(\omega_{\mathrm{K}}\right) \times \exp\left[-iu\omega_{\mathrm{K}} - \frac{1}{2}K^2\left(-iu + u^2/\beta\right)\right] \tag{61}$$

Replacement here of u by $u + i\beta/2$ shows that $\Gamma = \mu^{-1}$ from (45a) if $\Delta(u)$ takes on its free-particle value, $u^2/\beta + \beta/4$.

This result is what we expected but there are two points to be made. Firstly, we made no assumption that ν was small in solving the Boltzmann equation. Why then do we not find that $\Gamma = \operatorname{Im}\chi(\nu)/\nu$ as a function of frequency instead of a constant, the limit as $\nu \to 0$ of $\operatorname{Im}\chi(\nu)/\nu$? The answer does not lie in trying to solve (56) more exactly, for if we take a high-frequency case so
that the collision term in (56) is negligible compared to the $i\nu$ term, in first approximation $h = (\beta/i\nu)$ and is indeed constant as we assumed. That is, (58) is a closer approximation to

[8][19] If $\nu = 0$ (57) is a minimum, giving the useful variational principle for μ^{-1} discussed by Wilson [A. Wilson, Theory of Metals (Cambridge University Press, New York, 1959), p. 300].

the prediction of (56) the higher the value of ν relative to Γ. The answer is that the original formulation of the Boltzmann equation is faulty at high frequencies. It is assumed that the collisions are made and that between collisions the particle drifts in the electric field. But at higher frequencies new processes are possible in which, for example, the electron absorbs a quantum $\hbar\nu$ from the field and radiates a phonon. In the quantum theory for higher ν this cannot be analyzed as the succession of two independent events. Therefore, at the higher frequencies we may use our formulas (35). If the results deviate from that of the Boltzmann equation we must conclude the latter is inaccurate.

The second point to discuss is this. We did not solve the Boltzmann equation exactly; presumably, therefore, Γ is not exact. Why then is our result μ^{-1} from (51) not asymptotically exact as $\alpha \to 0$, in spite of our argument that our formulas should be correct in perturbation theory? The reason is easy to see from (57). For finite ν, as the coupling gets weaker the collision term falls below ν and Γ is in fact exact. Thus, for any ν other than zero in the limit of infinitesimal coupling our result (45) is exact. However, for $\nu = 0$, to get the exact answer no matter how small the coupling, the full Boltzmann equation must be solved and our result for μ, (45), is only an approximation. [Mathematically, the lack of uniform convergence arises when we invert G and expand, because the resistive part of $\chi(\nu)$ exceeds the leading (reactive) term ν^2 no matter how small the coupling is if $\nu = 0$.]

Although not exact, our result (45) for μ^{-1} is still a good approximation to the solution of the Boltzmann equation. The value of μ^{-1} obtained for Fröhlich's model at low temperature from (51) varies as $\beta^{-1}e^{-\beta}$, while from the Boltzmann equation we know that it should vary as a constant times $e^{-\beta}$.[5] But because of the rapid variation of the exponent these two are hard to distinguish (for example, the temperature at which the mobility reaches a given value is imperceptibly different in the two cases). At higher temperatures our results for μ^{-1} (46) no longer behaves as $e^{-\beta}/\beta$. In this case the values obtained from (46) and the Boltzamnn equation would come closer together. (At extremely low temperatures Fröhlich's model, of course, fails. Although acoustic phonons are not very effective, they cannot be disregarded for there are virtually no optical phonons excited.) As a test of our approximate solution of the Boltzmann equation we have also analyzed a system interacting at high temperature with acoustic phonons with $|C_{\mathrm{K}}|^2$ proportional to $K^2, \omega_{\mathrm{K}} = Kv_0$, and $\beta^{-1} > m{v_0}^2$. Such a coupling leads to a relaxation time for the electrons which varies inversely with their velocity. In this case μ is proportional to β in either theory, but Eq. (46) gives a result $32/9\pi$ or 13% higher than the more accurate solution of (56) given by (59).

11.3.7 VII. Suggestions for Improving Accuracy

The entire dependence of our result (35) for the polaron impedance on the imitating quadratic influence functional Φ_0 is contained in $D(u)$ which is expressed in terms of the model's response function, $Y_0(\nu)$. If in the expansion we used a more elaborate (but still quadratic) Φ_0, then all results would be the same but with a $D(u)$ coming from a different $Y_0(\nu)$ in (35). What is the best $Y_0(\nu)$ to take? We note that $Y_0(\nu)$ was also the first approximation to the desired function $Y(\nu) = [i\nu z(\nu)]^{-1}$. A natural suggestion, therefore, is that the best $Y_0(\nu)$ is the "true admittance function of the real polaron". Since the true $V(\nu)$ is unknown, perhaps the next best alternative would be to use a $Y_0(\nu)$ in (35) such that the $z(\nu)$ itself equals $[i\nu Y_0(\nu)]^{-1}$; that is to use a $Y_0(\nu)$ which satisfies (35) self-consistently.

To find a self-consistent $Y_0(\nu)$ is not, in general, easy. However, one might use the results calculated here, for example, and re-insert them as a new $Y_0(\nu)$ in (35) and recalculate $z(\nu)$ to find a second iteration, which might provide an even better impedance with which to recalculate again if necessary. Aside from the great amount of work involved and questions of convergence of the procedure, we cannot even be sure if a substantial improvement would result; however,

the following observations do suggest that a self-consistent solution of (35) could result in a considerable increase in accuracy.

In the variational principle of I , one can try a trial action functional S_0 which is more general than the two parameters one employed there and which describes an electron coupled to a general linear system,

$$S_0 = \frac{1}{2}\int\left(\frac{d\mathbf{X}(t)}{dt}\right)^2 dt + \frac{1}{2}\int h(t-s)x(t)x(s)dtds \tag{62}$$

Then, putting $h(t) = \int \mathbf{h}(\nu)e^{i\nu t}d\nu/2\pi$, one finds that the function $\mathbf{h}(\nu)$ which gives the lowest energy in the variational principal at zero temperature, satisfies the integral equation

$$\mathbf{h}(\mu) = \frac{2}{3(2\pi)^3}\iint K^2\left|C_{\mathrm{K}}\right|^2 d^3K(1-\cos\mu\tau) \times e^{-\omega\mathrm{K}^\tau}e^{-\frac{1}{2}K^2\varphi(\tau)}d\tau \tag{63}$$

where

$$\varphi(\tau) = \int^\infty 2(1-\cos\mu\tau)\frac{1}{-\mu^2+\mathbf{h}(\mu)}\frac{d\mu}{(2\pi)} \tag{64}$$

The Eqs. (35) treated as a self-consistent set with $D(u)$ generated from $Y(\nu) = [\nu^2+\chi(\nu)]^{-1}$ can be transformed for $\beta = 0$ at least, to exactly this same pair of Eqs. (63) and (64). In this case $\chi(-i\mu)$ replaces $\mathbf{h}(\mu)$. We therefore, can conclude (for $\beta = 0$) that if one tries as a trial action functional that for an electron coupled to a general linear system, no such system will produce a better result than one which has an impedance which is
the self-consistent solution of (35). [20] (Possibly the same is true for arbitrary β, but we have not checked this point.) These considerations substantiate further the interpretation of the expansion (38) in terms of an impedance rather than an admittance.

The above point, and the existence of a minimum principle for the Boltzmann equation, suggest that some minimum principle exists for the mobility $\chi(-i\mu)$ in quantum mechanics at arbitrary β.

Another way to improve accuracy is to try to include the next term $(\Phi-\Phi_0)^2$ in the expansion. The integrals to be performed still are of the form required for the evaluation of the ($\Phi-\Phi_0$) term but with more complicated driving forces E and E'. Although the calculation would proceed straightforwardly it would, in general, be very laborious. However, for certain values of ν and β, one could do what amounts to the same thing in a somewhat easier way, For example, for $\beta^{-1} < \nu < 1$ the various terms in (50) could be improved by calculating the appropriate cross sections more accurately. The cross section to absorb a quantum from the electric field and emit a single phonon requires matrix elements of quantities like $x_t \exp(i\mathbf{K}\cdot\mathbf{X}_s)$. Equation (50) corresponds to calculating these with the propagator $\exp(i\Phi_0)$, but an improvement can be made by calculating them with the propagator

$$[1+i(\Phi-\Phi_0)]\exp(i\Phi_0)$$

For zero frequency the Boltzmann equation can be used with the rates $\gamma(\mathbf{P}'\to\mathbf{P})$ calculated with the propagator $\exp(i\Phi_0)$; further improvement would again result by adding a correction for the difference of Φ and Φ_0.

11.3.8 Appendix A

In this appendix we discuss a fundamental path integral (or trace) such as (7) for a single one-dimensional oscillator, in terms of which all other path integrals can be immediately evaluated.

The oscillator Hamiltonian $H = p^2/2 + \omega^2 q^2/2$. Let

$$U = \exp\left\{-i\int_{-\infty}^{+\infty}\left[H_t + \gamma(t)q_t\right]dt\right\}$$
$$U' = \exp\left\{i\int_{-\infty}^{+\infty}\left[H'_t + \gamma'(t)q'_t\right]dt\right\}$$

and $\rho_a = e^{-\beta H}/Q$. The $\mathrm{Tr}\,(U\rho_a U'^{-1}) \equiv g$ may be done in several ways, for example by writing it in terms of path

integrals and performing the resulting Gaussian integrals. [12] As an alternative method we choose to represent the trace in free oscillator eigenfunctions. In this representation $(\rho_a)_{n,n} = e^{-n\beta\omega}\left(1 - e^{-\beta\omega}\right)$ and

$$g \equiv \sum_{m,n} G_{m,n} G_{m,n}{}^{*\prime} e^{-\beta\omega n}\left(1 - e^{-\beta\omega}\right), \tag{A1}$$

where $G_{m,n}$ is given in reference (9), Eq. (38) and $G_{m,n}{}'$ is the same expression with γ' replaced by γ.

By expanding

$$\exp\left[(x + i\xi)\,(y + i\xi^*)\right] = \sum_t (x + i\xi)^t\,(y + i\xi^*)^t\,/t!$$

in powers of x and y, one can show that $G_{m,n}$ may also be written as

$$G_{m,n} = G_{0,0}(m!n!)^{-1/2} e^{\xi\xi^*} \sum_t \frac{t!(i\xi)^{t-m}\,(i\xi^*)^{t-n}}{(t-m)!(t-n)!} \tag{A2}$$

where

$$\xi = i(2\omega)^{-1/2}\int_{-\infty}^{+\infty} e^{i\omega t}\gamma(t)dt \tag{A3}$$

The summation over m and n in our expression for g can be done by the binomial theorem if one uses this expression for $G_{m,n}$; but the one in reference (4), Eq. (38), for $G_{m,n}{}'$, calling $t = r + v$, where r is the free index in $G_{m,n}{}'$, permits summing first over r then over v. The final result is

$$\begin{aligned} g &= G_{00}G_{00}{}' e^{\xi\xi^*} \\ &\quad \times \exp\left[\left(1 - e^{-\beta\omega}\right)^{-1}(i\xi - i\xi')\left(i\xi^* - i\xi'^* e^{-\beta\omega}\right)\right] \end{aligned} \tag{A4}$$

Substituting in for G_{00} and $G_{00}{}'$, we find that

$$\begin{aligned} g = \exp\Bigg(\frac{1}{2}i\int_{-\infty}^{+\infty}\int_{-\infty}^{+\infty}&\left[\gamma(t) - \gamma'(t)\right]\left\{\left[\gamma(s) + \gamma'(s)\right]\right. \\ &\left.\times y(\omega, t-s) + i\left[\gamma(s) - \gamma'(s)\right]a(\omega, t-s)\right\}dtds\Bigg) \end{aligned} \tag{A5}$$

[820] One probably cannot get $\chi(\nu)$ from (63) and (64) by iteration for one finds $\chi(-i\mu)$ only approximately this way and one cannot pass to an accurate value on the real line from an imperfect knowledge on the negative imaginary axis alone.

where

$$\begin{aligned} y(\omega, t-s) &= (1/\omega)\sin\omega(t-s), & t > s \\ &= 0, & t < s \end{aligned} \tag{A6}$$

and

$$a(\omega, t-s) = (1/2\omega)\cos\omega(t-s)[1+2P(\beta\omega)] \tag{A7}$$

If $\gamma(\nu), \gamma'(\nu), y(\nu), a(\nu)$ are the Fourier transforms of $\gamma(t), \gamma'(t)$, etc., so that, for example,

$$\gamma(t) = \int \gamma(\nu) e^{i\nu t} d\nu/2\pi \tag{A8}$$

then the expression for g can be written in Fourier space as

$$\begin{aligned} g = \exp\Big(\tfrac{i}{4\pi}\textstyle\int_{-\infty}^{+\infty}[\gamma(-\nu)-\gamma'(-\nu)]\,\{[\gamma(\nu)+\gamma'(\nu)] \\ \times y(\omega,\nu) + i\,[\gamma(\nu)-\gamma'(\nu)]\,a(\omega,\nu)\}\,d\nu\Big) \end{aligned} \tag{A9}$$

Here, [11]

$$y(\omega,\nu) = 1/(\nu - i\varepsilon)^2 - \omega^2 \tag{A10}$$

and
$a(\omega,\nu) = (\pi/2\omega)[1+2P(\beta\omega)][\delta(\nu+\omega)+\delta(\nu-\omega)]$.

For the case of the Hamiltonian (11), we can represent the particle motion by a path integral on $\mathbf{X}(t)$. Then we have in fact a large number of independent oscillators, each coupled to the particle. The $\mathbf{K}$ mode of frequency ω_{K} is coupled by a $\gamma(t) = C_{\mathrm{K}}\exp[i\mathbf{K}\cdot\mathbf{X}(t)]$. Each of these modes contributes a factor like (A9) to g so that the final exponent is a sum of contributions from each oscillator mode.

We shall need the functions (A10), (A11) and superpositions of them (sums for various frequencies) which we call $Y(\nu), A(\nu)$. We shall also need another function $D(u)$ defined as

$$D(u) = \pi^{-1}\int_{-\infty}^{+\infty}\{\sin(\nu u)Y(\nu) + [1-\cos(\nu u)]A(\nu)\}d\nu \tag{A12}$$

and $\Delta(u)$ defined as $D(u+i\beta/2)$. All these functions are related to $Y(\nu)$, in fact to its imaginary part $\operatorname{Im} Y(\nu)$. We need it only for $\nu > 0$, since $\operatorname{Im} Y(-\nu) = -\operatorname{Im} Y(\nu)$. For a single oscillator, from (A5) as we have $\operatorname{Im} y(\nu) = -(\pi/2\omega)[\delta(\nu-\omega)-\delta(\nu+\omega)]$. But $a(\nu)$ can also be written as

$$\frac{\pi}{2\omega}\left(\frac{e^{\beta\nu}+1}{e^{\beta\nu}-1}\delta(\nu-\omega) + \frac{e^{-\beta\nu}+1}{e^{-\beta\nu}-1}\delta(\nu+\omega)\right)$$

hence, $a(\nu) = -\coth(\beta\nu/2)\operatorname{Im} y(\nu)$. Further, since the poles of a general $Y(\nu)$ lie above the real axis, the real part of $Y(\nu)$ can be obtained from the imaginary part. Proceeding in this way, we find the following expressions for all the functions in terms of $\operatorname{Im} Y(\nu)$:

$$Y(\nu) = \frac{2}{\pi}\int_0^\infty \frac{\operatorname{Im} Y(\mu)\mu d\mu}{(\nu - i\varepsilon)^2 - \mu^2} \tag{A13}$$

$$\mathrm{A}(\nu) = -\left(\frac{e^{\beta\nu}-1}{e^{\beta\nu}+1}\right)\operatorname{Im} Y(\nu) \tag{A41}$$

$$D(u) = -\frac{2}{\pi}\int_0^\infty\left(1 - e^{i\nu u} + \frac{2(1-\cos\nu u)}{e^{\beta\nu}-1}\right)\operatorname{Im} Y(\nu)d\nu \tag{A15}$$

and
$\Delta(u) = -\frac{2}{\pi}\int \frac{[\cosh(\beta\nu/2)-\cos(\nu u)]}{\sinh(\beta\nu/2)} \operatorname{Im} Y(\nu) d\nu$.

Although derived for a single oscillator, these relations are linear and hold for any superposition of oscillators.

11.3.9 Appendix B

We give here the details of the calculation of the first order correction to G_1. As explained in the text, we can calculate an expression like (28) by substituting (30) and (31) into (20). If we write

$$g^0 = \exp\left[\frac{i}{\pi}\int \eta e^{i\nu\tau}\left(\epsilon e^{-i\nu\sigma}Y_0 + i\eta A_0 e^{-i\nu\tau}\right) d\nu\right]$$

for the expression (20) calculated for $K = 0$, the result (20) with K included as in (30) and (31) is

$$\begin{aligned} &R(K,t,s) \\ &= g^0 \exp\left\{\frac{iK^2}{4\pi}\int \left|e^{i\nu t} - e^{i\nu s}\right|^2 (Y_0 + iA_0)\, d\nu \right. \\ &+ \frac{iK_x}{2\pi}\int \left(e^{i\nu t} - e^{i\nu s}\right)\left(\epsilon e^{-i\nu\sigma}Y_0 + i\eta A_0 e^{-i\nu r}\right) d\nu \\ &\left. + \frac{iK_x}{2\pi}\int \left(e^{-i\nu t} - e^{-i\nu s}\right)\eta e^{i\nu r}(Y_0 + iA_0)\, d\nu\right\} \end{aligned} \tag{B1}$$

We shall ultimately only need the result to the first order in $\epsilon\eta$ [see (9)], so differentiating R with respect to η and ϵ, putting $\epsilon = \eta = 0$ and calling the result $2r(K,t,s)$, we get (there is a 1/3 for averaging over directions of $\mathbf{K}$)[14]

$$\begin{aligned} r(K,t,s) = &\left\{\frac{i}{2\pi}\int Y_0 e^{iv(\tau-\sigma)} d\nu \right. \\ &- \frac{K^2}{3\,(8\pi^2)}\int \left(e^{ivt} - e^{ivs}\right) e^{-iv\sigma} Y_0 d\nu \\ &\times \int \left(e^{i\mu t} - e^{i\mu s}\right) iA_0(\mu) e^{-i\mu\tau} \\ &\left. + \left(e^{i\mu t} - e^{-i\mu s}\right) e^{i\mu\tau}\left[Y_0(\mu) + iA_0(\mu)\right] d\mu\right\} \\ &\times \exp\left[\frac{iK^2}{4\pi}\int \left|e^{ivt} - e^{ivs}\right|^2 (Y_0 + iA_0)\, d\nu\right] \end{aligned} \tag{B2}$$

The first term is $G_0(\tau - \sigma)$ times the path integral with $\epsilon = \eta = 0$. Such a term arises no matter what we integrate, so in total it gives $G_0(\tau - \sigma)\int e^{i\Phi_0}(\Phi - \Phi_0)\,\mathfrak{D}\mathbf{X}\mathfrak{D}\mathbf{X}'$. This term just cancels when we remember that we must divide ($\partial^2 g/\partial\eta\partial\epsilon$) by g evaluated at $\epsilon = \eta = 0$ for normalization. Therefore, this does not contribute to G_1, the first correction of G from G_0, and we omit it. The other terms are later to be multiplied by a function of $t - s = u$ only, and integrated on t and s. Hence, we let $t = u + s$ and integrate on all s 's to get [note $Y_0(-\nu) = Y_0{}^*(\nu)$,

$$
\begin{aligned}
&A_0(-\nu) = A_0(\nu)] \\
&r(K, t-s) = \left\{ -\frac{K^2}{12\pi^2} \int 2(1-\cos\nu u) Y_0(\nu) \right. \\
&\quad \left. [Y_0(\nu) + 2iA_0(\nu)]\, e^{i\nu(\tau-\sigma)} d\nu \right\} \\
&\quad \times \exp\left[\frac{iK^2}{2\pi} \int (1-\cos\nu u)\,(Y_0 + iA_0)\, d\nu \right]
\end{aligned} \tag{B3}
$$

This will make a contribution to $G_1(\tau-\sigma)$. It is already in the form of a Fourier transform so for the contribution to $G_1(\nu)$ we omit the integral on ν and the factor $e^{i\nu(\tau-\sigma)}$. According to (29) we must next multiply $r(K, t-s)$ by $y\,(\omega_K, u) + ia\,(\omega_K, u)$ and integrate on u. This is best done by dividing the range of u from 0 to ∞ and from $-\infty$ to 0 , and in the latter putting $u \to -u$ so that all integrals are over positive u only.

The integral in the exponent is $-K^2/2$ times

$$
\begin{aligned}
&-\frac{i}{\pi} \int (1-\cos\nu u)\,[Y_0(\nu) + iA_0(\nu)]\, d\nu \\
&\qquad = +i\,[\mathbf{Y}_0(u) + \mathbf{Y}_0(-u)] + 2\,[\mathbf{A}_0(0) - \mathbf{A}_0(u)]
\end{aligned} \tag{B4}
$$

[where $\mathbf{Y}_0(t), \mathbf{A}_0(t)$ are the inverse transforms of $Y_0(\nu),\ A_0(\nu)$]. Expression (46) is equal to $D(u)$, defined in (35c) for $u > 0$, and $D(-u)$ for $u < 0$, since $\mathbf{Y}_0(u) = 0$ for $u < 0$. Thus, this term in $r(K, t-s)$ contributes a piece

$$
\begin{aligned}
&-\frac{K^2}{3\pi} Y_0(\nu)[Y_0(\nu) + 2iA_0(\nu)] \\
&\times \int_0^\infty (1-\cos\nu u)\,[y\,(\omega_K, u) + y\,(\omega_K, -u) \\
&+2ia\,(\omega_K, u)]\, e^{-\frac{1}{2}K^2 D(u)} du
\end{aligned} \tag{B5}
$$

Adding the three other corresponding pieces from $\exp\{i\mathbf{K}\cdot[\mathbf{X}'(t) - \mathbf{X}'(s)]\}$, etc., multiplying by $|C_{\mathbf{K}}|^2$, and integrating over K [see Eq. (30)] gives the first term in (35). The second term is gotten in an analagous way from Φ_0. We need to expand our expression for $r(K, t-s)$ just to first order in K^2. The terms like $e^{-\frac{1}{2}K^2 D(u)}$ are replaced by one. The resulting expression is an integral on u, $\int_0^\infty (1 - e^{ivu})\, S_0(u) du$, where

$$
S_0(u) = \operatorname{Im} C \left(e^{iwu} + \frac{2\cos wu}{e^{\beta w} - 1} \right) = C \sin wu
$$

The integral on u gives $C\nu^2/w\,(\nu^2 - w^2)$, as in the last term of (34).

12 Old Articles that Are Used in Experiments

12.1 Optical Properties of Small Polarons in the Infrared by Reik, 1963

The mobility of small polarons is calculated as function of the temperature and the frequency. The frequency dependence is similar to the frequency dependence in the case of free electrons. For fixed frequencies the mobility increases strong ly with temperature, in contradistinction to the case of free electrons.

1. In a recent note [1] a derivation of Holstein's expression for the *d.c.* mobility of small polarons [2] from Kubo's formula [3] was given. In this note, an extension of the results for the case of finite frequencies will be presented. The optical properties under study are due to carriers in one small band in contradistinction to the recent treatment by Eagles [4] in which the effects due to interband transitions are studied.

The particular interest in the finite frequency case has been aroused by the apparent contradiction between the following two experimental results. a. Semi conducting Lanthanum-cobaltite $LaCoO_3$ shows, according to Gerthsen and Härdtl [5] a temperature dependence of the d. c. mobility which is characteristic for the hopping motion of small polarons. b. For the same substance, preliminary measurements of the reflectivity in the infrared by Kauer [6] give a frequency dependence of the real and imaginary part of the conductivity much the same as for free electrons. It will be shown, that conditions exist, under which these two experimental results can be reconciled from the theoretical point of view.
2. Kubo's expression for the a. c. conductivity is given by

$$\sigma(\omega) = \mathrm{Tr}\,\frac{1}{Z}\int_{-\infty}^{0} dn^{\rho}\int_{0}^{\beta} d\lambda \exp\left[(i\omega+\varepsilon)n^{\rho}\right] j \exp\left[-\frac{iH}{\hbar}(\vartheta - i\hbar\lambda)\right] j \exp\left[\frac{iH}{\hbar}(\vartheta - i\hbar[\lambda-\beta l)\right]$$

where Z is the partition sum, $\exp(\varepsilon\mathcal{Q})$ the adiabatic factor ($\varepsilon \to +0$) i the current density operator and H the Hamiltonian of the system.

For the l^2 - integration, a rectangular path $-\mathrm{t} \to -\mathrm{t} + \mathrm{i}\hbar(\lambda - \beta/2) \to i\hbar(\lambda-\beta/2) \to 0$ is used. Then the λ - integration can be carried out. The contributions to the conductivity

$$\sigma(\omega) = \sigma_1(\omega) + \sigma_2(\omega) + \sigma_3(\omega)$$

from the different parts of the path of integration are given by

$$\begin{aligned}
\sigma_1(\omega) =& 0\\
\sigma_2(\omega) =& \frac{\beta}{Z}\frac{\sinh \hbar\omega/\beta/2}{\hbar\omega/\beta/2}\,\mathrm{Tr}\int_{-\infty}^{0} d\zeta \exp[(i\omega+\varepsilon)\zeta]\times\\
&\times j\exp\left[-\frac{iH}{\hbar}\left(\zeta - \frac{i\hbar\beta}{2}\right)\right] j\exp\left[\frac{iH}{\hbar}\left(\zeta+\frac{i\hbar\beta}{2}\right)\right]\\
\sigma_3(\omega) =& \frac{2i}{\omega}\frac{\beta}{Z}\,\mathrm{Tr}_0^1\, d\eta \sinh^2\frac{\hbar\omega\beta\eta}{4} j\exp\left[-\frac{H\beta\eta}{2}\right] j\exp\left[\frac{H\beta(\eta-2)}{2}\right]
\end{aligned}$$

For the evaluation of the traces, the Hamiltonian for Holstein's linear chain model is used an the same simplifying assumptions for the density operator as in the previous note [1] are made. One then gets the following result for the mobility.

$$\begin{aligned}
\mu_2(\omega) =& \frac{\partial^2 e\beta}{4\hbar^2}\frac{\sinh\hbar\omega\beta/2}{\hbar\omega/\beta^{3/2}}\exp\left[-\sum_k \alpha_k \sin^2 k_{12}\coth\hbar\omega_k\beta/2\right]\times\\
&\times\int_{-\infty}^{0} d\zeta \exp\left[(i\omega+\varepsilon)\zeta + \sum_k \alpha_k \sin^2 k/2\frac{\cos\omega_k\zeta}{\sinh\hbar\omega_k\beta/2}\right] \qquad (1)\\
\mu_3(\omega) =& \frac{2i}{\omega}\frac{\partial^2 e\beta}{4\hbar^2}\exp\left[-\sum_k \alpha_k\sin^2 k/2\coth\hbar\omega_k\beta/2\right]\times\\
&\times\int_0^1 d\eta \sinh\frac{\hbar\omega\beta\eta}{4}\exp\left[\sum_k \alpha_k\sin^2 k/2\frac{\cosh\hbar\omega_k\beta(1-\eta)}{\sinh\hbar\omega_k\beta/2}\right] \qquad (2)
\end{aligned}$$

Here J is the resonance integral the sum over k extends over all wave vectors of the phonons $(-\pi \leq k < \pi)$, u_k is the frequency of an optical phonon with wave vector k and α_k is the contribution to the polaron selfenergy due to the interaction with the optical mode k divided by the energy of the phonon under consideration.
3. Equs. (1) and (2) can be greatly simplified, if the following conditions, relating the temperature, the phonon frequencies and the polaron self-energy, are met:

$$\frac{1}{n}\omega_k\beta < 4 \quad \text{for all } k \tag{3}$$

$$\frac{\sum_k \alpha_k \sin^2 k/2 \cos\frac{2\pi\omega_k}{\omega_0}}{\sum_k \sin^2 k/2} \ll 1 \tag{4}$$

$$\omega_0 = \frac{1}{2}\left[(\omega_k)_{\max} + (\omega_k)_{\min}\right]$$

Then the following results are found instead of (1) and (2)

$$\operatorname{Re}\mu_2(\omega) = \mu_2(0)\frac{\sinh\hbar\omega\beta/2}{\hbar\omega\beta/2}\exp\left[-(\omega\tau)^2\right] \tag{5}$$

$$\exists_m\mu_2(\omega) = -\mu_2(0)\frac{\sinh\hbar\omega\beta/2}{\hbar\omega\beta/2}\frac{2}{\pi^{1/2}}\omega\tau\int_0^{\hat{t}} d\tau \exp\left[-(\omega\tau)^2\left(1-\zeta^2\right)\right] \tag{6}$$

$$\exists_m\mu_3(\omega) = \mu_2(0)\frac{2}{\pi^{1/2}}\frac{1}{\omega\tau}\int_0^{\hat{t}} d\eta \sinh^2\frac{\hbar\omega\beta\eta}{4}\exp\left[\frac{1}{16}\left(\frac{\hbar\beta}{\tau}\right)^2\left(1-\eta'^2\right]\right. \tag{7}$$

$$\mu_2(0) = \frac{\pi^{1/2}}{2}\frac{\eta^2\,\mathrm{e}\,\beta\tau}{4\hbar^2}\exp\left[-\frac{\beta}{4}\sum_k \alpha_k \sin^2 k/2\hbar\omega_k\right] \tag{8}$$

$$\frac{1}{\tau^2} = 2\sum_k \alpha_k \sin^2 k/2\frac{\omega_k^2}{\sinh\hbar\omega_k\beta/2} \tag{9}$$

Under these conditions, the temperature dependence of $\mu_2(0)$ is characteristic for the hopping motion of small polarons. Furthermore, the frequency dependence of $\operatorname{Re}\mu(\omega)$ and $\operatorname{Jm}\mu(\omega)$ shows the same qualitative features as for free electrons. (See Fig. 1 and Fig. 2)

Notice that for $\omega\tau \gg 1$ the following asymptotic relation holds

$$\exists_m\mu(\omega) = -\frac{\mu_2(0)}{\pi^{1/2}\omega\tau}\int_0^1 \exp\left[\frac{1}{16}\left(\frac{\hbar\beta}{\tau}\right)^2\xi^2\right]d\xi$$

The experimental results of Gerthsen and Härdtl [5] and of Kauer [6] are therefore

FIG. 2

Frequency dependence of the imaginery part of the conductivity.
a) $h\beta/\tau = 4$; b) $h\beta/\tau = 2$; c) $h\beta/\tau = 0$; d) Drude theory for free electrons; a', b', c') asymptotes for a, b, c.

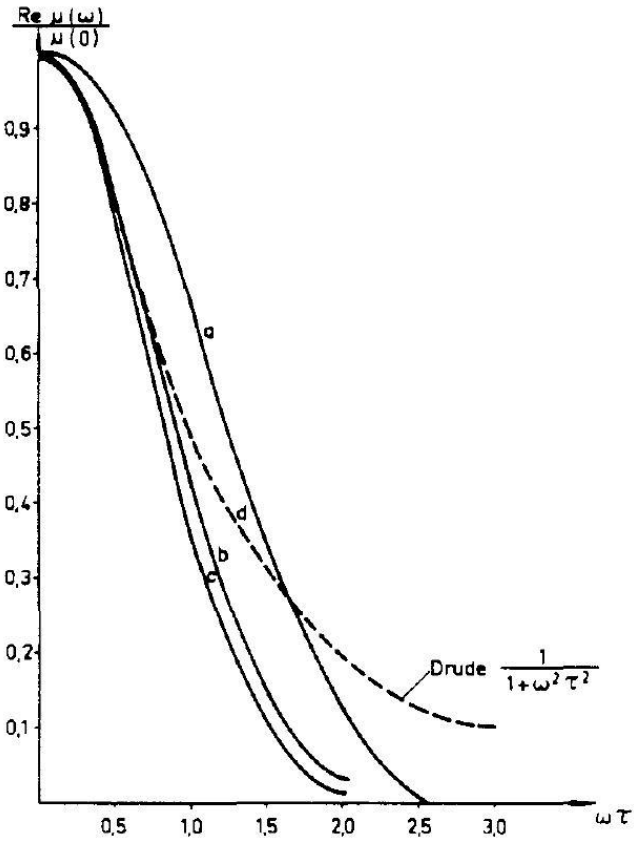

FIG. 1
Frequency dependence of the real part of the conductivity for small polarons.
a) $h\beta/\tau = 4$; b) $h\beta/\tau = 2$; c) $h\beta/\tau = 0$;
d) Drude theory for free electrons.

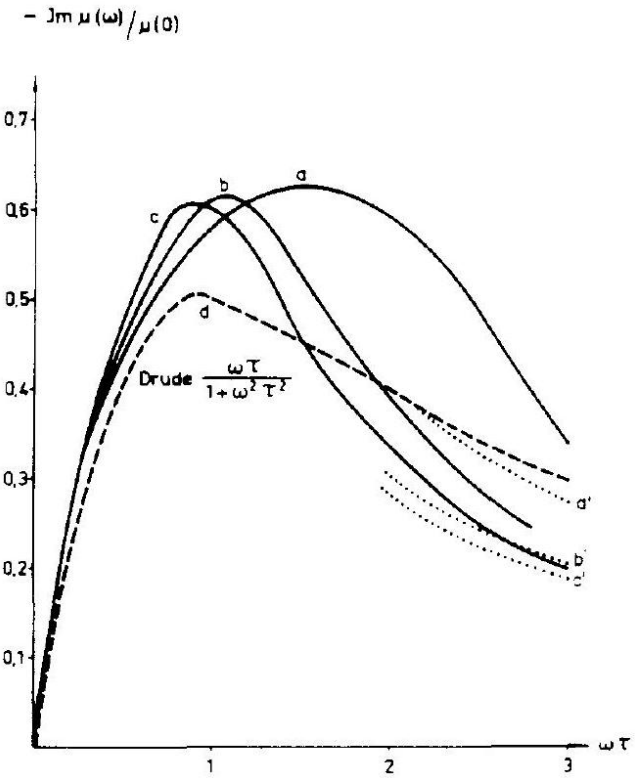

qualitatively consistent under these conditions. If condition (4) is no longer fulfilled, then

$\mathrm{Re}_2(\omega)$ and $\mathrm{Jm}_2(\omega)$ get more structured. The appearance of satellites at $\omega = 2, 3 \ldots \omega_0$ and their shape provide information concerning the dispersion of the optical phonons.

The author wishes to thank his colleagues W.J.A. Goossens, H.J.G. Meyer and D. Polder (Eindhoven) for helpful and stimulating discussions.

References

1. REIK H.G., Physics Letters 2, 236 (1963)
2. HOLSTEIN T., Ann. Physics N.Y. 8, 343 (1959)
3. KUBO R., J. Phys. Soc. Japan 12, 570 (1957)
4. EAGLES D.M., Phys. Rev. 130, 1381 (1963)
5. GERTHSEN P. and HARDTL K.H., Z. Naturforsch. 17a, 514 (1962)
6. KAUER E., private communication

Part VI
Special Effects: Useful, Selected Articles

Part VII
High Tc Polarons: Useful, Selected Articles

Part VIII
Experiments: Main Articles

13 Crystallization of polarons through charge and spin ordering transitions in 1T-TaS_2 by Bozin, Abeykoon, Conradson, Baldinozzi, Sutar, Mihailovic (2023)

(in this article it is shown that there are polarons at high temperature, and melting of polarons is discussed)

The interaction of electrons with the lattice in metals can lead to reduction of their kinetic energy to the point where they may form heavy, dressed quasi-particles-polarons. Unfortunately, polaronic lattice distortions are difficult to distinguish from more conventional charge- and spin-ordering phenomena at low temperatures. Here we present a study of local symmetry breaking of the lattice structure on the picosecond timescale in the prototype layered dichalcogenide Mott insulator 1T-TaS $_2$ using X-ray pair-distribution function measurements. We clearly identify symmetry-breaking polaronic lattice distortions at temperatures well above the ordered phases, and record the evolution of broken symmetry states from 915 K to 15 K . The data imply that charge ordering is driven by polaron crystallization into a Wigner crystal-like state, rather than Fermi surface nesting or conventional electron-phonon coupling. At intermediate temperatures the local lattice distortions are found to be consistent with a quantum spin liquid state.

Quasi-two dimensional quantum-ordered materials display very diverse and often exotic spin [1−3] and charge ordering behaviour [4], including exciton condensation [5], chiral spin liquids [6] and superconductivity [7,8]. They can also display hidden phases which can be manipulated by pressure [9,10], light [11−15], or doping [16−18]. An important aspect that determines spin ordering behaviour is the competition between Coulomb repulsion and interlayer interactions [19]. A common feature of these systems is that the strength of the electron phonon interaction (EPI) and electron density control the electron kinetic energy. Increasing the EPI leads to bandwidth narrowing, and lattice dressed electron quasiparticles - as originally introduced by Landau in 1933[20]. A further consequence of electron localization is an enhanced Coulomb interaction that leads to correlations, ubiquitous mesoscopic textures [21,22], charge-density wave (CDW) formation [23] and superconductivity at high critical temperatures in the fluctuation-dominated intermediate coupling regime of layered cuprate superconductors [24]. Recent model calculations [23] applied to wide range of transition metal dichalcogenide (TMD) materials and comparisons with scanning tunneling microsopy experiments highlighted the importance of the Coulomb interaction that lead to ubiquitous charge ordering at magic
filling fractions [23]. Specific features of the band structure may lead to further effects, such as exciton condensation [5] and CDW ordering aided by Fermi surface nesting [25] on top of the seemingly universal charge ordering [23]. Experimental evidence for polarons comes from many different techniques in a very wide variety of materials [26,27], but their role in forming quantum states, such as Wigner crystals, superconductivity and quantum spin liquids is not experimentally clear, particularly on the transition from the low to high density limit. Direct observation of symmetry-specific polaronic lattice distortions on the low- to high- density limit are crucial for progress in understanding a wide class of quantum materials.

As a prototypical example, the layered dichalcogenide 1T- TaS_2 in equilibrium is of interest as a Mott insulator [28], CDW system [4], polaronic superconductor [9] and quantum spin liquid [2]. Additional recent interest in the material comes from the discovery of hidden light- or charge

injection- induced mesoscopic metastable phases [12,29] that are important both fundamentally and for applications [30–32]. Structurally, it is a kinetically trapped 1T polymorph of TaS_2, with octahedral stacking (Fig. 1a) [4,33–35]. Its deceptively simple electronic band structure in the undistorted phase has a single Ta metal band crossing the Fermi

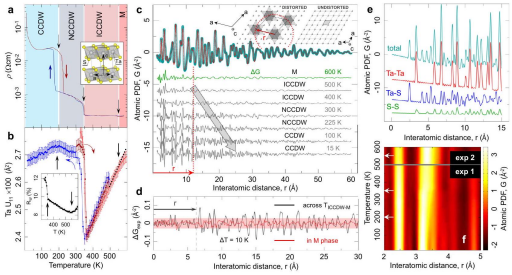

Fig. 1 | Electronic transitions & lattice symmetry breaking in 1T-TaS_2. a Temperature dependent resistivity, adopted from Sipos et al. [9], highlighting electronic phases in 1T-TaS_2. The insert shows the undistorted $P\overline{3}$ m lattice structure. **b** Temperature evolution of in-plane ADP of Ta from $P\overline{3}$ m model fit to PDF data over $20-60$Å range. Red color indicates heating, blue color indicates cooling. Sloping black dotted line is a reference. Inset: Fit residual, R_w, implicates IC-M and IC-NC transitions. c P $\overline{3}$ m model fit to 600 K data. Green difference trace (offset for clarity) reveals short range deviations. Stack of difference curves for the same model against data at different temperatures (as indicated) is shown underneath. Red arrow indicates a length-scale coarsely corresponding to the SoD polaron and the in-plane nearest neighbor inter-star center-to-center distance (inset). d Comparison of difference PDF between experimental data that are 10 K apart within metallic phase (T > 550 K) and across the IC-M transition, implicating existence of local distortions in the M phase over at least a radius r. e Calculated total PDF and partial pair-contributions in the P3 m structure. **f** False color plot of PDF intensity versus temperature over a short r-range.

level [12,34]. While nominally metallic at high temperatures, it shows an incommensurate (IC) CDW (ICCDW) along the principal crystal axes already at high temperatures (between 550 and 350 K), with an associated Kohn anomaly at a wavevector $q_{IC} \simeq (0.283, 0, 0)$ in units of the reciprocal lattice vector a_0^*[36,37] which implies a strong coupling between electrons and the lattice. Below 350 K , the IC state breaks up into a patchy periodic network of commensurate islands separated by discommensurations [38–40]. Upon further cooling, this nearly commensurate (NC) CDW (NCCDW) state becomes fully commensurate (C) CDW (CCDW) after a first order transition at $\sim$ 180 K, with the appearance of a Mott gap in the charge excitation spectrum observed by single-particle tunneling [41] and angle-resolved photoemission [25,42]. In contrast, gapless spin relaxation in the range $50-200$ K is attributed to a possible quantum spin liquid (QSL) phase, arising from the spin frustration on the triangular superlattice. While band structure calculations [3] suggest that the QSL phase may be suppressed by interlayer coupling [43], this cannot explain the marked difference of spin and charge excitation spectra [2]. A further intriguing feature is a discontinuity in the magnetic susceptibility and an anomalous peak in the spin-spin relaxation time concurrent with a crossover around $\sim$ 50 K of the spin-lattice relaxation time from a QSL-like, to a gapped T-dependence [44,45]. Near 50 K , a resistivity upturn from nearly T-independent resistivity to strongly T-dependent variable-range hopping behavior has been commonly reported, suggesting an onset of low-temperature charge localization [4,46]. The common picture of the IT- TaS_2 lattice structure in the C state assumes simple distortions from the average lattice structure (trigonal $P\overline{3}$ m, Fig. 1a), whereby 12 Ta atoms are attracted symmetrically towards the central Ta atom that carries an extra electronic charge, forming a star of David (SoD) pattern (Fig. 1c). The SoDs are arranged in a $\sqrt{\mathbf{13}} \times \sqrt{\mathbf{13}}$ unit cell superlattice structure ($P\overline{3}$ symmetry [47]). At such an electron density of 1/13,

the dimensionless ratio r_s of the Coulomb energy V to the kinetic (Fermi) energy $E_K r_s = \frac{V}{E_K} =$

$\frac{e^2 m}{\hbar^2 \sqrt{n}} \simeq 70 \sim 100$, where e is the elementary charge, n is the (2D) density, and $m \sim 3$ is the effective electron mass [25]. Considering that the Wigner crystal stability limit is $r_s = 31 \sim 38$[23,48–50], 1T- TaS_2 is comfortably in the Wigner crystal regime, which means that electronic superlattice ordering on the basis of dominant Coulomb interactions and tell-tale lattice deformations around localized carriers may be anticipated. Room temperature extended X-ray absorption fine structure (EXAFS) [51], high-resolution transmission electron microscopy (HRTEM) [52–54] and X-ray structural measurements [44] indeed suggest the existence of symmetry-breaking atomic displacements, but studies over a wide range of ordering temperatures have not yet been performed.

Here we present the first systematic measurements of the local lattice structure that covers temperatures from 15 to 915 K . The data reveal local symmetry breaking from the established $P\overline{3}$ m symmetry at all measured temperatures (Fig. 1a, inset), and unambiguous evidence for individual polarons in the dilute high-temperature limit, revising our current notions about the origin of charge and spin ordering, with clear implications for other materials of current interest.

Results

The local structure of 1 T$-TaS_2$ is investigated using X-ray pair distribution function (PDF) analysis [55,56], giving picosecond-timescale structural snapshots for 15 K $\leq$ T $\leq$ 915 K. This encompasses the known electronically ordered states below 600 K portrayed by the resistivity vs. temperature plot shown in Fig. 1a9 , as well as irreversible polytype transformations above 600 K .

The anisotropic atomic displacement parameters, U_{ij}, of Ta atoms were retrieved from a fit to the established $P\overline{3}$ m structure over a range of $20-60$Å (Fig. 1b). For T $<$ 600 K, the U_{ij}S, reveal an anomalously

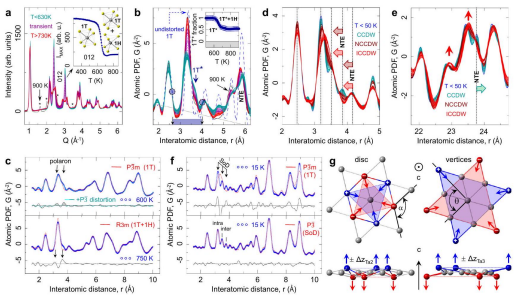

Fig. 2 | Temperature progression of atomic structure in 1T-TaS. a Stack of diffraction patterns revealing a polymporphic transformation on warming at $\sim$ 630 K. Inset: intensity collapse of the (012) $P\overline{3}$ m Bragg reflection during the restructuring from pure 1T to a hybrid 1T & 1H coordination. Further restructuring above 880 K results in additional Bragg reflections, marked by asterisk. b Corresponding PDFs over a narrow r-range. Data feature isosbestic points (circled) - nodes of temperature-invariant PDF intensity. Label 1T* indicates presence of local distortions in the 1T-type layers. Vertical blue arrow (1T*) marks polaronic distortion intensity. Inset: Change of fraction of distorted 1T* environments, relative to 600 K , estimated over the shaded region on the abscissa. c Polaron signature, seen in the M phase (top), persists in the restacked polymorph structure (bottom), and is associated with the 1T-type layers. Adding distortions, described in
g, as nanoscale inclusions results in improved fit (cyan trace). In d, e a stack of PDF data on different length scales is shown over the 15$-$500 K range, color-coded according to the electronic phase they belong to. At high temperature longer length-scale peaks sharpen (indicated by vertical arrows) due to apparent average symmetry increase, despite expected broadening due to ADP increase at elevated temperature and in contrast to the shorter length-scale behavior. Features exhibiting negative thermal expansion (NTE) are indicated by block arrows. f At 15 K clear distortions associated with the star of David (SoD) are seen in the local structure,

incompatible with the P$\overline{3}$ m symmetry (top) but explained well (bottom) by a simple P$\overline{3}$ broken symmetry model, depicted in **g** with focus on Ta atoms. Colored arrows show the Ta displacements. Out-of-plane degrees of freedom (exaggerated in the illustration for clarity) provide for puckering distortions.
large in-plane component, U_{11}, approximately a factor of 2 larger than the component along the stacking axis, U_{33} (e.g. at 500KU_{11} is 0.025Å^2 whereas U_{33} is 0.01Å^2). This is unusual for a layered system in which a larger out-of-plane component is expected to arise from interlayer disorder. At high T , in the metallic (M) phase, the large U_{11} signifies an apparent intralayer 'disorder', unaccounted for by the P$\overline{3}$ m structural model. At lower temperature, the P 3 m model is inadequate at any temperature, revealed by the difference PDFs shown in Fig. 1c. The spatial extent and character of this symmetry breaking changes across the cascade of CDW transitions, tracking complex correlations in different electronic regimes. Intriguingly, as we describe below, nanoscale symmetry breaking is also evident in the polymorphs above 630 K (Fig. 2b, c).

As an aid to understanding, pair-specific contributions to the total PDF within the P$\overline{3}$ m model are shown in Fig. 1e, where Ta-Ta pair contributions are dominant (see Methods). In the P$\overline{3}$ m structure, the undistorted Ta sublattice features a single-valued nearest-neighbor TaTa distance, seen as a sharp peak at -3.4Å, Fig. 1e. However, the data reveal a distinct additional shoulder, (e.g. Figs. 1e and 2b for 600 K), which is unexplained by the P$\overline{3}$ m model (Figs. 1c and 2c (top)). At high temperature this distortion is most likely dynamic, as expected for symmetry-specific lattice fluctuations associated with carrier localization and polaron formation. Very specific distributions of Ta$-$Ta and Ta$-$ S pairs in the 3.3$-$5.9Å range are expected for SoD polaronic distortions [47]. In the C phase with a single layer $\sqrt{\mathbf{13}} \times \sqrt{\mathbf{13}}$ supercell P$\overline{3}$
model (Methods and Supplementary Table 1) the SoD polaron structure is adequately described (Fig. 2f) [47,57]. However, for all other electronic regimes it was necessary to add P 3 m as a secondary phase to achieve good fits (see Fig. 3c, inset). The temperature dependence of the interatomic distances and bond angles, and deductions resulting from fits to the data are addressed sequentially below, starting from high temperatures, well above any known charge or spin ordered phase.

Polymorphic regime

Heating 1 T$-$$TaS_2$ above 600 K results in irreversible polymorphic transformations altering average symmetry and stacking [26,51], where nominally 50% of octahedrally coordinated 1 T layers convert into trigonal prismatically coordinated 1 H layers [35,58] (Fig. 2a inset). This is accompanied by polymorph-specific stacking of the two layer-types [4,45] and changes of the local Ta environment in the prismatic layers. Two such transformations are seen in the PDF data (Fig. 2b), at 630 and 880 K (see Supplementary Figure 1 for more details). Remarkably, a shoulder-signal ($\sim$ 3.5Å, Fig. 2b) associated with local lattice distortions (polarons) is observable for 730 K $<$ T $<$ 915 K. The distorted fraction does not vanish in the polymorphs but instead drops to half its value observed in the 1 T regime (T $<$ 630 K), with no significant reduction through the second transformation (Fig. 2b). Notably, PDF data above 730 K conform to the 6 R - TaS_2-like model (R3m symmetry) featuring equally abundant alternating 1 T and 1 H layers (Fig. 2c,

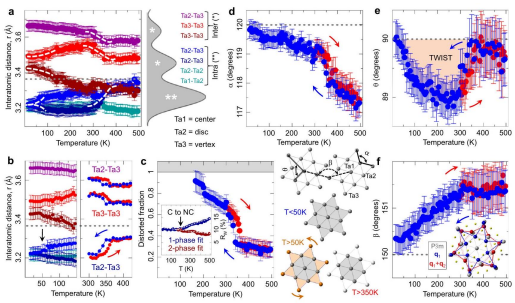

Fig. 3 | Local structure quantification from distorted local SoD model. a Local Ta-Ta distances from a P3 model fits to PDF data, obtained on cooling, over 1 nm length-scale in 15-500 K range. For reference, dashed horizontal gray line marks the undistorted P$\overline{3}$ m value at 300 K . Intra- and inter-star distances are color coded as indicated in the legend. **b** Closeup of C phase behavior (left) and hysteretic response across the IC-NC transition (right). c In NC and IC phases secondary undistorted P$\overline{3}$ m phase was necessary to reduce fit residual, R_w (inset). Distorted phase fraction, displaying thermal hysteresis consistent with one seen in resistivity, is calculated from atomic weight-based phase content obtained from the fits. $\mathbf{d}-\mathbf{f}$ show selected intra-SoD and inter-SoD bond angles, as indicated in the sketch.

In the IC phase the SoD motif is heavily distorted, with local distortions resembling discs. Upon entering the NC phase, the SoD distortion becomes better differentiated, with stars exhibit twists, and with interatomic angles beginning to evolve towards ideal values. In the C phase twists start to diminish. Below ~ 50 K a sharp regularization of stars is observed, with intra-star Ta-Ta distances becoming equal, intra-star angles approaching ideal values, and no twisting. Colored arrows in b-f indicate data collection on warming (red) and on cooling (blue) cycles. Inset to **f** : displacements of the Ta atoms for the $\mathbf{q}_1$ (blue) and $\mathbf{q}_1+\mathbf{q}_2$ (red) modes from symmetry analysis at 15 K , compared to the parent P 3 m phase (gray).
bottom) [59]. The model features undistorted 1 T and 1 H layers, but a clear distortion signal, albeit weaker, such as is seen at 600 K , persists in the fit differential, implying the existence of polaron-specific deformations in the 1T layers well above 600 K (Fig. 2c, top), with $\sim$ 10wt% distorted fraction (see below).

High-temperature metallic regime

The data at 600 K show multiple components at the position where the P3 m model predicts a single Ta-Ta peak (Fig. 1c and red trace fit in Fig. 2c, $R_w = 15\%$). The distortion spans ~ 5Å with weaker signal extending up to ~ 12Å, depicted by the difference PDFs. Such signatures, also seen in the IC phase, are weaker than in the NC and C regimes (Fig. 1c). However, their similarity and continuity imply a common origin and unambiguously reveal the presence of high temperature electron localization, detectable by charge-lattice coupling [60,61]. Despite similar P$\overline{3}$ m model misfits shown in Fig. 1c, explicit data differences, Fig. 1d, reveal subtle changes across the M-IC transition for $r > 5$Å. The electron localization results in incomplete breakup of the P$\overline{3}$ m matrix, but without the formation of the full SoD motif. The light red profile in Fig. 2d and the intensity band in Fig. 1e at ~ 3.3Å remain broad, consistent with incoherent distortions from weakly developed fluctuating charge correlations. In this diluted limit local distortions were approximated as P$\overline{3}$ nanoscale inclusions, Fig. 2 g , within the undistorted P$\overline{3}$ m matrix. This model (cyan traces in Fig. 2c (top), $R_w = 8\%$) accounts for the misfit, resulting in $\sim$ 20wt% of P$\overline{3}$ distortions involving heavily puckered hexagonal Ta discs surrounding
central tantalum. (This is consistent with $\sim$ 10wt% of locally distorted environments in the 1T-layers in the polymorphic regime above 630 K discussed in the previous section).

Incommensurate regime

The growth of charge correlations and structural coherence of associated distortions results in their signature extending over a longer length-scale (Fig. 1c). Stacks of experimental PDFs for 15-500 K (Fig. 2d, e) show that short length-scale peaks ($r < 5$Å) sharpen gradually on cooling. However, the data still do not show a clear SoD motif (Fig. 2d). The data at ~ 3.5Å are broad and unresolved, and at ~ 3.75Å are rather featureless. Conversely, peaks at higher distances show the opposite temperature trend. In the light red stack, Fig. 2 e , the signal at ~ 23.5Å is the sharpest just below the M-IC transition, portraying high symmetry, and systematically broadens with intensity reduction as temperature decreases, evidencing growth of broken-symmetry correlations. The change in slope of TeU_{11}(T) at 550 K (Fig. 1b) indicates an increased localized charge density. Model-derived Ta-Ta distances for T>350 K shown in Fig. 3a portray substantially distorted hexagonal SoD cluster cores comprised of short Ta-Ta contacts (Fig. 3d, f). The distorted fraction increases to ~ 30wt% compared to the M state (Fig. 3c). The PDF peaks which are sensitive to interlayer stacking are very broad, as shown in Fig. 4a, c, implying inhomogeneous stacking. The distribution centroids of the closest interlayer separation, Fig. 4a, are shifted to the left, well below 5.9Å, indicating local compression of layers which are, on average, closer together than they would be in the undistorted

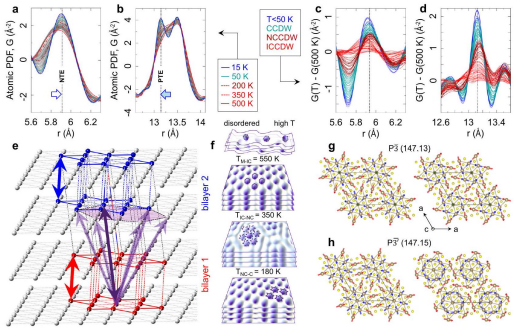

Fig. 4 | Model independent considerations of stacking correlations.
a Temperature stack of experimental PDFs around ~ 5.9Å peak containing intrabilayer correlations of SoDs, indicated in e by blue and red double arrows.
b Temperature stack of PDFs around ~ 13.1Å peak depicting inter-bilayer correlations of SoDs, indicated in e by purple double arrows. The contribution assignment is made based on features in P$\overline{3}$ m model, Fig. 1e. There, the 5.9Å feature is the c-axis lattice repeat distance involving strong signal from the nearest neighbor interlayer Ta-Ta correlations, whereas the 13.1Å feature is well isolated and dominated by the next nearest neighbor off-axis interlayer Ta -Ta correlations. In c, d temperature stacks of differential PDFs are shown for data in **a**, **b**, respectively, with differentials calculated using 500 K reference. Vertical dashed lines mark positions of apparent
maxima in the C phase. e Sketch of two bilayers highlighting correlations discussed in text. Inter-bilayer SoDs are separated by ~ 13.1Å at low temperature, a peak forming on cooling from a broad distribution at high temperature. This separation results from a SoD-shift by approximately one P$\overline{3}$ m lattice spacing in each P$\overline{3}$ m lattice direction. Note 6 possible choices of relative positioning of nearest bilayers, indicated by the purple shaded hexagon. f Schematics of distortions across different electronic phases in 1T-TaS $_2$.**g**, **h** magnetic moments consistent with the distortions of the SoDs as determined by the PDF analysis for two different settings. The arrows at the center Ta1 atom pointing along the z axis are shown in green (only in P 3 m).

1T structure. The observation of negative thermal expansion jumps along the stacking axis is relevant in this context [62] (see Supplementary Figs. 2 and 3 for discussion).

Nearly commensurate regime

Significant local structure changes occur at the IC-NC transition. The distortion fingerprint, Fig. 1c, grows dramatically and PDF intensities vividly redistribute below 5Å (Figs. 1f and 2d). The Ta-Ta peak at 3.25Å, which is broad in the IC phase, splits into an incompletely resolved triplet of unequal intensity peaks at -3.15Å, -3.3Å, and ~ 3.8Å, marking the formation of well-defined SoD clusters. The feature at -3.15Å corresponds to the Ta_{13}SoD intra-cluster configuration, whereas the other two features depict the inter-cluster correlations (Fig. 3). Residual intensity at ~ 3.4Å is associated with discommensuration regions of approximately P3 m character, separating hexagonal domains of wellordered SoD clusters within the Ta layers [63,64], well observable by STM. Multiphase modeling with coexisting P3 and P3 m phases confirms this picture (Fig. 3c inset, see Methods). As SoD clusters emerge, the distortion magnitude increases (Fig. 3a, b), consistent with increasingly resolved signal seen for 3Å $<$ r $<$ 4Å shown in Fig. 2d. Importantly, the star vertices exhibit sudden asymmetric contraction, accompanied by substantial puckering (Fig. 3d, f) and SoD twisting (Fig. 3e). The distorted $P\overline{3}$ phase becomes the dominant fraction below 350 K , at
$\sim$ 60wt% (Fig. 3c). This is consistent with the patchy nature of the discommensurate NCCDW phase. Narrow thermal hysteresis, shown in Fig. 3b-e, reflects the 1st order character of the IC-NC transition. As SoD local order is established in the NC state, they simultaneously form well defined bilayer correlations, Fig. 4a, c: The SoDs in adjacent layers couple and align along the c-axis. In contrast, inter-bilayer correlations are still fuzzy: different bilayers exhibit appreciable stacking disorder, evident from inter-bilayer sensitive peak, Fig. 4b, d, which probes off-axis correlations whose distribution is still considerably broad in the NC state.

Commensurate regime

At the NC-C transition, the PDF intensity at $\sim$ **3.4** Å diminishes, implying the gradual disappearance of the ordered domain walls, while the intra-SoD-cluster peak sharpens (Fig. 2d), consistent with increased SoD density and additional charge localization. Similar changes are observed in the far-r limit (Fig. 2e), as a homogeneous crystal structure forms in the commensurate state. Closer inspection of the data unveils an additional restructuring below $\sim$ 50 K, embodied in subtle peak shifts and sharpening observed in the dark blue traces in Figs. 2d and 4a. Modeling shows that the distribution of Ta-Ta distances depicting intra- and inter-SoD Ta-Ta contacts changes character in the C phase, with tightly bound SoDs structurally further regularizing below 50 K
(Fig. 3a, b). The intra-SoD angle θ reduces, approaching 120° at base temperature, Fig. 3e. The intra-star twist angle α increases, approaching 90° below 50 K (Fig. 3d), while the local inter-star angle β reaches 150° as SoDs align and form fully commensurate order (Fig. 3f) and the undistorted phase diminishes, consistent with vanishing domain walls (Fig. 3c). Simultaneously, well defined inter-bilayer correlations develop (Fig. 4b, d). The most dramatic changes are observed at $\sim$ 13.1Å where PDF intensity redistributes and sharpens, possibly indicating an offset of pairs of SoDs, going from one bilayer to another, by one P3m lattice spacing along both planar lattice vectors, Fig. 4e. Notably, there are 6 choices of such offsets, consistent with 13$\times$ stacking period and helical stacking arrangement suggested in some works [44]. Further qualitative changes are seen below 50 K in the PDF peak which includes the nearest neighbor intra-bilayer stacking peak just below 6 Å , whose intensity distinctly and abruptly shifts to lower distance (Fig. 4a, c). In contrast, the inter-bilayer peak at $\sim$ 13.1Å sharpens, but does not shift (Fig. 4b, d). This could imply enhanced intra-bilayer coupling, with neighboring bilayers presumably adjusting to preserve the interbilayer spacings [36].

Symmetry of the order parameter

On the basis of a symmetry analysis of the observed PDF displacements we can identify the symmetry of order parameters which transform as the A_{2u} and E_u irreducible representations in the parent P 3 m structure space group. The displacements are described by two modes with wavevectors of the form $\boldsymbol{q}_1 = (a, b, 0)$ and $\boldsymbol{q}_2 = (-b, a+b, 0)$ at 60° to $\boldsymbol{q}_1$. In the C phase, $\boldsymbol{q}_1 = \frac{3}{13}\boldsymbol{a}^* + \frac{1}{13}\boldsymbol{b}^*$, and $\boldsymbol{q}_2 = -\frac{1}{13}\boldsymbol{a}^* + \frac{4}{13}\boldsymbol{b}^*$, where $\boldsymbol{a}^*$ and $\boldsymbol{b}^*$ are the reciprocal lattice vectors of the undistorted lattice. It is possible to decompose the atomic displacements of the Ta atoms at any temperature in terms of the independent amplitudes of the A_{2u} and E_u modes described by $\boldsymbol{q}_1$ and $\boldsymbol{q}_1 + \boldsymbol{q}_2$. The displacements at 15 K are shown in the insert to Fig. 3f. In the NC phase at room temperature [44], $a_{NC} = 0.2448(2)$ and $b_{NC} = 0.0681(2)$, which is close to the C values ($a_C = 3/13$ and $b_C = 1/13$), while in the IC phase, $a_{IC} = 0.283(2)$, and b = 0, where a_{IC} is close to $2/7 = 0.2857$. Note that our PDF analysis does not reveal any information about long range order, and $\boldsymbol{q}_1$ and $\boldsymbol{q}_2$ should not be interpreted to imply its existence. Rather, they describe the symmetry of the lattice distortions associated with the twists and displacements of the Ta atoms in the distorted SoD polaron structures. (See Supplementary Fig. 4).

Discussion

The local structure data in 1 T$-$TaS$_2$ reveals symmetry-specific local structural fingerprints of polaron formation whose ordering evolves with temperature as shown schematically in Fig. 4f. Surprisingly, the polaron fingerprints are already identifiable in the polymorphic 6RTaS$_2$ regime (where individual 1T-monolayers appear between 1H layers), in the metallic phase (> 600 K), then successively through the IC, NC and C ordering transitions, and eventually in the non-QSL-like regime below 50 K , where-remarkably-SoD symmetry is restored in a layer-dimerized undistorted in-plane SoD structure. An important fundamental question arises in the context of conventional CDW viewpoint regarding the lattice distortions in the high-temperature M phase: Should the deformations be discussed in terms of a uniform reduced modulation amplitude in the IC-like phase, or in terms of dynamical polaron fluctuations? Fig. 1d indicates the range of the structural correlations. The black trace shows a difference across the IC-M transition, while the red trace is a difference corresponding to two PDFs in the same (M) phase separated by the same ΔT. This comparison shows that dominant changes across IC-M occur at $r > 5$Å, with smaller changes for $r < 5$Å (Supplementary Fig. 5). This implies that at the M to IC transition both the number of distorted sites and the extent of IC spatial correlations grow. The M phase thus looks like a sparse polaron gas, whereas the IC phase is a sparse polaron crystal (incommensurate with the lattice). We can now consider the three possible scenarios for the IC melting transition based on the PDF data: In the first one, in the M phase, the long-range IC-CDW becomes dynamic, with amplitude and phase fluctuations on a timescale faster than the lattice can respond. In the second scenario, all relevant charges become fully itinerant on all length scales in the M phase without lattice distortions. In the third, polaronic, scenario the IC-CDW breaks up in the M regime but the lattice follows the localized charge fluctuations, which is equivalent to thermally activated polaron hopping. In all three scenarios, we would see a disappearance of the reflections at the IC modulation wave vector on going from IC to M in Bragg reflections, with the third scenario leaving some diffuse scattering in the M phase. In the PDF data, the first and second scenario would result in no characteristic polaronic distortions in the M phase. The fact that we do see them implies that only the polaron fluctuation scenario is relevant in 1 T $-$ TaS$_2$. The persistence of polarons in the polymorphic regime (Fig. 2b, c) and the change from 20wt% to 10wt% on the transition from a uniform 1T to the 6R multilayer structure confirms this notion and implies that polarons exist only in individual 1T monolayers. These may be expected to appear also in free-standing monolayers or monolayers on substrates, provided that strain and interaction with the substrate

do not interfere.

Magnetic ordering

It is interesting to consider the symmetry of the magnetic polaron structures that are compatible with the two possible in-plane magnetic space groups P3 (#147.13) and P3' (147.15). Two (ferro)magnetic P3m subgroups can be derived from the analysis of the symmetric irreducible representation at the Γ point of the trigonal Brillouin zone of the 1 T stack. For $P\overline{3}$ m, inversion does not flip the magnetic moment, allowing a magnetic moment component along c for Ta1 and no constraints for the magnetic moments of the Ta 2 and Ta 3 atoms. In contrast, for the P″m magnetic space group, inversion reverses time and thus flips the magnetic moment, the magnetic moments of the Ta atoms of the same kind are not flipped by the symmetry operators. By choosing different components for Ta 2 and Ta 3 magnetic moments it is possible to create different motifs maintaining the same symmetry. Figure 4 g , h show the motifs compatible with the symmetry operations of the two magnetic groups for in-plane chiral and non-chiral arrangements of magnetic moments respectively. An in-plane QSLlike state is consistent with fluctuating in-plane moments, and c-axis antiparallel moments in the $P\overline{3}'$ magnetic group, consistent with dimerized stacking of CDW orders in the C state.

A remarkable feature of the data is that local in-plane mirror symmetries appear to be restored below 50 K , with $\alpha \simeq 120°$ and $\beta \simeq 150°$. The data below 50 K are strongly suggestive of dimerization along the c axis, consistent with inter-plane spin singlet formation and spin gap formation, that could explain the apparent cross-over from a $\sim T^2$ QSL-like spin relaxation above 50 K to a gapped, exponential T dependence below this temperature [2]. A plausible origin of the apparent symmetry restoration at low temperature comes from the disappearance of domain walls at low temperature. In-plane domain walls have been observed to persist well below the NC-C transition temperature, which topologically prevent interlayer stacking and spin dimerization. As long as domain walls exist, un-dimerized layers support an intra-layer QSL composed of spin structures shown in Fig. 4g, h, while regions with dimerized lattice layers are expected to exhibit inter-layer spin pairing [3]. The restoration of SoD symmetry at lowest temperatures may thus be considered to be associated with the disappearance of DWs. A slightly different situation occurs in the metastable 'hidden' domain state [65], where a QSL is allowed to form within domains whenever inter-layer stacking is indirect.

The polaron crystallization paradigm [66] emerging on the basis of these data has the benefit of providing a common framework for the understanding the polaronic physics in both the equilibrium and metastable phases of 1 T $-$ TaS_2 and numerous related materials that display similar charge and spin ordering [23]. The local structure symmetry analysis is particularly relevant for revealing the origin of the still poorly understood spin polaron structure and reconciles the observation of QSL-like behavior with theoretical band structure modelling, which commonly suggests a spin-paired dimerized ground state in a perfect crystal [3]. Finally, we note that it was shown theoretically that Wigner-crystal ordering is not limited to systems with a half-filled electronic band, but may be also present at other fillings [21,67], which suggest that the crystallization phenomenon reported here may be more general than previously thought.

Methods

Crystal growth and analysis

The 1 T $-$ TaS_2 samples were grown using iodine vapor transport reaction, grown at 850°C, and quenched to room temperature from the growth temperature. Single crystal XRD shows a pure single 1T phase is retained after the quench, with Ta:S composition determined by EDS to be $33 : 66 \pm 1at\%$.

Synchrotron X-ray atomic pair distribution function (PDF) measurements

Temperature dependent X-ray total scattering data were collected at 28-ID-1 beamline of the National Synchrotron Light Source II (NSLS II) at Brookhaven National Laboratory. Finely ground powders of 1 T$-TaS_2$ were sealed in 1 mm (outer diameter) polyimide capillary (referred to as experiment 1 or exp 1) and 1.5 mm (outer diameter) quartz capillary (experiment 2 or exp 2) within a glovebox under light vacuum. Measurements were carried out in capillary transmission geometry using a 2D PerkinElmer amorphous silicon area detector (2048×2048 pixels with 200μ m^2 pixel size) placed ~ 204 mm downstream of the sample. The setup utilized a monochromatic X-ray beam with 74.5 keV energy ($\lambda = 0.1665$Å). Sample temperature control was achieved using a Cryo Industries of America cryostat (exp 1, 15 K $\leq$ T $\leq$ 500 K) and a FMB Oxford Hot Air Blower model GSB1300 (exp 2, 300 K $\leq$ T $\leq$ 915 K). Data for each experiment were collected in 5 K steps using 5 K/min temperature ramp, 2 min thermalization, and 2 minutes data collection at each temperature. In exp1 data in temperature range 15 K $\leq$ T $\leq$ 300 K were collected on cooling, while these in temperature range 300 K $\leq$ T $\leq$ 500 K were collected on warming and cooling. In exp 2 data were collected on warming.

PDF data processing and analysis

Calibrations of the experimental geometry, momentum transfer range, and detector orientation were carried out by utilizing nickel standard measurements performed under the same conditions. Appropriate masking of the beam-stop shadow, inactive and outlier pixels, and subsequent azimuthal integration of the 2D images to obtain 1D diffraction patterns of intensity versus Q data were done using pyFAI software package [68,69] Standardized corrections to the data for experimental effects to obtain the reduced total scattering structure function, F(Q), and the subsequent sine Fourier transforms to obtain experimental PDFs, $G(r)$, with $Q_{\max} = 25$Å^{-1}(exp 1) and $Q_{\max} = 20$Å^{-1} (exp 2) were carried out using the PDFgetX3 program within the xPDFsuite software package [70] The PDF analysis was carried out using the PDFgui [71] modeling platform. The PDF, derived from powder diffraction-based Bragg and diffuse scattering data collected over a broad range of momentum transfer, describes direction-averaged distribution of atom pairs in a material as a function of interatomic distance, r, and provides structural information across different length scales. Uncertainties in reported model-derived parameters were estimated from their maximum variations observed by changing either the r-range of modelling (Figs. 1b, 3a-f) or integration (Fig. 2b, inset) by 10%. A double of the maximal values of such uncertainties was adopted as the error bars shown. Due to large X-ray scattering contrast (Z(Ta) = 73, Z(S) = 16) the dominant contribution to total PDF (Fig. 1e) originates from Ta-Ta pairs (red trace), followed by the Ta-S pairs' contribution (blue trace). The S-S (green trace) contribution is about 20 times weaker than the Ta-Ta contribution and 4 times weaker than that of Ta-S pairs.

Estimate of distorted fraction and structure modeling in polymorphic regime

By using a calculated PDF based on undistorted P3-m model as a reference, we form difference PDFs for all T > 600 K data. Such differences are then integrated over a $2.6 - 4$Å range (highlighted region on abscissa in Fig. 2b) and normalized to the 600 K value to quantify the relative change with temperature of the fraction of distorted sites across the polymorphic transformations, as shown in inset to Fig. 2b (for illustration see Supplementary Fig. 1). Above 730 K the short-range PDF data can be explained by a 6R-TaS $_2$-like model (R 3 m symmetry) featuring alternating 1T and 1H layers in equal abundance, Fig. 2c (bottom). Although the exact stacking and long-range character are likely more complex, as the model does not fully explain the data over longer length-scales, local analysis is rather robust. Importantly, the

6R − TaS_2 model features undistorted 1 T&1H layers, hence not accounting for local distortions responsible for nontrivial nearest neighbor Ta-Ta distance distribution.

Local structure model with P P symmetry

To map out temperature evolution of local interatomic distances, first data fits were carried out over 1 nm range and utilized a simple single S -Ta-S layer 1T-TaS $_2$ model conforming to P$\overline{3}$ symmetry. The model includes 19 independent structure parameters, constrained by symmetry to describe fractional coordinates of Ta (6 parameters) and S (13 parameters) atoms in the unit cell, two lattice parameters, two thermal parameters, and an overall scale factor. This explains the data features in the C state very well. The refinement range was established as a compromise between the model over-parametrization (data window too narrow) and the model deficiency (data window too wide) regimes. The 1 nm fitting range encompasses intra-bilayer correlations but excludes inter-bilayer correlations, which were subsequently explored in a model-independent manner as described below. (See Supplementary Table 1, Supplementary Figs. 6 and 7, and Section 2 for additional model details.)

Multiphase treatment

The fits using only the P**3** phase in the NC regime were noticeably worse compared to these in the C state, with observable increase of fit residual, as shown in inset to Fig. 3c. This is consistent with the presence of discommensuration domain walls and lower SoD density in the NC state whose atomic structure is less distorted and not accounted for in our simple distorted P$\overline{3}$ model. We approximated domain wall contribution by adding an undistorted P$\overline{3}$ m structure as a secondary (minority) phase to account for local environment of the discommensuration regions. We utilized this approach to fit the PDF data in the IC and M regimes as well, where the distorted and undistorted phases swap roles and the distorted phase becomes a minority phase.

Assignment and consideration of inter-layer PDF peaks

The inter-layer PDF peaks considered in this study were assigned based on undistorted P3m model as reported for 300 K and its supercell variants. In this, interlayer spacings along the stacking direction are defined by multiples of c-axis lattice parameter, including $\sim$ 5.9Å which corresponds to intra-bilayer separation. The $\sim$ 13.1Å peak in undistorted P$\overline{3}$ m structure corresponds to a well-defined off-axis Ta − Ta contribution connecting two Ta atoms that are 2 layers apart. These Ta atoms belong to next nearest neighbor Ta-layers and are offset within planes away from the stacking axis. In the high temperature regime, if structural distortions are incoherent, this peak in the data would be
smeared, as is observed. As order establishes, re-appearance (with respect to putative P$\overline{3}$ m structure that never materializes locally) of a sharp signal at $\sim$ 13.1Å implies re-emergence of structural coherence along this interatomic vector. The signal strength likely implies alignment of SoDs belonging to neighboring bilayers along this direction.

References

1. Law, K. T. & Lee, P. A. 1T-TaS2 as a quantum spin liquid. Proc. Natl Acad. Sci. USA 114, 6996-7000 (2017).

2. Klanjsek, M. et al. A high-temperature quantum spin liquid with polaron spins. Nat. Phys. 13, 1130-1134 (2017).

3. Darancet, P., Millis, A. J. & Marianetti, C. A. Three-dimensional metallic and two-dimensional insulating behavior in octahedral tantalum dichalcogenides. Phys. Rev. B 90, 045134 (2014).

4. Wilson, J. A., Salvo, F. J. D. & Mahajan, S. Charge-density waves and superlattices in the metallic layered transition metal dichalcogenides. Adv. Phys. 24, 117-201 (1975).

5. Kogar, A. et al. Signatures of exciton condensation in a transition metal dichalcogenide. Science 358, 1314-1317 (2017).

6. Persky, E. et al. Magnetic memory and spontaneous vortices in a van der Waals superconductor. Nature 607, 692-696 (2022).

7. Hamill, A. et al. Two-fold symmetric superconductivity in few-layer NbSe2. Nat. Phys. 17, 949-954 (2021).

8. Bednorz, J. G. & Müller, K. A. Possible high Tc superconductivity in the Ba-La-Cu-O system. Z. F.ür. Phys. B Condens Matter 64, 189-193 (1986).

9. Sipos, B., Berger, H., Forro, L., Tutis, E. & Kusmartseva, A. F. From Mott state to superconductivity in 1T-TaS2. Nat. Mater. 7, 960-965 (2008).

10. Dong, Q. et al. Structural phase transition and superconductivity hierarchy in 1 T -TaS2 under pressure up to 100 GPa . Npj Quantum Mater. 6, 20 (2021).

11. Zhang, P. et al. All-optical switching of magnetization in atomically thin Crl3. Nat. Mater. 1-6 https://doi.org/10.1038/s41563-022-01354-7 (2022).

12. Stojchevska, L. et al. Ultrafast switching to a stable hidden quantum state in an electronic crystal. Science 344, 177-180 (2014).

13. Ravnik, J. et al. A time-domain phase diagram of metastable states in a charge ordered quantum material. Nat. Commun. 12, 2323 (2021).

14. Dabrowski, M. et al. All-optical control of spin in a 2D van der Waals magnet. Nat. Commun. 13, 5976 (2022).

15. Kogar, A. et al. Light-induced charge density wave in LaTe3. Nat. Phys. 52, 1-6 (2019).

16. Tedstone, A. A., Lewis, D. J. & O'Brien, P. Synthesis, properties, and applications of transition metal-doped layered transition metal dichalcogenides. Chem. Mater. 28, 1965-1974 (2016).

17. Qiao, S. et al. Mottness collapse in 1T-TaS2-xSex transition-metal dichalcogenide: an interplay between localized and itinerant orbitals. Phys. Rev. X 7, 041054 (2017).

18. Li, L. J. et al. Fe-doping-induced superconductivity in the charge-density-wave system 1T-TaS2. Europhys. Lett. 97, 67005 (2012).

19. Wang, Y. D. et al. Band insulator to Mott insulator transition in 1TTaS2. Nat. Commun. 11, 1-7 (2020).

20. Landau, L. Electron motion in crystal lattices. Phys. Z. Sowjetunion 3, 644-645 (1933).

21. Camjayi, A., Haule, K., Dobrosavljević, V. & Kotliar, G. Coulomb correlations and the Wigner-Mott transition. Nat. Phys. 4, 932-935 (2008).

22. Mertelj, T., Kabanov, V. V., Mena, J. M. & Mihailovic, D. Selforganization of charged particles on a two-dimensional lattice subject to anisotropic Jahn-Teller-type interaction and threedimensional Coulomb repulsion. Phys. Rev. B 76, 9 (2007).

23. Vodeb, J. et al. Configurational electronic states in layered transition metal dichalcogenides. N. J. Phys. 21, 083001 (2019).

24. Mihailovic, D. Why Does Maximum T c Occur at the Crossover From Weak to Strong Electron-phonon Coupling in High-temperature Superconductors? https://doi.org/10.1007/s10948-022-06152-5.

25. Rossnagel, K. On the origin of charge-density waves in select layered transition-metal dichalcogenides. J. Phys. Condens. Matter 23, 213001 (2011).

26. Franchini, C., Reticcioli, M., Setvin, M. & Diebold, U. Polarons in materials. Nat. Rev. Mater. 6, 560-586 (2021).

27. Mihailovic, D. et al. Application of the polaron-transport theory to sigma (omega) in Tl2Ba2Ca1-xGdxCu2O8, YBa2Cu3O7-d, and La2xSrxCuO4. Phys. Rev. B 42, 7989-7993 (1990).

28. Fazekas, P. & Tosatti, E. Charge carrier localization in pure and doped 1t-Tas2. Phys. B C. 99, 183-187 (1980).

29. Gerasimenko, Y. A. et al. Quantum jamming transition to a correlated electron glass in 1T-TaS 2. Nat. Mater. 317, 505-1083 (2019).

30. Mraz, A. et al. Charge configuration memory devices: energy efficiency and switching speed. Nano Lett. 22, 4814-4821 (2022).

31. Mihailovic, D. et al. Ultrafast non-thermal and thermal switching in charge configuration memory devices based on 1T-TaS. APL 119, 013106 (2021).

32. Liu, G. et al. A charge-density-wave oscillator based on an integrated tantalum disulfide-boron nitride- graphene device operating at room temperature. Nat. Nanotechnol. 11, 845-850 (2016).

33. Landuyt, J. V., Tendeloo, G. V. & Amelinckx, S. Electron diffraction study of inter- and intrapolytypic phase transitions in transition metal dichalcogenides. IV Cinematogeraphic Observations of the 1 T$\beta \rightarrow$ 1 Tγ-Phase Transition in TaS2. Phys. Status Solidi A 42, 565-570 (1977).

34. Revelli, J. F. & Phillips, W. A. Studies of the system TaS2-xSex. J. Solid State Chem. 9, 176-186 (1974).

35. Givens, F. L. & Fredericks, G. E. Thermal expansion of NbSe 2 and TaS2. J. Phys. Chem. Solids 38, 1363-1365 (1977).

36. Ziebeck, K. R. A., Dorner, B., Stirling, W. G. & Schollhorn, R. Kohn anomaly in the 1T2phase of TaS 2. J. Phys. F. Met. Phys. 7, 1139-1143 (1977).

37. Machida, Y. et al. Observation of soft phonon modes in 1T-TaS2 by means of X-ray thermal diffuse scattering. J. Phys. Soc. Jpn 73, 3064-3069 (2004).

38. Nakanishi, K. & Shiba, H. Domain-like incommensurate charge-density-wave states and collective modes. J. Phys. Soc. Jpn 45, 1147-1156 (1978).

39. Nakanishi, K., Shiba, H., Takatera, H. & Yamada, Y. The nearly commensurate phase and effect of harmonics on the successive phase transition in 1 T-TaS 2. J. Phys. Soc. Jpn. 43, 1509-1517 (1977).

40. McMillan, W. L. Theory of discommensurations and the commensurate-incommensurate charge-density-wave phase transition. Phys. Rev. B 14, 1496-1502 (1976).

41. Butler, C. J., Yoshida, M., Hanaguri, T. & Iwasa, Y. Mottness versus unit-cell doubling as the driver of the insulating state in 1T-TaS2. Nat. Commun. 11, 2477 (2020).

42. Hellmann, S. et al. Time-domain classification of charge-densitywave insulators. Nat. Commun. 3, 1069-1069 (2012).

43. Ritschel, T. et al. Orbital textures and charge density waves in transition metal dichalcogenides. Nat. Phys. 11, 328-331 (2015).

44. Spijkerman, A., Boer, J., de, Meetsma, A. & Wiegers, G. X-ray crystalstructure refinement of the nearly commensurate phase of 1T-TaS2 in (3+ 2)-dimensional superspace. Phys. Rev. B 56, 13757 (1997).

45. Jellinek, F. The system tantalum-sulfur. J. Less Common Met. 4, 9-15 (1962).

46. Svetin, D., Vaskivskyi, I., Brazovskii, S. & Mihailović, D. Threedimensional resistivity and switching between correlated electronic states in 1T-TaS2. Sci. Rep. UK 7, 46048 (2017).

47. Brouwer, R. & Jellinek, F. Superstructure of 1s-TaS2. Mater. Res Bull. 9, 827-829 (1974).

48. Drummond, N. D. & Needs, R. J. Phase diagram of the low-density two-dimensional homogeneous electron gas. Phys. Rev. Lett. 102, 126402 (2008).

49. Pankov, S. & Dobrosavljević, V. Self-doping instability of the WignerMott insulator. Phys. Rev. B 77, 085104 (2008).

50. Radonjić, M. M., Tanasković, D., Dobrosavljević, V., Haule, K. & Kotliar, G. Wigner-Mott scaling of transport near the twodimensional metal-insulator transition. Phys. Rev. B 85, 085133-085137 (2012).

51. Kochubey, D. I., Kim, T. K., Babenko, V. P. & Shaikhutdinov, S. K. Charge density waves in 1T-TaS2: an EXAFS study. Phys. B Condens Matter 252, 15-20 (1998).

52. Ishiguro, T. & Sato, H. Electron microscopy of phase transformations in 1T-TaS2. Phys. Rev. B 44, 2046-2060 (1991).

53. Ishiguro, T. & Sato, H. High-resolution electron microscopy of discommensuration in the nearly commensurate phase on warming of 1 T- TaS2. Phys. Rev. B 52, 759-765 (1995).

54. Ishiguro, Y. et al. Layer number dependence of charge density wave phase transition between nearly-commensurate and incommensurate phases in 1T-TaS 2. J. Phys. Chem. C 124, 27176-27184 (2020).

55. Billinge, S. J. L. & Levin, I. The problem with determining atomic structure at the nanoscale. Science 316, 561-565 (2007).

56. Billinge, S. & Egami, T. Underneath the Bragg Peaks. https://doi.org/ 10.1016/s1470 − 1804(03)80011 − 1(2003).

57. Brouwer, R., C, F. J. P. B. & 1980. The low-temperature superstructures of 1T-TaSe2 and 2H-TaSe2. Phys. B C 99, 51-55 (1980).

58. Tidman, J. P. & Frindt, R. F. Resistivity of thin TaS2 crystals. Can. J. Phys. 54, 2306-2309 (1976).

59. Achari, A. et al. Alternating superconducting and charge density wave monolayers within bulk 6R-TaS2. Nano Lett. 22, 6268-6275 (2022).

60. Koch, R. J. et al. Dual orbital degeneracy lifting in a strongly correlated electron system. Phys. Rev. Lett. 126, 186402 (2021).

61. Bozin, E. S. et al. Local orbital degeneracy lifting as a precursor to an orbital-selective Peierls transition. Nat. Commun. 10, 3638 (2019).

62. Sezerman, O., Simpson, A. M. & Jericho, M. H. Thermal expansion of IT-TaS2 and 2H-NbSe2. Solid State Commun. 36, 737-740 (1980).

63. Ma, L. et al. A metallic mosaic phase and the origin of Mottinsulating state in 1T-TaS2. Nat. Commun. 7, 1-8 (2016).

64. Cho, D. et al. Nanoscale manipulation of the Mott insulating state coupled to charge order in 1T-TaS2. Nat. Commun. 7, 10453 (2016).

65. Gerasimenko, Y. A., Karpov, P., Vaskivskyi, I., Brazovskii, S. & Mihailovic, D. Intertwined chiral charge orders and topological stabilization of the light-induced state of a prototypical transition metal dichalcogenide. Npj Quantum Mater. 4, 1-9 (2019).

66. Fratini, S. & Quémerais, P. Polaron crystallization and melting: effects of the long-range Coulomb forces. Mod. Phys. Lett. B 12, 1003-1012 (1998).

67. Kapcia, K. J., Robaszkiewicz, S., Capone, M. & Amaricci, A. Dopingdriven metal-insulator transitions and charge orderings in the extended Hubbard model. Phys. Rev. B 95, 125112 (2017).

68. Ashiotis, G. et al. The fast azimuthal integration Python library: pyFAI. J. Appl. Crystallogr. 48, 510-519 (2015).

69. Kieffer, J., Valls, V., Blanc, N. & Hennig, C. New tools for calibrating diffraction setups. J. Synchrotron Radiat. 27, 558-566 (2020).

70. Juhás, P., Davis, T., Farrow, C. L. & Billinge, S. J. L. PDFgetX3: a rapid and highly automatable program for processing powder diffraction
data into total scattering pair distribution functions. J. Appl Crystallogr 46, 560-566 (2013).

71. Farrow, C. L. et al. PDFfit2 and PDFgui: computer programs for studying nanostructure in crystals. J. Phys. Condens Matter 19, 335219 (2007).

14 Observation of a two-dimensional liquid of Fröhlich polarons at the bare $SrTiO_3$ surface by Chen, Avila, Frantzeskakis, Levy, Asensio

(there is also a suppl info in the nature's webpage)

The polaron is a quasi-particle formed by a conduction electron (or hole) together with its self-induced polarization in a polar semiconductor or an ionic crystal. Among various polarizable examples of complex oxides, strontium titanate ($SrTiO_3$) is one of the most studied. Here we examine the carrier type and the interplay of inner degrees of freedom (for example, charge, lattice, orbital) in $SrTiO_3$. We report the experimental observation of Fröhlich polarons, or large polarons, at the bare $SrTiO_3$ surface prepared by vacuum annealing. Systematic analyses of angle-resolved photoemission spectroscopy and X-ray absorption spectra show that these Fröhlich polarons are two-dimensional and only exist with inversion symmetry breaking by two-dimensional oxygen vacancies. Our discovery provides a rare solvable field theoretical model, and suggests the relevance of large (bi)polarons for superconductivity in perovskite oxides, as well as in high-temperature superconductors.

T[s]he concept of a polaron was set forth by Landau [1] in 1933 and has attracted much attention over the following decades. It not only describes the specific physical properties of charge carriers in polarizable solid, but also constitutes an interesting field theoretical model consisting of a fermion interacting with a scalar boson field [2]. Even today, there is ongoing research on polarons, including the basic theory [3], as well as their behaviour in more compelling situations such as hightemperature superconductors [4–6] and colossal magnetoresistance in rare-earth manganites [7].

There are different types of polaron states in solids, such as Fröhlich polaron, small polaron, spin polaron, bipolaron and hydrated polaron [2]. Originally polaron describes interaction between charge carrier and long-wavelength optical phonons, namely, Fröhlich polaron [8], of which the spatial extension exceeds the lattice constant. Fröhlich polarons with low kinetic energy propagate through the lattice as free electrons but with an enhanced effective mass, thus directly measurable by spectroscopies like angle-resolved photoemission spectroscopy (ARPES). $SrTiO_3$ is the key material in the emerging field of oxide electronics [9]. Structurally or electronically modified $SrTiO_3$ presents a wide spectrum of phenomena such as superconductivity [10], twodimensional (2D) electron gas (2DEG) [11,12], ferroelectricity [13] and blue luminescence [14], indicating versatile interplay of charge, spin, orbital and lattice degree of freedom [15]. However, previous studies give controversial information about the carrier type in $SrTiO_3$ (see, for example, refs 16,17 and references therein), hampering the thorough distinction of these internal interplay. Recently, ARPES study on FeSe film grown on $SrTiO_3$ has revealed the enhancement of superconducting transition temperature T_c due to the coupling between FeSe electron and oxygen optical phonon in $SrTiO_3$ (ref. 6).

In this article, by examining the surface electronic structure of vacuum-annealed $SrTiO_3$, we report the observation of 2D liquid of Fröhlich polaron, a new quasi-particle formed by conduction band electron coupled with one polar longitudinal optical (LO) phonon mode. By controlling the annealing temperature, we can precisely tune the surface oxygen vacancy concentration, which develops from 2D to 3D distribution of charges. Moreover, by compiling partial electron yield (PEY) and total fluorescence yield (TFY) XAS spectrum, we are able

[81] Synchrotron SOLEIL, Beamline ANTARES, L'Orme des Merisiers, Saint Aubin-BP 48, Gif surYvette 91192, France. † Present addresses: Institute of Physics (IoP), University of Amsterdam, Science Park 904, 1098 XH Amsterdam, The Netherlands (E.F.); Sorbonne Universits, UPMC, Paris 06, CNRS, INSP, UMR 7588, INSP, F-75005 Paris, France (A.L.). Correspondence and requests for materials should be addressed to M.C.A. (email: asensio@synchrotron-soleil.fr).

to identify unambiguously these two distinctive distributions of oxygen vacancies. In the 2D case, oxygen defect dipoles break the inversion symmetry and initiate the coupling between electrons and polar LO phonons. This intermediate coupling leads to the formation of a new type of quasi-particles, Fröhlich polarons, whose spectra function contains multiple replicas of original bands, equally spaced ω_{LO} apart, with ω_{LO} the effective energy of LO phonons, as directly observed by ARPES here. Photon-energy-dependent ARPES measurements reveal the 2D nature of Fröhlich polarons. In the 3D oxygen vacancy case, the 2D polarons collapse into 3D electron liquid due to the reversal of symmetry. Our findings reveal the essential role of surface/interface LO-phonon-related large (bi)polarons in understanding superconductivity in perovskite oxides, as well as in high-temperature superconductors.

14.1 Results

Tunable oxygen vacancy concentration via vacuum annealing. Intrinsic $SrTiO_3$ is a band insulator with a $\sim$ 3.2eV gap, and experiences a second-order phase transition from cubic to tetragonal structure at the critical temperature of about 105 K (ref. 18). For the present study, both the XAS and ARPES measurements were performed $\sim$ 170 K while the low-energy-electrondiffraction (LEED) patterns were taken at room temperature.

Thus for our study, the bulk $SrTiO_3$ is in the centre-symmetric equilibrium structure, that is, the Ti atom lying in the centre of the regular octahedron of oxygen atoms in the cubic perovskite structure (Fig. 1a). All the experiment data is from the (001) surface as shown in Fig. 1b.

To start with, we present the precisely regulation of surface carriers by controlling the amount of oxygen vacancies via vacuum annealing. We prove the existence of oxygen vacancies by reproducing the well-known LEED patterns (Fig. 2a and also see, for example, ref. 19 and references in), which reflect the surface reconstruction due to the alignment of oxygen vacancies. Charge transfer from oxygen vacancies to Ti atoms (consequently, Ti^{4+} to Ti^{3+}) allow us to derive the oxygen vacancy concentration $[V_{\mathrm{O}}]$ from the XAS spectra of Ti $L_{2,3}$ edge, attributed to excitations of $2P_{3/2}$ and $2P_{1/2}$ subshells to unoccupied $t_{2\ \mathrm{g}}$ and e_{g} states, as shown in Fig. 2b,c. As indicated by the black arrow and more clearly shown in the insets, a 460 eV peak gradually increases with annealing temperature. According to the theoretical simulation [20] (Fig. 2f, top), this peak comes from the $Ti^{3+}L_3$ edge. Since X-ray absorption near-edge spectroscopy is an atomic probe, strongly sensitive to its formal oxidation state and coordination chemistry [21], we can calculate the Ti^{3+}/Ti^{4+} ratio by assuming the linear combination of Ti^{4+} and Ti^{3+} signals under the single inelastic electron scattering condition [22,23]. As exemplified in Fig. 2f (bottom) for the PEY XAS spectra from surface annealed at $1,000°$C, the experimental spectra can be decomposed into $85\%Ti^{4+}$ and $15\%Ti^{3+}$, using multiple leastsquares fit. Figure 2g schematically summarizes the fitted PEY ratio corresponding to surfaces with different annealing temperature. The monotonic increase of oxygen vacancies with annealing temperature clearly demonstrates that we can control and reproduce the carrier concentration of the $SrTiO_3$ samples. This point has been further corroborated by the agreement between the Ti^{3+}/Ti^{4+} ratio calculated by PEY XAS and Ti 3p core levels shown in the Supplementary Fig. 1. Notice that we have chosen a similar energy window ($\sim$ 40eV) to collect secondary electrons for XAS spectra and core level photoelectrons spectra, ensuring similar depth sensitivity in both data sets.

In addition, we can also prove the increase of surface oxygen vacancies from the OK-edge XAS spectra (Fig. 2d,e). As shown clearly in the insets, the A2 peak increases dramatically for the surface annealed at $1,200°$C. This peak arises from the $\mathrm{Ti}-\mathrm{O}pd-$ hybridization with a σ-bonding character. Its increase indicates the lattice distortion caused by oxygen vacancies, in qualitatively agreement with our conclusion based on Ti$L_{2,3}$-edge data. Given that each oxygen vacancy nominally transfers two electrons to the Tid band [24], and there are three O atoms but

only one Ti atom in the unit cell, Ti^{3+} ratio is six times the value of the oxygen vacancy concentration [V_O] (Fig. 2g), which allows XAS on Ti $L_{2,3}$ edge be much more sensitive than OK edge. Thus it is sensible to calculate the [V_O] from the XAS spectra of Ti $L_{2,3}$ edge.

More importantly, we show that the oxygen vacancy distribution displays a clear dimensionality change. Figure 2 g also summarizes $[V_O]$ values fitted from TFY-XAS spectra. For a given annealing temperature, both PEY and TFY spectra are recorded simultaneously from the same sample. Contrary to the monotonic increase of PEY [V_O], the TFY concentration remains at noise level at the beginning and only increases with annealing temperature above $1,000°$C. This distinctive behaviour is based on the different depth sensitivity of PEY and TFY spectra [25]. The PEY signals, that is, energy-selected secondary electrons in present case, typically from an average depth of < 1 nm (approximately two unit cells deep), are highly surface sensitive. In contrast, the TFY signals mainly give bulk information due to the long mean free path (MFP) of photons, (~ 100 nm). Thus, we

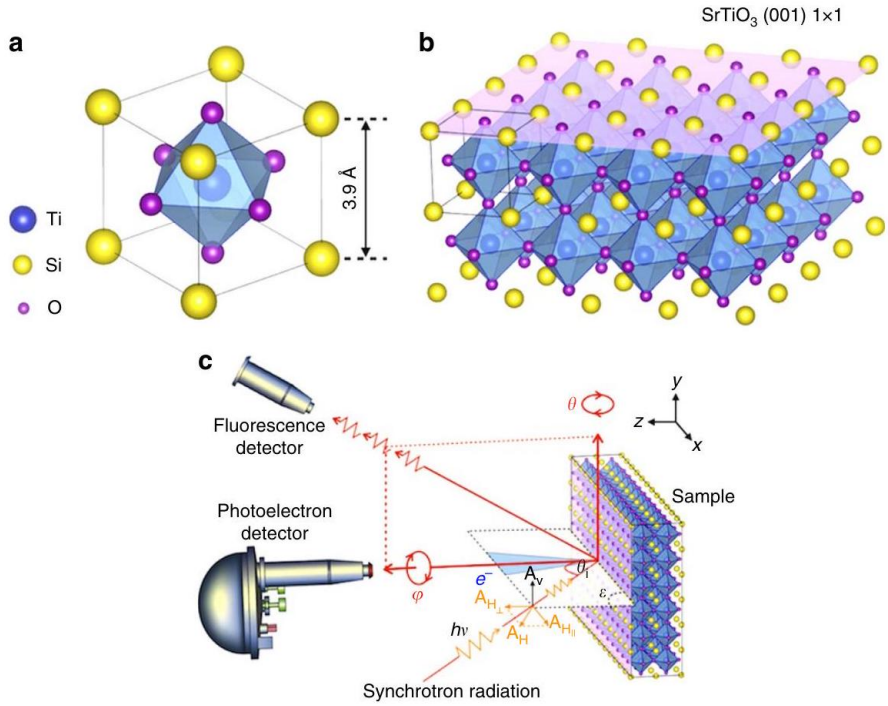

Figure 1 | Lattice structure of $\mathbf{SrTiO_3}$ and measurement geometry. (a) The cubic unit cell, with the TiO_6 octahedron shown as magenta surfaces. O atoms at O 1 cites have $\mathrm{Ti}-\mathrm{O}$ bonds along z direction, while O 2 cites have $\mathrm{Ti}-\mathrm{O}$ bonds parallel to the $x-y$ plane. (b) A $4\times4\times2$ block of unit cells. The top layer shown in light purple indicates the (001) surface. (c) Experimental geometry for XAS and ARPES measurements. $\mathbf{A}_\mathrm{H}$ ($\mathbf{A}_\mathrm{V}$) is the vector potential of the incident light with linear horizontal (vertical) polarization; θ and ϕ denote the polar and azimuthal degree of freedom and θ_i is the polar angle of incidence. The analyser slits permit photoelectron detection along the x axis. For all different θ, the incident photon momentum, the photoelectron momentum and the surface normal lie on the same plane (ε). For all the ARPES data, we set the $\theta_\mathrm{i} \sim 75°$, very close to the grazing angle, to enhance the surface contribution. We use linear horizontal polarization (LH). The beam polarization is even to the scattering plane. According to the matrix element effect (MEE), only orbitals with even symmetry respect to the scattering plane can be excited and detected.

conclude that vacuum annealing from $800°$C to $1,000°$C generates 2D oxygen vacancies confined at the surface. However, for samples annealed above $1,000°$C, the high concentration

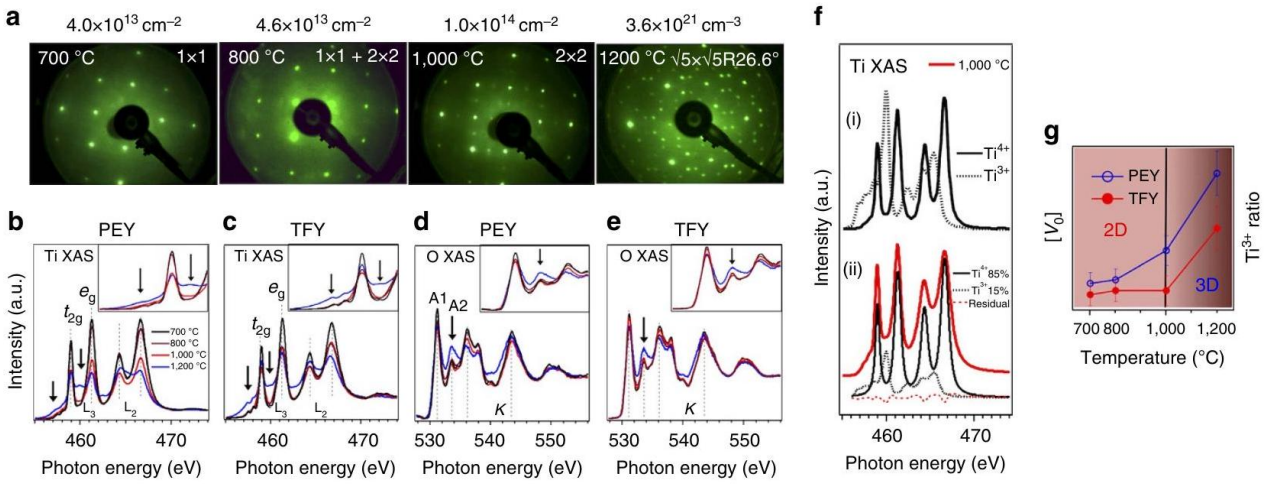

Figure 2 | Creating 2D and 3D oxygen vacancies. (a) LEED patterns with surface reconstruction labelled for $SrTiO_3$ surfaces prepared at different annealing temperature sequentially. The corresponding carrier densities are calculated by Ti^{3+} ratio from PEY XAS spectra for 2 D case ($\leq 1,000°C$) and TFY-XAS spectra for 3D case ($1,200°C$). See Methods for details. (b-e) Ti$L_{2,3}$-edge and OK-edge XAS spectra from different surfaces. Black arrows indicate the peak intensity coming from Ti^{3+}. (f) Top, numerically calculated XAS spectra of Ti^{3+} and Ti^{4+} ions in $SrTiO_3$. Bottom, decomposition of experimental XAS spectra, exemplified by the PEY spectra for surfaces annealed at $1,000°C$. (g) Schematic evolution of oxygen vacancy concentration and Ti^{3+} ratio from PEY and TFY spectra. Vertical black line indicates the boundary between 2D and 3D oxygen vacancies.

of oxygen vacancies presents a 3D distribution of
charges. For the whole annealing temperature range, the concentration of induced surface charge carriers (2D and 3D) increases monotonously with temperature. In addition, judged from the sharp LEED pattern, the vacancies are well-aligned.

These ordered defect dipoles break the local inversion symmetry, allow the Raman measurement of first-order phonons [26] and suggest a phase with ferroelectric-like polarization at the reduced surface of $SrTiO_3$ (ref. 27).

Observation of Fröhlich polaron spectra by ARPES. It is natural to ask what kind of electronic structure does this ferroelectric-like layer correspond to. Figure 3a shows the symmetrized Fermi surfaces (FSs) from the $SrTiO_3$ surface annealed at 700°C. Thanks to the matrix element effect, we can selectively excite electrons with different orbital symmetry (see Fig. 1c for measurement geometry). No ARPES spectral intensity can be detected at the first Brillouin zone centre (Γ and Γ_{00} specifically). FSs at Γ_{10} and Γ_{01} are elliptical, with d_{xz} (Fig. 3f) and d_{yz} orbital character, respectively. The circular FS at Γ_{11} are from d_{xy} orbital (Fig. 3b). Fitted dispersions (black dashed lines in Fig. 3b,c,f) show an effective mass of $\sim 0.6m_e$ (m_e the free electron mass) for d_{xy} band, and $\sim 6m_e$ for d_{xz} band (see Supplementary Fig. 2 for fitting details). These lighter effective masses will contribute to the high carrier mobility [12,28].

An extraordinary distinction is that there exist replica bands for each orbital (Fig. 3b,f), lying $\sim$ 90meV higher than the original, which can be clearly distinguished from the energy-second-derivative spectra in Fig. 3c. The replica forms one more higher-lying electron pocket, as shown by the constant-energy contours in Fig. 3e. These replicas are attributed to the many-body effect, specifically, the electron-phonon coupling
(EPC) [6,29]. The characteristic energy, $\sim$ 90meV, corresponds to one surface polar LO phonon mode [30]. These dispersions hence describe electrons weakly coupled to a lattice vibrational

mode by the Coulomb interaction, which together can move coherently through the solid and composite a new type of quasi-particle, that is, large polaron. We use the weak-coupling field-theoretical Fröhlich Hamiltonian [8] as the first approximation to describe EPC in both 3D and 2D cases:

$$H = \frac{\mathbf{p}^2}{2m_{\mathbf{b}}} + \sum_{\mathbf{k}j} \hbar\omega_{\mathrm{LO},j} a^{\dagger}_{\mathbf{k}j} a_{\mathbf{k}j} + \sum_{\mathbf{k}j} \left(V_{\mathbf{k},j} e^{i\mathbf{k}\vec{r}} a_{\mathbf{k}_j} + \text{ h.c. } \right) \tag{1}$$

Where $\mathbf{r}$ is the position coordinate operator of the electron with band mass $m_{\mathrm{b}}, \mathbf{p}$ is its canonically conjugate momentum operator; $a^{\dagger}_{\mathbf{k}j}$ $(a_{\mathbf{k}j})$ is the creation (annihilation) operator for the j-th LO phonons of wave vector $\mathbf{k}$ and energy $\hbar\omega_{\mathrm{LO},j}$. The $V_{\mathbf{k}j}$ is the Fourier component of the EP interaction. Considering one branch of dispersion-less LO-phonon (Einstein model) [31–33], this interaction system becomes one of the exactly solvable models in many-body physics [34]. The spectra can be well-described by a Franck-Condon model with Poisson distribution:

$$\frac{I_l}{I_0} = \frac{g^l}{l!} \tag{2}$$

Here I_0 is the quasi-particle peak intensity and I_l the l-th replica intensity with l phonon(s) dressed. g is a constant, related with the EP interaction in 3D.

Considering the ARPES spectra in Fig. 3b,f, the lower-lying band corresponds to charge carriers without dressing phonons, while the higher one corresponds to charge carriers dressing one phonon. Other higher-order bands are nearly invisible but can be deduced from the energy distribution curves (EDCs) fitted with Franck-Condon line shape as shown in Fig. 3h (refs 6,29). The fitting gives an energy separation $\omega_{\mathrm{LO}} \sim 90$meV and $g = 0.85$. We can also use other fitting parameters $\alpha_{3\mathrm{D}}$ and $\alpha_{2\mathrm{D}}$, to characterize the Fröhlich coupling constant. Inferred from the zero-phonon peak intensity fraction of total weight, according to the diagrammatic quantum Monte Carlo simulation [35], we have $\alpha_{3\mathrm{D}} \sim 2.5$. Using the scaling relation $Z_{2\mathrm{D}}(\alpha) = Z_{3\mathrm{D}}(3\pi\alpha/4)$ for 2D polarons [36], we have $\alpha_{2\mathrm{D}} \sim 1.1$. Notably, here we use a common and available approach to estimate the 2D coupling strength indirectly. However, although beyond the scheme of present work, a more accurate model directly describing 2D Fröhlich polaron spectra is highly desired.

It is worthy to note that the whole spectra with multiple bands we observed here describe the ground state of Fröhlich polaron, not the excited state, since the temperature is set to zero for the theoretical spectra function [34]. In the ground state of Fröhlich polaron, some probability exists that the charge carriers have different set of energy $\omega_l = \varepsilon_b - \Delta + \omega_{\mathrm{LO}}\, l$. Furthermore, this is different from the characteristic 'peak-dip-hump' spectra in cuprates [37,38], in which case localized small polarons show no high-order dispersion. Our discovery only becomes possible because of the intermediate coupling strength. The discrete phonon mode energy is bigger than the electron bandwidth and most crucially, because the forward scattering is dominating the EPC, as discussed in the recent literature. Figure 3d shows the simulated dispersion of Fröhlich polaron for both d_{xy} and $d_{xz/yz}$ orbitals, with the full width at half maximum (FWHM) set as constant, 25 meV and without multiple phonon contribution. Our discovery represents a 'rare' field theoretical model of Fröhlich polaron, which is exactly solvable [29,34].

One may wonder if these multiple bands arise from band bending effect due to the quantum confinement of the conduction band bottom. In fact, the 2D electron gases/liquids at $SrTiO_3$ surface have become model systems for engineering emergent behaviour and studying the quasi-particle dynamics in complex transition metal oxides [11,12,15]. Here we rule out this possibility due to the fact that the sub-bands in the quantum confinement picture are real electronic structure, crossing Fermi level, but our observed shadow bands are the 'echo' of EPC, without Fermi level crossing. See Supplementary Fig. 3 for schematic understanding. We also clarify that, contrary to previous works [12,39], during our experiments, all the surfaces displayed no

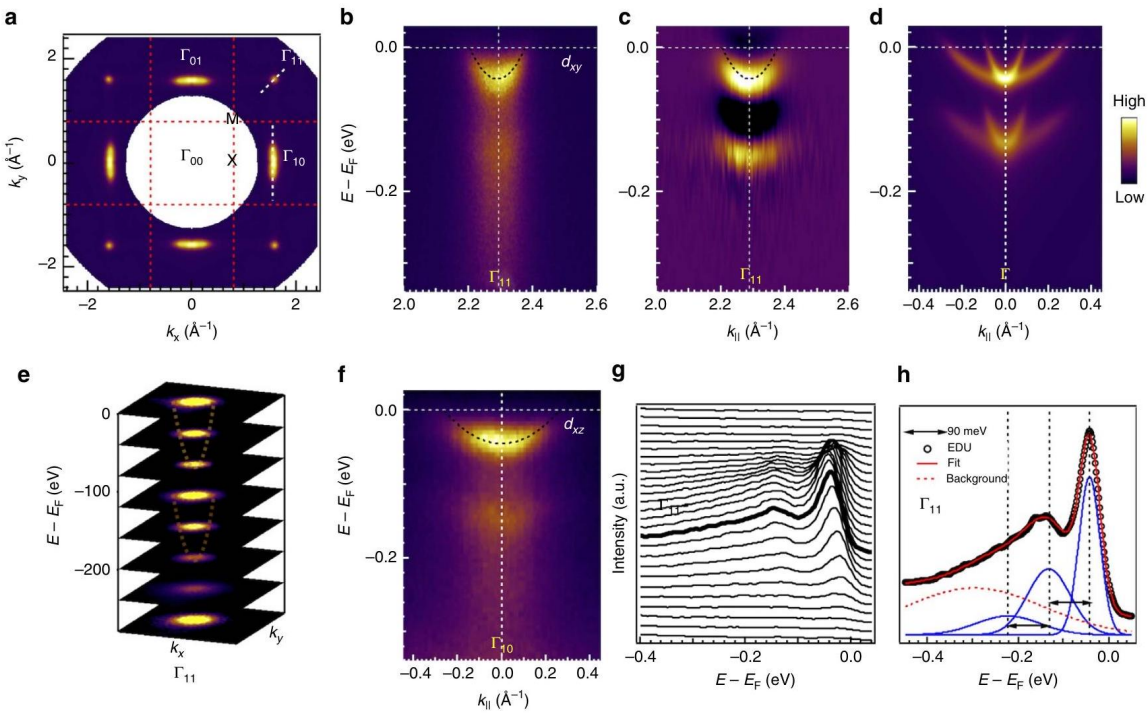

Figure 3 | Observation of Fröhlich polaron spectra by ARPES at $\mathbf{SrTiO_3}$ surface prepared at **700°C**. (a) Symmetrized Fermi surface of $SrTiO_3$ in $k_x - k_y$ space. $\Gamma_{10} = 2\pi/a(1,0) \sim (1.61,0)\text{Å}^{-1}$. (b) Dispersion from Γ_{11} along [11] direction with d_{xy} orbital character. Dispersion from Γ_{10} along [01] direction with d_{xz} orbital character is shown in **f**. The momentum cuts are shown in dashed while lines. (c) Energy-second-derivative image of spectra in **b**. (d) Simulated large polaron dispersions with d_{xy}/d_{yz} and d_{xz} orbital characters. (e) Constant-energy contours of large polaron electronic structure, characterized by two (or more) similar electron pockets, indicated by dashed lines. (g) EDC stacks of spectra in **b**. Black empty circles indicate the EDC shown in **h**. (h) Franck-Condon line shape fitting. The fitted EDC (red line) is composed of three Gaussian peaks (blue line), separated in energy by 90 meV , and a hump-like background (red dashed line). Black dashed lines in **b**, **c** and **f** are fitted dispersions for the zero-order bands. See Supplementary Fig. 2 for details.

detectable dependence on synchrotron irradiation, as demonstrated by the core level and XAS spectra in Supplementary Fig. 4.

Many seminal studies have been recently done describing the 2DEG scenario, which provide a lot of information even if many important aspects of this phenomenon are still under inflamed discussion. What is important, however, is that there is a quite robust consensus on the conditions in which the 2DEG is stable. Consequently, we have been able to identify three important parameters: carrier density, oxygen vacancy concentration and thickness of the surface layer where the 2DEG takes place. The reported value for the carrier density is close to 10^{14} cm^{-2} (see, for example, refs 11,15). For the oxygen vacancies, most of the works report a rather constant concentration [11,12,40]. Finally, the thickness is estimated in most of the important works around four to eight cell units [11,12,15,40]. For the 'polaron' scenario, however, the formation appears when the carrier density, the oxygen vacancies and the thickness of the surface layer are in rather different ranges. In our manuscript, we have demonstrated that the polarons only form when the carrier density is close to
10^{13} cm^{-2}, 1 order of magnitude lower than that for the case of 2DEG. For the oxygen concentration, the polarons appear for approximately half the concentration of oxygen vacancies

reported for 2DEG systems (Supplementary Fig. 1). Finally, for the thickness, thanks to the parallel detection of XAS and ARPES we can confirm that the thickness of the surface polarons is not larger than one to two cell units, at least four to eight times smaller than that for the 2DEG surface layer.

Dimensionality and stability of the Fröhlich polarons. As deduced from the XAS spectra, annealing below 1000°C creates 2D charge carrier localized mainly at the surface. From ARPES spectra we identify these charge carriers as Fröhlich polarons. We then directly demonstrate the 2D nature of Fröhlich polarons by ARPES. Photon-energy-dependent ARPES can map the FS at 3D momentum space (see Methods). Figure 4a shows the FS of d_{xy} orbital around one bulk Γ point in $k_x - k_y - k_z$ momentum space from surface annealed at 800°C. To highlight the detail, we plot the second-derivative photoemission intensity versus momentum. Its cylindrical shape and the lack of dispersion along k_z direction directly confirm the 2D nature of the FS. The projection of this 2D FS onto $k_x - k_y$ momentum space composes an open circle. On the contrary, for surface annealed at $1,200$°C, the corresponding k_z dispersion of the FS shows a ellipsoid-like shape, whose projection shows filled circle feature (Fig. 4d), composing evidence of 3D carriers. Consequently, the EDCs analysis as a function of the annealing temperature (Fig. 4c) shows the polaronic bands till the oxygen vacancies present a 3D distribution. In fact, only one Gaussian peak could be fitted to the $1,200$°C EDC, with a non-vanishing background connecting the oxygen vacancy band (Supplementary Fig. 1c). This higher binding energy spectral weight commonly results from electron interaction, reminiscent of liquid behaviour [12]. Thus, both FSs and EDCs spectral analysis prove the 2D nature of Fröhlich polarons. The transition from 2D Fröhlich polaron to 3D electron liquid will be discussed in detail later.

Despite its ultimate collapse, 2D Fröhlich polarons are relatively stable over a wide carrier density. The carrier density can be calculated from the Luttinger area of the FSs (see Methods), shown in Fig. 5a,b (see Supplementary Figs 5 and 2 for detailed FSs and fitting). For 2D Fröhlich polaron, we have $n_{2D} \sim 5.7 \times 10^{13}$ cm^{-2}, 7.4×10^{13} cm^{-2} and 7.6×10^{13} cm^{-2} for surfaces prepared at 700°C, 800°C and $1,000$°C, respectively. We have also estimated the carrier density according to the Ti^{3+}/Ti^{4+} ratio from PEY XAS spectra (see Methods). For 2D case, we got $n_{2D} \sim 4.0 \times 10^{13}$, 4.6×10^{13} and 1.0×10^{14} cm^{-2} for corresponding surfaces, in qualitative agreement with ARPES data. It is worthy to note that, for both ARPES and XAS, we assume an ideal 2D scenario. In reality the probe depth for our ARPES and XAS measurements are different since the photoelectron kinetic energy is about 95 eV for ARPES and 40 eV for XAS. As shown in Fig. 4c, from all samples annealed between 800°C and $1,000$°C, Franck-Condon line shape fitting gave similar second and third order polaronic peak weight, indicating a constant EPC and relatively stable polarons, regardless of the vacancies organization or charge concentration.

Estimated from the 2D carrier density for 700°C case, the Wigner-Seitz radius $r_s = (2\pi n_{2D})^{-1/2}$ is $\sim$ 5.3Å and the average separation between two Fröhlich polarons is $\sim$ 11Å (approximately three unit cells). Consequently, the momentum width Δk from ARPES spectra at Fermi momentum gives a polaron MFP $\lambda \sim$ 10Å. The Franck-Condon fitting in Fig. 4c also gave similar hump-like background for all the three surfaces. Note that, unlike the $1,200$°C case with oxygen vacancy band observed at higher binding energy, this background can only originate from the

conduction band, and most likely, attributed to the interaction between polarons. In addition, the effective mass for Fröhlich polaron ($\sim 0.6m_e$ for d_{xy} orbital) is even lighter than that both for 3D liquid in our case ($\sim 1.1m_e$) and for 2D electron gas from reported data ($\sim 0.7m_e$)[11], indicating its high mobility. Thus it is proper to conclude that 2D liquid of Fröhlich polarons with high mobility can be created and confined at the surface of $SrTiO_3$.

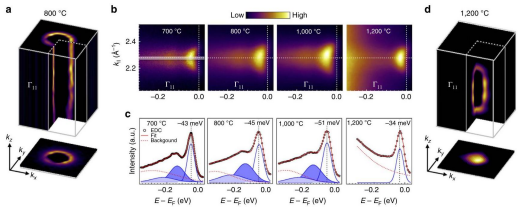

Figure 4 | 2D nature and stability of large polarons in **$SrTiO_3$**. (**a**, d) Fermi surface of $SrTiO_3$ in $k_x - k_y - k_z$ space with d_{xy} orbital character. The FSs are centred at one Brillouin zone centre, Γ, which is one high-symmetric point in three-dimensional momentum space with $(k_x, k_y, k_z) = 2\pi/a(1, 1, 3) \sim (1.61,\ 1.61, 4.83)\text{Å}^{-1}$. (b) Evolution of dispersions from the Γ_{11} cut as in Fig. 3b. (c) EDC curves (black empty circles) extracted from the momentum window shown in grey in b. Franck-Condon line shape fitted curves are shown with red lines. Blue lines represent individual Gaussian peaks.

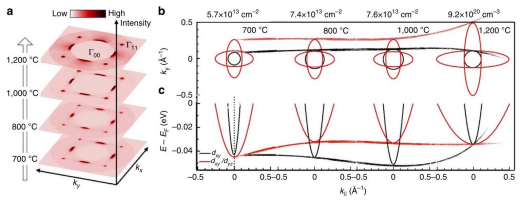

Figure 5 | Evolution of Fermi surfaces and dispersions. (a) Symmetrized Fermi surfaces of $SrTiO_3$ in $k_x - k_y$ space for (001) surfaces annealed at different temperature. The raw data is shown in Supplementary Fig. 5. (b) Fitted FSs for all the three orbitals. The calculated carrier densities are shown for corresponding FSs. See Methods for calculation formula. The superimposed red and black curves indicate the size change for d_{xz} FS and d_{xy} FS, respectively. (c) Fitted dispersions for different orbitals. See Supplementary Fig. 2 for fitting details. The superimposed red and black curves indicate the band bottom change for d_{xz} band and d_{xy} band (zero order), respectively.

14.2 Discussion

The ultimate collapse of 2D Fröhlich polaron to 3D liquid is puzzling and deserves further examination. Here we interpret it exclusively from the point of view of symmetry. Considering that the EPC is local and linear, in lattice with space inversion symmetry, only phonons with even parity can contribute to the EPC. The linear contribution from polar LO phonons becomes possible only with inducing symmetry breaking. Intrinsic $SrTiO_3$
has a centre-symmetric structure, with d_{xy} and $d_{xz/yz}$ orbitals degenerate at the bottom of conduction band [41]. As annealed from 800°C to 1,000°C, the oxygen vacancies mainly locate at the O1 site (Fig. 1a). These highly restricted 2D defect dipoles break the inversion symmetry along z direction, resulting in the level splitting between d_{xy} and d_{xz} orbitals as shown in Fig. 5c. The sign change of splitting between 700°C and 800°C cases may attribute to the alignment and correlation of dipolar moment. Nevertheless, Franck-Condon line shape fitting yields similar phonon energy and coupling strength (Fig. 4c), indicating the robustness of Fröhlich polaron with broken inversion symmetry. In the case of 1,200°C, oxygen vacancies expand to 3D and start to occupy O2 sites. These 3D defect dipoles generate relatively even potential along all the three directions. Thus somehow the surface lattices regain its symmetry, deduced by the re-degenerate orbital bands (see Fig. 5c for 1,200°C case). Consequently, EPC fails, and the many-body effect is dominated by electron-electron
interaction, forming 3D liquid. Our scenario suggests that, besides vacuum annealing, other

symmetry-breaking alternatives such as applying electric field [42] or capping layer [6,43] may also initiate the electron-LO phonon coupling and create Fröhlich polarons.

The 2D Fröhlich polaron density falls in the range of which superconductivity in perovskite oxide interfaces is observed [42,44]. It has been long proposed that a Bose-Einstein condensation of 2D bipolarons into a superconducting fluid be responsible for the high T_c in cuprates with multiple LO-phonon branches [45]. The recent discovery of high T_c in single unit cell thick iron selenide film (1UC FeSe) grown on $SrTiO_3$ substrate also suggests the intimate interplay between charge carriers in FeSe and LOphonon in $SrTiO_3$ (refs 6,46,47). The transport measurements [48] first confirm the very high- T_c superconductivity in single layer FeSe/STO system, in agreement with ref. 6. So if one considers these works together, it would be direct to deduce that this EPC is intrinsic for $SrTiO_3$ and be responsible for the enhanced superconductivity in FeSe/STO system. However, even if there are several articles suggesting that the EPC of the $SrTiO_3$ may be relevant in the mechanism of the high- T_c superconductivity, our manuscript is not dealing directly with this issue, in consequence further studies should be carried out to prove or disprove the relation between these two processes.

It is worthy to note that the phonon mode we observed here may not necessarily represent only one LO-branch, but could correspond to the approximation of multiple LO-phonon branches [49]. In this case, the calculated effective coupling constant α_{3D} is $2.34\,(m^\star)^{1/2}$. Using the band effective mass ($m^\star$) of d_{xy} orbital in 3D liquid case, we have $\alpha_{3D} \sim 2.45$, in excellent agreement with our experimental value. In this approximation, large bipolarons are found to have an extended stability region at low temperature. Thus our observation of Fröhlich polaron liquid in $SrTiO_3$ suggests significant relevance of large (bi)polaron for superconductivity and should stimulate broad interest in exploring polaron behaviour in a wide range of perovskite-related materials, especially high- T_c cuprates and iron-based superconducting film on $SrTiO_3$ substrate.

14.3 Methods

Sample preparation. $SrTiO_3(100)$ single crystals (crystal GmbH and SurfaceNet GmbH) were mounted on resistive Si heaters and cleaned by thermal annealing in vacuum conditions. Each sample was sequentially heated up to particular temperatures, and kept for 20 min , till characteristic LEED patterns are stabilized. At all stages of the cleaning procedure, the pressure was $< 10^{-9}$mbar. All samples presented reproducible and stable phases, with a series of typical reconstructions.

X-ray Absorption Spectroscopy (XAS). For the XAS measurements, from the same sample surface secondary electrons were recorded by Scienta energy analyzer, while fluorescence was recorded simultaneously by Bruker detector. XAS spectra simulation was performed by tetrahedral cluster model calculation. The cluster consists of a central Ti atom and its nearest neighbour ligand atoms, and the model calculation includes not only the full multiplets of $3d$ electrons but also configuration interaction.

ARPES. The angle and energy resolutions of the ARPES measurements (Scienta R4000) are set as 0.2° and $\sim$ 10meV. The photon energy-dependent ARPES experiments were performed with photon energy varying from 70 eV to 115 eV . The kz was calculated by $k_z = \hbar^{-1}\left(2m\left(E_k\cos^2\theta + V_0\right)\right)^{9/2}$. The inner potential $V_0 = 12$eV. Unless otherwise stated, we used photon energy at 100 eV for normal ARPES measurements. The 2D and 3D carrier density can be calculated from the Luttinger area of the FSs. $n_{2D} = k_F^2/2\pi$ and $n_{3D} = k_F^3/3\pi^2$. From the Ti^{3+} ratio, the carrier density can also be calculated by $n_{2D} =$ ratio $\times a^{-2}$ and $n_{3D} =$ ratio $\times a^{-3}$ with the lattice constant $\alpha = 3.9$Å.

14.4 References

1. Landau, L. D. On the motion of electrons in a crystal lattice. Phys. Z. Sowjetunion 3, 664-665 (1933).

2. Devreese, J. T. Polarons. Encyclopedia Appl. Phys. 14, 383-409 (1996).

3. Devreese, J. T. & Alexandre, S. A. Fröhlich polaron and bipolaron: recent developments. Rep. Prog. Phys. 72, 066501 (2009).

4. Alexandrov, A. S. Theory of high temperature superconductivity beyond bcs with realistic Coulomb and Fröhlich interactions. J. Supercond. Nov. Magn. 26, 1313-1317 (2013).

5. Alexandrov, A. S., Samson, J. H. & Sica, G. High-temperature superconductivity from realistic Coulomb and Frö hlich interactions. Europhys. Lett. 100, 17011 (2012).

6. Lee, J. J. et al. Interfacial mode coupling as the origin of the enhancement of T_c in FeSe films on $SrTiO_3$. Nature 515, 245-248 (2014).

7. Jooss, C. et al. Polaron melting and ordering as key mechanisms for colossal resistance effects in manganites. Proc. Natl Acad. Sci. USA 104, 13597-13602 (2007).

8. Fröhlich, H. Electrons in lattice fields. Adv. Phys. 3, 325-361 (1954).

9. Takagi, H. & Hwang, H. Y. An emergent change of phase for electronics. Science 327, 1601-1602 (2010).

10. Ueno, K. et al. Electric-field-induced superconductivity in an insulator. Nat. Mater. 7, 855-858 (2008).

11. Santander-Syro, A. F. et al. Two-dimensional electron gas with universal subbands at the sur- face of $SrTiO_3$. Nature 469, 189-193 (2011).

12. Meevasana, W. et al. Creation and control of a two-dimensional electron liquid at the bare $SrTiO_3$ surface. Nat. Mater. 10, 114-118 (2011).

13. Haeni, J. H. et al. Room-temperature ferroelectricity in strained $SrTiO_3$. Nature 430, 758-761 (2004).

14. Kan, D. S. et al. Blue-light emission at room temperature from Ar^+-irradiated $SrTiO_3$. Nat. Mater. 4, 816-819 (2005).

15. King, P. D. C. et al. Quasiparticle dynamics and spin-orbital texture of the SrTiO3 two-dimensional electron gas. Nat. Commun. 5, 3414 (2014).

16. Devreese, J. T., Klimin, S. N., van Mechelen, J. L. M. & van der Marel, D Manybody large polaron optical conductivity in $SrTi_{1-x}Nb_xO_3$. Phys. Rev. B 81, 125119 (2010).

17. Hao, X., Wang, Z., Schmid, M., Diebold, U. & Franchini, C. Coexistence of trapped and free excess electrons inSrTiO3. Phys. Rev. B 91, 085204 (2015).

18. Wang, F. Y. & Gupta, K. Phase transformation in the oxides. Metallurgical Transactions 4, 2767-2779 (1973).

19. Lin, Y. et al. The (2×2) reconstructions on the $SrTiO_3(001)$ surface: A combined scanning tunneling microscopy and density functional theory study. Surf. Sci. 605, L51-L55 (2011).

20. Cho, K. et al. X-ray absorption spectroscopy study of diluted magnetic semiconductors: $Zn_{1-x}M_xSe(M = Mn, Fe, Co)$ and $Zn_{1-x}Mn_xY(Y = Se, Te)$. Phys. Rev. B 63, 155203 (2001).

21. Newville, M. Fundamentals of XAFS. Rev. Mineral. Geochem. 78, 33-74 (2014).

22. Ohtomo, A., Muller, D. A., Grazul, J. L. & Hwang, H. Y. Artificial chargemodulation in atomic-scale perovskite titanate superlattices. Nature 419, 378-380 (2002).

23. Zhu, G. Z., Radtke, G. & Botton, G. A. Bonding and structure of a reconstructed (001) surface of $SrTiO_3$ from TEM. Nature 490, 384-387 (2012).

24. Muller, D. A., Nakagawa, N., Ohtomo, A., Grazul, J. L. & Hwang, H. Y. Atomicscale imaging of nanoengineered oxygen vacancy profiles in $SrTiO_3$. Nature 430, 657-661 (2004).

25. Stö hr, J. NEXAFS Spectroscopy (Springer Berlin Heidelberg, 2010).

26. Hanzig, J. et al. Migration-induced field-stabilized polar phase in strontium titanate single crystals at room temperature. Phys. Rev. B 88, 024104 (2013).

27. Uwe, H., Yamaguchi, H. & Sakudo, T. Ferroelectric microregion in $KTa_{1-x}Nb_xO_3$ and $SrTiO_3$. Ferroelectrics 96, 123-126 (1989).

28. Ohtomo, A. & Hwang, H. Y. A high-mobility electron gas at the $LaAlO_3/SrTiO_3$ heterointer- face. Nature 427, 423-426 (2004).

29. Moser, S. et al. Tunable polaronic conduction in anatase TiO2. Phys. Rev. Lett. 110, 196403 (2013).

30. Baden, A. D. et al. Observation of surface optical phonons on $SrTiO_3$ (100). J. Phys. C 14, L1081-L1084 (1981).

31. Fuchs, R. & Kliewer, K. L. Optical modes of vibration in an ionic crystal slab. Phys. Rev. 140, A2076-A2088 (1965).

32. Wu, X. G., Peeters, F. M. & Devreese, J. T. Exact and approximate results for the ground-state energy of a Frö hlich polaron in two dimensions. Phys. Rev. B 31, 3420-3426 (1985).

33. Mori, N. & Ando, T. Electron-optical-phonon interaction in single and double heterostructures. Phys. Rev. B 40, 6175-6188 (1989).

34. Mahan, G. D. Many-Particle Physics (Springer, 2000).

35. Mishchenko, A. S., Prokof'ev, N. V., Sakamoto, A. & Svistunov, B. V. Diagrammatic quantum Monte Carlo study of the Fröhlich polaron. Phys. Rev. B 62, 6317-6336 (2000).

36. Peeters, F. M. & Devreese, J. T. Scaling relations between the two- and threedimensional polarons for static and dynamical properties. Phys. Rev. B 36, 4442-4445 (1987).

37. Shen, K. M. et al. Missing quasiparticles and the chemical potential puzzle in the doping evolution of the cuprate superconductors. Phys. Rev. Lett. 93, 267002 (2004).

38. Mannella, N. et al. Nodal quasiparticle in pseudogapped colossal magnetoresistive manganites. Nature 438, 474-478 (2005).

39. Plumb, N. C. et al. Mixed dimensionality of confined conducting electrons in the surface region of $SrTiO_3$. Phys. Rev. Lett. 113, 086801 (2014).

40. McKeown Walker, S. et al. Control of a two-dimensional electron gas on$SrTiO_3$ (111)by atomic oxygen. Phys. Rev. Lett. 113, 177601 (2014).

41. Chang, Y. J., Bostwick, A., Kim, Y. S., Horn, K. & Rotenberg, E. Structure and correlation effects in semiconducting $SrTiO_3$. Phys. Rev. B 81, 235109 (2010).

42. Takahashi, K. S. et al. Local switching of two-dimensional superconductivity using the ferro- electric field effect. Nature 441, 195-198 (2006).

43. Sachs, R., Lin, Z.S. & Shi, J. Ferroelectric-like SrTiO3 surface dipoles probed by graphene. Sci. Rep. 4, 3657 (2014).

44. Reyren, N. et al. Superconducting interfaces between insulating oxides. Science 317, 1196-1199 (2007).

45. Emin, D. Formation, motion, and high-temperature superconductivity of large bipolarons. Phys. Rev. Lett. 62, 1544-1547 (1989).

46. He, S. et al. Phase diagram and electronic indication of high-temperature superconductivity at 65 K in single-layer FeSe films. Nat. Mater. 12, 605-610 (2013).

47. Tan, S. et al. Interface-induced superconductivity and strain-dependent spin density waves in $FeSe/SrTiO_3$ thin films. Nat. Mater. 12, 634-640 (2013).

48. Ge, J. F. et al. Superconductivity above 100 K in single-layer FeSe films on doped $SrTiO_3$. Nat. Mater. 14, 285-289 (2015).

49. Verbist, G., Peeters, F. M. & Devreese, J. T. Extended stability region for large bipolarons through interaction with multiple phonon branches. Ferroelectrics 130, 27-34 (1992).

15 Application of the polaron-transport theory to $\sigma(\omega)$ in $Tl_2Ba_2Ca_{1-x}Gd_xCu_2O_8$, $YBa_2Cu_3O_{7-8}$, and $La_{2-x}Sr_xCuO_4$ by Mihailovic, Foster, Voss, Heeger

Abstract

We analyze the frequency-dependent photoinduced infrared conductivity, $\sigma_P(\omega)$, obtained from photoinduced absorption measurements of the insulators $Tl_2Ba_2Ca_{0.98}Gd_{0.02}Cu_2O_8$, $YBa_2Cu_3O_{6.3}$, and La_2CuO_4 in terms of $\sigma_{\mathrm{PT}}(\omega)$ calculated from nonadiabatic polaron-transport theory. The calculated $\sigma_{\mathrm{PT}}(\omega)$ is in good agreement with the experimental $\sigma_P(\omega)$ in the midinfrared. We also compare $\sigma_P(\omega)$ with the infrared conductivity, $\sigma(\omega)$, of the high- T_c superconductors $Tl_2Ba_2CaCu_2O_8$, $YBa_2Cu_3O_7$, and $La_{1.85}Sr_{0.15}CuO_4$. The similar spectral shape and systematic trends in both $\sigma_P(\omega)$ and $\sigma(\omega)$ indicate that the carriers in the concentrated (metallic) regime retain much of the character of the carriers in the dilute (photoexcited) regime. Together, these results imply that in the superconducting cuprates and in their "parent" insulators, the carriers are polarons dressed with a phonon polarization cloud.

15.0.1 I. Introduction

An extensive body of infrared reflectance data has established that the normal-state frequency-dependent conductivity $\sigma(\omega)$ of the high-temperature superconductors, $Tl_2Ba_2CaCu_2O_8, YBa_2Cu_3O_7$, and $La_{1.85}Sr_{0.15}CuO_4$ consists of a narrow, temperature-dependent, Drude-like peak centered at zero frequency, and a broad, temperature-independent excitation in the midinfrared, the so-called "mid-ir" feature. [1–5] The systematic appearance of the mid-ir feature in $\sigma(\omega)$ and the direct correlation of its intensity with doping has been established experimentally for many perovskites (including Ba_{1-x} $Pb_xBiO_3, La_{2-x}Sr_xNiO_4, SrTiO_3$, and $BaTiO_3$) .[6–9] In the cuprate perovskites, similar correlations exist between the mid-ir peak and high-temperature superconductivity at moderate doping levels (less than $\approx$ 0.5 holes /Cu).[1] Further doping into a metallic phase reduces the intensity of the mid-ir feature [10] as well as T_c.[11,12] This close correspondence of the mid-ir intensity with T_c in cuprate perovskites suggests that the origin of $\sigma(\omega)$ in the mid-ir warrants further investigation, particularly in relation to the mechanism for high-temperature superconductivity.

The mid-ir feature in high- T_c superconductors has been interpreted by many groups. In the case of $YBa_2Cu_3O_{7-\delta}$, it has been attributed to a direct electronic transition distinct from the Drude-like free carrier contribution at low frequency, [2] to a contribution from free holes, but with an ω-dependent scattering rate arising from either a polaron shakeoff of dressed carriers (which are renormalized by strong interactions with phonons, spin waves, etc.), [2,4] or to an intrinsic ω dependence of the scattering mechanism. [3,13]

In systems which have large electronic bandwidth, carrier transport can be accurately described by adiabatic processes in which the crystal lattice is assumed to be
static with respect to carrier motion (i.e., the Drude model, Fermi liquid theory, etc.). In narrower band systems, carrier motion becomes nonadiabatic. When the sound velocity becomes comparable to the Fermi velocity, as has been shown to be the case in the cuprates, [14] carrier motion is intimately linked to lattice vibrations. In doped titanates, for example, $BaTiO_3$ and $SrTiO_3$, the origin of mid-ir features in $\sigma(\omega)$ and their relationship to transport mechanisms has been a subject of study for many years. [9,15–20] Both adiabatic and nonadiabatic mechanisms have been proposed for modeling the transport properties. The application of polaron transport theory (PTT), in which carriers move nonadiabatically with respect to the lattice, eventually proved successful as a model of carrier transport in these materials. [9,15–20]

In nonadiabatic PTT, carriers interact with both optical and acoustic phonons; the acoustic phonons determine the temperature-dependent contribution to $\sigma(\omega)$ near zero frequency [16] and the optical phonons give rise to a broad temperature-independent "shakeoff" peak in $\sigma(\omega)$ in the midinfrared for temperatures $T < T_D$, where T_D is the Debye temperature. [15,19,20] In addition to successfully describing the shape of the mid-ir peak in $\sigma(\omega)$ upon doping, [17,18] the model also correctly predicted the dc transport properties [16,18] of the doped titanates.

In this paper, we apply PTT as a model of the frequency-dependent transport process experimentally observed as the mid-ir features in $\sigma(\omega)$ in the high- T_c cuprates, restricting ourselves to carrier interactions with optical phonons. [15,17] The calculated $\sigma_{\rm PT}(\omega)$ is fit to the photoinduced infrared conductivity, $\sigma_P(\omega)$, obtained from photoinduced absorption (PIA) measurements of the insulating precursor materials, [21–24] where the carrier concentration is in the dilute limit and carrier-carrier interactions are thus assumed to be negligible. These spectra are compared to the infrared conductivity $\sigma(\omega)$ obtained from Kramers-Kronig analysis of reflectivity mea-
surements in the doped, metallic (superconducting) materials. The similar spectral shape and consistent trend toward lower energy of the mid-ir peak in both $\sigma_p(\omega)$ and $\sigma(\omega)$ indicate that carriers in the concentrated (metallic) regime retain much of the character of carriers in the dilute (photoexcited) regime. We conclude that the mid-ir absorption in

$Tl_2Ba_2CaCu_2O_8$, $YBa_2Cu_3O_{7-\delta}$, and La_2CuO_4 can be assigned to nonadiabatic polaron (or possibly bipolaron) transport and suggest that the differences between $\sigma_P(\omega)$ and $\sigma(\omega)$ can be attributed to the onset of carrier-carrier interactions in the concentrated regime. Since we cannot make any experimental distinction between polaron or bipolaron transport, we refer to the carriers simply as polarons.

15.0.2 II. Calculation of $\sigma(\omega)$ and Comparison with Experimental Results

The theoretical treatment of polaron transport is based on Holstein's molecular crystal Hamiltonian; [25]$\sigma_{\rm PT}(\omega)$ is calculated [15,16,19] in both the low-temperature ($T \to 0$) and high-temperature limit ($k_BT > \omega_D/2$), where ω_D is the Debye frequency and k_B is Boltzmann's constant. The $\sigma_{\rm PT}(\omega)$ spectrum reflects the shakeoff of the optical phonon cloud (the localized distortion) from the polaron as a result of nonadiabatic transport from site to site, with the peak [19] in the spectrum corresponding approximately to $2E_b$, where E_b is the polaron binding energy. Whereas the original calculation was done by Reik [15,17] in the limit of strong coupling, [i.e., with $(2E_b/k_BT)\,(a/r)^3 \gg 1$, where k_B is Boltzmann's constant, a is the lattice constant, and r is the polaron radius], the theory has been extended by Emin [19] to the weak-coupling regime to include large polarons where the range of the polaron extends beyond one unit cell.

In PTT, the polarons are considered as noninteracting particles [15−20] in the dilute limit. We can probe the transport of such isolated carriers by measurements of $\sigma_P(\omega)$, and we can probe the transport of carriers in the concentrated regime from measurements of $\sigma(\omega)$. However, we expect departures from the theoretically calculated $\sigma_{\rm PT}(\omega)$ in a system with a high density of carriers exhibiting collective phenomena (e.g., superconductivity), as is the case in the high- T_c cuprates where $\sigma(\omega)$ is the response of the carriers at a density in the range of $0.1 - 0.5$ per unit cell.

In the PIA technique, $\sigma_P(\omega)$ is derived from $(-\Delta T/T)$ of the insulating precursor compounds of the same materials, where T is the transmission, and ΔT is the change in transmission upon photoexcitation with weak laser light ($\cong 40$ mW/cm^2). In the insulator limit, where $\epsilon_1 \gg \epsilon_2$, the photoinduced infrared conductivity $\sigma_P(\omega)$ is related to $-\Delta T/T$ by

$$\sigma_P(\omega) = (nc/4\pi d)(-\Delta T/T)$$

where $n = \sqrt{\epsilon_1}$ is the refractive index, d is the absorption length, and c is the speed of light. The response of the system in the dilute limit, $\sigma_P(\omega)$, should correspond closely to the idealized theoretical model. Thus we compare $\sigma_P(\omega)$ with the predictions of PTT. We fit $\sigma_{\rm PT}(\omega)$ to the mid-ir $\sigma_P(\omega)$ in $Tl_2Ba_2Ca_{0.98}Gd_{0.02}Cu_2O_8$, [23]$YBa_2Cu_3O_{6.3}$, [22] and La_2CuO_4.[21] This approach is justified because of the observation of infrared active vibrational features in the PIA (which imply the existence of localized lattice distortions) and because the experimentally determined effective masses in the cuprates [21−24] (see Table I) are similar to the titanates ($3 < m^*/m_e < 30$) (Refs. 9 and 26) and thus suggest polaron formation.

The frequency-dependent conductivity $\sigma_{\rm PT}(\omega, T \to 0)$ in the low-temperature limit is given by [15,17]

$$\sigma_{\mathbf{PT}}(\omega, T \to 0) = \frac{\sqrt{2\pi}t^2e^2N}{\hbar^3\omega_0^2} e^{-\eta} \left(\frac{\omega_0}{\omega}\right)^{(\omega/\omega_0+2/3)} e^{(\omega/\omega_0)}\eta^{\omega/\omega_0} \tag{1}$$

where η is the number of phonons in the polaron polarization cloud, ω_0 is an averaged phonon frequency, t is the electronic resonance overlap integral, $\hbar$ is Planck's constant, and N

is the number density of carriers of charge e; η and ω_0 are parameters describing the electron-phonon interaction and are related to the electron-phonon coupling constant $\alpha_j(\mathbf{q})$ through the relations

$$\omega_0 = \frac{\sum_{j,q} \alpha_j(\mathbf{q}) \sin^2\left(\frac{1}{2}q\right) \omega_j^2(\mathbf{q})}{\sum_{j,q} \alpha_j(\mathbf{q}) \sin^2\left(\frac{1}{2}q\right) \omega_j(\mathbf{q})} \tag{2}$$

and

$$\eta = \frac{1}{\omega_0} \sum_{j,q} 2\alpha_j(\mathbf{q}) \sin^2\left(\frac{1}{2}q\right) \omega_j(\mathbf{q}) \tag{3}$$

with the sum over the wave vector $\mathbf{q}$ of the j th optical phonon branch. The characteristic frequency ω_0 represents an averaged phonon frequency involved in the carrier hopping, weighted by the electron-phonon interaction $\alpha_j(\mathbf{q})$. If the phonon dispersion is not too large, formula (3) can be approximated by the more familiar form, [17]

$$\eta \approx \sum_{j,q} 2\alpha_j(\mathbf{q}) \sin^2\left(\frac{1}{2}q\right) \tag{4}$$

which represents a weighted average of $\alpha_j(\mathbf{q})$ over the Brillouin zone. The two parameters η and ω_0 essentially determine the shape of the spectrum, and the prefactor is a constant proportional to the square of t.

The dashed curves in Fig. 1 show the calculated $\sigma_{\mathrm{PT}}(\omega)$ [Eq. (1)] using the parameters η and ω_0 listed in Table I. The fits to $\sigma_P(\omega)$ for $Tl_2Ba_2CaCu_2O_8$ and $YBa_2Cu_3O_{7-\delta}$ [Figs. 1(a) and 1(b)] are excellent over the entire frequency range. The value of $\omega_0 = 200$ cm^{-1} is

TABLE I. Effective masses and parameters describing the electron-phonon interaction.

	m^*/m_e	η	ω_0 (cm^{-1})
$La_{2-x}Sr_xCuO_4$	23	10	450
$YBa_2Cu_3O_7$	13	7	200
$Tl_2Ba_2CaCu_2O_8$	11	5.6	200

consistent with calculated values of $\alpha_j(\mathbf{q})$ obtained recently from a linearized-augmented-plane-wave calculation [27] for $YBa_2Cu_3O_{7-\delta}$ as well as with experimental evidence for strong coupling of the low-frequency modes from infrared spectroscopy. [28] In addition to the polaron shakeoff, we observe structure from photoinduced localized phonon modes in all three systems; for $Tl_2Ba_2CaCu_2O_8$ and $YBa_2Cu_3O_{7-\delta}$, they [21–24] distort the low-frequency edge of the peak in $\sigma_P(\omega)$. These vibrational modes are not described by Eqs. (1)-(3) (which are valid only above $\omega > \omega_D/2$) and will therefore be discussed elsewhere. In La_2CuO_4, the fit is good for $\omega > 3000$ cm^{-1}. The deviations at lower frequency possibly arise from the fact that the La_2CuO_4 PIA experiments [21] were carried out before highest quality materials were available.

In agreement with polaron theory, the values of η and ω_0 obtained from the theoretical fits for the three systems scale with the polaron effective masses obtained from the PIA data [24] (see Table I) reflecting a trend in $\alpha_j(\mathbf{q})$. In addition, as η and ω_0 (and the effective mass) decrease, T_c of the system increases. We have previously shown [24] that T_c is inversely proportional to m^* for the cuprates. This behavior is consistent with theories of bipolaronic super-

conductivity which predict $k_B T_c \cong \hbar^2 n^{2/3} m^*$ (Ref. 29), where n is the number of bipolarons of effective mass m^*.

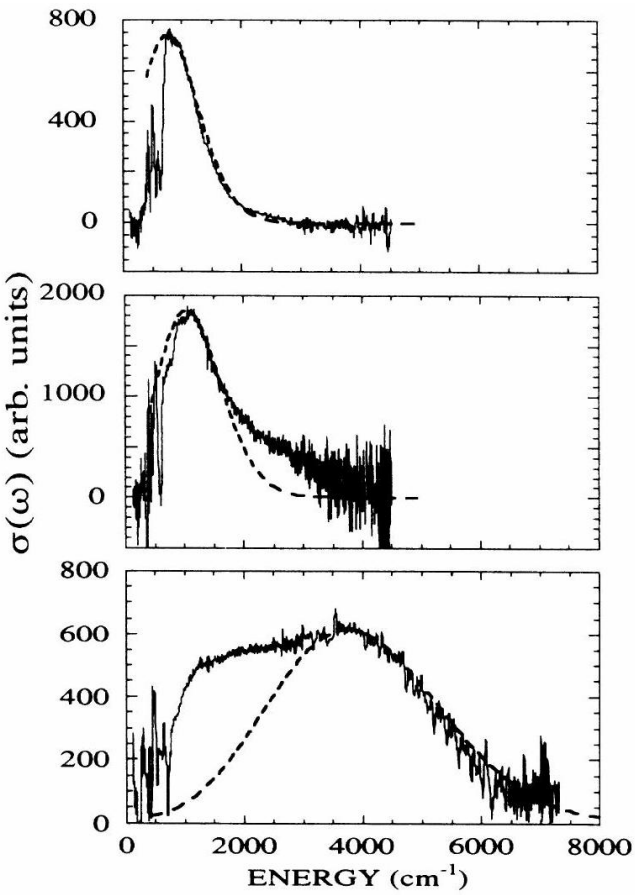

FIG. 1. The photoinduced infrared conductivity $\sigma_{P (\omega)$ (solid lines) in the insulator precursors for $Tl_2Ba_2CaCu_2O_8$ (top), $YBa_2Cu_3O_7$ (middle), and $La_{2-x}Sr_xCuO_3$ (bottom) compared with fits to polaron-transport theory $\sigma_{\rm PT}(\omega)$ as calculated using Eq. (1) (dashed lines).}

In Fig. 2, we compare the frequency-dependent conductivity $\sigma(\omega)$, obtained from reflectivity measurements of $Tl_2Ba_2CaCu_2O_8$ thin films [4] ($T_c = 100$ K), $YBa_2Cu_3O_7$ single crystals [5] ($T_c = 90$ K), and $La_{2-x}Sr_xCuO_4$ ceramic samples [30] ($T_c = 35$ K), with the photoinduced infrared conductivity $\sigma_P(\omega)$. The similar spectral shape and the consistent trend of the mid-ir peak toward lower energy in both $\sigma_P(\omega)$ and $\sigma(\omega)$ indicate that carriers in the concentrated (metallic) regime retain much of the character of carriers in the dilute (photoexcited) regime.

15.0.3 III. Discussion

A number of qualitative observations follow from the comparison of $\sigma(\omega)$ and $\sigma_P(\omega)$:
(i) In all perovskites exhibiting superconductivity, the peak energy in both $\sigma(\omega)$ and $\sigma_P(\omega)$ shifts toward lower energy as T_c of the material increases; from $\cong$ 1.2eV (12000 cm^{-1}) in Ba_{1-x} Pb_xBiO_3(Refs. 6 and 31) to $\simeq$ 0.5eV (4000 cm^{-1}) in $La_{2-x}Sr_xCuO_4$ (Refs. 1, 21, and 30) to 0.13eV (1300 cm^{-1}) in $YBa_2Cu_3O_7$(Refs. 1-3, 5, and 22) and to 0.09eV (950 cm^{-1}) in $Tl_2Ba_2CaCu_2O_8$ (Refs. 4 and
23) (see Table II).
(ii) The concurrent shift in energy of both $\sigma(\omega)$ and $\sigma_P(\omega)$ from system to system implies that both are intrinsic features of the frequency-dependent conductivity and that the origin of the mid-ir feature is the same in both the dilute and concentrated limits.
(iii) The primary difference between $\sigma_P(\omega)$ (the dilute limit) and $\sigma(\omega)$ (the concentrated limit)

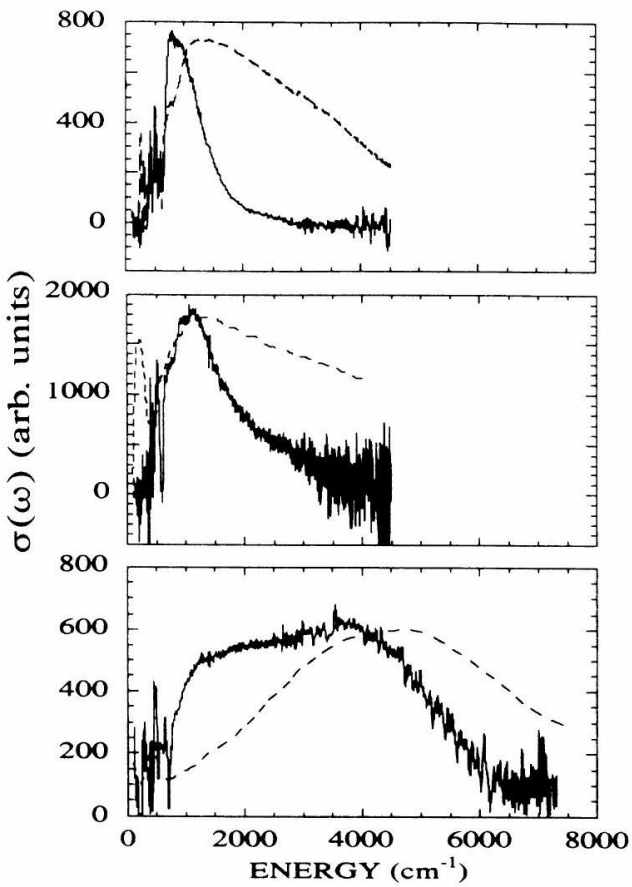

FIG. 2. The infrared conductivity $\sigma(\omega)$ (dashed lines) for $\mathrm{Tl *{2} \mathrm{Ba}*{2} \mathrm{CaCu}*{2} \mathrm{O}*{8}$ (top), $YBa_2Cu_3O_7$ (middle), and $La_{2-x}Sr_xCuO_4$ (bottom) compared with the photoinduced infrared conductivity $\sigma_P(\omega)$ (solid lines) in their respective insulator precursors.}

is the broadening of the mid-ir peak which we expect to occur as the carrier concentration increases to a level at which the exclusion principle and polaron-polaron interactions become important.

The differences between the experimental spectra obtained in the concentrated and the dilute limits (Fig. 2) imply that polaron-transport theory ceases to provide an accurate description of $\sigma(\omega)$ in the concentrated limit and emphasizes the need for generalization of the PTT to the concentrated regime appropriate to the metallic phases of the high- T_c cuprates.

In a given cuprate system, the energy of the mid-ir peak shifts only slightly to higher energy with increased carrier concentration. However, the intensity of the mid-ir peak significantly increases until the maximum T_c is reached at approximately $0.12 - 0.25$ holes /Cu.[1,11,30] A similar dependence of $\sigma(\omega)$ and T_c with doping concentration is seen in the titanates and bismuthates. [6,8,9] Recent data on $La_{2-x}Sr_xCuO_4$ show that upon further doping into the metallic region $(x > 0.2), T_c$ decreases [10,12] concurrent with a reduction of the intensity of the mid-ir feature. Table II compares the energy ($\approx 2E_b$) of the mid-ir peak and T_c for some cuprate, titanate, and bismuthate superconductors.

In the present analysis, we have not explicitly considered the effect of spin-wave "shakeoff" resulting from coupling of carriers to spin excitations (rather than phonons) as a source of $\sigma(\omega)$ in the mid-ir. The similarity of the line shapes of the $\sigma(\omega)$ spectra and the two-magnon spectra observed in Raman scattering of $Tl_2Ba_2CaCu_2O_8$, [32] $YBa_2Cu_3O_{7-\delta}$, [33] and La_2CuO_4 (Ref. 34) suggest that spin-polaron shakeoff might provide a contribution. A strong spin-

lattice interaction has recently been suggested by the temperature dependence of the two-magnon relaxation [35] via coupling to the lattice as inferred from Raman scattering experiments. However, since the electron-phonon interaction arises from the spatial dependence of the transfer integral t, it is expected to be larger than the spin-phonon interaction which originates in the spatial dependence of $d \cong t^2/4U$, where d is the magnetic coupling and U is the on-site Coulomb interaction strength. [36] Thus, any contribution to $\sigma(\omega)$ arising from magnon shakeoff should be significantly weaker

TABLE II. Critical temperatures and values of the mid-ir peak position in superconducting perovskites.

	T_c(K)	Mid-ir peak (eV)
$SrTiO_3$	0.3[8]	> 1[8]
Ba_{1-x} Pb_xBiO_3	13[6]	1.2[6]
La_2CuO_4	34	0.5
$YBa_2Cu_3O_7$	93	0.13
$Tl_2Ba_2CaCu_2O_8$	110	0.09

than the direct contribution to $\sigma(\omega)$ arising from electron-phonon coupling.

We have not discussed in detail the low-frequency, temperature-dependent part of the $\sigma(\omega)$ spectra, [1–5] which has been attributed to free carriers scattering in the weak-coupling limit of a quasimetallic system. In the context of polaron transport theory, these free carriers are dressed polarons with dc transport lifetime (and mean free path) limited by acoustic mode scattering for $k_BT < \hbar\omega_D$ and by a combination of acoustic and optical-mode scattering at higher temperatures.

15.0.4 IV. Conclusion

We conclude that the photoinduced infrared conductivity of dilute carriers photoinjected into $Tl_2Ba_2CaCu_2O_8$, $YBa_2Cu_3O_{7-\delta}$, and La_2CuO_4 is well described by nonadiabatic polaron hopping (polarontransport theory). The similar spectral shape and systematic trends in both $\sigma_P(\omega)$ and $\sigma(\omega)$ indicate that carriers in the concentrated (metallic) regime retain much of the character of carriers in the dilute (photoexcited) regime implying that the charge carriers in the normal state of high- T_c cuprates are polarons or bipolarons. This is in a general sense consistent with the evidence of ferroelectric distortions (doping-induced distortions correlated from cell to cell) in the high T_c cuprates. [37] Furthermore, the absence of a shift [2,4] in the mid-ir feature in $\sigma(\omega)$ at the superconducting transition suggests that if bipolaronic superconductivity is present in the cuprates, bipolarons are formed above T_c.

16 Holstein polaron in a valley-degenerate two-dimensional semiconductor by Kang, Jung, Shin, Sohn, Ryu, Kim, Hoesch, Kim

Two-dimensional (2D) crystals have emerged as a class of materials with tuneable carrier density [1]. Carrier doping to 2D semiconductors can be used to modulate manybody interactions [2] and to explore novel composite particles. Holstein polaron is a small composite particle of an electron carrying a cloud of self-induced lattice deformation (or phonons) [3–5], which has been proposed to play a key role in high-temperature superconductivity [6] and carrier mobility

in devices [7]. Here, we report the discovery of Holstein polarons in a surface-doped layered semiconductor, MoS_2, where a puzzling 2D superconducting dome with the critical temperature of **12 K** was found recently [8–11]. Using a high-resolution band mapping of charge carriers, we found strong band renormalizations collectively identified as a hitherto unobserved spectral function of Holstein polarons [12–18]. The unexpected short-range nature of electron-phonon ($e-ph$) coupling in MoS_2 can be explained by its valley degeneracy that enables strong intervalley coupling mediated by acoustic phonons. The coupling strength is found to gradually increase along the superconducting dome up to the intermediate regime, suggesting bipolaronic pairing in 2D superconductivity.

A key to understanding the dynamics of polarons is their spectral function that has been studied with two standard models, Frölich polaron [4] and Holstein polaron [5]. The latter is a more realistic lattice model for polarons whose spatial extent can be either short-ranged within few atoms (small polaron with the $e-ph$ coupling constant $\lambda > 1$) or long-ranged over several atoms (large polaron with $\lambda < 1$). Even this simple model is difficult to solve analytically, and the perturbation theory fails to account for the important intermediate regime ($\lambda \sim 1$) between small and large polarons. It was only recently that the spectral function of Holstein polaron at $\lambda \sim 1$ was successfully calculated in a nonperturbative manner by means of different theoretical techniques [12–18]. They have commonly predicted that electrons in a parabolic band (dotted lines in Fig. 1b) are scattered by the n number of phonons to form $e+n-ph$ continuums (orange and green regions). The state mixing with these continuums makes the parabolic band be separated into a series of sub-bands,
which is accompanied by small gaps and flatting of dispersion at the integer multiple of phonon energy ($-n\Omega_0, n = 1, 2, 3, \ldots$). The spectral weight is suppressed for the flat parts, so that the simulated spectral function (Fig. 1c) appears to be a series of broken bands, which is distinct from conventional kink [19], peak-dip-hump [19–21], and shake-off replica [22–25]. This characteristic spectral function of Holstein polarons should be observable with the use of angle-resolved photoemission spectroscopy (ARPES), but so far has been studied only in ultracold atomic gases [26] due to the lack of a suitable material system.

On the other hand, $2H$ transition-metal dichalcogenides (TMDs) have continued to attract broad interest as a class of two-dimensional (2D) van-der-Waals semiconductors with valley degeneracy [27,28]. This valley degree of freedom opens a channel of strong coupling between electronic states at two inequivalent valleys (K and K ' in Fig. 1d) mediated by short-wavelength phonons (arrows) [27–30], which can potentially be used to study shortrange e-ph coupling. Furthermore, electron doping to the surface of bulk (or multilayer) TMDs was found to develop the superconducting dome [8]. The critical temperature (T_c) as high as 12 K , which is a record among TMDs, was reported in MoS_2 (refs. 8-11), making it ideal to explore a signature of strong electron-boson coupling. There have been ARPES experiments on bulk or multilayer TMDs whose surface layer is chemically doped by the deposition of alkali-metals atoms [31–34], a well-known technique to form 2D electric dipole layers [34] as in ionic liquid gating [8–11] (Supplementary Fig. S1). However, no clear signature of electron-boson coupling has been reported so far. In this study, we carefully optimized samples and experimental conditions to measure ARPES data at high-resolution settings (see Methods for details), which can be used to detect a band-renormalization effect.

Figure 1d gives an overview of the low-energy band structure of surface-doped MoS_2, where ARPES intensity (shown in blue) is plotted as a function of energy and momentum (k). There is a well-defined valence band (VB) whose vertex is located at the zone centre ($k = 0$). Upon the deposition of Rb atoms, the donated electrons are known to be confined mostly within the topmost MoS_2 layer [34,35], leading to the formation of 2D electron gas, which is essentially the same situation where the 2D superconductivity was observed [8–11] (Supplementary Fig. S1). The band structure in the surface 2D layer of MoS_2 is shifted to the higher binding energy

(Supplementary Fig. S2), and two minima of the conduction band (CB) appear below the Fermi energy (E_F) mainly at K and K′ points and partly at T points, the latter of which can be more clearly identified in the Fermi surface map (upper panels). The CB minimum located at the T point for pristine bulk MoS_2 is moved to the K point due to the electric field effect [10], which is in agreement with the previous reports [33–35]. Below, we will focus on the K valleys of CBs, where $e - ph$ coupling is found to be greater than at T points (Supplementary Fig. S3).

In a non-interacting picture, the local band structure of CBs at the K (or K′) point can be approximated by a simple parabola with the effective mass $m_0 = 0.85m_e$, where m_e is the electron rest mass. This is shown by our spectral simulations in Fig. 1c for $\lambda = 0$ (left).

However, a striking deviation from this picture is observed in ARPES spectra (Fig. 1e) taken with high-resolution settings and low sample temperature (Methods). Instead of a simple parabolic band, we find strong distortions of the parabolic band at two energies (dotted lines), leading to three broken bands indicated by red, yellow, and green arrows. This unusual rearrangement of states is uniformly observed in different k cuts about the K point (Supplementary Fig. S4), and not expected for structural and electrostatic origins, such as quantum confinement (Supplementary Fig. S5).

The spectral function of MoS_2 can be more closely examined with a series of energydistributions curves (EDCs) shown in Fig. 2a. Whereas only a single pole is expected for each EDC in a non-interacting picture, even raw EDCs at k_1 and k_2 clearly show multiple poles separated by small gaps, a signature of band renormalizations by strong coupling to bosonic modes or polarons [12,13]. A curve fit to each EDC yields peak positions marked by closed circles whose size is scaled with their spectral weight in Fig. 2a,b. Around each small gap (δ_1 and δ_2 in Fig. 2b), the dispersion of poles is anti-crossing each other, and connected to flat branches with little spectral weight (Fig. 2c and Supplementary Fig. S6). A close pair of flat branches asymptotically approaches to either δ_1 at -26 ± 3meV or δ_2 at -53 ± 3meV, which are uniformly spaced at $-n\Omega_0$, where $\Omega_0 = 26$meV. That is, the experimental spectral function consists of three characteristic sub-bands (shown in red, yellow, and green) as summarized in Fig. 2b.

In comparison to Fig. 1b, such a series of band renormalizations at $-n\Omega_0$ is the hitherto unobserved characteristic signature of Holstein polarons [12–18]. We employed a simple model of k-average approximation [17] to simulate the spectral function of Holstein polarons at $\lambda = 0.5$ (Fig. 1c and Supplementary Fig. S7), which successfully reproduces our experimental observations in Fig. 1e. This can be further corroborated by the same simulations that predict a series of flat dispersions at the onset of $e + n - ph$ continuums, albeit their weak spectral weight, to be observable, as shown in Fig. 2d. Such flat dispersions with a weak intensity are indeed observed in our experimental data taken for the corresponding region (Fig. 2e), which are marked by red, yellow, green, and blue arrows. The latter is more clearly seen in Fig. 2f as a shoulder structure at -78 ± 3meV or $-3\Omega_0$, and the energy of band renormalizations is confirmed again to be located at the integer multiple of Ω_0. Consequently, our experimental data (Figs. 1e and 2 e) collectively identify key aspects of the Holstein spectral function shown in Figs. 1b and 2b.

On the other hand, there is another flat feature near E_F marked by the red arrow in Fig. 2e, which is not shown in Fig. 2d. A possible origin of this difference is a small gap opening at E_F, which is further supported by the subtle flattening of dispersion near E_F in Fig. 2b and Supplementary Fig. S6. This gap may arise from the onset of superconductivity [8–11] or the correlation of many polarons [36], which are not included in our simulations in Fig. 2d.

A key clue to understand the mechanism of Holstein polarons in MoS_2 can be obtained from the involved boson mode. From its energy value $\Omega_0 = 26$meV, we identify this mode as longitudinal acoustic (LA) phonons near zone corners (K and K′), where its phonon dispersion is locally flat like that of optical phonons (Supplementary Fig. S8). This short-wavelength branch of LA phonons has been proposed to mediate strong coupling between CBs at two

valleys [27,29], as illustrated by arrows in Fig. 1b,d. Since the k range of flat phonon dispersion is much wider than $\pm k_{\mathrm{F}}$, this intervalley e-ph coupling can be reasonably approximated by the standard Holstein model. Therefore, the emergence of Holstein polarons in MoS_2 can be accounted for by short-range intervalley e-ph coupling as a natural consequence of its intrinsic valley degeneracy.

The important physical parameters of Holstein polarons can be quantified from the observed spectral function. A series of band renormalizations at $-n\Omega_0$ comes from mixing with an electron plus n-phonons continuums (Fig. 1b). The sub-bands whose energy is greater than Ω_0 (yellow and green in Fig. 2b) are excited states of the resonant character, whereas that smaller than Ω_0 corresponds to the polaron band (red). Along its dispersion, the spectral weight of poles in EDCs is plotted as a function of k in Fig. 2c, which is proportional to quasiparticle residue Z_k. It abruptly drops from 1 at the dispersive to 0 at the flat branch, signalling a crossover from the e-like to the ph-like character within a single polaron band [12−18]. A polaron dragging a cloud of phonons (Fig. 1a) becomes heavier, and a fit to the polaron band with a simple quadratic function yields the mass enhancement factor as $m^*/m_0 \sim 3$. Comparing m^*/m_0 to theoretical simulations (those in Fig. 1c), we can roughly estimate λ at 0.5 ± 0.1.

We now discuss the evolution of Holstein polarons with the doping density ρ. In Fig. 3a for low ρ, there is a narrow band with a broad tail toward the higher binging energy. Its EDC at k_{F} in Fig. 3c consists of the main peak (in red) followed by a series of shake-off replicas, whose energy position is evenly spaced at $-n\Omega_0$ and whose intensity follows the Poisson distribution. This spectral function has been reported as a signature of long-range e-ph coupling or Frölich polarons in anatase TiO_2 (ref. 22) and $SrTiO_3$ (refs. 24,25). The long-range $e-ph$ interaction is screened as the band width of filled states (W) exceeds Ω_0 (ref. 37), that is, the inverse adiabaticity ratio $W/\Omega_0 > 1$. In contrast to conventional kinks within the framework of Migdal-Eliashberg theory [19,22,25], the valley degeneracy of MoS_2 enables a channel of strong short-range e-ph coupling, leading to the remarkably distinct signature of Holstein polarons (Fig. 3b). In this regime, the energy position of δ_1 and δ_2 remains nearly unchanged with ρ at $-n\Omega_0$ and $\Omega_0 = 26 \pm 3$meV (dotted lines in Fig. 3d). This shows the dominance of intervalley coupling to the lower-energy dispersionless part of acoustic phonons rather than to optical phonons, as predicted in theory [38].

On the other hand, the magnitude of δ_1 and δ_2 progressively increases with ρ (Fig. 3d), suggesting the enhancement of short-range $e-ph$ coupling. The corresponding m^* of polarons (black lines) is plotted as a function of ρ in Fig. 4a. While m_0/m_{e} shows little dependence on ρ in contrast to that of long-range $e-ph$ coupling [25], m^*/m_0 increases by more than a factor of 5 , much greater than theoretical predictions for many polarons at constant λ (ref. 39). This is consistent with the calculated intervalley $e-ph$ coupling matrix that increases with k relative to the K point (dashed line in Fig. 4a) [29] $\cdot\lambda$ is estimated from m^*/m_0 to increase in the intermediate coupling regime ($\lambda = 0.5 \sim 0.8$), where the formation of bipolaron bound states is predicted [6]. Shown together in Fig. 4a is the superconducting dome in surface-doped MoS_2 (green area) reported using the ionic liquid gating [8−11]. Although its superconducting gap is too small ($3-4$meV) to be resolved by our experiments, ρ at which we find Holstein polarons of $\lambda = 0.5 \sim 0.8$ coincides with the onset of superconductivity.

These experimental findings suggest that intervalley coupling of polarons in exchange of acoustic phonons (bipolaronic coupling) may play a key role in the formation of Cooper pairs (Fig. 4b), which is compatible to the picture of intervalley singlet pairing [9,10]. Thus, our observation of Holstein polarons in MoS_2, along with the recent observations of its long-range counterparts in high- T_{c}FeSe/$SrTiO_3$ (ref. 23) and $SrTiO_3$ (refs. 24,25), should be carefully considered in further discussions and theoretical studies on the mechanism of superconductivity [8−11]. The observation of Holstein polarons in MoS_2 may also be useful in understanding carrier mobility and dynamics in MoS_2-based devices (valleytronics) [27,28].

16.0.1 References

1. Novoselov, K. S. et al. Electric field effect in atomically thin carbon films. Science 306, 666-669 (2004).

2. Li, L. J., O'Farrell, E. C. T., Loh, K. P., Eda, G., Ozyilmaz, B. & Castro Neto, A. H. Controlling many-body states by the electric-field effect in a two-dimensional material. Nature 529, 185-189 (2016).

3. Landau, L. D. On the motion of electrons in a crystal lattice. Phys. Z. Sowjetunion 3, 664 (1933).

4. Fröhlich, H. Electrons in lattice fields. Adv. Phys. 3, 325 (1954).

5. Holstein, T. Studies on polaron motion. Ann. Phys. 8, 343 (1959).

6. Alexandrov, A. S. Polarons in Advanced Materials (Springer, Dordrecht, 2007).

7. Hulea, I. N. et al. Tunable Fröhlich polarons in organic single-crystal transistors. Nat. Mater. 5, 982-986 (2006).

8. Ye, J. T. et al. Superconducting dome in a gate-tuned band insulator. Science 338, 1193-1196 (2012).

9. Lu, J. M. et al. Evidence for two-dimensional Ising superconductivity in gated MoS_2. Science 350, 1353-1357 (2015).

10. Saito, Y. et al. Superconductivity protected by spin-valley locking in ion-gated MoS_2. Nat. Phys. 12, 144-149 (2016).

11. Costanzo, D., Jo, S., Berger, H. & Morpurgo, A. F. Gate-induced superconductivity in atomically thin MoS_2 crystals. Nat. Nanotech. 11, 339-344 (2016).

12. Engelsberg, S. & Schrieffer, J. R. Coupled electron-phonon system. Phys. Rev. 131, 993 (1963).

13. Meden, V., Schönhammer, K. & Gunnarsson, O. Electron-phonon interaction in one dimension: exact spectral properties. Phys. Rev. B 50, 11179 (1994).

14. Wellein, G. & Fehske, H. Polaron band formation in the Holstein model. Phys. Rev. B56, 4513 (1997).

15. Bonča, J., Trugman, S. A. & Batistić, I. Holstein polaron. Phys. Rev. B 60, 1633 (1999).

16. Hohenadler, M., Aichhorn, M. & von der Linden, W. Spectral function of electronphonon models by cluster perturbation theory. Phys. Rev. B 68, 184304 (2003).

17. Goodvin, G. L., Berciu, M. & Sawatzky, G. A. Green's function of the Holstein polaron. Phys. Rev. B 74, 245104 (2006).

18. Berciu, M. & Sawatzky, G. A. Light polarons and bipolarons for a highly inhomogeneous electron-boson coupling. Eur. Phys. Lett. 81, 57008 (2008).

19. Damascelli, A., Hussain, Z. & Shen, Z. -X. Angle-resolved photoemission studies of the cuprate superconductors. Rev. Mod. Phys. 75, 473 (2003).

20. Perfetti, L. et al. Mobile small polarons and the Peierls transition in the quasi-onedimensional conductor $K_{0.3}MoO_3$. Phys. Rev. B 66, 075107 (2002).

21. Shen, K. M. et al. Angle-resolved photoemission studies of lattice polaron formation in the cuprate $Ca_2CuO_2Cl_2$. Phys. Rev. B 75, 075115 (2007).

22. Moser, S. et al. Tunable polaronic conduction in anatase TiO_2. Phys. Rev. Lett. 110, 196403 (2013).

23. Lee, J. J. et al. Interfacial mode coupling as the origin of the enhancement of T_c in FeSe films on $SrTiO_3$. Nature 515, 245-248 (2014).

24. Chen, C., Avila, J., Frantzeskakis, E., Levy, A. & Asensio, M. C. Observation of a two-dimensional liquid of Fröhlich polarons at the bare $SrTiO_3$ surface. Nat. Commun. 6, 8585 (2015).

25. Wang, Z. et al. Tailoring the nature and strength of electron-phonon interactions in the $SrTiO_3$(001) 2D electron liquid. Nat. Mater. 15, 835-839 (2016).

26. Koschorreck, M. et al. Attractive and repulsive Fermi polarons in two dimensions. Nature 485, 619-622 (2012).

27. Zeng, H., Dai, J., Yao, W., Xiao, D. & Cui, X. Valley polarization in MoS $_2$ monolayers by optical pumping. Nat. Nanotech. 7, 490-493 (2012).

28. Mak, K. F., He, K., Shan, J. & Heinz, T. F. Nat. Nanotechnol. 7, 494-498 (2012).

29. Kaasbjerg, K., Thygesen, K. S. & Jacobsen, K. W. Phonon-limited mobility in n-type single-layer MoS_2 from first principles. Phys. Rev. B 85, 115317 (2012).

30. Yu, P. Y. & Cardona, M. Fundamentals of Semiconductors 4th Ed. (Springer, Heidelberg, 2010).

31. Eknapakul, T. et al. Electronic structure of a quasi-freestanding MoS_2 monolayer. Nano Lett. 14, 1312 (2014).

32. Zhang, Y. et al. Direct observation of the transition from indirect to direct bandgap in atomically thin epitaxial MoSe 2 . Nat. Nanotechnol. 9, 111-115 (2014).

33. Riley, J. M. et al. Negative electronic compressibility and tunable spin splitting in WSe_2. Nat. Nanotechnol. 10, 1043-1047 (2015).

34. Kang, M. et al. Universal mechanism of band-gap engineering in transition-metal dichalcogenides. Nano Lett. 17, 1610 (2017).

35. Brumme, T., Calandra, M. & Mauri, F. First-principles theory of field-effect doping in transition-metal dichalcogenides: Structural properties, electronic structure, Hall coefficient, and electrical conductivity. Phys. Rev. B 91, 155436 (2015).

36. Hohenadler, M., Neuber, D., von der Linden, W., Wellein, G., Loos, J. & Fehske, H. Photoemission spectra of many-polaron systems. Phys. Rev. B 71, 245111 (2005).

37. Verdi, C., Caruso, F. & Giustino, F. Origin of crossover from polarons to Fermi liquids in transition metal oxides. Nat. Commun. 8, 15769 (2017).

38. Covaci, L. & Berciu, M. Holstein polaron: the effect of coupling to multiple-phonon modes. Eur. Phys. Lett. 80, 67001 (2007).

39. Mishchenko, A. S., Nagaosa, N. & Prokof'ev, N. Diagrammatic Monte Carlo method for many-polaron problems. Phys. Rev. Lett. 113, 166402 (2014).

40. Covaci, L. & Berciu M. Polaron formation in the presence of Rashba spin-orbit coupling: Implications for spintronics. Phys. Rev. Lett. 102, 186403 (2009).

16.0.2 Additional Information

Supplementary information is available for this paper at.
Reprints and permissions information is available at www.nature.com/reprints.
Correspondence and requests for materials should be addressed to K.S.K.
Publisher's note: Springer Nature remains neutral with regard to jurisdictional claims in published maps and institutional affiliations.

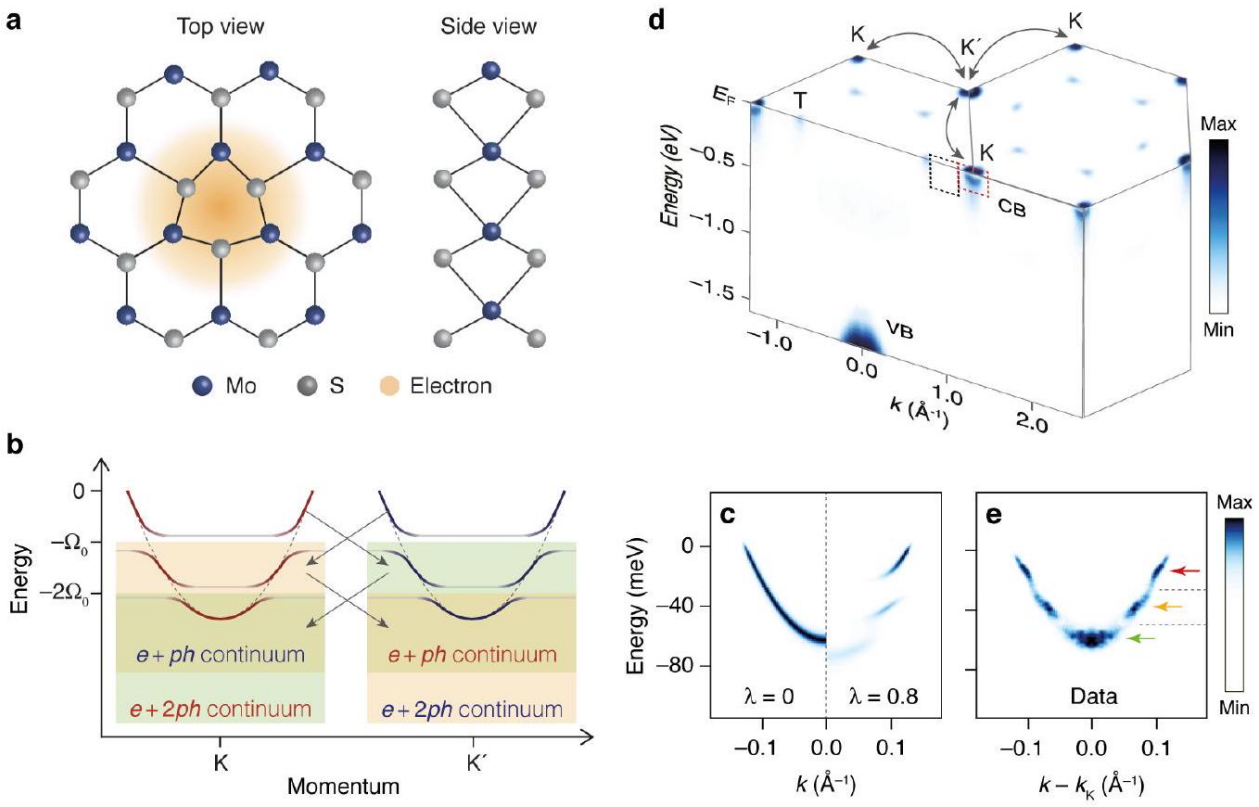

Figure 1 | Holstein polaron of $\mathbf{MoS_2}$. a, Schematic illustration of a polaron, an electron carrying its surrounding lattice deformation, in MoS_2.**b**, Energy spectrum of Holstein polarons in MoS_2 resulting from strong coupling between K and K′ valleys mediated by phonons (arrows). Dotted lines are the dispersion of bare bands in a non-interacting picture. Red and blue lines represent the electron character with $Z_k \sim 1$, whereas the thinner gray lines represent the phonon character with $Z_k \sim 0$. c, Simulated spectral function of Holstein polarons with zero ($\lambda = 0$) and intermediate ($\lambda = 0.5$)e-ph coupling based on k-average approximation (Methods) [17]. d, 3D representation of ARPES spectra taken for MoS_2 doped with Rb atoms at $\rho = 5 \times 10^{13}$ cm^{-2}. The photon energy was 54 eV , and the sample temperature was 80 K.**e**, High-resolution ARPES data taken at the region enclosed by the red dashed box in **d** and symmetrized with respect to the K point. Dotted lines indicate the energy position of gaps, while red, yellow, and green arrows indicate a series of sub-bands.

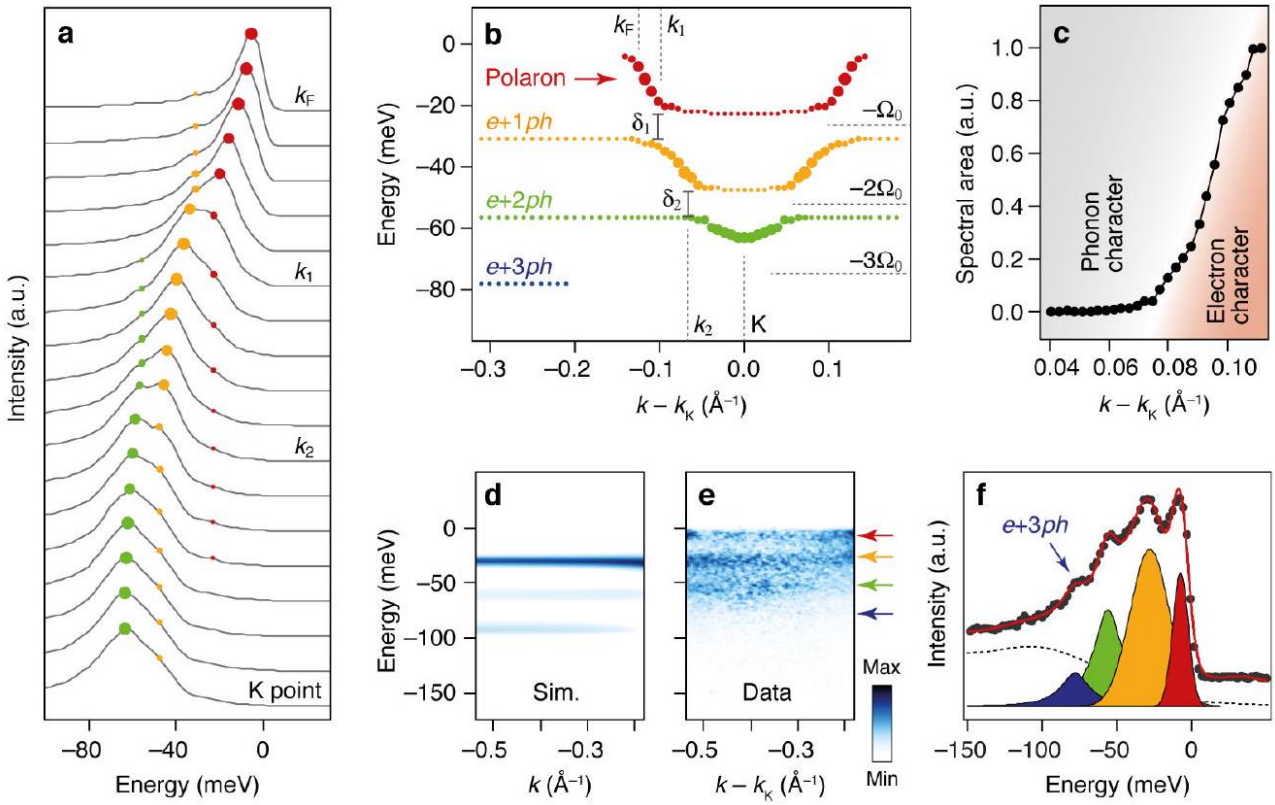

Figure 2 | Spectral function of Holstein polarons. a, Series of EDCs at k ranging from the K point to the Fermi momentum (k_F) with 0.007Å^{-1} steps. Closed circles mark the peak positions of three sub-bands shown in Fig. 1e, and their size is roughly proportional to the spectral weight. **b**, Energy position of poles plotted as a function of k.δ_n is an anticrossing gap at $-n\Omega_0$ and k_n. c, Spectral area of peaks plotted as a function of k along the polaron dispersion shown in red in **b**, which is proportional to Z_k. **d**, Simulated spectral function at $\lambda = 0.5$ for the region of flat dispersions in **b** (Methods) [17]. **e**, High-resolution ARPES data taken for the region enclosed by the black dashed box between the T and K points in Fig. 1d, which is the same region as in **d**. Red, yellow, green, and blue arrows indicate the energy position of flat sub-bands shown in the corresponding colour in **b**.**f**, k-integrated EDC of data shown in e. Red line overlaid is the best fit with a background (dotted line) and four components shown in corresponding colours with the arrows in **e**.

16.0.3 Methods

Samples and chemical doping. Single-crystal MoS_2 (99.995%, HQ Graphene) were glued by silver epoxy to sample holders, and cleaved in vacuum chambers with base pressure better than 4×10^{-11} torr. The high crystal quality of samples was confirmed from the extremely narrow spectral width as shown in Supplementary Fig. S2. Surface doping was achieved by the in situ deposition of alkali metals on the surface of MoS_2 using commercial dispensers (SAES). To avoid intercalation, we chose Rb deposited on MoS_2 samples kept under 30 K (refs. 31-34). A Rb atom on MoS_2 donates charges mostly to the topmost layer, leading to the formation of 2D dipole layers or electric double layers [34,35]. This is essentially the same mechanism as in the ionic liquid gating (Supplementary Fig S1), which is also accompanied by interlayer symmetry breaking. The signature of interlayer symmetry breaking was clearly observed in Supplementary Fig. S2, ruling out the possibility of intercalation that would generate only the doping effect with no strong interlayer symmetry breaking. The electron density at the surface

layer of MoS_2 is approximately estimated from the area enclosed by Fermi contours at E_F based on Luttinger's theorem.

ARPES experiments. We carried out ARPES measurements at two synchrotron radiations, Beamline I05 in the Diamond Light Source and at Beamline 7.0.2 in the Advance Light Source. ARPES end-stations are equipped with R4000 hemispherical electron analysers. The photon energy was used in the range of 46 $\sim$ 104eV, and 54 eV was chosen for the maximal yield of photoelectrons. The light polarization was set to be either linear (horizontal or vertical) or circular, but we found essentially the same results, as shown in Supplementary Fig. S4. We have optimized samples, photon energy, and photoexcitation cross-section to achieve an unusually high yield of photoelectrons. This allows us to have enough photoelectrons to measure at high-resolution analyzer settings (more specifically, the analyzer slit of 0.1 mm). Owing to this level of energy resolution, the key signature of Holstein polaron (Fig. 1b) could be clearly observed even in raw data (Figs. 1e and 2e) even without taking any background subtraction or second derivatives.

Spectral function analysis. To estimate physical parameters of Holstein polarons, we performed a systematic and quantitative analysis to a series of EDCs ranging from the K point to k_F (Fig. 2a and Supplementary Fig. S4). A fit to each EDC with multiple peaks (whose line shape is set to the Voight function, the use of either Lorentzian or Gaussian functions makes little difference) yields their energy positions (Fig. 2b) and spectral weight (Fig. 2c). The energy position of peaks is shown by closed circles, whose size is roughly proportional to their spectral weight in Fig. 2a,b. A fit to the bottom energy and $\pm k_F$ of CBs in Fig. 3d with a single quadratic function yields the effective mass of bare electrons m_0/m_e (blue circles in Fig. 4a). On the other hand, the same fit to only those shown in red in Fig. 3d yields the mass enhancement of polarons (red circles in Fig. 4a). A fit to the k-integrated EDC (the red curve in Fig. 2f) with a series of peaks yields their energy positions at $-n\Omega_0$, where $\Omega_0 = 26 \pm 3$meV. The relative intensity of satellite peaks ($n = 2, 3, \ldots$) to the main peak ($n = 1$) is additionally restricted to have the characteristic Poisson distribution as ${a_c}^{2n}/n!$ ($a_c =$ constant) in the fit to the EDC at k_F in Fig. 3c.

Spectral function simulations. To calculate the spectral function of Holstein polarons, we employed an efficient analytical model called the k-average (MA) approximation [17]. This model is based on the standard Hamiltonian that describes an electron interacting with a dispersionless phonon mode, that is, the Holstein polaron. For simplicity, we chose the 1D model, in which the k-averaged self-energy Σ_{MA} over the Brillouin zone is simplified as

$$\Sigma_{MA}(\omega) = \frac{g^2\Omega_0\bar{g}_0\,(\omega - \Omega_0)}{1 - \frac{2g^2\bar{g}_0(\omega-\Omega_0)\bar{g}_0(\omega-2\Omega_0)}{1-\frac{3g^2\bar{g}_0(\omega-2\Omega_0)\bar{g}_0(\omega-3\Omega_0)}{1-\cdots}}}$$

$$\bar{g}_0(\omega) = \frac{\mathrm{sgn}(\omega)}{\sqrt{(\omega + i\eta)^2 - 4t^2}}$$

where ω is the energy, Ω_0 is the photon energy taken from experimental data as 26 meV , $g^2 = 2t\Omega_0\lambda$, and t is the hopping amplitude. This k-averaged Σ_{MA} is taken to calculate the Green function as

$$G(k,\omega) = \frac{1}{\omega - E_k - \Sigma_{MA}(\omega) + i\eta}$$

where E_k is the dispersion of the bare (undressed) band obtained from experimental data (Fig. 1e) as $m_0 = 0.85m_e$ and $k_F = \pm 0.12\text{Å}^{-1}$. By taking the imaginary part of $G(k,\omega)$, we calculated the single-particle spectral function $A(k,\omega)$ as a function of $\lambda.\lambda$ is set to 0 for the non-interacting case and 0.5 $\sim$ 1.0 for the intermediate coupling regime.

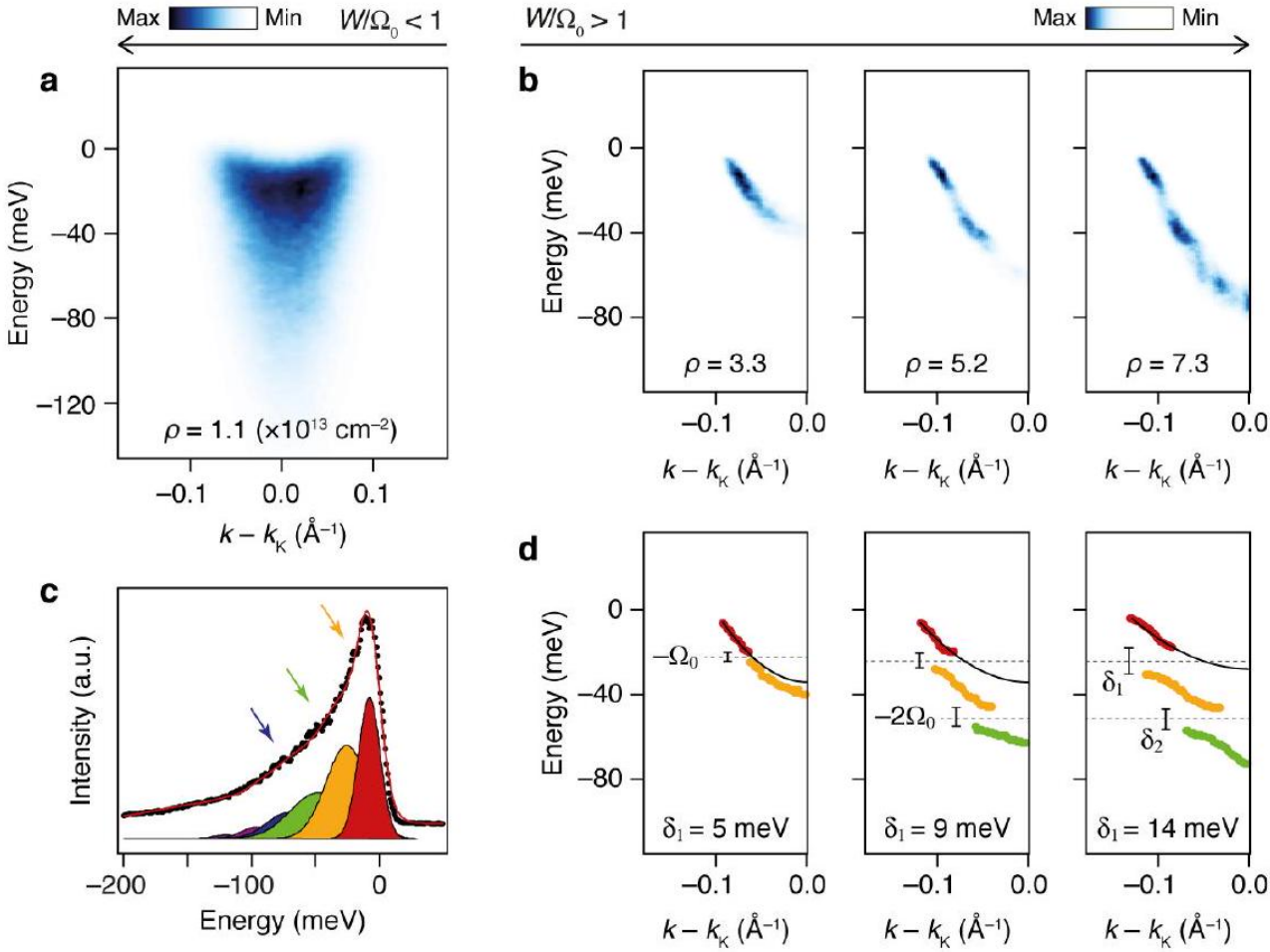

Figure 3 | Doping dependence of polarons. a,b, Series of ARPES spectra taken at ρ marked at the bottom of each panel with the photon energy of 54 eV and the sample temperature of 7 K . The ratio of W/Ω_0 separates two regimes, the unscreened (a) and the screened (b). **c**, **EDC** at k_{F} from data shown in **a**. The red line overlaid is the best fit with a series of peaks at $-n\Omega_0$, whose intensity follows the Poisson distribution (Methods). d, Corresponding peak positions of those in c. Dotted lines indicate the energy positions of $-n\Omega_0$. Scale bars show the magnitude of δ_1 and δ_2, the former of which is shown at the bottom of each panel. Black curves overlaid are a fit using a simple quadratic function to the polaron dispersion (red dots) with negative and positive velocity, but only half of them with negative velocity is shown in **d**.

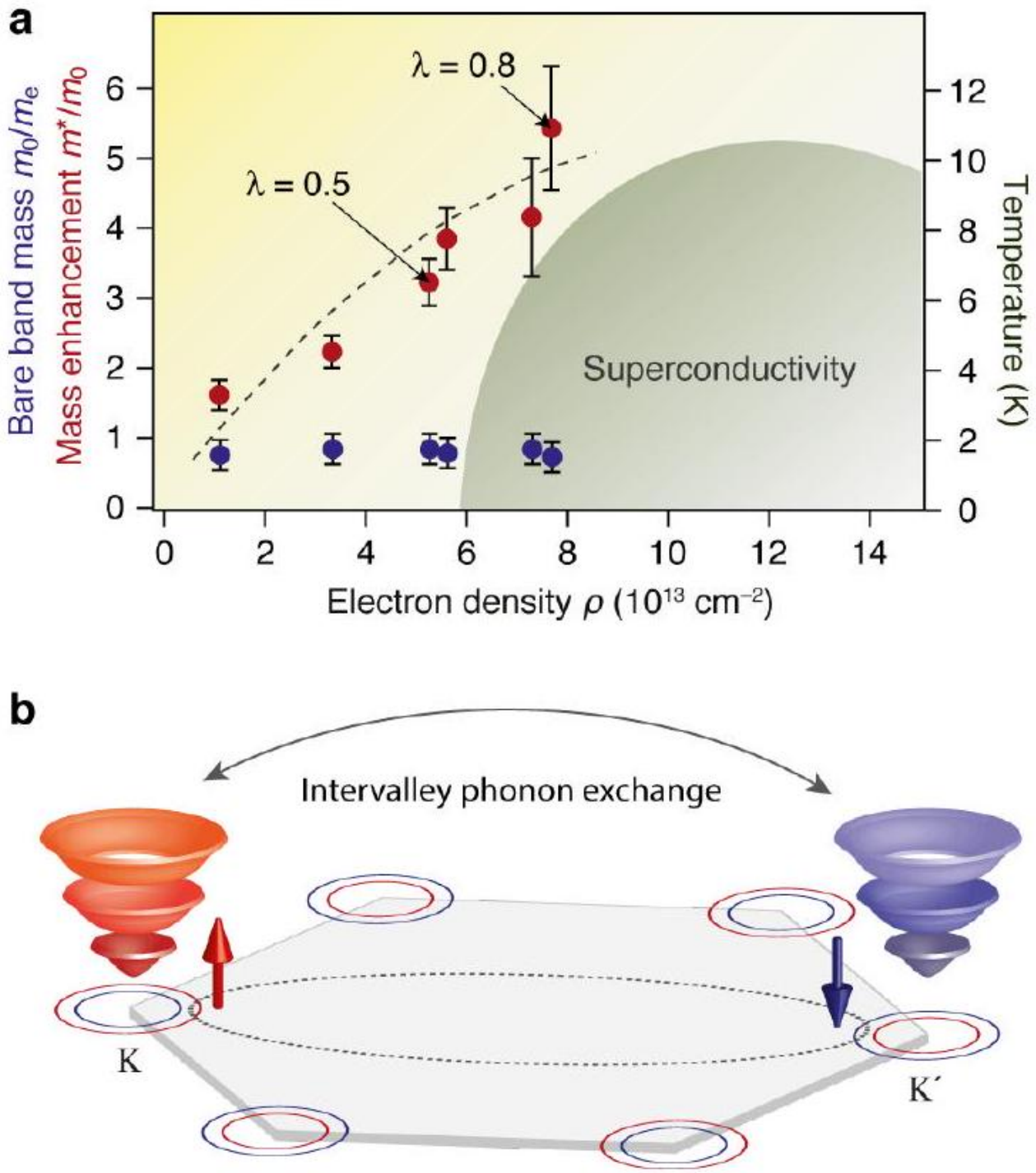

Figure 4 | Strength of $\boldsymbol{e}$-ph coupling and superconductivity. a, Effective mass of polaron bands (closed circles) and bare bands (open circles) plotted as a function of ρ. The error bars are the range of m^*/m_0 obtained by curve fitting to data points in Fig. 3d with a simple quadratic function. The dashed line is the intervalley $e-ph$ coupling matrix calculated for LA phonons near the K valleys of MoS_2 (ref. 29). The green region shows the superconducting dome of MoS_2 (ref. 9). b, Schematic illustration showing that two polarons with opposite spin at two K valleys are coupled via the exchange of phonons (bipolaronic coupling). Blue and red circles projected onto the Brillouin zone show the spin splitting in CB arising from spin-orbit coupling and interlayer symmetry breaking (Supplementary Fig. S2) [9,10]. The effect of this spin splitting to the spectral function of polarons is not considered here, since its energy scale is much lower than Ω_0 (ref. 40).

Bibliography

References

16.1 Bibliography from Most Useful Articles

References from Alexandrov, Mott

Abrikosov A A 1957 Zh.Eksp.Teor.Fiz. 1442.
Adamowski J 1989 Phys.Rev. B39, 3649-3652.
Alexandrov A S 1983 Zh.Fiz.Khim. 57, 273 (Russ.J.Phys.Chem.57, 167(1983));
1992a Phys.Rev. B46, 14932-35;
1992b Phys.Rev. B46, 2838-44;
1992c J.Low Temp. Phys. 87, 721-29;
1993 Phys.Rev B48, 10571-74;
1995 unpublished.
Alexandrov A S and Beere W H 1995 Phys.Rev. B51, 5887-91.
Alexandrov A S, Bratkovsky A M, and Mott N F 1994 Phys.Rev.Lett. 72, 1734-37.
Alexandrov A S, Bratkovsky A M, Mott N F and Salje E K H 1993 Physica C215, 359-70.
Alexandrov A S and Kabanov V V 1986 Fiz.Tverd.Tela (Leningrad) 28, 1129-35.
Alexandrov A S, Kabanov V V and Ranninger J 1995b unpublished.
Alexandrov A S, Kabanov V V and Ray D K 1994a Phys.Rev. B49, 9915-23; 1994b Physica C224, 247-55.
Alexandrov A S and Kornilovitch P E 1993 Z.Phys. B91, 47-50.
Alexandrov A S and Mazur E A 1989 Zh.Eksp.Teor.Fiz. 96, 1773-82.
Alexandrov A S and Mott N F 1993 Phys.Rev.Lett. 71, 1075-78; 1994 'High Temperature Superconductors and Other Superfluids',
Taylor & Francis;
ibid, Rep.Prog.Phys. 57, 1197-1290.
Alexandrov A S and Ranninger J 1981a Phys.Rev. B23, 1796-801;
1981b Phys.Rev. B24, 1164-69;
1992a Solid St.Commun.81, 403-406;
1992b Phys.Rev. B45, 13109-12.
Alexandrov A S, Ranninger J and Robaszkiewicz S 1986 Phys.Rev. B33, 4526-42;
Alexandrov A S, Samarchenko D A and Traven S V 1987 Zh. Eksp. Teor. Fiz. 93, 1007-19 (1987 Sov.Phys.JETP 66, 567).
Alexandrov A S, Zavaritsky V N, Liang W Y, and and Nevsky P L 1995 unpublished.
Allan N L and Mackrodt W C 1990 J.Chem.Soc., Faraday Trans. 86, 1227.
Allcock G R 1962 in 'Polarons and Excitons', eds. Kuper C G and Whitfield G D 45-70.
Anderson P W 1975 Phys.Rev.Lett. 34, 953-56;
Appel J 1968 in Solid State Physics, eds. Seitz F, Turnbull D and Ehrenreich H, Academic Press 21.
Aubry S 1995 in 'Polarons and Bipolarons in High- T_c Superconductors and Related Materials', eds. Salje E K H, Alexandrov A S and Liang W Y 271-308.
Austin I G and Mott N F 1969 Adv.Phys. 18, 41-102
Bardeen J, Cooper L N, and Schrieffer J R 1957 Phys.Rev. 108, 1175-1204.
Bassani F, Geddo M, Iadonisi G, and Ninno D 1991 Phys.Rev. B43, 5296-306.
Batlogg B, Hwang H Y, Takagi H, Cava R J, Kao H L and Kwo J 1995 unpublished.
Bednorz J G and Muller K A 1986 Z.Phys. B64, 189-93; 1988 Angew.Chem.Int.Ed.Engl. 27, 735-43.

Bishop R F 1974 J.Low Temp.Phys. 15, 601-35.
Bishop A R and Salkola M I 1995 in 'Polarons and Bipolarons in High- T_c Superconductors and Related Materials', eds. Salje E K H, Alexandrov A S and Liang W Y 353-366.
Bogoliubov N N 1947 J.Phys.USSR 11, 23-32;
1950 Ukr.Mat.Zh. 2 3;
1958 Zh.Eksp.Teor.Fiz. 34, 58, 73.
Bogoliubov Jr N N 1994 in 'Superconductivity and Strongly Correlated Electron Systems' eds. Noce C, Romano A and Scarpetta G, World Scientific 107-123.
Bogomolov V N, Kudinov E K and Firsov Yu A 1967 Fiz.Tverd.Tela (Leningrad) 9, 3175.
Bogomolov V N, Kudinov E K, Pavlov S T, and Sochawa L S 1968 Sov.Phys.Solid State 10, 2043.
Bornemann H J, Morris D E and Liu H B 1991a Physica C182, 132-36.
Bornemann H J, Morris D E, Liu H B, Sinha A P, Narwankar P
and Chandrachood M 1991b Physica C185-189, 1359-60.
Böttger H and Bryksin V V 1985 'Hopping Conduction in Solids', Academie-Verlag Berlin.
Brueckner K A 1967 Phys.Rev. 156, 204.
Bryksin V V and Gol'tsev A V 1988 Fiz.Tverd.Tela 30,1476-86 (1988 Sov.Phys.Solid State 30, 851-56).
Bryksin V V and Voloshin V S 1984 Fiz.Tverd.Tela (Leningrad) 26, 2357-65 (1984 Sov.Phys.Solid State 26, 1429-34).
Calvani P, Capizzi M, Lupi S, Maselli P, Paolone A, Roy P, Cheong S-W, Sadowski W, and Walker E 1994 Solid State Commun. 91, 113-16;
Calvani P, Lupi S, Roy P, Capizzi M, , Maselli P, Paolone A, Sadowski W, and Cheong S-W 1995 in 'Polarons and Bipolarons in High- T_c Superconductors and Related Materials', eds. Salje E K H, Alexandrov A S and Liang W Y 133-45.
Calvani P, Capizzi M, Lupi S, Maselli P, Paolone A, Roy P 1995 unpublished.
Catlow C R A 1989 J.Chem.Soc., Faraday Trans.2, 85, 335.
Chakraverty B K 1981 J.Physique 42, 1351-56.
Chen C Y, Branlund E C, Bae C-S, Yang K, Kastner M A, Cassanho A, and Birgeneau R J 1995 Phys.Rev. B51, 3671-77.
Cohen M H, Economou E N and Soukoulis C M Phys.Rev. B 29, 4496-99.
Cooper L N 1957 Phys.Rev. 104, 1189.
Crawford M K, Farneth W E, McCarron E M III, Harlow R L and Moudden A H 1990 Science 250, 1309-18.
Dagotto E 1994 Rev.Mod.Phys. 66, 763.
De Raedt H and Lagendijk Ad 1983 Phys.Rev. B27, 6097-109.
Devreese J T (ed) 1972 Polarons in Ionic Crystals and Polar Semiconductors, North-Holland (Amsterdam).
Devreese J T and Peeters (eds) 1984 Polarons and Excitons in Polar Semiconductors and Ionic Crystals, Plenum Press, New York.
Dewing H L and Salje E K H 1992 Supercond.Sci.Technol.5, 50-53.
Dolgov O V, Kirzhnits D A and Maximov E G 1981 Rev.Mod.Phys. 53, 81.
Eagles D M 1963 Phys.Rev. 130, 1381-1400; 1966 Phys.Rev. 145, 645-66;
1969 Phys. Rev. 186, 456-63.
Eliashberg G M 1960 Zh.Eksp.Teor.Fiz. 38, 966-76; 39, 1437-41
(1960 Sov.Phys.JETP 11, 696-702; 12, 1000-1002).
Emin D 1970 Phys.Rev.Lett. 25, 1751-54;
1971 Ann.Phys.(N.Y.) 64, 336.
1973 Adv.Phys. 22, 57;
1993 Phys.Rev. 48, 13691;

1995 in 'Polarons and Bipolarons in High- T_c Superconductors
and Related Materials', eds. Salje E K H, Alexandrov A S and Liang W Y 80-109.
Emin D and Holstein T 1969 Ann.Phys.N.Y. 53, 439-520.
Falk J P, Levy A, Kastner M A, and Birgeneau R J 1993 Phys.Rev. B48, 4043-48.
Fehske H, Röder H, Wellein G and Mistriotis A 1995 Phys.Rev. B51 16582-593.
Feinman R P 1955 Phys.Rev. 97660.
Feinman R P, Hellwarth R W, Iddings C K and Platzmann P M 1962 Phys.Rev. 127, 1004-17.
Fetter A L 1971 Ann.Phys.(N.Y.) 64,1.
Firsov Yu A (ed) 1975 Polarons, Nauka (Moscow).
Fisher A J, Hayes W and Wallace D S 1989 J. Phys.: Condens. Matter 15567-93.
Fisher R A, Kim S, Lacy S E, Phillips N E, Morris D E, Markelz
A G, Wei J Y T and Ginley D S 1988 Phys.Rev. B38, 11942-45.
Foldy L L 1961 Phys.Rev. 124, 649-51.
Franck J P et al. 1991 Physica C185-189, 1379-80.
Friedman L 1964 Phys.Rev. A 135, 233-46; 1995 in 'Polarons and Bipolarons in High- T_c Superconductors and Related Materials', eds. Salje E K H, Alexandrov A S and Liang W Y 180-87.
Friedman L and Holstein T 1963 Ann.Phys.(N.Y.) 21, 494.
Fröhlich H 1950 Phys.Rev. 79, 845;
1954 Adv.Phys. 3, 325-61;
Fröhlich H, Pelzer H an Zienau S 1950 Phil. Mag. 41221.
Geilikman B T 1975 Usp.Fiz.Nauk 115, 403-26 (1975 Sov.Phys.-Usp. 18, 190-202).
Gerlach B and Lowen H 1991 Rev. Mod. Phys. 63, 63-90.
Göbel U, Alexandrov A S and Capellmann H 1994 Z.Phys. B96, 47-52.
Gofron K, Campuzano J C, Abrikosov A A, Lindroos M, Bansil A, Ding H, Koelling D, and Dabrowski B 1994 Phys.Rev.Lett. 73, 3302-05.
Gogolin A A 1982 Phys.Status Solidi B109, 95-108.
Gold A 1991 Z.Phys. B83, 429.
Gor'kov L P 1958 Zh.Eksp.Teor. Fiz. 34, 735-39 (1958 Soviet Phys.JETP 7, 505-08).
Gunnarsson O, Handschuh H, Bechthold P S, Kessler B, Ganteför G, and Eberhardt W 1995 Phys.Rev.Lett. 74, 1875-78.
Gurari M 1953 Phil.Mag. 44329.
Harrison W A 1989 'Electronic Structure and the Properties of Solids', Dover Pub. (NY).
Hohenberg P and Kohn W 1964 Phys.Rev. B136, 864-72.
Hines D F and Frankel N 1979 Phys.Rev. B20, 972-83.
Hiramoto H and Toyozawa Y 1985 J.Phys.Soc.Jpn. 54, 245-59.
Hirsch J E and Fradkin E 1983 Phys.Rev. 27, 1680.
Holstein T 1959 Ann.Phys. 8, 325-42; ibid p. 343-89.
Holstein T and Friedman L 1968 Phys.Rev. 165, 1019-31.
Hore S R and Frankel N E 1975 Phys.Rev. B12, 2619-28; 1976 ibid 14, 1952-62.
Hwang H Y, Batlogg B, Takagi H, Kao H L, Kwo J, Cava R J, Krajewski J J, and Peck Jr W F 1994 Phys.Rev.Lett. 72, 2636-39.
Inderhees S E, Salamon M B, Goldenfeld N, Rice J P, Pazol B G and Ginzberg D M 1988 Phys.Rev.Lett. 60, 1178-81.
Junod A, Eckert D, Triscone G, Lee V Y and Muller J 1989 Physica C159, 215-25.
Kabanov V V and Mashtakov O Yu 1993 Phys.Rev. B47 6060-64.
Khomskii D 1995 in 'Polarons and Bipolarons in High- T_c Superconductors and Related Materials', eds. Salje E K H, Alexandrov A S and Liang W Y 375-84.
Kim Y H, Foster C M, Heeger A J, Cos S and Stucky G 1988 Phys.Rev. B38, 6478-82.
Klein B M, Boyer L L, Papaconstantopoulos D A 1978 Phys.Rev. B18, 6411-38.

Klinger M I 1961 Izv.Acad.Nauk SSSR, ser.Fiz. 25, 342-45; 1963 Phys.Letters 7, 102;
1979 Problems of electron (polaron) transport theory in semiconductors, Oxford: Pergamon Press.

Kochetov E A, Kuleshov S P, Mateev V A, and Smondyrev M A 1977 Teor.Mat.Fiz. 30, 183.

Kongeter A and Wagner M 1990 J.Chem.Phys. 92, 4003-11.

Kubo R 1957 J.Phys.Soc.Japan 12, 570.

Kubo K and Takada S 1983 J.Phys.Soc.Japan 52, 2108-17.

Kudinov E K, Mirlin D N and Firsov Yu A 1969 Fiz.Tverd.Tela (Leningrad) 11, 2789.

Lakkis S, Schlenker C, Chakraverty B K and Buder R 1976 Phys.Rev. B14, 1429-40.

Landau L D 1933 Phys.Z.Sowjetunion 3, 664.

Landau L D and Lifshitz E M 1977 'Quantum Mechanics - Non relativistic theory', third English edition, Pergamon Press.

Lang I G and Firsov Yu A 1962 Zh.Eksp.Teor.Fiz. 43, 1843-60 (1963 Sov.Phys.JETP 16, 1301-12).

Lee D K and Feenberg E 1965 Phys.Rev. 137, A731.

Lee T-D and Pines D 1952 Phys.Rev. 88960.

Lee T-D, Low F and Pines D 1953 Phys.Rev. 90297.

Loram J W, Mirza K A, Liang W Y and Osborne J 1988 Physica C162 - 164, 498-99.

Loram J W, Cooper J R, Wheatley J M, Mirza K A and Liu R S 1992 Phil. Mag. B65, 1405-17.

Mackenzie A P, Julian S R, Lonzarich G G, Carrington A, Hughes S D, Liu R S and Sinclair D C 1993 Phys.Rev.Lett. 71, 1238-41.

Marsiglio F 1995 Physica C 244, 21-34.

Matsubara T 1955 Prog.Theor.Phys. 14, 351-78.

McMillan W J 1968 Phys.Rev. B167, 331-44.

Migdal A B 1958 Zh.Eksp.Teor.Fiz. 34, 1438-46 (1958 Sov.Phys. JETP 7, 996-1001).

Mihailovic D, Foster C M, Voss K and Heeger A J 1990 Phys.Rev. B42, 7989-93.

Morel P and Anderson P W 1962 Phys.Rev. 125, 1263-71.

Mott N F 1990 Adv.Phys. 39, 55-81;
1993 Physica C205, 191-205;
1995 unpublished

Mott N F and Davis E A 1979 Electronic processes in non-crystalline materials, 2nd edn. Oxford University Press, Oxford.

Mott N F and Gurney R W 1940 Electronic Processes in Ionic Crystals, Oxford: Clarendon Press.

Mukhomorov V K 1982 Fiz.Tekh.Poluprovodn. 16, 1095-96 (1982 Sov.Phys.Semicond. 16, 700-701).

Nagaev E L 1979 Physics of Magnetic Semiconductors (Moscow) Mir.

Nambu Y 1960 Phys.Rev. 117, 648-63.

Nasu K 1985 J.Phys.Soc.Japan 54, 1933-43;
1991 in 'Electronic Conduction in Oxides', eds. Tsuda N, Nasu K, Yanase A, and Siratori K, Springer-Verlag, p. 81.

Nozieres, P. and Schmitt-Rink, J. J. 1985 Low Temp.Phys. 59, 195-211.

Osofsky M S et al. 1993 Phys.Rev.Lett. 71, 2315-18; 1994 ibid 72, 3292.

Overend N, Howson M A and Lawrie I D 1994 Phys.Rev.Lett. 72, 3238-41.

Peierls R E 1933 Z.Phys. 80, 763-91;
1955 in Quantum Theory of Solids (Oxford University Press, London).

Pekar S I 1946 Zh. Eksp. Teor. Fiz. 16, 335-339; 1951 (Russ.original Gostekhizdat), Research in Electron Theory of Crystals, US AEC Report AEC-tr- 5575 (1963).

Pines D 1961 The Many-Body Problem, Benjamin/Cummings, Reading, Massachusetts.

Ranninger J and Thibblin U 1992 Phys.Rev. B45, 773.
Rashba E I 1957 Opt.Spectr. 2, 75; 1985 in Excitons ed. by Rashba E I and Struge D M, Nauka (Moscow).
Robaszkiewicz S, Micnas R and Chao K A 1981 Phys.Rev. B23, 1447-58; ibid 24, 1579-82.
Reik H G 1963 Solid State Commun. 1, 67-71.
Salamon M B, Inderhees S E, Rice J P and Ginsberg D M 1990 Physica A168, 283.
Salje E K H 1995 in 'Polarons and Bipolarons in High- T_c Superconductors and Related Materials', eds. Salje E K H, Alexandrov A S and Liang W Y 110-31.
Scalapino D J 1969 in Superconductivity 1, ed. Parks R D, Marcel Deccer, 449-560.
Schafroth M R 1955 Phys.Rev. 100, 463-75
Schnelle W, Braun E, Broicher H, Dömel R, Ruppel S, Braunisch
W, Harnischmacher J and Wohlleben D 1990 Physica C168, 465-74.
Schultz T D 1962 in 'Polarons and Excitons', eds. Kuper C G and Whitfield G D 71-121.
Sewell G L 1958 Phil.Mag. 3, 1361-80.
Shluger A L and Stoneham A M 1993 J. Phys.: Condens. Matter 5, 3049-86.
Staunton J B 1994 Rep.Prog.Phys. 57, 1289-1344.
Street R A and Mott N F 1975 Phys.Rev.Lett. 35, 1293-96.
Suprun S G and Moizhes B Ya 1982 Fiz.Tverd.Tela (Leningrad) 24, 1571-73.
Takada Y Phys.Rev. B26 1223-32.
Taliani C, Pal A J, Ruani G, Zamboni R, Wei X and Vardini Z V 1990 Electronic Properties of HT_cSC and Related Compounds, Springer Series of Solid State Science (Springer-Verlag, Berlin) 99, 280.
Tjablikov S V 1952 Zh.Eksp.Teor.Fiz. 23, 381.
Tolmachev V V 1958 in Bogoliubov N N, Tolmachev V V and Shirkov D V 'A New Method in the Theory of Superconductivity', Academy of Science (Moscow) (1959 Consultant Bereau, New York).
Toyozawa Y 1961 Prog.Theor.Phys. 26, 29-44; 1990 Rev. Solid State Sci. 4133.
Uemura Y J 1995 in 'Polarons and Bipolarons in High- T_c Superconductors and Related Materials', eds. Salje E K H, Alexandrov A S and Liang W Y 453-59.
Verbist G, Peeters F M and Devreese J T 1991 Phys.Rev. B43, 2712-20.
Vinetskii V L and Giterman M Sh 1957 Zh. Eksp. Teor. Fiz. 33, 730 (1958 Sov.Phys. - JETP 6 560).
Vinetskii V L and Pashitskii E A 1983 Fiz. Tverd. Tela (Leningrad) 25, 1744-47 (1983 Sov.Phys.Solid State 25, 1005-06).
Von Molnar S and Methfessel S 1967 J. Appl. Phys. 38, 959.
Woo C-W and Ma S 1967 Phys.Rev. 159, 176-83.
Yagil Y, Zhang M, Baudenbacher F, and Salje E K H 1995 Phys.Rev. B, to be published.
Yamashita J and Kurosawa T 1958 J. Phys.Chem.Solids 5, 34.
Zhang X and Catlow C R A 1991 J.Mater.Chem. 1, 233-38.
Zhao G, K.K. Singh and D.E. Morris 1994 Phys.Rev. B50, 4112.
Zheng H 1988 Solid State Commun. 65, 731.
Zheng H, Feinberg D and Avignon M 1989 Phys.Rev. B39, 9405-22.

From Fröhlich Polarons: Lecture course including detailed theoretical derivations by Devreese.

Little bibliography

References

[1] W. Meevasana, X. J. Zhou, B. Moritz, C.-C. Chen, R. H. He, S.-I. Fujimori, D. H. Lu, S.-K. Mo, R. G. Moore, F. Baumberger, T. P. Devereaux, D. van der Marel, N. Nagaosa, J. Zaanen and Z.-X. Shen, New Journal of Physics **12**, 023004 (2010).

[2] J. L. M. van Mechelen, D. van der Marel, C. Grimaldi, A. B. Kuzmenko, N. P. Armitage, N. Reyren, H. Hagemann, and I. I. Mazin, Phys. Rev. Lett. **100**, 226403 (2008).

[3] M. Setvin, C. Franchini, X. Hao, M. Schmid, A. Janotti, M. Kaltak, C. G. Van de Walle, G. Kresse, and U. Diebold, Phys. Rev. Lett. **113**, 086402 (2014).

[4] X. Hao, Z. Wang, M. Schmid, U. Diebold, and C. Franchini, Phys. Rev. B **91**, 085204 (2015).

[5] J. T. Devreese, S. N. Klimin, J. L. M. van Mechelen, and D. van der Marel, Phys. Rev. B **81**, 125119 (2010).

[6] A. S. Mishchenko, N. V. Prokof'ev, A. Sakamoto, and B. V. Svistunov, Phys. Rev. *B* **62**, 6317 (2000).

[7] A. S. Mishchenko, N. Nagaosa, N. V. Prokof'ev, A. Sakamoto, and B. V. Svistunov, Phys. Rev. Lett. **91**, 236401 (2003).

[8] S. N. Klimin and J. T. Devreese, Phys. Rev. B **89**, 035201 (2014).

[9] G. L. Goodvin, A. S. Mishchenko, and M. Berciu, Phys. Rev. Lett. **107**, 076403 (2011).

[10] J. Tempere, W. Casteels, M. K. Oberthaler, S. Knoop, E. Timmermans, and J. T. Devreese, Phys. Rev. B **80**, 184504 (2009); **87**, 099903 (2013).

[11] J. Vlietinck, W. Casteels, K. Van Houcke, J. Tempere, J. Ryckebusch, and J. T. Devreese, New J. Phys. 17, 033023 (2015).

[12] F. Grusdt, Y. E. Shchadilova, A. N. Rubtsov, and E. Demler, Sci. Rep. **5,** 12124 (2015).

Selected publications on polarons in high-rating journals (Nature, Science, Physical Review Letters – 2005-2015)

1. *Method for Analyzing Second-Order Phase Transitions: Application to the Ferromagnetic Transition of a Polaronic System*, J. A. Souza, Yi-Kuo Yu, J. J. Neumeier, H. Terashita, and R. F. Jardim, Phys. Rev. Lett. **94**, 207209 (2005).
   Abstract
   A new method for analyzing second-order phase transitions is presented and applied to the polaronic system $La_{0.7}Ca_{0.3}MnO_3$. It utilizes heat capacity and thermal expansion data simultaneously to correctly predict the critical temperature's pressure dependence. Analysis of the critical phenomena reveals second-order behavior and an unusually large heat capacity exponent.

2. *Validity of the Franck-Condon Principle in the Optical Spectroscopy: Optical Conductivity of the Fröhlich Polaron*, G. De Filippis, V. Cataudella, A. S. Mishchenko, C. A. Perroni, and J. T. Devreese, Phys. Rev. Lett. **96**, 136405 (2006).
Abstract
The optical absorption of the Fröhlich polaron model is obtained by an approximation-free diagrammatic Monte Carlo method and compared with two new approximate approaches that treat lattice relaxation effects in different ways. We show that: (i) a strong coupling expansion, based on the Franck-Condon principle, well describes the optical conductivity for large coupling strengths ($\alpha > 10$); (ii) a memory function formalism with phonon broadened levels reproduces the optical response for weak coupling strengths ($\alpha < 6$) taking the dynamic lattice relaxation into account. In the coupling regime $6 < \alpha < 10$, the optical conductivity is a rapidly changing superposition of both Franck-Condon and dynamic contributions.

3. *Remanent Zero Field Spin Splitting of Self-Assembled Quantum Dots in a Paramagnetic Host*, C. Gould, A. Slobodskyy, D. Supp, T. Slobodskyy, P. Grabs, P. Hawrylak, F. Qu, G. Schmidt, and L. W. Molenkamp, Phys. Rev. Lett. **97**, 017202 (2006).

4. *Quantum Transport of Slow Charge Carriers in Quasicrystals and Correlated Systems*, Guy Trambly de Laissardière, Jean-Pierre Julien, and Didier Mayou, Phys. Rev. Lett. **97**, 026601 (2006).
Abstract
We show that the semiclassical model of conduction breaks down if the mean free path of charge carriers is smaller than a typical extension of their wave function. This situation is realized for sufficiently slow charge carriers and leads to a transition from a metalliclike to an insulatinglike regime when scattering by defects increases. This explains the unconventional conduction properties of quasicrystals and related alloys. The conduction properties of some heavy fermions or polaronic systems, where charge carriers are also slow, present a deep analogy.

5. *Occurrence of Intersubband Polaronic Repellons in a Two-Dimensional Electron Gas*, Stefan Butscher and Andreas Knorr, Phys. Rev. Lett. **97**, 197401 (2006).

6. *Subsecond Spin Relaxation Times in Quantum Dots at Zero Applied Magnetic Field Due to a Strong Electron-Nuclear Interaction*, R. Oulton, A. Greilich, S. Yu. Verbin, R. V. Cherbunin, T. Auer, D. R. Yakovlev, M. Bayer, I. A. Merkulov, V. Stavarache, D. Reuter, and A. D. Wieck, Phys. Rev. Lett. **98**, 107401 (2007).

7. *Exciton Dephasing in Quantum Dots due to LO-Phonon Coupling: An Exactly Solvable Model*, E. A. Muljarov and R. Zimmermann, Phys. Rev. Lett. **98**, 187401 (2007)

8. *Electron-Phonon Interaction and Charge Carrier Mass Enhancement in $SrTiO_3$*, J. L. M. van Mechelen, D. van der Marel, C. Grimaldi, A. B. Kuzmenko, N. P. Armitage, N. Reyren, H. Hagemann, and I. I. Mazin, Phys. Rev. Lett. **100**, 226403 (2008).
Abstract
We report a comprehensive THz, infrared and optical study of Nb-doped $SrTiO_3$ as well as dc conductivity and Hall effect measurements. Our THz spectra at 7 K show the presence of an unusually narrow (< 2meV) Drude peak. For all carrier concentrations the Drude spectral weight shows a factor of three mass enhancement relative to the effective mass in the local density approximation, whereas the spectral weight contained in the incoherent midinfrared response indicates that the mass enhancement is at least a factor two. We find no evidence of a particularly large electron-phonon coupling that would result in small polaron formation.

9. *Orbital and Charge-Resolved Polaron States in CdSe Dots and Rods Probed by Scanning Tunneling Spectroscopy*, Zhixiang Sun, Ingmar Swart, Christophe Delerue, Daniël Vanmaekelbergh, and Peter Liljeroth, Phys. Rev. Lett. **102**, 196401 (2009).

10. *Dynamical Response and Confinement of the Electrons at the $LaAlO_3/SrTiO_3$ Interface*, A. Dubroka, M. Rössle, K. W. Kim, V. K. Malik, L. Schultz, S. Thiel, C. W. Schneider, J. Mannhart, G. Herranz, O. Copie, M. Bibes, A. Barthélémy, and C. Bernhard, Phys. Rev. Lett. **104**, 156807 (2010).
Abstract
With infrared ellipsometry and transport measurements we investigated the electrons at the interface between $LaAlO_3$and $SrTiO_3$. We obtained a sheet carrier concentration of $N_s \approx 5-9\times 10^{13}$ cm^{-2}, an effective mass of $m^* = 3.2\pm 0.4m_e$, and a strongly frequency dependent mobility. The latter are similar as in bulk $SrTi_{1-x}Nb_xO_3$ and therefore suggestive of polaronic correlations. We also determined the vertical concentration profile which has a strongly asymmetric shape with a rapid initial decay over the first 2 nm and a pronounced tail that extends to about 11 nm.

11. *Bipolaron and N-Polaron Binding Energies*, Rupert L. Frank, Elliott H. Lieb, Robert Seiringer, and Lawrence E. Thomas, Phys. Rev. Lett. **104**, 210402 (2010).
Abstract
The binding of polarons, or its absence, is an old and subtle topic. Here we prove two things rigorously. First, the transition from many-body collapse to the existence of a thermodynamic limit for N polarons occurs precisely at $U = 2\alpha$, where U is the electronic Coulomb repulsion and $\alpha$is the polaron coupling constant. Second, if U is large enough, there is no multipolaron binding of any kind. Considering the known fact that there is binding for some $U > 2\alpha$, these conclusions are not obvious and their proof has been an open problem for some time.

12. *Polaronic Conductivity in the Photoinduced Phase of 1T-TaS_2*, N. Dean, J. C. Petersen, D. Fausti, R. I. Tobey, S. Kaiser, L. V. Gasparov, H. Berger, and A. Cavalleri, Phys. Rev. Lett. **106**, 016401 (2011).

13. *Spectroscopy of Single Donors at ZnO(0001) Surfaces*, Hao Zheng, Jörg Kröger, and Richard Berndt, Phys. Rev. Lett. **108**, 076801 (2012)

14. *Polarons in Suspended Carbon Nanotubes*, I. Snyman, and Yu. V. Nazarov, Phys. Rev. Lett. **108**, 076805 (2012)

15. *Two-Dimensional Polaronic Behavior in the Binary Oxides m-HfO_2 and m-ZrO_2*, K. P. McKenna, M. J. Wolf, A. L. Shluger, S. Lany, and A. Zunger, Phys. Rev. Lett. **108**, 116403 (2012)

16. *Polaron-to-Polaron Transitions in the Radio-Frequency Spectrum of a Quasi-Two-Dimensional Fermi Gas*, Y. Zhang, W. Ong, I. Arakelyan, and J. E. Thomas, Phys. Rev. Lett. **108**, 235302 (2012)
Abstract
We measure radio-frequency spectra for a two-component mixture of a ^{6}Li atomic Fermi gas in a quasi-two-dimensional regime with the Fermi energy comparable to the energy level spacing in the tightly confining potential. Near the Feshbach resonance, we find that the observed resonances do not correspond to transitions between confinement-induced dimers. The spectral shifts can be fit by assuming transitions between noninteracting polaron states in two dimensions.

17. *Model of the Electron-Phonon Interaction and Optical Conductivity of* $Ba_{1-x}K_xBiO_3$, R. Nourafkan, F. Marsiglio, and G. Kotliar, Phys. Rev. Lett. **109**, 017001 (2012)

18. *p-Wave Polaron*, Jesper Levinsen, Pietro Massignan, Frédéric Chevy, and Carlos Lobo, Phys. Rev. Lett. **109**, 075302 (2012)

19. *Effect of Electron-Phonon Interaction Range for a Half-Filled Band in One Dimension*, Martin Hohenadler, Fakher F. Assaad, and Holger Fehske, Phys. Rev. Lett. **109**, 116407 (2012)

20. *Digital Quantum Simulation of the Holstein Model in Trapped Ions*, A. Mezzacapo, J. Casanova, L. Lamata, and E. Solano, Phys. Rev. Lett. **109**, 200501 (2012)

21. *Bilayers of Rydberg Atoms as a Quantum Simulator for Unconventional Superconductors*, J. P. Hague and C. MacCormick, Phys. Rev. Lett. **109**, 223001 (2012)

22. *Relaxation Dynamics of the Holstein Polaron*, Denis Golež, Janez Bonča, Lev Vidmar, and Stuart A. Trugman, Phys. Rev. Lett. **109**, 236402 (2012)

23. *Quantum Simulation of Small-Polaron Formation with Trapped Ions*, Vladimir M. Stojanović, Tao Shi, C. Bruder, and J. Ignacio Cirac, Phys. Rev. Lett. **109**, 250501 (2012)

24. *Condensed-matter physics: Repulsive polarons found*, P. Hannaford, Nature **485**, 588 (2012)
Abstract
Quasiparticles known as repulsive polarons are predicted to occur when 'impurity' fermionic particles interact repulsively with a fermionic environment. They have now been detected in two widely differing systems. See Letters p.615 & p.619

25. *Quantum Breathing of an Impurity in a One-Dimensional Bath of Interacting Bosons*, Sebastiano Peotta, Davide Rossini, Marco Polini, Francesco Minardi, and Rosario Fazio, Phys. Rev. Lett. **110**, 015302 (2013)
Abstract
By means of the time-dependent density-matrix renormalization-group (TDMRG) method we are able to follow the real-time dynamics of a single impurity embedded in a one-dimensional bath of interacting bosons. We focus on the impurity breathing mode, which is found to be well described by a single oscillation frequency and a damping rate. If the impurity is very weakly coupled to the bath, a Luttinger-liquid description is valid and the impurity suffers an Abraham-Lorentz radiation-reaction friction. For a large portion of the explored parameter space, the TDMRG results fall well beyond the Luttinger-liquid paradigm.

26. *Measurement of Coherent Polarons in the Strongly Coupled Antiferromagnetically Ordered Iron-Chalcogenide* $Fe_{1.02}Te$ *using Angle-Resolved Photoemission Spectroscopy*, Z. K. Liu, R.-H. He, D. H. Lu, M. Yi, Y. L. Chen, M. Hashimoto, R. G. Moore, S.-K. Mo, E. A. Nowadnick, J. Hu, T. J. Liu, Z. Q. Mao, T. P. Devereaux, Z. Hussain, and Z.-X. Shen, Phys. Rev. Lett. **110**, 037003 (2013)

27. *Decoherence of a Single-Ion Qubit Immersed in a Spin-Polarized Atomic Bath*, L. Ratschbacher, C. Sias, L. Carcagni, J. M. Silver, C. Zipkes, and M. Köhl, Phys. Rev. Lett. **110**, 160402 (2013)

28. *Tunable Polaronic Conduction in Anatase* TiO_2, S. Moser, L. Moreschini, J. Jaćimović, O. S. Barišić, H. Berger, A. Magrez, Y. J. Chang, K. S. Kim, A. Bostwick, E. Rotenberg, L. Forró, and M. Grioni, Phys. Rev. Lett. **110**, 196403 (2013)

29. *Investigating Polaron Transitions with Polar Molecules*, Felipe Herrera, Kirk W. Madison, Roman V. Krems, and Mona Berciu, Phys. Rev. Lett. **110**, 223002 (2013)
Abstract
We determine the phase diagram of a polaron model with mixed breathing-mode and Su-Schrieffer-Heeger couplings and show that it has two sharp transitions, in contrast to pure models which exhibit one (for Su-Schrieffer-Heeger coupling) or no (for breathing-mode coupling) transition. We then show that ultracold molecules trapped in optical lattices can be used as a quantum simulator to study precisely this mixed Hamiltonian, and that the relative contributions of the two couplings can be tuned with external electric fields. The parameters of current experiments place them in the region where one of the transitions occurs. We also propose a scheme to measure the polaron dispersion using stimulated Raman spectroscopy.

30. *Electronic Instability in a Zero-Gap Semiconductor: The Charge-Density Wave in* $(TaSe_4)_2$, C. Tournier-Colletta, L. Moreschini, G. Autès, S. Moser, A. Crepaldi, H. Berger, A. L. Walter, K. S. Kim, A. Bostwick, P. Monceau, E. Rotenberg, O. V. Yazyev, and M. Grioni, Phys. Rev. Lett. **110**, 236401 (2013).

31. *Itinerant Ferromagnetism in a Polarized Two-Component Fermi Gas*, Pietro Massignan, Zhenhua Yu, and Georg M. Bruun, Phys. Rev. Lett. **110**, 230401 (2013).

32. *Suppression of the Hanle Effect in Organic Spintronic Devices*, Z. G. Yu, Phys. Rev. Lett. **111**, 016601 (2013).

33. *Energy and Contact of the One-Dimensional Fermi Polaron at Zero and Finite Temperature*, E. V. H. Doggen and J. J. Kinnunen, Phys. Rev. Lett. **111**, 025302 (2013).

34. *Measurement of the Femtosecond Optical Absorption of* $LaAlO_3/SrTiO_3$ *Heterostructures: Evidence for an Extremely Slow Electron Relaxation at the Interface*, Yasuhiro Yamada, Hiroki K. Sato, Yasuyuki Hikita, Harold Y. Hwang, and Yoshihiko Kanemitsu, Phys. Rev. Lett. **111**, 047403 (2013)
Abstract
The photocarrier relaxation dynamics of an n-type $LaAlO_3/SrTiO_3$ heterointerface is investigated using femtosecond transient absorption (TA) spectroscopy at low temperatures. In both $LaAlO_3/SrTiO_3$ heterostructures and electron-doped $SrTiO_3$ bulk crystals, the TA spectrum shows a Drude-like free carrier absorption immediately after excitation. In addition, a broad absorption band gradually appears within 40 ps, which corresponds to the energy relaxation of photoexcited free electrons into self-trapped polaron states. We reveal that the polaron formation time is enhanced considerably at the $LaAlO_3/SrTiO_3$ heterointerface as compared to bulk crystals. Further, we discuss the interface effects on the electron relaxation dynamics in conjunction with the splitting of the t_{2g} subbands due to the interface potential.

35. Pauli Spin Blockade and the Ultrasmall Magnetic Field Effect, Jeroen Danon, Xuhui Wang, and Aurélien Manchon, Phys. Rev. Lett. **111**, 066802 (2013)

36. *Tkachenko Polarons in Vortex Lattices*, M. A. Caracanhas, V. S. Bagnato, and R. G. Pereira, Phys. Rev. Lett. **111**, 115304 (2013).

37. *Impurity Problem in a Bilayer System of Dipoles*, N. Matveeva and S. Giorgini, Phys. Rev. Lett. **111**, 220405 (2013).

38. *Single-Polariton Optomechanics*, Juan Restrepo, Cristiano Ciuti, and Ivan Favero, Phys. Rev. Lett. **112**, 013601 (2014)

39. *Ferromagnetism of a Repulsive Atomic Fermi Gas in an Optical Lattice: A Quantum Monte Carlo Study*, S. Pilati, I. Zintchenko, and M. Troyer, Phys. Rev. Lett. **112**, 015301 (2014)

40. *Ultrafast Photoemission Spectroscopy of the Uranium Dioxide UO2 Mott Insulator: Evidence for a Robust Energy Gap Structure*, Steve M. Gilbertson, Tomasz Durakiewicz, Georgi L. Dakovski, Yinwan Li, Jian-Xin Zhu, Steven D. Conradson, Stuart A. Trugman, and George Rodriguez, Phys. Rev. Lett. **112**, 087402 (2014).

41. *Direct View at Excess Electrons in TiO_2 Rutile and Anatase*, Martin Setvin, Cesare Franchini, Xianfeng Hao, Michael Schmid, Anderson Janotti, Merzuk Kaltak, Chris G. Van de Walle, Georg Kresse, and Ulrike Diebold, Phys. Rev. Lett. **113**, 086402 (2014)
Abstract
A combination of scanning tunneling microscopy and spectroscopy and density functional theory is used to characterize excess electrons in TiO2 rutile and anatase, two prototypical materials with identical chemical composition but different crystal lattices. In rutile, excess electrons can localize at any lattice Ti atom, forming a small polaron, which can easily hop to neighboring sites. In contrast, electrons in anatase prefer a free-carrier state, and can only be trapped near oxygen vacancies or form shallow donor states bound to Nb dopants. The present study conclusively explains the differences between the two polymorphs and indicates that even small structural variations in the crystal lattice can lead to a very different behavior.

42. *Diagrammatic Monte Carlo Method for Many-Polaron Problems*, Andrey S. Mishchenko, Naoto Nagaosa, and Nikolay Prokof'ev, Phys. Rev. Lett. **113**, 166402 (2014)
Abstract
We introduce the first bold diagrammatic Monte Carlo approach to deal with polaron problems at a finite electron density nonperturbatively, i.e., by including vertex corrections to high orders. Using the Holstein model on a square lattice as a prototypical example, we demonstrate that our method is capable of providing accurate results in the thermodynamic limit in all regimes from a renormalized Fermi liquid to a single polaron, across the nonadiabatic region where Fermi and Debye energies are of the same order of magnitude. By accounting for vertex corrections, the accuracy of the theoretical description is increased by orders of magnitude relative to the lowest-order self-consistent Born approximation employed in most studies. We also find that for the electron-phonon coupling typical for real materials, the quasiparticle effective mass increases and the quasiparticle residue decreases with increasing the electron density at constant electron-phonon coupling strength.

43. *Polaron spin current transport in organic semiconductors*, Shun Watanabe, Kazuya Ando, Keehoon Kang, Sebastian Mooser, Yana Vaynzof, Hidekazu Kurebayashi, Eiji Saitoh, and Henning Sirringhaus, Nature Physics **10**, 308 (2014)

44. *Real Space Imaging of Spin Polarons in Zn-Doped $SrCu_2(BO_3)_2$*, M. Yoshida, H. Kobayashi, I. Yamauchi et al., Phys. Rev. Lett. **114**, 056402 (2015)

45. *Crossover from Super- to Subdiffusive Motion and Memory Effects in Crystalline Organic Semiconductors*, G. De Filippis, V. Cataudella, A. S. Mishchenko, N. Nagaosa, A. Fierro, and A. de Candia, Phys. Rev. Lett. **114**, 086601 (2015)
Abstract
The transport properties at finite temperature of crystalline organic semiconductors are investigated, within the Su-Schrieffer-Heeger model, by combining an exact diagonalization technique, Monte Carlo approaches, and a maximum entropy method. The temperature-dependent mobility data measured in single crystals of rubrene are successfully reproduced: a crossover from

super-to subdiffusive motion occurs in the range $150 < T < 200$K, where the mean free path becomes of the order of the lattice parameter and strong memory effects start to appear. We provide an effective model, which can successfully explain features of the absorption spectra at low frequencies. The observed response to slowly varying electric field is interpreted by means of a simple model where the interaction between the charge carrier and lattice polarization modes is simulated by a harmonic interaction between a fictitious particle and an electron embedded in a viscous fluid.

46. *Mobility of Holstein Polaron at Finite Temperature: An Unbiased Approach*, A. S. Mishchenko, N. Nagaosa, G. De Filippis, A. de Candia, and V. Cataudella, Phys. Rev. Lett. **114**, 146401 (2015).
Abstract
We present the first unbiased results for the mobility $\mu$of a one-dimensional Holstein polaron obtained by numerical analytic continuation combined with diagrammatic and worldline Monte Carlo methods in the thermodynamic limit. We have identified for the first time several distinct regimes in the $\lambda - T$plane including a band conduction region, incoherent metallic region, an activated hopping region, and a high-temperature saturation region. We observe that although mobilities and mean free paths at different values of λdiffer by many orders of magnitude at small temperatures, their values at Tlarger than the bandwidth become very close to each other.

47. *Band Structures of Plasmonic Polarons*, F. Caruso, H. Lambert, and F. Giustino, Phys. Rev. Lett. **114**, 146404 (2015)
Abstract
Using state-of-the-art many-body calculations based on the "GW plus cumulant" approach, we show that electron-plasmon interactions lead to the emergence of plasmonic polaron bands in the band structures of common semiconductors. Using silicon and group IV transition-metal dichalcogenide monolayers (AX(2) with A = Mo, W and X = S, Se) as prototypical examples, we demonstrate that these new bands are a general feature of systems characterized by well-defined plasmon resonances. We find that the energy versus momentum dispersion relations of these plasmonic structures closely follow the standard valence bands, although they appear broadened and blueshifted by the plasmon energy. Based on our results, we identify general criteria for observing plasmonic polaron bands in the angle-resolved photoelectron spectra of solids.

48. *Long-lived photoinduced polaron formation in conjugated polyelectrolyte-fullerene assemblies*, R. C. Huber, A. S. Ferreira, R. Thompson *et al.*, Science **348**, 1340 (2015)

49. *Electron-Phonon Interactions, Metal-Insulator Transitions, and Holographic Massive Gravity*, M. Baggioli and O. Pujolas, Phys. Rev. Lett. **114**, 251602 (2015)
Abstract
Massive gravity is holographically dual to "realistic" materials with momentum relaxation. The dual graviton potential encodes the phonon dynamics, and it allows for a much broader diversity than considered so far. We construct a simple family of isotropic and homogeneous materials that exhibit an interaction-driven metal-insulator transition. The transition relates to the formation of polarons – phonon-electron quasibound states that dominate the conductivities, shifting the spectral weight above a mass gap. We characterize the polaron gap, width, and dispersion.

50. *Electron-Phonon Coupling in the Bulk of Anatase TiO_2 Measured by Resonant Inelastic X-Ray Spectroscopy*, S. Moser, S. Fatale, P. Krueger *et al.*, Phys. Rev. Lett. **115**, 096404 (2015).

Abstract
We investigate the polaronic ground state of anatase TiO2 by bulk-sensitive resonant inelastic x-ray spectroscopy (RIXS) at the Ti L-3 edge. We find that the formation of the polaron cloud involves a single 95 meV phonon along the c axis, in addition to the 108 meV ab-plane mode previously identified by photoemission. The coupling strength to both modes is the same within error bars, and it is unaffected by the carrier density. These data establish RIXS as a directional bulk-sensitive probe of electron-phonon coupling in solids.

51. *Impurity in a Bose-Einstein Condensate and the Efimov Effect*, J. Levinsen, M. M. Parish, and G. M. Bruun, Phys. Rev. Lett. **115**, 125302 (2015).

52. *Decoherence of Impurities in a Fermi Sea of Ultracold Atoms*, M. Cetina, M. Jag, R. S. Lous, et al., Phys. Rev. Lett. **115**, 135302 (2015).

53. *Impurities in Bose-Einstein Condensates: From Polaron to Soliton*, S. Shadkhoo and R., Shahriar, Phys. Rev. Lett. **115**, 135305 (2015).
Abstract
We propose that impurities in a Bose-Einstein condensate which is coupled to a transversely laser-pumped multimode cavity form an experimentally accessible and analytically tractable model system for the study of impurities solvated in correlated liquids and the breakdown of linear-response theory. As the strength of the coupling constant between the impurity and the Bose-Einstein condensate is increased, which is possible through Feshbach resonance methods, the impurity passes from a large to a small polaron state, and then to an impurity-soliton state. This last transition marks the breakdown of linear-response theory.

54. *Quasiparticle Properties of a Mobile Impurity in a Bose-Einstein Condensate*, R. S. Christensen, J. Levinsen, and G. M. Bruun, Phys. Rev. Lett. **115**, 160401 (2015).
Abstract
We develop a systematic perturbation theory for the quasiparticle properties of a single impurity immersed in a Bose-Einstein condensate. Analytical results are derived for the impurity energy, effective mass, and residue to third order in the impurity-boson scattering length. The energy is shown to depend logarithmically on the scattering length to third order, whereas the residue and the effective mass are given by analytical power series. When the boson-boson scattering length equals the boson-impurity scattering length, the energy has the same structure as that of a weakly interacting Bose gas, including terms of the Lee-Huang-Yang and fourth order logarithmic form. Our results, which cannot be obtained within the canonical Frohlich model of an impurity interacting with phonons, provide valuable benchmarks for many-body theories and for experiments.

Bibliography

References

[1] L. D. Landau, *Phys. Z. Sowjetunion* **3**, 664 (1933) [English translation in *Collected Papers*, Gordon and Breach, New York, 1965, pp. 67-68].

[2] S. I. Pekar, Journal of Physics USSR **10**, 341 (1946).

[3] S. I. Pekar, Zh. Eksper. Teor. Fiz. **16**, 341 (1946).

[4] J. T. Devreese, in *Lectures on the Physics of Highly Correlated Electron Systems VII,* edited A. Avella and F. Mancini Proceedings of the 7th Training Course in the Physics of

Correlated Electron Systems&High-T_c Superconductors, Vietri sul Mare, Italy, October 14-16, 2002, AIP, Melville (2003), pp. 3 - 56.

[5] H. Fröhlich, *Adv. Phys.* **3**, 325 (1954).

[6] R. P. Feynman, R. B. Leiton and M. Sands, The Feynman Lectures on Physics (Addison-Wesley, 1972), Vol. II.

[7] E. Kartheuser, in *Polarons in Ionic Crystals and Polar Semiconductors* edited J. T. Devreese, North-Holland, Amsterdam (1972), pp. 717 - 733.

[8] M. Grynberg, S. Huant, G. Martinez, J. Kossut, T. Wojtowicz, G. Karczewski, J. M. Shi, F. M. Peeters, J. T. Devreese, *Phys. Rev. B* **54**, 1467 (1996).

[9] The spectra of the infrared-active LO (and TO) phonons in α-Al_2O_3 (sapphire) contain six modes. The values of the LO and TO phonon frequencies and of the high-frequency dielectric constants $\varepsilon_{\infty\parallel} = 3.072$, $\varepsilon_{\infty\perp} = 3.077$ are taken from Ref. [10]. Using these parameters and the electron band mass $m_b = 0.25m_e$ as estimated in Ref. [11], the effective value of the electron-phonon coupling constant α in Al_2O_3
has been calculated as

$$\alpha = \sum_j \alpha_j \left\langle \left(\mathbf{e}_j \cdot \frac{\mathbf{k}}{k} \right)^2 \right\rangle ,$$

where $\mathbf{e}_j$ is the polarization vector of the j-th LO-phonon branch, $\mathbf{k}$ is the phonon wave vector, $\langle\rangle$ denote the angular averaging, and the coupling constants α_j for each branch are obtained using the method [12]. The resulting value of the polaron coupling constant is $\alpha \approx 1.25$

[10] M. Schubert, T. E. Tiwald, and C. M. Herzinger, *Phys. Rev. B* **61**, 8187 (2000).

[11] J. Shan, F. Wang, E. Knoesel, M. Bonn, and T. F. Heinz, *Phys. Rev. Lett.* **90**, 247401 (2003).

[12] S. N. Klimin, V. M. Fomin, and J. T. Devreese, *to be published.*

[13] J. W. Hodby, G. P. Russell, F. Peeters, J. T. Devreese, and D. M. Larsen, *Phys. Rev. Lett.* **58**, 1471 (1987).

[14] The spectra of the LO (and TO) phonons in α-SiO_2 contain ten modes. The values of the LO and TO phonon frequencies are taken from Refs. [15, 16]. Using these frequencies and the value $\varepsilon_\infty = 2.40$ from Ref. [17] for the high-frequency dielectric constant, the effective value of the electron-phonon coupling constant α in SiO_2 has been calculated using the method of Ref. [12] as indicated in Ref. [9]. We use the estimated value of the electron band mass $m_b = 0.5m_e$ as in Refs. [18, 19, 20]. The resulting value of the polaron coupling constant is $\alpha \approx 1.59$.

[15] F. Gervais and B. Piriou, *Phys. Rev. B* **11**, 3944 (1975).

[16] J. L. Duarte, J. A. Sanjurjo, and R. S. Katiyar, *Phys. Rev. B* **36**, 3368 (1987).

[17] S. T. Pantelides and W. A. Harrison, *Phys. Rev. B* **13**, 2667 (1976).

[18] M. V. Fischetti, D. J. DiMaria, L. Dori, J. Batey, E. Tierney, and J. Stasiak, *Phys. Rev. B* **35**, 4404 (1987).

[19] D. Arnold, E. Cartier, and D. J. DiMaria, *Phys. Rev. B* **49**, 10278 (1994).

[20] P. Martin, S. Guizard, Ph. Daguzan, G. Petite, P. D'Oliveira, P. Meynadier, and M. Perdrix, *Phys. Rev. B* **55**, 5799 (1997).

[21] I. Biaggio, R. W. Hellwarth, and J. P. Partanen, *Phys. Rev. Lett.* **78**, 891 (1997) (for $m_b/m_e = 2$).

[22] G. Verbist, F. M. Peeters, and J. T. Devreese, *Ferroelectrics*, **130**, 27 (1992) (for $m_b/m_e = 2.6$).

[23] S. I. Pekar, *Issledovanija po Ekektronnoj Teorii Kristallov*, Gostekhizdat, Moskva, 1951 (in Russian) [German translation: *Untersuchungen über die Elektronentheorie der Kristalle*, Akademie Verlag, Berlin, 1951].

[24] G. C. Kuper and G. D. Whitfield (eds.), *Polarons and Excitons*, Oliver and Boyd, Edinburgh, 1963.

[25] J. Appel, in *Solid State Physics*, edited by F. Seitz, D. Turnbull, and H. Ehrenreich, Academic Press, New York, 1968, vol. 21, pp. 193-391.

[26] J. T. Devreese (ed.), *Polarons in Ionic Crystals and Polar Semiconductors*, North-Holland, Amsterdam, 1972.

[27] T. K. Mitra, A. Chatterjee, and S. Mukhopadhyay, *Phys. Rep.* **153**, 91 (1987).

[28] J. T. Devreese, in *Encyclopedia of Applied Physics*, edited by G. L. Trigg, VCH, Weinheim, 1996, vol. 14, pp. 383 - 413.

[29] A. S. Alexandrov and Sir Nevill Mott, *Polarons and Bipolarons*, World Scientific, Singapore, 1996.

[30] A. S. Mishchenko, N. V. Prokof'ev, A. Sakamoto, and B. V. Svistunov, *Phys. Rev. B* **62**, 6317 (2000).

[31] T. D. Lee, F. E. Low, and D. Pines, Phys. Rev. **90**, 297 (1953).

[32] J. Röseler, Phys. Stat. Sol.(b) **25**, 311 (1968)

[33] M. A. Smondyrev, Teor. Math. Fiz. **68**, 29 (1986) [English translation: Theor. Math. Phys. **68**, 653 (1986)]

[34] O. V. Selyugin and M. A. Smondyrev, Phys. Stat. Sol.(b)

[35] L. D. Landau and S. I. Pekar, Zh. Eksper. Teor. Fiz. **18**, 419 (1948)

[36] N. N. Bogolubov and S. V. Tyablikov, Zh. Eksp. i Teor. Fiz. **19**, 256 (1949)

[37] N. N. Bogolubov, Ukr. Matem. Zh. **2**, 3 (1950)

[38] S. V. Tyablikov, Zh. Eksp. i Theor. Phys. **21**, 377 (1951)

[39] R. Evrard, Phys. Letters **14**, 295 (1965)

[40] S. J. Miyake, J. Phys. Soc. Japan **38**, 181 (1975)

[41] J. T. Devreese and R. Evrard, Phys. Letters **11**, 278 (1964).

[42] E. Kartheuser, R. Evrard, and J. Devreese, in *Optical Properties of Solids*, edited by E. D. Haidemenakis, Gordon and Breach, New York, 1970, pp. 433-459 (Table 1).

[43] R. P. Feynman, *Phys. Rev.* **97**, 660 (1955).

[44] J. T. Devreese and R. Evrard, in *Proceedings of the British Ceramic Society* **10**, 151 (1968).

[45] J. T. Titantah, C. Pierleoni, and S. Ciuchi, *Phys. Rev. Lett.* **87**, 206406 (2001).

[46] G. De Filippis, V. Cataudella, V. Marigliano Ramaglia, C. A. Perroni, and D. Bercioux, *Eur. Phys. J. B* **36**, 65 (2003).

[47] R. P. Feynman, R. W. Hellwarth, C. K. Iddings, and P. M. Platzman, *Phys. Rev.* **127**, 1004 (1962).

[48] K. K. Thornber and R. P. Feynman, Phys. Rev. B **1**, 4099 (1970)

[49] E. Kartheuser, R. Evrard, and J. Devreese, Phys. Rev. Lett.**22**, 94 (1969).

[50] J. T. Devreese, J. De Sitter, and M. Goovaerts, Phys. Rev. B **5**, 2367 (1972)

[51] F. M. Peeters and J. T. Devreese *Phys. Rev. B* **34**, 7246 (1986).

[52] V. Cataudella, G. De Filippis, and G. Iadonisi, *Eur. Phys. J. B* **12**, 17 (1999).

[53] J. Tempere and J. T. Devreese, *Phys. Rev. B* **64**, 104504 (2001).

[54] J. Devreese, R. Evrard, and E. Kartheuser, *Phys. Rev. B* **12** 3353 (1975).

[55] W. Becker, B. Gerlach, H. Schliffke, Phys. Rev. B **28**, 5735 (1983).

[56] F. M. Peeters, J. T. Devreese, Phys. Rev. B **31**, 6826 (1985).

[57] Y. Osaka, Prog. Theor. Phys. **22**, 437 (1959).

[58] J. T. Devreese, *Contribution to the polaron theory*, Ph.D. Thesis, KU Leuven, 1964.

[59] J. T. Devreese and R. Evrard, in *Proceedings of the British Ceramic Society* **10**, 151 (1968). Reprinted in: *Path Integrals and Their Applications in Quantum, Statistical, and Solid State Physics*, edited by G. J. Papadopoulos and J. T. Devreese, NATO ASI Series B, Physics, vol. 34, Plenum, New York, 1977, pp. 344-357.

[60] F. M. Peeters and J. T. Devreese, in *Solid State Physics*, edited by F. Seitz and D. Turnbull, Academic Press, New York, 1984, vol. 38, pp. 81 - 133.

[61] H. Fröhlich, *Proc. R. Soc. (London) Ser. A* **160**, 230 (1937).

[62] D. J. Howarth and E. H. Sondheimer, *Proc. R. Soc. (London) Ser. A* **219**, 53 (1953).

[63] Y. Osaka, *Progr. Theoret. Phys.* **25**, 517 (1961).

[64] F. E. Low and D. Pines, *Phys. Rev.* **98**, 414 (1955).

[65] L. P. Kadanoff, *Phys. Rev.* **130**, 1364 (1963).

[66] D. C. Langreth and L. P. Kadanoff, *Phys. Rev.* **133**, A1070 (1964).

[67] F.M. Peeters, J.T. Devreese, *Phys. Stat. Sol. (b)* **115**, 539 (1983).

[68] R. W. Hellwarth and I. Biaggio, *Phys. Rev. B* **60**, 299 (1999).

[69] F. C. Brown, in *Point Defects in Solids*, edited by J. H. Crawford and L. M. Slifkin, Plenum, New York, 1972, vol. 1, p. 537.

[70] E. Hendry, F. Wang, J. Shan, T. F. Heinz, and M. Bonn, *Phys. Rev. B* **69**, 081101(R) (2004).

[71] V. L. Gurevich, I. G. Lang, and Yu. A. Firsov, *Fiz. Tverd. Tela* **4**, 1252 (1962) [English translation: *Sov. Phys. — Solid St.* **4**, 918 (1962)].

[72] G. D. Mahan, Many-Particle Physics, Kluwer/Plenum, New York, 2000.

[73] J. Devreese, W. Huybrechts, and L. Lemmens, Phys. Stat. Sol. (b) **48**, 77 (1971).

[74] H. Finkenrath, N. Uhle, and W. Waidelich, *Solid State Commun.* **7**, 11 (1969).

[75] M. J. Goovaerts, J. De Sitter, and J. T. Devreese, *Phys. Rev.* **7**, 2639 (1973).

[76] F. M. Peeters and J. T. Devreese, Phys. Rev. B **28**, 6051 (1983).

[77] D. Forster, *Hydrodynamic Fluctuations, Broken Symmetry and Correlation Functions,* Benjamin, New York, 1975.

[78] F. M. Peeters and J. T. Devreese, Phys. Rev. B **23**, 1936 (1981).

[79] A. S. Mishchenko, N. Nagaosa, N. V. Prokof'ev, A. Sakamoto, and B. V. Svistunov, *Phys. Rev. Lett.* **91**, 236401 (2003).

[80] W. Huybrechts and J.T. Devreese, Phys. Rev. B **8**, 5754 (1973).

[81] D. M. Eagles, R. P. S. M. Lobo, and F. Gervais, *Phys. Rev. B* **52**, 6440 (1995).

[82] J. T. Devreese, L. Lemmens, and J. Van Royen, Phys. Rev. B **15**, 1212 (1977).

[83] L. F. Lemmens, J. De Sitter, and J. T. Devreese, Phys. Rev. B **8**, 2717 (1973).

[84] F. M. Peeters, Wu Xiaoguang, J. T. Devreese, Phys. Rev. B **33**, 3926 (1986).

[85] Wu Xiaoguang, F. M. Peeters, J. T. Devreese, Phys. Rev. B **31**, 3420 (1985).

[86] F. M. Peeters, J. T. Devreese, Phys. Rev. B **36**, 4442 (1987).

[87] F. M. Peeters, J. T. Devreese, Phys. Rev. B **28**, 6051 (1983).

[88] J. T. Devreese, L. F. Lemmens, J. Van Royen, Phys. Rev. B **2**, 1212 (1977).

[89] F. M. Peeters, J. T. Devreese, Solid State Phys. **38**, 81 (1984).

[90] F. Brosens, S. N. Klimin, and J. T. Devreese, Phys. Rev. B **77**, 085308 (2008).

[91] L. F. Lemmens, J. T. Devreese, and F. Brosens, Phys. Stat. Sol. (b) **82**, 439 (1977).

[92] S. Lupi, P. Maselli, M. Capizzi, P. Calvani, P. Giura and P. Roy, Phys. Rev. Lett. **83**, 4852 (1999).

[93] Ch. Hartinger, F. Mayr, J. Deisenhofer, A. Loidl, and T. Kopp, Phys. Rev. B **69**, 100403(R) (2004).

[94] Ch. Hartinger, F. Mayr, A. Loidl, and T. Kopp, cond-mat/0406123.

[95] D. Emin, Phys. Rev. B **48**, 13691 (1993).

[96] G. P. Zhang, T. A. Callcott, G. T. Woods, L. Lin, B. Sales, D. Mandrus, and J. He, Phys. Rev. Lett. **88**, 077401 (2002).

[97] T. Hotta, Phys. Rev. B **67**, 104428 (2003).

[98] S. N. Klimin, V. M. Fomin, F. Brosens, and J. T. Devreese, Phys. Rev. B **69**, 235324 (2004).

[99] L. F. Lemmens, F. Brosens, and J. T. Devreese, Phys. Rev. E **53**, 4467 (1996).

[100] J. T. Devreese, S. N. Klimin, V. M. Fomin, and F. Brosens, Solid State Communications **114**, 305 (2000).

[101] F. Brosens, J. T. Devreese, and L. F. Lemmens, Phys. Rev. E **55**, 227 (1997); **55**, 6795 (1997); **58**, 1634 (1998).

[102] L. F. Lemmens, F. Brosens, and J. T. Devreese, Solid State Communications **109**, 615 (1999).

[103] G. De Filippis, V. Cataudella and G. Iadonisi, Eur. Phys. J. B **8**, 339 (1999).

[104] W.B. da Costa, N. Studart, Phys. Rev. B **47**, 6356 (1993).

[105] F. Brosens, S. N. Klimin, and J. T. Devreese, Phys. Rev. B **71**, 214301 (2005).

[106] S. N. Klimin, V. M. Fomin, F. Brosens, and J. T. Devreese, Physica E **22**, 494 (2004).

[107] J. T. Devreese, in: *Fluctuating Paths and Fields* (World Scientific, Singapore, 2001), pp. 289-304.

[108] G. Verbist, F. M. Peeters and J. T. Devreese, Phys. Rev. B **43**, 2712 (1991).

[109] M. A. Smondyrev, G. Verbist, F. M. Peeters, and J. T. Devreese, Phys. Rev. B **47**, 2596 (1993).

[110] N. I. Kashirina, V. D. Lakhno, and V. V. Sychyov, Phys. Stat. Sol. (b) **239**, 174 (2003).

[111] J. Tempere, S. N. Klimin, I. F. Silvera, J. T. Devreese, Eur. Phys. J. **32**, 329 (2003).

[112] A.P. Volodin, M.S. Khaikin, and V.S. Edelman, JETP Lett. **26**, 543 (1977); U. Albrecht and P. Leiderer, Europhys. Lett. **3**, 705 (1987).

[113] V.B. Shikin, JETP Lett. **27**, 39 (1978); M.M. Salomaa and G.A. Williams, Phys. Rev. Lett. **47**, 1730 (1981).

[114] I.F. Silvera, Bull. Am. Phys. Soc. **46**, 1016 (2001).

[115] J. Tempere, I.F. Silvera, and J.T. Devreese, Phys. Rev. Lett. **87**, 275301 (2001).

[116] S. Fratini and P. Quémerais, Eur. Phys. J. B **14**, 99 (2000).

[117] F. Lindemann, Z. Phys. **11**, 609 (1910); C.M. Care and N.H. March, Adv. Phys. **24**, 101 (1975).

[118] C.C. Grimes and G. Adams, Phys. Rev. Lett. **42**, 795 (1979).

[119] V.M. Bedanov and F.M. Peeters, Phys. Rev. B **49**, 2667 (1994).

[120] L.P. Gor'kov and D.M. Chernikova, Pis'ma Zh. Eksp. Teor. Fiz. **18**, 119 (1973) [JETP Lett. **18**, 68 (1973)].

[121] J. Tempere, I.F. Silvera, and J.T. Devreese, Phys. Rev. B **67**, 035402 (2003).

[122] D.S. Fisher, B.I. Halperin, and P.M. Platzman, Phys. Rev. Lett. **42**, 798 (1979).

[123] G. Deville *et al.*, Phys. Rev. Lett. **53**, 588 (1984).

[124] S. N. Klimin and J. T. Devreese (*to be published*).

[125] J. T. Devreese and A. S. Alexandrov, Rep. Prog. Phys. **72**, 066501 (2009); A. S. Alexandrov and J. T. Devreese, *Advances in Polaron Physics* (Springer, 2009).

[126] B. E. Sernelius, Phys. Rev. B **48**, 7043 (1993).

[127] G. De Filippis, V. Cataudella, A. S. Mishchenko, C. A. Perroni, and J. T. Devreese, Phys. Rev. Lett. **96**, 136405 (2006).

[128] G. R. Allcock, in *Polarons and Excitons*, edited by C. G. Kuper and G. D. Whitfield (Oliver and Boyd, Edinburgh, 1963), pp. 45 – 70.

[129] M. Born and K. Huang, *Dynamical theory of crystal lattices* (Oxford University Press, 2007).

[130] Yu. E. Perlin, Sov. Physics. Uspekhi. **6**, 542 (1964).

[131] H. Jahn and E. Teller, Proc. R. Soc. London A **161**, 220 (1937).

[132] H. Kleinert, *Path Integrals in Quantum Mechanics, Statistics, Polymer Physics, and Financial Markets* (5th edition, World Scientific, Singapore 2009).

[133] V. M. Fomin, V. N. Gladilin, J. T. Devreese, E. P. Pokatilov, S. N. Balaban, and S. N. Klimin, Phys. Rev. B **57**, 2415 (1998).

[134] E. N. Myasnikov, A. E. Myasnikova, and Z. P. Mastropas, Physics of the Solid State **48**, 1046 (2006).

[135] H. Spohn, Phys. Rev. B 33, 8906 (1986); Ann. Phys. **175**, 278 (1987).

[136] G. Wellein, H. Röder, and H. Fehske, Phys. Rev. B **53**, 9666 (1996).

[*] This work was presented at the $10^{\mathtt{th}}$ International Conference "Path Integrals – 2010", July 11 – 16, 2010, Washington DC, USA.

[138] N. N. Bogoliubov and N. N. Bogoliubov, Jr., *Some Aspects of Polaron Theory.* In: *Lecture Notes in Physics* vol. 4, World Scientific, Singapore (1988).

[139] K. Yamazaki, J. Phys. A **16**, 3675 (1983).

[140] V. Cataudella, G. De Filippis, and C. A. Perroni, in *Polarons in Advanced Materials*, Springer Series in Materials Science , Vol. 103, Edited by A. S. Alexandrov (Canopus and Springer, Bath, UK, 2007), pp. 149 – 189.

[141] J. T. Devreese and F. Brosens, Phys. Rev. B **45**, 6459 (1992).

[142] Y. Lépine and M. Charbonneau, Phys. Status Solidi B **122**, 151 (1984); Y. Frongillo and Y. Lépine, Phys. Rev. B **40**, 3570 (1989).

[143] J. T. Devreese and F. Brosens, Phys. Stat. Sol. (b) **108**, K29 (1981).

[144] T. D. Schultz, Phys. Rev. **116**, 596 (1959).

[145] J. T. Devreese and R. Evrard, Phys. Stat. Sol. (b) **78**, 85 (1976).

[146] J. T. Devreese, R. Evrard, and E. Kartheuser, Phys. Stat. Sol. (b) **90**, K73 (1978).

[147] J. T. Devreese and R. Evrard, in: *Linear and Nonlinear Electron Transport in Solids* (Plenum Press, New York, 1978).

[148] F. Brosens and J. T. Devreese, Phys. Stat. Sol. (b) **111**, 591 (1982).

[149] G. E. Volovik, V. I. Melnikov, and V. M. Edelshtein, JETP Letters **18**, 138 (1973).

[150] K. K. Thornber, *Phys. Rev.* B **3**, 1929 (1971).

[151] V. F. Los, Theor. and Math. Phys. **60**, 703 (1984).

[152] S. A. Sokolovsky, Theoretical and Mathematical Physics, **168**, 1150 (2011).

[153] D. Sels and F. Brosens, Phys. Rev. E **89**, 012124 (2014).

[154] D. Sels, F. Brosens, and W. Magnus, Physica A **392**, 326 (2013).

[155] D. Sels and F. Brosens, Phys. Rev. E **88**, 042101 (2013).

[156] H. Fröhlich and N. F. Mott, Proc. R. Soc. London, Ser. A **171**, 496 (1939).

[157] B. I. Davydov and I. M. Shmushkevich, Uspekhi Fiz. Nauk **24**, 21 (1940).

[158] A. Anselm, *Introduction to Semiconductor Theory* (English translation: Prentice Hall, 1981).

[159] G. De Filippis, V. Cataudella, A. de Candia, A. S. Mishchenko, and N. Nagaosa, Phys. Rev. B **90**, 014310 (2014).

Litreature from Prkar's book

1. Д. И. Блохинцеви Б. И. Давыдов, ДАН СССР, XX, 279, 1938.
2. С. И. Пекар, ЖЭТФ 9, 534, 1939.
3. N. F. Mot t, Proc. Roy. Soc. (A) 171, 27, 1939.
4. Б. И. Давыдов, ЖЭТФ 10, 1342, 1940; N. F. Mott. Proc. Cambr. Phil. Soc. 34, 568, 1938; С. И. Пекар, ЖЭТФ10, 1210, 1940; С. И. Пекар, ИАН СССР (сер. физ.) V, 422, 1941; Schottky und Spenke, Wissenschaftliche Veröffentlichungen aus den Siemens Werken, t. XVIII, 1939.
5. С. М. Рывкин, ЖТФ, XVIII, 1521, 1948; ДАН СССР, LXVIII, 487, 1949; ЖЭТФ 20, 139, 1950; В. П, Жузеи С. М. Рывкин, ДАН СССР, LXVIII, 673, 1949; ЖЭТФ 20, 152, 1950; В. Е. Лашкарёв, ЖЭТФ 18, 962, 1948; 19, 876, 1949; К. Б. Толпыго «Труды VII Совещания по свойствам полупроводников», Изд. АН СССР, 1951.

6. Л. Д. Ландау, Sow. Phys. 3, 664, 1933; Я. И. Френкель, Sow. Phys. 9, 158, 1936; Д. И. Блохинцев, ЖЭТФ 6, 1053, 1936.

7. M. Born. Zs. f. Phys. 40, 167, 1926; E. Fermiu. F. Persico, Rend. Lincei (6) 4, 452, 1926; M. Bornu. V. Fock, Zs. f. Phys. 51, 165, 1928; P. Güttinger, Zs. f. Phys. 73, 169, 1931.

8. F. Bloch, Zs. f. Phys. 52, 555, 1929; R. Peierls, Ann. d. Phys. 4, 123, 1930; 5, 244, 1930; R. de L. Kronig and W. C. Penney, Proc. Roy. Soc. (A) 130, 499, 1931.

9. Я. И. Френкель, Phys. Rev. 37, 17, 1931; 37, 1276, 1931; R. Peierls, Ann. d. Phys. 13, 905, 1932.

10. С. И. Пекар, ЖЭТФ 18, 525, 1948.

11. С. И. Пекар, ЖЭТФ 16, 933, 1946.

12. С. И. Пекар, ЖЭТФ 16, 341, 1946.

13. С. И. Пекар, ЖЭТФ 16, 335, 1946.

14. Н. Ф. Мотт и Р. В. Герни, Электронные процессы в ионных кристаллах, Гостехиздат, 1950.

15. С. И. Пекар, ЖЭТФ 17, 868, 1947.

16. С. И. Пекар и М. Ф. Дєйген, ЖЭТФ 18, 481, 1948.

17. С. И. Пекар, ЖЭТФ 18, 105, 1948.

18. Л. Д. Ландау и С. И. Пекар, ЖЭТФ 18, 419, 1948.

19. L ando1t, Phys. Chem. Tabellen III Ergänz. Band, стр. 1471.

20. Evans, Phys. Rev. 57, 47, 1940.

21. См., например, Борн и Гепперт-Мейер. Теория твёрдого тела.

22. С. И. Пекар, ЖЭТФ 19, 796, 1949.

23. D. R. Hartree, Cambr. Phyl. Soc. 24, 89, 1928.

24. В. Фок, Zs. f. Phys. 61, 126, 1930.

25. N. F. Mott, Proc. Roy. Soc. 167, 384, 1938.

26. А. С. Давыдов, ЖЭТФ 19, 168, 1949.

27. Ю. Е. Перлин, ЖЭТФ 21, 547, 1951.

28. Г. Бетеи А. Зоммерфельд, Электронная теорияметаллов, Гостехиздат, 1938.

29. И. Е. Тамм, Sow. Phys. 1, 733, 1932; Zs. f. Phys. 76, 849, 1932; Соколови Махалова, Zs. f. Phys. 99, 503, 1936.

30. W. C. Roentgen und A. F. Joffe, Ann. d. Phys. 64. 1, 1921.

31. С. А. Арцыбышев, Труды ФИАН, т. 1, вып. 3, 5, 1938.

32. Ф. Ф. Волькенштейн, Электропроводность полупроводников, Гостехиздат, 1947.

33. П. С. Тартаковский, Внутренний фотоэффект в диэлектриках, Гостехиздат, 1940.

34. А. Л. Ю з, Усп. физ. наук 17, 55, 1937.

35. F. Seitz, Rev. Mod. Phys. 18, 384, 1946.

36. R. Hilsch u. R. Pohl, Gött. Nachr. 11 (№ 46), 1933.

37. Mollwo, Gött. Nachr. 79, № 6, 1934.

38. С. И. Пекар, ЖЭТФ 20, 510, 1950.

39. J. M. Nuttal, Phys. Rev. 31, 742, 1928.

40. G. K1einschrod, Ann. d. Phys. 27, 97, 1936.

41. М. Ф. Дейген, ЖЭТФ 18, 818, 1948.

42. С. И. Пекар и О. Ф. Томасевич, ЖЭТФ 21, 1951.

43. Г. Е. Зильберман, ЖЭТФ 19, 135, 1949.

44. См., например, Д. И. Блохинцев, Основы квантовой механики, Гостехиздат, 1949.

45. Э. Рашба, Студ. науч. работы Киевского гос. университета X, 81, 1950.

46. К. Б. Толпыго, ЖЭТФ 21, 1951.

47. Н. Н. Боголюбов, Украинский математический журнал, т. II, № 2, 3, 1950.

48. К. Б. Толпыго, ЖЭТФ 20, 497, 1950.

49. Barnes, Zs. f. Phys. 75, 723, 1932.

50. B. Gudden und P. Henninger, Zs. f. Phys. 125, 757, 1949.

51. A. Smakula, Gött. Nachr. 1, 55, 1934.

52. Schönwa1d, Ann. d. Phys. 15, 395, 1932.

53. Джулай, Zs. f. Phys. 32, 103, 1925; А. Н. Арсеньева, Zs. f. Phys. 37, 701, 1926.

54. E. Engelgard, Ann. d. Phys. 17, 501, 1933.

55. R. W. Poh1, Proc. Roy. Soc. 49 (extra part), 3, 1937.

56. Г. И. Сканави, Физика диэлектриков, Гостехиздат, 1949.

57. С. И. Пекар, ЖЭТф 20, 267, 1950.

58. С. И. Пекар и М. Ф. Дейген, ЖЭТФ 21, в. 7, 1951.

59. С. И. Пекар и Ю. Е. Перлин, ЖЭТФ 20, 271, 1950.

60. H. Pick, Ann. d. Phys. 31, 365, 1938.

61. Ю. А. Перлин, ЖЭТФ 20, 274, 1950.

62. G. Glaser, Gött. Nachr. 2, 1937.

63. О. Ф. Томасевич, ЖЭТФ 51, 1951.

64. Г. Е. Зильберман, ЖЭТФ 19, 146, 1949.

65. Ю. А. Дунаеви Ю. П. Маслаковец, ЖЭТФ 17, 931, 1947.

66. Landolt, Phys. Chem. Tabellen.

67. Б. И. Давыдов и И. М. Шмушкевич, Усп. физ. наук 24, 21, 1940.

68. И. Курчатов, Т. Костинаи Л. Русинов, Sow. Phys. 7, 129, 1935.

69. Ф. Доманик, Ann. d. Phys. 43, 187, 1943.

70. А. С. Давыдов, ЖЭТФ 18, 913, 1948.

71. Э. И. Адирович, Труды ФИАН, т. V, 1950.

72. H. Fröhlich, H. Pelzer and S. Zienau, Phil. Mag. 41, 221, 1950.

73. С. В. Тябликов, ЖЭТФ 21, 377, 1951.

16.2 Bibliography from Old, Fundamental Articles

16.3 Bibliography from Articles about Special Models and Effects

16.4 Bibliography from articles about main experiments

From Application of the polaron-transport theory to $\sigma(\omega)$ in $Tl_2Ba_2Ca_{1-x}Gd_xCu_2O_8$, $YBa_2Cu_3O_{7-8}$, and $La_{2-x}Sr_xCuO_4$ by Mihailovic, Foster, Voss, Heeger

[1] For a review, see T. Timusk and D. B. Tanner, in Physical Properties of High Temperature Superconductors I, edited by Donald M. Ginsberg (World Scientific, Singapore, 1989), p. 339.
[2] K. Kamaras, S. L. Herr, C. D. Porter, N. Tache, D. B. Tanner, S. Etemad, T. Venkatesen, E. Chase, A. Inam, X. D. Wu, M. S. Hegde, and B. Dutta, Phys. Rev. Lett. 64, 84 (1990).
[3] R. T. Collins, Z. Schlesinger, F. Holtsberg, and C. Feild, Phys.
Rev. Lett. 63, 422 (1989); Z. Schlesinger, R. T. Collins, F. Holtsberg, C. Feild, S. H. Blanton, U. Welp, G. W. Crabtree, Y. Fang, and J. Z. Liu (unpublished).
[4] C. M. Foster, K. F. Voss, T. W. Hagler, D. Mihailovic, A. J. Heeger, M. M. Eddy, W. L. Olsen, and E. J. Smith, Solid State Commun. (to be published).
[5] G. A. Thomas, J. Orenstein, D. H. Rapkine, M. Capizzi, A. J. Millis, R. N. Bhatt, L. F. Schneemeyer, and J. V. Waszczak, Phys. Rev. Lett. 61, 1313 (1988).
[6] S. Tajima, S. Uchida, A. Masaki, H. Takagi, K. Kitazawa, S. Tanaka, and A. Katsui, Phys. Rev. B 32, 6302 (1985); S. Tajima, S. Uchida, A. Masaki, H. Takagi, K. Kitazawa, S. Tanaka, and S. Sugai, ibid. 35, 696 (1987).
[7] Xiang-Xin Bi, P. C. Eklund, E. McRae, Ji-Guang Zhang, P. Metcalf, J. Spalek, and J. M. Honig, Phys. Rev. B 42, 4756 (1990).
[8] J. F. Schooley, H. P. R. Frederikse, W. R. Hosler, and E. R. Pfeiffer, Phys. Rev. 159, 301 (1967).
[9] E. V. Bursian, Ya. G. Girshberg, and E. N. Starov, Phys. Status Solidi B 46, 529 (1971).
[10] J. Orenstein, G. A. Thomas, D. H. Rapkine, C. G. Bethea, B. F. Levine, B. Batlogg, R. J.

Cava, D. W. Johnson, Jr., and E. A. Rietman, Phys. Rev. B 36, 8892 (1987); S. L. Herr et al., in High Temperature Superconducting Materials: Preparation, Properties and Processing, edited by William Hatfield and J. J. Miller (Marcel Dekker, New York, 1988), p. 275.
[11] J. B. Torrance, Y. Tokura, A. I. Nazzal, A. Bezinge, T. C. Haung, and S. S. P. Parkin, Phys. Rev. Lett. 61, 1127 (1988).
[12] K. Sreedhar and P. Ganguly, Phys. Rev. B 41, 371 (1990).
[13] J. Ruvalds and A. Virosztek, Phys. Rev. B 42, 399 (1990); (unpublished).
[14] V. Z. Kresin and S. A. Wolf, Phys. Rev. B 41, 4278 (1990); W. Pickett, Rev. Mod. Phys. 61, 433 (1989); J. Fink, N. Nucker, H. Romberg, and J. C. Fuggle, J. Res. Dev. (to be published); M. Lang, T. Lechner, S. Riegel, F. Steglich, G. Weber, T. J. Kim, G. Luthi, B. Wolf, H. Rietschel, and M. Wilhelm, Z. Phys. B 69, 459 (1988).
[15] H. G. Reik and D. Heese, J. Phys. Chem. Solids 28, 581 (1967).
[16] H. G. Reik, Solid State Commun. 1, 67 (1963).
[17] H. G. Reik, Z. Phys. 203, 346 (1967).
[18] E. V. Bursian, Ya. G. Girshberg, and E. N. Starov, Fiz. Tverd. Tela (Leningrad) 14, 1019 (1972) [Sov. Phys. Solid State 14, 872 (1972)].
[19] D. Emin, Adv. Phys. 24, 305 (1975).
[20] M. Klinger, Phys. Lett. 7, 102 (1963).
[21] Y. H. Kim, A. J. Heeger, L. Acedo, G. Stucky, and F. Wudl, Phys. Rev. B 36, 7252 (1987).
[22] Y. H. Kim, C. H. Foster, A. J. Heeger, S. Cox, and G. Stucky, Phys. Rev. B 38, 6478 (1988); C. Taliani, R. Zamboni, G. Ruani, F. C. Matacotta, and K. I. Pokhodnya, Solid State Commun. 66, 487 (1988).
[23] C. M. Foster, A. J. Heeger, G. Stucky, and N. Herron, Solid State Commun. 71, 945 (1989).
[24] C. M. Foster, A. J. Heeger, Y. H. Kim, G. Stucky, and N. Herron, Synth. Met. 33, 171 (1989).
[25] T. Holstein, Ann. Phys. (N.Y.) 8, 343 (1959).
[26] H. G. Reik and D. Heese, Phys. Status Solidi 24, 281 (1967); also see Lines and Glass, Principles and Applications of Ferroelectrics and Related Materials (Clarendon, Oxford, England, 1977), and references therein.
[27] I. Batistic, A. R. Bishop, R. L. Martin, and Z. Tešanovic, Phys. Rev. B 40, 6896 (1989); R. E. Cohen, W. E. Pickett, and H. Krakauer, Phys. Rev. Lett. 64, 2575 (1990).
[28] L. Genzel, A. Wittlin, M. Bauer, M. Cardona, E. Schonherr, and A. Simon, Phys. Rev. B 40, 2170 (1989).
[29] D. Emin and M. S. Hillery, Phys. Rev. B 39, 6575 (1989); D. Emin, Ferroelectrics (to be published); A. S. Alexandrov, J. Ranninger, and S. Robaszkiewcz, Phys. Rev. B 33, 4526 (1986).
[30] S. L. Herr, K. Kamaras, C. D. Porter, M. G. Doss, D. B. Tanner, D. A. Bonn, J. E. Greedan, C. V. Stager, and T. Timusk, Phys. Rev. B 36, 733 (1987).
[31] C. Taliani, A. J. Pal, G. Ruani, and R. Zamboni, in Proceedings of the International Conference on Superconductors, Bangalore, India, 1990 [Bull. Mater. Sci. (to be published)].
[32] P. E. Sulewski, P. A. Fleury, K. B. Lyons, S-W. Cheong, and Z. Fisk, Phys. Rev. B 41, 225 (1990).
[33] K. B. Lyons, P. A. Fleury, L. F. Schneemeyer, and J. V. Waszczak, Phys. Rev. Lett. 60, 732 (1988).
[34] K. F. McCarty, E. L. Venturini, D. S. Ginley, B. Morosin, and J. F. Kwak, Physica C 159, 603 (1989).
[35] P. Knoll, C. Thomsem, M. Cardona, and P. Murugaraj, Phys. Rev. B 42, 4842 (1990).
[36] F. C. Zhang and T. M. Rice, Phys. Rev. B 37, 3759 (1988).
[37] D. Mihailovic and A. J. Heeger, Solid State Commun. 75, 319 (1990).